

PROCEEDINGS
VETERINARY PATHOLOGY SERVICE
WEDNESDAY SLIDE CONFERENCE
2018-2019



JOINT PATHOLOGY CENTER
SILVER SPRING, MD 20910
2018-2019

JOINT PATHOLOGY CENTER
VETERINARY PATHOLOGY SERVICE

*This year's edition of the Wednesday Slide Conference
is dedicated to*

COL Robert Moses "Bob" McCully.

Husband, father, officer, veterinarian, pathologist.

*"You spend your life studying pathology, and at the
end, you are pathology." ...RMM*

In Memoriam: Robert M. McCully (1927–2017)

Veterinary Pathology
2018, Vol. 55(5) 759-761
© The Author(s) 2018
Article reuse guidelines:
sagepub.com/journals-permissions
DOI: 10.1177/0300985818776053
journals.sagepub.com/home/vet



Bruce Williams¹



The long mission of Bob McCully is now complete. The senior surviving alumnus of the Armed Forces Institute of Pathology (AFIP) Department of Veterinary Pathology and likely its most colorful personality, Col Robert Moses “Bob” McCully, USAF, lived a life and successfully pursued a rich and varied career that most pathologists simply dream about. Col McCully was also one of the Department’s most prolific authors, with over 50 first-author papers to his credit. He passed on 24 March 2017, having left his mark and singular impression on generations of pathologists on

2 continents, and on 16 March 2018 was interred with honors at Arlington National Cemetery, alongside many other American heroes. The last line of his gravestone in

¹Joint Pathology Center, Rockville, MD, USA

Corresponding Author:

Bruce Williams, Joint Pathology Center, 606 Stephen Sitter Ave, Rockville, MD 20852, USA.

Email: bruce.h.williams@hotmail.com

Arlington bears the achievement he was most proud of—“Veterinary Pathologist.”

A lanky Mississippian, Bob McCully enlisted in the US Merchant Marine in 1945 immediately upon graduation from high school. With the war over, he returned to civilian life and enrolled in pre-vet studies at Mississippi State College, entering veterinary school at Iowa State University in 1949. He graduated from veterinary school at Iowa State in 1953, did a 2-year internship at Angell Memorial, and was recruited to join the Air Force in 1955, with an initial assignment at the Armed Forces Institute of Pathology (which was to ultimately become his one and only duty station in a 20+-year Air Force career). While serving as the chief of both the Lab Animal Colony and Experimental Surgery Section in the brand-new AFIP building on the campus of Walter Reed, 1st Lt McCully simultaneously trained as a veterinary pathologist under Drs T.C. Jones and Charlie Barron, forming the first AFIP resident class in 1958 with Capt F.M. Garner. As a resident, he not only worked with NASA's fledgling space program but was also an observer during 3 separate nuclear tests at the Nevada Proving Grounds (proudly displaying, years later, the certificate he received from the US government in the 1980s stating he had not received a dangerous dose of radiation during his observer days.)

He culminated his official 3-year residency with ACVP certification in 1961. (His ACVP “class” of 6 was a memorable one, including John King and David Dodd, among others.) Following 2 years as the training officer at the AFIP, Capt McCully was the first AFIP-Onderstepoort Exchange Officer, a program that was to change the course of his career and life.

In December 1963, Maj McCully, his wife Elaine, and 4 children traveled to South Africa, a country that captured their hearts and they would truly never leave. While studying foreign animal diseases for the US government and sending incredible amounts of material back to the AFIP for teaching and research, Bob also accompanied local guides, rangers, and African natives on their excursions in Kruger national park and elsewhere around the country, doing field autopsies on culled hippopotami, large cats, and many and varied hoofstock, cataloguing diseases that few non-Africans had ever seen. Dr McCully investigated and eventually published over 40 peer-reviewed articles dealing primarily with the pathology and parasitology of African wildlife and domestic livestock. In 1969, he returned to the AFIP to manage the exchange program until 1975, when he retired from the Air Force. His family remained behind in South Africa, beginning for him a 40-year quasi-nomadic life that would take him between South Africa, Washington, DC, and his childhood home in Lewisville, Mississippi, each year.

In South Africa, where he primarily lived and watched his family grow to 8 members (all graduating college and most entering various aspects of medicine), he continued to interact and work with the Department of Veterinary Pathology at Onderstepoort, attending rounds, assisting in autopsies, and collecting additional photographs and data on almost every disease of local livestock. His dedication to pathology was

evidenced by his electronic publication of his ultimate work, the *The AFIP-Onderstepoort Program Color Atlas of Foreign and Domestic Diseases of Pastoral Animals and Other Selected Species*, a volume 30 years in the making and ultimately financed, completed, and distributed (a copy handposted to each member of the ACVP) by Dr McCully himself.

These are the facts of the man, most set in stone before I met “Dr Mac,” but certainly not his measure. I met him first in the early 1990s when the incessant delays of the AFIP's publishing of his *Atlas* made him a much feared figure whenever he would turn up in its hallways, but I was later to find out that his anger was righteous and his treatment (and more importantly to him, those of his fellow authors) by my organization was most unconscionable. (The aforementioned delays totaled 16 years before Col McCully was able to wrest back his manuscript from the government and publish it himself.)

I was not to meet the real Bob McCully until almost 20 years later, when the AFIP was closed and its successor, the Joint Pathology Center (JPC), established miles away on the old Forest Glen Campus. On the day we opened the JPC doors, I noticed a lanky, albeit stooped older gentleman in a leather bomber jacket and USAF retiree ballcap walking laps around our parking lot behind a grocery cart (the JPC shares a building with the Army commissary, so grocery carts are a common sight). My memories of Dr McCully were vivid enough to allow me the temerity of reintroducing myself after many years, and my invitation to come see the “new AFIP” was met with enthusiasm and grace, but only “after I finish my two miles.” From that day on, Bob McCully, at least when he was in the US, was a fixture in our department—attending lectures, looking at cases, and telling stories as only he could about his days at the AFIP and in South Africa, to the delight of residents 50 years his junior.

At the JPC, he was considered family, which made it all the more difficult when he returned from South Africa in 2015 with a diagnosis of melanoma and a tumor on his ear and face that made all of us gasp. Fearful of a surgery that might leave him with facial paralysis, Bob handled the situation as only Bob would—he informed his doctors at Walter Reed that he would endure no surgery, no chemo, and no radiation. After 6 weeks of additional rapid tumor growth, his doctors started Bob on an experimental monoclonal antibody (nivolumab), which combined with several biopsies and tumor debulking (under local anesthetic and Bob's very watchful eye) resulted in an almost miraculous recovery and ultimately, a cure. During this time, even though he often suffered great pain from the tumor, he insisted on biweekly biopsies to document the tumor's response to treatment and doing the pathologic observations and descriptions himself. He continued to put in a full day each day at the microscope, poring over his own biopsies, interrupting his work only for lectures and slide rounds. His case, a rare success in melanoma treatment, has been written up in surgical journals, where the rapid regression of his tumor once he insisted on surgical debulking and repeated biopsy (contrary to all AMA oncologic directives) has been published as “the McCully effect.” His work during this most trying of times was


an inspiration to our staff, our residents, and even the visitors lucky enough to share the study spaces with him.

For me, the Bob McCully I met in his last 5 years will always be larger than life. His stories of Africa and the AFIP in its heyday, his incredible work ethic—a full day at the JPC at the age of 88, and then home to work on his memoir or his beloved *Atlas*, his endless graciousness to everyone in the Department (the secretaries were as fond of him as he was of them) and his generosity—“Bruce, go buy sandwiches for everyone in the department, as long as they all want Reubens” (as half of the department had the first Reuben sandwich in their lives that day), will always be fond memories. He was also a true man of letters—writing constantly (his memoir stands at 530 pages, his *Atlas* even more), as well as writing several letters to friends and family each day. Everything was written in beautiful longhand—while Bob loved the Internet, especially YouTube, he eschewed email and refused to ever

get an email account. Most of all, those who knew Bob in those last years will remember his love of life and that omnipresent smile.

Perhaps my most lasting memory will be the last day I saw Bob, as the hyperstimulated immune system that cured his melanoma turned on his body, attacked his lungs, and made the great man weak. “Time is short, and we still have work to do,” he told me, as we set up his laptop one last time and, side by side, made some final changes to his memoir. Changes made, he got back into the hospital bed, and we talked and laughed a bit more about pathology and pathologists and finally about the nature of family and the universe. His work finished, and his long mission complete, my friend Bob McCully passed peacefully early the next morning, surrounded by family.

ORCID iD

Bruce Williams  <http://orcid.org/0000-0002-8419-3553>

WEDNESDAY SLIDE CONFERENCE 2018-2019

Case No.	JPC No.	Contr. No.	Species	Tissue	Diagnosis
Conference 1 – August 15, 2018					
1	4020132	RUSVM Case1	African Green Monkey	Liver, Spleen	Yersiniosis
2	4023574	VF247 0900677-d	Rat	Mesenteric artery	Polyarteritis nodosa
3	4102985	PV2017	Mouse	Kidney	Mouse kidney parvovirus
4	4068156	15/191	Horse	Cranial nerve	Craniopharyngioma
Conference 2 – August 22, 2018					
1	4019882	21-168-14 12-168-17	Ferret	Lung	Coronavirus-associated disease
2	4034956	13V1542	Ox	Liver	Acute bovine liver disease
3	4066919	#191301	Dog	Tonsil	Lymphangiomatous tonsillar polyp
4	4017185	1/12	Dog	Haired skin	<i>Straelensia cynotis</i>
Conference 3 – September 5, 2018					
1	4067411	15-13332	Cat	Colon	<i>Clostridium piliforme</i> AEEC
2	4068388	Case 1	Sheep	Brainstem	<i>Listeria monocytogenes</i>
3	4023564	12L1581	Cat	Liver	Mastocytosis
4	4066086	3150102012	Dog	Lung	<i>Angiostrongylus vasorum</i>
Conference 4 – September 19, 2018					
1	4049562	N14-111	Dog	Kidney	Lyme disease
2	4066460	Case 1	Cynomolgus macaque	Kidney EM	Immune-complex glomerulonephritis
3	4048996	P2551-13	Horse	Kidney	Hemolytic-uremic syndrome
4	4056733	252464	Dog	Kidney	Renal dysplasia
Conference 5 - September 26, 2018					
1	4066664	1505184	Ox	Cerebellum Trachea	Ovine herpesvirus-2 MCF
2	4066395	S1408459	Ox	Heart, thymus	<i>Pajaroellobacter abortibovis</i>
3	4033383	13749	Mouse	Salivary gland	Botryomycosis
4	4068765	Case 2	Rat	Zymbal's gland	Zymbal's gland adenoma
Conference 6 – October 3, 2018					
1	4089879	21609	Rat	Cerebrum	Glioma
2	4102645	A16-38521	Dog	Brainstem	Astrocytoma, low grade
3	4048997	P3213-13	Cat	Cerebellum	Abiotrophy
4	4068932	V15-09895	Ox	Cerebellum	Locoism
Conference 7 – October 17, 2018					
1	4084541	UW Case 1 2016	Cat	Eye	Chondrosarcoma
2	4102435	16RD2093	Dog	Optic nerve	Astrocytoma, low-grade
3	4068158	15/444	Horse	Eye	Ciliary body amyloid Recurrent uveitis
4	4019356	AVC C5181-11	Dog	Eye	Orbital meningioma

WEDNESDAY SLIDE CONFERENCE 2018-2019

Conference 8 – October 24, 2018					
1	4084541	UW Case 1 2016	Red squirrel	Skin	<i>Mycobacterium lepromatis</i>
2	4102435	16RD2093	Bald eagle	Heart	Lead toxicity
3	4068158	15/444	Alligator	Liver	<i>Chlamydia</i> sp.
4	4019356	AVC C5181-11	Dog	Mandible	<i>Ophidiomyces ophiodiicola</i>
Conference 9 - November 1, 2018					
1	4050022	13-12484	Horse	Small intestine	<i>Clostridium difficile</i>
2	4085384	H1507887-83	Dog	Stomach	Canine hemorrhagic gastritis
3	4105936	H17-1982	Calf	Abomasum	<i>Sarcina ventriculi</i>
4	4048573	13101599	Ox	Colon	Bovine coronavirus
Conference 10 - November 9, 2018					
1	4006380	Case 1	Dog	Ocular cytology	<i>Prototheca</i> sp.
2	4048660	9428-12	Cat	Spleen	<i>Francisella tularensis</i>
3	4066393	11136	Cynomolgus macaque	Kidney	Fatal fasting syndrome
4	4084546	15-H700012	Rabbit	Cerebrum	<i>Encephalitozoon cuniculi</i>
Conference 11 – December 5, 2018					
1	4066260	P15/141	Ox	Skin	<i>Besnoitia besnoitii</i>
2	4085967	Case #1	Cat	Skin	Cowpox
3	4090973	E2337	Cat	Skin	Bowenoid in situ SCC
4	4084013	16-859	Cat	Gingiva	Peripheral giant cell granuloma
Conference 12 – December 12, 2018					
1	4049888	Case 1 2014	Common marmoset	Tongue, brain	Human herpesvirus 1
2	4039359	V1312663	Ox	Cerebrum	Polioencephalomalacia
3	4084217	K9 CNS1	Dog	Cerebrum	Hypnatremia
4	4100730	16H9445	Dog	Cerebrum	Gm2-gangliosidosis
Conference 13 – January 2, 2019					
1	4100984	A-475-4	C57BL/6Ncr1 mouse	Liver	Ebola virus
2	4105937	N130/176	Cat	Heart	Hypertrophic cardiomyopathy
3	4033739	317048	Horse	Heart	Arrhythmogenic right ventricular cardiomyopathy
4	4049160		Cat	Heart	Reactive angioendotheliomatosis
Conference 14 – January 9, 2019					
1	<u>4101745</u>	<u>NE17-176</u>	Dog	Thyroid gland	Lymphocytic thyroiditis Atherosclerosis
2	<u>4084299</u>	<u>S1603556</u>	Horse	Lung	<i>Acanthamoeba</i> sp.
3	<u>4101314</u>	<u>17-612</u>	Goat	Lung	<i>Rhodococcus equi</i>
4	<u>4103659</u>	<u>Case 1</u>	Sprague-Dawley rat	Lung	Alveolar-bronchiolar carcinoma

WEDNESDAY SLIDE CONFERENCE 2018-2019

Conference 15 –January 15, 2018					
1	4102152	16153E	Rhesus macaque	Heart	<i>Spiroucleus</i> sp.
2	4067571	NCDS-2203/1003-17	Sprague-Dawley rat	Eye	Linear retinopathy
3	4048861	13004	Wister Crlj rat	Kidney	Alloxan toxicity
4	4085317	16-10769	Dog	Tongue	Embedded burdock spines
Conference 16 – January 23, 2019					
1	4019118	FMZV USP Case 1	Dog	Liver	Canine adenovirus-1 Infectious hepatitis
2	4084299	14-7470-10	Horse	Liver	Hemochromatosis
3	4019850	11727	Ox	Liver	Fasciola hepatica
4	4018823	UW SVM Case 2	Dog	Liver	<i>Toxoplasma gondii</i>
Conference 17 – January 30, 2019					
1	4084248	S1501813	Dog	Testis	<i>Rickettsia rickettsii</i>
2	4066258	L14-10949	Pig	Heart	Porcine circovirus-2
3	4032592	D12-044205	Guinea pig	Lung	Guinea pig adenovirus
4	4083744	14A310	Rhesus macaque	Adrenal gland	Waterhouse-Friedrichsen syndrome
Conference 18 – February 6, 2019					
1	4048673	13-161654	African Grey Parrot	Great arteries	Atherosclerosis
2	4066242	B	Orange-winged amazon	Liver	<i>Mycobacterium genavense</i>
3	4085103	1013/15	Blue-eyed cockatoo	Lung	<i>Sarcocystis falcatula</i>
4	4035109	BA214/11 B1	Bearded dragon	Skin	<i>Chrysosporium anamorph of Nannizziopsis vriesii</i>
Conference 19 – February 13, 2019					
1	4048498	08-36807	Soft-shelled turtle	Heart	<i>Spirorchis</i> sp.
2	4054746	TAMU-2 2014	Leopard tortoise	Heart, thymus	<i>Entamoeba histolytica</i> <i>Intranuclear coccidia</i>
3	4084545	15-41009	Tiger	Lung	Canine morbillivirus, CDV
4	4102647	M17-69	American paddlefish	Stomach	<i>Anisakis</i> sp.
Conference 20 – March 20, 2019					
1	4041970	D12-49 3	Dog	Skin	Mast cell tumor, hi grade
2	4117533	SB-18-1846 1	Horse	Eyelid	Clear cell SCC
3	4070611	Case 2	Cat	Prepuce	Transmissible venereal tumor
4	4101757	C9969-15	Ox	Penile urethra	Transitional cell carcinoma
Conference 21 – March 27, 2019					
1	4033381	NCAH 2013-1	Chicken	Trachea	Gallid herpesvirus-1
2	4066708	A231/15	Chicken	Liver	Avian adenovirus
3	4085106	1	Roman duck	Esophagus	Anatid herpesvirus-1
4	4101757	16-5448	Chicken	Gonad	Ovotestis
Conference 22 – April 3, 2019					
1	4113194	Case 2	Norway rat	Liver	<i>Cysticercus fasciolaris</i> <i>Capillaria hepatica</i>
2	4103280	401324	Ox	Lung	<i>Dictyocaulus viviparus</i>
3	4074226	NP545M3	Dog	Skeletal muscle	<i>Ancylostoma caninum</i>
4	4116731	S15/8162	Dog	Small intestine	<i>Echinococcus granulosus</i> adults

WEDNESDAY SLIDE CONFERENCE 2018-2019

Conference 23 – April 10, 2019					
1	<u>4032713</u>	<u>12-324 3</u>	Dog	Liver	Malignant plasma cell tumor
2	<u>4066543</u>	<u>2014910070</u>	Dog	Skin	Erythrocytic plasmablastic lymphoma
3	<u>4066455</u>	<u>66619</u>	Dog	Cerebrum	Histiocytic sarcoma
4	<u>4099791</u>	<u>UMC172</u>	Horse	Lung, liver	Intravascular lymphoma
Conference 24 – April 24, 2019					
1	<u>4088206</u>	<u>W837-12</u>	Horse	Colon	Lethal white foal syndrome
2	<u>4066219</u>	<u>P/2014 95</u>	Horse	Skeletal muscle, fat	Vit E/Se imbalance
3	<u>4101752</u>	<u>S643/17</u>	Horse	Liver	<i>Clostridium difficile</i>
4	<u>4085442</u>	<u>16L-2013</u>	Dog	Lung, heart	Metastatic rhabdomyosarcoma
Conference 25 – May 1, 2019					
1	<u>4037902</u>	<u>N261/13</u>	Cat	Lung	<i>Bordetella bronchiseptica</i>
2	<u>4050143</u>	2014 Case 2	Ox	Lymph node	<i>Mycobacterium bovis</i>
3	<u>4100993</u>	<u>S-2017-20</u>	Dog	Omentum	<i>Actinomyces</i> sp.
4	<u>4032439</u>	<u>12H5674</u>	Dog	Lung	Plexiform arteriopathy

**Joint Pathology Center
Veterinary Pathology Services**



WEDNESDAY SLIDE CONFERENCE 2018-2019

C o n f e r e n c e 1

22 August 2018

CASE I: RUSVM-1 (JPC 4020132).

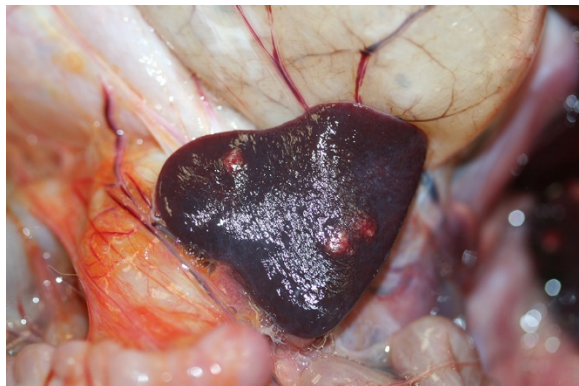
Signalment: 4-year-old, male, African green monkey (*Chlorocebus aethiops sabaesus*)

History: This monkey was euthanized during a recent outbreak of acutely fatal enteric disease in a colony of captive African green monkeys (*Chlorocebus aethiops sabaesus*) in the island of St. Kitts, West Indies. On clinical examination, the monkey had bloody diarrhea, was pyrexia and severely dehydrated. Previous to this case submission, multiple monkeys in the same enclosure had died after a short period of illness characterized by depression, diarrhea and dehydration, or had been found dead in the enclosure. Necropsies performed by the referring veterinarian revealed multifocal, variably-sized, white foci throughout the splenic and hepatic parenchyma. All affected monkeys were part of a large, breeding population maintained by the Behavioral Sciences Foundation, Estridge Estate, St. Kitts, West Indies. Maintenance, testing and all procedures carried out in this facility are approved by the Animal Care Committee of the Behavioral Sciences Foundation, acting under the auspices of the Canadian Council on Animal Care.



Liver, African green monkey. There are multifocal to coalescing variably sized 2-8mm white foci scattered throughout the liver. (Photo courtesy of: Department of Pathobiology, Ross University School of Veterinary Medicine, St. Kitts, West Indies, www.rossu.edu)

Gross Pathology: At necropsy, the monkey was in poor body condition (BCS 2/5), with scant fat reserves and muscle mass. The carcass was moderately dehydrated and the perineum was stained with blood-tinged feces. Multifocal areas of petechiation were present throughout the subcutaneous tissue, and mucous membranes were diffusely pale. The liver and the spleen had multifocal, variably-sized (2 mm-8mm) white foci. The spleen was slightly enlarged. On cut surface, the foci were moderately firm and had a caseated appearance (abscessation /necrosis). The stomach was markedly distended with gas. The mucosa of the small intestine was



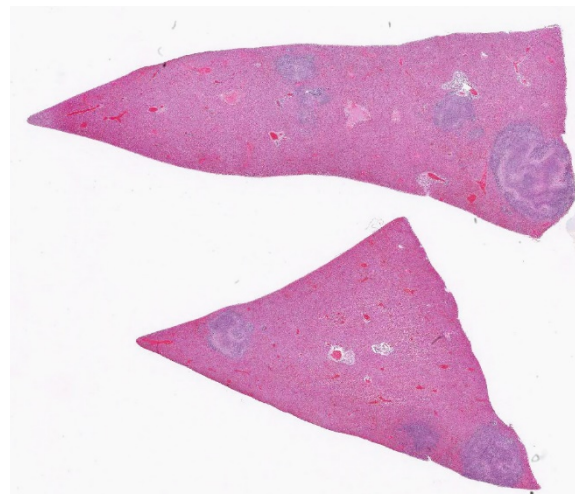
Spleen, African green monkey. There are similar foci scattered throughout the spleen. (Photo courtesy of: Department of Pathobiology, Ross University School of Veterinary Medicine, St. Kitts, West Indies, www.rossu.edu)

diffusely reddened. The cecum and the colon contained blood-tinged mucus and there were numerous 1-2 cm white, slender nematodes present (*Trichuris* sp.). The mesenteric lymph nodes were moderately enlarged and slightly edematous. No other gross lesions were present elsewhere.

Laboratory results: Bacteria recovered from hepatic and splenic swabs collected during necropsy examination were identified by routine culture and biochemical methods as gram-negative, cytochrome oxidase-negative rods. MicroID kits identified the isolates as *Yersinia* spp. Further molecular diagnosis provided by amplification and sequencing of the 16S SSU rRNA gene confirmed the isolates as *Y. enterocolitica*. Leukograms of affected monkeys indicated a leukocytosis most commonly composed of monocytosis, basophilia, lymphocytosis (combined increase in lymphocytes and large granular lymphocytes), an occasional mature neutrophilia, and rarely a left shift. Monocytes were commonly vacuolated. Lymphocytes commonly had increased amounts of pale blue glassy cytoplasm, an occasional reniform nucleus, and more open chromatin. Large granular lymphocytes were

commonly larger than a neutrophil with variable numbers of granules and reniform to amoeboid nuclei. Neutrophils commonly had open chromatin and were pale staining. Döhle bodies, cytoplasmic basophilia, and vacuolation (toxic changes) were not common. Many ruptured cells (“basket cells”) were observed. Increased PCV was uncommon, and red cell abnormalities included schistocytes and microcytes; plasma was often pink-tinged. Platelet clumping was common. The biochemical profile occasionally indicated cholestasis, less commonly, hepatocellular damage, and infrequent increases in UN and phosphorus.

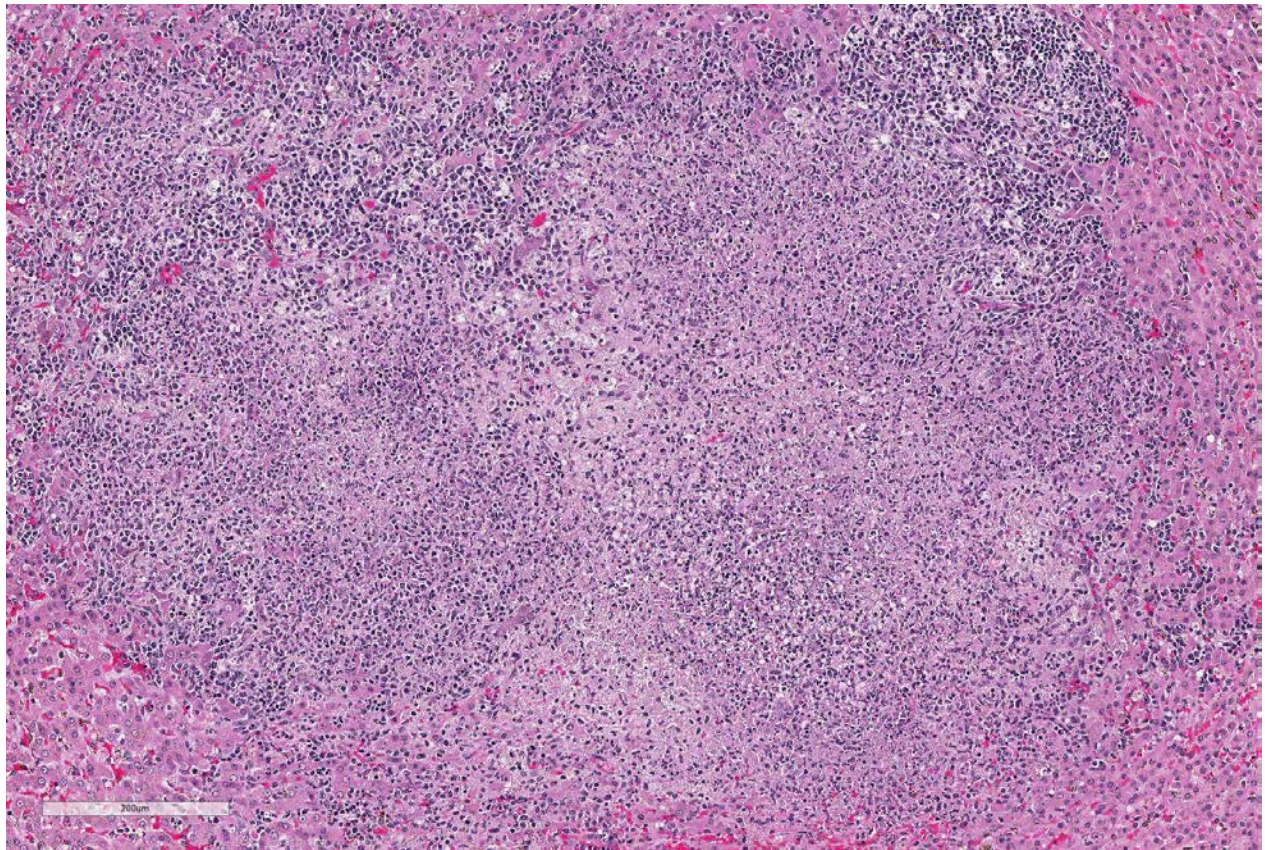
Microscopic Description: Sections of the liver and the spleen reveal random, multifocal to coalescing areas of liquefactive necrosis characterized by extensive loss of normal tissue architecture and cellular detail. Areas of necrosis consisted of a central core of pale eosinophilic and karyorrhectic cellular debris, degenerate neutrophils and a pale, eosinophilic, fibrillar material (fibrin) associated with variably-sized gram-negative colonies (up to 200µm in diameter) of coccobacilli. Numerous macrophages, and



Liver, African green monkey. There are multifocal to coalescing areas of lytic necrosis scattered throughout the two sections of liver. (HE, 5X).

lesser numbers of lymphocytes and plasma cells surrounded the areas of necrosis. Additional microscopic lesions present in the liver include disorganization of hepatic cords, centrilobular and sinusoidal congestion and a mild periportal lymphocytic and plasmacytic hepatitis. Numerous hepatocytes and Kupffer cells contained a yellow-brown granular pigment in the cytoplasm and small bile casts were occasionally observed in canaliculi. Additional microscopic lesions present in the spleen included follicular lymphoid hyperplasia and splenic histiocytosis (please note that not all slides contain a section of the spleen). Similar microscopic lesions were present in the mesenteric lymph nodes and the small intestine (not submitted).

Extramedullary hematopoiesis is present.



Liver, African green monkey. Higher magnification of an area of lytic necrosis. (HE, 130X)

Contributor's Morphologic Diagnoses:

Liver and spleen: Necrotizing and suppurative hepatosplenitis, multifocal, subacute, with gram-negative bacterial colonies, African green monkey.

Contributor's Comment:

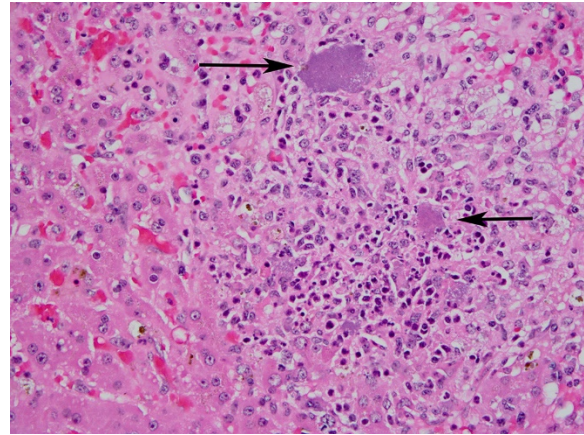
Yersinia enterocolitica is a member of the genus *Yersinia*, a facultative anaerobic bacterium from the Enterobacteriaceae family. *Yersinia enterocolitica* is associated with diverse clinical disease manifestations in humans and a variety of animal species, including non-human primates.^{6,7}

Yersiniosis is an important condition in non-human primates. Non-human primates are very sensitive to pathogenic *Yersinia*, and yersiniosis has been described in these species as an acutely fatal enteric disease, or

as a chronic, debilitating, primarily enteric disease characterized by anorexia, diarrhea and weight loss.^{1,3-5} Enteric yersiniosis in non-human primates is caused by *Y. pseudotuberculosis* and *Y. enterocolitica*. *Yersinia pestis*, the causative organism of plague, is thought to have evolved from *Y. pseudotuberculosis* and initially was considered an enteric pathogen.⁶ Numerous reports have been published describing outbreaks of acute fatal yersiniosis with high morbidity and mortality in captive colonies of non-human primates.^{1,3,5} Host susceptibility to *Yersinia* may differ depending on monkey species.⁶ Outbreaks are characterized by variable degrees of weight loss, anorexia, diarrhea and dehydration. Clinical disease manifestation is variable, and highly dependent on bacterial strains.^{5,6}

Yersinia spp. are widespread in the environment. Fecal contamination of water and the environment, as well as food contamination, are commonly recognized sources of infection.^{1,3} Pigs, wild rodents, and wild birds are major reservoirs of pathogenic *Yersinia* spp. From the point of view of public and animal health, additional sanitary precautions and extreme caution are necessary in order to avoid intra and interspecies transmission of pathogenic *Yersinia* spp.

The source of infection in this outbreak has yet to be established, however, wild birds and rodents were commonly observed around the enclosures. It has also been postulated that stress and behavioral factors may precipitate the presentation of severe clinical disease in captive populations of non-human primates since prevalence of infection appears to be high.^{1,4} Age may also be an important factor in clinical disease manifestation, with asymptomatic infections being common in adults.⁵ In the outbreak described, the majority of mortalities occurred in juveniles; however as the outbreak progressed, adult



Liver, African green monkey. Large colonies of bacilli (arrows) are scattered throughout areas of necrosis. (HE, 200X) (Photo courtesy of: Department of Pathobiology, Ross University School of Veterinary Medicine, St. Kitts, West Indies, www.rossu.edu)

monkeys were also clinically affected.

Characteristic postmortem findings reported in non-human primates include severe enterocolitis, necrotic foci in the liver and the spleen and mesenteric lymphadenitis.³⁻⁵ Microscopic findings are characterized by the presence of multiple necrotic foci of variable size, containing cellular debris and large gram-negative colonies of coccobacilli. Differential diagnoses for bacteria that appear microscopically as large colonies include *Yersinia* spp., *Actinomyces* spp., *Actinobacillus* spp., *Corynebacterium* spp., *Staphylococcus* spp. and *Streptococcus* spp. (resulting in the mnemonic YAACS).

In this case, the clinical signs, the gross findings and the characteristic microscopic lesions were consistent with *Yersinia* spp. infection. Amplification and sequencing of the 16S SSU rRNA gene confirmed the isolates as *Y. enterocolitica*. Antimicrobial susceptibility testing of bacterial isolates obtained indicated tetracycline, gentamycin, chloramphenicol, amikacin, imipenem, ceftiofur, kanamycin, trimethoprim/sulfamethoxazole, ceftriaxone, ciprofloxacin, ceftazidime, pip/tazo con 4, aztreonam, levofloxacin, and cefepime susceptibility. Isolates were resistant to

sulfisoxazole, amoxicillin/clavulanic acid 2:1 ratio, ampicillin, amoxicillin, erythromycin, vancomycin, and clindamycin. Outbreak mortalities were significantly reduced after tetracycline administration.

JPC Diagnosis: 1. Liver: Hepatitis, necrotizing, multifocal to coalescing, marked, with large colonies of bacilli.

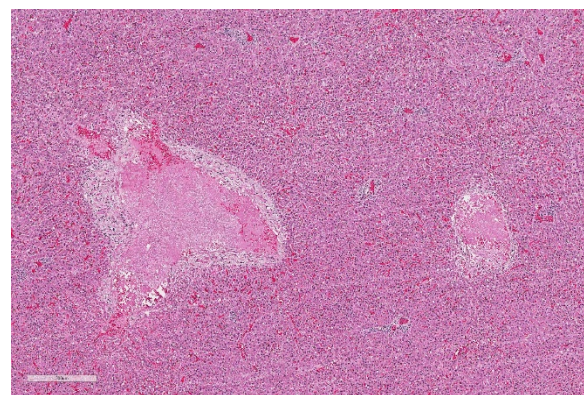
2. Spleen: Splenitis, necrotizing, multifocal, marked with large colonies of bacilli. (spleen not present on all slides.)

Conference Comment:

The genus *Yersinia* is a member of the family Enterobacteriaceae and consists of 14 species and gram-negative bacilli, three of which, *Y. enterocolitica*, *Y. pseudotuberculosis*, and the causative agent of plague, *Yersinia pestis* are pathogenic for humans and nonhuman primates. An additional species, *Y. ruckeri* is a pathogen of fish. Nonhuman primates and man are considered extremely susceptible to infection by these pathogens, although *Y. enterocolitica* was not considered as a human or veterinary pathogen until the late 1960s.⁶ In contrast, a number of domestic and wildlife species including pigs, rodents, and wild birds, are and important reservoirs of these pathogens and considered significantly less susceptible to their pathogenic effects. (Interestingly, pork chitterlings (intestine) have been often identified as a source of food-borne illness to young children, during the cleaning and preparation phase.) *Y. enterocolitica* has over 60 serotypes, but less than ten are pathogenic in management and nonhuman primates. Stress and behavioral factors may also precipitate the conversion of asymptomatic carriage of pathogenic *Yersinia* serotypes to active infection; one case report describing an outbreak of fatal yersiniosis was attributed to the administration of metronidazole to treat colony trichomonad infections.¹

It is difficult, if not impossible, to distinguish the lesions caused by *Y. enterocolitica* from those caused by *Y. pseudotuberculosis* either grossly or histologically, and advanced diagnostics (as done in this case) are recommended in all cases where definitive speciation is required. One study⁵ suggested that the pathogenicity of *Y. enterocolitica* is lower than that of *Y. pseudotuberculosis*, as sudden death may occur in the absence of clinical signs with the latter. This study postulates that the *ypm* gene carried by *Y. pseudotuberculosis* (but not *Y. enterocolitica*) may encode a superantigenic toxin resulting in enhanced pathogenicity.

An interesting historical fact about *Y. enterocolitica* serogroup 0:8 (a particularly pathogenic serogroup in both man and non-human primates) is the story of some of its earliest outbreaks. In September 1976, two hundred school children in Holland Patent, NY, developed nausea, vomiting, diarrhea, and abdominal cramping. Thirty-six children were hospitalized, sixteen of whom subsequently had an appendectomy. Contaminated chocolate milk was identified as the common source in this outbreak.⁸ A second major outbreak occurred in a coed summer camp in Liberty, NY, five years later. At least 35% of 455 campers and staff members had similar GI signs as the previous



Liver, African green monkey. Arterioles and venules are multifocally occluded by fibrin thrombi. (HE, 100X)

outbreak, with 53% complaining of abdominal pain. Appendectomies were performed on five of the seven campers who were hospitalized.⁸ This likely reflects the affinity of “hot” gram-negative bacilli for lymphoid tissue, and the ability of this particular bacterium to mimic a surgical emergency.

Conference participants discussed various aspects of the pathogenesis of yersinial invasion into the GI tract and its affinity for M cells (similar to other “hot” gram-negatives), as well as similarities and differences of *Y. pseudotuberculosis* and *enterocolitica* as compared to *Y. pestis* (which has an enteric form with lesions quite similar to those seen in this case.) Additionally, another ruleout for abdominal infection in African green monkeys, hypermucoviscous *Klebsiella pneumoniae* (WSC 2015, Conference 1, Case 2) was briefly discussed.

Contributing Institution:

Department of Pathobiology
Ross University School of Veterinary
Medicine, St. Kitts, West Indies
www.rossu.edu

References:

1. Bakker J, Kondova I, de Groot CW, Remarque EJ, Heidt, PJ. A report on Yersinia-related mortality in a colony of new world monkeys. *Lab Prim Newsletter*. 2007; 46(3):11-15.
2. Bronson R, May B, Ruebner. An outbreak of infection with *Yersinia pseudotuberculosis* in nonhuman primates. *Am. J. Pathol*. 1972; 69(2):289-308.
3. Iwata T, Hayashidani H. Epidemiological

findings on yersiniosis in nonhuman primates in zoological gardens in Japan. *Japan Agricultural Research Quarterly*. 2011; 45(1):83-90.

4. MacArthur JA, Wood M. Yersiniosis in a breeding unit of *Macaca fascicularis* (cynomolgus monkeys). *Laboratory Animals*. 1983; 17:51-155.

5. Nakamura S, Hayashidani H, Iwata T, Namae S., Une Y. Pathological changes in captive monkeys with spontaneous yersiniosis due to infection by *Yersinia enterocolitica* serovar O8. *J. Comp Path* 2010; 143(2–3):150-156.

6. Sabina Y, Rahman A, Ray RC, Montet, D. *Yersinia enterocolitica*: Mode of transmission, molecular insights of virulence and pathogenesis of infection. *J Path* 2011; 1:1-10.

7. Shayegani M, Stone WB, Deforge I, Deforge I, Root T, Parsons LM, Maupin P. *Yersinia enterocolitica* and related species isolated from wildlife in New York State. *Appl Environ Microbiol* 1986; 52: 420-424.

8. Sheyegani M, Morse D, DeForge I, Root T, Parsons, LM, Maupin PS. Microbiology of a major foodborne outbreak of gastroenteritis caused by *Yersinia enterocolitica* serogroup O:8. *J Clin Micro* 1983; 35-40.

CASE II: BC/EP/NTP (JPC 4023574).

Signalment: 2-year-old female, Wistar-Han, *Rattus norvegicus*, rat

History: Tissue from a rat used in used in a National Toxicology Program (NTP) chronic toxicity/carcinogenesis study submitted for peer review. Clinically, the rat was reported as thin, lethargic, breathing abnormally and having a ruffled hair coat.



Mesentery, rat. Mesenteric arteries are tortuous and markedly increased in size. (Photo courtesy of: Experimental Pathology Laboratories, Inc., www.epl-inc.com)

Gross Pathology: The individual animal necropsy record stated that multiple mesenteric blood vessels were enlarged (up to 10 x 5 x 5 mm). Other findings included bilateral granular appearing renal cortices and a 2 x 15 x 15 mm mass in the left inguinal mammary gland. The right ovary contained a 10mm diameter clear, fluid-filled cyst.

Laboratory results: None.

Microscopic Description: The section is of small intestine (ileum) and attached mesentery. The mesenteric artery is dilated and has a thickened wall surrounded by a varying amount of neovascularized connective tissue (granulation tissue). There is margination of neutrophils with focal necrosis of endothelium, inflammatory cell infiltrates, and variable amounts of fibrinoid material in some segments/sections. The tunica media is thickened by fibromuscular tissue and focal accumulations of lymphocytes and plasma cells are present at the periphery. Marked medial hypertrophy and thrombosis are present in some sections.

Contributor's Morphologic Diagnoses: Artery, mesenteric – arteritis and periarteritis, chronic-active and proliferative, severe with multifocal necrosis and thrombosis.

Contributor's Comment: The slide presents a typical case of spontaneous periarteritis (polyarteritis) nodosa of rats. Polyarteritis nodosa (PN) is a multisystemic, transmural necrotizing vasculitis of small or medium-sized muscular arteries.¹¹ PN is the most conspicuous inflammatory vascular lesion of rats; the incidence varies among different strains. Incidences have been reported in the August (45.4% in males and 43.0% in females), Fischer 344 (1.8% in male and 0.9% in females), Long-Evans (4.5% in males and 2.6% in females) and in Wistar (9.1% in males and 2.6% in females)⁷ and spontaneously hypertensive rats (SHR) (76.1% in males and 10.3% in females).¹¹

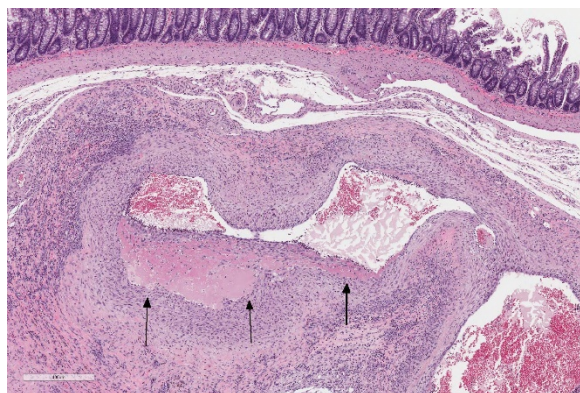
In the well-studied SHR rat, PN mainly affects the spermatic artery, mesenteric arteries, kidney, adrenal, and pancreas and is seen less frequently in the tongue, paratracheal tissue, salivary gland, liver, esophagus, thyroid, spleen, urinary bladder and intestine.¹² Suzuki, et al. reported that PN was never seen in the lung, brain and aorta.¹² Though PN lesions develop later in the mesenteric arteries than in testicular arterioles, the lesions of PN progress much faster in mesenteric arteries.¹⁰ Lesions of PN develop earlier and have a higher incidence



Mesentery, rat. At subgross magnifications, mesenteric vessels are tortuous and walls are thickened up to 5 times normal. (HE, 5X).

in stroke-prone spontaneously hypertensive rats (SHRSP) than in stroke resistant (SHRSR) SHRs.¹² PN lesions are often found at bifurcations of medium-sized arteries, small arteries and arterioles.¹²

A number of chemicals have been reported to produce vascular lesions.^{5,6,9,10,12} Fenoldopam mesylate (FM), a selective post-junctional dopaminergic (DA₁) vasodilator, causes lesions of large caliber splanchnic arteries (100-180 micrometers) in the rat characterized by necrosis of medial smooth muscle cells and hemorrhage.⁵ FM does not induce lesions in other vascular beds of the rat, or in dogs or monkeys.⁵ Dopamine is an alpha- and beta-adrenoreceptor and dopaminergic receptor agonist.⁵ Dopamine, like FM, causes hemorrhagic lesions of large caliber splanchnic arteries in the rat, as well as fibrinoid necrosis of small caliber arteries (less than 100 micrometer) of the splanchnic, cerebral, coronary and renal vascular beds.⁵ Co-exposure to dopamine and an alpha adrenoreceptor antagonist (phenoxybenzamine) blocked fibrinoid necrosis of distal branches of the mesenteric arcade but increased severity of hemorrhagic lesions of larger arteries.⁵ Dopamine alone did not induce medial necrosis and hemorrhage of the rat pancreatic artery but



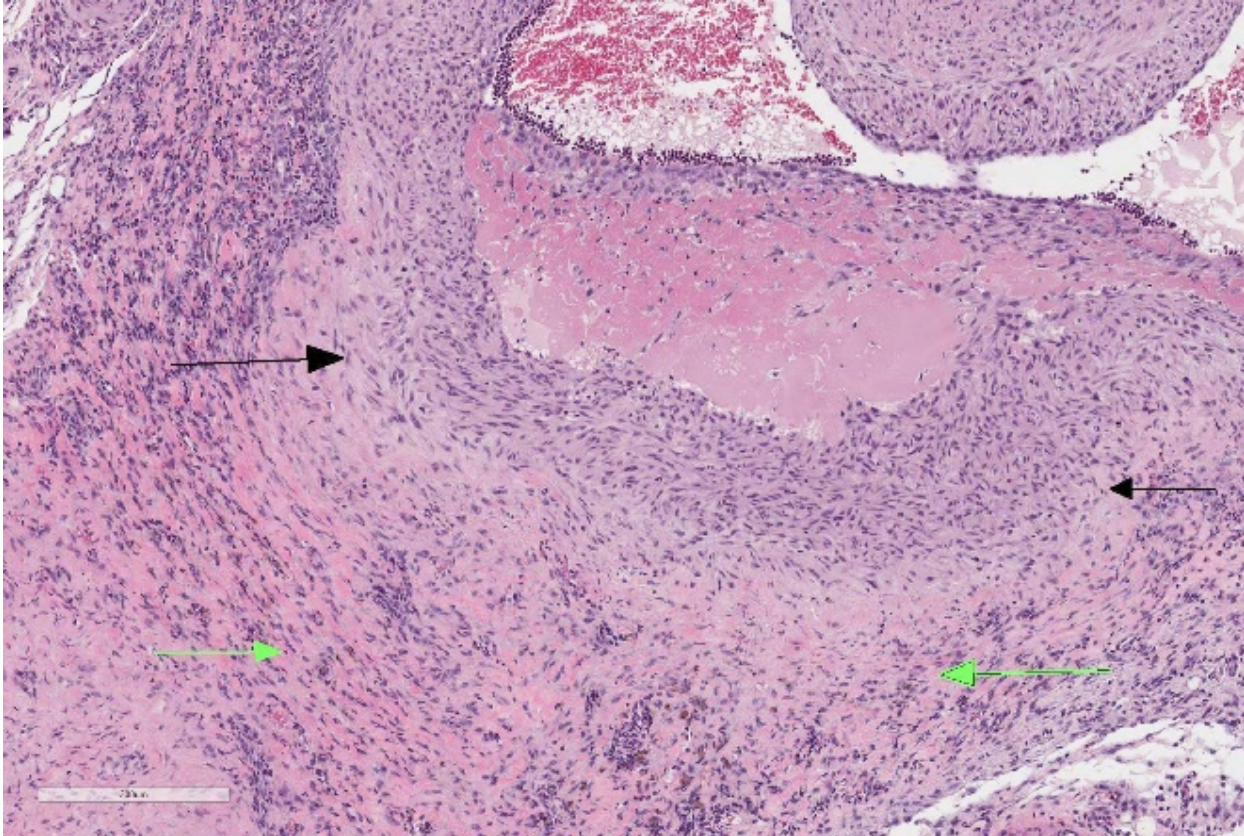
Mesenteric artery, rat. Segmentally, the tunica intima is effaced by bright pink extruded protein which extends in the tunica media (arrows). (HE, 52X).

phenoxybenzamine pretreatment resulted in characteristic lesions of the type induced by FM at this site.⁵ No rats exposed to dopamine and a combination of phenoxybenzamine and a DA₁ receptor antagonist developed arterial lesions of any kind.⁶ The arterial lesion produced by FM and dopamine was not the result of alpha-adrenoreceptor-mediated vasoconstriction because phenoxybenzamine pretreatment provided no protection.⁵

Phosphodiesterases (PDE) are a family of enzymes responsible for the metabolism of the intracellular second messengers cyclic adenosine monophosphate (cAMP) and cyclic guanosine monophosphate (cGMP). Phosphodiesterase-4 (PDE4) is the major cAMP metabolizing enzyme in inflammatory and immune cells and makes a significant contribution to cAMP metabolism in airway smooth muscle cells.⁶ PDE4 inhibition produces bronchodilation, reduces vascular leakage in airways and modulates airway inflammation.⁶ Some PDE4 inhibitors produce arterial lesions in the mesentery of the rat; however, the lesions appear to begin in the mesenteric fat rather than in the arterial wall.⁶

Theophylline, an alkylxanthine and non-specific phosphodiesterase inhibitor found in cocoa and tea, is used medicinally as a bronchodilator and has been reported to induce mesenteric arteritis in male F344/N rats exposed chronically for 2 years at 75mg/kg and in both sexes in acute (16 day) studies at 40mg/kg given once daily.⁷ The mesenteric and pancreatic arteries of rats are particularly sensitive to excessive vasodilator activity.⁷

JPC Diagnosis: Mesenteric artery: Arteritis, necrotizing and proliferative, multifocal, chronic-active, marked, with fibrinoid



Mesenteric artery, rat. Subjacent to the lakes of extruded protein, the tunica media is hypercellular and smooth muscle is disordered (black arrows) and the tunica adventitia is markedly thickened with abundant fibrosis and aggregates of lymphocytes and macrophages (green arrows). (HE, 52X).

necrosis, mural smooth muscle hyperplasia and marked medial and adventitial fibrosis.

Conference Comment: Lesions consistent with polyarteritis nodosa are not exclusive to the rat but have been documented in a wide range of species including mice, sheep, raccoons, pigs, dogs, non-human primates, and man.

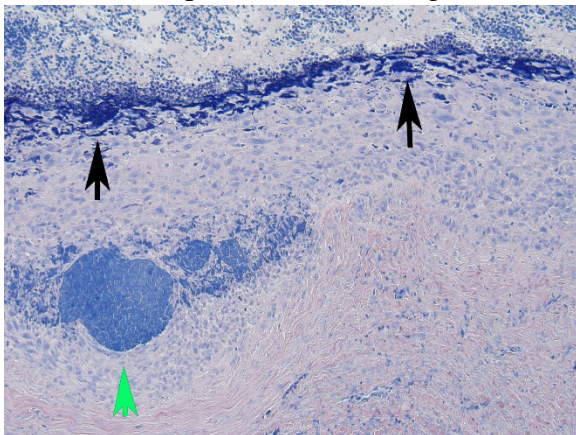
While PN in many instances and in many species is idiopathic, a number of plausible theories have been purported to explain its cause. In humans, PN is a disease primarily of young adults which affects the small-or medium-sized muscular arteries typically involving renal vessels but sparing the pulmonary circulation.² Lesions are very similar to those seen in this case, down to the

often segmental, non-circumferential areas of fibrinoid necrosis, with a predilection for vascular branching points.¹ Approximately 30% of PN cases in humans are the result of infection with hepatitis B, as antigen-antibody complex is within affected vessels off and are immunopositive for hepatitis B antigen.² The lesions of PN blue foxes infected with *Encephalitozoon cuniculi*⁷ have also been suggested as a potential infectious cause for the classic Type III hypersensitivity lesions in this condition.

A number of related theories abound regarding the development of PN in rats administered a variety of structurally unrelated vasodilators listed in the contributor's comments. The reduction in mural tension of splanchnic vessels in the

face of the positive inotropy caused by these drugs may result in increased shear forces to endothelium and damage to the underlying tunica media, as well as the possibility of interference with the diffusion of essential nutrient's into the wall affected arteries increasing there are susceptibility to injury.⁹ In affected rats, mesenteric and pancreatic arteries are particularly sensitive to these types of drugs, which may be the result of the lack of supporting tissue for the splanchnic vasculature.⁹ It has also been suggested that arterial necrosis develops due to alternating dilation and vasoconstriction of these muscles, which may help to explain the prevalence of this condition in spontaneously hypertensive rats.

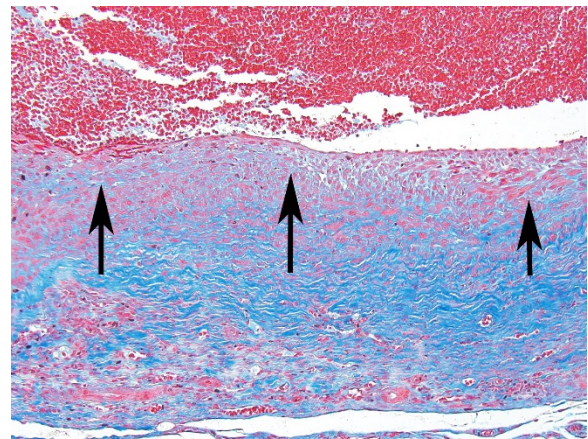
Phosphodiesterase-inhibiting drugs, which have positive inotropic effects on the heart, have also been shown to produce distinctive arterial changes of the extramural coronary arteries with subsequent myocardial necrosis and atrial and endocardial hemorrhage in the dogs as well.³ (See [WSC 2009-2010, Conference 2, case III](#)). At 7 days of treatment or less histologic changes include medial necrosis and hemorrhage, and more chronic treatment protocols are required to achieve the proliferative changes of the



Mesenteric artery, rat. In areas of endothelial loss, there is polymerized fibrin within the inner tunica media which stains dark blue (black arrows). A lake of extruded protein within the tunica media stains less intensely with this stain (green arrow) (PTAH, 200X)

intima and adventitia which characterize PN. Interestingly, associated clinical signs of fever, weight loss, cervical neck pain, and neutrophilic leukocytosis are seen in idiopathic polyarteritis of beagles (“beagle pain syndrome”), but not with administration of vasoactive compounds.²

An interesting view on the development of



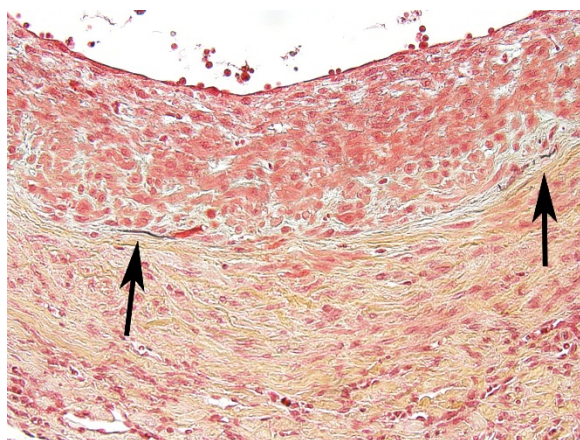
Mesenteric artery, rat. There is moderate amount of fibrosis separating medial smooth muscle cells and extensive collagen deposition and aggregates of lymphocytes, macrophages, and plasma cells within the tunica adventitia (Masson's trichrome, 200X)

PN in rats following administration of a phosphodiesterase type for inhibitor was put forth an article by Mecklenburg et al.⁶ In a timed dosage study, rats administered a phosphodiesterase inhibitor developed a mesenteritis as early as 3 days after the initiation of drug treatment, which was characterized by macrophage infiltration, fibroblast proliferation, neovascularization, and atrophy and loss of adipocytes (similar to that seen in this case). A segmental necrotizing panarteritis was subsequently seen but only after 3 or 4 weeks of treatment, and only in a limited subset of individuals. The authors of this study⁵ postulate that phosphodiesterase inhibitors do not cause a primary vasculitis in rats but the predominant toxic effects are seen in the mesentery, and that cytokines, growth factors, and other mediated results of inflammation in the

adjacent mesentery may result in vascular lesions.

A recent article has been published on spontaneous arteritis and its comparison with drug-induced arteritis in Gottingen minipigs.³ Arteritis is a common background finding in Gottingen minipigs used in preclinical safety studies, and is most often seen in cardiac vessels, vagina, oviduct, rectum, epididymis, spinal cord, pancreas, urinary bladder, kidney, and stomach. It is of unknown etiology, and may be seen in association with thrombocytopenic purpura syndrome, an often fatal disease in this breed. The article discusses the relative resistance of minipigs to drug-induced arteritis as compared to the rats, dogs, and monkeys, and the absence of lesions associated with administration of endothelin receptor antagonists and phosphodiesterase inhibitors.³

The moderator started the discussion by reviewing a recent article by Bacares¹, detailing an excellent method for the histologic examination of mesenteric artery of the rat. A review of special stains for this case (Masson's trichrome and Movat pentachrome) demonstrated a number of important features including the loss of the



Mesentery artery rat. The external elastic lamina is largely effaced with small remnants (arrows). (Movat Pentachrome, 400X).

internal elastic lamina, discontinuity of the external elastic lamina, and the marked fibrosis of the tunica media and adventitia.

Contributing Institution:

Experimental Pathology Laboratories, Inc.,
www.epl-inc.com

References:

1. Bacares, MEP. Sampling the rat mesenteric artery: a simple technique. *Toxicol Pathol* 2016; 44(8): 1166-1169.
2. Clemo FAS, Evering W, Snyder PW, Albassam MA: Differentiating spontaneous from drug-induced vascular injury in the dog. *Toxicol Pathol* 31(Suppl.):25-31, 2003.
3. Dincer AD, Piccicuo V, Walker UJ, Mahl A, McKeag S: Spontaneous and drug-induced arteritis/polyarteritis in the Gottingen minipig – review. *Toxicol Pathol*, 2018; 46(2):121-130.
4. Ferreras MC, Benavides J, Fuertes M, et al. Pathological features of systemic necrotizing vasculitis (polyarteritis nodosa) in sheep. *J Comp Pathol*. 2013;149:74-81.
5. Kerns WD, Arena E, Macia RA, Bugelski PJ, Matthews WD, Morgan GD: Pathogenesis of arterial lesions induced by dopaminergic compounds in the rat. *Toxicol Pathol* 1989; 17:203-213.
6. Mecklenburg L, Heuser A, Juengling T, Kohler M, Foell, R, Ockert D, Tuch K, Bode G: Mesenteritis precedes vasculitis in the rat mesentery after subacute administration of a Phosphodiesterase type 4 inhibitor. *Toxicol Ltt* 2006; 163:54-64.

7. Mitsumori K: Blood and lymphatic vessels. In: Boorman GA, Eustis SL, Elwell MR, Montgomery CA, MacKenzie WF. *Pathology of the Fischer Rat*. San Diego, CA: Academic Press; 1990:475-477.
8. Nordstoga K, Westbye K. Polyarteritis nodosa associated with nosematosis in blue foxes. *Acta Pathol Microbiol Scand A* 1976; 84(3):291-296
9. Nyska A, Herbert RA, Chan PC, Haseman JK, Hailey JR: Theophylline-induced mesenteric periarteritis in F344/N rats. *Arch Toxicol* 1998; 72: 731-737.
10. Saito N, Kawamura H: The incidence and development of periarteritis nodosa in testicular arterioles and mesenteric arteries of spontaneously hypertensive rats. *Hypertens Res* 1999; 22:105-112.
11. Schoen FJ, Cotran RS: Blood vessels. In: Cotran RS, Kumar V, Collins T, eds. *Robbins Pathologic Basis of Disease*. 6th ed. Philadelphia, PA: W.B. Saunders Company; 1999: 520-521.
12. Suzuki T, Oboshi S, Sato R: Periarteritis nodosa in spontaneously hypertensive rats – incidence and distribution. *Act Path Jap* 1979; 29:697-703.
13. Wessels I, Strugnell B, Woodger N, Peat M, La Rocca SA, Dastjerdi A. Systemic necrotizing polyarteritis in three weaned lambs from one flock. *J Vet Diagn Invest* 2017; 29(5) 733–737

CASE III: PV2017 (JPC 4102985).

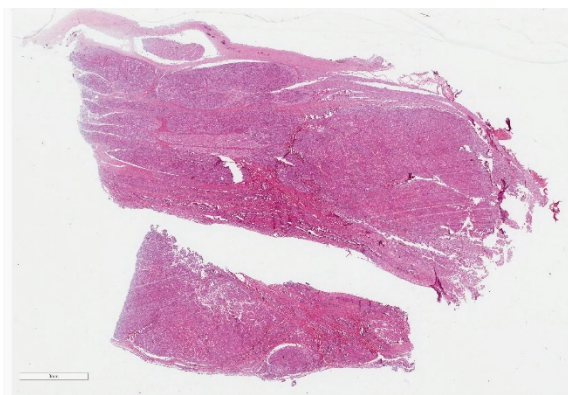
Signalment: Female NOD-SCID mouse

History: N/A.

Gross Pathology: The kidneys were described as pale by the technician.

Laboratory results: None.

Microscopic Description: Kidney: The kidney appears reduced in size. The capsular surface is irregular and there is a marked reduction in the number of normal proximal convoluted tubules. Most of the cortex is occupied by small tubules lined by cells that stain more lightly than normal. Many of these cells have karyomegalic nuclei with chromatin margination and eosinophilic intranuclear inclusion bodies. Their cytoplasm is pale and contains granular eosinophilic material. Other degenerative changes seen in the pale tubules include lining by a reduced number of cells, flattening, loss and anisokaryosis and anisocytosis of lining cells and accumulation of intraluminal debris. There is multifocal mild to moderate tubular dilation and the



Kidney, mouse: Subgross examination reveals an irregular outline to the kidney, with the majority of tubules in all levels of the cortex are hypercellular and basophilic. (Areas of normal tubules are marked by arrows.) There are numerous ectatic tubules, primarily in the deeper areas of the cortex. (HE, 5X)

dilated tubules show similar degenerative changes. There is mild multifocal interstitial fibrosis and scattered accumulation of granular brown material in tubular lining cells, and possibly in macrophages.

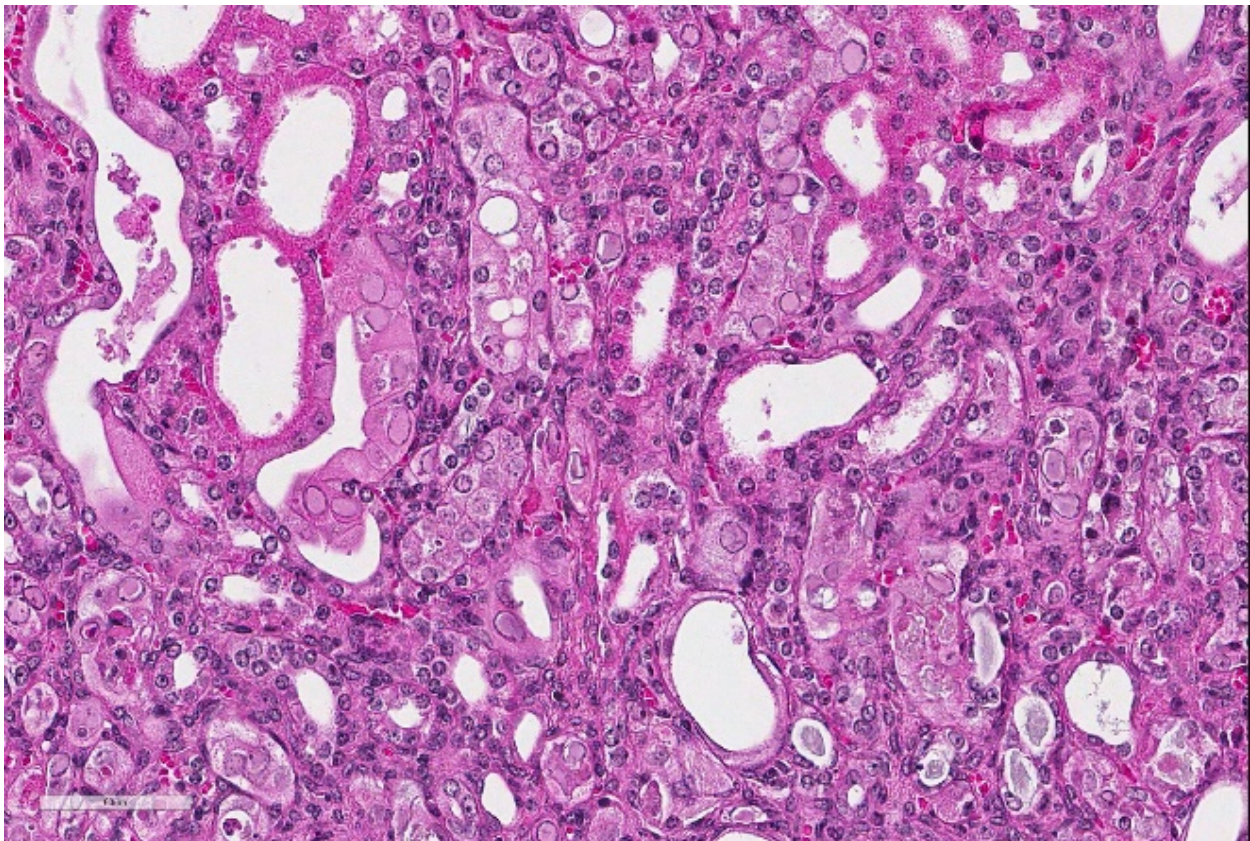
Contributor's Morphologic Diagnoses: Multifocal severe tubular degeneration and loss with karyomegalic and intranuclear inclusion bodies

Contributor's Comment: Karyomegalic with intranuclear inclusion bodies (INIB) and chromatin margination in renal epithelial cells is reported in different types of immunodeficient mice.^{1,2} The condition appears to affect female more than male mice and was termed murine inclusion body

nephropathy in one reference.² The distribution of the INIB is reportedly random but they are more common in the cortex than in the medulla and concentrate near the corticomedullary junction.^{1,2}

Ultrastructurally, the INIB consist of a collection of flocculent electron-lucent material. No viral particles or other pathogens haven been identified.^{1,2} Histochemical analysis showed that they are not composed of nucleic acid or carbohydrate, leaving protein as the most likely major chemical constituent.³

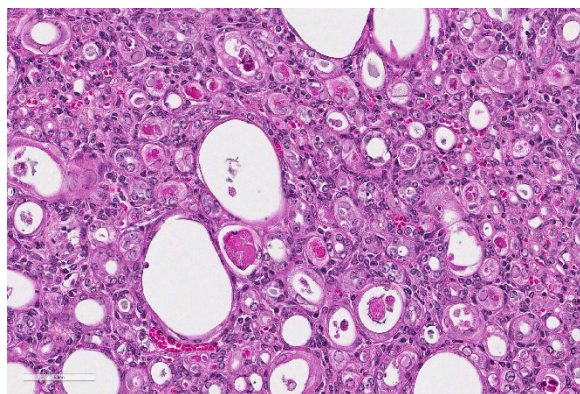
Investigations using PCR (murine polyomavirus, papillomaviruses, circoviruses, anelloviruses), immuno-



Kidney, mouse. Tubular epithelial cells are multifocally and markedly enlarged, with nuclear expansion by a homogenous karyomegalic intranuclear inclusion which peripheralizes the chromatin. Inclusions may or may not fill the expanded nucleus. (HE, 232X)

histochemistry (adenovirus) and serologic tests for a broad range of murine pathogens were negative.^{1,2} Toxic etiology was suspected, and indeed, cannot be ruled out. Lead poisoning is a well-known cause of inclusion bodies in multiple species, but the INIB in immunodeficient mice are not acid fast and their ultrastructural features differ from lead inclusion bodies which have an electron-dense core surrounded by a zone of fibrillar structures.^{1,2}

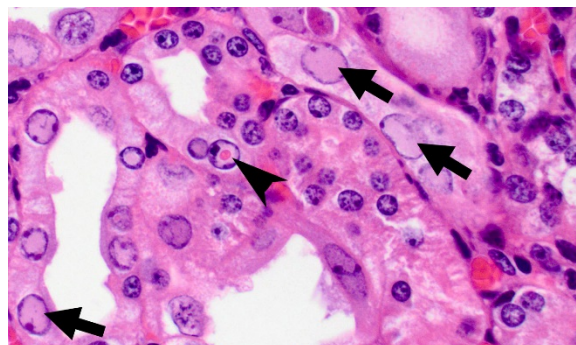
Interestingly, the INIB were positive in immunohistochemistry for heat shock cognate 70 (Hsc70). This protein is a molecular chaperone that protects cells from physical and chemical damage. It is normally located in the cytoplasm but it can be recruited to the nucleus, where in concert with other cellular proteins, it assists repair. Once nuclear damage has been corrected, Hsc70 exits the nucleus. Thus, detection of HSc70 in nuclei with INIB indicates nuclear damage in these cells, but does not shed light on the underlying cause.^{1,2} The same study also found that the INIB react specifically with anti-bovine papillomavirus type 1 L1 antibody, but the weight of the evidence suggests that the binding is due to a shared epitope rather than an indication of infection with murine papilloma virus.²



Kidney, mouse. Tubules within deeper levels of the cortex are often ectatic, and contain various amounts of eosinophilic protein and sloughed granular cellular debris. (HE, 232X)

Both reports describe inclusion body nephropathy in sentinel mice.^{1,2} and one report states that the nephropathy did not appear to affect the health of the mice.¹ In our samples, the nephropathic changes are pronounced and it seems likely that they would cause compromised renal function. Unfortunately, biochemical and urinalysis of this mouse were not carried out. The occurrence of other lesions in kidneys with inclusion body nephropathy appears to be inconsistent.^{1,2}

In summary, the cause of murine inclusion body nephropathy is currently not

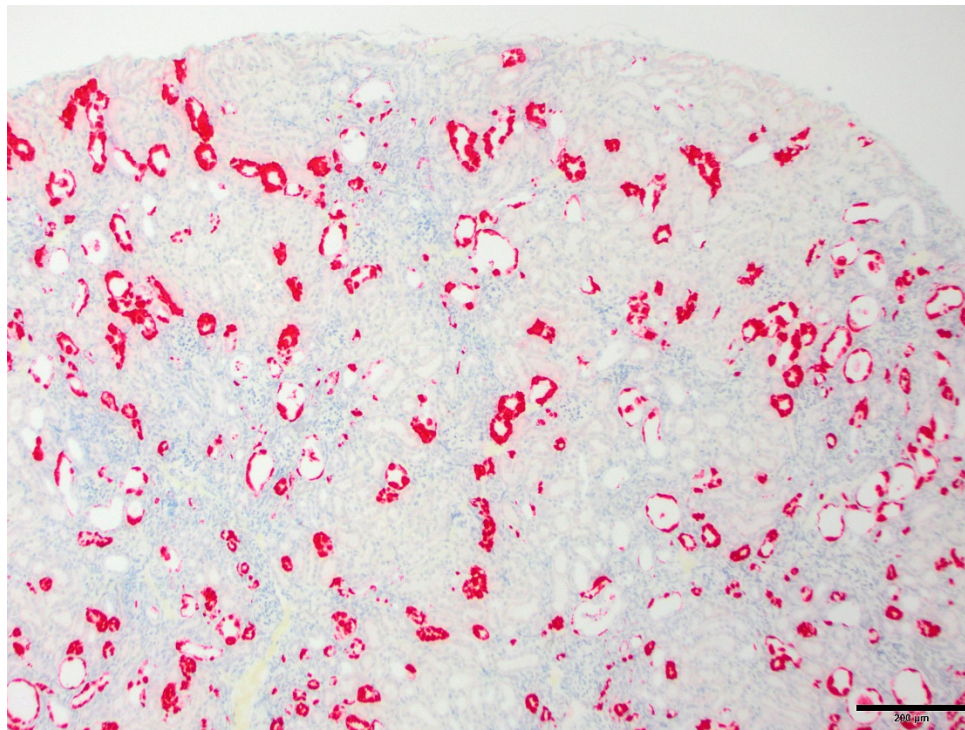


Kidney, mouse. Two types of inclusions are present in this section: many large pale amphophilic inclusions filling the nucleus (arrows) but also occasional (much fewer) small densely eosinophilic inclusions (arrowheads). (HE, 400X) (Image courtesy of: Dr. S. Monette, Memorial Sloan Kettering Cancer Center).

understood. From a practical point of view the authors of the papers describing this condition suggested to view them as a “degenerative change”¹ or as part of the “normal background pathology of immunodeficient mice”.²

JPC Diagnosis: Kidney, tubular epithelium: Karyomegaly, with numerous eosinophilic intranuclear inclusions.

Conference Comment: Shortly after the publication of the first version of the results for this conference, the JPC was contacted by



Kidney, mouse. There is intense staining for viral RNA in abnormal tubules displaying karyomegaly (1) or ectasia, epithelial attenuation, and luminal debris (2) while morphologically normal tubules (3) are not stained (Mouse kidney parvovirus RNA ISH, 600x). (Image courtesy of: Dr. S. Monette, Memorial Sloan Kettering Cancer Center).

Dr. Sébastien Monette, who is part of a multi-institutional research group that has been investigating this condition over a number of years. (Much of the discussion below is the result of personal communications from Dr. Monette and Dr. Ben Roediger).

While milder lesions associated with renal tubular inclusions were previously reported in mice^{1,2}, as discussed by the contributor, description of the severe form of murine inclusion body nephropathy (IBN), as seen in the present case, was first reported in 2017⁴ as part of an article on aging changes in NOD *scid* gamma (NSG) female mice. The article described moderate to marked renal tubular degeneration and necrosis with two types of intranuclear inclusions within renal cortical and medullary tubular epithelial cells (numerous large pale inclusions filling the nucleus, and occasional small densely staining inclusions surrounded by a clear

halo; as observed in this case – the presence of these two distinct types of inclusions may be of diagnostic value to pathologists encountering these lesion for the first time.) These lesions were associated with marked elevation of serum BUN and creatinine concentrations, and were determined to be a significant cause of morbidity and mortality in the colony being studied. Renal samples were negative on PCR for mouse adenovirus 1

and 2, murine cytomegalovirus, and murine polyomavirus. TEM performed on 2 cases failed to identify viral particles (similar to the results obtained on this case at the JPC following the conference).

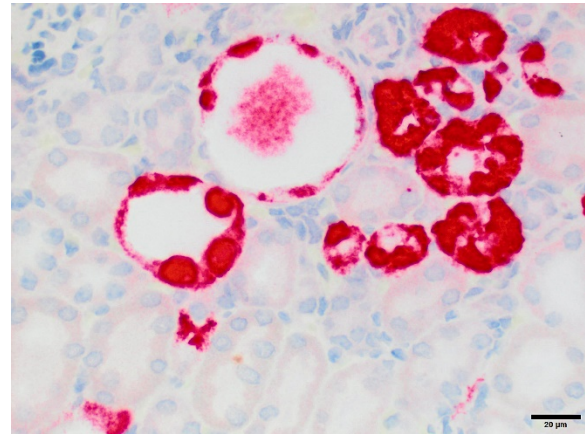
Unbiased viral metagenomic analysis of affected kidneys samples lead to the discovery of a novel viral sequence, and this virus was shown to be the cause of murine IBN in a series of observational and experimental transmission studies, performed by scientists in multiple organizations, and described in the paper by Roediger et al³, published a month after the conference. These findings have finally shed light on the elusive etiology of a lesion that has puzzled pathologists for decades. The etiology of the lesion, an atypical parvovirus, was shown to cause naturally occurring morbidity, mortality, and marked lesions in highly immunodeficient mice such as NSG

and Rag1 knockout mice, and subclinical infection and mild lesions in immunocompetent mice and athymic nude mice.

The novel parvovirus, termed “mouse kidney parvovirus” (MKPV), is highly divergent from the known mouse parvoviruses, mouse parvovirus (MPV) and the minute virus of mice (MVM) and is not detected by serology and PCR for these viruses. Based on analysis of its sequence, this virus apparently belongs to a new genus with the proposed name chapparvovirus, recently found in bats, wild rats, and pigs, but without disease association. In mice, it causes unusual pathology compared to typical parvoviruses. Unlike most parvoviruses which tend to require actively dividing cells to replicate (intestinal crypts, hematopoietic cells, external germinal cells of the developing cerebellum) this virus replicates predominantly in renal tubular cells, an unusual target for a virus of this family. The infection is chronic, and in immunodeficient strains leads to progressive tubular injury and loss, with interstitial fibrosis in advanced stages, over a period of months.

Attempts at isolating the virus in several cell lines have failed; therefore a pure inoculum could not be obtained and Koch’s postulate could not be fulfilled. The causal relationship between MKPV and IBN was demonstrated in this article by a sum of evidence³, including:

- MKPV virus was detected by PCR from kidney tissues in cases of IBN and never detected in the kidneys of normal mice.
- By in situ hybridization (ISH) staining for viral RNA, the virus was detected in kidneys with IBN but not in normal kidneys. Importantly, within affected kidneys the staining was localized to abnormal tubules with karyomegaly and degenerative changes but not present in normal tubules, suggesting that the viruses causes the lesions and is



Kidney, mouse. There is intense staining for viral RNA of numerous tubules in the cortex (Mouse kidney parvovirus RNA ISH, 100x). (Image courtesy of: Dr. S. Monette, Memorial Sloan Kettering Cancer Center).

not simply a bystander. - Viral load in urine and kidney, as measured by quantitative PCR, showed concordance with clinical progression, histopathologic severity of lesions, and serum BUN concentration.

The investigators have found evidence of this virus in laboratory mice in multiple research facilities in the US and Australia, in samples collected over a period of eleven years. Material from this particular case was sent to Dr. Monette and evaluated via RNA ISH and was strongly positive for this virus, with a staining pattern as previously described, adding evidence that this pathogen is likely widespread throughout the world.

While the virus has been identified in laboratory mice in several facilities, the prevalence of infection by MKPV within these facilities was not clear, as detection of cases was primarily based on histopathological observation of the lesions followed by confirmation by PCR and ISH. Because immunocompetent mice develop much milder lesions that may be missed, and no clinical signs, determination of the true prevalence will require surveys by PCR or

serology. Nevertheless, these findings suggest that MKPV may have significant negative impacts on research performed with mouse models, as it can cause unexpected morbidity and mortality in highly immunodeficient strains, but also because it may have subtle, but potentially significant effect on the outcome of research performed in all mice, including immunocompetent strains. Further research is ongoing to determine the impact on this virus on biomedical research that relies on mouse models.

Contributing Institution:

Department of Veterinary Resources,
Weizmann Institute of Science
Rehovot 76100, Israel
<http://www.weizmann.ac.il/vet/>

References:

1. Baze WB, Steinbach TJ, Fleetwood ML, Blanchard TW, Barnhart KF, McArthur MJ. Karyomegaly and intranuclear inclusions in the renal tubules of sentinel ICR mice (*mus musculus*). *Comp Med*. 2006; 56:435-8.
2. McInnes E, et al. Intranuclear Inclusions in Renal Tubular Epithelium in Immunodeficient Mice Stain with Antibodies for Bovine Papillomavirus Type 1 L1 Protein. *Vet. Sci*. 2015; 2: 84-96
3. Roediger B, Lee Q, Tikoo S, Cobbin JCA, Henderson JM, Jormakka M, O'Rourke MB, Padula MP, Pinello N, Henry Marisa, Wynne M, Santagostino SF, Brayton CF, Rasmussen L, Lisowski L, Tay SS, Harris DC, Bertram JF, Dowling JP, Bertolino P, Lai JH, Wu W, Bachovchin WW, Wong JJJ, Gorrel MD, Shaban B, Holmes EC, Jolly CJ, Monette S, Weninger W. An atypical parvovirus drives chronic tubulointerstitial nephropathy and

kidney fibrosis. *Cell*; 2018.
<https://doi.org/10.1016/j.cell.2018.08.013>

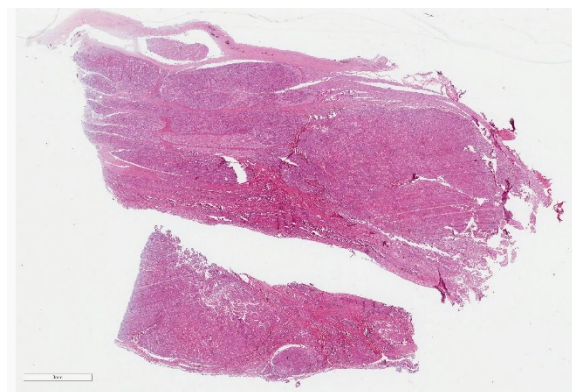
4. Santagostino SF, Arbona RJR, Nashat MA, White JR, Monette S. Pathology of aging in NOD scid gamma female mice. *Vet Pathol* 2017; 54(5): 855-869.

CASE IV: 15/191 (JPC 4068156).

Signalment: 19 years old sportpony mare (*Equus caballus*)

History: The pony had a history of eye problems of 2-3 weeks (exact duration not known). It had a corneal ulcer of the left eye that increased in severity, with left sided progressive neurological clinical signs, external ophthalmoplegia, ceased tear production, absent corneal sensitivity, dry mucosal membranes of the left nasal cavity. Keratitis and uveitis were also noted clinically. The neurological clinical examination indication a lesion affecting multiple cranial nerves associated with the ipsilateral fissure orbitalis.

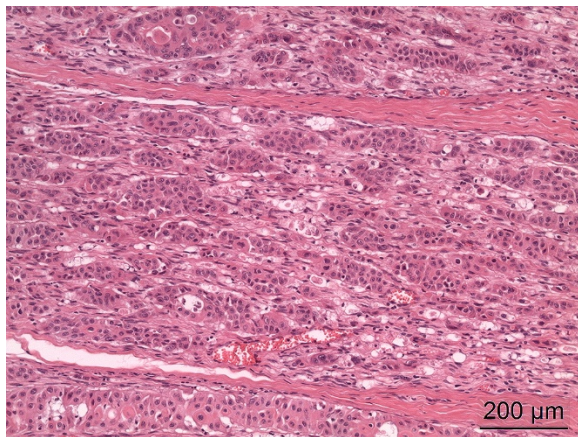
Gross Pathology: In the left eye, there was a focal extensive ulceration of the cornea with



Cranial nerve and ganglion, horse: Sections of a cranial nerve (top) and the associated ganglion (bottom) are largely effaced by a moderately cellular infiltrative neoplasm. (HE, 5X)

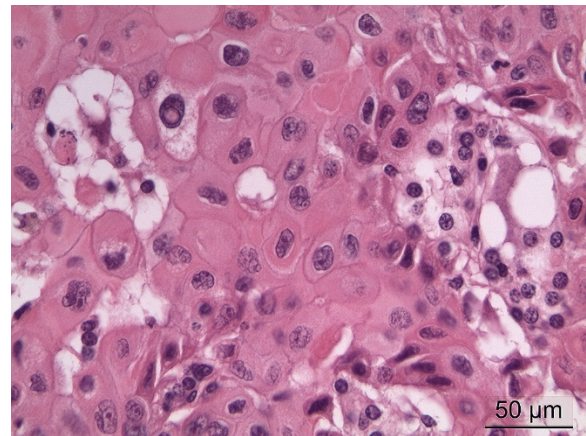
yellow discoloration of the central and ventral areas and a narrow rim of intact cornea laterally and dorsally. At the lower limbus, there was severe hyperemia. After removal of the eye, the mandible and the arcus zygomaticus of the maxilla, the orbital fissure was inspected. A few small nodular proliferations, 2-3 mm in diameter, of a light grey firm tissue was detected associated with nerves in the area. Multiple sections was made in the cranium parallel to the optical canal, cutting the canal from the fissura orbitalis to the cranial cavity obliquely in several sections. Nerves within this canal was thickened with a light grey to white firm tissue and, in continuation with this, similar tumor-like tissue was also detected laterally to the infundibulum of the pituitary gland and optical chiasm. The left trigeminal ganglion also appeared grossly to be involved. The same structures on the right side was unaffected.

Laboratory results: None.



Cranial nerve and ganglion, horse. Nests of polygonal cells, rarely making tubules, infiltrate the nerve. Between nests of neoplastic cells, remaining axons are swollen (spheroids) with dilated axon sheaths. (HE, 100X) (Photo courtesy of: Institute of Basic Sciences and Aquatic Medicine, Norwegian University of Life Science, School of Veterinary Medicine, www.nmbu.no)

Microscopic Description: In the trigeminal ganglion, the tumor tissue to the left of the pituitary gland, and the above-mentioned cranial nerves, there was a non-encapsulated, infiltrative, cell-rich tumor consisting of squamous epithelial tumor cells growing in islands and trabeculae with moderate amount of stroma. The tumor cells were large with abundant amphophilic to eosinophilic cytoplasm with keratinization of single cells or groups of cells, and large round, oval to irregular nucleus with coarsely stippled



Cranial nerve and ganglion, horse. Neoplastic cells have distinct cell borders and a moderate amount of brightly eosinophilic keratinizing cytoplasm. Similar to keratinizing squamous epithelium, some neoplastic cells have numerous vacuoles in proximity (Photo courtesy of: Institute of Basic Sciences and Aquatic Medicine, Norwegian University of Life Science, School of Veterinary Medicine, www.nmbu.no)

chromatin and 1-2 nucleoli with variable size. Anisocytosis and anisokaryosis were prominent, and there was one mitotic figure per 10 40X HPFs. In multiple areas, the tumor cells formed narrow slit-like or larger irregular cyst-like lumens, often with papillary epithelial formations. There was a multifocal mild mononuclear inflammatory cell infiltrate dominated by lymphocytes and multifocal mild mineralization in the stroma. In nerves and in the ganglion remnants surrounding the tumor tissue, there were multifocal degenerative changes.

Contributor's Morphologic Diagnoses:

Cranial nerves and trigeminal ganglion: malignant craniopharyngioma, papillary

Contributor's Comment: Craniopharyngiomas are rare epithelial tumors of humans and animals arising in the sellar or suprasellar region. They are thought to arise in remnants of craniopharyngeal duct ectoderm that normally forms the Rathke's pouch,^{1,4,8} and they may occur in two forms, adamantinomatous and papillary, the former shows morphologic similarities with odontogenic lesions.⁶ In animals, they usually consist of solid and cystic areas composed of cuboidal, columnar to squamous epithelial cells.¹ Craniopharyngiomas are usually described as benign tumors, but some malignant examples of the tumor have been reported in humans and animals.^{1,5,6}

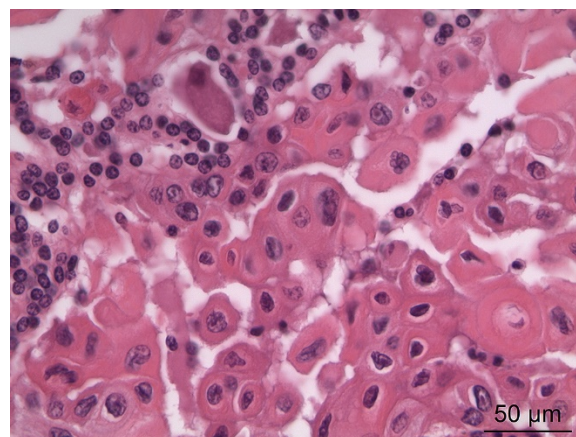
The tumor in this horse was diagnosed as malignant based on severe pleomorphism and extensive infiltrative growth. Tumors arising in the sellar or suprasellar region may cause different clinical signs depending on which structures they involve; pituitary hormone secretion may be affected either due to compression or involvement of the pituitary gland itself, cranial nerve function deficits and CNS dysfunction due to extension into the overlying brain.¹ In this horse, the cranial nerve dysfunction was most prominent, and the clinicians suspected that nerves associated with the fissura orbitalis were involved. Several cranial nerves enter the lower medial orbita associated with the fissura orbitalis and the foramen rotundum, including the ophthalmic nerve (V1 of trigeminal nerve, cranial nerve no. 5), maxillary nerve (V2 of trigeminal nerve), trochlear nerve (cranial nerve no. 4), oculomotor (cranial nerve no. 3) and

abducent nerves (cranial nerve no. 6), however in the horse there is a separate foramen for the trochlear nerve, the foramen trochleare.^{2,3} Most, if not all, of these nerves were affected by the tumor tissue. The tumor did not exert any pressure on the optic chiasm and the optic nerve was unaffected. The pituitary infundibulum and overlying brain tissue was also unaffected, and in the pituitary gland there was diffuse hypertrophy and hyperplasia of the pars intermedia in addition to a microadenoma of 2 mm in diameter.

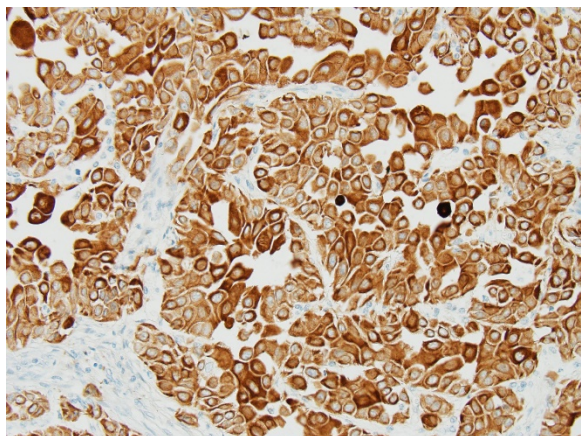
JPC Diagnosis: Cranial nerve and ganglion: Craniopharyngioma.

Conference Comment:

Craniopharyngiomas are benign tumors that have primarily been identified in small animals and laboratory species. Their sellar or suprasellar location may make them grossly indistinguishable from other tumors of the hypophysis such as pituitary adenomas, and their growth may result in destruction of the pituitary gland or hypophysis resulting in clinical signs of



Cranial nerve and ganglion, horse. Some areas of the neoplasm are populated by smaller, less differentiated neoplastic cells (upper left). (HE, 100X) (Photo courtesy of: Institute of Basic Sciences and Aquatic Medicine, Norwegian University of Life Science, School of Veterinary Medicine, www.nmbu.no)



Cranial nerve and ganglion, horse: Neoplastic cells are strongly immunopositive for cytokeratin. (anti - AE1-AE3, 400X)

hypopituitarism or diabetes insipidus. These neoplasms, however, tend to arise in individuals much younger than expected to develop tumors of the pituitary pars intermedia or glandularis.⁷

Grossly, these neoplasms may advance along the ventral aspect of the brain incorporating and effacing cranial nerves as seen in this case. Extensive growth should not be interpreted as a sign of malignancy.⁷

The histological characteristics of this tumor is unique and does not replicate any other neoplasm that may be found in this location of the cranial vault. The distinct features of keratinization results from the ectodermal origin of this tumor as previously discussed by the contributor; and cytokeratin (as performed in this case at the JPC) should be strongly positive. Neoplastic cells are also immunopositive for alpha-fetoprotein suggesting their embryonic level of differentiation; however the AFP stain performed by the JPC was noncontributory, as it is likely not optimized for equine tissues.

Both solid and cystic areas are often seen in these neoplasms.⁷ Neoplastic cells will occasionally form colloid-like structures containing eosinophilic secretory material

(but this was not a significant feature in this case).

Valentine et al.⁹ has suggested that these tumors be classified as germ cell tumors rather than craniopharyngiomas. In a study of five craniopharyngiomas in young dogs, diagnosis of germ cell tumor is based on 3 criteria: A) a midline suprasellar location, B) the presence of several distinct cell types within the tumor, a germ cell phenotype being one, as well as other cells suggesting differentiation into a secretory or squamous phenotype, and C) positive staining for alpha-fetoprotein.⁹ The AFP run at the JPC was non-contributory, and neoplastic cells were negative for NSE, GFAP, and S-100. (Interestingly, satellite glial cells were strongly positive for GFAP; enhanced expression of which has been reported by satellite glia in response to nerve injury).

Conference participants discussed potential differentials based on location in the hypothalamus: pituitary adenoma, suprasellar germ cell tumor, and craniopharyngioma. While we strongly considered the contributor's diagnosis of malignant craniopharyngioma, conference attendees favored a benign neoplasm due to the lack of appreciable pleomorphism or vascular invasion in the distributed sections or any description of metastasis in the submitted history.

Contributing Institution:

Institute of Basic Sciences and Aquatic Medicine
Norwegian University of Life Science,
School of Veterinary Medicine
www.nmbu.no

References:

1. La Perle KMD. Endocrine system. In: Zachary JF, McGavin MD, ed.

- Pathologic basis of veterinary disease*. 5th ed. St. Louis, USA: 2012: 660-697.
2. Liebich HG, König HE. Axial skeleton (skeleton axiale). In: Liebich HG, König HE, eds. *Veterinary anatomy of domestic animals*. 4th ed. Stuttgart, Germany: Schattauer; 2009:49-112.
 3. Liebich HG, König HE, Cervený C. Nervous system (systema nervosum). In: Liebich HG, König HE, eds. *Veterinary anatomy of domestic animals*. 4th ed. Stuttgart, Germany: Schattauer; 2009:489-560-
 4. Maxie MG, Youssef S. Nervous system. In: Maxie MG, ed. *Jubb, Kennedy and Palmer's pathology of domestic animals*, Vol 1, 5th ed. Philadelphia, USA: Elsevier Saunders; 2007:281-457.
 5. Pace V, Heider K, Persohn E, Schaetti P. Spontaneous malignant cranio-pharyngioma in an albino rat. *Vet Pathol*. 1997;24:146-149.
 6. Rodriguez FJ, Scheithauer BW, Tsunoda S, Kovacs K, Vidal S, Piepgras DG. The spectrum of malignancy in craniopharyngioma. *Am J Surg Pathol*. 2007;31:1020-1028.
 7. Rosol TJ, Meuten DJ. Tumors of the endocrine glands. In: Meuten DJ, ed., *Tumors in domestic animals*, 5th ed. Ames, IA. Wiley Blackwellpp 70-781.
 8. Summers BA, Cummings, JF, de Lahunta A. Tumors of the central nervous system. In: Summers BA, ed. *Veterinary neuropathology*. 1st ed. St. Louis, USA: Mosby-Year Book; 1995:351-401.
 9. Valentine BA, Summers BA, de Lahunta A. Suprasellar germ cell tumors in the dog: a report of five cases and review of the literature. *Acta Neuropathol* 1988; 76:94-100.

Self-Assessment - WSC 2017-2018 Conference 1

1. Which of the following is considered an extremely susceptible species to pathogenic *Yersinia*?
 - a. Swine
 - b. Rodents
 - c. Nonhuman primates
 - d. Birds

2. Polyarteritis nodosa is seen with the highest frequency in which of the following strains?
 - a. Wistar-Han
 - b. August
 - c. Sprague-Dawley
 - d. Fischer 344

3. Which of the following is inconsistent with phosphodiesterase inhibitor administration in the rat?
 - a. Positive inotropy
 - b. Vasodilation of splanchnic vessels
 - c. Increase endothelial shear stresses
 - d. Weight loss and fever

4. What is the primary component in non-viral intranuclear inclusions in immunodeficient mice?
 - a. Protein
 - b. Viral DNA
 - c. Cholesterol
 - d. Lipid

5. Craniopharyngiomas arise from which embryological structure?
 - a. Mesonephros
 - b. Rathke's pouch ectoderm
 - c. Proctodeum
 - d. Optic vesicle

Please email your completed assessment to Ms. Jessica Gold at Jessica.d.gold2.ctr@mail.mil for grading. Passing score is 80%. This program (RACE program number) is approved by the AAVSB RACE to offer a total of 0.5 CE Credits, with a maximum of 12.5 CE Credits being available to any individual Veterinary Medical Professionals for the 2017-2018 Wednesday Slide Conference. This RACE approval is for the subject matter categories of: SCIENTIFIC using the delivery method of NON-INTERACTIVE DISTANCE. This approval is valid in jurisdictions which recognize AAVSB RACE; however, participants are responsible for ascertaining each board's CE requirements. RACE does not "accredit", "endorse" or "certify" any program or person, nor does RACE approval validate the content of the program.

**Joint Pathology Center
Veterinary Pathology Services**



WEDNESDAY SLIDE CONFERENCE 2018-2019

C o n f e r e n c e 2

5 September 2018

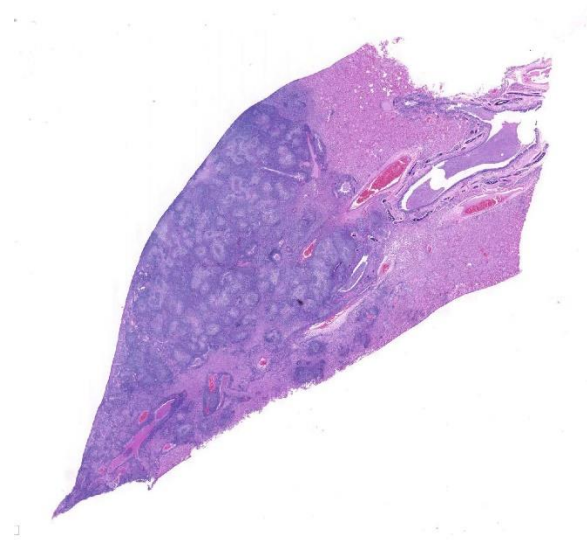
Conference Moderator:

Bruce H. Williams, DVM, DACVP
Senior Pathologist
Veterinary Pathology Services, Joint Pathology Center
Silver Spring, MD 20910

CASE I: 21-168-14/12-168-17 (JPC 4019882).

Signalment: 18-month-old male ferret (*Mustela putorius furo*)

History: This ferret was first initially diagnosed with ferret granulomatous coronavirus-associated disease at about six months of age at the private veterinary referral clinic. Initial clinical findings at that time included diarrhea, lethargy, anorexia, and a 4 cm mesenteric mass. Biopsy of this mass confirmed a diagnosis of granulomatous coronavirus-associated disease. The ferret was maintained by supportive care including occasional antimicrobial therapy to treat diarrhea and lethargy, sucralfate, potassium supplements, and hand feedings of highly palatable soft foods. After continued decline over many months, the ferret was euthanized one year after the initial diagnosis and the carcass submitted for gross and histopathological examination.



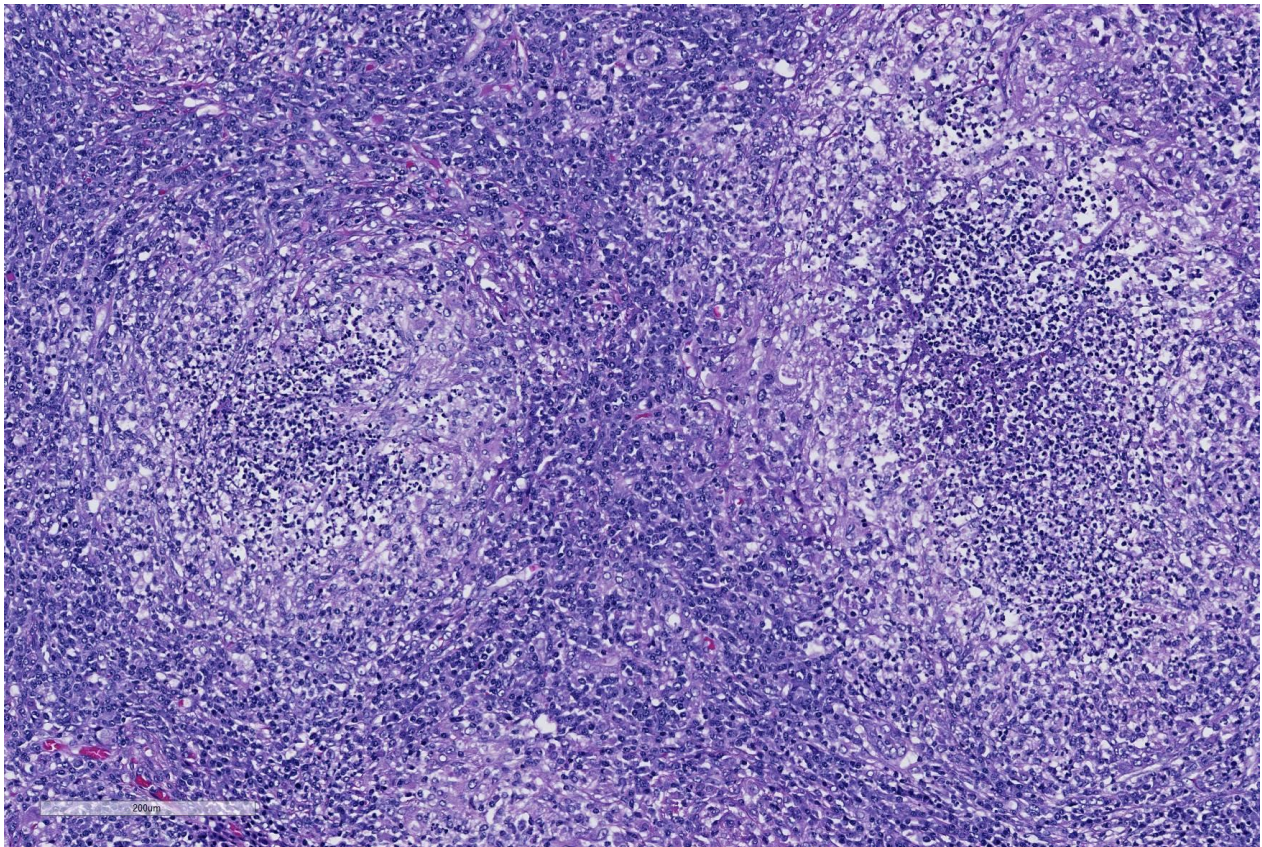
Lung, ferret. Approximately 50% of the section is effaced by multifocal to coalescing granulomas. (HE 5X)

Gross Pathology: Gross postmortem findings included multiple firm tan 1-5 m diameter nodules throughout the mesentery, bilateral pale cortical pitting lesions on the kidneys, multifocal coalescing raised white nodules on the lungs with complete consolidation of the accessory lobe, and splenomegaly with pinpoint pitted lesions.

Laboratory results: CBC and serum chemistry analysis performed at a commercial diagnostic laboratory revealed anemia (PCV 23%, reference, 43-55), leukocytosis ($14 \times 10^3/\mu\text{m/L}$) with 89% lymphocytes, mild hypoalbuminemia (1.6 g/dL; reference, 2.6 to 3.8 g/dL) and mild hyperglobulinemia (3.6 g/dL; reference, 1.8 to 3.1 g/dL). Abdominal radiographs revealed a poorly defined area of increased opacity in the midabdomen apparent on the lateral but not ventrodorsal views.²

Microscopic Description: Lung: Depending upon the section examined, there is either marked diffuse or severe large segmental effacement and expansion of the normal pulmonary parenchymal architecture by variably sized discrete and fairly well organized nodular foci (granulomas). The

granulomas/granulomatous foci are comprised of a central variable sized core of necrotic cellular debris surrounded by numerous large epithelioid macrophages with indistinct cell borders, abundant granular to vacuolated to clear cytoplasm, and large oval indented to marginated nucleus. The macrophages are in turn encircled by numerous plasma cells, lymphocytes and fewer neutrophils, which are in turn encircled by fibroblasts and variably thick band dissecting fibrous connective tissue. Variably within the sections, sparse to abundant non-staining clear needle like acicular crystals (cholesterol clefts) are often associated closely with multinucleated (macrophages) giant cells (Langhans' and foreign body type) within the granulomatous foci. The remaining



Lung, ferret. The inflammatory process is characterized by confluent, poorly formed pyogranulomas or granulomas with a central core of degenerate neutrophils and cellular debris, surrounded by layers of epithelioid macrophages, in turn surrounded by lymphocytes and plasma cells. HE, 200X)

discernible alveolar septa and lumen are expanded by numerous type II pneumocytes and large epithelioid macrophages, variable numbers of plasma cells/lymphocytes, degenerate neutrophils and necrotic cellular debris and low to abundant intraluminal proteinaceous material (edema). The bronchial and bronchiolar lumen when discernible are filled with eosinophilic proteinaceous material, mucous, epithelial and inflammatory cellular debris, associated variable bronchial epithelial hyperplasia, dense peribronchial aggregates of lymphocytes and plasma cells. In many regions, the bronchioles are obliterated by fibrosis or are severely necrotic and replaced by inflammatory cellular debris. There is also prominent lymphoplasmacytic and histiocytic perivascularitis (mostly perivenular), and in some instances, vasculitis characterized by adventitial and medial expansion by edema and inflammatory cells and/or mild mural/degeneration/necrosis. Multifocal moderate alveolar septal necrosis and interstitial and pleural fibrosis is also noticed. Rarely, dystrophic calcification and bone formation is noticed within the granulomatous foci.

Special stains:

PAS/ GMS:

- Lung: Negative for fungal organisms

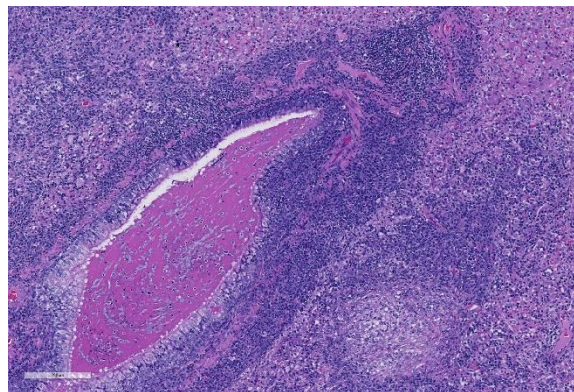
Ziehl-Neelson Acid fast stain

- Lung, mesenteric lymph node, stomach, intestine: Negative for acid fast bacilli.

Electron Microscopy:

Mesenteric lymph node:

Ultrastructurally, coronavirus-like particles were identified in examined tissues inside macrophages, either within cytoplasmic vacuoles or free in the cytosol (Representative images provided).



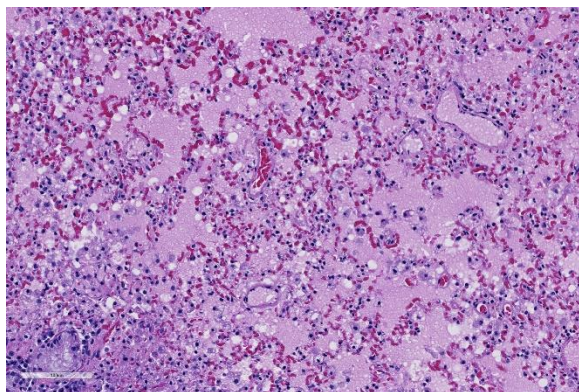
Lung, ferret. Airways contain abundant proteinaceous material, moderate numbers of degenerate neutrophils and are surrounded by profound BALT hyperplasia, consistent with the clinical history of aspiration. (HE, 100X)

Contributor's Morphologic Diagnoses:

Lung: Pneumonia, severe, coalescing to diffuse, chronic, organizing, necrogranulomatous with multinucleated giant cells, cholesterol clefts, pulmonary edema and fibrosis.

Contributor's Comment: This case is an interesting example of the recently recognized ferret systemic coronavirus-associated disease resembling feline infectious peritonitis (FIP)-like disease syndrome in ferrets. This relatively new disease entity in ferrets was first recognized in Europe in late 2005-early 2006^{5,8} and since then has been systemically characterized in the US^{5,12,17} and more recently identified in Japan⁹. The clinical disease and the lesions in all these described cases are similar to those observed with the "dry" form of FIP.¹ The differentials considered for this case include mycobacteriosis and systemic fungal infections, however no acid-fast bacilli nor fungal organisms were identified.

Coronaviruses are enveloped, pleomorphic, positive-strand RNA viruses with a diameter of 60-220 nm and classified under the genus *Coronavirus* within the family Coronaviridae, order Nidovirales.¹ The viral particles typically develop in the



Lung, ferret. Alveoli in less affected areas are filled with abundant foamy edema fluid. (HE 211X)

cytoplasm of affected epithelial cells and macrophages inside vacuoles and form characteristic radiating peplomer spikes on the surface of the envelope, a diagnostic feature in EM,^{5,8-9,16}

Ferret coronaviruses can cause two distinct clinical conditions, namely epizootic catarrhal enteritis (ECE) in association with ferret enteric coronavirus (FECV)^{8,12,15-16} and the more recent ferret systemic coronal viral disease caused by ferret systemic corona virus (FRSCV) with a clinical picture resembling the “dry” form of feline Infectious peritonitis (FIP)^{5,12,16}. ECE was first observed in the spring of 1993 on the East Coast of United States and a detailed description of the disease and its association with corona virus was first published in 2000.¹⁵ Unlike FRSCV associated FIP-like disease in ferrets, ECE affects all age groups and is more severe in aged ferrets.¹⁵ ECE is primarily an enteric disease with lesions consistent with intestinal coronaviral infection such as vacuolar degeneration and necrosis of villous enterocytes, villous atrophy, blunting and fusion, and lymphocytic enteritis.^{8,12,15-16}

Feline coronavirus (FCoV) typically infects domestic and exotic felids. Two biotypes of FCoV include feline enteric coronavirus (FECV) and feline Infectious peritonitis virus (FIPV). FECV replicates in

enterocytes causing clinical disease resulting in diarrhea or an asymptomatic infection, whereas FIPV replicates in macrophages resulting in a systemic infection. Both “wet” and “dry” forms of feline infectious peritonitis (FIP) occur depending upon the immune status of the animal. Histologically, pyogranulomatous inflammation involves multiple tissues predominantly with a vasculocentric distribution targeting small arterioles and venules are hallmarks of this disease.¹ In a similar fashion, ferret systemic coronaviral disease also causes pyogranulomatous to granulomatous lesions and /or vasculitis in multiple organs including the spleen, mesenteric lymph nodes, intestine, kidneys, brain etc. The common clinical signs associated with the systemic form include anorexia, weight loss, diarrhea and large palpable intraabdominal masses. Less frequent findings included hind limb paresis and central nervous system signs. Immunoreactivity with FIP feline coronaviral antigen (FCoV) on paraffin sections and/or serum samples has been demonstrated by immunohistochemistry in all these cases within the granulomas.^{5,9,12,15} It is thought that the positive immunoreactivity is due to cross-reactivity from common antigenic determinants within different host specific corona viruses.

In this case, in addition to the lung lesions, discrete granulomas or coalescing granulomatous inflammatory foci were also observed in the mesenteric nodes, mesentery, pancreas, intestinal serosa and the spleen. Cholesterol clefts were not observed within these tissues and multinucleated cells were also sparse. It is of interest to note that cholesterol clefts and the associated presence of numerous multinucleated cells are not typical of earlier descriptions of this disease and even in these cases it was primarily a feature of the lung lesions only and the underlying pathophysiological basis is

unclear. Immunohistochemistry for feline coronavirus antigen (FCoV) was not performed on this case for confirmation time of submission. However, on electron microscopic evaluation of the mesenteric lymph node granulomas, enveloped coronavirus-like particles, some with radiating spikes were identified within macrophages, either inside cytoplasmic vacuoles or free in the cytosol.

In this individual, the kidneys exhibited predominant plasmacytic interstitial nephritis with occasional granulomatous foci and severe chronic glomerulonephritis and mild perivascularitis. The distribution and nature of the lesions can mimic those seen with chronic Aleutian disease (AD) caused by distinct parvoviruses in minks and ferrets. AD is characterized by progressive wasting, weight loss, hypergammaglobulinemia, plasmacytosis, interstitial pneumonia in young kits, chronic glomerulonephritis, lymphoplasmacytic interstitial nephritis and prominent arteritis involving kidneys and other organs.¹³⁻¹⁴ However, in this case we did not have information on the tests for immunoglobulin levels nor additional serology or viral diagnostic tests to rule out a concomitant chronic Aleutian disease.

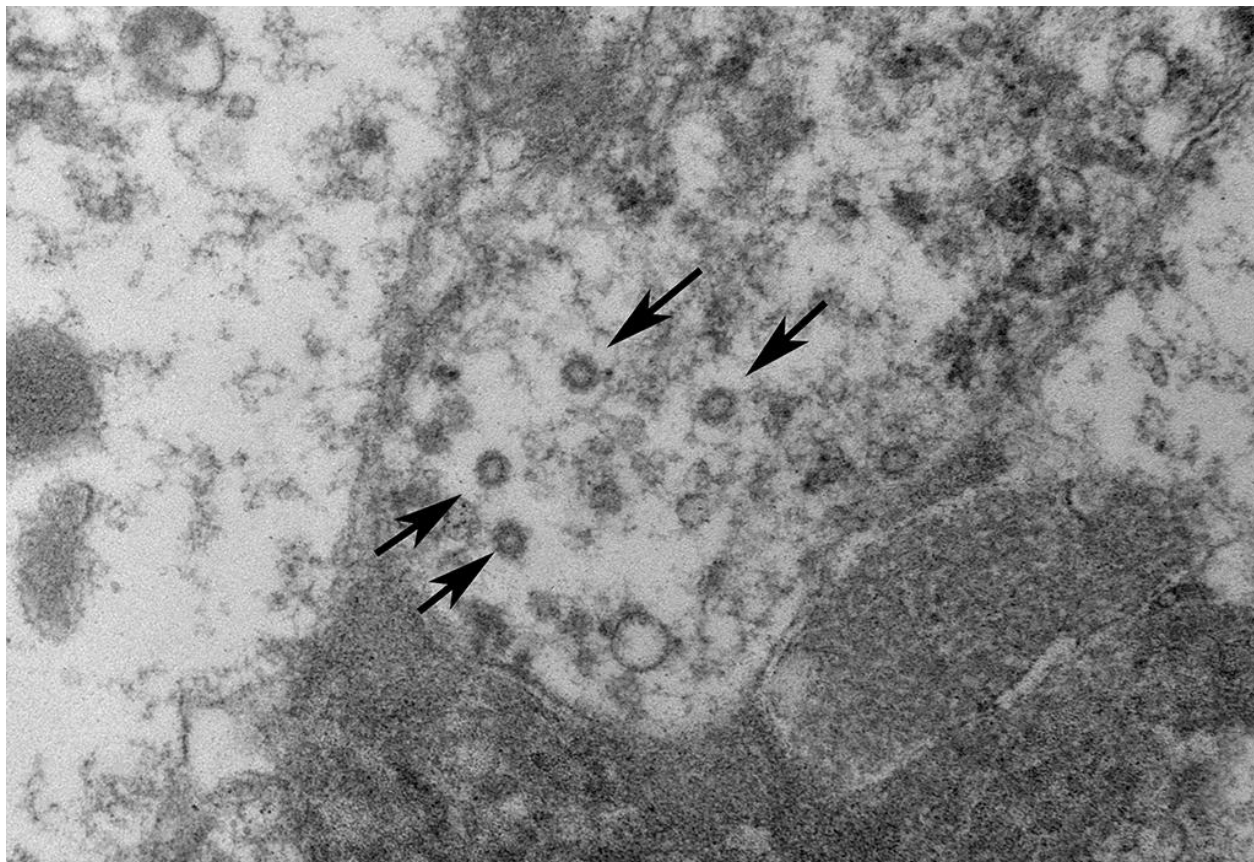
JPC Diagnosis:

1. Lung: Pneumonia, interstitial, pyogranulomatous, multifocal to coalescing, severe.
2. Lung: Bronchopneumonia, neutrophilic and necrotizing, multifocal, mild, with marked BAL hyperplasia and intrabronchiolar proteinaceous material.
3. Lung: Pneumonia, interstitial, histiocytic, multifocal, mild, with intraalveolar *Pneumocystis* trophozoites and cysts.
4. Lung, subpleural alveoli: Histiocytosis, focally extensive, mild (endogenous lipid pneumonia.)

Conference Comment:

Since the submission of this case and 2012 for consideration in the Wednesday Slide Conference, there has been extensive additional work in the investigation of this important disease of both patent and laboratory ferrets. This particular case itself was published as part of a 5 case study by Autieri et al. in 2015.² This review was composed of animals from multiple sources including private pets as well as laboratory animals from accredited facility. In addition to identifying cases from seven countries on four continents. The literature review for this publication also identified an interesting report from Denmark in 1951¹¹ of a syndrome in 142 ferrets, many less than a year of age, with strikingly similar clinical signs and pathologic findings. The syndrome, known as ends are wanted malignant granulomatosis, demonstrated granulomatous inflammatory changes in lymph nodes, spleen, and liver and histochemical stains failed to disclose the presence of bacteria, fungi, and protozoa as well as negative cultures for aerobic, anaerobic, and mycobacterial bacilli.¹¹

Continuing investigation of ferret coronavirus-associated disease, which has no definitive treatment and is considered invariably fatal in affected individuals, has resulted in the sequencing of the viral genome of two different FECRV strains in Japan.⁶ This work has determined that the virus shares 50-69% nucleotide sequencing with known coronaviruses suggest doing that the ferret enteric coronavirus (FRCoV) might be classified as a new species in the genus *Alphacoronavirus*.⁶ additionally, and enzyme-linked immunosorbent assay (ELISA) using recombinant partial nucleocapsid proteins of the FRCoV Yamaguchi-1 strain was developed to establish a method for detection of FRCoV from blood sampling.¹⁰ Not



Lung, ferret. Ultrastructural examination of macrophages from the center of one of the granulomas reveals coronavirus particles free within the cytoplasm. (Photo courtesy of: Massachusetts Institute of Technology, 16- 849, Division of Comparative Medicine, 77 Massachusetts Ave, Cambridge, MA 02139. <https://web.mit.edu/comp-med/>)

surprisingly, as anyone who was worked with this virus can understand, 89% of tested ferrets in Japan have been infected with ferret coronavirus.¹⁰

In Spain, Doria-Torr et al³ investigated the inflammatory response and antigen distribution of FRCoV infection and compared it to similar studies of FIP in cats. The group identified four distinct types of granulomas in affected animals including those with necrosis, without necrosis, with neutrophils as a central core, and diffuse granulomatous inflammation, very similar to the inflammatory response demonstrated by cats infected with mutated coronavirus. Close inspection of the slide submitted for this case will demonstrate most, if not all of the various types of granulomas discussed in

this paper. The authors³ postulate that the various morphologies might be a consequence of different episodes of viremia, as described in cats with FIP. The authors also noted that vasculitis was an uncommon finding, which has been noted in other reviews of this disease. Other FIP-like syndromes that have recently been described in single case reports since the submission of this case include pyogranulomatous panophthalmitis as well as membrano-proliferative glomerulonephritis.

Additional clinicopathologic features of ferret coronavirus infection that bear mention in review includes the progressive nature of this disease of juvenile and young adult ferrets which has an average survival time following diagnosis of 69 days⁵. The most

common clinical signs of affected ferrets include weight loss, a palpable intra-abdominal mass or masses, lethargy and anorexia.⁵ Hematologic findings are nonspecific for this disease and many may be within normal reference levels; the most common hematologic abnormality in affected animals is a polyclonal gammopathy.⁵ Histologically, Garner et al review many of the same lesions noted in this particular case, however their study identified inflammation involving the adventitial and medial tissue next of small veins and venules⁵, which was not particularly prominent in this slide. The EM findings in this study⁵ are similar to those noted by the contributor of this case, with intracytoplasmic virus particles found free within the cytoplasm of macrophages within the center of granulomas.

Careful inspection of the regions of the section in which granulomatous inflammation is not present (and in which the primary lesion is marked alveolar edema, will disclose the presence of numerous vacuolated histiocytes admixed with fewer lymphocytes in the alveoli immediately (<1mm) subjacent to the pleura. This is a characteristic incidental finding in ferrets, resulting from endogenous lipid pneumonia.

The composition of the JPC morphologic diagnosis above, due to multiple simultaneous pathogeneses in the submitted tissues, was a subject of spirited debate. The attribution of secondary inflammatory changes to a particular etiology was further complicated due to the history of prolonged therapeutic immunosuppression. The JPC tradition of assigning a separate morphologic diagnosis to each distinct process was ultimately upheld in the post-conference signout session.

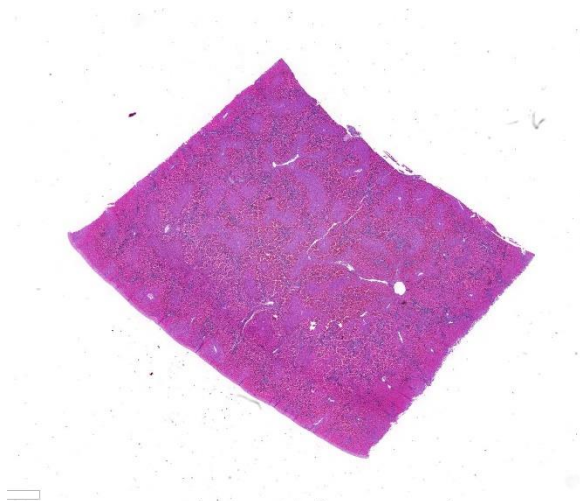
Contributing Institution:

Massachusetts Institute of Technology,
16- 849, Division of Comparative Medicine
77 Massachusetts Ave,
Cambridge, MA 02139
<https://web.mit.edu/comp-med/>

References:

1. Addie DD. Feline coronavirus infections. In Greene CE, ed. (2012). *Infectious Diseases of the Dog and Cat*, 4th Edition. St Louis, MO, pp. 92-108.
2. Autieri CR, Miller CI, Scott KE, Kilgore A, Papscoe VA, Garner MM, Haupt JL, Bakthavatchalu V, Muthupalani S, Fox JG. Systemic coronaviral disease in five ferrets. *Comp Med* 2015; 65(6):508-516.
3. Doria-Torra G, Viana B, Ramis A, Amarilla SP, Martinez J. Coronavirus infection in ferrets: antigen distribution and inflammatory response. *Vet Pathol* 2016, 53(6):1180-1186.
4. Fujii Y, Tochtani T, Kouchi M, Matsumoto, I, Yamada T, Funabashi H. Glomerulonephritis in a ferret with feline coronavirus infection. *J Vet Diagn Invest* 2015;27(5):637-640
5. Garner MM, Ramsell K, Morera N, Juan-Sallés C, Jiménez J, Ardiaca M, Montesinos A, Teifke JP, Löhr CV, Evermann JF, Baszler TV, Nordhausen RW, Wise AG, Maes RK, Kiupel M. Clinicopathologic features of a systemic coronavirus-associated disease resembling feline infectious peritonitis in the domestic ferret (*Mustela putorius*). *Vet Pathol* 2008 45(2):236-46.

6. Li, TVC, Yoshizaki S, Kataoka M, Doan YH, Ami Y, Suzaki Y, Nakamura T, Takeda N, Wakita. Determination of ferret enteric coronavirus genome in laboratory ferrets. *Emerg Inf Dis* 2017; 23(9) 1568-1570
 7. Lindemann DM, Eshar D, Schumacher LL, Almes KM, Rankin AJ. Pyogranulomatous panophthalmitis with systemic coronavirus diease in a domestic ferret (*Mustela putorius furo*). *Vet Ophthalmol* 2016; 19(2):167-171.
 8. Martinez J, Ramis A, Reinacher M, Perpignan D. Detection of feline infectious peritonitis virus-like antigen in ferrets. *Vet Record* 2006: p. 523.
 9. Michimae Y, Mikami S, Okimoto K, Toyosawa K, Matsumoto I, Kouchi M, Koujitani T, Inoue T, Seki T. The first case of feline infectious peritonitis-like pyogranuloma in a ferret infected by coronavirus in Japan. *J Toxicol Pathol* 2010; 23(2):99-101.
 10. Minami S, Terada Y, Shimoda H, Takazawa M, Onuma M, Ota, A, Ota Y, Akabane Y, Tamukai K, Watanabe K, Naganuma Y, Kanagawa E, Nakamura K, Ohashi M, Takami Y, Miwa Y, Tanoue T, Ohwaki M, Ohta J, Une Y, Maeda, H. Establishment of serological test to detect antibody against ferret coronavirus. *J Vet Med Sci* 2016; 78(6):1013-1017.
 11. Momberg-Jorgensen HC. Enzoitic malignant granulomatosis in ferrets. *Acta Pathol Microbiol Scand* 1951;29:297-306.
 12. Murray J, Kiupel M, Maes RK. Ferret coronavirus-associated diseases. *Vet Clin North Am Exot Anim Pract* 2010; 13(3):543-60.
 13. Palley LS, Corning BF, Fox JG, Murphy JC, Gould DH. Parvovirus-associated syndrome (Aleutian disease) in two ferrets. *J Am Vet Med Assoc* 1992;201(1):100-6.
 14. Porter HG, Porter DD, Larsen AE. Aleutian Disease in Ferrets. *Infect Immun* 1982; 36(1):379.
 15. Williams BH, Kiupel M, West KH, Raymond JT, Grant CK, Glickman LT. Coronavirus-associated epizootic catarrhal enteritis in ferrets. *J Am Assoc Vet Med* 2000; 217(4):526-530.
 16. Wise AG, Kiupel M, Garner MM, Clark AK, Maes RK. Comparative sequence analysis of the distal one-third of the genomes of a systemic and an enteric ferret coronavirus. *Virus Res* 2010; 149(1):42-50.
 17. Wise AG, Kiupel M, Maes RK. Molecular characterization of a novel coronavirus associated with epizootic catarrhal enteritis (ECE) in ferrets. *Virology* 2006; 349:164-174.
- CASE II:** 13V1542 (JPC 4034956).
- Signalment:** 1 year old, female, Hereford heifer
- History:** Tissue samples sent in formalin from a post-mortem done by the referring veterinarian from Victoria, Australia, in March 2013 with the following history. 14 months old Hereford heifers in good condition in high country on lush green pasture. Vaccination program and management good and properly done. 1 x died 6 days ago. Lost 6 last year from this



Liver, ox. A section of liver with a retiform pattern of periportal hemorrhage is submitted. (HE, 5X)

paddock. Dead on arrival. Showed ataxia before died.

Gross Pathology: Submitted by referring veterinarian. Petechiae through omentum. Abomasum petechiae and filled with brownish blood-tinged fluid. Petechiae and ecchimoses on pericardium, epicardium and endocardium.

Laboratory results: None.

Microscopic Description: Liver; severe periportal hepatocellular necrosis extended throughout all liver sections examined and involved up to 50% of the hepatocytes in each lobe. The degenerate hepatocytes had been replaced with blood and neutrophils. Portal areas contained moderate biliary hyperplasia and mild neutrophil infiltration.

An unidentified artifact similar to acid hematin was present throughout all sections.

Contributor's Morphologic Diagnoses: Liver; severe acute disseminated periportal hepatocellular necrosis, moderate biliary

hyperplasia and moderate neutrophilic hepatitis.

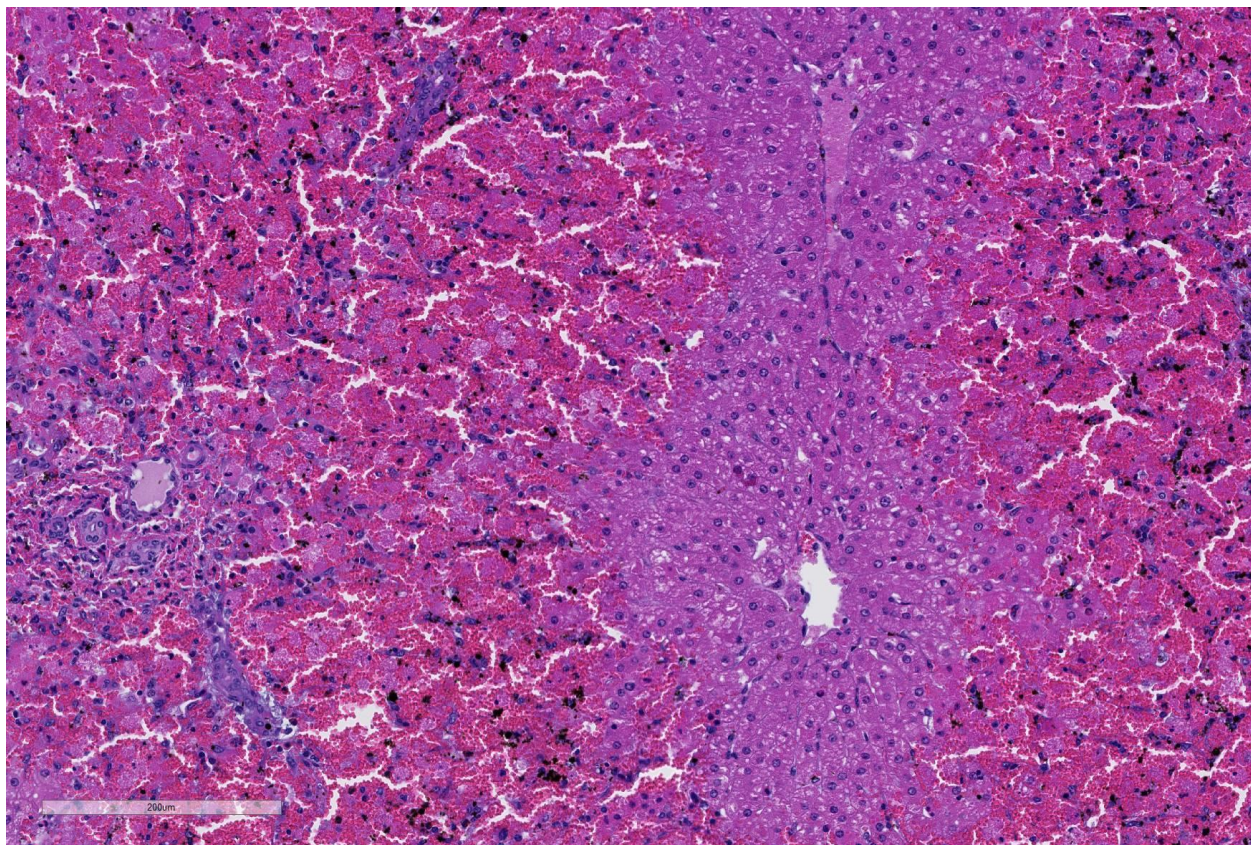
Contributor's Comment: The hepatic lesion is very severe and sufficient to explain the sudden death of the heifer. Periportal hepatocellular necrosis is a relatively rare lesion in cattle and is typical of ABLD (acute bovine liver disease). ABLD typically strikes in autumn in the south eastern areas of Victoria, Australia and affects dairy and beef cattle. Clinical signs of the disease include decreased milk yield and sudden death with photosensitization developing in survivors. The cause is presumed toxic but the agent has never been defined.

It has been associated with rough dog's tail grass (*Cynosurus echinatus*), but no toxic agent has been found in this grass. The known phytopathogenic fungus *Drechslera biseptata* has been isolated from *C. echinatus* collected at the time of, and from the sites of, outbreaks of ABLD and is tentatively associated with its pathogenesis¹. Whether there are other hepatotoxins involved is not known. An attempt to reproduce the disease in cattle by feeding *Cynosurus echinatus* mixed with an inoculum of *Drechslera biseptata* grown from an isolate taken from a previous outbreak of ABLD was not successful².

The petechiation described in the history is also a common PM change of this condition. The slides contained an artifact similar to acid hematin but could not be removed with the usual laboratory treatment for acid hematin. The artifact was not identified.

JPC Diagnosis: Liver: Hepatocellular necrosis, periportal to midzonal, diffuse, with hemorrhage.

Conference Comment: Although there is current heightened sensitivity among cattle



Liver, ox. A portal area is at left, and centrilobular vein at right. Periportal hepatocytes are individualized, many lost, and largely replaced by hemorrhage. Kupffer cells and sinusoidal architecture remains. Hemorrhage extends into the portal areas as well. At right, midzonal and centrilobular hepatocytes are mildly swollen by numerous distinct small lipid vacuoles, occluding sinusoids. There is abundant acid hematin. (HE, 167X)

producers in Australia and New Zealand to the clinical effects and implications of acute bovine liver disease, intensive research into its pathogenesis has not yet been published. An excellent review by Reed et al.⁴ was published subsequent to the submission of this case and is summarized below.

Acute bovine liver disease (ABLD) commonly formerly known as phytotoxic hepatitis, affects grazing beef and dairy cattle regardless of age, sex or breed. Clinical signs consistently include an initial drop in milk production, photosensitization, an altered behavior such as seeking shade on overcast days. Depression, pyrexia, appetite loss, and agitation may be observed in some cattle, and acute cases may result in death prior to display of clinical signs. Serum

biochemistries are nonspecific, including marked elevation of aspartate transaminase, glutamate dehydrogenase, and moderate increases in gamma-glutamyl transpeptidase activity. Histologic features of acute disease are as seen in this slide, with periportal necrosis as a characteristic feature. The pathology seen in chronic cases has yet to be described.⁴

The nonspecific signs and lesions as well as the sporadic and unpredictable nature of deaths with this condition complicate the investigation of ABLD occurrences. Outbreaks often occur on pastures which contains senescent rough dog's tail grass (*Cynosurus echinatus*), however this plant is found worldwide and does not appear to cause illness on its own. Feeding trials with

this plant have demonstrated no ill effects in several studies.

Because of the similarity of the epidemiology of ABLD to other mycotoxicoses, fungal infections of rough dog's tail grass are suspected. The most common fungal species identified in ABLD occurrences include *Colletotrichum graminicola* and *Drechslera* sp. aff. *siccans*, with *D. biseptata* and *Colleotrichum* sp. aff. *coccodes* were also identified less commonly. As *Colletotrichum* sp., has not been reported to produce mycotoxins, leaving *Drechslera* as the more likely candidate. Aslani et al.¹ identified *in vivo* hepatotoxicity from extracts of the spores and mycelia of *D. biseptata* whose mass spectral profile implies a cytochalasin-like activity in rat hepatocytes *in vivo*. This research also demonstrated a lower level of toxicity from spores alone as compared to extracts from mycelia, or mycelia and spores combined.

As most ABLD occurrences occur in the autumn, current thought is that weather change may stimulate production of fungal toxins or toxic spores in infected grasses. Cattle producers are recommended to be vigilant for signs of disease in this time of the year when cattle are grazing high risk pasture. Additionally, sheep may be used to graze out a high risk pasture, as they do not appear to be susceptible, or at least less susceptible to the effects of the putative toxin.

Periportal hepatocellular necrosis is an uncommon pattern of hepatocellular injury caused by a limited subset of toxins in veterinary medicine.² The majority of these toxins may not require metabolism by the mixed function oxidases of centrilobular hepatocytes, and simply overwhelm the initial hepatocytes they encounter as they enter the liver from the portal venous circulation. Other toxins may simply require

metabolism by the limited amounts of biotransforming enzymes present within periportal hepatocytes to exert their effect. Additionally, periportal necrosis may be seen in toxins that are excreted in the bile, and there is damage enhanced by cholestatic disease. Toxins which have been identified in veterinarian medicine as characteristically resulting in periportal necrosis include elemental phosphorus, allyl alcohol, and boobialla (*Myoporum tetandrum*) another toxic plant found in Australia which contains furanoid sesquiterpene oils as the toxic principle.¹

The lack of traditional descriptors for chronicity and severity is a consequence of the choice of the term "necrosis" as the main feature of this slide. As necrosis is neither acute nor chronic, nor are there levels of severity of necrosis, we generally do not use these terms as modifiers. An estimation of extent of necrosis is probably more appropriate than "severity" in these cases, and diffuse gives an excellent picture of the extent of necrosis seen here, with all periportal hepatocytes in the section being necrotic.

Contributing Institution:

Gribbles Veterinary Pathology
1868 Dandenong Rd,
Clayton VIC 3168
Australia

References:

1. Aslani, Pascoe, Kowalski, Michalewicz, Retallick and Colegate. In vitro detection of hepatocytotoxic metabolites from *Drechslera biseptata*: a contributing factor to acute bovine liver disease? *Aust J Experimental Agriculture*. 2006; **46**: 599–604.

2. Brown DL, Van Wettere AJ, Cullen JM. Hepatobiliary system and exocrine pancreas. In: Zachary, J, ed, 6 Ed. *Pathologic Basis of Veterinary Disease*. Elsevier, St. Louis MO, 2017, p. 423.
3. Lancaster, Jubb and Pascoe. Lack of toxicity of rough dog's tail grass (*Cynosurus echinatus*) and the fungus *Drechslera biseptata* for cattle. *Aust. Vet J.* **84** (3):98-100.
4. Read E, Edwards J, Deseo M, Rawlin, G, Rochfort, S. Current understanding of acute bovine liver disease in Australia. *Toxins* 2017; 9(8)

CASE III: VPL 1 (JPC 4066919-00).

Signalment: A 12-year-old female spayed Galgo Español, dog, *Canis lupus familiaris*

History: During a routine dental cleaning procedure, a polypoid pedunculated mass on the left palatine tonsil was discovered. The mass has been removed surgically. There have been no other signs of illness during clinical examination.

Gross Pathology: Submitted by referring veterinarian. Petechiation was seen throughout the omentum. There were petechiae in the abomasum which was also



Tonsil, dog: Gross morphology reveals a pedunculated and polypoid appearance and a delicately nodular surface. (Photo courtesy of: Institute of Pathology, Faculty of Veterinary Medicine, University of Leipzig, Germany <http://patho.vetmed.uni-leipzig.de>)

filled with brownish blood-tinged fluid. There were petechiae and ecchymoses on pericardium, epicardium and endocardium.

Laboratory results: None.

Microscopic Description: The mass mainly consists of soft tissue and is covered by a nonkeratinized pluristratified epithelium showing variable degrees of hyperplasia. The epithelium multifocally shows mild to moderate intracellular oedema and there also is a mild to mainly moderate epitheliotropism of mainly lymphocytes but also some neutrophils. Multifocally, the epithelium tends to form crypts which are filled with an eosinophilic material, scaled off epithelial cells, lymphocytes, neutrophils and cellular debris. There are multiple densely-arranged subepithelial areas consisting of mononuclear cells, which can be identified as well-differentiated slightly anisocytotic lymphocytes and a few plasma cells. Partially, the lymphocytes form follicular nodules which show an appearance of primary and secondary lymphoid follicles. Altogether, the histomorphologic structures resemble tonsillar tissue, which is consistent with the localization of the tumor. The center of the mass is formed by collagenous connective tissue, which shows mild to moderate edema. Embedded in that fibrous stroma, numerous dilated and ectatic vascular structures can be seen. Some of them are filled with erythrocytes and resemble arterial and venous blood vessels. Others, mostly thin-walled, are filled with varying amounts of slightly eosinophilic fluid and a few cellular components (lymphocytes and macrophages) or they appear to be empty. These vascular structures may be identified as lymphatic vessels. All of the vessels are lined by a one-layered well-differentiated endothelium. In some slides, there are seromucous glands at the base of the mass, which seem to be salivary glands.

Contributor's Morphologic Diagnoses:

Tonsil: lymphangiomatous tonsillar polyp

Contributor's Comment: To characterize the involved cellular components an immunohistological examination was performed. The lymphocytes were immunopositive for CD3 and CD79a and showed the expected distribution patterns for tonsillar tissue. Some of the cells mostly adjacent to small vessels or inside of supposedly lymphatic vessels could be identified as macrophages via expression of MAC387 and lysozyme. While blood vessels often could easily be identified due to the presence of intravascular erythrocytes or thick vascular walls, there were some difficulties in the direct differentiation of lymphatic vessels and thin-walled venous vessels, especially when they appeared to be empty. For that reason, the endothelium was immunolabeled using markers specific for lymphatic endothelium (LYVE-1 and Prox1.⁹ While not all lymphatic vessels were immunopositive regarding LYVE-1 (Lymphatic vessel endothelial hyaluronan receptor 1), Prox1 (Prospero homeobox 1) was widely expressed by the lymphatic vessels in the tissue sample, which is

consistent with the findings of previously performed studies on immunohistochemical labelling of blood and lymphatic vessels in dogs⁹.

The pathogenesis of lymphangiomatous tonsillar polyps is still unclear. There are different theories about the origin of this benign proliferation. Because of the haphazard proliferation of components which are usually found in the tonsil they are discussed to be hamartomatous proliferations⁵ and therefore classified as malformations. One author sees them as the result of lymphatic obstruction with consecutive congestion and mucosal prolapse finally forming the polyp¹¹. In veterinary medicine those polyps are also considered being a result of chronic recurrent tonsillitis and are regarded as inflammatory polyps which occur infrequently in old dogs⁵. Anyhow, the definite cause remains uncertain.

As in this case such polyps are often undiscovered for a long period of time. They can be asymptomatic or, probably when large enough, they may cause dysphagia⁶, non-productive cough¹¹ or a sore throat¹. In



Tonsil, dog: The cut surface shows an oedematous fibrous stock and multinodular white foci in the margin areas. (Photo courtesy of: Institute of Pathology, Faculty of Veterinary Medicine, University of Leipzig, Germany <http://patho.vetmed.uni-leipzig.de>)

human medicine, the complete surgical excision is normally curative and there usually are no recrudescences.⁵

This case shows that such benign proliferations might be considered as differential diagnosis when there is a unilateral mass of the tonsils, especially concerning tonsillar squamous cell carcinoma, even though regional lymph nodes are usually enlarged early in such cases.⁷

JPC Diagnosis: Tonsil: Lymphangiomatous polyp.

Conference Comment: The contributor has provided an excellent review of this uncommon but morphologically unique lesion often seen in association with chronic tonsillitis in older dogs.

The tonsil samples antigens which are dissolved in the saliva, and develops immune responses akin to other lymphoid organs throughout the body. A layer of non-keratinizing squamous epithelium provide barrier function for the tonsil.¹⁰

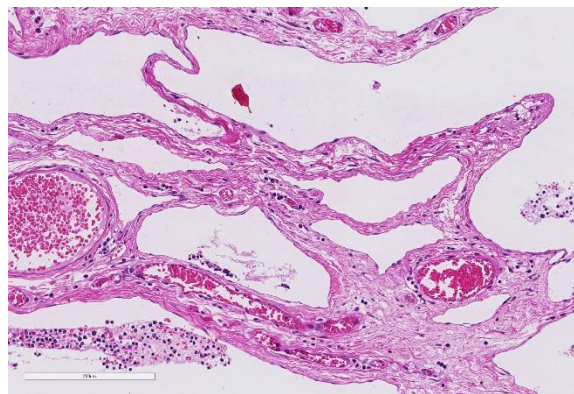
A unique feature of the tonsils is their lack of afferent lymphatic vessels. This prevents them from being effective lymphoid filter for structures in the oral cavity (which drains instead primarily to pharyngeal and



Tonsil, dog: Subgross examination of the submitted polyp reveals a marked expansion of the connective tissue component by abundant clear space. There is moderate follicular hyperplasia. (HE, 7X)

submandibular nodes)³, but also significantly reduces the possibility of finding metastatic tumors within the tonsils. As a general rule, tonsillar neoplasms arise from tissues native to the tonsil itself- squamous cell carcinoma, lymphoma, and rare tumors of the vascular and lymphatic endothelium.

The tonsils also serve as a reservoir or portal vein treated for a variety of viral and bacterial



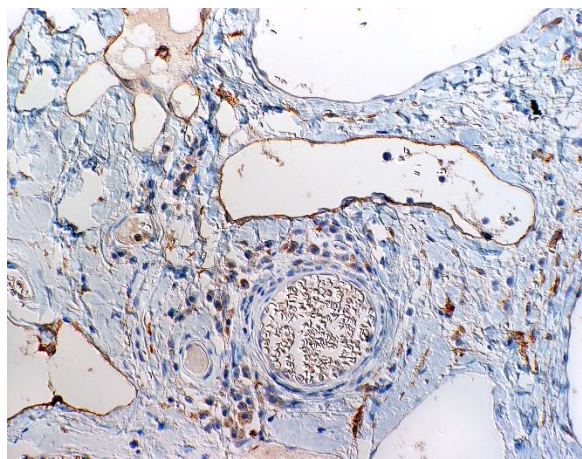
Tonsil, dog. Clear spaces are endothelial lines (presumably lymphatics) and are separated by loosely arranged fibrous connective tissue which contains few lymphocytes and plasma cells. (HE, 198X)

agents.¹⁰ A number of viral agents including pseudorabies in swine and parvovirus in carnivores may utilize the tonsil as an initial site of replication and dissemination. Depending upon the particular virus and stage infection, either involution or hyperplasia of tonsillar follicles may be the result. A significant percentage of swine carry *Erysipelothrix rhusiopathae*, *Streptococcus suis*, and various species of salmonellae within the tonsils as well.¹⁰ Additionally, the scrapie-associated prion protein has been identified in tonsillar tissue as well.¹⁰

The lymphoid changes seen in the tonsils parallel those seen in reactive lymph nodes with a number of primary follicles surrounding tonsillar crypts. Following antigenic stimulation, development of secondary follicles with mantle zones

extending in the direction of the antigenic stimulus will occur, as well as marked expansion of the interfollicular lymphoid tissue. The majority of histologic changes seen in the biopsy samples of excised tonsils will be chronic in nature; acute tonsillitis is rarely if ever seen. The presence of neutrophils within crypts, crypt epithelium and most importantly with in the parenchyma of the tonsils is required for the diagnosis of acute tonsillitis. The histologic changes of chronic tonsillitis are indistinguishable in most cases from tonsillar hyperplasia.

An appropriate ruleout in this case would be that of a lymphangioma. Lymphangiomas are uncommon benign proliferations of lymphatic derived thin walled cystic spaces often filled with pink, watery proteinaceous fluid.¹² These benign tumors may be found as isolated findings in lymphoid tissues including the lymph node and spleen. The abundant fibrous connective tissue seen in lymphangiomatous polyps is generally not a feature of lymphangiomas, and provides additional support as tonsillar lymphan-



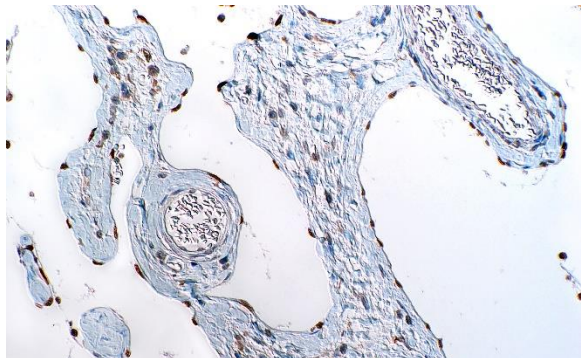
Tonsil, dog: Endothelial cells of dilated lymphatic vessels exhibit strong immunopositivity for LYVE-1, while endothelial cells of blood vessels are immunonegative. (Nomarski Differential Interference Contrast microscopy, 400x) (Photo courtesy of: Institute of Pathology, Faculty of Veterinary Medicine, University of Leipzig, Germany, <http://patho.vetmed.uni-leipzig.de>)

giomatous polyps are hamartomatous lesions rather than true neoplasms.⁵

A very interesting, morphologically distinct lesion of lymphoid tissue that is occasionally seen in the dog and cat is vascular transformation of lymph node sinuses (previously referred to as nodal angiomatosis). This lesion has not yet been reported in the tonsil as of yet. Gelberg and Valentine reported this change in association with thyroid carcinoma in a dog.⁴ Vascular transformation of lymph node sinuses is a pressure-induced non-neoplastic conversion of nodal sinuses into anastomosing vascular channels. The inciting pressure is often the result of obstruction of venous or hilar lymphatic drainage and has been reported in humans in association with a variety of neoplasms, as well as various forms of venous obstruction. Vascular transformation may take a variety of appearances believed to be the result of a continual related to the duration and degree of venous or lymphatic obstruction.⁴ The plexiform pattern, the most commonly reported in animals, presents as a mass lesion composed of interconnected mature vascular channels, a flat endothelial cell lining, and a low mitotic rate.¹⁰ More chronic cases are associated with increased amounts of collagen separating proliferating vessels. In a second variant, the round vascular type, vascular changes are usually empty or contain amorphous material presumed to be lymph¹⁰. A recently published review by Xu et al., excellently describes this and other vascular and stromal proliferations in the lymph nodes of humans.¹²

Contributing Institution:

Institute of Pathology, Faculty of Veterinary Medicine, University of Leipzig, Germany
<http://patho.vetmed.uni-leipzig.de>



Tonsil, dog: Endothelial cells of dilated lymphatic vessels label intranuclear immunopositive for Prox1, while endothelial cells of blood vessels are immunonegative (Nomarski Differential Interference Contrast microscopy, 400x) (Photo courtesy of: Institute of Pathology, Faculty of Veterinary Medicine, University of Leipzig, Germany, <http://patho.vetmed.uni-leipzig.de>)

References:

1. Al Samarrae SM, Amr SS, Hyams, VJ. Polypoid lymphangioma of the tonsil: report of two cases and review of the literature. *J of Laryngol Otol* 1985; 99(8): 819-823.
2. Bauchet A, Balme E, Thibault J, Fontaine J, Cordonnier N. Lymphangiectatic fibrous polyp of the tonsil in a dog. *ECVP/ESCVP 2009 Proceedings*; 141(4):284.
3. Gelberg HB. Alimentary system and the peritoneum, omentum, mesentery, and peritoneal cavity. In: Zachary, JF, ed. *Pathologic Basis of Veterinary Disease, 6th ed.* 2017. St. Louis, MO, pp. 324-411.
4. Gelberg HB, Valentine BA. Lymphadenopathy associated with a thyroid carcinoma in a dog. *Vet Pathol* 2011; 48(2): 530-534.
5. Kardon DE, Wenig BM, Heffner DK, Thompson LDR. Tonsillar lymphangiomatous polyps: a clinopathologic series of 26 cases. *Mod Pathol* 2000; 13(10):1128-1133.
6. Kuhnemund M, Wernert N, Gevensleben H, Gerstner AO. Lymphangiomatoser Tonsillenpolyp. *HNO* 2010; 58(4):409-412.
7. Meuten DJ, ed.. *Tumors in Domestic Animals, 4th ed.* 2002; Ames IA; Iowa State Press.
8. Miller A, Alcaraz, A, McDonough S. Tonsillar lymphangiomatous polyp in an adult dog. *J Comp Pathol* 2008; 138(4): 215-217.
9. Sleenckx N, van Brantegem L., Fransen E. Evaluation of immunohistochemical markers for lymphatic and blood vessels in canine mammary tumors. *J Comp Pathol* 2013; 148(4): 307-317.
10. Uzal FA, Plattner BL, Hotstetter JM. Alimentary System, In: Maxie MG, ed. *Jubb Kennedy and Palmer's Pathology of Domestic Animals, 6th ed.* 2016; St. Louis MO, Elsevier Press, vol 2, p. 20
11. Visvanathan PG. A pedunculated tonsillar lymphangioma. *J Laryngol Otol* 1971; 85(1):93-96.
12. Xu ML, O'Malley D. Lymph node stromal and vascular proliferations. *Seminars Diagn Pathol* 2018; (67-75).

CASE IV: 1/12 (JPC 4066919-00).

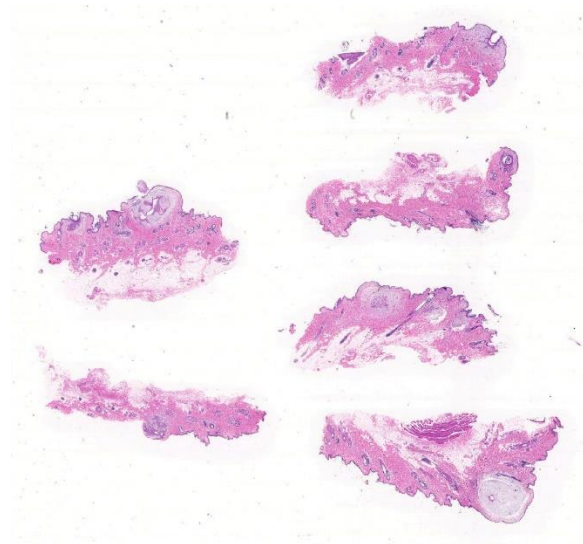
Signalment: Ten-month old, mixed breed, female spayed, canine

History: Multiple diffuse papules. No pruritus.

Gross Pathology: Not available.

Laboratory results: None.

Microscopic Description: Haired skin: All sections have similar histological



Haired skin, dog. Multiple expansile nodules containing proliferative follicular epithelium are present within the superficial dermis. (HE, 5X)

characteristics with variations in intensity. The epidermis is minimally hyperplastic to normal. There is formation of multiple raised dermal nodules, varying from 0.5 to 2mm in diameter. The nodules consist of a large dilated hair follicle with hyperplastic epithelium forming arborizing cords growing into a perifollicular accumulation of myxomatous material. The latter constitutes the bulk of the mass and produces its nodular shape. In several nodules there is a central 20-50µm thick band of deep eosinophilic hyaline material. This hyaline band surrounds a focus of necrotic debris, or, in rare follicles, a degenerated mite larva. There is minimal superficial perivascular dermal mononuclear cell infiltration.

Contributor's Morphologic Diagnoses:

Skin, Arborizing follicular hyperplasia with myxomatous degeneration and dilation, intrafollicular hyaline material and arthropod larvae, canine, mixed breed - findings typical of canine straelensiosis

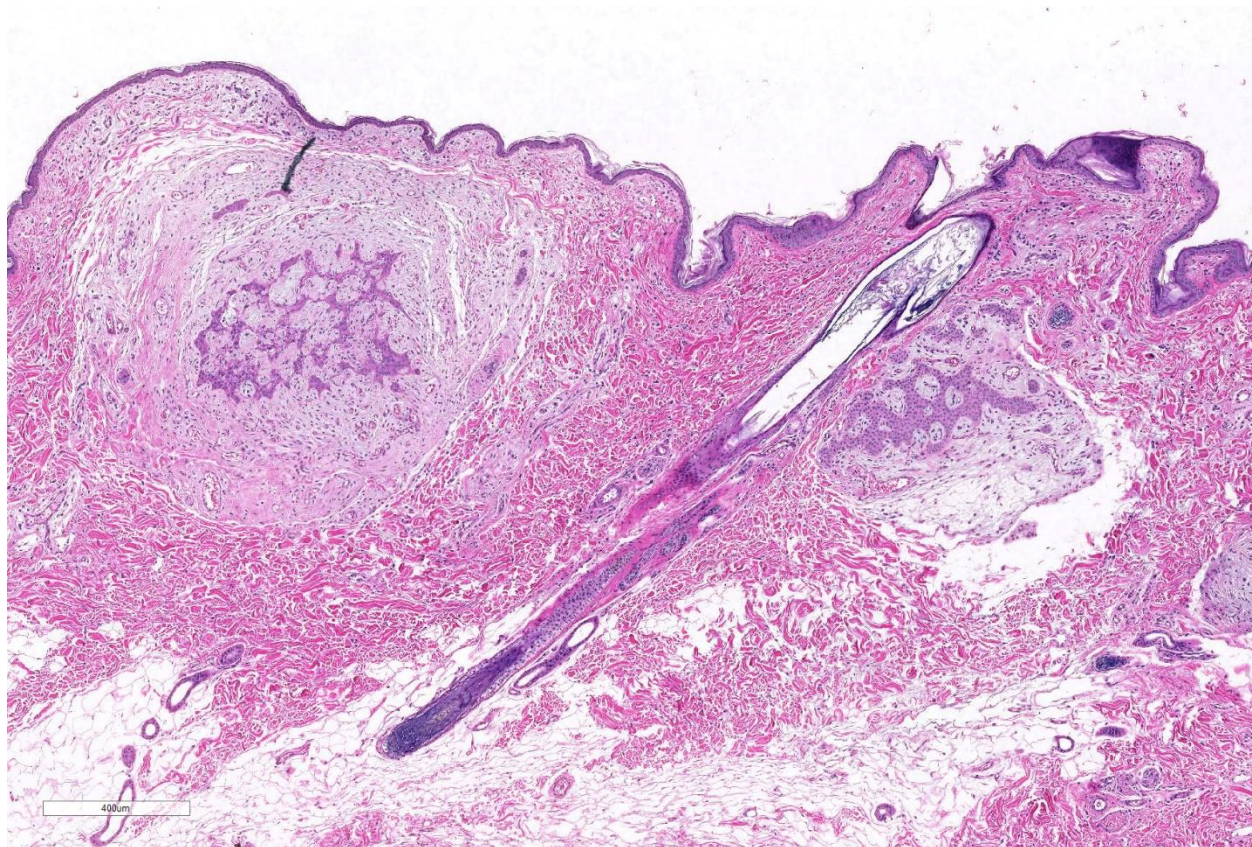
Contributor's Comment: Infection with the trombidoid mite *Straelensia cynotis* has been

reported in dogs in France, Portugal and Spain.^{2,4,10} The findings described in these reports are virtually identical to several cases we have seen in Israel.

Straelensiosis is a trombidiosis caused by the "chigger" mite *Straelensia cynotis*, and is a relatively newly described etiology for nodular dermatitis in dogs in the Old World.^{2,4,10} Nodular trombiculiasis has also been described in white tailed deer and birds.^{5,7} The findings are similar to those described for the dog. The first publication of the morphologic characteristics of these mites was by Le Net and Fain who proposed the classification of a new species: *S. cynotis*, superfamily Trombidoi, family Leeuwenhoekidae. Straelensiosis was first identified as a cause of nodular dermatitis in dogs in France by Le Net et al.^{1,4}

In general, the nymphs and adults of trombiculid arthropods are free-living, or parasitize plants or other arthropods. The parasitic stage is the larvae which are known as 'harvest mites', 'chiggers' or 'red bugs'.^{3,9} Infected animals may present with accumulation of orange granular material or pin-sized red spider-like foci in the canthi of the eyes.^{3,5,9} The larvae attach themselves to areas of the host's skin in contact with the ground e.g. legs, feet, head, ears or ventrum and make a tunnel to the epidermis, called stylosome, through which salivary enzymes are injected and digested tissue fluids are withdrawn. The larvae engorge through a period of 3-5 days after which they drop off to become nymphs and complete their life cycle in the soil. Wild mammals are the usual hosts for trombiculid mite larvae, but pets and people may be accidentally infected.^{3,9}

The histologic finding in skin infection with trombiculid larvae is the presence of tunnels within the stratum spinosum or stratum corneum, inducing degenerative and hyperplastic changes in the epidermis. The



Haired skin, dog. Higher magnification of the perifollicular nodules shows marked pseudoepitheliomatous hyperplasia of follicular epithelium. (HE, 51X)

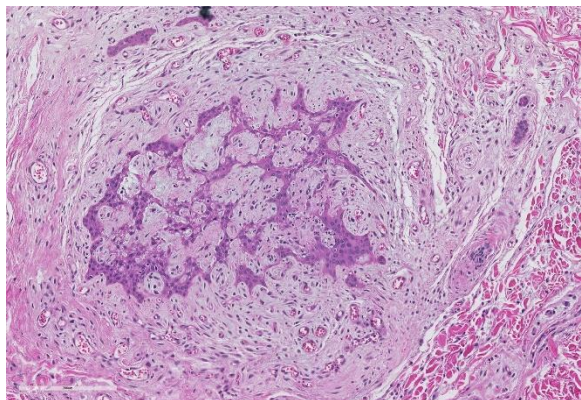
stylostome is described as a hyalinized tube oriented vertical to the skin surface.³

It is thought that the fox is the normal host for *Straelensia* and that hunting and rural dogs are predisposed to aberrant infection.⁴ There is a clear geographical pattern of infection in certain areas within the countries reported and an obvious tendency for infection to occur in the fall and spring.⁷ The nodules may last 1 to 12 months. On average, they are reported to last 3 months,⁴ which is much longer than the course described for chiggers in the US. The follicular reaction to the presence of the larvae is highly characteristic and allows diagnosis to be made in the absence of larvae in the section. The follicle is dilated and contains a ring of hyalinized material identified as the stylosome.^{4,8,10} The follicles exhibit epithelial hyperplasia with

formation of arborizing epithelial cords within a perifollicular accumulation of myxomatous material.^{4,8,10} Associated pyogranulomatous, suppurative and eosinophilic perifollicular infiltration is described.^{4,8,10}

In this particular case inflammation is negligible, but we have observed pyogranulomatous and suppurative perifollicular inflammation in most of the dogs infected in Israel.

Prognosis is variable.^{2, 4,8,10} Some dogs may run the course of the infection and have spontaneous regression. Some respond well to antiparasitic shampoos or Ivermectin injections, but some dogs are reported to present with persistent infection and no



Haired skin, dog. Further magnification of a dermal nodule demonstrate pseudoepitheliomatous hyperplasia of follicular epithelium which is bounded by a vascular myxomatous dermis. Inflammation, however, is minimal. (HE, 100X)

apparent response to therapy.^{2, 4, 8, 10} This may represent continuous exposure.

In our experience in Israel, infection is most common in the northern and in the Jerusalem areas, (both of higher altitude), in the spring and winter. Response, as described in the European reports, is variable but most dogs appear to respond well to pesticide shampoos.

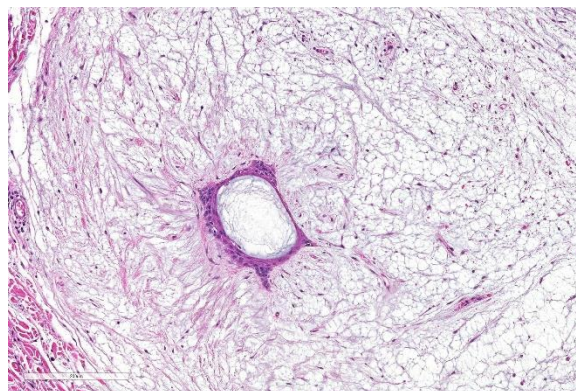
JPC Diagnosis: Haired skin, follicles: Pseudoepitheliomatous hyperplasia, multifocal, severe, with marked perifollicular mucin, and occasional intrafollicular trombiculid larvae.

Conference Comment: The contributor provides an excellent description of changes associated with most common trombiculid mite infections, however the histologic findings of *S. cynotis* are quite different than traditional trombiculid mite infections. While other trombiculid mites generally attach to the surface epidermis, the larva of *S. cynotis* live and feed with in follicular ostia. They are separated from the wall of the follicle by the highly characteristic stylosome, a proteinaceous tube secreted by the mouthparts of the larval mite, through

which the larva feeds by repeated cycles of extrusion of digestive salivary fluids followed by suction of digested tissue and tissue fluids.⁵ The extensive pseudoepitheliomatous hyperplasia of follicular epithelium and perifollicular mucinosis are additional histologic features which allow for the diagnosis of *S. cynotis* infection even in the absence of the larval arthropods. The larval forms of this parasites may be absent in treated cases or following the completion of the larval stage (as nymphs and adults are free living stages).⁸

Another interesting fact about infection by *S. cynotis* is the almost total lack of dermal inflammation in response to the presence of the parasite. This may be the result of the intra-follicular location of the mites as well as a total enclosure by the presence of the stylosome.⁸

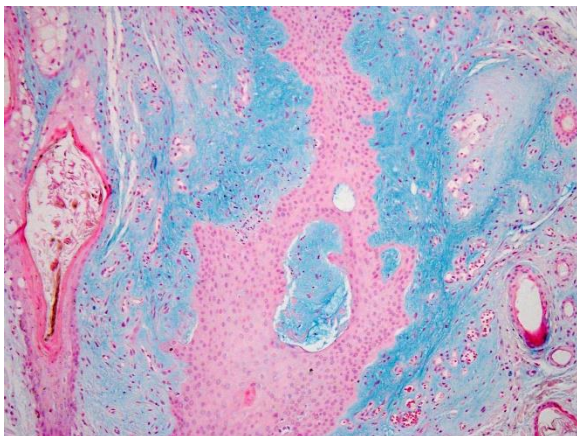
A number of arthropod and helminth parasites inhabit hair follicles. By far the most common genus is that of *Demodex*, which are normal inhabitants of hair follicles and sebaceous glands in most mammals, including humans. Interestingly, their position within the hair follicle is invariably head down.⁶ *Demodex* sp. are obligate parasites which complete their entire life



Haired skin, dog. The adjacent perifollicular dermis is extremely myxomatous with infiltration of few muciphages. (HE, 122X)

cycle on the host and are usually transmitted from mother to offspring within the first 3 days of life through close physical contact while nursing. *Demodex* mites, unlike trombiculid mites, feed harmlessly on sloughed cells, sebum, and epidermal debris. These mites may move from follicle to follicle, and transmission likely occurs while in transit. Prolonged sojourns on the epidermis may result in death of the mite through desiccation.⁶

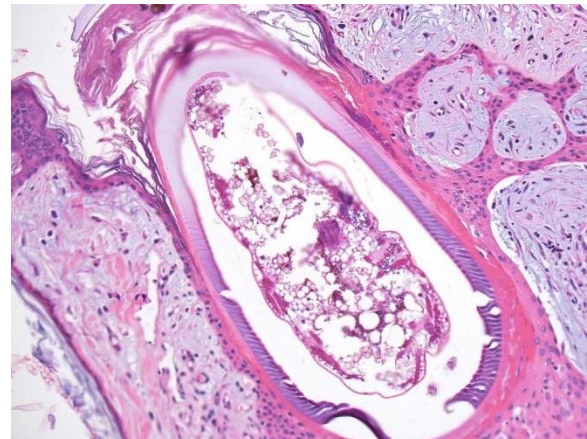
Two important helminth species parasitize hair follicles in mammals. Parasitic females of the species *Pelodera* (*Rhabditis*) *strongyloides*, normally also free-living indicating plant matter, may indicate the skin and reside within hair follicles.⁶ *Pelodera* dermatitis occurs most often the dogs but cases are well documented in cattle, sheep, horses, and humans.⁶ Affected dogs are often victim supportive husband 3 and straw embedding is a common finding. *Stephanofilaria* species are uncommon cutaneous parasites of a wide range of ruminant species; with *S. stilesi* occurring in Western and Southwestern North America. While abdominal skin is characteristic for this particular species, other species each



Haired skin, dog. An Alcian blue 2.5 stain demonstrates the mucinous nature of the perifollicular substance. (AB, 200X)

have particular sites where they affect their

respective host.⁶ Flies are intermediate hosts for these parasites and deposit infective larva on both intact and broken skin of the host species. The adults of *S. stilesi* and similar species live within cystic hair follicles and microfilariae occur free in the dermis or within dermal lymphatics, where they may be



Haired skin, dog. This is a section through the degenerate larva occupying the infundibulum and surrounded by a band of hyaline material (stylosome). (HE, 100X) (Photo courtesy of: Department Vet Resources, Weizmann Institute, Rehovot, Israel <http://www.weizmann.ac.il/vet/>)

ingested by flies and complete their life cycle. Maturation from microfilaria to infective larva occurs within the intermediate host. A marked inflammatory reaction occurs if the adults exit the hair follicles, resulting in profound lymphoplasmacytic and eosinophilic inflammation, epidermal hyperplasia, and often alopecia. The presence of the adults within the follicle or of microfilariae within the dermis generally results in little inflammation.⁶

Contributing Institution:

Department Vet Resources, Weizmann Institute, Rehovot, Israel

<http://www.weizmann.ac.il/vet/>

References:

- Fain A, Le Net JL. A new larval mite of the genus *Straelensia* Vercammen-Grandjean and Kolebinova, 1968 (acari: Leeuwenhoekiidae) causing nodular dermatitis of dogs in France. *Int Jour of Acarology* . 2000;**26**: 339–45.
1. Font A, Straelensiosis in a dog in Spain. *Vet Derm*. 2007;**18**: 67-68.
 2. Ginn PE *et al*, Skin and appendages. In: Jubb, Kennedy and Palmer's *Pathology of Domestic Animals*, 5th ed. Maxie Ed. Saunders Elsevier 2007;Vol. 1:7272-728.
 3. Le Net JL *et al*. Straelensiosis in dogs: a new deA hyalscribed nodular dermatitis induced by *Straelensia cynotis*. *Vet Rec*. 2002; **150**:205-209.
 4. Little SE *et al*, Trombidiosis-induced Dermatitis in White-tailed Deer (*Odocoileus virginianus*). *Vet Pathol* 1997;**34**:350-352.
 5. Mauldin EA, Peters-Kennedy J.. Integumentary System, In: Maxie MG, ed. *Jubb, Kennedy and Palmer's Pathology of Domestic Animals*, 6th ed. 2016; St. Louis MO, Elsevier Press, vol 1, pp. 666-690.
 6. Ornelas-Almeida MA *et al*. Nodular trombiculosis caused by *Apolonia tigipioensis*, Torres and Braga (1938), in an ostrich (*Struthio camelus*) and a house sparrow (*Passer domesticus*). *Vet Parasit*. 2007;**150**: 374–377.
 7. Ramirez GA, Clinical, histopathological and epidemiological study of canine Straelensiosis in the Iberian Peninsula (2003-2007). *Vet Derm*. 2009;**20**:35-41.
 8. Scott *et al*, Parasitic skin diseases. In: *Muller and Kirk's Small Animal Dermatology*. 5th ed. Saunders 1995; 407-408.

Self-Assessment - WSC 2017-2018 Conference 2

1. Infection with ferret enteric coronavirus closely resembles coronavirus infection in what other species?
 - a. Cats
 - b. Rodents
 - c. Ruminants
 - d. Viverrids

2. Which of the following is not a characteristic finding in ferret coronavirus-associated disease ?
 - a. Palpable intraabdominal mass
 - b. Polyclonal gammopathy
 - c. Anemia
 - d. Weight loss

3. Which of the following is not an important mechanism of periportal hepatocellular necrosis?
 - a. Overwhelming toxicity coming out of portal venous system
 - b. Toxins that are excreted in bile
 - c. Highly lipid soluble toxins
 - d. Toxins that do not need to be metabolized by mixed function oxidases

4. Which of the following is a specific immunohistochemical marker for lymphatic endothelium?
 - a. MAC 387
 - b. CD 31
 - c. LYVE-1
 - d. Factor VII

5. With regard to infection by trombiculid mites, what is a stylosome?
 - a. The excretory tube of the mite
 - b. A channel within the epidermis where eggs are laid.
 - c. A proboscis used to pierce the dermis and suck tissue fluids
 - d. A hyalinized tube within the follicle or epidermis that surrounds the mite

Please email your completed assessment to Ms. Jessica Gold at Jessica.d.gold2.ctr@mail.mil for grading. Passing score is 80%. This program (RACE program number) is approved by the AA VSB RACE to offer a total of 0.5 CE Credits, with a maximum of 12.5 CE Credits being available to any individual Veterinary Medical Professionals for the 2017-2018 Wednesday Slide Conference. This RACE approval is for the subject matter categories of: SCIENTIFIC using the delivery method of NON-INTERACTIVE DISTANCE. This approval is valid in jurisdictions which recognize AA VSB RACE; however, participants are responsible for ascertaining each board's CE requirements. RACE does not "accredit", "endorse" or "certify" any program or person, nor does RACE approval validate the content of the program.

Please email your completed assessment to Ms. Jessica Gold at Jessica.d.gold2.ctr@mail.mil for grading. Passing score is 80%. This program (RACE program number) is approved by the AAVSB RACE to offer a total of 0.5 CE Credits, with a maximum of 12.5 CE Credits being available to any individual Veterinary Medical Professionals for the 2017-2018 Wednesday Slide Conference. This RACE approval is for the subject matter categories of: SCIENTIFIC using the delivery method of NON-INTERACTIVE DISTANCE. This approval is valid in jurisdictions which recognize AAVSB RACE; however, participants are responsible for ascertaining each board's CE requirements. RACE does not "accredit", "endorse" or "certify" any program or person, nor does RACE approval validate the content of the program.

**Joint Pathology Center
Veterinary Pathology Services**



WEDNESDAY SLIDE CONFERENCE 2018-2019

C o n f e r e n c e 3

12 September 2018

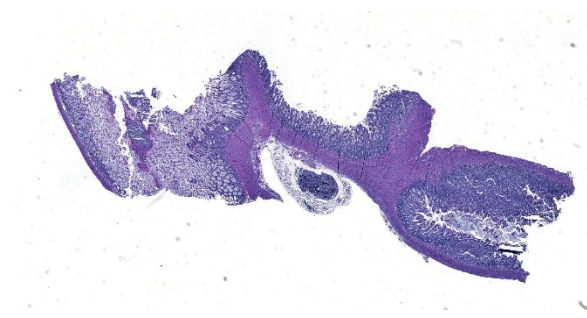
CASE I: AFIP 15-13332 (JPC 4067411-00).

Signalment: 3-week-old male domestic shorthair kitten

History: A 3-week-old male domestic short hair kitten was one of 8 kittens found before taken to a cat rescue. The litter was split into two different foster homes. All kittens developed diarrhea with lethargy and inappetence. The kitten in this case was euthanized after a week of developing symptoms and two more died subsequently (exact timing unknown). The remaining two surviving kittens are alive and thriving.

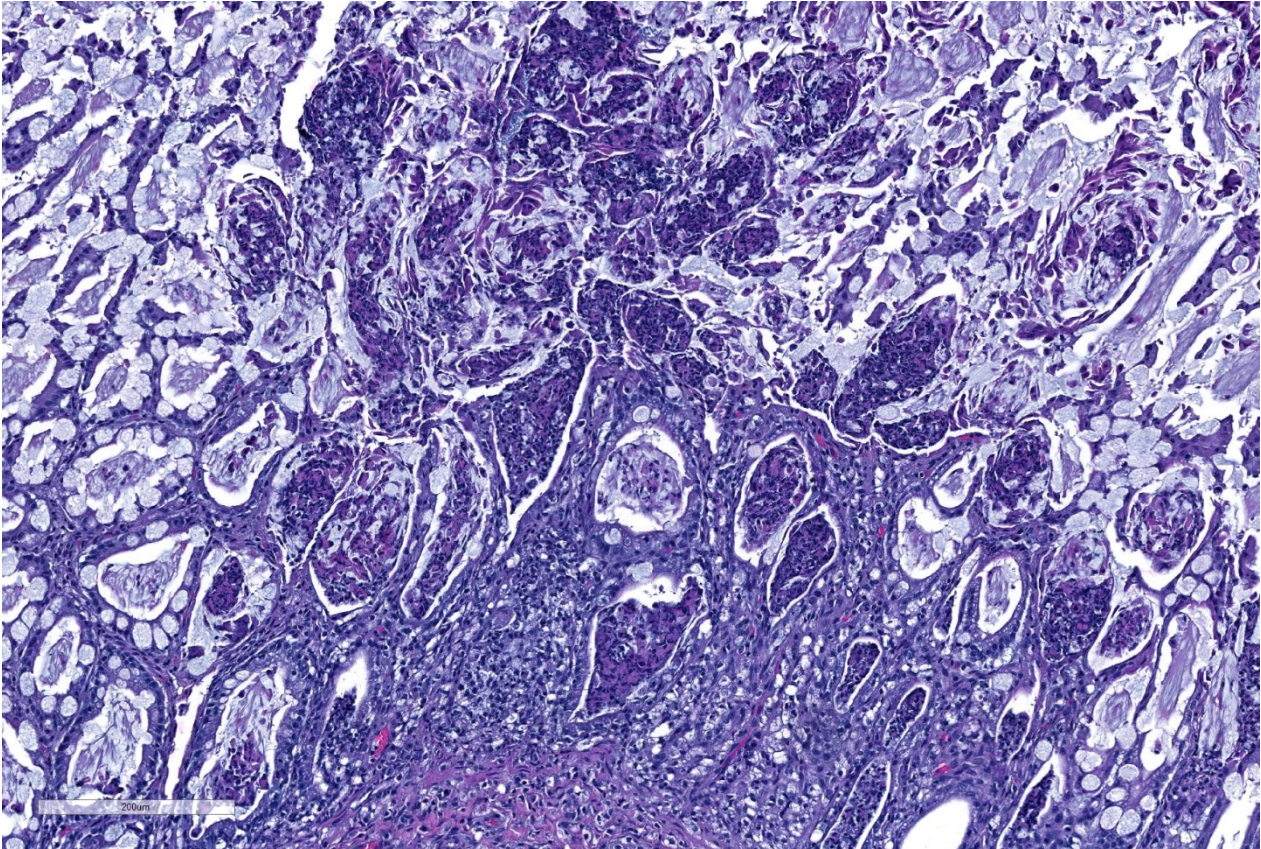
Gross Pathology: A male kitten (0.11 kg) in fair body and postmortem condition was presented for autopsy. The umbilicus has no lesions. The stomach is expanded by ~ 5 ml of curdled milk. The rectum and distal colon contain yellow-green dry string-like fecal material. Both lungs are wet and mottled dark and pale pink with areas of hyperinflation. No other significant gross lesions identified.

Laboratory results: Hemolytic *E. coli* and group G beta-hemolytic *Streptococcus* were both cultured from pulmonary tissue.



Ileocolic junction, kitten. A section of the ileocolic junction with ileum on the left and the colon on the right is submitted. (HE 12X)

Microscopic Description: Ileum and colon. The section of ileum contains frequent crypt necrosis and ~50% intestinal villi blunted with occasional complete villous loss. There are large numbers of cocci and rod bacteria within the lumen and crypts of the tunica mucosa, both extracellularly and intracellularly, throughout the majority of stained sections. Slender rod-shaped bacteria are arranged in one or more parallel stacks within the cytoplasm of numerous enterocytes. The lumen of the ileum is heavily colonized by a mixed population of gram-negative rods and cocci, with moderate numbers of cocci directly associated with the surface of mucosal epithelial cells. The tunica muscularis and serosa appear unaffected. The section of intact colon is included to



Colon, kitten. There is necrosis of colonic glands with replacement by neutrophils and macrophages. Remaining colonic glands are dilated and filled with variable combinations and concentrations of necrotic glandular epithelium, degenerate neutrophils, cellular debris, and mucin. (HE, 137X)

demonstrate that the changes to the ileum are not likely due to autolysis. The colon contains few luminal bacteria, but moderate numbers of enterocytes contain slender rod bacteria as described above.

Contributor's Morphologic Diagnoses:

Ileum and colon: Marked multifocal to coalescing necrotizing enterocolitis with extracellular, adherent and intracellular mixed bacteria.

Contributor's Comment: Differentials to consider in a case of enterocolitis in neonatal kittens include: bacteria (*E. coli*, *Salmonella*), primary viral enteritis (parvovirus, enteric coronavirus), protozoa (*Isospora*, *Giardia*) or severe systemic disease, such as caused by feline immunodeficiency virus (FIV) and feline

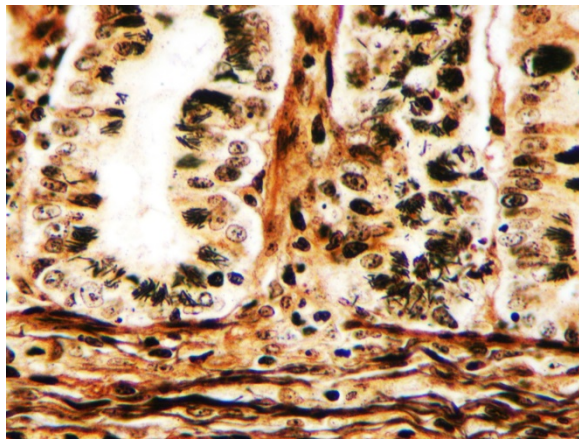
leukemia virus (FeLV). The two surviving kittens were 8 weeksold at the time of this submission and both had tested negative for FIV and FeLV the week prior. Culture of fecal samples from both kittens yielded *E. coli*, however only one harbored the hemolytic phenotype. Salmonellae were not recovered using routine media.

In the case presented here, there are concurrent intestinal bacterial infections by *C. piliforme* and *E. coli*. *E.coli* had primarily colonized the small intestine while *C. piliforme* was associated with crypt necrosis in the large intestine. An area of overlap within the ileum, as highlighted in the submitted slide, shows the co-existence of both bacteria. There have been few published feline cases of Tyzzer's disease, and a

bacterial co-infection in a cat has not yet been reported. A recent publication, however, describes dual infection by *C. piliforme* and enteropathic and effacing *E. coli* causing enterotyphlocolitis in a Syrian hamster.¹

Tyzzler's disease in cats has been associated with viral co-infection with FIP and FeLV.^{2,5} Coronaviral protein was not detected in the small intestine or colon by immunohistochemistry in this kitten (a quantity of fecal material sufficient for testing could not be obtained during necropsy); thus, a concurrent or underlying and predisposing viral infection, while unlikely, cannot be completely ruled out. Other factors that are more likely to have predisposed this kitten to Tyzzler's disease are failure of passive transfer, environmental stress (exposure, relocation), immune compromise, or concurrent disease.

Suboptimal immune competency of the host has been associated with the dissemination of extraintestinal pathogenic *E. coli*.⁴ Colonization of the small intestine with *E.*



Colon, kitten. Glandular epithelial cells contain numerous slender bacilli in haphazard stacks within their cytoplasm, consistent with *C. piliforme*. (Warthin-Starry 4.0, 400X) (Photo courtesy of: Oregon State University Diagnostic Laboratory, <http://vetmed.oregonstate.edu/diagnostic>)

coli and subsequent sepsis could have been a primary event in this case. Bacterial culture identified moderate numbers of hemolytic *E. coli* and low numbers of group G beta-hemolytic *Streptococcus* in the lungs. Histopathology of the lung identified mild, diffuse, interstitial pneumonia consistent with sepsis.

E. coli is a constituent of the normal feline intestinal microflora and does not normally produce disease. When provided with a compliment of virulence factors, however, *E. coli* may become an opportunistic pathogen resulting in local and systemic infection and even death. At least seven distinct pathotypes have been identified, including enteropathogenic (EPEC), enterotoxigenic (ETEC), and shiga-toxin producing *E. coli* (STEC; also referred to as enterohemorrhagic *E. coli* or EHEC).⁸ Shiga toxin-producing Escherichia coli (STEC) causes hemolytic uremic syndrome (HUS) in humans and has zoonotic potential. Most shiga-toxin producing *E. coli* belong to various serotypes including O26, O103, O111, O145, and O157, the latter being the most commonly identified.⁷ A study of cats and dogs in Buenos Aires, Argentina, where STEC is an endemic pathogen, identified O157 in 4/149 (2.7%) cats and 34/450 (7.5%) dogs (3). Testing of the *E. coli* isolate did not detect O157:H7 antigen in this case.

Group G beta-hemolytic *Streptococcus* isolates include: *Streptococcus dysgalactiae* subspecies *equisimilis*, *S. milleri*, *S. canis*, and *S. intestinalis*. Both *S. dysgalactiae* subspecies *equisimilis* and *S. milleri* are associated with human infection, while dogs and pigs are reservoirs for *S. canis* and *S. intestinalis*, respectively. *S. canis* is the most likely strain to be identified in this case and is typically considered a commensal and extracellular pathogen in cats, however it has been shown to cause severe feline disease

such as necrotizing fasciitis, sinusitis, bacteremia, and toxic shock–like syndrome.⁹ Because of the low numbers of *Streptococcus* organisms isolated from the lungs, and absence of pathogenic changes consistent with primary *Streptococcus* infection, we consider this an opportunistic colonization in this cat.

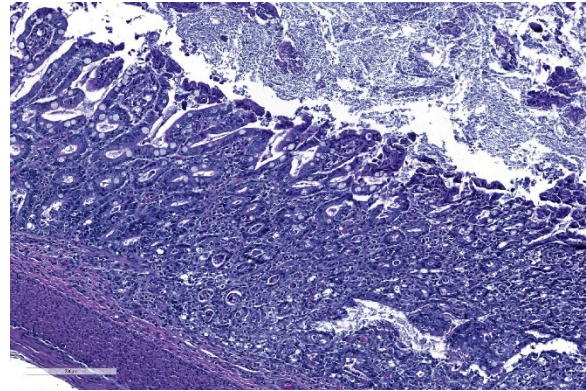
The clinical presentation of Tyzzer’s disease can range from subclinical infection and incidental finding to mild to marked mucoid diarrhea or death without premonitory signs. The mechanism of host cell attachment and entry by *C. piliforme* is not fully understood. Following colonization of the distal ileum, cecum, and colon, bacteria can penetrate into the portal vasculature to seed the liver.⁷ Neither necrotizing inflammation nor clostridial forms were identified within the liver in this kitten. *C. piliforme* infection limited to the intestinal tract could reflect an early stage of infection, prior to hematogenous spread, and would suggest that *C. piliforme* colonization occurred secondary to *E. coli* infection.

JPC Diagnosis: 1. Colon: Colitis, necrotizing, diffuse, marked with numerous crypt abscesses, crypt hyperplasia and intracytoplasmic bacilli within crypt epithelium.

2. Ileum: Ileitis, necrotizing, diffuse, mild to moderate with numerous surface-adherent bacilli.

Conference Comment:

Ernest Edward Tyzzer (1895-1965) was an American pathologist whose investigations far exceeded the disease which today bears his name. A graduate of Harvard medical school in 1902, many of his discoveries impacted veterinary science far more than human medicine. In 1901, he received a



Ileum, kitten. Crypt abscesses are also present within the ileum as well, indicating a necrotizing enteritis. (HE 137X)

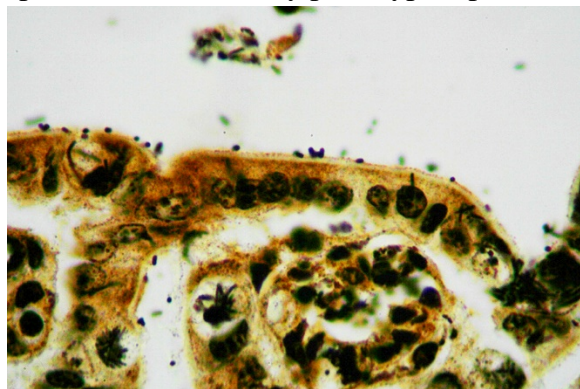
master’s degree studying myxosporidian infections in menhaden. Between 1905 and 1916, he was research director for the Harvard Cancer Commission, investigating spontaneous and transplanted tumors in mice, but continuing his interest in infectious diseases as well.¹⁰ In 1910, he identified the genus *Cryptosporidium* sp. for the first time. He was responsible for the development of the DBA inbred strain of mouse during this time, as well as the identification of *Leishmania* sp. as the cause of Oroya fever.¹⁰

In 1916, Dr. Tyzzer became the head of the Department of Comparative Pathology at Harvard, a chair he held until his retirement in 1942.¹⁰ In 1917, he first identified the disease that now bears his name in Japanese waltzing mice, a strain he was utilizing in cancer research. In this position, he correctly identified the flagellate *Histomonas meleagridis* as the causative agent of blackhead, as well as detailing its life cycle. (The principles which he used to raise turkeys on his experimental farm were subsequently published by the Massachusetts Department of Agriculture and he was given a citation by the Governor of Massachusetts for “saving the turkey industry of Massachusetts”).¹⁰ Additional investigations during his career provided seminal work in equine

encephalomyelitis as well as coccidiosis in gallinaceous birds.

Over a century following its identification, many questions remain about *C. piliforme*. A common commensal in rodents, disease has been difficult to reproduce in healthy dogs and cats. Concomitant disease, especially infection with immunosuppressive viruses such as FELV, FIV, feline panleukopenia, and the mutated coronavirus of feline infectious peritonitis have been incriminated in the majority of feline infections, and experimental immunosuppression by glucocorticoids or cyclophosphamide has also been used to enhance experimental infections.⁶ Transmission from the feces of rodents has been suggested as a source of infection of dogs and cats, but has not been proven. Basic information about the pathogenesis of *C. piliforme* infection, such as the mechanisms of attachment and entry into cells by *C. piliforme*, have not yet been identified, and inability to culture the organism on artificial media further hampers laboratory research.⁶

Attaching and effacing *E. coli* (AEEC), which has been reported in a wide variety of species (and is the only pathotype reported in



Ileum, kitten. Bacilli are adhered to the luminal surface of ileal enterocytes. (Warthin-Starry 4.0, 400X) (Photo courtesy of: Oregon State University Diagnostic Laboratory, <http://vetmed.oregonstate.edu/diagnostic>)

the rabbit), employs a unique procedure for colonization of the intestine. The classic “cup and pedestal” attachment to the luminal surface results from the bacteria’s ability to manipulate the host cytoskeleton, in particular the recruitment of actin filaments beneath adherent bacteria.⁸ An additional virulence factor of AEEC is intimin and its receptor-translocated intimin receptor (TIR). TIR is secreted directly by AEEC into the cytoplasm of intestinal epithelium via injectisomes (aka, needle complexes or T3SS apparatus), whereupon intimin expressed on the bacterial surface.⁸

Conference participants reviewed the pathogenesis of Tyzzer’s disease in a variety of animal species, as well as reviewed the various common pathotypes of *E. coli* which produce disease in domestic species. A Giemsa stain run on this slide demonstrated both the mucosal-adherent *E. coli* as well as the intracellular *C. piliforme* extremely well.

Contributing Institution:

Oregon State University Diagnostic Laboratory
<http://vetmed.oregonstate.edu/diagnostic>

References:

1. Aboellail TA, Hk N, Mahapatra D. A Naturally Occurring Enterotyphlocolitis Associated with Dual Infection by *Clostridium piliforme* and Enteropathogenic Attaching and Effacing *Escherichia coli* in Syrian Hamsters. *J Vet Sci Med* 2013;1.
2. Bennett AM, Huxtable CR, Love D. Tyzzer’s Disease in Cats Experimentally Infected with Feline Leukaemia Virus. *Vet Microbiol* 1977;2:49–56.
3. Bentancor A, Rumi MV, Gentilini MV, Sardoy C, Irino K, Agostini A et

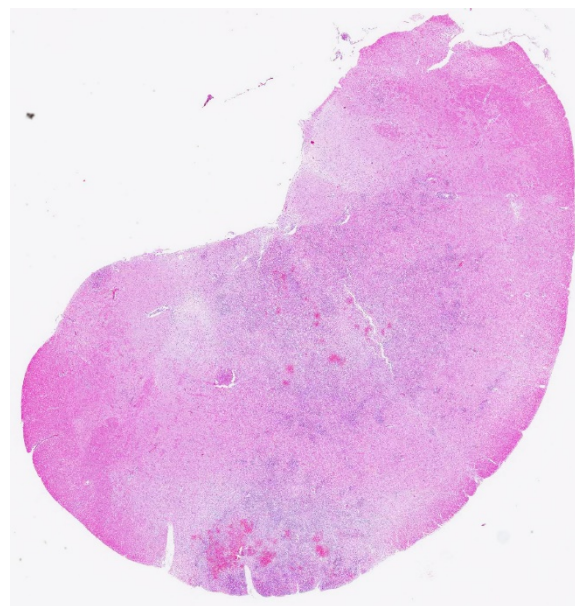
- al. Shiga toxin-producing and attaching and effacing *Escherichia coli* in cats and dogs in a high hemolytic uremic syndrome incidence region in Argentina. *FEMS Microbiol Lett* 2007;267:251–256.
4. Bleibtreu A, Gros P-A, Laouénan C, Clermont O, Le Nagard H, Picard B et al. Fitness, stress resistance, and extraintestinal virulence in *Escherichia coli*. *Infect Immun* 2013;81:2733–2742.
 5. Ikegami T, Shiota K, Goto K, Takakura A, Itoh T, Kawamura S et al. Enterocolitis associated with dual infection by *Clostridium piliforme* and feline panleukopenia virus in three kittens. *Vet Pathol* 1999;36:613–615.
 6. Jones BR, Greene CE. Tyzzer's Disease. In Greene, CE, ed. *Infectious Diseases of the Dog and Cat, 4th edition*. St. Louis, MO. Elsevier Saunders, 2012 pp. 391-393.
 7. Kumar V, Abbas AK, Fausto N, Aster JC. Robbins and Cotran's Pathologic Basis of Disease, Professional Edition: Expert Consult-Online.
 8. Marks SL, Rankin SC, Byrne BA, Weese JS. Enteropathogenic Bacteria in Dogs and Cats: Diagnosis, Epidemiology, Treatment, and Control. *J Vet Intern Med* 2011;25:1195–1208.
 9. Pesavento PA, Bannasch MJ, Bachmann R, Byrne BA, Hurley KF. Fatal *Streptococcus canis* infections in intensively housed shelter cats. *Vet Pathol* 2007;44:218–221.
 10. Weller TH. Ernest Edward Tyzzer 1875-1965, A biographical memoir. *Nat Acad Sci* 1978; 49(14):351-373.

CASE II: AFIP 15-13332 (JPC 4067411-00).

Signalment: 8-month-old Romney ewe lamb (*Ovis aries*)

History: The ewe lamb was found recumbent and unable to stand. Paddling movements and spasms were observed prior to euthanasia.

Gross Pathology: The 8-month-old Romney ewe lamb was in good body condition (BCS 3/5), with good muscle mass, fat reserves, and adequately hydrated. Numerous variably-sized (2 mm-5mm) areas of hemorrhage were present in the medulla oblongata and extended caudally to the level of the obex and cranial cervical spinal cord. No other gross lesions were present elsewhere.



Brainstem, sheep. There is rarefaction, hemorrhage and a cellular infiltrate in up to 50% of the section. (HE, 5X)

Laboratory results: None.

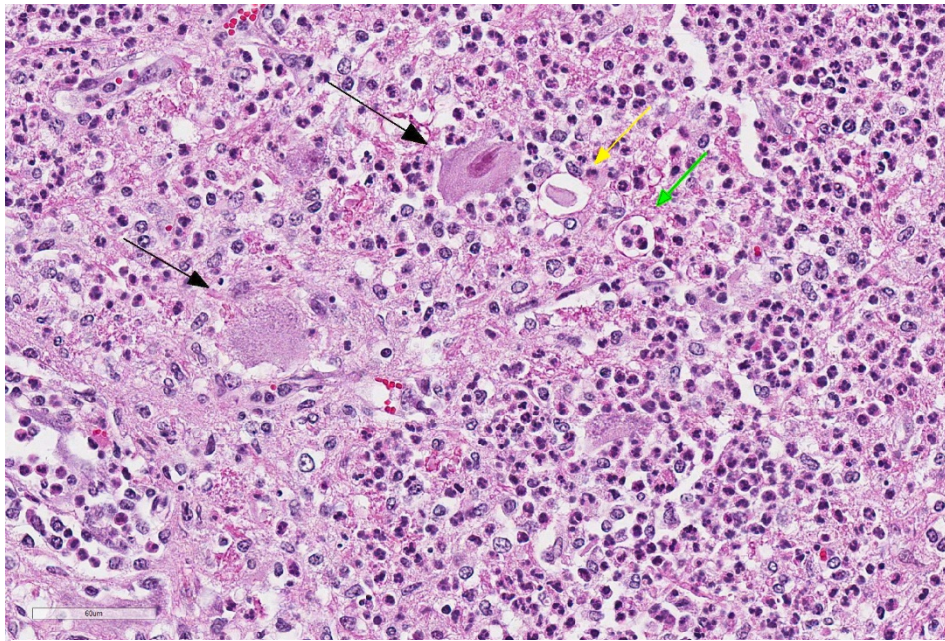
Microscopic Description: Within the brainstem and affecting both gray and white matter, are multifocal to coalescing, variably-sized aggregates of numerous intact and degenerate neutrophils and lesser numbers of macrophages and gitter cells (microabscesses) surrounded by small areas of gliosis. Within and adjacent to the areas of inflammation, numerous axons are swollen and eosinophilic (spheroids) and rare hypereosinophilic, shrunken neurons with pyknotic nuclei surrounded by neutrophils are present (neuronal necrosis and neuronophagia). Multifocally, the white matter is edematous and rarefied. Within the parenchyma, there are numerous densely cellular perivascular cuffs mainly composed of lymphocytes and plasma cells, with lesser number of macrophages, neutrophils and rare eosinophils. A Gram stain reveals moderate numbers of predominantly intracellular, short, plump gram-positive coccobacilli. Additionally, there are multifocal areas of

hemorrhage in the parenchyma and locally extensive regions of leptomeningeal hemorrhage. Multifocally, lymphocytes and plasma cells, and lesser numbers of neutrophils and macrophages, surround and disrupt meningeal blood vessels.

Contributor's Morphologic Diagnoses: Brainstem.

Meningoencephalitis, necrosuppurative, subacute, multifocal to coalescing with gram-positive coccobacilli (Listeric encephalitis)

Contributor's Comment: The clinical signs and the microscopic findings in the brain of this ewe lamb are consistent with listeric encephalitis.^{1-6,9} *Listeria monocytogenes* belongs to the bacterial genus *Listeria*, which are gram-positive, non-spore-forming, facultative anaerobic, intracellular coccobacilli ubiquitously found in the environment and commonly present in the faeces of healthy animals.^{1,3,5,6} It has been suggested that domesticated ruminants play a key role in the maintenance of *Listeria* spp.



Brainstem, sheep. The brainstem is infiltrated by large numbers of neutrophils. There are swollen, degenerating axons (black arrows), dilated myelin sheaths with swollen axons (spheroids – yellow arrow), and a myelin sheath which contains neutrophils and debris (green arrow). (HE, 379X)

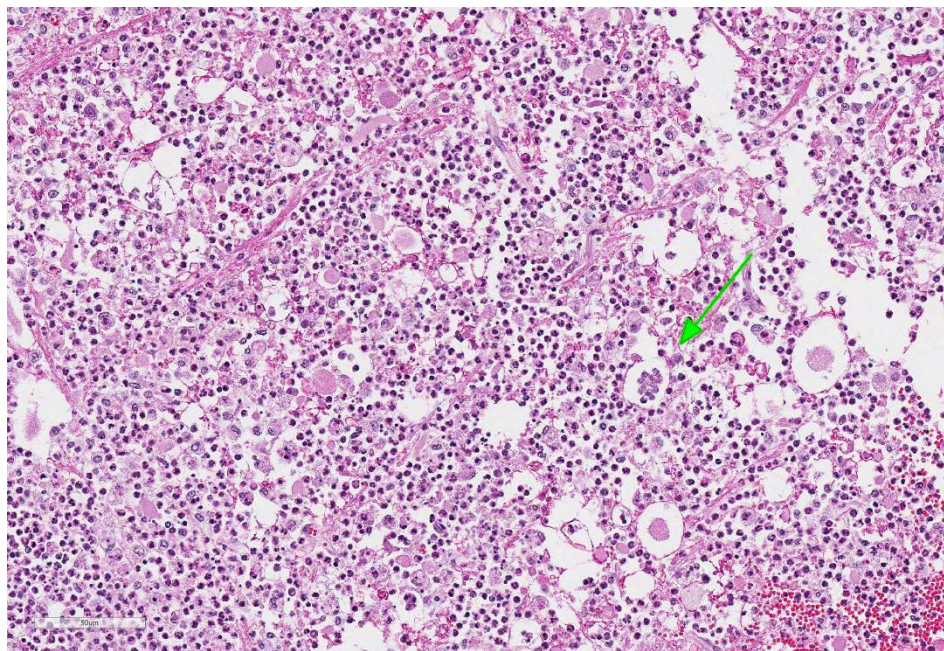
in the environment through a continuous faecal–oral enrichment cycle.¹ There are currently six species in the genus *Listeria*, but only *L. monocytogenes* and *L. ivanovii* are considered pathogenic for domestic animals.⁵⁻⁷

Virulent strains possess a group of virulence genes such as the positive regulatory factor A, internalins, hemolysins (such as

listeriolysin O), phospholipases, a hexose phosphate transporter and others, which allow them to replicate within and spread between eukaryotic cells.^{1,4-8} Critical to the virulence of *Listeria*, is the ability to escape intracellular killing within macrophages by lysis of the phagosomal membrane and escape into the cytoplasm, actions mediated by the secretion of listeriolysin O.⁵⁻⁷ The importance and role of these genes in neurovirulence and neuroinvasion in natural infections, whether by hematogenous infection or axonal migration, is yet to be determined.⁶⁻⁷

In ruminants, the main clinical features of *Listeria* infection are encephalitis, septicaemia, abortion, mastitis and gastroenteritis.^{1-6,9} Listeriosis in ruminants occurs primarily in sporadic cases and is considered to be non-contagious.^{1,5} In general, the disease is more frequent in winter and early spring and outbreaks of disease are known to occur when animals are exposed to

a single contaminated source such as silage.^{1,3-6} However, outbreaks of listeric encephalitis have been described unrelated to silage feeding.⁸⁻⁹ Pathogenesis of listeric encephalitis in sheep, goats and cattle suggests that *L. monocytogenes* gains access to the brainstem via migration through axons of various cranial nerves (most commonly the trigeminal nerve), using the oropharyngeal mucosae as the port of entry.⁶⁻⁸ Once the bacteria has accessed the CNS it spreads further from the brainstem into other brain regions probably by intracerebral axonal migration.⁷⁻⁸ Clinical signs of listeric encephalitis are similar in ruminants and vary depending on the topography of the CNS lesions.¹⁻³ The neurologic signs of listeriosis in sheep reflect dysfunction of caudal brainstem, cerebellar peduncles and/or cranial nerves III through XII.¹⁻³ Gross lesions of the brain are generally absent, or limited to mild meningeal congestion, unilateral or bilateral areas of malacia in the brainstem or spinal cord, and mild clouding

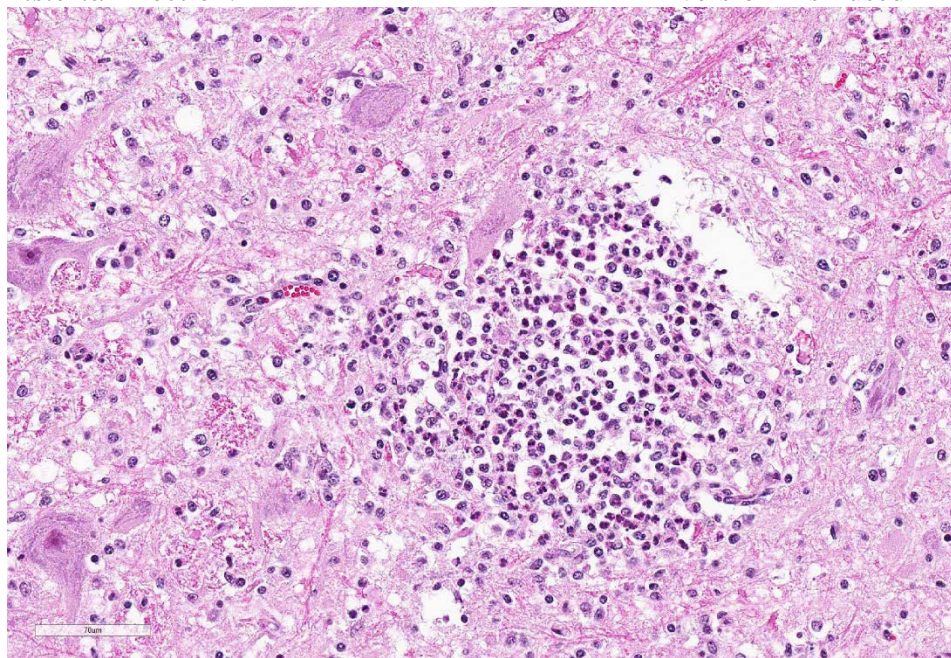


Brainstem, sheep. Large numbers of neutrophils infiltrate areas of white matter, resulting in necrosis and formation of large numbers of spheroids. Several dilated myelin sheaths (HE, 226X)

of the cerebrospinal fluid.^{1,3,5-8} In this case the gross lesions consisted of variably-sized areas of hemorrhage in the medulla oblongata that extended caudally to the level of the obex and cranial cervical spinal cord. Histologically, microabscesses, focal gliosis with adjacent perivascular cuffs consisting predominantly of lymphocytes with histiocytes, plasma cells and occasional neutrophils characterize listerial

encephalitis.^{1,6-8} In severe cases, such as the present case, lesions may coalesce to affect large areas of brain tissue.⁷ Meningitis is often present, and thought to develop secondary to parenchymal lesions.⁵⁻⁷ Species differences can be observed in lesion distribution throughout the CNS, and in the extent and cellular composition of the inflammatory reactions.⁷ Although the characteristic lesion is the presence of microabscesses both in cattle and small ruminants, cattle tend to have relatively more macrophages and more prominent mononuclear perivascular cuffs than small ruminants. Neuronal necrosis appears to be more frequent in small ruminants than in cattle.⁷

In this case, bacterial culture was not attempted since the clinical presentation, together with the gross and histological lesions, and the demonstration of gram-positive, intracellular coccobacilli in histological sections, were consistent with *Listeria* infection.



Brainstem, sheep. Focal areas of lytic necrosis (microabscesses) are scattered throughout the brainstem. (HE, 379X)

JPC Diagnosis: Brainstem: Rhombencephalitis, necrotizing and suppurative, multifocal to coalescing, severe, with microabscesses and mild lymphohistiocytic meningitis.

Conference Comment: The contributor has done an excellent job in describing the general aspects, virulence factors, and pathogenesis of the encephalitic form of listeriosis in small ruminants. A number of other syndromes have been identified in small ruminants infected with *Listeria monocytogenes*, to include enteritis, septicemia, abortion, mastitis, and ophthalmitis. In addition, the contributor has correctly utilized the various, often non-intuitive spellings of the tissue Gram stain, named after Dr. Hans Christian Gram, who developed the method in 1884. When describing the particular stain, the upper case “Gram” is used – “She performed a Gram stain on each section”. When describing the stain’s positivity or negativity, the lowercase version is used – “The bacteria were consistent gram-positive in every section.”

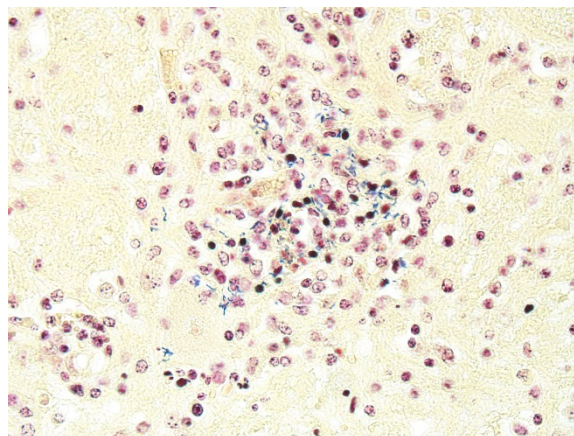
While the portal of entry for pathogenic *Listeria* sp. in cases of encephalitis is presumed to be the buccal mucosa, all other forms of disease caused by this pathogen in ruminants are presumed to develop through the lower gastrointestinal tract. Enteritis, the most common presentation in humans, has been

rarely identified in sheep.⁵ Adult sheep may develop a marked enteritis with extensive necrosis of Peyer's patches as well as necrohemorrhagic enteritis and abomasitis.⁵

Within the gut, bacteria will enter macrophages, often via M cells, whereupon they escape from phagolysosomes and are transported throughout the body. This bacteremia may develop into a listerial septicemia - septicemia occurs most often in immunosuppressed animals and pregnant animals, and its characteristic lesions are most often seen in the fetus. In the fetus, multiple foci of necrosis are seen in the liver and spleen and the organism is readily demonstrated within these lesions. Occasional massive outbreaks of septicemia involving pregnant mucinuous have been described with clinically affected animals exhibiting fever and profuse diarrhea.⁵

The gravid uterus appears to be highly susceptible to infection during listerial septicemia in ruminants and many other species. Another pathogenic form of *Listeria*, *L. ivanovii*, has been recorded as a cause of abortion in cattle and sheep, albeit with less frequency than *L. monocytogenes*. In cases of listerial abortion, there are necrotic lesions within cotyledons as well as a diffuse intercondylar urinary placentitis characterized by a reddish brown exudate.⁵ The fetus is usually autolytic with evidence of septicemia as discussed previously.

Less common but documented listerial syndromes include iritis and keratoconjunctivitis in both cattle in sheep (likely complications of cranial nerve infection), as well as subclinical or clinical mastitis, both seen in silage-fed animals during winter.



Brainstem, sheep. Microabscesses contain numerous gram-positive bacilli, characteristic of L. monocytogenes. (HE, 379X)

Conference participants discussed the various virulence factors associated with *Listeria*, including internalin (initiates E-cadherin-facilitated entry into the cell), listeriolysin (a perforin which lyses the phagosomes of neutrophils and macrophages), and act A protein (which co-opts actin within the cytoskeleton to facilitate cell-to-cell transfer). Major differences between *L. monocytogenes* and *H. somni*, another neurotropic bacillus in ruminants, were identified as vasculitis in cases of *H. somni*, microabscess formation by *L. monocytogenes*, and *L. monocytogenes*' preference for the brainstem as a result of transaxonal migration from the oral cavity along the cranial nerves.

Contributing Institution:

Massey University
Institute of Veterinary, Animal and
Biomedical Sciences
<http://ivabs.massey.ac.nz>
<http://vet-school.massey.ac.nz>

References:

1. Brugere-Picoux. Ovine listeriosis. *Small Ruminant Res.* 2008;**76**:12–20.

2. Constable PD. Clinical examination of the ruminant nervous system. *Vet Clin North Am Food Anim.* 2004;**20**:185–214.
3. Fentahun T, Fresebehat A. Listeriosis in small ruminants: A review. *Advances in Biological Research.* 2012;**6**:202-209.
4. Hamon MA, Ribet D, Starvu F et al. Listeriolysin O: the Swiss army knife of *Listeria*. *Trends Microbiol.* 2012;**20**:36-368.
5. Low JC, Donachie W. A review on *Listeria monocytogenes* and Listeriosis. *Vet J.* 1997;**153**:9-29.
6. Maxie MG, Youssef S. Nervous system. In: Maxie MG, ed. *Jubb, Kennedy, and Palmer's Pathology of Domestic Animals.* 5th ed. Vol. 1. Philadelphia, PA: Elsevier; 2007:282–457.
7. Oevermann A, Di Palma S, Doherr MG, et al. Neuropathogenesis of naturally occurring encephalitis caused by *Listeria monocytogenes* in ruminants. *Brain Pathol.* 2010;**20**:378–390.
8. Oevermann A, Zurbriggen A, Vandeveld M. Rhombencephalitis Caused by *Listeria monocytogenes* in Humans and Ruminants: A Zoonosis on the Rise? *Interdiscip Perspect Infect Dis.* 2010;**2010**:1-22
9. Reuter R, Bowden M, Palmer M. Ovine listeriosis in south coastal Western Australia. *Aust Vet J.* 1989;**66**:223–224.

CASE III: 12L-15812 (JPC 4067411-00).

Signalment: 12-year-old, female, Ragdoll cat, (*Felis catus*)

History: Three days period of nausea and vomiting, followed by unconsciousness, convulsions and finally death.

Gross Pathology: Spleen: Splenomegaly, with pale pink / white marbled parenchyme. The liver showed disseminated, 2-5 mm sized, partly confluent pale white subcapsular and parenchymal areas. Within the gastrointestinal tract, a focal acute ulcerative gastritis, and a multifocal chronic ulcerative duodenitis was present. The duodenal lymph nodes showed mild enlargement and a homogeneous pale cream cut surface.

Laboratory results: None.

Microscopic Description: Section of spleen with mild mesothelial hyperplasia and mild capsular fibrosis. The splenic architecture (red and white pulp) is widely effaced by infiltration of a population of monomorphic large, approximately 20-40µm sized, plump, round cells with fine granular eosinophilic cytoplasm and round, small, hypochromatic, eccentric nuclei with one nucleolus. Mitotic figures are rare, focal apoptotic cells, mild diffuse hemosiderosis and hyperaemia is present.



Spleen, cat: The spleen was diffusely enlarged with a pink-white marbled surface. (Photo courtesy of: University of Liverpool, <http://www.liv.ac.uk/vetpathology/index.htm>)

Special stains: Toluidine blue stain:
Neoplastic cells reveal variable amounts of metachromatic fine cytoplasmic granula.

Immunohistochemistry:

- Anti-Mast Cell Tryptase: Neoplastic cells exhibit variable degrees of weak positive reaction
- CD3: Neoplastic cells: negative reaction
- CD45R: Neoplastic cells: negative reaction

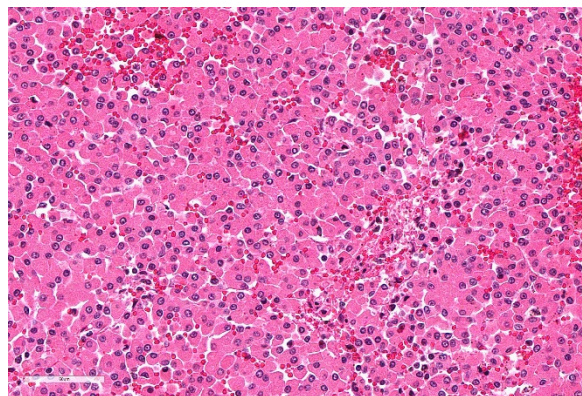
Contributor's Morphologic Diagnoses:

Diffuse visceral (splenic) mast cell tumor with mild mesothelial hyperplasia and capsular fibrosis, Ragdoll, *Felis catus*.

Contributor's Comment: According to the information sheet of Veterinary Society of Surgical Oncology (VSSO, http://www.vssso.org/Splenic_MCT.html), about 50% of feline visceral mast cell tumours are located in the spleen. Other sites of visceral mast cell tumours are the mediastinum, lymph nodes, and intestines. Visceral mast cell tumours present in three forms, smooth, diffuse, and nodular. These



Spleen, cat: The splenic parenchyma is replaced by sheets of round cells with multifocal hemorrhage. (HE, 9X)



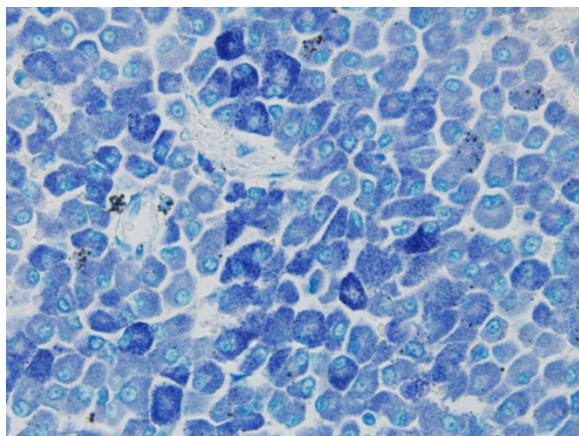
Spleen, cat: Neoplastic cells have abundant granulated eosinophilic cytoplasm and nuclei are often excentric. (HE, 400X)

neoplasms often metastasize to liver (90%), visceral lymph nodes (73%), bone marrow (23%-40%), lung (20%), and intestine (17%), often accompanied by pleural and peritoneal effusions. The cutaneous involvement of mast cell tumours in cats with primary visceral MCT is less frequent (18%).

In the present case, metastases in mesenteric lymph nodes and bone marrow was observed. Within sections of stomach and duodenal ulcerations, no neoplastic mast cells could be demonstrated. large numbers of neoplastic mast cells as observed in the spleen, were observed within hepatic sinuses.

JPC Diagnosis: Spleen: Mast cell tumor.

Conference Comment: Review of the recent literature reveals a number of terms which are interchangeably used to describe non-cutaneous mast cell tumors in the cat. Visceral mast cell tumor, systemic mastocytosis, and mast cell leukemia are all in common usage; the use of the term mast cell leukemia implies mastocytemia. Mastocytemia is not uncommon in cats with visceral mast cell tumors; rates of up to 68% have been reported.⁴



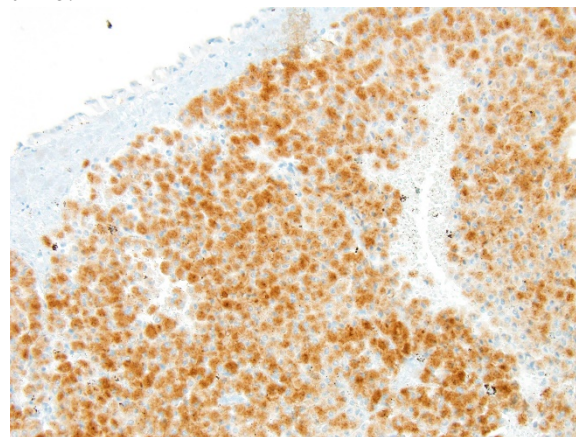
Spleen, cat: Neoplastic cells have numerous cytoplasmic metachromatic granules. (Toluidine blue, 400X)

Splenic involvement of mast cell tumors ranges from 15-50% in various reviews.^{1,5} The liver and intestine are also common sites, and multiorgan disease is also seen. Although cats with visceral tumors may have concomitant cutaneous tumors as well, visceral mast cell tumors are considered a separate disease from cutaneous mast cell tumor; evidence that visceral tumors arise from a cutaneous primary is lacking in the veterinary literature.

Grossly, visceral mast cell tumors often cause diffuse organ enlargement, but may sometimes appear nodular.¹ Histologically, neoplastic mast cells have a finely granulated poorly stained cytoplasm and granules may not be recognizable on hematoxylin and eosin stained sections. Moreover, cytoplasmic granules may not stain with Toluidine blue or Giemsa. This is thought to be the case when neoplastic mast cells arise from the intestinal mucosa; special fixation in media other than formalin may be required for their cytoplasmic granules to be metachromatic.¹

Immunohistochemical evaluation of feline mast cell tumors may be frustrating. Reported rates of cytoplasmic expression of c-Kit ranges from 35³ to 85%⁵. In the

submitted case, Toluidine blue and Giemsa stains run at the JPC were strongly positive, and the tumors showed diffuse strong cytoplasmic expression of c-kit (toluidine blue and c-Kit illustrated in images 3-4 and 3-5, respectively.) One study demonstrated 14 missense c-kit mutations in 13 of 20 tumors; with 11 mutations located in exon 8, and 3 in exon 9.⁵ No correlation was observed between c-kit mutations and tumor differentiation, mitotic activity, or survival time.⁵



Spleen, cat: Neoplastic cells have are strongly immunopositive for c-kit. (200X)

Contributing Institution:

University of Liverpool

<http://www.liv.ac.uk/vetpathology/index.htm>

References:

1. Kiupel, M. Mast Cell Tumors. In: Meuten DJ, ed. *Tumors in Domestic Animals, 5th ed.* Ames IA, Wiley and Sons 2017. pp 195-199.
2. Lamm CG, Stern AW, Smith AJ, Cooper EJ, Ullom SW, Campbell GA. Disseminated cutaneous mast cell tumors with epitheliotropism and systemic mastocytosis in a domestic cat. *J Vet Diagn Invest* 2009; 21:710-715.

3. Mallett CL, Northrup NC, Saba CF, Rodriguez CO, Rassnick KM, Gieger TL, Childress MO, Howerth EW. Immunohistochemical characterization of feline mast cell tumors. *Vet Pathol* 2012; 50(1): 106-109.
4. Piviani M, Walton RM. Significance of mastocytosis in cats. *Vet Clin Pathol* 2013; 42:4-10.
5. Sabattini S, Barzon G, Giantin M, Lopparelli RM, Dacasto M, Prata D, Bettini G. Kit receptor tyrosine kinase dysregulations in feline splenic mast cell tumors. *Vet Comp Oncol* 2017; 15(3):1051-1056.
6. Veterinary Society of Surgical Oncology.
http://www.vssso.org/Splenic_MCT.html



Lung, dog. The lungs have a mottled appearance due to areas of hemorrhage, collapse, consolidation, and emphysema. (Photo courtesy of: Utrecht University, Faculty of Veterinary Medicine, Department of Pathobiology, www.uu.nl/faculty/veterinarymedicine/EN/labs_services/pdc)

CASE IV: AFIP Canine 315010212 lungs (JPC 4067411-00).

Signalment: 1 year-old female Weimeraner dog, *Canis lupis familiaris*.

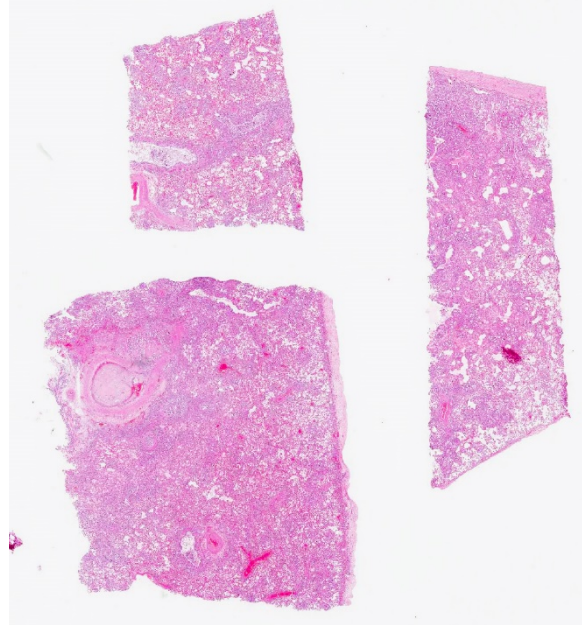
History: After undergoing anesthesia for laminectomy of T10 this dog failed to regain independent breathing and was euthanized during recovery.

Gross Pathology: The lungs have a mottled appearance composed of small areas of hemorrhage intermixed with coalescing areas of pale grey to tan tissue with multifocally slightly raised whitish nodules of a few millimeters in diameter. Both lungs are markedly oedematous, have an increased consistency and are firm to touch. There is a small amount of fibrin on the pleura of the cranioventral lobes.

Laboratory results: None.

Microscopic Description: Lung: The normal architecture of the lung is severely distorted by the presence of a predominantly granulomatous interstitial infiltrate associated with the presence of numerous *Angiostrongylus vasorum* larvae and eggs.

In both the alveolar interstitium and free within the alveolar spaces are moderate to large numbers of transverse or longitudinal sections of nematode larvae measuring approximately 20x80 μm and fewer multinuclear (embryonated) and uninuclear (non-embryonated) eggs, recognizable as approximately 60x90 μm , oval-shaped accumulations of coarsely granular eosinophilic material. These are typically surrounded by moderate numbers of extravascular erythrocytes, epithelioid macrophages (which occasionally show erythrophagy and contain cytoplasmic hemosiderin granules) and scattered multinucleated giant cells. The alveolar septa are often indistinct and are markedly expanded by moderate numbers of macrophages, fewer plasma cells and lymphocytes, and occasional eosinophils as



Haired skin, dog. Several sections of lung are submitted for examination. At subgross magnification, a large arteriolar thrombus is visible as well as hypercellularity and exudation within a large airway. (HE, 5X)

well as moderate edema, and parasites. Alveoli are frequently lined by plump cuboidal epithelial cells (type 2 pneumocyte hyperplasia).

Throughout the section, there are mild to moderate vascular changes including moderate hypertrophy of the lamina media, separation of the collagen fibers of the tunica adventitia by fine reticular eosinophilic material (edema), and the presence of parasites within the vascular lumen. In the adventitia of some vessels, there are increased numbers of small-caliber blood vessels.

In some sections, adult nematodes are present within the lumen of large blood vessels; these are approximately 300 μ m in diameter and are characterized by a thin eosinophilic cuticle surrounding coelomyarian musculature and a pseudocoelom containing digestive and reproductive tracts. In some cases this is associated with partial occlusion of the lumen

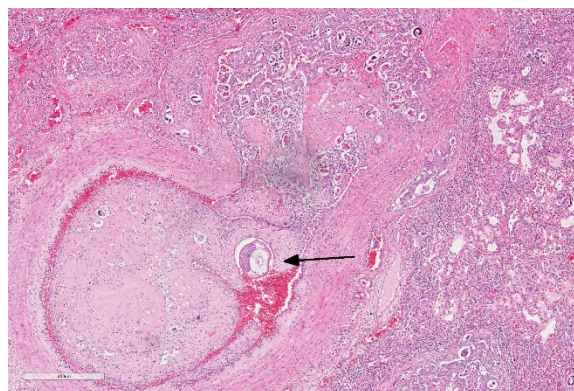
by an organizing thrombus composed of haphazardly arranged collagen bundles and fibroblasts, with endothelial cells forming small vascular channels (recanalisation) and scattered parasite eggs. Throughout the thrombotic material are moderate numbers of mixed inflammatory cells, predominantly plasma cells and macrophages. The lamina intima is markedly expanded by edema and moderate numbers of plasma cells and macrophages with fewer lymphocytes and occasional neutrophils. There is intimal hyperplasia characterized by the formation of multiple, endothelium-lined small, rounded, projections into the vessel lumen (proliferative endoarteritis).

Also in the less-severely affected areas, alveolar spaces and bronchiolar lumens contain moderate numbers of epithelioid macrophages, erythrocytes and protein-rich material. Bronchial epithelium shows mild hypertrophy and there are scattered intramucosal neutrophils.

The pleura is moderately expanded by mild fibrosis and edema and in some sections there are scattered groups of parasite eggs and larvae surrounded by macrophages, plasma cells and lymphocytes.

Contributor's Morphologic Diagnoses:

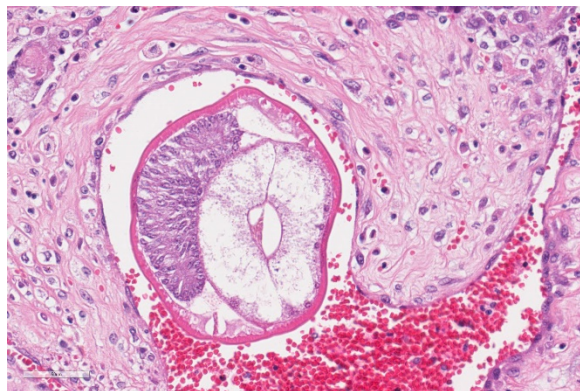
Lung: Severe, chronic, multifocal to



Lung, dog. An arteriole is thrombosed and recanalized at the periphery. There is a cross section of an adult helminth within the thrombus (arrow) (HE, 54X)

coalescing interstitial granulomatous pneumonia with *Angiostrongylus vasorum* in different stages of development, interarterial thrombosis and marked pleural fibrosis.

Contributor's Comment: *Angiostrongylus vasorum*, or French heartworm, is endemic in the Americas, parts of Africa and some European countries but until the end of the last decade was not considered endemic in the Netherlands.⁵ The few cases reported before this time were typically seen in dogs which had been travelled outside of the country. Following the emergence of the disease in dogs which had never been outside the Netherlands, research was carried out to determine the prevalence of this parasite in Dutch foxes and intermediate hosts. Interestingly, concurrent to the increase in cases of *A. vasorum* seen in domestic dogs there has been an expansion of the range and population of foxes reported in the Netherlands. Combined with the wet Dutch environment that is conducive to the survival of the gastropod intermediate hosts, establishment of *A. vasorum* in the Netherlands is not surprising.⁵ Of particular importance is the finding that L3 or the infective stage can be released from the intermediate host in fresh water meaning that infection may occur not only by ingestion of

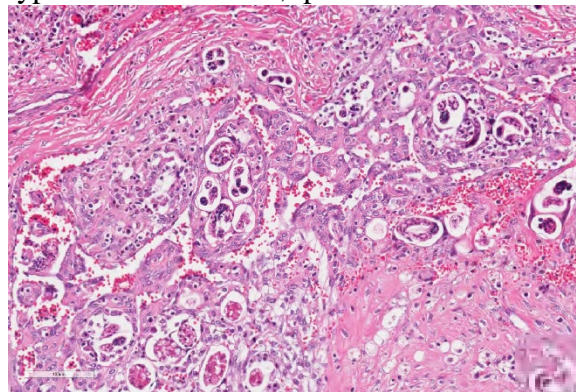


Lung, dog. The adult helminth as a thin hyaline cuticle, low polymyarian-coelomyarian musculature, lateral cords, a pseudocoelom, and cross sections of a gonad and intestine. (HE, 400X)

slugs and snails but by drinking water from the many canals and ditches that are prominent features of the Dutch countryside.⁵

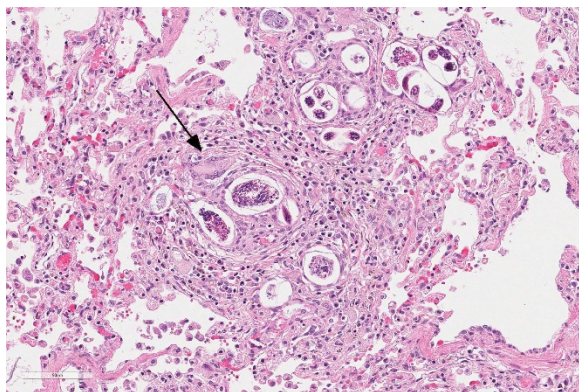
There was no history available for this young dog which underwent surgery for suspected lymphoma of the spinal cord from which it did not recover. The severe parasitic pneumonia may explain the post-surgical failure to resume independent breathing.

The histological lesions in this case are typical of a chronic, patent infection with



Lung, dog. There is a plexiform area of recanalization in the adjacent artery which contains numerous cross-sections of embryonated and larvated metastrongyle eggs. (HE, 210X)

multiple stages of parasite present and organizing thrombosis seen in the pulmonary vessels. The adults inhabit the right ventricle and pulmonary arteries releasing eggs after a pre-patency period of 35-60 days.² These are transported to the pulmonary capillaries from which L1 larvae hatch and penetrate into the alveolar spaces before being coughed up and excreted in the faeces. L1 are taken up by intermediate hosts (including snails, slugs and frogs) in which larval development continues to the infectious L3 stage and infection occurs in definitive hosts when these are ingested and mature larvae and young adult worms migrate via the circulatory system ultimately inhabiting the right ventricle. The presence of adult worms



Lung, dog. There are numerous granulomas scattered throughout the pulmonary parenchyma centered on helminth larvae and eggs. Rare multinucleated macrophages (arrows) are seen. (HE, 280X)

in the circulatory system is thought to activate both intrinsic and extrinsic coagulation pathways resulting in intravascular consumptive coagulopathy and bleeding tendencies.⁴ This may explain the persistent bleeding at the that was noted incision site during the operation preceding the death of this dog.

Whilst infection with *A. vasorum* can cause a range of other clinical signs the majority of cases develop cardiorespiratory problems, typically culminating in heart failure.^{2,3} Other clinical presentations may reflect aberrant larval migration to organs such as the eye and brain.^{2,3,5}

JPC Diagnosis: Lung: Pneumonia, interstitial, granulomatous, diffuse, severe, with proliferative endarteritis, thrombosis, and recanalization, and rare adult and numerous metastrongyle larvae and eggs.

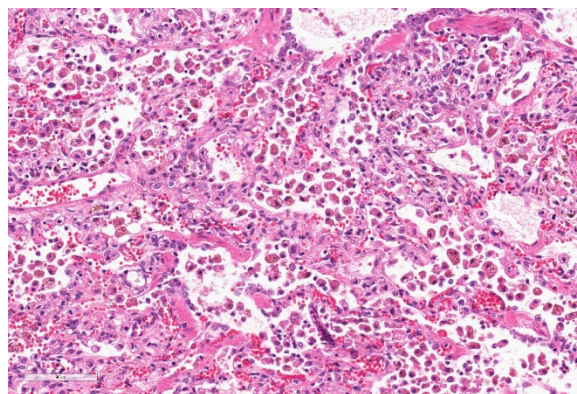
Conference Comment:

Angiostrongylus vasorum, termed French heartworm because it was reported first in France in the 1800s¹, is a metastrongyle nematode considered to be the most pathogenic lungworm of dogs. *A. vasorum* has a worldwide distribution and the

infection seems to be increasing in recent decades. Red foxes are the natural definitive hosts and are important reservoirs of infection for domestic dogs, however, natural infection has also been reported in other species including wolves, coyotes, and Eurasian badgers.¹

Adults reside in the pulmonary artery and right heart ventricle in canids. Clinical signs run a gamut from mild coughing and exercise intolerance to fatal cardiopulmonary disease which may manifest as sudden death.

A. vasorum may cause right heart failure and extensive pulmonary lesions as a consequence of egg embolization. Prepatent lesions are mild with adult worms in the pulmonary arteries and a few 1-2 mm diameter, red, firm, multinodular to confluent areas of hemorrhage and edema at the lung periphery.² Female adults have a “barber pole” appearance due to their intertwined red intestine and white ovaries. At patency, lesions are more severe including proliferative endarteritis and interstitial granulomatous pneumonia, as displayed in this case. Vascular lesions are characterized by proliferative endarteritis, including thrombosis, thickening of tunica intima by

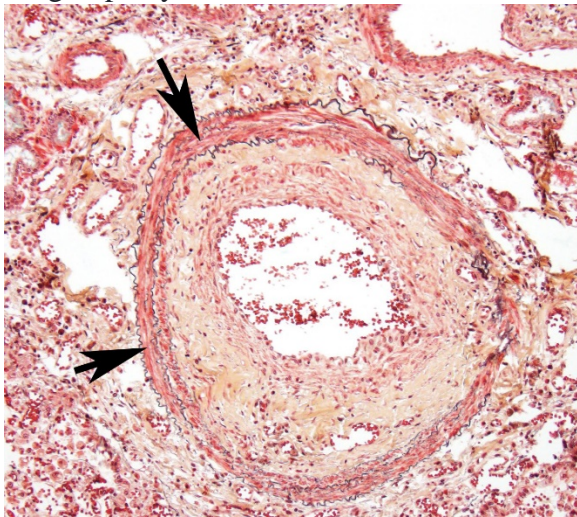


Lung, dog. Throughout the remainder of the section, alveolar septa are expanded by intraseptal macrophages, collagen, and patchy Type II pneumocyte hyperplasia. Alveoli contain numerous macrophages (often hemosiderin-laden), hemorrhage, edema, and rare migrating helminth larvae. (HE, 250X)

fibromuscular tissue, and medial hypertrophy with infiltration of eosinophils, lymphocytes and plasma cells.²

Coagulation abnormalities are commonly seen in association with *A. vasorum* infection. A prolonged activated partial thromboplastin or prothrombin times, thrombocytopenia, and increases in circulating D-dimers and fibrin degradation products suggests disseminated intravascular coagulation.^{2,4} Affected dogs may have petechiae and ecchymoses in multiple tissues. The cause of this coagulopathy is unknown but may represent thrombosis triggered by parasite proteins or endothelial damage from adult and larval nematodes.²

Cerebral lesions to include mass lesions and areas of hemorrhage are noted as a combination of aberrant larval migration as well as the previously described coagulopathy.



Lung, dog. Pulmonary arterioles exhibit marked myointimal proliferation – within the tunica intima, there is proliferation of smooth muscle cells on the luminal side, with deposition of collagen centrifugally. The internal elastic lamina is marked by black arrows. (Movat pentachrome. 200X)

The moderator reviewed a Movat's pentachrome stain and demonstrated a mural change in the branches of the pulmonary arteries which the moderator interpreted as myointimal proliferation. In this condition, vascular smooth muscle cells migrate into the tunica intima, undergoing both proliferation and secretion of extracellular matrix and collagen. This non-specific change results from endothelial activation and is often seen in cases of heartworm infection.

Contributing Institution:

Utrecht University
Faculty of Veterinary Medicine
Department of Pathobiology
Yalelaan 1
3584 CL Utrecht
The Netherlands

www.uu.nl/faculty/veterinarymedicine/EN/1abs_services/vpdc

References:

1. Bourque AC, Conboy G, Miller LM, et al. Pathological findings in dogs naturally infected with *Angiostrongylus vasorum* in Newfoundland and Labrador, Canada. *J Vet Diagn Invest.* 2008;**20**(1):11–20.
2. Caswell JL, Williams KG: In: Jubb, Kennedy and Palmer's Pathology of Domestic Animals, ed. Maxie MG, 5th ed., pp. 648. Elsevier Limited, Philadelphia, PA, 2007.
3. Gallagher B, Brennan SF, Zarelli M, et al. Geographical, clinical, clinicopathological and radiographic features of canine angiostrongylosis in Irish dogs: a retrospective study. *Ir Vet J.* 2012;**65**(1):5.
4. Ramsey IK, Littlewood JD, Dunn JK, et al. Role of chronic disseminated

- intravascular coagulation in a case of canine angiostrongylosis. *Vet Rec.* 1996;**138**:360–363.
5. van Doorn DCK, van de Sande AH, Nijse ER, et al. Autochthonous *Angiostrongylus vasorum* infection in dogs in The Netherlands. *Vet Parasitol.* 2009;**162**:163–166.

Self-Assessment - WSC 2017-2018 Conference 3

1. Attaching and effacing E.coli is the only pathotype of E.coli reported in which species?
 - a. Horses
 - b. Cats
 - c. Hamsters
 - d. Rabbits

2. Which of the following is NOT true about *Clostridium piliforme* ?
 - a. It can only be grown on artificial media.
 - b. Immunosuppression is a major factor in small animal infection.
 - c. It is a common commensal in rodents.
 - d. It was first identified as a rodent pathogen.

3. Which of the following is not a documented syndrome associated with *Listeria* infection in small ruminants?
 - a. Abortion
 - b. Arthritis
 - c. Encephalitis
 - d. Septicemia

4. Which of the following organs is not a common site for visceral mast cell tumors in cats?
 - a. Lung
 - b. Spleen
 - c. Intestine
 - d. Liver

5. Which of the following is not an intermediate or paratenic host of *Angiostrongylus vasorum*??
 - a. Ducks
 - b. Snails
 - c. Frogs
 - d. Slugs

Please email your completed assessment to Ms. Jessica Gold at Jessica.d.gold2.ctr@mail.mil for grading. Passing score is 80%. This program (RACE program number) is approved by the AAVSB RACE to offer a total of 0.5 CE Credits, with a maximum of 12.5 CE Credits being available to any individual Veterinary Medical Professionals for the 2017-2018 Wednesday Slide Conference. This RACE approval is for the subject matter categories of: SCIENTIFIC using the delivery method of NON-INTERACTIVE DISTANCE. This approval is valid in jurisdictions which recognize AAVSB RACE; however, participants are responsible for ascertaining each board's CE requirements. RACE does not "accredit", "endorse" or "certify" any program or person, nor does RACE approval validate the content of the program.

**Joint Pathology Center
Veterinary Pathology Services**



WEDNESDAY SLIDE CONFERENCE 2018-2019

C o n f e r e n c e 4

19 September 2018

Conference Moderator:

Rachel Cianciolo, VMD PhD, DACVP
Assistant Professor (Clinical)
Co-Director, International Veterinary Renal Pathology Service
The Ohio State University
301 Goss Laboratory
1925 Coffey Road
Columbus, Ohio 43210

CASE I: N14-111 (JPC 4049562-00).

Signalment: Three-year-old castrated male, Scottish terrier cross canine

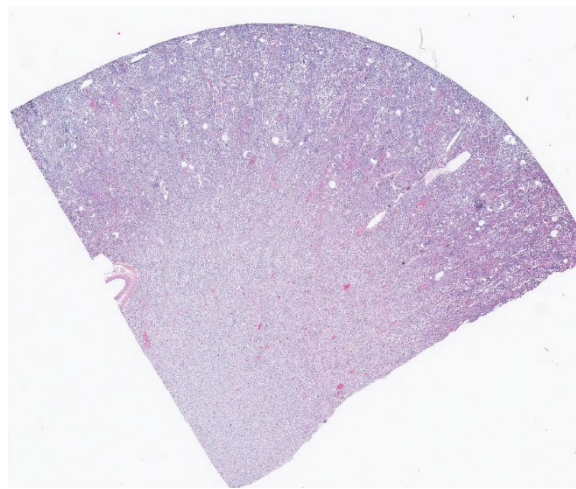
History: Presented with a history of renal failure and protein-losing nephropathy

Gross Pathology: Enlarged pale kidneys with dozens of red pinpoint foci in the cortex.

Laboratory results: None.

Microscopic Description: Kidney: Diffusely, glomeruli fill Bowman's space and are segmented. They are globally hypercellular with markedly increased mesangial matrix, typically with obliteration of capillary lumina. Syneciae are present multifocally. Tufts occasionally contain

karyorrhectic debris, intravascular or intramesangial leukocytes, or exhibit exudation of fibrin and/or proteinaceous fluid

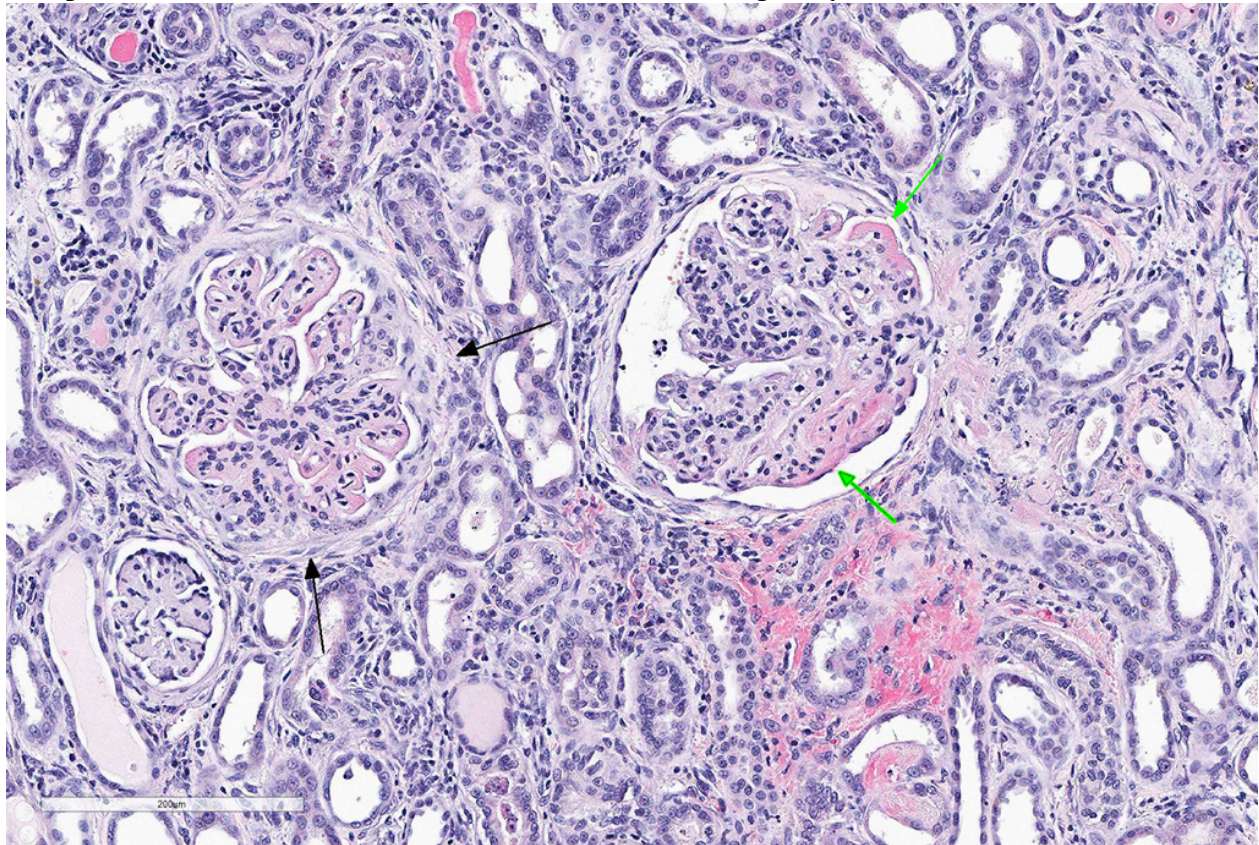


Kidney, dog. A section of kidney is submitted for examination. Tubular ectasia, proteinosis, and cystic glomeruli are evident at low magnification. (HE 6X)

into Bowman's space. Podocytes and parietal epithelial cells are frequently hypertrophied. There is multifocal, mild to moderate periglomerular fibrosis. Diffusely, tubules vary from dilated and lined by attenuated to regenerating epithelium to lined by swollen, vacuolated epithelial cells undergoing hydropic degeneration and necrosis with cytoplasmic hyper eosinophilia, nuclear pyknosis, and cellular sloughing. Many tubules contain proteinaceous fluid or casts with fewer containing cellular casts. Occasional tubules are mineralized. The interstitium multifocally contains moderate numbers of lymphocytes and plasma cells with mild interstitial fibrosis. Rare arterioles exhibit fibrinoid necrosis and are surrounded by hemorrhage and fibrin (too infrequent to be a point in these slides).

- Contributor's Morphologic Diagnoses:**
1. Marked, diffuse, global, membranoproliferative glomerulonephritis with moderate tubular proteinosis
 2. Moderate, multifocal, lymphoplasmacytic, interstitial nephritis
 3. Moderate, multifocal, tubular necrosis, degeneration, and regeneration

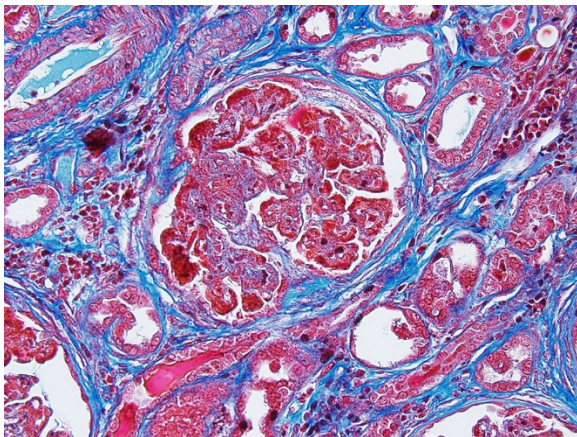
Contributor's Comment: Lyme disease, caused by *Borrelia burgdorferi* is one of the most common tick-borne diseases in the world. The organism is a spirochete, is transmitted by *Ixodes* ticks and lives extracellularly near collagen and fibroblasts usually causing little inflammation in most hosts. Lyme nephritis, which is the most serious form of Lyme disease in dogs is incompletely understood, as recent evidence



Kidney, dog. Glomerular changes include synechia and crescent formation (black arrows), expansion of the glomerular capillary loops by a granular eosinophilic material (green arrows), endocapillary and mesangial hypercellularity, and marked periglomerular fibrosis. (HE, 183X)

has shown that there is no consistent evidence of the presence of *B. burgdorferi* in the renal tissue of dogs with Lyme nephritis. Koch's postulates have not been satisfied and there is no experimental model to study the disease.

As compared with cases of arthritis, fewer dogs (<1-2%) with Lyme-positive status develop severe acute progressive and often fatal protein-losing nephropathy. Labradors, Golden Retrievers and younger dogs are predisposed. Unlike leptospirosis, Lyme nephritis is not due to renal invasion by the spirochete but rather due to immune-mediated glomerulonephritis with Lyme-specific antigen-antibody deposition.^{5,7} The microscopic findings of the kidney from Lyme-positive dogs with severe proteinuria, hypoalbuminemia and kidney failure exhibit membranoproliferative glomerulonephritis with subendothelial C3, IgG and IgM deposits, diffuse tubular necrosis/regeneration and lymphoplasmacytic interstitial nephritis.³ The breed predisposition, younger age of onset and histopathologic findings are different when compared to previously described types of



Kidney, dog. A trichrome stain demonstrates coalescing brightly eosinophilic immune complexes within subepithelial locations. There is mature collagen within a crescent, as well as periglomerular fibrosis. There is extensive fibrosis of the interstitium as well. (Masson's trichrome, 200X)

glomerulonephritis. It is thought that the secondary tubular changes may be due to hypertension and efferent arteriole vasoconstriction, tubular hypoxia or toxic proteins in the glomerular filtrate. Very few if any organisms are found by silver stain or PCR in kidneys of dogs with Lyme nephritis. However, Lyme antigen, DNA and occasionally organisms have been found in tubular cells and in urine.^{5,7}

JPC Diagnosis: Kidney: Glomerulonephritis, membranoproliferative, diffuse and global, severe, with synechia and crescent formation, tubular epithelial necrosis, thrombotic microangiopathy of vascular poles, and moderate lymphoplasmacytic interstitial nephritis.

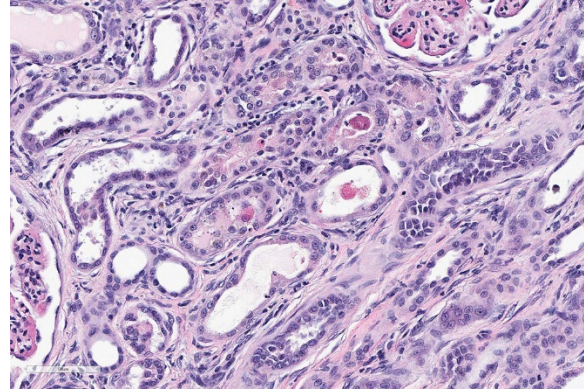
Conference Comment: The contributor provides a concise summary of much as is known about the renal effects of Lyme borreliosis in dogs. Retrievers are predisposed but many breeds are affected in endemic areas.² Renal disease has been reported to occur in less than 2% of dogs of serologically positive for Lyme disease; approximately 30% of patients with Lyme disease had concurrent or prior lameness.² Antigen-antibody complexes against bacterial outer surface proteins (OSP) OspA, OSPB, and flagellin are thought to be causative for glomerular disease.²

Lyme disease and other chronic infectious agents most often result in membranoproliferative patterns of glomerulonephritis (MPGN) in the dog. From the recent online atlas published by the moderator and other members of the WSAVA study group on renal standardization (<https://ohiostate.pressbooks.pub/vetrenalpat/hatlas/chapter/membranoproliferative-glomerulonephritis/>): "...In the MPGN pattern, lesion progression is not straightforward. The lesions are dependent

on the duration/magnitude of immune complex deposition and the severity of the resultant inflammatory response (inflammatory cells and inflammatory mediators). Features that should be assessed include: a) Hypercellularity – this dimension involves the number, location, and types of cells that are present in the glomeruli in excess of what is expected in normal glomeruli, as well as evidence of cellular injury (e.g., pyknotic debris); b) capillary wall remodeling – this dimension involves the degree and extensiveness of changes in the structures that compose the peripheral capillary wall; namely wall thickening, double contours of the GBM, cellular interpositioning; and c) sclerosis – this dimension involves the degree and extent of changes that are thought to be irreversible, namely synechia and segmental or global sclerosis.”¹

Equine borreliosis due to *B. burgdorferi* is an emerging disease in many parts of the world. The American College of Veterinary Internal Medicine has recently published a consensus statement about *B. burgdorferi* infection in horses in North America.⁴ Documented syndromes in the horse attributed to *B. burgdorferi* infection include neuroborreliosis, uveitis, and cutaneous pseudolymphoma.⁴ Although other cases exhibiting lameness and stiffness have been identified in horses, these are often not well documented. Diagnosis of Lyme disease in the horse requires cytology or histopathology of infected fluid or tissue as well as antigen detection.⁴

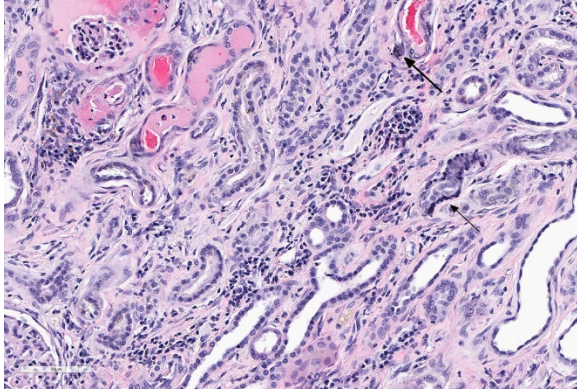
Neuroborreliosis in horses parallels a similar syndrome in humans which generally results in a triad of meningitis, cranial or peripheral neuritis and radiculitis; while clinical signs may be extremely variable, the histologic lesions seen in the horse are unique in equine



Kidney, dog. There is multifocal, often single cell necrosis of tubular epithelium with sloughing into the lumen. Granular and cellular casts are present with many ectatic tubules. (HE, 281X)

neuropathology.⁴ Gross lesions are limited to meninges and include opacification, yellowish discoloration, and plaques of hyperemia and edema.⁶ Microscopically, horses display variable infiltration of the leptomeninges as well as perivascularitis and segmental vasculitis.⁶ Lymphohistiocytic infiltrates predominate but neutrophilic, eosinophilic, and plasmacytic inflammation is also seen inflammatory cells may infiltrate cranial nerves and ganglia resulting in Wallerian degeneration and spheroid formation.⁶ Five reports of equine uveitis are present in the veterinary literature.⁴ Of these, 3/5 infected horses also displayed neurologic signs and neural inflammation.⁴ Organisms were detected within the leptomeninges and vitreous of the eye through the use of Warthin-Starry stains as well as PCR performed on shavings from formalin-fixed paraffin-embedded tissue sections.⁴

Cutaneous pseudolymphoma is a rare condition associated with *B. burgdorferi* infection in the horse, but has also been replicated in experimentally infected colonies.⁴ Papular to nodular lesions occurring most often at the site of the tick bite and florid mixed lymphoid hyperplasia are microscopically suggestive of lymphoma in



Kidney, dog. There is multifocal expansion of the interstitium by collagen and loss of tubules. Additional changes include tubular necrosis, proteinosis (with hemorrhage) and mineralization (arrows), and aggregates of lymphocytes and plasma cells. (HE, 281X)

these cases. PCR performed on these lesions will be positive for *B. burgdorferi*.⁴

The moderator discussed a number of potential ruleouts for immune-complex glomerulonephritis in the dog, including *Dirofilaria immitis* infection (which does not always present as a MPGN), tick-borne diseases. The glomerular lesions seen with leishmaniasis are similar to that seen in this case. The moderator identified the widespread single cell necrosis in occurring in many tubules as a prominent feature in this particular condition, but also suggested that tubulointerstitial nephritis is not particularly specific for Lyme disease (as has been previously published) and many cases of very active MPGN may result in tubular necrosis resulting from concurrent simultaneous deposition of immune complexes in peritubular capillaries.

The moderator identified the hypercellularity in the glomeruli as being both endocapillary and in the mesangium. A Masson's trichrome run at the JPC on this case highlighted large bright red, often coalescing immune complexes within the subendothelial locations. ("Wire loops" is a term used in human medicine for the appearance of

thickened capillary wall due to large coalescing immune complexes.)

The moderator also discussed the changes noted in approximately 20% of the vascular poles, which often display necrosis and intramural protein and erythrocytes (suggestive of possible concurrent hypertension in this patient.) As well as the two potential ways that crescents can form – from rupture of glomerular capillaries or less commonly, due to the rupture of Bowman's capsule.

Contributing Institution:

Tufts Cummings School of Veterinary Medicine
Department of Biomedical Sciences
200 Westboro Road
North Grafton
MA 01536
<http://vet.tufts.edu/dbs/>

References:

1. Cianciolo R, Brown CM, Mohr C, Mabity M, Van der Lugt J, McLeland S, Aresu L, Benali S, Spangler B, Amerman H, Lees G. *In Atlas of Renal Lesions in Proteinuric Dogs.* <https://ohiostate.pressbooks.pub/vetr-enalpathatlas/chapter/membranoproliferative-glomerulonephritis/>
2. Cianciolo RE and Mohr FC. Urinary System. In: Maxie MG, ed. *Jubb Kennedy and Palmer's Pathology of Domestic Animals, 6th ed.* 2016; St. Louis MO, Elsevier Press, vol 2, p. 411-412.
3. Dambach DM, Smith CA, Lewis RM, Van Winkle TJ. Morphologic, Immunohistochemical and ultrastructural characterization of a distinctive renal lesion in dogs putatively associated with *Borrelia burgdorferi* infection: 49 Cases

- (1987-1992). *Vet Pathol.* 1997; 34:85-96
4. Divers TJ, Gardner RB, Madigan JE, Witonsky SG, Bertone JJ, Swinebroad EL, Schutzer SE, Johnson. *Borrelia burgdorferi* infection and Lyme disease in North American Horses: A consensus statement. *J. Vet Intern Med* 2018;617-683.
 5. Hutton TA, Goldstein RE, Njaa BL, Atwater DZ, Chang YF, Simpson KW. Search for *Borrelia burgdorferi* in kidneys of dogs with suspected "Lyme Nephritis". *J Vet Intern Med.* 2008; 22(4):860-5
 6. Johnston LK, Engiles, JB, Aceto H, Buchner-Maxwell V, Divers T, Gardiner R%, Levine, R, Shceere N, Tewai D, Tomlinson J Johnson AL. Retrospective evaluation of horses diagnosed with neuroborreliosis on postmortem examination: 16 cases (2004–2015). *J Vet Intern Med* 2016; 30:1305-1312.
 7. Littman MP. Lyme nephritis. *J Vet Emerg Crit Care.* 2013; 23(2):163-73

CASE II: NA (JPC 4066460-00).

Signalment: Adult (>2.5 years) male cynomolgus monkey, *Macaca fascicularis*

History: This study was conducted in accordance with the current guidelines for animal welfare. All procedures performed on these animals were in accordance with regulations and established guidelines and were reviewed and approved by the Institutional Animal Care and Use Committee. For further information, please see Contributor's Comments.

Gross Pathology: No macroscopic findings

Laboratory results:

Clinical pathology findings:

Increased from pre-study baseline:
AST, Urine volume, Urine protein and protein ratio, Urine blood, Urine creatinine, Urine NAG, and Urine microalbumin

Decreased from pre-study baseline:
GGT, Total protein, Albumin, Ca

Light microscopic findings:

Glomerulus: Moderate mesangial and podocyte hyperplasia, mild eosinophilic inclusions in podocytes, mild granulocytes in capillary lumens, marked increase in mesangial matrix, moderate synechia, moderate parietal epithelial cell hyperplasia, marked C5b-9 granular staining of capillary walls and podocytes (IHC)

Tubules: Mild distal tubular dilation, minimal distal tubular luminal hyaline casts, moderate erythrocyte casts in proximal and distal tubular lumens

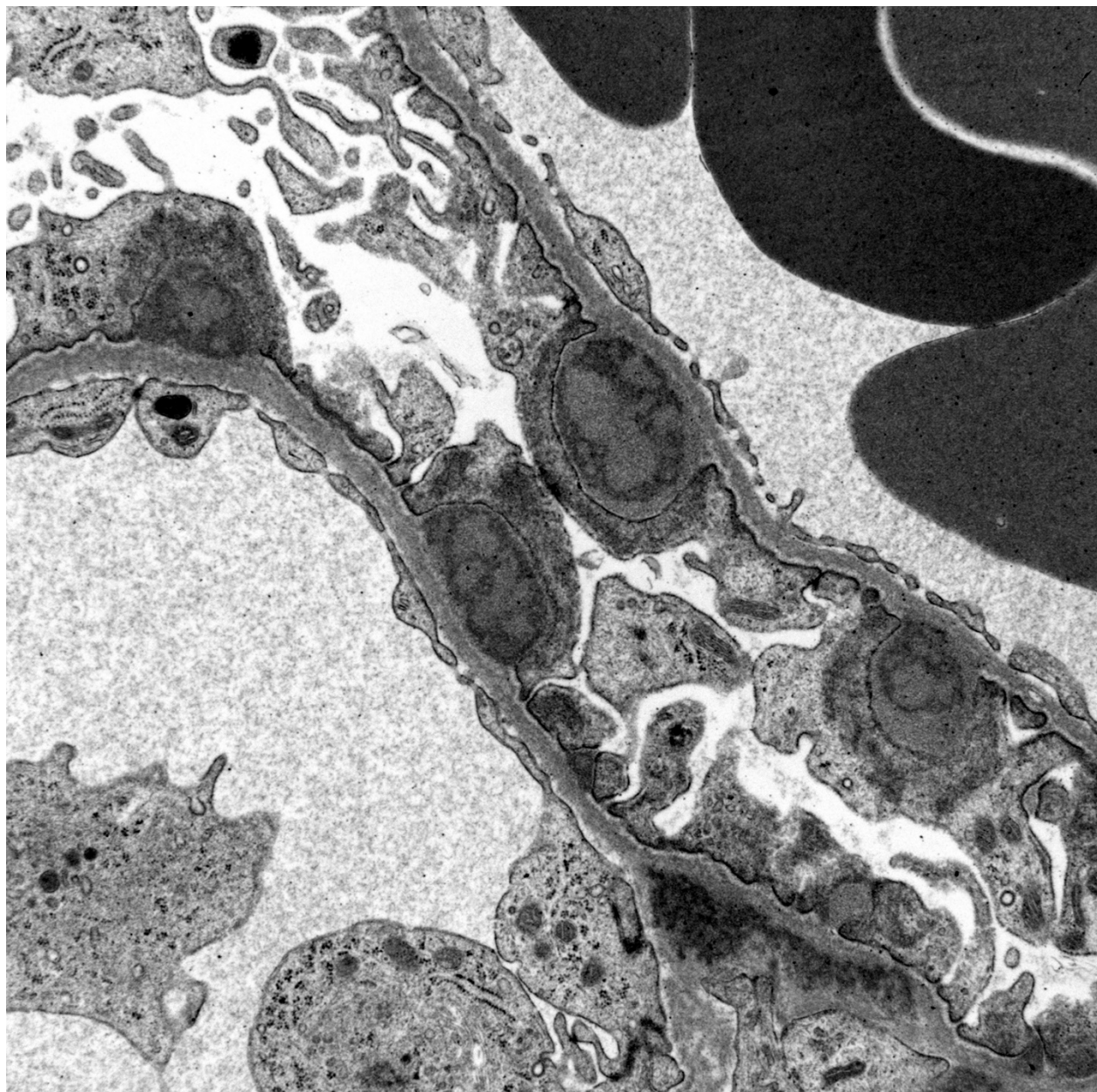
Ureter: Minimal luminal erythrocytes

Ultrastructural Description: Kidney, portions of two glomerular capillary loops (5,000x original negative magnification) - There are four large generally similar, approximately 500-700 nm diameter, oval-to-spherical, subepithelial, electron dense deposits morphologically consistent with immune complexes. Each consists of an irregular mixture of darker and less dark areas. Facing the capillary lumen, these deposits contact the lamina rara externa of the glomerular basement membranes, and facing the urinary space, deposits contact and are encircled by fused podocyte foot processes (foot process effacement). Podocyte foot process cytoplasm adjacent to these deposits

contains flocculent electron dense material. One smaller subepithelial roughly-triangular dense deposit is also present, and there is also an irregular intramembranous electron dense deposit on one border of the image. Podocyte foot processes adjacent to this intramembranous deposit and in capillary loop

sites not adjacent to deposits are also effaced, but less severely so.

There are narrow branching cytoplasmic projections extending from podocytes into the urinary space (podocyte hypertrophy), light accumulations of flocculent material in the urinary space (interpreted as protein



Glomerulus, macaque. The photomicrograph contains cross sections of two capillaries and the intervening uriniferous space. Numerous subepithelial dense deposits are present within the glomerular basement membrane and the overlying podocyte foot processes are effaced.

leakage), and a circular intensely electron dense spherical inclusion in one podocyte pedicle (interpreted as resorbed protein). Glomerular capillary endothelium of one capillary lacks most of its fenestrations, and endothelial cells lining this capillary are enlarged and protruding into the capillary lumen.

Contributor's Morphologic Diagnoses:

Kidney: Glomerulopathy, with subepithelial and intramembranous electron dense deposits, podocyte foot process effacement, and podocyte hypertrophy

Contributor's Comment: The overall experimental design employed in this study was adapted from that described by Hebert,⁴ In that study, animals administered bovine gamma globulin (BGG) intravenously at 5.5 mg/kg/day (dosed five days per week) developed glomerulopathy beginning as early as after six weeks of dosing. In a previous pilot study conducted by the contributor, the methods and dose levels outlined below successfully induced immune complex-mediated glomerulopathy. This

animal was immunized with, and then dosed with, BGG according to the schedule outlined in the table below.

Immunization: On pre-study Day -48, 1.3 mL of Complete Freund's Adjuvant (CFA) at 0.5 mg/mL was combined with 1.3 mL of BGG, reconstituted in PBS, formulated to deliver 1 mg/kg, and administered subcutaneously at 10 different sites along the upper portion of the dorsal thorax. Total volume administered was 2 mL. On pre-study Day -22, 1.3 mL of Incomplete Freund's Adjuvant (IFA) was combined with 1.3 mL of BGG reconstituted in PBS, formulated to deliver 1 mg/kg, and administered subcutaneously at 10 different sites along the upper portion of the dorsal thorax. Total volume administered was 2 mL. All animals were anesthetized with ketamine for CFA and IFA administration and given buprenorphine.

Antigen dosing: BGG was administered once daily over 30 minutes through a vascular access port. On each BGG dosing day, 5 mg/kg of diphenhydramine (DPH) was administered intramuscularly approximately 15-30 minutes prior to BGG administration.

Day 1		Day 2	Day 3	Day 4
5 mg/kg DPH 0.5 mg/kg (0.1)		5 mg/kg DPH 0.5 mg/kg (0.1)	5 mg/kg DPH 1.0 mg/kg (0.2)	5 mg/kg DPH 1.0 mg/kg (0.2)
Day 5		Day 6	Day 7	Day 8 to Study End
5 mg/kg DPH 2.0 mg/kg (0.4)		5 mg/kg DPH 3.0 mg/kg (0.6)	5 mg/kg DPH 4.0 mg/kg (0.8)	5 mg/kg DPH 5.5 mg/kg (1.1)

BGG immunization followed by daily BGG dosing was tolerated with antihistamine pre-treatment and induced proteinuria and immune complex glomerulopathy in this animal after 8 weeks.

JPC Diagnosis:

Glomerulonephritis, membranous, diffuse, marked, with subepithelial dense deposits,



Glomerulus, macaque. Higher magnification of the variegated dense deposits within the glomerular basement membrane. The overlying foot processes of the podocyte are fused (effaced). There is a dark cytoplasmic condensation of actin within podocyte cytoplasm overlying each immune deposit.

At the bottom corner of the image, a more traditional appearance of dense deposits is seen, which do not result in the bulging of the basement membrane; however podocytes overlying these deposits are similarly effaced. It also demonstrates the uncommon lesion of villous transformation of podocytes, which is usually seen in advanced stages of podocyte effacement.

Immune complex glomerulonephritis (ICGN) is the classic type III hypersensitivity

Kidney: effacement of podocyte foot processes, and podocyte villar hypertrophy.

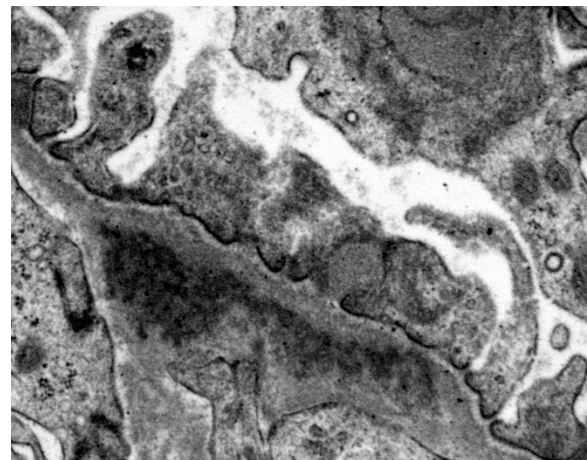
Conference Comment:

This outstanding electron micrograph excellently demonstrates immune complex deposition in subepithelial areas and effacement of the overlying podocytes.

reaction resulting from long-standing inflammation, formation of large amounts of antigen-antibody complexes in circulation, and their deposition within the glomerular basement membrane (GBM). The offending antigen may be that of an infectious organism causing a chronic infection (i.e. *D. immitis*) or may be endogenous in nature (as is seen in systemic lupus erythematosus in humans).¹ Other non-ICGN types of glomerulonephritis include anti-GBM disease as well as those forms which fix complement.¹ This particular model, of periodic injections of bovine serum albumin, mimics the continued antigenemia of infectious disease.

The basic theory of ICGN is somewhat controversial, as many animals with circulating soluble immune complexes may present without glomerulonephritis; others believe that the deposition of immune complexes may be secondary to previous glomerular injury.¹ Additionally other molecules such as C3, capital C1q, and IgM may also adhere to previously injured tissue.¹

Localization of immune complexes are generally described as subendothelial,

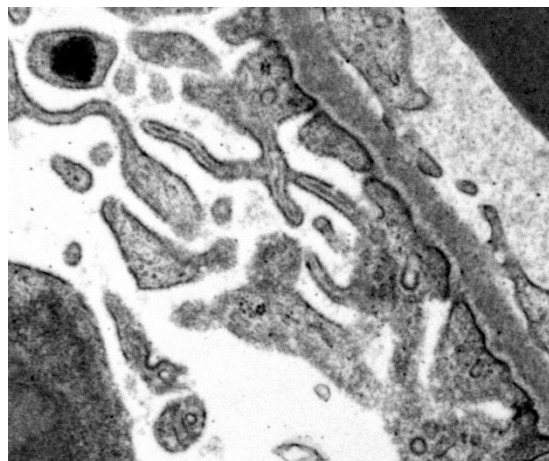


Glomerulus, macaque. Higher magnification of a dense deposits within the glomerular basement membrane.

subepithelial, intramembranous, and mesangial. Their localization within the GBM is predicated on a number of factors including their size, shape, charge, and chemical composition as well as the presence of local mediators of inflammation which may affect transport across endothelium or within the basement membrane.¹ A number of features may also impact the persistence of immune complexes within the basement membrane. Phagocytosis by neutrophils or macrophages, removal of the source of the persistent antigenemia, extracellular degradation by proteases, and even egress from the basement membrane may result in elimination.¹ At the other end of the spectrum, immune complexes may enlarge within the basement membrane through addition of small amounts of antigen or antibody, complement, or by addition of similar immune complexes.¹

A recently published classification of glomerular disease in the dog² identified immune complex-mediated glomerulonephritis as one of the two large categories of glomerular disease, with the other major category characterized by the absence of immune complexes and largely composed of cases of glomerular amyloidosis or focal segmental glomerulosclerosis. When examined only by light microscopy, 22/89 cases were misdiagnosed, emphasizing the importance of additional diagnostic modalities (especially electron microscopy) beyond light microscopy alone.²

The WSAVA Classification denotes the characteristic subepithelial location of ICs in cases of membranous glomerulonephritis (as seen in this case), and subendothelial or mesangial locations in cases of membranoproliferative glomerulonephritis. The subepithelial location of the immune complexes results in characteristic glomerular changes. The interposition of



Glomerulus, macaque. "Villar transformation" or hypertrophy of podocytes is seen in cases of severe effacement.

basement membrane between the ICs and the capillary lumen does not engender endocapillary hypercellularity (an increase in the number of leukocytes, endothelial cells and interposed mesangial cells internal to the GBM) which ultimately encroaches or obliterates the lumina of glomerular capillaries.² The ability of these subepithelial complexes to fix complement, however, does result in effacement of podocyte foot processes.² Conversely, subendothelial locations of ICs results in activation of endothelium and transcapillary recruitment of inflammatory cells and peripheral capillary hypercellularity as previously described.²

Interestingly, reports of ICGN in nonhuman primates are relatively scarce within the last decade. Membranoproliferative glomerulonephritis with crescent formation was reported in cynomolgus macaques injected with obinutuzumab, a monoclonal antibody targeted against CD20,⁵ exemplary of the immunogenicity of foreign antibodies in primate models. Membranoproliferative glomerulonephritis was also attributed to chronic SHIV infection in a rhesus macaque.³

A potential differential on ultrastructure for the immune complexes would in this case would be “hump-like” deposits of complement, as seen in post-infectious glomerulonephritis in humans with a history of recent infectious disease. These “humps” are primarily composed of the third component of complement with little immunoglobulin present.

Contributing Institution:

Pfizer
588 Eastern Point Rd
Groton, CT 06340

References:

1. Cianciolo RE and Mohr FC. Urinary System. In: Maxie MG, ed. *Jubb Kennedy and Palmer's Pathology of Domestic Animals, 6th ed.* 2016; St. Louis MO, Elsevier Press, vol 2, p. 411-412.
2. Cianciolo RE, Mohr FC, Aresu L, Brown CA, James C, Jansen JH, Spangler WL, van der Lugt JJ, Kass PH, Brovida C, Cowgill LD, Heiene R, Polzin DJ, Syme H, Vaden SL, van Dongen AM, Lees GE. World Small Animal Veterinary Association Renal Pathology Initiative: Classification of Glomerular Diseases in Dogs. *Vet Pathol* 2016; 53(1): 113-135.
3. Clarke CL, Eckhaus MA, Zerfas PM, Elkins WR. Peripheral edema with hypoalbuminemia in a nonhuman primate infected with simian-human immunodeficiency virus: a case report. *J Am Assoc for Lab Anim Sci* 2008; 47(1):42-48.
4. Hebert L, Cosio F, Birmingham D. Experimental immune complex-mediated glomerulonephritis in the nonhuman primate. *Kid Intern.* 1991; 39:44-56.

5. Husar E, Solonets M, Kuhlmann, O, Schick E, Piper-Leputre H, Singer T, Tyagi G. Hypersensitivity reactions to obinutuzumaba in cynomolgus monkeys and relevance to humans. *Toxicol Pathol* 2017; 45(5):676-686.

CASE III: P2551-13 (JPC 4048996-00).

Signalment: 3 year-old, female, Standardbred, *Equus caballus*, horse

History: This mare had a history of decreased racing performances of a few weeks duration. A week prior to its last race, an endoscopic examination was performed and revealed excessive tracheal mucus; it was treated with enrofloxacin for a week. The morning after its last race, the horse was anorectic and listless/depressed; it was treated with IV trimethoprim-sulfa, DMSO and electrolytes. The condition rapidly worsened over the next 24 hours, with tachypnea, marked weakness and fever. Clinical biochemistry revealed hypercreatininemia (800 µmol/L; normal range: 87-150). Tracheobronchial washing results were within normal limits. Acute renal failure was strongly suspected. Due to the poor

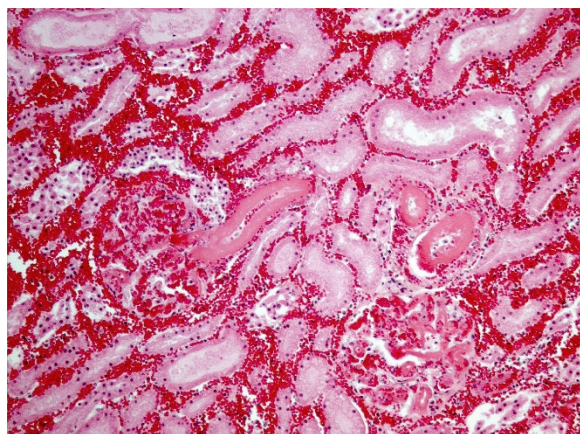


Right kidney; horse. The cortex is diffusely hemorrhagic. (Photo courtesy of: Université de Montréal, Faculty of veterinary medicine, St-Hyacinthe, Québec, Canada. <http://www.medvet.umontreal.ca>)

prognosis, the owners elected for euthanasia and a full necropsy was performed.

Gross Pathology: There was subcutaneous edema with multifocal petechiation in the dependent portions of the abdomen. Approximately 1.5 L of blood-tinged serous fluid was present in the thoracic cavity. The lungs showed moderate diffuse congestion and edema with a few small (< 1 cm) randomly distributed dark red foci. The liver was pale and appeared slightly yellowish. The cortex of both kidneys was diffusely hemorrhagic. Petechiae were present multifocally on the small intestinal mucosa, sometimes accompanied by mild submucosal edema. Colonic contents were slightly more fluid than normal, without any associated lesions.

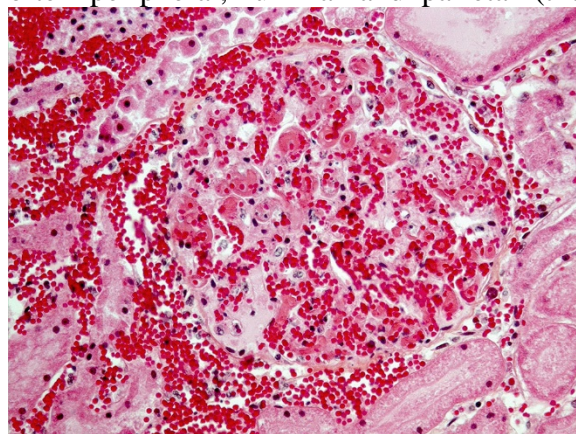
Laboratory results: Routine aerobic bacteriology on ileum and colon yielded 4+ of an α -hemolytic *Streptococcus* (not further identified) and 1+ of *E.coli* (negative for *Salmonella*). The latter was negative by PCR



Kidney, horse: There is thrombosis and thickening of vascular walls by fibrinoid material, involving glomerular capillaries, and interlobular and afferent glomerular arterioles. Multifocal acute tubular necrosis is also present. (Hematoxylin-eosin-phloxine-saffron, 400X). (Photo courtesy of: Université de Montréal, Faculty of veterinary medicine, St-Hyacinthe, Quebec, Canada. <http://www.medvet.umontreal.ca>)

for all tested virulence factors including Stx1 and Stx2.

Microscopic Description: On low magnification, the renal cortex has a variegated appearance. There are severe and extensive cortical interstitial hemorrhages associated with vascular lesions involving glomerular capillaries, interlobular and (afferent) glomerular arterioles, and fewer venules. These lesions consist of hyaline thrombi and thickening of vascular walls by fibrinoid material with nuclear debris (fibrinoid necrosis). The fibrinoid material is often peripheral, luminal and parietal (the



Kidney, horse: A glomerulus shows several hyaline thrombi associated with erythrocytes, and thickening of glomerular loops by fibrinoid material and rare nuclear debris. (Hematoxylin-eosin-phloxine-saffron, 400). (Photo courtesy of: Université de Montréal, Faculty of veterinary medicine, St-Hyacinthe, Quebec, Canada. <http://www.medvet.umontreal.ca>)

limit is often blurred), and associated with erythrocytes; the fibrinous nature is supported by its Martius scarlet blue positivity. The fibrinoid vascular material is PAS-positive and Jones' silver-negative. Especially in non-hemorrhagic areas, the capillaries in some glomeruli contain granular material (possible platelets), fragmented erythrocytes and/or thrombi. There is multifocal acute tubular necrosis in the cortex and superficial medulla, the extent of which is hard to evaluate (some post-

mortem change and very acute), and tubular proteinosis. Inflammation is minimal: occasionally a few interstitial degenerate neutrophils and small lymphocytes.

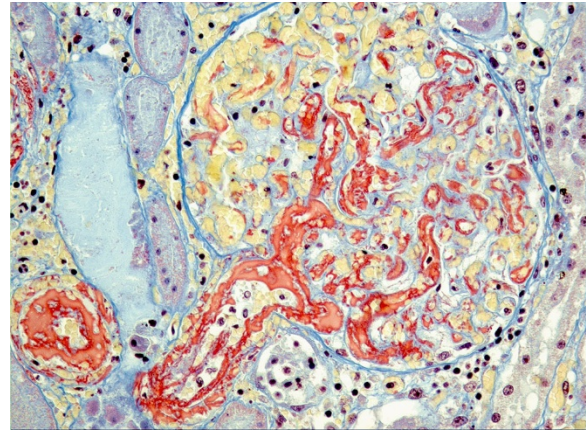
Contributor's Morphologic Diagnoses:

Severe, extensive renal necrotizing vasculopathy with fibrin thrombi (glomerular capillaries, interlobular and afferent glomerular arterioles) and extensive hemorrhage (consistent with hemolytic-uremic syndrome).

Multifocal, acute tubular necrosis (ischemic, secondary to vascular lesions).

Contributor's Comment: Even though hematological data was not available (i.e. to assess microangiopathic hemolytic anemia and thrombocytopenia), hemolytic-uremic syndrome was the final diagnosis, based on the renal lesions associated with acute renal failure. Unfortunately, no cause was found, but only Shiga toxin-producing *E. coli* (STEC) were investigated.

Hemolytic-uremic syndrome (HUS) and thrombotic thrombocytopenic purpura (TTP) are the two best-known thrombotic microangiopathies, which are clinical syndromes characterized by microangiopathic hemolytic anemia, thrombocytopenia and dysfunction of one or more organs, the result of microvascular thrombosis and endothelial damage. Both HUS and TTP cause the formation of platelet-rich thrombi in the microcirculation and endothelial swelling, which cause erythrocyte fragmentation (leading to anemia) and excessive platelet consumption (leading to thrombocytopenia).^{1,7,10} In their original description, HUS involved mostly or only the kidney, with acute renal failure as a prominent feature, while TTP involved mostly the brain, with mainly neurologic manifestations. However, it is now known



Kidney, horse: Kidney; horse. A Martius scarlet blue stain shows the luminal and parietal distribution of fibrin (red staining) in glomerular capillaries, and interlobular and afferent glomerular arterioles. Martius scarlet blue. (Martius, 400X) Photo courtesy of: Université de Montréal, Faculty of veterinary medicine, St-Hyacinthe, Quebec, Canada. <http://www.medvet.umontreal.ca>)

that HUS can involve organs other than the kidney, including the brain (and thus cause neurologic dysfunction), and TTP patients often have renal involvement; thus, these two clinical syndromes often overlap.^{7,10} Thrombotic microangiopathies in humans are now classified, based on known causes/pathogenesis or associations, as 1) **typical HUS** (epidemic, classic or diarrhea-positive HUS), **atypical HUS** (non-epidemic or diarrhea-negative HUS) and **TTP**. **Typical HUS (tHUS)** is caused by intestinal Shiga toxin-producing bacteria, in most cases *E. coli* producing Stx1 or Stx2 (STEC), and occasionally other bacteria like *Shigella dysenteriae* type 1; the best known STEC serotype is the O157:H7, which is most often acquired by ingestion of undercooked contaminated ground beef (thus its sometimes epidemic nature). **Atypical HUS (aHUS)** is often associated with a genetic (mutation) or, less commonly, acquired (autoantibodies) deficiency of complement regulatory proteins, mostly factor H (CFH), predisposing to hyperactivation of the alternative complement pathway. **Thrombotic thrombocytopenic purpura**

(TTP) is associated with an acquired (autoantibodies) or, less commonly, a genetic (mutation) deficiency in ADAMTS13, a metalloproteinase which degrades high-molecular-weight multimers of von Willebrand Factor (vWF); subsequent accumulation of ultralarge vWF multimers (UL-VWF) in plasma promotes platelet aggregation and activation. Triggering conditions or exposures associated with aHUS and TTP include pregnancy, autoimmune diseases and certain drugs (e.g. cyclophosphamide).^{1,7,10} The pathogenesis of these syndromes is complex and incompletely understood. The initiating factor in tHUS is endothelial damage by Shiga toxins while it seems to be platelet aggregation in TTP.^{1,7,10} In recent years, complement hyperactivation has been proposed as an important common pathogenetic factor, due to its prothrombotic and proinflammatory effects (platelets are activated by complement); the glomerular endothelium, which is targeted in aHUS, is highly susceptible to complement. In tHUS, P-selectin upregulation in endothelial cells by Shiga toxins results in complement deposition on these. Hyperactivation of the alternative complement pathway is central to aHUS pathogenesis. In TTP, the large platelet thrombi may contribute to complement activation. This hypothesis is supported by the clinical efficiency of an anti-C5 antibody in aHUS and some cases of tHUS and TTP.¹⁰

The pathology of tHUS, aHUS and TTP is essentially similar. Microscopic hallmarks of the acute phase of these conditions in the kidney are: 1) occlusion of glomerular capillaries by platelet-rich fibrin thrombi, 2) capillary wall thickening due to endothelial cell swelling and subendothelial cell debris and fibrin deposits, 3) mesangial damage (cells and matrix), and 4) often fibrinoid necrosis of interlobular and afferent

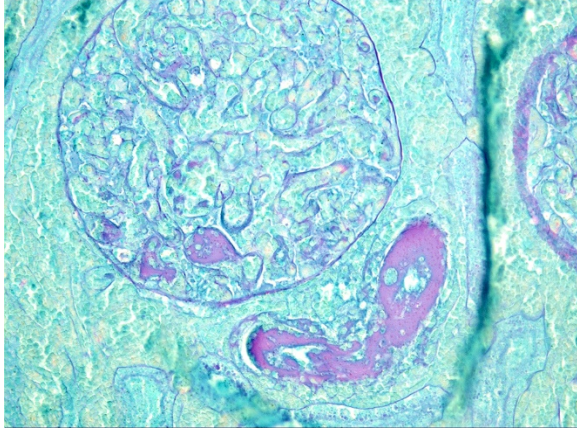
glomerular arterioles. These vascular lesions may lead to variably extensive cortical necrosis. Chronic lesions are only seen in aHUS and TTP.¹

Hemolytic-uremic syndrome is better known in human medicine, but natural cases have been reported in horses and dogs;^{2,3,4,6,8,9} the cause was not determined except in one equine case, involving a mare and her foal, in which a 0138:H2 STEC was isolated from the mare's uterus and both animal's gastrointestinal tract.⁴

JPC Diagnosis: Kidney, cortex: Necrosis and hemorrhage, diffuse, severe with fibrinoid vascular necrosis and numerous fibrin thrombi.

Conference Comment: The contributor has provided an excellent review for hemolytic-uremic syndrome in humans. As previously discussed, "typical" hemolytic-uremic syndrome may result from endothelial damage by Shiga toxins produced by several strains of enteropathogenic *E. coli* (EPEC). This toxin, encoded in the genome of bacteriophages in these strains, binds to the glycolipid receptor globotriaosylceramide (Gb3) on the surface of endothelial cells.¹³ A number of mechanisms result in necrosis of infected cells, including the inhibition of protein synthesis, leading to vascular permeability and cell lysis. The concomitant exposure of endothelial cells to lipopolysaccharides or various inflammatory cytokines (TNF- α , IL-1) increases the sensitivity of endothelial cells to the cytotoxic effects of Shiga toxin.

The susceptibility of a particular cell or tissue to the effects of Shiga toxin is directly proportional to the concentration of the Gb3 receptor in a particular tissue. The classic lesions of edema disease in swine, a



Kidney, horse: Kidney; horse. The fibrin/fibrinoid vascular material is PAS-positive. (Periodic acid-Schiff, 400X). (Photo courtesy of: Université de Montréal, Faculty of veterinary medicine, St-Hyacinthe, Quebec, Canada. <http://www.medvet.umontreal.ca>)

disease associated with enterohemorrhagic O serotypes of *E. coli* (O138, O139, O140)—edema of the eyelids, gastric wall, mesocolon, larynx, and cerebrum — are directly related to the high concentrations of Gb3 receptors in these tissues.

The most widely recognized Shiga-toxin producing *E. coli* (STEC) is O157:H7, a major human pathogen, although over 200 other STEC serotypes have been identified.¹³ In calves less than four weeks of age, STEC have been associated with ulcerative fibrinohemorrhagic enterocolitis and dysentery. Lesions are most commonly seen in the spiral colon and rectum, although occasionally the ileum and cecum are involved. In a review of outbreaks of human enterohemorrhagic *E. coli* (EHEC), cattle were identified as a natural reservoir of STEC and approximately 75% of outbreaks in humans are limited to the consumption of contaminated beef.¹¹

In dogs, STEC have been associated with dysentery and in greyhounds, the syndrome of cutaneous and renal glomerular vasculopathy has been attributed to the consumption of STEC-contaminated beef.¹³

A similar condition of cutaneous and renal glomerular vasculopathy has been recently identified in the UK in dogs, although STEC were not identified in feces from affected dogs.⁵

Another very interesting lesion resembling those caused by STEC has been identified in the mesentery of horses with naturally and experimental endotoxemia. The lesion consists of marked necrosis and loss of medial smooth muscle cells in the mesenteric arterioles with fibrinoid degeneration and intramural hemorrhage.¹²

The moderator discussed thrombotic microangiopathy, a term which covers a wide range of conditions (infectious disease, drug reactions, and hypertension among others) in which there is direct damage to endothelial cells. The morphology of renal damage among the disparate forms of TMA does not always target the same vessels in the kidney, as “not all endothelial cells are alike.” While the large areas of infarction are the overwhelming feature of this particular slide, careful inspection of will reveal inflammatory cells and cellular debris within the walls of radial arteries (a change referred to in some quarters as “necrotizing arteritis of Weisbrode”) as well as the present of occlusive thrombi; thrombi are also present in glomerular tuft capillaries as well. The possibility of purpura hemorrhagica as an etiology (which would cause a lesion more similar to TTP than HUS) was also discussed in this case.

While the clinical picture and lesion morphology is consistent with documented cases of hemolytic-uremic syndrome in the horse, the unavailability of hematologic data, coupled with the inability to identify Shiga toxins (and only a section of kidney to review) may call for a less specific diagnosis than hemolytic-uremia syndrome in this

particular

case.

Contributing Institution:

Université de Montréal, Faculty of veterinary medicine, St-Hyacinthe, Quebec, Canada.
<http://www.medvet.umontreal.ca>

References:

1. Alpers CE. The kidney. In: *Robbins and Cotran Pathologic Basis of Disease*. 8th ed. Philadelphia: Saunders Elsevier; 2010:905-969.
2. Chantrey J, Chapman PS, Patterson-Kane. Haemolytic-uraemic syndrome in a dog. *J Vet Med A*. 2002;49:470-472.
3. Dell'Orco M, Bertazzolo W, Pagliaro L et al. Hemolytic-uremic syndrome in a dog. *Vet Clin Pathol*. 2005;34(3): 264-269.
4. Dickinson CE, Gould DH, Davidson AH et al. Hemolytic-uremic syndrome in a postpartum mare concurrent with encephalopathy in the neonatal foal. *J Vet Diagn Invest*. 2008;20:239-242.
5. Holm, LP, Hawkins I, Robin C, Newton RJ, Stanzani G, McMahon LA, Pesavento P, Carr T, Cogen T, Gouto CG, Cianciolo R, Walker \$. Cutaneous and renal glomerular vasculopathy as a cause of acute kidney injury in dogs in the UK. *Vet Rec* 2015; 176(15):384
6. Holloway S, Senior D, Roth L et al. Hemolytic uremic syndrome in dogs. *J Vet Intern Med*. 1993; 7(4):220-227.
7. Kumar V, Abbas AK, Fausto N et al. Diseases of white blood cells, lymph nodes, spleen, and thymus. In: *Robbins and Cotran Pathologic Basis of Disease*. 8th ed. Philadelphia: Saunders Elsevier; 2010:589-638.
8. MacLachlan NJ, Divers TJ. Hemolytic anemia and fibrinoid change of renal vessels in a horse. *J Am Vet Med Assoc*. 1982 Oct 1;181(7):716-717.
9. Morris CF, Robertson JL, Mann PC et al. Hemolytic uremic-like syndrome in two

horses. *J Am Vet Med Assoc*. 1987 Dec 1;191(11):1453-1454.

10. Noris M, Mescia F, Remuzzi G. STEC-HUS, atypical HUS and TTP are all diseases of complement activation. *Nat Rev Nephrol* 2012 Nov;8(11):622-33.
11. Nguyen Y, Sperandio V. Enterohemorrhagic *E. coli* pathogenesis. *Front Cell Infect Micro* 2012; 2:1-7.
12. Oikawa M, Ueno T, Yoshikawa H. Arterionecrosis of the equine mesentery in naturally occurring endotoxaemia. *J Comp Path* 2004; 150:75-79.
13. Uzal FA, Plattner BL, Hosstetter JM. Alimentary System. In: Maxie MG, ed. *Jubb Kennedy and Palmer's Pathology of Domestic Animals*, 6th ed. 2016; St. Louis MO, Elsevier Press, vol 2, p. 162-163.

CASE IV: 13-555-21 (JPC 4034756-00).

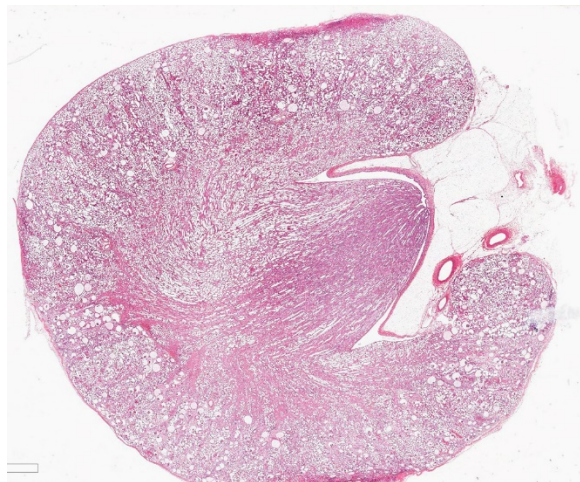
Signalment: 8-month-old, neutered male Airedale, *Canis familiaris*, canine.

History: Presented with depression, vomiting and diarrhea. Significantly raised urea, creatinine, phosphate, sodium, calcium. Did not improve with three days of intravenous fluid therapy and was euthanised. Only the kidneys were sent by the clinician via the surgical biopsy service.

Gross Pathology: Irregularly pitted with an undulating capsular surface.

Laboratory results: None.

Microscopic Description: Kidney. Diffusely, the renal capsule is moderately thickened and multifocally depressed. The subjacent parenchyma consists of irregular foci of loose primitive stroma that contains small caliber vessels, primitive tubules and tubules lined by irregularly tall



Kidney, dog. At subgross magnification, the kidney is characterized by diffuse ectasia of tubules and glomeruli. (HE, 5X)

columnar epithelium with basilar nuclear location (persistent metanephric ducts). Extending radially from the outer cortex to the medulla are multifocally extensive areas of loose fibrous stroma (interstitial fibrosis; confirmed with trichrome staining). Predominantly within these areas and affecting over 80% of glomeruli, Bowman's spaces are markedly dilated and multifocally contain a moderately shrunken glomerulus. Multifocally within the superficial cortex glomeruli are small with peripheral nuclei and indistinct capillary tufts (fetal glomeruli). Multifocally Bowman's capsules contain intramural, spherical (2-15 μ m diameter) basophilic material (mineral; confirmed with von Kossa staining). Diffusely cortical tubules are markedly dilated (up to 120 μ m in diameter). Tubules are multifocally lined either by plump cuboidal to flattened (attenuated) tubular epithelium or epithelium that is enlarged and hypereosinophilic (tubular degeneration) or multifocally by enlarged, severely vacuolated epithelium with karyorrhesis and karyolysis (tubular necrosis). Multifocally tubules contain amorphous hyaline to granular hypereosinophilic material (protein casts) and tubular epithelium is multifocally

replaced or deviated by amorphous basophilic material (mineral; confirmed with Von Kossa staining). Collecting ducts range in diameter from 20 to 140 μ m and are variously lined by attenuated to plump cuboidal and columnar epithelium, which multifocally partially occludes the lumen (atypical epithelium). Multifocally collecting ducts are surrounded by areas of loose, undifferentiated mesenchyme that is focally infiltrated by low numbers of neutrophils; multifocally lumina contain sloughed pyknotic and karyorrhectic debris (necrosis). The cortical interstitium is infiltrated by low numbers of lymphocytes and plasma cells.

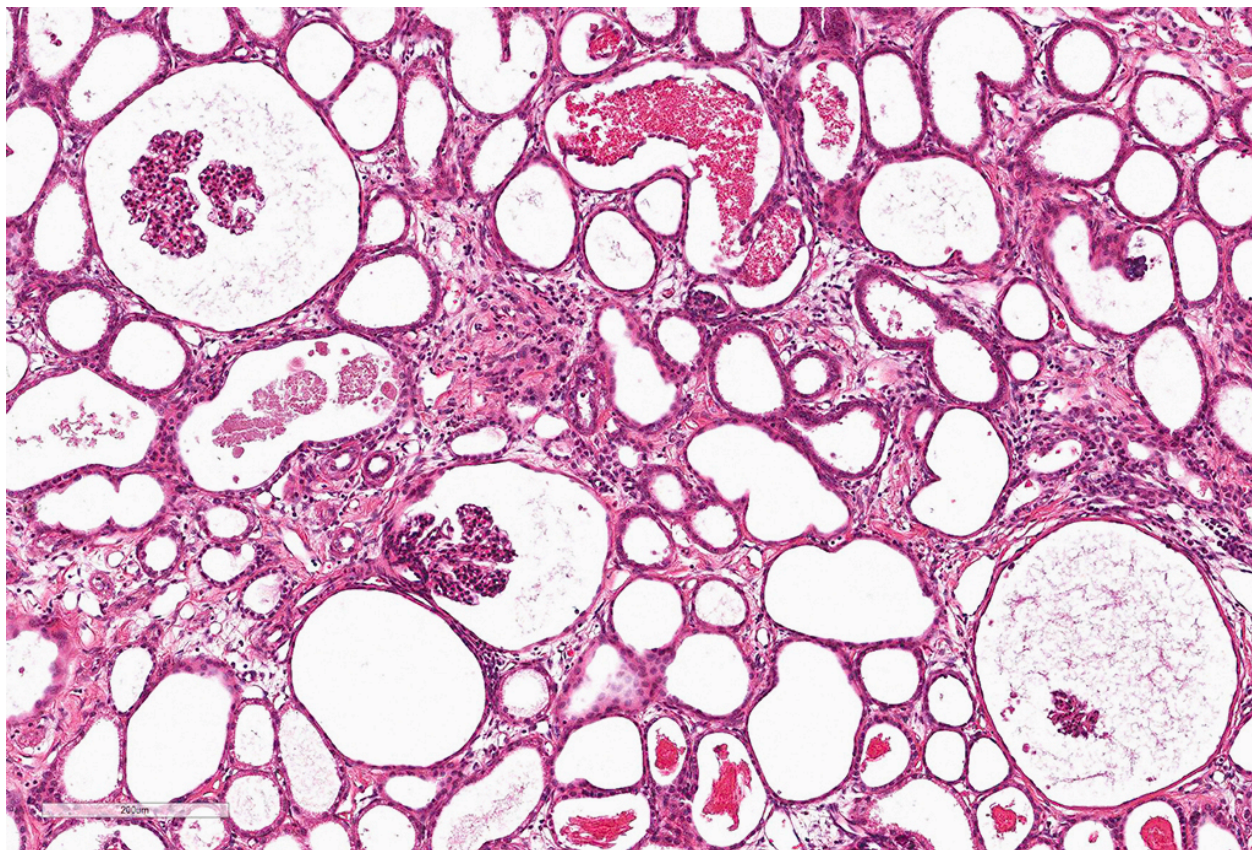
Contributor's Morphologic Diagnoses: 1. Kidney; dysplasia with fetal glomeruli, persistent metanephric ducts, primitive mesenchyme and atypical tubular epithelium.

2. Kidney; marked diffuse tubular and Bowman's space ectasia with multifocal tubular degeneration, necrosis and mineralization and moderate interstitial fibrosis

Contributor's Comment:

Canine renal dysplasia is usually congenital and often thought to be hereditary resulting in disorganized development of renal parenchyma due to anomalous differentiation.⁴ It has been reported in many breeds including the Golden Retriever, Beagle, Dutch Kookier, Miniature Schnauzer, Shih Tzu, Lhasa Apso, Great Dane, Samoyed, Alaskan Malamute, Cavalier King Charles Spaniel and Bulldog.^{1,2,3,5,9,11}

Disease in the early neonatal period may also cause renal dysplasia by affecting incompletely differentiated renal tissue. This has been reported in puppies that survived intraperitoneal infection with canine herpesvirus at 2 days of age and were



Kidney, dog. Higher magnification shows a marked dilation of Bowman's space and atrophy of glomerular tufts. There is diffuse loss of tubules, ectasia of many remaining tubules with attenuated epithelium, marked interstitial fibrosis, and mild interstitial lymphocytic interstitial inflammation. (HE, 130X)

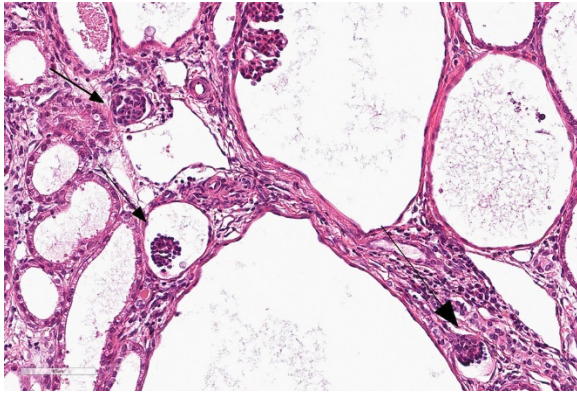
sacrificed at 11 and 16 days post infection.⁸ Similarly renal dysplasia has been reported in calves and kittens following infection with bovine pestivirus and feline parvovirus, respectively.⁴

The kidney develops from successive structures, which overlap in their formation. Renal malformation can therefore occur in many patterns. The developing structures include the pronephros, mesonephros and ultimately, the metanephros. The pronephros and mesonephros degenerate to vestigial remnants but are crucial in the correct formation of the metanephros. The metanephros or 'definitive kidney' forms from complex interaction of the ureteral bud and metanephric blastema. This may explain why malformations of the kidney are often

accompanied by ureteral anomalies in man, although this is not commonly reported in dogs.^{4, 10}

The clinical presentation and the age at which signs develop are variable. Renal dysplasia in neonates has been associated with reduced appetite, intermittent vomiting, dullness, poor growth and polyuria/polydipsia. Puppies may not survive to weaning; longer survival (over 4 months) results in clinical signs that can be attributed to uremia such as vomiting, diarrhea, anemia, nervous signs and fibrous osteodystrophy ("rubber jaw").⁶

Renal dysplasia may be uni- or bilateral. Grossly, affected kidneys may be small and therefore potentially they could be misdiagnosed as hypoplastic. They may also be



Kidney, dog. Glomeruli near the capsular surface have a fetal appearance without glomerular capillaries, and a peripheral rim of primitive podocytes with hyperchromatic nuclei. (HE, 183X)

misshapen, lobulated, contain an irregularly thin cortex or thick walled cysts and they may be associated with dilated tortuous ureters.^{4,9} They can be indistinguishable from end stage renal lesions in old dogs.⁹ Alternatively, they may appear grossly normal, and therefore histopathological examination is required for diagnosis.⁴

In the largest case series available, 45 dogs of various breeds were diagnosed with renal dysplasia. Histological features were described as primary, compensatory and degenerative or inflammatory. At least one of the following primary features was identified in each case:

- 1) Asynchronous differentiation of nephrons, defined by the presence of fetal or immature glomeruli and/or tubules (40/45 cases).
- 2) Persistent mesenchyme: a loose stroma found in the medulla, which is alcian blue positive and trichrome stain negative (25/45 cases).
- 3) Atypical tubular epithelium reported as adenomatoid cuboidal or clusters of

squamous epithelial cells (7/45 cases).

4) Persistent metanephric ducts, which are ducts in the outer medulla lined by tall pseudostratified columnar epithelium and often dilated (6/45 cases).

5) Dysontogenic metaplasia: represented as cartilaginous or osseous metaplasia (2/45 cases).⁷

There is disagreement between authors on the features required for a diagnosis of renal dysplasia. Some authors believe juvenile nephropathy or juvenile renal disease is a more appropriate term for cases of renal dysplasia which do not exhibit primitive ducts or dysontogenic metaplasia. Dysontogenic metaplasia and primitive metanephric ducts are the least commonly observed features in 'renal dysplasia', therefore making the classification restrictive and excluding many cases where fetal glomeruli alone are observed. Juvenile nephropathy is a general term that includes non-inflammatory, degenerative, developmental and chronic renal disease of unknown pathogenesis and is therefore non-specific. However this may be a more appropriate term for cases whereby the pathogenesis of the dysplasia is unknown or unclear. Further increasing the confusion, 'familial renal disease' has been used interchangeably with renal dysplasia in the literature.^{4,5,9}

Compensatory features were described in 20/45 cases and included enlarged glomeruli with mesangial hyperplasia and cortical tubular dilation with hypertrophic and hyperplastic cuboidal epithelial lining. Degeneration and inflammatory changes may be severe and therefore obscure primary features required for diagnosis.

Degenerative/inflammatory features were present in all cases and predominantly included interstitial fibrosis, which was often segmental and within areas of fetal glomeruli. The appearance of tubulointerstitial nephritis and pyelonephritis was in parallel with the severity of fibrosis. Other changes observed included dystrophic mineralization, cystic glomerular atrophy, microcystic tubules, retention cysts and glomerular lipidosis.⁸

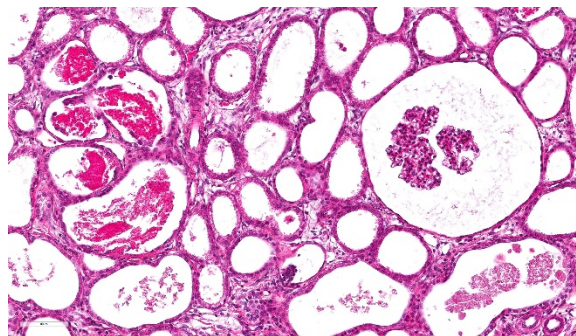
JPC Diagnosis: 1. Kidney: Asynchronous maturation, diffuse, marked, with glomerulocystic atrophy, fetal glomeruli, marked tubular ectasia, and mild chronic interstitial nephritis.
2. Kidney: Tubular loss, diffuse, moderate, with granular cast formation and rare epithelial necrosis.

Conference Comment: The contributor has provided a concise but relatively thorough discussion of renal dysplasia in the dog.

A slightly more detailed review of renal embryogenesis may help in understanding its development. During fetal development, the ureteric bud, an evagination of the mesonephric duct, develops into the metanephros. The ureteric bud extends cranial dorsally into the overlying metanephric blastema whereupon successive divisions of the ureteric bud result in formation of the collecting ducts. Interaction with mesenchymal cells within the metanephric blastema results of the formation of the remainder of the nephron, including glomeruli and tubules. The structures initially form at the cortical medullary junction, but as the collecting ducts elongate, or subsequently formed in the superior aspects of the cortex. The first few weeks of life see additional development of renal structures.⁹

As the importance of the ureteric bud in the overall development of the kidney now becomes clear, it can be understood how ureteral abnormalities during development have such a profound impact on the developing kidney. Abnormal placement of the ureters during development as well as lower urinary tract obstruction have both been identified as major contributors to renal dysplasia in humans.^{7, 10} Such extra-renal abnormalities are not commonly reported in dogs, but this may be the result of incomplete autopsy examination of the entire urinary tract.⁹

As renal dysplasia is a complex, multifactorial disease, obviously there are many other contributors than simply the placement of the ureteric bud. Regulation of “renal branching morphogenesis” is controlled by a wide range of transcription factors, growth factors, and cell surface signaling peptides which, if deficient, results in improper induction of the metanephric blastema and ultimately, renal dysplasia.⁴ Subsequent to the observation that cyclooxygenase-2 (Cox-2) deficient mice exhibit renal changes similar to renal dysplasia in dogs, the Cox-2 genes of Lhasa Apso affected with familiar renal dysplasia were sequenced and compared to that of



Kidney, dog. The presence of granular and cellular casts within dilated tubules is not common in canine juvenile nephropathy, and suggests a superimposed second insult to the abnormal renal development in this case. (HE, 285X)

normal dogs.¹² Small insertions and the deletions of GC boxes upstream of the ATG translation start site (which are putative SP1 transcription factor binding sites) were found upstream of the A translation start site in affected animals.¹²

During the slide description, the moderator commented on the difficulty on the precise identification of primitive mesenchyme and metanephric tubules in cases of juvenile nephropathy, as well as the spirited discussions that it often engenders among experts in renal disease. Without precise definitions for these terms even among experts, their identification in many cases is often quite subjective and fraught with peril. In this particular case, after some discussion, the “primitive mesenchyme” identified by some attendees was determined to be edematous mature collagen, and immature tubules more likely to be the result of interesting sectioning of collecting ducts.

The moderator also commented on the amount of debris within tubules which is uncommon in cases of juvenile dysplasia. In this case, this cellular debris is more suggestive of a second, more recent tubular insult, resulting in this animal’s acute uremic presentation. The developmental abnormalities seen in this kidney, although dramatic, likely would not have resulted in a death at 8 months on their own. She also commented on the profound ectasia of Bowman’s capsules in this case, strongly suggesting downstream obstruction (which is corroborated by the marked tubular ectasia also seen in this case.)

The term “renal dysplasia” itself appears to be falling from favor today among pathologists and clinicians, with other terms such as “juvenile nephropathy” and “renal maldevelopment” gaining favor.

Contributing Institution:

The Royal Veterinary College,
PPB, Hawkshead Campus,
Hawkshead Lane,
South Mymms,
AL9 7TA
www.rvc.ac.uk/pathology-and-diagnostic-laboratories

References:

1. Bruder MC, Shoieb AM, Shirai N, Boucher GG, Brodie TA. Renal dysplasia in beagle dogs: four cases. *Toxicol Pathol.* 2010; 38:1051-1057.
2. Hoppe A, Swenson L, Jonsson L, Hedhammar A. Progressive nephropathy due to renal dysplasia in shih tzu dogs in Sweden: a clinical pathological and genetic study. *J Small Anim Pract.* 1990; 31:83-91.
3. Kerlin RL, Van Winkle TJ. Renal dysplasia in golden retrievers. *Vet Pathol.* 1995; 32: 327-329.
4. Maxie MG. Urinary system. In: Jubb, Kennedy, and Palmer's *Pathology of Domestic Animals*. 5th, ed. Philadelphia, PA: Elsevier Saunders; 2007; Vol 2, pp. 437-442
5. Morton LD, Sanecki RK, Gordon DE, Sopiaryz RL, Bell JS, Sakas PS. Juvenile renal disease in miniature schnauzer dogs. *Vet Pathol* 1990; 27:455-458.
6. Nash AS. Familial renal disease in dogs. *J Small Anim Pract* 1989; 30:178-183.
7. Nagata M, Sawako S, Shu Y. Pathogenesis of dysplastic kidney associated with urinary tract obstruction *in utero*. *Nephrol Dial Transplant* 2002; 17(Suppl 9): 37-38.
8. Percy DH, Carmichael LE, Albert DM, King JM, Jonas AM. Lesions in puppies surviving

- infection with canine herpesvirus. *Vet Pathol* 1971; 8:37-53.
9. Picut CA, Lewis RM. Microscopic features of canine renal dysplasia. *Vet Pathol* 1987; 24:156-163.
10. Risdon RA. Renal dysplasia. *J Clin Path* 1971; 24:57-71.
11. Schulze C, Meyer HP, Blok AL, Schipper K, Van Den Ingh TS. Renal dysplasia in three young adult dutch kookier dogs. *Vet Quart* 1998; 20:146-148
12. Whitely MH, Bell JS, Rothman DA. Novel allelic variants in the canine cyclooxygenase-(Cox-2) promoter are associated with renal dysplasia in dogs. *PLoS One* 2011, 6(2) e16684.

Self-Assessment - WSC 2018-2019 Conference 4

1. Which of the following has not been reported in association with equine infection with *B. burgdorferi*?
 - a. Skin infection
 - b. Kidney infection
 - c. Neural infection
 - d. Eye infection

2. Which of the following is NOT a cause of immune-complex glomerulonephritis?
 - a. *D. immitis*
 - b. Systemic lupus
 - c. Chronic SIV infection
 - d. Anti-GBM disease

3. Which of the following is associated with a Shiga-toxin producing strain of *E. coli*?
 - a. Microangiopathic hemolytic anemia
 - b. Typical hemolytic-uremic syndrome
 - c. Atypical hemolytic-uremic syndrome
 - d. Thrombocytopathic thrombocytopenic purpura

4. Which of the following is not considered a primary feature of renal dysplasia?
 - a. Persistent mesenchyme
 - b. Hydronephrosis
 - c. Fetal glomeruli
 - d. Presence of cartilaginous or osseous metaplasia

5. Which of the following is a common cause of renal dysplasia in humans?
 - a. p53 mutation
 - b. In utero trauma
 - c. Abnormal placement of the ureter during development
 - d. Cox-2 mutation

Please email your completed assessment to Ms. Jessica Gold at Jessica.d.gold2.ctr@mail.mil for grading. Passing score is 80%. This program (RACE program number) is approved by the AAVSB RACE to offer a total of 0.5 CE Credits, with a maximum of 12.5 CE Credits being available to any individual Veterinary Medical Professionals for the 2017-2018 Wednesday Slide Conference. This RACE approval is for the subject matter categories of: SCIENTIFIC using the delivery method of NON-INTERACTIVE DISTANCE. This approval is valid in jurisdictions which recognize AAVSB RACE; however, participants are responsible for ascertaining each board's CE requirements. RACE does not "accredit", "endorse" or "certify" any program or person, nor does RACE approval validate the content of the program.

Please email your completed assessment to Ms. Jessica Gold at Jessica.d.gold2.ctr@mail.mil for grading. Passing score is 80%. This program (RACE program number) is approved by the AAVSB RACE to offer a total of 0.5 CE Credits, with a maximum of 12.5 CE Credits being available to any individual Veterinary Medical Professionals for the 2017-2018 Wednesday Slide Conference. This RACE approval is for the subject matter categories of: SCIENTIFIC using the delivery method of NON-INTERACTIVE DISTANCE. This approval is valid in jurisdictions which recognize AAVSB RACE; however, participants are responsible for ascertaining each board's CE requirements. RACE does not "accredit", "endorse" or "certify" any program or person, nor does RACE approval validate the content of the program.

**Joint Pathology Center
Veterinary Pathology Services**



WEDNESDAY SLIDE CONFERENCE 2018-2019

C o n f e r e n c e 5

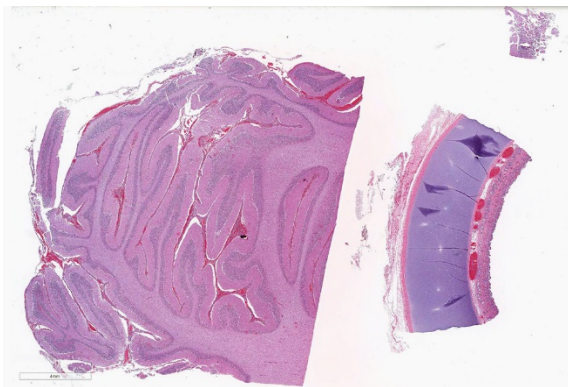
26 September 2018

CASE I: 1505184 (JPC 4066664-00).

Signalment: 14-month-old Holstein heifer.

History: Two 14-month-old Holstein heifers were presented to the large animal clinic as representatives from a heard outbreak, which affected five other heifers on the farm who had more severe signs and had subsequently died or were euthanized. This heifer (heifer A) died immediately prior to transit to the clinic, and had no known clinical signs. Her live herdmate (heifer B) had a 2-week-duration of clinical signs of unthriftiness, oral and cutaneous ulcers with ptyalism, and ocular signs including squinting, epiphora, and corneal ulcers. On physical exam, this heifer B was tachycardic and tachypneic with a rectal temperature of 103° Fahrenheit and generalized peripheral lymphadenomegaly. Heifers involved in the outbreak were also reported to have had cloudy eyes and appeared to be blind. Also housed in close physical proximity to the heifer herd were 5 sheep that had recently lambed. No treatments were performed at this time, and due to suspicion for malignant catarrhal fever, the live herdmate was euthanized without further clinical diagnostics or treatment.

Gross Pathology: Autopsy of the euthanized herdmate (heifer B) revealed severe crusting and ulcerative dermatitis and stomatitis including the following locations: perineal/perivulvar, periocular, mammary, perinasal/perioral and tongue. In addition, large raised to crateriform ulcers with adherent diphtheritic membranes were present throughout the rumen, as well as generalized lymphadenopathy, splenomegaly and corneal edema. Autopsy of the spontaneously dead heifer (heifer A) revealed meningeal edema and hyperemia with cerebellar coning, consistent with cerebellar



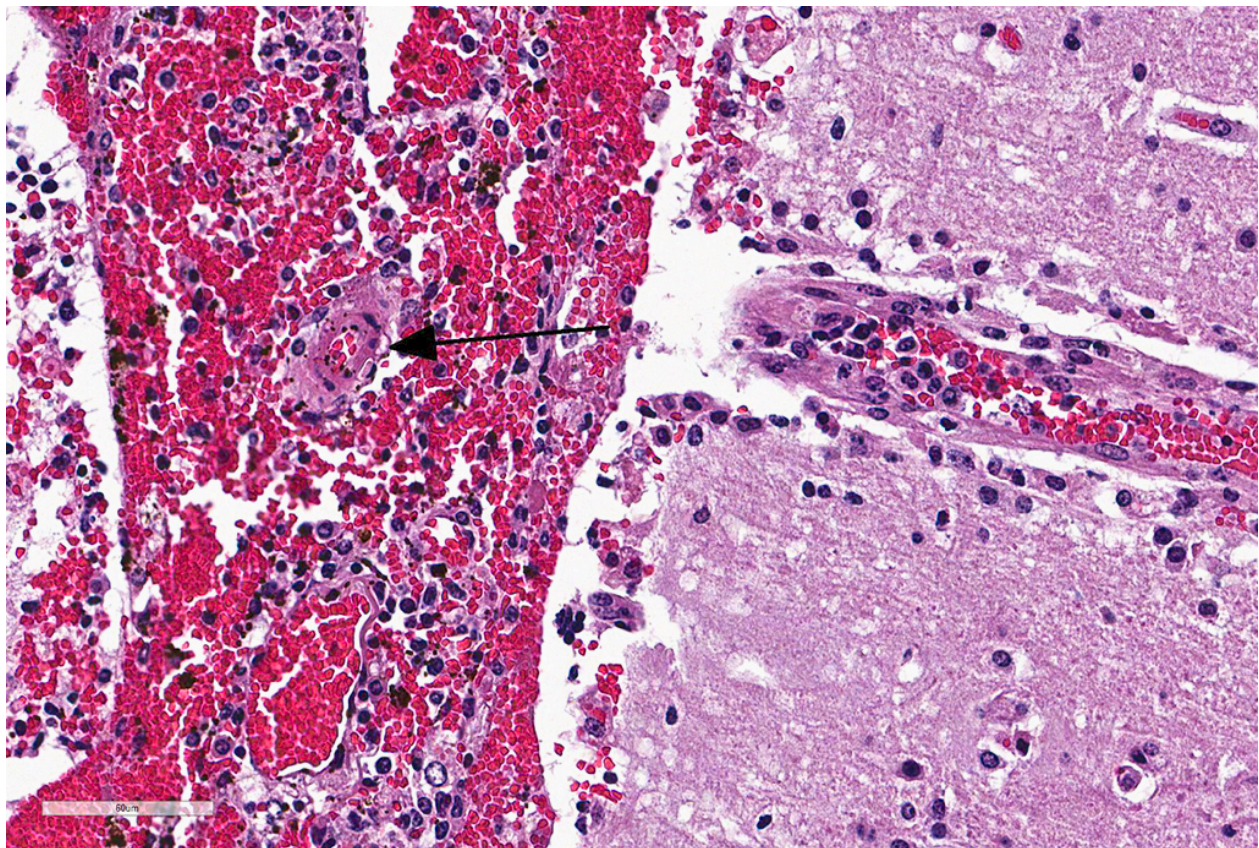
Cerebellum and trachea, ox. Sections of cerebellum and trachea are submitted for examination. Congestion and hemorrhage within the cerebellar leptomeninges as well as the tracheal submucosa are evident at low magnification. (HE, 5X)

herniation. The brain did not autofluoresce under exposure to ultraviolet light.

Laboratory results: A panel including serology and PCR tests was submitted on blood drawn from the live heifer (heifer B) immediately prior to euthanasia. A nested PCR test was positive for ovine herpesvirus-2 malignant catarrhal fever (MCF) virus, and negative for the alcelaphine herpesvirus-1 and 2 MCF viruses. Coronavirus PCR tests performed on intestinal contents were also negative. ELISA serology tests detected antibodies for bluetongue virus; however, PCR tests performed on serum for bluetongue virus were negative. No serum antibodies were detected by ELISA for foot and mouth disease virus, vesicular stomatitis

virus (Indiana or New Jersey strains) or epizootic hemorrhagic disease of deer virus. Virus isolation performed on fresh lung, liver, kidney and spleen sections harvested immediately postmortem were negative for bovine viral diarrhea virus (BVDV) and infectious bovine rhinotracheitis (IBR) virus.

Microscopic Description: Cerebellum, Trachea (heifer A): Within the cerebellar leptomeninges and tracheal mucosa and submucosa, there is marked vasculitis with edema, multifocal to coalescing lymphohistiocytic infiltrates and hemorrhagic foci. The vasculitis is characterized by moderate numbers of lymphocytes, histiocytes, plasma cells and neutrophils that expand the tunica adventitia and transmigrate through the walls

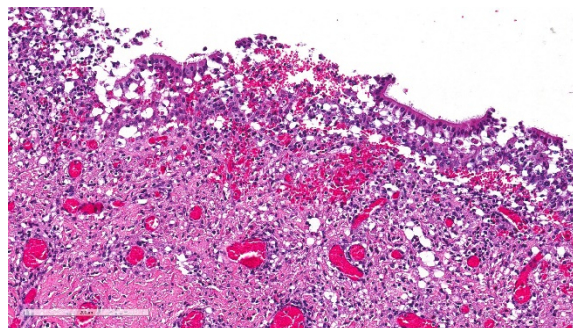


Cerebellum, ox. Higher magnification of the leptomeninges with abundant hemorrhage, and a lymphohistiocytic infiltration which extends down into Virchow-Robin's Space. There is protein and cellular debris in the wall of a small arteriole (vasculitis) and an infiltrate of lymphocytes and plasma cells in the leptomeninges as well as the adjacent Virchow-Robins' space. (HE, 215X)

of varying caliber arterioles and venules. Segments of vascular walls demonstrate pyknosis and karyorrhexis with fibrinoid necrosis and hemorrhagic foci that are also scattered within the cerebellar parenchyma.

Numerous discrete clear vacuoles surround Purkinje cells, which often demonstrate cytoplasmic hypereosinophilia (degeneration). The tracheal mucosal epithelium is multifocally attenuated, with loss of apical cilia, or necrotic and denuded and replaced by eosinophilic and karyorrhectic debris, necrotic neutrophils and extravasated erythrocytes. Similar inflammatory populations surround and infiltrate seromucinous glands.

The kidney and urinary bladder from heifer A had similar vascular changes as described above in addition to multifocal associated interstitial inflammation with tubular necrosis and regeneration in the kidneys, and ulceration of the transitional epithelium of the urinary bladder with submucosal hemorrhage. Similar vascular changes and inflammatory infiltrates were also present in the cutaneous, oral and rumen lesions of heifer B, and the choroid of both eyes. In skin and mucosal lesions, inflammatory infiltrates often extended from the submucosa and dermis into the overlying epidermis/epithelium, occasionally blurring the basement membrane. The epidermis and squamous mucosa of the tongue and rumen frequently contained deep erosions to ulcers covered by waves of serocellular crusts containing colonies of bacteria, grit and fragments of plant material. In other regions there was multifocal keratinocyte necrosis within all layers of the epidermis/epithelium characterized by cytoplasmic hyper-eosinophilia with loss of intercellular desmosomes and pyknosis. Marked paracortical hyperplasia was observed within enlarged peripheral lymph nodes of heifer B.



Trachea, ox. There is segmental necrosis of ciliated epithelium, and infiltration of the mucosa and underlying submucosa with numerous lymphocytes, and fewer histiocytes and neutrophils. There is also submucosal hemorrhage and edema. (HE, 216X)

Contributor's Morphologic Diagnoses:

Cerebellum: Moderate-severe lymphohistiocytic meningitis and segmental necrotizing vasculitis with multifocal acute-subacute hemorrhage.

Trachea: Moderate multifocal acute erosive and ulcerative tracheitis with severe lymphohistiocytic necrotizing vasculitis, perivasculitis and adenitis.

Contributor's Comment: Malignant catarrhal fever (MCF) is a highly fatal lymphoproliferative viral disease reported worldwide affecting many wild and captive species of the order *Artiodactyla*.^{5,9} The MCF virus group comprises ten gamma-herpesviruses, belonging to the recently assigned *Macavirus* genus^{4,6,7}, six of which are naturally pathogenic.^{5,8} These include alcelaphine herpesvirus-1 (AIHV-1), alcelaphine herpesvirus-2 (AIHV-2), ovine herpesvirus-2 (OvHV-2), caprine herpesvirus-2, (CpHV-2), MCF of white-tailed deer (*Odocoileus virginianus*) (MCFV-WTD), and ibex-MCFV. Experimental infection with hippotragine herpesvirus-1 (HipHV-1) in domestic rabbits (*Oryctolagus cuniculus*) is documented, but no natural infections have been reported.^{5,9} Non-pathogenic members include: gemsbok-MCF, muskox-MCF, and aoudad-MCF, also named

after their respective carrier species.^{5,9} Identified natural host species including wildebeest (*Connochaetes taurinus*), domestic sheep (*Ovis aries*), wild and domestic goats (*Capra hircus*) and roan antelope (*Hippotragus equinus*) are a source of infection for susceptible, poorly adapted species such as American bison (*Bison bison*), many cervids, and domestic cattle (*Bos taurus*).

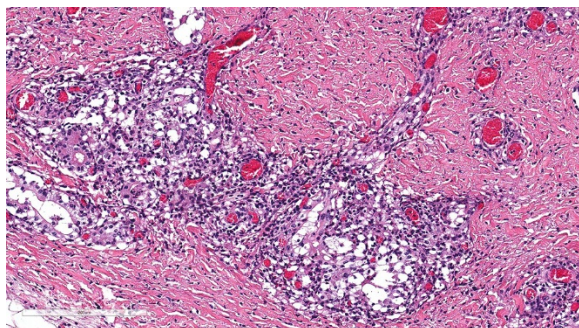
Of paramount economic importance to those managing bison, deer, and exotic game farms, as well as zoological collections, are alcelaphine herpesvirus-1 (AIHV-1) and ovine herpesvirus-2 (OvHV-2), the causative agents of wildebeest-associated MCF (WA-MCF), and sheep-associated MCF (SA-MCF) respectively. Susceptibility to infection by pathogenic MCF viruses and development of disease in non-reservoir hosts varies.⁵ In general, Bali cattle/banteng (*Bos javanicus*), white-tailed deer (*Odocoileus virginianus*), Pere David's deer (*Elaphurus davidianus*), and American bison are highly susceptible to disease following infection; water buffalo (*Bubalus bubalis*), and many cervids are intermediately susceptible; domestic cattle and pigs (*Sus scrofa*) are mildly susceptible; and fallow deer (*Dama dama*) are resistant.^{5,9} Additionally, laboratory animals such as rabbits (*Oryctolagus cuniculus*) and hamsters (*Mesocricetus auratus*) are susceptible to experimental infection.⁵

The clinical signs associated with WA-MCF and SA-MCF are indistinguishable.^{5,9} In most cases, animals present with fever, depression, anorexia, and a constellation of clinical signs, termed the "head and eye" form, which includes: oral mucosal ulcers, ptyalism, oculonasal discharge, dyspnea, corneal edema, hypopyon and photophobia. Additionally, dysentery, profuse catarrhal and mucopurulent nasal discharge and

generalized lymphadenopathy are characteristic of the intestinal form, and severe nasal mucosal inflammation and hemorrhagic gastroenteritis are characteristic of the peracute form. Hematuria, stranguria, and convulsions can also be seen.⁹ In cattle infected with OvHV-2, there is usually an acute onset of clinical signs, but experimental studies show that some animals may present with disease months after infection.⁹

Bison are 100 times more likely to become infected, and 10,000 times more susceptible to developing MCF than cattle⁵, but experimentally-induced MCF with OvHV-2 in bison yields milder clinical signs (oculonasal discharge, peripheral lymphadenopathy) and vascular lesions (arteritis, phlebitis) than in cattle.⁹ CpHV-2 harbored asymptotically in wild and domestic goats infects many species of deer and manifests usually as chronic weight loss, dermatitis and alopecia.⁵ Goats also harbor OvHV-2, and may be the source of infection for white-tailed deer in MCFV-WTD, which is now known to affect other cervids such as the red brocket deer (*Mazama americana*).⁵ CpHV-2 has also been linked to a recent report of MCF in a captive pudu (*Pudu puda*). It is important to note that viral shedding of OvHV-2 and AIHV-1 does not occur in clinically infected susceptible hosts^{5,9}, so an infected animal is not a threat to its herd mates.

Common histopathological findings include: mononuclear mucosal inflammation and necrosis in the gastrointestinal tract, respiratory tract and skin; lymphocytic arteritis/phlebitis and perivasculitis in several tissues; lymphoid hyperplasia (paracortical and interfollicular); and panophthalmitis. Other distinguishing histologic features of MCF in American bison are



Trachea, ox. There is diffuse necrosis of submucosal gland and infiltration by numerous neutrophils and perivascular accumulation of lymphocytes. (HE, 188X)

degeneration and apoptosis of urothelium and hemorrhagic cystitis.⁹ In cervids, most notably sika deer (*Cervus nippon*), granulomatous hyperplastic dermatitis and mural to perforating folliculitis are also seen. Widespread necrosis, intracytoplasmic viral inclusions and formation of syncytia, typical of herpesviral infections, are not observed in MCF.

Differential diagnoses include: mucosa! disease/bovine viral diarrhea virus (BVDV), infectious

bovine rhinotracheitis (IBR), bluetongue virus, epizootic hemorrhagic disease, vesicular stomatitis, foot and mouth disease, rinderpest, and photosensitization. In this case, the clinical history, gross and histologic lesions, and positive PCR and serology tests confirmed Ovine herpesviral-2 associated MCF. Ancillary diagnostic tests in conjunction with histologic lesions allowed rule-out of the other differential etiologies listed above. Although the heifer had antibodies against Bluetongue virus, the negative PCR test was most consistent of prior exposure to the virus, but not active infection. Definitive diagnosis requires a combination of clinical signs in conjunction with positive serological test and/or confirmation with virus DNA detection in fresh or fixed tissue. This is due to the fact that infected, highly susceptible hosts may

have negative titers, and that low levels of OvHV-2 have been detected in clinically healthy cattle.^{5,9}

Key similarities and differences in transmission between alcelaphine and ovine gammaherpesvirus infections in reservoir hosts are listed below.^{5,9}

AIHV-1:

- Harbored in wildebeest as lifelong asymptomatic infection.
- Vertical and horizontal transmission is possible, though most infections are transmitted horizontally.
- Newborn calves are infected and continuously shed virus via ocular and nasal secretions. Viral shedding declines after about 3 months. Outbreaks in susceptible hosts are usually a seasonal phenomenon, corresponding to calving season in reservoir hosts.

OvHV-2:

- Harbored in sheep (and goats) as lifelong asymptomatic infection.
- Transmission via placenta or through milk/colostrum is rare, most infections transmitted horizontally.
- Lambs are born uninfected. Most are infected by 2 months of age from carrier adults. 6-9-month adolescents are responsible for most viral shedding predominantly via nasal secretions. Uninfected lambs remain susceptible to infection as adults.
- Sporadic outbreaks in susceptible hosts as well as seasonal outbreaks corresponding to calving season in carrier hosts.

Most of our understanding of MCF is derived from in vitro studies of AIHV-1, WA-MCF.^{5,12}

Though OvHV-2 has yet to be cultured in vitro, the discovery that OvHV-2 viral particles are shed copiously in sheep nasal secretions has helped elucidate the pathogenesis of SA-MCF, and will be the focus of this discussion. We now know that the pathogenesis of OvHV-2 infection in sheep (the natural host) involves a 3-stage replication cycle, characterized by entry and initial replication in the lung, maintenance with latent infection in lymphocytes, and exit via replication and shedding in nasal mucosal epithelium.⁵ This differs from the 2-stage replication cycle in susceptible hosts with only entry, and maintenance (with latent and lytic viral replication), and no viral shedding.⁵

In general, sheep are better adapted to controlling the initial respiratory infection with OvHV-2, as evidenced by a significant increase in the level of expression of multiple immune-related genes when compared to susceptible species like bison and rabbits, who seem to have a less effective initial immune response in the lung.^{5,9} The products of the following viral genes are used to determine infection patterns in OvHV-2: open reading frame (ORF) 25 (a major capsid protein associated with lytic viral replication), ORF73 (a latency-associated nuclear antigen), ORF50 (R-transactivator that induces latent to productive cell cycle switch), and ORF9 (a DNA polymerase)^{5,9}

In sheep, lytic replication in the lower respiratory tract after initial infection is associated with detection of ORF25 transcripts. This is followed by a change in viral tropism from alveolar epithelial cells to lymphoid cells, and subsequent dissemination of latently infected T-lymphocytes. Although viral DNA may be detected in many tissues in sheep, ORF25 transcripts are rarely detected, indicating the

prevalence of a latent stage in tissues in the natural host.⁵ Although mechanisms of reactivation are unclear, shedding following reactivation occurs in the nasal mucosal epithelium.⁵ Conversely, in MCF-susceptible species such as bison and rabbits infected with OvHV-2, dissemination occurs with a latent and lytic pattern of viral gene expression, with viral gene transcripts ORF25, 50 and 73 detected in multiple organs during MCF disease.⁵ Systemic viral lytic replication is positively associated with severe illness in OvHV-2 infection as evidenced in bison and rabbits with SAMCF.⁵ In contrast to OvHV-2, studies with AIHV-1 infection in rabbits (a susceptible species) indicate that the virus is not productive during MCF disease, with low expression of viral genes (< 10% of viral genome) and very low detection of viral particles in tissues.¹⁰ Palmeira et al. (2013) confirmed the expression of ORF73 (the latency-associated nuclear antigen) during active MCF disease, without detectable expression of other ORF genes necessary for viral production, giving supportive evidence that active WA-MCF disease occurs with a latent viral infection. These findings were further confirmed when experimental nebulization of rabbits with an ORF73-deleted recombinant virus, showed effective initial host infection *without* the development of MCF lesions. Since it was also demonstrated at this time that AIHV-1 ORF73-null viral infection elicits an antibody response, this null-virus is currently being explored as a potential candidate for vaccine development.¹⁰

In susceptible host species, lesions are associated with multisystemic lymphohistiocytic vasculitis and vascular necrosis, producing multiorgan inflammation, hemorrhage and ulcers. It is controversial whether the lympho-proliferation that results in generalized lymphadenopathy and

immunosuppression is a direct result of viral infection of T lymphocytes, or a triggered dysregulation of uninfected I- lymphocytes.⁵ In MCF disease, cytotoxic T lymphocytes are the incriminated cell type in vascular lesions.^{5,11} In OvHV-2, CD8+ perforin+ cytotoxic T cells

as well as CD4+ perforin- regulatory T-cells and B-cells, are involved in vascular lesions.^{5,8}

IL-10, *TNF α* , IFN γ , and IL-4 are demonstrated, with no expression of IL-1~ and IL-2 in OvHV-2 cell lines.⁵ In AIHV-1, CD3+ CD8+ CD4-cytotoxic T-cells with increased expression of activated surface markers CD25 and CD44, high levels of IFN γ , and perforin, and reduced levels IL-2 are characteristic.^{4,5} It appears that suppression of IL-2 production and signaling, and thus, suppression of immune regulation is common to the pathogenesis of disease in both ALHV-1 and OvHV-2 MCF infections.⁵

Interestingly, in a recent study of OvHV-2 in bison, cytoplasmic ORF25 protein was demonstrated in perivascular fibroblasts, with no detection in endothelium, vascular leiomyocytes or transmigrating leukocytes, presenting yet another potential avenue for the pathogenesis of vascular lesions in MCF.⁷

The lesions in these two heifers included a wide spectrum of clinical signs, as well as gross and histologic lesions seen with MCF disease, including cutaneous, gastrointestinal (tongue and rumen), urinary, respiratory, ocular and neurologic manifestations. This herd outbreak serves as a reminder of the various forms of MCF, the importance of biosecurity regarding separation of ruminant species in a production operation, and emphasizes the multiple modalities required to make a definitive etiologic diagnosis.

JPC Diagnosis: 1. Cerebellum: Vasculitis, necrotizing and lymphocytic, multifocal, moderate, with hemorrhage, neuronal

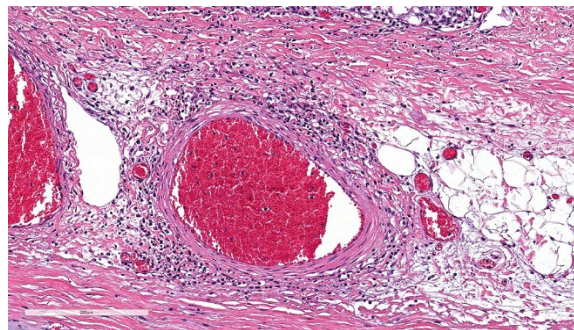
necrosis, and diffuse lymphohistiocytic meningitis.

2. Trachea: Vasculitis, necrotizing and lymphocytic, diffuse, moderate, with hemorrhage and mucosal and submucosal gland necrosis.

Conference Comment: The contributor has done an excellent job summarizing the condition known as malignant catarrhal fever, from species affected, basic pathogenesis, and molecular aspects of this disease.

American bison are considered one of the most sensitive species to the various viruses which may cause MCF, particularly that of OHV-2. Dr. Donal O'Toole has written and published extensively on this topic^{7,8,9}, and his comments certainly bear summarization for this species, one of the U.S. most majestic symbols.

Bison with MCF due to OvHV-2 are most often found dead or dying, due to the large size of bison pastures and the inherent difficulties in patrolling these large areas of land. Mortality among bison heard approaches 100%, especially in those in feedlots. Some feedlots experience up to 75% of all deaths as a result of MCF. Aerosol transmission is an important route of exposure between bison in sheep, especially in sale barns.⁹



Trachea, ox. Submucosal arterioles often are surrounded by a lymphocytic infiltrate.

Acute clinical disease in bison predominates over subclinical and chronic forms. In natural outbreaks, preclinical pneumonia is inconspicuous or may be masked by aspiration pneumonia of the clinical disease. Characteristic gross findings in terminal animals include oculonasal discharge, hemorrhagic cystitis, necrohemorrhagic typhlocolitis, ulcerative rhinitis, stomatitis, pharyngitis, laryngitis, and esophagitis.⁹ Abortions may also occur. Due to its prevalence in affected animals and rarity in other conditions, hemorrhagic cystitis may be used by owners in making a provisional diagnosis of this condition. Generalized lymph node hyperplasia is usually present, but rarely as pronounced as in cattle. Ulceration in the forestomachs and alimentary tract is common. Traumatic lesions due to goring may be seen and may be incorrectly assumed to be the sole cause of illness.

Histologic lesions are similar to that discussed with cattle; in addition, degeneration of urothelium is a consistent and helpful feature in fresh carcasses. Fibrinoid necrosis is less common in bison than in cattle. Myocardial necrosis may be seen in more longstanding cases as a result of exertional myopathy.⁹

Sampling for OHV-2 is occasionally problematic as the distribution of OHV-2 antigen may not necessarily reflect the pansystemic nature of disease. Sampling a minimum of 2 tissues, both lymphoid and nonlymphoid is recommended, and OHV-2 DNA may also be found in peripheral blood of clinically healthy bison. Interestingly in spite of the widespread and often severe lesions, no viral particles are detectable ultrastructurally, and the expression of viral antigens in tissue is limited. It is generally assumed that the small fraction of infected lymphocytes induces proliferation and

deregulation of uninfected cells, which may induce lesions due to non-specific cytotoxic effects.⁹

Contributing Institution:

University of Pennsylvania, School of Veterinary Medicine, Department of Pathobiology
<http://www.vet.upenn.edu/research/academic-departments/pathobiology/pathology-toxicology>

References:

1. Ackermann, M et al. Pathogenesis of gammaherpesvirus infections. *Vet Micro* 2006; 153(3): 211-222.
2. Cunha, CW et al. Antibodies to ovine herpesvirus 2 glycoproteins decrease virus infectivity and prevent malignant catarrhal fever in rabbits. *Vet Micro* 2012; 175(2):349-355.
3. Cunha, CW et al. Ovine herpesvirus 2 infection in American bison: virus and host dynamics in the development of sheep-associated malignant catarrhal fever *Vet Micro* 2012; 159(3):307-319.
4. Dewals, B. "Malignant catarrhal fever induced by Alcelaphine herpesvirus I is characterized by an expansion of activated CD3 CD8 CD4-T cells expressing a cytotoxic phenotype in both lymphoid and non-lymphoid tissues." *Vet Res* 2011; 22:42-95.
5. Li, Hong, et al. Malignant Catarrhal Fever: Inching Toward Understanding *Ann Rev Anim Biosci* 2014; 2(1):209-233.
6. Modesto P et al. First report of malignant catarrhal fever in a captive pudu (*Pudu pudu*). *Res Vet Sci* 2015; 99: 212-214.
7. Nelson, DD et al. Fibroblasts express OvHV-2 capsid protein in vasculitis lesions of American bison (*Bison bison*) with experimental sheep-

- associated malignant catarrhal fever. *Vet Micro* 2013; 166(3): 486-492.
8. Nelson, DD et al. "D8+/perforin+/WCl- γ T cells, not CDS+ α - T cells, infiltrate vasculitis lesions of American bison (*Bison bison*) with experimental sheep-associated malignant catarrhal fever." *Vet Immunol and Immunopathol* 2010; 136(3):284-291
 9. O'Toole, D, Li, H. The pathology of malignant catarrhal fever, with an emphasis on ovine herpesvirus-2. *Vet Pathol* 2014; 51(2):437-452.
 10. Palmeira L et al. "An essential role for γ -herpesvirus latency-associated nuclear antigen homolog in an acute lymphoproliferative disease of cattle. *Proc Nat Acad Sci* 2013; 110(21): E1933-E1942.
 11. Simon S, et al. The vascular lesions of a cow and bison with sheep-associated malignant catarrhal fever contain ovine herpesvirus 2-infected CDS+ T lymphocytes. *J Gen Virol* 2003; 84(8):2009-2013.
 12. Taus, NS et al. Malignant catarrhal fever in American bison (*Bison bison*) experimentally infected with alcelaphine herpesvirus 2." *Vet Microbiol* 2014; 172(1):318-322.
 13. Vikoren T et al. A geographic cluster of malignant catarrhal fever in moose (*Alces alces*) in Norway. *J Wildl Dis* 2015; 51(2):471-474.

CASE II: S1408459 (JPC 4066395-00).

Signalment: An aborted Angus bull calf, *Bos taurus*, bovine

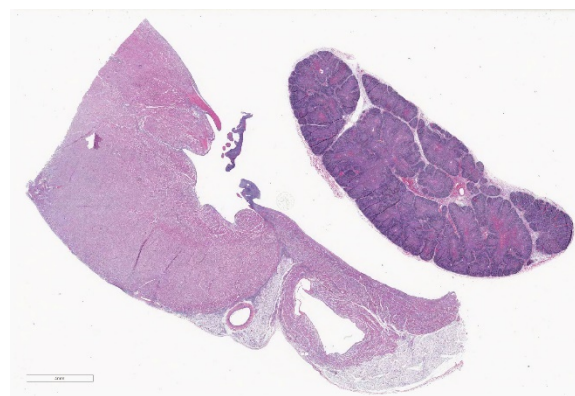
History: An aborted Angus bull calf of approximately 6 month gestation; second first time heifer to have aborted fetus on the previously non-grazed ranch.

Gross Pathology: A 10.56 kg Angus bull calf fetus with crown-to-rump length of 54 cm and in good post-mortem state. Lung lobes were diffusely red and samples sank in 10% formalin [non-inflated lung]. The liver weighed 0.84 kg, was deep red-brown, nodular, markedly enlarged with rounded margins, and had a cobblestone appearance with multiple, pinpoint white foci scattered throughout. Spleen and thymus were markedly enlarged and diffusely lymph nodes were enlarged and prominent.

No gross lesions / abnormalities were noted in other viscera, brain, umbilicus, cranial vault and in bones and joints of all limbs. Placenta was not submitted.

Laboratory results: Tissues tested negative for multiple agents on a full bovine abortion panel which included *Leptospira* sp., *Salmonella* sp., *Campylobacter* sp., *Brucella* sp., bovine herpes virus 1, and bovine viral diarrhea virus [BVDv]. Liver minerals including selenium were within acceptable concentrations.

Submitted dam serum had marginally low magnesium levels, and was negative for antibodies to *Leptospira* spp., BVDv-1,



Heart and thymus, aborted calf: There is multifocal thymic hemorrhage (incidental), and a cellular infiltrate can be seen within the myocardium and epicardium and infiltrating epicardial fat. (HE, 5X)

BVDv-2, BHV-1, *Neospora caninum* and *Brucella abortus*.

Microscopic Description: Slides contain a section each of thymus and heart.

Thymus: There is marked depletion of cortical thymocytes affecting most if not all follicles, scattered foci of lymphocytolysis, marked histiocytic infiltration of the medulla and septa with occasional giant cell formation, and focal interlobular hemorrhages.

Heart: There are mild to moderate histiocytic infiltrates and fewer numbers of lymphocytes and plasma cells around small and medium caliber vessels throughout the epicardium, myocardium and epicardial fat.

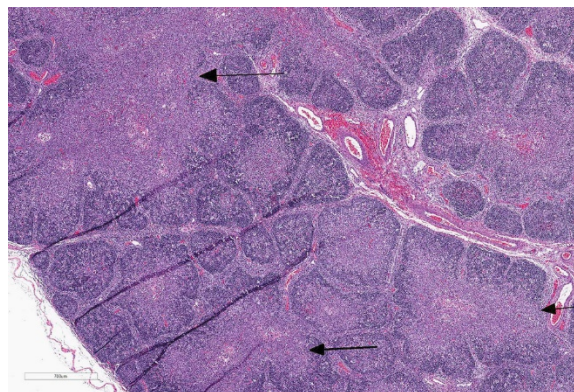
Other findings: Mild to marked perivascular [vasculitis] and interstitial predominantly histiocytic infiltrates [fewer lymphocytes and plasma cells] in brain, lung, liver, kidney, spleen, lymph node, intestine, diaphragm, adrenal gland, and urinary bladder. There was marked lymphoid hyperplasia in spleen and lymph nodes in addition to infiltration by macrophages. Tissues were negative for *Mycobacterium* sp. on acid-fast stains.

Contributor's Morphologic Diagnoses:

Thymus: Thymitis, histiocytic to granulomatous, marked, diffuse with loss of cortical thymocytes and lymphocytolysis, consistent with epizootic bovine abortion.

Heart: Vasculitis, histiocytic and lymphoplasmacytic, multifocal, moderate.

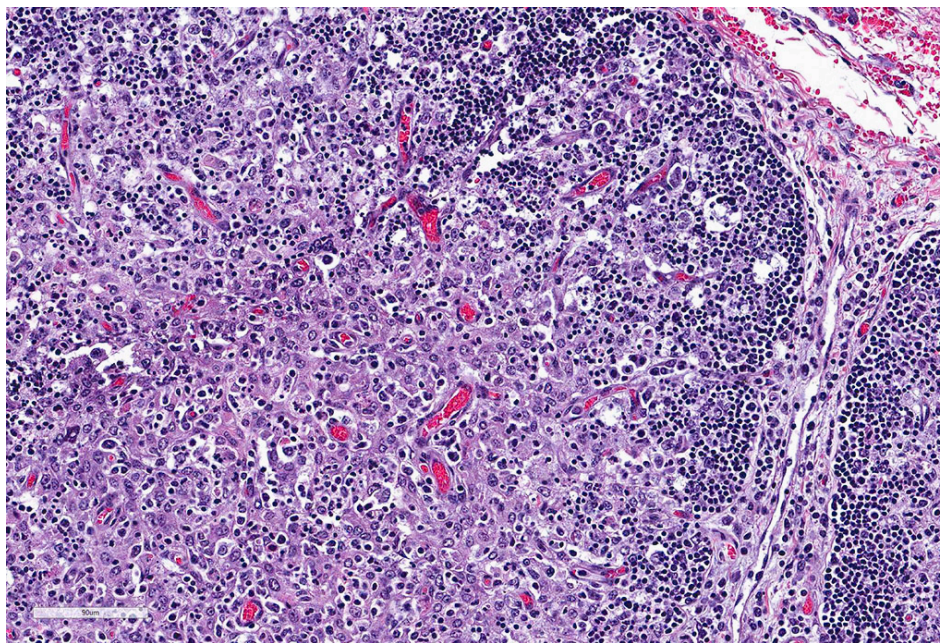
Contributor's Comment: Lesions are similar in submitted slides though there may be some variation in severity and extent. The clinical history, gross findings and microscopic lesions particularly those noted in the thymus, spleen and lymph nodes are



Thymus, aborted calf: The thymic medulla is markedly expanded by an infiltrate of large numbers of macrophages (arrows). (HE, 32X)

considered characteristic of epizootic bovine abortion [EBA].

EBA, also known as foothill abortion, is a tick-borne infection of cattle that results in late term abortions of fetuses, stillbirths, or the birth of weak calves. The name of the disease is misleading given that the disease is endemic, and distribution is confined to the range of the vector, the argasid tick *Ornithodoros coriaceus*, which includes foothills of California, and adjacent states of Nevada, Oregon and Northern Mexico.^{1,6,13} The tick is thought to transmit the agent from deer to cattle, and naïve cattle i.e. first time heifers or pregnant cows mainly beef cattle grazing for the first time in a tick-infested area, are primarily at risk.^{7,10} Infection from dam to fetus commonly occurs at 2-6 months gestation resulting in chronic disease in the fetus.⁷ The etiologic agent of EBA (aoEBA) has been identified as a novel organism in the



Heart and thymus, aborted calf: Higher magnification of the numerous macrophages infiltrating the thymic medulla. (HE, 320X)

class Deltaproteobacteria in the order *Myxococcales*.¹⁰

Clinical findings include petechial hemorrhages of conjunctiva, tongue, oral mucous membranes and tracheal mucosa, palpable lymph nodes, and often ascites. Grossly there is splenomegaly, lymphadenomegaly, enlarged nodular liver, and enlarged thymus with hemorrhages.^{1,7,9}

Microscopic lesions consist of marked lymphoid hyperplasia of lymph nodes and spleen accompanied by mononuclear, predominantly histiocytic, infiltration of medulla and sinuses. Histiocytes diffusely infiltrate medulla and septae of the thymus, and are present around vessels in multiple organs sometimes with giant cell formation.^{1,7,8,11} Bacterial rods, 1.5 to 3 μm long can often be seen in cytoplasm of histiocytes using Steiner's silver stains, and there is positive cytoplasmic EBA immunohistochemical staining confined to foci of inflammation in multiple tissues.¹

Diagnosis is based on compatible clinical history, gross and microscopic lesions, elevated fetal immunoglobulins particularly IgG, and exclusion of other agents commonly associated with bovine abortion.^{2,3}

Supplemental diagnostic tests to identify agent in tissues include histochemical [Steiner's silver] and immunohistochemical stains,¹ and TaqMan

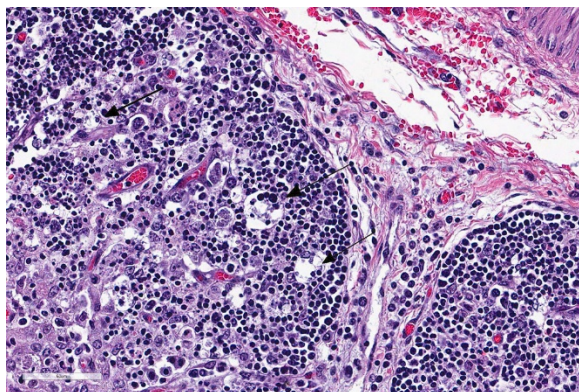
polymerase chain reaction.^{4,10}

Successful transmission of the disease has been achieved by inoculation of thymus from EBA-positive fetuses in naïve pregnant cows¹², and viability of the agent had been proved following serial passages and propagation of deltaproteobacterium in immunodeficient mice.² While the tick *O. coriaceus* is identified as the known vector for the deltaproteobacterium, co-infection of the tick with *Borrelia coriaceae* has been reported, and antibody cross-reaction with *Borrelia* spp. in fetal tissues is possible.¹⁴

JPC Diagnosis: 1. Thymus: Fine mild tenderness, granulomatous, diffuse, marked, with marked lymphoid depletion.

2. Heart: Pancarditis, granulomatous, diffuse, mild.

Conference Comment: Since the submission of this case in 2015, additional characterization of this agent and a name change has occurred. The organism is



Thymus, aborted calf: The cortex is markedly depleted, with lymphocyte karyorrhexis and tingible body macrophages (HE, 400X)

currently identified as *Pajaroellobacter abortibovis*, after the Pajaroello tick, (*Ornithodoros coriaceus*) which transmits the disease (and which was identified as the vector in 1976). The name “Pajaroello” (pa-har-way”-o) comes from the Spanish “paja” meaning straw and “huello” meaning the underside of a hoof, is also called to the grayback or leatherback tick, and is found only in California and Mexico extending from Humboldt County on the north to the Mexican isthmus of Tehuantepec.⁷

Phylogenetic characterization of this yet-to-be-cultured bacterium is currently based on analysis of the 16S ribosomal RNA gene, which places the bacterium in the order Myxococcales, suborder Sorangiineae, family Polyangiaceae and the bacterium is most closely related to *Sorangium cellulosum*.⁵ Modified Gram staining, combined with transmission electron microscopy, provides strong evidence that the bacteria is gram-negative.⁵ PCR analysis has demonstrated *P. abortibovis* to be a myxobacterium a member of a family of gram-negative rods typically inhabiting soil. These bacteria are referred to as “gliding” bacteria as many produce a polysaccharide slime layer to aid in their motility.⁵ Its most closely related relative, *S. cellulosum* carries the largest genome of any known bacterium.

In addition, its 16S ribosomal sequence establishes a distant connection to another deltaproteobacterium, *Lawsonia intracellularis*.⁵

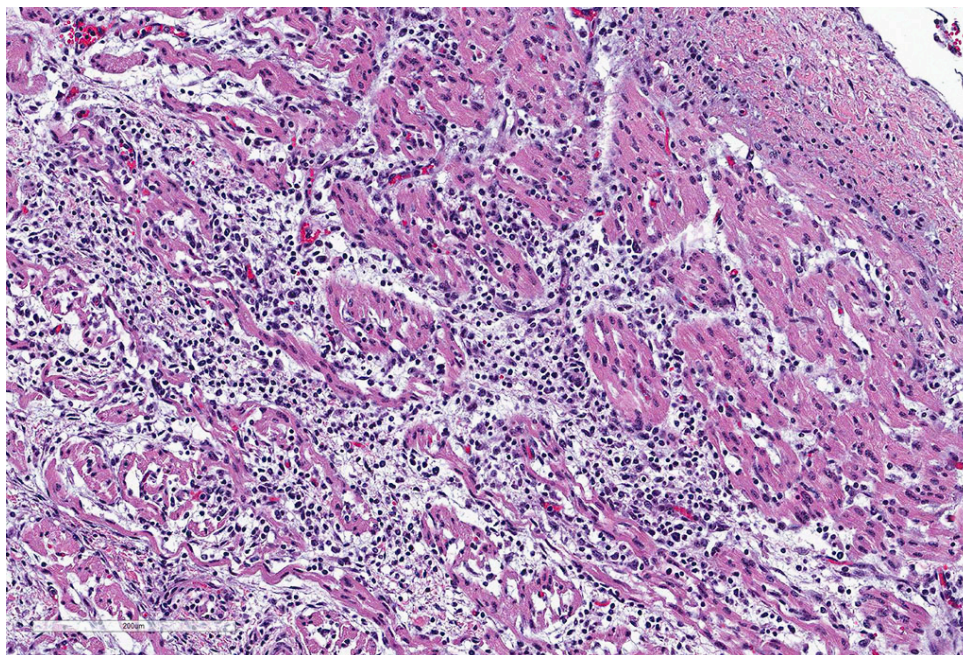
Interestingly, the bite of the pajaroella tick (*Ornithodoros coriaceus*) has for many years been the subject of much misinformation and great myth. “A bite more severe to than that of the rattlesnake” is largely the product of the overactive imagination of the lay press, with hyperbolic early reports describing the bite as “intolerably sharp and painful... with intermittent irritation, irritability, and numbness” persisting for weeks to months. Local folklore in one area reported that “three bites would result in certain death.”⁷ The truth of the matter is that the macule or papule resulting from the bite of this tick is similar grossly and histologically to those of other ticks of a similar size.⁷

Contributing Institution:

California Animal Health and Food Safety
Laboratory, University of California
Davis, 105 W.
Central Avenue, San Bernardino, CA 92374
<http://www.vetmed.ucdavis.edu/cahfs/>

References:

1. Anderson ML, Kennedy PC, Blanchard MT, et al. Histochemical and immunohistochemical evidence of a bacterium associated with lesions of epizootic bovine abortion. *J Vet Diagn Invest* 2006; 18:76–80.
2. Blanchard MT, Chen C-I, Anderson M, et al. Serial passage of the etiologic agent of epizootic bovine abortion in immunodeficient mice. *Vet Microbiol* 2010; 144: 177-182.
3. Blanchard MT, Anderson ML, Hoar BR et al. Assessment of a fluorescent antibody test for detection of



Heart, aborted calf: There is patchy infiltration of the myocardium and separation of myofibers by moderate numbers of histiocytes and lymphocytes. (HE, 183X).

disease. *Calif Med* 1972; 116(5):16-19.
 8. Foster, RA: Epizootic bovine abortion. In: *Pathologic Basis of Veterinary Disease*, 2007, McGavin MD, Zachary JF, eds., 4th ed., pp.1296, Elsevier, St. Louis, MO.
 9. Hall MR, Hanks D, Kvasnicka W et al. Diagnosis of epizootic bovine abortion in Nevada and identification of the vector. *J Vet Diagn Invest* 2002; 14: 205-210.

- antibodies against epizootic bovine abortion. *J Vet Diagn Invest* 2014; 26: 622-630.
4. Brooks RS, Blanchard MT, Anderson ML, et al. Quantitative duplex TaqMan real-time polymerase chain reaction for the assessment of the etiologic agent of epizootic bovine abortion. *J Vet Diagn Invest* 2011; 23: 1153 – 1159
 5. Brooks RD, Blanchard MT, Clothier KA, fish S, Anderson ML, Stott JL. Characterization of *Pajaroellobacter abortibovis*, the etiologic agent of epizootic bovine abortion. *Vet Microbiol* 2016; 192:73-80.
 6. Chen C-I, et al. Identification of the etiologic agent of epizootic bovine abortion in field-collected *Ornithodoros coriaceus* Koch ticks. *Vet Microbiol* 2007; 120:320-327.
 7. Failing RM, Lyon CB, McKittrick JE. The pajaroello tick bite – the frightening folklore and the mild
 10. King DP, Chen C-I, Blanchard MT, et al. Molecular identification of a novel deltaproteobacterium as the etiologic agent of epizootic bovine abortion (foothill abortion). *J Clin Microbiol* 2005; 43:604–609
 11. Schlafer DH, Miller RB, Epizootic bovine abortion In: *Female genital system. Jubb Kennedy, and Palmer's Pathology of Domestic Animals*, Maxie MG ed., 5th ed., vol 3, pp .510-512, Elsevier , Philadelphia, PA.
 12. Stott JL, Blanchard MT, Anderson M, et al. Experimental transmission of epizootic bovine abortion [foothill abortion]. *Vet Microbiol* 2002; 88: 161-173.
 13. Teglas MB, Drazenovich NL, Stott J, Foley JE: The geographic distribution of the putative agent of epizootic bovine abortion in the tick vector, *Ornithodoros coriaceus*. *Vet Parasitol* 2006; 140: 327-333.

14. Teglas MB, Mapes S, Hodzic E, et al. Co-infection of *Ornithodoros coriaceus* with the relapsing fever spirochete *Borrelia coriaceus*, and the agent of epizootic bovine abortion. *Med Vet Entom* 2011; 25: 337-343.

CASE III: 13749 (JPC 4033383-00).

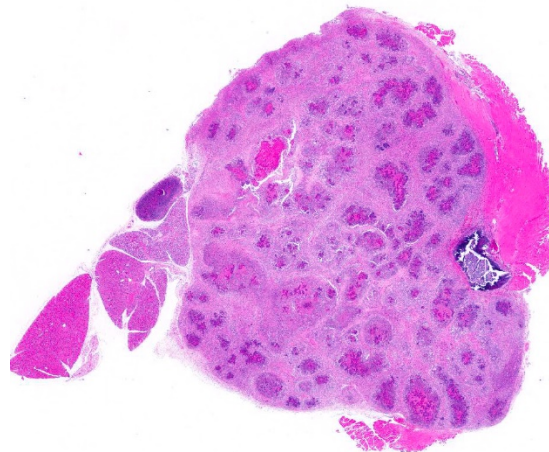
Signalment: 7-month-old B6;129 wild type mice (hybrid C57BL/6J; 129X1/SvJ), male.

History: The mouse belonged to a WT +/+ control group in a study using genetically engineered mice on a B6;129 background. It was euthanatized at the age of 7 months for ethical reasons due to a rapidly growing submandibular mass. No other animal of the study was affected.

Gross Pathology: A multinodular tan mass replaced and destroyed most of the left submandibular salivary gland. After section the mass, measuring 2cmx1cm, appeared encapsulated and filled with white to tan caseous material.

Laboratory results: None provided.

Microscopic Description: The submandibular salivary gland is almost entirely replaced by a well-circumscribed multifocal coalescing inflammatory lesion. Most foci are identical and centered on a core of eosinophilic karyolytic or karyorrhectic necrotic cell debris, pyknotic and karyorrhectic neutrophils (suppuration) and cocci colonies circumscribed by a radiating band of hyaline eosinophilic material (Splendore-Hoeppli phenomenon). A peripheral rim of activated macrophages, epithelioid macrophages, multinucleated giant cells, lymphocytes, fibroplasia and



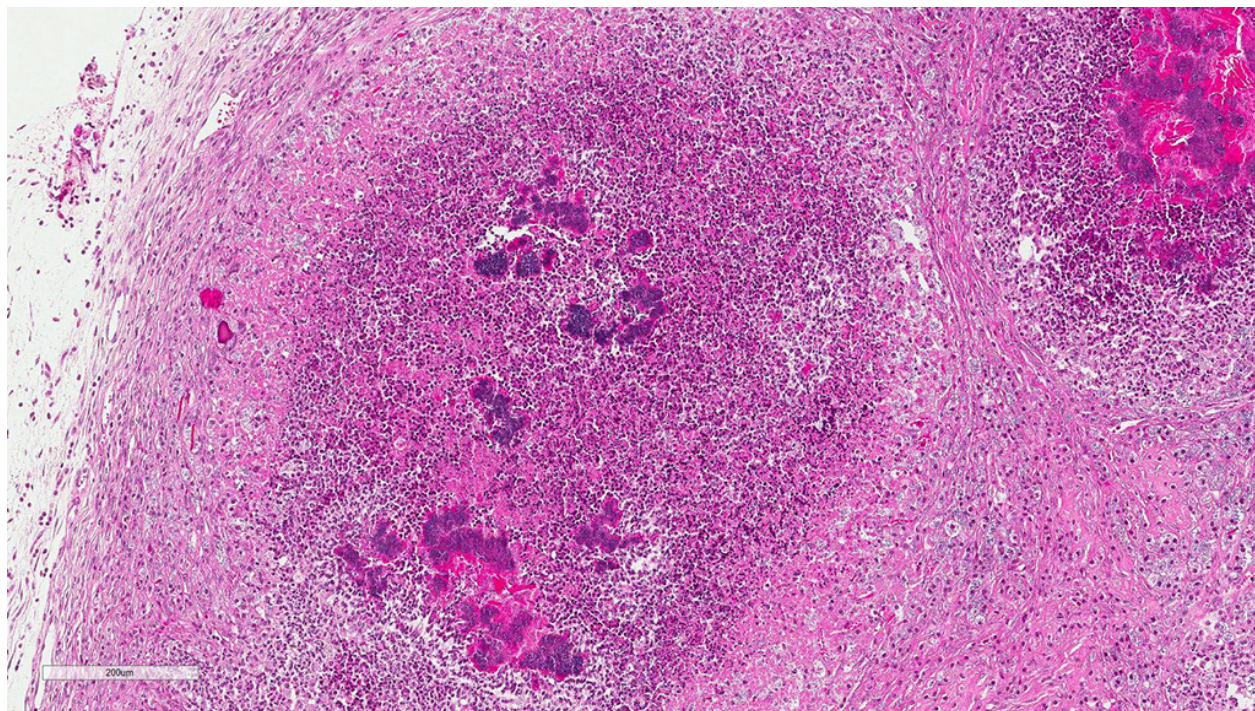
Subcutaneous tissue, mouse: The subcutis ventral to the ear is expanded by numerous coalescing pyogranulomas which infiltrate the adjacent salivary gland and lymph node. (HE, 5X)

fibrosis form the external limit of those pyogranulomas. Macrophages and giant multinucleated cells often display a markedly enlarged cytoplasm filled with myriads of cocci. Those bacteria-filled macrophages are also observed within the fibrotic bands. Necrotic centers display multifocal dystrophic mineralization.

Eosinophilic macrophages and acicular or rectangular eosinophilic birefringent crystals are observed within the pyogranulomas. Crystals are found free in the extracellular space and less commonly in the cytoplasm of activated macrophages and giant cells.

A Gram coloration was performed and revealed the presence of abundant gram-positive cocci, 1 to 2 um in diameter, consistent with staphylococci.

Contributor's Morphologic Diagnoses: 1. Multifocal coalescing chronic pyogranulomatous sialoadenitis with cocci circumscribed by Splendore-Hoeppli phenomenon (botryomycosis).



Subcutaneous tissue, mouse: Pyogranulomas are centered on colonies of cocci which are surrounded by eosinophilic Splendore-Hoeppli material. (HE, 108X)

2. Presence of acicular and rectangular eosinophilic crystals into macrophages, giant cells, and extracellular space.

Contributor's Comment: Botryomycosis is a chronic suppurative infection characterized by a granulomatous inflammatory response to bacterial pathogens; it may present with cutaneous or, less commonly, visceral involvement. The term botryomycosis is derived from the Greek word *botrys* (meaning "bunch of grapes") and *mycosis* (a misnomer, due to the presumed fungal etiology in early descriptions). In Human, the major etiologic agent of botryomycosis is *Staphylococcus aureus* (40%) followed by *Pseudomonas aeruginosa* (20%), *coagulase-negative staphylococci*, *Streptococcus spp*, *Escherichia coli*, and *Proteus spp*¹. The Splendore-Hoeppli phenomenon consists of antigen-antibody precipitates, immunoglobulin G, C3 complement, tissue debris and fibrin¹.

Staphylococci are commensal bacteria that inhabit the skin and mucous membrane and that can become pathogenic under certain circumstances. In the mouse, disease has been associated with *Staphylococcus aureus* and *S. xylosus*, causing necrotizing dermatitis, chronic suppurative infection of cutaneous adnexae, conjunctiva, periorbital tissues, preputial glands and regional lymph nodes². The Splendore-Hoeppli phenomenon is classically observed in staphylococcal lymphadenitis² and in chronic skin infection affecting immune compromised mice such as agammaglobulinemic or nude mice³. Botryoid abscess of a salivary gland is to our knowledge uncommon, especially in immunocompetent mice, and has not yet been documented.

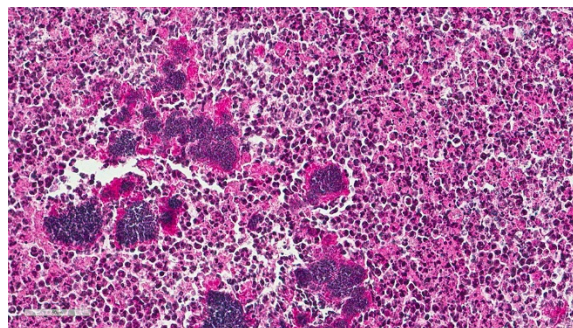
The incidence of eosinophilic crystals is high in aging B6;129 mice, a hybrid background often encountered in studies using genetically engineered mice. It is observed in lungs (36% of males and 65% of females) and nasal

turbinates (4% of males and 12% of females)⁴. The so-called eosinophilic crystalline pneumonia is a major cause of death in 129/SvJ mice and immunohistochemical studies show that crystals are composed predominantly of Ym1 protein, a chitinase-like protein known to be secreted by activated macrophages⁵. In our case, the context of chronic granulomatous inflammation with numerous activated macrophages is very likely the direct cause of Ym1 protein accumulation and crystallization.

JPC Diagnosis: Subcutis: Cellulitis, pyogranulomatous, focally extensive, severe with numerous colonies of cocci, Splendore-Hoeppli material, with mild to moderate granulomatous lymphadenitis and sialoadenitis.

Conference Comment: Botryomycosis is a chronic pyogranulomatous disease which is as well known in mice as it is poorly named. This inflammatory lesion is seen in a wide range of mammals including man, mice, dogs, cattle⁶, swine, apes, and elephants, and likely many other in species. The lesion, which consists of colonies of bacteria surrounded by aggregates of antigen-antibody complexes (known as Splendore-Hoeppli material), goes also by the name of “bacterial pseudomycetoma”, “bacterial pseudomycosis”, “bacterial granuloma”, and “granulomatosis”. It has no connection to fungal infections, other than a passing resemblance to mycetomas, or deep fungal infections which are characterized by “grains”.

Historically, the first cases of botryomycosis were observed in the late 1800s in post-surgical cattle and horses, with the first actual description of botryomycosis in a horse in 1870 by Bollinger. The first human case of botryomycosis was not reported until 1913.



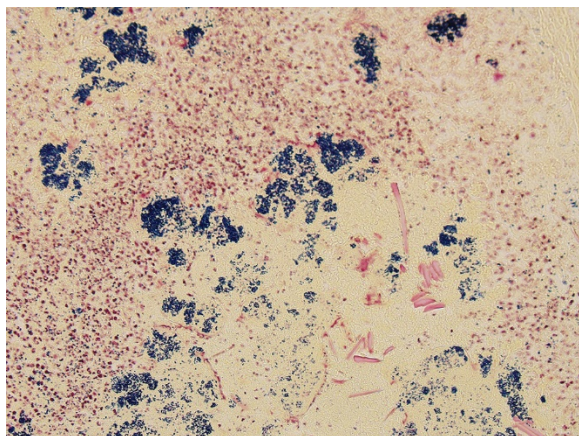
Subcutaneous tissue, mouse: Higher magnification of the center of the pyogranulomas. (HE, 108X)

The causality of *Staphylococcus aureus* and description of Splendore-Hoeppli phenomenon was first made in 1919.⁴

Botryomycosis is an uncommon disease in humans with approximately 200 cases reported to date. Case distribution is worldwide, and the disease predominates 2:1 men with no age predilection. 75% of reported cases are cutaneous, with the rest visceral. Accidental or postoperative skin trauma and altered immune function are considered major contributing factors.⁴

The pathogenesis of botryomycosis in humans and animals has not been explicitly defined, but several factors appear to be necessary. Most causative microorganisms are of low virulence. The contributor lists the commonly implicated organisms (above). Implicated anaerobes include *Propionibacterium acnes* and *Bacteroides* species. Rare causes include *Actinobacillus lignieresii*, *Serratia marcescens*, *Pneumocystis jirovecii*, and *Moraxella* sp.⁴

A wide range of immune dysfunctions have been associated with the development of botryomycosis in humans and animals.⁴ It has been found more often in animals with deficient cellular immune responses including lymphopenia (nude mice) and various hypoglobulinemic syndromes (agammaglobulinemic mice).



Subcutaneous tissue, mouse. A tissue Gram stain demonstrates the gram-positivity of the cocci, as well as highlighting shards of crystalline protein within the pyogranulomas. (Brown-Brenn, 200X)

Cutaneous botryomycosis require skin trauma in most cases, as low-virulence bacteria are generally unable to cross an intact barrier. The inoculum of bacteria must be high enough to evade the body's immediate immune response, yet low enough not to cause massive necrosis or systemic disease. In all but severely immunosuppressed patients, the Splendore-Hoeppli phenomenon (SHP) is present. SHP assists in clustering the bacteria to create a stage of resistance. The major component of SHP is antigen-antibody complexes, but other substances are often present, to include immunoglobulin G, C3 fragments of complement, fibrin, and cellular debris.⁴

Both cutaneous and visceral forms of botryomycosis are well documented in man in animals. In humans, cutaneous forms most often affect exposed parts of the body including the hands, feet, head, and neck. Visceral forms may be seen in almost 10 organs and in humans often accompanies prolonged hospital stays, especially in immunosuppressed patients. The most frequent visceral organs involved are the lungs, and are often associated with patients suffering from cystic fibrosis. HIV/AIDS is also a common predisposing condition.⁴

Contributing Institution:

Department of Pathology, Nantes-Atlantic National College of Veterinary Medicine, Food Science and Engineering - ONIRIS, 44 307 Nantes Cedex 03, France.
www.oniris-nantes.fr

References:

1. Bridgeford EC, Fox JG, Nambiar PR, Rogers A B. Agammaglobulinemia and *Staphylococcus aureus* botryomycosis in a cohort of related sentinel Swiss Webster mice. *J Clin Microbiol* 2006; 46, 1881–1884.
2. Haines DC, Chattopadhyay S, Ward, JM. Pathology of aging B6;129 mice. *Toxicol Pathol* 2001; 29: 653–661 (2001).
3. Hoenerhoff MJ, Starost MF, Ward JM. Eosinophilic crystalline pneumonia as a major cause of death in 129S4/SvJae mice. *Vet Pathol* 2006; 43, 682–688.
4. Padilla-Desgarenes C, Vázquez-González D., Bonifaz A. Botryomycosis. *Clin Dermatol* 2012; 30, 397–402.
5. Percy DH, Barthold SW. Mouse. In *Pathology of Laboratory Rodents and Rabbits* 73–76 (2007).
6. Spagnoli S, Reilly TJ, Calcutt MJ, Fales WH, Kim DY. Subcutaneous botryomycosis due to *Bibersteinia trehalosi* in a Texas longhorn steer. *Vet Pathol* 49(5):775-778.

CASE IV: Case 2 (JPC 4068765-00).

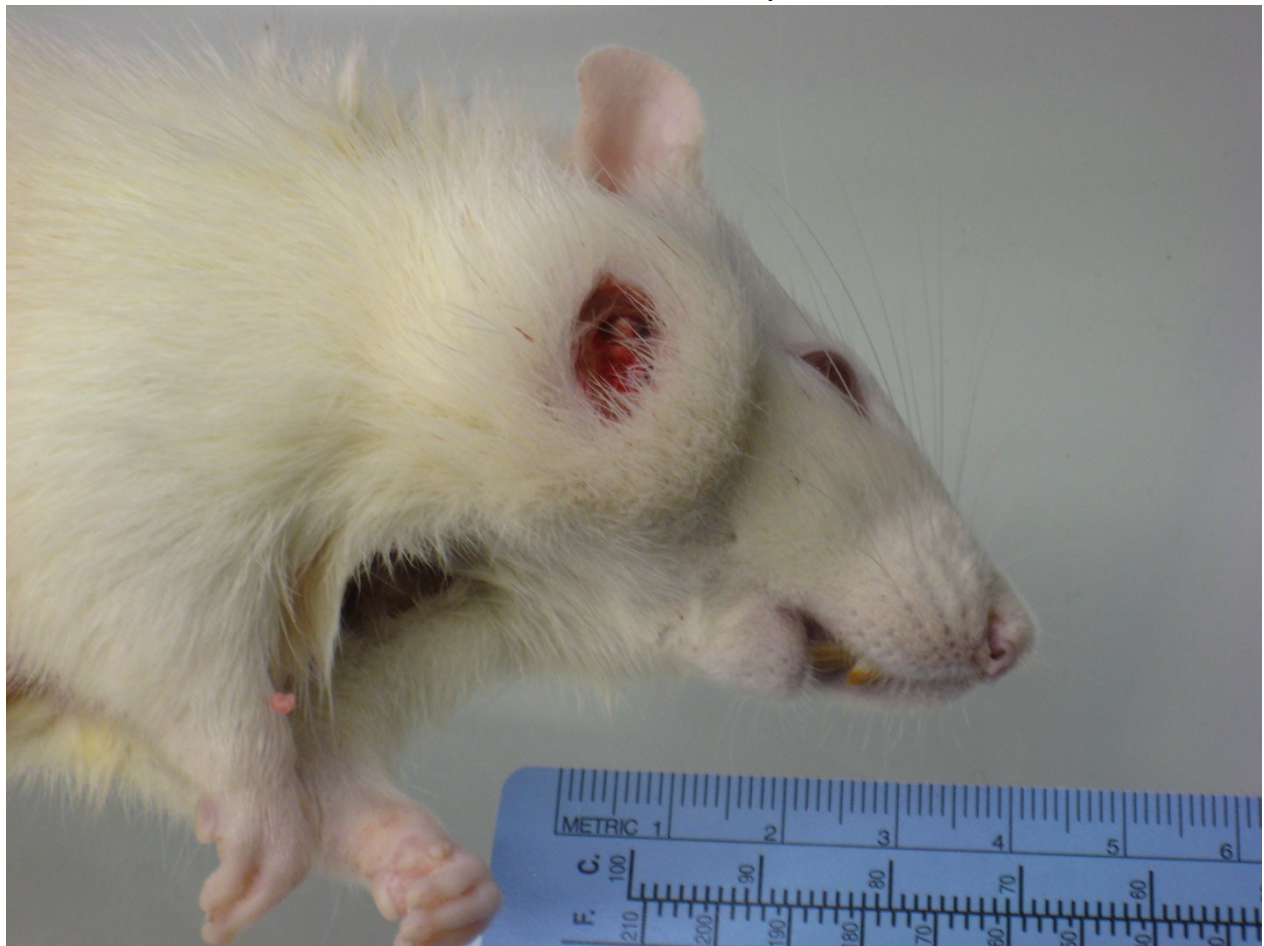
Signalment: 6 month old, female, Harlan Sprague-Dawley rat, (*Rattus norvegicus*)

History: Moribund sacrifice due to ulcerated facial mass; several animals affected.

Gross Pathology: A multinodular tan mass replaced and destroyed most of the left submandibular salivary gland. After section the mass, measuring 2cmx1cm, appeared encapsulated and filled with white to tan caseous material.

Laboratory results: None provided.

Microscopic Description: Facial mass: An approximately 2 x 2cm, well-circumscribed, unencapsulated, multilobular, and cystic neoplasm is expanding and compressing the subcutis. The neoplasm is composed of polygonal cells arranged in islands, cords, and trabeculae supported by moderate fibrovascular stroma. Neoplastic islands and trabeculae are often bordered by a peripheral layer of flattened to cuboidal epithelial cells with scant, eosinophilic cytoplasm, and condensed round to oval nuclei (basaloid reserve cells) and also contain a central area comprised of polygonal cells with abundant, microvacuolated cytoplasm and round nuclei with finely stippled chromatin and 1-3 variably distinct nucleoli (sebaceous

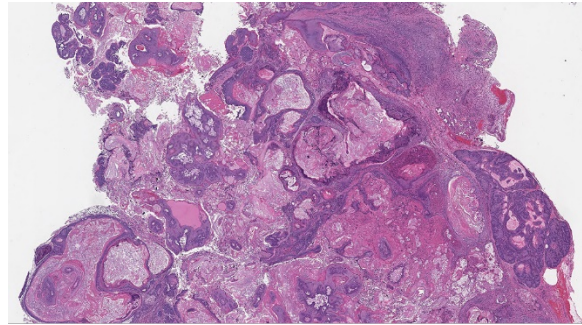


Facial mass, rat. An approximately 2 x 2cm, ulcerated nodule is at the base of the right ear. (Photo courtesy of: NIEHS/NTP, <http://ntp.niehs.nih.gov/nnl/>)

differentiation). Anisocytosis and anisokaryosis are minimal and the mitotic rate for both cell populations is less than 1 mitotic figure per 40X field. Also within the neoplasm, are multifocal areas of squamous epithelial cells undergoing gradual keratinization, lining cystic spaces filled with lamellar whorls of keratin, moderate numbers of viable and degenerative neutrophils, smooth proteinaceous material (sebum), and variable amounts of necrotic debris (cystic degeneration and ductal differentiation). The neoplasm is focally disrupted and replaced by large numbers of epithelioid macrophages with scattered neutrophils and multinucleated giant cells (pyogranulomatous inflammation), reactive fibroblasts with perpendicularly arranged small caliber vessels lined by hypertrophied endothelium (granulation tissue) admixed with collagen, lamellations of keratin, and necrotic and proteinaceous debris. Some of these areas appear to be associated with focally extensive ulceration. There are also multifocal areas of mild hemorrhage scattered throughout the neoplasm.

Contributor's Morphologic Diagnoses:
Zymbal's gland: Adenoma.

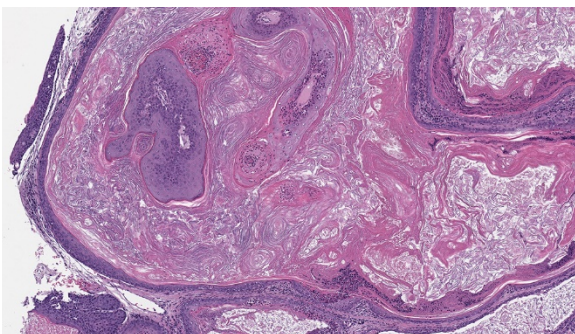
Contributor's Comment: The Zymbal's gland or auditory sebaceous gland is a specialized sebaceous gland unique to rodents and insectivores.^{3,6,7} This compound branched acinar gland sits anteroventral to the external ear meatus and is composed of 3-4 triangular lobes. These lobes are characterized by clusters of saccular acini surrounding a prominent interlobular duct that drains into a short excretory duct. The periphery of each acinus is lined by an incomplete layer of flattened to cuboidal cells containing hyperchromatic nuclei and scant cytoplasm (basaloid reserve cells) while the center is comprised of large polygonal cells with pale, foamy cytoplasm due to the



Facial mass, rat. A well-circumscribed, multilobular, unencapsulated, and cystic neoplasm is expanding and compressing the subcutaneous tissue. Note remnants of more normal sebaceous (Zymbal's) gland along the periphery. (HE, 1X) (Photo courtesy of: NIEHS/NTP, <http://ntp.niehs.nih.gov/nml/>)

progressive accumulation of lipid vacuoles.⁶ Two smaller sebaceous glands underlying the ear canal epithelium are sometimes considered to be a component of the Zymbal's gland; these glands are holocrine glands, as their secretory products are formed from degenerative mature acinar cells that disintegrate and discharge into the ducts.^{3,4,6}

Spontaneous neoplasms of the Zymbal's gland are uncommon in Fisher 344 (F344) and Harlan-Sprague Dawley rats and rarely occur in the mouse.^{1,5,6} The classic presentation for a Zymbal's gland tumor is an ulcerated mass on the side of the face or the base of the ear. Early neoplasms are typically firm, well-circumscribed, freely moveable, subcutaneous masses whereas larger neoplasms are frequently ulcerated, with or without extension into the ear canal, and may exude caseous or purulent material on cut section. Most Zymbal's gland neoplasms exhibit histological features of malignancy with local invasion, cellular atypia, necrosis and high mitotic activity, however, metastasis is not reported to occur.^{3,4,6} Benign neoplasms, adenomas or papillomas, are generally smaller, well-circumscribed masses with minimal cellular atypia and



Facial mass, rat. Higher magnification of one of the lobules with a central cystic area lined by proliferating squamous epithelium which largely recapitulates normal epidermal maturation in verrucous projections into the cystic space. (HE. 10X) (Photo courtesy of: NIEHS/NTP, <http://ntp.niehs.nih.gov/nnl/>)

invasion. Zymbal's gland carcinomas are less well-circumscribed with invasion of the surrounding tissues and frequent cystic cavities filled with mixtures of proteinaceous fluid (sebum), keratin and necrotic debris. The neoplastic sebaceous and squamous cells that comprise the malignant neoplasms are very pleomorphic and anaplastic and some tumors are composed almost entirely of squamous epithelium.^{4,6}

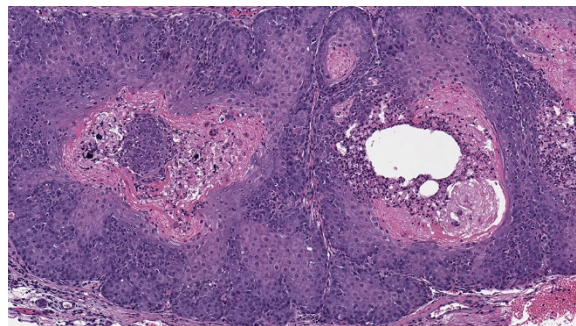
While spontaneous Zymbal's gland neoplasms are infrequently observed, these types of tumors are easily induced by a variety of carcinogens, particularly aromatic amines like benzene.^{3,4,7} The Zymbal's gland lacks transacylase and sulfotransferase activity, but is able to hydroxylate compounds via cytochrome p450-dependent enzymatic pathways. Detectable cytochrome p450 activity within these tumors suggests that the formation of active metabolites within the affected gland may contribute to tumorigenesis. In a survey conducted by the National Cancer Institute, 8% of rats treated with carcinogenic compounds developed Zymbal's gland neoplasms (where N = 526 different chemical studies), yet tumor incidence increased to 14% among rats treated with those chemicals known to be mutagenic for *Salmonella typhimurium* (N =

214); this indicates that those chemicals typically causing neoplastic transformation in specialized sebaceous glands, like the Zymbal's gland, are typically mutagenic compounds.^{2,6} The rat in this case was part of an 18-month carcinogenicity study for a known carcinogen with no reported mutagenic activity.

JPC Diagnosis: Zymbal's gland: Adenoma.

Conference Comment: Due to their unique location and fairly characteristic histologic presentation, Zymbal's gland neoplasms are one of the most well-known neoplasms in the rat. The contributor has provided a concise but thorough review of Zymbal's gland neoplasia in the rat. However, it should be noted that the Zymbal's gland undergoes other degenerative, inflammatory, vascular and other non-neoplastic changes, most similar to those observed in the mammary gland.

Non-neoplastic changes of degeneration, single cell necrosis (apoptosis), necrosis, and regeneration changes may all be seen in the ductal and sebaceous epithelium⁴ following administration of toxins, and cystic



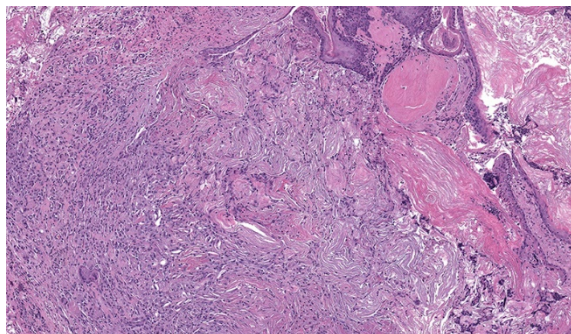
Facial mass, rat. Squamous epithelial cells exhibit gradual keratinization and line cystic spaces filled with lamellar whorls of keratin, moderate numbers of viable and degenerative neutrophils, smooth proteinaceous material (sebum), and variable amounts of necrotic debris (cystic degeneration and ductal differentiation). HE. 10X. (Photo courtesy of: NIEHS/NTP, <http://ntp.niehs.nih.gov/nnl/>)

degeneration of the ducts may be seen as an aging change. Zymbal's glands are uncommonly inflamed, but may be home to the typical range of inflammatory cells, largely depending upon the chronicity of the insult. It may be a site for metastasis in lymphoma or other neoplasms of hematopoietic origin.⁴ Both hyperplastic and atrophic changes are occasionally observed in acinar epithelium. The retention of normal tissue architecture aids in differentiating adenoma from hyperplastic lesions, and adenomas will also have increased numbers of basal cells.⁴

Neoplasms of Zymbal's glands include adenomas (as seen in this case), carcinomas, and squamous papillomas, which may closely resemble tumors of the glandular epithelium, and often pose a diagnostic dilemma.

Carcinomas may be differentiated from adenomas due to the presence of large, irregular acini lacking ducts, and the presence of invasive growth with nests or cords of squamous epithelium penetrating the basal lamina and invading the underlying dermis and skeletal muscle.⁴ Close examination will reveal abnormalities in cellular differentiation of cells above the basal layer; there is variation in size and staining of nuclei, atypical mitotic figures, and loss of intracellular bridges.⁴

A more difficult differential diagnosis is squamous papilloma of the Zymbal's gland (WSC 2015-2016, Conference 22, Case 3.) These neoplasms arise from the main duct epithelium and have a complex arborizing structure with maturing squamous epithelium overlying fibrous cores. One of the keys for the diagnosis of squamous papilloma of the Zymbal's gland is the absence of sebaceous differentiation and the entirely keratinaceous



Facial mass, rat. Marked granulomatous inflammation in areas of ulceration and extrusion of keratin debris into the fibrovascular core of the neoplasm (HE. 10X.)
(Photo courtesy of: NIEHS/NTP, <http://ntp.niehs.nih.gov/nnl/>)

nature of the contents in the cystic area of the neoplasm.⁴

Contributing Institution:

NIEHS/NTP

<http://ntp.niehs.nih.gov/nnl/>

References:

1. Brix A, Nyska A, Haseman JK, Sells DM, Jokinen MP, Walker NJ. Incidences of Selected Lesions in Control Female Harlan Sprague-Dawley Rats from Two-Year Studies Performed by the National Toxicology Program. *Toxicologic Pathology* 2005;33:477-483.
2. Gold LW, Manley NB, Slone TH, Ward JM. Review Article: Compendium of Chemical Carcinogens by Target Organ: Results of Chronic Bioassays in Rats, Mice, Hamsters, Dogs, and Monkeys. *Toxicologic Pathology* 2001;29:639-352.
3. Percy DH and Barthold SW. Rat: Zymbal's gland tumors. In: Percy DH and Barthold SW, eds. *Pathology of Laboratory Rodents and Rabbits*. 3rd ed. Ames, IA: Blackwell Publishing, 2007:175.

4. Rudman D, Cardiff R, Chouinard L, Goodman D, Küttler K, Marxfeld H, Molinolo A, Treumann S, Yoshizawa K, For the INHAND Mammary, Zymbal's, Preputial, and Clitoral Gland Working Group. Proliferative and Nonproliferative Lesions of the Rat and Mouse Mammary, Zymbal's, Preputial, and Clitoral Glands. *Toxicologic Pathology* 2012; 40:7S-39S.
5. Son W and Gopinath C. Early Occurrence of Spontaneous Tumors in CD-1 Mice and Sprague--Dawley Rats. *Toxicologic Pathology* 2004;32:371-374.
6. Yoshizawa K. Specialized Sebaceous Glands. In: Suttie AW, ed. *Boorman's Pathology of the Fisher Rat*. San Diego, CA: Academic Press, Inc., 2018: 348-356.
7. The Joint Pathology Center (JPC). (2015). Veterinary Systemic Pathology Online (VSPO): I-N11 – Zymbal's gland adenoma – Zymbal's gland – rat. Available at: http://www.askjpc.org/vspo/show_page.php?id=355

Self-Assessment - WSC 2018-2019 Conference 5

1. Which of the following does not harbor a herpesvirus which may cause malignant catarrhal fever in susceptible hosts?
 - a. White-tailed deer
 - b. Wildebeest
 - c. Pigs
 - d. Sheep

2. Which of the following is a consistent and characteristic gross finding in American bison with MCF?
 - a. Hemorrhagic cystitis
 - b. Hypopyon
 - c. Interdigital vesicles
 - d. Profound suppurative rhinitis

3. Which of the following is the causative agent of foothill abortion?
 - a. *Pajaroellobacter abortibovis*
 - b. *Ornithodoros coriaceae*
 - c. *Lawsonia intracellularis*
 - d. *Sorangium cellulosum*

4. Which of the following is the most common bacteria identified in cases of botryomycosis in the mouse?
 - a. *Staphylococcus aureus*
 - b. *Corynebacterium bovis*
 - c. *Proteus mirabilis*
 - d. *Escherichia coli*

5. Besides rodents, which other mammals have Zymbal's glands?
 - a. Mustelids
 - b. Insectivores
 - c. Bats
 - d. Viverrids

Please email your completed assessment to Ms. Jessica Gold at Jessica.d.gold2.ctr@mail.mil for grading. Passing score is 80%. This program (RACE program number) is approved by the AAVSB RACE to offer a total of 0.5 CE Credits, with a maximum of 12.5 CE Credits being available to any individual Veterinary Medical Professionals for the 2017-2018 Wednesday Slide Conference. This RACE approval is for the subject matter categories of: SCIENTIFIC using the delivery method of NON-INTERACTIVE DISTANCE. This approval is valid in jurisdictions which recognize AAVSB RACE; however, participants are responsible for ascertaining each board's CE requirements. RACE does not "accredit", "endorse" or "certify" any program or person, nor does RACE approval validate the content of the program.

Please email your completed assessment to Ms. Jessica Gold at Jessica.d.gold2.ctr@mail.mil for grading. Passing score is 80%. This program (RACE program number) is approved by the AAVSB RACE to offer a total of 0.5 CE Credits, with a maximum of 12.5 CE Credits being available to any individual Veterinary Medical Professionals for the 2017-2018 Wednesday Slide Conference. This RACE approval is for the subject matter categories of: SCIENTIFIC using the delivery method of NON-INTERACTIVE DISTANCE. This approval is valid in jurisdictions which recognize AAVSB RACE; however, participants are responsible for ascertaining each board's CE requirements. RACE does not "accredit", "endorse" or "certify" any program or person, nor does RACE approval validate the content of the program.



WEDNESDAY SLIDE CONFERENCE 2018-2019

Conference 6

3 October 2018

Jennifer (Jey) Koehler, DVM, Ph.D, DACVP
Assistant Professor of Pathology
Auburn University College of Veterinary Medicine
Auburn, AL

CASE I: 21608 (JPC 4089879-00).

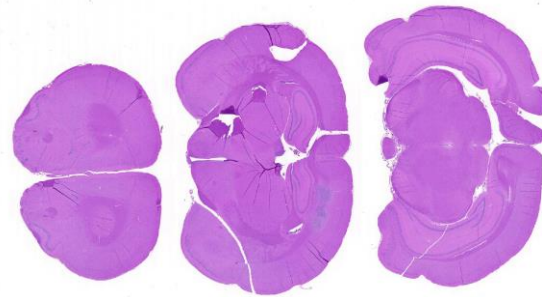
Signalment: 22 week old female
Crl:WI(Han) rat (*Rattus norvegicus*)

History: Tissues were routinely collected from this control female rat at the terminal sacrifice of a 13 week oral gavage study of a drug candidate. No clinical observations were noted prior to sacrifice.

Gross Pathology: No macroscopic observations were noted.

Laboratory results: None given.

Microscopic Description: Brain: In the cerebrum, subcortical white matter in one hemisphere is focally replaced by a poorly demarcated mass composed of densely packed round to fusiform cells. These cells are often arranged in small palisades, rarely form perivascular whorls, and have indistinct cytoplasmic margins, scant to abundant abundant pale amphophilic fibrillar

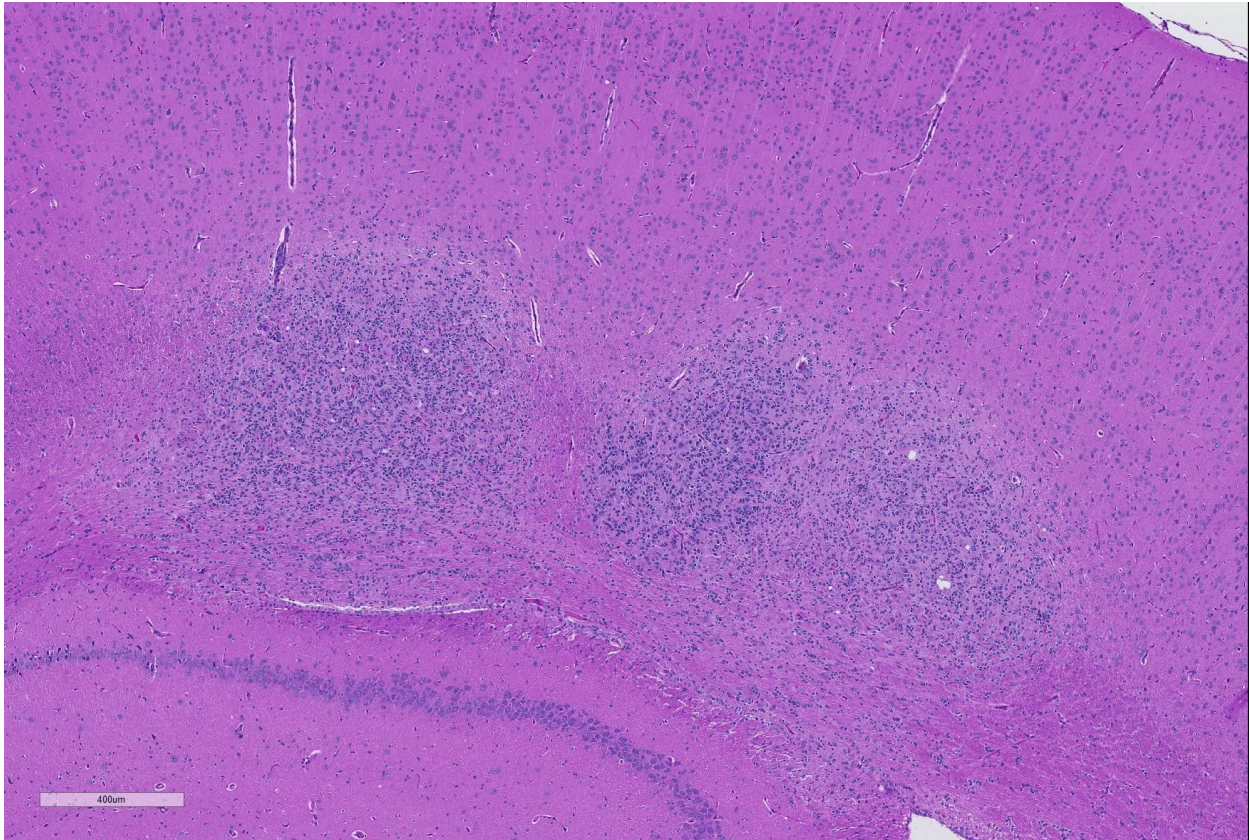


Cerebrum, rat. Three section of brain from telencephalon (left) to diencephalon (right) are submitted for examination. The middle section has a focal unilateral hypercellular mass. (HE, 5X)

cytoplasm, and round to oval euchromatic nuclei that often contain one or two nucleoli.

There is marked anisokaryosis and there are rare mitotic figures. Interspersed among these neoplastic cells are cells with large nuclei and abundant eosinophilic cytoplasm (interpreted as gemistocytic astrocytes).

Contributor's Morphologic Diagnoses:
Glioma, brain.



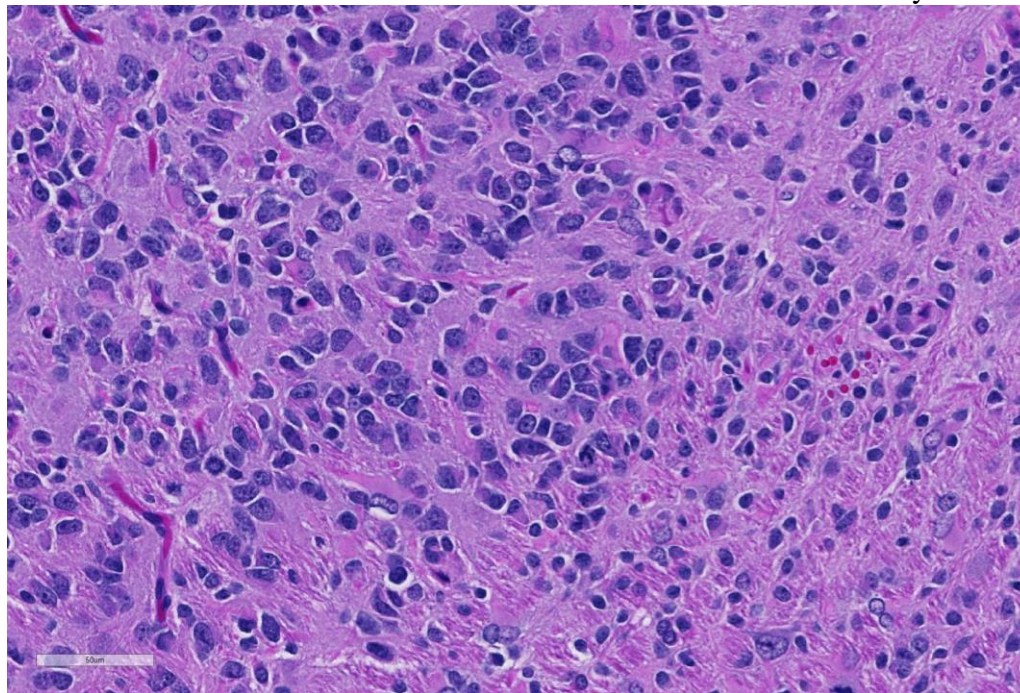
Cerebrum, rat. There is a focal, unencapsulated, minimally infiltrative neoplasm within the deep cortex immediately above the hippocampus. (HE, 67X)

Contributor's Comment: Glial neoplasms are the most commonly occurring spontaneous brain neoplasms in Sprague Dawley (SD) rats, with a reported incidence of approximately 1.5 – 2.0% in control rats in carcinogenicity studies, and are generally more common in males. Most of these tumors have been classified as malignant astrocytomas.^{1,6} Although rarely fatal during the first year of life, spontaneous glial neoplasms have been reported in SD rats as young as 21 or 32 weeks of age.^{3,8}

Recent immunohistochemical studies of rat glial neoplasms have demonstrated that the vast majority of spontaneous and chemically induced tumors traditionally termed “astrocytomas” do not express detectable glial fibrillary acidic protein (GFAP) or other astrocyte markers,^{2,4,5} although GFAP positive neoplastic astrocytes have been

demonstrated in oligodendrogliomas and mixed gliomas of rats.⁷ In contrast, most rat “astrocytomas” are immunopositive for markers of microglia and monocytes/macrophages such as ionized calcium-binding adapter molecule-1 (Iba-1) and bind the lectin *Ricinus communis* agglutinin type 1 (RCA-1).^{2,4,5} Based on these studies, the majority of rat “astrocytomas” are more appropriately termed malignant microglial tumors. It has been recommended that these tumors be diagnosed as “gliomas” in routine toxicology or carcinogenicity studies, and that more specific diagnosis as to cell of origin should be based on immunohistochemical findings.²

and 3) the relative resistance of post-natal rats to chemical induction of tumors in the central nervous system. Most brain cancer



Cerebrum, rat. Neoplastic cells resemble both astrocytes (large open-raced nuclei with moderate amounts of granular eosinophilic cytoplasm), oligodendroglia (scant cytoplasm and round or deeply cleaved nuclei) and are admixed with few reactive astrocytes (marginated chromatin, ovoid nuclei) and activated microglia (small cells with minimal cytoplasm and triangular hyperchromatic nuclei. (HE, 400X)

Covance Laboratories, Inc, Madison, Wisconsin,

USA.<http://www.covance.com/industry-solutions/drug-development/services/safety-assessment/nonclinical-pathology-services.html>

JPC Diagnosis: Cerebrum: Glioma.

JPC Comment: As recently as the early 2000's, texts referred to primary tumors of the central nervous system in rats as "uncommon" neoplasms.² This somewhat questionable statement may have resulted from the fact that 1) many of these tumors are not grossly visible, 2) brain sampling protocols generally only require three coronal sections of grossly normal brains,

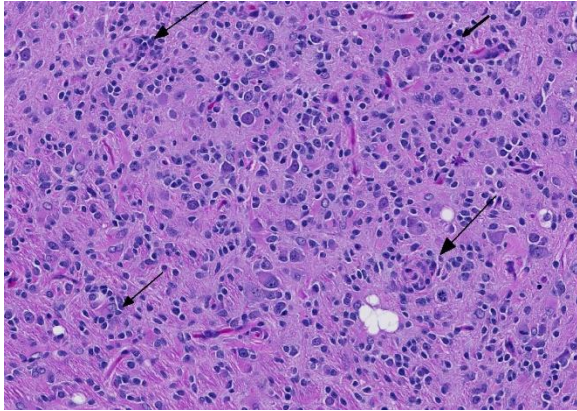
models have traditionally required intrauterine exposure at critical stages of development to carcinogenic substances.²

In the last decade, a growing body of literature, improved sampling techniques as promoted by the Society for

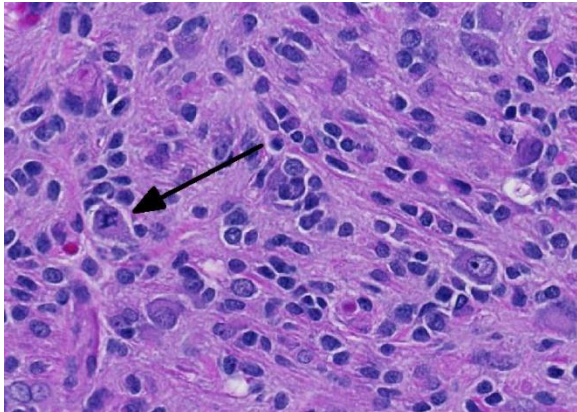
Toxicologic Pathologists, and the publication of historical

control databases has shed more light on CNS tumors in rats.³ In general, the incidence of spontaneous CNS tumors is higher than in mice and spontaneous tumors are found more frequently in males than in females. Incidence does not differ significantly between strains. Tumors of with glial and meningeal differentiation are more commonly seen than those with

neuronal



Cerebrum, rat. Smaller cells form clusters/pseudorosettes in perivascular areas. (HE, 216X)



Cerebrum, rat: An atypical mitotic figure is present. (HE, 400X)

or primitive neuroepithelial differentiation.³

Glial cell tumors are believed to arise from neoplastic radial glial cells (RGCs).³ These neoplasms may move within the CSF into the spinal cord but metastasis outside the nervous system has not yet been reported. For this reason, the terms “benign” and “malignant” have largely been replaced in the toxicologic pathology community with the terms “low-grade” and “high-grade”.³

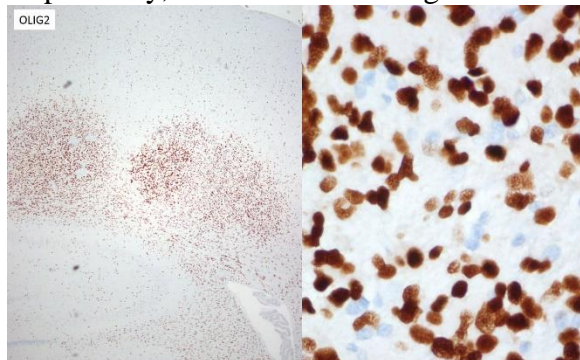
Before the advent of immunohistochemistry and other advanced diagnostics that allowed for more precise identification of the cell of origin, most glial tumors were identified as “glioma”.² Today, immunohistochemical protocols are allowing pathologists to sort

glial tumors into more specific categories with precision. Immunohistochemical and lectin profiles exist for astrocytomas and oligodendrogliomas. The term “glioma” is largely reserved for mixed tumors in which cells fitting the morphology and the immunohistochemical and lectin profiles of both astrocytoma and oligodendroglioma are present in the neoplasm. These neoplasms may be either low- or high-grade tumors. High-grade gliomas are characterized by infiltration into multiple areas of the brain, cellular atypia and pleomorphism, necrosis, and rarely giant cell formation (most likely of astrocytic origin). If these changes are present and each glial cell provides at least 20% of the neoplasm, the tumor is diagnosed as a high-grade mixed glioma. Interestingly, experimental studies have indicated that gliomas in adult rats are initially composed of either differentiated astrocytes or oligodendrocytes. As these neoplasms increase in size, cellular composition becomes mixed and anaplastic over time.³ These high-grade mixed gliomas share some histologic features with the so-called glioblastoma multiforme of humans.³

The conference moderator commented on the heterogeneous nature of the neoplastic cells, with cells resembling both astrocytes and oligodendrocytes in the neoplasm, as well as accompanying activated microglia and reactive astrocytes, ultimately forming a complicated mix of morphologies. The JPC diagnosis of glioma in this case is largely based on the HE appearance.

The majority of neoplastic cells were strongly immunopositive for an OLIG2 stain run at the JPC and is consistent with the diagnosis of glioma. (OLIG2, counterintuitively to its name, will stain both oligodendrocytes and astrocytes.) While there was extensive staining with the JPC-run GFAP and Iba1 within the neoplasm, the

moderator believes that this reflects reactive astrocytes and infiltrating microglia respectively, and the staining excluded



Cerebrum, rat: Neoplastic cells are strongly positive for OLIG2, denoting a glial origin.

neoplastic cells. Based on this additional data, the moderator believes that a diagnosis of glioma is appropriate for the HE appearance of this neoplasm, and that the immunohistochemical findings are consistent with a primitive glial tumor, but does not enable a more specific diagnosis.

References:

- Bertrand L, Mukaratirwa S, Bradley A. Incidence of spontaneous central nervous system tumors in CD-1 mice and Sprague-Dawley, Han-Wistar, and Wistar Rats used in carcinogenicity studies. *Toxicol Pathol.* 2014;42:1168-1173.
- Elmore SA, Farman CA, Hailey JR, et al. Proceedings of the 2015 National Toxicology Program Satellite Symposium. *Toxicol Pathol.* 2016;44:502-35.
- Ikezaki S, Takagi M, Tamura K. Natural occurrence of neoplastic lesions in young Sprague-Dawley rats. *J Toxicol Pathol.* 2011;24:37-40.
- Kolenda-Roberts HM, Harris N, Singletary E, Hardisty JF. Immunohistochemical characterization of spontaneous and acrylonitrile-induced brain tumors in the rat. *Toxicol Pathol.* 2013;41:98-108.
- Nagatani M, Ando R, Yamakawa S, Saito T, Tamura K. Histological and immunohistochemical studies on spontaneous rat astrocytomas and malignant reticulosis. *Toxicol Pathol.* 2009;37:599-605.
- Nagatani M, Kudo K, Yamakawa S. Occurrence of spontaneous tumors in the central nervous system (CNS) of F344 and SD rats. *J Toxicol Pathol.* 2013;26:263-273.
- Nagatani M, Yamakawa S, Saito T, et al. GFAP-positive neoplastic astrocytes in spontaneous oligodendrogliomas and mixed gliomas in rats. *Toxicol Pathol.* 2013;41:653-661.
- Son W-C, Gopinath C. Early occurrence of spontaneous tumors in CD-1 mice and Sprague-Dawley rats. *Toxicol Pathol.* 2004;32:371-374.

CASE II: A16-38521 (JPC 4102645-00).

Signalment: Seven-year-old neutered male mixed breed dog, *Canis familiaris*

History: The dog presented to a veterinary college neurology service one month prior to

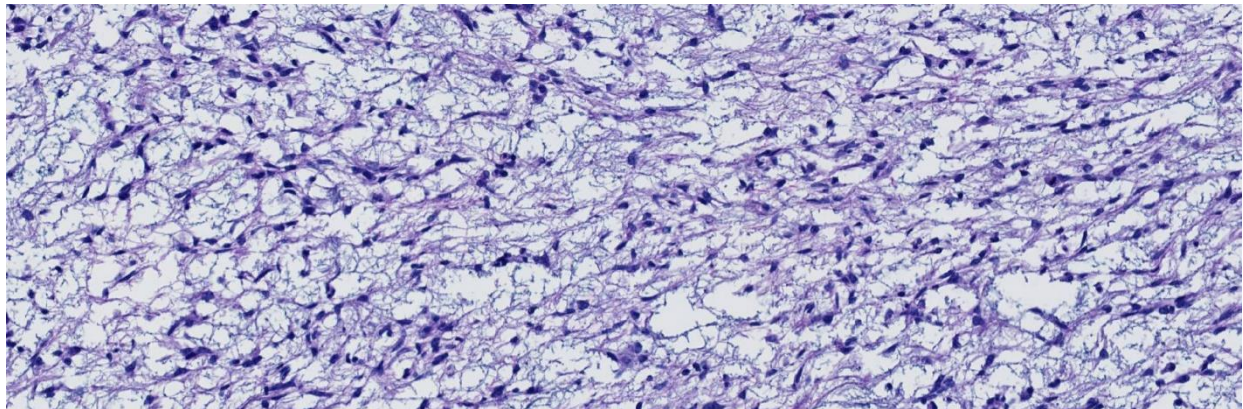


Brainstem, dog: A large well-demarcated, non-infiltrative neoplasm within the brainstem compresses the fourth ventricle and extends across the midline. (HE, 5X)

homogenously hyperintense, non-contrast enhancing mass lesion within the left thalamus and midbrain with secondary obstructive hydrocephalus, characterized by distension of the lateral and third ventricles. The dog was started on corticosteroid therapy, but gradually declined until the owners elected to euthanize.

Gross Pathology: The brain was mildly edematous and there was thinning of the cerebral cortex bilaterally with distension of the lateral ventricles. Serial sectioning revealed a well-circumscribed, well demarcated, pale, gelatinous mass on the left side effacing the mesencephalon with compression of the third ventricle and mesencephalic aqueduct.

Laboratory results: None given.

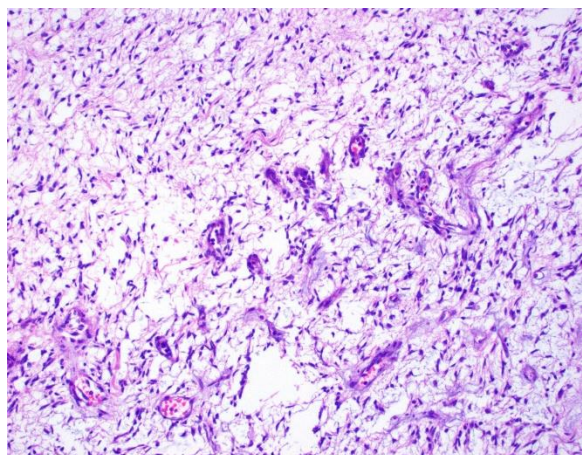


Brainstem, dog. The neoplasm is primarily composed of streams of bipolar elongate spindle cells which are widely separated by a granular amphiphilic myxoid matrix. (HE, 207X)

necropsy following a 3-week history of circling toward the left and altered mentation. On neurologic examination, the dog had inappropriate, dull mentation and a left head turn. He was ambulatory with no weakness or ataxia but circled to the left with right-sided postural reaction deficits in the thoracic and pelvic limbs. There was an inconsistent menace response on the right side. His neuroanatomic localization was to the left prosencephalon. Magnetic resonance imaging (MRI) revealed a T2-weighted

Microscopic Description: Extending from the thalamus caudally to the cerebellar peduncles caudally and expanding the mesencephalon with compression of the lateral ventricles and mesencephalic aqueduct was a well demarcated, unencapsulated, expansile, moderately cellular mass. There were two morphologically distinct cellular populations within the mass: bipolar, spindloid cells with

small ovoid nuclei and long thin wispy cytoplasmic processes, and proliferative, small, round, individualized cells with round to indented, condensed nuclei and scant, granular cytoplasm. Cells were embedded within an abundant loose myxoid matrix that was positive on Alcian blue pH 2.5. Throughout the mass, there were scattered proliferations of hypertrophied endothelial cells, frequently forming glomeruloid capillary loops. There was pallor and mild vacuolation of the surrounding neuroparenchyma. Most of the large, bipolar cells and their associated spindloid processes were strongly positive for GFAP on immunohistochemistry. The nuclei of the smaller round cells stained positively for Olig2, but did not stain with GFAP.



Brainstem, dog. There is robust neovascularization in some areas of the tumor. (HE, 200X)

Contributor's Morphologic Diagnoses: Neoplasia, oligoastrocytoma, thalamus to brain stem, left side with bilateral hydrocephalus

Contributor's Comment: There is a diffuse mixture of GFAP-positive and Olig2-positive cells within the mass. The Olig2-positive cells, interpreted as oligodendrocytes, are too proliferative to be considered reactive cells and therefore are likely neoplastic. There is also proliferation

of GFAP-positive astrocytic cells, but it is less clear whether these are reactive or neoplastic. Astrocytes will commonly proliferate into and around oligodendrogliomas in response to the neuroparenchymal destruction⁵. This reactive response should comprise no more than 30% of the mass, which is far less than the proportion of astrocytic, GFAP-positive cells observed in this mass, which led us to the diagnosis of oligoastrocytoma. Oligoastrocytomas, or mixed gliomas, have been described previously in dogs, where both glial lineages have neoplastic features. These two populations are often separated and distinguishable within the mass, but more heterogeneous and mixed masses are reported.^{2,5,6} It has also been proposed gliomas originating from more primitive cell lines may be dually positive for astrocytic and oligodendroglial markers.⁵ In this case, however, there appear to be two distinct populations.

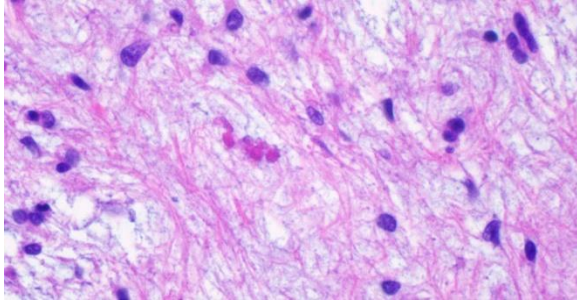
Contributing Institution:

University of Georgia, College of Veterinary Medicine, Department of Pathology, (www.vet.uga.edu/VPP)

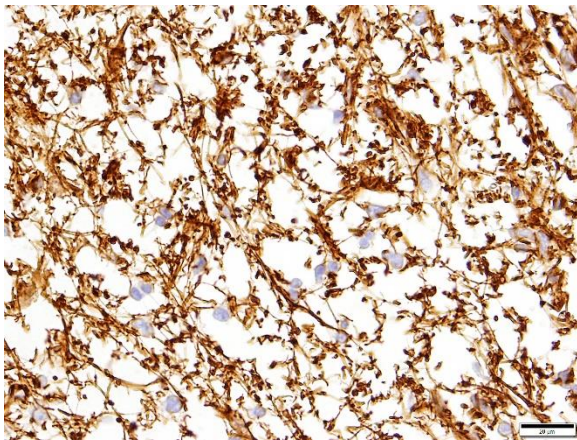
JPC Diagnosis: Brainstem, adjacent to 4th ventricle: Astrocytoma, noninfiltrative, low grade.

JPC Comment: A 2018 publication by the Comparative Brain Tumor Consortium⁴ has laid the groundwork for a sweeping reclassification of canine glial tumors. Currently the World Health Organization (WHO) Tumor Fascicle Histological Classification of Tumors of the Nervous

System of Domestic Animals, published in 1999, still serves as the gold standard for diagnosis of canine glial tumors; however, its diagnostic content is based largely on morphology alone (with a small amount of immunohistochemical data— then in its infancy – on some of the more common neoplasms). The human side of the WHO has published not one, but two editions in their



Brainstem, dog. Neoplastic cells for small Rosenthal fibers. (HE, 400X)



Brainstem, dog. Bipolar spindle cells and multipolar cells stain strongly positive for glial fibrillary acidic protein, a marker of astrocytes. (GFAP, 400X) (Photo courtesy of: University of Georgia, College of Veterinary Medicine, Department of Pathology, (www.vet.uga.edu/VPP))

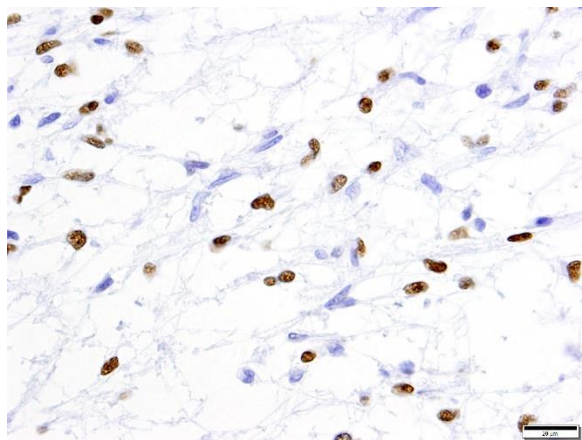
series on Tumors of the CNS, grouping these neoplasms into expected outcomes based on morphologic features, but also incorporating molecular data as part of the diagnostic and prognostic algorithms. This new publication on canine tumors lays the

important groundwork for similar advances when they become more widely available.

The new publication also has an immediate impact on the current methods of diagnosis of canine glial tumors, simplifying the classification of these tumors into three groups: astrocytoma, oligodendroglioma, and “undefined glioma”. A takeaway message that will immediately simplify classification is the recommendation that any tumor in which greater than 80% of the neoplastic cells exhibit morphology and immunoreactivity of either astrocytic or oligodendroglial differentiation, that the tumor be classified into one of those two groups. “Undefined” gliomas are characterized as glial neoplasms which do not have predominant features of either an oligodendroglioma or an astrocytoma; the geographic distribution of the neoplastic cells in these tumors might be either segregated or intermingled.⁴

A number of excellent tips regarding the interpretation of immunohistochemistry on canine gliomas is also presented in this article. The authors recommend the following panel in the diagnosis of canine gliomas: GFAP, Olig2, CNPase (a component of myelin expressed exclusively by oligodendroglia in the CNS), and Ki67. It should be noted that despite its name, Olig2 is not specific for oligodendroglia and may be expressed by neoplastic astrocytes as well. A lack of Olig2 staining is of diagnostic importance as well as a result of its specificity for oligodendro- and astroglia, and a lack of staining should lead the pathologist to strongly consider non-glial tumors at that point in the diagnostic process. The article also comments on the interpretation of immunohistochemical results, with decreased staining of GFAP, CNPase and Ki67 all being negatively impacted by time to fixation (which may be important in the processing of necropsy

samples) as well as time in fixation, and fixation buffering. ⁴



Brainstem, dog. Scattered neoplastic cells stain strongly positive with OLIG-2 (a non-specific glial marker). (Olig-2, 400X) (Photo courtesy of: University of Georgia, College of Veterinary Medicine, Department of Pathology, (www.vet.uga.edu/VPP))

Finally, the paper suggests morphologic criteria (albeit subjective) that may be useful in classifying gliomas into low- or high-grade, to include necrosis, pseudo-palisading of neoplastic cells along areas of necrosis, mitotic activity, microvascular proliferation, and cellular features of malignancy (atypia, anisocytosis, anisokaryosis, and nuclear pleomorphism). Interestingly, in this study, oligodendrogliomas had an overall increased rate of high-grade tumors than astrocytomas, and in keeping with anecdotal observations by many veterinary neuropathologists, oligodendroglial tumors in general far outnumbered astrocytic tumors. ⁴

A number of features in this particular neoplasm are key to its classification as an astrocytoma (notwithstanding the diffuse immunoreactivity for GFAP, as this information was not provided to attendees.). The minimal amount of cytoplasm of the neoplastic cells, elongate nuclei, bipolar cell morphology, lack of necrosis, and lack of

any apparent nuclear rowing (aka “interfascicular queuing”) were considered more appropriate for the diagnosis of astrocytoma in this case. It is important to note that in pilocytic astrocytomas in humans (which this neoplasm strongly resembles in appearance and location), smaller Olig2 cells can be interspersed with the bipolar astrocyte population and do not confer a diagnosis of oligoastrocytoma. The presence of microcysts and formation of Rosenthal fibers by some of the neoplastic cells was also considered of diagnostic importance (a feature that has been well established in human astrocytomas)

During the discussion of this case, the moderator acknowledged the difficulty of identifying true edema in neurologic sections and the lack of well-defined criteria for it, but believes that the area of rarefaction surrounding the neoplasm and extending into the adjacent parenchyma in this case is a good example of spongiosis.

References:

1. Ide T, Uchida K, Kikuta, F, Suzuki K, Nakayama H. Immunohistochemical characterization of canine neuroepithelial tumors. *Vet Pathol* 2010; 47:741-50.
2. LeCouteur RA, Withrow SJ. Tumors of the nervous system. In: Withrow SJ, Vail DM, eds. *Small Animal Clinical Oncology*. St Louis, MO: Saunders Elsevier; 2007:659-670.
3. Higgins RJ, Bollen AW, Dickinson PJ, Siso-Lonch S. Tumors of the nervous system. In: Meuten DJ, ed, *Tumors of Domestic Animals, 5th ed*. Ames IA, Wiley-Blackwell, 2017: 848-849.
4. Koehler JW, Miller AD, Miller CR, Porter BR, Aldape K, Beck J, Brat D, Cornax I, Corps K, Frank C, Giannini, Horbinski C, Huse JT, O’Sullivan MG, Rissi

DR, Simpson RM, Woolard K, Shih JH, Mazcko C, Gilbert MR, LeBlanc AK. A revised diagnostic classification of canine glioma: towards validation of the canine glioma patient as a naturally occurring preclinical model for human glioma. *J Neuropathol Exp Neurol* 2018; doi 10.1093/jnen/nly085

5. Summers BA, Cummings JF, deLaunta A. *Veterinary Neuropathology*. St. Louis, MO: Mosby, 1995:370-373.

6. Vandvelde M, Higgins RJ, Oevermann O. Neoplasia. In *Veterinary Neuropathology*. West Sussex, United Kingdom, Wiley-Blackwell; 2012: 139-140.

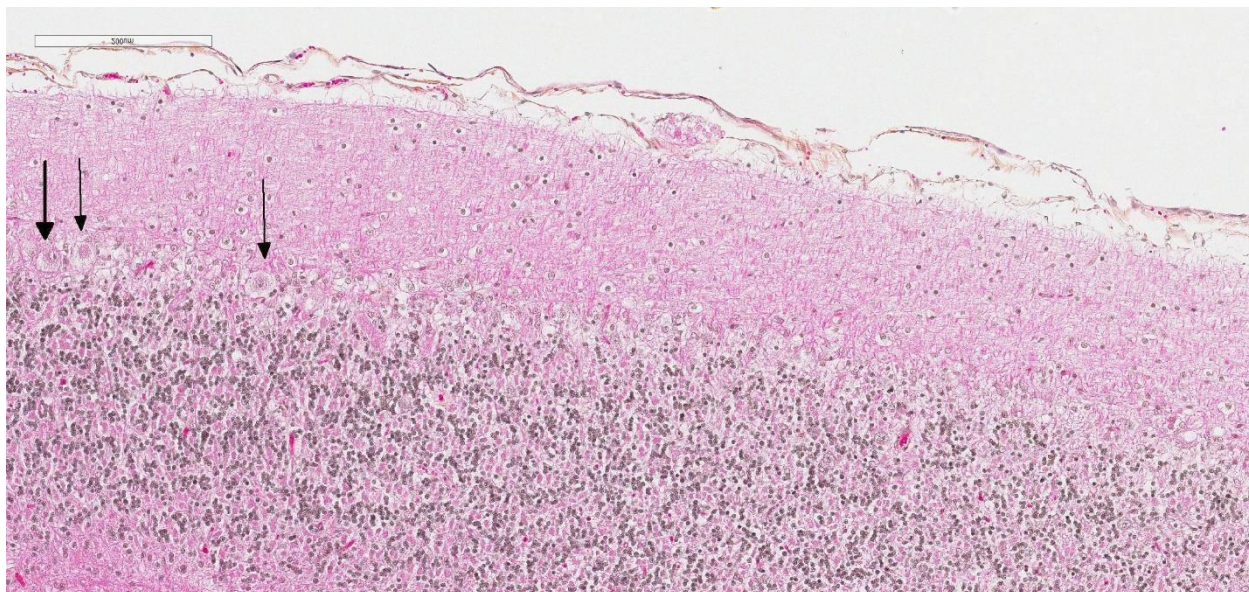
CASE III: P3213-13 (JPC 4048997-00).

Signalment: 1½ year-old, male neutered, Domestic shorthair, (*Felis catus*), cat



Cerebellum, cat. At subgross magnification, there is mild thinning of the cerebellar cortex. (HE, 12X)

History: This cat was reported to be normal at birth. At 7 months of age, it started showing progressive signs of cerebellar disturbance, i.e. abnormal gait and balance. Another cat from the same litter developed similar symptoms. Two MRI examinations of the head/brain were performed. The first one, on April 2013, only showed a slightly smaller than normal cerebellar size with a small suspicion of cerebellar abiotrophy. The second one, on December 2013, revealed a reduced cerebellar size with moderate diffuse widening of the cerebellar sulci, consistent with a diagnosis of cerebellar abiotrophy. The neurological examination also supported a disease process affecting all portions of the cerebellum. Due to progression of the illness, the cat was euthanized and a full



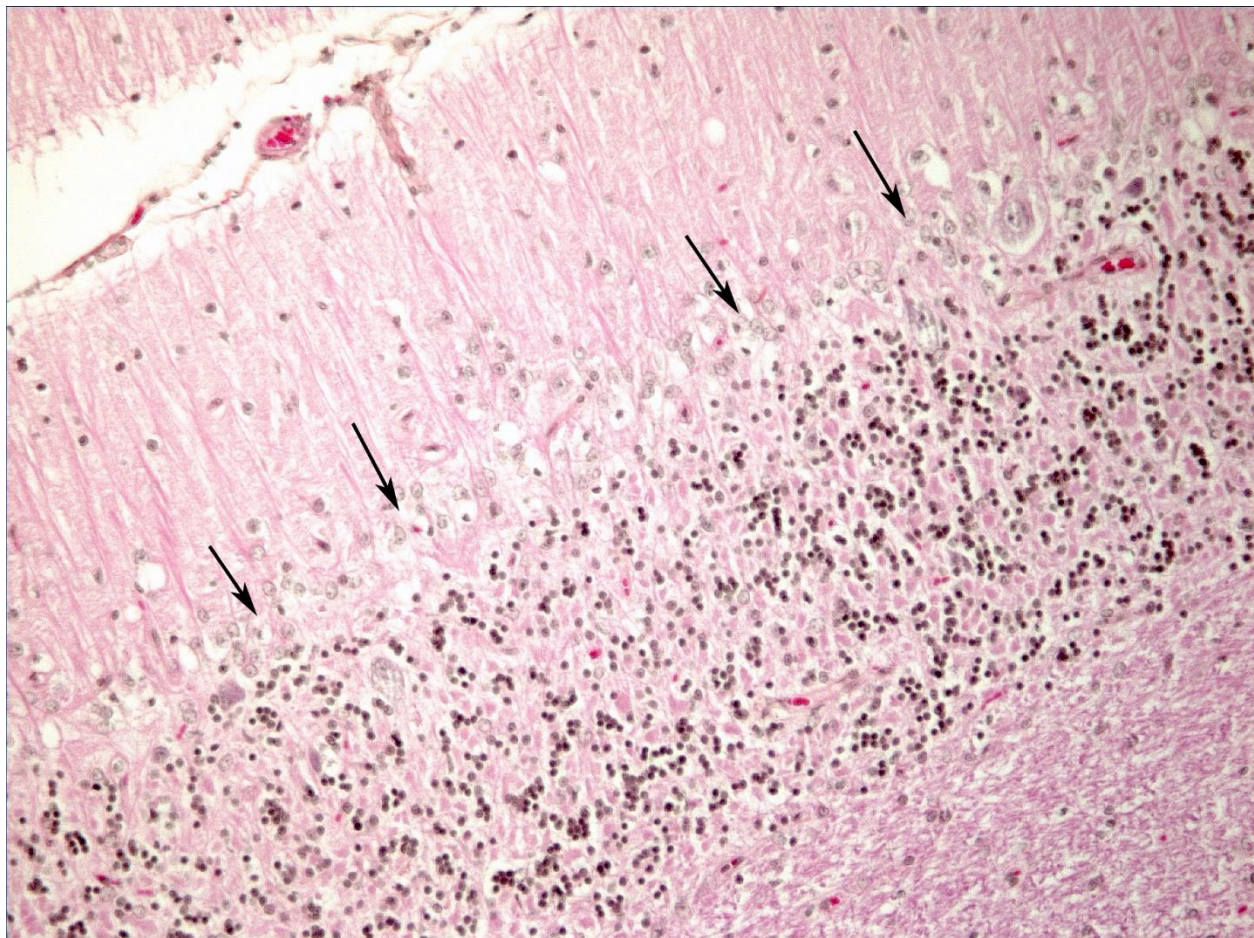
Cerebellum, cat. There is significant segmental loss of Purkinje cells (note three at left and none to the right). Remaining Purkinje cells are swollen and vacuolated. (HE, 163X)

necropsy was performed.

Gross Pathology: The only significant change was observed in the cerebellum which had diffusely widened sulci (more conspicuous when compared with an age-matched control), consistent with atrophy of folia.

Laboratory results: None given.

(astrogliosis), often with prominent processes extending radially in the molecular layer to the pia mater (isomorphic gliosis); this was confirmed by GFAP immunohistochemistry. The molecular and granular layers are irregularly thin; the granular layer has a variably decreased density (loss of granule cells). Rare torpedoes can sometimes be seen. In some sections, there is Wallerian degeneration (mostly digestion chambers) in the



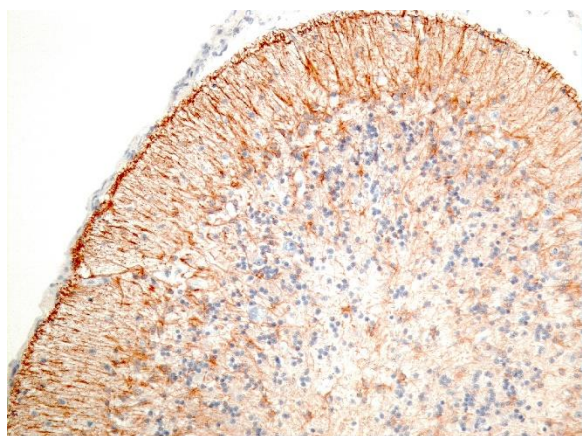
Cerebellum, cat. There is a proliferation of Bergmann's glia at the level previously occupied by Purkinje cells. Their prominent processes run perpendicularly to the overlying pia mater. (HE, 400X) (Photo courtesy of: Université de Montréal, Faculty of veterinary medicine, St-Hyacinthe, Quebec, Canada. <http://www.medvet.umontreal.ca>)

Microscopic Description: Diffusely in the cerebellar cortex, there is a severe loss of Purkinje cells, leaving multiple “empty baskets”; most of the persistent Purkinje cells have a pale and vacuolar cytoplasm (degeneration). There is an associated proliferation of Bergmann astrocytes

in the cerebellar white matter; this change was also present bilaterally and symmetrically in the lateral and superficial portions of the medulla (not submitted). In the cerebellar nuclei (present in some sections), there is mild diffuse gliosis with some neuropil vacuolation, but no obvious neuronal

changes. These lesions were present in all portions of the cerebellum.

Spinal cord (not submitted): There is bilateral and symmetrical Wallerian degeneration affecting all portions (cervical, thoracic and lumbar) of the spinal cord, with variation in the affected tracts/fasciculi depending on the level examined. In some dorsal spinal ganglia, a few neurons were chromatolytic.



Cerebellum, cat. A GFAP stain demonstrates the dense parallel network of fibers of the Bergmann's glia (i.e., Bergmann's astrocytes) (isomorphic gliosis). (anti GFAP, 100X). (Photo courtesy of: Université de Montréal, Faculty of veterinary medicine, St-Hyacinthe, Quebec, Canada. <http://www.medvet.umontreal.ca>)

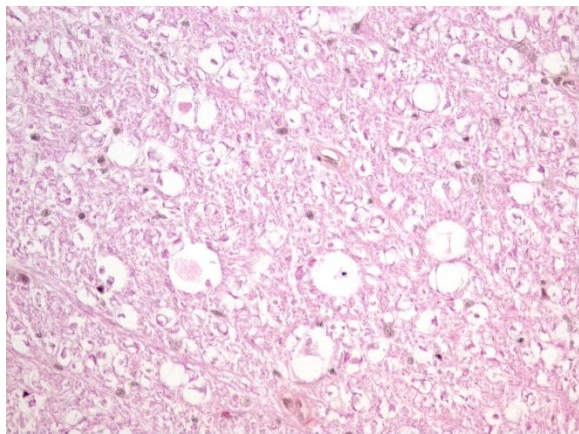
Contributor's Morphologic Diagnoses:
Diffuse, severe loss of Purkinje cells
(cerebellar abiotrophy)

Bilateral and symmetrical degenerative myeloencephalopathy (spinal cord and medulla; not submitted)

Contributor's Comment: Based on the lesions in the cerebellum, medulla and spinal cord, this case was diagnosed as cerebellar abiotrophy and degenerative myeloencephalopathy, consistent with spinocerebellar ataxia; a genetic component is strongly suspected as one littermate had

similar clinical signs. The cerebellar lesion is characteristic of cerebellar abiotrophy or cerebellar cortical abiotrophy. In veterinary medicine, cerebellar abiotrophy is a rare condition described in most domestic animals, non-human primates and a few rodent species.¹⁻¹² Contrary to cerebellar hypoplasia – a condition targeting the cerebellar outer germinal layer and resulting in failure to reach normal organ size (e.g. *in utero* infection with feline panleukopenia parvovirus or BVDV) – cerebellar abiotrophy is characterized by the loss of neuronal populations after full development of the organ. Thus, a hallmark of this condition is normal function at birth, followed by progressive signs of cerebellar disease of variable onset.¹⁰

Cerebellar abiotrophy is well recognized in dogs, with reports in several different breeds (e.g. English bulldog, American Staffordshire terrier, Border collie),^{2,3,5,7,10} and often a suspicion of primary genetic origin. Affected animals usually show progressive neurological signs including cerebellar ataxia, head tremors and symmetrical hypermetria. At necropsy, the cerebellum is usually of normal size but shrinkage of cerebellar folia and broadening of sulci may be present in chronically affected dogs. Microscopic examination reveals an ongoing loss of neurons associated with reactive gliosis. Purkinje cells are severely depleted, leaving clear space (“empty baskets”); Bergmann astrogliosis is a common associated finding. Depletion of the different neuronal populations eventually leads to shrinkage of the molecular and granular layers.¹⁰



Spinal cord, cat. Mild Wallerian degeneration was present throughout the spinal cord. (HE, 400X). (Photo courtesy of: Université de Montréal, Faculty of veterinary medicine, St-Hyacinthe, Quebec, Canada. <http://www.medvet.umontreal.ca>)

In cats, cerebellar abiotrophy is uncommon, with only a few cases published^{1,6,9,10,11,12}. However, the present feline case is to our knowledge unique as reported feline cases did not describe spinal cord lesions.

Contributing Institution:

Université de Montréal, Faculty of veterinary medicine, St-Hyacinthe, Quebec, Canada. <http://www.medvet.umontreal.ca>

JPC Diagnosis: Cerebellum: Purkinje cell degeneration and loss, diffuse, severe, with marked granular cell loss and Bergmann gliosis.

JPC Comment: Cerebellar cortical degeneration, also referred to as cerebellar abiotrophy, encompasses a group of diseases characterized by degeneration of formed neurons within the cerebellar cortex. As opposed to cerebellar hypoplasia, in which viral infection in utero damages the external granular cell layer (the source of formation of Purkinje cells and neurons that populate the granule cell layer), the cerebellar cortex is grossly and histologically normal at birth,

and progressively degenerates over time. While many of the mutations associated with both autosomal dominant and recessive forms of cerebellar cortical degeneration (CCD) have been elucidated in humans, this work is yet in its early stages in veterinary medicine. Mutations in the SEL1L gene have been associated with early onset progressive cerebellar ataxia in Finnish Hounds, and PARK2 gene mutations are common to hereditary striatonigral and cerebello-olivary degeneration in Kerry Blue Terriers and humans.

In the absence of such genetic information, most forms of CCD in veterinary medicine continue to be classified largely based on the locations in which degenerative changes are noted. Most cases of cerebellar cortical degeneration involve Purkinje cells, and the spontaneous depletion of granule cells (neurons populating the adjacent granular cell layer) is often a concurrent, although less obvious finding. Primary degeneration of neurons of the granule cell layer (also referred to as cerebellar granuloprival degeneration) has been reported in a number of canine breeds, including the Coton de Tulear (see WSC 2016-2017, Conference 12, Case 1). A number of syndromes, such as hereditary striatonigral and cerebello-olivary degeneration, as mentioned above, involve neuronal degeneration outside of the cerebellar cortex as well.

While well-documented in a wide variety of dog breeds, far fewer cases of cerebellar abiotrophy have been identified in cats. The disease has been reported both in kittens and in adult cats, with adult-onset “late” onset disease appearing in animals from 1.5 to 9 years. (Biolatti) A syndrome of olivopontocerebellar atrophy in two possibly related cats involved loss of neurons in the cerebellar cortex, olivary complex, and the pontine nuclei in an unusual orderly and progressive fashion. Subtle differences

between the human and the feline disease exist, to include depletion of the granular cell layer in the feline variant and an absence of ubiquitinated intranuclear inclusions within degenerating Purkinje cells. A report of three sibling kittens described severe Purkinje cell loss as well as vacuolation of the neuropil in the cervical spinal cord (as described by the contributor in this case.)

Prominent in this section is the proliferation of Bergmann's glia (often referred to as Bergmann's astrocytes) in the areas of Purkinje cell loss. The cell bodies of Bergmann's glia are found in the Purkinje cell layer, and their processes extend through the molecular layer with endfeet located on the pia mater. In addition to traditional tasks of gray matter protoplasmic astrocytes following injury to Purkinje cells, they have numerous other functions. In the developing cerebellum, they contribute to the layering of the cerebellar cortex - proneurons migrate along their processes from the external germinal layer to populate the granule cell layer. At the late stage of Purkinje cell development, Bergmann's glia form an intricate interwoven network to provide physical and trophic support to the developing Purkinje dendrite tree. Bergmann's glia even assist in information processing in the mature molecular layer – clearing neurotransmitters from synaptic cleft (particularly excitotoxic glutamates), buffering potassium, and even coupling neuronal activity with energy supply and blood flow.

The moderator noted the marked depletion of granular cells as well as that of Purkinje cells, but identified the Purkinje cell loss as the primary lesion, both in terms of importance to the clinical picture as well as the first of the two lesions to occur temporally.

References:

1. Biolatti C, Gianella P, Capucchio MT, Borrelli A, D'Angelo A. Late onset and rapid progression of cerebellar abiotrophy in a domestic shorthair cat. *J Small Anim Pract.* 2010;**51**:123-126
2. Buffo A, Rossi, F. Origin, lineage, and function of cerebellar glia. *Prog Neurobiol,* 2013; 109:42-63.
3. Gandini G, Botteron C, Brini E, Fatzed R, Diana J, Jaggy A. Cerebellar cortical degeneration in three English bulldogs: clinical and neuropathological findings. *J Small Anim Pract.* 2005;**46**:291-294
4. Gumber S, Cho DY, Morgan TW. Late onset of cerebellar abiotrophy in a Boxer dog. *Vet Med Inter.* 2010; Article ID 406275
5. Mouser P, Lévy M, Sojka J.E, Ramos-vara J.A. Cerebellar abiotrophy in an Alpaca (lama pacos). *Vet Pathol.* 2009;**46**:1133-1137
6. Olby N, Blot S, Thibaud JL, et al. Cerebellar cortical degeneration in adult American Staffordshire terriers. *J Vet Intern Med.* 2004;**18**:201-208
7. Résibois A, Poncelet L. Olivopontocerebellar atrophy in two adults cats, sporadic cases or new genetic entity. *Vet Pathol* 2004;**41**:20-29
8. Sandy JR, Slocombe RF, Mitten RW, Jedwab D. Cerebellar abiotrophy in a family of border collie dogs. *Vet Pathol.* 2002;**39**:736-

738

9. Sato J, Sasaki S, Yamada N, Tsuchitani M. Hereditary cerebellar degenerative disease (cerebellar cortical abiotrophy) in rabbits. *Vet Pathol.* 2012, **49**:621-628
10. Shamir M, Perl S, Sharon L. Late onset of cerebellar abiotrophy in a Siamese cat. *J Small Anim Pract.* 1999;**40**:343-345
11. Summers BA, Cummings JF, DeLahunta A. Degenerative diseases of the central nervous system, neuronal abiotrophy. In: Summers BA, Cummings JF, DeLahunta A . ed. *Veterinary Neuropathology*. St Louis, MO: Mosby-Year Book; 1995:300-347
12. Taniyama H, Takayanagi S, Izumisawa Y, Kotani T, Kaji Y, Okada H, Matsukawa K. Cerebellar cortical atrophy in a kitten. *Vet Pathol.* 1994; **31**:710-713
13. Willoughby K, Kelly D.F. Hereditary cerebellar degeneration in three full sibling kittens. *Vet Rec.* 2002,**151**:295-298

CASE II: V15-09895-X (JPC 4068932-00).

Signalment: 1 day old, male, Maine Anjou mixed breed, *Bos taurus taurus*, cattle



A plant submitted was identified as Astragalus species by the faculty in New Mexico State University Range Sciences. (Photo courtesy of: New Mexico Department of Agriculture Veterinary Diagnostic Services; www.nmda.nmsu.edu)

History: The owner stated that a large percentage of the spring calf crop was born three to four weeks prematurely. Approximately one half of the calves that lived were lethargic at birth and die. A few of the cows had lost weight and thin despite of eating well.

Gross Pathology: The only significant gross lesion was the thyroid gland was equivocally enlarged.

Laboratory results: A plant submitted was identified as *Astragalus* species by faculty in New Mexico State University Range Sciences.

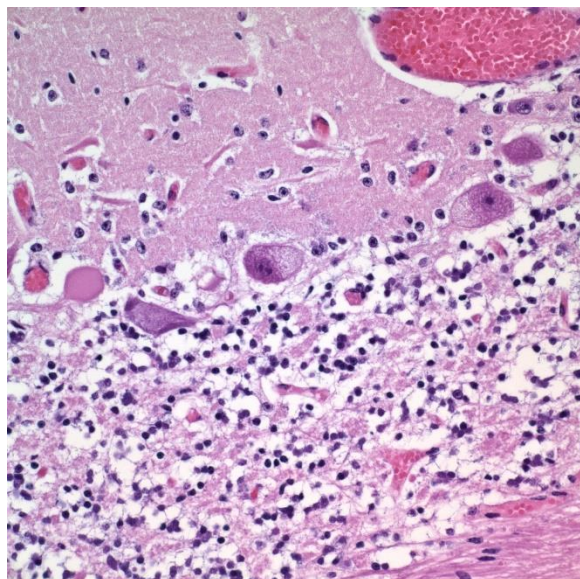
Microscopic Description: The Purkinje cells of the cerebellum are swollen by clear cytoplasmic vacuoles that are most prevalent at axon hillocks (Figure 2). There are rare

necrotic Purkinje cells. There are rare affected neurons in the granule cell layer.

Contributor's Morphologic Diagnoses:

Diffuse, severe loss of Purkinje cells (cerebellar abiotrophy)

Contributor's Comment: Locoism in livestock is caused by the chronic ingestion of legumes of the genera *Astragalus* and *Oxytropis*.^{7,11} There are over 2000 species of *Astragalus* and *Oxytropis* worldwide with 370 known species of these legumes occurring in North America.⁷ Most livestock poisonings caused by these two genera of plants in the United States occur in the western United States.¹¹ Common names for plants of *Astragalus* and *Oxytropis* genera are locoweeds, milk vetches or vetches. Not all species of *Astragalus* and *Oxytropis* cause locoism. However, these plant species can cause other toxicities as they can contain toxic nitro compounds and can be selenium accumulators.^{7,11} Identification of a specific species of locoweed is difficult and is best performed by experienced botanists after the



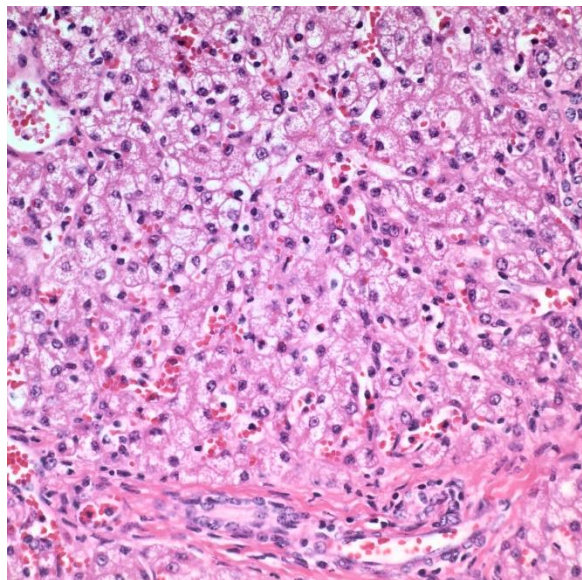
Cerebellum, calf. Purkinje cells are swollen by numerous discrete cytoplasmic vacuoles, most predominantly seen at the axon hillock. (HE, 400X) (Photo courtesy of: New Mexico Department of Agriculture Veterinary Diagnostic Services; www.nmda.nmsu.edu)

plant has flowered and/or produced seed pods.¹¹

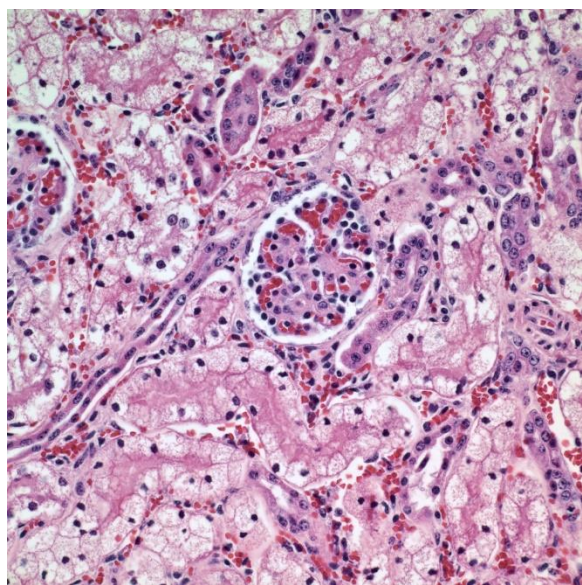
The locoweed population is cyclical with the highest number of locoweeds occurring in wet years such as the fall of 2014 and the spring of 2015 in New Mexico.¹¹ Contrary to prior belief, locoweeds are palatable and some animals will preferentially graze locoweeds in the spring over dormant warm season grasses due to the nutritional value of locoweeds, which in some species is comparable to alfalfa.^{7,11} Animals grazing locoweeds can become habituated to locoweeds, but do not become addicted.^{7,11} Toxicity occurs when the level of the locoweed toxin reaches the toxic threshold.

The toxic principle of locoweeds is the indolizidine alkaloid swainsonine.^{7,11} Swainsonine can be found in all parts of the plant with higher concentrations in the above ground portion of the plants particularly the flowers and seeds.^{5,7} Production of swainsonine by the plant is dependent on infection of the plant by commensal endophyte fungi of the genera *Undifilum*.³⁻⁶ Swainsonine inhibits α -D-mannosidase and Golgi mannosidase II causing cells to accumulate oligosaccharides.^{7,11} The result is a systemic lysosomal storage disease with cytoplasmic accumulations of oligosaccharides manifesting microscopically as clear cytoplasmic vacuoles in multiple organs including but not limited to the neurons of the brain mainly in the axon hillock, liver, kidney and thyroid gland.^{7,8,11} In fetuses, the accumulation of oligosaccharides can also occur in trophoblasts of the placenta.⁸ If the cellular damage is not severe, then preventing livestock from ingesting locoweeds can result in recovery of the animal with cellular changes remaining the longest in the liver and neurons.⁷ The cytoplasmic vacuoles can persist for one year in the Purkinje cells of the cerebellum.⁷

That being said, it is recommended to not ever return horses with locoism to work such as riding due to the potential dangers associated with residual neurological effects.⁷



Liver, calf. Hepatocytes are diffusely expanded by similar clear cytoplasmic vacuoles, obscuring normal sinusoidal architecture. (HE, 400X) (Photo courtesy of: New Mexico Department of Agriculture Veterinary Diagnostic Services; www.nmda.nmsu.edu)



Kidney, calf. Proximal convoluted tubular epithelium is markedly swollen due to numerous clear cytoplasmic vacuoles. (HE, 400X) (Photo courtesy of: New Mexico Department of Agriculture Veterinary Diagnostic

Services; www.nmda.nmsu.edu)

The most widely known manifestation of locoweed toxicity in livestock is neurological disease (locoism). However, locoism in livestock can manifest as chronic weight loss/ill thrift, reproductive losses and worsening the cardiac disease associated with high-mountain disease in cattle.^{7,11} The reproductive losses can be devastating to a producer with losses of close to fifty percent of offspring occurring in some cases. Chronic ingestion of locoweeds has been known to prolong the estrus cycle, result in the failure to conceive and cause early embryonic death.^{2,7-9} Some pregnant cows with locoism develop hydrops.⁷ Abortion may occur at all stages of gestation with cytoplasmic vacuoles present in fetal tissues such as in this case.^{2,7,8} In addition, neonates may be born small and weak. Congenital abnormalities such as limb and head deformities can occur in affected fetuses.^{2,7,8,9} Testicular atrophy and decreased spermatogenesis can occur in adult males with locoism.⁷

The moderator pointed out that the cytoplasmic vacuolation is especially prominent in the area of the axon hillock of Purkinje cells in this particular case, a feature often described in this particular entity. Some participant noted the relative paucity of nuclei within the granular layer; the cause of this finding was ascribed by some to the young age of the animal (one day, and with a prominent external granular cell layer, and likely continued maturation of this region), and some preferred to ascribe it to poor tissue preservation.

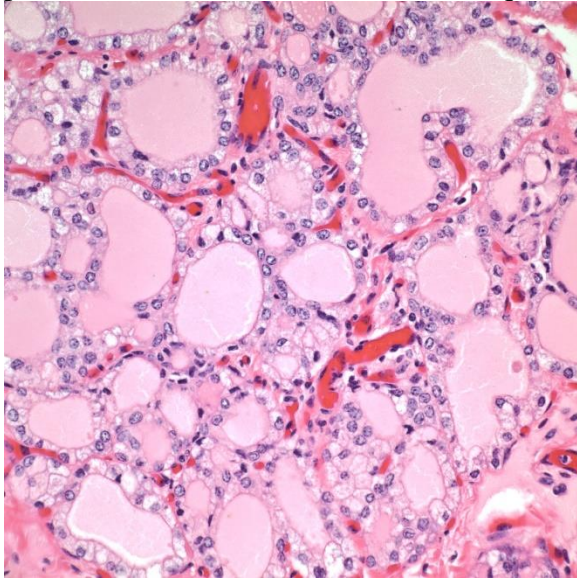
Contributing Institution:

New Mexico Department of Agriculture
Veterinary Diagnostic Services

www.nmda.nmsu.edu

JPC Diagnosis: Cerebellum, Purkinje and granular cells: Cytoplasmic vacuolation, diffuse, marked.

JPC Comment: The contributor has provided an excellent review of the acquired



Thyroid, calf. Follicular epithelium is swollen from numerous clear cytoplasmic vacuoles. (HE, 400X)
(Photo courtesy of: New Mexico Department of Agriculture Veterinary Diagnostic Services;
www.nmda.nmsu.edu)

lysosomal storage disease known as locoism in cattle.

Lysosomal storage diseases are a group of inherited and acquired disorders. Over 50 genetically-determined lysosomal storage diseases have been identified in veterinary medicine.¹ The majority of these diseases result from mutations of genes coding specific lysosomal hydrolases which contribute to the activation of lysosomal enzymes. Moreover, infantile and adult types of inherited diseases may result from different mutations of the same gene. Infantile disease results in early death due to a total absence of enzymatic activity, while adult disease may have late presentation and

mild-to-moderate manifestations as partial enzyme activity is present. Rare cases of congenital disease may result in the absence of hydroxylase activator proteins, recognition markers (which results in lysosomal enzymes being aberrantly secreted into the extracellular milieu), or protector proteins which results in rapid degradation of hydrolytic enzymes.¹ A list of the more common inherited lysosomal storage disease is present Table 1. A more complete review is available in the excellent review by Alroy and Lyons.¹

Acquired lysosomal storage diseases share a common mechanism in the inhibition of alpha-mannosidase II by ingestion of a number of plants from the genera *Astragalus*, *Swainsona*, *Oxytropis*, and *Ipomoea* as well as a number of amphiphilic cationic drugs, including amiodarone and chloroquine.¹

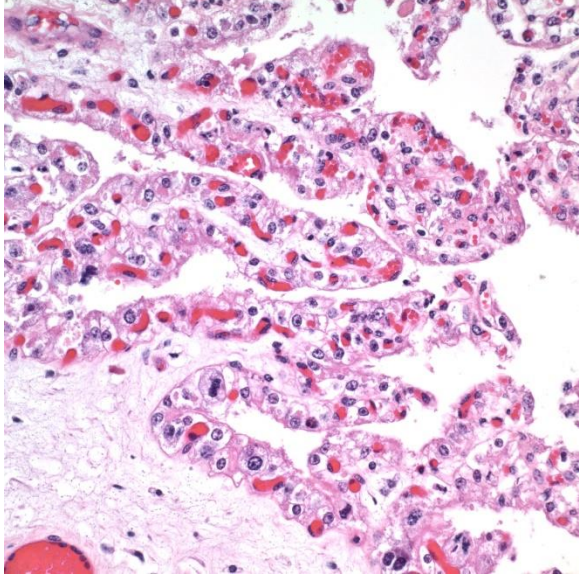
As a general rule, the accumulation of undigested substrate in cells occurs when residual activity of deficient enzymes is less than 10 to 15% of normal levels. There is wide variation in the cell types and organs affected by different types of lysosomal storage diseases; neuronal vacuolation, (as seen in this case), is seen in approximately two thirds of all lysosomal storage diseases.¹

Histochemical stains have traditionally been involved in the differentiation of many types of lysosomal storage diseases. Periodic acid-Schiff stains (with and without diastase digestion), Alcian blue, and colloidal iron (with and without hyaluronidase treatment) are useful for identifying oligosaccharide and glycolipids. Sudan Black, oil red O, and Luxol fast blue stains are helpful in the characterization of abnormally stored lipids. Normal ceroid lipofuscinosis is diagnosed by autofluorescence and rarely requires ultrastructure. Definitive identification of enzyme deficiencies is most commonly

performed on white blood cells or cultured fibroblasts by measuring activity of specific enzymes.¹

Diagnostic Services; www.nmda.nmsu.edu

The moderator noted that the axon hillock was part of the neuron that was most



Placenta, ox. Trophoblasts contain numerous intracytoplasmic vacuoles. (HE, 400X) (Photo courtesy of: New Mexico Department of Agriculture Veterinary

⊕ Table 1: Select inherited lysosomal storage diseases⁸

Condition	Enzyme Defect	Storage Material	Inheritance/species
GM1 gangliosidosis	β -galactosidase	GM1 ganglioside in lysosomes of neurons, glial cells, macrophages	- autosomal recessive - dogs, cats, Friesian cattle; - suffolk sheep - deficiencies in β 1-galactosidase AND α -neuraminidase.
GM2 gangliosidosis (Tay-Sachs and Sandhoff diseases)	-hexosaminidase ($\alpha\beta$ - or $\beta\beta$ -dimer) -activator protein	GM2 ganglioside in lysosomes of neurons, glial cells, macrophages	- autosomal recessive 1. domestic and Korat cats, German shorthaired pointers, golden retrievers: β -subunit deficiency 2. Japanese spaniel dogs, Yorkshire pigs: activator protein deficiency
Sphingomyelinosis (Niemann-Pick disease)	sphingomyelinase	sphingomyelin in lysosomes of neurons and macrophages	- autosomal recessive in cat and dog
Globoid cell leukodystrophy (galactocerebroside)	galactocerebroside	galactocerebroside in oligodendrocytes/Schwann cells, globoid cell macrophages (NOT in neurons) demyelination, axonal loss	- autosomal recessive - dogs, cats and polled Dorset sheep
Glucocerebroside (Gaucher disease)	glucocerebroside	glucocerebroside in lysosomes of hepatic/lymph node sinusoidal macrophages, some neurons (NOT in Purkinje cells or the spinal cord)	- Sydney Silky Terriers
α -Mannosidosis	α -mannosidase	mannose/N-acetylglucosamine oligosaccharide in lysosomes of neurons, macrophages, secretory epithelial cells	- Angus cattle
β -Mannosidosis	β -mannosidase	oligosaccharides in lysosomes of neurons, macrophages, secretory epithelial cells	- Salers cattle and Nubian goats
α -L-fucosidosis	α -L-fucosidase	- fucose containing glycoconjugates in lysosomes of neurons - similar appearance to α/β -Mannosidosis	- autosomal recessive - English springer spaniels
MPS I	α -L-iduronidase	mucopolysaccharide storage in mesoderm derived cells	- domestic shorthair cats and Plott hounds
MPS III	N-acetylglucosamine-6-sulfatase	heparan sulfate in mesoderm-derived cells; neurons contain gangliosides	- Nubian goats
MPS VI	arylsulfatase-B	mucopolysaccharide storage in mesoderm derived cells; neuronal storage does not occur	- Siamese and domestic shorthair cats
MPS VII	β -glucuronidase	widespread neurovisceral storage	- dogs and cats
Glycogenosis (type II in humans)	α -1,4-glucosidase	widespread glycogen storage within lysosomes and intracytoplasmically: including neurons	- autosomal recessive in shorthorn and Brahman beef cattle

obviously vacuolated and this was very apparent in this particular specimen. The participants also discussed the possibility of decreased numbers of nuclei within the granular cell layer in this individual and its potential causes, to include the possibility of

incomplete maturation in a 1 day old calf (with a very visible external granular cell layer in this case) as well as the possibility of autolysis in the particular specimen.

References:

1. Alroy J, Lyons JA. Lysosomal storage diseases. *J Inborn Errors of Metabol Screening* 2014; pp 1-20.
2. Anderson MA. Disorders of Cattle. In: Njaa BL, ed. *Kirkbride's Diagnosis of Abortion and Neonatal Loss in Animals*. 4th ed. Ames, IA. Wiley-Blackwell. 2012 13-48
3. Baucom DL, Romero M, Belfon R, Creamer R. Two new species of *Undilifum*, fungal endophytes of *Astragalus* (locoweeds) in the United States. *Botany*. 2012; 90(9): 866-875.
4. Braun K, Romero J, Liddell C, Creamer R. Production of swainsonine by fungal endophytes of locoweed. *Mycol Res*. 2003; 107(8): 980-988.
5. Cook D, Gardner DR, Grum D, et al. Swainsonine and endophyte relationships in *Astragalus mollissimus* and *Astragalus lentiginosus*. *J Agric Food Chem*. 2011; 59: 1281-1287.
6. Creamer R, Baucom D. Fungal endophytes of locoweeds: a commensal relationship? *J Plant Physiol Pathol* 2013; 1(2): doi:10.4172/2329-955X.1000104.
7. Knight AP, Walter RG. Locoism. In: *A Guide to Plant Poisoning of Animals in North America*. 1st ed. Jackson, WY: Teton New Media: 2001; 204-211.
8. Maxie MG, Youssef S. Nervous system. In: Maxie MG, ed. *Jubb, Kennedy and Palmers Pathology of Domestic Animals*. 5th ed. Vol 1. St. Louis, MO: Elsevier; 2007:322-332, 381.
9. Moeller RJ. Disorders of Sheep and Goats. In: Njaa BL, ed. *Kirkbride's Diagnosis of Abortion and Neonatal Loss in Animals*. 4th ed. Ames, IA. Wiley-Blackwell. 2012; 49-87.
10. Panter KE, Stegelmeier BL. Reproductive toxicoses of food animals. *Vet Clin North Am Food Anim Pract*. 2000; 16(3): 531-544.
11. Panter KE, Welch KD, Gardner DR, et al. Poisonous Plants of the United States. In: Gupta RC, ed. *Veterinary Toxicology*. 2nd ed. Waltham, MA: Academic Press Elsevier: 2012; 1031-1079

Self-Assessment - WSC 2018-2019 Conference 6

1. Some neoplasms of the rat brain traditionally diagnosed as astrocytomas via morphologic features have more recently been identified as having an immunohistochemical profile suggestive of what cellular origin?
 - a. Microglia
 - b. Neurons
 - c. Oligodendroglia
 - d. Astrocytes

2. Which of the following is the most common pairing of cell morphologies in canine mixed gliomas ?
 - a. Neurons and astrocytes
 - b. Astrocytes and ependyma
 - c. Astrocytes and oligodendroglia
 - d. Neurons and oligodendroglia

3. Which of the following cell types is most commonly affected in cerebellar abiotrophy?
 - a. Purkinje cells
 - b. Granular cell layer neurons
 - c. Bergmann's glia
 - d. White matter oligodendroglia

4. Which of the following is not a function of Bergmann's astrocytes?
 - a. Serving as scaffolding for migration of the proneurons during development
 - b. Provide support to Purkinje dendritic tree
 - c. Provide structural repair following Purkinje cell loss
 - d. Provide nourishment to neurons of the granular cell layer

5. Which of the following enzymes is inhibited by ingestion of *Astragalus* and *Swainsona*?
 - a. α -L-fucosidase
 - b. β -mannosidase
 - c. Sphingomyelinase
 - d. β -galactosidase

Please email your completed assessment to Ms. Jessica Gold at Jessica.d.gold2.ctr@mail.mil for grading. Passing score is 80%. This program (RACE program number) is approved by the AAVSB RACE to offer a total of 0.5 CE Credits, with a maximum of 12.5 CE Credits being available to any individual Veterinary Medical Professionals for the 2017-2018 Wednesday Slide Conference. This RACE approval is for the subject matter categories of: SCIENTIFIC using the delivery method of NON-INTERACTIVE DISTANCE. This approval is valid in jurisdictions which recognize AAVSB RACE; however, participants are responsible for ascertaining each board's CE requirements. RACE does not "accredit", "endorse" or "certify" any program or person, nor does RACE approval validate the content of the program.

**Joint Pathology Center
Veterinary Pathology Services**



WEDNESDAY SLIDE CONFERENCE 2018-2019

Conference 7

17 October 2018

Conference Moderator:

Leandro Teixeira, DVM, PhD, DACVP

Assistant Professor, Department of Pathobiological Sciences

Director, COPLOW

University of Wisconsin School of Veterinary Medicine

Madison, WI 53706

CASE I: UW Case 1 (JPC 4084541-00).

Signalment: 15-year-old female spayed Himalayan feline, *Felis catus*

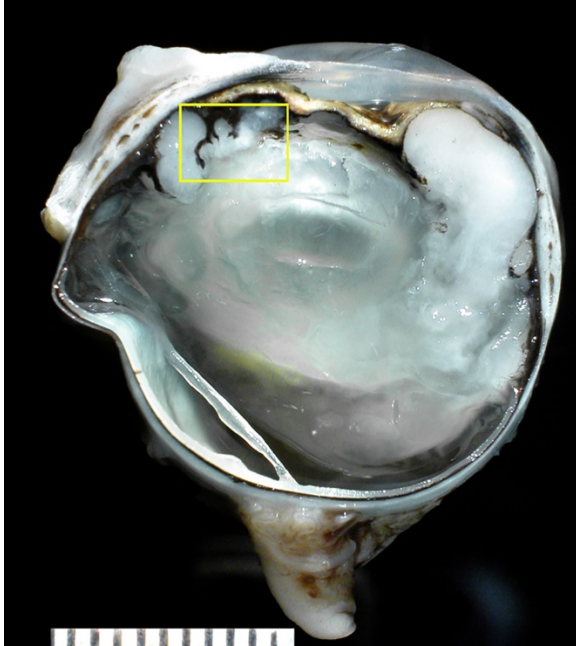
History: The patient presented to the University of Wisconsin–Madison Veterinary Medical Teaching Hospital and was diagnosed with a blind left eye (OS), granulomatous infiltrate in the anterior chamber, posterior chamber and vitreous (OS) and bilateral corneal ulcers. The left eye was enucleated, formalin-fixed and submitted for histopathology.

Gross Pathology: The formalin-fixed left eye was section at the dorsoventral plane. There was a white homogeneous tissue carpeting the surfaces of the iris and ciliary body and extending into the posterior

chamber and anterior vitreous, cradling the lens.

Laboratory results: Thoracic radiographic studies and abdominal ultrasound were within normal limits.

Microscopic Description: There is a poorly delineated, moderately cellular and hyper-eosinophilic neoplastic mass carpeting the posterior iris and ciliary body surfaces, infiltrating and expanding the inferior iris leaflet stroma and extending into the anterior chamber, posterior chamber and anterior vitreous, surrounding the lens capsule. The mass is composed of haphazardly arranged plump neoplastic cells surrounded by dense, highly basophilic chondromatous matrix. Neoplastic cells are individualized or aggregated in lacunae within the matrix and have a moderate amount of granular



Globe, cat. A white homogenous tissue carpets the surfaces of the iris and ciliary body and extends into the posterior chamber and anterior vitreous, encircling the lens. (Photo courtesy of: Comparative Ocular Pathology Laboratory of Wisconsin – COPLOW, School of Veterinary Medicine, Department of Pathobiological Sciences, University of Wisconsin – Madison. <http://www.vetmed.wisc.edu/departments/pathobiological-sciences/>)

eosinophilic to basophilic cytoplasm. Nuclei are oval, have 1-2 magenta nucleoli and finely stippled chromatin. The mitotic rate averages less than one per 10 HPF. There are focally extensive areas of necrosis comprising approximately 20% of the mass. There is a fibrovascular membrane carpeting the anterior surface of the iris (preiridal fibrovascular membrane). There is moderate liquefaction of the cortical lens fibers with accumulation of round and lightly eosinophilic degenerated fibers (Morgagnian globules) and migration of the lens epithelial cells over the inner aspect of the posterior lens capsule. The retina is artifactually detached. The inner retina is devoid of ganglion cells and that are diminished numbers of nuclei in the inner nuclear layer. The optic nerve is markedly gliotic and

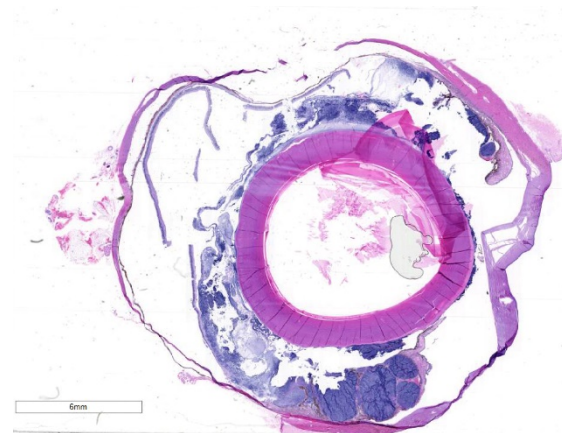
atrophied (optic nerve not present in all sections).

Contributor's Morphologic Diagnoses:

Left eye:

- a. Chondrosarcoma, primary.
- b. Lens, circumferential and moderate cortical lens fiber degeneration and posterior lens epithelial migration (mature cortical cataract).
- c. Retina, marked and diffuse inner retinal atrophy (secondary chronic glaucoma).
- d. Optic nerve, marked and diffuse optic nerve gliosis and atrophy (secondary chronic glaucoma).

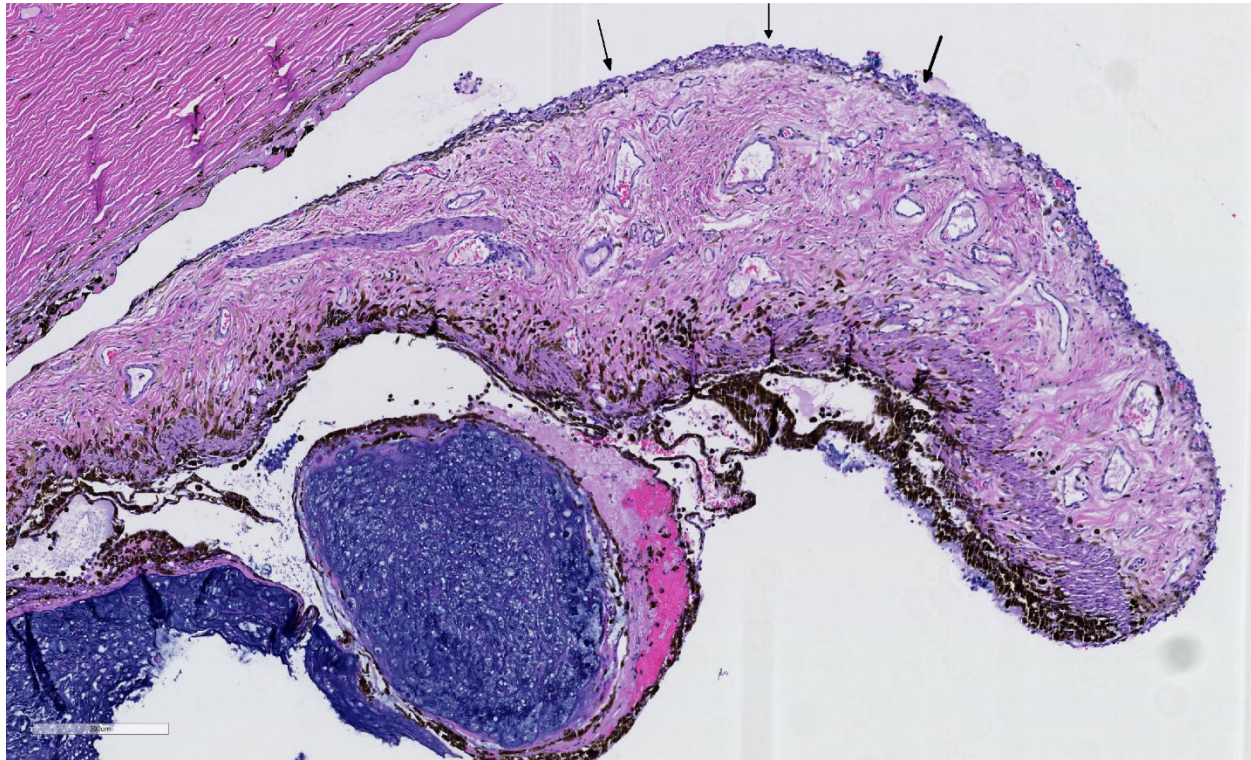
Contributor's Comment: Chondrosarcomas are uncommon malignant neoplasms with predominating cartilaginous matrix that account for the second most common primary skeletal tumor after osteosarcoma in both veterinary and human medicine.⁵ The average age of cats affected by chondrosarcomas is 9.6 years, and there is



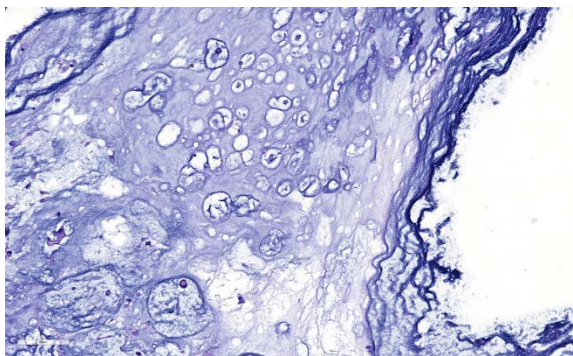
Globe, cat. At subgross magnification, a multilobular dark blue neoplasm carpets the iris, ciliary body and peripheral retinal surfaces, multifocally infiltrating the iris and ciliary body and surrounds the lens. (HE, 5X)

a slight male predilection for the development of these tumors.⁵ Extraskeletal chondrosarcomas, and visceral ones in particular, are rare tumors in dogs, cats and people.^{5,7} In a case series of 67 cats with chondrosarcomas, 47 were tumors of skeletal origin and 20 presented in subcutaneous sites, several of which were thought to be vaccine-site sarcomas.⁵ Intraocular chondrosarcoma is reported in two dogs as a primary¹¹ or metastatic⁸ neoplasm. Metastatic intraocular chondrosarcoma was also reported in one human patient.⁶ In 1959, a single account was published describing an intraocular chondrosarcoma in a cat presenting with multiple intraocular tumors.² Recently, we reported 4 cases of presumed primary intraocular chondrosarcoma in cats (including the present case).² The mean age of the animals was 12.5 (range 9-16) and the tumors presented unilaterally as coalescing, poorly demarcated, white, friable masses

filling the vitreous and intraocular chambers. One tumor presented as a solitary, well-demarcated, tan mass involving the iris and ciliary body. All four neoplasms were composed of haphazardly arranged plump neoplastic spindle cells surrounded by irregular islands and thick trabeculae of abundant, variably basophilic and Alcian-blue-positive chondromatous matrix. No other tumors or skeletal lesions were identified in these four cats that could suggest a metastatic tumor to the eye. Two of the four cats diagnosed with primary ocular chondrosarcoma are still alive and healthy 2.5 years and 5 years following enucleation. One cat died 6 months after enucleation due to chronic kidney disease and diabetes and although no necropsy was performed, imaging done in the follow-up visits still did



Globe, cat. The neoplasm (at left) carpets the posterior iris surface and the ciliary body. The anterior surface of the iris leaflet is covered by a fibrovascular membrane (arrows) (HE, 84X)



Globe, cat. Higher magnification of the neoplasm demonstrates variably sized cartilage lacunae containing polygonal cells. (HE, 260X)

not revealed other masses. The last cat was lost to follow-up.

Due to the distribution of the neoplastic tissue on the eye (posterior chamber and anterior vitreous, surrounding the lens) and because of the chondromatous nature of the mass a post-traumatic sarcoma (chondro-sarcoma) is a possible differential diagnosis. Feline post-traumatic sarcomas (FPTS) are malignant, intraocular neoplasms that are usually associated with trauma that can be evidenced from the clinical history and/or histologic findings (e.g. lens capsule rupture, retinal detachment, and corneal perforation)^{3,4}. We ruled out the diagnosis of FPTS in the present case based on the absence of a history of trauma and/or histologic features of trauma, especially lens capsule rupture, which appears to be a major step on the development of the post-traumatic sarcoma, allowing the lens epithelial cells to gain access to the extra-capsular space, proliferate over the ocular tissues and eventually become neoplastic.^{1,11}

Cats, similar to all mammals, do not have cartilage or bone within their globes and, therefore, the tissue of origin of the primary ocular chondrosarcoma is unclear. It is likely that primary intraocular chondrosarcomas arise from ocular multipotent mesenchymal stem cells or cancer stem cells.⁹ In human eyes, multipotent mesenchymal stem cells

have been derived from the trabecular meshwork.⁹ The trabecular meshwork could be a likely origin of the tumors seen in these cases, all of which showed extensive involvement in the vicinity of the iris, ciliary body and ciliary cleft.

Contributing Institution:

Comparative Ocular Pathology Laboratory of Wisconsin - COPLOW

School of Veterinary Medicine

Department of Pathobiological Sciences

University of Wisconsin – Madison

<http://www.vetmed.wisc.edu/>

<http://www.vetmed.wisc.edu/departments/pathobiological-sciences/>

<http://uwveterinarycare.wisc.edu/>

<http://uwveterinarycare.wisc.edu/support-services/laboratory/anatomic-pathology/>

JPC Diagnosis: Eye, iris and ciliary body: Chondrosarcoma.

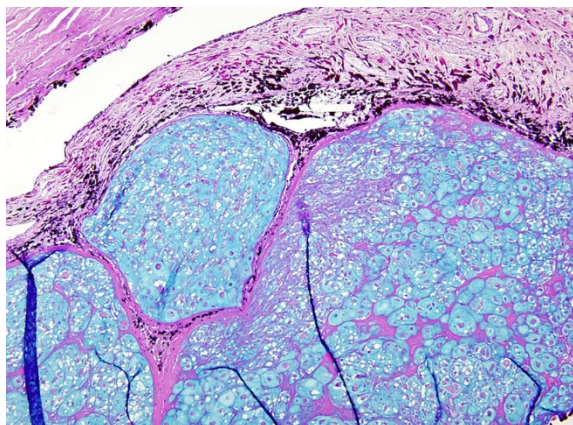
JPC Comment: The moderator, who was also the contributor of this case, has provided an excellent review of this uncommon lesion, as well as the primary differential diagnosis and secondary changes in the section.

In bone and beyond, a diagnosis of chondrosarcoma may be complicated by a number of factors, not the least of which is small sampling. Both the production of osteoid (which changes a diagnosis of chondrosarcoma to a diagnosis of osteosarcoma) as well as malignant features of neoplastic chondrocytes may be lacking in small samples and present in more liberal ones.¹⁰ Due to their poorly vascularized nature, many sarcomas contain extensive areas of necrosis and/or mineralization, and these areas should be avoided when evaluating the malignant features of a potential chondrosarcoma.¹⁰ When evaluating for potential malignancy, the most obviously atypical area of the tumor deserves primary focus. Malignant features

include: more than an occasional binucleated cell (as seen in this case), numerous cells with prominent nuclei, and mitotic figures (which may be extremely rare in more well differentiated malignancies).¹⁰ Chondrosarcomas often contain cellular populations of great morphological variety, including small cells with hyperchromatic nuclei resembling the mesenchymal precursors of cartilage,¹⁰ which were seen in this section as well. Intercellular matrix may range in color from pink to blue, as well as the amount present, and mucinous or myxoid matrix may predominate.

In conference, the moderator discussed three potential diagnoses for this case of an obvious chondromatous neoplasm within the globe: a) a primary ocular chondrosarcoma, b) a chondrosarcoma metastatic to the globe, and c) a post-traumatic sarcoma. The moderator noted the absence of any variation in the morphology of the neoplasm particularly that of in the absence of a spindle cell or osseous component, which would be unusual for a post-traumatic sarcoma, which often has a mix of morphologies. In addition, post traumatic sarcomas are often associated with a tear in the lenticular capsule, which is absent in this specimen.

He also noted that the pattern of “carpeting” of posterior aspect of the ciliary body, as well as the lack of infiltration into this tissue suggests a metastatic process. Other characteristics of ocular metastasis is the formation of a well-demarcated mass within the globe. Presence of neoplastic emboli within the vessels of the choroid or uvea may or may be seen with metastatic tumors. The presence of a primary process elsewhere in the body is ultimately a major consideration, and this was a case submitted by the moderator, who was were unable to identify a primary process elsewhere in the body. COPLOW currently has a total of 7 similar



Globe cat: An Alcian blue/PAS stain highlights the composition of the chondromatous matrix. (Alcian blue/PAS 2.5, 100X). (Photo courtesy of: Comparative Ocular Pathology Laboratory of Wisconsin – COPLOW, School of Veterinary Medicine, Department of Pathobiological Sciences, University of Wisconsin – Madison.

<http://www.vetmed.wisc.edu/departments/pathobiological-sciences/>

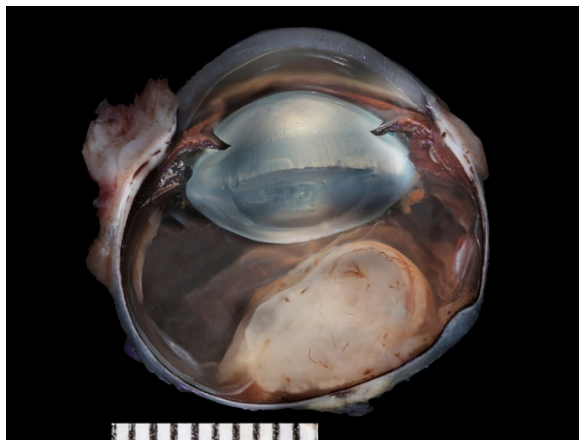
lesions in cats in their database – 5/7 were alive after 2.5 years, the remaining two died of unrelated causes.

Another discussion centered upon whether the retina was artifactually or truly detached. For most of its circumference, photoreceptors remained attached to the RPE, suggesting artifactual detachment. However, there are focal areas in of RPE hypertrophy (tombstoning) as well scattered along the retina, suggesting the possibility of focal areas of detachment prior to processing.

References:

1. Albert DM, Phelps PO, Surapaneni KR, Thuro BA, MD, Potter HAD, Ikeda A, Teixeira LBC, Dubielzig, RR. The Significance of the Discordant Occurrence of Lens Tumors in Humans versus Other Species. *Ophthalmology*; 2015122(9):1765-1770.
2. Beckwith-Cohen B, Teixeira LBC, Dubielzig RR. Presumed primary

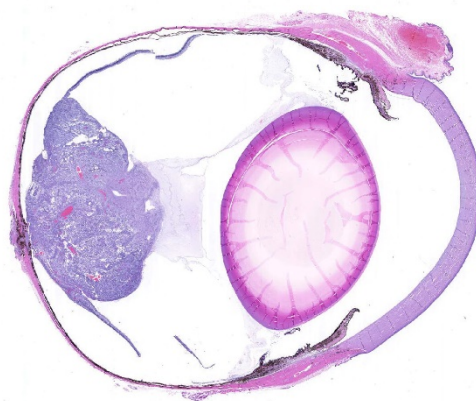
- intraocular chondrosarcoma in cats. *J Vet Diag Invest.* 2014; 26(5):664-668.
3. Dubielzig RR, Everitt J, Shaddock JA, Albert DM. Clinical and morphologic features of post-traumatic ocular sarcomas in cats. *Vet Pathol.* 1990; 27:62-65.
 4. Dubielzig RR. Non-surgical trauma. In: Dubielzig RR, Ketring KL, McLellan GJ, Albert DM, ed. *Veterinary Ocular Pathology: A Comparative Review.* Philadelphia, PA: Saunders Elsevier; 2010:81-114.
 5. Durham AC, Popovitch CA, Goldschmidt MH. Feline chondrosarcoma: a retrospective study of 67 cats (1987-2005). *J Am Anim Hosp Assoc.* 2008; 44:124-130.
 6. George DP, Zamber RW. Chondrosarcoma metastatic to the eye. *Arch Ophthalmol* 1996; 114:349-351.
 7. Rozeman LB, Cleton-Jansen AM, Hogendoorn PC. Pathology of primary malignant bone and cartilage tumours. *Int Orthop.* 2006; 30:437-444.
 8. Rodrigues EF, Jr., Ribeiro AP, Perlmann E, et al. Metastatic intraocular chondrosarcoma in a dog. *Vet Ophthalmol.* 2009; 12:254-258.
 9. Tay CY, Sathiyathan P, Chu SW, et al. Identification and characterization of mesenchymal stem cells derived from the trabecular meshwork of the human eye. *Stem Cells Dev.* 2012; 21:1381-1390.
 10. Thompson KG, Dittmer KE. Tumors of Bone. In: Meuten DJ, ed, *Tumors of Domestic Animals, 5th ed.* Ames IA, Wiley-Blackwell, 2017: 848-849.
 11. Zeiss CJ, Johnson EM, Dubielzig RR. Feline intraocular tumors may arise from transformation of lens epithelium. *Vet Pathol.* 2003; 40:355-362.
- CASE II: 16RD2093 (JPC 4102435-00).**
- Signalment:** 8-year-old male neutered Yorkshire terrier dog, *Canis familiaris*
- History:** The patient presented to a veterinary ophthalmologist and was diagnosed with a blind right eye (OD) with retinal detachment and potentially an opaque structure posterior to the lens with areas of hemorrhage. The right eye was enucleated, formalin-fixed, and submitted for histopathology.
- Gross Pathology:** The formalin-fixed left eye was section at the dorsoventral plane. There was a soft, tan and homogeneous mass adjacent to the optic nerve protruding into the vitreous.
- Laboratory results:** Ocular ultrasound revealed a soft tissue opacity extending from the optic nerve into the vitreal space.
- Microscopic Description:** There is an unencapsulated, well-delineated and densely cellular neoplastic mass infiltrating,



Eye, dog: A neoplasm arises from and effaces the central retina and optic nerve head protruding into the vitreous. (Photo courtesy of: Comparative Ocular Pathology Laboratory of Wisconsin – COPLOW, School of Veterinary Medicine, Department of Pathobiological Sciences, University of Wisconsin – Madison. <http://www.vetmed.wisc.edu/departments/pathobiological-sciences/>)

expanding and partially effacing the optic nerve head and central retina, protruding into the vitreous. The mass is composed of a mixture of polygonal, spindle and round cells arranged in short interlacing streams and bundles supported by a moderately dense fibrovascular stroma. The neoplastic cells have indistinct cell borders, a variable amount of pale eosinophilic fibrillar cytoplasm, oval to elongate nuclei with finely stippled chromatin and 1-3 variably distinct nucleoli. A subset of neoplastic cells presents vacuolated cytoplasm with round and eccentrically located nuclei. Anisocytosis and anisokaryosis are marked; with moderate numbers of karyomegalic cells and a few bi and multinucleated cells. There are 6 mitotic figures in 10 HPFs. There are multifocal to focally extensive areas of necrosis, characterized by tissue hypereosinophilia and accumulation of karyorrhectic debris that are surrounded by palisading neoplastic cells (not in all sections). There are multifocal cavitated areas filled with light amphophilic material thought the mass. At the periphery of the neoplasm and in the inner aspects of the retina adjacent to the mass there is prominent capillary proliferation with

occasional formation of glomerular-like tufts. There is a mild accumulation of red blood cells in the anterior vitreous. The retina is diffusely detached and there is moderate hypertrophy of the RPE cells and mild subretinal hemorrhage. The detached retina presents diffuse loss of ganglion cells, atrophy of the inner nuclear layer, and mild and multifocal hemorrhage. The post-laminar portion of the optic nerve (not present in all slides) is markedly atrophied and presents increased numbers of non-neoplastic glial



Eye, dog Subgross magnification of the retinal mass infiltrating, expanding and partially effacing the central retina and optic nerve head and its placement within the vitreous.

cells (gliosis).

Contributor's Morphologic Diagnoses:

Left eye:

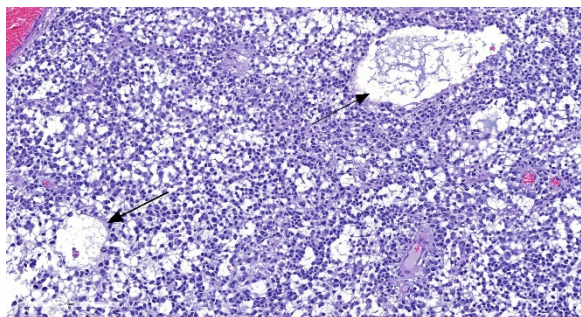
- e. Optic nerve and retinal glioma/astrocytoma, high-grade.
- f. Retina, diffuse retinal detachment with inner retinal atrophy.
- g. Post-laminar optic nerve, moderate and diffuse atrophy and gliosis.

Additional results: Neoplastic cells

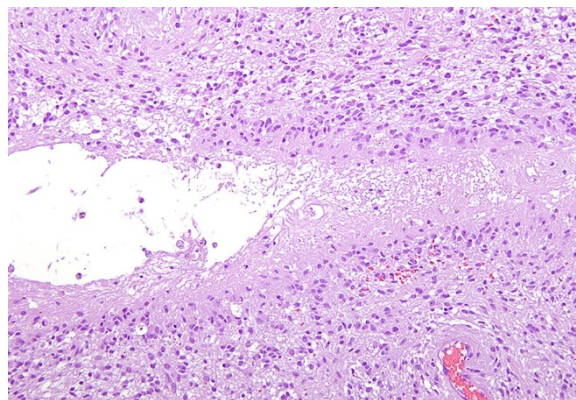
present strong immunohistochemical cytoplasmic positivity for glial fibrillary acidic protein (GFAP).

Contributor's Comment: Gliomas are among the most common primary tumors of the CNS in dogs, their prevalence being only exceeded by meningiomas.⁴ Based on the World Health Organization (WHO) classification for domestic animal tumors,⁶ which, in turn, is based on classification of human neoplasms, these tumors are classified according to their cell of origin into astrocytomas, oligodendrogliomas, mixed tumors (oligoastrocytomas), and ependymomas. According to their cytologic characteristics, astrocytomas are further classified into low-grade or well-differentiated, medium-grade or anaplastic, and high-grade or glioblastoma. Low-grade astrocytomas are classified as fibrillary, protoplasmic, or gemistocytic.^{4,6}

Optic nerve and retinal glioma are rare neoplasms that have been sporadically reported in dogs and cats.^{2,3,9} These tumors can originate and infiltrate the retina, optic nerve head and the post-laminar optic nerve. Most optic nerve and retinal gliomas present morphologic features similar to astrocytomas as seen in other areas of the central nervous system, but rarely these tumors can resemble



Eye, dog Neoplastic cells are polygonal to spindle on a mucinous matrix. There are large areas of dropout scattered throughout the mass (arrows) (HE, 286X)



Eye, dog. Neoplastic cells palisade around areas of dropout and necrosis. (HE, 100X) (Photo courtesy of: Comparative Ocular Pathology Laboratory of Wisconsin – COPLOW, School of Veterinary Medicine, Department of Pathobiological Sciences, University of Wisconsin – Madison.

<http://www.vetmed.wisc.edu/departments/pathobiological-sciences/>

oligodendrogliomas or present a mixture of astrocytoma and oligodendroglioma features.^{3,9}

Optic nerve/retinal gliomas with predominantly astrocytic phenotype present immunohistochemical positivity for glial fibrillary acidic protein (GFAP) and the rare cases of oligodendrogliomas reported were GFAP-negative.^{3,9} The present case is an example of a mixed glioma, with the tumor presenting predominantly astrocytic cells with areas of oligodendroglial differentiation. The decision to classify the present tumor as an astrocytoma was based on the predominance of the astrocytic component and the strong immunoreactivity to GFAP.

Regarding tumor grading, it has been reported that, based on the WHO classification,⁶ the majority of optic nerve/retinal gliomas in dogs fit into the high-grade astrocytoma category.⁹ Similarly, the hypercellularity, cellular pleomorphism, relatively high mitotic count (6/10 HPF) and the presence of intratumoral vascular proliferation and necrosis identified on the present tumor led to the classification of a

high-grade astrocytoma. Interestingly, despite the high-grade classification of the majority of canine optic nerve/retinal gliomas these tumors rarely metastasize or recur when surgical margins are clean.^{2,3,9} The most important prognostic feature is the presence of tumor invasion beyond the optic nerve surgical margins, which correlated with tumor recurrence (in the remaining optic pathways) and, in rare cases, tumor extension to the brain.⁴

Contributing Institution:

Comparative Ocular Pathology Laboratory of Wisconsin - COPLOW

School of Veterinary Medicine

Department of Pathobiological Sciences

University of Wisconsin – Madison

<http://www.vetmed.wisc.edu/>

<http://www.vetmed.wisc.edu/departments/pathobiological-sciences/>

<http://uwveterinarycare.wisc.edu/>

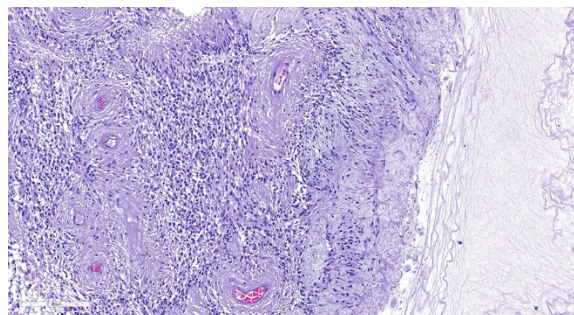
<http://uwveterinarycare.wisc.edu/support-services/laboratory/anatomic-pathology/>

JPC Diagnosis: Eye, retina and optic nerve: Astrocytoma, low-grade.

JPC Comment: The moderator, who was also the contributor of this case, has provided an excellent review of this uncommon lesion as well, and this case brings our two-week run of three gliomas(!) to an end.

The JPC ran GFAP and Olig-2 on sections from this case and well over 80% of the neoplastic cells were strongly positive for both markers in this particular case.

The naming of Olig2, like many other immunohistochemical markers, implies a specificity for oligodendroglia that is unfortunately lacking in the real world of the diagnostic pathologist. Immunohistochemical markers are largely named for



Eye, dog Neoplastic cells palisade around vessels with numerous cytoplasmic projections adjacent to vessel walls. (HE, 134X)

their targeted gene product. (Another example of this “false advertising” for immunohistochemical markers is thyroid transcription factor 1, which not only labels both thyroid follicular and C-cells, but also is an excellent marker for pulmonary carcinomas.)

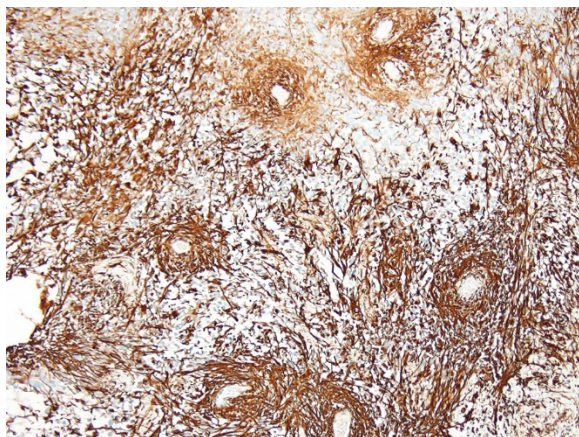
Within the subcutaneous ventricular zone of the developing brain, undifferentiated progenitor cells may ultimately developing to neurons, astrocytes, or oligodendroglia. Expression of Olig2 specifies progenitor cells to pattern glial versus neuronal lineage. By reprocessing the neuronal phenotype in these progenitor cells, only two expression permits production of astrocyte and oligodendrocyte precursors.⁷ Undifferentiated retinal progenitor cells may also express Olig-2, although oligodendroglia are not found in the retina. In the retina it functions to maintain retinal progenitor cells in an undifferentiated state.⁸

Olig-2 expression is downregulated in mature astrocytes.⁷ This may explain the increased expression of Olig 2 in the progression of malignant astrocytomas¹, with highest levels in glioblastomas and anaplastic gliomas. A review of labeling indices (LI) in neuroepithelial tumors in humans revealed Olig-2 LI at 43.7% in diffuse astrocytomas, 59.3 in oligoastrocytomas (mixed gliomas), and 76.1% in oligodendrogliomas.¹⁰

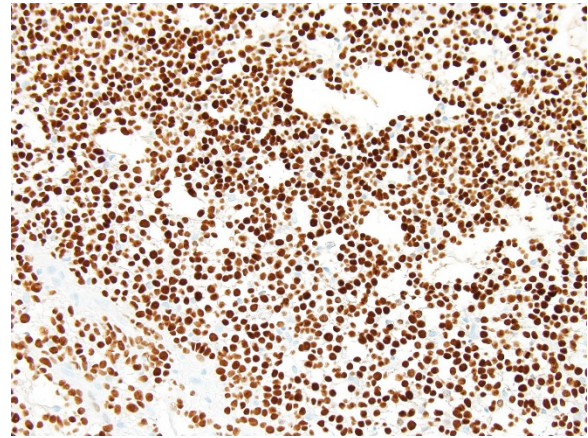
From a diagnostic standpoint, Olig2 is obviously widely expressed in both astrocytomas and oligodendrocytomas. It is not expressed in ependymomas, so a negative finding may help to differentiate pilocytic astrocytomas and glioblastomas which morphologically resemble ependymomas from tumors of true ependymal origin.⁵

While most species do not have oligodendroglia in the retina, dogs and rabbits have a myelinated optic nerve head which and may contain oligodendroglia. However, the strongly positive GFAP in this case rules out the possibility of an oligodendroglioma in the case.

In the conference, the moderator drew the attendees' attention to the proliferation of



Eye, dog Palisading neoplastic cells and their projections demonstrate strong cytoplasmic immunopositivity for glial fibrillary acidic protein. (anti-GFAP, 134X)



Eye, dog Neoplastic cells demonstrate strong nuclear immunopositivity for OLIG-2. (anti-OLIG-2, 200X)

blood vessels within the inner layers of the retina (particularly the ganglion cell layer and inner nerve fiber layer) similar to that seen within the tumor as well, suggesting the possibility of local diffusion of growth factors produced by tumor cells. Another incidental change noted by the moderator is the presence of melanin within the connective tissues of the drainage angle, suggestion previous damage to the pigmented epithelium of the ciliary body. While not a problem in this globe at this particular time, infiltration of macrophages may occur at some point in the future to phagocytize the pigment and initiate inflammatory changes that may ultimately result in fibrosis and closure of the drainage angle.

The moderator commented on the thickness of the sclera, which some participants had interpreted as thinned. Three points are helpful in evaluation of scleral thickness – first the moderator says that evaluation of thickness should be made at the limbus. Second, the normal spatial relationship of other structures, such as the iridal leaves will be abnormal in buphthalmic eyes, and finally, comparison to suspected buphthalmic globes to globes from other dogs (even other breeds) may be useful, as the difference in globe size

between dogs, even of different breeds, is not very significant.

The JPC diagnosis of astrocytoma, low grade is based on the presence of over 80% of cells which are morphologically identifiable of astrocytes on the HE, a mitotic rate of 2 per 2.37mm² field, and strong GFAP and Olig2+ positivity (not available to participants before the conference). The moderator said that COPLOW would likely call this a mixed glioma of the retina/optic nerve but the JPC diagnosis was essentially the same.

References:

12. Bozinov O, Hohler S, Samans B, Benes L, Miller D, Ritter M, Sure U, Bertalanffy H. Candidate genes for the progression of malignant gliomas identified by microarray analysis. *Neurosurg Rev* 2008; 31(1):83-90
13. Dubielzig RR. The optic nerve. In: Dubielzig RR, Ketring KL, McLellan GJ, Albert DM, ed. *Veterinary Ocular Pathology: A Comparative Review*. Philadelphia, PA: Saunders Elsevier; 2010:399-417.
14. Dubielzig RR. Tumors of the eye. In: Meuten DJ. *Tumors in domestic animals*. 5ed. Ames, IA: John Wiley and sons Inc.; 2017:892-922.
15. Higgins RJ, Bollen AW, Dickinson PJ and Siso-Llonch S. Tumors of the nervous system. In: Meuten DJ. *Tumors in domestic animals*. 5ed. Ames, IA: John Wiley and sons Inc.; 2017:834-891.
16. Ishizawa K, Komori T, Shimada S, Hirose. Olig2 and CD99 are useful negative markers for the diagnosis of brain tumors. *Clin Neuropathol*, 27: 118-128.
17. Koestner A, Bilzer T, Fatzer R. *et al*. Tumors of neuroepithelial tissue. In: World Health Organization.

International Histological Classification of Tumors of Domestic Animals. *Histological Classification of the Tumors of the Nervous System of Domestic Animals*, 2nd series, Vol. V. Armed Forces Institute of Pathology, Washington, DC, 1999; 17-27.

18. Marshall CAG, Novitch BG, Goldman JE. Olig2 directs astrocyte and oligodendrocyte formation in postnatal subventricular zone cells. *J Neuroscience* 2005; 25(32):7289-7298.
19. Nakamura K, Harada C, Namekata K, Harada T. Expression of olig2 in retinal progenitor cells. *Develop Neurosci* 2006; 17(4):345-349.
20. Naranjo C, Schobert C, Dubielzig RR. Canine ocular gliomas: a retrospective study. *Vet Ophthalmol*. 2008; 11:356-362.
21. Suzuki A, Nobusawa S, Natsume A, Suzuki H, Kim Y, Yokoo H, Nagaishi, M, Ikota, H, Nakazawa T, Wakabyashi T, Ohgaki H, Makazato Y. Olig2 labeling index is correlated with histological and molecular classifications in low-grade diffuse gliomas. *J Neuro-oncol* 2014; 120(2):283-291

CASE III: 15/444 (JPC 4068158-00).

Signalment: 20-year-old horse, Appaloosa, unknown sex (*Equus caballus*)

History: The horse was blind on the left eye, and had glaucoma that was suspected to be secondary to chronic (possibly recurrent) uveitis and posterior lens luxation. The eye was enucleated due to increased ocular pressure that could not be medically



Eye, horse. A partial section of eye containing cornea, sclera, iris, ciliary body and iridocorneal angle structures is submitted for examination. (HE, 8X)

controlled, and submitted for histopathological examination.

Gross Pathology: The lens of the eye was posteriorly luxated and attached in only a few lens fibers. Other gross changes were not detected.

Laboratory results: N/A.

Microscopic Description: Eye, horse: In the conjunctiva, there was a mild lymphoplasmacytic infiltration. Multiple ruptures was observed in the Descemet's membrane in conjunctiva. The filtration angle appeared to be pressed posteriorly, and consisted of compact tissue without obvious trabecular tissue. The iris appeared normal. Along the non-pigmented epithelium of the ciliary body, there was a diffuse thick membrane consisting of eosinophilic homogeneous to slightly fibrillar material. Intensely eosinophilic rod-shaped inclusions were found in some of the non-pigmented epithelial cells. There was a very mild multifocal infiltration of lymphocytes and plasma cells in the ciliary body. The retina was atrophic, with few ganglion cells, a thin inner nuclear layer that multifocally merged with the outer nuclear layer. In the lens, there was mild multifocal degenerative changes.

In Congo-red stained sections, there was intense positive apple green birefringence under polarized light (amyloid) in the

eosinophilic membrane associated with the non-pigmented epithelium. Small amounts of positive material was also detected in the filtration angle and the iris. In some sections, there are vascular invasion in the cornea and corneal edema.

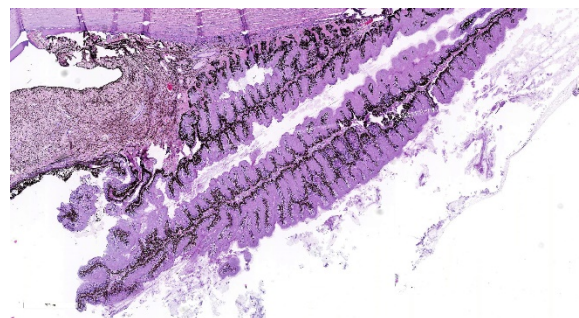
Due to the large size of the eye, pieces containing limbal cornea, iris, ciliary body and anterior sclera, choroid and retina was excised for submission for Wednesday Slide Conference. In a few sections the tip of the iris is missing in the slide, however as described above this area of the ocular tissue was without morphological lesions. The number of intracytoplasmic inclusion and inflammatory infiltrates were few, and thus not present in every slide. The main lesion, the amyloid, was extensive and is present in every slide.

Contributor's Morphologic Diagnoses:

Eye, ciliary body: amyloidosis, severe, diffuse with mild multifocal lymphoplasmacytic uveitis and ciliary non-pigmented epithelial intracytoplasmic inclusions

Eye: secondary glaucoma and posterior lens luxation

Contributor's Comment: Equine recurrent uveitis is a leading cause of blindness in horses. The cause is unknown, and autoimmune disease, infection with



Eye, horse: The ciliary processes are markedly expanded. (HE, 14X)

leptospire or a stereotypic response to chronic intraocular inflammation following a variety of insults have been proposed to cause the disease.^{2,5,6,11,12} Inflammation in the ciliary body of this horse was very mild and consisted of multifocal infiltration of few lymphocytes and plasma cells. Another histopathologic feature of equine recurrent uveitis in the horse is rod-shaped intracytoplasmic inclusions in the non-pigmented ciliary epithelium,^{1,4} and although sparse, such inclusions were present in this case.

The most striking lesion was the thick eosinophilic membrane associated with the non-pigmented ciliary epithelium that was confirmed to be amyloid in Congo red stained slides viewed under polarized light. This finding is by some authors considered to be specific for equine recurrent uveitis and diagnostic for the condition.^{4,13} The ocular amyloid in two horses suffering from equine recurrent uveitis was characterized immunohistochemically and by mass spectrometry to be localized ocular AA amyloid.⁹ Several morphologic features in the ciliary body in the eye from this horse was consistent with

equine recurrent uveitis: amyloid deposition - lymphoplasmacytic uveitis and intraepithelial eosinophilic rod shaped inclusions - although the two latter were very mild.

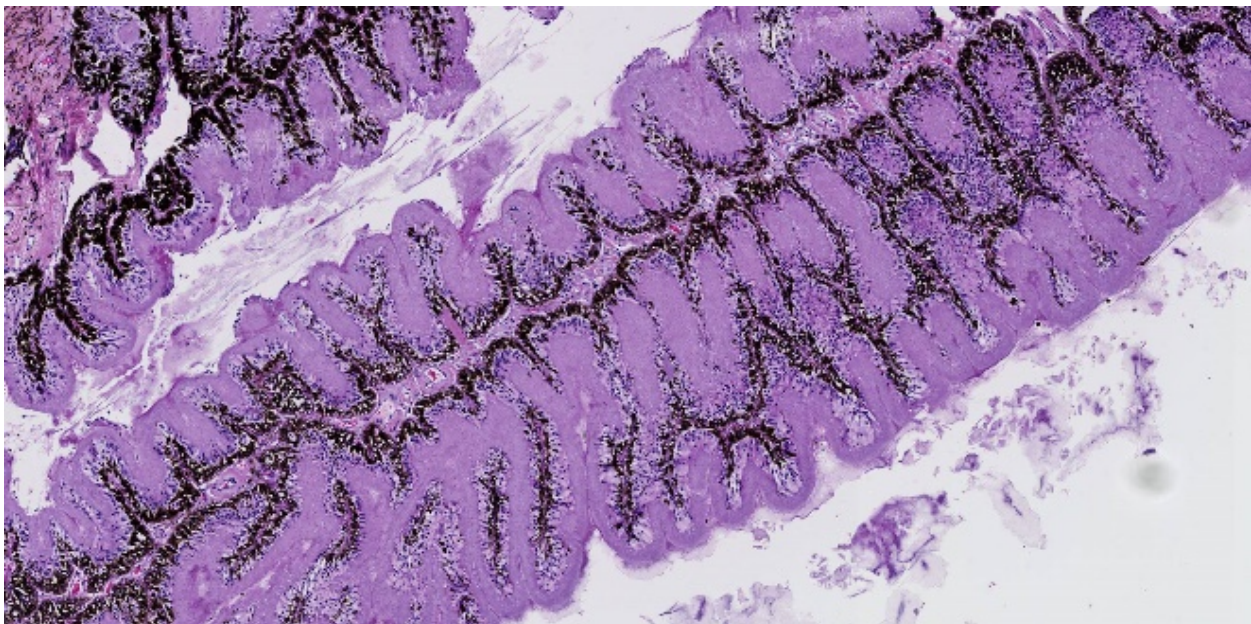
Contributing Institution:

Institute of Basic Sciences and Aquatic Medicine,
Norwegian University of Life Science,
School of Veterinary Medicine
www.nmbu.no

JPC Diagnosis: 1. Eye, surface of ciliary body: Amyloidosis, diffuse, severe.

2. Eye, iris: Anterior synechiae with occlusion of the iridocorneal angle.

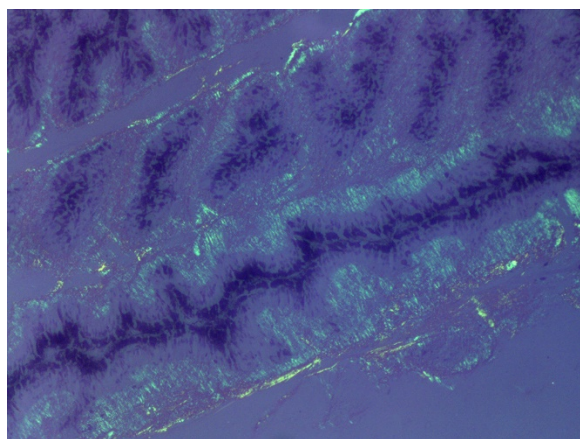
JPC Comment: Ocular amyloidosis is an uncommon finding in the horse; to date, all reported cases of intraocular amyloid have been associated with equine recurrent uveitis. Conjunctival amyloid has also been identified in the horse eye, most often in conjunction with nasal amyloidosis.¹⁰



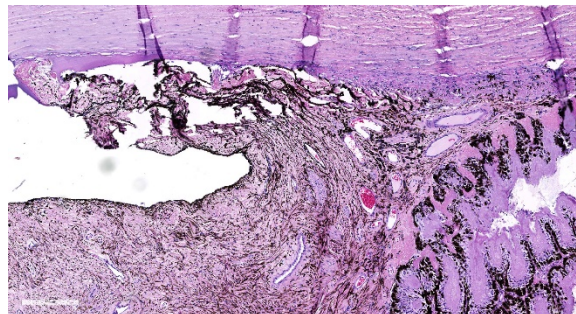
Eye, ciliary processes, horse: A 35µm-thick layer of amyloid carpets the non-pigmented epithelium. (HE, 73X)

Several syndromes have been identified with amyloidosis in the horse. Systemic amyloidosis occur secondary to chronic inflammatory conditions, horses used for the production of immunoglobulins, and neoplasia. Reactive systemic amyloidosis (seen in chronic inflammatory conditions and immunoglobulin-producing horses) results from the production of excessive serum amyloid A (SAA), and deposition of the non-degradable protein within tissues. SAA is preferentially deposited in the liver but may also be seen in the spleen, kidneys, GI tract, adrenal glands, and lymph nodes. Systemic amyloidosis resulting from the deposition of amyloid light chains (AL) is rare in the horse and has been seen in association with multiple myeloma.⁶

There are several forms of localized amyloidosis in the horse as well. Nasal amyloidosis results from the nodular deposition of AL amyloid within the nasal cavity and elsewhere in the respiratory system. These deposits may result in epistaxis, stertor, exercise intolerance, and nasal obstruction. Conjunctival amyloid



Eye, ciliary processes, horse: The amyloid displays marked apple green birefringence under polarized light. (Congo Red, 100X). (Photo courtesy of: Institute of Basic Sciences and Aquatic Medicine, Norwegian University of Life Science, School of Veterinary Medicine, www.nmbu.no)

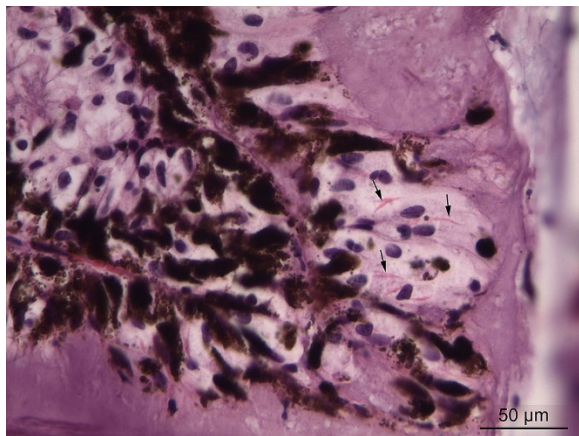


Eye, drainage angle, horse: The drainage angle presents a narrowed ciliary cleft and a collapsed trabecular meshwork (HE, 73X).

deposits have been seen in two cases. Progression to systemic AL amyloidosis has not been reported in the horse.¹⁰

A final type of localized AL-amyloidosis seen in the horse is cutaneous amyloidosis (and has also been documented in man, dogs, and cats. In the horse, these nodules are most often seen within the panniculus of the head, neck, shoulders and chest, and may be associated with granulomatous dermatitis and panniculitis.⁸ They may wax and wane, and of the cases that have been associated with extraskeletal plasmacytoma and lymphoma, a pathogenesis for most cases has not yet been identified. They are occasionally seen with other forms of localized amyloid, but not with systemic forms of amyloid in the horse.⁸

According to the pathologists of the Comparative Ocular Pathology Laboratory of Wisconsin (COPLOW), equine recurrent uveitis (ERU) is the most common cause of cataract, glaucoma, phthisis bulbi, and blindness in the horse. It is characterized by recurrent bouts of inflammatory disease resulting in progressive ocular degeneration. Its pathogenesis has not been definitively established, although previous infection with various *Leptospira* serovars, breakdown of the ocular-blood barrier, and autoimmunity all play a significant part. The involvement



Eye, non-pigmented ciliary body epithelium: Linear inclusions of hypereosinophilic crystalline proteins are present within non-pigmented ciliary body epithelium. (HE, 400X) (Photo courtesy of: Institute of Basic Sciences and Aquatic Medicine, Norwegian University of Life Science, School of Veterinary Medicine, www.nmbu.no)

of *Leptospira* sp. is a well-known yet often inconsistent finding, and the latter two factors are likely the most important driver in this disease. Appaloosas have a yet undefined breed predisposition.³

Affected eyes have a wide range of morphologic appearances, but the following have been noted with regularity in this condition: lymphoplasmacytic uveitis with lymphoid follicle formation; lymphocytes and/or plasma cells within the nonpigmented ciliary epithelium; eosinophilic linear inclusions within the cytoplasm of nonpigmented ciliary body epithelial cells, amyloid; and the deposition of a cell-poor hyaline protein on the inner surface of the nonpigmented ciliary body epithelium.⁴ A wide range of non-specific secondary changes may be seen in affected eyes, including cataracts, anterior and posterior synechiae, iridal fibrovascular membranes, retinal degeneration and attachment, and optic neuritis.⁴

On a cellular level, the distribution of lymphocytes is characteristic of a TH1-like

inflammatory response with a predominance of CD4 plus T cells and increased transcription of IL-2 and interferon gamma. Retinal autoantigens, including intra-photo receptor binding protein, cellular rectum aldehyde binding protein, recoverin, and retinal S antigen have been demonstrated in experimental models and spontaneous cases of the ERU.⁴

The presence of corpora nigra (a normal structure in the eye of the horse which assists in filtering light coming into the globe) is useful in orienting horse eyes, as they are primarily found in the dorsal iris leaflet.

The formation of the JPC morphologic was a subject of spirited discussion. Due to the lack of significant inflammation, the term “uveitis” was not considered appropriate in this case. The combination of amyloid and crystalline inclusions within non-pigmented ciliary body epithelium in the first morphologic diagnosis above was made more out of convention than a shared pathogenesis. While references refer to the inclusions as “amyloid-like”¹³, amyloid is an extracellular protein, and ultrastructurally, many of these inclusions are present in the mitochondria in ciliary body epithelium. The true nature of these inclusions is yet to be determined. The second morphologic diagnosis of anterior Synechiae with drainage angle occlusion is likely the result of recurrent episodes of now-resolved inflammation and subsequent fibrosis within the drainage angle. While this change is certainly consistent with the contributor’s diagnosis of secondary glaucoma, we are unable to confirm this finding with the limited number of intraocular tissue available on the slide. While the contributor identified retinal atrophy (possibly from being able to evaluate the whole globe), the conference slides only contain peripheral retina, the evaluation of

which, in the moderator's (and JPC staff) experience, for atrophy is problematic at best.

References:

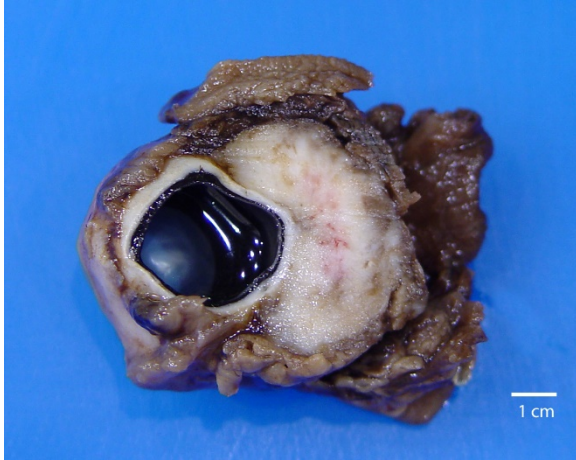
1. Cooley PL, Wyman M, Kindig O. Pars plicata in equine recurrent uveitis. *Vet Pathol* 1990; 27:138-140.
2. Deeg CA. Ocular immunology in equine recurrent uveitis. *Vet Ophthalmol* 2008; 11, Suppl.1,61-54.
3. Dubielzig RR. The uvea. In: Dubielzig RR, Ketring KL, McLellan GJ, Albert DM, ed. *Veterinary Ocular Pathology: A Comparative Review*. Philadelphia, PA: Saunders Elsevier; 2010:245-322..
4. Dubielzig RR, Render JA, Morreale RJ. Distinctive morphologic features of the ciliary body in equine recurrent uveitis. *Vet Comp Ophthalmol* 1997; 7:163-167.
5. Frellstedt L. Equine recurrent uveitis: A clinical manifestation of leptospirosis. *Equine Vet Educ* 2009; 21:546-552.
6. Hines MT. Immunologically mediated ocular disease in the horse. *Vet Clin North Am Large Anim Pract* 1984; 6:501-512.
7. Kim, DY, Taylor HW, Eades SC, Cho DY. Systemic AL amyloidosis associated with multiple myeloma in a horse. *Vet Pathol* 2005; 42(1):81-84.
8. Mauldin EA, Peters-Kennedy J. Integumentary system. In: Maxie MG, ed. *Jubb, Kennedy and Palmer's Pathology of domestic animals*, Vol 1, 6th ed. Philadelphia, USA: Elsevier Saunders; 2017:509-735.
9. Østevik L, de Souza GA, Wien TN, Gunnes G, Sørby R. Characterization of amyloid in equine recurrent uveitis as AA amyloid. *J Comp Path* 2014; 151:228-233.
10. Ostevik L, Gjermund Gunnes, de Souza GA, Wien TN, Sorby R. Nasal and ocular amyloidosis in a 15-year-old horse. *Acta Vet Scand* 2014; 56:50-59.
11. Pearce JW, Galle LE, Kleiboeker SB, et al. Detection of *Leptospira interrogans* DNA and antigen in fixed equine eyes affected with end-stage equine recurrent uveitis. *J Vet Diagn Invest* 2007; 19:686-690.
12. Romeike A, Brugmann M, Drommer W. Immunohistochemical studies in equine recurrent uveitis (ERU). *Vet Pathol* 1998; 35:515-526.
13. Wilcock BP. Eye and ear. In: Maxie MG, ed. *Jubb, Kennedy and Palmer's Pathology of domestic animals*, Vol 1, 5th ed. Philadelphia, USA: Elsevier Saunders; 2007:459-552.
14. Wogemeskell, M. A concise review of amyloidosis in animals. *Vet Med Int* 2012; Article is ID, 427296.

CASE IV: AVC C5181-11 (JPC 4019356-00).

Signalment: 5 year old, castrated male Boxer, (*Canis familiaris*)

History: A mass was located behind the eye in the region of the optic nerve resulting in exophthalmia. It was noticed 4 months prior to presentation. There was no evidence of metastasis.

Gross Pathology: A globe with attached orbital soft tissue and eyelids was submitted. A firm to hard lobulated white mass which measured approximately 2 cm x 3 cm x 3 cm surrounded the optic nerve and infiltrated the



Eye, dog. A whitish conical neoplasm encircles the optic nerve and infiltrates the orbital connective tissue but does not infiltrate the posterior sclera. (Photo courtesy of: Atlantic Veterinary College, University of Prince Edward Island <http://avc.upei.ca>)

orbital soft tissues on the posterior aspect of the globe.

Laboratory results: NA

Microscopic Description: The non-encapsulated, well-delineated, moderately cellular mass surrounds the optic nerve, invades the orbital adipose and skeletal tissue, and extends slightly into the sclera. The mass is composed of nests and sheets of moderately densely packed neoplastic cells separated into lobules by fibrous connective tissue septa with scattered nodules of myxoid tissue and multifocal osseous and chondroid metaplasia. The majority of the neoplastic cells are large and polygonal with distinct cell margins, a moderate to abundant amount of glassy eosinophilic cytoplasm, and a large eccentric ovoid vesicular nucleus, occasionally with peripheralized chromatin, and one or two small distinct nucleoli. Scattered neoplastic cells contain intranuclear cytoplasmic invaginations. There is moderate to marked anisocytosis and anisokaryosis and scattered cells contain lobulated or multiple nuclei. Five mitotic figures are counted in 10 randomly selected

HPF (40x) and rare mitotic atypia is noted. Small foci of necrosis, suppurative infiltration, and hemorrhage are present multifocally and small aggregates of lymphocytes are scattered amongst the neoplastic cells.

Contributor's Morphologic Diagnoses:
Orbital (retrobulbar) meningioma

Contributor's Comment: Along with the gross appearance and location (surrounding the optic nerve), the histomorphologic features, which include dense aggregates of large epithelioid cells and foci of cartilaginous and osseous metaplasia, are characteristic of orbital (retrobulbar) meningioma.⁸

Meningiomas are considered common tumors of dogs and Boxers may be one of several breeds with a predilection for developing these masses.^{9,10} Most meningiomas arise intracranially; tumors in the retrobulbar location are considered rare^{1,3,9,14} accounting for only 3% of meningiomas in the dog.⁷ Retrobulbar meningiomas may be primary (also called orbital meningioma), arising from the arachnoidal cap cells of optic nerve sheath, or

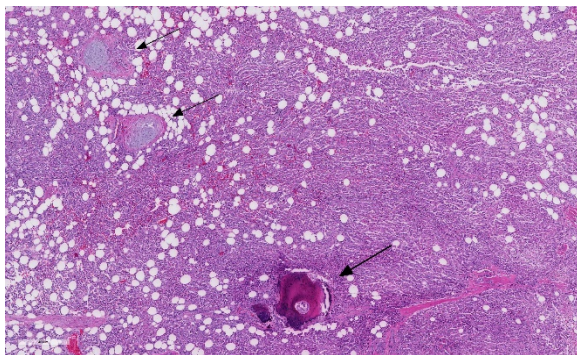


Eye, dog. Subgross image of the neoplasm, better demonstrating infiltration of the orbital connective tissue and compression, but not invasion, of the posterior globe. (HE, 5X)

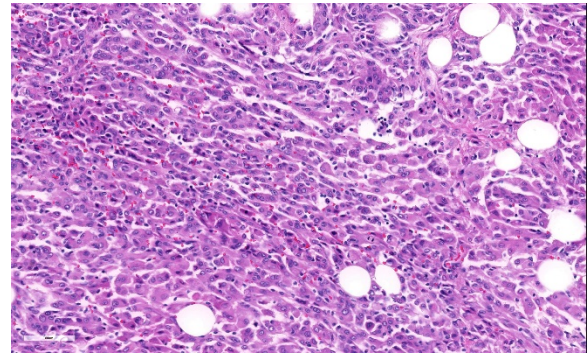
secondary, representing extension of an intracranial neoplasm along the optic nerve.^{6,7} In addition to dogs^{1,2,4,8,9,11,12} and humans⁶, meningiomas arising from the optic nerve have been reported in a cat,⁵ F334 rats,¹⁶ and a Simmental cow.¹³

Grossly orbital meningiomas are tan solid conical masses that surround the optic nerve and are firmly adhered to the posterior aspect of the globe with tapering towards the optic canal.³ These tumors compress the optic nerve and circumferentially invade the adipose and muscular tissue of the orbit.³

Several histomorphologic subtypes of meningioma have been recognized in domestic species including: meningothelial, fibroblastic, transitional, psammomatous, papillary, microcystic, myxoid, angiomatous/angioblastic, and atypical/anaplastic.^{7,9,14} Histologically, orbital meningiomas of dogs (and humans) fit best within the meningothelial and/or transitional types.^{1,3,6,8,12} Granular cell differentiation, which has previously been described in meningothelial meningiomas,⁷ has recently been recognized within a retrobulbar meningioma in a Golden Retriever dog.¹¹ More typically however, the neoplastic cells form lobules and dense aggregates and are epithelioid in appearance being polygonal with moderate to abundant



Eye, dog. There are scattered foci of cartilaginous and osseous metaplasia throughout the neoplasm. The adipose tissue is pre-existent orbital fat. (HE, 52X)



Eye, dog. Neoplastic cells range from polygonal (epithelioid) to spindled. (HE, 260X)

eosinophilic cytoplasm and round to oval, often vesicular, nuclei.^{1,3,8,9,12,15} The presence of myxoid, cartilaginous and osseous metaplasia are common features^{1,2,4,8,9,11,15} and may be useful aids in both the histologic and radiographic or ultrasound diagnosis of these tumours.^{3,8}

Immunohistochemistry is useful in ruling out carcinoma, an important differential diagnosis in these cases.^{3,14} Unlike carcinomas, the cells of orbital meningioma typically stain positively for vimentin and S-100 (although variably) and are usually negative for cytokeratin.^{8,11} In one reported case,¹² tumor cells stained positively for vimentin (cytoplasmic), E-cadherin (membranous), and were negative for S100, pancytokeratin, and cytokeratins AE1 and AE3. Ultrastructurally, these masses have the typical features of meningioma¹⁴ with interdigitating processes containing intermediate filaments and occasional desmosomes present between the cell membranes.⁸

Dogs with orbital meningioma are usually aged (mean age of 9 years)⁸ and present with orbital swelling or exophthalmos with^{2,4,8,12} or without^{1,8} blindness. These tumors are generally thought to be slow-growing and benign, however tumor recurrence following extenoration,^{2,4,11} intraocular invasion,^{1,2} and

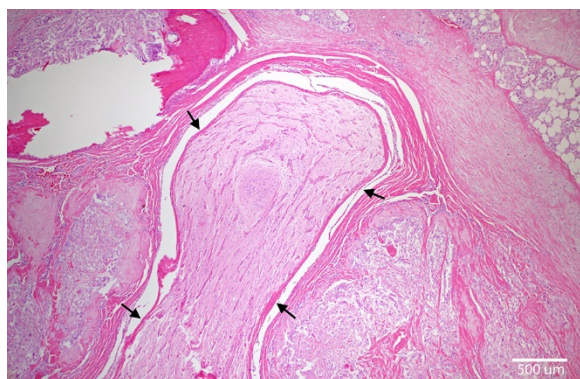
malignant variants with extracranial metastasis (mainly to the lungs)^{2,4,11} have been reported. In one review paper⁸ evaluating orbital meningioma in 22 dogs, follow-up information was available in 17 cases: enucleation with excisional biopsy was therapeutically effective in 11 cases (median follow-up time 1.7 years) and local recurrence was reported in 6 cases. While none of the 22 dogs had evidence of metastases, 2 of the 6 dogs with tumor recurrence developed central blindness in the opposite eye, suggesting spread along the optic nerve to the level of the optic chiasm.⁸

Contributing Institution:

Atlantic Veterinary College, University of Prince Edward Island
<http://avc.upei.ca>

JPC Diagnosis: Eye: Orbital meningioma.

JPC Comment: The contributor has done an outstanding job in describing this unique classification of meningioma. There are few differentials for this fairly characteristic neoplasm of the orbit; the morphologic appearance of epithelioid to spindle cells infiltrating the periorbital tissues with multiple areas of osseous and chondroid differentiation is unique, even in the absence of immunohistochemical findings. In



Eye, dog. The neoplasm surrounds the optic nerve (arrows). (Photo courtesy of: Atlantic Veterinary College, University of Prince Edward Island
<http://avc.upei.ca>)

addition to being strongly immunopositive for vimentin, canine meningiomas may be multifocally positive for other neural markers, such as S-100 and NSE (WSC 2015-2016, Conference 20, Case 4). An S-100 immunostain was performed on this case at the JPC; neoplastic cells were strongly immunopositive.

Differential diagnosis would include malignant peripheral nerve sheath tumor (especially epithelioid variants), multilobular tumor of bone, and possibly orbital lobular adenoma. Of these three, only the multilobular tumor of bone would be expected to have any significant osseous or cartilaginous differentiation, and obviously far exceeding that which is seen in this slide. Histiocytic sarcoma commonly metastasizes to the eye and may also have a dimorphic appearance with both epithelioid and spindle cells, but lacks osseous and chondrous metaplasia and possesses a different immunohistochemical profile (immunopositive for vimentin and IBA-1 and other leukocyte markers, while negative for S-100 and NSE.)

The conical gross appearance of orbital meningiomas is a characteristic finding, tapering in proximity to the brain. Infiltration through the optic foramen may be life-threatening; metastasis of this tumor is extremely rare.³

References:

1. Barnett KC, Kelly DF, Singleton WB. Retrobulbar and chiasmal meningioma in a dog. *J Small Anim Pract.* 1967; **8**: 391-394
2. Buyukmichi N. Orbital meningioma with intraocular invasion in a dog: histology and ultrastructure. *Vet Pathol.* 1977; **14**: 521-523.

3. Dubielzig RR. Tumours of the eye. In Meuten DJ, ed. *Tumors In Domestic Animals*. 5th ed. Ames, IA: Blackwell Publishing; 2017: 892-922.
4. Geib LW. Ossifying meningioma with extracranial metastasis in a dog. *Vet Pathol*. 1966; **3**: 247-254
5. Grahn BH, Stewart WA, Towner RA, Noseworthy MD. Magnetic resonance imaging of the canine and feline eye, orbit, and optic nerves and its clinical application. *Can Vet J*. 1993; **34**: 418-424.
6. Jain D, Ebrahimi KB, Miller NR, Eberhart CG. Intraorbital meningiomas: a pathologic review using the current World Health Organization criteria. *Arch Pathol Lab Med*. 2010; **134**: 766-770
7. Koester A, Higgins RJ. Tumours of the nervous system. In Meuten DJ, ed. *Tumors In Domestic Animals*. 4th ed. Ames, IA: Blackwell Publishing; 2002: 697-738.
8. Mauldin EA, Deehr AJ, Hertzke D, Dubielzig RR. Canine orbital meningiomas: a review of 22 cases. *Vet Ophthalmol*. 2000; **3**: 11-16.
9. Montoliu P, Anor S, Vidal E, Pumarola M. Histologic and immunohistochemical study of 30 cases of canine meningioma. *J Comp Path*. 2006; **135**: 200-207
10. Patnaik AK, Kay WJ, Hurvitz AI. Intracranial meningioma: a comparative pathologic study of 28 dogs. *Vet Pathol*. 1986; **23**: 369-373.
11. Perez V, Vidal E, Gonzalez N, Benavides J, Ferreras MC, Villagrasa M, Pumarola M. Orbital meningioma with a granular cell component in a dog, with extracranial metastasis. *J Comp Path*. 2005; **133**: 212-217.
12. Regan DP, Kent M, Mathes R, Almy FS, Moore PA, Howerth EW. Clinicopathologic findings in a dog with retrobulbar meningioma. *J Vet Diagn Inves*. 2011; **23**: 857-862.
13. Reis JL, Kanamura CT, Machado GM, Franca RO, Borges JRJ, Santos RL. Orbital (retrobulbar) meningioma in a Simmental cow. *Vet Pathol*. 2007; **44**: 504 - 507.
14. Summers BA, Cummings JF, de Lahunta A. Tumors of the central nervous system. In: Summers BA, Cummings JF, de Lahunta A, eds. *Veterinary Neuropathology*. St Louis, MO: Mosby; 1995: 351-401.
15. Wilcock BP. Eye and ear. In: Maxie MG, ed. *Jubb, Kennedy and Palmer's Pathology of Domestic Animals*. 4th ed. Vol 1. St Louis, MO: Elsevier; 2007: 459-552.
16. Yoshitomi K, Everitt JI, Boorman GA. Primary optic nerve meningioma in F344 rats. *Vet Pathol*. 1991; **28**: 79-81.

Self-Assessment - WSC 2017-2018 Conference 7

1. Which of the following is not a malignant microscopic feature of chondrosarcoma?
 - a. Numerous cells with prominent nuclei
 - b. Occasional binucleated cells
 - c. Numerous mitotic figures
 - d. Mucinous intercellular matrix

2. Which of the following would not be expected to exhibit Olig-2 labeling ?
 - a. Ependymoma
 - b. Astrocytoma
 - c. Oligodendroglioma
 - d. Mixed glial tumor

3. Which of the following horse breeds is overrepresented in cases of equine recurrent uveitis?
 - a. Paso Fino
 - b. Appaloosa
 - c. Thoroughbred
 - d. Arabian

4. Intracytoplasmic rod-shaped inclusions are seen in which cell type in cases of equine recurrent uveitis?
 - a. Retinal ganglion cells
 - b. Corneal endothelium
 - c. Non-pigmented ciliary epithelium
 - d. Retinal pigmented epithelium

5. What is the typical gross shape of an orbital meningioma?
 - a. Ovoid
 - b. Conical
 - c. Spherical
 - d. Hourglass

Please email your completed assessment to Ms. Jessica Gold at Jessica.d.gold2.ctr@mail.mil for grading. Passing score is 80%. This program (RACE program number) is approved by the AAVSB RACE to offer a total of 0.5 CE Credits, with a maximum of 12.5 CE Credits being available to any individual Veterinary Medical Professionals for the 2017-2018 Wednesday Slide Conference. This RACE approval is for the subject matter categories of: SCIENTIFIC using the delivery method of NON-INTERACTIVE DISTANCE. This approval is valid in jurisdictions which recognize AAVSB RACE; however, participants are responsible for ascertaining each board's CE requirements. RACE does not "accredit", "endorse" or "certify" any program or person, nor does RACE approval validate the content of the program.

Please email your completed assessment to Ms. Jessica Gold at Jessica.d.gold2.ctr@mail.mil for grading. Passing score is 80%. This program (RACE program number) is approved by the AAVSB RACE to offer a total of 0.5 CE Credits, with a maximum of 12.5 CE Credits being available to any individual Veterinary Medical Professionals for the 2017-2018 Wednesday Slide Conference. This RACE approval is for the subject matter categories of: SCIENTIFIC using the delivery method of NON-INTERACTIVE DISTANCE. This approval is valid in jurisdictions which recognize AAVSB RACE; however, participants are responsible for ascertaining each board's CE requirements. RACE does not "accredit", "endorse" or "certify" any program or person, nor does RACE approval validate the content of the program.

**Joint Pathology Center
Veterinary Pathology Services**



WEDNESDAY SLIDE CONFERENCE 2018-2019

C o n f e r e n c e 8

24 October 2018

CASE I: Case 1 6981 R23 (JPC 41078788-00).

Signalment: Adult, female, N/A, *Sciurus vulgaris*, red Eurasian squirrel

History: A frozen, adult red squirrel was presented for postmortem examination as part of a surveillance scheme aiming to understand the causes behind the decline in red squirrel populations in the UK.⁴

Gross Pathology: This squirrel had bilateral areas of alopecia and cutaneous swelling at the snout, lips, eyelids, pinna and the ventral and distal aspect of all limbs (figure 1). Internally, the thoracic cavity was filled by a moderate amount of pale pink, opaque fluid (chylothorax).

Laboratory results: Hsp65 PCR followed by sequencing⁶, and ulterior whole genome sequence work¹ were positive for *Mycobacterium lepromatosis*.

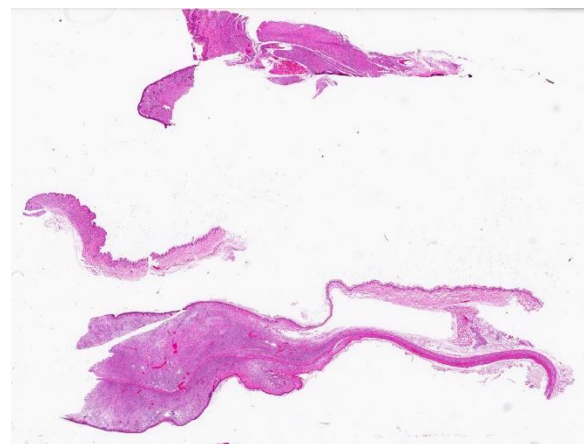
Microscopic Description: Description of the pinna only: At the tip of the pinna, extending from the aural cartilage to the superficial dermis, there is severe, focally extensive expansion by intercellular spacing (oedema)



Pinna, squirrel. The squirrel had bilateral areas of alopecia and swelling on the snout, lips, eyelids, and pinnae. (Photo courtesy of: Easter Bush Pathology, College of Medicine and Veterinary Medicine, University of Edinburgh, UK (<http://www.ed.ac.uk/vet/services/easter-bush-pathology>).

and severe infiltration by inflammatory cells. The latter are mostly foamy macrophages, with fewer lymphocytes and plasma cells and rare multinucleated giant cells. Scattered throughout this area, there are spindle shaped cells (fibroblasts – fibrosis, suspected) and accumulation of loose eosinophilic fibrillary material (collagen). Within this there are clear spaces containing 50-150µm wide, loose aggregates of pale basophilic cotton-like material. In the superficial dermis, all the hair follicles are small to non-existent (follicular atrophy, suspected). The overlying epidermis is approximately 5 cells thick (mild, focally extensive, epidermal hyperplasia), and has a thick stratum corneum composed of several, parallel layers of keratin (lamellar hyperkeratosis).

In areas of skin adjacent to the above described lesion (at the base of the pinna), the superficial dermis is diffusely infiltrated by small numbers of lymphocytes and fewer eosinophils. In the panniculus and subcutaneous muscle associated, there is mostly perivascular infiltration by lymphocytes, with very rare mast cells.



Pinna, squirrel. A section of haired skin and a cross-section of the pinna is submitted for examination. The dermis of both is markedly expanded by a dermal infiltrate that causes marked thickening of the pinna. (HE, 5X)

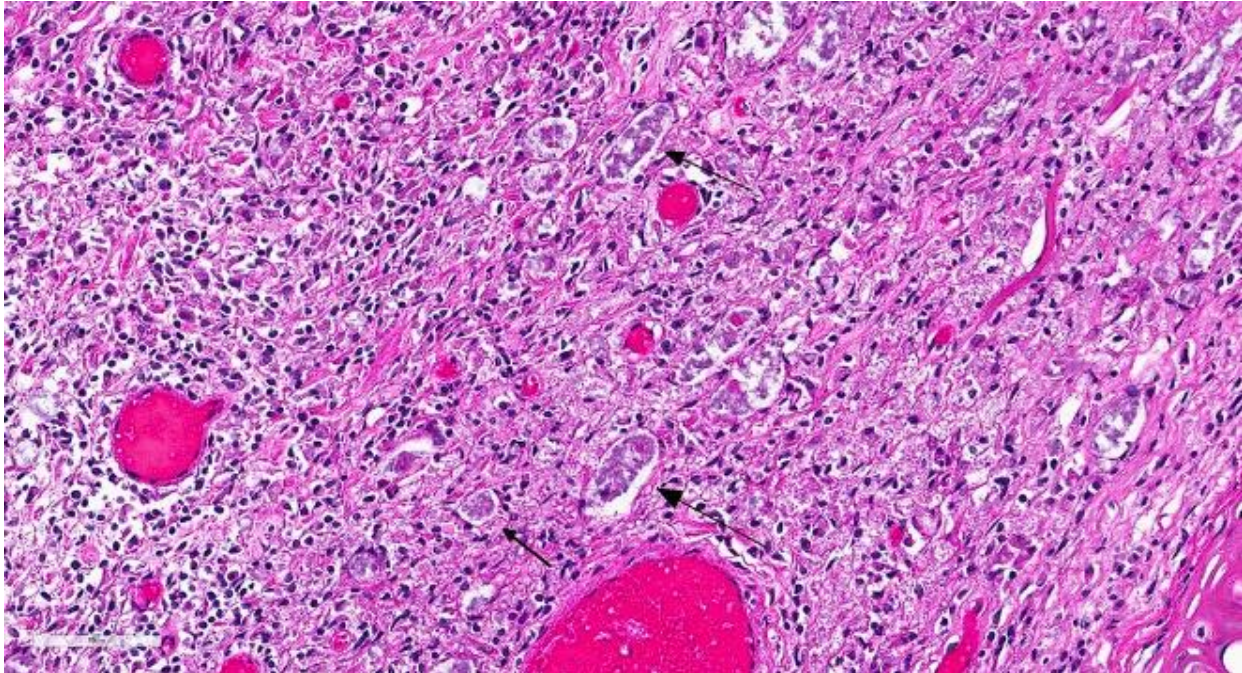
Contributor's Morphologic Diagnoses:

Severe, focally extensive, granulomatous dermatitis with fibrosis, superficial oedema, epidermal hyperkeratosis and basophilic bacteria – haired skin, pinna

Contributor's Comment: This is the first red squirrel that was diagnosed with squirrel leprosy a novel disease of red squirrels that has only been detected in the UK so far.⁷

In this case, the diagnosis of mycobacterial disease was first confirmed by Ziehl-Neelsen staining, which revealed intrahistiocytic and intraneural acid-fast bacteria. The role of the gram-positive filamentous bacteria noted within the pinnal lesions was interpreted at first either as a co-infection, or as a secondary infection. Since this first diagnosis, we have recorded the presence of filamentous bacteria in some -but not all- further cases of squirrel leprosy, frequently associated with ulceration of the lepromatous lesions. This suggests that the primary etiological agent are the acid-fast bacteria. Work on the characterization of this sporadic association, as well as the taxonomical identity of these filamentous bacteria is pending.

Following this diagnosis, further sporadic red squirrel cases with similar gross lesions were submitted for examination from diverse areas of Scotland, and we were able to collect six cases from 2006 to 2013. Three of these cases were lost to follow up due to freezer break down, and the gross and histological examination was followed by PCR analyses for the three remaining squirrels (including this case). Briefly, fresh and fixed samples from these were analyzed by PCR for the detection of IS900 and F57 (specific for *Mycobacterium avium* subspecies *paratuberculosis* [MAP]), IS901 (specific for MAP), and the gene encoding heat shock protein 65 (hsp65=vgg – present in all *Mycobacterium* spp). Only hsp65 yielded



Pinna, squirrel. The infiltrate is composed of numerous epithelial macrophages with vacuolated cytoplasm, admixed with fewer lymphocytes and plasma cells. Some macrophages are up to 60µm in diameter with stacks of greyish filamentous bacilli and cellular debris in their cytoplasm (lepra cells) (arrows). (HE, 320X)

positive results, and of the amplicons revealed 99% sequence homology with *Mycobacterium lepromatosis* (FJ924). This was an unexpected finding, as *M. lepromatosis* had only been reported in human leprosy patients in Mexico from 2008,³ and since then in other human cases from additional locations (e.g. Costa Rica and Singapore).² There are no human cases of *M. lepromatosis* reported in the United Kingdom, or any report of *M. lepromatosis* in other non-human mammal worldwide.

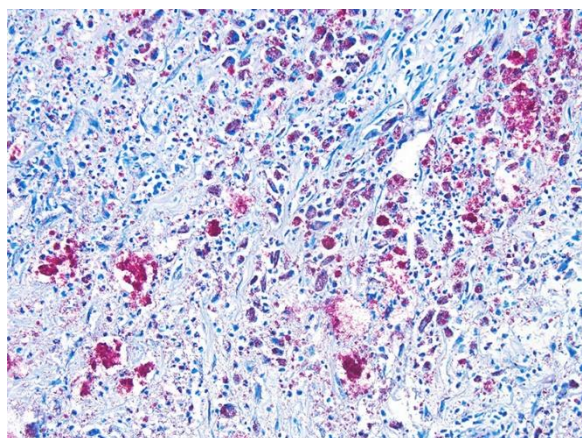
The first report of human leprosy by *M. lepromatosis* in 2008 has expanded the range of etiological agents of human leprosy to two bacterial species (previously only *Mycobacterium leprae* was known to cause human leprosy). Human infection with *M. lepromatosis* is associated with diffuse leprosy, a severe form of leprosy with spreading lesions containing foamy macrophages laden with large numbers of intracytoplasmic acid fast bacteria. The

histological presentation we saw in these squirrels is consistent with lepromatous leprosy. The spectrum of human leprosy lesions as described for *Mycobacterium leprae* is summarized in figure 6. At the extremes of this spectrum *M. leprae* causes two distinct histological patterns⁵:

- *Tuberculoid leprosy*, with dry, insensitive, scaly cutaneous lesions, which histologically feature asymmetric involvement of large peripheral nerves, which are enclosed within granulomas containing low numbers of intracellular acid fast bacilli (paucibacillary). This is associated with a Th1 response, with production of IL-2 and IFN- γ .
- *Lepromatous leprosy*, with symmetric skin thickening and nodules in distal areas (earlobes, feet). This presentation involves widespread nervous invasion of nerves by Mycobacteria, which are found within Schwann cells, endoneurial and perineural macrophages with minimal

inflammation. The lesions are composed of large, dermal aggregates of lipid-laden macrophages containing large numbers of acid-fast bacteria (multibacillary). Other organs that may be involved are regional lymph nodes, spleen, liver and testicles. This presentation is also known as anergic leprosy, because of immune unresponsiveness, and features a weak Th1 response and relative increase in Th2 response.

The spectrum contain intermediate categories between the two poles, and is described by the Ridley-Joplin classification scheme.⁷ This scheme also includes early indeterminate leprosy (IL – usually early lesions that may evolve to one or another pole). The entire scale includes polar tuberculoid leprosy (TT), borderline tuberculoid leprosy (BT), mid-borderline leprosy (BB), borderline lepromatous leprosy (BL), and polar lepromatous leprosy (LL). A further layer of information is provided by the determination of the number of acid-fast bacilli present in the lesions, which is expressed on a 1 to 6 score based on a logarithmic scale called the bacteriologic index (BI). At the extremes are score 1= 1-10 bacilli in 100 oil immersion fields



Pinna, squirrel. Epithelioid macrophages and lepra cells contain numerous intracytoplasmic acid-fast bacilli. (Fite-Furaco, 200X)

(paucibacillary) to score 6= ≥ 1000 bacilli in 1 oil immersion field (multibacillary).

An important diagnostic feature of leprosy, is the presence of neural lesions, as noted in the red squirrel cases. Intranural acid fast bacteria are a diagnostic feature, and these may be associated with neuritis or perineuritis.⁵ Neural lesions are present throughout the spectrum of leprosy lesions, and lead to skin anaesthesia and muscular atrophy that render affected areas susceptible to trauma-associated lesions. It is possible to hypothesize that the filamentous bacteria noted in red squirrels may have entered the skin lesion after trauma, as their presence is associated with ulceration.

Other patterns may be associated with human leprosy, which have not been reported in red squirrels. The Type I reaction, or reversal reaction, involves an increase in cell-mediated immunity in lesions at the borderline part of the spectrum. This leads to progression towards the tuberculoid pole, but also to reactivation of the lesions. This reactivation in results in pain, the appearance of new lesions, erythema/oedema of old lesions, and nerve tenderness and swelling. The type II reaction, or erythema nodosum, is a type III hypersensitivity that occurs on patients with lepromatoid leprosy. These patients develop neutrophilic infiltration of the lesions, oedema, vasculitis/panniculitis, and visceral manifestations.

Raised awareness as a result of the work on Scottish squirrels infected with *M. lepromatosis* led to the detection of a cluster of similar cases in Brownsea Island, a small island off the south coast of England. Strikingly, sampling and PCR analysis of these cases revealed infection of 25 red squirrels with *M. leprae*¹. This expands the range of possible *M. leprae* hosts previously, which were humans and nine-banded

armadillos.⁹ Another isolated case of *M. lepromatosis* was detected in Ireland as part of this further work. The gross and microscopic lesions are very similar in red squirrels infected with *M. leprae* or *M. lepromatosis* (indistinguishable in the sample set available).

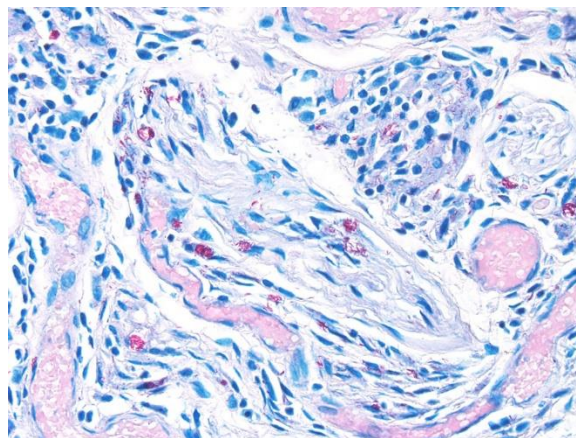
Further mycobacterial whole genome analysis was possible using enriched techniques (e.g. host DNA depletion tools) on tissues from all the squirrel samples.¹ This enabled whole genome sequencing of these bacteria, and phylogenetic comparisons using Bayesian statistics. Comparison of British and Irish *M. lepromatosis* with two Mexican strains from humans show that they diverged from a common ancestor around 27,000 years ago, whereas the *M. leprae* strain is closest to one that circulated in Medieval England. Furthermore, comparison between the English and Irish *M. lepromatosis* isolates revealed divergence approximately 300 years ago, coinciding with the reintroduction of red squirrels in Ireland from British stocks.

Contributing Institution:

Easter Bush Pathology, College of Medicine and Veterinary Medicine, University of Edinburgh, UK
(<http://www.ed.ac.uk/vet/services/easter-bush-pathology>).

JPC Diagnosis:

1. Ear, pinna: Dermatitis and neuritis, granulomatous, multifocal to coalescing, severe, with numerous intracytoplasmic bacilli.
2. Ear, pinna: Dermatitis, superficial, hyperkeratotic, multifocal to coalescing, moderate, with rare arthropods (acarasis).



Haired skin, squirrel. Macrophages containing acid-fast bacilli are present within rootlets of peripheral nerves. (HE, 320X)

JPC Comment: The contributor has provided an outstanding write up on this emerging disease a unique species as well as a fine review on the various types of leprosy, allowing us to examine the history of one of the world's oldest scourges.

In 2005, genetic analysis was performed on the incredibly stable genome of MA in order to map its origins.⁶ Incredibly, a cases of leprosy throughout history are derived from a single clone throughout history, and very rare polymorphisms in single nucleotides allow for insight into the disease's roots. The disease originated in Eastern Africa or the Near East, and spread into Asia and Europe with progressive human migrations, often accompanying patterns of colonization and the slave trade. Leprosy was introduced into the Americas with the advent of slavery, either by Europeans or Western Africans.

Sadly, no disease has resulted in more transiently or social stigmata than leprosy. The etymology of the word "leprosy" is derived from Greek or from old English, meaning (scaly skin). While it is difficult to make retrospective diagnoses from symptoms of diseases in ancient writings, lesions strongly suggestive of leprosy known

as “tzaraath” (and reputed to be healed by Jesus in the New Testament) are found in the Bible and the Talmud, and similar lesions are described in the Feng Zhen Shi (266-246 B.C., China). In 2009, a 4000-year old skeleton was uncovered in India demonstrating patterned lesions of leprosy.

The stigmata associated with leprosy began in the Middle Ages – afflicted individuals were often required to wear bells on their persons to announce their passage in the streets and literally thousands of leprosariums sheltered the infected (as well as many others with other diseases whose only affront was being a family member of an infected individual or simply indigent. Mandatory segregation of afflicted individuals was practice in a number of countries (with Japan in 1996 being the final country to rescind this stigmatizing law) and many countries (including the UK) made it a practice to segregate patients by gender in leprosaria, in the unfounded belief that children arising from two infected individuals would be born with the disease. Some of the most restrictive practices were the norm in India which in the 1900s regionally prohibited infected individuals from traveling by train, diving, running in local elections and even made it a legal justification for divorce. Some of these laws, written prior to the development of successful multidrug therapy and the Indian healthcare’s systems very successful campaign against the diseases, still remain on the books.

In 1873, Dr. G.H Armauer Hansen discovered the causative agent, making leprosy the first disease to be recognized as being caused by a bacterium. The disease today is often referred to as “Hansen’s disease”, a term preferred by patients over the term “leper”. In the 1940’s the sulfone drug promin became the first effecting therapy.

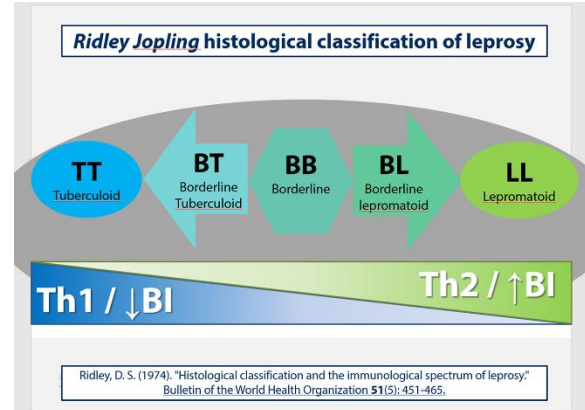


Diagram of the Ridley-Jopling histological classification of leprosy. (Image courtesy of: Easter Bush Pathology, College of Medicine and Veterinary Medicine, University of Edinburgh, UK (<http://www.ed.ac.uk/vet/services/easter-bush-pathology>)).

Today, multidrug therapy of rifampicin, clofazimine, and dapsone (a derivative of promin) are highly affected in treating leprosy.

Due to effectiveness of multidrug therapies, the sole remaining leprosarium in the US in Carville, Louisiana was closed in 1999 in favor of outpatient treatment of those afflicted with Hansen’s disease. Approximately 200 cases are diagnosed yearly in the U.S, and treated effectively if the disease is recognized early. Interestingly, zoonotic leprosy, transmitted from armadillos to humans has been confirmed in parts of the southern U.S.⁹

In this case, the amount of hyperkeratosis and superficial inflammation seemed excessive for mycobacteriosis. In the electronic disc provided with this series, there are rare cross sections of a chitinous exoskeleton, suggestive of an arthropod, overlying the epidermis. On serial sections of the slide provided for special stains, multiple intact arthropods were identified within regions of hyperkeratosis. This is consistent with acarasis in addition to leprosy in this animal.

A recent publication on “atypical histiocytosis” in red squirrels described animals with similar gross and histologic lesions to those in this case, but IHC, special stains, and PCR were negative for *Mycobacterium* spp.⁸

Following the review of the case, the moderator discussed the widespread distribution of mycobacteria in a number of other species including fish, reptiles and amphibians. Other species of note for mycobacterial infections include elephants, which are often infected by *M. tuberculosis*, noting that it may be advantageous to wear personal protective gear when performing necropsies on elephants. She also noted the prevalence and severity of mycobacterial in syngnathid fish, including sea horses, sea dragons, and pipefish.

References:

- 1 Avanzi C, del-Pozo J, Benjak A, et al. Red squirrels in the British Isles are infected with leprosy bacilli. *Science*. 354(6313) 2016: 744-747.
- 2 Han XY, Aung FM, Choon SE, Werner B. Analysis of the leprosy agents *Mycobacterium leprae* and *Mycobacterium lepromatosis* in four countries. *Am J Clin Pathol*. 142(4) 2014: 524-532.
- 3 Han XY, Seo YH, Sizer KC, et al. A new *Mycobacterium* species causing diffuse lepromatous leprosy. *Am J Clin Pathol*. 130(6) 2008: 856-864.
- 4 LaRose JP, Meredith AL, Everest DJ, et al. Epidemiological and postmortem findings in 262 red squirrels (*Sciurus vulgaris*) in Scotland, 2005 to 2009. *Vet Rec*. 167(8) 2010: 297-302.
- 5 McAdam AJ, Sharpe AH. Leprosy. In: Kumar V, Abbas AK, Fausto N, Aster JC, ed. *Robbins & Cotran pathologic basis of disease*. 8th ed. Philadelphia, US: Saunders Elsevier; 2010:372-373
6. Monot M, Honore N, Darnier T, Araoz R, Coppee JY, Lacroix C, Sow S. On the origin of leprosy. *Science*; 2005, 308:1040-1042.
7. Meredith A, Pozo JD, Smith S, et al. Leprosy in red squirrels in Scotland. *Veterinary Record*. 175(11) 2014: 285-286.
8. Ridley DS. Histological classification and the immunological spectrum of leprosy. *Bull World Health Organ*. 51(5) 1974: 451-465.
9. Smith SH, Stevenson K, del-Pozo J, Moss S, Meredith. Atypical histiocytosis in red squirrels (*Sciurus vulgaris*). *J Comp Path* 2017; 156:446-450.
10. Truman RW, Singh P, Sharma R, et al. Probable Zoonotic Leprosy in the Southern United States. *New England Journal of Medicine*. 364(17) 2011: 1626-1633.

CASE II: D15-060481 (JPC 4082891-00).

Signalment: Hatch-year female bald eagle (*Haliaeetus leucocephalus*)

History: This animal was admitted to The Raptor Center (TRC) of the University of Minnesota on December 13, 2015. It was recumbent and had head tremors. The animal was severely dyspneic. Small radio-dense fragments were detected in the ventriculus by x-ray. The animal had a PCV of 27% (considered to be anemic). It was euthanized the same day after blood analysis revealed a markedly elevated lead level (3.3ppm).

Gross Pathology: The bird was in a good nutritional state. It was anemic. The pericardial sac contained 45ml of clear



Heart, bald eagle: A cross section of the myocardium is submitted. Subgross examination does not reveal any significant lesions. (HE, 6X)

yellowish watery fluid with a small amount of flocculent material (heart weight: 53g). The myocardium of the left and right ventricle was multifocally beige discolored. Approximately 30% of the myocardium, particularly subjacent to the endocardium of the left ventricle, were affected. The proventriculus and ventriculus contained multiple small metallic fragments.

Laboratory results: None performed.

Microscopic Description: Heart (left ventricle) – The lesions are most pronounced in one papillary muscle of the left ventriculus but to a lesser degree are present at other sites of the myocardium (eg subepicardial myocardium). Cardiomyocytes in numerous fascicles of the aforementioned papillary muscle are shrunken and slightly hyper-eosinophilic containing homogenous (“hyalinized”) material. Occasional pyknotic nuclei of cardiomyocytes are present. The number of cardiomyocytes in some fascicles appears to be reduced and the endomysium appears more prominent and slightly vacuolated. The number of fibrocytes in the endomysium is slightly increased in few locations with subtle deposition of

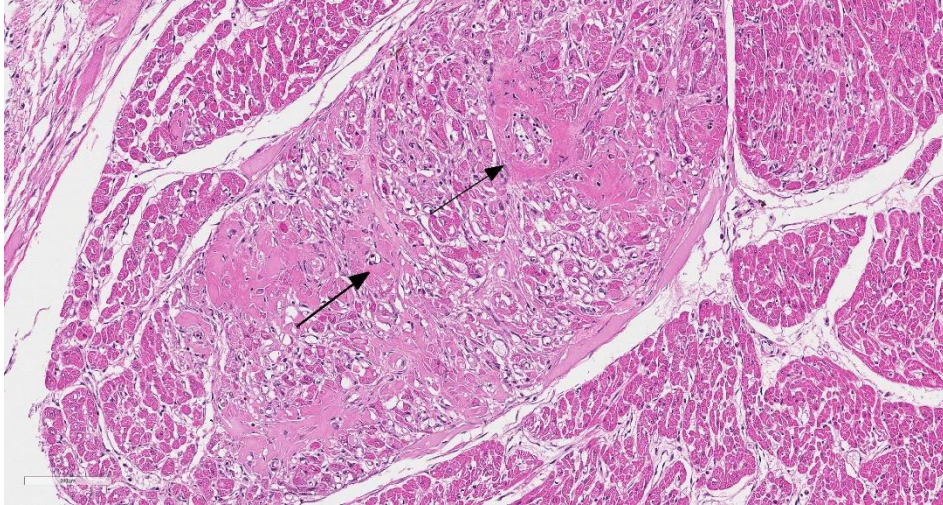
collagenous matrix. In more affected fascicles, groups of cardiomyocytes are replaced by pools of homogenous eosinophilic acellular (“hyalinized”) material. The smooth muscle cells in the media of occasional small to medium caliber myocardial arteries are mildly vacuolated. The endothelial cells of these arteries are slightly hypertrophied. In few arteries, homogenous eosinophilic (“hyalinized”) material replaced the media or portions of the media and adventitia.

Contributor’s Morphologic Diagnoses:
Heart:

- a. fibrinoid necrosis of small and medium caliber myocardial arteries, multifocal, acute
- b. myocardial necrosis, multifocal, moderate, acute.
- c. myocardial fibrosis, multifocal, mild.

Contributor’s Comment: The cardiac lesions in this case are most consistent with a degenerative or toxic cardiomyopathy. The result of the blood lead analysis is diagnostic of lead poisoning. The blood lead level of 3.3ppm is high considering that bald eagles with levels above 1ppm have a poor prognosis for survival even when treated by chelation and are frequently euthanized at admission.¹² The good nutritional state of the bird at the time of death suggests a fairly acute course of the disease. Accordingly, the myocardial lesions were dominated by rather acute changes with only subtle early myocardial fibrosis.

Lead toxicity is a common cause of death in scavenging raptors such as eagles and vultures as well as waterfowl worldwide. Cardiac lesions including hydropericardium, myocardial necrosis, fibrinoid necrosis of myocardial vessels and myocardial fibrosis



Heart, bald eagle: Multifocally, the walls of arterioles near the endocardial surface are effaced by a dense hyaline material with admixed cellular debris (fibrinoid necrosis).

have been described in bald eagles.^{2,6,7,10} Approximately 36% of lead intoxicated eagles submitted to the National Wildlife Health Center (Madison, Wisconsin, USA) had microscopic cardiac lesions. Myocardial infarction with angiopathy is also common in waterfowl with fatal lead intoxication.⁴ Besides the cardiac lesions, tubulonephrosis and brain lesions, including hemorrhages and parenchymal necrosis, have been reported in eagles with plumbism.^{8,10} Anemia, bile stasis and bile staining of gastrointestinal mucosa are considered to be common gross findings in lead intoxicated eagles but are unspecific as to the cause and highly subjective findings.⁷ Lead is known to have a wide range of pathophysiologic effects. Lead interferes in the avian host with sulfhydryl-dependent enzyme function (eg, delta aminolevulinic acid dehydrase); mimics calcium hereby interfering with neurologic function and mitochondrial respiration; and adversely affects DNA and RNA synthesis.³ However, the exact pathogenesis of the lead-associated fibrinoid vascular necrosis, cardiomyocyte degeneration, and myocardial fibrosis is uncertain.

While waterfowl pick up lead pellets (accumulated in lakes after hundreds of years of hunting with lead-based ammunition and ongoing illegal use of lead-based ammunition), lead sinkers, etc. while dabbling, lead exposure in eagles and scavenging birds occurs almost exclusively by ingestion of carcasses and offal of animals (upland birds and ungulates) killed with lead-based ammunition.¹ Despite the ban of lead-based ammunition for waterfowl hunting in the USA and Canada in the seventies, the flow of cases of lead-intoxicated scavenging birds to wildlife rehabilitation centers and diagnostic labs has not slowed.⁵ Extending the ban of lead-based ammunition to hunting of upland birds, wild turkey and ungulates would prevent lead poisoning in scavenging birds.¹

Contributing Institution:

University of Minnesota Veterinary Diagnostic Laboratory
<http://www.vdl.umn.edu>

JPC Diagnosis: Heart, small- and medium-sized arteries: Fibrinoid necrosis, multifocal, severe, with myofiber degeneration, necrosis and atrophy and marked myocardial fibrosis.

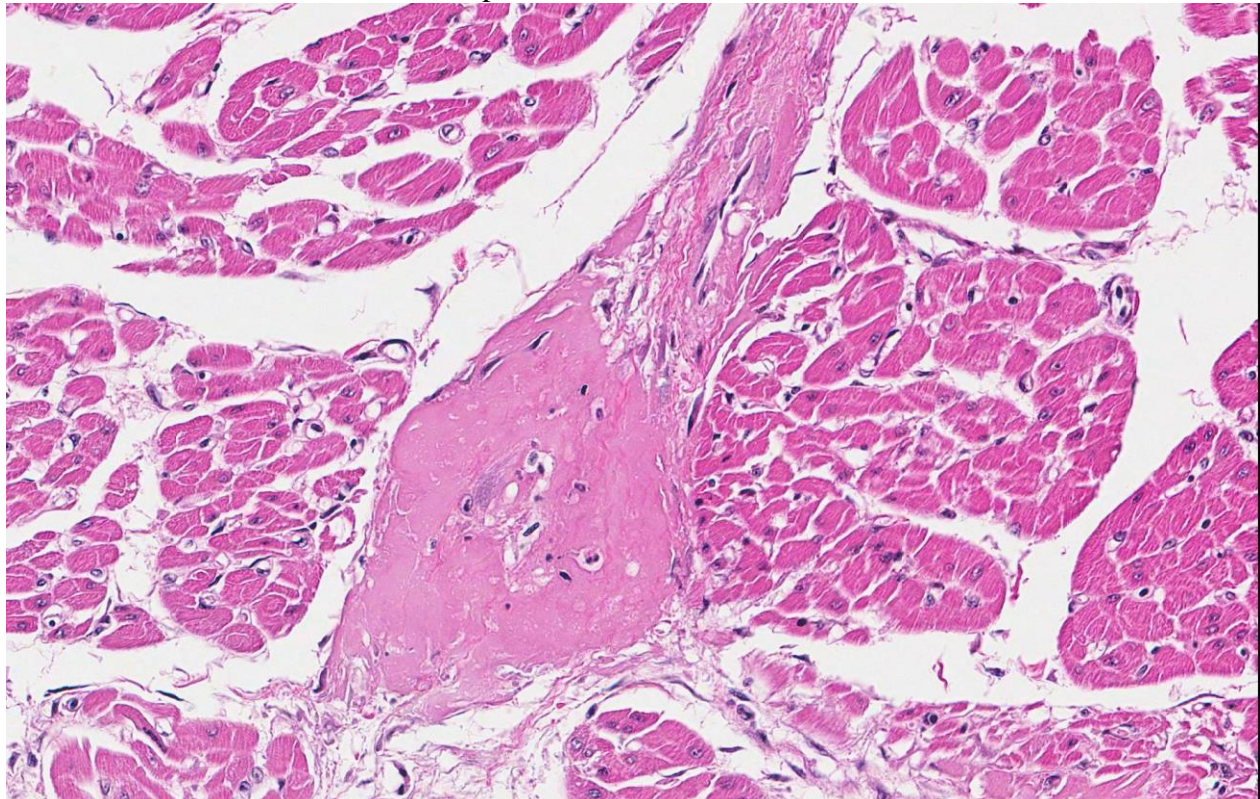
JPC Comment: Lead is a well-known and potent environmental and industrial contaminant. It is widely distributed in the body and stored in the kidney, liver, and bone (where it may reside for up to 35 years!). Its effects in the hematopoietic, urinary, musculoskeletal, and nervous systems are

well known, even if many gaps yet persist in our knowledge of its pathophysiology in these systems.

One of the more recent areas of investigation in lead toxicosis are its effects upon the cardiovascular system. Damage to the vascular system as a result of lead intoxication is likely multifactorial, and lead exposure in humans has been identified in an increased incidence of cardiovascular disorders such as hypertension, organic heart disease, and peripheral arterial diseases, including atherosclerosis.⁹ Research in animal models and human populations has also shown a direct and causal relationship between low-level lead exposure and hypertension.¹¹

At the cellular level, lead is a major driver in free radical damage affecting both endothelial cells and smooth muscle cells. Entering the cells through normal calcium channels, lead inhibits endoplasmic

reticulum (ER) Ca^{2+} -ATPase, resulting a release of calcium into the cytoplasm, and triggering ER stress as a result of release of calcium-dependent signaling and chaperone proteins contained within the ER.¹¹ In addition, it can bind directly to the calcium-binding protein, glucose-regulated protein 78 (GRP78), another ER-based chaperone protein involved in ER stress.¹¹ Activation of these proteins results in elevated levels of reactive nitrogen species in damaged cells and measurable increases in the cytotoxic effects of lead. *In vitro* studies of cardiofibroblasts has also shown that administration of lead induces autophagy (a protective response) through inhibiting the mammalian target of rapamycin complex 1 (mTORC1) pathway.¹³ While speculative, the vascular changes seen in this case suggest a correlation between hypertension, endothelial damage and the toxic principles of lead at the cellular level. The arterial lesions seen in this case are similar to those



Heart, bald eagle: Higher magnification of affected vessels with loss of endothelium, partial to total occlusion, and effacement of the media and adventitia. (HE, 354X)

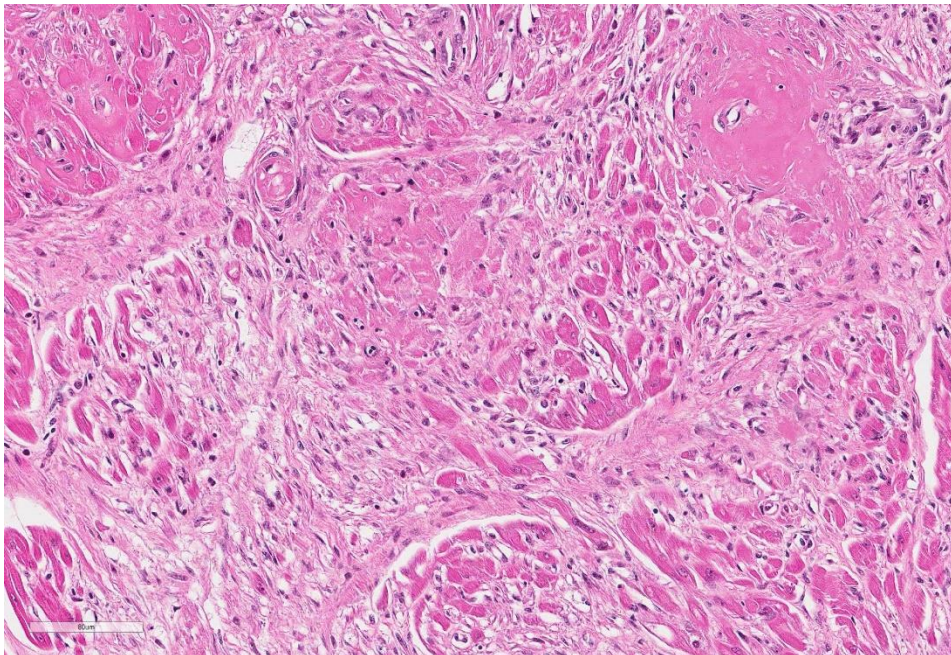
of polyarteritis nodosa (PN), a change often seen in hypertensive rat models. A vicious cycle of endothelial damage and hypertension may result in similar lesions. (One difference between this lesion and PN, however, is the lack of cellular proliferation in the adventitia associated with many cases of PN).

In this section, myocardial damage appears most severe in the areas of vascular necrosis, suggesting a cause-and-effect scenario, bolstered by the concurrent presence of myofiber degeneration, necrosis, and fibrosis, denoting a polyphasic timeline consistent with a toxic vascular injury. It is certainly possible that a similar direct effect of lead on cardiocytes, in addition to that seen in the vessels may have contributed to the widespread myocardial damage in this section.

The most diagnostic tissue to submit for lead toxicosis post mortem is the liver. Although

lead accumulates in bone, bone levels of lead represent a lifetime accumulation of this metal and therefore are difficult to correlate to point in time toxicosis if acute toxicity is suspected. As stated by the contributor, exposure to lead in these animals is via ingestion. Although embedded lead shot is common in wildlife, intramuscular lead does not readily dissolve, and poses little risk for toxicosis. It is unusual that presumptive lead fragments were identified in the proventriculus and ventriculus in this case as birds of prey with plumbism frequently cast out metallic fragments prior to death. An additional histologic finding of lead toxicosis, though rare, is intranuclear, acid-fast inclusions in renal tubular epithelial cells. These lead inclusions have not been reported in eagles or California condors, but have been seen in turkey vultures and Andean condors.

Attendees discussed a number of differential diagnoses for this case including West Nile virus, capture myopathy, nutritional imbalance of Vitamin E and selenium, and even electrocution (which may result in hemopericardium at necropsy). The absence of significant inflammation argues against West Nile Virus infection (although interestingly, the heart, brain, and eye are preferentially affected - the same triad of organs that exhibit vasculitis in



Heart, bald eagle: Scattered throughout the myocardium, and often within papillary muscles, there are areas of myocardial necrosis with myofiber swelling, loss of cross striations, and rare pyknotic nuclei. (HE, 400X)

lead-intoxicated birds.) The polyphasic nature of the lesion and concomitant vasculitis argues against the possibility of capture myopathy, and vasculitis is uncommon in most species with Vitamin E/Se imbalance (with the possible exception of swine).

It is not uncommon for particulate matter containing lead to be absent from poisoned birds at autopsy. When submitting avian tissues for lead measurement, most reference ranges are based on liver accumulation, which would best represent acute lead storage (as opposed to bone levels, which may reflect a lifetime accumulation of lead). When searching histologically for evidence of lead toxicosis, kidneys are a good choice for the identification of intranuclear inclusions.

References:

1. Clark AJ, Scheuhammer AM. Lead poisoning in upland-foraging birds of prey in Canada. *Ecotoxicol.* 2003;12: 23-30.
2. Franson RE, Russell JC. Causes of mortality in eagles submitted to the National Wildlife Health Center 1975-2013. *Wildl. Soc. Bull.* 2014;38: 697-704.
3. Haig SM, D'Elia J, Eagles-Smith C, Fair JM, Gervais J, Herring G, Rivers JW, Schulz JH. The persistent problem of lead poisoning from ammunition and fishing tackle. *The Condor* 2014;116: 408-428.
4. Karstad L. Angiopathy and cardiomyopathy in wild waterfowl from ingestion of lead shot. *Conn. Med.* 1971;35: 355-360.
5. Kramer JL, Redig PT. Sixteen years of lead poisoning in eagles: 1980-95: an epizootiologic view. *J. Raptor Res.* 1997;31: 327-332.
6. Langelier KM, Andress CE, Grey TK, Wooldridge C, Lewis RJ, Marschetti R. Lead poisoning in bald eagles in British Columbia. *Can. Vet. J.* 1991;32:108-109.
7. LaDouceur EE, Kagan R, Scanlan M, Viner T. . Chronically embedded lead projectiles in wildlife: a case series investigating the potential for lead toxicosis. *J Zoo Wild Med* 2015; 46(2):438-442.
8. Locke LN, Thomas NJ. Lead poisoning in waterfowl and raptors. In: Fairbrother N, Locke LN, Hoff GL, eds. *Non-Infectious Diseases of Wildlife*. 2nd ed. Iowa State University Press. Ames, Iowa, USA; 1996: 108-117.
9. Nicolas de Francisco O, Feeney D, Armien A, Wunschmann A, Redig PT. Correlation of brain magnetic resonance imaging of spontaneously lead poisoned bald eagles (*Haliaeetus leucocephalus*) with histologic lesions: a pilot study. *Res. Vet. Sci.* 2016;105: 236-242.
10. Patrick, N. Lead toxicity part II: The role of free radical damage and the use of antioxidants in the pathology and treatment of lead toxicity. *Alt Med Rev* 2006; 11(2):114-126.
11. Pattee OH, Wiemeyer SN, Mulhern BN, Sileo L, Carpenter JW. Experimental lead shot poisoning in bald eagles. *J. Wildl. Manage.* 1981;45: 806-810.
12. Shinkae Y, Kaji T. Cellular defense mechanisms against lead toxicity in the vascular system. *Biol Pharm Bull* 2012; 35(11): 1885-1891.
13. Stauber E, Finch N, Talcott PA, Gay JM. Lead poisoning of bald (*Haliaeetus leucocephalus*) and golden (*Aquila chrysaetos*) eagles in the the US inland pacific northwest region – an 18-year retrospective study: 1991-2008. *J. Avian Med. Surg.* 2010;24: 279-287.
14. Sui L, Zhang RH, Zhang P, Yunj, KL, Zhang HC, Liu L, Hu MX. Lead toxicity induces autophagy to protect against cell death through the mTORC1 pathway in cardiofibroblasts. *Biosci Rep*

2015; 31;35(2). pii: e00186

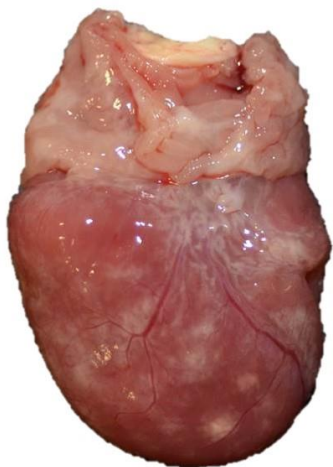
15. Wunschmann A. Birds of Prey. *In: Pathology of Wildlife and Zoo Animals.* Terio K, McAloose D, St. Leger J, eds. London, Academic Press, pp. 717-740

CASE III: L16-618 (JPC 4083860-00).

Signalment: One juvenile female alligator (*Alligator mississippiensis*)

History: Out of a cohort of 5,000 alligators, five had decreased appetite but no associated mortalities had been recorded at the time of submission. Alligators of this farm had previously been diagnosed with chlamydia infection. The client also requested testing for West Nile Virus.

Gross Pathology: The alligator was in good body condition, weighing 2.8 kg. A scant amount of clear free fluid was in the coelomic cavity. The liver was pale tan to green on cut surface. The spleen measured 4 x 1.5 x 1 cm (approximately twice the expected size), was



Heart, alligator. Multiple pale tan foci are on the epicardial surface. (Image courtesy of: Louisiana Animal Disease Diagnostic Laboratory, <http://www1.vetmed.lsu.edu/laddl/index.html>).

mottled red to dark red, and bulged on cut surface. On the epicardial surface were multiple 1 mm, pale tan foci that did not extend into the myocardium. Minimal red-tinged fluid was in the lower trachea.

Laboratory results:

Molecular (PCR):

Liver, heart, conjunctiva (pooled) and conjunctival swab: Positive for Chlamydiaceae

Liver, kidney, heart, brain, spleen (pooled): Negative for West Nile Virus

Special stains:

Liver: Gimenez-positive microorganisms

Immunohistochemistry

Liver: Microorganisms are



Liver, alligator. On cut surface the hepatic parenchyma is slightly orange to brown with multiple pinpoint pale tan-to-yellow foci. (Image courtesy of: Louisiana Animal Disease Diagnostic Laboratory, <http://www1.vetmed.lsu.edu/laddl/index.html>).

immunopositive using a monoclonal anti-chlamydia lipopolysaccharide antibody

Microscopic Description: Liver: There are multifocal to coalescing areas of hepatocellular vacuolar degeneration, necrosis, and loss and replacement by aggregates of fibrin, cellular debris, and heterophils. Clusters of basophilic, Gimenez-positive microorganisms are present in multiple remaining hepatocytes. Aggregates

of lymphocytes and plasma cells infiltrate portal areas. Biliary epithelial cells, Kupffer cells and, to a lesser extent, hepatocytes contain intracytoplasmic golden yellow-to-dark brown, iron stain-positive and bile stain-negative pigment granules.

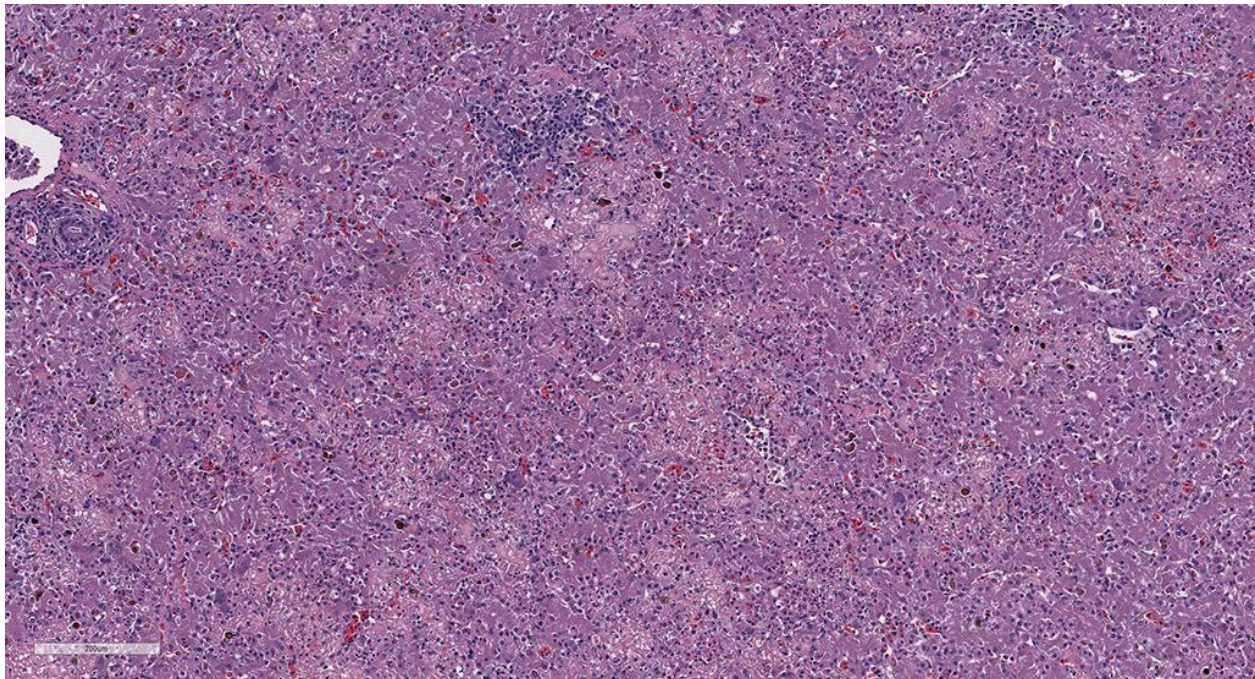
Contributor's Morphologic Diagnoses:

Liver: Hepatitis, necrotizing, multifocal-to-coalescing, marked, acute, with intrahepatocellular coccobacilli

Contributor's Comment:

Chlamydiae represent a phylum of obligate, intracellular bacteria that parasitize an array of hosts including vertebrates, a few arthropod species, and several free-living amoebae.² Ubiquitous in the environment, chlamydiae are further classified into nine different families, all of which share similar developmental cycles and reproductive requirements but differ in their morphology, host specificity and capacity for disease.⁴ Chlamydiae exist in either one of three stages: an extracellular infectious elementary body (or the dispersal form, analogous to a

spore), an intracellular vegetative reticulate body, or, rarely, as described for the Parachlamydiaceae family, a crescent body (also an infective stage).² The family Chlamydiaceae is comprised of the genera *Chlamydia* and *Chlamydophila*. The most significant human pathogens include *Chlamydia trachomatis* (responsible for urogenital infections and the agent of trachoma) and *Chlamydophila pneumoniae* (associated with respiratory infections and neurodegenerative syndromes). The majority of the other related species are veterinary pathogens with few anthroponotic exceptions, notably *Chlamydophila psittaci* (psittacosis) and *Chlamydophila abortus* (spontaneous fetal loss).⁶ Besides mammals, *Chlamydophila* also targets birds, amphibians, and reptiles, and chlamydiosis has been described in both free-ranging and captive cold-blooded animals including a variety of snakes, frogs, crocodiles, chameleons, and tortoises.⁶ Associated lesions in these species are commonly observed in the spleen, heart, lung and liver, characterized by granulomatous



Liver, alligator. A retiform pattern of pallor resulting from coalescing areas of lytic necrosis is present across the section. (HE, 100X)

inflammation within whichever organ is infected. There are also rare reported incidences of wasting disease; gastrointestinal involvement; and necrotizing myocarditis, enteritis and splenitis.⁶

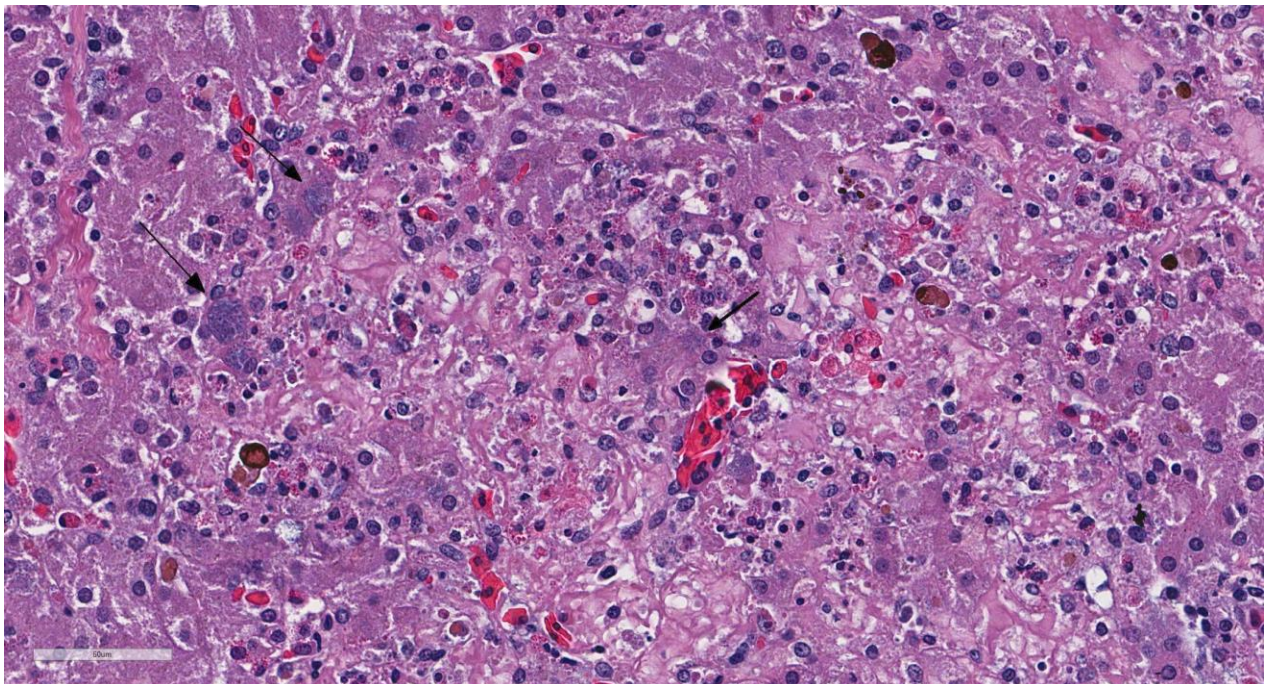
The Louisiana Animal Disease Diagnostic Laboratory has recently diagnosed an outbreak of chlamydiosis with high mortalities in a group of farmed American alligators, the first documented report of chlamydiosis in the species.⁶ A novel reptilian *Chlamydophila* isolate was identified via PCR with 86% homology to *C. psittaci* using OmpA gene sequencing. The main pathological findings included necrotizing, heterophilic and granulomatous hepatitis with intracellular bacteria, necrotizing myocarditis, and lymphoplasmacytic, mixed histiocytic and heterophilic conjunctivitis. The alligator of the present submission had similar lesions in both the liver and heart (namely a heterophilic and lymphoplasmacytic necrotizing hepatitis, epicarditis and

pericarditis). Additional molecular characterization of this novel *Chlamydophila* species is warranted to understand its host specificity and infective potential.

In conference, the moderator reviewed some anatomic peculiarities of the reptile liver. The reptile liver is not organized into distinct lobules as in mammals, and hepatic cores are not always seen radially around central veins. Hepatic veins and bile ductules mark the edge of a lobule, and hepatic arteries may or may not be present. She also commented on the difficulty of precisely identifying pigments within the liver of reptiles, which in this case, the attendees variously identified as bile, hemosiderin, or melanin. In reality, many of the aggregates of pigment may stain positively for none, one, or more of these particular pigments on a variety of histochemical stains.

Contributing Institution:

Louisiana Animal Disease Diagnostic Laboratory



Liver, alligator. At the periphery of areas of necrosis, hepatocytes contain an intracytoplasmic bacterial inclusion characteristic of chlamydiae. (HE, 400X)

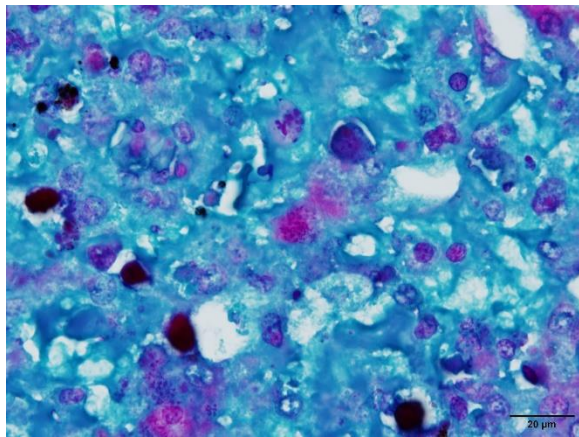
<http://www1.vetmed.lsu.edu/laddl/index.html>

JPC Diagnosis: Liver: Hepatitis, necrotizing, multifocal to coalescing, severe, with rare intrahepatocellular intracytoplasmic bacterial inclusions.

JPC Comment: Prior to any further discussion on this case, it appears (to the delight of pathologists everywhere), all members of the genus *Chlamydophila* have been replaced in the genus *Chlamydia*, and the controversial creation of the genus *Chlamydophila* has been reversed.¹

While largely known as an intracellular “energy parasite” of mammals and birds, chlamydiae are also well-established as parasites of reptiles, fish, insects, crustaceans, and bivalves. Chlamydia (or *Chlamydia*-related bacteria) are the causative agent of “epitheliocystis”, a poorly-named but common parasitic gill disease of fresh and saltwater fish species.¹

One of the most interesting parts of the life cycle of chlamydiae is their dependence on



Liver, alligator. A Gimenez stain highlights the clusters of microorganisms within the hepatocytes (Gimenez, 400X)(Image courtesy of: Louisiana Animal Disease Diagnostic Laboratory, <http://www1.vetmed.lsu.edu/laddl/index.html>).

host cells for energy. Traditionally, chlamydiae have been considered “energy

parasites”, entirely dependent on host cells to supply ATP requirements. Much of this early research was apparently performed on elementary body life stages (a rather metabolically inert form) revealing a lack of flavoproteins and cytochromes associated with traditional mitochondrial function, as well as the presence of two ATP-ADP translocases which allow for energy uptake from the host cell. Recent genomic investigations of other life stages have revealed genetic encoding for many energy pathways, including glycolysis, the Krebs cycle, and the pentose phosphate pathway. Enzymes in these pathways have been identified in reticulate bodies suggesting a potential for inherent energy creation in more metabolically active life stages than previously thought.⁵

Another interesting feature of many species of chlamydiae is their symbiotic relationship in the absence of a suitable host with free-living amoeba, to include *Acanthamoeba* and *Hartmannella*. While present within the cytoplasm of amoeba, the bacteria are not digested or harmed, and some species may even continue to excrete elementary bodies (the environmentally resistant life stage) into the surrounding extracellular environment. The presence of intracellular chlamydiae have differential effects on the growth rate of various host amoebae, and have been documented to increase the cytopathic effects of certain amoeba species. In human medicine, combined free-living amoebic and chlamydial infections have been documented, likely as a result of infection of susceptible individuals by amoeba/chlamydial symbionts.²

Since the submission of this case, a second report of fatal systemic *Chlamydia* infection in juvenile Siamese crocodiles, with lesions in the heart, liver and spleen similar to those reported in this outbreak, has been published.

PCR also suggested a novel *Chlamydia* sp. The lesions seen in this case, as well as the subsequent report by Thongkamkoon *et al.*, are similar to the lesions seen in estuarine and Nile crocodiles, in which hepatitis is the predominant lesion of systemic chlamydiosis⁸ and differs from other types of chlamydia-associated disease previously identified in crocodiles, which include infection of the conjunctiva and upper respiratory tract, and death as a result of fibrinous suppurative upper airway and tracheal disease.³

References:

1. Borel N, Polkinghorne A, Pospischil A. A review on chlamydial diseases in animals: still a challenge for pathologists: *Vet Pathol* 2018; 55(3):374-390.
2. Corsaro, D. & G. Greub (2006). Pathogenic potential of novel chlamydiae and diagnostic approaches to infections due to these obligate intracellular bacteria. *Clinical Microbiology Reviews*. 19(2): 283-297.
3. Conley KJ, Chilton CM. Crocodilia. *In: Pathology of Wildlife and Zoo Animals*. Terio K, McAloose D, St. Leger J, eds. London, Academic Press., Pp. 849-864.
4. Huchzermeyer, F.W., E. Langelet, & J.F. Putterill (2008). An outbreak of chlamydiosis in farmed Indopacific crocodiles (*Crocodylus porosus*): Clinical communication. *Journal of the South African Veterinary Association*. 79(2): 99-100.
5. Liang P, Rosas-Lemus M, Patel D, Fang X, Tuz K, Juarez O. Dynamic energy dependency of *Chlamydia trachomatis* on host cell metabolism during different stages of intracellular growth: Possible role of sodium-

based energetics in chlamydial ATP generation.

6. Sakaguchi, K., Nevarez J, Paulsen D, Bauer R, Crossland N, Langohr I, J. Ferracone J, Ritchi B, Del Piero F. Chlamydiosis in farmed American alligators (*Alligator mississippiensis*). Poster presented at the 2015 Annual Meeting of the American College of Veterinary Pathologists, Minneapolis, Minnesota, 2015..
7. Taylor-Brown, A., S. Rüegg, A. Polkinghorne & N. Borel (2015). Characterisation of *Chlamydia pneumoniae* and other novel chlamydial infections in captive snakes. *Veterinary Microbiology*. 178(1-2): 88-93.
8. Thongkamkoon P, Tohnee N, Morris EK, Inamniay K, Lombardini ED. Combined fatal systemic *Chlamydia* sp. and *Aeromonas sobria* infection in Juvenile Siamese crocodiles (*Crocodylus siamensis*). *Vet Pathol* 2018; doi:10.1177/0300985818768382.

CASE IV: 13-46415 (JPC 4048668-00).

Signalment: Adult, male, eastern massasauga rattlesnake (*Sistrurus catenatus catenatus*)

History: Free-ranging eastern massasauga rattlesnake from Michigan.

Gross Pathology: The mandible is markedly enlarged and distorted by firm swelling of the subcutis, up to 0.9 cm in thickness. Along the rostral aspect of mandible, a 1.5 cm x 0.4 cm region of the oral mucosa is red-brown and ulcerated. The spectacles are bilaterally light blue and opaque. Adhered along the entire length of the body, there are focally extensive regions of dull, retained scales (dysecdysis).



Mandible, rattlesnake. A 1.5x04cm ulcerated nodule involves the oral mucosa. The spectacle is moderately opaque. (Photo courtesy of: University of Illinois College of Veterinary Medicine Department of Pathobiology and Veterinary Diagnostic Laboratory. <http://vetmed.illinois.edu/path/>)

Laboratory results:

Real time PCR positive for *Ophidiomyces ophiodiicola*

Microscopic Description: Effacing and expanding the dermis and subcutis of the right caudoventral mandible, compressing the adjacent skeletal muscle and dorsally elevating the overlying mucosa of the oral cavity are multiple coalescing granulomas centered on eosinophilic necrotic debris and small numbers of fungal hyphae. The hyphae are 3-5 um in diameter, parallel walled, septate, and occasionally branching. Areas of necrosis are surrounded by numerous epithelioid macrophages and few multinucleated giant cells containing up to 6 nuclei. The granulomas are further circumscribed by plump fibroblasts and dense bands of fibrous connective tissue that are infiltrated by many heterophils, fewer

lymphocytes and plasma cells. There is also a free crust composed of numerous degenerate and viable heterophils, necrotic cellular debris, myriad small coccobacilli and a few fungal hyphae. The fungal hyphae stain black with Grocott's Methenamine Silver (GMS).

Contributor's Morphologic Diagnoses:

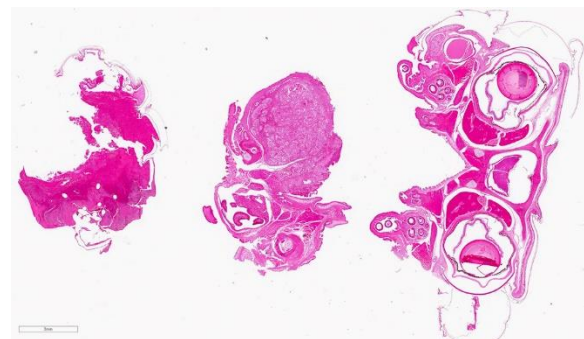
Head, mandible:
Dermatitis and cellulitis,

heterophilic and granulomatous, focally extensive, severe with fungi

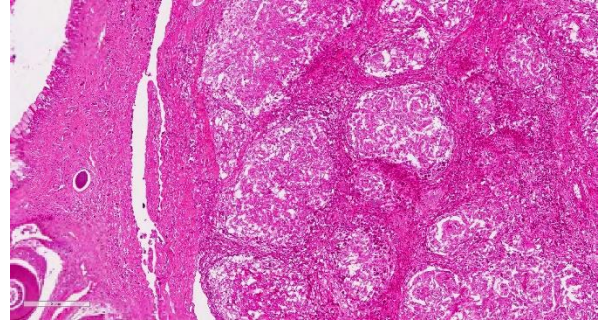
Contributor's Comment: Over the last decade, Snake Fungal disease (SFD) has become an emerging skin disease in certain populations of wild snakes in the Eastern and Midwestern United States. The keratinophilic fungus *Ophidiomyces* (formerly *Chrysosporium*) *ophiodiicola* has been consistently associated with SFD. Unlike other fungal members of the family Onygenaceae (order Onygenales), *O. ophiodiicola* has been recovered only from snakes. Published reports of fungal isolates confirmed via DNA sequencing or PCR assays have been reported in at least 12 different snake species.^{2,10}

While clinical signs and disease severity may vary by species, fungal infection often leads to a fatal outcome, especially in eastern massasauga rattlesnakes.² The most common clinical signs of *O. ophioidicola* are severe facial swelling and disfiguration. Other cutaneous lesions include scabs or crusty scales, subcutaneous nodules, skin ulcers, dysecdysis, and hyperkeratosis.^{2,9-11} Occasionally, fungal invasion may further progress to disseminated or systemic mycosis. Histologic lesions typically consist of cutaneous ulcers with thick adherent serocellular crusts and multiple granulomas within deeper tissues that are centered on variable numbers of fungal hyphae.^{2,9} Although not seen histologically in this snake, notable morphological characteristics for *O. ophioidicola* may include formation of short, undulate, sparsely septate lateral branches and chains of cylindrical arthroconidia usually along the epidermal surface.⁷

The origin, transmission, and predisposing factors of infection with *O. ophioidicola* remain poorly understood. Occurrence of infection across different locations over a span of years suggests fungal presence within the environment. Histopathologic evidence of primary skin involvement is also



Head, rattlesnake. Three sections of decalcified head are submitted. The middle section contains a large inflammatory nodule. The section on the right is primarily composed of a serocellular crust. (HE, 5X)



Mandible, rattlesnake. The inflammatory nodule is composed on well-defined coalescing granulomas ("a granuloma composed of smaller granulomas"). (HE, 122X)

consistent with environmental acquisition of infection.² Recent culture and molecular based surveys of healthy captive and wild snakes have shown that the fungus is not a common constituent of the normal snake skin microflora.^{1,3}

Aside from presence of the fungal elements in disease-associated lesions, specific pathological criteria for *O. ophioidicola* associated SFD have not yet been established. Differentials for dermatomycosis of snakes include dermatophytes and members of the *Chrysosporium* anamorph *Nannizziopsis viresii* (CANV) complex, which share similar fungal morphologies. Therefore, diagnosis of *O. ophioidicola* typically requires a combination of physical examination, histopathology, culture and/or molecular analysis such as PCR or DNA sequencing.^{9,10}

Contributing Institution:

University of Illinois College of Veterinary Medicine Department of Pathobiology and Veterinary Diagnostic Laboratory.
<http://vetmed.illinois.edu/path/>

JPC Diagnosis: Mandible: Osteomyelitis, rhabdomyositis, cellulitis, and stomatitis, granulomatous, focally extensive, severe, with myofiber atrophy, ulcerative stomatitis, and fungal hyphae.

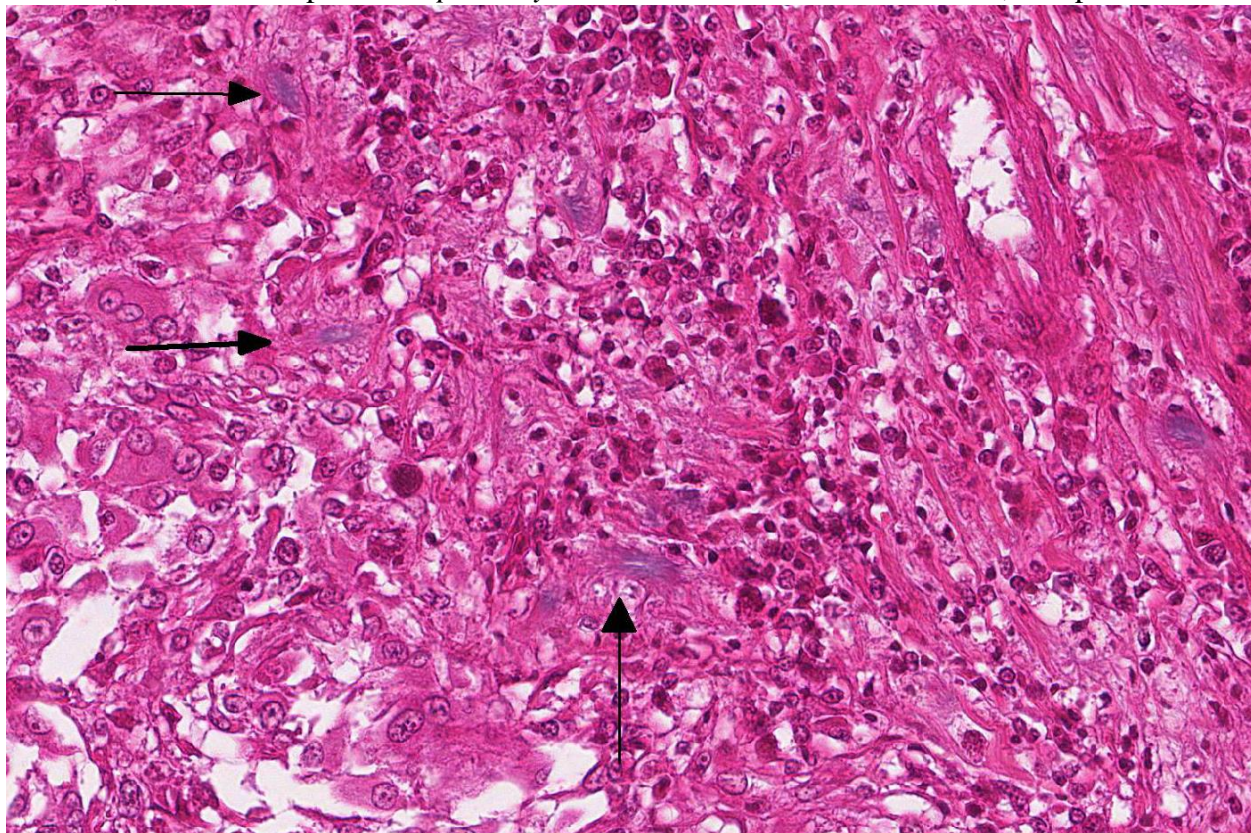
JPC Comment:

Within the last generation, cutaneous and systemic fungal infections have resulted in dramatic declines of various animal species on a global scale – *Batrachochytridium dendrobatidis* in amphibians (and a related species, *B salamandrivorans* in European salamanders), *Pseudogymnoascus destructans* in bats, and now, related species of *Chrysosporium* (*Nannizziopsis*) in various species of reptiles.³

Three lineages of closely related genera cause dermal or systemic infections in reptiles: the genus *Nannizziopsis* (*N. vriesis*, *N. guarroi*, and six additional species) infect various lizard species. *Paranannizziopsis* has three species which affect squamates and tuataras, and the species *Ophidomyces*

ophiodiicola affects snakes.⁸

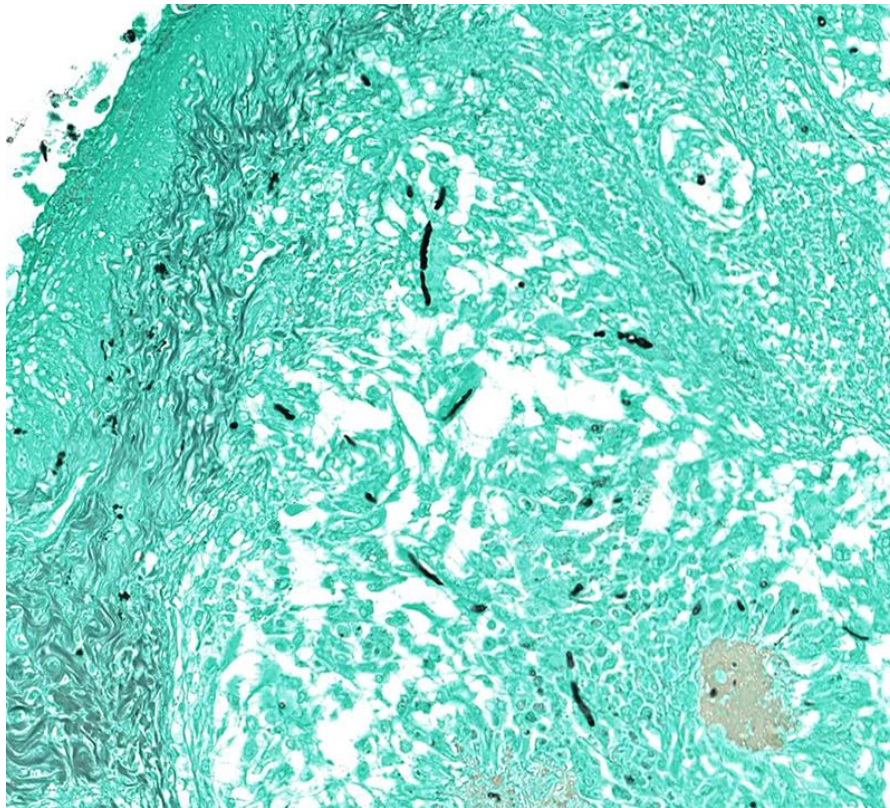
While considered an emerging threat, opinions differ as to whether *O. ophiodiicola* is a recently introduced pathogen, or a pathogen which has emerged and spread as a result of recent environmental changes.⁴ The agent was first identified in 2006 as an outbreak in timber rattlesnakes, but since then has been identified in over 30 snake species, 6 families, and outbreaks in wild snakes in almost every state in eastern half of the United States. While this rapid emergence of the disease suggests a newly introduced pathogen, subsequent cases may be identified 500-1000 miles distant from the closest report, activity not consistent with the “new pathogen” theory. Moreover, investigation of historical outbreaks of skin disease in wild snakes, couple with new



Mandible, rattlesnake. Scattered randomly throughout the granulomas are cross sections of negatively stained, 3-5um diameter fungal hyphae (arrows) (HE, 400X)

molecular techniques has identified *O. ophiodiicola* in previous cases. One recent study documented a 74% incidence of *O. ophiodiicola* in cases of “hibernation sores” – a condition well known to herpetologists for decades.⁴

On a comparative note, invasive, occasionally fatal infections caused by *Nannizziopsis* sp. have been rarely identified in humans, often in immunosuppressed patients. *N. obscura*, *N. infrequens* (both good names for rare pathogens) have been



Mandible, rattlesnake. A silver stain highlights the presence of non-branching fungal hyphae with non-parallel walls (GMS, 200X).

identified in patients sharing risk factors of HIV infection and/or recent travel to Africa. Abscesses in the brain, bone, viscera or soft tissues predominate; treatment with antifungals were successful in several cases. There is currently no evidence of zoonotic infections associated with *Nannizziopsis* sp.⁵ Reptiles have a diverse array of normal mycobiota of the skin. As such, PCR or culture should never be performed to

diagnose fungal disease without paired histologic samples. Many fungi colonize the shed of snakes, and ecdysis may be a mechanism for snakes to prevent pathogenic fungal infections. Fungi that are primary pathogens in snakes are uncommon.⁷ Invasiveness, granulomatous dermatitis, and arthroconidia may increase the index of suspicion for SFD (and warrant culture) and help the pathologist to diagnose this condition over other, common, secondary fungal infections. Secondary, opportunistic,

fungi are very common in snakes, and are frequently caused by hyalo-hyphomycotic fungi; this underscores the importance of evaluating fungal morphology and using ancillary diagnostics to screen for primary fungal diseases, such as SFD.⁶

The moderator discussed the diverse mycobiota of the skin of snakes, which is often composed of a number of secondary pathogens; however, subcutaneous infection and granuloma formation is very characteristic of this particular pathogen. Acid-fast staining to rule out mycobacteriosis is advisable in these cases

from a practical aspect.

References:

1. Allender MC, Dreslik MJ, Wylie DB, et al. Ongoing health assessment and prevalence of *Chrysosporium* in the eastern massasauga (*Sistrurus catenatus* *catenatus*). *Copeia*.2013;1:97–102.

2. Allender MC, Dreslik M, Wylie S, et al. *Chrysosporium* sp. infection in eastern massasauga rattlesnakes. *Emerg. Infect. Dis.* 2011;17(12):2383-2384.
3. Last LL, Fenton H, Gonyour-McGuire J, Moore M, Yabsley MJ. Snake fungal disease caused by *Ophiomyces ophidiicola* in a free ranging mud snake. *J Vet Diagn Invest* 2016 28(6):709-713.
4. Lorch JM, Knowles S, Lankton JS, Mitchell K, Edwards JL, Kapfer JM, Staffen RA, Wild ER, Schmidt KZ, Ballmann AE, Blodgett D, Farrell TM, Glorioso BM, Last LA, Price SJ, Schuler KL, Smith CE, Wellehan JFX, Bleher DS. Snake fungal disease: an emerging threat to wild snakes. *Phil Trans R Soc B* 2016; 371:20150547.
5. Nourisseon C, Vidal-Roux, M, Cayot S, Jacomeet C, Bothorel C, Ledoux-Pilon A, Anthony-Moumoni F, Lesens O, Poirier P. Invasive infections caused by *Nannizziopsis* sp. molds in immunocompromised patients. *Emerg Inf Dis* 24(3):549-552
6. Ossiboff, R. Reptilia. *In: Pathology of Wildlife and Zoo Animals*. Terio K, McAloose D, St. Leger J, eds. London, Academic Press,
7. Pare JA, ER Jacobson. Mycotic Diseases of Reptiles. *In: Jacobson ER, ed. Infectious Diseases and Pathology of Reptiles*. Boca Raton: CRC Press; 2007;527-570.
8. Paré JA, Rypien KL, Gibas CF. Cutaneous mycobiota of captive squamate reptiles with notes on the scarcity of *Chrysosporium* anamorph *Nannizziopsis vriesii*. *J. Herpetol. Med. Surg.* 2003;13(4): 10-15.
9. Rajeev S, Sutton DA, Wickes BL, et al. Isolation and characterization of a new fungal species, *Chrysosporium ophidiicola*, from a mycotic granuloma of a Black Rat Snake (*Elaphe obsoleta obsoleta*). *J. Clin. Microbiol.* 2009;47(4):1264-1268.
10. Sigler L, Hambleton S, Paré JA. Molecular characterization of reptile pathogens currently known as members of the *Chrysosporium* anamorph of *Nannizziopsis vriesii* (CANV) complex and relationship with some human-associated isolates. *J. Clin. Microbiol.* 2013;51(10):3338-3357.
11. Sleeman J. Snake fungal disease in the United States. National Wildlife Health Center Wildlife Health Bulletin 2013-02. http://www.nwhc.usgs.gov/disease_information/other_diseases/snake_fungal_disease.jsp. Updated May 21, 2013.

Self-Assessment - WSC 2017-2018 Conference 8

1. Which of the following is a characteristic finding in leprosy?
 - a. Intraneural acid-fast bacilli
 - b. Granulomatous inflammation destroying the nasal septum
 - c. Langhans' giant cells
 - d. Rare intrahistiocytic acid-fast bacilli

2. Which of the following cardiac lesions has NOT been seen in lead-intoxicated bald eagles?
 - a. Hydropericardium
 - b. Lymphocytic inflammation of the conduction system
 - c. Scattered myocardial necrosis
 - d. Myocardial fibrosis

3. Which of the following may form a symbiotic relationship with *Chlamydia* sp?
 - a. Amoebae
 - b. Swine
 - c. Mushrooms
 - d. Fruit bats

4. Which of the following is the environmentally resistant, metabolically inactive form of *Chlamydia* sp?
 - a. Intermediate body
 - b. Elementary body
 - c. Reticulate body
 - d. Crescentic body

5. Which of the following is infected by *Ophidiomyces ophiodiicola*?
 - a. Snakes
 - b. Crocodilians
 - c. Turtles
 - d. Chameleons

Please email your completed assessment to Ms. Jessica Gold at Jessica.d.gold2.ctr@mail.mil for grading. Passing score is 80%. This program (RACE program number) is approved by the AAVSB RACE to offer a total of 0.5 CE Credits, with a maximum of 12.5 CE Credits being available to any individual Veterinary Medical Professionals for the 2017-2018 Wednesday Slide Conference. This RACE approval is for the subject matter categories of: SCIENTIFIC using the delivery method of NON-INTERACTIVE DISTANCE. This approval is valid in jurisdictions which recognize AAVSB RACE; however, participants are responsible for ascertaining each board's CE requirements. RACE does not "accredit", "endorse" or "certify" any program or person, nor does RACE approval validate the content of the program.

Please email your completed assessment to Ms. Jessica Gold at Jessica.d.gold2.ctr@mail.mil for grading. Passing score is 80%. This program (RACE program number) is approved by the AAVSB RACE to offer a total of 0.5 CE Credits, with a maximum of 12.5 CE Credits being available to any individual Veterinary Medical Professionals for the 2017-2018 Wednesday Slide Conference. This RACE approval is for the subject matter categories of: SCIENTIFIC using the delivery method of NON-INTERACTIVE DISTANCE. This approval is valid in jurisdictions which recognize AAVSB RACE; however, participants are responsible for ascertaining each board's CE requirements. RACE does not "accredit", "endorse" or "certify" any program or person, nor does RACE approval validate the content of the program.

**Joint Pathology Center
Veterinary Pathology Services**



WEDNESDAY SLIDE CONFERENCE 2018-2019

C o n f e r e n c e 9

1 November 2018

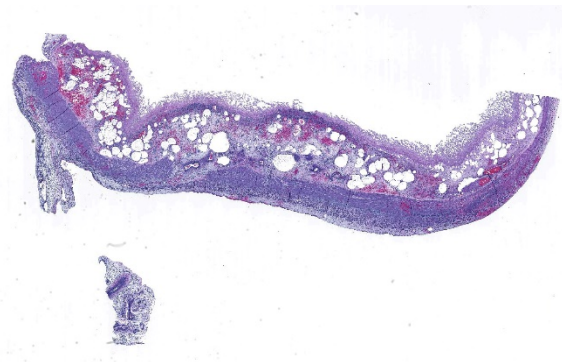
Conference Moderator:

Francisco A. Uzal, DVM, PhD, DACVP
Professor of Pathology
California Animal Health and Food Safety Lab
San Bernardino Lab
San Bernardino, CA 92408

CASE I: 13-12484 (JPC 4050022-00).

Signalment: Two day old male warmblood horse, *Equus caballus*

History: This colt presented for bloody diarrhea, lethargy, and anorexia for ~1 day. His birth was not witnessed and he was noticed to be standing and nursing although the mare's udder was tight and he was not nursing well. He passed tan diarrhea at that time. Later that morning the diarrhea became bloody and he was increasingly lethargic. At presentation to Oregon State University Lois Bates Acheson Veterinary Teaching Hospital he was lateral, dull, ~ 5-10% dehydrated, and minimally responsive. Mucous membranes were pale, tacky, cold, and injected with a prolonged CRT. There were petechiae in the oral mucous membranes and in the pinna. Preliminary diagnosis was sepsis and despite supportive care there was little improvement. Due to the guarded prognosis the foal was euthanized and a necropsy was performed.



Intestine, foal: A section of intestine is submitted for examination. At subgross magnification, a linear band of cellular debris is present at the base of the mucosa, and the submucosa is markedly expanded by edema, hemorrhage, and multifocal emphysema. (HE, 6X)

Gross Pathology: Jejunal content was hemorrhagic, with multifocal zones of mucosal necrosis up to 50 x 15 cm throughout. There were multiple gastric ulcers with hemorrhagic gastric content and bloody liquid material throughout the small and large intestine. Petechiae and ecchymoses were present in the endocardium and kidneys.

Laboratory results: CBC: Leukopenia (2810; RI: 6000-120000/ul), HCT 48.7% RI: 32-48%), hypoproteinemia (5.4; RI: 6.0-8.5 g/dL), hyperfibrinogenemia (400; RI: 100-400 mg/dl), lymphopenia (1208; RI: 1500-5000/ul), moderate neutropenia with a left shift (674; RI: 3000-6000/ul; bands 141 RI: 0-100ul).

Complete Chemistry: Mild azotemia (BUN 30; RI: 8-23 mg/dl, Crea 2.3; RI: 0.9-1.7 mg/dl), mild hypoglycemia (Glu 51; RI: 79-109), mild hyperbilirubinemia (3.4 RI: 0.8-2.6 mg/dl), moderate to marked hyperphosphatemia (10.1; RI: 1.9-4.1 mg/dl), increased SDH (12.9; RI: 2.4-7.2 U/L

IgG > 800 mg/dl

Blood culture: *Actinobacillus equuli* two colony types

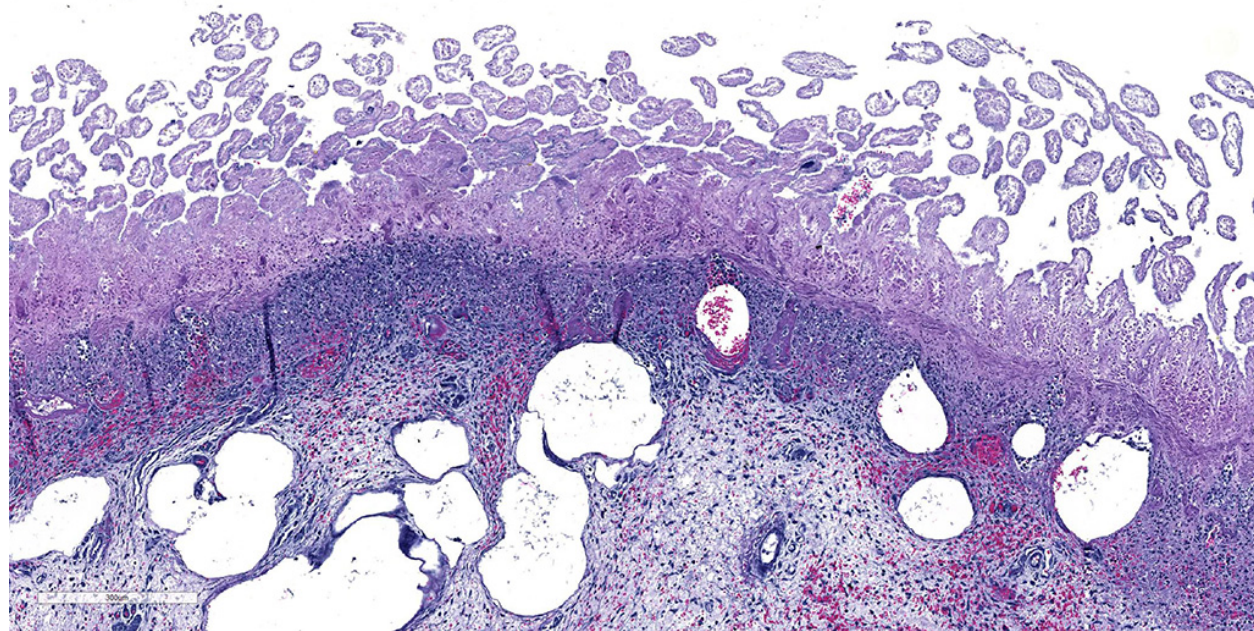
Fecal *c. difficile* enterotoxin ELISA: positive

Fecal *c. perfringens* enterotoxin ELISA: negative

Microscopic Description: Small intestine: There are multifocal extensive areas of transmural hemorrhage. The submucosa is markedly edematous and there are multifocal fibrin thrombi with overlying mucosal necrosis. Within areas of necrosis there are numerous vessels occluded with amorphous, smudgy, eosinophilic deposition (fibrin thrombi) in the lamina propria and the tips of the villi are hypereosinophilic with necrosis and cellular debris. Also within affected areas there are multiple colonies of bacilli. The tissue is inflamed with mixed degenerate inflammatory cells and the base of the mucosa is expanded by plump fibroblasts (proliferative fibroplasia) and numerous small vessels lined by plump endothelium (reactive vasculature).

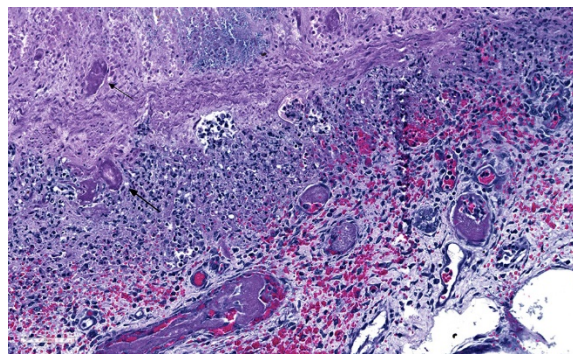
Contributor's Morphologic Diagnoses:

Small intestine: Severe multifocal transmural necrohemorrhagic enteritis with fibrin thrombi and bacilli consistent with clostridia



Intestine, foal: There is diffuse coagulative necrosis of the mucosa (top). There is a line of cellular debris immediately subjacent to the muscularis mucosae. The submucosa is multifocally diffusely expanded by edema, multifocal hemorrhage, and clear space (emphysema). (HE, 60X)

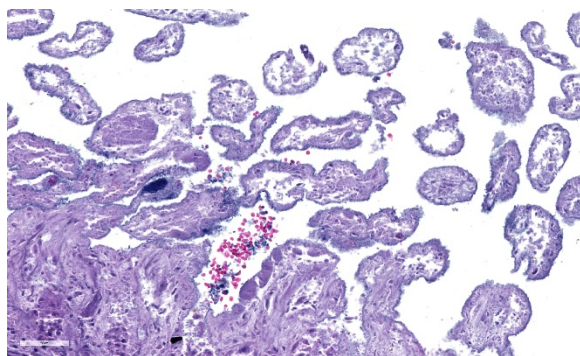
Contributor's Comment: *Clostridium difficile* is a gram-positive, anaerobic, spore-forming bacillus associated with diarrhea and (entero)colitis in humans and other mammals³. Colitis is most common in most species but the small intestine is affected in rabbits and foals³. In horses, *Clostridium difficile*, has been incriminated in hemorrhagic enteritis in foals and colitis in all ages and foals may be affected within the first few days of life⁵. The disease causes severe acute-to-peracute enterocolitis likely due to dysbacteriosis with clostridial overgrowth secondary to antibiotic therapy, stress, or dietary changes³. Although prior antibiotic treatment and/or hospitalization are significant predisposing factors in horses that develop *C. difficile*-associated disease (CDAD), disease may occur without prior treatment or hospitalization^{1,2}. Foals < 7 days old without prior antibiotic therapy or hospitalization may frequently develop CDAD². The primary virulence factors of *C. difficile* are toxin A (TcdA) and toxin B (TcdB) which act synergistically³. TcdA causes widespread damage to the mucosa (enterotoxic) allowing TcdB to affect epithelial cells (cytotoxic)³. TcdA enters the epithelial cell through endocytosis by coated pits and escapes into the cytoplasm by acidification of the endolysosome. In the cytoplasm, toxin inactivates Rho and other GTPase necessary for the regulation of cytosolic actin filaments leading to a loss of cell-to-cell contacts, increased paracellular permeability, and ultimately cell death³. TcdA and TcdB also initiate the inflammatory cascade including generation of reactive oxygen intermediates and elaboration of IL-8 and macrophage inhibitory protein 2 (MIP-2), both of which cause influx of neutrophils leading to host tissue damage³. TcdA also causes monocyte production of IL-1, IL-6, IL-8, and TNF α , and macrophage expression of COX-2 leading to release of prostaglandin E₂ which



Intestine, foal: Proprial vessels are often thrombosed; vessels in areas of necrosis have hyalinized walls, but this does not represent true vasculitis, but simply being in the wrong place at the wrong time. (HE, 275X)

inhibits sodium chloride and water absorption in the intestine and enterocyte chloride secretion³. *Clostridium perfringens* is also an important cause of enteric disease but usually causes disease in more proximal segments of the gastrointestinal tract³. In foals, enteritis with extensive necrosis can occur in the small intestine due to both *C. difficile* and *C. perfringens*³. In this case the ELISA for *C. perfringens* toxin was negative. This case demonstrates classic gross and histologic lesions of CDAD. Additional lesions, petechiation and ecchymosis, have been described in horses with CDAD and have been attributed to endotoxic shock and/or disseminated intravascular coagulation¹. The most common histologic findings in foals with confirmed *C. difficile* infection are necrotizing or necro-hemorrhagic enteritis and submucosal thrombosis,¹ which were features of this case. Other infectious differentials for this type of enteritis in horses includes *C. perfringens* type C enterotoxemia, salmonellosis, or ehrlichial enteritis¹. Culture and toxin assay should be interpreted together because culture sensitivity is below 100% and *C. difficile* can be isolated from a small number of healthy horses¹.

Actinobacillus equuli was isolated from the blood culture. *A. equuli* is a common cause



Intestine, foal: Close inspection of the HE section will disclose the presence of robust bacilli adherent to the necrotic remnants of the villi. (HE, 400X)

of neonatal septicemia and death, with disease course ranging from abortion to early neonatal death to survival for several days with development of microabscesses in many organs⁵. *A. equuli* can occasionally be found as an opportunist in pathological tissue⁵. In this case there were fibrin thrombi identified in the kidney and edema of the choroid plexus that may have been caused by septicemia by *A. equuli*. The lesions in the intestine were most significant and the positive ELISA for *C. difficile* confirmed the diagnosis of CDAD. Mucosal damage due to *Clostridium* infection with subsequent *A. equuli* entry and sepsis is a likely sequence of events and has been suggested in a report of a foal with multiple concurrent diseases including CDAD and *A. equuli*⁴.

Contributing Institution:

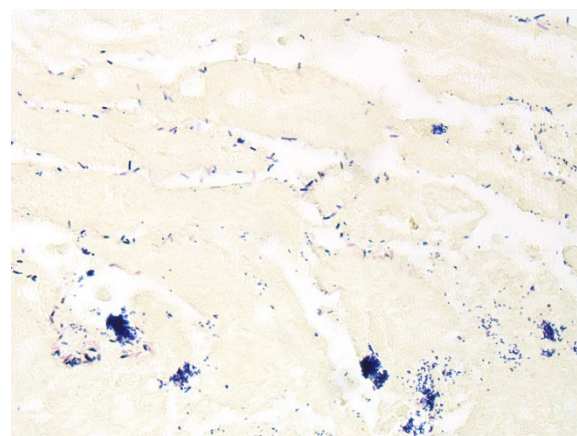
Oregon State University College of Veterinary Medicine
Department of Biomedical Sciences and Veterinary Diagnostic Laboratory
<http://vetmed.oregonstate.edu/diagnostic>

JPC Diagnosis: Small intestine: Enteritis, necrotizing, diffuse, severe, with submucosal hemorrhage, edema and emphysema and numerous adherent robust bacilli.

JPC Comment: The contributor provides an excellent review of the subcellular events

associated with *C. difficile* infection in foals. In this species, both foals and horses are equally susceptible to infection, with antibiotic therapy and hospitalization being the main predisposing factors for the development of this disease in adult horses.² *C. difficile* has been the cause of disease in a wide variety of mammalian species. First identified from feces of clinically healthy human babies in the 1930s, the organism was originally named *Bacillus difficilis* because of the difficulties encountered in cultivating it. In humans, most infected people will remain symptomatic, with the remainder developing variable GI signs ranging from watery diarrhea to pseudomembranous colitis.² As in horses, hospitalization and antibiotic administration is a predisposing factor. Most *C. difficile*-positive infants, however, lack clinical signs, possibly due to lacking receptors for the toxin.

In humans, *C. difficile* associated disease (CDAD) was always assumed to affect individuals of any age, except during the neonatal period as it was thought that this specific group may lack specific *C. difficile* toxin receptors. Although between 25 and 70% of human neonates are colonized with *C. difficile*, these microorganisms have been largely considered part of the commensal microbiota. Recently, however, two 9 or 18



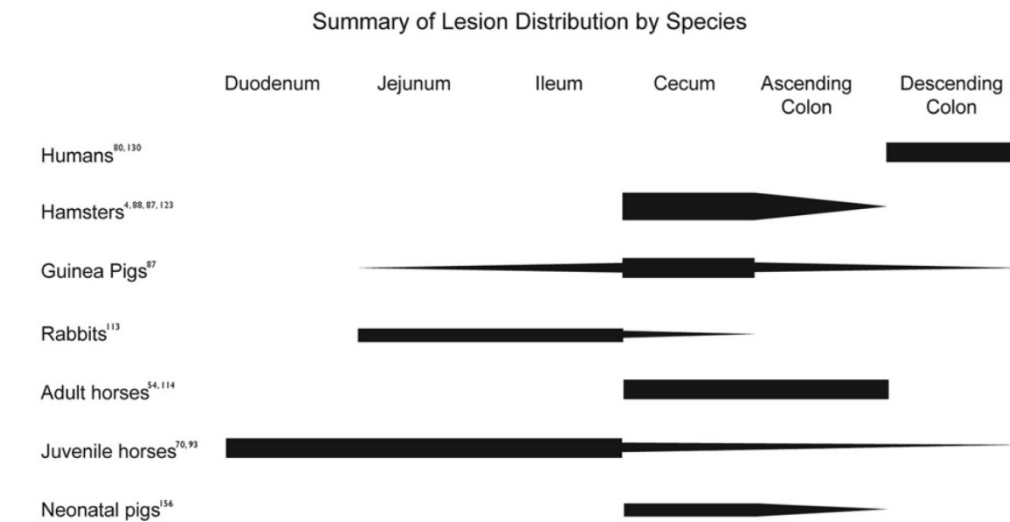
Intestine, foal: Gram-positive bacilli are adherent to the necrotic remnants of the villi. (Brown-Hopps, 400X)

month-old children were diagnosed with CDAD, providing evidence that *C. difficile* is a potential cause of bloody diarrhea in neonates and young infants. In most animal species, CDAD is not age-dependent. The exception to this are pigs, which are almost exclusively affected during the neonatal period, up to approximately one week of

age.⁶

C. difficile-associated disease (CDAD) affects a wide range of other mammals – while always resulting in enterocolitis, its manifestation varies widely with the affected species. Table 1 summarizes the severity of disease in various species by enteron segment.

Table 1. Summary of lesion distribution by species.³



1 Fig. 1. Summary of the species-dependent distribution of intestinal lesions induced by *Clostridium difficile*. The thickness of the bars represents the severity of lesions typically seen in an infected individual of a given species at a particular site. The figure lists only those species for which the distribution of spontaneous lesions of *Clostridium difficile*-associated disease (CDAD) is well documented.

In rodents, CDAD is primarily cecal, resulting in ulcerative and rarely proliferative typhlitis and death. In pigs, the disease results in ulcerative typhlitis or colitis with development of “volcano ulcers”. An additional gross finding of mesocolonic edema (as well as diarrhea) makes CDAD a differential diagnosis for edema disease in swine.² The difference is that *C. difficile* infections occurs in young piglets (1-7 days of age), while edema disease is a disease of weanling age pigs. In rabbits, the lesion is

primarily seen in the small intestine and concentrated in the ileum, often following antibiotic administration. It has also been reported sporadically in dogs, cats, ostriches, prairie dogs, and experimentally in non-human primates.³

Diagnosis of CDAD is usually based on a combination of clinical history, often with previous antibiotic administration or hospitalization, characteristic microscopic lesions in appropriate segments of the enteron, and most importantly, ELISA testing

of feces and/or intestinal for *C. difficile*-specific TcdA of TcdB toxins. Culture is useful because the carrier rate in horses is low, but care should be taken as: a) a few healthy horses (usually up to 5% although there is great variation in the literature) can be carriers of *C. difficile*, and b) occasionally non-toxigenic strains may be present in the intestine of horses, so any isolate should ideally be typed by PCR to confirm the presence of the genes encoding the major toxins of this microorganism. The latter is not routinely done in most veterinary diagnostic laboratories. Gross lesions, and to a lesser extent microscopic lesions are non-specific as to etiology, and in the horse, may resemble those of other diseases such as *C. perfringens* type C, salmonellosis, Potomac horse fever, and NSAID toxicity.²

In reviewing the slide, the moderator commented on the presence of numerous bacilli lining the necrotic villi as a relatively non-specific finding that should NOT be interpreted as evidence of clostridial infection, unless an appropriate immunohistochemical stain discloses that they are all of the same etiology. Many bacilli (and not just clostridia) will adhere to denuded mucosa. In addition, The moderator also pointed out that the presence of fibrin thrombi in the submucosa as evidence that the changes in the mucosa are truly antemortem and not simple autolysis.

References:

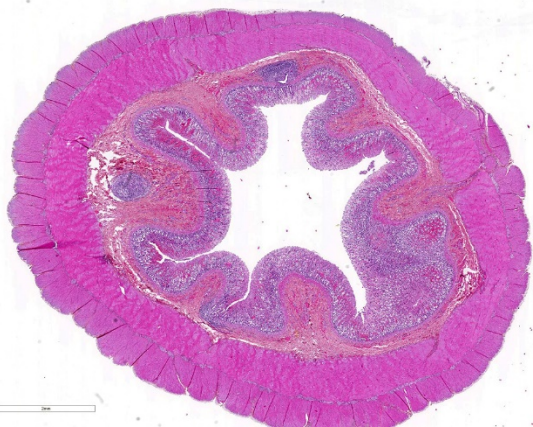
1. Diab SS, Rodriguez-Bertos A, Uzal FA: Pathology and diagnostic criteria of *Clostridium difficile* enteric infection in horses. *Vet Pathol* 2013;50(6):1028-1036.
2. Diab SS, Songer G, Uzal FA: *Clostridium difficile* infection in horses: a review. *Vet Microbiol* 2013;167(1-2):42-49.
3. Keel MK, Songer JG: The comparative pathology of *Clostridium difficile*-associated disease. *Vet Pathol* 2006;43(3):225-240.
4. Lohr CV, Polster U, Kuhnert P, Karger A, Rurangirwa FR, Teifke JP: Mesenteric lymphangitis and sepsis due to RTX toxin-producing *Actinobacillus* spp in 2 foals with hypothyroidism-dysmaturity syndrome. *Vet Pathol* 2012;49(4):592-601.
5. Maxie MG: Jubb, Kennedy, and Palmer's Pathology of Domestic Animals 5th ed. Philadelphia: Elsevier Limited; 2007.
6. Uzal FA, Navarro MA, Li J, Freedman JC, Shrestha A, McCline BA. Comparative pathogenesis of enteric clostridial infections in humans and animals. *Anaerobe* 2018; 53:11-20.

CASE II: H150787-83 (JPC 4085384-00).

Signalment: Dog (*Canis lupus familiaris*), intact female, 5-year-old, Chihuahua

History: The dog developed acute diarrhea and died suddenly. The dog was already dead at arrival to our teaching hospital and no further clinical investigations could be performed. The owner suspected intoxication and asked for a necropsy.

Gross Pathology: This dog was in good body condition but showed marked dehydration. The stomach contained two plastic fragments and the mucosa was brown to green. A thick viscous content was in the small intestine



Colon, dog: A cross section of colon is submitted for evaluation. There is diffuse pallor (indicating necrosis) of the superficial mucosa and scattered hemorrhage. (H/E and Saffron, 6X).

associated with a diffuse and moderately congested mucosa.

The cecum, colon and rectum were moderately thickened with a severely and diffusely congested mucosa. The content was scant, hemorrhagic and thick.

A concentric hypertrophy of the left ventricle, a moderate distal tracheal collapse, a discrete mesenteric lymph node hypertrophy and a mild meningeal congestion were also noted. All other organs and tissue were within normal gross limits.

Laboratory results: None given.

Microscopic Description: Colon: There is diffuse necrosis of the superficial mucosa, characterized by superficial mucosal hyper eosinophilia with loss of cellular borders, pyknotic nuclei and loss of the mucosal epithelial lining. On the mucosal surface, admixed with necrotic debris, there are numerous 1- μ m-long rod-shaped bacteria. The lamina propria and the submucosa present moderate to marked hyperemia and hemorrhage, and moderate infiltration by lymphocytes, plasma cells and degenerated neutrophils. There is multifocal thrombosis of small-sized blood vessels in the mucosa and submucosa. A Gram stain

revealed numerous positive rods attached to the necrotic mucosal surface.

Contributor's Morphologic Diagnoses:

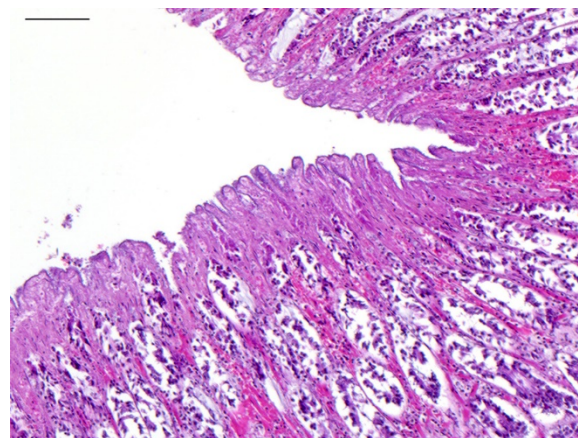
Colon: Colitis, necrotizing and hemorrhagic, acute, diffuse, severe, with mucosal and submucosal vascular thrombosis and numerous gram-positive rod-shaped bacteria (consistent with *Clostridium sp.*) on to the mucosal surface

Name of the disease: Canine Hemorrhagic Gastroenteritis

Etiology: *Clostridium perfringens* type A (putative)

Contributor's Comment: Canine Hemorrhagic Gastroenteritis (CHG) is a sporadic, peracute, hemorrhagic gastroenteritis of dogs. The etiology is not always identified, but *Clostridium perfringens* type A can be identified in some cases. A predilection for small breeds is described.⁶

Clostridium perfringens type A is responsible for mild and self-limiting diarrhea to fatal acute necrotizing and hemorrhagic enteritis



Colon, dog. The mucosa shows superficial necrosis and hemorrhage. (H/E/Saffron, 200X) (Photo courtesy of: Unité d'Histologie, d'Embryologie et d'Anatomie pathologique, Département des Sciences Biologiques et Pharmaceutiques, Ecole Nationale Vétérinaire d'Alfort, FRANCE: www.vet-alfort.fr)

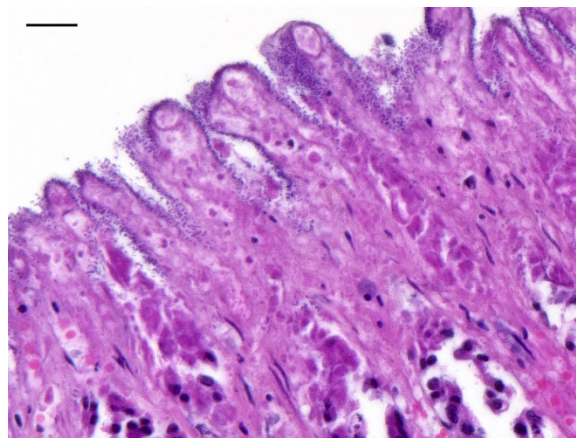
in dogs and cats. It is also known to cause food poisoning in humans, necrotic enteritis in chickens, enterocolitis in horses and neonatal piglets, and enterotoxemia and hemorrhagic enteritis in lambs and calves.⁹

Clostridium perfringens is a gram-positive obligate anaerobic, spore-forming bacteria. It is part of the normal microbiota of human and animals, and a common enteric pathogen. It is separated into 5 types (A through E) based on the production of α , β , ϵ , and I toxins. Other important toxins, such as β_2 and enterotoxin (CPE) may be produced by any of the five types, but the production of CPE is most commonly associated with type A strains.¹¹

Clostridium perfringens type A major toxin is alpha toxin. Enterotoxin and β_2 toxin may be produced by some strains. The bacteria require an anaerobic environment to sporulate and produce enterotoxin.¹¹

CPE is a cytotoxic enterotoxin only elaborated during sporulation. It causes tissue damage and fluid secretion by binding to intestinal epithelial cells, forming pores in the plasma membrane that initiate cell death signaling pathway, and inducing structural damage to intercellular tight junctions resulting in increased epithelial permeability.⁴ However, the pathogenesis remains poorly understood because CPE can be demonstrated in the feces without sporulation and in the feces of healthy dogs.¹⁰

In 2015, three novel putative toxin genes encoding proteins related to the pore-forming Leukocidin/Hemolysin Superfamily were identified, and named netE, netF, and netG. Only netF was associated with cytotoxicity. There was a highly significant association between the presence of netF with type A strains isolated from cases of canine acute hemorrhagic gastroenteritis.⁴

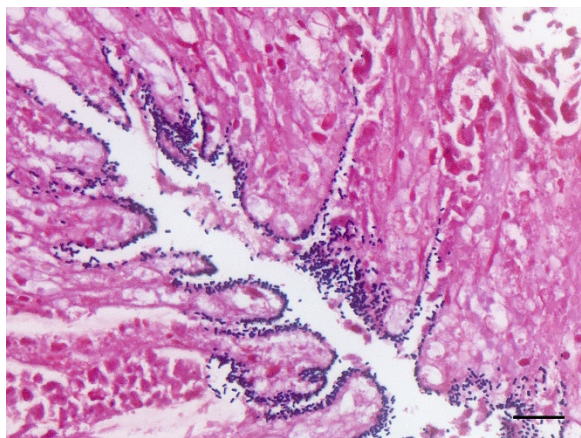


Colon, dog. Numerous rod-shaped bacteria are adherent to the mucosal surface. (H/E/Saffron, 1000X) (Photo courtesy of: Unité d'Histologie, d'Embryologie et d'Anatomie pathologique, Département des Sciences Biologiques et Pharmaceutiques, Ecole Nationale Vétérinaire d'Alfort, FRANCE: www.vet-alfort.fr)

Three predisposing factors for CHG are described: enteric infection by another pathogen (such as canine parvovirus), antibiotic administration, and disruption of the normal microbiota (for example by a sudden change to a high protein diet). Dogs present with hemorrhagic diarrhea. In the acute form, dogs are often found dead lying in a pool of blood excreta. Gross lesions consist of necrotizing and hemorrhagic enterocolitis, and sometimes gastritis. Lesions in the colon tend to be more severe, as so well demonstrated in this case.

The histologic lesions consist of mural hemorrhagic necrosis of the gastrointestinal mucosa. Necrotic mucosal surface is lined by many gram-positive bacilli in association with fibrin and debris. The bacilli do not invade the lamina propria and can also be found within necrotic debris.¹⁰

Definitive diagnosis of CHG due to *Cl. perfringens* type A is not an easy task and cannot be based on macroscopic and microscopic lesions only. It requires combined testing for the CPE gene by PCR and for the *Cl. perfringens* enterotoxin by fecal enzyme-linked immunosorbent assay,



Colon, dog. The bacteria are gram-positive. (Gram, 1000X)(Photo courtesy of: Unité d'Histologie, d'Embryologie et d'Anatomie pathologique, Département des Sciences Biologiques et Pharmaceutiques, Ecole Nationale Vétérinaire d'Alfort, FRANCE: www.vet-alfort.fr)

and exclusion of other potential enteropathogens.^{11,13,16} In our case, such investigations could not be performed. However, the finding of an acute, fatal, necrotizing and hemorrhagic enterocolitis in a small-breed dog associated with numerous gram-positive bacilli is highly suggestive of CHG due to *Cl. perfringens* type A.

Contributing Institution:

Unité d'Histologie, d'Embryologie et d'Anatomie pathologique, Département des Sciences Biologiques et Pharmaceutiques, Ecole Nationale Vétérinaire d'Alfort, FRANCE : www.vet-alfort.fr

JPC Diagnosis: Colon: Colitis, necrohemorrhagic, diffuse, moderate, with thrombosis of submucosal vessels.

JPC Comment: The contributor provides an excellent review of this condition, which is well known to practitioners, but may be less well-known to veterinary pathologists. While the histologic lesion in this case is consistent with that seen in reported cases of acute canine hemorrhagic diarrhea syndrome (AHDS - a new and likely temporary name

for this condition), the inability to either culture the pathogen or perform toxin identification is somewhat problematic in terms of a definitive identification of the etiologic agent. Mostly problematic is that the etiology remains unknown. *C. difficile* is identified in an equal or increased number of cases of hemorrhagic enteritis in dogs with similar predisposing factors to AHDS (previous antibiotic therapy, concurrent intestinal pathogens, and rapid dietary change.)³ However, *C. difficile* is found in similar prevalence in healthy dogs and its role in enteric canine disease remains undetermined.²

Since the submission of this case to the WSC, a review of lesions in endoscopic biopsies obtained from dogs with acute hemorrhagic diarrhea syndrome (a name chosen to reflect the lack of gastric lesions in affected animals) has been published.⁸ In endoscopic biopsies taken from 10 dogs with clinical AHDS, 9/10 demonstrate acute lesions of necrosis and neutrophilic infiltrate within the duodenum, 7/8 in the ileum, and 9/9 in the colon. Robust bacilli were identified in 5/6 duodenal samples, 5/8 ileal samples, and 7/9 colon samples.

C. perfringens type A was recently reported as a cause of necrotizing myositis in a German Shepherd Dog.¹² A large mass of crepitant necrotic muscle developed on the right hindlimb over a period of 72 hours which necessitated radical surgical excision, drainage, and prolonged antibiotics; the animal survived. Multiplex PCR identified the agent in initial aspirates as *Clostridium perfringens* type A with a cpA toxin.¹² *C. perfringens* type A is, beyond any doubt, responsible for human gas gangrene; alpha toxin is the main virulence factor of this type involved in gas gangrene.^{1,14}

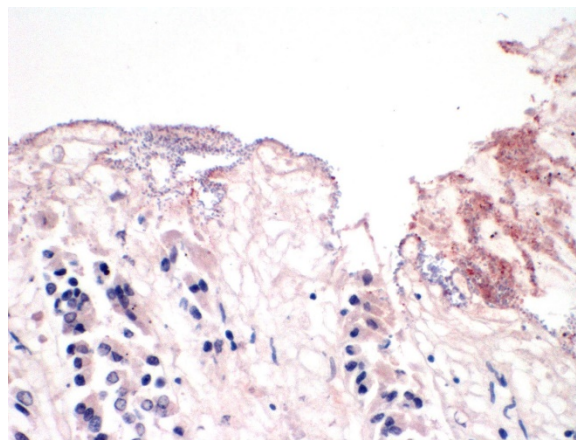
NetF is a novel toxin produced by some strains of *C. perfringens* type A. While

preliminary evidence indicate that there seems to be a higher prevalence of NetF+ strains in dogs with AHDS than in healthy dogs^{2,4}, final proof of the role of this toxin in this or other enteric conditions is lacking.

Upon review of the slide, the moderator discussed parameters which might be used in determining the presence of inflammation within the lamina propria versus a normal inflammatory population. While various criteria exist, but the separation of crypts and or lifting of crypts off of the muscularis mucosa by more than 3 layers of inflammatory cells suggests the presence of a true inflammatory infiltrate within the lamina propria.

Attendees discussed the possibility of parvoviral in this case based on morphologic finding, but the group consensus is that this differential diagnosis is not morphologically supported by the lack of profound crypt necrosis, necrosis of superficial mucosa and sparing of lymphoid tissue.

An immunohistochemical stain was performed for *Clostridium perfringens* type A at the San Bernardino lab of the California Animal Health and Food Safety system, and only a small percentage of the mucosal-adherent bacilli stained positively. The role of *C. perfringens* type A in enterocolitis and/or enterotoxemia of mammalian species is controversial and poorly supported by scientific evidence.¹⁵ The fact that *C. perfringens* type A has been identified in some cases (most cases actually) does not support a causal role in the disease, as this microorganism may be isolated from a large percentage of normal animals as well. One possible exception to the relationship between *C. perfringens* type A is perhaps yellow lamb disease.¹⁵ The contributor's assertion that combined testing for the CPE gene by PCR and for the *Cl. perfringens*



Colon, dog: In areas of necrosis, numerous robust bacilli are adherent to the devitalized mucosa. Numerous (but certainly not all) of these bacilli stain immunopositively for a stain for C. perfringens (which does not differentiate for toxinotype). (pan-C. perfringens, 400X)(Photo courtesy of: California Animal Health and Food Safety Laboratory, San Bernardino Branch.)

enterotoxin by fecal enzyme-linked immunosorbent assay would be helpful in this diagnosis is problematic as well in light of recent developments in the field as the production of *C. perfringens* enterotoxin is now restricted only to *C. perfringens* type F in humans, a common cause of food poisoning which has not been identified in animals.¹⁰

The consensus diagnosis of the attendees in this particular case is that, without any other submitted diagnostics, the etiology of this particular case remains in question.

References:

1. Awad MM, Ellemor DM, Boyd RL, Emmins JJ, Rood JJ. Synergistic effects of alpha-toxin and perfringolysin O in Clostridium perfringens-mediated gas gangrene; Infect Immun. 2001 Dec;69(12):7904-10).
2. Busch K, Suchodolski JS, Kühner KA, Minamoto Y, Steiner JM, Mueller RS, Hartmann K, Unterer S. Clostridium perfringens enterotoxin and

- Clostridium difficile* toxin A/B do not play a role in acute haemorrhagic diarrhoea syndrome in dogs. *Vet Rec* 2015; Mar 7;176(10):253. doi: 10.1136/vr.102738.
3. Diniz AN, Coura FM, Rupnik M, Adams V, Stent TI, Rood JI, de Oliveira Jr. CA, Lobator FCF, Silva ROS. The incidence of *Clostridioides difficile* and *Clostridium perfringens* netF-positive strains in diarrheic dogs. *Anaerobe* 2018; 49:58-62.
 4. Finley A, Gohari IM, Parreira VR, Abrahams M, Staempfli HR, Prescott JF. Prevalence of netF-positive *Clostridium perfringens* in foals in southwestern Ontario. *Can J Vet Res.* 2016; 80(3):242-4.
 5. Gohari IM, Parreira VR, Nowell VJ. A novel pore-forming toxin in Type A *Clostridium perfringens* is associated with both fatal canine hemorrhagic gastroenteritis and fatal foal necrotizing enterocolitis. PLOS ONE. 2015;10:e0122684.
 6. Iii JGS, Fisher DJ, Sayeed S, et al. The enteric toxins of *Clostridium perfringens*. in: *Reviews of Physiology, Biochemistry and Pharmacology*. Springer Berlin Heidelberg, 2004:183–204.
 7. Lawson PA, Citron DM, Tyrrell KL, Finegold SM. Reclassification of *Clostridium difficile* as *Clostridioides difficile* (Hall and O'Toole 1935) Prévot 1938. *Anaerobe*. 2016 Aug;40:95-9. doi: 10.1016/j.anaerobe.2016.06.008. Epub 2016 Jun 28.
 8. Leipid-Rudolph M, Busch K, Prescott JF, Gohari M, Leutenegger CH, Hemranns W, Wolf G, Hartmann K, Verspohl J, Unterer S. Intestinal lesions in dogs with acute hemorrhagic diarrhea syndrome associated with InetF-positive *Clostridium perfringens* type A. *J Vet Diagn Invest* 2018; 30(4):495-503.
 9. Maxie G. Alimentary system. *Jubb, Kennedy & Palmer's Pathology of Domestic Animals*. 6th ed. Saunders Ltd; 2015;2:183-185.
 10. Rood JI, Adams V, Lacey J, Lyras D, McClane BA, Melville SB, Moore RJ, Popoff MR, Sarker MR, Songer JG, Uzal FA, Van Immerseel F. Expansion of the *Clostridium perfringens* toxin-based typing scheme. *Anaerobe*; 2018 pii: S1075-9964(18)30068-4. doi: 10.1016/j.anaerobe.2018.04.011.
 11. Schlegel BJ, Van Dreumel T, Slavić D. et al. *Clostridium perfringens* type A fatal acute hemorrhagic gastroenteritis in a dog. *Can. Vet. J.* 2012;53:555-557.
 12. Sedigh HS, Rajabloun M, Razmyar J, Mehrjerdi HK. An unusual necrotic myositis by *Clostridium perfringens* in a German Shepherd dog: a clinical report, bacteriological and molecular identification.
 13. Silva ROS, Lobato FC. *Clostridium perfringens*: A review of enteric diseases in dogs, cats and wild animals. *Anaerobe*. 2015;33:14–17.
 14. Uzal FA, McClane BA, Cheung JK, Theoret J, Garcia JP, Moore RJ, Rood JI. Animal models to study the pathogenesis of human and animal ***Clostridium perfringens*** infections. *Vet Microbiol*. 2015 Aug 31;179(1-2):23-33. doi: 10.1016/j.vetmic.2015.02.013.
 15. Uzal FA, Plattner BL, Hostetter JM. In: Maxie MG, ed. *Jubb, Kennedy, and Palmer's Pathology of Domestic Animals*. Vol 2. 6th ed. Philadelphia, PA: Elsevier;2016:216-217.

16. Washabau RJ, Day MJ. Disease of the gastrointestinal tract. In: *Canine and Feline Gastroenterology*, Saunders; 2012.

CASE III: H17-1982 (JPC 4105936-00).

Signalment: 16 day-old Holstein-Friesian male (*Bos taurus*).

History: The calf became acutely dull and lethargic, with subnormal body temperature, despite being placed under a heating lamp. The animal did not feed and died overnight.

Gross Pathology: The calf was in reasonable body condition. Bilaterally, sunken eyeballs within sockets. Abundant serofibrinous fluid in abdominal cavity with fibrin adherent to a large (4 cm diameter) non-penetrating serosal tear along the greater curvature of the abomasum. Within the abomasum, the mucosa was diffusely congested, with two large (approximately 5 cm diameter) areas of ulceration. Diffusely, there was marked thickening, edema and emphysema of the abomasal folds.



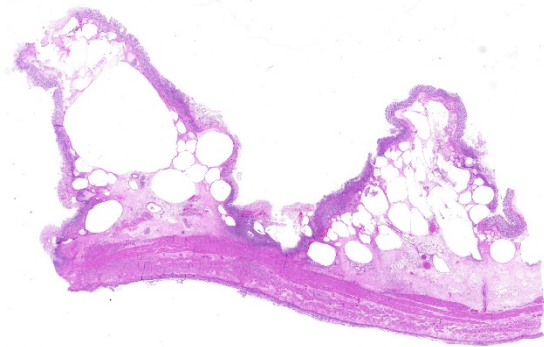
Abomasum, calf. The submucosa is markedly expanded by edema, hemorrhage, and emphysema with multiple areas of mucosal ulceration. (Photo courtesy of: UCD School of Veterinary Medicine, University College Dublin, Belfield, Dublin 4, Ireland, <http://www.ucd.ie/vetmed/>)

Laboratory results:

Abomasal tissue *Clostridium sordellii* FAT – negative

Abomasal tissue *Clostridium septicum* FAT – negative

Microscopic Description: Abomasum: There are marked multifocal areas of degeneration, necrosis and loss of the glandular mucosa and gastric pits. Necrotic areas contain amorphous eosinophilic cellular debris, basophilic karyorrhectic debris and are infiltrated by large numbers of



Abomasum, calf. Subgross examination details the extent of the emphysema within the submucosa and areas of mucosal necrosis. (HE, 5X)

viable and degenerate neutrophils and some macrophages. Occasionally both within and overlying necrotic areas there are tetrad packets of basophilic cuboidal 2-3 um bacteria (*Sarcina spp.*). Diffusely, the abomasal leaves are thickened with severe submucosal expansion by large (up to 6mm) multifocal-coalescing clear spaces (emphysema), abundant finely fibrillar eosinophilic mesh (fibrinous exudate) and dilated lymphatics. There is marked submucosal infiltration of numerous neutrophils. The neutrophilic infiltrate and fibrinous oedema obscures the muscularis mucosa and extends through the submucosa, muscularis externa and serosa. The external serosa is covered by a thick mat of fibrin and neutrophils.

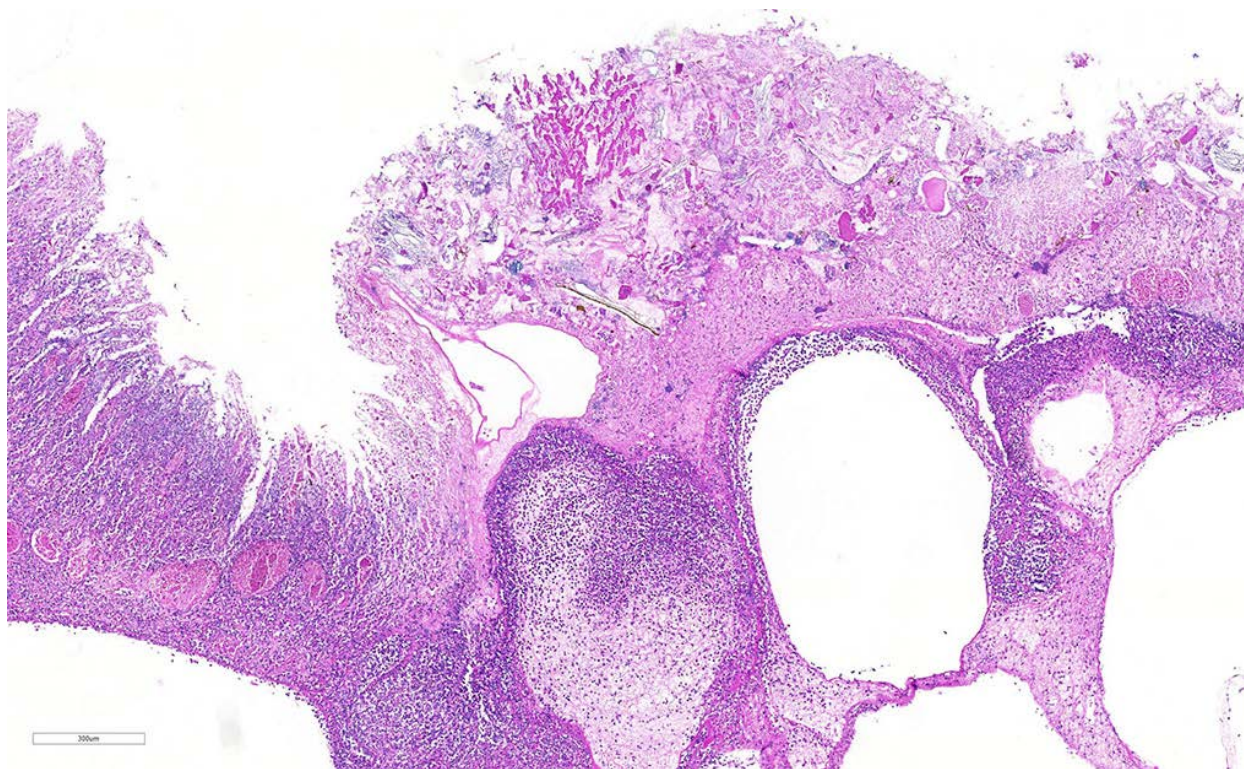
Contributor's Morphologic Diagnoses:

Abomasum: Severe, acute, diffuse, necrosuppurative and emphysematous abomasitis with *Sarcina* spp.

Etiology: *Sarcina* spp. (putative)

Contributor's Comment: The association of *Sarcina* spp. with fatal emphysematous abomasitis, abomasal bloat and abomasal ulceration in both young calves and lambs has been reported.^{2,3} The current case demonstrates a number of typical features; submucosal emphysematous bullae, fibrinous exudate, neutrophilic infiltrates, foci of mucosal necrosis and the characteristic colonies of *Sarcina* spp. bacteria^{2,5}. *Sarcina* spp. are gram-positive anaerobic cocci, are carbohydrate fermenters and can grow in an acid environment (as low as pH 1.0). They have a characteristic microscopic morphology: basophilic, cuboidal bacteria with flattened walls

occurring in tetrad packets. They are not invasive and are typically found along the mucosal surface.¹ The main products of *Sarcina* carbohydrate fermentation are ethanol, acetaldehyde, carbon dioxide and hydrogen. In human gastritis associated with *Sarcina ventriculi*, it is postulated that the mucosal damage is the result of alcohol production, as the lesions are reminiscent of acute alcohol poisoning¹. In animals it is postulated that production of large volumes of carbon dioxide induce abomasal bloat and emphysema² with the distension in turn inducing ulceration, edema and haemorrhage⁵. *Sarcina* spp. are present in the soil and environment. When ingested by pre-ruminant calves the milk diet provides a rich fermentative substrate, and the low pH



Abomasum, calf. Area of full-thickness mucosal necrosis overlying an emphysematous submucosa infiltrated by large numbers of neutrophils enmeshed in edema and polymerized fibrin. (HE, 69X)

environment favoured by the bacteria, enabling them to outgrow the commensal abomasal flora and cause gas accumulation. Although *Sarcina spp.* are difficult to culture under routine conditions, their histological features are quite characteristic/pathognomonic.

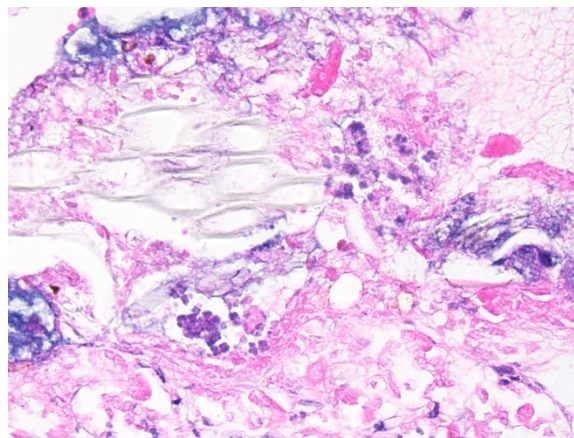
Contributing Institution:

UCD School of Veterinary Medicine,
University College Dublin, Belfield, Dublin
4, Ireland

<http://www.ucd.ie/vetmed/>

JPC Diagnosis: Abomasum: Abomasitis, necrotizing and neutrophilic, transmural, diffuse, severe, with marked submucosal emphysema and edema, and numerous bacterial tetrads and colonies of bacilli.

JPC Comment: *Sarcina ventriculi* is an interesting presumptive pathogen of young ruminants, and occasionally in humans. Since its original association with abomasal bloat in goat kids and lambs in the 1990s, it has been incriminated as a cause of various syndromes of abomasal bloat, tympany, and necrotizing abomasitis. It is a relatively fastidious anaerobe and notoriously difficult to culture, rendering inoculation studies difficult at best, and the additional observation that it may be found in the stomachs of healthy as well as diseased animals has led to great consternation for pathologist trying to add it to the established pathogens *Clostridium septicum* and *Clostridium perfringens type A* in the development of braxy or braxy-like syndromes in young ruminants. The concurrent identification of various clostridial species, notably *C. sordelli*, in affected animals has further clouded the diagnostic picture⁵; hence, the role of this microorganism in abomasitis of calves has, however, not been definitely demonstrated



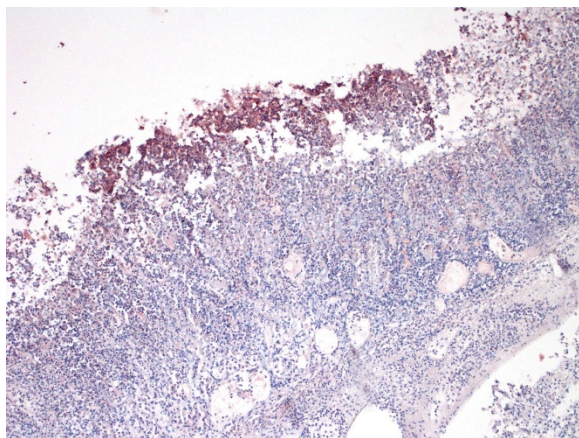
Abomasum, calf: In areas of necrosis, bacterial tetrads consistent with S. ventriculi are present among cellular debris and colonies of bacilli. (HE, 200X).

and it is possible that *Sarcina* is part of a multifactorial etiology.^{3,4}

To complicate the etiology of the lesion in this individual even more, several rods identified in the lumen of this abomasum were immunopositive for *C. perfringens* IHC at the San Bernardino laboratory of the California Animal Health and Food Safety System.

In humans, *S. ventriculi* was first identified as a gastric pathogen by Dr. John Goodsir in 1842, while only 19 cases of gastritis due to *S. ventriculi* infection have been confirmed since, with more than half of these cases occurring in patients with a history of previous gastric surgery resulting in outflow impairment. The term “sarcinous vomiting” referring to a characteristic “obstinate, frothy” vomit has been described in these patients as well as others with chronic gastritis.¹

Sarcina is a genus of three species of gram-positive coccobacteria in the family Clostridiaceae which are known commensals of human skin and GI tract, and synthesize microbial cellulose. It derives its name from “sarcina” from the Latin meaning a pack or



Abomasum, calf: In areas of necrosis, numerous robust bacilli are adherent to the devitalized mucosa. Numerous (but certainly not all) of these bacilli stain immunopositively for a stain for C. perfringens (which does not differentiate for toxinotype). (pan-C. perfringens, 400X)(Photo courtesy of: California Animal Health and Food Safety Laboratory, San Bernardino Branch.)

bundle (similar to that worn by Roman legionaries). The bacteria grow in two planes, resulting in characteristic tetrads, with cell wall compression against adjacent bacilli giving them a cuboidal appearance. (A similar tetrad appearance may also be seen with the much smaller *Micrococcus*.) Interestingly, they are purportedly refractile (not demonstrated in this slide), mimicking plant material.¹

Sarcina sp. are naturally present in the soil and is likely ingested with feedstuffs. *Sarcina* sp. possess an exclusive carbohydrate fermentative metabolism, producing ethanol, acetaldehyde, carbon dioxide and hydrogen. Theories of pathogenesis include the production of large amounts of carbon dioxide resulting in bloat and emphysema, with production of ethanol and acetaldehyde resulting in mucosal necrosis. Abomasal tympany may additionally result in secondary damage to the overstretched mucosa.²

References:

1. Al Rasheed M, Senseng CG. *Sarcina ventriculi*: Review of the Literature. *Arch Pathol Lab Med*; 2016 140: 1441-1445.
2. Edwards GT, Woodger NGA, et al. Sarcina-like bacteria associated with bloat in young lambs and calves. *Vet Rec*; 2008; 163: 391-393, 2008.
3. Panciera RJ, Boileau MJ, Step DL. Tympany, acidosis, and mural emphysema of the stomach in calves: report of cases and experimental induction. *J Vet Diagn Invest*; 2007 19(4):392-5.
4. John F. Prescott, Paula I. Menzies and Russell S. Fraser. Clostridial abomasitis. In: Uzal FA, Songer WG, Prescott J, Popoff M eds. *Clostridial Diseases of animals*. Wiley Blackwell, Ames, IA, 2016.
5. Vatn S, Tranulis MA, Hofshagen M. Sarcina-like bacteria, *Clostridium fallax* and *Clostridium sordellii* in lambs with abomasal bloat, haemorrhage and ulcers. *J Comp Path* 1999; 122: 193-200.

CASE IV: 13101599 (JPC 4048573-00).

Signalment: 13-month-old, intact male, Angus, *Bos taurus*, bovine

History: Two, 13-month-old, Angus bulls from the same farm presented for acute, voluminous, red, watery diarrhea. The diarrhea was noticed by the owner while animals were being gathered into the barn for a routine testing procedure. Both bulls were in excellent body condition (body condition score of 5/9) and one of the two was said to be the owners fastest grower. Both bulls were routinely vaccinated and dewormed. One of



Colon, ox. There was extensive blood and a large clot within the lumen. (Photo courtesy of: Department of Veterinary Pathobiology, Center for Veterinary Health Sciences, Oklahoma State University, www.cvm.okstate.edu)

the bulls died while in transit to Oklahoma State University and a necropsy was performed at the Oklahoma Animal Disease Diagnostic Laboratory. Multiple diagnostic tests were performed on the other bull and the only significant finding on rectal examination was frank blood within the colon and a CBC measuring a PCV of 19%. This bull fully recovered with symptomatic care.

Gross Pathology: On gross examination, the bull was in excellent body condition. Approximately 7cm proximal to the spiral colon, there was an abrupt change in the intestinal content from normal to watery dark red fluid containing blood clots. This continued throughout the remainder of the spiral and descending colon. Segmentally (30 cm), the distal colonic mucosa had a mild cobblestone appearance with innumerable pinpoint to coalescing petechiae and ecchymosis and approximately four 0.5 x 0.2 cm, elliptical, shallow mucosal ulcers. Otherwise, the colonic mucosa outside of this segment was within normal limits.

Laboratory results:

Fluorescent antibody (FA) staining for coronaviral antigens was conspicuously positive in the colonic mucosal sections. Immunostains (IHC) were also strongly positive (13101599 BCoV IHC). Positive and negative controls for both FA and IHC stains behaved as expected.

Bacterial culture of distal colon, spiral colon, and feces yielded large numbers of growth of *E. coli* and *Streptococcus bovis*. A *Clostridium perfringens* Type A was also isolated, but was determined opportunistic with little contributory role to death.

Fecal floatation was negative for parasites, including coccidia.

Microscopic Description: Histologically, colonic sections exhibited multifocal loss of colonic glands with scattered remnant glands present in an uneven distribution. The remnant glandular epithelium was either hyperplastic or was exhibiting features of degeneration and necrosis with occasional sloughing of necrotic epithelial cells into the glandular lumen. The hyperplastic epithelium exhibited re-epithelialization of expansive



Colon, ox. A section of colon is presented for examination – there are no obvious lesions at subgross examination. (HE, 5X)

sections of the surface mucosa. In most regions, goblet cells were absent. The lamina propria had a moderate infiltrate of lymphocytes and plasma cells. Multifocally, hemorrhage was present within the lamina propria.

Contributor's Morphologic Diagnoses:

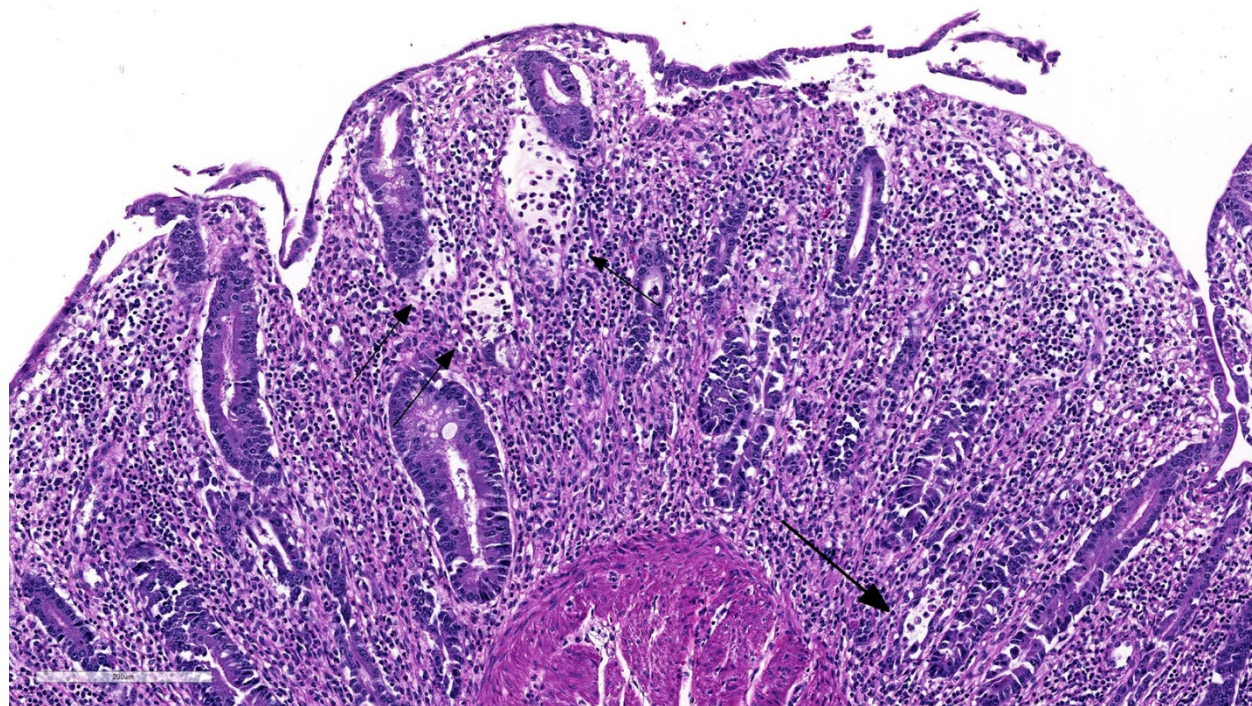
Large intestine, distal colon: Ulcerative colitis, lymphoplasmacytic and hemorrhagic with multifocal colonic epithelial necrosis and colonic gland collapse, severe

Contributor's Comment:

Coronavirus has been implemented in causing three diseases in cattle: neonatal diarrhea in calves (between 1 day and 30 months old, with diarrhea most common at 1 to 2 weeks of age), respiratory disease in a wide age range of calves (between 2 and 19 weeks of age), and winter dysentery, which affects adult dairy and beef cattle.¹

Genus *Coronavirus* is found in the family Coronaviridae within the genus *Torovirus*. They have a single-stranded, positive sense, RNA genome, are pleomorphic and vary in size from 70 to 200 nm in diameter.² They contain four major structural proteins: the nucleocapsid protein N, the integral membrane glycoprotein M, the spike glycoprotein S, and the hemagglutinin-esterase glycoprotein HE. N protein is associated with the genome to form the nucleocapsid. M glycoproteins are found within the virus envelope. S and HE glycoprotein receptors are used in attachment of the virus to the target cell membrane.¹

The exact cause of winter dysentery has not yet been determined; however mounting scientific evidence strongly suggests the etiologic agent to be coronavirus. Winter dysentery has been described in cattle worldwide, and in the United States, is more common in the northern states.^{1,3} Typically, this disease occurs in cattle during the cooler



Colon, ox. There is marked necrosis and loss of glands with numerous crypt abscesses (arrows).

winter months and is associated with multiple environmental risk factors, including low drop in atmospheric temperature, close confinement, poor ventilation, and using manure handling equipment to handle feed.³ Viral transmission is by respiratory or oral routes.

Winter dysentery is a sporadic, acute, contagious, hemorrhagic enterocolitis that predominately affects adult dairy cows, and infrequently adult beef cattle. Clinical signs include dark brown, hemorrhagic, watery, and commonly profuse diarrhea, often with concurrent anorexia, depression, and dehydration. The disease typically has a high morbidity (50-100%) and low mortality (1-2%). Significant economic losses are associated with this disease, especially regarding milk drops in lactating dairy cows.³ The length of acute disease is brief, often with spontaneous recovery within a few days. Persistent diarrhea can lead to dehydration, with secondary polydipsia and reduced ruminal motility. Rarely, hemorrhage from the large colon leads to acute, severe anemia and death⁴, as seen in this case.

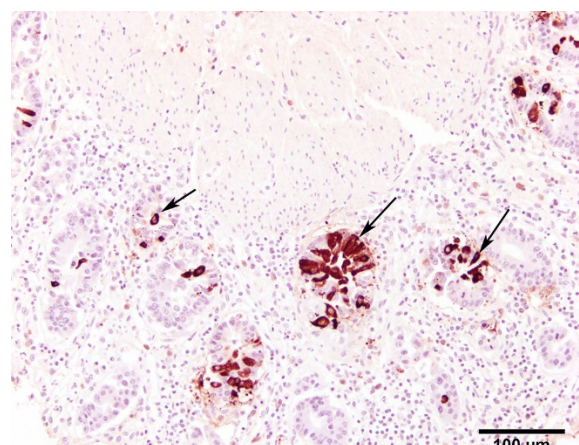
Differential diagnoses for adult cattle with acute, profuse, watery, diarrhea include BVDV, coccidiosis, and salmonellosis. Diagnosis of winter dysentery requires physical examination and exclusion of the above causes of acute and contagious diarrhea in cattle. Diagnostic tests include PCR, virus isolation, or IHC on ear notch to rule out BVDV, fecal floatation to rule out coccidiosis, and fecal bacterial culture to rule out salmonellosis. At necropsy, spiral colon is the ideal sample for virus detection because the virus persists for the longest time here after oral infection.³ Immunohistochemistry was used in this case to detect BCoV antigen in positively staining crypts within the colonic mucosal epithelium.

Coronavirus has a tropism for respiratory and intestinal epithelium.⁴ Coronavirus implicated in winter dysentery causes lesions comparable to neonatal calves with coronaviral diarrhea. In winter dysentery, epithelial cells of colonic crypts are destroyed by virus, leading to degeneration and necrosis of crypt epithelium. Sloughing of damaged and necrotic epithelium can be seen grossly as massive quantities of frank, often clotted, blood within the spiral and distal colon. Viral particles leave the cell by exocytosis at the apical or lateral cell surface, or by lysis of the cell.^{2,3} As in this case, marked mucosal atrophy and re-epithelialization can also be seen. In addition, fine streaks of hemorrhage were noted along the edges of the mucosal folds in the distal colon.^{2,3}

The diarrhea that occurs in winter dysentery is a malabsorptive diarrhea and death in this case was most likely due to severe, acute anemia from profound colonic hemorrhages.

Contributing Institution:

Department of Veterinary Pathobiology
Center for Veterinary Health Sciences



Colon, ox. Immunohistochemistry for bovine coronavirus showing variably intense positive staining for epithelial intracytoplasmic viral antigen (arrows). BCoV, HRP method, counterstained with hematoxylin. Bar = 100µm. (Photo courtesy of: Department of Veterinary Pathobiology, Center for Veterinary Health Sciences, Oklahoma State University, www.cvm.okstate.edu)

Oklahoma State University
www.cvm.okstate.edu

JPC Diagnosis: Colon: Colitis, necroulcerative and hemorrhagic, diffuse, severe with marked loss of glands and multifocal crypt abscessation.

JPC Comment: The contributors provide an excellent review of this case, and subsequent to its submission for the Wednesday Slide Conference, published this is a case report including three additional cases, from which further details are now publicly available. In 2012-2013, four calves from two herds died of acute necro-hemorrhagic colitis. Colonic tissue from all calves were positive by fluorescent antibody and IHC for BoCV. The virus was isolated, and the genomic information from a variable region of the Spike gene revealed BoCV clade 2 in all cases, which had been previously seen as a respiratory infection in postweaned beef calves. (To date, 4 separate clades of BoCV have been isolated.)

Coronaviruses are well known as pathogens of both the digestive system (dog, swine, mice, rats) as well as the respiratory system (humans, cattle, rats). In the early 2000s, SARS-CoVs was discovered in civet cats, raccoon dogs, and bats) that were associated with both respiratory and enteric infections, and were subsequently identified in humans, camelids, and a wide variety of species. BoCV in itself is a pneumoenteric virus infecting both the upper and lower respiratory tract in respiratory infections.

BoCV is ubiquitous worldwide based on antibody seroprevalence data. In a study of 2311 calves with diarrhea in Tulare, CA, 30.5% were positive for BCV; the age range of affected animals was 1-30 days with an average of 10.4 days.¹ BoCV is also commonly incriminated as one of the inciting

agents in the bovine respiratory disease complex in feedlot cattle with some studies identifying the virus through the use of RT-PCR testing in up to 96% of feedlot cattle. A number of wild species may serve as wildlife reservoirs for BoCV, including white-tailed deer, Sambar deer, elk, waterbuck, and giraffes; isolates from each of these species share amino acid sequences with over 99% homology to BoCV. Dogs have also been implicated as a potential reservoir for a coronavirus which may potentially infect ruminants.

In 2-6 month old calves, respiratory infections are associated with coughing, rhinitis, and pneumonia, which may or may not be accompanied by enteric signs; fecal shedding of the virus is commonly documented. It has been proposed by researchers following the time course of pneumoenteric infections that following clinical upper respiratory infection, large amounts of the virus, coated in mucus, may be swallowed, facilitating infection of the intestinal epithelium. A number of intra-nasal modified live vaccines designed primarily to protect against coronavirus-associated “calf scours” have been released on the market in the last five years.

The moderator gave the following differentials – BoCV, BRotaV, Coccidiosis (gross appearance, but too old an animal), and salmonellosis. The moderator commented on the age of the affected (13 months) in this case, which is consistent with “winter dysentery” (which is another misnomer as it may occur in hot months or in tropical climates which do not see a cold season as well.)⁷

References:

1. **Blanchard PC.** [Diagnostics of dairy and beef cattle diarrhea.](#) Vet Clin

- North Am Food Anim Pract. 2012 Nov;28(3):443-64. doi: 10.1016/j.cvfa.2012.07.002.
2. Boileau M, Kapil S: Bovine coronavirus associated syndromes. *Vet Clin North Am Food Anim Pract* **26**:123-146, 2010.
 3. Brown CC, Baker DC, Barker IK: *Bovine Coronavirus. In: Alimentary system, in Jubb, Kennedy, and Palmer's Pathology of Domestic Animals*, M.G. Maxie, Editor. 2007, Elsevier Saunders: Philadelphia, PA. p. 172-173.
 4. Clark, MA: Bovine Coronavirus. *Br Vet J* **149**:51-70,1993.
 5. Fulton RW, Herd HR, Sorensen NJ, Confer AW, Ritchey JW, Ridpath JF, Burge LJ. Enteric disease in postweaned beef calves associated with bovine coronavirus clade 2. *J Vet Diagn Invest* 2015; 27(1):97-101.
 6. Natsuaki S, Goto K, Nakamura K, Yamada M, Ueo H, Komori T, Shirakawa H, Uchinuno Y: Fatal Winter Dysentery with Severe Anemia in An Adult Cow. *J Vet Med Sci* **69**:957-960, 2007.
 7. Uzal FA, Plattner BL, Hostetter JM. In: Maxie MG, ed. *Jubb, Kennedy, and Palmer's Pathology of Domestic Animals*. Vol 2. 6th ed. Philadelphia, PA: Elsevier;2016:216-217.)

Self-Assessment - WSC 2018-2019 Conference 9

1. Which of the following is a predisposing factor for the development of *C. difficile* infection in adult horses?
 - a. NSAID therapy
 - b. Gastric ulceration
 - c. Antibiotic therapy
 - d. Conditioning for racing

2. Which of the following is the most specific indication of *C. difficile* toxicity in the horse?
 - a. History of antibiotic administration
 - b. Bacterial culture of *C. difficile* from intestinal contents
 - c. ELISA test for C difficile A and B toxins in intestinal contents
 - d. Microscopic finding of numerous robust bacilli adherent to villi

3. Which of the following biopsy sites would NOT display lesions associated with Acute Hemorrhagic Diarrhea Syndrome in dogs?
 - a. Stomach
 - b. Duodenum
 - c. Ileum
 - d. Colon

4. Which of the following is NOT true about *Sarcina ventriculi*?
 - a. Inoculation studies have fulfilled Koch's postulates about its effects in the abomasum of young ruminants.
 - b. It is a gram-positive coccobacillus.
 - c. Its characteristic tetrad pattern is not unique.
 - d. It produces ethanol as a byproduct of energy metabolism.

5. Which of the following is true concerning winter dysentery in cattle?
 - a. Large amounts of hemorrhage is found within the duodenum and jejunum.
 - b. In outbreaks, the disease has a low morbidity and high mortality.
 - c. The diarrhea is a malabsorptive in nature.
 - d. Coronaviruses are single-stranded, positive sense DNA viruses.

Please email your completed assessment to Ms. Jessica Gold at Jessica.d.gold2.ctr@mail.mil for grading. Passing score is 80%. This program (RACE program number) is approved by the AAVSB RACE to offer a total of 0.5 CE Credits, with a maximum of 12.5 CE Credits being available to any individual Veterinary Medical Professionals for the 2017-2018 Wednesday Slide Conference. This RACE approval is for the subject matter categories of: SCIENTIFIC using the delivery method of NON-INTERACTIVE DISTANCE. This approval is valid in jurisdictions which recognize AAVSB RACE; however, participants are responsible for ascertaining each board's CE requirements. RACE does not "accredit", "endorse" or "certify" any program or person, nor does RACE approval validate the content of the program.

Please email your completed assessment to Ms. Jessica Gold at Jessica.d.gold2.ctr@mail.mil for grading. Passing score is 80%. This program (RACE program number) is approved by the AAVSB RACE to offer a total of 0.5 CE Credits, with a maximum of 12.5 CE Credits being available to any individual Veterinary Medical Professionals for the 2017-2018 Wednesday Slide Conference. This RACE approval is for the subject matter categories of: SCIENTIFIC using the delivery method of NON-INTERACTIVE DISTANCE. This approval is valid in jurisdictions which recognize AAVSB RACE; however, participants are responsible for ascertaining each board's CE requirements. RACE does not "accredit", "endorse" or "certify" any program or person, nor does RACE approval validate the content of the program.

**Joint Pathology Center
Veterinary Pathology Services**



WEDNESDAY SLIDE CONFERENCE 2018-2019

C o n f e r e n c e 1 0

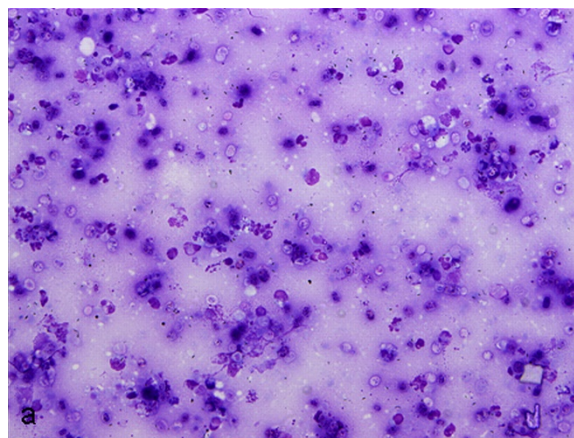
28 November 2018

CASE I: Case 1 (JPC 4006380)

Signalment: 3-year old, boxer, dog (*Canis familiaris*)

History: The patient initially presented to the internal medicine service at the University of Glasgow with a 1 year history of protracted colitis. An endoscopic biopsy of the colon was taken at that time. Five weeks following biopsy, the patient re-presented for acute onset of blindness. The owners reported a slight vision loss beginning roughly 1 month prior that progressed rapidly to complete blindness within the previous 24 hours.

On physical examination, there was subtle ocular hyperemia. The menace responses were absent and the PLRs very weak and sluggish. There was mild corneal edema and significant deep stromal vascularization in both eyes. There was marked aqueous flare



Subretinal aspirate, dog: A good quality, moderately cellular aspirate on a proteinaceous background is submitted. At this magnification, degenerate neutrophils are evident and a single rhomboidal cholesterol crystal is present at bottom left. . (Photo courtesy of: School of Veterinary Medicine, University of Glasgow, Garscube Estate, Bearsden, Glasgow, G611QH, United Kingdom, <http://www.gla.ac.uk/schools/vet/>) (May-Grunwalds, 100X)

and swollen irides. The right eye had a reddish tapetal reflex with a blood tinged and murky posterior segment with no detail

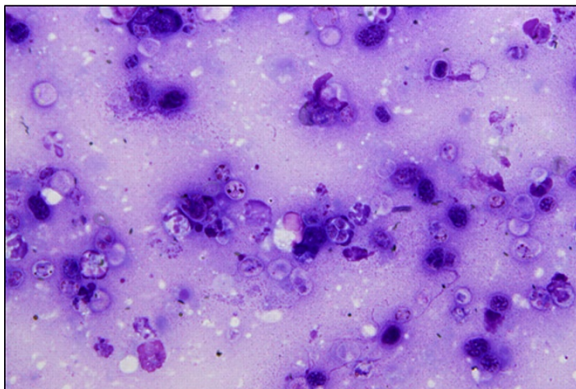
discernible. The left eye had a good tapetal reflex but there was profound posterior segment disturbance with thickened folds of hyperemic and hypervascular detached retina present throughout and the impression of a cellular retinal infiltrate. A subretinal aspirate was collected and submitted to Veterinary Diagnostic Services at the University of Glasgow for cytologic analysis and routine cultures. Cytology smears were routinely stained with May-Grünwalds and Giemsa.

Gross Pathology: None given.

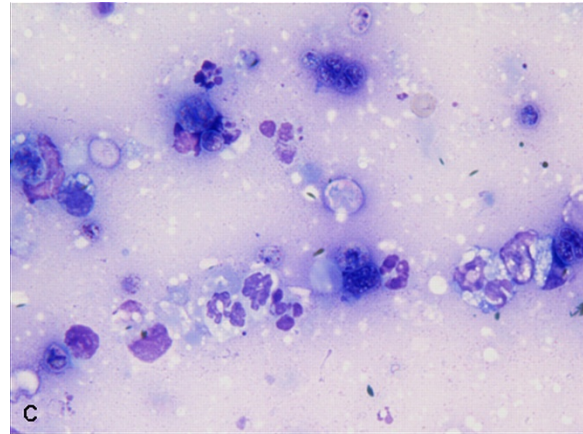
Laboratory results: *Prototheca* sp. was cultured on routine aerobic cultures. The organism was not further speciated.

Cytologic Description:

Examined is a highly cellular smear of good quality. There is a dense, faintly basophilic proteinaceous background containing many free rod-shaped melanin granules. There are large numbers of degenerate neutrophils admixed with low numbers macrophages and occasional erythrocytes. Abundant intracellular and extracellular algal organisms are present, both intact and as



Subretinal aspirate, dog: Individual alga (sporangia) and clusters of deeply basophilic proliferating endospores are present among the inflammatory cells. A single sporangiospore at center exhibits tripartite division characteristic of Prototheca (arrow). (Photo courtesy of: School of Veterinary Medicine, University of Glasgow, Garscube Estate, Bearsden, Glasgow, G611QH, United Kingdom, <http://www.gla.ac.uk/schools/vet/>) (May-Grunwalds, 200X)



Subretinal aspirate, dog: Neutrophils contain vacuolated cytoplasm and degeneration is characterized by hypersegmented, hyperchromatic and mildly shrunken nuclei. At left, a macrophage contains an engulfed alga. Empty cyst forms are scattered throughout the image. Rod-shaped melanin granules are present within the proteinaceous background. (Photo courtesy of: School of Veterinary Medicine, University of Glasgow, Garscube Estate, Bearsden, Glasgow, G611QH, United Kingdom, <http://www.gla.ac.uk/schools/vet/>) (May-Grunwalds, 400X)

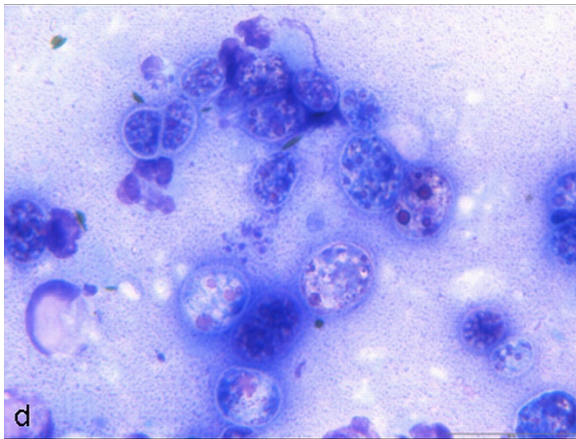
ruptured empty cell casings. Algal organisms are variably sized, 5-10 μm diameter, round to oval, have a thin, clear cell wall and have deeply basophilic cytoplasm (consistent with *Prototheca* spp.). Early endospore replication is characterized by clusters of 3-5 endospores with deeply magenta nuclei and internal septation. Sporangia are 20 μm in diameter, have pale basophilic cytoplasm and contain up to 20, magenta, 5 μm diameter sporangiospores. Occasional organisms are seen intracellularly within the cytoplasm of degenerate cells. Organisms are Periodic Acid-Schiff (PAS) positive.

Contributor's Morphologic Diagnoses: Purulent inflammation with extracellular algal organisms (consistent with *Prototheca* spp.)

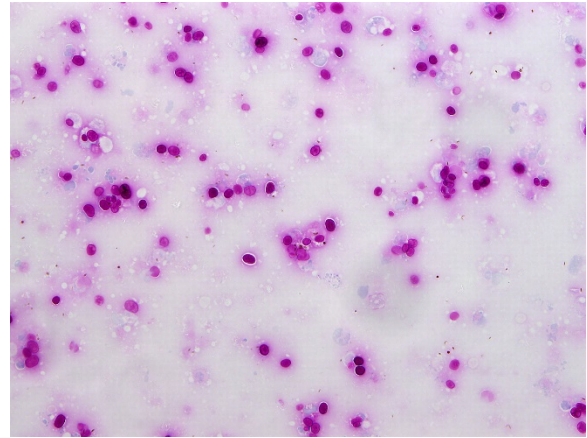
Contributor's Comment: *Prototheca* spp. are unicellular, colorless, saprophytic algae that can be found within the environment, particularly with standing water and sewage

effluent.⁶ Protothecosis is a rare disease of people and animals that can be localized, such as in the intestine or skin, or disseminated, resulting in widespread granulomatous and/or necrotizing lesions throughout the body.¹ In people, infection is primarily within the skin or joints.⁶ Protothecosis is a relatively uncommon cause of mastitis in cattle.¹ In dogs, the intestine and the eye are the most common organs affected.^{2,5,6}

Colitis is the most common presenting complaint in dogs with protothecosis and the clinical course is often protracted.⁶ Dogs can also present with acute blindness.⁹ The dog in this case initially presented with colitis, followed by acute blindness and had a clinical presentation typical of protothecosis. In dogs, protothecal organisms first invade and colonize the colon, with further spread through both lymphatics and blood vessels to other organ systems. In this case, biopsies from the colon in this dog revealed a marked pyogranulomatous and ulcerative colitis. Rare protothecal organisms were detected



Subretinal aspirate, dog: Clusters of deeply basophilic endospores and interspersed with larger individualized sporangia containing 2-3µm eosinophilic sporangiospores. (Photo courtesy of: School of Veterinary Medicine, University of Glasgow, Garscube Estate, Bearsden, Glasgow, G611QH, United Kingdom, <http://www.gla.ac.uk/schools/vet/>) (May-Grunwalds, 600X)



Subretinal aspirate, dog: Algae stain positively with a periodic acid-Schiff preparation. (Photo courtesy of: School of Veterinary Medicine, University of Glasgow, Garscube Estate, Bearsden, Glasgow, G611QH, United Kingdom, <http://www.gla.ac.uk/schools/vet/>) (PAS, 100X)

within the sections, confirming infection in both the intestine and the eye. The dog initially responded to treatment with partial resolution of the colitis, which included amphotericin B and itraconazole; however, vision never returned. The dog was eventually euthanized due to financial constraints. Disseminated infection could not be documented because post-mortem examination was declined.

Protothecal organisms can be highlighted with special stains, such as PAS and Gomori's Methenamine-Silver, in both cytological and histopathology sections.¹ Algal organisms of the *Chlorella* species can be morphologically similar to *Prototheca* spp. *Chlorella* spp. can be differentiated by the often green tinge to the organisms and the presence of PAS positive cytoplasmic granules that are negative following amylase digestion.¹ The two main species of *Prototheca* known to cause infection in dogs are *P. zopfii* and *P. wickerhamii*. Though these species of *Prototheca* differ slightly morphologically (size and number of sporangiospores), PCR is required for definitive differentiation.

Differentials for suppurative or pyogranulomatous inflammation in ocular fluid include both bacterial and fungal infections.⁹ Rarely, protozoa, such as *Toxoplasma gondii*, can result in endophthalmitis.⁹ Any case of bacteremia has the potential to develop bacterial endophthalmitis and the list of potential agents is extremely long.⁹ Fungal endophthalmitis is also typically secondary to a mycotic septicemia. Fungal organisms most commonly associated with eye infections include *Cryptococcus neoformans*, *Blastomyces dermatitidis*, *Histoplasma capsulatum* (particularly in cats), and, less likely, *Coccidioides immitis*.⁹ Both bacterial and fungal infections of the eye are often differentiated based on morphology of the organism, including size and presence of budding, and/or culture. Cultures can be obtained from endoscopy samples, ocular fluid, and/or urine of living patients, depending on the organ systems involved clinically.

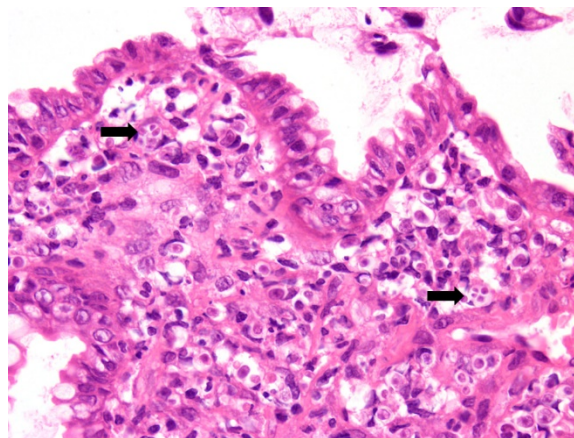
Contributing Institution:

School of Veterinary Medicine
University of Glasgow
Garscube Estate
Bearsden, Glasgow
G61 1QH, United Kingdom
<http://www.gla.ac.uk/schools/vet/>

JPC Diagnosis: Fine needle subretinal aspirate: Pyogranulomatous inflammation with numerous endosporulating alga.

JPC Comment:

Four species of *Prototheca* exist: *P. zopfii*, *P. wickerhamii* (the two pathogenic forms), *P. stagnora*, and a proposed form, *P. salmonis*. They are found in abundance in nature in animal waste, sewage, soil, food, and flowing or standing water and have a worldwide distribution. Additional ribosomal sequencing further divided *P.*



Colon, dog: Numerous algal life stages (arrows) are admixed with neutrophils, macrophages, lymphocytes, and plasma cells (HE, 400X). (Photo courtesy of: School of Veterinary Medicine, University of Glasgow, Garscube Estate, Bearsden, Glasgow, G611QH, United Kingdom, <http://www.gla.ac.uk/schools/vet/>) (PAS, 100X)

zopfii into biotypes, with *P. zopfii* biotype one being present in bovine liquid manure, biotype 2 present in many cases of bovine mastitis, and biotype 3 isolated from swine manure (and recently renamed *P. blaschkeae*.)⁴ A novel *Prototheca* (*P. cutis* sp. nov) has been tentatively identified based on ribosomal RNA sequencing of a single human isolate.⁴

Despite its ubiquity, animal infections are rare, with dogs, cats and cattle predominantly reported in the literature. Cats are most commonly infected cutaneously with large firm nodules on the limbs and feet, and *P. wickerhamii* is most commonly isolated.⁷ In cattle, *P. zopfii* is an uncommon cause of pyogranulomatous lesions of the bovine mastitis and associated lymph nodes.⁴ In goats, *P. wickerhamii* causes ulcerative nodules of the mucocutaneous junction of the nasal vestibule, nostrils, and subcutis of the face and head.⁴

Human infections are uncommon and usually manifest as erythematous vesicobullous rashes which may occasionally be crusting and purulent. Risk factors include immune

suppression from HIV, prolonged steroid use, diabetes mellitus, and underlying malignancy.² The frequency of cases increases with age. Most human cases are the result of infection with *Prototheca wickerhamii*. Disseminated infections, although uncommon and usually seen only in patients with severe immunodeficiency, and demonstrate a mortality rate of 60% (in a limited number of reported cases).²

A related non-photosynthetic of algae, *Helicosporidium*, has recently been identified as a specialized parasite from a variety of dipteran, coleopteran, and lepidopteran insects, primarily infecting larvae.⁸

References:

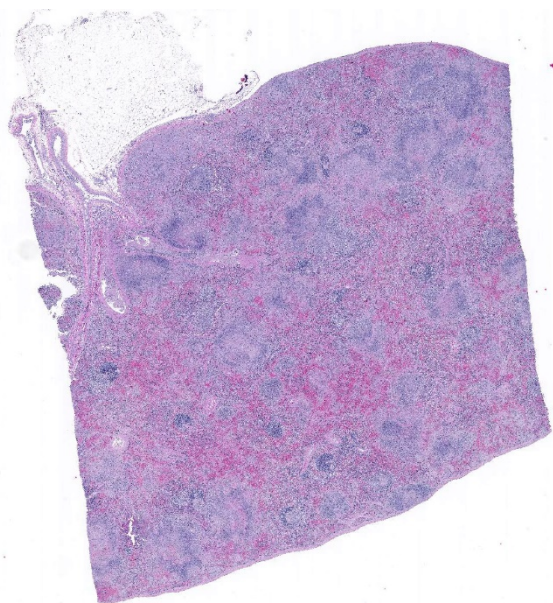
1. Brown CC, Baker DC, Barker IK. Alimentary System. In: Maxie MG ed. *Pathology of Domestic Animals*. 5th ed. Edinburgh, UK: Saunders Elsevier; 2007: 231-232.
2. Hillsheim PB, Bahrami S. Cutaneous protothecosis. *Arch Pathol Lab Med* 2011; 135: 941-946.
3. Hollingsworth SR: Canine protothecosis. *Vet Clin North Am Small Animal Pract*. 2000; 30:1091-1101.
4. Pal M, Abraha A, Rahman MT, Dave P. Protothecosis: an emerging algal disease of humans and animals. *Int J Life Sc Bt Pharm Res* 2014.
5. Pier AC, Cabañes FJ, Chermette R, Ferreira L, Guillot J, Jensen HE, Santurio JM. Prominent animal mycoses from various regions of the world. *Med Mycol*. 2000; 38 Suppl 1:47-58.
6. Stenner VJ, Mackay B, King T, Barrs VR, Irwin P, Abraham L, Swift N, Langer N, Bernays M, Hampson E, Martin P, Krockenberger MB, Bosward K, Latter M, Malik R. Protothecosis in 17 Australian dogs and a review of the canine literature. *Med Mycol*. 2007; May;45(3):249-66.
7. Strunck E, Billups L, Avgeris S. Canine protothecosis. *Compendium* 2004; 96-102
8. Tartar, A. The non-photosynthetic algase *Helicosporidium* spp.: emergence of a novel group of insect pathogens. *Insects* 2013; 4:375-391.
9. 5. Wilcock BP. Eye and Ear. In: Maxie MG ed. *Pathology of Domestic Animals*. 5th ed. Edinburgh, UK: Saunders Elsevier; 2007: 231-232.

CASE II: 9428-12 (JPC 4048660).

Signalment: Two-years-old, neutered, male, domestic shorthair cat, (*Felis domesticus*)

History: Patient presented to emergency clinic in lateral recumbency with oral ulcers, mild dyspnea, hypothermia, and mild nystagmus. Reportedly, the patient had been anorexic. The patient died within one hour of presentation.

Gross Pathology: Spleen was enlarged with a roughened serosal surface. Multiple white pinpoint foci were observed on the serosal surface. The cut surface bulged and had a granular appearance. Liver was swollen with rounded margins and multiple white pinpoint foci were present on the serosal and cut surfaces.



Spleen, cat. At subgross, pallor (necrosis) of the white pulp, extending into the adjacent red pulp is prominent.

Laboratory results: Neutropenia, hyperbilirubinemia, elevated ALT. *Francisella tularensis* was isolated from the spleen and from a lymph node sample.

Microscopic Description:

In sections of spleen, there is disseminated and coalescing necrosis of germinal centers which extends into adjacent red pulp. Foci of necrosis are accompanied by an inflammatory response comprised of neutrophils and macrophages. Scattered thrombosed blood vessels can be seen mainly associated with the capsule and near the hilus. Variably sized and shaped aggregates of homogenous eosinophilic material is present in many germinal centers. Mesothelial cells on the serosa are reactive characterized by cuboidal appearance.

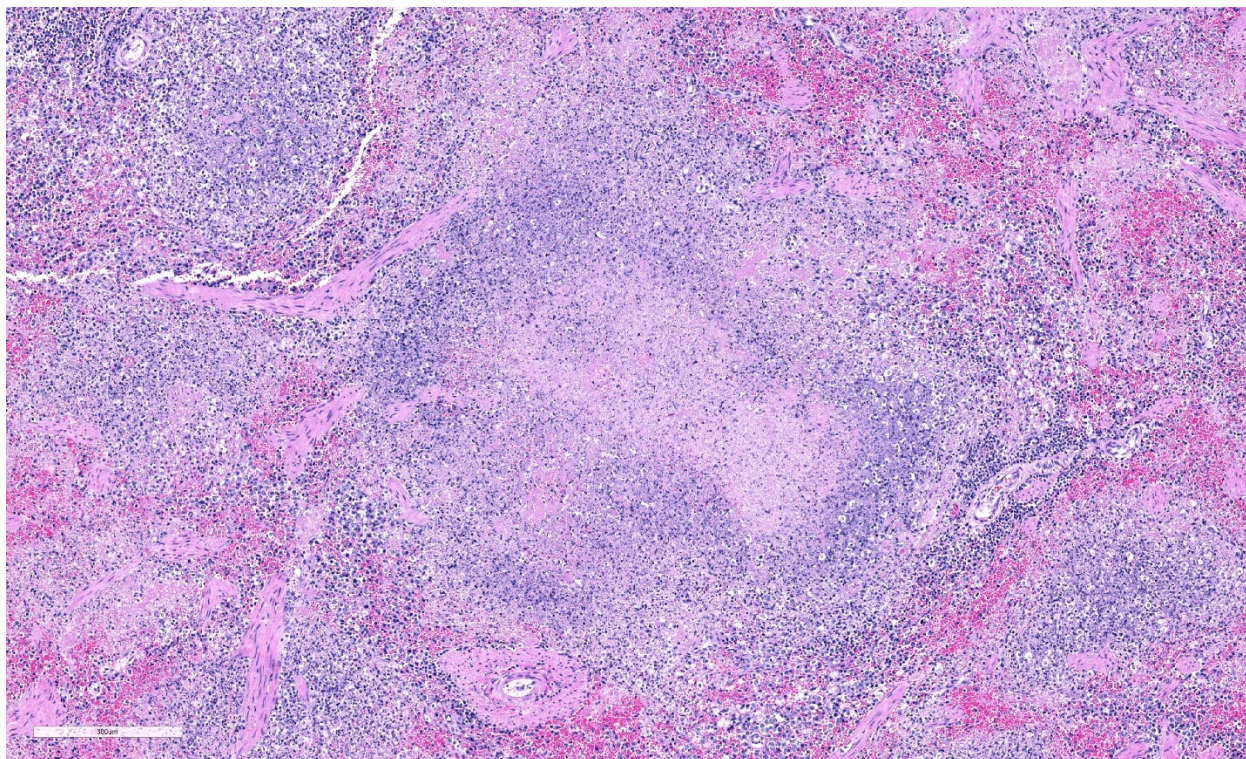
Contributor's Morphologic Diagnoses:

1. Severe, subacute, multifocal, coalescing, necrotic, splenitis.
2. Splenic amyloidosis – germinal centers

Contributor's Comment: *Francisella tularensis* is a gram-negative, encapsulated, facultative intracellular pathogen.⁷ *F. tularensis* is subdivided into two subtypes. Type A is *F. tularensis* subsp. *tularensis* and has an infectious dose in humans of <math><10^3</math> CFU's, whereas type B is *F. tularensis* subsp. *holarctica* which has an infectious dose of <math><10^3</math> CFU and a milder form of tularemia in humans.⁷ The organism is abundant in nature and infects many mammalian and arthropod species.¹¹ *F. tularensis* type A has been isolated from cats on numerous occasions and can be transmitted from cats and other animals (deer, personal experience) to humans.^{5,10,13}

Diagnosis, in some cases may be difficult, but culture appears to be more sensitive than immunohistochemistry.¹ Gross lesions consist of multiple pinpoint white foci on the spleen, liver, and lymph nodes. As a facultative intracellular parasite, it may persist for years as a latent infection.¹¹ The genes for several virulence factors have been identified and shown to share some features with the intracellular parasite, *Listeria monocytogenes*.¹ Tularemia in other mammalian species such as horses and sheep are often associated with heavy infestation by ticks such as *Dermacentor andersoni* and *Amblyoma americanum*.¹² One serologic survey indicated 12 – 24 percent of cats had antibodies to *F. tularensis* due to natural exposure.⁶ Those serologically positive animals were negative for *F. tularensis* DNA, indicating infection may have been cleared naturally. Tularemia should be considered in a differential diagnosis of unexplained febrile illness in cats.

Amyloidosis in the spleen is considered an incidental finding in this case. Amyloidosis of splenic germinal centers is reportedly a rare finding in cats and particularly domestic



Spleen cat. At higher magnification, white pulp is largely effaced by lytic necrosis extending into the surrounding red pulp. There is abundant fibrin in the adjacent necrotic red pulp, replacing (HE, 93X)

shorthair cats.¹¹ Generalized amyloidosis is more common in Abyssinian cats and has been reported in Siamese cats and wild black-footed cats as well.⁹

Contributing Institution:

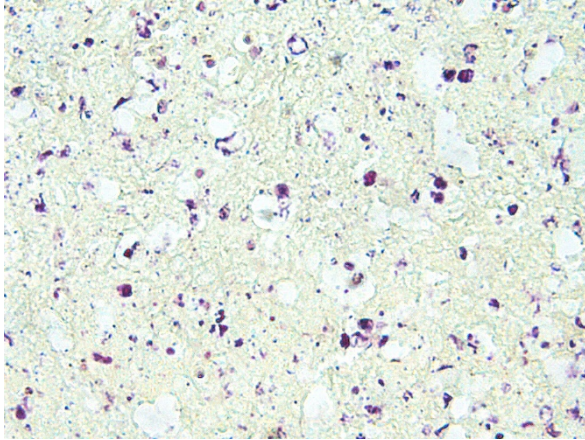
Veterinary Diagnostic Center, University of Nebraska-Lincoln, Lincoln, NE.
vbms.unl.edu/nvdl

JPC Diagnosis: Spleen, lymphoid tissue: Necrosis, diffuse, with multifocal red pulp necrosis, hemorrhage, fibrin, and edema.

JPC Comment: *Francisella tularensis* is a global pathogen that has been classically divided into three distinct subspecies: *F. tularensis* subsp. *tularensis*, *F. tularensis* subsp. *holarctica*, and *F. tularensis* subsp. *mediasiatica*. A fourth, *F. tularensis* subsp. *novocida*, which is non-pathogenic for humans, was recently separated into a separate species, *F. novocida*, and is

extensively used in *Francisella* research.⁷ Additional research has divided *F. tularensis* into genetically distinct clades, Type A and Type B, with the highly pathogenic type A (*F. tularensis* subsp. *tularensis*) found in the USA and the less virulent type B (*F. tularensis* subsp. *holarctica*) found throughout the Northern Hemisphere.⁷ The first report of *F. tularensis* subsp. *holarctica* in Australia was recently published.³ Both Type A and Type B infections of *F. tularensis* subsp. *tularensis* have been identified in cats.¹²

The first case of *Francisella tularensis*-mediated disease was recognized as a plague-like illness in rodents during an outbreak in Tulare County, California in 1911, and the first human cases were described three years later in two patients in Ohio, who had recently had contact with wild rabbits.⁴ In 1919, Dr. Edward Francis established that the disease was caused by *Bacterium tularensis*



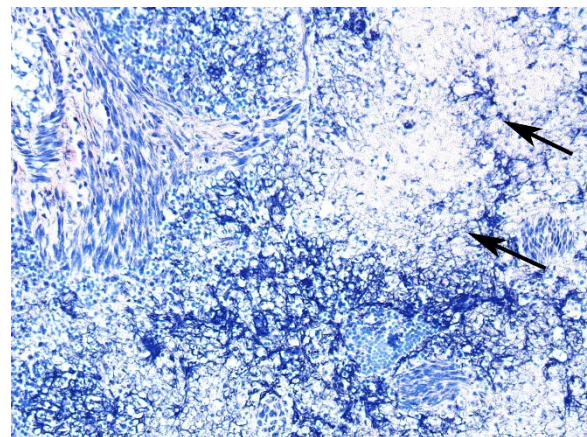
Spleen, cat. Areas of necrosis contain large numbers of small 1-2µm gram-negative coccobacilli. (Brown-Hopps, 600X).

(named for the county in which the disease was originally identified) and appended the name “tularemia” to the disease.⁴ The number of cases of tularemia in the US peaked in 1939-1940 with 2,291 documented cases, but has decreased to a current average of 125 cases over the last two decades.⁸ Tularemia cases in both humans and animals have been identified in 49 US states; with Hawaii being the only exception.⁸

While the transmission of tularemia has classically been associated with contact with rodents and rabbits, giving rise to the colloquialisms “rabbit fever”, “market men’s disease”, and “meat-cutter’s disease”,⁷ a number of important methods of transmission also exist: transmission by insect vectors including ticks, biting flies, and mosquitoes, and water-borne outbreaks.⁷ Aerosol-born outbreaks have accounted for some of the largest number of cases, from a 1967 outbreak and a farming area of Sweden involving more than 600 individuals⁷, as well as a more recent outbreak in Martha’s Vineyard, which involved 15 individuals and 1 fatality, with a common factor of lawn mowing or brush cutting a week prior to illness⁴.

There are three basic clinical syndromes associated with tularemia: pneumonic (exemplified by aerosol born disease as previously described), typhoidal, and ulceroglandular. Typhoidal tularemia is the result of entry of the bacteria into breaks in the skin or mucous membranes, with vascular dissemination, sepsis, and necrosis in any involved organs (as exemplified in this case). Approximately three quarters of tularemia cases in the US are localized, manifested by a tender regional lymph node a local papule which involves to a chancreform lesion; such cases are referred to as ulceroglandular tularemia.¹² A single case of localized cutaneous infection resembling ulceroglandular disease has been reported in a cat with localized swellings of the right submandibular salivary gland and mandibular lymph node but lack signs of systemic illness.¹⁰

Classic association with rodents and rabbits is woefully inadequate to describe the potential for transmission from infected mammalian species. Bites, especially from asymptomatic individuals other than cats may transmit the disease, and human cases have been documented from the bites of



Spleen cat. Areas of necrosis (arrows) are surrounded by abundant polymerized fibrin and hemorrhage. (PTAH, 100X)

dogs, coyotes, raccoon, skunks, opossums, squirrel monkeys, tamarins, and swine.²

F. tularensis has an interesting method of surviving macrophage ingestion. Following internalization into phagocytic cells, the bacilli reside in membrane-bound endosomal compartment known as the *F. tularensis*-containing vacuole (FCV) which acquires both early-and late-lysosomal markers but not acid hydrolase cathepsin-D, preventing its fusion with lysosomes, and escaping the bactericidal respiratory burst.⁷

Within the laboratory, *F. tularensis* requires the use of a minimum standard biosafety level II has recommended by the American Society for microbiology. Biosafety level III facility some protocols are recommended for handling. All suspect cultures are isolated, experimental animal studies, and animal autopsies.⁸

References:

1. Brotcke A, Weiss DS, Kim CC, Chain P, Malfatti S, Garcia E, Monack DM: Identification of MglA-regulated genes reveals novel virulence factors in *Francisella tularensis*. *Infect Immun* **74**: 6642-6655, 2006
2. Chomel BB, Morton JA, Kastern RQ, Chang CC. First pediatric case of tularemia after a coyote bite. *Case Rep Inf Dis* 2016; <http://dx.doi.org/10.1144/2016/8095> 138.
3. Eden JS, RoseK, Ng J, Shi M, Wang Q, Sintchenko, V HolmesEC. *Francisella tularensis* ssp. holarctica in ringtail possums, Australia. *Emerg Infect Dis* 2017; 23(7):1198-1201.
4. Feldman KA, enscore RE, Lathrop SL, Matyas BT, McGill M, Schriefer ME, Stiles-Enos D, Dennis DT, Petersen LR, Hayes EB. An outbreak of primary pneumonia tularemia on Martha's Vineyard. *N Engl J Med* 2001, 345(22): 1601-1606.
5. Inzana TJ, Glindemann GE, Snider G, Gardner S, Crofton L, Byrne B, Harper J: Characterization of a wild-type strain of *Francisella tularensis* isolated from a cat. *J Vet Diagn Invest* **16**: 374-381, 2004
6. Magnarelli L, Levy S, Koski R: Detection of antibodies to *Francisella tularensis* in cats. *Res Vet Sci* **82**: 22-26, 2007
7. Pechous RD, McCarthy TR, Zahrt TC: Working toward the future: insights into *Francisella tularensis* pathogenesis and vaccine development. *Microbiol Mol Biol Rev* **73**: 684-711, 2009
8. Stidham RA, Freeman DB, Tostenson SD Epidemiological review of *Francisella tularensis*: A case study in the complications dual diagnoses. *PLoS Curr* doi: 10.1371/currents.outbreaks.8eb0b55f377abc2d250314bbb8fc9d6d.
9. Terio KA, O'Brien T, Lamberski N, Famula TR, Munson L: Amyloidosis in black-footed cats (*Felis nigripes*). *Vet Pathol* **45**: 393-400, 2008
10. Valentine BA, DeBey BM, Sonn RJ, Stauffer LR, Pielstick LG: Localized cutaneous infection with *Francisella tularensis* resembling ulceroglandular tularemia in a cat. *J Vet Diagn Invest* **16**: 83-85, 2004
11. Valli VEO: Jubb, Kennedy, and Palmer's Pathology of Domestic Animals, 5th ed., vol. 3, Saunders Selsevier, Philadelphia, PA, 2007
12. van der Linde-Sipman JS, Niewold TA, Tooten PC, de Neijs-Backer M, Gruys E: Generalized AA-

amyloidosis in Siamese and Oriental cats. *Vet Immunol Immunopathol* **56**: 1-10, 1997

13. Weinberg AN, Branda JA: Case records of the Massachusetts General Hospital. Case 31-2010. A 29-year-old woman with fever after a cat bite. *N Engl J Med* **363**: 1560-1568, 2010

CASE III: 11136 (JPC 4066393).

Signalment: 21-year-old male Indonesian origin cynomolgus macaque (*Macaca fascicularis*).

History: Following sedation for an experimental procedure two weeks prior to death, this female macaque lost 6% of its body weight. It had a 4 year history of eating an atherogenic diet and was in obese body condition. The day prior to death, the animal presented with lethargy, dehydration and hypothermia (94.4°F). Following an unsuccessful attempt at supportive care, the animal died and was submitted for necropsy.



Kidney, cynomolgus macaque. The renal cortices are diffusely pale tan. (Photo courtesy of: Wake Forest School of Medicine, Department of Pathology/Comparative Medicine, Medical Center Boulevard, Winston Salem, NC 27157-1040 <http://www.wakehealth.edu/School/Comparative-Medicine/Training-Programs/ACVP.htm>)

Gross Pathology: The animal was obese with abundant visceral and subcutaneous adipose tissue. The kidneys were diffusely tan. The liver was diffusely pale yellow with a slight reticular pattern, had slightly rounded edges, and cut sections floated in formalin. The luminal surface of the aortic intima was irregularly thickened by pale yellow to tan plaques (atherosclerosis). The stomach and small intestine contained only clear mucinous fluid, flecked with ingesta.

Laboratory results: Blood chemistry values acquired the day prior to death revealed marked azotemia (BUN 107mg/dL; creatinine 8.4mg/dL) with hyperphosphatemia (13.60mg/dL), mildly elevated ALP (239U/L), and moderate hypoproteinemia (total protein 5g/dL; albumen 2.1g/dL).

Microscopic Description:

The renal cortical proximal tubular epithelial cells were markedly dilated by variably-sized clear cytoplasmic vacuoles (lipid), up to 40 microns in diameter. Tubular lumina were often reduced by these plump cells and occasionally contained neutrophils or sloughed epithelial cells. The epithelial cells in some tubules were attenuated and widely spaced indicative of epithelial loss. Scattered tubules contained round lamellar basophilic material (mineral). A few glomeruli had thickened basement membranes and, rarely, glomeruli were atrophic.

Contributor's Morphologic Diagnoses:

Kidney: Vacuolar degeneration, diffuse, marked with epithelial loss and intraluminal mineral, renal tubular epithelium (renal lipidosis)

Kidney: Glomerulonephritis, diffuse, chronic, minimal



Liver, cynomolgus macaque. The liver is diffusely pale yellow with rounded edges. (Photo courtesy of: Wake Forest School of Medicine, Department of Pathology/Comparative Medicine, Medical Center Boulevard, Winston Salem, NC 27157-1040 <http://www.wakehealth.edu/School/Comparative-Medicine/Training-Programs/ACVP.htm>)

Contributor's Comment: Additional relevant microscopic findings included vacuolar hepatocellular degeneration (hepatic lipidosis) and necrosis of adipose tissue. Death was attributed to acute renal failure due to the massive accumulation of lipid and the associated metabolic derangements, all consistent with fatal fasting syndrome of obese macaques. The necropsy findings, along with the marked azotemia, hyperphosphatemia, advanced age, recent stressors and obesity with rapid weight loss are all consistent with this syndrome.⁸

Fatal fasting syndrome has been reported in African green monkeys (*Cercopithecus aethiops*), cynomolgus macaques (*Macaca fascicularis*) and rhesus macaques (*Macaca mulatta*), and shares similarities with conditions in other species, including hyperlipidemia in Shetland ponies, hepatic lipidosis in cats and guinea pigs, and pregnancy toxemia in ruminants.² Obese, female, aged macaques are particularly susceptible to this syndrome, which is often precipitated by a period of anorexia, weight loss, or stress.^{2,3,7,8} The pathogenesis has not yet been fully elucidated, but a period of

inadequate caloric intake in obese animals is a common theme among the disease profiles of the all the aforementioned species. Regardless of the initiating factor, an over-compensation of the liver results in fatty acid mobilization beyond the body's ability to metabolize, resulting in a metabolic imbalance with an inability to process the excessive triglycerides and lipoproteins.^{4,7}

The most common associated clinical pathology finding is renal azotemia.⁸ Hypertriglyceridemia is a common associated finding among the similar metabolic derangements across species. Triglycerides are not considered inherently toxic, but the products produced with triglyceride breakdown or failure of esterification (non-esterified fatty acids, ceramides, diacylglycerols) have detrimental effects on cells.¹⁰ Lipotoxicity has been described in a several animal models throughout non-adipose tissues including cardiac and skeletal myocytes, hepatocytes, pancreatic B-cells and renal tubules.⁹ Lipotoxic mechanisms leading to cellular dysfunction and injury may involve reactive oxygen species, intra-cellular pathway disruption, organellar damage, and lipid-induced apoptosis.¹ Renal tubular degeneration and detachment can lead to luminal tubule obstruction, increasing the interstitial pressure and ultimately reducing the glomerular filtration rate with subsequent acute renal failure.⁴

The reason for the female predisposition to this syndrome is unclear, but hyperlipidemia in Shetland ponies is similarly gender predisposed.⁵ In cats with hepatic lipidosis, males and females are equally represented.⁶

Contributing Institution:

Wake Forest School of Medicine
Department of Pathology/Comparative Medicine of

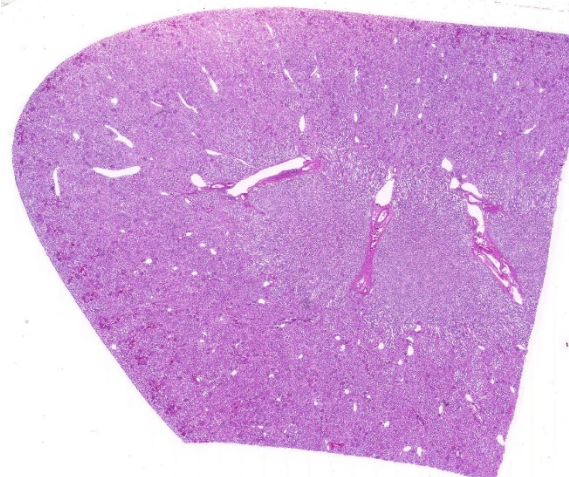
Medical Center Boulevard
 Winston Salem, NC 27157-1040
<http://www.wakehealth.edu/School/Comparative-Medicine/Training-Programs/ACVP.htm>

JPC Diagnosis: Kidney, proximal convoluted tubular epithelium: Lipidosis, diffuse, severe with mild tubular proteinosis.

JPC Comment: The contributor has done an excellent job describing this classic metabolic condition in the macaque.

One of the obvious morphologic abnormalities in this section is the disproportionate amount of lipid within the cells of the proximal convoluted tubules. As the proximal convoluted tubules are the site of albumin resorption in the kidney, and free fatty acids (FSA) are normally complexed to albumin¹, this may explain the predominance of lipid within cells of the proximal convoluted tubules. Whether significant lipid synthesis from non-lipid substrates occurs in renal tubular epithelium and pathways of lipid export from the kidney are subjects of current conjecture and research.¹

The link between lipidosis and kidney disease was first suggested more than 150 years ago by Rudolph Virchow, and the association between kidney disease and renal lipid accumulation has been demonstrated in the number of rodent models including mice on high fat diets, mice and rats with leptin deficiency, Type 1 diabetes and various transgenic models.¹ Lipotoxicity is usually accompanied by accumulation of neutral lipids in renal tubular epithelium and other cells as triglycerides. Triglycerides in themselves are non-toxic, with toxicity deriving mainly from long-chain non-esterified fatty acids (NEFA) and other breakdown products such as ceramides and

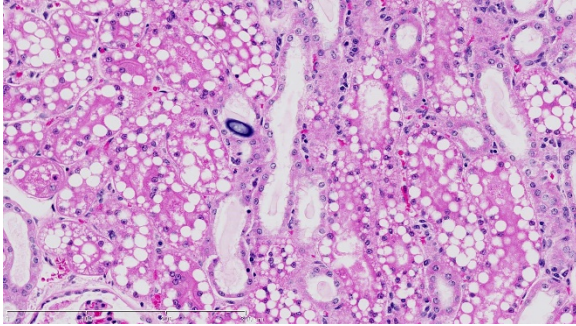


Kidney, cynomolgus macaque. A section of renal cortex and medulla is submitted for examination. There is mild diffuse pallor of the renal cortex. (HE, 6X)

diglycerols, and the association with NEFA-induced mitochondrial de-energization or persistent ATP depletion has been well-documented in renal reperfusion injury as well other forms of lipid-induced nephrotoxicity.²

Fatal fasting syndrome in macaques present in numbers of similarities to syndromes associated with stress, anorexia and lipidosis of multiple organs in both the cat and the horse. Hepatic lipidosis is a well-known metabolic condition in cats resulting from severe prolonged caloric and protein restriction. Carbohydrate restriction is the primary driver of mobilization of peripheral fat stores and flooding of the liver with NEFA. In the normal state, NEFA enter the mitochondria and are converted to energy. In excess, NEFA are either stored within the hepatocyte, or esterified with lipoproteins and re-secreted as VLDLs. In cats with hepatic lipidosis, concurrent protein starvation precludes production of lipoproteins and retention of massive amounts of triglycerides as lipid vacuoles within the hepatocyte.

In horses, hyperlipidemia is associated with



Kidney, cynomolgus macaque. The renal cortical proximal tubular epithelium is diffusely vacuolated with occasional epithelial cell attenuation and nuclear pyknosis. Intraluminal mineral is present in some tubules. (Photo courtesy of: Wake Forest School of Medicine, Department of Pathology/Comparative Medicine, Medical Center Boulevard, Winston Salem, NC 27157-1040

<http://www.wakehealth.edu/School/Comparative-Medicine/Training-Programs/ACVP.htm>

additional risk factors including breed (ponies, donkeys, and miniature breeds), gender (with mares accounting for between 75 and 100% of cases) and stress (more commonly associated with late pregnancy and early lactation). In ponies and donkeys, hyperlipidemias usually a primary disease process with stress and obesity appearing to be particularly important predisposing factors. Gross and histologic findings mirror similar syndromes in macaques and cats with gross lipidosis of multiple organs - hepatic lipidosis in affected animals may be severe enough to result in signs of colic from overstretching of the hepatic capsule.⁵

On a peripherally related subject, a recent article identified interstitial lipid accumulation as a long-term histologic findings in cats with chronic renal disease.⁸ Data from the study suggests that the interstitial lipid accumulation may be the result of tubular epithelial degeneration and lysis as well as tubular basement membrane fragmentation in a species in which tubular lipidosis is often seen in the normal state. In the animals of the study, interstitial lipid was

not equally distributed between the right and left kidneys, but all was found in the cortical regions. In light of recent research on mechanisms of renal lipoma toxicity, this is an interesting finding which may contribute to the overall progression of this common disease in cats.⁸

Within the seminar, there was discussion about the use of the term “vacuolar degeneration, lipid-type” versus “lipidosis” in the morphologic diagnosis for this particular lesion. There was general agreement that the former is better reserved for situations in which morphologic evidence of cellular degeneration is noted beyond simple lipid vacuolation or swelling. In this case, without either clinicopathologic evidence of tubular damage, or morphologic evidence of tubular damage, it was thought that lipidosis (or vacuolar change) would be most a more appropriate choice..

References:

1. Bobulescu, Ion Alexandru. "Renal lipid metabolism and lipotoxicity." *Curr Opin in Nephr Hypertens* 19.4 (2010): 393.
2. Bronson RT, O'Connell M, Klepper-Kilgore N, Chalifoux LV, Sehgal P: Fatal fasting syndrome of obese macaques. *Lab Anim Sci* 32(2):187-191, 1982
3. Christie KL, Valverde CR: The use of a percutaneous endoscopic gastrostomy (PEG) tube to reverse fatal fasting syndrome in a cynomolgus macaque (*Macaca fascicularis*). *Contemp Topics* 38(4):12-15, 1999

4. Cotran RS, Kumar V, Collins T: Cellular pathology II: adaptations, intracellular accumulations, and cell aging. In: Robbins' Pathologic Basis of Disease, 6th ed., pp. 38-40, 993-995. WB Saunders, Co., Philadelphia, PA, 1999
5. Hughes, K. J., D. R. Hodgson, and A. J. Dart. "Equine hyperlipaemia: a review." *Aust Vet J* 82.3 (2004): 136-142.
6. Kelly WR: The liver and biliary system. In: Pathology of Domestic Animals, ed. Jubb KVF, Kennedy PC, Palmer N, 4th ed., vol. 2, pp. 335-336. Academic Press, Inc., New York, NY, 1993
7. Laber-Laird KE, Jokinen MP, Lehner NDM: Fatal fasting liver-kidney syndrome in obese monkeys. *Lab Anim Sci* 37(2):205-209, 1987
8. Lewis AD, Colgin L: Pathology of Noninfectious Diseases of the Laboratory Primate. In: The Laboratory Primate: Wolfe-Coote, Sonia. pp. 65-66. Academic Press, 2005.
9. Martino-Costa AL, Malhao F, Lopes C, Dias-Pereira P. Renal interstitial lipid accumulation in cats with chronic kidney disease. *J Comp Path* 2017; 157:75-79.
10. Weinberg JM. Lipotoxicity. *Kidney Int* 70: 1560–1566, 2006.

CASE IV: 15-H700012 (JPC 4084546).

Signalment: 21 week old, intact male, domestic rabbit (*Oryctolagus cuniculus*)

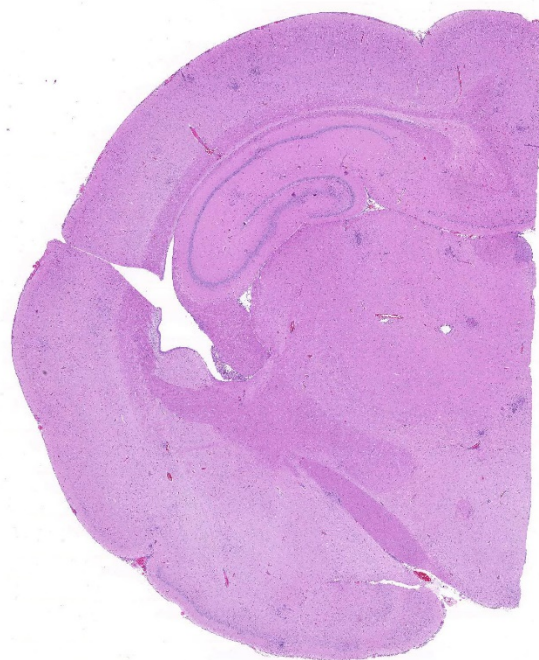
History: 1 day history of sneezing with acute onset on respiratory distress.

Gross Pathology: The animal was in poor nutritional condition characterized by a near-complete lack of subcutaneous, perirenal and mesenteric adipose tissue. The right nasal cavity was nearly completely filled with a tan, viscous material.

Laboratory results: None given

Microscopic Description:

BRAIN (Some slides contain cerebrum while others contain hippocampus and cerebellum,



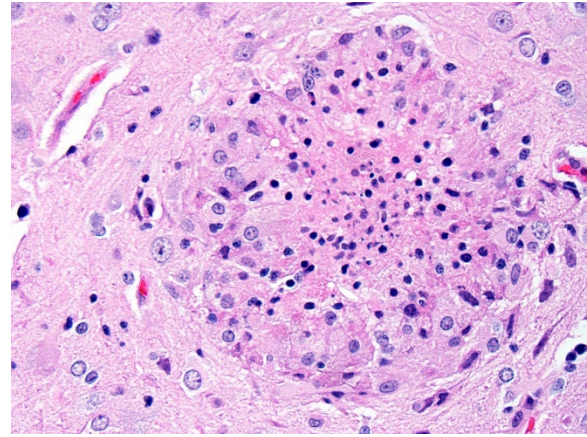
Cerebrum, rabbit. Inflammatory foci are visible within both grey and white matter at subgross magnification. (HE, 5X)

but the lesions are identical): Infiltrating both grey and white matter, there are multiple aggregates of epithelioid macrophages with lesser numbers of lymphocytes and plasma cells and rare heterophils. The inflammatory infiltrates frequently surround accumulations of eosinophilic cellular and karyorrhectic nuclear debris (necrosis). Occasional necrotic foci contain irregular, fragmented, basophilic material (mineral). Within inflammatory foci, there are rare, 20-30 μm pseudocysts that contain numerous 1x3 μm refractile spores with a small, basophilic nucleus. The neuropil surrounding the necrotic and inflammatory foci contains moderate numbers of reactive glial cells (gliosis). Vascular endothelial cells are frequently plump (reactive), and Virchow-Robin spaces often are expanded with macrophages, lymphocytes and plasma cells. The leptomeninges are expanded with moderate numbers of lymphocytes and plasma cells.

Contributor's Morphologic Diagnoses:

Brain (cerebrum, hippocampus, and cerebellum): Meningoencephalitis, granulomatous and necrotizing, multifocal with microsporidial spores (*Encephalitozoon cuniculi*).

Contributor's Comment: Wright and Craighead initially identified *Encephalitozoon cuniculi* in 1922 as the agent responsible for "infectious motor paralysis" in rabbits exhibiting lethargy, tremors and paresis.¹⁴ *E. cuniculi* are members of the phylum Microspora, which contain a diverse collection of obligate intracellular organisms which can exist as environmentally resistant spores outside of the host.¹² There has been considerable debate and reclassification with regards to the evolutionary origin of Microspora. These intracellular eukaryotes lack mitochondria and peroxisomes, and were originally

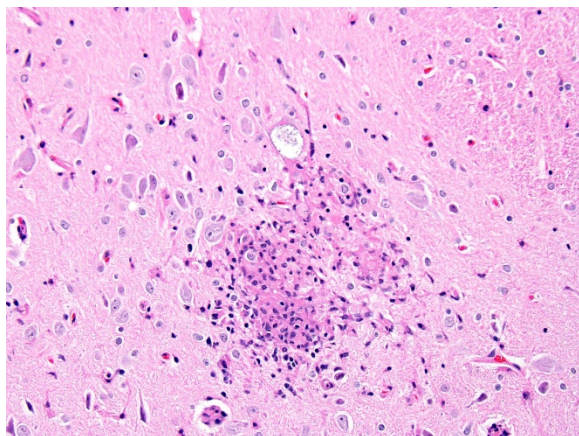


Cerebrum, rabbit. Inflammatory foci are composed of a combination of activated glia and epithelioid macrophages which are centered on cellular debris (and likely Encephalitozoon spores.) (HE, 400X)

thought to belong to a deeply branching protist lineage diverging prior to the emergence of the mitochondria as an endosymbiont (11). Modern phylogenetic analysis reveals that Microsporida are actually more closely related to the fungal domain.⁵ Phenotypically, the defining criterion for inclusion is the phylum is an organelle found coiled within the spore termed a "polar filament" or a "polar tube".¹

Besides *E. cuniculi*, two other species with the genus *Encephalitozoon* are also known to infect mammals: *Encephalitozoon hellum* and *Encephalitozoon intestinalis*.⁸ *E. cuniculi* is capable of infecting a wide range of mammalian hosts, including rabbits, rodents, horses, carnivores and humans.⁷ In humans, *E. cuniculi* and other microsporidia have been identified as opportunistic pathogens in immunocompromised patients, though not causing the same epidemiological human morbidity and mortality as other parasites such as *Plasmodia*, *Trypanosoma*, *Leishmania* and *Toxoplasma gondii*. At one time, *E. cuniculi* was thought to be the agent responsible for rabies and polio.¹²

The main host for *E. cuniculi* is the rabbit, and infections are mostly subclinical, and the



Cerebrum, rabbit. Cells with cytoplasmic parasitophorous vacuoles containing spores are present in close apposition to "granulomas". (HE, 400X)

course is typically chronic, taking weeks to months to develop a parasite burden sufficient to cause clinical signs.⁷ The seroprevalence in pet populations is high (between 37% and 68%) due to proximity.⁴ Historically, in laboratory rabbit colonies, *E. cuniculi* was a significant problem that resulted in interference with experiments and affected the overall health of the colonies.¹⁰ Generally, infected rabbits will exhibit the non-specific signs of weight loss and failure to thrive, but can also manifest neurological signs such as ataxia, opisthosomas, torticollis, hyperesthesia, or paralysis.⁶ Phacoclastic uveitis is also possible, and is characterized by a mixed inflammatory response (granulocytes, macrophages and multinucleate giant cells) causing lens capsule rupture, with organisms found only within the lens.³

In naturally infected rabbits, transmission occurs through organisms shed in the urine that are orally consumed, although transplacental infections are documented.^{9,12} In experimental conditions, rabbits are also capable of being infected via a respiratory route in addition to oral. Following exposure, spores infect mononuclear cells and thereby enter they systemic circulation via leukocyte

trafficking.⁹ The first organs affected are the lung, liver and kidney, but later (approximately 3 months post-exposure), the lesions in the lung and liver subside and there are significant changes to the brain as well as the kidneys.⁷ Gross lesions are not typically seen, although rarely there can be focal, irregular and depressed regions in the renal cortex.²

Reliable histological lesions in the brain consist of focal to multifocal, non-suppurative meningoencephalitis with gliosis and perivascular accumulations of lymphocytes and plasma cells. In some instances, there can be foci of necrosis surrounded by epithelioid macrophages with lesser numbers of lymphocytes and plasma cells.¹³ Lesions in the kidneys include focal to segmental interstitial nephritis with tubular epithelial degeneration, necrosis and sloughing. There is little to no glomerular involvement.^{9,13} Spores can be identified using Gram stain an ovoid, 1.5 x 2.5-5 um diameter structures, which also stain purple with carbol fuchsin.⁹

Contributing Institution:

University of Illinois College of Veterinary Medicine, Department of Pathobiology, 2522 Veterinary Medicine Basic Science Building, 2001 S. Lincoln Ave., Urbana, IL 61802

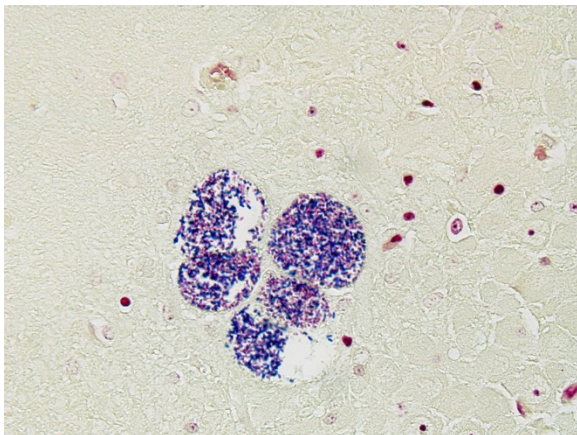
<http://vetmed.illinois.edu/research/departments/pathobiology/>

JPC Diagnosis: Cerebrum: Encephalitis, granulomatous and necrotizing, multifocal, moderate with lymphoplasmacytic meningitis and numerous microsporidian spores.

JPC Comment: Microsporidia are unique organisms which apparently have evolved from fungi, being most closely related to the zygomycetes.⁷ Other similarities between

microsporidia and fungi include the presence of chitin and trehalose, similarities between the cell cycles, and the organization of certain genes. Other unique factors include their lack of mitochondria (although enzymes with mitochondrial functions have been conserved), and ribosomal RNA which more closely resembles that of prokaryotes than eukaryotes. Particularly impressive is their extremely small genome, comprising 2.9 Mbp, which has been accomplished due to the compression of genetic information within chromosomes, resulting from a virtual absence of introns, a low number of repetitive sequences and many single-copy genes, an overall shortening of genes as well as of non-coding sequences, as well as the absence of genetic information regarding certain metabolic pathways that are unnecessary for the organism's parasitic lifestyle.^{7,8}

The unicellular spores of these parasites are unique within the animal kingdom with incorporation of the nucleus, the posterior vacuole, and ribosomes into "sporoplasm", which is injected into new host cells by virtue of a polar tube, a specialized invasion apparatus which works much like a



Cerebrum, rabbit. Spores of Encephalitozoon within intact pseudocysts stain gram-variable (predominantly gram-positive) on tissue gram stains. (Brown-Hopps, 400X)

hypodermic needle. In addition, the polar tube may stain positively with a number of histochemical stains, including modified trichrome, Luna, PAS, and Giemsa facilitating identification of microsporidia in tissue section.

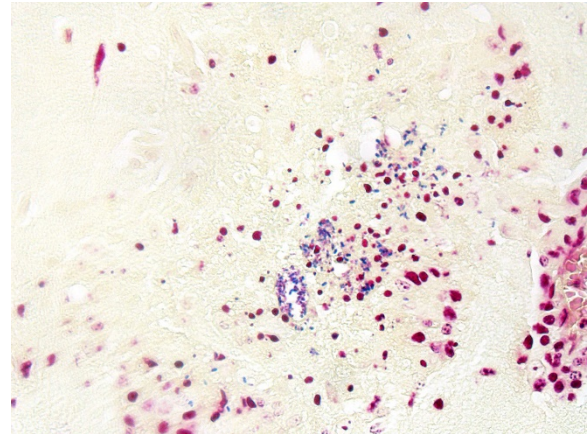
E. cuniculi may parasitize a wide range of mammals, but is most commonly associated with infections in rabbits, rodents, dogs, and primates. Based on the number of short repeats in the ribosomal internal transcribe spacer region, three different strains of *E. cuniculi* have been identified: the "rabbit" (type I), the "mouse" (type 2), and the "dog" strain (type 3). These strains are useful in identifying the source of human outbreaks (with only infections with dog and rabbit strains being previously identified). Outbreaks in rabbits appear to occur solely from rabbit strains.⁸

The contributor has an excellent job in detailing infection in the rabbit. While lesions in the rabbit are classically considered to be limited to the CNS and kidney, acute infections may result in cysts and spores within the lung, liver and heart, sites which are clear of organisms when the clinical signs of neurologic disease or renal failure become evident. Lenticular invasion is a particularly interesting phenomenon which appears to be restricted to dwarf rabbits; unlike normal horizontal infections, this syndrome results from vertical transmission to the developing lens via a peculiar homing mechanism for *E. cuniculi* to the developing optic cup where it takes residence within the lens. Delayed replication results in destruction of lens fibers and leaching of lens protein into the globe, ultimately causing severe granulomatous inflammation and phthisis.

Infections with *Encephalitozoon* sp. and a related microsporidian genus, *Enterocytozoon*, have been reported in

humans. While most cases of infection of *E. cuniculi* are associated with severe immunodeficiency, a number of cases have occurred in immunocompetent individuals in close contact with rabbits and dogs. As spores of *E. cuniculi* are resistant within the environment, waterborne infections could not be totally excluded in such cases.⁸ Other related species of *Encephalitozoon*, to include *E. hellem* and *E. intestinalis*, are also well reported in the literature. *E. hellem*, is a microsporidian parasite primarily of psittacine birds which has been almost exclusively diagnosed in HIV-infected individuals. *E. intestinalis* is the second most prevalent microsporidian species infecting humans and is a common cause of diarrhea and other gastrointestinal complaints in HIV-infected individuals.⁸

A related microsporidia parasite, the most common species known to cause human disease, is *Enterocytozoon bienusi*. This pathogen was first described in HIV-infected patients in 1985 and may be found in up to 50% of HIV infected patients.⁸ It has also been identified in immunocompetent patients associated with traveler's diarrhea in Europe. *E. bienusi* has also been identified in immunocompetent diarrhea patients in concert with *E. hellem* and *E. intestinalis*.⁸ Over the last decade, evidence has accumulated that this parasite may persist as an asymptomatic infection in immunocompetent humans. Eleven years after its discovery as a human pathogen, *Enterocytozoon* was detected in animals for the first time and seems to be a common parasite in asymptomatic pigs.⁸ It has also been reported as a common finding in SIV-infected macaques, but may also be seen in immunocompetent macaques as well. It has not been documented in macaques in the wild.⁸



Cerebrum, rabbit. Gram stains delineate extracellular spores within inflammatory foci which resemble cellular debris. (Brown-Hopps, 400X)

The determination of the morphologic diagnosis in this case was met with spirited discussion, and other descriptive features of the morphology of this disease were also greeted with some skepticism (including the oft-used term “pseudocyst”). Granulomatous encephalitis is a classic description of the inflammation associated with cerebral encephalitozoonosis (and is used in some very recent textbooks on laboratory animal disease, yet the true composition of the inflammatory foci surrounding extracellular spores is difficult to elucidate on morphologic grounds alone, and a more in-depth analysis of cell types contained in these foci is not available. The lack of multinucleated cells, lymphocytes, and plasma cells in inflammatory foci do not support granulomatous inflammation, and pathologists who refer to these foci as “glial nodules” may in fact be closer to the truth. Our morphologic diagnosis above is a combination of tradition and morphology – granulomatous on faith to excellent morphologists who preceded us, and necrotizing on evidence.

References:

1. Canning EU, Lom J: *The Microsporidia of Vertebrates*. Harcourt Brace Jovanovich, New York, NY, 1986.
2. Flatt RE, Jackson SJ: Renal nosematosis in young rabbits. *Vet Pathol*. 1970;7:492–497.
3. Giordano C, Weigt A, Vercelli A, Rondena M, Grilli G, Giudice C. Immunohistochemical identification of *Encephalitozoon cuniculi* in phacoclastic uveitis in four rabbits. *Vet Ophthalmol*. 2005;8:271–275.
4. Harcourt-Brown FM, Holloway HKR (2003) *Encephalitozoon cuniculi* in pet rabbits. *Vet Rec*. 2003;152:427–431.
5. Katinka, MD, et al. Genome sequence and gene compaction of the eukaryote parasite *Encephalitozoon cuniculi*. *Nature*, 2001;414, 450-453.
6. Kunstyr I, Naumann S: Head tilt in rabbits caused by pasteurellosis and encephalitozoonosis. *Lab Anim*. 1985;19: 208–213.
7. Kunzel F, Joachin A: Encephalitozoonosis in Rabbits. *Parasitol Res*. 2010;106:299-309.
8. Mathis A, Weber R, Deplazes P. Zoonotic potential of the microsporidia. *Clin Microbiol Rev*. 2005;18:423–445.
9. Percy DH, Barthold SW, Griffey SM. In: *Pathology of Laboratory Rodents and Rabbits*. 4th ed. Ames, IA: Blackwell Publishing; 2016: 293-295.
10. Shadduck JA. Effect of fumagillin on in vitro multiplication of *Encephalitozoon cuniculi*. *J Protozool*. 1980;27(2):202–208.
11. Vossbrinck, C. R., Maddox, J. V., Friedman, S., Debrunner-Vossbrinck, B. A. & Woese, C. R. Ribosomal RNA sequence suggests microsporidia are extremely ancient eukaryotes. *Nature*, 1987;326, 411-414.
12. Wasson K, Peper RL. Mammalian Microsporidiosis. *Vet Pathol*. 2000; 37(2): 113-128.
13. Wicher V, Baughn RE, Fuentealba C, Shadduck JA, Abbruscato F, Wicher K (1991) Enteric infection with an obligate intracellular parasite, *Encephalitozoon cuniculi*, in an experimental model. *Infect Immun*. 1991; 59:2225–2231.
14. Wright JH, Craighead EM. Infectious motor paralysis in young rabbits. *J Exp Med*. 1922;36:135–140.

Self-Assessment - WSC 2018-2019 Conference 10

1. Which of the following is true concerning protothecosis in the dog?
 - a. *P. wickerhamii* and *P. zopfii* may be distinguished morphologically from each other by their marked size difference.
 - b. Colitis is the most common presentation of canine protothecosis.
 - c. Prototheca has PAS-positive cytoplasmic granules that are negative following amylase digestion.
 - d. Prototheca infections may have a green tinge grossly.

2. Which of the following syndromes is associated with necrotic foci in multiple organs?
 - a. Typhoidal tularemia
 - b. Ulceroglandular tularemia
 - c. Septic tularemia
 - d. Pneumonic tularemia

3. Which is the minimum recommended for working with *F. tularensis* sp. in the laboratory?
 - a. BSL 1
 - b. BSL 2
 - c. BSL 3
 - d. BSL 4

4. Which of the following is NOT a consistent finding in fatal fasting system in macaques?
 - a. Diabetes mellitus
 - b. Stress
 - c. Hypertriglyceridemia
 - d. Obesity

5. Which of the following is not found in microsporidia?
 - a. Ribosomes
 - b. Golgi apparatus
 - c. Nuclei
 - d. Mitochondria

Please email your completed assessment to Ms. Jessica Gold at Jessica.d.gold2.ctr@mail.mil for grading. Passing score is 80%. This program (RACE program number) is approved by the AAVSB RACE to offer a total of 0.5 CE Credits, with a maximum of 12.5 CE Credits being available to any individual Veterinary Medical Professionals for the 2017-2018 Wednesday Slide Conference. This RACE approval is for the subject matter categories of: SCIENTIFIC using the delivery method of NON-INTERACTIVE DISTANCE. This approval is valid in jurisdictions which recognize AAVSB RACE; however, participants are responsible for ascertaining each board's CE requirements. RACE does not "accredit", "endorse" or "certify" any program or person, nor does RACE approval validate the content of the program.

Please email your completed assessment to Ms. Jessica Gold at Jessica.d.gold2.ctr@mail.mil for grading. Passing score is 80%. This program (RACE program number) is approved by the AAVSB RACE to offer a total of 0.5 CE Credits, with a maximum of 12.5 CE Credits being available to any individual Veterinary Medical Professionals for the 2017-2018 Wednesday Slide Conference. This RACE approval is for the subject matter categories of: SCIENTIFIC using the delivery method of NON-INTERACTIVE DISTANCE. This approval is valid in jurisdictions which recognize AAVSB RACE; however, participants are responsible for ascertaining each board's CE requirements. RACE does not "accredit", "endorse" or "certify" any program or person, nor does RACE approval validate the content of the program.

**Joint Pathology Center
Veterinary Pathology Services**



WEDNESDAY SLIDE CONFERENCE 2018-2019

C o n f e r e n c e 1 1

5 December 2018

Conference Moderator:

Charles W. Bradley, VMD, DACVP
Assistant Professor, Pathobiology
University of Pennsylvania School of Veterinary Medicine
4005 MJR-VHUP
3900 Delancey Street
Philadelphia, PA, 19104

CASE I: P15/141 JPC 4066260)

Signalment: 2.5-year-old, Aubrac bull, *Bos taurus*

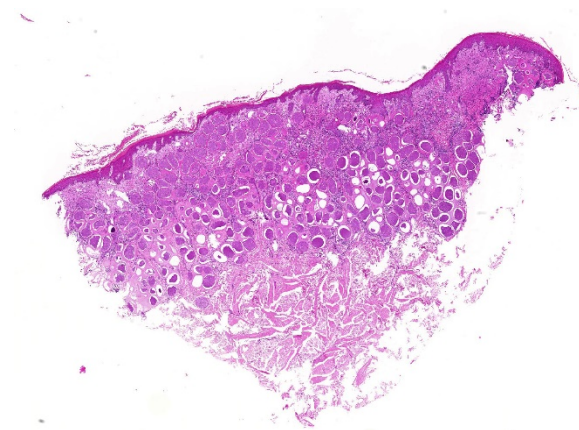
History: The bull presented to Veterinary Teaching Hospital with history of chronic skin lesions of unknown reason.

Gross Pathology: Multifocal areas of alopecia

Laboratory results: PCR positive for *B. besnoiti*, ELISA positive for *B. besnoiti*

Microscopic Description:

Haired skin. The epidermis displays low to moderate, diffuse, orthokeratotic hyperkeratosis, moderate, diffuse, epidermal hyperplasia characterized by acanthosis and irregular rete ridge formation, rare, multifocal, individual, intraepidermal



Haired skin, ox. The dermis is diffusely expanded by numerous apicomplexan tissue cysts ranging from 200-400um. (HE, 5X)

macrophages, eosinophils and neutrophils (exocytosis), and rare, multifocal, discrete, shrunken, hypereosinophilic keratinocytes with pyknotic nuclei (apoptosis). The superficial dermis and a variable part of the adjacent deep dermis are markedly and diffusely expanded by a moderate,

coalescing, perivascular, and nodular to diffuse infiltration of macrophages, plasma cells, lymphocytes, eosinophilic granulocytes and to a locally variable extent also neutrophilic granulocytes, as well as a low to moderate, coalescing amount of bundles of fibroblasts and fibrocytes within a collagenous stroma (fibrosis). There is a marked coalescing to diffuse loss of follicular and adnexal structures (alopecia). Within the superficial and upper deep dermis are numerous round protozoal cysts characterized by a diameter of ~ 250 µm, a ~ 12 µm thick, distinctly bordered, pale eosinophilic, hyaline outer capsule, a subcapsular ~ 10 µm thick ring of eosinophilic cytoplasm containing multiple fusiform nuclei, and a central round vacuole containing myriads of densely packed, ~ 4 µm in diameter, distinctly bordered, crescent-shaped bradyzoites with pale eosinophilic cytoplasm and a central, hyperchromatic nucleus. The dermal collagenous stroma, adjacent to the cysts show a mild, laminar zone of shrinkage and hypereosinophilia (compression atrophy).

Contributor's Morphologic Diagnoses:

Haired skin. Dermatitis nodular to diffuse, granulomatous and eosinophilic, chronic, coalescing, moderate with numerous intradermal, intracellular, apicomplexan cysts (etiology consistent with *Besnoitia besnoiti*), adjacent laminar compression atrophy, dermal fibrosis, alopecia, epidermal hyperplasia and orthokeratotic hyperkeratosis.

Contributor's Comment: Etiology: The apicomplexan protozoan parasite *Besnoitia besnoiti* (*B. besnoiti*; Family: *Sarcocystidae*) is the etiologic agent of bovine besnoitiosis (Synonyms: bovine cutaneous globidiosis, bovine cutaneous sarcosporidiosis, elephant skin disease of cattle) and has been described first by Cadéac in 1884.¹ The closely related

Besnoitia species *B. caprae*, *B. bennetti* and *B. tarandi* induce a comparable disease mainly in goats, equids and wild ruminants, respectively (Table 1).¹¹

Besnoitiosis is an endemic disease in the southern part of Europe, the subtropical areas of Asia, and sub-Saharan Africa, but has also been reported as an emerging disease in the central and northern part of Europe.^{1,5,7,8} In endemic areas seroprevalence rates are ~ 50% whereas the incidence of clinical cases of 1-10% per year, as well as the mortality rate of less than 1% are obviously low. Prevalence and incidence may be higher in areas where the disease is emerging.^{1,11}

B. besnoiti is commonly believed to have a heteroxenous life cycle, however until today only homoxenous transmission from intermediate to intermediate host has been shown experimentally. The most important intermediate host are cattle, but wildebeest, kudu and impala are also affected.¹¹ The epidemiological importance of wild ruminants in northern Europe is currently unknown. Although roe deer and red deer can be seropositive in areas of endemic bovine besnoitiosis, the strong cross reactivity of *B. besnoiti*, *B. tarandi* and *B. bennetti* prevents differentiation of these species employing serological methods.⁶ Although many authors have suggested that the final host of *B. besnoiti* could be the domestic cat or wild carnivores, attempts to proof this hypothesis have been unsuccessful so far.¹⁰ Therefore the final host of *B. besnoiti* remains currently unknown, as is true for most other species of the genus *Besnoitia* (Table 1).

Whether transmission from the currently unknown definitive host to the intermediate host occurs in via oocytes shed in the feces remains unknown. In contrast, horizontal mechanical transfer between intermediate hosts by blood-sucking insects including

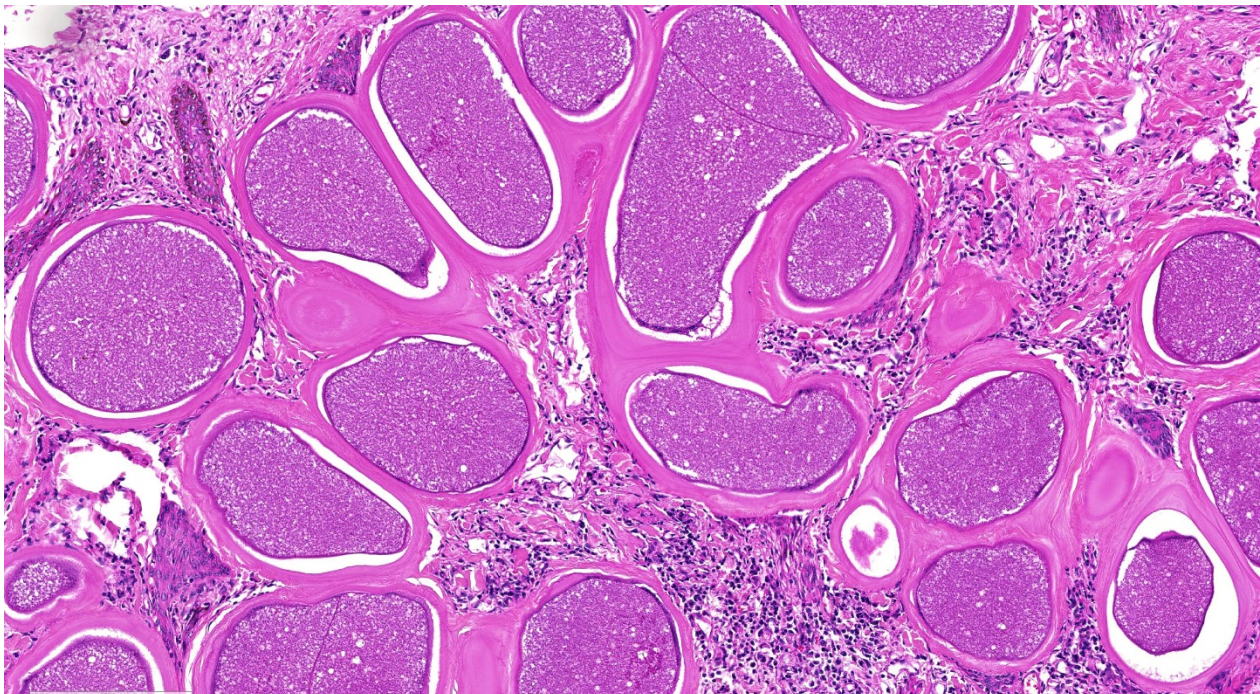
tsetse flies (*Glossina brevipalpis*), tabanids (*Tabanocella denticornis*, *Atylotus nigromaculatus*, *Haematopota albihirta*), mosquitoes (*Culex simpsoni*, *Culex spp.*) and stable flies (*Stomoxys calcitrans*) has been experimentally proven and is suggested to be an important mode of transmission.⁵ Furthermore, transmission by other arthropods, iatrogenic transfer and direct contact including sexual transfer are possible other routes of transmission.¹

Rapid asexual intracellular proliferation of *B. besnoiti* tachyzoites occurs mainly within the intermediate host's endothelial cells during the acute phase after the first infection. This leads to vasculitis and thrombosis of capillaries and smaller veins, especially within the dermis, and subsequent generalized subcutaneous edema.^{2,8} One to two weeks after the onset of the acute phase, the infection reaches the subacute to chronic stage which is characterized by evolving intracellular tissue cysts containing myriads

of bradyzoites within vimentin-positive, MAC387-negative, mesenchymal cells (suggested to be fibroblasts or myofibroblasts), especially within the dermis and submucosa, as well as various other tissues.⁸ A detailed description of the sequential steps of tissue cyst formation can be found in Langenmayer et al. (2015).⁸

The clinical disease can be subdivided into two phases. The acute phase ("anasarca phase") of bovine besnoitiosis occurs 11-13 days after infection and lasts for 6-10 days, and is characterized by fever, subcutaneous edema, lymphadenitis, conjunctivitis, nasal discharge, salivation, laminitis and depression.^{2,8}

In contrast, the chronic phase (scleroderma phase) is characterized by macroscopically detectable tissue cysts in connective tissues, especially the pathognomonic pin-head sized cysts in the dermis and submucosa of conjunctiva, nasal cavity and vagina, as well



Haired skin, ox. Tissue cysts are surrounding by the thick hyaline wall ranging from 10 to 20um. Within cyst the wall, a thin rim of cell cytoplasm with peripheralized nuclei surrounds a parasitophorous vacuole contain innumerable zites. Tissue cysts are separated by moderate numbers of lymphocytes, histiocytes, and eosinophils, as well as down projecting rete ridges of the hyperplastic epithelium (HE, 159X)

as lichenification, hyperkeratosis and alopecia.^{5,8}

Overt clinical disease most often affects 2- to 4-year old adults and chronically infected animals may partially recover but are thought to remain infected for the rest of their lives.¹ Although only a small percentage of less than 1% of the affected cattle die, bovine besnoitiosis may lead to major economic losses due to weight loss and decreased milk production, abortion, male infertility, and reduced value of the hides. Currently there are no therapeutic treatment options available. An attenuated live vaccine is available in some countries for prophylaxis.

Macroscopic changes in the acute phase of besnoitiosis are rather unspecific and include coalescing to generalized subcutaneous edema (anasarca), multifocal to coalescing, lymphohistioplasmacytic and eosinophilic perivascular dermatitis, dermal hemorrhages, generalized swelling of lymph nodes (lymphadenopathy), and swollen testicles (orchitis).^{2,8}

The characteristic tissue cysts start to develop in the subacute stage concurrent with the decline of dermal edema. The tissue cysts become clearly macroscopically visible as pin-head sized, pearl white tissue cysts with a diameter of up to 1 mm within the conjunctiva and mucous membranes of the vagina, nose, pharynx and upper respiratory tract in the chronic phase of besnoitiosis.⁸ The dermis exhibits multifocal to coalescing palpable indurations with a diameter of initially 3-5 mm and later up to 1 cm, especially at the teats, eyelids, neck and limbs, as well as hypotrichosis, alopecia, seborrhea, lichenification and partially erosions, exudations and crusts. Other affected tissues include the connective tissue of the subcutis, intermuscular fascia, mesentery and scrotum.^{2,4,5}

Histologically, crescent-shaped 6-7,5 x 2,5-3,9 μm sized *B. besnoiti* tachyzoites with eosinophilic cytoplasm and a round basophilic nucleus may be visible within endothelial cells, blood and lymph vessels, and extracellular spaces during the acute stage. Notably, these tachyzoites are indistinguishable from *Neospora caninum* or *Toxoplasma gondii* by light microscopy.^{2,4,8}

The *B. besnoiti* tissue cysts of the chronic phase exhibit a diameter of up to 600 μm , and a characteristic double-walled morphology which allows differentiation from the similar cysts of *Sarcocystis spp.* and *Eimeria spp.*¹¹ The outer 10-12 μm , pale eosinophilic, hyaline cyst wall is comprised of host-derived collagenous material and its outer surface blends irregularly into the surrounding connective tissue. The inner cyst wall is a thin pale gray-bluish band with distinct histochemical staining characteristics in between the outer cyst wall and the outer cell membrane of the host cell. The outer cyst wall stains blue with Masson's trichrome and pale white with Giemsa stain, whereas the inner cyst wall stains pale white with Masson's trichrome stain and deeply violet with Giemsa stain.⁸ The large host cell is multinucleated and forms a peripheral rim of cytoplasm, which in turn encompasses the central parasitophorous vacuole. The parasitophorous vacuole is filled with thousands of 6,0-7,5 x 1,9-2,3 μm sized bradyzoites.² The cysts are often surrounded by a granulomatous and eosinophilic, nodular to diffuse dermatitis with fibrosis, compression atrophy of adnexa, and hyperkeratosis.^{4,7} Occasional multinucleated giant cells of the foreign body type can be present in the inflammatory infiltrate.⁸ Other lesions include focal or multifocal myositis, keratitis, periostitis, endosteitis, lymphadenitis, pneumonia, periorchitis, orchitis, epididymitis, arteritis, perineuritis, and laminitis.^{4,8}

A comprehensive ultrastructural description of the tachyzoites, bradyzoites and tissue cysts in bovine besnoitiosis has been published recently.⁹

The gold standard for the diagnosis of bovine besnoitiosis seems to be the histologic demonstration of the pathognomonic *Besnoitia* spp. tissue cysts. Obvious microscopic differentials for *B. besnoiti* include the indistinguishable cysts of other species of the genus *Besnoitia* as well as the confusable cysts of *Sarcocystis* spp., *Eimeria* spp., and the sporangia of the fungal agents *Rhinosporidium seeberi*, *Emmonsia crescens*, *Sporothrix schenkii*, *Coccidioides immitis* and *Loboa lobo*.³

Immunohistochemistry can be used to differentiate *B. besnoiti* bradyzoites and cysts from those of *Toxoplasma gondii*, *Neospora caninum* and, although with minor cross reactivity, also *Sarcocystis* spp.⁸ Due to the serological cross reactivity of the various species of the genus *Besnoitia*, it seems reasonable that it is also not possible to differentiate between these species using immunohistochemistry.⁶ Therefore molecular genetic methods are the method of choice if a diagnosis at the species level is needed.¹¹

Table 1. Species of the genus *Besnoitia* and their main hosts.

Species name	Main intermediate host	Main final host
<i>Besnoitia besnoiti</i>	Cattle, kudu, blue wildebeest, impala	?
<i>Besnoitia caprae</i>	Goat	?
<i>Besnoitia tarandi</i>	Reindeer, caribou, mule deer, roe deer, muskox	?
<i>Besnoitia bennetti</i>	Horse, donkey, mule, (zebra)	?
<i>Besnoitia jellisoni</i>	Mouse, rat, other rodents	?
<i>Besnoitia akodoni</i>	Montane grass mouse	?
<i>Besnoitia oryctofelisi</i>	Rabbit	Cat
<i>Besnoitia darlingi</i>	Virginia opossum	Cat
<i>Babesia neotomofelis</i>	Southern plains woodrat	Cat
<i>Besnoitia wallacei</i>	?	Cat

Data based on the review of Olias et al. (2011).¹¹

Contributing Institution:

Friedrich-Loeffler-Institut, Federal Research Institute for Animal Health, 17493 Greifswald-Insel Riems, Germany (www.fli.bund.de)

JPC Diagnosis: Hairless skin: Dermatitis, lymphoplasmacytic, histiocytic, and eosinophilic, diffuse, moderate, with numerous apicomplexan cysts and mild diffuse epidermal hyperplasia and

hyperkeratosis.

JPC Comment: The contributor has provided a thorough discussion of this disease which is currently considered of great economic importance in cattle in Europe. Historically, the disease was first described by Cadeac in 1884 and named ‘Telephanitiasis el l’anasarque du bouef.’ Although initially misdiagnosed by Besnoit (a professor of veterinary medicine in Toulouse) and Robin as a species of

Sarcocystis (*S. besnoiti*) in 1912, and in 1916, Franco and Borges proposed the name *Besnoitia besnoiti*. The disease is gone by many names, including bovine subcutaneous globidiosis, bovine cutaneous cervical spongiosis, and elephant skin disease of cattle.

While the definitive host of *B. besnoiti* remains unproven, domestic and wild felines have been shown to be the definitive host for *Besnoitia* species of rodents. A recent publication by Verma et al. has identified the bobcat (*Lynx rufus*) as the definitive host of *B. darlingi*, a species which parasitizes the opossum.

While orchitis and a marked decrease in fertility in bulls has been well documented this disease, chronically infected cows may still become pregnant, and give birth, with no reports to date of vertical transmission of *B. besnoiti*. Subsequent rearing is problematic, as the disease causes a negative impact on milk production, as well as the calf's nursing opening painful wounds on infected teats.² Another clinical finding in chronic cases of disease in cattle include laminitis, likely as a result of interference with dermal vasculature and pressure put on epidermal laminae by the presence of tissue cysts. Inappropriate weight bearing ultimately results in rotation of P3 and the development of sole ulcers.⁵

On a microscopic level, the composition of the two cysts walls, the inner cyst wall (which lies outside the host cell membrane), and the hyalin outer cyst wall (composed of type I collagen as evidenced by a deep blue staining on a Masson's trichrome and orange birefringence on picosirius red), was recently described by Langenmeyer et al. The pale white staining of the ICW on Masson's and a blue-green color in picosirius red/Alcian blue strongly suggests that the ICW is composed of elements of the

extracellular matrix. This interesting histochemical discovery further supports myofibroblasts as the cell of origin for tissue cysts as myofibroblasts are capable of producing both extracellular matrix components as well as type I collagen.

To date, no member of the genus *Besnoitia* have been demonstrated to elicit disease in humans.

References:

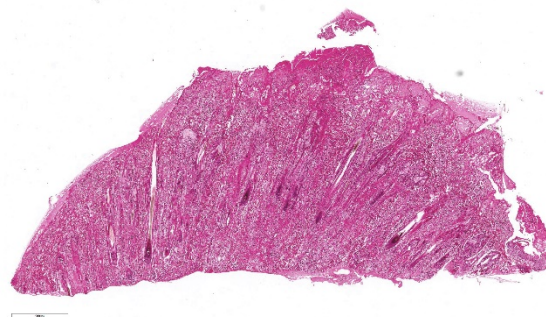
- 1 Alvarez-Garcia G, Frey CF, Mora LM, Schares G: A century of bovine besnoitiosis: an unknown disease re-emerging in Europe. *Trends Parasitol* 2013;29(8):407-415.
- 2 Cortes H, Leitao A, Gottstein B, Hemphill A: A review on bovine besnoitiosis: a disease with economic impact in herd health management, caused by *Besnoitia besnoiti* (Franco and Borges,). *Parasitology* 2014;141(11):1406-1417.
- 3 Gardiner CH, Fayer R, Dubey JP: *An Atlas of Protozoan Parasites in Animal Tissues*: Armed Forces Institute of Pathology, 1998.
- 4 Ginn PE, Mensett JEKL, Rukich PM: Skin and appedages. In: Maxie MG, ed. *Jubb, Kennedy, and Palmer's Pathology of Domestic Animals*. 5 ed.: Saunders Elsevier; 2007: 556-781.
- 5 Gollnick NS, Scharr JC, Schares G, Langenmeyer MC: Natural *Besnoitia besnoiti* infections in cattle: chronology of disease progression. *BMC Vet Res* 2015;11(1):35.
- 6 Gutierrez-Exposito D, Ortega-Mora LM, Marco I, Boadella M, Gortazar C, San Miguel-Ayanz JM, et al.: First serosurvey of *Besnoitia* spp. infection in wild European ruminants in Spain. *Vet Parasitol* 2013;197(3-4):557-564.

- 7 Hornok S, Fedak A, Baska F, Hofmann-Lehmann R, Basso W: Bovine besnoitiosis emerging in Central-Eastern Europe, Hungary. *Parasit Vectors* 2014;7:20.
- 8 Langenmayer MC, Gollnick NS, Majzoub-Altweck M, Scharr JC, Schares G, Hermanns W: Naturally acquired bovine besnoitiosis: histological and immunohistochemical findings in acute, subacute, and chronic disease. *Vet Pathol* 2015;52(3):476-488.
- 9 Langenmayer MC, Gollnick NS, Scharr JC, Schares G, Herrmann DC, Majzoub-Altweck M, et al.: Besnoitia besnoiti infection in cattle and mice: ultrastructural pathology in acute and chronic besnoitiosis. *Parasitol Res* 2015;114(3):955-963.
- 10 Millan J, Sobrino R, Rodriguez A, Oleaga A, Gortazar C, Schares G: Large-scale serosurvey of *Besnoitia besnoiti* in free-living carnivores in Spain. *Vet Parasitol* 2012;190(1-2):241-245.
- 11 Olias P, Schade B, Mehlhorn H: Molecular pathology, taxonomy and epidemiology of *Besnoitia* species (Protozoa: Sarcocystidae). *Infect Genet Evol* 2011;11(7):1564-1576.
12. Verma SK, Cerquiera-Cezar CK, Murata FHA, Loavallo MJ, Rosenthal BM, Dubey JP. Bobcats (*Lynx rufus*) are natural definitive hosts of *Besnoitia darlingi*. *Vet Parasitol* 2017; 248:84-89.

CASE II: Case #1 (JPC 4085967)

Signalment: 16-month-old, female, European shorthair cat

History: The cat showed a non-healing wound at the right forelimb over a few weeks. A treatment with NSAID's and antibiotics



Haired skin: At subgross examination, the submitted section of skin is ulcerated and the dermis is hypercellular. (HE, %x)

didn't show any improvement. Therefore a biopsy was taken for microscopic investigation.

Gross Pathology: The specimens showed a moderate alopecia and some crusts.

Laboratory results: Molecular biological examination:

- PCR for Cowpox virus: positive

Microscopic Description:

- Epidermis: diffusely covered by plasmatic components; nearly diffuse severe erosions and ulcerations multifocal with serocellular crusts containing a high mount of neutrophils; multifocal moderate intracellular edema up to ballooning degeneration and necrosis of the keratinocytes; multifocal eosinophilic intracytoplasmic inclusion bodies within the keratinocytes
- Dermis: severe infiltration with marked numbers of neutrophils, some lymphocytes, plasma cells and macrophages; multifocal severe necrosis with degenerate neutrophils and cellular and karyorrhectic debris; multifocal moderate hemorrhages
- Adnexa: disseminated severe perifollicular infiltration with marked numbers of neutrophils, some

lymphocytes, plasma cells and macrophages, multifocal with complete destruction of the adnexa; multifocal eosinophilic intracytoplasmic inclusion bodies within the keratinocytes of the hair follicle

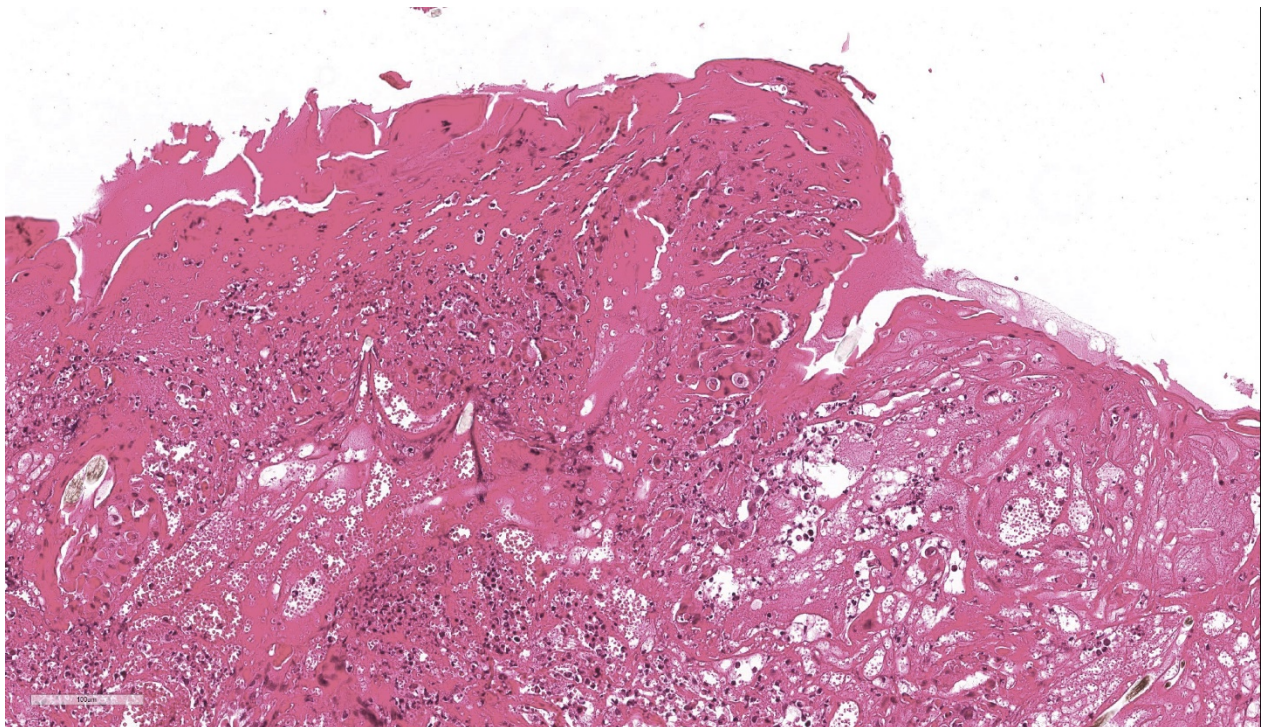
Contributor's Morphologic Diagnoses:

Haired skin: Dermatitis, purulent and necrotizing, erosive and ulcerative, severe, with eosinophilic intracytoplasmic inclusion bodies within keratinocytes

Contributor's Comment: Etiology: The cowpox virus is a member of the genus Orthopoxvirus in the family Poxviridae. The reservoir hosts are rodents from which the virus spreads to other animals, for example cows, cats (including large felids), zoo animals (rhinoceroses, elephants, okapis) and humans.⁹ In cats, it usually causes a regional

viral dermatitis and is often a more severe disease than in cattle or humans. There is an increased incidence in the autumn, which may reflect the increased size and activity of wild rodents in this time of the year.¹

The primary lesion after cutaneous infection is usually an ulcerating, erythematous, crusted macule or plaque on the head, neck, or forelegs that occurs after 3-6 days.⁹ After a viremia, pyrexia, anorexia and depression widespread secondary lesions develop within 10 days to a few weeks.^{1,5} Like the primary lesion, these first appear as small erythematous macules, ultimately forming ulcerated papules. Sometimes, vesicles are found on the tongue, the mouth or inner aspect of the pinna. Approximately 20 per cent of affected cats show a mild infection of the upper respiratory tract. After three weeks the cutaneous scabs dry and fall off.² Typical microscopic findings are ulceration,



Haired skin, cat. There is diffuse full thickness necrosis of the epithelium of the superficial dermis which extends into the follicular epithelium. Large pools of serocellular exudate expand the intercellular space. The dermis is infiltrated by large numbers of degenerate neutrophils admixed with cellular debris, hemorrhage, edema, and fibrin. (HE, 182X)

serocellular crusts, ballooning degeneration of keratinocytes in epidermis and hair follicles with large intracytoplasmic eosinophilic inclusions and a secondary necrosis and infiltration with inflammatory cells.⁶

There are reports about some cases with more severe clinical signs, especially with a severe necrotizing or interstitial pneumonia, necrotizing rhinitis and/or generalized skin lesions. These are either described as atypical infections or are associated with secondary bacterial infection or an underlying immunosuppression like FIV, parvovirus and FeLV infections, debilitating disease or treatment with corticosteroids.^{8,12,13,14} Macroscopic differential diagnoses for this condition are facial and nasal dermatitis and stomatitis associated to feline herpesvirus 1, cutaneous lymphoma, autoimmune dermatoses, such as pemphigus foliaceus, cutaneous bacterial, fungal or parasitic infections and physicochemical injuries.^{7,8} Because of the intracytoplasmic inclusion bodies, there are no histological differential diagnoses.

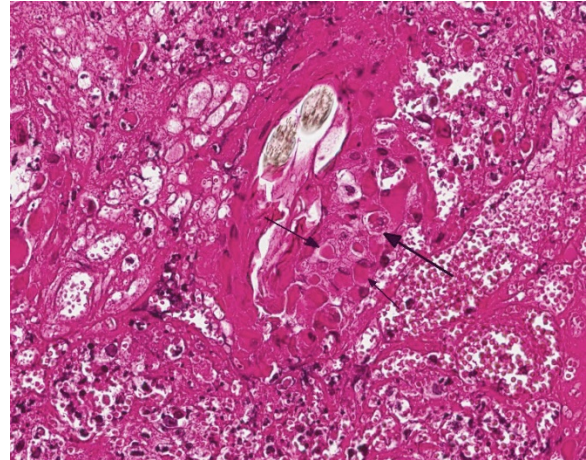
Furthermore, cowpox virus infection is zoonotic and there exist several reports of the virus being transmitted from cats to human beings.^{8,14,15} Lesions are similar to those in cats and are usually associated with a cat scratch.^{8,14}

Contributing Institution:

Institut für Veterinär-Pathologie,
Veterinärmedizinische Fakultät Leipzig,
Universität Leipzig,

Germany (<http://www.vetmed.uni-leipzig.de/ik/wpathologie>)

JPC Diagnosis: Haired skin: Dermatitis, necrotizing, diffuse, severe with epithelial



Haired skin, cat. There is diffuse full thickness necrosis of the epithelium of the superficial dermis which extends into the follicular epithelium. Large pools of serocellular exudate expand the intercellular space. The dermis is infiltrated by large numbers of degenerate neutrophils admixed with cellular debris, hemorrhage, edema, and fibrin. (HE, 132X)

ballooning degeneration, and numerous intracytoplasmic viral inclusions.

JPC Comment: Few medical or veterinary students have not heard the story of Edward Jenner, the milkmaids, and his discovery of the correlation between inoculation with cowpox and resistance to smallpox. In a time in which myths fall quickly and hard, the long-held attribution of one of the early vaccine discoveries has been recently called into question. A 2018 article in the *New England Journal of Medicine*³ ascribes the important observation to the physician to whom Jenner was actually apprenticed, Dr. John Fuster, who two years earlier in 1768, began inoculating people against smallpox.” It was a conversation with a farmer that Fuster inoculated ineffectually that led to the connection between smallpox and cowpox, when the farmer exclaimed, “I have had the Cow Pox lately to a violent degree, if that’s any odds.” Jenner confided about the finding to a friend later that year, but would not travel to London to gain fame as the inventor of the vaccine until 1770.

Even the identity of the virus used by Jenner et al. has been called into question. While the story of the “unrivaled” (i.e., unpocked) complexions of the milkmaids in the area at that time is legend, even the use of the cowpox virus in early vaccinations has been called in to question. The widespread exchange and mixing of vaccines and “lymph” in the US in the early 1900s resulted in vaccines today that likely would contain viral determinants of many vaccines in use around the world at that time. Interestingly, no trace of cowpox has been identified in vaccines tested from that time or today’s derivatives. The active virus appears to be the vaccinia virus, closely related to cowpox, but instead isolated from horses.⁵

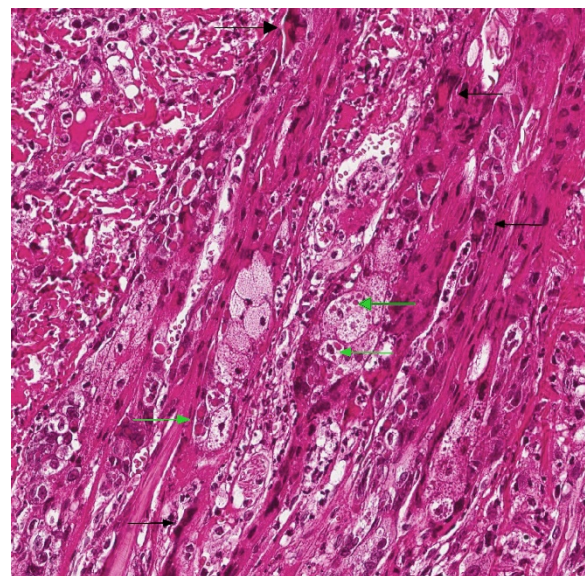
Today, cowpox viruses are distributed throughout Asia and Europe, except for Ireland. Wild rodents, predominantly voles, are the reservoir of these viruses; hunting cats are accidentally infected by their prey.⁹ Historically, cattle (likely infected by rodent contact) have been the primary source for zoonotic infections; however, within the last decade, cats have been primarily described as the source of human infections. Wild rodents are the primary source for the cat; pet rats have been rarely been incriminated in human infections.⁹

While generally considered to be a cutaneous infection, fatal generalized systemic infections with cowpox virus have been seen in immunosuppressed cats, as well as a single human case report following immunosuppressive corticosteroid therapy. The effects of concurrent immunosuppressive viruses such as feline T virus, retrovirus, parvovirus may also exerts adverse effects by promulgated concurrent bacterial infections.⁹

A number of atypical cases of cowpox in cats have been identified in the literature.

Necrotizing and proliferative pneumonia has been seen in the absence of cutaneous lesions in domestic cats and wild felids. A series of cases in cats in which the cutaneous lesions were present on the hindlimbs or tail was reported by Jungwirth et al.¹⁰ In a Denmark zoo which has reported seasonal recurrence of cowpox virus outbreaks in captive cheetahs, two of nine (22%) died of generalized disease or pulmonary infection.¹⁷

Finally, a fatal outbreak of a novel orthopoxvirus was reported in 2017, in which phylogenetic analysis revealed the virus to be distantly related to cowpox, and more closely related to ectromelia virus.⁴ Autopsied macaques demonstrated interstitial pneumonia with necrosis of bronchial epithelium; lymphoid necrosis of the spleen and lymph node, and numerous ulcers in the skin and upper GI tract. Rodents in the facility demonstrated serologic (IGG) to the putative poxvirus, but the virus was not isolated from trapped rodents. A subsequent report of cutaneous infection by a virus within the same cluster as this putative novel orthomyxovirus was subsequently reported.¹¹



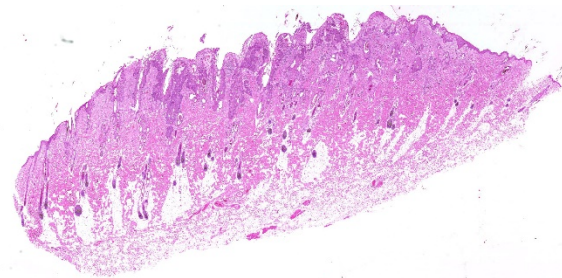
Haired skin, cat. Within surviving follicular epithelium, there are numerous multinucleated viral syncytia (black arrows). Degenerating sebaceous epithelium also contains intracytoplasmic viral inclusions. (HE, 351X)

The attendees noted the presence of numerous multinucleated epithelial cells, which are not commonly seen in poxviral infections; their significance or etiology in this case is not apparent. The large areas of profound necrosis of the epidermis led some attendees to question whether vascular lesions, such as may be seen in other orthopoxviral infections, such as ectromelia, might have been present.

References:

- (1) Bennett M, Gaskell CJ, Gaskell R M, Baxby D, Gruffydd-Jones TJ. Poxvirus infection in the domestic cat; some clinical and epidemiological observations. *Vet Rec.* 1986;118:387–390
- (2) Bennett M, Gaskell CJ, Baxby D et al. Feline cowpox virus infection. *J Small Anim Pract* 1990; 31:167–73.
- (3) Boylston, AW. The myth of the milkmaid. *NEJM* 2018; 378(5):414-415.
- (4) Cardeti G, Gruber CEM, Eleni C, Carietti F, Castiletti C, Manna G, Rsoone F, Giombini E, Seileri M, Lapa D, Puro V, Di Caro A, Lorenzetti R, Scicluna MT, Grifoni G, Rizzoli A, Tagliapietra V, De Marco L, Capobianchi MR, Autorinao GL. Fatal outbreak in Tonkean macaques caused by possibly novel orthopoxvirus, Italy, January 2015. *Emerg Inf Dis* 2017; 23(12):1941-1949.
- (5) Damaso CR. Revisiting Jenner's mysteries, the role of the Baugency lympho in the evolutionary path of ancient smallpox vaccine. *Hist Rev* 2018; 18(2): 55-63. For the
- (6) Gaskell RM, Gaskell CJ, Evans RJ, Dennis PE, Bennett AM, Udall ND, Voyle C, Hill TJ. Natural and experimental poxvirus infection in the domestic cat. *Vet Rec.* 1983;112:164–170.
- (7) Gross TL, Ihrke P, Walder E, Affolter VK. Ulcerative and crusting diseases of the epidermis. In: *Skin diseases of the dog and cat: clinical and histopathologic diagnosis.* 2nd ed. Blackwell Science. 2005; 116-135.
- (8) Hargis AM, Ginn PE. Feline herpesvirus 1-associated facial and nasal dermatitis and stomatitis in domestic cats. *Veterinary Clinics of North America: Small Animal Practice Vet Clin N Am-Small* 1999; 29:1281–90.
- (9) Herder V, Wohlsein P, Grunwald D et al. Poxvirus infection in a cat with presumptive human transmission. *Vet Dermatol* 2011; 22:220–4.
- (10) Jungwirth N, Puff C, Koster K, Mischke R, Meyer, H, Stark, A, Thoma, B, Zoller G, Seehusen F, Hewicker-Trautwein M, Beineke A, Baumgartner W, Wohlsein P. Atypical Cowpox virus infection in a series of cats. *J Comp Path;* 2018 158:71-76
- (11) Lanave G, Dowdglar, Decaro N, Albanese F, Brogi E, Parisi A, Losurdo M, Lavazza A, Martella V, Buonavoglia C, Elia G. Novel orthopoxvirus and lethal disease in cat, Italy.
- (12) Osterrieder K. Familie Poxviridae. In: Selbitz H-J, Truyen U, Peter V-W, eds. *Tiermedizinische Mikrobiologie, Infektions- und Seuchenlehre.* 9. Auflage. Stuttgart: Enke-Verlag. 2011;420-434.
- (13) Schaudien D, Meyer H, Grunwald D et al. Concurrent infection of a cat with cowpox virus and feline parvovirus. *J Comp Pathol.* 2007;137:151–4.

- (14) Schöniger S, Chan DL, Hollinshead M et al. Cowpox virus pneumonia in a domestic cat in Great Britain. *Vet Rec.* 2007;160:522–3.
- (15) Schulze C, Alex M, Schirmeier H et al. Generalized fatal Cowpox virus infection in a cat with transmission to a human contact case. *Zoonoses Public Hlth.* 2007; 54:31–7
- (16) Schupp P, Pfeffer M, Meyer H, Burck G, Kolmel K, Neumann C. Cowpox virus in a 12-year-old boy: rapid identification by an orthopoxvirus-specific polymerase chain reaction. *Brit J Dermatol* 2001;145:146-150
- (17) Stagegard J, Kurth A, Stern D, Dabrowski PW, Pocknell A, Nitsche A, Schrick L. Seasonal recurrence of cowpox virus outbreaks in captive cheetahs (*Acinonyx jubatus*). *PLOS One*; 2017; 12(11)e0187089.



Haired skin, cat. Higher magnification demonstrates the profound epidermal hyperplasia with nodular downward growth of rete ridges. Erosion of the epidermis has resulted in marked intercellular edema, and there is marked dermal inflammation. (HE, 88X)

infundibulum; part of the lesion is covered by a serocellular crust. There is a mild hyperkeratosis and mild to severe hyperpigmentation. In most areas, the basement membrane is intact with neoplastic cells confined to the epidermis with dysplasia of all layers with loss of the polarity of the cell nuclei and loss of the normal stratification of the keratinocytes. Some keratinocytes are small with hyperchromatic nuclei, others are rather large with vesicular nuclei.

Groups of cells are dorsoventrally protracted and bent in one direction, exhibiting a "wind-blown" appearance. Nuclei are large, round to oval, centrally placed, and vesicular with finely stippled chromatin and one to two prominent round magenta nucleoli. There is a mild to moderate anisocytosis and anisokaryosis. The number of mitotic figures range from 0 to 4 per high power field. Multifocally, dark basophilic round structures are present within the neoplastic cells, interpreted as apoptotic bodies. In the dermis a mild, perivascular infiltration of neutrophils, lymphocytes and macrophages is present and few mast cells are observed. Multifocally there is moderate dermal fibrosis.

Contributor's Morphologic Diagnoses: Epidermal hyperplasia and dysplasia, focally

CASE III: E2337 (JPC 4090973)

Signalment: 13-year old female domestic European shorthair cat (*Felis catus*)

History: The affected skin displayed a plaque-like lesion with irregular edges.

Gross Pathology: The tissue sample submitted for histopathological examination had an extension of 1,2 cm consisting of skin and subcutis.

Laboratory results: None given.

Microscopic Description:

Haired skin: There is an area of irregular epidermal hyperplasia with formation of rete ridges, also affecting the hair follicle

extensive, severe (Bowenoid *in situ* carcinoma – BISC)

Contributor's Comment: The morphologic findings are compatible with a Bowenoid *in situ* carcinoma (BISC) or Bowen-like disease, an uncommon premalignant lesion in middle-aged to old cats, that has been rarely reported in dogs.^{5,6}

Grossly, irregular, slightly elevated to heavily-crusting plaques and verrucous or papillary lesions up to 5.0 cm in diameter are found on haired, pigmented or non-pigmented skin at any site of the body.^{3,5,6} Usually, multiple lesions occur, but also solitary lesions are seen infrequently.⁴ Lesions are reported to be chronic, not painful, and only mild pruritus is noted.³ There is neither a causal correlation to sunlight exposure nor a breed or sex predilection.^{5,6}

Several studies suspect that papillomavirus infection may be associated with feline BISC *in situ*.^{3,7,8} In two studies, papillomavirus-antigen was detected in 11% and 48% of BISC *in situ*, respectively, using immunohistochemistry.^{7,8}

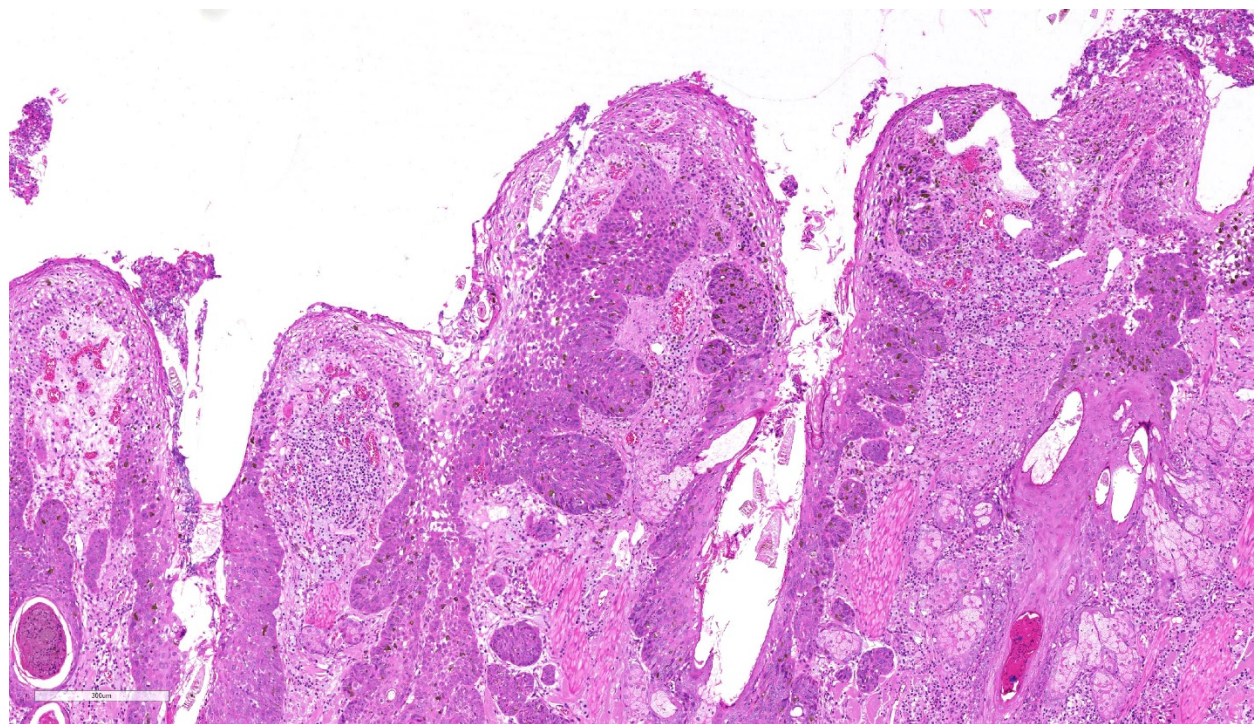
Contributing Institution:

Institute of Veterinary Pathology at the Centre for Clinical Veterinary Medicine LMU, Munich

Veterinaerstr. 13; 80539 Munich Germany

JPC Diagnosis: Haired skin: Bowenoid squamous cell carcinoma *in situ*.

JPC Comment: John Templeton Bowen, MD was a quiet professor of dermatology who spent his days at Harvard Medical School dodging patients, preferring to read slides. In 1912, he published a paper on a particular form of precancerous chronic dermatosis. As his proposed name of



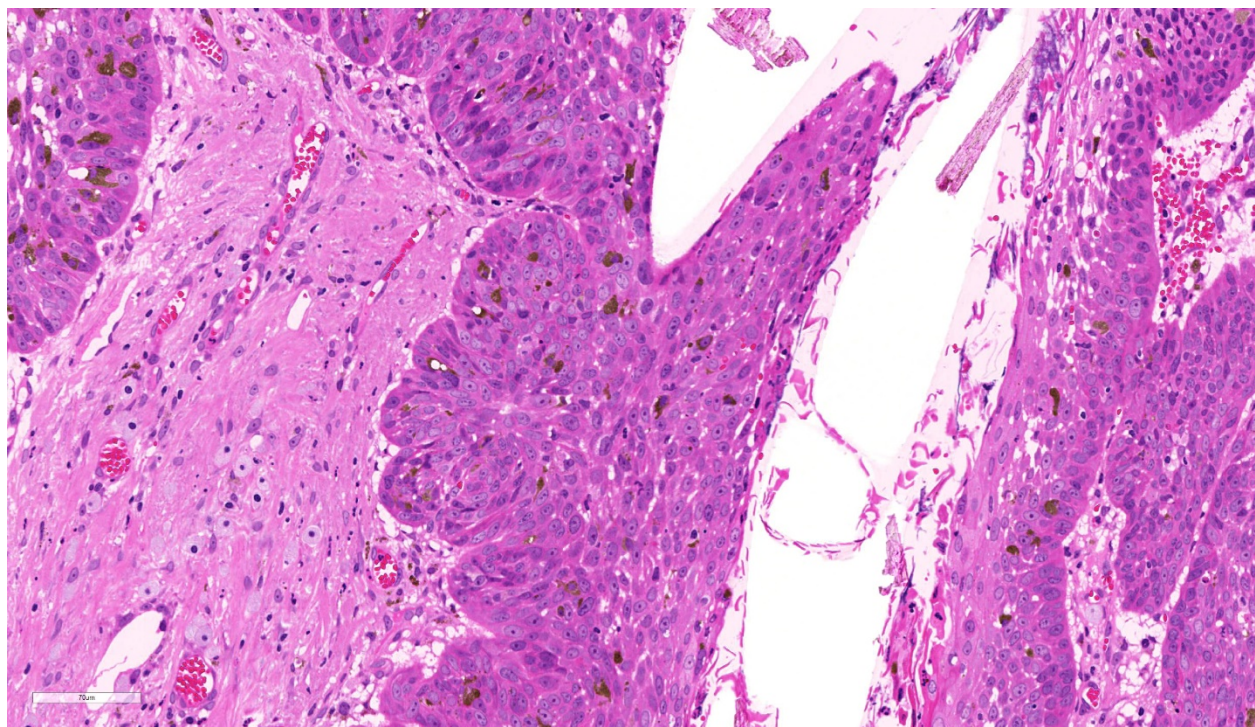
Haired skin, cat. At subgross magnification, there is marked thickening of the epidermis and follicular epithelium within the center of the section. (HE, 88X)

“dyskeratosis lenticularis et discoides” didn’t appear to catch on widely, Dr. Jean Darier (who already had Darier’s disease named after him, so he wasn’t really in the game anymore) suggested in his rather aptly named 1914 textbook on dermatology, *A Textbook on Dermatology*, that this condition simply be called Bowen’s disease.¹ Bowenoid papulosis, a proliferative lesion of the genitals resulting from infection by human papillomavirus 16 or 18, was named in Bowen’s honor in 1977, 37 years after his death, when he couldn’t refuse.

In humans, Bowen’s disease is the eponym commonly applied to cutaneous squamous cell carcinoma *in situ*. It appears as a sharply margined erythematous scaly or verrucous, often pigmented plaque. It may be appear in sun-exposed areas of skin, or other areas where it may be associated with HPV infection or exposure to inorganic arsenic.⁹

In the cat, Bowenoid *in situ* carcinoma (BISC) presents as one or multiple thickened areas of the epidermis, which may present as a thick plate of keratin due to its propensity for overlying orthokeratotic or parakeratotic hyperkeratosis.⁴ This keratinization may extend into follicles which may become dilated and plugged with keratin debris. Over time, BISCs may progress to a nodular mass which bulges into the underlying dermis.⁴

The histologic features of the risks are characteristic. Poorly lesions display basal cell crowding and a loss of nuclear polarity and stratification. Cells within the stratum spinosum and even more superficial levels are enlarged with prominent nuclei and nucleoli are more consistent with cells of the basal layer. Mitoses may be present at any level in the dermis. Alternatively, as seen in this case discs may demonstrate a more basaloid pattern, with proliferation of epithelial cells with minimal cytoplasm and



Haired skin, cat. Within the affected epidermal and follicular epithelium, there is inappropriate maturation (dysplasia) with a similarity of nuclei at all levels, lack of keratohyaline granules, and mitotic figures at all levels of the epidermis. (HE, 137X)

large often hyperchromatic nuclei. Melanization of these of the epithelial cells as well as macrophages in the underlying dermis is often seen in these lesions.⁴

Feline papilloma virus has been repeatedly isolated from lesions in this type, and cytopathic effects, such as koilocyte formation, associated with papillomavirus infection may be seen in early lesions. Similar changes are rarely seen in advanced lesions.⁴

Cats that develop one BISC are likely to develop additional lesions over time. Histologic differentials include invasive squamous cell carcinoma and actinic keratosis. The differentiation between a BISC and a SCC is made by careful examination to insure that all cells are confined within the basement membrane. Differentiation between actinic keratosis and a BISC may be more difficult unless papilloma virus-induced cell changes are present. As opposed to the BISC, actinic keratosis demonstrates random loss of nuclear polarity of the basal cells only, a poorly defined interface between normal and affected epidermis, and most importantly a lack of thickening and dysplasia of the follicular infundibulum.⁴

The association between feline papilloma virus infection in the cat in the development of BISC is well-known and consistent with an emerging body of knowledge associating papillomavirus infection and malignant transformation of epithelial neoplasms in cats and many other species. In the cat, *Felis catus* papilloma virus 2 and 3 (FcPV-2 and -3) have been isolated from BISC lesions. Other lesions associated with feline papillomavirus infection including feline viral plaques (FcPV-1 and -2) and FcPV-2 been detected not only in BISCs but in up to 50% of invasive SCC lesions in this species.

Feline sarcoid is a rare neoplasms of the skin of the nose limbs, or digits of young to middle-aged cats; however, the papillomavirus that has been isolated from these lesions has extensive similarity in the DNA to bovine papillomavirus 1 and 2 and may represent a novel bovine papilloma virus.

The moderator discussed the requirements and methods for differentiation between papillomavirus-induced lesion and similar lesions that might be induced by actinic damage. The moderator suggested that the cellular proliferation extending deep into hair follicles as well as the bulbous outgrowth of neoplastic cells perpendicularly outward from the affected follicles is more suggestive of viral induction than actinic induction.

References:

1. Arora H, Arora S, Sha V, Nouri K. John Templeton Bown. *JAMA Derm*; 2015; 191(13):1329.
2. Baer KE, Helton K. Multicentric squamous cell carcinomas *in situ* resembling Bowen's disease in cats. *Vet Pathol*.1993; 30: 535-543.
3. Favrot C, Welle M, Heimann M, Godson DL, Guscetti F. Clinical, histologic and immunohistochemical analyses of feline squamous cell carcinoma *in situ*. *Vet Pathol*. 2009; 46:25-33.
4. Goldschmidt MH. Munday JS, Scruggs JL, Klopffleisch R. Kiupel M. In *Surgical Pathology of Tumors of Domestic Animals Vol. 1: Epithelial tumors of the skin*. 3rd ed., Gurnee, IL: C.L. Davis and S.W. Thompson Foundation; 2018: 47-51.
5. Gross TL, Ihrke PJ, Walder EJ, Affolter VK. *Skin diseases of the dog and cat: clinical and histopathological diagnosis*, 2nd ed.

Oxford, UK: Blackwell science; 2005: 148-151, 575-584.

6. Mauldin EA, Peters-Kennedy J. Integumentary System. In: Maxie MG, Hrsg. Jubb, Kennedy, and Palmer's Pathology of Domestic Animals. 6. Aufl. Edinburgh: Elsevier; 2016; 706-714.

7. Munday JS, Kiupel M. Papillomavirus-associated cutaneous neoplasia in mammals. *Vet Pathol.* 2010; 47: 254-264.

8. Nicholls PK, Stanley MA. The immunology of animal papillomaviruses. *Veterinary Immunology and Immunopathology* 2000; 73: 101-27.

9. Patterson JW, Wick MR. Epidermal tumors. In AFIP Atlas of Tumor Pathology, Fourth Series. Non-melanocytic lesions of the skin. ARP Press, Bethesda MD. 2006: pp. 32-35.

CASE IV: 16-859 ((JPC 4084013))

Signalment: 8-year-old castrated male domestic shorthair cat, *Felis catus*

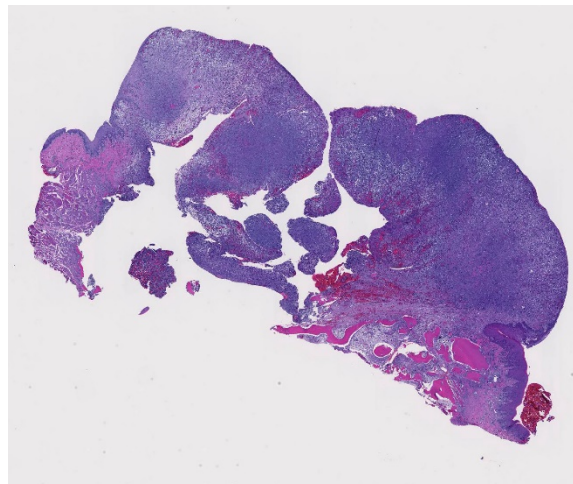
History: Presented with a 1cm mass around the right lower canine. The referring veterinarian removed the mass, tooth, and part of the mandible.

Gross Pathology: None given.

Laboratory results: None given.

Microscopic Description:

There is almost diffuse gingival ulceration with necrosis of the exposed lamina propria, fibrin deposition, and neutrophil infiltration. Underlying this there is early granulation



Gingiva, cat. A 1.2 x 0.5cm mass expands the submucosa and elevates the overlying ulcerate mucosa. (HE, 5X)

tissue proliferation that blends into a deeper, poorly-demarcated population of plump spindle cells arranged in streams and admixed with large numbers of multinucleated giant cells. Cells are occasionally separated by amorphous eosinophilic material (presumed osteoid). The nuclei have finely stippled chromatin and a central prominent nucleolus. This area is surrounded by fibrosis with scattered lymphocytes and plasma cells. Occasionally there are central areas of necrosis with hemorrhage, neutrophils, and rarely a raft of filamentous bacteria is present (in some slides). At the periphery of the mass there are fragments of pre-existing lamellar bone with varying amounts of woven bone. Bone fragments are lined by primarily by osteoblasts with rare osteoclasts in Howship's lacunae. There are also tooth fragments surrounded by fibrosis. The remaining gingival epithelium is hyperplastic.

Contributor's Morphologic Diagnoses:

Gingiva: Peripheral giant cell granuloma

Contributor's Comment: Peripheral giant cell granulomas were previously referred to as giant cell epulides.⁷ These are ulcerated

masses composed of a poorly demarcated proliferation of fibroblasts and blood vessels (resembling granulation tissue) with prominent multinucleated giant cells. Osteoid-like material may be present. Cellular pleomorphism, mitoses and anaplastic cells are absent. Unlike the fibromatous epulis and acanthomatous ameloblastoma, these tumors lack an epithelial component, although the gingival epithelium adjacent to the areas of ulceration is, as expected, hyperplastic.¹

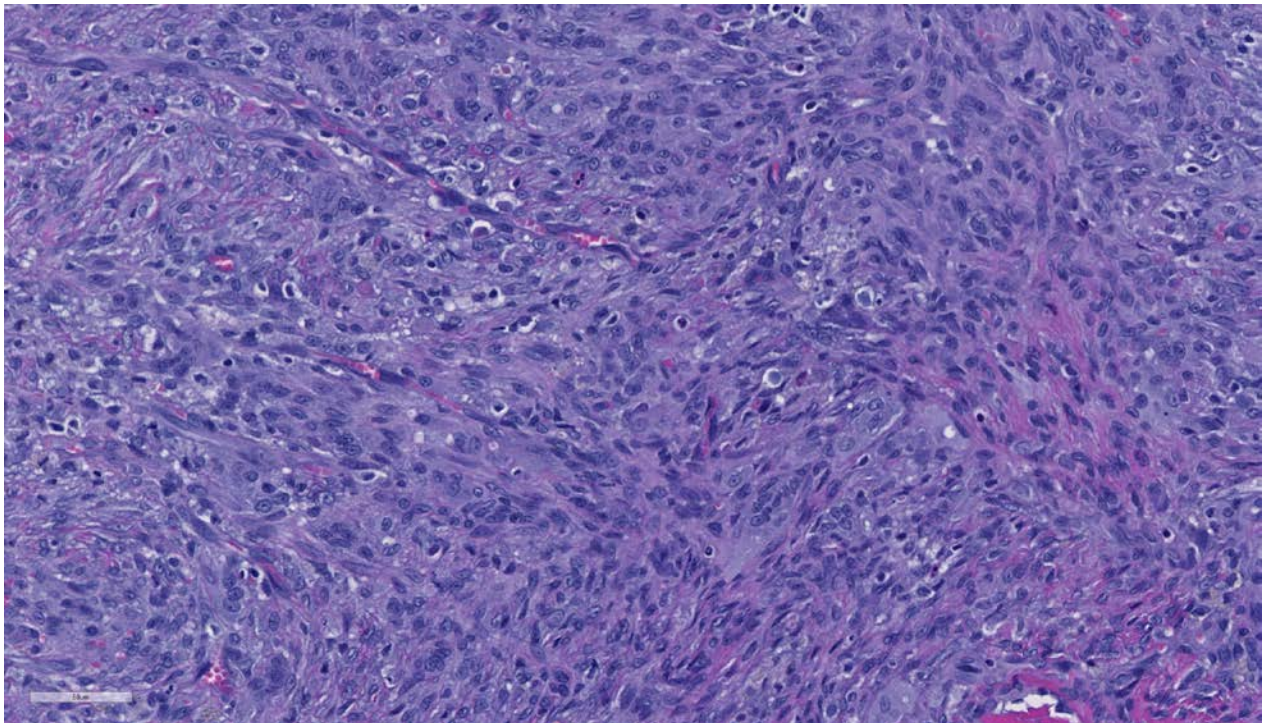
In cats, peripheral giant cell granulomas (giant cell epulis) are the second most common gingival tumor (28.8%) after fibromatous epulis (57.7%). The reported range for age of onset is 4-19 years. Compared to the fibromatous epulis, giant cell epulides are more likely to be ulcerated, grow more rapidly, rapidly recur following

excision, and are more likely to result in the death or euthanasia of the cat.¹

Immunohistochemical stains have shown the multinucleated giant cells to be positive for vimentin, tartrate-resistant acid phosphatase (TRAP; osteoclast marker) and the polyclonal antibody receptor activator of nuclear factor $\kappa\beta$ (RANK; involved in osteoclast maturation)³ while being negative for smooth muscle actin, MIB-1 (proliferation marker) and factor VIII. These findings suggest an osteoclastic, as opposed to macrophage, origin for the multinucleated giant cells.¹

Peripheral giant cell granulomas are regarded as hyperplastic (reactive) and have occurred at sites of tooth extraction.⁷

Contributing Institution:



Gingiva, cat. The lesion is composed primarily of plump fibroblasts forming tightly packed short streams and bundles oriented in various planes. (HE, 400X)

University of Tennessee, College of Veterinary Medicine, Department of Biomedical and Diagnostic Sciences
<http://www.vet.utk.edu/departments/path/index.php>

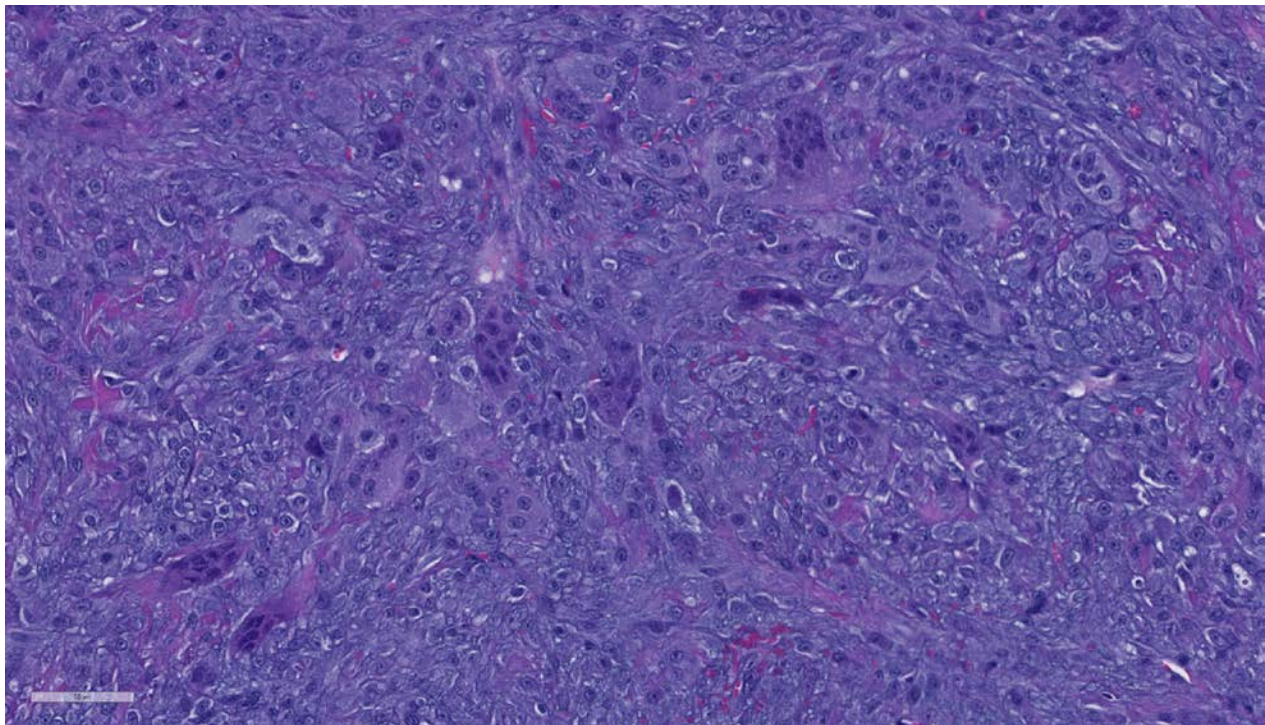
JPC Diagnosis: Gingiva: Peripheral giant cell granuloma.

JPC Comment:

The contributor does an excellent job of describing this poorly-named reactive lesion. The term “peripheral giant cell granuloma” has been lifted from the human literature, although this lesion bears no resemblance to a true granuloma. The term “peripheral” is used to differentiate this lesion from its identical intraosseous or “central” counterpart. It has been classified previously as an epulis³, another relatively non-specific term for a “tumor-like mass on the gingiva” which also appears to be falling from common usage today.

In the human, where this lesion is best defined, it represents an exuberant reparative response to local trauma or irritation. These lesions are seen exclusively in the gingiva and presumably arises from the periodontal ligament or periosteum. They typically present as red-blue, broad-based masses in the gingiva around the incisors and premolars (a location that is shared in the cat and dog as well).⁵ They are seen at any age in the human and tends to be seen more commonly in females than in males. . The appearance of multinucleated giant cells is unusual and the reason for the presence of this cell type remains unknown; they appear to be nonfunctional in the usual sets of either phagocytosis or bone resorption. Islands of metaplastic bone may occasionally be seen in this lesion.

A number of peripheral giant cell granulomas have been published in the dog as well^{2,4} An article by DeSoutter et al.⁴ demonstrates an



Gingiva, cat. Numerous multinucleated polygonal cells are scattered throughout the lesion. (HE, 400X)

almost identical lesion in the area of the incisors or premolars (the characteristic lesion in humans as well) described as an “classic” peripheral giant cell granuloma, as well as a number of open “collision” peripheral giant cell granulomas, with features of both a peripheral giant cell granuloma and a fibromatous epulis of periodontal ligament origin. In contrast to the lesion in cats, peripheral giant cell granulomas in the dog behave more like fibromatous epulides of periodontal ligament origin and seldom recur after excision. Multinucleated cells in the canine lesion also exhibits positive staining with tartrate-resistant acid phosphatase (TRAP).

The ultimate diagnosis of this case engendered spirited discussion. A number of attendees identified osteoid amidst the spindle cell population, favoring a diagnosis of osteosarcoma in this case. Consultation from the oral pathology human subspecialists confirmed the lesion to a peripheral giant cell granuloma; the presence of osteoid is not uncommon in their experience. The presence of large islands of dental and woven bone in one area of the section, was attributed to products of the extracted tooth and section of manible surrounding it..

References:

1. DeBruijn ND, Kirpensteijn J, Neyens IJS, et al. A clinicopathological study of 52 feline epulides. *Vet Pathol.* 2007;44:161-169.
2. DeSoutter AV, Goldschmidt MH, Sanchez MD. Clinical and histologic features of 26 canine peripheral giant cell granulomas (formerly giant cell epulis). *Vet Pathol* 2012; 49(6): 1018-1023.
3. Dubielzig RR. Tumors of Odontogenic Origin. *In* Head KW, Cullen JM, Dubielzig RR, Else RW, Misdorp W, Patnaik AK, Tateyama S, van der Gaag I., *Histological Classification of Tumors of the Alimentary System of Domestic Animals; Second Series, Volume X.* ARP Press, Bethesda, MD 2002: pp 56-57.
4. Hiscox LA, Dumais Y. Peripheral Giant Cell Granuloma in a Dog. *J Vet Dent*; 2015 32(2): 103-110.
5. Munday JS, Lohr CV, Kiupel MK. Tumors of the Alimentary Tract. *In*: Meuten DJ ed, *Tomorsin Domestic Animals*, 5th ed. Wiley-Blackwell, Ames IA, 2017; pp: 542-543.
6. Regezi JA, Sciubba JJ, Jordan RCK. Red-blue lesions. *In* *Oral Pathology: Clinical Pathologic Correlations*, 7th Ed. Elsevier Press, St. Louis MO 2017; 119-121
7. Uzal FA, Plattner BL, Hostetter JM. Alimentary system. *In*: Jubb, Kennedy and Palmer’s *Pathology of Domestic Animals*. 6th ed. Elsevier 2016: vol.2 p.21.

Self-Assessment - WSC 2017-2018 Conference 11

1. Infection of which of the following mesenchymal cell most likely develops into tissue cysts of *Benoitia besnoiti*?
 - a. Tissue histiocytes
 - b. Fibroblasts or myofibroblasts
 - c. Vascular endothelium
 - d. Lymphatic endothelium

2. Which of the following is NOT associate with the acute phase of besnoitiosis?
 - a. Formation of tissue cysts
 - b. Orchitis
 - c. Generalized subcutaneous edema
 - d. Lymphadenopathy

3. Which organ is the primary target for cowpox in the cat?
 - a. Lung
 - b. Mammary gland
 - c. Skin
 - d. Kidney

4. Which of the following viruses has been associated with Bowenoid squamous cell carcinoma in the cat:?
 - a. Herpesvirus
 - b. Retrovirus
 - c. Polyomavirus
 - d. Papillomavirus

5. Giant cells in peripheral giant cell granuloma will stain with which of the following immunohistochemical markers?
 - a. Cytokeratin
 - b. TRAP
 - c. S-100
 - d. Synaptophysin

Please email your completed assessment to Ms. Jessica Gold at Jessica.d.gold2.ctr@mail.mil for grading. Passing score is 80%. This program (RACE program number) is approved by the AAVSB RACE to offer a total of 0.5 CE Credits, with a maximum of 12.5 CE Credits being available to any individual Veterinary Medical Professionals for the 2017-2018 Wednesday Slide Conference. This RACE approval is for the subject matter categories of: SCIENTIFIC using the delivery method of NON-INTERACTIVE DISTANCE. This approval is valid in jurisdictions which recognize AAVSB RACE; however, participants are responsible for ascertaining each board's CE requirements. RACE does not "accredit", "endorse" or "certify" any program or person, nor does RACE approval validate the content of the program.

Please email your completed assessment to Ms. Jessica Gold at Jessica.d.gold2.ctr@mail.mil for grading. Passing score is 80%. This program (RACE program number) is approved by the AAVSB RACE to offer a total of 0.5 CE Credits, with a maximum of 12.5 CE Credits being available to any individual Veterinary Medical Professionals for the 2017-2018 Wednesday Slide Conference. This RACE approval is for the subject matter categories of: SCIENTIFIC using the delivery method of NON-INTERACTIVE DISTANCE. This approval is valid in jurisdictions which recognize AAVSB RACE; however, participants are responsible for ascertaining each board's CE requirements. RACE does not "accredit", "endorse" or "certify" any program or person, nor does RACE approval validate the content of the program.

**Joint Pathology Center
Veterinary Pathology Services**



WEDNESDAY SLIDE CONFERENCE 2018-2019

C o n f e r e n c e 1 2

12 December 2018

Conference Moderator:

Mark T. Butt, DVM, DACVP
President, Tox Path Specialists (TPS), LLC
8420 Gas House Pike, Suite G
Frederick, MD 21701

CASE I: 065/Case 1 (JPC 4049888)

Signalment: Juvenile female common marmoset (*Callithrix jacchus*).

History: Two juvenile common marmosets (*Callithrix jacchus*) from the German Primate Center were presented to the veterinarian. They showed depression, pyrexia, anorexia, and multiple facial skin ulcerations. Neither animal responded to antibiotic and analgesic treatment and both developed severe neurological signs including clonic seizures, disorientation, and circular movements before they died within few days after disease onset.

Gross Pathology: Both monkeys revealed multiple erosions and ulcerations of the facial skin, especially at mucocutaneous junctions, and on the tongue. Lingual lesions presented as multifocal to coalescing dark red mucosal indentations with distinct, variably raised margins, measuring between 0.5 and 1 cm in

diameter, and sometimes covered by a fibrinosuppurative exsudate. Besides severe lymphadenopathy of the associated mandibular and cervical lymph nodes and mild splenomegaly, no other gross lesions were detected.

Laboratory results: Brain, tongue and skin tissues were positive for HHV1 antigen, detected by immunohistochemistry (particularly in central neurons and



Tongue, common marmoset: There are multifocal areas of lingual necrosis, some with a raised white rim. (Photo courtesy of: German Primate Center, Pathology Unit, Kellnerweg 4, 37077 Göttingen, Germany, www.dpz.eu)

keratinocytes). Transmission electron microscopy revealed numerous 1 herpes virions with characteristic electron-dense core, capsid and envelope in cutaneous keratinocytes.

Microscopic Description:

Brain: Multifocally throughout the grey and to a lesser extent in the white matter of cerebrum, brainstem and cerebellum, there are mild to moderate inflammatory foci, either concentrated around blood vessels (perivascular cuffing) or scattered within the neuropil. The inflammatory infiltrate consists of lymphocytes, histiocytes, neutrophils and fewer plasma cells, often admixed with mild karyorrhexis, karyolysis and pyknosis (necrotic neutrophils). The affected neuropil in addition reveals mild to moderate scattered to nodular gliosis and several shrunken, angular and hypereosinophilic neurons with hyperchromatic nuclei (neuronal necrosis). Within very few glia cells and degenerate neurons, there are conspicuous large basophilic intranuclear inclusions, which marginate the chromatin. Perivascular cuffing is often associated with mild endothelial hypertrophy. Meningeal blood vessels are often engorged with erythrocytes (hyperemia) together with moderate to marked intravascular stasis of leucocytes, mainly neutrophils, and multifocal mild to moderate perivascular inflammatory infiltration as previously described. Multifocally within the cerebral white matter, there is also mild to moderate dilation and vacuolation of Virchow-Robin spaces (edema).

Tongue: There is multifocal to coalescing ulceration of the lingual surface with the extensively lost mucosal epithelium being replaced by a thick serocellular crust composed of fibrin, varying amounts of viable and degenerate neutrophils and multifocal coccoid bacterial colonies. In



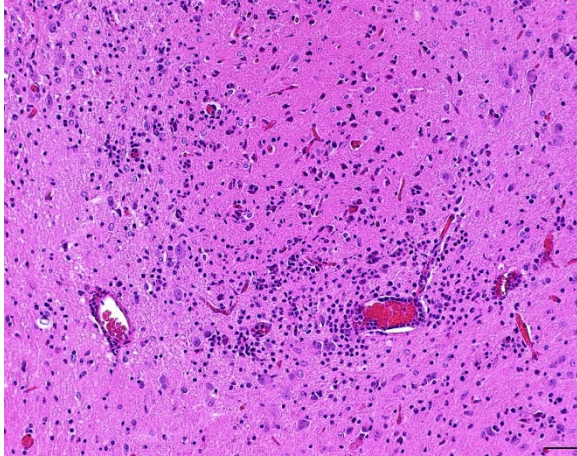
Brain, common marmoset: A section of cerebrum and cerebellum/brainstem are submitted for examination. There are no visible lesions at subgross examination. (HE, 5X)

areas with less extensive ulceration, circumvallate papillae are multifocally expanded by intraepithelial clefts filled with variable amounts of viable and degenerate neutrophils, fibrin, edema, and few acantholytic keratinocytes (vesicopustules). Ulcerations and pustules are multifocally flanked by groups of degenerate or necrotic keratinocytes, often bearing large eosinophilic to amphophilic, homogenous intranuclear inclusions with marked margination of chromatin. The adjacent epithelium is mild to moderately hyperplastic, characterized by acanthosis and intracellular edema. Fibrin, mild hemorrhage and edema together with varying numbers of neutrophils, histiocytes, fewer lymphocytes and plasma cells moderately expand the adjacent subepithelial connective tissue and separate superficial skeletal muscle fibers and individual myocytes.

Contributor's Morphologic Diagnoses:

Central nervous system:

Cerebrum, cerebellum and brainstem: Meningoencephalitis, lymphohistiocytic and neutrophilic, multifocal, moderate, subacute



Brainstem, common marmoset: Within the brainstem white matter, there are focal areas of gliosis with formation of glial nodules as well as mild lymphocytic perivascular cuffing. (HE, 100X) (Photo courtesy of: German Primate Center, Pathology Unit, Kellnerweg 4, 37077 Göttingen, Germany, www.dpz.eu)

with neuronal necrosis, gliosis and very few glial and neuronal homogenous basophilic intranuclear inclusion bodies; common marmoset (*Callithrix jacchus*), nonhuman primate.

Tongue:

Glossitis, vesicopustular to ulcerative, multifocal to coalescing, subacute, marked with fibrinous to serocellular crusting and epithelial homogenous eosinophilic to amphophilic intranuclear inclusion bodies; common marmoset (*Callithrix jacchus*), nonhuman primate.

Contributor's Comment: Herpesviridae are global pathogens of almost every vertebrate species. In their natural hosts, they do not cause fatal disease, but cross-species infection can cause acute death^{1,10}.

Infection with Human Herpesvirus 1 (HHV1), an alphaherpesvirus, leads to mild mucosal lesions or an inapparent course in the natural host (human).^{9,13} Fatal encephalitis and/or systemic disease can occur in neonates or immune compromised individuals.^{7,14} In humans, infection with

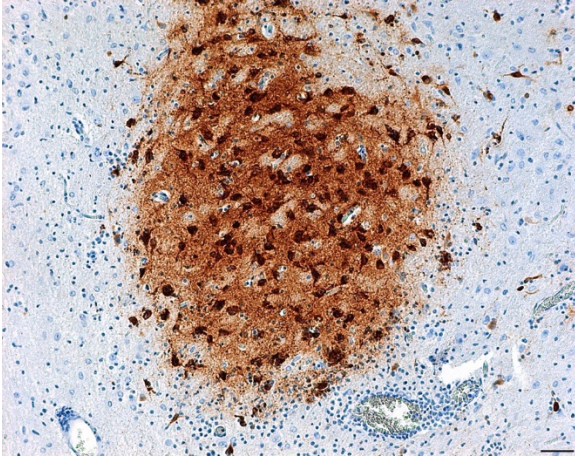
HHV1 persists lifelong because of viral latency in sensory neurons. When immunity is compromised through stress or disease, it becomes activated through suppression of the latency-associated transcript gene.¹¹ It can be shed even in the absence of visible lesions.

Several nonhuman primate species are susceptible to infection with human herpesviruses. Old World Primates like gorillas (*Gorilla gorilla*), bonobos (*Pan paniscus*), white handed gibbons (*Hylobates lar*) and chimpanzees (*Pan troglodytes*), can be naturally infected with HHV1. Although single fatal disease outcomes have been described,^{2,6} their virus-host relationship seems to be similar to that in humans, as they usually show only mild symptoms (lesions in mucocutaneous tissue, skin, conjunctiva).¹⁰

However, New World monkey species and prosimians are highly susceptible to HHV 1 infections.^{1,4,5,9,10} Typical lesions in these species are erosions and ulcers of oral mucous membranes, especially the tongue, and mucocutaneous junctions of the lips. Severe necrotizing hepatitis and multifocal nonsuppurative meningoencephalitis often occur in these species.^{5,10} Thus, in cases of ulcerative skin lesions in nonhuman primates, HHV1 has to be considered as a possible cause and callitrichids represent a highly susceptible species for HHV1 infections.

The exact route of transmission is unknown, but likely occurs via direct mucosal contact, wounds, saliva, maternal milk, contaminated fomites and through airborne and waterborne routes.⁶ Additionally, direct transmission from latently infected humans to their monkey pets is described.

In the present case, possible sources of virulent HHV1 are animal keepers or visitors. HHV1 specific PCR can be used for



Brainstem, common marmoset: Multifocally, brainstem neurons within areas of gliosis stain strongly positive for human herpesvirus-1. (Photo courtesy of: German Primate Center, Pathology Unit, Kellnerweg 4, 37077 Göttingen, Germany, www.dpz.eu)

antemortem diagnostics to allow appropriate treatment with antiviral drugs. Viral antigen can be detected in histological sections of lesions by immunohistochemistry and Transmission electron microscopy can serve as a useful tool to seek for viral particles.

Contributing Institution:

German Primate Center, Pathology Unit, Kellnerweg 4, 37077 Göttingen, Germany www.dpz.eu

JPC Diagnosis: 1. Tongue: Glossitis, necrotizing, focally extensive, moderate, with ulceration, epithelial syncytia and intranuclear viral inclusions.

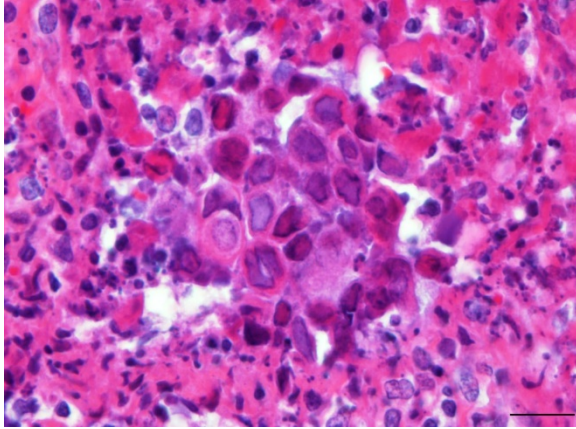
2. Cerebrum and brainstem: Encephalitis, necrotizing, multifocal, mild to moderate with gliosis, perivascular cuffing, and rare intranuclear viral inclusions.

JPC Comment: The contributor has provided an excellent overview of cross-species herpesviral infection, in this case human herpesvirus 1 (human simplex virus 1) and its devastating effects on New World primates.

Cross species infection by alphaherpesviruses has been well known to result in tragic circumstances, via zoonotic and reverse-zoonotic (as seen here) means, as well as between diverse animal species. A review of the literature is replete with interesting cases, some of which are recounted here.

Perhaps the most famous case of interspecies transmission of herpesvirus was described in a case report by Albert Sabin, MD (who would go on to develop the oral polio vaccine) in 1932, who described an ascending paralysis in an accomplished young physician and research colleague following a “monkey bite”. For many years, this researcher was simply known as “W.B”, while the agent isolated from his neural tissue gained great renown as the “B virus” (now known as macacine herpesvirus-1) which has claimed 70% of its known victims over the years due to fatal encephalitis. In 1985, that young researcher’s name was finally published, Dr. William Barlett Brebner (1903-1932).¹²

Equine herpesvirus-1 (EHV-1) is a well-known pathogen of horses that is known to cause a wide range of disease in its natural host, but may also result in disease in widely disparate mammalian species as well. A 2011 article¹⁵ details fatal encephalitides characterized by non-suppurative meningo-encephalitis, which were shown to be caused equine herpesvirus 1 in four black bears (*Ursus americanus*), two Thompson gazelles (*Eudorcas thomsoni*) and eighteen guinea pigs (*Cavia porcellus*). In addition, a closely-related herpesvirus, equine herpesvirus-9 (EHV-9), thought to have originated in the plains zebra (*Equus burchelli*), has been known to cause fatal encephalitis in polar bears.³ Pseudorabies virus (*Suid herpesvirus-1*) is another alphaherpesvirus with a wide host range. Primarily infecting swine (who are the natural reservoir),



Tongue, common marmoset: Nuclei of basal epithelium of the lingual mucosa contain viral inclusions and rare syncytia are present. (HE, 400X) (Photo courtesy of: German Primate Center, Pathology Unit, Kellnerweg 4, 37077 Göttingen, Germany, www.dpz.eu)

secondary mammalian hosts abound, including cattle, horses, dogs, mink, and cats. Human infection, although possible in immunocompetent humans has been limited to non-fatal conditions.

One final tragic cross-species herpesviral infection has resulted in the death of over 100 young captive and wild Asian elephants from a rapid-onset, acute hemorrhagic disease caused primarily by multiple distinct strains of two closely related chimeric variants of a novel herpesvirus species designated elephant endotheliotropic herpesvirus (EEHV1A and EEHV1B). These and two other species of *Probosciviruses* (EEHV4 and EEHV5) are evidently ancient and also result in commonly asymptomatic infections of adult Asian. Although only a few similar cases have been observed in African elephants, they harbor similar viruses—EEHV2, EEHV3, EEHV6, and EEHV7—have been isolated in African elephants in lung and skin nodules or saliva. For reasons not yet understood, approximately 20% of Asian elephant calves appear to be susceptible to the disease when primary infections are not controlled by normal innate cellular and humoral immune responses.⁸

References:

1. Costa EA, Luppi MM, Malta Mde C et al. Outbreak of human herpesvirus type 1 infection in nonhuman primates (*Callithrix penincillata*). *J Wildl Dis.* 2011;**47**:690-693.
2. Emmons RW, Lennette EH: Natural herpesvirus hominis infection of a gibbon (*Hylobates lar*). *Arch Gesamte Virusforsch.* 1970; **31**:215-218.
3. Greenwood AD, Tsangaras K, Ho SYW, Szentiks CA, Nikolin VM, Ma G, Daminani A, East ML, Lawrenz A, Hofer h, Oserrieder N. A potentially fatal mix of herpes in zoos. *Curr Biol* 2012; **22**:1727-1732.
4. Huemer HP, Larcher C, Czedik-Eysenberg T, Nowotny N, Reifinger M. Fatal infection of a pet monkey with Human herpesvirus. *Emerg Infect Dis.* 2002;**8**:639-642.
5. Juan-Salles C, Ramos-Vara JA, Prats N, Sole-Nicolas J, Segales J, Marco AJ. Spontaneous herpes simplex virus infection in common marmosets (*Callithrix jacchus*). *J Vet Diagn Invest.* 1997;**9**:341-345.
6. Kik MJ, Bos JH, Groen J, Dorrestein GM. Herpes simplex infection in a juvenile orangutan (*Pongo pygmaeus pygmaeus*). *J Zoo Wildl Med.* 2005;**36**:131-134.
7. Kleinschmidt-DeMasters BK, Gilden DH. The expanding spectrum of herpesvirus infections of the nervous system. *Brain Pathol.* 2001;**11**:440-451.
8. Long SY, Latimer EM, Hayward GS. Review of elephant endotheliotropic herpesviruses and acute hemorrhagic disease. *ILAR J;* 2016;**56**(3):283-296.
9. Longa CS, Bruno SF, Pires AR, et al. Human herpesvirus 1 in wild marmosets, Brazil, 2008. *Emerg Infect Dis.* 2011;**17**:1308-1310.

10. Mätz-Rensing K, Jentsch KD, Rensing S, et al. Fatal herpes simplex infection in a group of common marmosets (*Callithrix jacchus*). *Vet Pathol.* 2003;**40**:405-411.
11. Perng GC, Jones C, Ciacci-Zanella J, et al. Virus-induced neuronal apoptosis blocked by the herpes simplex virus latency-associated transcript. *Science.* 2000;**287**:1500-1503.
12. Pimmentel JD. Past professive: Herpes B virus – “B” is for Brebner: Dr. William Barlet Brebner (1903-1932), *Can Med Assoc J* 2018: 178(6):726.
13. Schrenzel MD, Osborn KG, Shima A, Klieforth RB, Maalouf GA. Naturally occurring fatal herpes simplex virus 1 infection in a family of white-faced saki monkeys (*Pithecia pithecia pithecia*). *J Med Primatol.* 2003;**32**:7-14.
14. Whitley RJ, Roizman B. Herpes simplex virus infections. *Lancet.* 2001;**357**:1513-1518.
15. Wohlsein P, Lehmecker A, Spitzbarth I, Algermissen D, Baumgartner W, Boer M, Kummrow M, aas L, Grummer B. Fatal epizootic equine herpesvirus 1 infections in new and unnatural hosts. *Vet Microbiol* 2011 149(3-4):456-460.

CASE II V13-12663 (JPC 4039359)

Signalment: Four year old female, Angus cow, *Bos taurus*,

History: The owner moved a herd of about 60 cattle from a pasture that was getting short of grass and water to an adjacent pasture with a separate water source. The environmental temperature for the time period was over 90° Fahrenheit (32° Celsius). The cattle had been on this pasture in the past. Two days after moving the cattle, two cows had died, two cows were recumbent and could not stand, and 11 head of cattle were staggering when walking. The two recumbent cows and



Cerebrum, ox. There are multifocal areas of malacia within the cortex. (Photo courtesy of: NMDA Veterinary Diagnostic Services, <http://www.nmda.nmsu.edu/vds/>)

eventually the 11 head of cattle that were staggering showed neurologic signs of blindness and “seizures” as described by the owner. All of these cattle with neurologic signs eventually died. In total, the owner lost 15 head of cattle. The owner had lost 22 head of cattle with a similar scenario about 3 years prior to this loss of cattle. The horses on the pasture were healthy with no clinical signs of illness.

Gross Pathology: The submitting veterinarian performed the postmortem examination with no significant gross findings. He submitted fresh and fixed tissues for examination. Upon arrival at the diagnostic laboratory, the fresh tissues were severely autolyzed. In the fixed brain, there were light yellow areas of malacia in the cerebral gray matter that fluoresced when placed under an ultraviolet light with a wavelength of 365 nm.

Laboratory results: The water on the pasture was determined to be of unsuitable quality and possibly toxic for cattle with a sulfate concentration of at least 4000 mg/L (ppm), which is the upper reference limit for sulfate at the laboratory testing the water.

Microscopic Description:

The cerebral gray matter of the brain contained multiple foci where the neuropil is pale-staining and vacuolated with prominent vasculature with swollen endothelial cells. The affected areas tend to involve the deep and middle lamina associated with the sulci, but often extend to the superficial lamina and extend up to the middle of the gyri. Within the affected foci, the neurons are often necrotic and are shrunken and hyper eosinophilic with angular borders and dark pyknotic nuclei. There are occasional areas in the affected foci and associated leptomeninges where there are perivascular infiltrates of small numbers of macrophages, lymphocytes, and glial cells.

Contributor's Morphologic Diagnoses:

Brain, cerebrum, gray matter -
Polioencephalomalacia

Contributor's Comment: Necrosis of the neurons in the lamina of the cerebral gray matter in cattle can be caused by sulfur toxicosis, thiamine deficiency, water deprivation/sodium ion toxicosis, lead intoxication, and ischemia/anoxia.^{1,4} The polioencephalomalacia in this case was most likely the result of sulfur toxicosis.

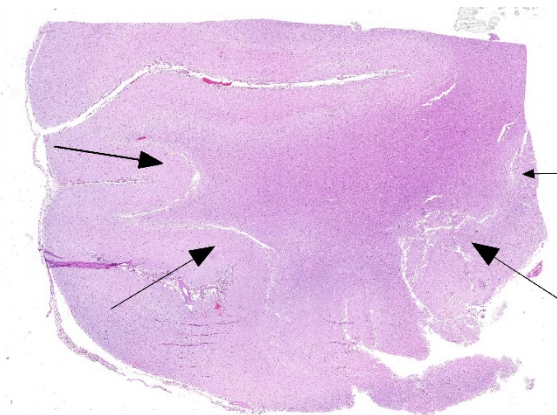
When calculating the sulfur content within ruminant diets, all sources including feedstuffs and water need to be considered and calculated into the total dietary consumption of sulfur.^{1,2} The dietary requirement of sulfur in beef cattle diets is not well defined. According to the National Research Council, the recommended concentration of sulfur in beef cattle diets is 1500 ppm with 4000 ppm being the maximum tolerable limit for sulfur in the diet.⁵ Thus, a 1000 pound (454 kg) cow consuming approximately 2% body weight of feed (9.08 kg) daily would have a maximum tolerable daily limit of 36.32 g of sulfur. At

90° F (32° C), it is estimated that a 454 kg cow would consume 20.6 gallons (78.0 liters) of water per day. In this case, the water contained at least 4000 mg/L sulfate. Thus, the cow consumed an estimated 104 g of sulfur in the water, which is almost 3 times the recommended tolerable daily limit of sulfur in the beef cattle diet.

The pathogenesis of how sulfur results in neuronal necrosis is not well defined. In the rumen, the excess sulfur is converted to hydrogen sulfide gas, which can be found in the rumen gas cap.^{1,2,4} There is evidence that sulfide inhibits cellular respiration, which could result in neuronal hypoxia sufficient enough to result in neuronal necrosis.² However, some have theorized that sulfite (an intermediate in the reduction of sulfate) cleaves thiamine into pyrimidine and thiazole rendering thiamine inactive thereby resulting in thiamine deficiency.⁴

Contributing Institution:

NMDA Veterinary Diagnostic Services,
<http://www.nmda.nmsu.edu/vds/>

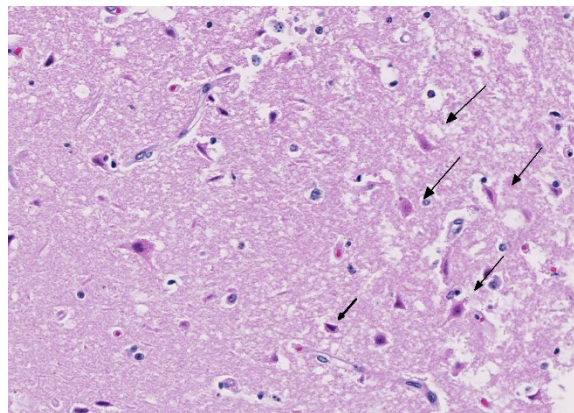


Cerebrum, ox. There is segmental areas of laminar necrosis within the deep laminae of the cerebral cortex. (HE, 6X)

JPC Diagnosis: Cerebrum: Necrosis and, cortical, laminar, multifocal to coalescing, with cavitation, spongiosis and gliosis.

JPC Comment: The contributor provides a concise yet thorough review of sulfur-induced polioencephalomalacia (PEM) in cattle. Although the first reports of PEM were published in the early 1900s, it was not until the 1970s that thiamine, or more properly its deficiency, was identified as a cause. Sulfur was first linked to PEM in the 1980s, when it was linked to the gypsum (calcium sulfate) added to cattle reactions to control feed intake would cause cerebral lesions, and its removal, decrease the incidence of PEM.⁵ While an interaction with thiamine was initially suspected, it is now known that PEM may be caused by the direct action of excess dietary sulfur independent of thiamine status.⁵

Thiamine, or vitamin B₁ is a dietary requirement in carnivores (unlike in ruminants, where it is produced via rumen microbes). Deficiency in carnivores may be the result of starvation or eating a diet high in finish that contains thiamine-splitting enzymes. High levels of sulfur in the diet may also destroys thiamine after it is metabolized into sulfate. As opposed to ruminants in which necrosis is generally seen within the cerebrum, the necrosis seen in carnivores on thiamine-deficient diets is seen in the primarily seen in basal areas including nuclei of the caudal colliculi, medial vestibular nuclei and the periventricular gray matter. The term “Chastek paralysis” applied to this constellation of lesions was coined in the 1930’s with the first outbreak of the condition in silver foxes on the Chastek fur farm in Minnesota. The outbreak, which killed a third of the farm’s population of silver foxes, was linked to the feeding of fresh fish.



Cerebrum, ox. At the edges of cavitation, neurons are dark, angular, and necrotic. (HE, 291X)

Thiamine encephalopathy is also well known in human medicine, where it is referred to as Wernicke’s encephalopathy. First described by Carl Wernicke in 1881, the condition is often seen in long-term alcoholics. Wernicke’s original cases initially underwent a subacute course of fatigue, unsteadiness, photophobia, vomiting, and weight loss. Initial neurologic syndromes manifested as acute gaze palsies, somnolence, and waxing and waning levels of orientation. These patient’s rapidly deteriorated into stupor and died within 7-14 days of admission, as thiamine was not discovered either as a vitamin or as the cause of this illness, during Wernicke’s lifetime.³ The lesions of Wernicke’s encephalopathy are similar to those seen in carnivores with Chastek paralysis, with bilaterally symmetrical lesions of the periventricular and periaqueductal gray matter, and the mammillary bodies.³

Another very interesting manifestation of thiamine deficiency is that of Alaskan Husky encephalopathy.⁶ This lethal syndrome in Huskies is associated with a mutation in the SLC19A3.1 gene which encodes a thiamine transporter-2 with a predominantly central nervous system distribution. This brain-specific thiamine deficiency ultimately leads to mitochondrial dysfunction and increased

oxidative stress in certain areas of the brain. Affected Huskies present with seizures, altered mentation, dysphagia, central blindness, hypermetria, and proprioception positioning deficits. Cavitory lesions are present in the thalamus, and smaller lesions are often present in the putamen, claustrum, and that the junction of the gray and white matter in the cortex, brainstem, and midline cerebellar vermis.⁶

From a terminology point of view, the moderator reminded the group that the term “cortex” should be applied to the cerebral gray matter and does not include the underlying white matter. There are six levels to the cortex (which are best seen in man and non-human primates).

References:

1. Gould DH. Polioencephalomalacia. *J Anim Sci.* 1998; 76: 309-314
2. Gould DH, Dargatz DA, Garry FG, et. al. *J Am Vet Med Assoc.* 2002; 221: 673-677
3. Isenberg-Grzeda E, Hsu AJ, Hatzoglou V, Nelso C, Breitbard W. Palliative treatment of thiamine-related encephalopathy (Wernicke’s encephalopathy) in cancer: a case series and review of the literature. *Palliat Support Care* 2015; 12(5): 1241-1249.
4. Maxie MG, Youssef S. Nervous system. In: Maxie MG, ed. *Pathology of Domestic Animals.* 5th ed. Philadelphia, PA: Elsevier Saunders; 2007: 281-457
5. Niles GA, Morgan SE, Edwards WC, The relationship between sulfur, thiamine and polioencephalomalacia – a review. *Bovine Practice.* 2002; 36: 93-99.

6. Vernau K, Napoli E, Wong S, Ross-Inta C, Cameron J, Bannasch D, Boilen, Dickenson P, Giulivi C. thiamine deficiency-mediated brain mitochondrial pathology in Alaskan Huskies with mutation in SLC19A3.1. *Brain Pathol* 2015; 25(4):441-453.

CASE III 111474 (JPC 4084217)

Signalment: 7-year-old, male castrated, Shih Tzu dog (*Canis familiaris*)

History: A 7-year-old, male castrated, Shih Tzu dog was referred to the Cornell University Hospital for Animals for acute neurologic signs after 4 episodes of vomiting. The dog had a 4-5 year history of polyuria and polydipsia (PU/PD).

After vomiting overnight, the following day the dog showed signs of lethargy and ataxia which progressed to disorientation and lateral recumbency. The dog was brought to the referring veterinarian where blood work showed > 180 mmol/μl of sodium [144-160 mmol/μl]. Initial fluid therapy consisting of lactated Ringer’s solution (LRS) was administered (unknown dose); however, the dog began head pressing. Furosemide (5 mg/kg) was administered. Soon after the patient had a focal seizure and received an additional 4 mg/kg of furosemide. The dog was referred to Cornell University Hospital for Animals’ Emergency Service. He had an additional seizure during transit.

On examination, the patient was stuporous, hyperthermic (104.6 F), and tachycardic (200 bpm) with a weak femoral pulse. The patient was approximately 9% dehydrated and had tacky, injected mucous membranes with a capillary refill time of 1 second. The initial blood pressure was 97/24 with a mean of 43.

Anisocoria was present (meiosis OD). A neurologic consultation revealed a forebrain neurolocalization. The patient was recumbent with an absent menace response and nasal sensation, bilaterally. Proprioception was absent in all four limbs with intact spinal reflexes. No head or neck pain was noted.

Point of care blood work (PCV, total solids and venous blood gas) revealed severe hyponatremia (182 mEq/L; 140–154 mEq/L) and hyperchloremia (134 mEq/L; 104–119 mEq/L) with normokalemia (3.04 mEq/L; 3.8–5.4 mEq/L).



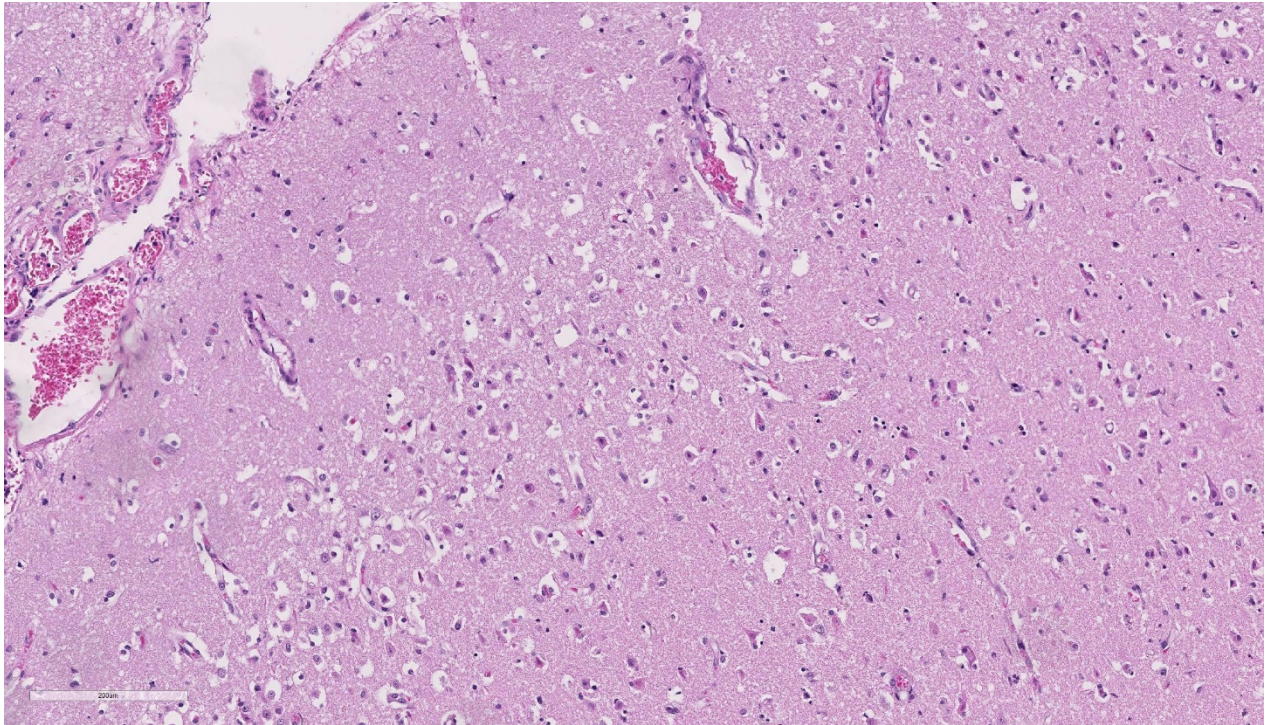
Cerebrum, dog. (Section at the level of the rostral commissure.) Lesions are minimal at subgross examination. (HE, 4X)

The patient was started on a custom fluid containing 175 mEq/L of sodium. A recheck of venous blood gas analysis revealed sodium of 191 mEq/L. On the basis of the history, physical examination findings, and biochemical abnormalities, central diabetes insipidus was suspected. Fluid therapy was changed to a hyponatremic solution and with continued fluid adjustments and subcutaneous administration of 1 mcg/kg of desmopressin, the serum sodium decreased to 177.7 mEq/L over the course of 12 hours. The patient's mental status remained unchanged with an additional seizure. MRI revealed bilateral grey matter swelling characterized by a reduced size of the subarachnoid space, effacement of the sulci and compression of the adjacent white matter tracts consistent with moderate, diffuse, cerebral edema, which was primarily cytotoxic.

The sodium level improved steadily over the 48 hours of hospitalization and fluid therapy and there was a transient improvement of mentation, but the patient became bradycardic and nonresponsive to atropine and experienced cardiac arrest. No cardiopulmonary resuscitation efforts were made at the request of the owner.

Gross Pathology: The submitting veterinarian performed the postmortem examination with no significant gross findings. He submitted fresh and fixed tissues for examination. Upon arrival at the diagnostic laboratory, the fresh tissues were severely autolyzed. In the fixed brain, there were light yellow areas of malacia in the cerebral gray matter that fluoresced when placed under an ultraviolet light with a wavelength of 365 nm.

Laboratory results: The sodium level of the brain tissue was 13,850 ppm (reference



Cerebrum, dog. There is segmental laminar necrosis, edema, and gliosis of the middle and deep laminae of the cortex. (HE, 154X)

interval, calculated on a dry matter basis, 6000-8000 ppm).

Microscopic Description:

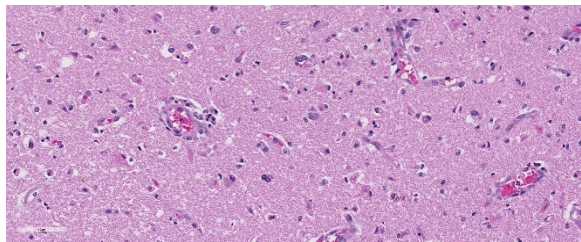
Brain, cerebral cortex: Diffusely, the blood vessels throughout all the sections are prominent, severely congested, lined by plump, reactive endothelial cells, and occasionally surrounded by small numbers of macrophages and fewer lymphocytes, hemorrhage, and fibrin within the Virchow-Robbin space. In the neuropil are scattered pyknotic and karyorrhectic cellular debris, most frequent in the mid to deep cerebral gray matter. In this area, there are frequent necrotic neurons: 1) angular with hypereosinophilic, variably microvacuolated cytoplasm that lack Nissl substance, with a smudgy nucleus without a nucleolus, or 2) appear as faint angular eosinophilic shadows of ghost neurons that lack a nucleus. The necrosis is most prominent in the mid to deep cerebral gray matter, while the perivascular

cuffing, vascular branching, and perivascular fibrin and hemorrhage are most prominent in the caudate nucleus.

Pituitary gland (image not included): The pituitary gland is severely distorted by multifocal to coalescing cysts replacing and expanding 60% of the pars distalis, most of the pars intermedia, and 10% of the pars nervosa. The cysts are filled with variably eosinophilic, fibrillar to homogenous material, and lined by attenuated to low columnar, pseudostratified ciliated epithelium.

A variety of immunohistochemical and histochemical stains were applied to the brain sections. All positive and negative controls were adequate.

Microtubule associated protein 2 for neurons (MAP2) demonstrated strong but infrequent cytoplasmic immunoreactivity of the soma



Cerebrum, dog. Neurons multifocally exhibit ischemic damage characterized by variable amounts of swelling, pallor (degeneration), fading, and pyknosis (necrosis). (HE, 308X)

and moderate immunoreactivity of cytoplasmic processes in neurons of the mid to deep cerebral gray matter indicative of neuronal necrosis. An image of a positive control from a normal dog is included as an inset. In this image, the neuropil exhibits widespread moderate immunoreactivity with moderate to strong immunoreactivity of the neuronal soma and processes. The internal negative control is adequate highlighted by the negative glial cells and blood vessels.

Glial fibrillary acidic protein (GFAP) for astrocytes highlights the well-demarcated cortical laminar necrosis affecting the mid to deep gray matter with very few remaining astrocytes in this area.

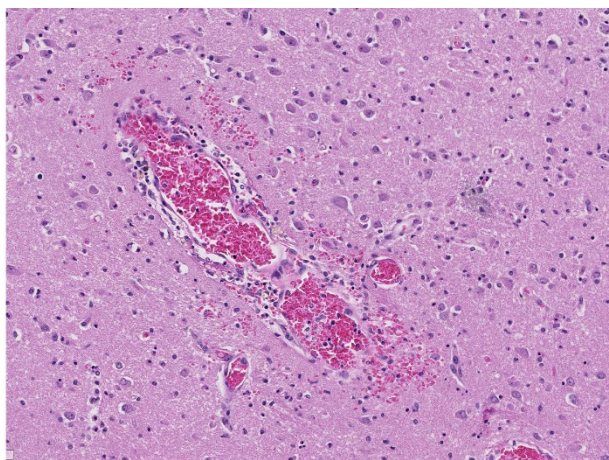
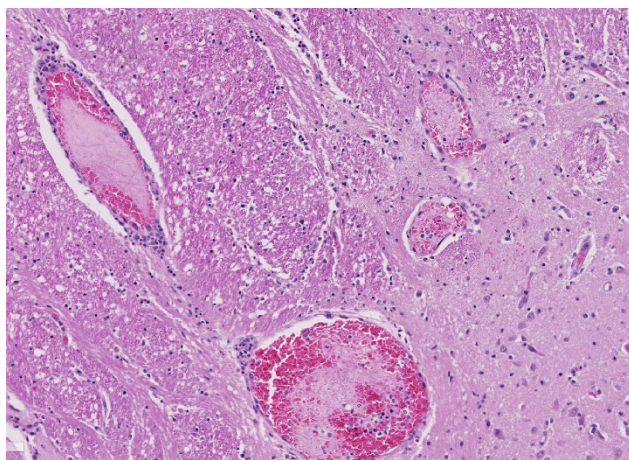
Olig2 for oligodendrocytes maps the GFAP in the mid to deep gray matter.

Ionized calcium binding adaptor molecule 1 (Iba1) for microglia and histiocytes in the affected mid to deep cerebral gray matter revealed three different populations of microglia. The first population is round, ameboid, or nonramified with strong cytoplasmic immunoreactivity interpreted as reactive microglia. The second population is stellate or ramified with strong cytoplasmic immunoreactivity interpreted as quiescent microglia. The third is a background population of small and round microglia and exhibits weak cytoplasmic immunoreactivity and were considered degenerate. Note perivascular mononuclear cells are predominantly macrophages.

Contributor's Morphologic Diagnoses:

Brain: Severe, acute, cortical laminar necrosis with reactive microgliosis, reactive endothelium, histiocytic perivascular cuffing, perivascular hemorrhage and fibrin exudation

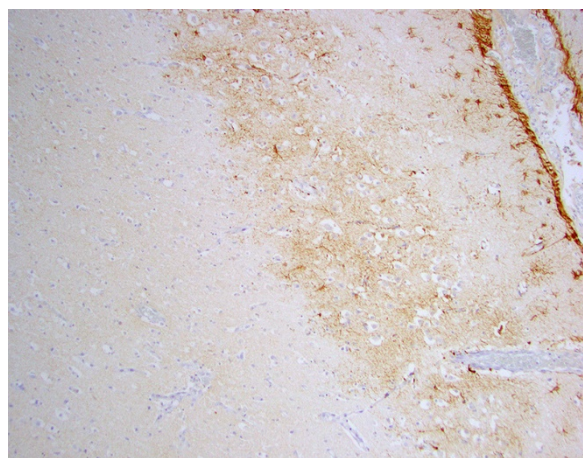
Contributor's Comment: Hypernatremia is an infrequently encountered condition in dogs caused by decreased body fluid or



Cerebrum, dog. (Left) Non-occlusive thrombi are present scattered throughout the section. Vessels are cuffed by low to moderate numbers of lymphocytes and macrophages. (Right) There are rare ring hemorrhages. (HE, 308X)

sodium gain.¹⁴ Causes of hypernatremia include diabetes insipidus, insensible loss such as hyperventilation or fever¹⁴, lack of water intake due to hypothalamic defect resulting in a defective thirst response,¹³ iatrogenic administration of hypertonic saline or sodium bicarbonate or consumption of high salt content material,⁹ and decreased renal excretion of sodium due to hyperaldosteronism.³

In a recent retrospective study, the three most common causes of severe hypernatremia in dogs were central diabetes insipidus, alimentary loss, and fever/hyperthermia.¹⁴ Central diabetes insipidus (CDI) is characterized by diminished activity or lack of the antidiuretic hormone (ADH) due to damage of neuroanatomic sites involved in ADH secretion including the neurohypophysis, hypothalamic osmoreceptors, the supraoptic or para-ventricular nuclei, or the superior portion of the supraopticohypophyseal tract.¹² Underlying causes include vascular, autoimmune, infection, drugs, surgery, trauma, benign or



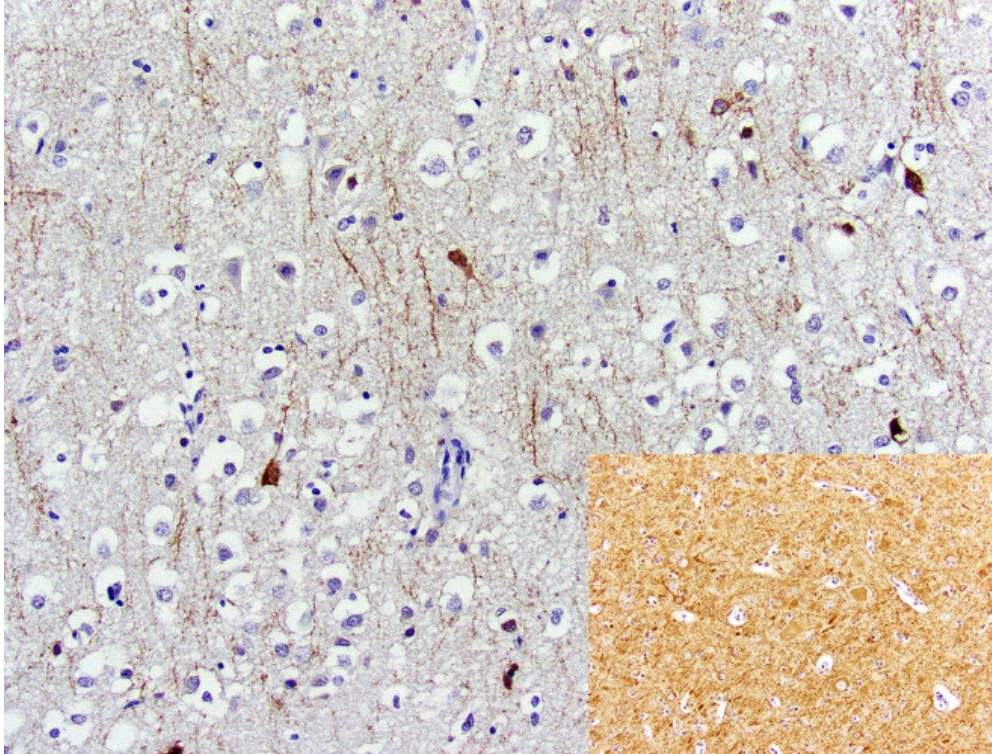
Cerebrum, dog. Glial fibrillary acidic protein (GFAP) for astrocytes highlights the few remaining astrocytes in areas of necrosis. (anti-glial fibrillary acidic protein, 400X). (Photo courtesy of: Cornell University, College of Veterinary Medicine, Department of Biomedical Sciences, Section of Anatomic Pathology, Ithaca, New York, <http://www.vet.cornell.edu/biosci/pathology/>)

metastatic pituitary-hypothalamic tumors. Patients with a normal thirst mechanism and free access to water generally do not present clinically; however, when water intake is restricted, hypernatremia occurs.¹ In this case, the central diabetes insipidus was attributed to craniopharyngeal duct cysts and predisposed this dog to severe hypernatremia. However, given the widespread, severe lesions of the brain, the aggressive fluid therapy likely contributed to the severe histologic lesions.

Clinically, hypernatremia primarily affects the central nervous system and rapid changes in plasma sodium concentrations can cause severe, permanent, and lethal brain injury.² The pathogenesis of these lesions is due to the failure to retain brain osmolarity. As the plasma osmolarity decreases with fluid therapy when these cases are recognized, the brain osmolarity fails to decrease at a similar rate due to failure of idiogenic osmoles to dissipate leading to cerebral edema.

Salt toxicity and water deprivation and its histologic features have been widely documented in other domestic animals including pigs, poultry, and ruminants.⁹ Most cases are caused by indirect salt poisoning which occurs when consumption of high levels of salt, followed by water deprivation, and then excessive water consumption occurs.⁹ Direct salt poisoning is in general rare, but primarily has been reported in cattle.¹⁵ The histopathologic lesions shared across these species include cerebral cortical laminar necrosis, perivascular mononuclear cuffing, and cerebral edema.⁸ Indirect salt poisoning in pigs is a well-known pathologic characterized by eosinophilic meningitis and perivascular eosinophilic cuffing.¹³

Neuropathologic alterations of hypernatremia in the dog have mostly been extrapolated from human and rodent studies



Cerebrum, dog. Microtubule-associated protein 2, a neuron stain, demonstrates the marked loss of neurons in the affected area. A positive control (normal cerebrum) is presented as the inset. (anti-MAP2, 600X). (Photo courtesy of: Cornell University, College of Veterinary Medicine, Department of Biomedical Sciences, Section of Anatomic Pathology, Ithaca, New York, <http://www.vet.cornell.edu/biosci/pathology/>)

with only brief descriptions in the literature. Most of the histologic description in canine cases has been quite variable. Cerebrocortical neuronal necrosis with symmetrical encephalomalacia of the brain stem has been reported in a dog diagnosed with pituitary-dependent hyperadrenocorticism that was euthanized due to hypernatremia 4 weeks post hypophysectomy.⁹ Neuronal degeneration and astrocytosis of the thalamus and hypothalamus has been reported in a young dog with hypodipsic hypernatremia.⁴ In a case of acute salt toxicity by ingestion of salt-flour mixture used as clay, diffuse white matter vacuolation with occasional perivascular cuffing by necrotic hyperchromatic mononuclear leukocytes with a thin ring of hemorrhage was observed with no evidence of axonal or neuronal necrosis.⁶

This case described the range of histologic changes that can be seen in dogs with hypernatremic encephalopathy which includes 1) cortical laminar necrosis, 2) reactive and necrotic endothelium with perivascular histiocytic cuffing, edema, fibrin, and hemorrhage, 3) reactive microgliosis, 4) white matter vacuolization, and 5) Purkinje

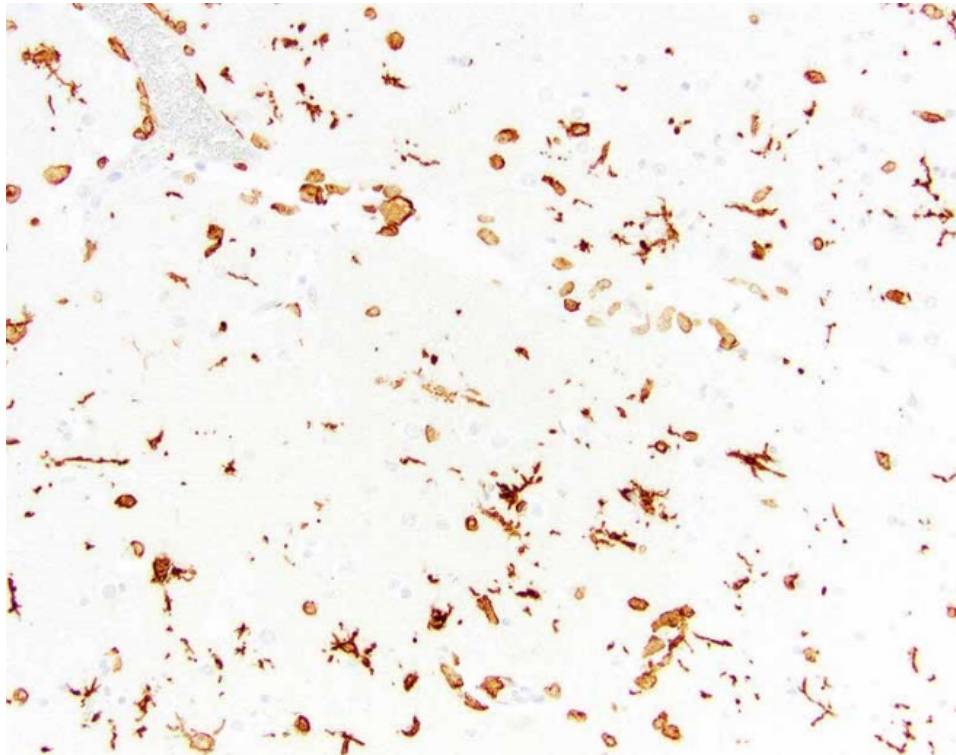
cell necrosis. In the absence of relevant history, toxic-metabolic encephalopathies or global ischemic encephalopathy where widespread bilateral ischemic damage can occur in anesthetic deaths, cardiac arrest, severe anemia, hypotension, hypovolemic shock, and neonatal maladjustment syndrome may be considered. In this case, the sudden and aggressive ion alterations likely account for the brain lesions and the neurologic signs. In conclusion, severe hypernatremia should be considered as a differential in dogs with cortical laminar necrosis.

Contributing Institution:

Cornell University, College of Veterinary Medicine, Department of Biomedical Sciences, Section of Anatomic Pathology, Ithaca, New York, USA
<http://www.vet.cornell.edu/biosci/pathology/>

JPC Diagnosis: Cerebrum: Necrosis, cortical, laminar and segmental, multifocal to coalescing, with gliosis.

JPC Comment: The contributor provides an excellent review of hypernatremia in the dog. To add to the extensive list of differentials for polioencephalomalacia in the dog, other potential causes to be considered in the dog include lead, cyanide, thiamine deficiency, hypoglycemia, canine distemper infection, head trauma, cardiac arrest, and following portosystemic shunt ligation.⁸ Seizure activity has been documented to result in cortical damage in man and domestic and experimental animals, and the moderator discussed the possibility of this being the root cause of the laminar cortical necrosis in this animal.⁸



Cerebrum, dog. IBA1 stain for microglia and histiocytes demonstrates strongly staining reactive and quiescent glia as well as weakly positive degenerating microglia. (anti-MAP2, 600X). (Photo courtesy of: Cornell University, College of Veterinary Medicine, Department of Biomedical Sciences, Section of Anatomic Pathology, Ithaca, New York, <http://www.vet.cornell.edu/biosci/pathology/>)

One of the classic symptoms of salt toxicity in affected animal species is blindness. In a previous WSC case of salt toxicity in a Vietnamese potbellied pig (WSC 2012-2013, Conference 21, Case 1), resulting from eating potato chips (this has been reported several times in the literature!), blindness was a long-term sequela following hospitalization and treatment and ultimately resulted in his euthanasia. While a number of changes occur in the brain following the development of hypernatremia and hyperosmolality and may result in dysfunction of the optic pathway, equally severe and irreparable changes also result in the globe. Following ingestion of diet with 3% salt concentration (the minimum concentration associated with changes in the globe) for 3-4 days, the following ocular changes were noted in study

pigs, rats, and rabbits – conjunctival injection, corneal and lens opacities, swelling of the optic disc, blindness, vitreous collapse, and ultimately progress to phthisis bulbi. Due to hyperosmolality, fluid loss from the vitreous resulted in vitreous shrinkage resulting in vascular damage, retinal and vitreous hemorrhage, posterior vitreal detachment, and retinal detachment.⁶ This suggests that while many of the CNS signs in salt-intoxicated animals may resolve with successful therapy to

combat hyperosmolality, the changes in the eye may be irreversible and blindness, if present, permanent.

In the hospitalized dog and cat, hypernatremia is associated with a significant decrease in prognosis.¹³ Case fatality rates of dogs and cats with hypernatremia was 20.6 and 28.1% respectively compared to 4.4 and 4.5% with a normal blood or serum sodium concentration. In a review case histories in this study, 50% of the dogs and 38.5% of cats presented with hypernatremia, and the remaining animals developed hospital acquired hypernatremia.

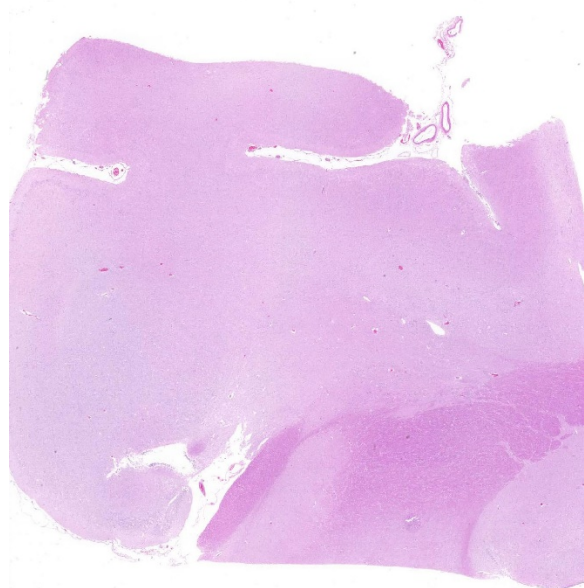
References:

1. Adroge, H.J., and N.E. Madias. 2000. Hypernatremia. *N Engl J Med* 342: 1493-1499.
2. Ayus, J.C., D.L. Armstrong, and A.I. Arieff. 1996. Effects of hypernatraemia in the central nervous system and its therapy in rats and rabbits. *J Physiol* 492 (Pt 1): 243-255.
3. Breitschwerdt, E.B., D.J. Meuten, C.L. Greenfield, L.W. Anson, C.S. Cook, and R.E. Fulghum. 1985. Idiopathic hyperaldosteronism in a dog. *J Am Vet Med Assoc* 187: 841-845.
4. Crawford, M.A., M.D. Kittleson, and G.D. Fink. 1984. Hypernatremia and adipsia in a dog. *J Am Vet Med Assoc* 184: 818-821.
5. Greco, D.S. 2012. Pituitary deficiencies. *Top Companion Anim Med* 27: 2-7.
6. Heydarpour F, Derakhshandeh J, Fekn A, Heydarpour P. Salt poisoning blindness in Wistar rat, rabbit, and pig. *Toxicol Environ Chem* 2008; 90(5):1035-1042.
7. Khanna, C., H.J. Boermans, and B. Wilcock. 1997. Fatal hypernatremia in a dog from salt ingestion. *J Am Anim Hosp Assoc* 33: 113-117.
8. Mariana, CL, Platt SR, Newell SM, Terrell SP, Chrisman CL, Clemmons RM. Magnetic resonance imaging of cerebral cortical encrosis (polioencephalomalacia) in a dog.
9. Maxie, M.G., editor. 2015. *Jubb, Kennedy, and Palmer's Pathology of Domestic Animals*. Elsevier, St. Louis, MO. 314-315 pp.
10. Meij, B.P., G. Voorhout, T.S. van den Ingh, H.A. Hazewinkel, E. Teske, and A. Rijnberk.. Results of transsphenoidal hypophysectomy in 52 dogs with pituitary-dependent hyperadrenocorticism. *Vet Surg* 1998; 27: 246-261.
11. Qureshi, S., S. Galiveeti, D.G. Bichet, and J. Roth. 2014. Diabetes insipidus: celebrating a century of vasopressin therapy. *Endocrinology* 155: 4605-4621.
12. Shimokawa Miyama, T., E. Iwamoto, S. Umeki, M. Nakaichi, M. Okuda, and T. Mizuno. 2009. Magnetic resonance imaging and clinical findings in a miniature Schnauzer with hypodipsic hypernatremia. *J Vet Med Sci* 71: 1387-1391.
13. Smith, D.L. 1957. Poisoning by sodium salt; a cause of eosinophilic meningoencephalitis in swine. *Am J Vet Res* 18: 825-850.
14. Ueda, Y., K. Hopper, and S.E. Epstein. 2015. Incidence, severity and prognosis associated with hypernatremia in dogs and cats. *J Vet Intern Med* 29: 794-800.
15. Van Leeuwen, J.A. 1999. Salt poisoning in beef cattle on coastal pasture on Prince Edward Island. *Can Vet J* 40: 347-348.

CASE IV 16H94455 or blank (JPC 4100730)

Signalment: Canine, Golden Retriever, 0.5 years old, male

History: This dog was purchased through a breeder at 7 weeks of age. At around 4 months of age, the dog started having uncontrolled watery–mucoïd diarrhea that was large volume and frequent. He was placed on Metronidazole and Provable and



Cerebrum, dog. Subgross examination of a coronal section from the area above the pyriform lobe shows no abnormalities. (HE, 5X)

needed to stay on the medication as diarrhea would return when the drugs were not used. The dog was diagnosed with carpal flexure deformity at 3 months of age. Radiographs of the cervical spine and hips revealed mild hip dysplasia and shortened distal cervical vertebral bodies. The dog developed urinary accidents (normal volume) at home. On presentation to Iowa State University Teaching Hospital, the dog had lateral strabismus, vertical nystagmus, ataxia that was worse in hindlimbs with normal reflexes and placement and hopping, head tremor, and rectal mucosa felt very irregular on rectal palpation. The owner did not allow many additional tests; only creatine kinase, which was mildly increased at 378, and blood smear which showed possible granules in lymphocytes. The dog's condition deteriorated over a week and was euthanized.

Gross Pathology: Small intestine: A small number (approximately 10) of 2–5 cm in length and 2 mm in diameter, white, elongate nematodes with tapered ends (roundworms)

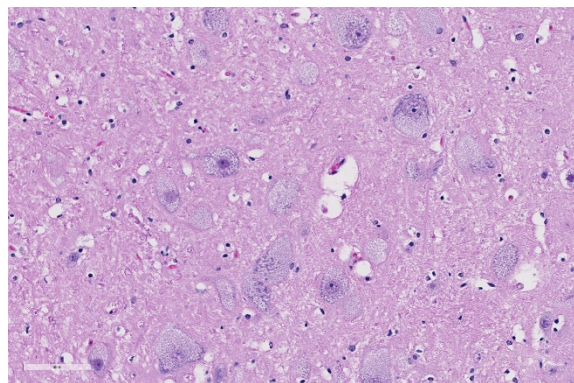
were present multifocally within the small intestinal lumen.

Laboratory results: Hepatic β -hexosaminidase A (HexA) enzyme activity was assayed. Enzyme activity levels were increased compared to the normal canine liver standard.

Electron microscopy was performed on sections of brain. The vacuoles appeared as round to ovoid membrane bound bodies with, most frequently, internal concentric whorls of membrane with a periodicity of 6-8 nanometers.

Microscopic Description:

Spinal cord (cervical; thoracic;lumbar, sacral): All spinal cord segments are similarly affected. Diffusely, neurons are variably expanded by abundant finely vacuolated cytoplasm, which often peripheralizes the nucleus and Nissl substance. Multifocal neurons contain larger vacuoles, up to 8 microns in diameter, containing pale eosinophilic material. Some neurons contain both foamy microvacuolated cytoplasm and larger vacuoles. Glia appear unaffected. White matter and nerve rootlets



Cerebrum, dog: Neurons are swollen up to 50um due to by abundant vacuolated cytoplasm that often peripheralizes the nucleus and Nissl substance. (HE, 400X) Cerebrum, dog: Neurons are swollen up to 50um due to by abundant vacuolated cytoplasm that often peripheralizes the nucleus and Nissl substance. (HE, 400X)

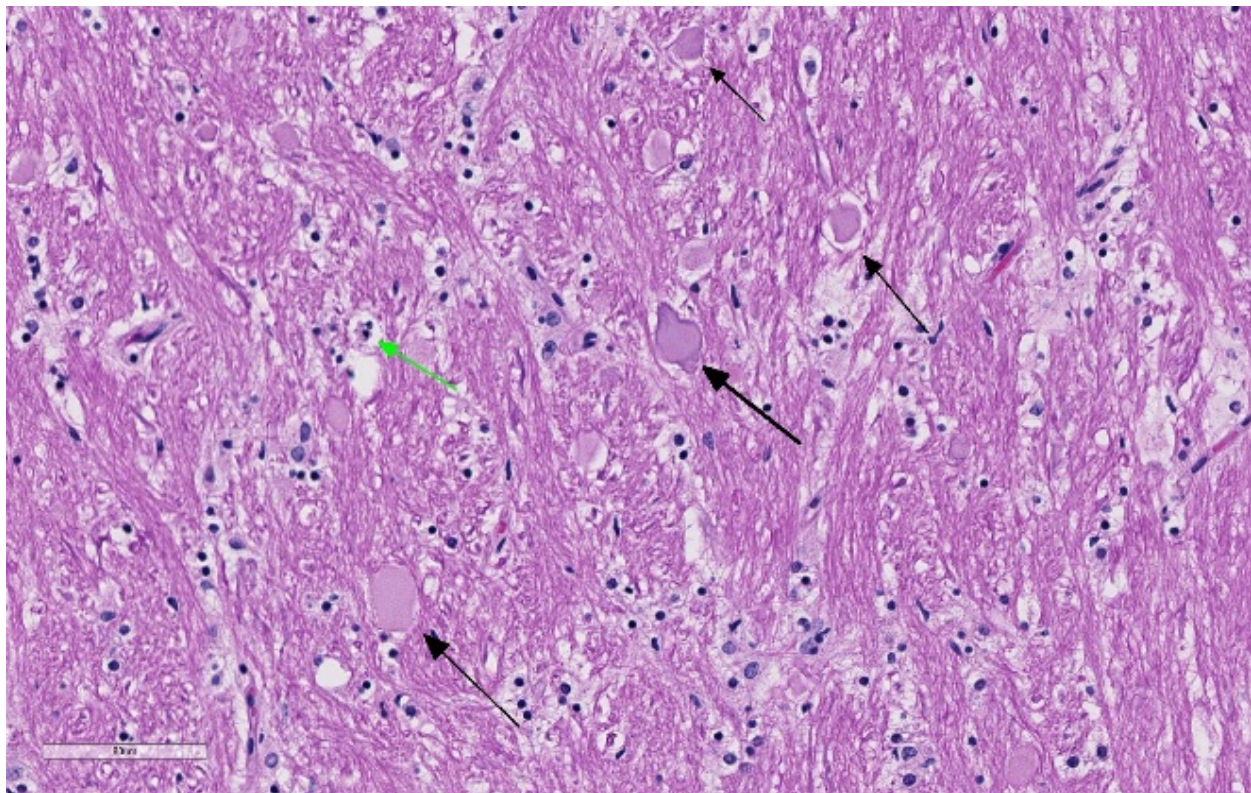
contain scattered dilated and often empty axon sheaths. Meninges, blood vessels – no specific pathologic findings.

Brain: thalamus, hippocampus; level of caudate nucleus; cerebrum; midbrain; cerebellum; rostral cerebral cortex; pons: diffusely, neurons are moderately to markedly expanded by similar microvacuolated cytoplasm, which often peripheralizes the nucleus and occasionally extends into and expands proximal processes. Infrequently, neurons also contain larger vacuoles up to 8 microns in diameter. Microglia are subjectively increased in number. There is rare neuronal necrosis, and rare (two) blood vessels are cuffed by few lymphocytes. White matter is mildly vacuolated with occasional spheroids and few vacuolated cells (small neuron or astrocyte morphology). Neuronal

vacuolation in diencephalon and brainstem nuclei is especially pronounced. The caudate nucleus is regionally strikingly hypercellular with vascular proliferation and gliosis – extant neurons are similarly vacuolated. Purkinje cells are similarly vacuolated; PC density appears normal. Cerebellar nuclei are hypercellular with marked gliosis, similarly vacuolated neurons, and moderate numbers of spheroids in white matter tracts. Meninges, blood vessels – no specific pathologic findings.

Eye: Retinal ganglion cells are similarly enlarged and vacuolated with margination of the nucleus.

Intestine (duodenum, colon): Myenteric and submucosal plexus neurons occasionally appear enlarged with microvacuolated clear



Cerebrum, dog: There are numerous swollen axons (spheroids) (black arrows) within the white matter and occasional dilated myelin sheaths containing cellular debris (digestion chambers) (green arrow). (HE, 400X)

to eosinophilic cytoplasm with marginated nuclei.

Urinary bladder: Ganglion cells within the bladder wall are similarly enlarged and vacuolated.

Liver: Diffusely, hepatocytes contain coarse, coalescing vacuoles with ragged margins.

Mesenteric ganglion: Ganglion cells are markedly distended by similar microvacuolated cytoplasm as described above.

No significant microscopic changes were identified in the following tissues: kidney, colon, skeletal muscle (rare protozoal cysts), ileum, cecum (advanced mucosal autolysis), trachea, sciatic nerve, prostate, testis, tongue, heart, lung (marked congestion with RBC extravasation), spleen (moderate to advanced autolysis), thymus, thyroid gland, adrenal gland, pituitary (pars distalis), mandibular salivary gland.

Contributor's Morphologic Diagnoses:

Brain, spinal cord, mesenteric ganglia: Neuronal cytoplasmic vacuolation, diffuse, moderate to severe.

Retina: Retinal ganglion cell vacuolation, cytoplasmic, diffuse, moderate.

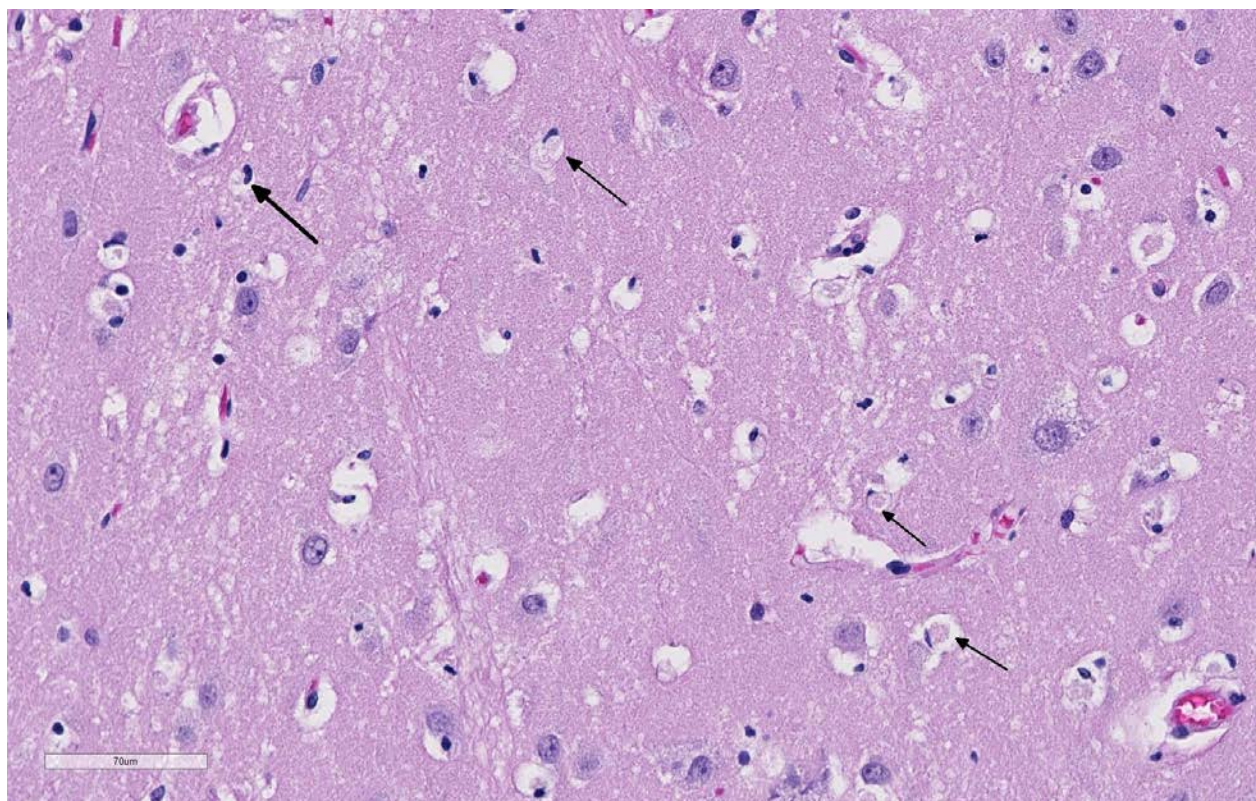
Small intestine: Mild endoparasitism (roundworms)

Contributor's Comment: Lysosomal storage diseases (LSD) are inherited (often autosomal recessive) or acquired (from ingested plant or other toxins) disorders that result in accumulation of macromolecules in lysosomes due to defective catabolism.^{1,2} Most are due to deficient or inactive hydrolytic enzymes or defects such as inactive proteins, impaired posttranslational

processing, lack of enzyme activator, lack of substrate and lack of transport proteins.³ Types of LSDs of veterinary importance include: Sphingomyelin lipidosis (e.g., GM1 and GM2 gangliosidosis and globoid cell leukodystrophy), glycoproteinoses (alpha and beta mannosidosis, l-fucosidosis), mucopolysaccharidoses (MPSI, MPSII, MPS III, VI, and VII), glycogenoses (alpha 1, 4 glucosidase), and neuronal ceroid lipofuscinoses (infantile, late infantile, juvenile, and adult variants).

Microscopic changes in this dog were consistent with a lysosomal storage disease. Vacuolation was predominantly, if not solely, intraneuronal affecting the central and autonomic nervous systems, and retina. Hepatocellular vacuolation was also present, but vacuole morphology appeared more consistent with glycogen than a storage disease enzyme product. Biochemical and/or genetic testing is required for diagnosis of the specific type of LSD.

By electron microscopy, vacuoles appeared most commonly as concentric lamellated inclusions, most typical of the gangliosidoses. Restriction of disease to the nervous system in this case makes a GM2-gangliosidosis more likely. GM2 gangliosidoses reported in animals include Tay-Sachs/variant B (caused by *HEXA* mutations), Sandhoff/variant 0 (*HEXB* mutations), and GM2 activator deficiency/Variant AB (*GM2A* mutations). The finding of increased HexA activity in this case is inconsistent with Tay-Sachs and Sandhoff. In the AB variant, hexosaminidase activity is retained, but there is deficiency of an activator protein (GM2A) that is required for degradation of GM2 ganglioside by HexA. The AB variant has been reported in a Japanese Spaniel.⁵ Additionally, a novel *HEXA* missense mutation has been recently identified in Japanese Chin dogs that have a



Cerebrum, dog: Microglia also are also expanded by abundant vacuolated cytoplasm (arrows). (HE, 400X)

phenotype similar to the AB variant.⁶ DNA was isolated from this dog and is being tested for known LSD mutations.

Contributing Institution:

<https://vetmed.iastate.edu/vpath>

JPC Diagnosis: Cerebrum: Neuronal and glial vacuolation, diffuse, marked, with gliosis.

JPC Comment: GM2 ganglioside is a cell membrane glycolipid which is catabolized by the action of N-acetylhexosaminidase and GM2 activator (GM2A) protein. N-acetylhexosaminidase exists as a dimer in two forms, hexosaminidase A and hexosaminidase B. Improper functioning of either one of these subunits, or GM2A, results in accumulation of GM2 gangliosides in the lysosomes of neurons leading to a progressive deterioration of the central

nervous system (GM2 gangliosidosis, monosialoganglioside gangliosidosis). Tay-Sachs disease of humans is a GM2 gangliosidosis caused by a mutation in the HexA gene and deficient production of the hexosaminidase A dimer, while Sandhoff disease is caused by mutation of the Hex B gene and deficiency of both hexosaminidase A and B dimers.⁴ GM2 gangliosidosis has been previously described in toy poodles, German shorthaired pointers and Japanese Spaniel dogs, domestic short haired and Korat cats, Jacob sheep, Yorkshire pigs, and Muntjak deer.

Three forms of GM2 gangliosidosis are defined based on the age of onset and subsequent disease severity a) infantile (classical), b) juvenile, and c) adult onset (a more heterogeneous progression). The most frequent initial signs are developmental arrest, abnormal startling responses, and low

muscle tone, ultimately progressing to seizures, blindness, and coma. Gross lesions in affected animals may include macrocephaly, cortical atrophy, broadening of gyri and shallow sulci.⁴ Histologic lesions include neuronal vacuolation with displacement of Nissl substance. As gangliosides figure prominently in synaptic transmission, spheroids may be numerous in white matter, as seen in this case. Cytoplasmic vacuolation may be seen in other cells throughout the body including hepatocytes, leukocytes, renal tubular epithelium, pancreatic acinar cells, and corneal stromal cells (corneal clouding has been identified grossly in Portuguese water dogs and cats).

Recent therapeutic studies in treatment of feline GM2-gangliosidosis cats resembling Sandhoff's disease have shown promise in ameliorating the signs of disease and extending life span. Treatment requires intrathalamic or intraventricular injection of an adenovirus associated virus vehicle encoding both the human HEX A and HEX B genes. Sandhoff-type cats were treated between 4 and 6 weeks of age prior to the onset of clinical signs. Treated cats in this study demonstrated increase Hex activity up to 4-fold, had twice the life-span of untreated cats, and demonstrated up to 90% decreased GM2 ganglioside storage in all CNS regions analyzed.¹

The attendees noted that in the submitted sections of slides, it appears that microglia cells are also swollen by vacuolated cytoplasm, which is not inconsistent with a clinical diagnosis of GM2-gangliosidosis, in which vacuolation of perivascular macrophages and glial cells has been described.

References:

1. Bradbury AM, Gurda BL, Casal ML, Ponder KP, Vite CH, Haskins ME: A review of gene therapy in canine and

feline models of lysosomal storage disorders. *H Gene Ther Clin Devel* 2015; 26:27-37.

2. Cummings JF, Wood PA, Walkley SU, de Lahunta A, DeForest ME: GM2 gangliosidosis in a Japanese Spaniel. *Acta Neuropathol*, 1985; 67(3):247-253.
3. Haskins ME, Giger U, Patterson DF. Animal models of lysosomal storage diseases: their development and clinical relevance. *In: Mehta A, Beck M, Sunder-Plassmann G, editors. Fabry Disease: Perspectives from 5 years of FOS. Oxford: Oxford PharmaGenesis; 2006*
4. Jolly RD, Walkley SU. Lysosomal storage diseases of animals: an essay in comparative pathology. *Vet Pathol* 1997; 34:527-548
5. Miller AD, Zachary JF. Nervous system. *In: Zachary JF, ed. Pathologic basis of veterinary disease, Elsevier, 2017, pp. 858-861.*
6. Sanders DN, Zeng R, Wenger DA, Johnson GS, Johnson GC, Decker JE, Katz ML, Platte SR, O'Brien DP: GM2 gangliosidosis associated with a *HEXA* missense mutation in Japanese Chin dogs: A potential model for Tay Sachs disease. *Molecular Genetics and Metabolism* 2013; 108(1):70-75.

Self-Assessment - WSC 2018-2019 Conference 12

1. Which of the following is most likely to develop encephalitis following infection with human herpesvirus-8 (HHV-8)?
 - a. Gorilla
 - b. Golden lion tamarin
 - c. White-handed gibbon
 - d. Can of Campbell's soup

2. Which of the following is considered the reservoir species for pseudorabies?
 - a. Dogs
 - b. Bats
 - c. Swine
 - d. Birds

3. Which of the following is NOT considered a potential cause for Polioencephalomalacia in the ruminant?
 - a. Sulfur toxicosis
 - b. Copper toxicosis
 - c. Lead toxicosis
 - d. Water deprivation

4. Which of the following is a classic symptom of salt toxicity in domestic species?
 - a. Anosmia
 - b. Deafness
 - c. Blindness
 - d. Gangrene of the extremities

5. Which of the following diseases is characterized by the accumulation of cytoplasmic clear vacuoles primarily in neurons?
 - a. Ceroid lipofuscinosis
 - b. Beta mannosidosis
 - c. GM2-gangliosidosis
 - d. Mucopolysacchidosis 1

Please email your completed assessment to Ms. Jessica Gold at Jessica.d.gold2.ctr@mail.mil for grading. Passing score is 80%. This program (RACE program number) is approved by the AA VSB RACE to offer a total of 0.5 CE Credits, with a maximum of 12.5 CE Credits being available to any individual Veterinary Medical Professionals for the 2017-2018 Wednesday Slide Conference. This RACE approval is for the subject matter categories of: SCIENTIFIC using the delivery method of NON-INTERACTIVE DISTANCE. This approval is valid in jurisdictions which recognize AA VSB RACE; however, participants are responsible for ascertaining each board's CE requirements. RACE does not "accredit", "endorse" or "certify" any program or person, nor does RACE approval validate the content of the program.

Please email your completed assessment to Ms. Jessica Gold at Jessica.d.gold2.ctr@mail.mil for grading. Passing score is 80%. This program (RACE program number) is approved by the AAVSB RACE to offer a total of 0.5 CE Credits, with a maximum of 12.5 CE Credits being available to any individual Veterinary Medical Professionals for the 2017-2018 Wednesday Slide Conference. This RACE approval is for the subject matter categories of: SCIENTIFIC using the delivery method of NON-INTERACTIVE DISTANCE. This approval is valid in jurisdictions which recognize AAVSB RACE; however, participants are responsible for ascertaining each board's CE requirements. RACE does not "accredit", "endorse" or "certify" any program or person, nor does RACE approval validate the content of the program.

**Joint Pathology Center
Veterinary Pathology Services**



WEDNESDAY SLIDE CONFERENCE 2018-2019

Conference 13

2 January 2018

Conference Moderator:

Timothy Cooper, DVM, DACVP
Pathology Department
NIH/NIAID
Integrated Research Facility
Frederick, MD

CASE I: A-475-4 (JPC 4100984).

Signalment: 4-8 week old female
C57BL/6NCrl mouse (*Mus musculus*)

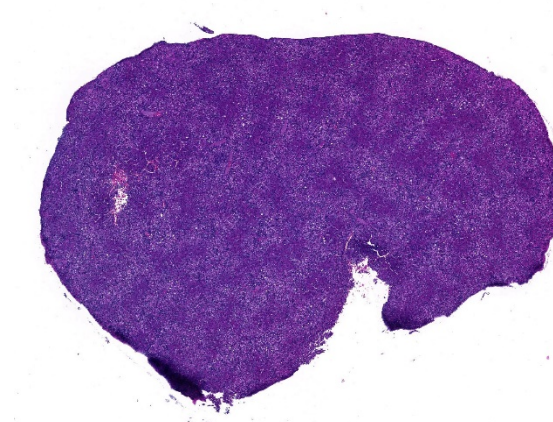
History: Experimentally infected with
mouse adapted Ebola virus (ma-EBOV) by
intraperitoneal route

Gross Pathology: Gross lesions included a
pale and friable liver, pale kidneys, enlarged
spleen and hemorrhagic/congested
gastrointestinal tract

Laboratory results: N/A

Microscopic Description:

Slide contains a single section of liver. There
is severe multifocal to coalescing
predominantly periportal and midzonal
hepatocellular degeneration and necrosis
with moderate to severe mixed inflammation.



Liver, mouse. There is a retiform pattern of hepatocellular necrosis evident at low magnification (HE, 36X)

In approximately 30% of lobules there is massive panlobular degeneration and inflammation. There is abundant periportal to midzonal microvesicular lipid type cytoplasmic vacuolation of hepatocytes, with frequent hyaline eosinophilic cytoplasmic inclusions (resembling Councilman bodies) and cell swelling. There are several foci of

hepatocyte dissociation and loss with acute hemorrhage. Apoptotic and necrotic hepatocytes are common. Small to large eosinophilic intracytoplasmic (viral) inclusions are present within viable and degenerate hepatocytes, Kupffer cells and rarely endothelial cells. Inflammatory cell infiltrate includes large numbers of macrophages and viable and degenerate neutrophils. Within central veins there are frequent vacuolated monocytes, occasionally with phagocytosed apoptotic debris or eosinophilic intracytoplasmic inclusions. There are scattered linear to branching fine olive green bile plugs within canaliculi between hepatocytes.

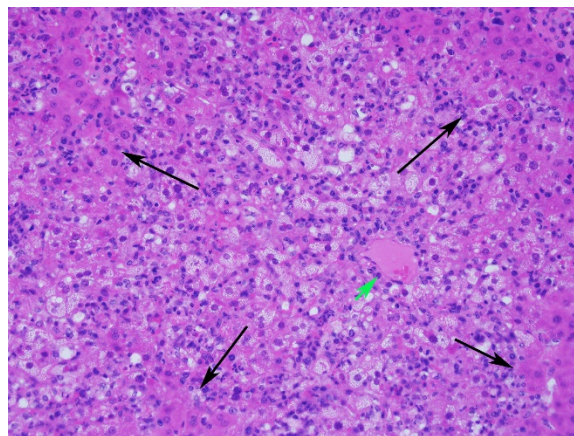
Contributor's Morphologic Diagnoses:

Liver, hepatitis, necrotizing and histiocytic, multifocal to coalescing, acute, severe with intracytoplasmic inclusion bodies

Contributor's Comment:

Liver lesions are severe and consistent with experimental mouse-adapted Ebola virus infection.^{2,3} Ebola virus, a filovirus, is an important high consequence pathogen causing significant human disease, most recently a large outbreak in west Africa from 2014 to 2016, with a smaller outbreak in 2017. Ebola targets hepatocytes and Kupffer cells of the liver, resulting in widespread hepatocellular degeneration and necrosis. Liver lesions in human and non-human primate infections are conspicuous for the minimal to absent leukocytic infiltrate, in contradistinction to the lesion presented here.^{1,7}

The extensive inflammation and absence of a distinct zonal (lobular/acinar) pattern point toward an infectious/inflammatory rather than toxic etiology. Not knowing the strain of mouse, immune status, experimental manipulation or other tissue lesions, reasonable differential etiologies for severe necrotizing hepatitis in a (usually



Liver, mouse. There is diffuse vacuolar degeneration and widespread necrosis of centrilobular (central vein marked with a green arrow) and midzonal hepatocytes. . Portal areas are mildly vacuolated to morphologically normal (black arrows.) (HE, 200X)

immunodeficient) mouse would include mouse hepatitis virus (MHV, type species of *Betacoronavirus*), mouse adenovirus (MAdV-1 or -2, *Mastadenovirus*), mouse cytomegalovirus (MCMV, *murid betaherpesvirus-1*, type species of *Muromegalovirus*), lymphocytic choriomeningitis virus (LCMV, type species of *Mammarenavirus*), or ectromelia virus (mousepox, *Orthopoxvirus*).¹ Mouse adenovirus and MCMV have intranuclear rather than intracytoplasmic inclusions, and mouse hepatitis virus lacks inclusions but forms characteristic syncytia. Ectromelia does form cytoplasmic inclusions in hepatocytes, but these tend to be difficult to visualize without prolonged hematoxylin staining. Viral cytoplasmic inclusions in hepatocytes must also be differentiated from phagocytosed neighboring apoptotic hepatocytes (Councilman bodies). Acute salmonellosis and Tyzzer's disease would be additional differential etiologies, although the lesions tend to be more nodular, with intracellular bacterial stacks in the latter.¹

Contributing Institution:

Pathology Department
NIH/NIAID

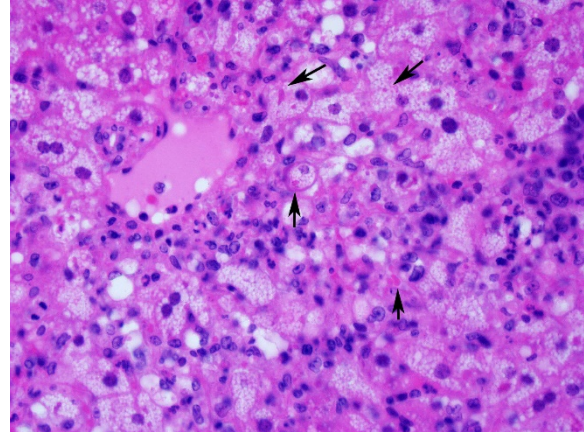
Integrated Research Facility

<https://www.niaid.nih.gov/about/integrated-research-facility>

JPC Diagnosis: Liver: Hepatitis, necrotizing and neutrophilic, random, diffuse, severe, with numerous intracytoplasmic viral inclusions.

JPC Comment: The first Ebola virus outbreak occurred in the Democratic Republic of the Congo (DRC) in 1976, resulting in 280 cases as a result of close contact and use of contaminated needles. A large outbreak in Western Africa from 2013-2015 claimed over 11,000 lives in multiple countries, with the majority of deaths in Sierra Leone, Liberia and Guinea with cases exported to other countries in Europe and North America for the first time.⁴ At the time of this writing, another outbreak occurs in the DRC, with 130 confirmed cases. Outbreak control has been the key to the decreased in lives claimed by this disease over the last forty years, effective treatment and vaccination for this hemorrhagic fever of humans is still woefully inadequate.

The genus *Ebolavirus* is divided into five distinct species: Zaire ebolavirus (EBOV), Sudan ebolavirus, Tai Forest ebolavirus, Bundibugyo ebolavirus, and Reston ebolavirus (a species of ebolavirus that is fatal in macaques but not in humans.) The ebolaviruses can infect a number of animal species including non-human primates (chimpanzees, monkeys, macaques, orangutans, baboons), fruit bats, dogs, rodents, porcupines, and a range of laboratory rodents.⁴ During human epizootics, bats have served as reservoirs in the source for infection. Bats are subclinical carriers, and do not show clinical signs of infection. Studies on arthropods have shown that they are not vectors of EBOV.⁴



Liver, mouse. Degenerating hepatocytes contain one or more brightly eosinophilic intracytoplasmic viral protein inclusions (arrows). Moderate numbers of neutrophils infiltrate areas of necrosis. (HE,400X)

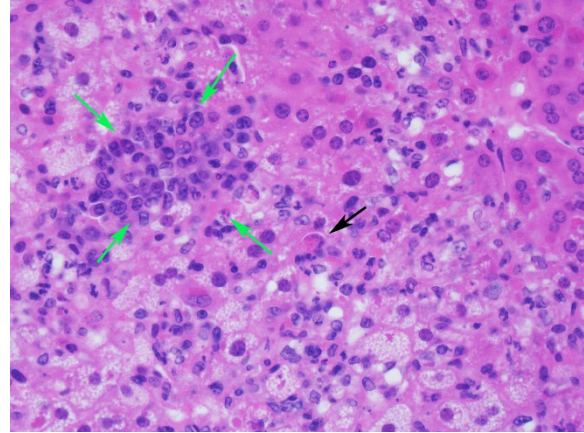
Shortly after the initial outbreak in the DRC, nonhuman primate and guinea pig models were developed for infection with Zaire ebolavirus. The hemorrhagic fever seen in nonhuman primates closely resemble the human disease.² However the complications of working with nonhuman primate models, as well as their expense, demonstrated the need for the development of murine models. In addition, the possibility of using genetically engineered murine models to study specific cytokine interactions in a very complex viral pathogenesis further reinforced a call for development of an appropriate murine model. Ultimately, an appropriate murine model was eventually developed by passaging Zaire ebolavirus from the original outbreak through progressively older suckling mice until it could be transmitted to adult, immunocompetent BALB/c mice.²

Mouse models such as the BALB/C share many similarities with guinea pig and NHPS models with cells of the mononuclear phagocyte system being target by the virus early in the disease. Viral replication may be seen in macrophages in lymph nodes and the spleen within 2 days of infection. On day three, when mice first show signs of clinical illness, virus replication is widespread, with

infection of hepatocytes, adrenocortical cells, fibroblasts, adipocytes, and cells of the monocyte-macrophage system in all organs. Histologic changes on day five include marked lymphocytolysis in multiple organs. Endothelial cell infection, even in late stages of disease, is uncommon. One notable difference in the mouse model as compared to humans and the NHP model is the noticeable paucity of fibrin thrombi within the spleen of infected mice (a very prominent finding in other model species as well as humans.)²

Since the development of the first murine model, flaws in the model have become apparent, as mouse models do not display other consequences of disease noted in humans, such as disseminated intravascular coagulation or death from shock, as seen in non-human primates. (An excellent 2015 article by Martines et al.⁵ from the Centers for Disease Control and Prevention reviews the disease caused by ebolaviruses and the related Marburg virus in humans). Since that time, research in a wide variety of inbred mouse strains have identified resistant and susceptible strains and potentially responsible resistance genes which may reflect the apparent genetic susceptibility displayed in humans when a large population is infected by the virus.⁶

The moderator noted the difference between Ebola infections in mice and in primates, with the almost total lack of inflammatory cells within primate specimens. Ebola is not a virus that can be simply injected in mouse models – it is serially passaged, and mouse-adapted strains need to be injected IP for infection. He also discussed the peculiar abnormalities associated with C57BL/6N strains, including retinal dysplasia, and if they are 6Nhsd, a mutation which causes an impaired immune response.



Liver, mouse. Apoptotic hepatocytes are rounded up and individualized. An aggregate of immature granulocytes (extramedullary hematopoiesis) is present at upper left (green arrows) (HE, 400X)

The moderator cautioned about over interpreting the lipid change in this particular animal – it may be quite variable based on time of day, elapsed time since last meal, and in sick mice, inability to feed.

References:

1. Barthold, S.W., S.M. Griffey, and D.H. Percy, *Mouse*, in *Pathology of Laboratory Rodents and Rabbits*, S.W. Barthold, S.M. Griffey, and D.H. Percy, Editors. 2016, Wiley Blackwell: Ames, IA. p. 1-118.
2. Bray M, Davis K, Geisbert T, Schmaljohn C, Huggins J. A mouse model for evaluation of prophylaxis and therapy of Ebola hemorrhagic fever. *J Infect Dis* 1998; 178(3): 651-61.
3. Gibb TR, Bray M, Geisbert TW, Steele KE, Kell WM, Davis KJ, Jaax NK. Pathogenesis of experimental Ebola Zaire virus infection in BALB/c mice. *J Comp Pathol* 2001. 125(4):233-42.
4. Gumusova S, Sunbul M, Lebecicioglu. Ebola virus disease and the veterinary perspective. *Ann Clin Microbiol and Antimicrobials* 2015; 14:30-35.

5. Martines RB, Ng DL, Greer PW, Rollin PE, Zaki SR. Tissue and cellular tropism, pathology and pathogenesis of Ebola and Marburg viruses. *J Pathol* 2015. 235(2):153-74.
6. Rasmussen AL, Okumura A, Ferris MT, Green R, Feldmann F, Kelly SM, Scott DP, Safronetz D, Haddock E, LaCase R, Thomas MJ, Sova P, Carter VS, Weiss JM, Miller DR, Shaw GD, Korth MJ, Heise MY, Baris RS, deVilena FPD, Feldmann H, Katze MG. Host genetic diversity enables Ebola hemorrhagic fever pathogenesis and resistance. *Science* 2014; 346(6212):987-991.
7. Ryabchikova, E.I., L.V. Kolesnikova, and S.V. Luchko, An analysis of features of pathogenesis in two animal models of Ebola virus infection. *J Infect Dis* 1999; 179 Suppl 1: S199-202.

CASE II: N1301/17B: (JPC 4105937).

Signalment: 4.5 years, male-neutered, Domestic Shorthaired, *Felis catus*, cat

History: A 4.5 year-old male-neutered cat was submitted to post mortem examination. Found dead unexpectedly.

Gross Pathology: The cat weighed 4.5 kg and was in a good body condition with adequate subcutaneous and intraabdominal fat deposits. Skeletal musculature of both hind limbs was mottled pale to red. The thoracic cavity contained 30 ml of translucent serosanguinous fluid. The trachea contained moderate amounts of white froth and both lungs were diffusely heavy and wet with copious frothy fluid on cut surface. The heart weighed 35g and the left atrium was subjectively enlarged. The left to right free ventricular wall ratio was 3:1 (9:3 mm). The septum measured 9 mm in thickness. Located

at the aortic bifurcation was a 3 cm plug of friable dark red to tan material, completely occluding the vessel lumen and extending along both iliac arteries. Thyroid glands were bilaterally unremarkable.

Laboratory results: None.

Microscopic Description:

Heart: Affecting approximately 10-20% of the myocardium of the left ventricular free wall are broad bands of mature and developing fibrous tissue extensively replacing and dissecting between cardiac myocytes. Myocytes entrapped within fibrous tissue are often shrunken and hypereosinophilic and have lost cross-striation (segmental degeneration). Fibrosis affects mainly the middle aspect of the left free ventricular wall and smaller foci within the septum. Furthermore, cardiac myocytes of the left ventricle are multifocally arranged in an interwoven pattern (myofiber disarray). Within the left ventricular wall and extending into the right ventricular wall, myocytes frequently measure 2-3 times normal diameter and show vesicular nuclei (hypertrophy).

Contributor's Morphologic Diagnoses:

Heart: Hypertrophic cardiomyopathy, domestic shorthaired cat, *Felis catus*.

Contributor's Comment: Hypertrophic cardiomyopathy (HCM) is the most frequent feline cardiomyopathy, accounting for almost two thirds of cases.³ In affected cats, a thickened and remodeled ventricular cardiac muscle, unable to relax completely during diastole, leads to incomplete ventricular filling and thus a decreased preload (diastolic dysfunction).² Common clinical signs include lethargy, heart murmurs, tachycardia and/or may be secondary to pulmonary oedema (dyspnea, coughing) or



Heart, cat. A cross section of heart at the level of the papillary muscle is submitted. The left ventricular free wall and interventricular septum (black arrow) is thickened. There are multiple areas of myocardial fibrosis (green arrows) visible at subgross magnification. (HE, 5X)

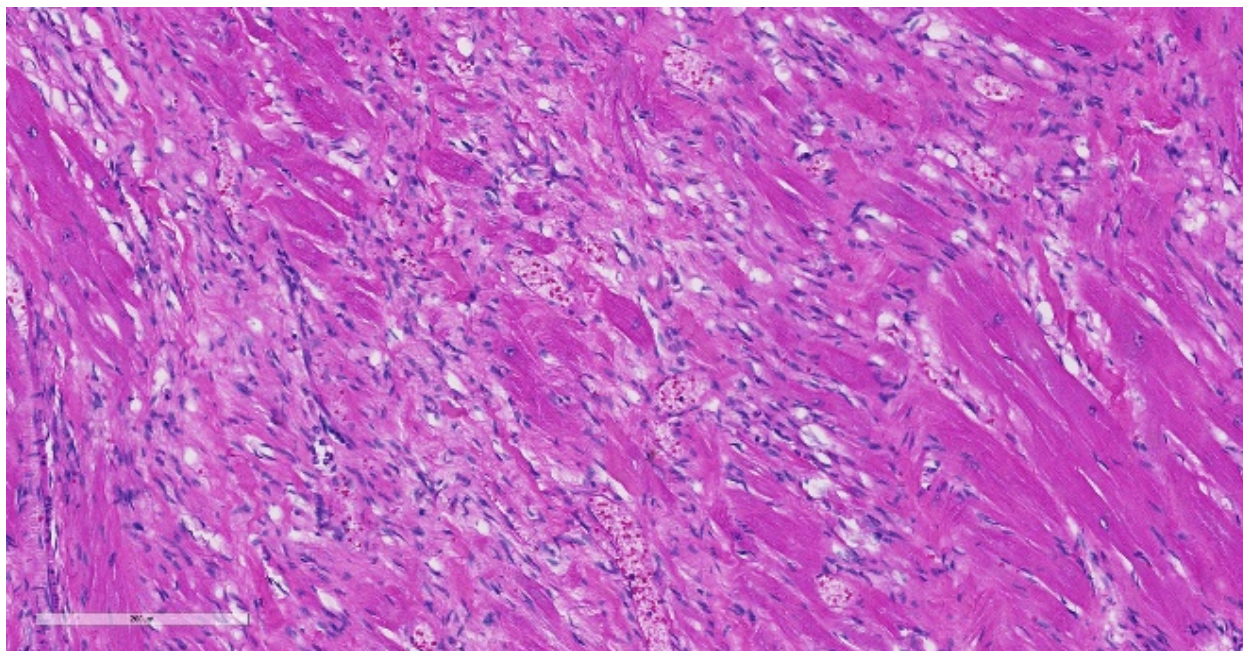
thromboembolism (hindlimb paresis).^{1,3,9} Sudden death may also occur.¹

This case illustrates classical features of idiopathic feline HCM, including subsequent aortic thromboembolism. At 35g, the heart was markedly heavier than normal in adult cats (<20-25g) and within the upper range of values reported for cats that died of HCM (29-37g).² As in the present case, symmetrical and concentric hypertrophy of the myocardium is most common, thus retaining a 'normal' left:right ventricular free wall ratio of 3:1, while wall thicknesses are absolutely increased.

Alterations in blood flow and velocity, especially within the often dilated left atrium, may lead to turbulence and produce focal thrombi, which may subsequently be flushed

into circulation, where they become lodged most frequently at the aortic-iliac junction.⁹ At this location, thromboembolism leads to acute hindlimb paraparesis with clinical signs classically termed the five 'p's' (paresis-pain-pallor-pulselessness-poikilothermy), which may be the first presenting clinical sign of a cat with HCM.¹⁰ Renal cortical infarcts may also be a feature indicating previous thromboembolism of renal arteries (not present in this case).

Histological hallmarks of feline HCM are hypertrophied cardiac myocytes with vesicular nuclei, myofiber disarray, especially within the left free ventricular wall and septum, and replacement fibrosis, all of which can be observed in this case.⁹ Further, medial hypertrophy of intramyocardial arteries with or without perivascular mononuclear infiltrates may be present.⁹ If performed antemortem, immunoassays for cardiac biomarkers often reveal increased levels of cardiac troponin I, indicating ongoing myocardial damage.⁴ A familial predisposition for HCM is best characterized in the Maine Coon and Ragdoll breeds.^{7,8} Two separate mutations have been identified affecting the gene coding for myosin binding protein C3 (MYBPC3): an alanine for proline substitution in exon 3 of the MYBPC3 gene



Heart, cat. There are numerous areas of myocardial loss with replacement by fibroblasts and mature collagen. (HE, 320X)

was identified as the causative mutation in Main Coons, whereas in Ragdolls, an arginine to tryptophan mutation in codon 820 occurs, indicating that mutation events occurred independently from each other in each breed.^{7,8} While hypertrophy of the cardiac muscle also occurs secondarily in cases of hyperthyroidism, this entity should not be confused with primary (idiopathic) HCM.⁵ More recently, feline panleukopenia virus has been implicated as a possible cause of HCM in cats.⁶

Contributing Institution:

UCD School of Veterinary Medicine,
University College Dublin, Belfield, Dublin
4, Ireland

<http://www.ucd.ie/vetmed/>

JPC Diagnosis: Heart,
myocardium: Fibrosis, multifocal, moderate,
with myofiber hypertrophy, disarray,
degeneration and loss.

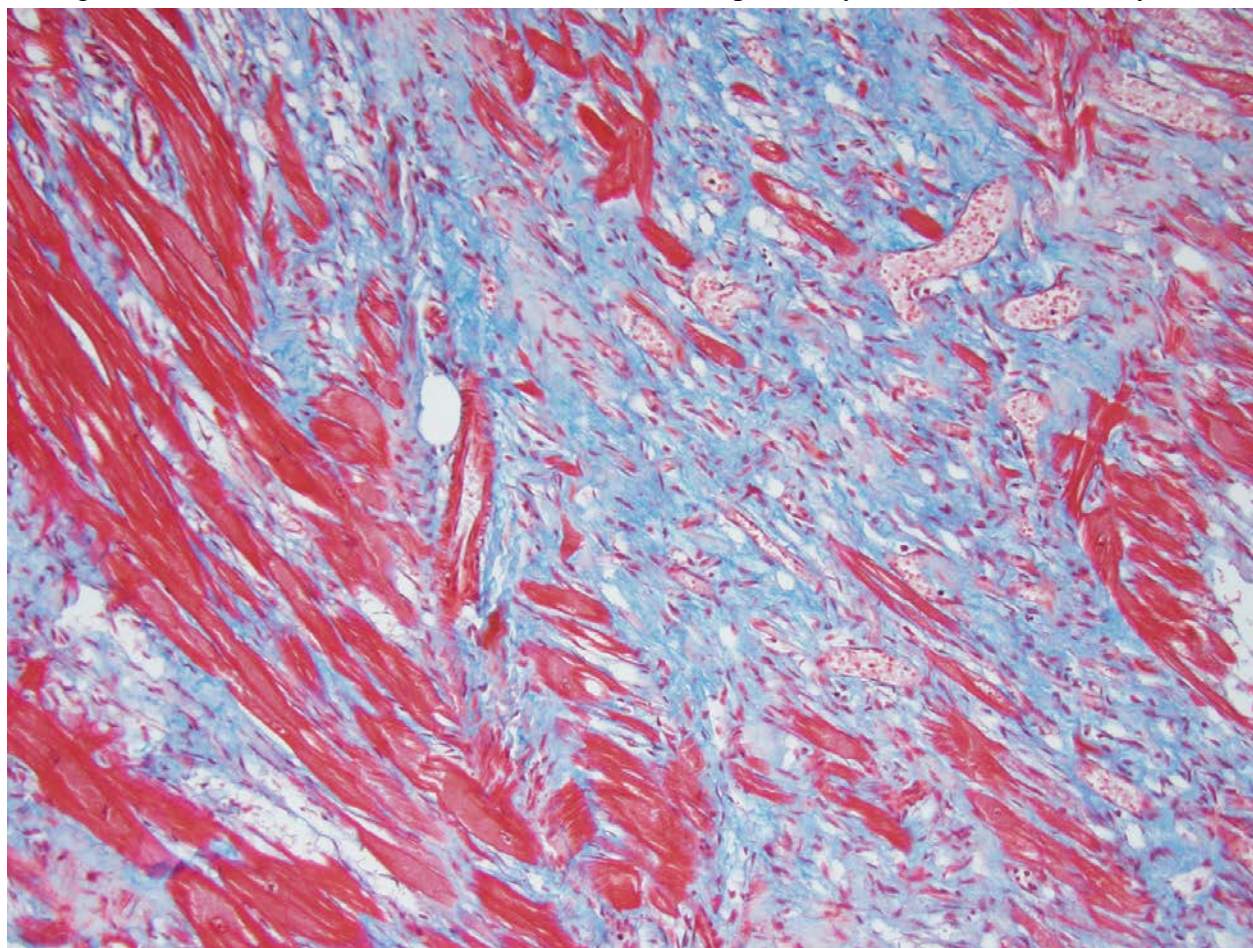
JPC Comment: Hypertrophic
cardiomyopathy (HCM), first diagnosed in

humans in the 1950's is an autosomal dominant primary myocardial disease with incomplete penetrance⁶ that affects approximately 1 in every 500 humans. It is characterized by increased left ventricular mass in the absence of a metabolic cause or pressure overload. Causative mutations for this disease have been identified as single base substitutions in a variety of sarcomeric genes, including beta-myosin heavy chains, cardiac myosin binding protein C, cardiac troponins T, I and C, alpha-tropomyosin, the essential and regulatory light chains, actin, and titin.⁷ In humans, the two most common genes affected by HCM mutations are the myosin heavy chain gene MYH7 (the gene that encodes for the motor protein beta-myosin heavy chain - - the sarcomeric protein that splits ATP to generate force) and the cardiac myosin binding protein C (cMyBP-C) – the same defective protein as seen in Maine Coon and ragdoll cats with HCM.⁶ In the human, approximately 70% of cases are the result of 11 identified sarcomeric genes, suggesting other mutations in proteins are associated with sarcomeric function. A

similar case exists in Maine Coon cats, as not all affected individuals demonstrate known mutations.¹

Cardiac troponin I (cTnI) is commonly used as a measurement for ongoing myocardial damage in cats (and humans) with HCM; this protein, which inhibits the structural interaction of the myosin heads with the actin-binding sites in cardiac and skeletal muscle, has been shown to increase rapidly in the serum after cardiomyocyte injury and is a sensitive and specific marker for cats with moderate to severe HCM as compared to normal cats whether or not congestive heart failure is present. Although there is still some debate, increased levels of cTnI are generally consistent with irreversible myocardial damage.⁵

One of the characteristic histologic changes associated with HCM is cardiomyocyte loss and fibrosis, which often starts in proximity to myocardial vessels. A number of vascular changes have been identified in cats and humans with HCM, to include microvascular or intramural coronary arterial disease, which likely result in areas of ischemic damage and resulting fibrosis, initially localized to perivascular areas within the myocardium.⁵ In humans with HCM, abnormal coronary flow dynamics, decreased coronary artery diastolic reserve, and systolic compression of the septal perforator arteries have been documented as contributory to myocardial ischemia. Furthermore, the increase in myocardial muscle mass without compensatory increase in myocardial



Heart, cat. A Masson's trichrome demonstrates the areas of fibrosis as blue against the red background of viable cardiomyocytes. (HE, 320X)

capillary density is also likely to contribute to ischemic damage in the myocardium of affected individuals.⁴

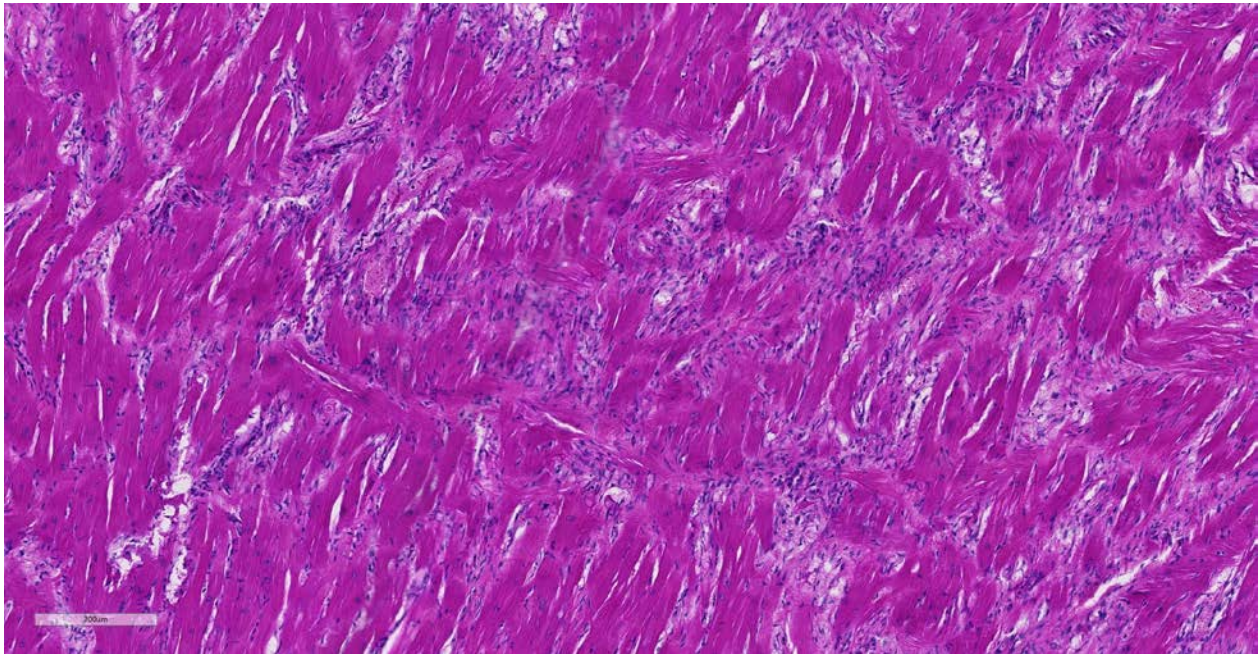
Since 1960, surgical intervention and septal myomectomy have been common approaches to relieving left ventricular outflow tract obstruction. Alcohol septal ablation (a less invasive procedure in which ethanol is injected to the first or second perforator artery, resulting in localized myocardial infarction) was introduced in 1994, and its surgical complication rate has proven to be similar to that of surgical myomectomy.⁴

During the conference, the moderator cautioned about interpretation of luminal diameter in these cases, based on a lack of knowing the level of section within the heart as well as the status of rigor during fixation.

In the normal heart, myofibers are often maloriented to each other at the area in which ventricles meet the interventricular septum – this may be misinterpreted. The described

feature of ‘myofiber disarray’ in HCM is most appropriately evaluated wholly within the left ventricular free wall or septum. In cases of microscopic examination of the heart, it would be unusual to be able to take a cross-section through the ventricles and septum and not find disarrayed fiber, but emphasized the need to take multiple sections to completely evaluate the heart. Without the presence of the disarrayed fibers, a diagnosis of HCM cannot be made; the hypertrophic changes seen in a number of fibers such as markedly enlarged nuclei are non-specific and may be seen in a number of heart diseases.

Microscopically, the moderator briefly discussed the differentiation between “interstitial” and “replacement” fibrosis for complete description of this lesion, and highlighted the need for a Masson’s trichrome to fully appreciate the amount of fibrosis in this case.



Heart, cat. Within the left ventricle of this section, there is a large focal area in which myofibers assuming an interlacing “basket-weave” appearance. (HE, 320X)

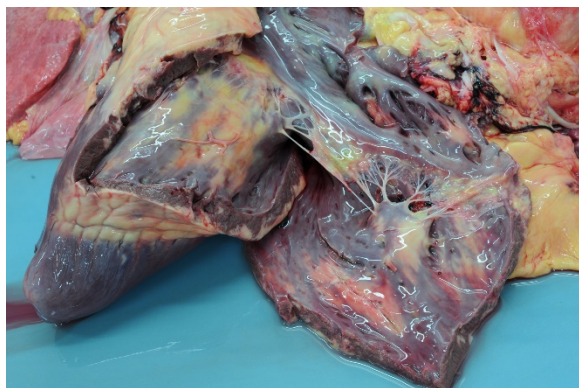
References:

1. Abbott JA. Feline hypertrophic cardiomyopathy: an update. *Vet Clin North Am Small Anim Pract* 2010; 40(4):685-700.
2. Côté E, MacDonald KA, Meurs KM, Sleeper MM. *Feline Cardiology*. 1st ed. Wiley-Blackwell, West Sussex, UK, 2011:110-112.
3. Ferasin L, Sturgess CP, Cannon MJ, Caney SM, Gruffydd-Jones TJ, Wotton PR. Feline idiopathic cardiomyopathy: a retrospective study of 106 cats (1994-2001). *J Feline Med Surg* 2003; 5(3):151-159.
4. Hang DH, Nguyen A, Schaff HY. Surgical treatment of hypertrophic cardiomyopathy: a historical perspective. *Ann Cardiothor Surg* 2017; 6(4):318-328.
5. Herndon WE, Kittleson MD, Sanderson K, Drobatz KJ, Clifford CA, Gelzer A, Summerfield NJ, Linde A, Sleeper MM. Cardiac troponin I in feline hypertrophic cardiomyopathy. *J Vet Intern Med* 2002; 16(5):558-564.
6. Kittleson MD, Meurs K, Harris S. The genetic basis of hypertrophic cardiomyopathy in cats and humans. *J Vet Cardiol* 2015; 17(Suppl 1):S53-S73.
7. Liu SK, Peterson ME, Fox PR: Hypertrophic cardiomyopathy and hyperthyroidism in the cat. *J Am Vet Med Assoc* 1984; 185(1):52-57.
8. Meurs KM, Fox PR, Magnon AL, Liu S, Towbin JA. Molecular screening by polymerase chain reaction detects panleukopenia virus DNA in formalin-fixed hearts from cats with idiopathic cardiomyopathy and myocarditis. *Cardiovasc Pathol* 2000; 9(2):119-126.
9. Meurs KM, Norgard MM, Ederer MM, Hendrix KP, Kittleson MD. A substitution mutation in the myosin binding protein C gene in ragdoll hypertrophic cardiomyopathy. *Genomics* 2007; 90(2):261-264.
10. Meurs KM, Sanchez X, David RM, Bowles NE, Towbin JA, Reiser PJ, Kittleson JA, Munro MJ, Dryburgh K, Macdonald KA, Kittleson MD. A cardiac myosin binding protein C mutation in the Maine Coon cat with familial hypertrophic cardiomyopathy. *Hum Mol Genet*; 2005 14(23):3587-3593.
11. Robinson WF, Robinson NA. Cardiovascular System. In: Maxie MG, ed. *Jubb, Kennedy and Palmer's Pathology of Domestic Animals*. 6th ed. Elsevier, St. Louis, MO, USA, 2016:46-47.
12. Smith SA, Tobias AH. Feline arterial thromboembolism: an update. *Vet Clin North Am Small Anim Pract*; 2004; 34(5):1245-1271.

CASE III: 317048 (JPC 4033739).

Signalment: 15-year-old, Clydesdale-Cob cross, male castrated, horse (*Equus caballus*).

History: The animal presented to the Weipers Centre at the University of Glasgow for re-evaluation of episodes of syncope that had been noted sporadically over the preceding two years. The horse had been investigated for syncope associated with polycythaemia and elevation of cardiac



Heart, horse. Grossly, the right ventricular wall is multifocally and rarely transmurally infiltrated by fat; similar changes are seen in the interventricular septum as well. (Photo courtesy of: Veterinary Diagnostic Services, School of Veterinary Medicine, College of Medical, Veterinary and Life Sciences, University of Glasgow, Bearsden Road, G61 1QH, Glasgow, United Kingdom, www.glasgow.ac.uk/vds)

troponin (CTnI). Cardiac dysrhythmias had resolved over time, with correction of red cell count and CTnI levels. Since then, the horse had returned to ridden exercise with no observed collapses until one week before presentation when it went down into lateral recumbency, paddled with his front legs and chomped his lips, appearing to have lost consciousness, the eyes appeared vacant and the horse remained down for two to three minutes after which he recovered and appeared normal. On presentation the horse was bright and alert and in good body condition (613kg). The syncopal episodes had implications for horse welfare and human safety, therefore the owner elected euthanasia.

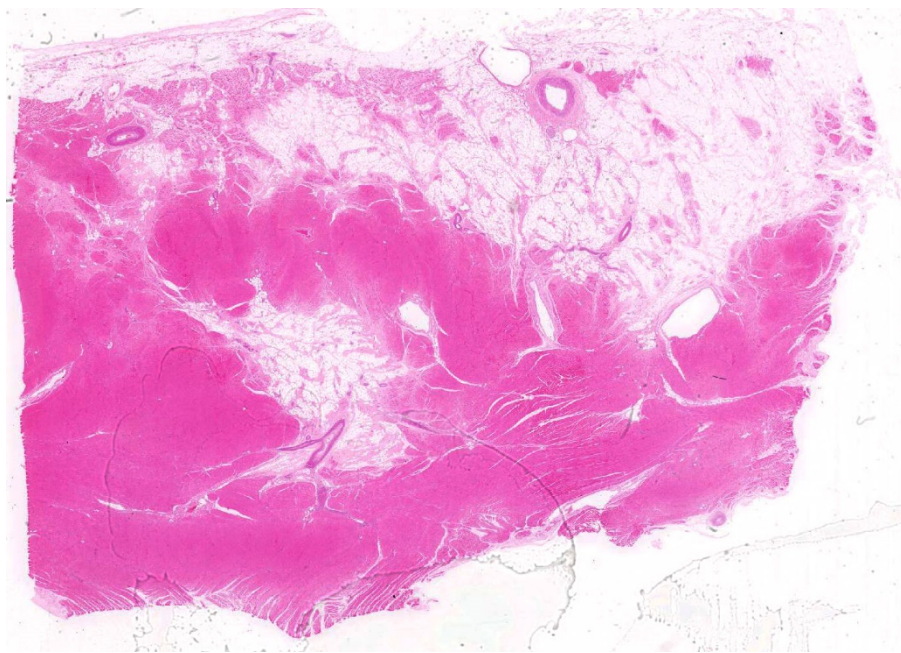
Gross Pathology: On macroscopic examination, the epicardium of the right ventricular free wall was replaced by a yellowish soft material that expanded extensively from the coronary arteries towards the center of the ventricle and was also multifocally distributed in small foci within the remaining myocardial fibers, which accounted for less than 40% of the total right ventricle. Upon opening the right ventricle, the endocardium was similarly

replaced by this abnormal tissue extending multifocally up to 1cm deep into the myocardium from both the epicardium and endocardium. The left ventricle was similarly affected, with approximately 20% of the myocardial tissue being replaced by yellowish soft tissue. Small foci of this yellowish tissue were also multifocally observed in both the left and right atria. No other significant gross pathologic findings were observed in other organ systems.

Laboratory results: Haematology and biochemistry profiles were unremarkable. Serum amyloid A and fibrinogen were within normal limits. CTnI was within reference range. On ECG examination there were multiple short periods of sinus tachycardia with no apparent external stimuli and also one episode of profound tachycardia, four ventricular premature complexes were also present. Echocardiography and neurological evaluation were unremarkable.

Microscopic Description:

Microscopic findings were similar in both ventricles, being more extensive in the right ventricular free wall; and similar to those previously described in horses. Cardiomyocytes extensively within subepicardial zone and multifocally within the myocardial and subendocardial areas are markedly reduced in number and replaced by abundant adipose tissue intermixed with variably thickened bundles of fibrous connective tissue. Residual cardiomyocytes within the adipose tissue or surrounding it are highly vacuolated, and often with loss of myofibrils and nuclear detail (degeneration). Interspersed within the fibrous and adipose tissue infiltrate are low numbers of mononuclear inflammatory cells, mainly lymphocytes and macrophages. Periodic acid-Schiff (PAS) stain highlighted the disruption of Purkinje fibres by adipose tissue. Masson's trichrome stain highlighted



Heart, horse. The epicardium (at top) and the myocardium in subepicardial and superficial myocardium is infiltrated by well-differentiated adipocytes. (HE, 6X)

the variably thickened bundles of fibrous connective tissue dissecting the myofibers.

Contributor's Morphologic Diagnoses:

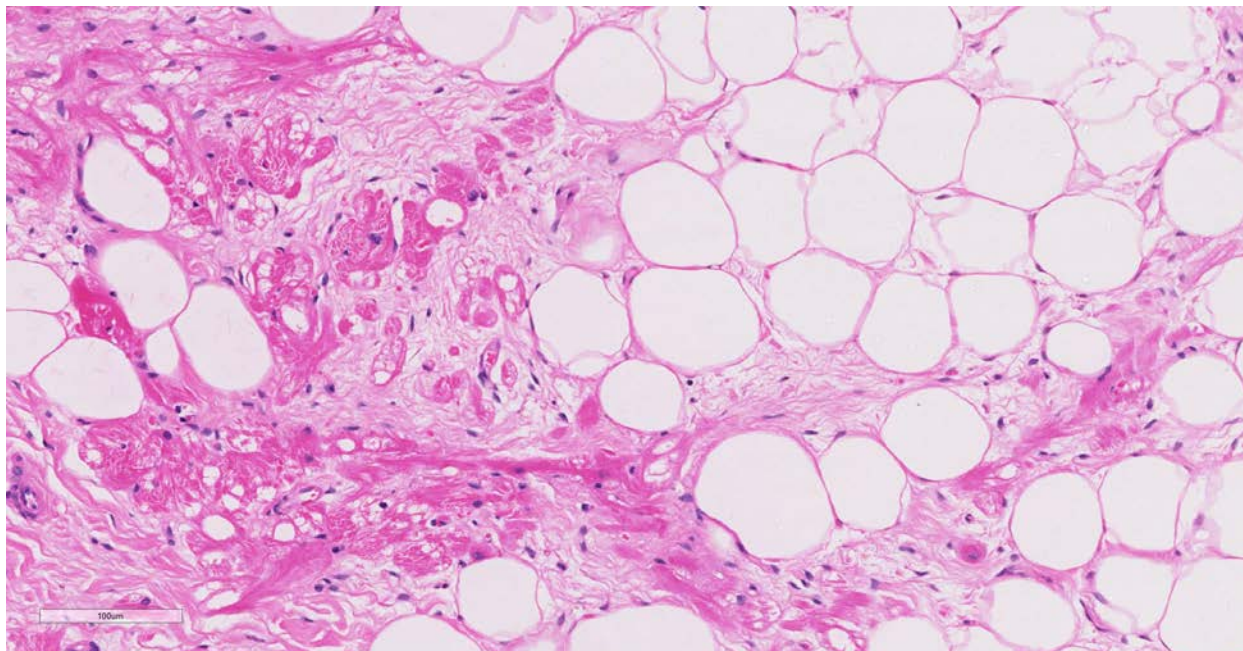
Myocardial degeneration, focally extensive, severe, chronic; with marked adipose tissue replacement with fibrosis, myocardium, Clydesdale-Cob cross, male castrated, horse (*Equus caballus*).

Contributor's Comment: Arrhythmogenic right ventricular cardiomyopathy is a well-recognized entity in human beings from which clinicopathological features were described in 1982.^{5,15} The condition has also been described in Boxer dogs^{1,6} and cats² with similar gross and histological appearances; reports of this similar condition in breeds of dogs other than Boxer has also been described.⁹ Recently, a similar condition was diagnosed in two horses³ that died with no previous signs and in which both hearts were bearing fibro-fatty replacement similar to the case we present here.

While the two previous equine cases died without showing clinical signs, in this case there is a prolonged history of collapse and cardiac dysrhythmias. Young human cases are presented most commonly with cardiomegaly, congestive heart failure or sudden death^{5,14} while adult patients usually have a more extensive history of recurrent ventricular arrhythmias and ventricular

tachycardia.⁵ Clinical signs in Boxer dogs vary widely from sudden death to congestive heart failure with or without arrhythmias⁶ while cats usually do not present any signs of arrhythmia and die due to congestive heart failure.²

This cardiomyopathy is a human familial condition of autosomal dominant inheritance with various degrees of penetrance.⁴ Mutations in genes involved in cell adhesion complexes such as desmoglein-2 (GSG2) or plakophilin-2 (PKP2) have been found to be associated with ARVC in humans¹, which supports the hypothesis that this condition is caused by inadequate cell-to-cell adhesion between cardiac myofibers leading to detachment of cardiomyocytes, cell death and replacement by adipose tissue with fibrosis.⁴ Several desmosomal genes and the cardiac ryanodine receptor (RyR2) gene (involved in excitation-contraction coupling across the ventricles and mutated in some unique forms of human ARVC) have been investigated in boxer dogs with no positive



Heart, horse. The myocardium is multifocally infiltrated by well-differentiated adipocytes (right), as well as poorly cellular fibrous connective tissue. Entrapped and degenerating cardiomyocytes contain large clear vacuoles, and are often shrunken and hyalinized (atrophy). (HE 181X)

relationship established.^{7,8,16} This could be, however, due to the substantial genetic heterogeneity of the disease.

With only three cases reported in horses, it is difficult to determine correlation between sex, age or exercise. However, the three cases were all male horses of heavy breeds (Clydesdale and Cob) in the same geographic region, which could possibly indicate a genetic relationship as is observed in many human cases.¹⁴

Contributing Institution:

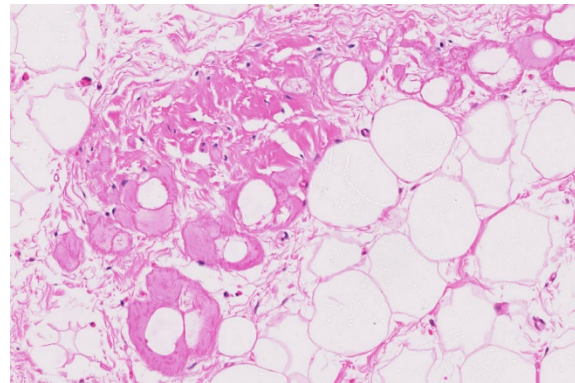
Veterinary Diagnostic Services, School of Veterinary Medicine
College of Medical, Veterinary and Life Sciences, University of Glasgow
Bearsden Road
G61 1QH
Glasgow, United Kingdom
www.glasgow.ac.uk/vds

JPC Diagnosis:

Heart, ventricle: Fibrofatty infiltration, subepicardial and myocardial, multifocal to coalescing, severe, with cardiomyocyte, atrophy, and loss.

JPC Comment:

The uncommon syndrome of humans and Boxer dogs (often referred to as “Boxer cardiomyopathy”) of arrhythmogenic right ventricular cardiomyopathy is poorly named, as the evolving literature has identified cases



Heart, horse. Entrapped Purkinje fibers also contain large clear cytoplasmic vacuoles. (HE, 282X)

in which degenerative lesions (and subsequent generation of arrhythmias) may arise in the atria and frequently, the left ventricle.

While mutations in several desmosomal genes have been identified as causative in the human condition, and a loss of desmosomal integrity has been identified in affected Boxers, mutations of desmosomal genes have not yet been identified in the Boxer model.¹⁰ Striatin, a scaffolding protein localized to intermediate filaments and the intercalated disk has been proposed as a potential cause in the Boxer. Decreased Wnt signaling in the myocardium of genetically engineered mouse models of ARVC appears to be responsible for increased myocardial adipogenesis, stimulating abnormal cell proliferation and differentiation as a result of beta-catenin accumulation in the cytoplasm of cardiac progenitor cells. Abnormal levels of beta catenin and mislocalization of this protein as well as striatin have been identified in affected Boxers.¹⁰

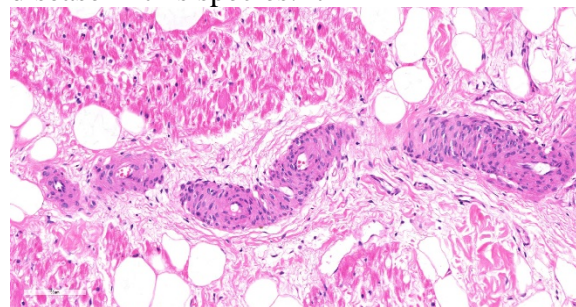
The veterinary literature is sparse with regard to this entity in the horse. This particular case was reported in the literature in 2015¹², bringing the total number of reported equine cases to three. In previous studies of cardiac muscle in several equine populations, including racing, working, and a general



Heart, horse. There is subintimal fibrosis of intramyocardial coronary arteries. (HE, 128X)

population, fibrofatty infiltration has not been identified as a post-mortem finding. Similar changes were noted within the right ventricle of the two other reported equine cases.¹² The microscopic changes noted in this entrapped myofibers are also commonly seen in the human cases, to include cytoplasmic vacuolation and nuclear dysmorphism.¹¹

ARVC has also been reported in two related chimps in a zoo collection (14 and 16 years of age) with no premonitory signs. A predominance of fibrofatty infiltration over the traditional interstitial fibrosis of the so-called “fibrosing cardiomyopathy”, considered the predominant form of heart disease in this species.¹⁷



Heart, horse. There is multifocal mural smooth muscle hyperplasia of intramyocardial arterioles. (HE, 128X)

A number of questions remain about the pathophysiology of this fascinating disease. Why are changes most prominent in the right ventricle? Current theory points to the thin wall and increased distensibility of the right ventricle which predisposes it to desmosomal failure;¹³ the identified cases of ARVC involving the atria as well as left ventricle does not put this pathogenesis into dispute. There is dispute within the literature as to whether the lesion is the result of abnormal proliferation or an aberrative repair response – earlier studies such as the one in the feline model of ARVC identified a much higher number of cases with myocardial inflammation to a level not identified in other models²; their association of inflammation and fibrofatty repair was made prior to

identification of causative genes in human cases and generation of genetically engineered mouse models.

References:

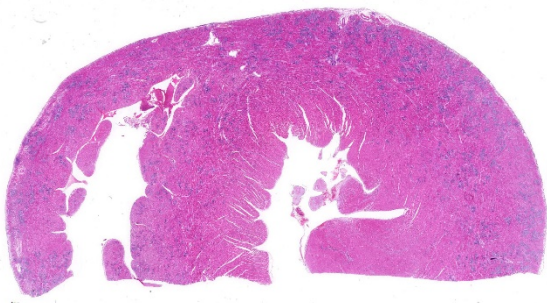
1. Basso C, Fox PR, Meurs KR. Arrhythmogenic right ventricular cardiomyopathy causing sudden cardiac death in Boxer dogs: a new animal model of human disease. *Circulation* 2004; 109:1180-1185.
2. Fox PR, Maron BJ, Basso C.. Spontaneously occurring arrhythmogenic right ventricular cardiomyopathy in the domestic cat: A new animal model similar to the human disease. *Circulation* 2000; 102:1863-1870.
3. Freel KM, Morrison LR, Thompson H, et al. Arrhythmogenic right ventricular cardiomyopathy as a cause of unexpected cardiac death in two horses. *Veterinary Record*. 2010; 166:718-722.
4. Kies P, Bootsma M, Bax J, et al. Arrhythmogenic right ventricular dysplasia/cardiomyopathy: Screening, diagnosis and treatment. *Heart Rhythm*. 2006; 3(2):225-234.
5. Marcus FI, Fontain GH, Guiraudon G. . Right ventricular dysplasia: a report of 24 adult cases. *Circulation*. 1982; 65: 384-398.
6. Meurs KM, Spier AW, Miller MW. Familial ventricular arrhythmias in boxers. *J Vet Intern Med*. 1999; 13:437-439.
7. Meurs KM, Lacombe VA, Dryburgh K, et al. Differential expression of the cardiac ryanodine receptor in normal and arrhythmogenic right ventricular cardiomyopathy canine hearts. *Hum Genet* 2006; 120:111–118.
8. Meurs KM, Erderer MM, Stern JA, et al. Desmosomal gene evaluation in Boxers with arrhythmogenic right ventricular cardiomyopathy. *Am J Vet Res*. 2007; 68(12):1338-1341.
9. Nakao S, Hirakawa A, Yamamoto S, et al. Pathologic features of arrhythmogenic right ventricular cardiomyopathy in middle-aged dogs. *J Vet Med Sci* 2011; 73(8):1031-6.
10. Oxford EM, Danko CG, Fox PR, Kornrich BG, Moise NS. Change in beta catenin localization suggests involvement of the canonical Wnt pathway in Boxer dogs with arrhythmogenic right ventricular cardiomyopathy. *J Vet Intern Med* 2014; 28:92-101.
11. Pilichou K, Nava A, Basso C, et al. Mutations in Desmoglein-2 Gene Are Associated With Arrhythmogenic Right Ventricular Cardiomyopathy. *Circulation*. 2006; 113:1171-1179.
12. Raftery AG, Garcin NC, Thompson HT, Sutton DGM. Arrhythmogenic right ventricular cardiomyopathy secondary to adipose infiltration as a cause of episodic collapse in a horse. *Irish Vet J* 2015;68:24. Doi 10.1186/s13620-015-0052-3.
13. Sen-Chowdry S, Morgan RD, Chamber JC. Arrhythmogenic cardiomyopathy: etiology diagnosis, and treatment. *Ann Rev Med* 2010; 61:233-253.
14. Thiene G, Nava A, Corrado D, et al. Right ventricular cardiomyopathy and sudden death in young people. *N Engl J Med*. 1988; 318(3):129-133.
15. Thiene G, Basso C. Arrhythmogenic right ventricular cardiomyopathy: An update. *Cardiovascular pathology*. 2001; 10:109-117.
16. Tiso N, Stephan DA, Nava A, et al. Identification of mutations in the cardiac ryanodine receptor gene in families affected with arrhythmogenic right ventricular cardiomyopathy type 2 (ARVC2). *Human molecular genetics*. 2001; 10(3):189-194.

17. Tong LJ, Flach EJ Sheppard MN, Pocknell A, aenerjee AA, Boswood A, Bouts T, Routh A, Feltrer. Fatal Arrhythmogenic right ventricular cardiomyopathy in two related subadult chimpanzees (*Pan troglodytes*). *Vet Pathol* 2014; 51(4): 858-887.

CASE IV: 317048 (JPC 4033739).

Signalment: 2-year and 6-month old female neutered domestic shorthair cat (*Felis catus*)

History: The animal was presented to the Internal Medicine department of the University Small Animal Hospital in the University of Glasgow School of Veterinary Medicine. The animal had a 6 week history of pica (licking coal) with a more recent history of reduced appetite and lethargy culminating to progressive deterioration of body condition. The animal was again referred to the Small Animal Hospital of the University and found to be tachypnoeic and lethargic. An echocardiogram showed thickening of the left ventricular wall and interventricular septum, mild pericardial effusion and a moderate pleural effusion. 45ml of blood tinged fluid was drained from the thorax. The fluid had a high protein count with clotting protein noted within the syringes. The respiratory rate improved but



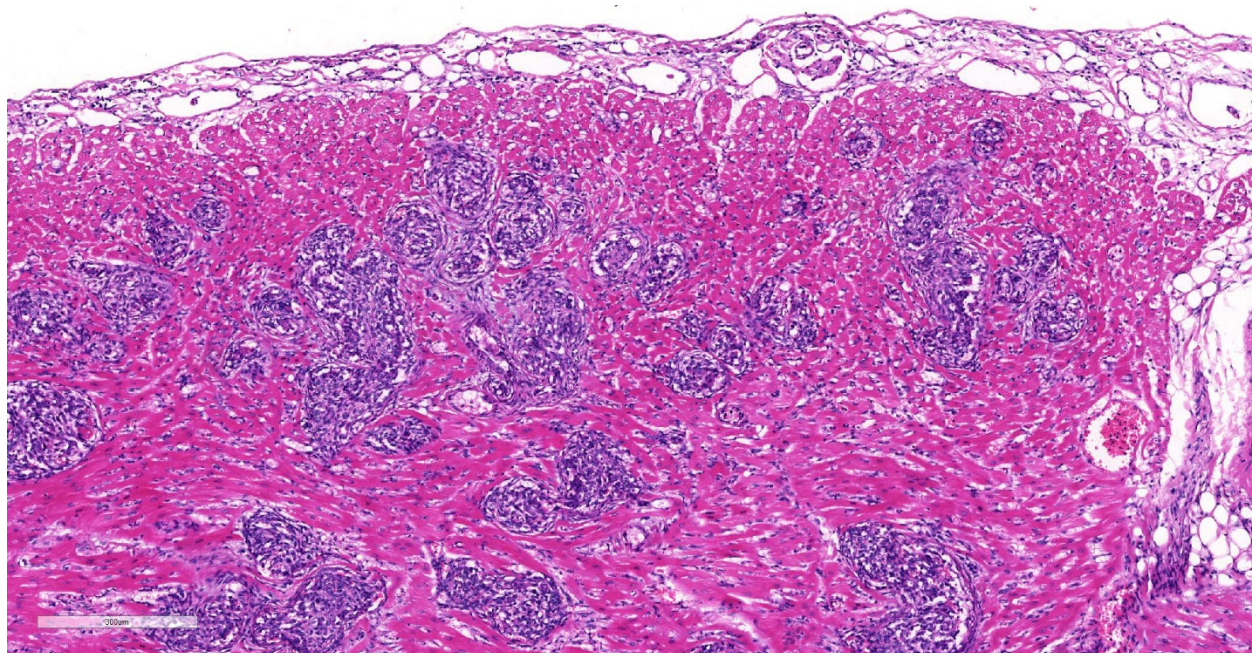
Heart, cat: (HE, 5X) Areas of hypercellularity outline the distribution of myocardial vessels within the outer half of the left ventricle, interventricular septum, and right ventricular wall (HE, 7X)

shortly after respiratory and cardiac arrest ensued. The owners decided for the resuscitation procedure to be interrupted.

Gross Pathology: The animal was in fairly good general condition with considerable visceral deposits of adipose tissue. Within the pleural cavity there were approximately 50 ml of reddish fluid. Moderate amount of pinkish fluid is present within the trachea and extend to the bifurcation and bronchi. Multifocal areas of collapse are noted affecting multiple pulmonary lobes. Within the pericardial cavity there was a small amount (less than 10 ml) of reddish fluid. Thin fibrin tags were noted on the surface of the left atrium, and few 2x3 mm irregular areas of dark red discoloration were present on the epicardium in the upper portion of the left ventricle. The heart appeared moderately elongated and enlarged, and weighed 20.44 gr. The heart was fixed whole and re-evaluated a few days after fixation. Multiple transverse sections in the mid to lower portion of the ventricles were taken. The left ventricular wall and interventricular septum appeared moderately thickened with substantial reduction of the left ventricle lumen.

The spleen was moderately enlarged. The femoral bone marrow was diffusely plum red in color. In the urinary bladder there were multifocal ectatic venous vessels visible from the mucosal surface.

Laboratory results: Hematology evaluation showed a haematocrit of 20.8%, mild leukocytosis with a normal neutrophil count and thrombocytopenia. A blood smear examination revealed moderate regeneration with polychromasia, anisocytosis and circulating red blood cell precursors. Testing for *Mycoplasma haemofelis* on a sample of peripheral blood was negative. There were some platelet aggregates on examination and



Heart, cat: Arterioles are expanded by concentric to haphazard arrangement of spindle cells. (HE, 88X)

on visual examination her platelet count was between 45-60x10⁹/l.

Clinical chemistry revealed a mild azotemia, increases in ALT (290U/l) and AST (219U/l) and a mild increase in total bilirubin.

Slide agglutination test was unremarkable and Coombs test was negative.

Microscopic Description:

Involving approximately 30-40% of the tissue within the myocardium of the left and right ventricle and interventricular septum, there are proliferative changes multifocally affecting small to medium sized vessels. The vascular changes are characterised by proliferation of haphazardly arranged spindle cells frequently delimiting small slit-like spaces frequently showing the presence of erythrocytes and occasional fibrin thrombi. Some proliferations, characterised by a round shape and irregularly anastomosed vascular spaces, are reminiscent of glomeruloid structures. Multifocal variably sized areas of

oedema with separation and disruption of cardiomyocytes are detectable, in some instances characterised by accumulation of small numbers of extravasated erythrocytes (microhaemorrhages). Scattered foci or small areas of cardiomyocyte condensation, shrinkage and fragmentation (degeneration and necrosis) are detectable with some variation among the sections. Focal areas of myocardial and subendocardial haemorrhage affecting a portion of a papillary muscle of the left ventricle are noted (but not present in all sections). Numerous small infiltrates of moderate numbers of lymphocytes, plasma cells and few macrophages are noted multifocally along the epicardium.

The plump spindloid cells comprising the vascular proliferative lesions were characterised by consistent moderate to strong cytoplasmic immunoreactivity for alpha smooth muscle actin (αSMA) and only occasional positive staining for van Willebrand Factor (vWF). On the other hand, strong vWF immunolabeling was consistently observed in fibrin and platelet thrombi associated with the small irregular

and slit-like lumens of the vascular proliferative lesions.

Vascular proliferative changes similar to those observed in the heart were also noted in the spleen, in the bone marrow, and in the kidney, affecting the afferent arterioles at the vascular pole of the glomeruli, and to variable extents the of glomerular tuft capillaries.

Contributor's Morphologic Diagnoses:

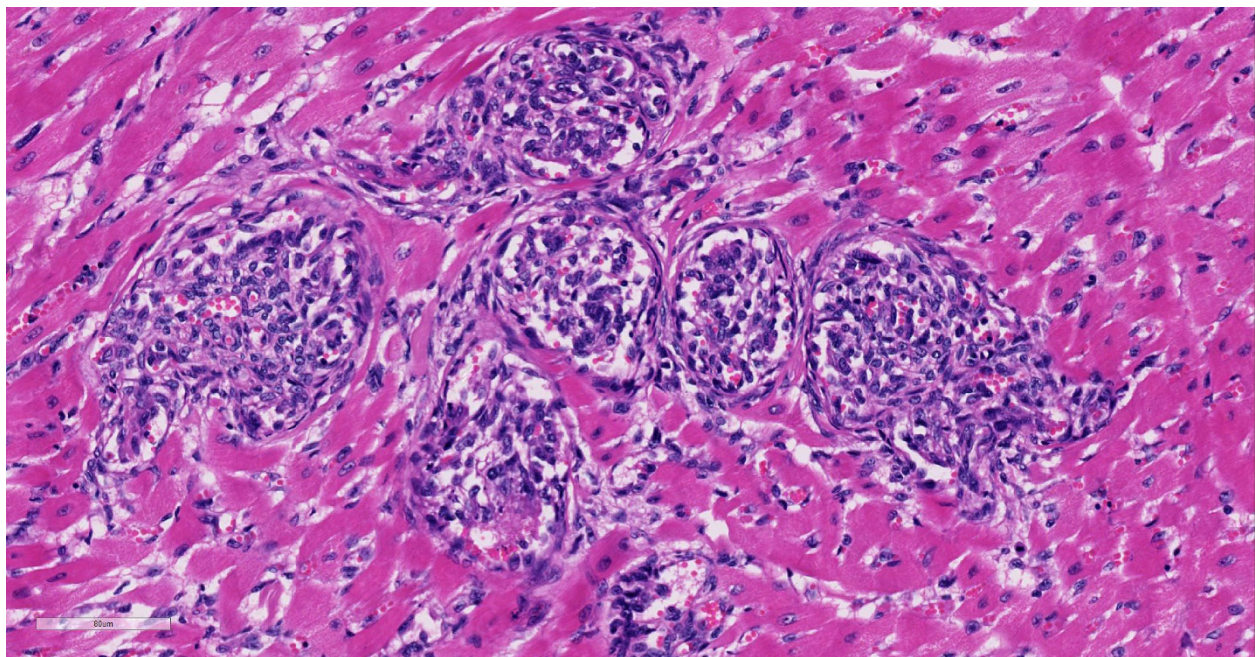
Heart, intravascular endothelial and pericyte proliferation, marked, multifocal, consistent with reactive angioendotheliomatosis

Contributor's Comment: The term "angioendotheliomatosis" in human medicine has been a subject of controversy and confusion, resolved with the recognition of two distinct conditions: "malignant angioendotheliomatosis" form representing a type of aggressive intravascular lymphoma, and "reactive angioendotheliomatosis" (RAE) which

consists of endothelial cells and pericyte proliferation. 15 proliferative changes mainly affecting small to medium sized vessels of the skin. Notably, two cases of intravascular disseminated angiosarcoma were also reported in humans and discussed as examples of "true neoplastic angioendotheliomatosis".⁸

Seventeen cases of "malignant angioendotheliomatosis" (intravascular lymphoma) were described in the dog, with consistent involvement of the central nervous system and variable involvement of other tissues,⁹ and a single case was described in the cat.⁶ Sporadic cases of feline multisystemic disease characterized by vascular endothelial and pericyte proliferative lesions have been reported, addressing comparisons with different vasoproliferative conditions in humans and other animal species.^{4,11,12}

A subsequent report describing a case series of cats affected by similar multisystemic



Heart, cat: Higher magnification of affected vessels. Slit-like lumina containing erythrocytes are present between spindle cells, and dilated vessels compress adjacent hyalinized cardiomyocytes. (HE, 278X)

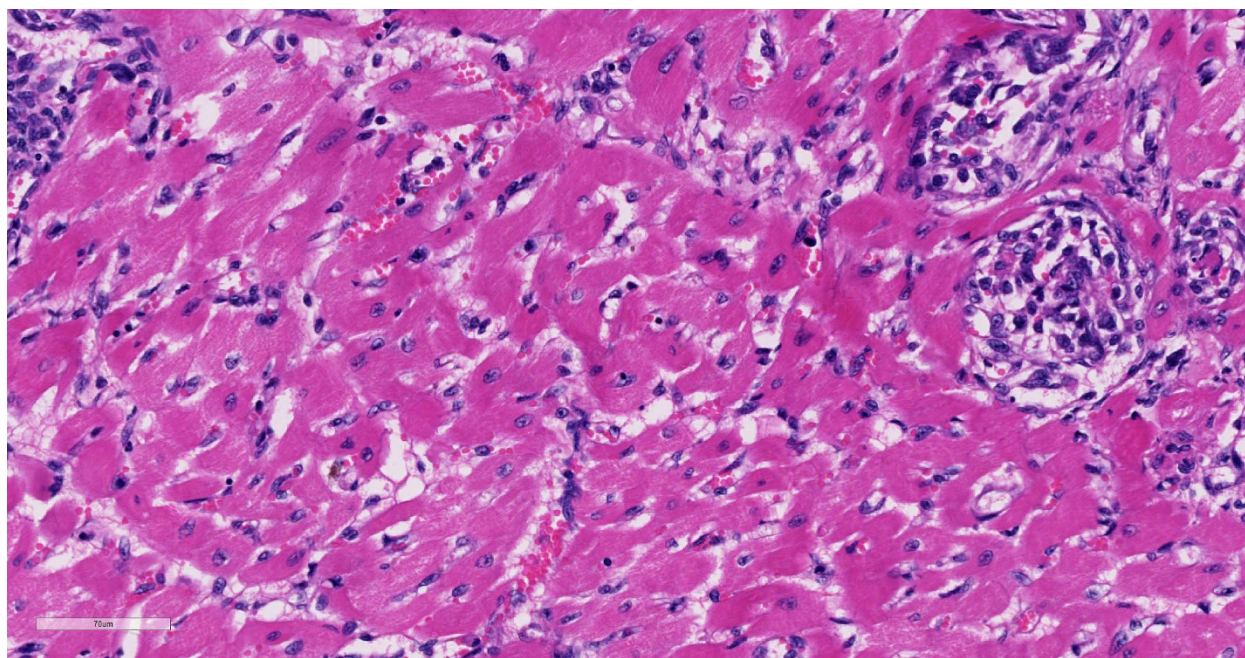
vascular proliferative lesions and addressing a review of the literature, defined the criteria for the classification of this condition as feline systemic reactive angioendotheliomatosis.⁵ This rare condition in cats proves invariably fatal and frequently characterized by cardiac dysfunction and/or failure, variably associated with respiratory distress, in some cases hematological alterations. Serosanguinous and/or fibrinous pericardial effusions were reported in some instances, similar to those observed in our case. Microscopic evidence of vascular proliferative changes was most consistently observed in the heart in all cases. Spleen, kidney and lymph nodes were also frequently involved. Other organs affected at lower frequency included pancreas, gastrointestinal tract, brain, meninges, eyes, adrenals, spinal cord, liver, subcutis, thyroids, sciatic nerve and bone marrow.^{4-5,11-12}

The etiopathogenesis of reactive angioendotheliomatosis remains obscure in both humans and cats. The possible

association of reactive angioendotheliomatosis with underlying infection, thrombotic thrombocytopenic purpura (TTP), autoimmune disorders, hypersensitivity, cryoglobulinemia, renal and liver failure, post liver transplantation, bone marrow transplantation-related graft versus host disease has been discussed in humans^{7,10,15}

A recent report described the detection of DNA of different *Bartonella* species, including *B. vinsonii* subsp. *berkhoffii*, *B. henselae*, and *B. koehlerae* from tissues of cats affected by systemic reactive angioendotheliomatosis.¹ The authors also provide evidence for *B. vinsonii* subsp. *berkhoffii* causing upregulation of hypoxia inducible factor-1 α (HIF-1 α) with resulting increased production of vascular endothelial growth factor (VEGF) in an *in vitro* cell culture system.¹

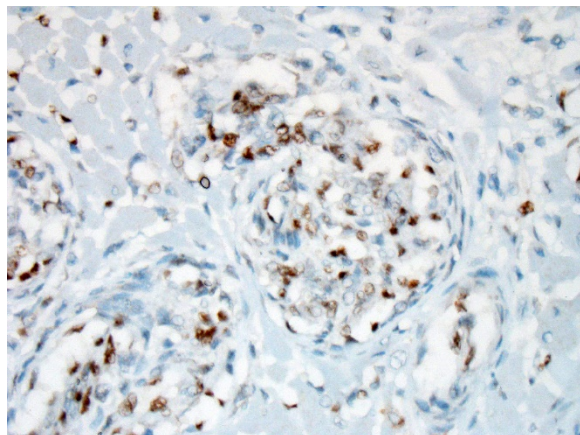
Lesions with features strikingly similar to feline systemic reactive angioendotheliomatosis were reported in a 2-year



Heart, cat: Cardiomyocytes adjacent to affected arterioles often show evidence of degeneration (hyalinization and loss of cross striations) and necrosis (pyknosis). (HE, 317X)

old steer presumed to be persistently infected with bovine viral diarrhea virus (BVDV). BVDV antigen was detected in a proportion of the glomeruloid intravascular proliferations.³ The authors addressed a possible comparison between the multisystemic vascular proliferative changes and a TTP-like condition ensuing in the animal. The possibility of relationship between BVDV infection and the development of the intravascular proliferative lesions was also discussed although a causal connection could not be definitively demonstrated.³ Interestingly, tissue samples from this animal were also submitted for molecular analysis and *B. henselae* DNA was isolated from the vascular proliferative lesions affecting that steer.¹ These results offer interesting perspectives on the postulated association between infection with *Bartonella* spp. and the development of vascular proliferative changes including bacillary angiomatosis,¹⁶ epithelioid haemangioendothelioma,² and hemangiosarcoma.²

However, a later study demonstrated that, in the context of diagnostic histopathology laboratories, multiple potential sources of cross-contamination associated with tissue



Heart, cat: A portion of cells within the arteriolar lumina demonstrate strong nuclear immunopositivity for ERG transcription factor) (anti-ERG, 400X)

processing may result in *Bartonella* spp. DNA carryover and need to be carefully monitored and excluded to ensure the validity and significance of *Bartonella* spp. isolation from paraffin embedded tissues.¹³

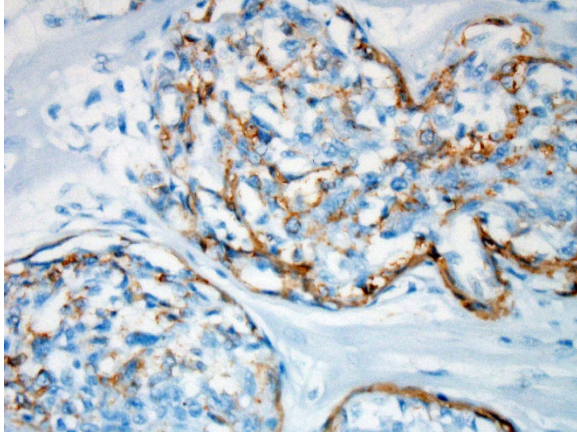
Immunohistochemical labeling performed at the JPC showed that some of the proliferative cells within the arterioles were positive for smooth muscle actin, while a second population within the proliferative masses were simultaneous immunopositive for Factor VIII antigen as well as ERG transcription factor.

Contributing Institution:

Veterinary Diagnostic Services, School of Veterinary Medicine
College of Medical, Veterinary and Life Sciences, University of Glasgow
Bearsden Road
G61 1QH
Glasgow, United Kingdom
www.glasgow.ac.uk/vds

JPC Diagnosis: Heart arterioles: Atypical endothelial and pericyte proliferation (angioendotheliomatosis), diffuse, severe, with cardiomyocyte degeneration, necrosis, and myocardial fibrosis.

JPC Comment: The contributor excellently summarizes the available literature on this rare condition of cats. Since 1985, the veterinary literature is limited to a total of 15 cases, not including two WSC submissions during this time (WSC 2008 Conf. 3 Case 2 and WSC 2014 Conf. 21, Case 3). Since the submission of this case, a single case report was published on this particular entity.¹⁷ Immunohistochemical results for this condition have been published in several articles on this condition in the cat,^{5,11,17} with intraluminal spindle cells staining strongly positive for Factor-VIII related antigen and VWF, and occasionally for smooth muscle



Heart, cat: A portion of cells within the arteriolar lumina demonstrate strong cytoplasmic immunoreactivity for smooth muscle actin. (anti-SMA, 400X)

actin (suggesting that some of the cells within the proliferation are of pericyte origin.) Immunohistochemical stains for FVIIIra and smooth muscle actin run at the JPC are in agreement with these findings. Because of the dual cell population, lesions of FSRA are considered to be an aberrant reactive process rather than a neoplasm.

The contributor also points out potential confusion in the naming of this particular condition. A very different condition, intravascular lymphoma, is presented in the veterinary literature as “malignant angioendotheliomatosis” (aka “intravascular lymphomatosis” and “angiotropic large-cell lymphoma”). While the syndrome of FRSA does bear a similar morphology to the human disease of reactive endotheliomatosis (which in humans is restricted to the skin), there does not appear to be a human precedent for the unfortunate name of “malignant angioendotheliomatosis.”

References:

1. Beerlage C, Varanat M, Linder K, Maggi RG, Cooley J, Kempf VA, Breitschwerdt EB. Bartonella vinsonii subsp. berkhoffii and Bartonella henselae as potential causes of proliferative vascular

- diseases in animals. *Med Microbiol Immunol.* 2012; 201(3): 319- 326.
2. Breitschwerdt EB, Maggi RG, Varanat M, Linder KE, Weinberg G. Isolation of Bartonella vinsonii subsp. berkhoffii genotype II from a boy with epithelioid hemangioendothelioma and a dog with hemangiopericytoma. *J Clin Microbiol.* 2009; 47 (6): 1957-1960.
3. Breshears MA, Johnson BJ. Systemic reactive angioendotheliomatosis-like syndrome in a steer presumed to be persistently infected with bovine viral diarrhea virus. *Vet Pathol.* 2008; 45 (5): 645-649.
4. Dunn KA, Smith KC, Blunden AS. Fatal multisystemic intravascular lesions in a cat. *Vet Rec.* 1997; 140(5): 128-129.
5. Fuji RN, Patton KM, Steinbach TJ, Schulman FY, Bradley GA, Brown TT, Wilson EA, Summers BA. Feline systemic reactive angioendotheliomatosis: eight cases and literature review. *Vet Pathol.* 2005; 42(5): 608-617.
6. Lapointe JM, Higgins RJ, Kortz GD, Bailey CS, Moore PF. Intravascular malignant T-cell lymphoma (malignant angioendotheliomatosis) in a cat. *Vet Pathol.* 1997; 34(3): 247-250
7. Lazova R, Slater C, Scott G. Reactive angioendotheliomatosis. Case report and review of the literature. *Am J Dermatopathol.* 1996; 18 (1): 63-69.
8. Lin BT, Weiss LM, Battifora H. Intravascularly disseminated angiosarcoma: true neoplastic angioendotheliomatosis? Report of two cases. *Am J Surg Pathol.* 1997 21(10): 1138-1143.

9. McDonough SP, Van Winkle TJ, Valentine BA, vanGessel YA, Summers BA. Clinicopathological and immunophenotypical features of canine intravascular lymphoma (malignant angioendotheliomatosis). *J Comp Pathol.* 2002; 126 (4): 277-288.
 10. McMenamin ME, Fletcher CD. Reactive angioendotheliomatosis: a study of 15 cases demonstrating a wide clinicopathologic spectrum. *Am J Surg Pathol.* 2002; 26 (6): 685-697.
 11. Rothwell TL, Xu FN, Wills EJ, Middleton DJ, Bow JL, Smith JS, Davies JS. Unusual multisystemic vascular lesions in a cat. *Vet Pathol.* 1985; 22(5): 510-512.
 12. Straumann Kunz U, Ossent P, Lott-Stolz G. Generalized intravascular proliferation in two cats: endotheliosis or intravascular pseudoangiosarcoma? *J Comp Pathol.* 1993; 109 (1): 99-102.
 13. Varanat M, Maggi RG, Linder KE, Horton S, Breitschwerdt EB. Cross-contamination in the molecular detection of Bartonella from paraffin-embedded tissues. *Vet Pathol.* 2009; 46 (5): 940-944.
 14. Varanat M, Maggi RG, Linder KE, Breitschwerdt EB. Molecular prevalence of Bartonella, Babesia and hemotropic Mycoplasma sp. in dogs with splenic disease. *J Vet Intern Med.* 2011; 25 (6): 1284-1291
 15. Wick MR, Rocamora A. Reactive and malignant "angioendotheliomatosis": a discriminant clinicopathological study. *J Cutan Pathol.* 1988; 15 (5): 260-271.
 16. Yager JA, Best SJ, Maggi RG, Varanat M, Znajda N, Breitschwerdt EB. Bacillary angiomatosis in an immunosuppressed dog. *Vet Dermatol.* 2010; 21 (4): 420-428
- Yamamoto S, Shimoyana Y, Haruyama T. A case of feline systemic reactive angioendotheliomatosis. *J Fel Med Surg* 2015; doi: 10.1177/2044116915579684.

Self-Assessment - WSC 2018-2019 Conference 13

1. Which of the following is NOT a finding in the mouse model for ebolavirus infection?
 - a. Early targeting of macrophages
 - b. Widespread lymphocytolysis by day 5
 - c. Extensive fibrin thrombi within the spleen
 - d. Limited infection of endothelial cells

2. Which of the following histologic findings have NOT been identified in cases of hypertrophic cardiomyopathy in the cat?
 - a. Medial hypertrophy of intramyocardial arteries
 - b. Increased vascular density per square centimeter of myocardium
 - c. Myocardial fibrosis
 - d. Myofiber disarray

3. Which of the following proteins is useful in the diagnosis of hypertrophic cardiomyopathy in the cat?
 - a. Aspartate aminotransferase
 - b. Creatine kinase
 - c. Beta myosin
 - d. Cardiac troponin I

4. Failure in which of the following organelles has been identified as important in the pathogenesis of arrhythmogenic right ventricular cardiomyopathy?
 - a. Desmosome
 - b. Mitochondrion
 - c. Ribosome
 - d. Golgi apparatus

5. Reactive angioendotheliomatosis has most often been reported in which of the following species?
 - a. Cat
 - b. Dog
 - c. Cattle
 - d. Swine

Please email your completed assessment to Ms. Jessica Gold at Jessica.d.gold2.ctr@mail.mil for grading. Passing score is 80%. This program (RACE program number) is approved by the AAVSB RACE to offer a total of 0.5 CE Credits, with a maximum of 12.5 CE Credits being available to any individual Veterinary Medical Professionals for the 2017-2018 Wednesday Slide Conference. This RACE approval is for the subject matter categories of: SCIENTIFIC using the delivery method of NON-INTERACTIVE DISTANCE. This approval is valid in jurisdictions which recognize AAVSB RACE; however, participants are responsible for ascertaining each board's CE requirements. RACE does not "accredit", "endorse" or "certify" any program or person, nor does RACE approval validate the content of the program.

Please email your completed assessment to Ms. Jessica Gold at Jessica.d.gold2.ctr@mail.mil for grading. Passing score is 80%. This program (RACE program number) is approved by the AAVSB RACE to offer a total of 0.5 CE Credits, with a maximum of 12.5 CE Credits being available to any individual Veterinary Medical Professionals for the 2017-2018 Wednesday Slide Conference. This RACE approval is for the subject matter categories of: SCIENTIFIC using the delivery method of NON-INTERACTIVE DISTANCE. This approval is valid in jurisdictions which recognize AAVSB RACE; however, participants are responsible for ascertaining each board's CE requirements. RACE does not "accredit", "endorse" or "certify" any program or person, nor does RACE approval validate the content of the program.

Joint Pathology Center
Veterinary Pathology Services



WEDNESDAY SLIDE CONFERENCE 2018-2019

Conference 14

9 January 2018

CASE I: NE 17-176 (JPC 4101745).

Signalment: 6-year-old neutered male brindle Mastiff dog, *Canis familiaris*



Thyroid gland, dog. The thyroid glands were small. Vessels within the gland and fibroadipose tissue are occasional opaque and whitish-yellow prominent due to mural accumulation of cholesterol and inflammatory cells. (Photo courtesy of: University of Tennessee College of Veterinary Medicine, Department of Biomedical and Diagnostic Sciences, 2407 River Drive, Room A205, Knoxville, TN 37996, https://vetmed.tennessee.edu/departments/Pages/biomedical_diagnostic_sciences.aspx)

History: This dog had a 10-minute seizure at home and afterwards he was blind. He had had a similar, but less severe episode of altered mental status several weeks prior. Physical exam findings included dull mentation, circling to the right, and negative menace response. After premedication for imaging, the dog developed ventricular tachycardia and was euthanized.

Gross Pathology: The dog was in obese nutritional condition (body condition score 4.5/5) and the tail was alopecic. The thyroid glands were small (right 3x2x32mm; left 5x3x30mm). The walls of many vessels including the coronary arteries, prostatic vessels, and meningeal vessels had white opaque firm walls. The myocardium adjacent to affected coronary vessels was often red.

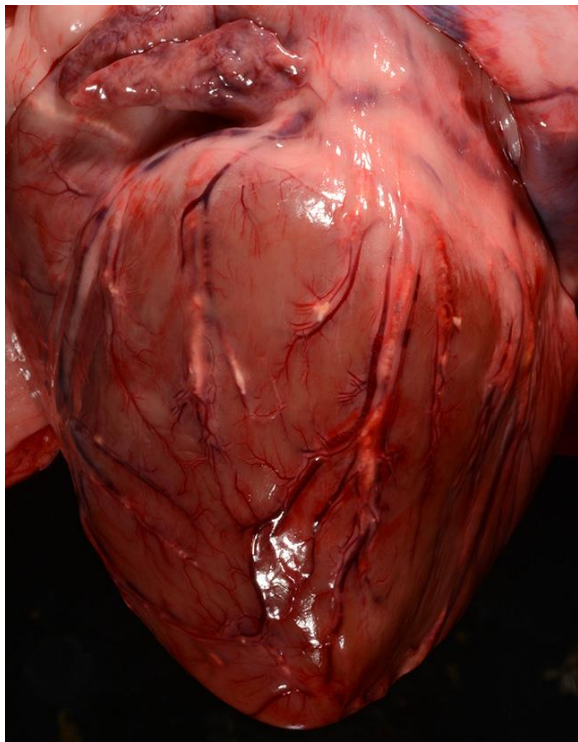
Laboratory results: None.

Microscopic Description:

Thyroid: The thyroid glands are small and lack follicles. The follicles are replaced by dense infiltrates of small lymphocytes and plasma cells. The remaining C (parafollicular) cells are prominent. The vessels within and around the gland have

foamy macrophages and acicular (cholesterol) clefts replacing and expanding their walls, often resulting in occlusion of the lumen. The parathyroid gland is unremarkable.

Artery and surrounding vessels: The muscular artery at the center of the section (taken from the hilus of the liver) has mild multifocal expansion of the tunica muscularis by foamy macrophages and small acicular clefts (not present in all sections). The surrounding smaller vessels have severe replacement and expansion of their walls by foamy macrophages and acicular (cholesterol) clefts. The deposits often narrow or occlude the lumens, which occasionally contain thrombi. There is mild lymphoplasmacytic inflammation within the adventitia of the affected vessels.



Heart, dog. Atherosclerotic plaques are prominent within coronary arteries. (Photo courtesy of: University of Tennessee College of Veterinary Medicine, Department of Biomedical and Diagnostic Sciences, 2407 River Drive, Room A205, Knoxville, TN 37996, https://vetmed.tennessee.edu/departments/Pages/biomedical_diagnostic_sciences.aspx)



Prostate gland. Atherosclerotic plaques are prominent within prostatic and paraprostatic arterioles. (Photo courtesy of: University of Tennessee College of Veterinary Medicine, Department of Biomedical and Diagnostic Sciences, 2407 River Drive, Room A205, Knoxville, TN 37996, https://vetmed.tennessee.edu/departments/Pages/biomedical_diagnostic_sciences.aspx)

Contributor's Morphologic Diagnoses:

Severe chronic diffuse lymphocytic thyroiditis with follicular atrophy
Severe multifocal chronic vascular atherosclerosis with thrombosis.

Contributor's Comment: Lymphocytic thyroiditis in dogs is similar to Hashimoto's disease of humans. Both are thought to have a polygenic inheritance. Predisposed dog breeds include: boxers, bulldogs, dachshunds, great Danes, Doberman pinschers, golden and Labrador retrievers. Circulating autoantibodies to thyroglobulin are present in affected humans and dogs. Interestingly, the infiltrating lymphocytes and plasma cells are thought to mechanically dislodge the thyroid follicular epithelial cells from their basement membranes resulting in destruction of the follicle.³

The vessel (and nerve) bundle on the submitted slides was taken from the hilus of

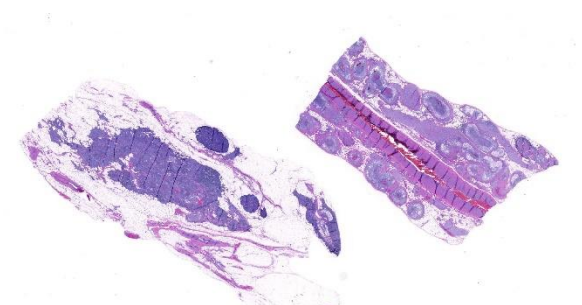
the liver. The central vessel is presumed to be the hepatic artery (although pretty small for a mastiff). The surrounding more severely affected vessels were presumed to be veins, but veins are reportedly unaffected in canine atherosclerosis.⁴ Grossly, they resembled lymphatic vessels, but those are also presumably unaffected by atherosclerosis.

This dog had a history of hypothyroidism and had been recently restarted (too late) on his thyroid supplementation in response to his clinical signs. The seizures were likely due to ischemic brain lesions; meningeal and cerebral vessels were occluded by atherosclerosis. Coronary artery atherosclerosis and the resulting myocardial ischemia likely caused the arrhythmia. Externally the findings consistent with hypothyroidism were obesity and tail alopecia.

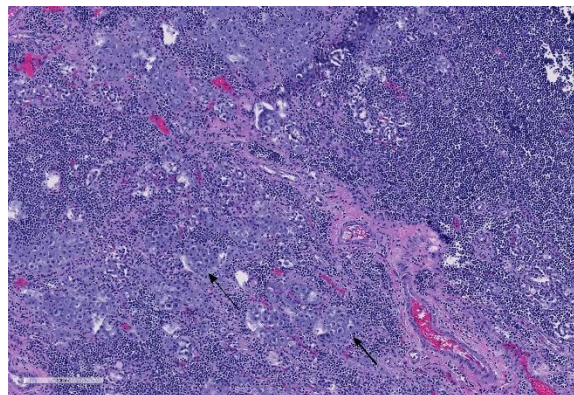
In summary, this was a case of lymphocytic thyroiditis which led to hypothyroidism which led to hyperlipidemia which led to widespread atherosclerosis which led to cerebral and myocardial ischemia which led to seizures and arrhythmia, respectively.

Contributing Institution:

University of Tennessee College of Veterinary Medicine
Department of Biomedical and Diagnostic Sciences
2407 River Drive, Room A205



Thyroid gland (left) and hepatic hilar vessels: The thyroid gland (left) is largely effaced by an inflammatory infiltrate. At right, hepatic hilar arterioles are tortuous and markedly expanded. (HE, 5X)



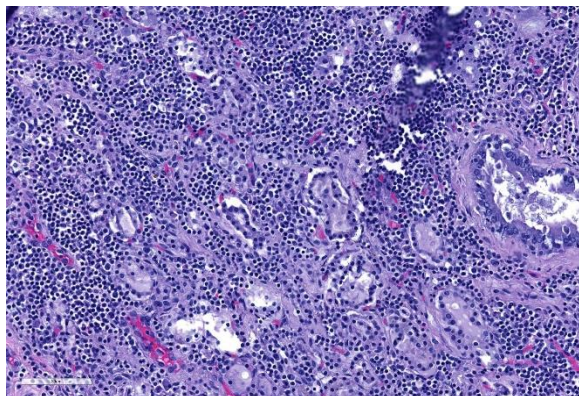
Thyroid gland: Follicular architecture is lost and replaced by marked lymphoplasmacytic inflammation. Large nests of interfollicular cells remain (arrows). (HE 154X)

Knoxville, TN 37996

https://vetmed.tennessee.edu/departments/Pages/biomedical_diagnostic_sciences.aspx

JPC Diagnosis: 1. Thyroid gland: Thyroiditis, lymphoplasmacytic, diffuse, severe with severe follicular atrophy and moderate parafollicular hyperplasia.
2. Thyroid gland, adjacent perivascular fibroadipose tissue, arterioles: Atherosclerosis, diffuse, severe with thrombosis and recanalization.

JPC Comment: As discussed above, this case is an excellent example of primary hypothyroidism due to canine lymphocytic thyroiditis (CLT) in the dog. According to various studies, 65-80% of cases are the result of autoimmune disease, with resulting lymphoplasmacytic thyroiditis and destruction of the thyroid gland.² A number of breeds show a breed predisposition for hypothyroidism, including dobermans, Great Danes, poodles, Irish Setters, miniature and giant schnauzers, boxers, golden retrievers, dachshunds, Shetland Sheepdogs, Pomeranians, Cocker Spaniels and Airedales and Hovawarts.¹ Both cellular and humoral mechanisms of immunity are involved in this pathogenesis. Affected animals generally exhibit decreased thyroxine and 75% will



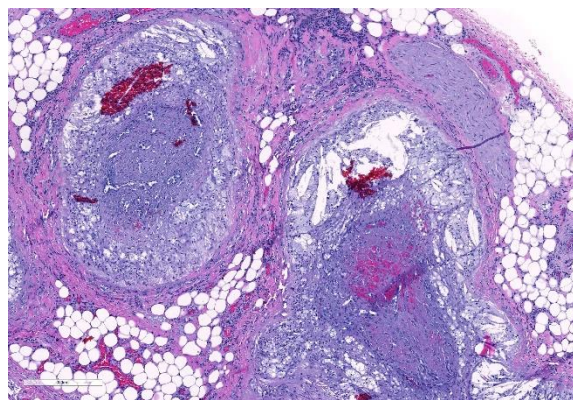
Thyroid gland: Remaining follicles are lined by cuboidal, often detached epithelium and do not contain colloid. A cross section through a Kursteiner's cyst is present at right. (HE, 190X)

demonstrate decreased serum TSH levels. Autoantibodies against thyroglobulin, thyroxine, and triiodothyronine correlate well with lymphocytic thyroid inflammation. In humans, immune complexes containing thyroglobulin have been identified in the basement membrane of thyroid follicles, which may induce NK cell activity and/or complement activation.¹

A sensitive assay for thyroglobulin autoantibodies (TGAA) is available and may be positive in animals at a young age, but progression of the disease is variable and cannot be accurately predicted. TGAA positivity has been identified as the first stage of subclinical canine lymphocytic thyroiditis.¹ Even when up to 60%-70% of the thyroid has been replaced by lymphocytic inflammation, hypothyroidism may yet be subclinical as a result of overstimulation of remaining follicles by elevated TSH.¹ In end stage hypothyroidism, in which almost all thyroid follicles are destroyed (similar to that seen in this case), TGAA may decrease, but TSH, T3, and T4 levels remain abnormal.¹ Boxers, Giant Schnauzers, and Hovawarts have been shown to develop CLT with elevated TGAA levels.¹

The foamy basophilic to amphophilic cells

within the thyroid were discussed during the conference. Some participants thought they represented “oncocytes” (thyroid follicular cells), others believed they were macrophages, while others still thought there were parafollicular c-cells. Participants reviewed a battery of immunohistochemical stains (TTF-1, Iba-1, and synaptophysin and chromogranin-A). The cells in question are diffusely immunoreactive to neuroendocrine markers (chromogranin-A) indicating c-cell origin. It was unclear to the participants whether these cells were hyperplastic, hypertrophic, or simply remnants of normal cells.



Hepatic hilus, dog: The walls of hilar arterioles is markedly expanded by plaques of foam cells and cholesterol clefts admixed with cellular debris. The tunica intima is effaced and the lumen has been remodeled and recanalized. (HE, 85X)

References:

1. Ferm K, Bjornerfeldt S, Karlsson A, Andersson G, Nacrtiner R, Hedhammar A. Prevalence of diagnostic characteristics indicating canine autoimmune lymphocytic thyroiditis in giant schnauzer and hovawart dogs. *J Small Anim Pract* 2009; 50:176-179.
2. Mansfield CS, Mooney CT. Lymphocytic-plasmacytic thyroiditis and glomerulonephritis in a boxer. *J*

Small Anim Pract 2006: 47:396-399.

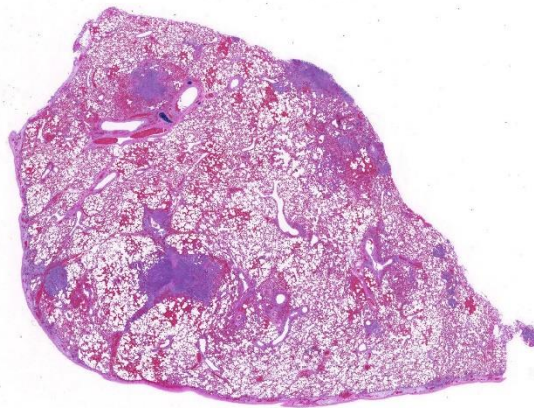
3. Rosol TJ, Grone A. Endocrine Glands. In: Maxie MG, ed. *Jubb, Kennedy, and Palmer's Pathology of Domestic Animals*. Vol 3, 6th ed. St. Louis Elsevier; 2016:315-319.
4. Robinson WF, Robinson NA. Cardiovascular System. In: Maxie MG, ed. *Jubb, Kennedy, and Palmer's Pathology of Domestic Animals*. Vol 3, 6th ed. St. Louis Elsevier; 2016:57-59.

CASE II: S1603556 (JPC 4084299).

Signalment: A 1-year-old Quarter horse filly

History: The filly had a history of 10-day lethargy. The owner was suspicious of a rattlesnake bite.

Gross Pathology: The lip was diffusely thickened with edema. Both submandibular lymph node were enlarged, firm and dark red. Bilaterally, the parietal pleura had multiple petechiae and ecchymoses. Multifocally in both lungs there were numerous white, firm nodules, approximately 2 to 3mm in diameter, surrounded by a dark red halo. The parenchyma between these nodules was dark red and firm. The pericardium, mainly in proximity to the coronary vessels and paragonal septum, also showed several multiple petechiae and ecchymoses. The kidneys had several multifocal white, firm cortical spots of approximately 1 to 3mm in diameter. The cortex was diffusely pale. The mesentery had multifocal random white firm nodules of approximately 3 to 5 mm in diameter surrounded by a dark red halo.



Lung, horse. At subgross magnification, areas of a dense cellular infiltrate as well as foci of hemorrhage are scattered randomly throughout the section. (HE, 4X)

Laboratory results: No bacterial pathogens were isolated from liver, lung, spleen and submandibular lymph node on aerobic culture.

Microscopic Description:

Lung: centering in small caliber vessels and extending into the adjacent alveolar spaces and septa, there is a multifocal and random inflammatory infiltrate composed by large numbers of viable and degenerated neutrophils, fewer histiocytes and occasional multinucleated giant cells that are admixed with basophilic cellular debris and several rounded eosinophilic protozoa of approximately 15 to 20 μm in diameter, with an eccentric single round nucleus. In addition, there are numerous fibrin thrombi and segments of alveolar necrosis. A few blood vessels display transmural necrosis, with fibrinoid degeneration and the presence of pyknotic debris. The remaining parenchyma shows moderate congestion, occasional small hemorrhages and multiple focal areas of intra-alveolar edema.

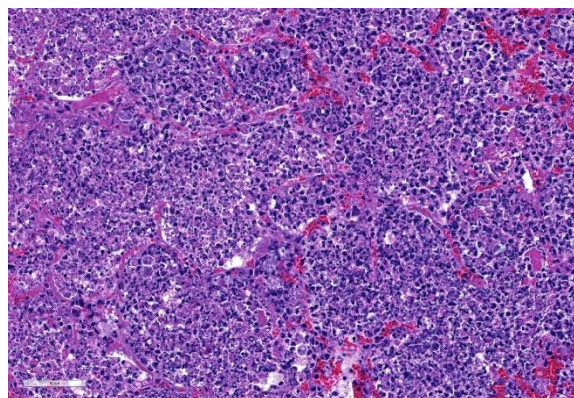
Contributor's Morphologic Diagnosis: Embolic pneumonia, necrosuppurative, severe, multifocal, with numerous trophozoites.

Etiology: *Acanthamoeba sp.*

Additional Findings: Trophozoites were immunolabeled for *Acanthamoeba sp.* in the lung, kidney and lymph node via immunohistochemistry test. In addition, a lymphohistiocytic to granulomatous interstitial nephritis, myocardial necrosis and mineralization, focal suppurative myositis; moderate to severe suppurative, lymphoplasmacytic and histiocytic, necrotizing peritonitis, gastritis and hepatitis, with protozoa consistent with *Acanthamoeba sp.* were also observed.

Contributor's Comment: *Acanthamoeba sp.* are ubiquitous free-living amoebae distributed in the environment.^{2,3} Disease produced by these amoebae have been described in cows, dogs, pigs, rabbits, pigeons, sheep, reptiles, fish, turkeys, rhesus macaque and toucans.^{7,8} Amoebic infection in horses is very rare and it has been reported in Southern California, USA, causing pneumonia, meningoencephalitis⁴ or systemic infections, and in placentitis in the state of New South Wales, Australia¹. The reason for these presentations is still not clear. Amoebas can be easily missed in histology sections because of the morphology of their trophozoites, which resemble macrophages¹. Reports of human infection with *Acanthamoeba sp.* have traditionally been limited to cases of systemic disease in the immunocompromised, granulomatous encephalitis, keratitis and cutaneous and sinus lesions.²

Acanthamoeba has two stages in its life cycle, a vegetative trophozoite stage with a diameter of 13-23 μm and dormant cyst stage of 13-23 μm . During the trophozoite stage, *Acanthamoeba* feeds on organic particles as well as other microbes and divides mitotically under optimal conditions.⁵ It has



Lung, horse: Hypercellular areas consist of areas of lytic necrosis with discontinuous, thrombosed, and necrotic alveolar septa and expansion of alveoli by innumerable degenerate neutrophils admixed with cellular debris. (HE, 335X)

been proposed as a reservoir of several microorganisms as *Legionella pneumophila*, *Pseudomonas aeruginosa*, *Enterobacter cloacae*, *Escherichia coli*, *Serratia marcescens*, *Klebsiella spp.* and *Streptococcus pneumoniae*.²

Amoebae can be cultured from lesions by special methods, which are not available in most diagnostic laboratories. Speciation may be accomplished by fluorescent antibody testing and immunohistochemistry.³

Information on treating topical and systemic amoebic infections in animals is lacking.³

Contributing Institution:

California Animal Health and Food Safety Lab. San Bernardino Branch. University of California, Davis

JPC Diagnosis: Lung: Pneumonia, necrosuppurative, multifocal to coalescing, moderate, with numerous extracellular amebic trophozoites.

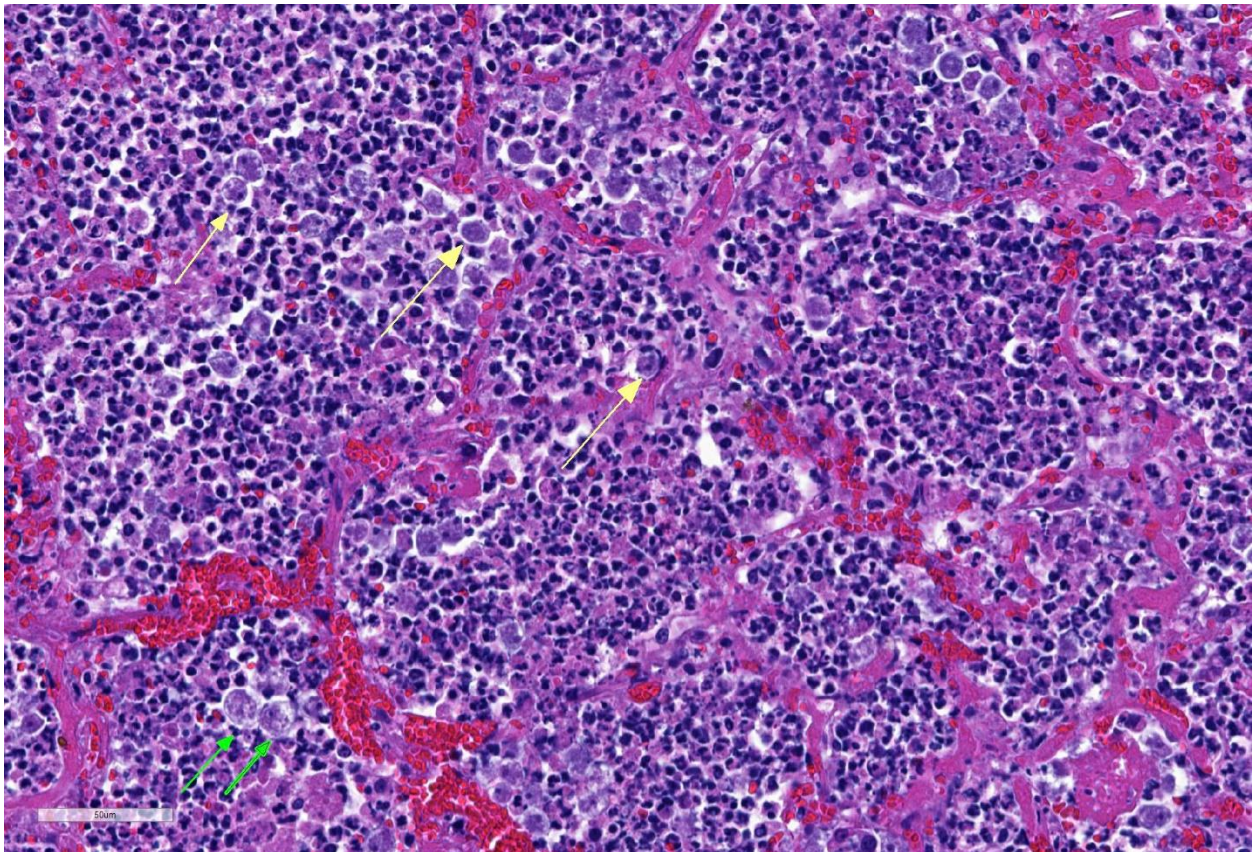
JPC Comment: Free-living ameba are ubiquitous protozoans in the environment, of which four generally are considered pathogenic for humans and animals:

Acanthamoeba, *Balamuthia*, *Naegleria*, and *Sappinia*.¹

Acanthamoeba appear to be most often associated with disease in humans and animals, with 18 distinct genotypes based on nuclear small-subunit ribosomal DNA rather than morphology. The most common condition associated with infection in humans is a chronic keratitis, seen in immunocompetent patients associated with improper handling of contact lenses, exposure to contaminated water, or trauma. Risk factors of contact lens users include the use of all-in-one solutions, showering while wearing contact lenses, and poor contact lens hygiene.⁵ Granulomatous amebic encephalitis is a well-documented syndrome in humans resulting from hematogenous

spread, often from the lower respiratory tract or skin lesions. It shows a chronic fatal progression with luckily only 150 documented cases worldwide.⁵ Due to its hematogenous origins, areas of granulomatous inflammation are seen throughout all parts of the brain. Cutaneous acanthamoebiasis is also an uncommon opportunistic condition primarily seen in immunosuppressed patients, resulting in erythematous sores and skin ulcers.¹

Primary amebic meningoencephalitis (PAM) is another rare fatal disease in humans caused by *Naegleria fowleri*. This condition generally occurs in healthy children and adults swimming or bathing in warm freshwater ponds. Infective amebae migrate along olfactory nerves from the nose to the



Lung, horse. Areas of necrosis contain numerous 15-20um amebic trophozoites with prominent nuclei and karyosomes (green arrow) and 20-30 amebic cysts. (HE, 400X)

brain; fatal infection proceeds rapidly and is almost always fatal. Due to this unique entry portal, areas of lytic necrosis are clustered at the base of the brain; hypothalamus, pons, and occasionally seen in posterior areas such as the medulla oblongata.

Balamuthia mandrillaris is also a cause of granulomatous amebic encephalitis which ranges in duration between *Acanthamoeba* and *Naegleria*, which usually results from hematogenous spread from soil-contaminated wounds.

Other species of free-living amoeba which may have been identified in cases of keratitis include *Hartmanella*, *Vahlkampfi*, and *Allovalkampi*¹ *sp.*

As the contributor mentioned above, free-living amoebae may act as vectors for a wide range of pathogenic bacilli. They may also act as hosts for a range of viruses, including coxsackieviruses and adenoviridae pathogenic for humans. Other viruses, the so-called giant viruses, may act as endocytobionts, including representatives of the *Mimi*-, *Moumo*- and *Megaviridae*, as well as *Pandoviridae*. Co-cultivation in amoebae has been of great benefit in the eventual isolation of these putative human pathogens.

The moderator and participants could not definitively identify cysts in tissues although PAS and GMS were run, they were of no help in identifying cysts. Megakaryocytes were identified in the alveolar capillaries. The moderator noted that they can normally be found there as the lungs are a site of thrombopoiesis and as such can serve as reservoirs for platelet production and release them in response to various stimuli.⁹ Finally, the moderator reviewed the various types of free-living amoebae, and participants discussed the associated syndromes in humans and animals.

References:

1. Balczun C, Scheid PL. Free-living amoebae as hosts for and vectors of intracellular microorganisms with public health significance. *Viruses* 2017; 9:1-10, doi 10-3390/v9040065.
2. Begg A., Todhunter, K., Donahoe, S, Krockenberger, M., Slapeta J. Severe amoebic placentitis in a horse caused by an *Acanthamoeba hatchetti* isolate identified using next generation sequencing. *Journal of clinical microbiology*. 3101-3104. 2014
3. Bradbury R S, French L.P., Blizzard L. Prevalence of *Acanthamoeba spp* in Tasmanian intensive care clinical specimen. *Journal of Hospital Infection* 86, 178-181. 2014.
4. Greene C.E. Infectious diseases of the dog and cat. 802-804. Fourth edition. 2012
5. Krol-Turminska K, Olendar A. Human infections caused by free-living amoebae. *Ann Agric Env Med* 2016 24(2):240-260
6. Kinde, H., Read D.H., Daft, B., Manzer, M., Nordhausen R., Kelly D., Fuerst P.A., Booton G., Visvesvara G.S. Infections caused by pathogenic free-living amoebae (*Balamuthia mandrillaris* and *Acanthamoeba sp.*) in horses. *J Vet Diagn Invest* 19:317-322. 2007.
7. Siddiqui R and Khan N A. Biology and pathogenesis of *Acanthamoeba*. Review. *Parasites and vectors*. 5:6. 2012.
8. Westmoreland S.V., Rosen J., MacKey J., Romsey C., Xia D.L., Visvesvera G.S., Mansfield K.G.. Necrotizing Meningoencephalitis and Pneumonitis in a Simian Immunodeficiency Virus-Infected Rhesus Macaque due to

Acanthamoeba. Veterinary Pathology. July 2004. vol 41 398-404.

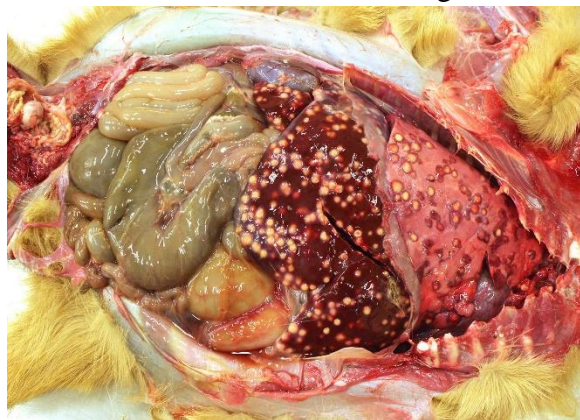
9. Weyrich AS, Zimmerman GA. Platelets in lung biology. *Annu Rev Physiol.* 2013;75:569-591.

CASE III: S1603556 (JPC 4084299).

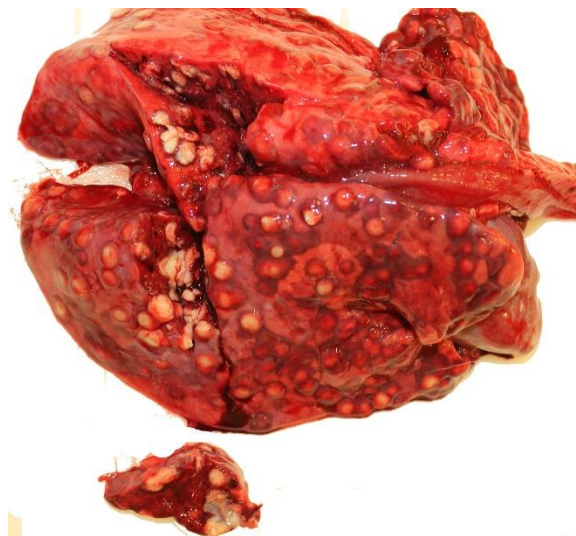
Signalment: A 14-month-old, 5 kg, female, Nigerian dwarf goat (*Capra hircus*)

History: A total of 4 goats in an original herd of 8, died in a period of 8 months with a history of limping, progressive loss of body condition, and difficulty in getting up. Three goats died naturally and one was euthanized. This goat died naturally.

Gross Pathology: The thoracic cavity contained approximately 25 mL of thin, pink fluid. The lungs and liver had innumerable disseminated, soft to semi-firm, pale yellow, 0.3-0.6 cm diameter, occasionally raised nodular foci scattered throughout the



Viscera, goat: The lungs and liver had innumerable disseminated, soft to semi-firm, pale yellow, 0.3-0.6 cm diameter, occasionally raised nodular foci scattered throughout the parenchyma. (Photo courtesy of: University of Connecticut, Connecticut Veterinary Medical Diagnostic Laboratory, Department of Pathobiology and Veterinary Science, College of Agriculture, Health and Natural Resources <http://patho.uconn.edu/>)



Lung, goat. The lungs had innumerable disseminated, soft to semi-firm, pale yellow, occasionally raised nodular foci scattered throughout the parenchyma, which frequently oozed pale yellow, thick liquid upon sectioning. (Photo courtesy of: University of Connecticut, Connecticut Veterinary Medical Diagnostic Laboratory, Department of Pathobiology and Veterinary Science, College of Agriculture, Health and Natural Resources <http://patho.uconn.edu/>)

parenchyma, which frequently oozed pale yellow, thick liquid upon sectioning. The spleen had a few similar foci.

Laboratory results: Bacteriology: aerobic bacterial culture of the liver yielded heavy growth of *Rhodococcus equi*, *Streptococcus sp.* and *Staphylococcus sp.*

Microscopic Description:

Lung: centering in small caliber vessels and extending into the adjacent alveolar spaces and septa, there is a multifocal and random inflammatory infiltrate composed by large numbers of viable and degenerated neutrophils, fewer histiocytes and occasional multinucleated giant cells that are admixed with basophilic cellular debris and several rounded eosinophilic protozoa of approximately 15 to 20 μm in diameter, with an eccentric single round nucleus. In addition, there are numerous fibrin thrombi and segments of alveolar necrosis. A few

blood vessels display transmural necrosis, with fibrinoid degeneration and the presence of pyknotic debris. The remaining parenchyma shows moderate congestion, occasional small hemorrhages and multiple focal areas of intra-alveolar edema.

Contributor's Morphologic Diagnosis:

Lung: marked, multifocal to coalescing, pyogranulomatous, pneumonia with myriad intrahistiocytic, gram-positive, coccobacillary bacteria

Other tissues (Slides not submitted):

Liver: marked, multifocal to coalescing, pyogranulomatous, hepatitis with intrahistiocytic, gram-positive, coccobacillary bacteria

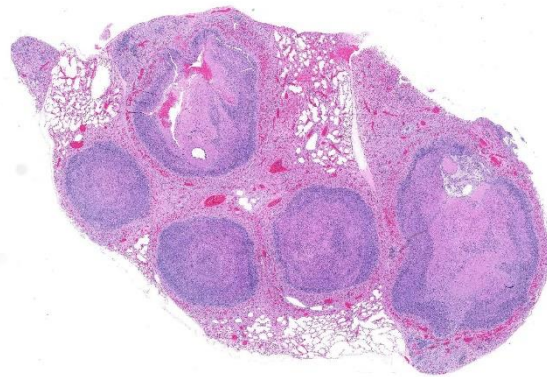
Spleen: 1. mild, multifocal, nodular, pyogranulomatous, splenitis with multifocal mineral deposition, intrahistiocytic, gram-positive, coccobacillary bacteria; 2. marked histiocytosis

Skeletal muscle: marked, focally extensive, pyogranulomatous, myositis with myriad



Liver, goat. The liver had innumerable disseminated, soft to semi-firm, pale yellow, occasionally raised nodular foci scattered throughout the parenchyma. (Photo courtesy of: University of Connecticut, Connecticut Veterinary Medical Diagnostic Laboratory, Department of Pathobiology and Veterinary Science, College of Agriculture, Health and Natural Resources <http://patho.uconn.edu/>)

intra-histiocytic coccobacillary bacteria



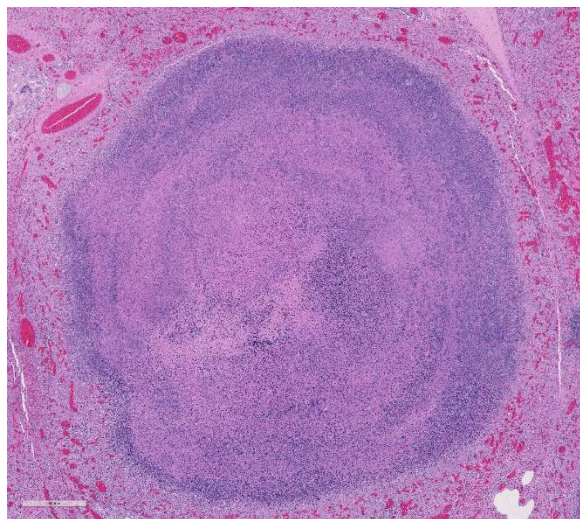
Lung, goat. 75% of the section is replaced by discrete pyogranulomas. Intervening alveoli are expanded by edema, an inflammatory infiltrate, and multifocal emphysema. (HE, 5X)

Contributor's Comment: The morphology and distribution of the lesions found in this goat were consistent with a disseminated rhodococcal infection. In goats, this is a recognized cause of disseminated pulmonary and hepatic abscesses^{2, 4}. *Rhodococcus equi* is classified largely as a soil organism, but has been isolated from the feces of birds and grazing herbivores. It has been suggested that *R. equi* may be widespread in herbivores and their environment because their manure supplies the substrates on which the organism thrives⁵. Inhalation or ingestion of the bacteria is thought to be the major mode of transmission, causing the development of respiratory or enteric infections, respectively⁸. Subsequent bacteremia and hematogenous dissemination within macrophages to other sites in the body then occurs⁸.

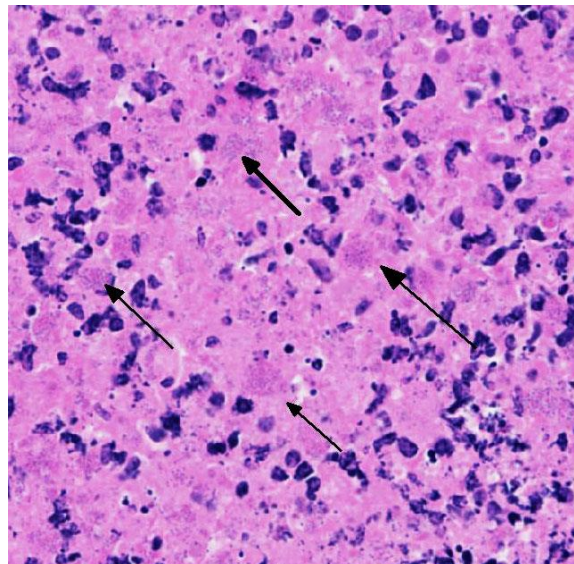
Rhodococcus equi is a facultative intracellular gram-positive bacterium which proliferates in macrophages and multinucleated giant cells⁸. *R. equi* causes two primary forms of disease in foals which are pyogranulomatous bronchopneumonia

and ulcerative enterocolitis. In addition, ulcerative typhlitis with suppurative or granulomatous lymphadenitis, osteomyelitis, synovitis, septic arthritis, and rarely abortion are reported in horses with *R. equi* infection^{6, 8}. *R. equi* has also been reported to cause pneumonia in immunosuppressed people, especially in AIDS patients³. *R. equi* infections are rarely reported in cattle, sheep, pigs, cats, dogs and camelids^{1, 8}. In goats, *R. equi* typically causes pyogranulomatous lesions in the liver and lungs^{2, 4}. Occasionally, osteomyelitis of the vertebra and skull and fibrinous enterocolitis have also been reported in goats⁴.

The virulent forms of *R. equi* contain a plasmid containing a vapA gene (virulence associated protein A) which encodes a 15-17 kDa cell surface lipid protein. This protein can elicit an intense humoral response^{7, 8}. The bacterium is able to prevent phagosome-lysosome fusion by inhibiting opsonization or activation of macrophages by IFN-gamma resulting in bacterial survival within the macrophage, therefore, an intense Th-1



Lung, goat: Higher magnification of a pyogranuloma with a lamellated center of eosinophilic and basophilic cellular debris. Viable inflammatory cells populate the periphery, enmeshed in collagen and dilated capillaries. (HE, 34X)



Lung, goat: Scattered throughout the necrotic center are numerous macrophages containing 1-3 coccobacilli within their cytoplasm (arrows). (HE, 400X)

response is required to clear an established infection⁸.

Contributing Institution:

University of Connecticut
Connecticut Veterinary Medical Diagnostic Laboratory,
Department of Pathobiology and Veterinary Science
College of Agriculture, Health and Natural Resources
<http://patho.uconn.edu/>

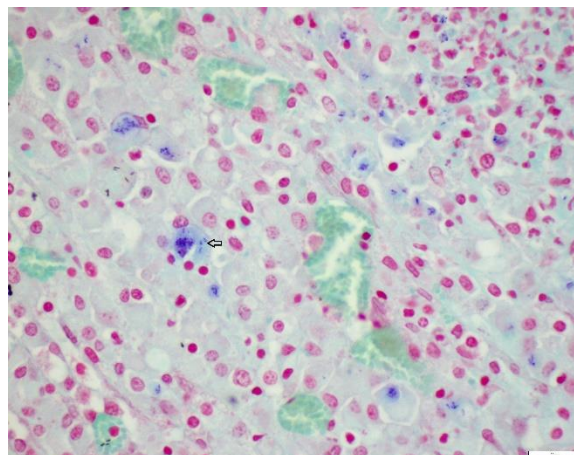
JPC Diagnosis: Lung: Pyogranulomas, multiple, with numerous intrahistiocytic coccobacilli.

JPC Comment: *R. equi*'s virulence-associated proteins (vapA in virulent strains, and vapB in intermediately virulent strains) are encoded on circular and linear plasmids. Strains that do not contain these proteins are classified as avirulent. Recently, a novel *R. equi* host-adapted linear virulence plasmid, pVAPN was characterized in cattle isolates,

which encodes another virulence –associated protein (vapN). VapG, another protein identified in virulent strains has recently been identified as a potential vaccinal protein which has shown efficacy in the partial protection of *R. equi* in mice (in addition to current vaccinal work with vapA). In addition, a highly conserved conjugal transfer protein gene (traA) is common to all strains which carry these plasmids and may now be used to identify pathogenic strains.¹ In previous studies, the virulent and intermediately virulent strains are primarily identified in foals and pigs, while most reports of *R. equi* isolated from cattle and dogs appear to be of avirulent (non-vapA, non-vapB) strains.¹

A recent article by Bryan et al¹ describes the clinical syndrome associated with *R. equi* infection in five dogs. Two of the isolated strains were avirulent, one was vap-A positive, and one carried the vapN virulence-associated plasmid. Four dogs were on immunosuppressive drugs or had endocrinopathies. The varied presentation and distribution of disease in the five dogs reflects the systemic and almost random nature of *R. equi* infection of the dog, with granulomatous dermatitis, aortic vegetative valvular endocarditis, pulmonary abscessation, and lymphadenitis the most common presentation, but each only being present in two out of five cases.

Considered an emerging pathogen in humans, over 100 cases of *R. equi* infection have been reported since the first description of its occurrence in 1967, likely as a result of improvement in isolation techniques and recognition of this bacterium as a human pathogen.⁹ The vast majority of cases have occurred in immunosuppressed patients with over 66% in cases in AIDS patients, and an



Lung, goat: The bacteria within the macrophages (arrow) stain positively with a tissue Gram stain (Twort's, 600X)

additional 10% in transplant recipients as a late complication (mean 49 months post-transplant) of immunomodulation. 80% of cases involved pulmonary infection, most commonly abscesses with necrotic centers, although pulmonary disease characterized by microabscesses is also common. As in other species, pyogranulomatous infection may occur in a wide range of organs. Treatment involves regimes of multiple antibiotics (often including rifampin) and is complicated by the typical presence of immunosuppression in affected individuals.⁹

The moderator reviewed the differences between *Corynebacterium pseudotuberculosis* and *Rhodococcus equi*. Additionally, he identified several recent review articles discussing rhodococcal infection in several atypical species such as dogs¹ and goats^{2,4}.

References:

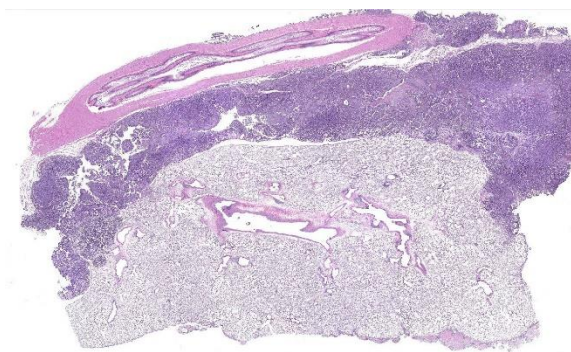
1. Bryan LK, Clark SD, Diaz-Delgado J. *Rhodococcus equi* Infections in Dogs. *Vet Pathol.* 2017; 54(1):159-163.
2. Davis WP, Steficek BA, Watson GL. Disseminated *Rhodococcus equi* infection in two goats. *Vet Pathol.* 1999;36(4):336-339.

3. Ferretti F, Boschini A, Iabichino C. Disseminated *Rhodococcus equi* infection in HIV infection despite highly active antiretroviral therapy. *BMC Infect Dis* 2011; 11:343-2334-11-343.
4. Jeckel S, Holmes P, King S. Disseminated *Rhodococcus equi* infection in goats in the UK. *Vet Rec* 2011; 169(2):56.
5. Muscatello G. *Rhodococcus equi* pneumonia in the foal--part 1: pathogenesis and epidemiology. *Vet J* 2012; 192(1):20-26.
6. Szeredi L, Molnar T, Glavits R. Two cases of equine abortion caused by *Rhodococcus equi*. *Vet Pathol* 2006; 43(2):208-211.
7. Trevisani MM, Hanna ES, Oliveira AF, et al. Vaccination of Mice with Virulence-Associated Protein G (VapG) Antigen Confers Partial Protection against *Rhodococcus equi* Infection through Induced Humoral Immunity. *Front Microbiol* 2017; 8:857.
8. Vazquez-Boland JA, Giguere S, Hapeshi A, et al. *Rhodococcus equi*: the many facets of a pathogenic actinomycete. *Vet Microbiol* 2013; 167(1-2):9-33.
9. Weinstock DM, Brown AE. *Rhodococcus equi*: an emerging pathogen. *Clin Inf Dis* 2002; 34:1379-85.

CASE IV: Case 1 (JPC 4103659).

Signalment: 2-year old, male, NCTR Sprague Dawley (CD) rat, (*Rattus rattus*)

History: This male rat was part of a 2-year carcinogenesis study that included prenatal and perinatal exposure to the test article. The animal survived to terminal sacrifice and was euthanized via CO₂ inhalation.



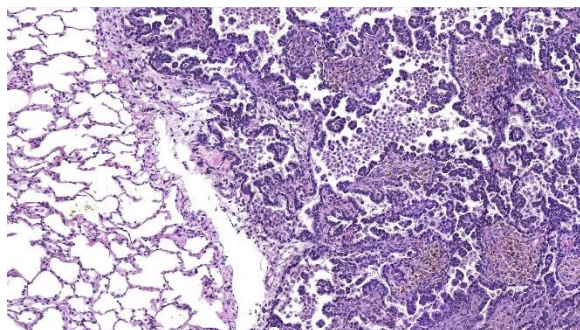
Lung, NCTR Sprague Dawley (CD) rat. Subgross image of an expansile neoplasm involving the lung, pleura, and adjacent rib. (HE, 6X) (Photo courtesy of: EPL, Inc., P.O. Box 12766, Research Triangle Park, NC 27709 <http://epl-inc.com/>)

Gross Pathology: At necropsy, an extensive tumor was identified within the thoracic cavity that involved the lung, pleura, pericardium, diaphragm, and rib.

Laboratory results: None.

Microscopic Description:

Lung: a multifocal, unencapsulated, expansile, neoplasm is diffusely expanding the pleural surface, compressing the adjacent lung parenchyma and adhering to the costal pleura of the adjacent rib. The neoplasm is composed of epithelial cells, arranged in tubules and cords, as well as papillary and alveolar-like structures that are supported by small amounts of fine, fibrovascular stroma. Neoplastic cells are cuboidal to columnar, with moderate amounts of finely fibrillar, eosinophilic cytoplasm and a single, round to oval, central to basilar nucleus, with 1-3 variably distinct nucleoli and stippled chromatin. Anisocytosis and anisokaryosis are minimal and the mitotic rate is low with 0-2 mitotic figures per 40X field. Some areas within the neoplasm contain abundant fibrous connective tissue (schirrous response) infiltrated by large numbers of hemosiderin-laden macrophages. Large influxes of foamy, alveolar macrophages are frequently



Lung, NCTR Sprague Dawley (CD) rat. The neoplasm is composed of cuboidal to columnar cells arranged in tubules and cords as well as papillary and alveolar-like structures. (HE, 100X) (Photo courtesy of: EPL, Inc., P.O. Box 12766, Research Triangle Park, NC 27709 <http://epl-inc.com/>)

observed within the neoplasm. Multifocal areas of hemorrhage, emphysema and edema are also present.

Immunohistochemistry: neoplastic cells exhibit a similar staining pattern to that of alveolar-bronchiolar (AB carcinoma) with positive cytoplasmic staining with SPC and cytokeratin 18 antibodies and negative staining with vimentin and CC10.

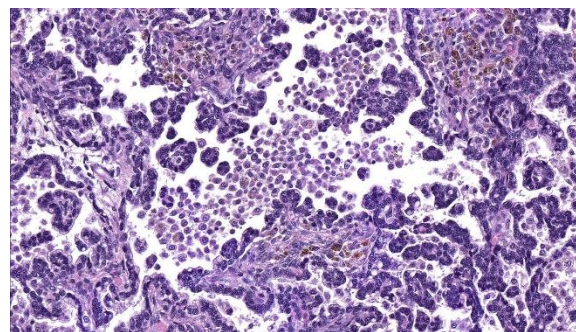
Contributor's Morphologic Diagnosis:
Lung: Alveolar-bronchiolar carcinoma (bronchiolo-alveolar carcinoma)

Contributor's Comment: Alveolar-bronchiolar carcinomas (AB carcinomas), are the most commonly induced pulmonary malignancies in rodent studies conducted by the National Toxicology Program (NTP).² However, the current literature now refers to these types of tumors as bronchiolo-alveolar carcinomas.² Although the cell of origin for bronchiolo-alveolar tumors remains somewhat controversial, the International Harmonization of Nomenclature and Diagnostic Criteria (INHAND) guidance document on rodent respiratory lesions indicates that bronchiolo-alveolar carcinoma may originate from club cells (formerly known as Clara cells) or type II alveolar cells,

but more commonly arise from type II alveolar cells.^{2,5} These types of tumors typically invade the lung parenchyma as poorly circumscribed, nodular masses that may occupy an entire lung lobe and infiltrate adjacent tissues.¹ However, extra-pulmonary AB carcinomas that are largely mediastinal have been reported.⁴

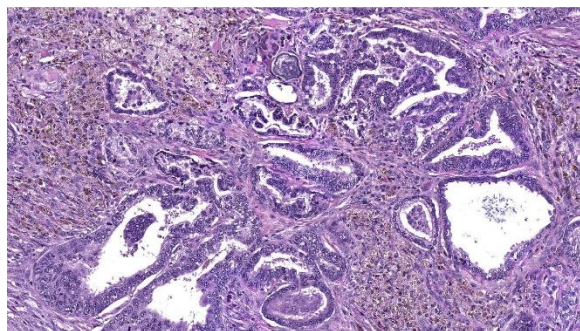
Several growth patterns for AB carcinoma have been described in the rat, these include: Alveolar (glandular) patterns - consisting of cuboidal to columnar cells forming glandular structures, papillary growth - cuboidal to columnar cells forming papillary structures supported by a connective tissue core, tubular patterns - prominent elongated tubules, solid-composed of tightly arranged round cells with no visible space in-between or mixed patterns where multiple patterns are apparent. Marked pleomorphism, areas of squamous metaplasia or abundant fibrosis (schirrous response) are additional features that have been described in rats and mice as well as large influxes of macrophages into the tumor and adjacent alveoli, as observed in this case.^{1,5}

This case was presented to a pathology working group (PWG) because the study and reviewing pathologists were torn between a



Lung, NCTR Sprague Dawley (CD) rat. Areas of abundant fibrous connective tissue (schirrous response) with large numbers of hemosiderin-laden macrophages are also observed. (HE, 200X) (Photo courtesy of: EPL, Inc., P.O. Box 12766, Research Triangle Park, NC 27709 <http://epl-inc.com/>)

diagnosis of AB carcinoma or malignant mesothelioma. Immunohistochemistry was applied to help determine the cell of origin. The neoplasm exhibited IHC staining characteristics similar to a positive AB Carcinoma control that was pulled from the NCTR archives. The majority of neoplastic cells demonstrated positive cytoplasmic staining for SPC (surfactant protein C, alveolar type II cells) and CK18 (cytokeratin 18, epithelial cells) markers, confirming that the neoplasm was most likely an epithelial tumor arising from type II alveolar cells. The cells lining the pleural surface of the neoplasm appeared to represent a layer of reactive mesothelium, as these cells stained positive with both CK18 and vimentin stains, similar to a malignant mesothelioma control also pulled from the NCTR archives; most of the neoplasm was negative for vimentin. Based on the IHC profile, the tumor was diagnosed an AB carcinoma. However, it should be noted, that not every pathologist that reviewed these findings were convinced of the diagnosis.



Lung, NCTR Sprague Dawley (CD) rat. Lung, NCTR Sprague Dawley (CD) rat. Large influxes of foamy alveolar macrophages are frequently found within neoplastic structures. (HE, 400X) (Photo courtesy of: EPL, Inc., P.O. Box 12766, Research Triangle Park, NC 27709 <http://epl-inc.com/>)

Contributing Institution:

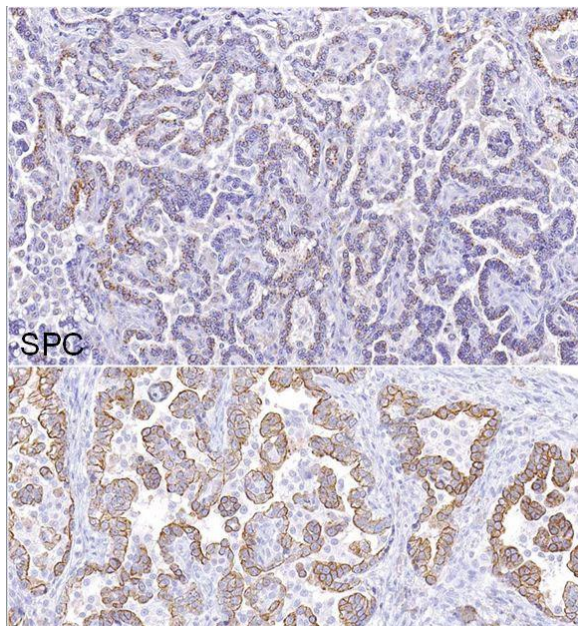
EPL, Inc., P.O. Box 12766, Research Triangle Park, NC 27709 <http://epl-inc.com/>

JPC Diagnosis: Lung: Alveolar-bronchiolar carcinoma, papillary type.

JPC Comment: A review of the archives of the National Toxicology Program (NTP) almost a decade ago identified the lung as the organ that is third most common target site of chemical carcinogens in the female rat (with liver and mammary gland preceding it) and as an uncommon site in male rats.² Inhalation and gavage studies account for 70% of tumors at approximately 35% each, with water-dosing, IP, topical, and *in utero* exposure accounting for the remainder. Spontaneous A/B neoplasms of the lung occur at incidences of less than 4% in both genders of F344 rats, but over 90% of chemically induced pulmonary neoplasm. The most common site of pulmonary metastases in these rats, interestingly, the skin.²

Alveolar-bronchiolar adenocarcinoma is considered one of the best models for non-small cell lung cancer (NSCLC) in humans. K-RAS, EGFR, and TP53 are the three most commonly altered genes “driver mutations” in NSCLC, with TP53 genes exhibit the highest frequency of mutations in lung tumors (both squamous cell and NSCLC) in smokers.

Differentials for alveolar-bronchiolar adenocarcinoma in the rat should include AB adenomas, acinar carcinomas, adenosquamous carcinoma, mesothelioma, and neoplasms metastatic to the lung.⁵ AB adenomas, which may represent a continuum with AB carcinoma, are often diagnose based on size, as well as a lack of cellular pleomorphism or atypia as well as a lack of invasive growth.⁵ Acinar carcinoma grow in a glandular pattern utilizing pre-existent alveolar walls, and may contained mixed populations of pleomorphic cuboidal cells, mucous cells, or ciliated cells.



Lung, NCTR Sprague Dawley (CD) rat. Neoplastic cells exhibit positive cytoplasmic staining with SPC (surfactant protein C) and CK18 (cytokeratin 18) consistent with AB carcinoma. (HE, 200X) (Photo courtesy of: EPL, Inc., P.O. Box 12766, Research Triangle Park, NC 27709 <http://epl-inc.com/>)

Adenosquamous carcinoma has areas of malignant squamous cells or is composed entirely of squamous cell carcinoma. Metastatic foci of primary adenocarcinoma from other organs may be multifocal and often present within vessels or in perivascular locations. Finally, mesothelioma may be the most difficult of these tumors to differentiate from A/B carcinoma due to its similar predilection to grow along pleural surfaces or within the mediastinum, as well as the variability of cellular morphology.⁵

References:

1. Boorman GA, Eustis SL. Lung. In: Boorman GA, ed. *Pathology of the Fisher Rat*. San Diego, CA: Academic Press, Inc., 1990: 351-357.
2. Dixon D, Herbert RA, Kissling GE, Brix AE, Miller RA, Maronpot R. Summary of chemically induced pulmonary lesions in the National Toxicology Program (NTP) toxicology and carcinogenesis studies. *Toxicol Pathol*, 36: 428-439, 2008.
3. Hong, H, Hoenerhoff MJ, Ton T, Herbert R, Kissling GE, Hooth MJ, Behl M, Witt KL, Smith-Roe SL, Sills RC, Pandiri AR. Kras, Egfr, and Tp53 mutations in B6C3F1/N Mouse and F344/NTac rat alveolar/bronchiolar carcinomas resulting from chronic inhalation exposure to cobalt metal. *Toxicol Pathol* 2015; 43(6):872-882.
4. Howroyd P, Allison N, Foley JF, Hardisty J. Apparent Alveolar Bronchiolar Tumors Arising in the Mediastinum of F344 Rats. *Toxicologic Pathology*, 37: 351-358, 2009.
5. Renne R, Brix A, Harkema J, Herbert R, Kittel B, Lewis D, March T, Nagano K, Pino M, Rittinhausen S, Rosenbruch M, Tellier P, Wohrmann T. Proliferative and Nonproliferative Lesions of the Rat and Mouse Respiratory Tract. *Toxicologic Pathology*, 5S-73S, 2009.

Self-Assessment - WSC 2018-2019 Conference 14

1. Which of the following may be used as an early test for diagnosis of canine lymphoplasmacytic thyroiditis in the dog
 - a. Serum T3
 - b. Thyroglobulin autoantibodies
 - c. Free T4
 - d. Serum TSH

2. Which of the following ameba have NOT been identified in cases of meningitis in humans??
 - a. *Hartmannella* sp.
 - b. *Acanthamoeba* sp.
 - c. *Naegleria* sp.
 - d. *Balamuthia* sp.

3. Which of the following proteins is most closely associated with virulent forms of *R. equi*?
 - a. vapA
 - b. vapB
 - c. vapG
 - d. pVAPN

4. Which of the following is a common predisposing factor for *R. equi* infection in the dog?
 - a. Hospitalization
 - b. Endocrinopathy
 - c. Infected skin wounds
 - d. Co-habitation with horses

5. Which of the following is NOT a growth pattern in A/B carcinoma in the rat?
 - a. Tubular
 - b. Papillary
 - c. Lepidic
 - d. Alveolar (glandular)

Please email your completed assessment to Ms. Jessica Gold at Jessica.d.gold2.ctr@mail.mil for grading. Passing score is 80%. This program (RACE program number) is approved by the AAVSB RACE to offer a total of 0.5 CE Credits, with a maximum of 12.5 CE Credits being available to any individual Veterinary Medical Professionals for the 2017-2018 Wednesday Slide Conference. This RACE approval is for the subject matter categories of: SCIENTIFIC using the delivery method of NON-INTERACTIVE DISTANCE. This approval is valid in jurisdictions which recognize AAVSB RACE; however, participants are responsible for ascertaining each board's CE requirements. RACE does not "accredit", "endorse" or "certify" any program or person, nor does RACE approval validate the content of the program.

Please email your completed assessment to Ms. Jessica Gold at Jessica.d.gold2.ctr@mail.mil for grading. Passing score is 80%. This program (RACE program number) is approved by the AAVSB RACE to offer a total of 0.5 CE Credits, with a maximum of 12.5 CE Credits being available to any individual Veterinary Medical Professionals for the 2017-2018 Wednesday Slide Conference. This RACE approval is for the subject matter categories of: SCIENTIFIC using the delivery method of NON-INTERACTIVE DISTANCE. This approval is valid in jurisdictions which recognize AAVSB RACE; however, participants are responsible for ascertaining each board's CE requirements. RACE does not "accredit", "endorse" or "certify" any program or person, nor does RACE approval validate the content of the program.

**Joint Pathology Center
Veterinary Pathology Services**



WEDNESDAY SLIDE CONFERENCE 2018-2019

C o n f e r e n c e 1 5

16 January 2018

CASE I: 16153 E (JPC 4102152).

Signalment: 7 year old, male, rhesus macaque (*Macaca mulatta*)

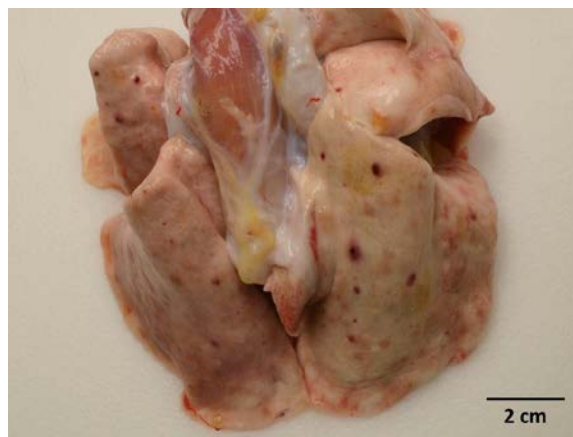
History: This animal received total body irradiation (4 Gy) as part of an experimental protocol, and demonstrated persistent pyrexia (104 °-105 ° F), inappetence, weight loss and was persistently pancytopenic despite aggressive supportive care, blood transfusions and antibiotic therapy (Enrofloxacin, Ceftiofur and Ertepenem). The animal was euthanized 47 days post-irradiation due to poor prognosis and non-response to treatment.

Gross Pathology: Dozens of petechiae, ecchymoses and pinpoint to 1.4 mm diameter, soft, yellow-tan foci and were scattered throughout the parenchyma of both lungs. Additional petechiae and ecchymoses were scattered throughout the left lateral lobe of the liver and urinary bladder. The epicardium of the right ventricle was irregularly thickened by off-white opaque material.

Gross Pathology: Dozens of petechiae, ecchymoses and pinpoint to 1.4 mm diameter, soft, yellow-tan foci and were scattered throughout the parenchyma of both

lungs. Additional petechiae and ecchymoses were scattered throughout the left lateral lobe of the liver and urinary bladder. The epicardium of the right ventricle was irregularly thickened by off-white opaque material.

Laboratory results: Blood culture: No growth
Transmission electron microscopy, epicardial adipose tissue: There were numerous 3-4µm diameter extracellular and intrahistiocytic protozoa with cilia projecting

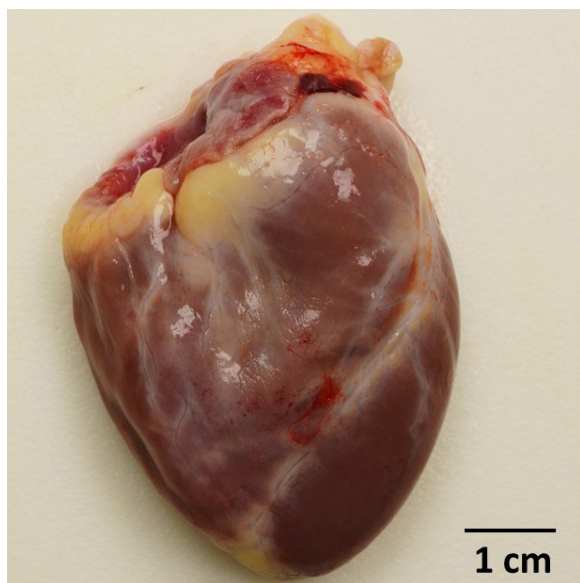


Lungs, rhesus macaque. Ecchymoses, petechiae and soft, yellow-tan foci are scattered throughout the parenchyma of all lung lobes. (Photo courtesy of: Wake Forest School of Medicine Department of Pathology, Section on Comparative Medicine, Medical Center Boulevard, Winston-Salem, NC 27157 www.wakehealth.edu)

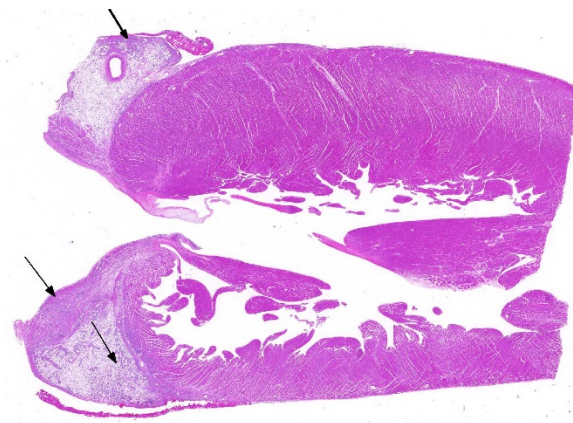
from the lateral margins, often arranged in parallel rows, moderately electron dense grainy cytoplasm, two electron dense nuclei, and a single internal marginated flagellum.

Microscopic Description:

The epicardium and epicardial adipose tissue is infiltrated by coalescing aggregates of lymphocytes, plasma cells, macrophages, and scattered foci of neutrophils, all of which dissect between and separate adipocytes, and extend into the underlying myocardium. Innumerable, free and intrahistiocytic, 3-4 μ m diameter, oval, eosinophilic to amphophilic protozoa are scattered throughout the affected tissue. The protozoa are surrounded by a 10 μ m diameter clear space within the matrix. The protozoa stain positively with Heidenhain iron hematoxylin (HIH); and are negative for periodic acid-Schiff (PAS), Groncott-Gomori methenamine silver stain (GMS), and mucicarmin.



Heart, rhesus macaque. The epicardium of the right ventricle is variably thickened by opaque off-white material. (Photo courtesy of: Wake Forest School of Medicine Department of Pathology, Section on Comparative Medicine, Medical Center Boulevard, Winston-Salem, NC 27157 www.wakehealth.edu)



Heart, rhesus macaque. The epicardial fat, epicardium, and right atrial and ventricular myocardium contains a cellular infiltrate. (HE, 5X)

The epicardial surface is overlain by sheets of loose, fibrillar eosinophilic material (fibrin), containing scattered lymphocytes and histiocytes.

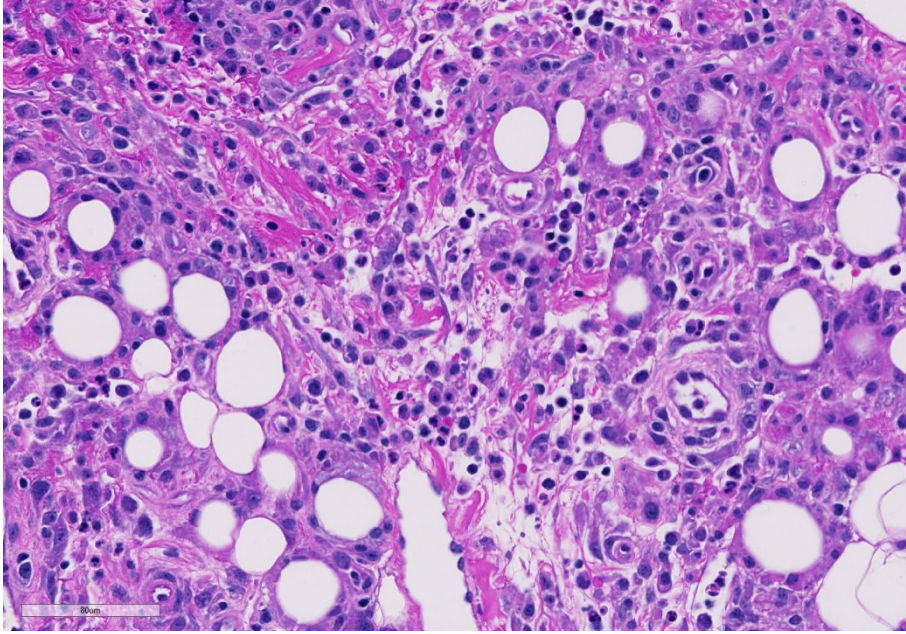
Contributor's Morphologic Diagnoses:

Epicarditis, pericarditis, myocarditis, and epicardial steatitis, regionally extensive, chronic, severe, lymphohistiocytic with protozoa

Contributor's Comment:

Spironucleus species are flagellated diplomonad protozoans which are found as gastrointestinal (GI) commensals and may also act as opportunistic parasites in an array of hosts including birds, fish, and mammals. Generally, the parasites live within the intestinal lumen or crypts, with clinical signs in infected animals either not observed or limited to GI-related symptoms including diarrhea, anorexia, and wasting^{4,11}. Gross pathologic changes depend on the severity of disease, and may include gas-distended intestines, enteritis, and ascites.³

While *Spironucleus* species rarely cause extra-intestinal disease, such incidents have been previously documented in Atlantic salmon¹², Atlantic char¹³, Siamese fighting



Heart, rhesus macaque. Epicardial fibroadipose tissue is infiltrated by moderate numbers of neutrophils, macrophages, lymphocytes, and plasma cells. (HE, 282X)

fish, cichlids¹⁰, and rhesus macaques². Immunocompromised animals have a greater risk of developing an overwhelming infection; for example, athymic mice infected with *Spironucleus* have increased mortality.⁴ Reported pathogenic infections in macaques have been in animals infected with Simian Immunodeficiency virus.^{2,8}

This animal was one of three in a cohort of animals that had received experimental whole body irradiation. All three animals had systemic *Spironucleus* infection where protozoa were positively identified and confirmed by PCR. Speciation is pending. Lesions included polyserositis, epicarditis, ureteritis, cystitis, epididymitis, and pneumonia. One animal had protozoa in the cerebrospinal fluid.

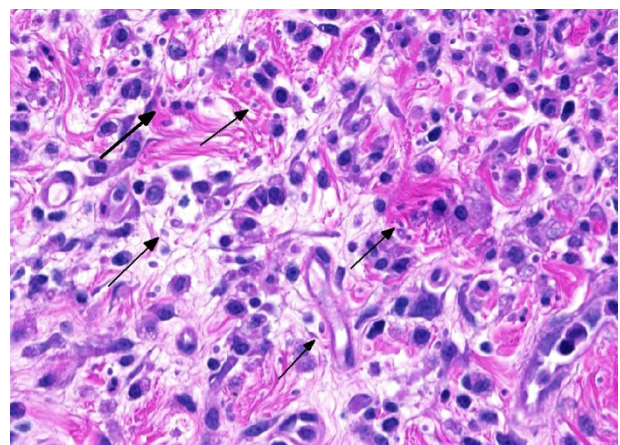
Spironucleus, formerly classed as *Hexamita* or *Octomitus* in some species^{9,11}, may be difficult to detect on routine histologic sections. Histologic stains used to identify them are hematoxylin and eosin (H&E), Giemsa, Gomori's methenamine silver

(GMS), and Heidenhain iron hematoxylin (HIH).¹⁴ The protozoa from the three cases from our institution appeared amphophilic on H&E and Giemsa, were negative for GMS, and prominently stained deep purple with HIH. Other previously utilized techniques for diagnosis include direct smear of intestinal contents, immunochemical techniques on feces, and polymerase chain reaction.^{5,6} Electron microscopy (EM) has also been used as a tool

to positively identify *Spironucleus* species, which, on TEM depending on speciation, range from 2-4x4-20µm have lateral cilia and a recurrent flagellum which arises from an indent in the nuclear membrane near two nuclei, which form an 'S'-shape.^{2,12}

Contributing Institution:

Wake Forest School of Medicine
Department of Pathology, Section on
Comparative Medicine
Medical Center Boulevard



Heart, rhesus macaque. Numerous oval 2-4 extracellular flagellated protozoans are present extracellularly (arrows). Close inspection will also demonstrate one or multiple protozoa within the cytoplasm of macrophages as well. (HE.

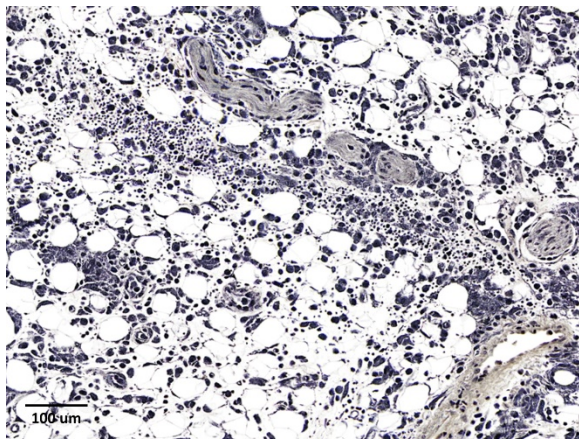
Winston-Salem, NC 27157

www.wakehealth.edu

JPC Diagnosis: Heart: Epicarditis and steatitis, histiocytic and neutrophilic, multifocal to coalescing, marked with mild myocarditis and endocarditis and numerous intrahistiocytic and extracellular protozoa.

JPC Comment: The contributor has provided an excellent discussion of this rarely reported systemic condition in immunosuppressed macaques. A very similar case of systemic spironucleosis was included in the 2011-2012 Wednesday Slide Conference (Conference 19, case 3) although the submitted tissue was colon.⁸

Reports of *Spironucleus* in non-human primates are rare in both health and disease. To date, the rhesus macaque appears to be the only species of non-human primate in which this genus (specifically, *S. pitheci*) has been identified², and all other reports of *Spironucleus* (largely that as a gut commensal) are in laboratory rodent species. Immunosuppression in rodent species may



Heart, rhesus macaque. A Heidenhain iron hematoxylin stain demonstrates the presence of numerous protozoa within the pericardial fat. (Photo courtesy of: Wake Forest School of Medicine Department of Pathology, Section on Comparative Medicine, Medical Center Boulevard, Winston-Salem, NC 27157 www.wakehealth.edu) (HIH, 200X)

also lead to systemic infection.

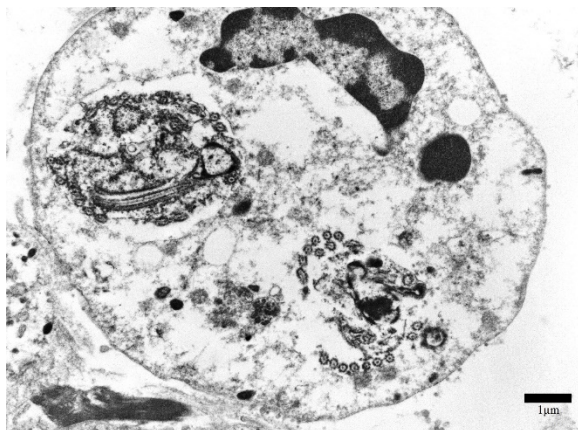
Spironucleus and other related flagellates such as *Giardia* and *Entamoeba* are interesting in their evolutionary development of a highly reductive organelle to take the place of mitochondria, known as a “mitosome” (or in the case of *Spironucleus*, the “hydrogenosome”).¹ These organelles, like mitochondria, have a double membrane, and are associated with a number of proteins closely related to those found in mitochondria. Unlike mitochondria, mitosomes do not contain their own genes; genes for their genesis and function are



Heart, rhesus monkey: Transmission electron microscope (TEM) image of the pericardial fat: There is a 4x3µm protozoan with cilia extending from the margins, moderately electron-dense grainy cytoplasm with multiple 500nm electron lucent bodies and two moderately electron-dense nuclei. (Photo courtesy of: Wake Forest School of Medicine Department of Pathology, Section on Comparative Medicine, Medical Center Boulevard, Winston-Salem, NC 27157 www.wakehealth.edu)

present in the nuclear genome. Mitosomes do not generate ATP through the process of oxidative phosphorylation similar to other eukaryotes. Energy generation in these species is largely a process of anaerobic glycolysis with the conversion of glucose to pyruvate occurring in the cytosol, and further oxidation of pyruvate occurring in the hydrogenosome.¹

An extremely important component of this



Heart, rhesus monkey: TEM image of the pericardial fat: An ~11 μ m diameter macrophage, with a stippled electron-dense cytoplasm and an irregular 5.5x2 μ m electron-dense nucleus contains two 3x4 μ m protozoa as described in figure 4. One protozoal profile has a recurring flagellum arising from the edge of the nucleus. (Photo courtesy of: Wake Forest School of Medicine Department of Pathology, Section on Comparative Medicine, Medical Center Boulevard, Winston-Salem, NC 27157 www.wakehealth.edu)

particular case is the immunosuppression required for systemic infection by the offending diplomonad. The hematopoietic syndrome is a well-recognized subsyndrome of acute radiation exposure (along with the gastrointestinal and cerebrovascular subsyndromes).⁶ Lymphocytes are extremely sensitive to ionizing radiation and rapidly disappear from the circulation following whole-body irradiation. This is followed by neutrophil loss and then finally platelet loss over the course of several days as existing populations are used up and not replaced by the damaged marrow.⁶ At this point, impaired immunity may result in a wide range of opportunistic infections, or the animal may succumb to fatal hemorrhage as a result of thrombocytopenia.⁶

References:

1. Adam R. Biology of *Giardia lamblia*. Clin Microbiol Rev 2001; 14(3):447-445.
2. Bailey C, Kramer J, Mejia A, MacKey A, Mansfield KG, and Miller AD. Systemic Spironucleosis In two immunodeficient rhesus macaques (*Macaca mulatta*). Vet Pathol. 2010;47(3):488–494.
3. Baker D. Natural pathogens of laboratory mice, rats, and rabbits and their effects on research. Clin Microbiol Rev. 1998;11:231-66.
4. Boorman GA, Lina PHC, Zurcher C, and Nieuwerkerk HTM. *Hexamita* and *Giardia* as a cause of mortality in congenitally thymusless mice. Clin Exp Immunol. 1973;15:623–627.
5. Fain MA, Karjala Z, Perdue KA, Copeland MK, Cheng LI, and Elkins WR. Detection of *Spironucleus muris* in unpreserved mouse tissue and fecal samples by using a PCR assay. J Am Assoc Lab Anim Sci. 2008;47:39–43.
6. Gulani J, Koch A, Chappell MG, Christensen CL, Facemire P, Singh V, Ossetrova NI, Srinivasan V, Holt RK. Cercopithecine herpesvirus-9 (Simian varicella virus) infection after total-body irradiation in a rhesus macaque. *Comp Med* 2016; 66(2):150-153
7. Jackson GA, Livingston RS, Riley LK, Livingston BA, and Franklin CL. Development of a PCR assay for the detection of *Spironucleus muris*. J Am Assoc Lab Anim Sci. 2013;52(2):165-170.
8. Joint Pathology Center Veterinary Pathology Services Wednesday Slide Conference: Conference: 19 - 2011 Case: 03 Colon – Macaque. c2011. Cited 2017 June 5. Available from: https://www.askjpc.org/wsc/wsc_showconference.php?id=492
9. Jørgensen A, Sterud E. Phylogeny of *Spironucleus* (Eopharyngia: Diplomonadida: Hexamitinae) Protist. 2007;158:247–254.

10. Paull GC MR: Spironucleus vortens, a possible cause of hole-in-the-head disease in cichlids. *Diseases of Aquatic Organisms* 2001;45:197-202.

11. Poynton S. Diplomonad (Hexamitid) Flagellates: Diplomonadiasis, Hexamitosis, Spironucleosis. In: AFS-FHS (American Fisheries Society-Fish Health Section), FHS Blue Book: Suggested Procedures for the Detection and Identification of Certain Finfish and Shellfish Pathogens, 2007 ed., AFS-FHS, Bethesda, MD.

12. Sterud E, Atle Mo T, Poppe TT. Systemic spironucleosis in sea-farmed Atlantic salmon *Salmo salar*, caused by *Spironucleus barkhanus* transmitted from feral Arctic char *Salvelinus alpinus*. *Dis Aquat Org.* 1998;33:63-66.

13. Sterud E, Poppe TT, Bornø G. Intracellular infection with *Spironucleus barkhanus* (Diplomonadida, Hexamitidae) in farmed Arctic char *Salvelinus alpinus*. *Dis Aquat Org.* 2003;56:155–61.

14. Wood AM, Smith VH. Spironucleosis (Heramitiasis, Hexamitosis) in the ring-necked pheasant (*Phasianus colchicus*): Detection of cysts and description of *Spironucleus meleagridis* in stained smears. *Avian Dis.* 2005;49:138–143.

CASE II: NCDS-2203/1003-17 (JPC 4067571).

Signalment: 10-12 week old male Sprague-Dawley rat (*Rattus norvegicus*, SD:CrI)

History: This animal was a control animal in a 1 week study for an oncology agent.

Gross Pathology: Dozens of petechiae, ecchymoses and pinpoint to 1.4mm diameter, soft, yellow-tan foci and were scattered throughout the parenchyma of both lungs. Additional petechiae and ecchymoses were scattered throughout the left lateral lobe of the liver and urinary bladder. The epicardium of the right ventricle was irregularly thickened by off-white opaque material.

Gross Pathology: None.

Laboratory results: Ophthalmic examinations were not performed in this study.

Microscopic Description:

Eye: Unilaterally, a locally extensive area spanning the central to peripheral retina, there is thinning of the retina characterized by vacuolation of the photoreceptor layer, shortening and loss of the photoreceptor layer, decreased cellularity to loss of the outer nuclear layer and occasional infiltrating macrophages.

Contributor's Morphologic Diagnoses:

Eye: Unilateral, focal, mild retinal degeneration, photoreceptor layer/outer nuclear layer



Eyes, rat. Sections of two globes are presented for examination. (HE, 4X)

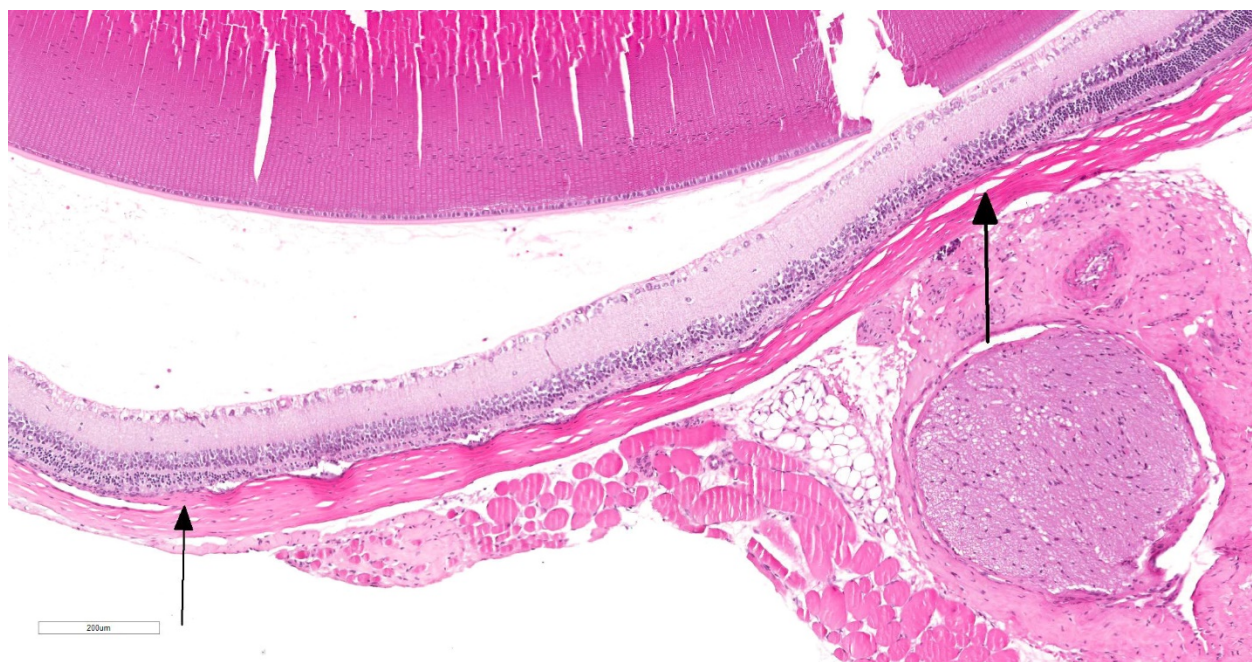
Contributor's Comment: Spontaneous or background retinal findings in the Sprague-Dawley (SD) rat have been attributed to heritable and environmental factors, as well as aging. These findings may be present unilaterally or bilaterally. Spontaneous retinal findings may include dysplasia, dystrophy, and degeneration. Dysplasia is defined as disorganization of the sensory retina with or without degeneration and is also known as "linear retinopathy" in the rat. This is the most common background finding in SD rats greater than 11 weeks of age with 3% incidence in one study.¹ Dystrophy is defined by photoreceptor and/or retinal pigmented epithelium alterations with variable time to onset and progression.

Degeneration is a non-specific term and can encompass a variety of changes in the retina. In the context of spontaneous changes associated with aging, degeneration is defined by decreased numbers of photoreceptor cells and thinning of the outer nuclear layer especially in the peripheral

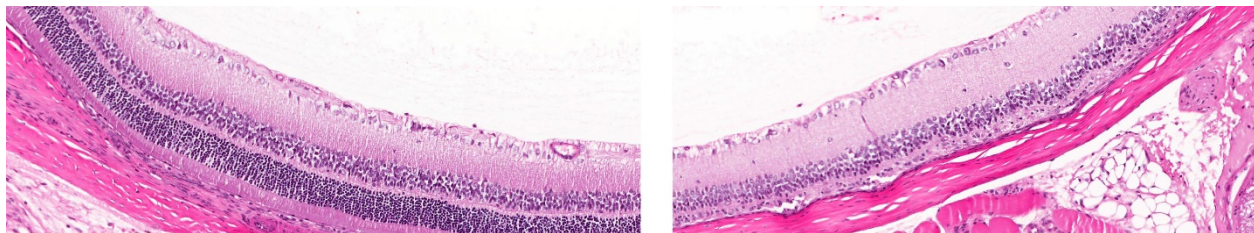
retina. Degeneration associated with excess light exposure is generally more prominent in the central retina and in albino animals. The development of retinal photoxicity can be influenced by a number of factors including gender, light wavelength and diet.² The rate of spontaneous degeneration in SD rats over a broad age range (6 to 24 months, males and females) in one study is 3.7% .⁴ An understanding of the background incidence of retinal degeneration is important since this is the most common manifestation of retinal toxicity. Retinal toxicity can appear microscopically similar to spontaneously occurring retinal degeneration so the incidence and severity must be evaluated to determine the relevance of the finding in given treatment group.²

Contributing Institution:

Wake Forest School of Medicine
Department of Pathology, Section on
Comparative Medicine, Medical Center
Boulevard, Winston-Salem, NC 27157
www.wakehealth.edu



Eye, rat. There is a segmental area at the edge of the central retina (delimited by arrows) in which the outer nuclear layer as well as the photoreceptor layer is lost. (HE, 200X)



Eye, rat. Comparison of normal retina (left) and area of retinal degeneration with subtotal loss of the outer nuclear layer and the photoreceptor layer (right). (HE, 400X)

JPC Diagnosis: Retina: Degeneration of the outer nuclear and photoreceptor layer, focal, severe.

JPC Comment: The lesion described above appears to be consistent with “linear retinopathy” – one of the more frequently observed lesions in the rat retina in toxicologic studies, and reportedly prevalent in the Sprague-Dawley rat. This lesion was first reported in 1975 by Schardein et al, under the name “retinal dystrophy” and has also been recorded in the literature as “retinal or retinchoroidal degeneration and atrophy”, “retinal dysplasia/dystrophy”, or “choroidal defect” in Sprague Dawley rats. While most commonly reported in SD rats, it has also been categorized in Crl:CD BR rats.²

This particular lesion, usually unilateral, is the most frequently observed change in rats from 7-10 weeks of age, achieving maximum frequency (around 3%) in animals from 11-14 weeks of age. This frequency appears to be maintained until 110 weeks of age. Fundoscopic examination of affected rats reveals a sharply demarcated, pale, linear area of pallor in varying locations. Histologically, these lesions result in abutment of the inner nuclear layer directly on the underlying choroid or uvea, much as seen in this case.² Early reports describe a 38% incidence of diffuse lesions, which appears rare in subsequent studies and may

simply reflect evolving diagnostic criteria over time. The earliest study in SD rats theorized the possibility of retinal reattachment as a cause for this particular lesion; although other causes, such as genetic or environmental factors have not been ruled out.²

Another form of retinal degeneration not discussed by the contributor is associated with aging. Age-related degeneration includes retinal thinning with a loss of nuclei in the outer and inner nuclear layers, fusion of the nuclear layers, hypertrophy of the retinal pigmentation and possibly migration of RPE cells or macrophages into the sensory retina. Changes are noticed first in the RPE, and often in the peripheral retina, as it is thinner than the central portion.²

Other retinal diseases of a focal nature which may be seen in the retinas of Sprague-Dawley rats. Retinal folds are unilateral lesions that occur at a prevalence of 0.3% at 7-10 weeks of age. They are difficult to see on fundoscopic exam as liner elevations. Histologically, they present as multilayered rosettes.³ Colobomas may be seen at a frequency of approximately 0.5% at 7-10 weeks, and are also generally unilateral. On fundoscopic exam, they often appear as a white discoloration of the fundus in a ventral location, with an abnormal optic disc. Histologically, they present with disordered retinal layers, rosette formation, and ectasia of the optic disk.^{1,3}

References:

1. Hubert M.F., Gillet J.P., Durand-Cavagna G. (1994). Spontaneous retinal changes in Sprague Dawley rats. *Lab Anim Sci.* Dec;44(6):561-7.
2. Render J.A., Schafer K.A. and Altschuler R.A. (2013). Special senses: Eye and ear. In *Toxicologic Pathology: Nonclinical Safety Assessment* (P.S. Sahota, J.A. Popp, J.F. Hardisty and C. Gopinath, eds) pp. 942-948. CRC Press, Boca Raton.
3. Render, J. The eye in safety studies – ocular conditions and issues. C.L. Davis and S.W. Thompson Foundation, *NE Division Symposium on Toxicologic Pathology of the Eye.* <https://www.cldavis.org/cgi-bin/download.cgi?pid=331>.
4. Weisse I. (1994). Aging and Ocular Changes. In *Pathobiology of the*

Aging Rat, vol. 2 (U. Mohr, D.L. Dungworth and C.C. Capen, eds.) p.81

CASE III: 13004 (JPC 4048861).

Signalment: 8 weeks, male, Wistar/Crlj, *Rattus norvegicus*, rat

History: The rat was administered alloxan (50mg/kg) by an intra-vein injection for single time at the 7 weeks. The rat lost its body weigh gradually after injection. Both the food intake and the urine volume were also less than other diabetic rats. It was sacrificed at the 8 weeks.

Gross Pathology: Both kidneys were enlarged at the time of necropsy.

Laboratory results:

General parameters and blood glucose (BG)

time	Purchased day	injective day	Day1	Day 2	Day 3	Day 4	Day 5	Day 6	Day 7
BW(g)	237.3	239.6	/	232.4	/	/	/	/	202.4

Food Consumption(g)	23.38	13.36	10.55	1.51	3.09	5.76	9.95	14.45	
Urine volume (ml)	28	28	42	22	22	32	26	36	56
BG (mg/dl)	92	/	418	/	/	/	/	/	455

Microscopic Description:

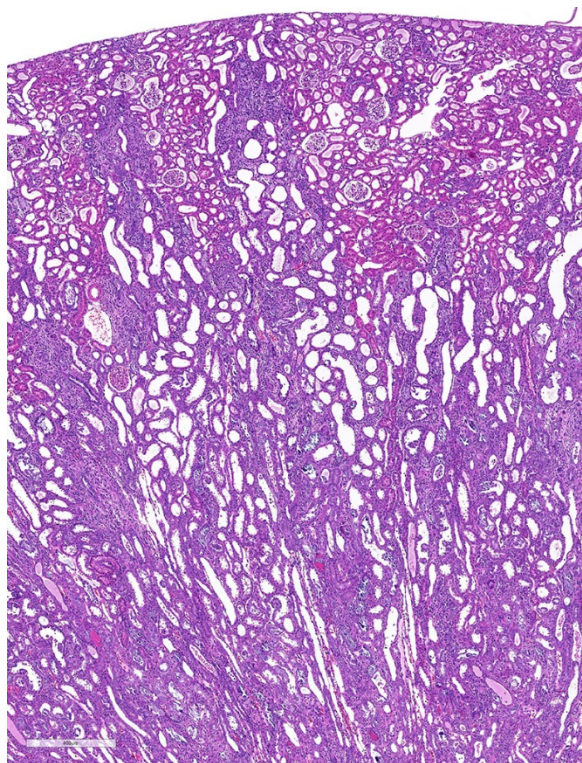
Both two kidneys showed similar lesions. Many dilated and occluded tubules were segmentally observed in inner cortex and outer medulla. Degeneration and necrosis of tubular epithelial cells were seen with/without tubular obstruction by cell debris and crystal/mineral. Dilated tubules were lined with flattened- and attenuated-epithelium with basophilic cytoplasm. In the interstitium around degenerated tubules, multinuclear giant cells, macrophages and lymphocytes infiltrated with fibrosis. Some multinuclear giant cells formed granuloma containing the crystal and mineral. The crystals and minerals located mainly inside the tubules, and some occluded the tubular lumen. In some tubules, they were enveloped by tubular epithelial cells, and tubular basement membrane was disrupted by these crystals and minerals. Mineral was positive for von Kossa's method, but crystal was negative, and both showed non-birefringence with polarized microscopy. Mineral was confirmed as calcium salt. Damaged tubules were mainly the proximal tubules that have brush border and immunopositive for

aquaporin-1, but some were distal tubules that were negative for aquaporin-1 and positive for Na⁺/K⁺ pomp.

Contributor's Morphologic Diagnoses:

Kidney: Granulomatous tubulointerstitial nephritis with tubular necrosis, degeneration and regeneration, and mineralization.

Contributor's Comment: Type 1 diabetes in the rat induced by intravenous injection of alloxan is one of the most common experimental diabetic model which was firstly discovered by Dunn et al. Alloxan induces selectively necrosis of pancreatic



Kidney, rat. There are significant changes within the renal cortex visible within the inner cortex and outer medulla which spares glomeruli and proximal segments of the proximal convoluted tubules. (HE, 20X)

beta cells. Alloxan molecule is structurally similar to glucose, and it can enter beta cells via glucose transporter 2 (GLUT2).² In the presence of intracellular thiols, especially glutathione, alloxan generates reactive oxygen species (ROS) in a cyclic redox reaction with its reduction product, dialuric acid. Autoxidation of dialuric acid generates superoxide radicals, hydrogen peroxide and, in a final iron-catalyzed reaction step, hydroxyl radicals. These hydroxyl radicals are ultimately responsible for the death of the beta cells.⁴ Nephrotoxicity is a dominating feature of the toxicity of alloxan after systemic administration.⁴ As alloxan is an unstable substance, it disappears within five minutes and almost entirely converted to the relative stable alloxanic acid or alloxanates in plasma and these might exist in the largest amount in urine. Therefore nephrotoxicity is so severe that it causes fatal renal failure in

the animals before diabetes can develop.⁴ The expression of GLUT2 in tubular epithelial cells may explain why the toxins can cause damage to the kidney.⁴

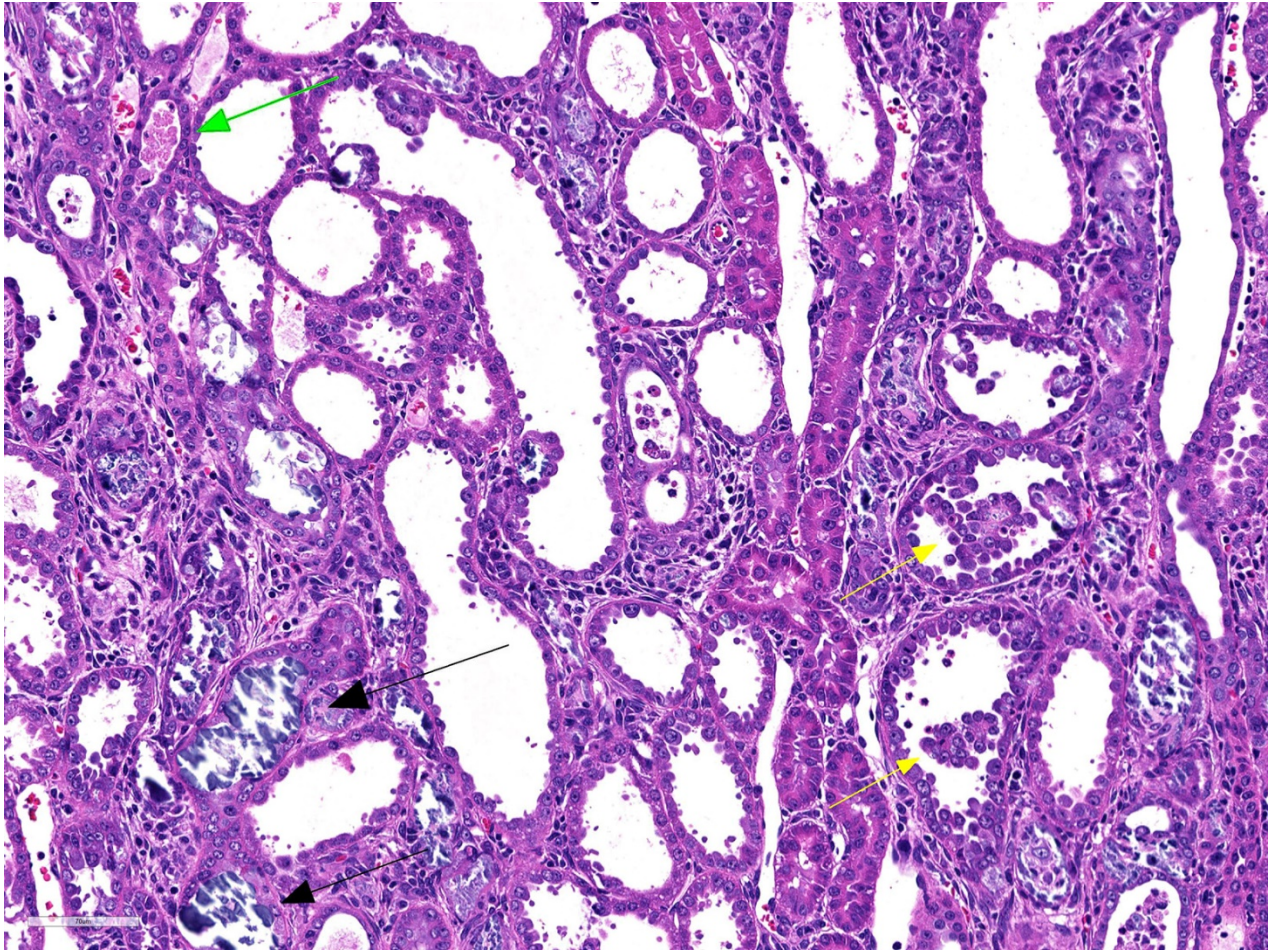
The nephrotoxic changes induced by alloxan include extensive swelling and vacuolar degeneration of renal tubular cells, necrosis of tubular cells with disappearance of brush border and tubular dilation, cellular infiltrates resembling granuloma in the interstitium from the third day to fourteen days.⁵ Histological changes of the kidney observed in alloxan-induced diabetic rats were vacuolar change/ glycogen deposition of the tubular cells and glomerular lesions. Thus, the histologic changes in our case could be differentiated from diabetic change.

Alloxan promotes intratubular mineral deposition and granulomatous interstitial nephritis. These minerals were also localized in the interstitium. The mechanism of translocation of mineral from tubular lumen to interstitium might be similar to that of calcium oxalate crystals¹. Crystal in the tubules is surrounded by tubular epithelial cells and then entered the interstitium through disrupted basement membrane of the tubules and then engulfed by macrophages to form foreign granuloma.

Contributing Institution:

Department of Pathology, Faculty of Pharmaceutical Sciences, Setsunan University,
45-1 Nagaotohge-cho, Hirakata, Osaka 573-0101, Japan
<http://www.setsunan.ac.jp/~p-byori/>

JPC Diagnosis: Kidney, distal convoluted tubules and collecting ducts: Tubular degeneration, necrosis and regeneration, diffuse, severe, with granulomatous tubular interstitial nephritis, rare intratubular crystals, and marked tubular mineralization.

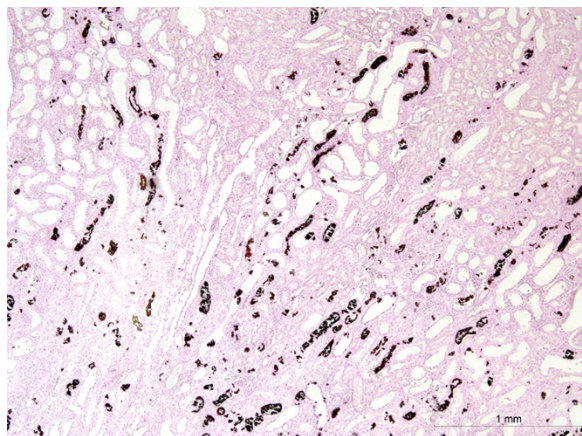


Kidney, rat. A wide variety of changes affect tubules and the interstitium, to include tubular ectasia with epithelial attenuation with granular and cellular casts (green arrow), marked intraluminal proliferation of the tubular epithelium, and the formation of intraluminal oxalate crystals. The interstitium is expanded by variable combinations and concentrations of lymphocytes, plasma cells, histiocytes and neutrophils, collagen, and plump fibroblasts. (HE, 325X)

Conference Comment: Alloxan, a pyrimidine derivative is one of the world's oldest named organic compounds. It was originally derived by the oxidation of uric acid by nitric acid, with early investigators using various sources of uric acid, including human kidney stones as well as boa constrictor excrement (which contains up to 90% ammonium acid urate) The compound was named by Wohler and von Leibig in 1838, who began with the synthesis of urea in 1828, then of uric acid, and some additional 13 derivatives of uric acid of which alloxan is one.⁴ In another one of those cruel twists of fate over naming compounds, Wohler and Leibig were previously aware of similar

research conducted in 1818 by Brugnatelli (working in Italy and publishing in Italian) who created the compound almost two decades previously and had named it "erythric acid" as a result of the red staining it caused on his fingers. The word "alloxan" is derived from a combination of "allantoin", and oxalic acid. A number of reductive products from alloxan exist, including dialuric acid (also diabetogenic in animals), and an anhydrous dimer, alloxantin (produced by the partial reduction of alloxan with hydrogen sulfide.)⁴

As discussed by the contributor, alloxan's similarity to glucose allows it to be taken up

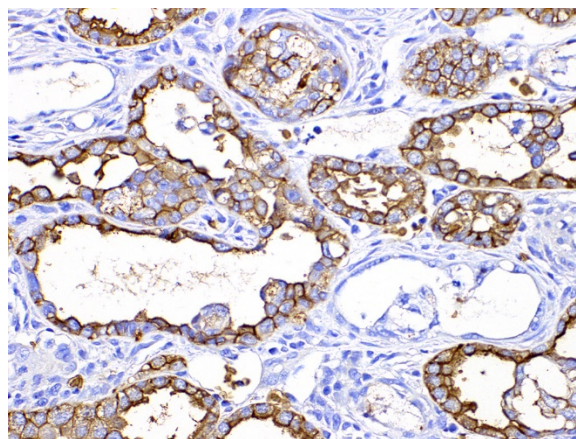


Kidney, rat. A Von Kossa stain demonstrates the prevalence of the mineral within tubules. (HE, 100X 181X) (Photo courtesy of: Department of Pathology, Faculty of Pharmaceutical Sciences, Setsunan University, 45-1 Nagaotohge-cho, Hirakata, Osaka 573-0101, Japan <http://www.setsunan.ac.jp/~p-byori/>)

by GLUT2 glucose transporters in pancreatic beta cells, as well as renal tubular epithelium, resulting in the characteristic necrosis in both cell types, and ultimately “alloxan diabetes” and a change in the kidney initially referred to as “cortical sponge kidney”⁵ (an appellation that like erythric acid, has fortunately not survived the test of time.) Without its structural similarity to glucose, alloxan would not be able to penetrate the cell membrane as it is not lipid soluble.

The basic mechanism of action of alloxan is its generation of reactive oxygen species and selective necrosis of beta cells. The reduction of alloxan within beta cells to dialuric acid results in the generation of the superoxide radical as well as hydrogen peroxide, and in the presence of iron, hydroxyl radicals via the Fenton reaction.³ In addition, alloxan also inhibits glucokinase, inhibiting glucose-induced insulin secretion. This action occurs within a minute of alloxan administration, following alloxan’s almost immediate inhibition of glucose oxidation and generation of ATP necessary to stimulate insulin release from beta cells.³

Another commonly used diabetogenic agent is streptozotocin, a chemotherapeutic alkylating agent and antineoplastic, which was first identified as a diabetogenic agent in 1963.³ This nitrosourea analogue exhibits its effects of beta cells through methylation, or a damaging transfer of a methyl group from streptozotocin to the DNA and other protein molecules of the beta cell following selective uptake through the GLUT2 glucose transporter.³



Kidney, rat. Damaged tubules stain immunopositively for aquaporin. (Photo courtesy of: Department of Pathology, Faculty of Pharmaceutical Sciences, Setsunan University, 45-1 Nagaotohge-cho, Hirakata, Osaka 573-0101, Japan <http://www.setsunan.ac.jp/~p-byori/>)

References:

- 1 de Water R, Noordermeer C, van der Kwast TH, Nizze H, Boeve ER, Kok DJ, Schroder FH: Calcium oxalate nephrolithiasis: effect of renal crystal deposition on the cellular composition of the renal interstitium. *Am J Kidney Dis* **33**: 761-771, 1999
- 2 Elsner M, Tiedge M, Guldbakke B, Munday R, Lenzen S: Importance of the GLUT2 glucose transporter for pancreatic beta cell toxicity of alloxan. *Diabetologia* **45**: 1542-1549, 2002

- 3 Lenzen S: The mechanisms of alloxan- and streptozotocin-induced diabetes. *Diabetologia* **51**: 216-226, 2008
4. McLetchie NGB. : Alloxan diabetes: a discovery albeit a minor one. *J Rou Coll Physicans Edinb* 2002; 32:134-142.
5. Vargas L, Friederici HH, Maibenco HC: Cortical sponge kidneys induced in rats by alloxan. *Diabetes* **19**: 33-44, 1970

CASE IV: 16-10769 (JPC 4085317).

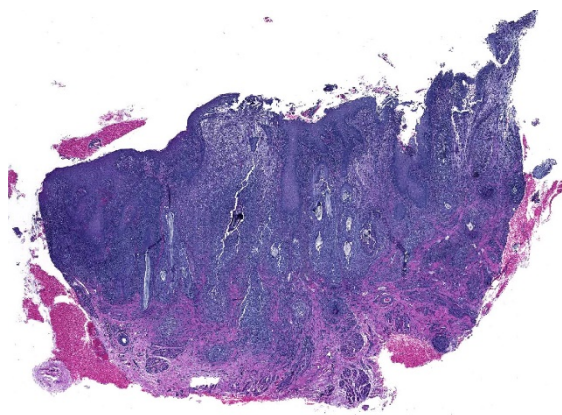
Signalment: 3-year-old, neutered male, mixed breed dog.

History: A 3-year-old mixed breed, neutered male dog had a 6-month history of glossitis with firm raised plaques affecting the proximal third of the tongue. The animal initially responded to prednisone and antibiotic therapy, but improvement stagnated, and two surgical debridements were needed to remove plant material and accelerate the healing process. On follow-up consultation, the dog presented a 95% improvement with only a small focal residual



lesion still present.

Tongue, dog. The dog presented with firm, raised plaques on the dorsal surface of the tongue. (Photo courtesy of: Oregon State University Diagnostic Laboratory, <http://vetmed.oregonstate.edu/diagnostic>)



Tongue, dog. The lingual submucosa is effaced by multifocal to coalescing areas of pyogranulomatous inflammation and granulation tissue which extends deeply into the skeletal muscle and into the overlying hyperplastic and ulcerated mucosa. (HE, 7X)

Gross Pathology: A 3-year-old male dog presented with lesions on the tongue. The rostral third of the tongue had multifocal to coalescing raised, firm and irregular plaques, painful to the touch.

Laboratory results: N/A

Microscopic Description:

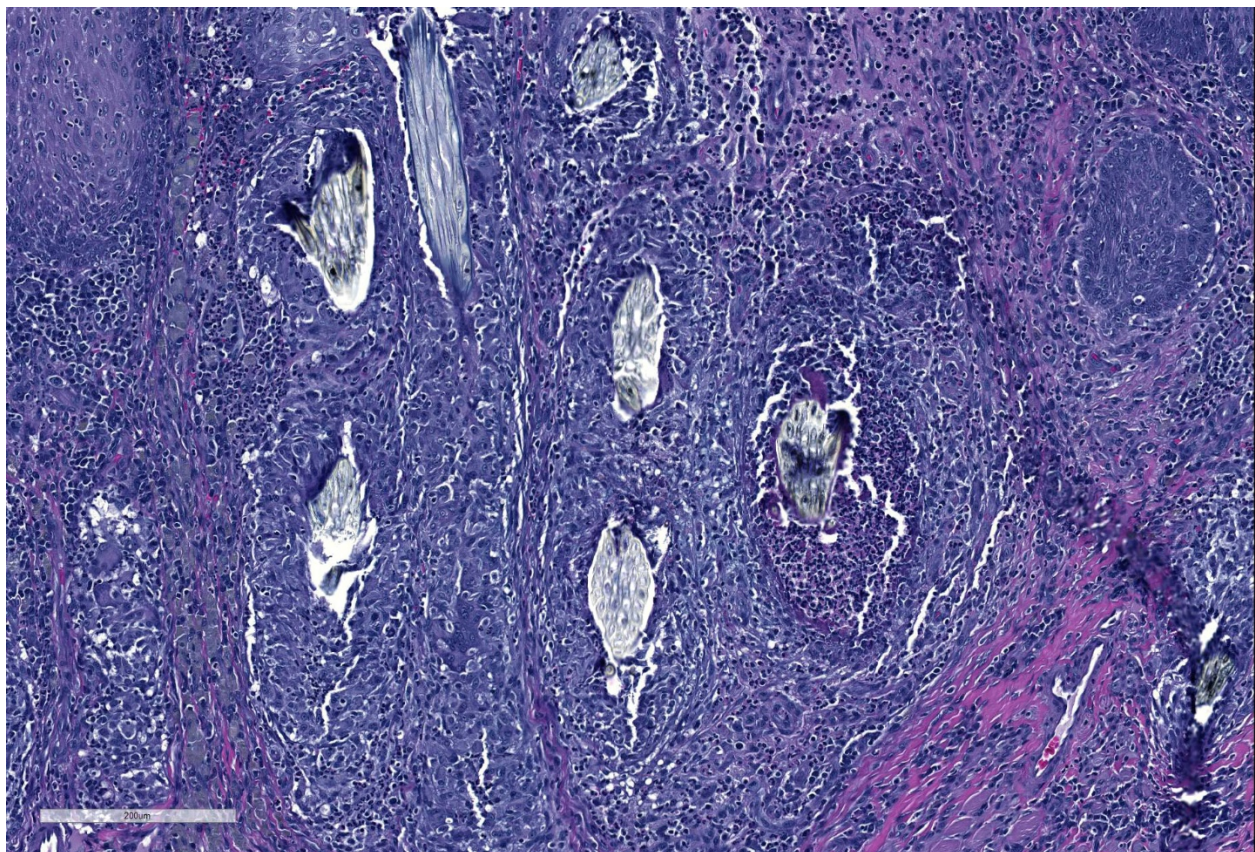
Tissue sections of mucous membrane consistent with tongue. Expanding and elevating the submucosa, and infiltrating deeper layers of muscular bundles are severe, multifocal to coalescing, nodular infiltrates of epithelioid macrophages, degenerate neutrophils, and eosinophils surrounding fragments of embedded plant material. Many of the plant fragments have visible spiny projections. The submucosa is multifocally severely edematous with dilated lymphatics and scattered areas of hemorrhage. The surface epithelium is irregularly thickened with scattered intra-corneal pustules, areas of ulceration and is occasionally covered by a 5 to 10 layers of a thick serocellular crust.

Contributor's Morphologic Diagnoses: Tongue: Severe, multifocal to coalescing, chronic, pyogranulomatous and eosinophilic

ulcerative glossitis associated with foreign plant material.

Contributor's Comment: Lingual lesions are relatively infrequent in dogs; they mostly consist of neoplasms and glossitis associated with trauma or infections. This case is an example of the latter, a severe granulomatous inflammation associated with foreign plant material. The extension of the lesion combined with spiny projections of the plant is highly suggestive of burdock glossitis ("burr-tongue")¹. *Arctium lappa* L., also known as greater burdock, was introduced to the United States and can be currently found throughout the country, except for a few Southeastern and Southwestern states.⁵

Burdock blooms during the summer (July and August). As a result, there is an increase in the incidence of "burr glossitis" particularly in long haired dogs; plant structures tend to accumulate and stick to the coat around the mouth. The flower has a pappus with numerous exposed bristles with sharp hooks that firmly stick to clothes and animal coats.¹



Tongue, dog. Coalescing pyogranulomas are centered on embedded fragments of plant material with evenly spaced barbules. Some have cores of degenerate neutrophils immediately surrounding the plant material (right). (HE, 145X)

Although *Arctium* sp. are the predominant etiology for this type of lesion, other plants such as cactus glochids and *Setaria* sp. have also been associated with burr-tongue in multiple species.⁴ Different structures of the plant such as burrs, fibers or quills can perforate the tongue and lodge itself in deeper layers of connective or muscular tissue, eliciting an inflammatory response. Oral lesions most often occur on the tip and edges of the tongue, anterior parts of the upper lip and gum, and may also affect the philtrum. Clinical signs vary according to the severity of inflammation and the number of lodged bristles, but they include salivation, anorexia, drooling with mild oral discomfort, halitosis, sensitive mouth, and polydipsia.⁴

Differential diagnosis in these cases include the ingestion of caustic chemicals leading to ulcerative lesions, and ulcerated oral neoplasms such as squamous cell carcinoma, melanoma, and granular cell tumor.

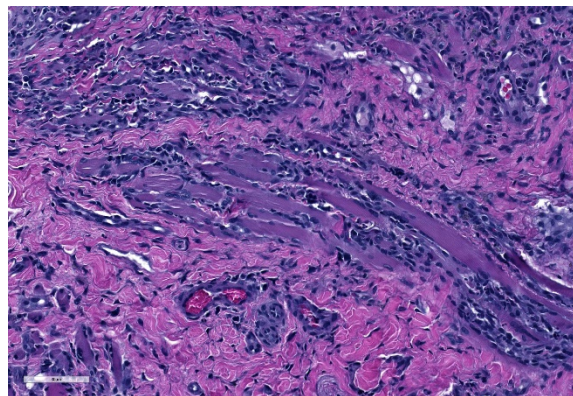
Contributing Institution:

Oregon State University Diagnostic Laboratory
<http://vetmed.oregonstate.edu/diagnostic>

JPC Diagnosis: Tongue: Glossitis, pyogranulomatous and ulcerative, multifocal to coalescing, chronic, with granulation tissue, and abundant plant material.

JPC Comment: The veterinary literature actually contains few reports of plant-induced stomatitis, and the human literature apparently contains none at all (at least based on a very recent Pubmed search.)

“Burr tongue” is a condition which is apparently well-known to practitioners in areas in which *Arctium* sp. grows widely, and is likely a concomitant lesion in animals presented for other complaints.⁴ Clinical signs of careful and slow eating and drinking



Tongue, dog. Atrophic skeletal muscle fibers are surrounded by dense collagen, plump fibroblasts, and abundant perivascular lymphocytic inflammation. Some have cores of degenerate neutrophils immediately surrounding the plant material (right). (HE, 264X)

may not be noticed by the owner. Volcanic ulcers with necrotic centers on the tip and edges of the tongue may require deep curetting or excision to remove the plant scales and the granulation tissue that they are embedded in, and this procedure may need to be repeated several times.⁴

Setaria sp., another common genus of plants referred to as “foxtails” or “bristlegrass”, is well known for causing ulcerative stomatitis in horses when unwittingly incorporated into forage hay. Veterinarians may be consulted for “outbreaks” of stomatitis that may mimic vesicular diseases of the horse, such as vesicular stomatitis, but careful history often reveals the introduction of a new hay source.⁵ *Setaria* stomatitis results in varying degrees of gingivitis, ranging from mild periodontal swelling to marked ulceration, as well as that of labial mucosa in contact with the affected gingiva. Similar, but more severe lesions throughout the oral cavity have also been identified in horse and experimentally in cattle fed a Satu variant of triticale hay in Australia.² Affected animals became totally anorexic and displayed submandibular edema due to the severity of ulcerative lesions throughout the pharynx. A single case report of migrating awns from barley clusters

was reported to cause lingual arteritis, meningoencephalitis, and uveitis in a two-year-old heifer.

Histologically, the lesions of this and other plant awns, such as glochids from prickly pear cacti and foxtail awns from *Setaria* sp. have been reported to be identical both with regard to the characteristic chronic and pyogranulomatous inflammation as well as the appearance of the plant material itself. While the barbs on the bristles of these plants may be oriented either anteriorly or posteriorly, this bit of identifying information is generally useful only in examining the plants themselves under a dissecting microscope and not in examining tissue histologically.

References:

1. Georgi, M. E., Harper, P., Hyypio, P. A., Pritchard, D. K., & Scherline, E. D. Pappus bristles: the cause of burdock stomatitis in dogs. *The Cornell veterinarian*, 1982;72(1), 43-48.
2. McCosker, JE, Keenan DM. Ulcerative stomatitis in horses and cattle caused by triticale hay. *Austr Vet J* 1983; 60:259.
3. Sorden SD, Radostits OM. Lingual arteritis, multifocal meningoencephalitis and uveitis induced by barley spikelet clustes in a two-year-old heifer. *Can Vet J* 1996; 37:227-229.
4. Thivierge, G., 1973. Granular stomatitis in dogs due to Burdock. *The Canadian Veterinary Journal*, 14(4), p.96.
5. Turnquist, SE, Ostlund EN, Kreegar JM, Turk JR. Foxtail-induced ulcerative stomatitis outbreak in a Missouri stable. *J Vet Diagn Invest* 2001: 13-238-240.
6. United States Department of Agriculture: (USDA)
<http://plants.usda.gov/core/profile?symbol=ARLA3>

Self-Assessment - WSC 2018-2019 Conference 15

1. Which of the following is most commonly infected with *Spironucleus* as an extra-intestinal infection?
 - a. Birds
 - b. Primates
 - c. Reptiles
 - d. Fish

2. Which of the following mammals have *Spironucleus* as a common intestinal commensal?
 - a. Rodents
 - b. Primates
 - c. Marsupials
 - d. Swine

3. Which of the following is seen in direct apposition to the choroid or uvea in linear retinopathy of Sprague Dawley rats?
 - a. Retinal pigmented epithelium
 - b. Outer nuclear layer
 - c. Inner nuclear layer
 - d. Ganglion cell layer

4. Which of the following is the primary cellular target for alloxan?
 - a. Schwann cells
 - b. Beta cells
 - c. Articular chondrocytes
 - d. Adrenocortical cells

5. Which of the following is likely not a ruleout for embedded plant material in the tongue of a domestic animal?
 - a. *Setaria sp.*
 - b. *Arctium sp.*
 - c. *Astragalus sp.*
 - d. Triticale hay

Please email your completed assessment to Ms. Jessica Gold at Jessica.d.gold2.ctr@mail.mil for grading. Passing score is 80%. This program (RACE program number) is approved by the AA VSB RACE to offer a total of 0.5 CE Credits, with a maximum of 12.5 CE Credits being available to any individual Veterinary Medical Professionals for the 2017-2018 Wednesday Slide Conference. This RACE approval is for the subject matter categories of: SCIENTIFIC using the delivery method of NON-INTERACTIVE DISTANCE. This approval is valid in jurisdictions which recognize AA VSB RACE; however, participants are responsible for ascertaining each board's CE requirements. RACE does not "accredit", "endorse" or "certify" any program or person, nor does RACE approval validate the content of the program.

Please email your completed assessment to Ms. Jessica Gold at Jessica.d.gold2.ctr@mail.mil for grading. Passing score is 80%. This program (RACE program number) is approved by the AAVSB RACE to offer a total of 0.5 CE Credits, with a maximum of 12.5 CE Credits being available to any individual Veterinary Medical Professionals for the 2017-2018 Wednesday Slide Conference. This RACE approval is for the subject matter categories of: SCIENTIFIC using the delivery method of NON-INTERACTIVE DISTANCE. This approval is valid in jurisdictions which recognize AAVSB RACE; however, participants are responsible for ascertaining each board's CE requirements. RACE does not "accredit", "endorse" or "certify" any program or person, nor does RACE approval validate the content of the program.

**Joint Pathology Center
Veterinary Pathology Services**



WEDNESDAY SLIDE CONFERENCE 2018-2019

C o n f e r e n c e 1 6

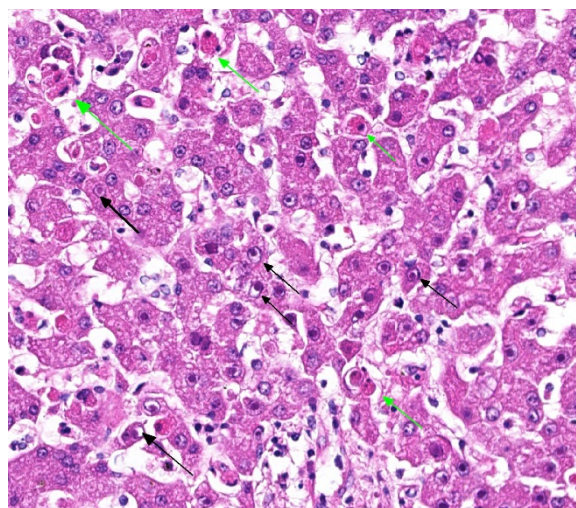
16 January 2019

CASE I: FMVZ USP Case 16 (JPC 4019118).

Signalment: 2-month-old, female, Bernese Mountain Dog, *Canis familiaris*.

History: A 2-month-old female asymptomatic Bernese Mountain dog from a private kennel with sudden death few minutes after second vaccination using polyvalent vaccine (Recombitek C6/CV, Merial®) was sent to necropsy. The kennel's vaccination protocol with Recombitek was: adults, yearly; puppies, beginning at 4 weeks of age with boosters after each 2 to 4 weeks until 12 weeks of age.

Gross Pathology: The puppy was in regular body condition, weighing 4Kg. The lungs were diffusely marked dark red, distended, edematous; trachea's lumen contained transparent fluid. The liver was enlarged, diffuse dark red and friable. All the other organs were within normal limits of shape, size, color and consistency. The death cause being diagnosed as acute pulmonary insufficiency.



Liver, dog. There are individualized and aggregates of shrunken, brightly eosinophilic necrotic hepatocytes, scattered randomly throughout the section (green arrows). The nuclei of numerous hepatocytes contain a 4-6µm eosinophilic intranuclear inclusions surrounded by a clear halo (black arrows).

Laboratory results: None.

Microscopic Description:

Histopathologic evaluation of the liver section showed mild disseminated periarterial (or centrilobular) necrosis and multiple midzonal foci of single-cell necrosis (apoptosis) of hepatocytes, with few neutrophils surrounding them. Numerous large eosinophilic intranuclear inclusion

bodies are present in hepatocytes and in few Kupffer's cells. Other findings include moderate congestion and diffuse mild microvesicular fatty change. The reticulin framework showed intact by reticulin stain; no changes were observed by picrossirius and Perls' stain. The microscopical evaluation of lungs revealed acute diffuse hemorrhage, congestion and edema (lesion not showed).

Contributor's Morphologic Diagnoses:

Liver: hepatitis, acute, neutrophilic, necrotic, periacinar, disseminated, mild with eosinophilic intranuclear inclusion bodies in hepatocytes and in Kupffer's cells, etiology consistent with canine adenovirus 1, Bernese Mountain dog.

Contributor's Comment:

Canine adenoviruses (CAV) have been pathogens of dogs. There are two types, type 1 (CAV-1) and type 2 (CAV-2), which are responsible for infectious canine hepatitis (ICH) and infectious tracheobronchitis (ITB), respectively.² CAV-1 causes infectious disease in dogs and other canids, has worldwide distribution and serologic homogeneity. The wild species affected are Canidae and Ursidae such as coyotes, foxes, wolves, and different species of bears. In addition, adenoviruses have been reported in otters (*Lutra lutra*) and marine mammals such as walruses (*Odobenus rosmarus*) and sea lions (*Eumetopias jubatus*)⁴. In Brazil the frequency of CAV infections in domestic dogs and wild canids is unknown.

Synonyms for ICH include epizootic fox encephalitis and Rubarth's disease and it was first recognized in dogs in 1930. CAV-1 and CAV-2, a DNA virus, are members of the genus *Mastadenovirus*, family Adenoviridae, and are antigenically and genetically closely related (75% identity at the nucleotide level). Despite of this, they are easily distinguishable by restriction endonuclease

analysis and DNA hybridization. They also exhibit different hemagglutination patterns and cell tropism: CAV-1 replicates in the vascular endothelial cells, hepatic and renal parenchymal cells, whereas CAV-2 replicates in the respiratory tract and to a limited extent in the intestinal epithelia.

Transmission occurs directly by animal-to-animal contact or indirectly through exposure to infectious saliva, feces, urine, or respiratory secretions. Viral spread occurs by contact of fomites and hands. Ectoparasites can harbor CAV-1 and may be involved in the natural transmission of the disease. The incubation period in dogs is 4 to 6 days after ingestion of infectious material and 6 to 9 days after direct contact with infected dogs. Viremia lasts 4 to 8 days postinfection and an antibody response clears the virus from blood and liver by day 7 postinfection and restricts the extent of hepatic damage. However, experiments show that dogs with partial neutralizing titer by day 4 or 5 postinfection may develop chronic active hepatitis and hepatic fibrosis. The mortality rate is 10% to 30%. Coinfections with canine coronavirus, canine distemper virus, or canine parvovirus can exacerbate the disease, increasing the mortality rates.

The virus enters the host through oronasal route and initially localizes in the tonsils, where it spreads to lymph nodes and lymphatics before reaching the bloodstream through the thoracic duct.³ The prime targets of viral localization and injury are hepatic parenchymal cells and vascular endothelial cells of many tissues, including the central nervous system (SNC). After 10 to 14 days postinoculation the virus can be found only in the kidneys and is excreted in the urine of carrier animals for up to 6 to 9 months. CAV-1 is highly resistant to environmental inactivation, surviving disinfection with chemicals such as chloroform, ether, acid,

formalin and certain frequencies of ultraviolet radiation. It is inactivated after 5 minutes at 50°C to 60°C, which allows steam cleaning a mean of disinfection.³

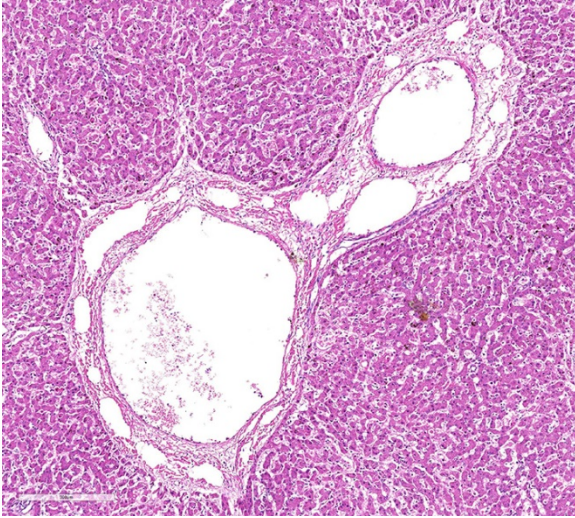
Adenovirus is capable of infecting multiple organ systems; however, most infections are asymptomatic, and infections that result in disease may not be fatal. Clinical findings in the early phase of infection include increased rectal temperature (39.4°C to 41.1°C) and accelerated pulse and respiratory rates. Abdominal tenderness and hepatomegaly are usually apparent in the acutely ill dog and hemorrhagic diathesis may occur. Depression, disorientation, seizures or terminal coma can develop at any time after infection. Severely affected dogs die within a few hours after the onset of clinical signs, while mildly affected dogs may recover after the first febrile episode. Classic symptoms, such as corneal edema and anterior uveitis (“blue eye”), occur when clinical recovery begins and may be the only clinical abnormalities seen in dogs with unapparent infection. Death cause of ICH is uncertain. Although the liver is a primary site of viral injury some dogs die so suddenly that liver damage with resulting hepatic failure does not occur. Death in these dogs can result from damage to the brain, lungs, and other vital parenchymatous organs, or from the development of disseminated intravascular coagulation (DIC) during the early viremic phase of the disease.

Corneal opacity (“blue eye”) and interstitial nephritis may occur 1 to 3 weeks after recovery because of deposition of immune complexes. Hematologic findings include leukopenia (<2000 cells/IL of blood; mainly attributable to a decrease in neutrophil count), increase in the serum transaminases (only in the severe forms of disease), and coagulation disorders associated with disseminated intravascular coagulation (DIC;

thrombocytopenia, altered platelet formation, and prolonged prothrombin time). Proteinuria (albuminuria) can easily reach values greater than 50 mg/dL because of immunomediated glomerulonephritis. Icterus is uncommon in acute ICH, but it is found in some dogs that survive the acute fulminant phase of the disease.

Necropsy and biopsy of liver from dogs can usually confirm a diagnosis of ICH. During acute phase dogs are often in good flesh, with edema and hemorrhage of superficial lymph nodes and cervical subcutaneous tissue. Blotchy hemorrhages may be present on the serous membranes, as well as a small quantity of fluid in the abdomen. The liver is slightly enlarged, with sharp edges, turgid and friable, sometimes congested and spotted with small round areas of necrosis; the gallbladder appears thickened, edematous, and grayish or bluish white opaque in color. Edema of the gallbladder wall is a constant finding. Red strands of fibrin can be found on its capsule, especially between the lobes. Intraluminal gastrointestinal hemorrhage is a frequent finding. Gross lesions in other organs are inconstant and include multifocal hemorrhagic renal cortical infarcts, areas of pulmonary consolidation and edematous bronchial lymph nodes. The brain can be slightly swollen and on cut surface multifocal petechial hemorrhage and gray discoloration of brainstem can be observed. The Bernese puppy necropsy showed only enlarged and friable liver and edematous and dark red lungs which means that the puppy was in acute phase of CAV 1 infection.

Histopathologic changes in the liver of dogs that died of acute hepatitis include widespread centrilobular (periacinar) to panlobular necrosis and individual hepatocellular necrosis, along with neutrophilic and mononuclear cell infiltration and intranuclear inclusions in the hepatocytes



Liver, dog. Marked dilation of lymphatics surrounding sublobular veins give a "rose window" appearance and attest to hepatic edema. (HE, 97X)

and Kupffer's cells. Fatty changes are common but not constant. Multifocal areas of congestion, hemorrhage, and leukocyte infiltration can be observed in several organs, mainly in the lymphoid organs and kidneys, because of vascular damage and inflammation. Interstitial nephritis and iridocyclitis with corneal edema are also present in dogs recovering from ICH. Viral inclusions are initially found in the renal glomeruli and later in renal tubular vascular endothelium. Lymphoid follicles are dispersed with central areas of necrotic foci. The lungs have thickened alveoli with septal cell and peribronchial lymphoid accumulations. Alveoli in consolidated areas are filled with an exudate consisting of erythrocytes, fibrin, and fluid. Swollen, desquamated endothelial cells in meningeal vessels contain intranuclear inclusions. Mononuclear cuffing is present around small vessels throughout the parenchyma of the CNS. Mild endothelial proliferation and mononuclear perivascular infiltration persist for at least 3 weeks after clinical recovery. The histopathologic specificity of the lesions is based on the demonstration of large, intranuclear inclusion bodies. They can be

also found in vascular endothelial cells and histiocytes.

The Bernese puppy had no previously symptoms and died quickly after second vaccination. The CAV 1 infection diagnosis was made based on characteristic microscopic liver lesions. The death cause was acute pulmonary insufficiency consistent with anaphylaxis, a vaccine-associated adverse event and CAV infection was considered a finding not directly correlated to death. The lung lesions were interpreted as immediate hypersensitivity reaction to polyvalent vaccine that overlapped virus infection. Generally, in the dog, clinical signs of type I hypersensitivity include facial edema ("big head"), pruritus, hypotensive shock, weakness, dyspnea, and vomiting with or without diarrhea that can be hemorrhagic. Local or systemic reactions can occur in young puppies within 1 to 24 hours after their second or third vaccination and can result in acute clinical signs such as previously described, and death.

The ICH diagnosis can be helped by hematologic findings (eg, leukopenia, prolonged blood clotting, increased activities of alanine aminotransferase [ALT] and aspartate aminotransferase [AST]), although the increase of transaminases is commonly observed only in severely affected or moribund dogs. Postmortem findings and histopathologic changes are highly consistent of CAV-1 infection when the *inclusion bodies*, which have been classified as Cowdry type A, are present in both ectodermal and mesodermal tissues. Confirmation of a diagnosis of ICH is obtained by virus isolation on permissive cell lines, such as Madin Darby canine kidney (MDCK) cells.² A polymerase chain reaction (PCR) protocol has recently been developed for molecular diagnosis. Ocular swabs, feces, and urine can be collected in vivo for virus

isolation and PCR. Postmortem samples can be withdrawn from the kidney, lung, and lymphoid tissues. The liver is rich in arginase, which inhibits viral growth in cell cultures, but it represents the most important organ for histopathologic examination. Viral growth in cells is revealed by rounding cells that form clusters and detach from the monolayer. Immunofluorescence (IF) can detect viral antigens in infected cell cultures and in acetone-fixed tissue sections or smears. Viral replication can also be demonstrated by detection of nuclear inclusion bodies in the cells after hematoxylin-eosin staining. Neither virus isolation nor IF is able to distinguish between the two adenovirus types.² Because CAV-2 can also be detected in the internal organs and feces of vaccinated or acutely infected dogs and CAV-1 is also frequently isolated from respiratory secretions, trachea, and lungs, distinction between CAV-1 and CAV-2 necessarily deserves laboratory examination. Restriction fragment length polymorphism analysis on viral genomes using the endonucleases PstI and HpaII generates differential patterns. Detection and differentiation of CAV-1 and CAV-2 by PCR with a single primer pair are also possible.² Although CAVs agglutinate erythrocytes of several species, hemagglutination is not used in routine diagnosis. Because most dogs are vaccinated and since CAV-2 infection is frequent in dogs, serology has low diagnostic relevance.

Vaccination has controlled the disease and turned it rare in domestic dog population, although severe outbreaks can be still observed in countries in which CAV vaccines are not used routinely or as a consequence of uncontrolled importation of dogs from endemic areas. Clinical management of dogs that develop ICH is primarily symptomatic and supportive expecting hepatocellular repair. Vaccination usually is repeated

yearly, although after administration of two doses of CAV-2 vaccine, immunity seems to persist for more than 3 years. Even extensive vaccination has greatly reduced the incidence of CAV infections, re-emergence of ICH has been described in some countries such Italy, probably do to trading of pups with uncertain sanitary status from Eastern Europe. At the moment, there are few data on the molecular epidemiology of CAVs, but it is commonly accepted that vaccine breaks occur rarely with CAV vaccines, because the viruses are genetically stable. Accordingly, CAV infection in vaccinated dogs has been associated with maternally derived antibody (MDA) interference in the early life of the pups rather than with emergence of variants genetically distant from the prototype strains contained in CAV-2 vaccines.

We assumed first vaccination failure in the Bernese puppy due to maternally derived antibody interference. Regarding that maternally derived antibody (MDA) titers decrease below 100 around 5 to 7 weeks of age .Sporadic cases in which dogs do not get adequate vaccination during puppyhood are still seen. The duration of passively acquired immunity in the pup is dependent on the antibody concentration of the bitch. The half-life of CAV-1 antibodies is 8.6 days, and these values correlate well with the half-life for canine globulin. The recommended schedule with any vaccine for protection against ICH involves at least two doses, given 3 to 4 weeks apart, at 8 to 10 and 12 to 14 weeks of age.

The intensification of surveillance activity using new diagnostic techniques and molecular analysis tools may help to investigate the epidemiology of CAV infections more thoroughly and plan adequate measures of control in different countries.

Contributing Institution:

Faculdade de Medicina Veterinária e Zootecnia da Universidade de São Paulo
Av. Prof. Dr. Orlando Marques de Paiva, 87
CEP 05508 270
Cidade Universitária
São Paulo/SP – Brasil

JPC Diagnosis: Liver: Hepatitis, necrotizing, multifocal, centrilobular to midzonal, mild to moderate, with edema and numerous hepatocytic and endothelial intranuclear viral inclusions.

JPC Comment: The contributor has provided an excellent and wide-ranging discussion of canine adenovirus-1 in the dog and in a wide range of other species.

A purported viral disease that shows a number of similarities to infectious canine hepatitis was identified in Great Britain in 1985, but may not be well-known (or even heard of by WSC participants). “Canine acidophil cell hepatitis” gets its name from the shrunken necrotic hepatocytes scattered throughout the liver, but lacks the intranuclear inclusions and CAV-1 and CAV-2 have not been identified. Transmission studies of liver homogenates induced reproducible disease, suggesting a viral agent which has not yet been characterized. Also, unlike infectious canine hepatitis, the chronic disease characterized by cirrhosis and in some cases hepatocellular carcinoma have been identified in suspect cases.³

References:

1. Caudell D, Confer AW, Fulton RW, et al. Diagnosis of infectious canine hepatitis virus (CAV-1) infection in puppies with

encephalopathy. *J Vet Diagn Invest.* 2005; (17):58-61.

2. Decaro N, Martella V, Buonavoglia C. Canine adenoviruses and herpesvirus. *Vet Clin Small Anim* 2008; (38): 799–814.

3. Greene CE. Infectious Canine Hepatitis and Canine Acidophil Cell Hepatitis. In: Greene CE, ed. *Infectious Diseases of the dog and cat.* 4th ed. Philadelphia, PA: Saunders; 2011:42-47.

4. Greene, CE, Levy, JK. Immunoprofilaxy. In: Greene CE, ed. *Infectious Diseases of the dog and cat.* 4th ed. Philadelphia, PA: Saunders; 2011:1163-1205.

5. Stalker MJ, Hayes MA. Liver and biliary system. In: Maxie MG, ed. *Jubb, Kennedy and Palmer’s Pathology of Domestic Animals.* 5th ed. Vol 2. New York, NY: Elsevier Saunders; 2007:348-351.

6. Thompson H, O’Keeffe AM, Lewis JCM, et al. Infectious canine hepatitis in red foxes (*Vulpes vulpes*) in the United Kingdom. *Veterinary Record*, 2010; (166)111-114.

7. Watson PJ. Chronic hepatitis in dogs: a review of current understanding of the aetiology, progression, and treatment. *The Veterinary Journal.* 2004; (167)228-241.

CASE II: 1407470-10 (JPC 4050020).

Signalment: 16 year old Male castrated Shetland pony

History: A 16 year old castrated male Shetland pony presented to Oregon State University large animal emergency service for acute onset of respiratory distress. He had an eight-month history of hind end staggering, inappetence, and difficulty maintaining weight.

On physical exam, the gelding was ataxic, dyspneic, tachycardic, tachypneic, and febrile. The complete blood count with

unremarkable. Blood gas revealed a high pCO₂, bicarbonate, and lactate with low chlorine. Endoscopy revealed bilaterally closed arytenoids on inspiration. Due the history of chronic neurologic disease, plus poor condition, euthanasia was performed and the body was submitted for necropsy.

Gross Pathology: At necropsy, the animal was in poor body condition with no subcutaneous, visceral, or pericardial fat. Approximately 200 mL of straw colored fluid was within the thorax and 1 liter of fluid within the abdomen. The liver was markedly

enlarged (2x) with swollen, rounded edges, and an irregularly nodular visceral surface. The parenchyma bulged when cut and had a prominent micronodular pattern. The right adrenal gland was swollen by a blood filled 1.5 cm diameter cyst which expanded the medullary area. A few ecchymotic hemorrhages were present on the epiglottis and in the tissue surrounding the trachea. The lungs were diffusely congested and edematous. No significant gross findings were present within the brain, spinal cord, or vertebral column.

Laboratory results: Following histopathology examination a frozen liver specimen was submitted for trace mineral concentration:

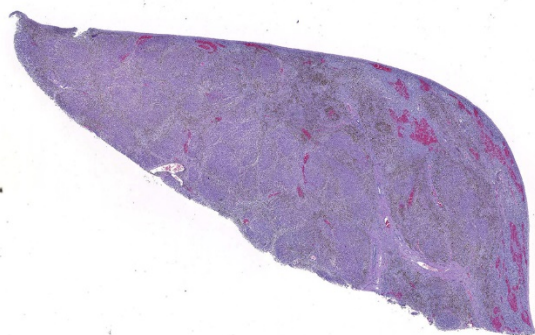
Mineral	Horse values	Reference Range	Units
Iron	27,048 High	[300-900]	ug/g
Zinc	81 Low	[120-375]	ug/g
Copper	25	[12-25]	ug/g
Selenium	0.5 Low	[1.0-2.5]	ug/g
Cobalt	0.12 Low	[0.30-0.60]	ug/g
Molybdenum	23.7 High	[1.5-3.0]	ug/g
Manganese	9.6	[6.0-18.0]	ug/g

Frozen serum was retrieved and submitted for ferritin levels at Michigan State University. A limited biochemical profile was analyzed at the OSU VDL.:

Mineral	Horse values	Reference Range	Units
Ferritin	46,539 High	[43-261]	ng/mL

Liver chemistry profile

Analyte	Result	Reference Range	Units
Bun	7 Low	[8-23]	mg/dL
Total protein	6.5	[5.9-7.6]	g/dL
Albumin	3.0	[2.9-3.8]	g/dL
Total bilirubin	2.9 High	[0.8-2.6]	mg/dL
Ck	3530 High	[145-633]	U/L
Alkaline Phosphatase	742 High	[80-240]	U/L
GGT	430 High	[7-25]	U/L
AST (SGOT)	764 High	[212-453]	U/L
SDH	>170 High	[2.4-7.2]	U/L



Liver, horse. At subgross magnification, the liver parenchyma is divided into variably sized lobules by bands of dense fibrous connective tissue bridging between portal areas. There is aggregates of large amounts of a brown pigment at the periphery of the lobules (especially in subcapsular areas) and multifocal congestion and hemorrhage. (HE, 7X)

Liver. The hepatic architecture is markedly distorted by severe fibrosis. Pseudolobules are formed from periportal bridging fibrosis with large amounts of collagen in these areas. Along the subcapsular surface, the sinusoidal patterns are disorganized. Infrequently, megalocytes are present but nuclei are generally unremarkable. An abundance of hemosiderin pigment is within stromal macrophages and Kupffer cells while hepatocytes also contain large amounts of iron positive granules. There is moderate cholangiolar hyperplasia.

The thyroid, kidney, pituitary gland, salivary gland, spleen, adrenal gland, pancreas, and colonic epithelial cells as well as mononuclear phagocytes contain the similar brown to golden pigment. Prussian blue staining of the histologic section demonstrated the pigment to be iron.

Cervical, thoracic, lumbar spinal cord (not submitted). All white matter spinal tracts, are vacuolated to some extent, with some vacuoles containing macrophages (digestion chambers). In longitudinal sections, myelin

sheaths are disrupted and axons are swollen with spheroid formation.

Cerebrum (not submitted) There are single or 2-3 cell clusters of swollen astrocytes with dispersed chromatin, and scant cytoplasm (Alzheimer type II cells).

Skeletal muscle. Multifocally, the myocytes are hypereosinophilic, with internalization of nuclei and loss of cross-striations.

Contributor's Morphologic Diagnoses:

Liver: Severe, diffuse hepatocellular degeneration and loss, with bridging portal fibrosis, marked iron accumulation, and mild biliary hyperplasia

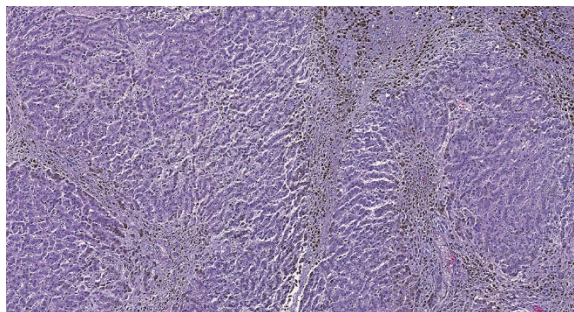
Condition: Hemochromatosis

Spinal cord: Moderate myelopathy, consistent with equine degenerative myelopathy

Cerebrum: Mild encephalopathy with Alzheimer type II cells: consistent with hepatic encephalopathy

Skeletal muscle: Mild multifocal myocyte degeneration

Contributor's Comment: Hemochromatosis is a well described disease affecting humans, fruit-eating and insect-

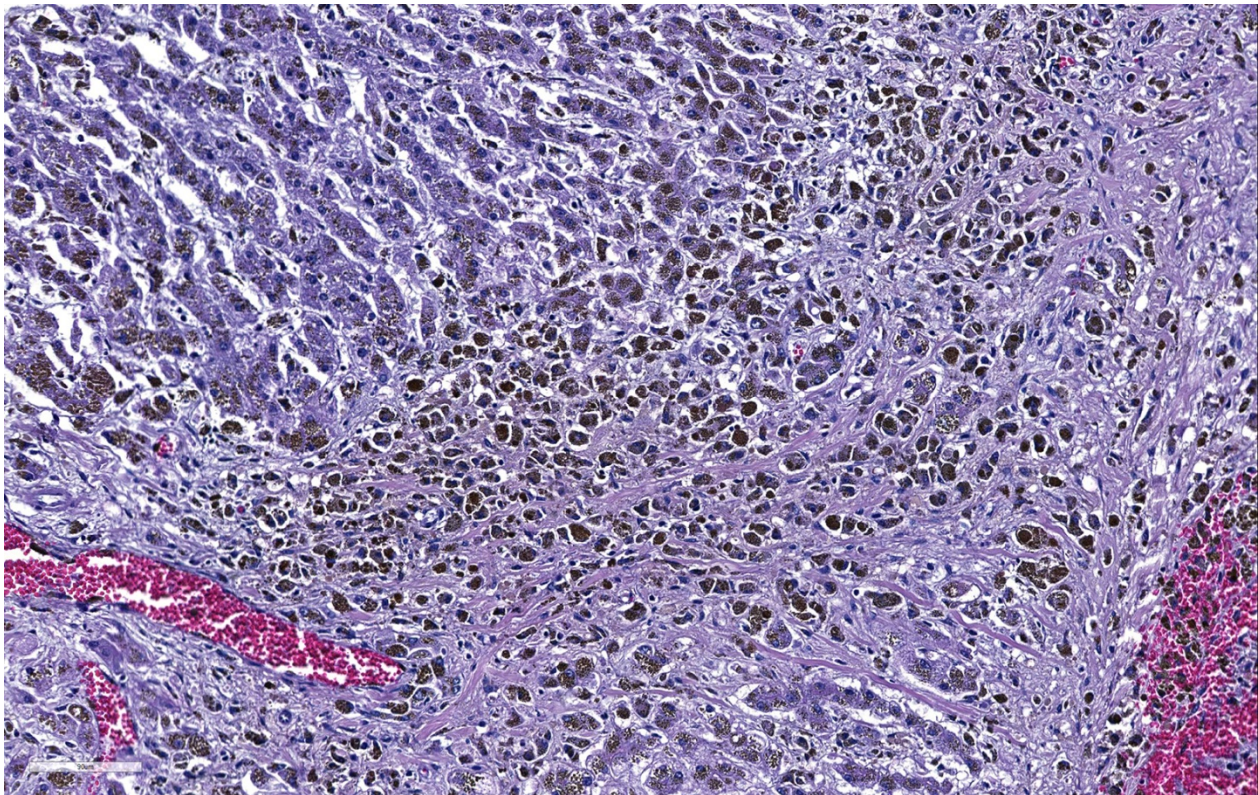


Liver, horse. Higher magnification demonstrating irregularly lobules, bridging portal fibrosis and abundant iron pigment. (HE, 97X)

eating birds and in Salers cattle.^{2,9,10} In humans, hereditary (primary) hemochromatosis is an autosomal recessive disorder characterized by hyperabsorption of dietary iron and accelerated recycling of iron by macrophages.¹ The excessive iron is stored in the parenchymal organs, especially the liver, causing damage which may result in fibrosis, cirrhosis and hepatocellular carcinoma.⁹ Mynah birds are one of the most frequently reported avian species to have hemochromatosis. Affected livers have marked chronic active cholangiohepatitis with fibrosis and iron granules within hepatocytes, Kupffer cells, and macrophages.⁸ Iron is also deposited in the other organs. In this present case, Prussian blue stains of histology sections demonstrated excessive iron pigment in the thyroid gland, kidney, pituitary gland, salivary gland, spleen, adrenal glands,

pancreas and colon. The serum and hepatic iron levels showed tremendous elevations.

Hemochromatosis patients and mynahs have a defect in the gene encoding for iron proteins (HFE) responsible in the iron sensing mechanism.^{3,12} The mechanism is well described in humans.¹⁰ Dietary iron is used by enteric cells in enzymatic reactions, stored as ferritin, excreted in sloughed enterocytes, or transferred to plasma. Iron absorption is mainly influenced by the hepatic protein hepcidin³. It works by blocking ferroportin channels located in enterocytes (and macrophages), preventing iron from reaching the plasma. Dysregulation of this pathway, which is dependent on several genes, can lead to primary hemochromatosis, as low hepcidin levels allow excessive influx and storage of iron³. The mechanism of secondary hemochromatosis is unclear, but occurs in



Liver, horse. Portal areas are markedly expanded by abundant collagen which extends into the periportal parenchyma entrapping individual and small groups of hepatocytes. Portal hepatocytes, entrapped hepatocytes, macrophages, and Kupffer cells contain abundant brown granular pigment. (HE, 247X)

humans as a result of chronic liver disease and hemolytic anemias.¹⁵ Untreated, hereditary hemochromatosis patients may develop severe iron overload, whereas in secondary hemochromatosis iron overload is minimal to modest. Also, the pattern of iron accumulation differs in primary and secondary hemochromatosis.^{5,15} In primary hemochromatosis, iron accumulates within hepatocytes in the periportal region (acinar zone 1) whereas in secondary hemochromatosis iron accumulation is within macrophages and endothelial sinusoidal cells. The pattern observed in this case is more consistent with primary hemochromatosis.^{2,15} This pony was not on any iron supplements. No other equid in this group has developed liver disease in the year since the diagnosis was made. This suggests that inappropriate intestinal iron absorption as seen with primary hemochromatosis may have been the underlying disease process in this case.

The most common signs of liver disease in horses are non-specific and include icterus, behavioral changes and weight loss.^{13,15} Histopathology is vital for the definitive diagnosis of hepatic diseases. Potential causes include the acute liver disease known as serum sickness or Theiler's disease, Tyzzer's disease, cholangiohepatitis, and hepatic lipidosis.⁴ Hepatotoxic disease in equids can be separated into pharmaceutical-induced (such as carbon tetrachloride, pentachlorophenols, etc) and plant/environmental exposure (pyrrolizidine alkaloidosis, blue-green algae, *Fusarium*

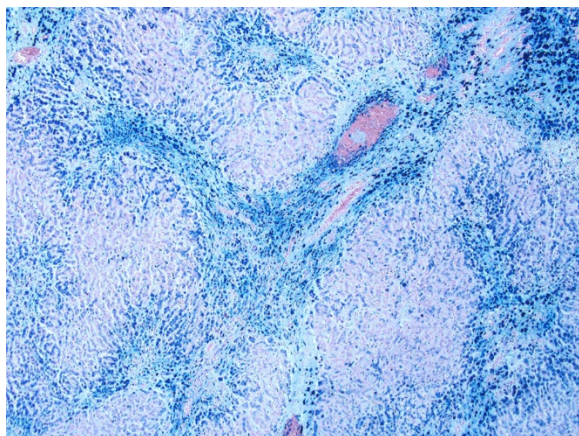
Contributing Institution:

Oregon State University Veterinary
Diagnostic Laboratory
<http://vetmed.oregonstate.edu/diagnostic>

toxicosis, etc). Iron toxicity has been reported as a cause of hepatotoxicity in orally supplemented foals.¹⁰ Biliary calculi (choleliths), liver lobe torsion, and hepatic amyloidosis are other differentials for hepatic disease. Animals with severe destructive hepatic disease may show signs of or acute or chronic hepatic failure (wasting, jaundice) as well as neurological signs.¹² Microscopic changes of hepatic encephalopathy may include polymicrocavitation or spongiform changes of white matter (not observed in this case) and Alzheimer type II cells (present in the cerebrum). Spinal cord lesions observed in hepatic encephalopathy include vacuolation at the fasciculus proprius with no histiocytic response. This does not fit with the more widespread microscopic lesions observed in this case.

Excess iron is toxic, causing increased oxidative stress and the production of reactive oxygen species.¹³ We suspect that excess iron may have promoted oxidative damage, depleting levels of antioxidants such as Vitamin E, leading to the degenerative changes to the myelinated tracks as seen in equine degenerative myelopathy. Acute onset of respiratory distress due to laryngeal and/or pharyngeal paralysis is a proposed, uncommon manifestation of hepatic disease in ponies.¹³ In this instance, there is a concurrent depression in hepatic selenium levels, and high CK levels, as may be seen with nutritional myopathy, another potential cause of laryngeal malfunction in horses. Sections of heart in this pony had mild multifocal degeneration of cardiomyocytes.

JPC Diagnosis: Liver: Fibrosis, bridging and portal, diffuse, severe, with periportal hepatocellular degeneration and loss, edema, biliary hyperplasia and marked hepatocellular and histiocytic siderosis.



Liver, horse. A Perl's iron stain discloses the identity and location of the pigment within hepatocytes and macrophages. (Perl's, 100X)

JPC Comment: A number of mechanisms are responsible for the excessive storage of iron within the liver in man and many other species of animal. The term hemosiderosis is defined as excessive storage of iron, while the term hemochromatosis, as applied to the liver, indicates a cellular injury resulting from this storage. Primary hemochromatosis is considered to be the result of genetic mutations involving proteins regulating iron metabolism; additional information on the importance of these proteins have been studied in a series of genetic-engineered mutant mice, as well as red deer,⁶ black rhinoceroses,⁶ and bottle-nosed dolphins.¹⁴

Secondary forms of hemosiderosis result from excessive absorption of iron from sources high in iron, or may result from lack of iron chelators normally found in the diet, which allow iron normal bound in the intestinal lumen, to be freely absorbed (a mechanism which is often commonly identified as a cause of excessive liver iron in a number of zoo and wildlife species in captivity.) Affected zoo species in which hemochromatosis is routinely reported include mynah birds, toucans, birds of paradise, New World monkeys, bottle-nose dolphins and black rhinoceroses.⁹

A number of studies have been published since the submission of this case to the WSC which have helped to shed light on the pathology and potential pathogenesis of hemochromatosis in a number of species.

A 2018 case report of hemochromatosis from the University of Utrecht¹⁶ reported a case of secondary hemochromatosis in 21 horses and one donkey housed together for a minimum of 9 years. Clinical pathology of affected animals revealed blood transferrin saturation levels of >80% and increased gamma-glutamyltransferase levels. Hepatic biopsy demonstrated excessive iron storage in hepatocytes and macrophages, hepatitis and fibrosis. Necropsy of seven animals revealed siderosis in other organs. Excessive levels of iron in drinking water was identified as a the cause, and the remaining 13 animals from 17 to 79 months post diagnosis.

A 2014 study of bottlenose dolphins resulted in the sequence of the hfe gene in this species. The hfe gene is a common cause of primary (hereditary) hemochromatosis in man. The hfe gene's product regulates the amount of hepcidin produced by hepatocytes. The point mutation of hfe in humans results in improper binding to beta2-macroglobulin preventing the transport of hfe to the hepatocyte surface, where it ultimately upregulates the expression of hepcidin. While a point mutation was not identified in affected dolphins, genomic sequencing is now a tool that may be used to pinpoint hereditary causes of hemochromatosis in animals outside the realm of human and lab animal medicine.¹⁴

A recent study of 83 adult Egyptian fruit bats not only documented excessive storage of iron in a number of organs including liver and spleen, but also pancreas, kidney, skeletal muscle, heart, and lung. In addition, 11

animals also had hepatocellular carcinoma, and this represents the first positive correlation between hemochromatosis and hepatocellular carcinoma in a species other than humans.⁷

References:

1. Ajioka R, Kushner J. Clinical consequences of iron overload in hemochromatosis homozygotes. *Blood* 2003; 3351-3354
2. Brown PJ. Haemosiderin deposition in donkey (*Equus asinus*) livers: comparison of quantitative histochemistry for iron and liver iron content. *Res Vet Sci* 2011; 284-287
3. Coates, T. Physiology and pathophysiology of iron in hemoglobin-associated diseases. *Free Radic Biol Med* 2014; 1-12
4. Cullen J. Liver and biliary system. *In: Jubb, Kennedy, and Palmer's Pathology of Domestic Animals*, 5th ed. Philadelphia, PA: Elsevier; 2007.
5. Klopfleisch R, Olias P. The pathology of comparative animal models of human haemochromatosis. *J Comp Path* 2012; 147:460-478.
6. Lavoie JP, Teushcher E: Massive iron overload and liver fibrosis resembling haemochromatosis in a racing pony. *Eq Vet J* 1993; (6) 552-554.
7. Leone AM, Crawshaw GJ, Garner MM, Frasca S, Stasiak I, Rose K, Neal D, Farina LL. A retrospective study of the lesions associated with iron storage disease in captive Egyptian fruit bats. *J Zoo Wildl Med* 2016; 47(1):45-55.
8. Mete A, Hendriks HG, Klaren PHM, Dorrestein GM, van Dijk JE, Marx JJM. Iron metabolism in mynah birds (*Gracula religiosa*) resembles human hereditary haemochromatosis. *Avian Path* 2003; 625-632

9. Mullaney TP, Brown CM. Iron toxicity in neonatal foals. *Eq Vet J* 1988; (20):119.
10. O'Toole D, Kelly EJ, McAllister MM, Layton AW, Norrdin RW, Russell WC, Saeb-Parsy K, Walker WP: Hepatic failure and hemochromatosis of Salers and Salers-cross cattle. *Vet Pathol* 2001; 372-389.
11. Pearson E, Hedstrom R, Poppenga R. Hepatic cirrhosis and hemochromatosis in three horses. *JAVMA* 1994; 1053-1056
12. Pearson, EG. Liver failure attributable to pyrrolizidine alkaloid toxicosis and associated with inspiratory dyspnea in ponies: three cases. *JAVMA* 1991; 198:1651-1654.
13. Pearson, EG. Liver disease in the mature horse. *Eq Vet Educ* 1999; 11:(2) 87-96
14. Phillips BE, Venn-Watson S, Archer LL, Nollens HH, Wellehan JFX. Preliminary investigation of bottlenose dolphins (*Tursiops truncatus*) for hfe gene-related hemochromatosis. *J Wildl Dis*; 2014; 50(4):891-895.
15. Sebastiani G, Walker A: HFE gene in primary and secondary hepatic iron overload. *World J of Gastroent* 2007; 4673-4689
16. Theelen MJP, Beukers M, Grinwis GCM, Oldruitenborgh-Oosterbaan MM. Chronic iron overload causing haemochromatosis and hepatopathy in 21 horses and one donkey. *Eq Vet J* 2018; epub doi: 10.1111/evj.13029.

CASE III: 11727 (JPC 4019850).

Signalment: 3-years-old, female, crossbreed, heifer (*Bos taurus*)

History: A herd of 70 heifers were in a wetland during the summer (since February 2010). These three-years-old heifers had been transferred to two years rice stubble, next to a facility to calve (August 2011). In



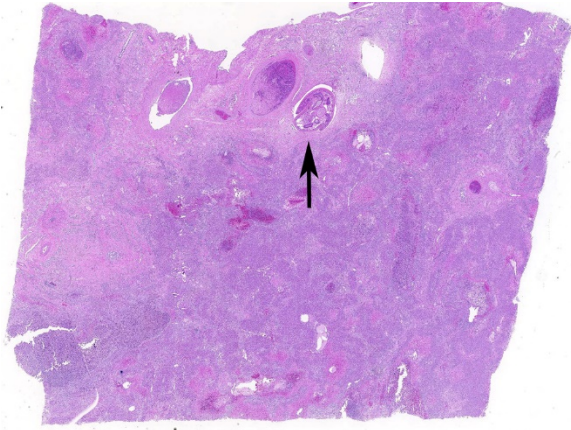
Liver, ox: On cut section, the liver is fibrosis, and hemorrhagic with hemorrhagic tract and immature flukes within the parenchyma. (Photo courtesy of: Animal Pathology Department / Veterinary Diagnostic Laboratory, Veterinary Faculty; Federal University of Pelotas. 96010-900 Pelotas, RS, Brazil. <http://www.ufpel.edu.br/fvet/oncovet/>)

December 2011, five animals died after 30-40 days of weight loss. The heifers had been treated with Nitroxynil in May and September 2011 before calving and with Ivermectin in October 2011 after calving. One heifer was recumbent for 12 hour and was euthanized due to unfavorable prognosis and was immediately necropsied.

Gross Pathology: At necropsy, mucosae showed mild anemia and jaundice. Dark brown ascitic fluid was present in abdominal cavity and there were a thick layer of fibrin among peritoneum, intestines, diaphragm and liver. The liver was enlarged with rounded edges and the capsular surface was irregular with adhered fibrin and red strips

interspersed with clear areas and petechiae. Liver cut surface was irregular, friable and hemorrhagic and white channels could be observed through the parenchyma. There were some dark foci filled with debris and adult forms of *Fasciola hepatica*. The gallbladder was enlarged and the wall was thick and edematous and contained some adult forms of *F. hepatica*. Hepatic lymph nodes were enlarged and wet and fluid was drained on the cut hemorrhagic surface. Renal infarction was also observed. Fibrin and clotted blood were observed adhered to the pericardium and lung, mainly in diaphragmatic lobes.

Laboratory results: no tests were performed



Liver, ox: A large area of fibrosis (at top) contains a cross section of an immature trematode and several cross-sections of a thrombosed artery. Bridging portal fibrosis is evident at low magnification and at bottom areas of coagulative necrosis within several lobules. (HE, 8X)

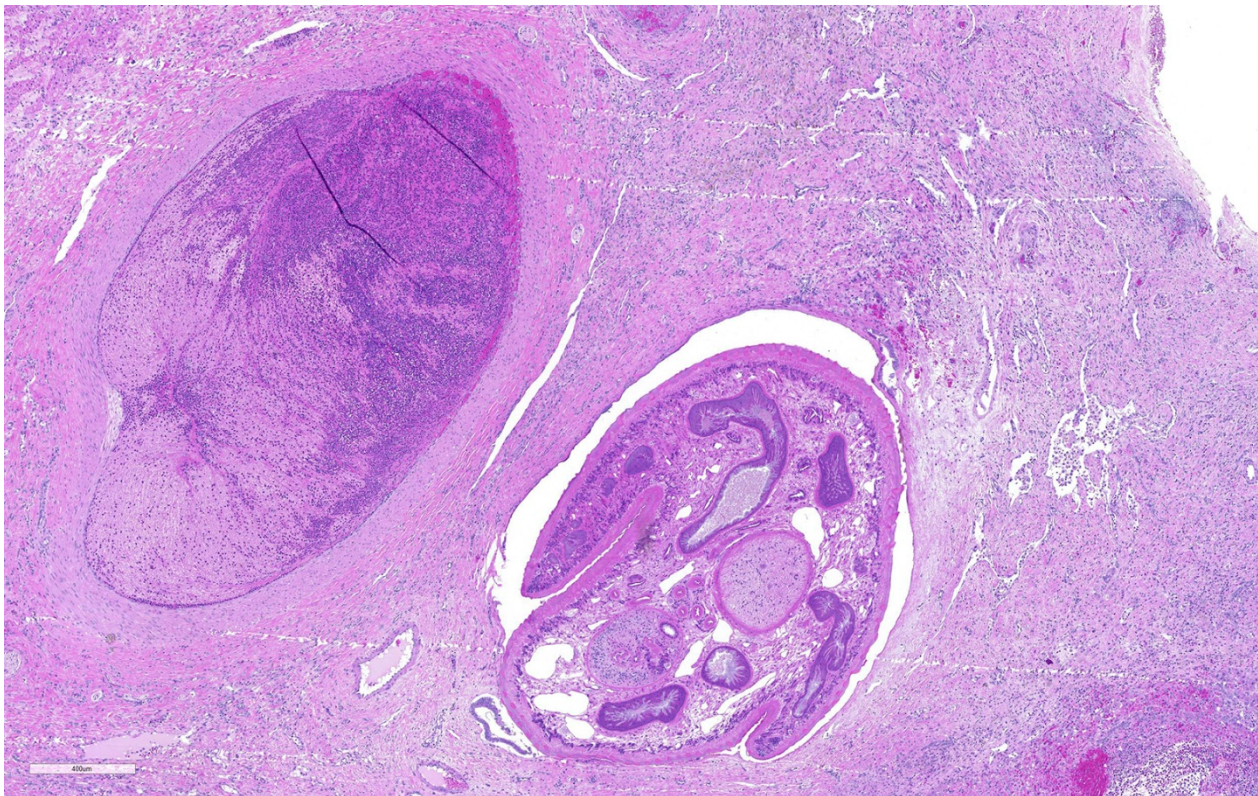
Microscopic Description:

Liver: areas of coagulative necrosis and extensive hemorrhage in streaks or foci and disruption of the parenchyma with neutrophil and eosinophil infiltration. There was also fibrosis and bile duct hyperplasia in some areas. Immature forms of *F. hepatica* were observed in the parenchyma surrounded by degenerated hepatocytes, neutrophil, eosinophil and hemorrhage.

Additional findings (organs not submitted): peritonitis with fibrinohemorrhagic deposits on the serous surfaces of abdominal cavity. Multifocal fibrosis, hemorrhage and neutrophil infiltration were observed in renal cortex and some hyaline casts were present in renal tubules.

Contributor's Morphologic Diagnoses:

Hepatitis with extensive hemorrhages

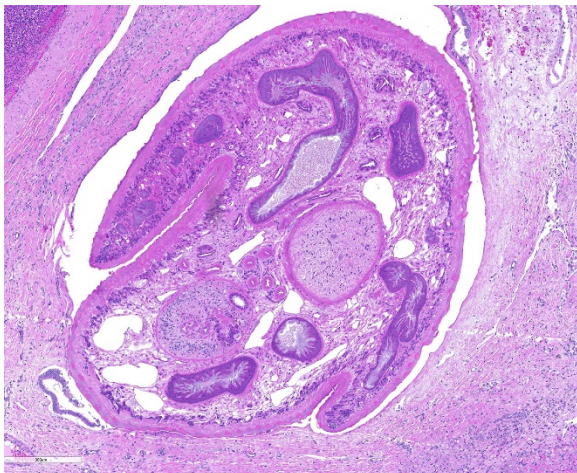


Liver, ox: At left, a large fibrinocellular thrombus occludes a hepatic arteriole, at right is a cross section of an immature trematode. (HE, 52X)

associated with infiltration of neutrophils and eosinophils and the presence of immature forms of *F. hepatica*. Fibrosis and bile duct hyperplasia

Contributor's Comment: Fasciolosis is a common parasitic disease of domestic ruminants throughout the world. The disease is caused most commonly by the trematode *Fasciola hepatica* that has a cosmopolitan distribution.¹⁰ Liver fluke infections affect farm animals especially in terms of poor productivity, reduced milk yield and livers condemned at slaughter¹¹. *F. hepatica* remains an economically significant parasite of livestock and is emerging as an important zoonotic infection of humans.⁶ In southern Brazil, the rate of liver condemnation at slaughter due to infection by *F. hepatica* is 10.34% for cattle and 20% for buffaloes⁵, 38% for cattle and 7% for sheep.²

Infection occurs by ingestion; excystment occurs in the duodenum. The young flukes penetrate the intestinal wall and cross the peritoneal cavity, attaching here and there to suck blood and penetrate the liver through its capsule.¹⁰ The acute phase follows and



Liver, ox: The trematode parasite has a thick cuticle with spikes, cross sections of two suckers, and numerous cross section of an intestine. The lack of a uterus, vitellarian glands and eggs indicates that this is a larval fluke. (HE, 88X)

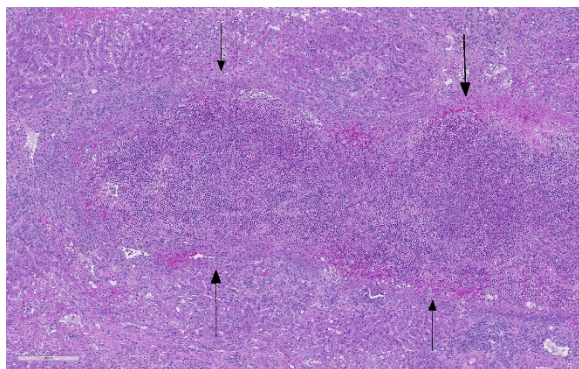
coincides with active liver migration of immature parasites.⁶ Parasites digest hepatic tissue and cause extensive parenchymal destruction with intensive hemorrhagic lesions and immunological reactions. On the other hand, the injury of the liver can be also induced chemically by factors produced or induced by the fluke. Immature flukes wander in the liver for a month or more before settling down in the bile ducts to mature, which they do in 2-3 months.¹⁰ The chronic phase begins 30 to 40 days after exposure as the parasites enter the bile ducts.⁶

Usually there is no obvious reaction to the passage of young flukes through the intestinal wall and across the peritoneal cavity and parasites may be found in ascitic fluid. Acute and exudative or chronic and proliferative peritonitis occurs in heavy and repeat infections.¹⁰

Wet environments with temperature between 10-25°C are necessary for proliferation of the parasite as well the intermediate host (snail).⁹ Precipitation may favor the accumulation of water that is a prerequisite for the disease cycle. Generally, this buildup occurs in flat or less mountainous terrain, as in Santa Vitória city (latitude S32°58'50.4"), extreme southern of Brazil, where this case occurred.

This case occurred in a recognized endemic area.⁵ Acute outbreaks are not common in cattle of this region where outbreaks with high mortality are only common in sheep.⁴ It seems possible that cattle from this area shows a relative resistance to the agent. A long time ago, resistance to *F. hepatica* infection in cattle has been reported.⁹

In the present case, the disease probably occurred as a result of consecutive infections since cows remained for a long period in a snail infected wetland on the farm. However, the cattle had been treated in May and



Liver, ox: Large linear areas of lytic necrosis (migration tracts) course through the hepatic parenchyma. (HE, 70X)

September with drugs of nitroxylnil group, it is possible that these drugs cannot be effective, since does not act in the young forms of the parasite. Moreover, *F. hepatica* resistance has been reported to these drugs.^{7,8} In mice secondary infections, the inflammatory response was faster and shorter. Resolution also was more rapid and often complete in 30 days.⁶

Contributing Institution:

Animal Pathology Department/
Veterinary Diagnostic Laboratory,
Veterinary Faculty; Federal University of
Pelotas. 96010-900 Pelotas, RS, Brazil.

<http://www.ufpel.edu.br/fvet/oncovet/>

<http://www.ufpel.edu.br/fvet/lrd/>

JPC Diagnosis: Liver: Fibrosis, portal, bridging and random, diffuse, moderate to severe, with arteriolar thrombosis, larval trematodes, and migration tracts

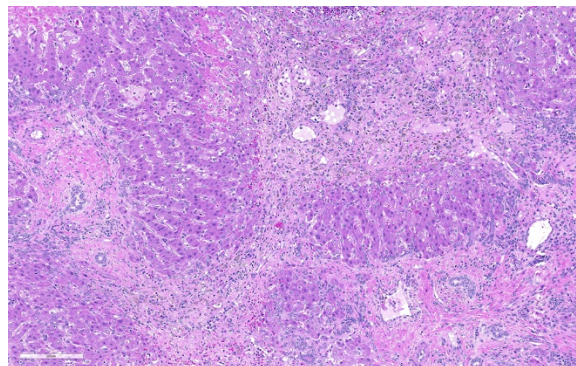
2. Liver, centrilobular hepatocytes: Necrosis, multifocal.

JPC Comment: The contributor does an excellent job of describing the pathogenesis and clinical issues surrounding *F. hepatica* in cattle. While most commonly associated with infection in ruminants, *F. hepatica* (and a second related species, *F. gigantea*) can result in fascioliasis in a much wider range of

species, including pigs, dogs, cats, capybara, and humans. (WSC 2010-2011, Conference 10 Case 1, details a case of *F. hepatica* in a pony from Ireland.)

F. hepatica, termed the temperate fluke, is found on every inhabited continent, while *F. gigantean* is found in tropical areas of Asia and Africa.³ The life cycle (as described above) is similar for both flukes. Interestingly, in areas of Japan, Vietnam, and Korea, a number of intermediate hybrids between the two species have been identified by morphometric and molecular analysis.³

Two possible sequelae to hepatic trematodiasis are black disease (*C. novyi*) in sheep and bacillary hemoglobinuria (*C. hemolyticum*) in sheep and cattle. The migration of immature flukes through the hepatic parenchyma may result in the generation of necessary ischemic conditions for the proliferation of *C. novyi* spores, already within the liver, to proliferate. Once active, *C. novyi* produces a necrotizing beta toxin and a hemolytic phospholipase C, resulting in large areas of coagulative necrosis in the liver and death, often with no premonitory signs. The pathogenesis of bacillary hemoglobinuria, caused by *Clostridium haemolyticum*, is similar to black disease with respect to the fluke involved, germination of spores, and toxin production. The toxins

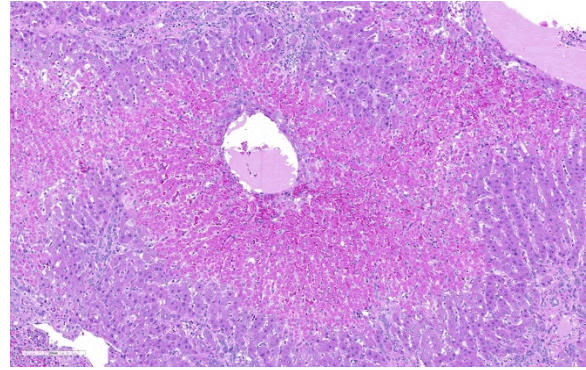


Liver, ox: There is marked expansion of portal areas with fibrosis and biliary hyperplasia, as well as bridging portal fibrosis. (HE, 137X)

of *C. haemolyticum* also produces intravascular hemolysis with associated anemia and hemoglobinuria.

Fascioliasis is a tropical disease in humans whose prevalence is likely underestimated given the lack of surveys in endemic areas. Humans may be infected as a result of ingesting metacercariae-infected water or aquatic salad vegetation, such as watercress.³ Two main phases exist in the human disease. The acute phase of the disease coincides with the migration of immature flukes through liver liver, One to three months following ingestion of the metacercariae, the course of disease is marked by fever, right quadrant pain, hepatomegaly, eosinophilia and hypergammaglobulinemia. The second, or biliary stage, corresponds to active cholangitis with or without cholestasis, and the presence of flukes within biliary radicles.¹ Diagnosis may be accomplished by stool examination for ova and parasites, but is unreliable during acute stages. The most widely used diagnostic technique is an ELISA test for antibodies against secretory/excretory products from the flukes themselves. Ultrasound or CT results may demonstrate the hyperplastic changes in bile ducts and periductal fibrosis, as well as capsular fibrosis and subcapsular hemorrhage, changes quite similar to that seen in affected animals.¹ While generally easily treated with anti-fluke drugs such as triclabendazole and bithionol, developing resistance to these drugs poses a significant problem for both animals and humans and poses a “One Health” problem for veterinarians and physicians alike.

There is significant slide variation in this case, with not all sections having the arteriolar thrombosis and areas of coagulative centrilobular necrosis. The etiology of the centrilobular necrosis was largely attributed to vascular insufficiency resulting from



Liver, ox: Multifocally, there are areas of centrilobular and midzonal coagulative necrosis. (HE, 137X)

arteriolar thrombosis, however the possibility of shock as a cause could not be completely excluded.

References:

1. Aksoy DY, Kermolglu U, Oto A, Erguven S, Arslan S, Unal S, Batman F and Bayraktar Y. Infection with *Fasciola hepatica*. *Clin Microbiol Infect* 2005; 11:859-861.
- 2.
3. Cunha FOV, Marques SMT, Mattos MJT. Prevalence of slaughter and liver condemnation due to *Fasciola hepatica* among sheep in the state of Rio Grande do Sul, Brazil 2000 and 2005. *Parasitol Latinoam.* 2007; 62: 188 - 191
4. Cwiklinski K, O'Neill SM, Donnelly S, Dalton JP. A prospective view of animal and human fasciolosis. *Parasite Immunol* 2016; 38:558-568.
5. Fairweather, I. 2011. Reducing the future threat from (liver) fluke: realistic prospect or quixotic fantasy? *Vet. Parasitol.* 180: 133-143
6. Marques, S.M., Scroferneker, M.L. 2003. *Fasciola hepatica* infection in cattle and buffaloes in the state of Rio Grande do Sul, Brazil. *Parasitol Lationam.* 58: 169-172

7. Masake RA, Wescott RB, Spencer GR, Lang BZ. The pathogenesis of primary and secondary infection with *Fasciola hepatica* in mice. *Vet Pathol.* 1978; 15: 763-769

8. Moll L, Gaasenbeek CPH, Vellema P, Borgsteede FHM. Resistance of *Fasciola hepatica* against triclabendazole in cattle and sheep in The Netherlands. *Vet Parasitol.* 2000; 91: 153–158

9. Olaechea F, Lovera V, Larroza M, Raffo F, Cabrera R. Resistance of *Fasciola hepatica* against triclabendazole in cattle in Patagonia (Argentina). *Vet Parasitol.* 2011; 178: 364–366

10. Smithers SR, Terry RJ. Resistance of the host to *Fasciola hepatica*. *Proc. R. Soc. Med.* 1967; 60:168-169

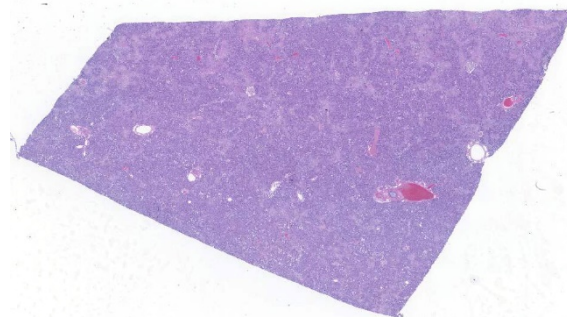
11. Stalker MJ, Hayes MA. Liver and biliary system. In: Maxie MG, ed. *Jubb, Kennedy and Palmer's Pathology of Domestic Animals.* 5th ed., vol. 2. Philadelphia, PA: Saunders Elsevier; 2007:359-362

12. van Dijk, J, Sargison, ND, Kenyon, F, Skuce, PJ. Climate change and infectious disease: helminthological challenges to farmed ruminants in temperate regions. *Animal.* 2010. 4(3): 377–392

CASE IV: UW-SVM Case 2 (JPC 4018823).

Signalment: 1-year-old, intact male, Boxer, canine (*Canis lupus familiaris*)

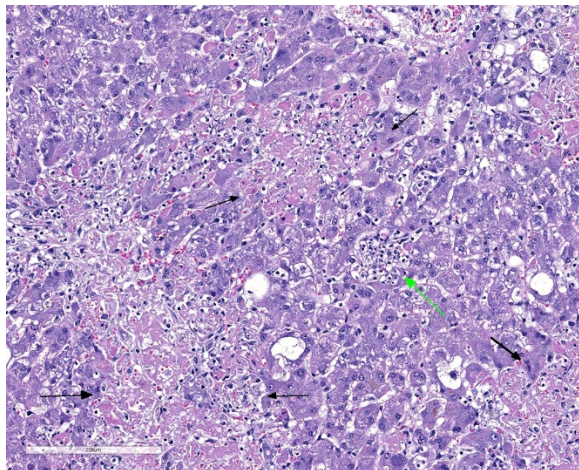
History: This dog was under treatment for 4 months for waxing and waning episodes of pyrexia, cervical pain and ataxia (cerebellar and proprioceptive), which progressed to a non-ambulatory state. In addition, valvular endocarditis was diagnosed 2 months following the initial presentation, based on a



Liver, dog. A retiform pattern of pallor delineates coalescing areas of necrosis throughout the section. (HE, 5X)

2/6 cardiac murmur and an echocardiogram which showed a vegetative lesion on the aortic valve. Complete blood count showed a neutrophilic leukocytosis. Treatment included non-steroidal anti-inflammatory drugs and various antibiotics (amoxicillin/clavulanic acid, sulfadimethoxine, cephalexin, ciprofloxacin) for suspected bacterial endocarditis. When negative test results were obtained for a variety of infectious diseases (see laboratory results), a presumptive diagnosis of immune-mediated meningoencephalomyelitis was made and the dog was placed on an immunosuppressive dose of prednisone; antibiotic treatment was continued. There was clinical improvement which then mildly regressed. Azathioprine was added to the immunosuppressive protocol; dramatic clinical improvement ensued which lasted approximately 6 weeks. The dog then showed signs of profound lethargy, weakness, a return of ataxia and mild cervical pain, dyspnea, tachycardia, and pale mucus membranes. The cardiac murmur had resolved. Further testing and treatment were declined and the dog was euthanized.

Gross Pathology: The dog was in poor body condition with marked skeletal muscle wasting and scant adipose stores. The liver was diffusely tan, variably friable to mildly firm, and enlarged (4.8% body weight). The lungs were diffusely rubbery, wet, and heavy,



Liver, dog. Areas of both coagulative (black arrows) and lytic (green arrow) necrosis are present within the section. (HE, 176X)

and oozed abundant serosanguinous fluid on section; the parenchyma contained four poorly demarcated tan to grey semi-firm nodules ranging from 0.7 cm to 2.5 cm in widest dimension. The trachea contained pink foam and dark red, cloudy watery fluid from the larynx to the carina. The sternal and tracheobronchial lymph nodes were moderately enlarged. The pancreas was pink mottled tan and adjacent fat and omental fat had multifocal firm yellow foci (pancreatitis with fat necrosis). Adrenal cortices were bilaterally thin. There were few small raised crusted foci on metatarsal and metacarpal skin. Cardiac valves were grossly normal, indicating resolution of previous valvular endocarditis.

Laboratory results:

Antemortem results:

Complete blood count: Neutrophilic leukocytosis at initial presentation. Mild anemia and mild neutrophilia 1 week prior to euthanasia. Blood culture, urine culture: no growth. Cerebrospinal fluid (CSF) analysis: increased protein, neutrophilic pleocytosis, no organisms seen. Blastomyces EIA negative. *Neospora caninum* IFA negative.

Rocky Mountain Spotted. Fever titer negative. Lyme C6 4DX SNAP: negative for *Ehrlichia canis*, *Dirofilaria immitis*, *Borrelia burgdorferi*, *Anaplasma phagocytophilum*.

Postmortem results:

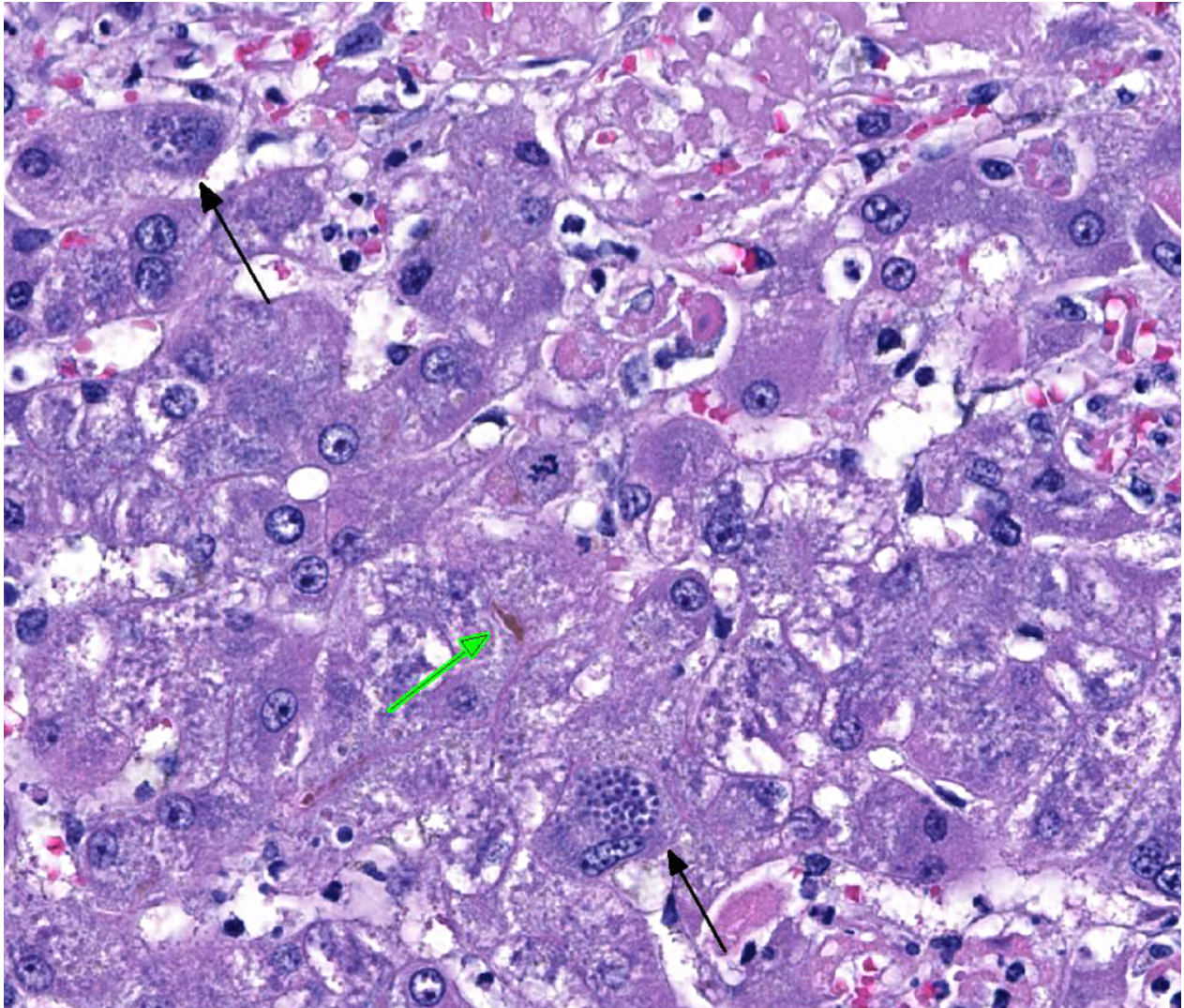
Cytology on lung nodules, impression smear: The sample contained many oval to crescentic protozoal organisms, approximately 2x6 microns, with a 1-2 micron diameter basophilic nucleus, along with many macrophages, fewer degenerate neutrophils, and a heavy background of erythrocytes.

CSF cytology: The sample contained many neutrophils and macrophages; no organisms were seen.

PCR on lung tissue for *Toxoplasma gondii*: positive (Ct=16.92). *Neospora caninum* PCR negative.

Microscopic Description:

Liver: Multifocally throughout the liver are many random, occasionally coalescing foci of hepatocellular necrosis, in total affecting up to ~1/3-1/2 of the parenchyma. Hepatocellular necrosis is characterized by one or more of the following: pale eosinophilic cytoplasm with loss of cellular detail and retention of cellular outlines (coagulation necrosis), fragmentation of cytoplasm, karyolysis or karyorrhexis, and replacement of cells by cellular and karyorrhectic debris, fibrin, and few to moderate numbers of neutrophils with fewer macrophages and erythrocytes. Within few hepatocytes, Kupffer cells, and macrophages are small clusters or variable numbers of individual 2-4 micron, round to oval protozoal organisms with a small round basophilic nucleus. Most remaining hepatocytes are mildly to moderately swollen and contain irregular, variably sized cytoplasmic clearings (glycogen-type



Liver, dog. Numerous zoites bounded by a visible parasitophorous vacuole are present within hepatocytes (and potentially a Kupffer cell at lower right). Bile canaliculi are expanded (cholestasis – green arrow) (HE 400X)

vacuolar change), with few small random foci and individual cells showing severe swelling and vacuolar degeneration. Multifocally few bile canaliculi are dilated by green-orange bile. Few portal areas are mildly expanded by immature fibrous connective tissue which occasionally extends along surrounding sinusoids; these areas are often bordered by a focus of necrosis.

Additional histologic findings: Multiple other organs also had necrosis with protozoa, including the lung, pancreas, and myocardium, and accompanied by varying amounts of inflammation. The central

nervous system had minimal to mild multifocal non-suppurative meningoencephalomyelitis with microglial nodules and few protozoal cysts that were usually not associated with areas of inflammation. Skeletal muscle had mild myonecrosis with protozoal cysts in few viable myocytes. A focal necrosuppurative skin lesion on the metatarsus contained angioinvasive pigmented fungal hyphae (phaeohyphomycosis). There was bilateral adrenocortical atrophy.

Contributor's Morphologic Diagnoses:

Liver: 1. Multifocal to coalescing random

hepatocellular necrosis with protozoal organisms

Moderate to marked diffuse hepatocellular vacuolar degeneration, glycogen-type (steroid-induced hepatopathy)

Mild multifocal portal fibrosis; mild extracellular cholestasis

Contributor's Comment: *Toxoplasma gondii* is a coccidian protozoal parasite found worldwide that can cause systemic infection in the definitive hosts (members of the Felidae) as well as intermediate hosts (other warm-blooded animals, including humans), though subclinical infections are more common.^{3,6}

The life cycle includes an asexual and sexual enteroepithelial cycle that occurs only in felids, and a tissue cycle that occurs in felids and intermediate hosts.^{3,6} The host becomes infected by ingesting the organism in the form of sporulated oocysts in cat feces or in material contaminated by cat feces, or in the form of tachyzoites or encysted bradyzoites in tissues of intermediate hosts.^{3,4} Vertical transmission can also occur. Tachyzoites replicate in a wide variety of host cells, and spread throughout the body from the intestine via lymphatics or the portal system, within leukocytes or free in plasma.³ Intracellular replication of tachyzoites causes focal necrosis, which may be followed by inflammation. Tissue cysts containing bradyzoites tend to form in brain and skeletal muscle; immunocompromise may cause these latent tissue cysts to release the zoites and reinitiate systemic infection.³

Systemic infection occurs most often in young animals and immunocompromised animals, and in dogs can accompany diseases such as canine distemper, lymphoma, or ehrlichiosis.³ It has also been reported in dogs undergoing immunosuppressive therapy.^{3,6}

Lesions of toxoplasmosis are typically necrosis followed by inflammation, and organs most often affected include the lungs and central nervous system; neurologic and respiratory signs are most common and can be confounding in cases of dual infection with canine distemper.³ Pulmonary lesions include necrosis of the alveolar septa and interstitial pneumonia. Central nervous system lesions include multifocal necrosis and non-suppurative inflammation, with microglial nodules forming in more chronic cases, but as rapidly as 1-2 weeks following infection. Cysts can form in chronic cases as the infection becomes quiescent.

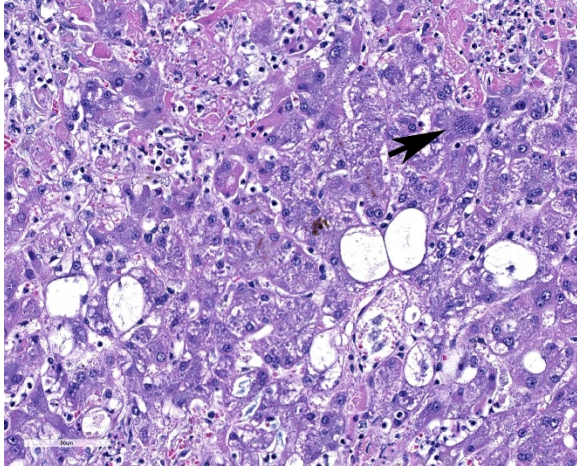
Hepatocellular glycogen-type vacuolar degeneration (hepatic glycogenosis, glucocorticoid hepatopathy) is due to excess exogenous or endogenous corticosteroids.⁵ In this case, an immunosuppressive dose of prednisone caused steroid-induced hepatopathy as well as adrenocortical atrophy. Focal necrotizing dermatitis due to phaeohyphomycosis was presumably an opportunistic infection in this immunocompromised dog.

Contributing Institution: Department of Pathobiological Sciences

School of Veterinary Medicine University of Wisconsin–Madison
<http://www.vetmed.wisc.edu>

JPC Diagnosis: 1. Liver: Hepatitis, necrotizing, random, multifocal to coalescing, moderate, with edema and intrahepatocytic, intrahistiocytic, and extracellular apicomplexan zoites. 2. Liver, hepatocytes: Glycogenosis, multifocal, moderate.

JPC Comment: The contributor has presented an excellent review of the systemic infection associated with *T. gondii*. Within the 15 years, much has been learned about the *T. gondii* infection at the cellular level as well



Liver, dog. Small groups of hepatocytes are markedly swollen by cytoplasmic glycogen granules ("spider cells"). An intracytoplasmic cyst containing numerous tachyzoites is present (black arrow) and bile canaliculi at center are distended (cholestasis)

including mechanisms of invasion, replication, and egress, as well as the body's mechanisms to control *T. gondii* and mechanisms that it has evolved to escape those mechanisms.²

Interestingly, the parasite forms found intracellularly and extracellularly represent distinct biological states. Extracellular parasites are motile, non-replicative, and designed to extrude the conoid and secrete the contents of their microneme organelles. Intracellular parasites divide, are non-motile and do not secrete micronemes or extrude their conoid. Marked changes in gene expression, mRNA production and translation, and changes in glycolytic pathways of energy production are required from the transition between the two stages.²

IFN γ appears to be the lynchpin of mammalian resistance to *T. gondii* infection.² IFN γ upregulates a variety of anti-parasite genes whose expression kills the parasite by a number of mechanisms. These include autophagy-dependent degradation of the parasitophorous vacuolar membrane by the p47 family of IFN γ -regulated GTPases

(IRGs) as well as the degradation of essential nutrients such as tryptophan by indoleamine dioxygenase. *Toxoplasma* has developed two primary ways of evading these IFN γ -mediated effects. *Toxoplasma* has evolved the ability to produce and secrete proteins which directly inactivate IFN γ -stimulated mediators, including the aforementioned GTPases (effective in most species except higher primates, which do not apparently produce them. Moreover, it can also directly interfere with IFN γ -regulated gene expression, by blocking the binding of STAT1 transcription factors from binding to their target genes.²

A number of other cases of toxoplasmosis have been included in the WSC within the last ten years: dog (Liver; WSC 2014 Conf 10 Case 1), cat (Duodenum, WSC 2009-2010, Conference 16 Case 2), and mole (Liver, WSC 2016 Conf 11, Case 4).

References:

1. Bernstein L, Gregory CR, Aronson LR, Lirtzman RA, Brummer DG: Acute toxoplasmosis following renal transplantation in three cats and a dog. *JAVMA* 1999; 15:1123-1126,
2. Blader I, Coleman B, Chen C, Gubbles M. The lytic cycle of *Toxoplasma gondii*: 15 years later. *Annu Rev Microbiol* 2015; 69:463-485.
3. Brown CC, Baker DC, Barker IK: Alimentary system. In: Jubb Kennedy and Palmer's Pathology of Domestic Animals, ed. Maxie MG, 5th ed., vol 2, pp. 270-273. Elsevier Limited, Philadelphia, PA, 2007.
4. Gardiner CH, Fayer R, Dubey JP: Apicomplexa: *Toxoplasma* and *Hammondia*. In: An atlas of protozoan parasites in animal tissues, 2nd ed., pp. 53-56, Armed Forces Institute of Pathology, Washington, DC, 1998.

5. Stalker MJ, Hayes MA: Liver and biliary system. *In*: Jubb Kennedy and Palmer's Pathology of Domestic Animals, ed. Maxie MG, 5th ed., vol 2, pp.309-310. Elsevier Limited, Philadelphia, PA, 2007

6. Webb JA, Keller SL, Southorn EP, Armstrong J, Allen DG, Peregrine AS, Dubey JP: Cutaneous manifestations of disseminated toxoplasmosis in an immunosuppressed dog. *J Am Anim Hosp Assoc* **41**:198-202, 2005

Self-Assessment - WSC 2018-2019 Conference 16

1. Which of the following tests may be used to differentiate between canine adenovirus-1 and canine adenovirus-2 infection?
 - a. Serology
 - b. Immunofluorescence
 - c. Virus isolation
 - d. Polymerase chain reaction

2. Which of the following acts to regulate iron absorption by blocking ferroportin channels on enterocytes?
 - a. Hepcidin
 - b. Transferrin
 - c. HFE
 - d. Psilocybin

3. In which of the following species has hepatocellular carcinoma been positively correlated with elevated levels of liver iron?
 - a. Egyptian fruit bat
 - b. Black rhinoceros
 - c. Mynah birds
 - d. Bottle-nosed dolphins

4. Which of the following species of fluke has formed hybrid species with *Fasciola hepatica*?
 - a. *Fascioloides magna*
 - b. *Dicrocoelium dendriticum*
 - c. *Fasciola gigantica*
 - d. *Schistosoma haematobium*

5. Which of the following is not a method of transmission of *Toxoplasma gondii*?
 - a. Vertical transmission
 - b. Ingestion of tissue from an intermediate host
 - c. Arthropod bite
 - d. Ingestion of feces from the definitive host

Please email your completed assessment to Ms. Jessica Gold at Jessica.d.gold2.ctr@mail.mil for grading. Passing score is 80%. This program (RACE program number) is approved by the AA VSB RACE to offer a total of 0.5 CE Credits, with a maximum of 12.5 CE Credits being available to any individual Veterinary Medical Professionals for the 2017-2018 Wednesday Slide Conference. This RACE approval is for the subject matter categories of: SCIENTIFIC using the delivery method of NON-INTERACTIVE DISTANCE. This approval is valid in jurisdictions which recognize AA VSB RACE; however, participants are responsible for ascertaining each board's CE requirements. RACE does not "accredit", "endorse" or "certify" any program or person, nor does RACE approval validate the content of the program.

Please email your completed assessment to Ms. Jessica Gold at Jessica.d.gold2.ctr@mail.mil for grading. Passing score is 80%. This program (RACE program number) is approved by the AAVSB RACE to offer a total of 0.5 CE Credits, with a maximum of 12.5 CE Credits being available to any individual Veterinary Medical Professionals for the 2017-2018 Wednesday Slide Conference. This RACE approval is for the subject matter categories of: SCIENTIFIC using the delivery method of NON-INTERACTIVE DISTANCE. This approval is valid in jurisdictions which recognize AAVSB RACE; however, participants are responsible for ascertaining each board's CE requirements. RACE does not "accredit", "endorse" or "certify" any program or person, nor does RACE approval validate the content of the program.

**Joint Pathology Center
Veterinary Pathology Services**



WEDNESDAY SLIDE CONFERENCE 2018-2019

C o n f e r e n c e 1 7

30 January 2019

Conference Moderator:

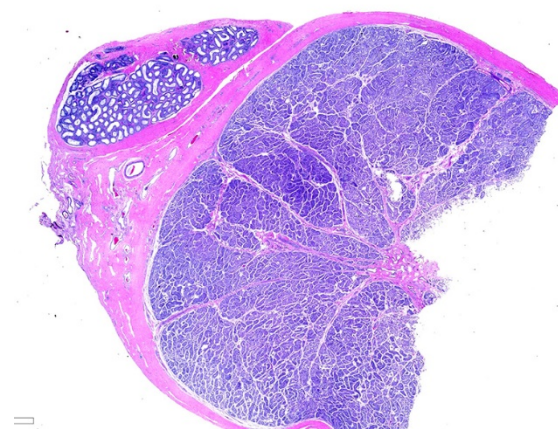
Patricia Pesavento, DVM, PhD, DACVP
Professor of Pathology, Microbiology & Immunology
UC Davis School of Veterinary Medicine
Davis, CA

CASE I: S1501813 (JPC 4084248).

Signalment: Six-year-old, intact male German shepherd dog (*Canis familiaris*)

History: This animal was born in the East coast of the US and then moved to the West coast, close to the border with Mexico. Up to date with vaccination. Presented to the clinic with signs of lethargy, anorexia and swelling of the right thoracic limb. Treated with antibiotics (Rilexine/cephalexine). The dog showed improvement, but a few days later developed diarrhea and neurological signs. On clinical examination, the dog evidenced disorientation, ataxia, nystagmus, generalized lymphadenomegaly, edema of the limbs and scrotum and peripheral neuropathy. The animal was treated with doxycycline and enrofloxacin intravenously, but died a few hours later.

Gross Pathology: The carcass was in good body condition. The subcutis of the distal limbs displayed small amounts of edema. The prescapular, popliteal and submandibular lymph nodes were mildly enlarged and



Testis, dog. There are no visible lesions at subgross. (HE, 5X)

fleshy. Lungs were diffusely red and wet, and the heart appeared rounded due to marked dilation of the right ventricle. The spleen was markedly enlarged with dark red fleshy parenchyma. Mesenteric lymph nodes were minimally enlarged.

Laboratory results: The blood chemistry (Table 1) revealed hypoalbuminemia without alteration of the A/G ratio. Alkaline phosphatase was mildly elevated and hypocalcemia was detected. The CBC (table

2) revealed leukocytosis due to neutrophilia and monocytosis, plus thrombocytopenia.

The canine tick borne PCR panel (Table 3) was positive for *Rickettsia rickettsii*.

Table 1: Blood chemistry:

Test	Result	Ref range	Units
Total protein	5.1	5.0-7.4	g/dL
Albumin	2.1 (LOW)	2.7-4.4	g/dL
Globulin	3.0	1.6-3.6	g/dL
A/G ratio	0.7 (LOW)	0.8-2.0	
AST	58	15-66	IU/L
ALT	38	12-118	IU/L
Alk Phosphatase	210 (HIGH)	5-131	IU/L
GGT	5	1-12	IU/L
Total bilirubin	0.3	0.1-0.3	mg/dl
BUN	15	6-31	mg/dl
Creatinine	0.6	0.5-1.6	mg/dl
BUN/Creatinine ratio	25	4-27	
Phosphorus	4.7	2.5-6.0	mg/dl
Glucose	96	70-138	mg/dl

Calcium	8.5 (LOW)	8.9-11.4	mg/dl
Corrected calcium	9.9		
Magnesium	1.5	1.5-2.5	mEq/L
Sodium	141	139-154	mEq/L
Potassium	4.2	3.6-5.5	mEq/L
NA/K ratio	34	27-38	
Chloride	111	102-120	mEq/L
Cholesterol	277	92-324	mg/dl
Trygliceride	88	29-291	mg/dl
Amylase	723	290-1125	IU/L
Lipase	65 (LOW)	77-695	IU/L
CPK	107	59-895	IU/L

Table 2: CBC:

Test	Result	Ref range	Units
WBC	15.6 (HIGH)	4.0-15.5	10³/uL
RBC	5.5	4.8-9.3	10 ⁶ /uL
HGB	12.5	12.1-20.3	g/dL
HCT	38	36-60	%
MCV	69	58-79	fL

MCH	22.7	19-28	pg
MCHC	33	30-38	g/dL
Blood parasites	None seen		
RBC morphology	Normal		
Platelet count	75 (LOW)	170-400	10³/uL
Platelet Est	Adequate		
Neutrophils (HIGH)	13260	2060-10600	/uL
Bands	0		
Lymphocytes	1248	690-4500	/uL
Monocytes (HIGH)	1092	0-840	/uL
Eosinophils	0	0-1200	/uL
Basophils	0	0-150	/uL

Table 3. Canine tick borne PCR panel profile:

Anaplasma phagocytophylum	Negative
Anaplasma platys	Negative
Babesia canis	Negative
Babesia spp (non-canis)	Negative
Bartinella henselae	Negative
Bartonella vinsonii	Negative

Ehrlichia canis	Negative
M haemocanis/hematoparvum	Negative
Neorickettsia risticii	Negative
Rickettsia rickettsii	Positive

Microscopic Description:

Testicle: Section include testicle and tunica albuginea, head of epididymis and vascular plexus. Scattered throughout the section, numerous vessels display segmental inflammatory changes, characterized by fibrinoid degeneration of the vascular media and transmural inflammatory infiltrates, composed mostly of lymphocytes, plasma cells and macrophages. Endothelial cells are plump and frequently detached. In addition to the inflammatory component, necrotic cellular debris are identified within the media and adventitia of the affected vessels. Occasionally, the adventitia is also expanded with fibrin. These findings were more prominent at the testicular vein (pampiniform venous plexus), but could be found in any medium and small caliber vessel. Other findings within the testicle is segmental tubular degeneration, characterized by the presence of multinucleated cells in the lumen of seminiferous tubules.

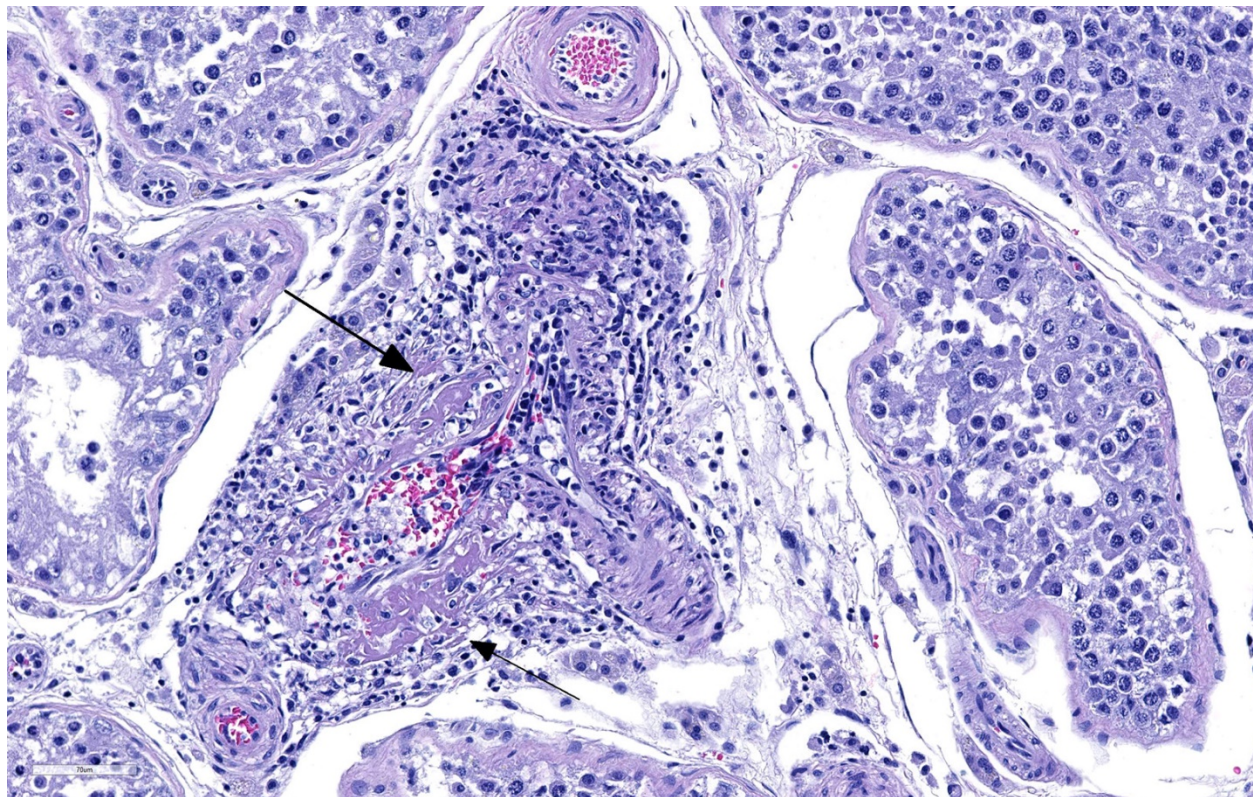
Similar vascular findings with varying degrees of severity were also identified (but not included in the section) in: brain, subcutis of distal limbs, eye, lung, heart, skeletal muscle, tongue and gastrointestinal wall. Other significant histological findings included meningoencephalitis, mild hepatitis and dermatitis (the latter presumably associated with tick bite site).

Contributor's Morphologic Diagnoses:

Testicle: 1. Vasculitis, lymphohistiocytic to necrotizing, marked, sub-acute, segmental.
2. Testicular degeneration, mild, multifocal.

Contributor's Comment: "Rocky Mountain Spotted fever" (RMSF) is a tick-transmitted zoonotic infectious disease caused by *Rickettsia rickettsii*. Of the tick-borne diseases in America, RMSF is the most severe, and can result in rapid course of disease and high mortality rate. This disease can be transmitted by ticks of the *Dermacentor*, *Rhipicephalus* and *Amblyomma* genera.⁷ In the USA, *Dermacentor variabilis* and *Dermacentor andersoni* are most commonly responsible for the transmission of the disease and they act as vectors, reservoirs and natural hosts for *R. rickettsii*. In its natural cycle, *R. rickettsii* is maintained in persistently infected tick population and small rodent reservoir hosts. Interestingly, transovarial transmission from infected females to eggs and transmission between adult ticks during mating can maintain the infection in a population without additional infectious feedings.⁵

Once a dog is bitten by infected ticks, there is invasion of small vessels and replication, with damage of endothelial cells. Rickettsiae use phospholipase A proteases and free radicals to induce oxidative and peroxidative damage to the host cell membrane, which



Testis dog. Multifocally, the walls of small- and medium caliber arterioles are necrotic and effaced by abundant extruded protein, necrotic smooth muscle, low to moderate numbers of infiltrating neutrophils, macrophages, and lymphocytes and cellular debris (fibrinoid necrosis). (HE, 205X)

will finally result in cell death. In addition, cell mediated immunity induces apoptosis in cells infected with rickettsiae via mechanisms such as the CD8 T lymphocyte cytotoxicity.¹ The net effect of these mechanisms is endothelial cell damage, which is followed by immune and phagocytic cellular responses plus platelet activation and activation of the coagulation and fibrinolytic systems, resulting in thrombosis.^{1,7} Platelet consumption is considered as the primary cause of thrombocytopenia in dogs. However, antiplatelet antibodies has also been identified in infected animals.³ Hypoalbuminemia is often observed and is probably caused by leakage associated with generalized vascular damage.²

Because RMSF lesions are characteristically associated with vasculitis throughout the body, it is not surprising that disease can

manifest with a wide variety of clinical signs and can be mistaken for an undifferentiated viral illness during the first days of manifestation.¹ Clinical signs includes fever (early manifestation), edema and hyperemia of the lips, penile sheath, scrotum (with abnormal gait), pinna and ventral abdomen. Petechial and ecchymotic hemorrhages may develop subsequent to the acute illness in mucous membranes, skin, pleura and gastric wall, in addition to hemorrhagic colitis and generalized lymphadenopathy.^{2,7} Histologically, the most prominent lesion in necrotizing vasculitis of small veins, capillaries and arterioles with perivascular accumulation of mononuclear cells. This lesion is frequently seen in the skin, testicle, alimentary tract, pancreas, kidney, urinary bladder, myocardium, retina and skeletal muscle. In addition, acute meningo-encephalitis, interstitial pneumonia and

necrosis of the myocardium, adrenal gland and liver can be present.⁷

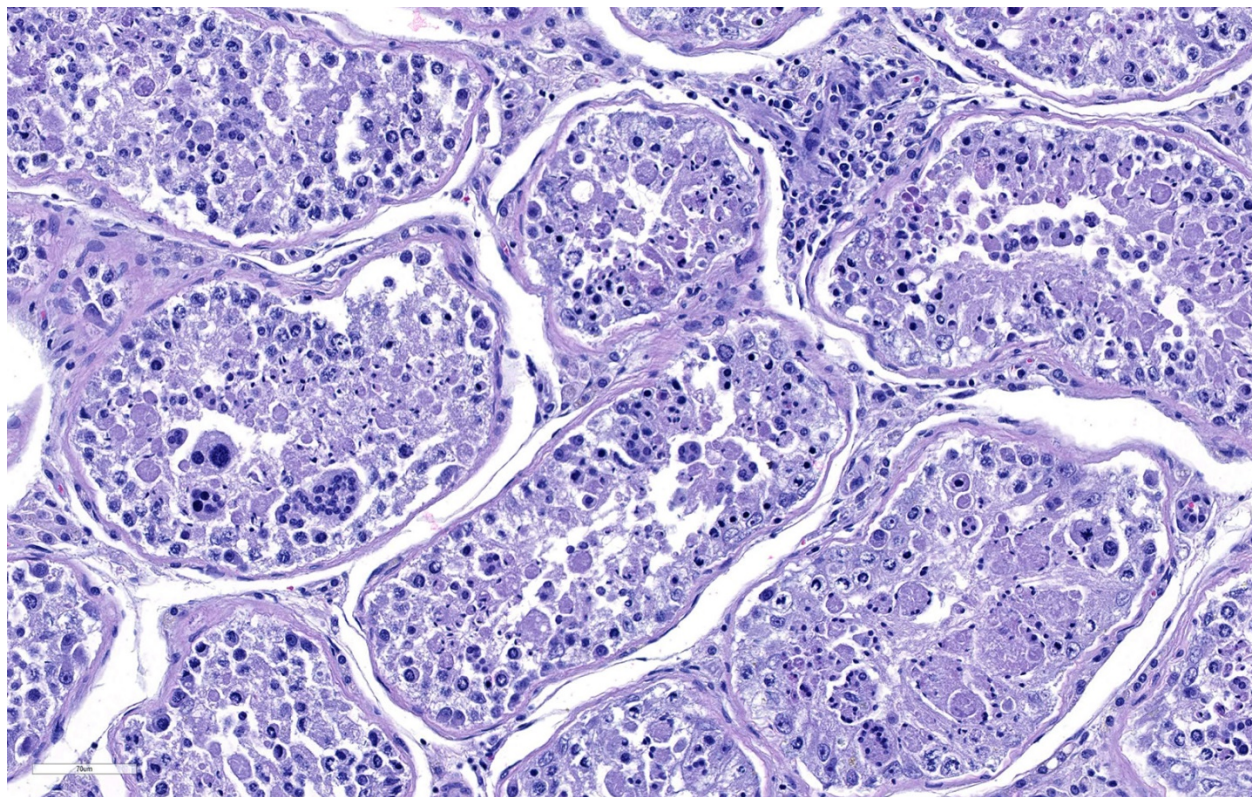
Among the differential diagnosis for vasculitis in dogs, other causes of secondary vasculitis should be considered, such as autoimmune diseases (such as lupus erythematosus), infections with canine circovirus, *Leishmania* spp, *Angiostrongylus vasorum* and *Dirofilaria immitis*, and exposure to therapeutic products, such as carprofen and meloxicam.^{4,9}

Contributing Institution:

California Animal Health and Food Safety Laboratory
San Bernardino Branch
105 W Central Ave
San Bernardino, CA 92408
www.cahfs.ucdavis.edu

JPC Diagnosis: 1. Testis, arterioles: Vasculitis, necrotizing, random, multifocal, severe, with seminiferous tubule necrosis. 2. Testis, seminiferous tubules: Degeneration and atrophy, diffuse, moderate, with spermatid giant cell formation.

JPC Comment: The contributor has provided an excellent discussion of Rocky Mountain spotted fever in the dog. Humans and dogs are the only two species in which clinical disease (and life threatening infections) may result from *Rickettsia rickettsiae* infection. While a number of small mammals, including rodents, rabbits, and opossums may provide a reservoir for the bacterium, clinical disease has not been documented in these species. Recent inoculation studies in horses failed to elicit clinical disease.



Testis dog. There is necrosis of spermatogonia and Sertoli cells within seminiferous tubules. The presence of spermatid giant cells is likely a pre-existent degenerative change. (HE, 295X)

Clinical symptoms of RMSF in humans arise abruptly and generally include high fever, headache, nausea, vomiting, and generalized myalgia. A generalized macular rash appears two to four days later which may or may not be accompanied by eschar at the site of the tick bite, and often starts on the wrists, ankles, and forearms. In 50-60% of patients, the lesions evolved into petechiae or purpura. More severe lesions include gangrene, pulmonary and cerebral edema, myocarditis, renal failure and disseminated intravascular coagulation. 5-10% of patients will die despite treatment.⁶

The contributor refers to “secondary vasculitis”. This particular nomenclature comes from human medicine. The term “primary” vasculitis refers to blood vessel wall injury arising without an apparent cause, and “secondary” vasculitis in which an apparent cause (infectious, immune-mediated, or neoplastic) is identified. Few well-defined syndromes of primary vasculitis exist in veterinary medicine, to include the so-called “beagle pain syndrome”, as well as a number cutaneous vasculitides in the dog. The vasculitis seen in this case, secondary to *R. rickettsii* infection, would be classified as “secondary” vasculitis. A retrospective study of 42 cases by Swann et al in 2015, compared cases of vasculitis which fell into both categories. Significant differences between the two groups were not many, with female dogs more likely to develop primary vasculitis, and dogs with primary vasculitis were more likely to have elevated serum globulin concentrations. The authors concluded that there does not appear to be well-defined syndromes of primary and secondary vasculitis in the dog as there are in humans.⁹

In veterinary medicine, the determination of “small” vs. “medium” arterioles is not well defined, due to the range of species we often

examine (i.e., in a gerbil, all arteries are small). In human medicine, the definition is much more well defined, with luminal measurements defining “large”, “medium”, and “small”. The moderator suggested that in any animal species, the aorta and the pulmonary artery are should be considered large, direct branches off of them would be “medium” and a third or more distal branches represent “small” arteries.

References:

1. Chen LF, Sexton DK. What’s new in Rocky Mountain spotted fever? *Infect Dis Clin N Am* 2008; 22 (3): 415-432.
2. Greene CE, Kidd L, Breitschwerdt EB. Rocky Mountain and Mediterranean spotted fevers, and typhus. In: Greene CE, ed. *Infectious diseases of the dog and cat*. 4th ed. St Louis, MO: Elsevier; 2012: 259-276.
3. Grindem CB, Breitschwerdt EB, Perkins PC, Culins LD, Thomas TJ, Hegarty BC. Platelet-associated immunoglobulin (antiplatelet antibody) in canine Rocky Mountain spotted fever and Ehrlichiosis. *J Am Anim Hosp Assoc* 1999; 35 (1): 56-61.
4. Li L, McGraw S, Zhu K, Leutenegger CM, Marks SL et al. Circovirus in tissues of dogs with vasculitis and hemorrhage. *Emerg Infect Dis* 2013; 19 (4): 534-541.
5. Nicholson WL, Allen KE, McQuiston JH, Breitschwerdt EB, Little SE. The increasing recognition of rickettsial pathogens in dogs and people. *Trends Parasitol* 2010; 26 (4): 205-2012.
6. Parola P, Paddock DC, Socolovschi C, Labruna MG, Mediannikov O, Kernif T, Abdad MY, Stenos J, Bitam I, Fournier P, Raoult. Update on tick-borne rickettsioses around the world: a geographic approach. *Clin Microbiol Rev* 2013; 26(4):657-702

7. Robinson WF, Robinson NA. Cardiovascular system. In: Maxie MG, ed. Jubb, Kennedy and Palmer's Pathology of domestic animals. 6th ed Vol 3. St. Louis, MO: Elsevier; 2015: 1-101.
8. Shaw SE, Day MJ, Birtles RJ, Breitschwerdt EB. Tick borne infectious diseases of dogs. *Trends Parasitol* 2001; 17 (1): 74-80.
9. Swann JW, Priestnall SL, Dawson C, Chang YM, Garden OA. Histologic and clinical features of primary and secondary vasculitis: A retrospective study of 42 dogs (2004-2011). *J Vet Diagn Invest* 2015; 27 (4): 489-496.
10. Ueno TE, Costa FB, Moraes-Filho J, Agostinho WC, Fernandes WR, Labruna MB. Experimental infection of horses with *Rickettsia rickettsii*. *Parasit Vectors* 2016; 9(1):499.

CASE II: L14 10949 (JPC 4066258).

Signalment: Two 2.5 week old male intact, Spots breed, *Suidae*, domestic pigs (litter mates).

History: Healthy litter of pigs - 2 1/2 weeks old. Owner noticed rapid breathing in one piglet, and it was given penicillin G and iron dextran injections. The pig died immediately. A second pig in the litter developed similar



Heart, piglet. There is a dense cellular infiltrate most prominently along the epicardial surface which replaces up to 40% of the parenchyma. (HE, 7X)

breathing problems and died after being given Florfenicol. A third piglet with similar signs received Florfenicol, Flunixin and Dexamethasone with some improvement noted. All three piglets developed signs in the span of a few hours. The two dead piglets were submitted for necropsy.

Gross Pathology: Gross alterations were similar in both pigs. The pericardial sac contained approximately 5 ml of serosanguinous fluid. The epicardium had multifocal to coalescing white areas that on cut surface extended into the myocardium. The lungs were diffusely wet, non-collapsing and mottled light red to light purple, with prominent interlobular septa. Approximately 30 ml of serosanguinous fluid was present in the peritoneal cavity, and scattered delicate fibrin strands covered the serosal surface of the intestines. Diffuse accentuated lobular pattern was evident throughout the liver, which appeared to be more friable than usual.

Laboratory results: Bacteriology: Lung - No bacteria isolated

Parasitology: Colon contents - No parasite eggs seen

Virology:

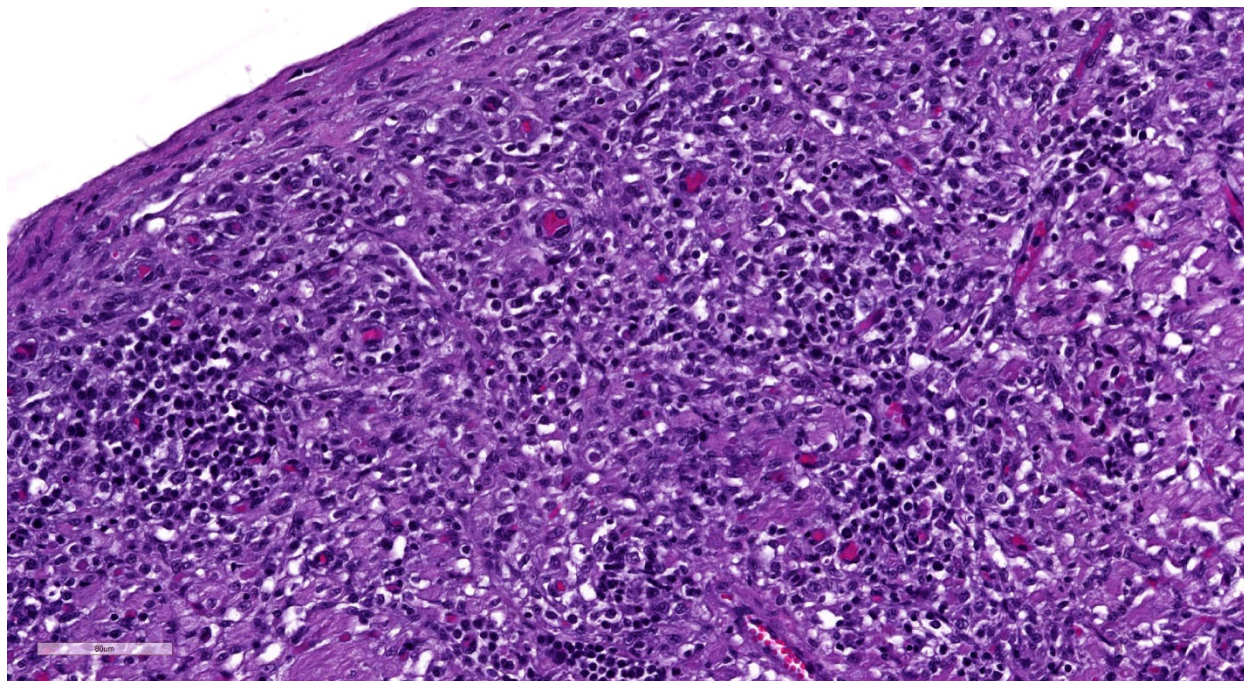
Lung and spleen - Negative for Porcine Reproductive and Respiratory Syndrome virus (PRRSV) by fluorescent antibody

Lung, intestine, and spleen - Negative for Porcine Circovirus-2 (PCV2) by fluorescent antibody

Intestine - Negative for Transmissible Gastroenteritis (TGE) virus and Porcine Rotavirus by fluorescent antibody assay, and for enteric viruses by electron microscopy

Heart - Negative for Encephalomyocarditis virus (EMCV) by PCR

Immunohistochemistry (performed at the University of Pennsylvania):



Heart, piglet. The cellular infiltrate is composed primarily of lymphocytes, with fewer macrophages and plasma cells. (HE, 278X)

Heart - Immunopositive for PCV2 antigen in cardiomyocytes, endothelial cells, and infiltrating macrophages

Microscopic Description:

Heart: Approximately fifty percent of the myocardium of the right and left free ventricular walls as well as of the interventricular septum is multifocally disrupted and replaced by inflammatory infiltrates of lymphocytes and plasma cells, fewer histiocytes and eosinophils, and sporadic multinucleated giant cells. Inflammatory cells also multifocally infiltrate the epicardium and endocardium. Cardiomyocytes are frequently characterized by loss of cross-striations, sarcoplasmic vacuolation and fragmentation, and nuclear swelling or pyknosis (myocardial degeneration and necrosis). Occasional cardiomyocyte abortive regeneration is suspected based on the presence of some giant cells with mildly basophilic cytoplasm and clusters of large euchromatic nuclei. Lost

myocardium is often replaced by fibrous connective tissue.

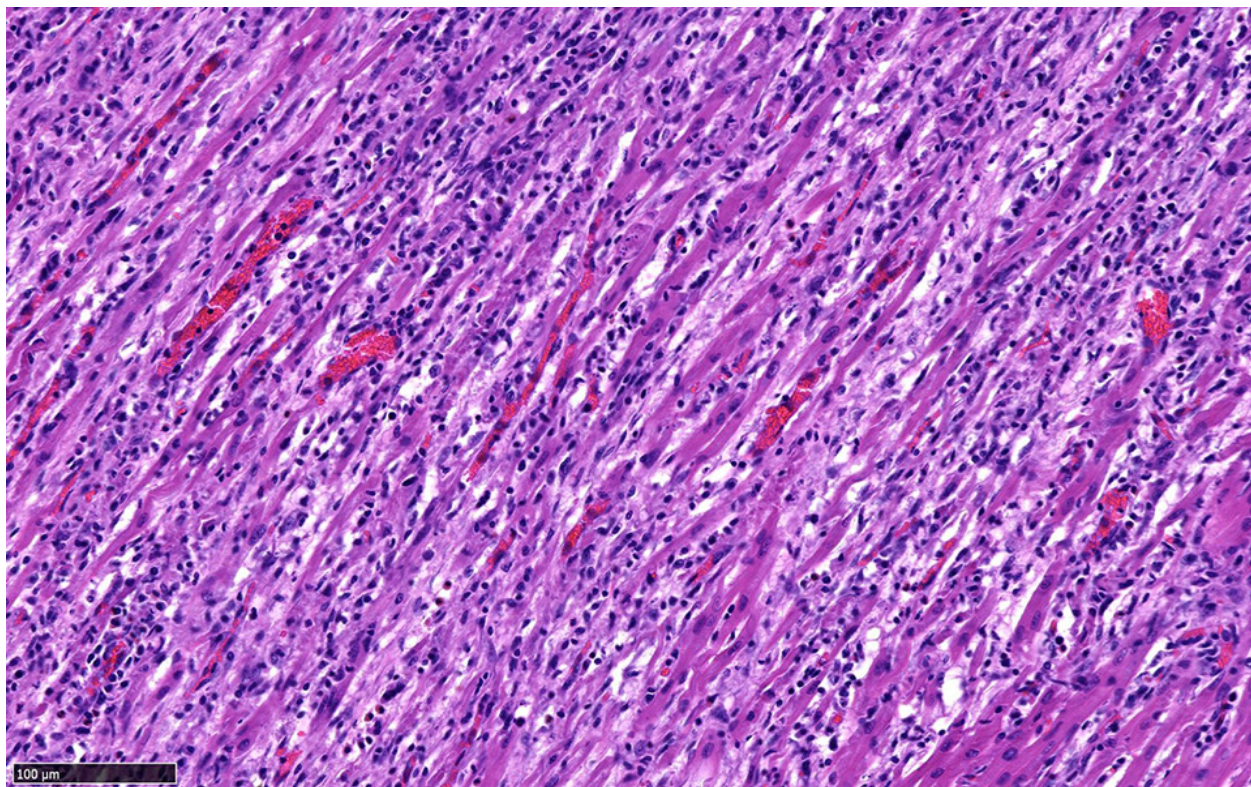
Additional not shown histologic findings in both pigs consisted of centrilobular hepatocellular degeneration and necrosis, erythroid hyperplasia in the bone marrow, and extramedullary hematopoiesis in multiple tissues suggestive of anemia, as well as subacute pulmonary edema and congestion consistent with subclinical cardiac insufficiency.

Contributor's Morphologic Diagnoses:

Heart: Myocarditis, lymphoplasmacytic and histiocytic, multifocal to coalescing, chronic, severe, with fibrosis

Contributor's Comment:

Porcine circovirus type 2 (PCV2) is a small, non-enveloped DNA virus. It was first described as the causative agent of postweaning multisystemic wasting syndrome (PMWS), a disease with a wide variety of clinical signs and lesions in multiple organ systems. Classically, PMWS is characterized by



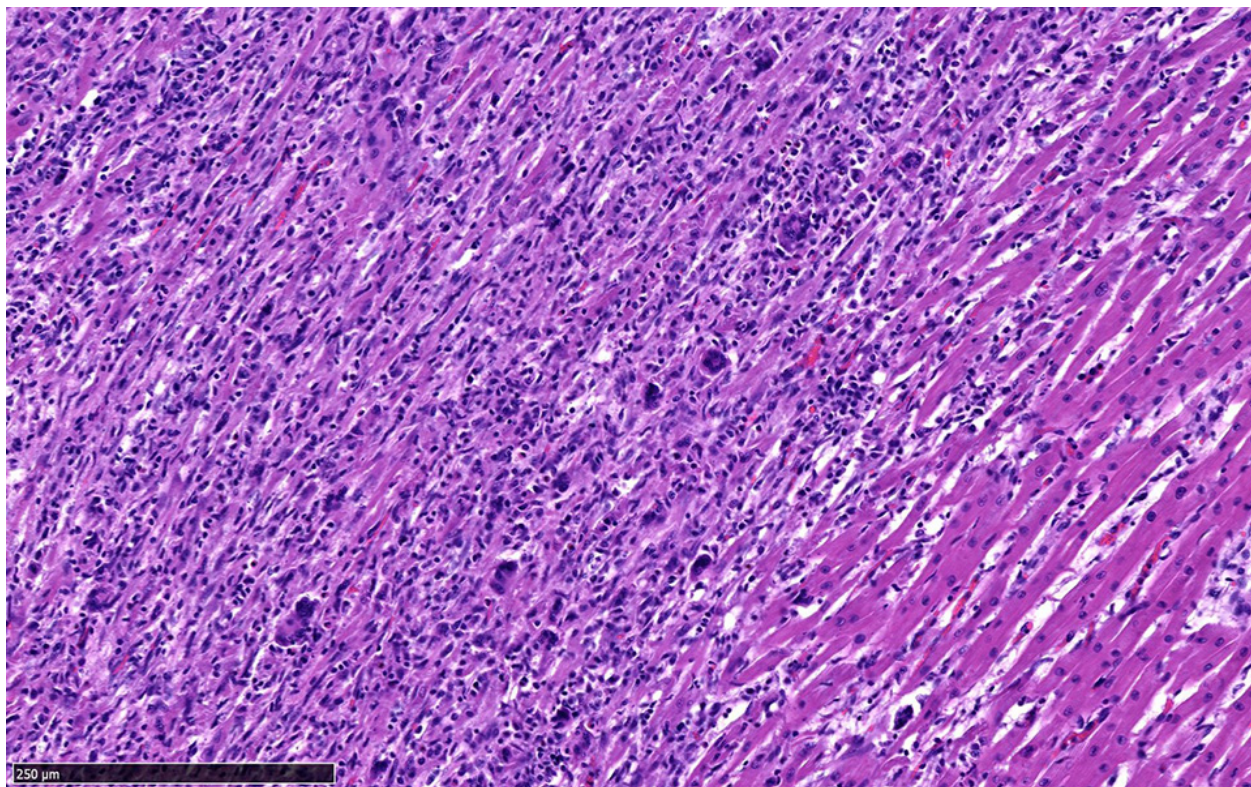
Heart, piglet. Cardiomyocytes exhibit marked variation in fiber size, fragmentation, and are separated by loosely arranged collagen fibers. (HE, 200X)

dyspnea, diarrhea, pallor, and jaundice with severe lymphoid depletion in pigs between 5 and 8 weeks of age. In addition to causing PMWS, PCV2-infection has been associated with an array of conditions, including respiratory and enteric diseases, porcine dermatitis and nephropathy syndrome (PDNS), and reproductive failure.⁷

The submitted case is an example of PCV2-associated myocarditis. PCV-associated myocarditis is most commonly seen in aborted, mummified, and weak-born fetuses that were infected during gestation.^{6,7,11} However, chronic myocarditis has also rarely been reported in piglets infected at 1-3 days of age,^{2,3,4,8} and we believe that this is what occurred in the current case. In previous reports, cardiac lesions tended to be more severe in animals co-infected with porcine parvovirus.^{2,8} We did not test for parvovirus; we can therefore not rule it out as a contributing factor to disease in our case.

Additional causes of myocarditis in swine including bacteria (e.g. *Streptococcus suis* and other bacteria associated with septicemia) and other viruses (e.g. PRRSV and EMCV) were ruled out by negative test results.⁵

In the current case, tissues routinely tested for the presence of PCV2 antigen (multiple lymph nodes, spleen, and lung) yielded negative results by immunofluorescence. These tissues also had no inflammatory lesions on histology. The heart, however, was positive by immunohistochemistry for PCV2 antigen, and this correlated well with the presence of the cardiac lesions. These findings illustrate the importance of being able to recognize potential PCV2-associated lesions in order to then submitting the affected tissues to PCV2 antigen testing. Similarly, only affected tissues should be used for detection of PCV2 by PCR, since the mere presence of PCV2 DNA in the absence



Heart, piglet. Numerous multinucleated giant cells are scattered throughout the areas of inflammation. (HE, 200X)

of lesions is not sufficient for a definitive disease diagnosis.⁷

Contributing Institution:

Louisiana Animal Disease Diagnostic Laboratory

<http://www1.vetmed.lsu.edu/laddl/index.htm>

1

JPC Diagnosis: Heart: Pancarditis, lymphoplasmacytic, histiocytic, and necrotizing, multifocal to coalescing, severe with multinucleated giant cells.

JPC Comment: The family Circoviridae is a rapidly expanding family of small, non-enveloped, circular, single-stranded, DNA viruses. Although chicken anemia agent, an early addition, has now been booted to the Anelloviridae, circoviruses have been identified in swine, a wide variety of bird species (including psittacine beak and feather

disease), dogs, bats, mink, pandas, hermit crabs, and insects.¹²

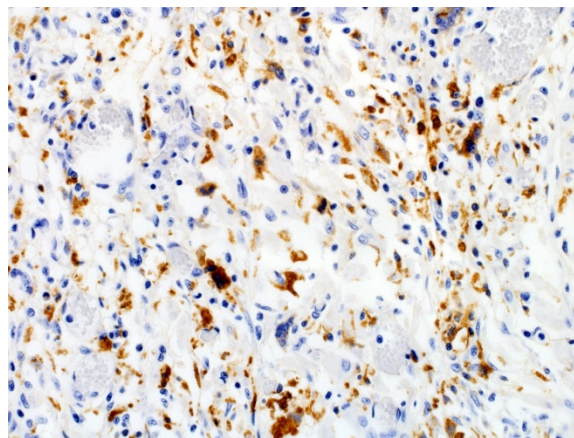
A number of interesting syndromes have been ascribed to PCV-associated diseases (PCVAD). Previous WSC submissions falling into this category include a previous case of PCV-associated myocarditis (which also has an excellent comment on PCVAD and post-weaning multisystemic wasting syndrome (PMWS) – WSC 2016, Conf 8, Case 2), cerebellar vasculitis and necrosis (WSC 2014, Conf 21, Case 4), granulomatous lymphadenitis and hepatitis (WSC 2013 Conf 25 Case1) and tubulointerstitial nephritis (WSC 2011, Conference 7, Case 3).

Lymphohistiocytic myocarditis is considered a hallmark lesion in the prenatal infection of pigs with porcine circovirus-2 (PCV-2). Experimental infection of swine fetuses at

day 52 is associated with myocardial viral tropism versus later infection (after day 92) which is generally associated with lymphoid tropism.¹ In affected fetuses, myofiber degeneration, necrosis, and loss and replacement by collagen and mineral, as well as inflammatory changes similar to those seen in this case and considered hallmark signs. Classic PCV-2-associated botryoid intranuclear inclusions (not seen in this section) may also be present. Cardiomegaly (predominantly right sided and associated with pericardial effusion) has been reported in piglets aged 4-7 weeks in heart failure.⁷

Vasculitis is also a well-described lesion in association with PCV-2 infection. Porcine dermatitis and nephritis syndrome is characterized by a necrotizing and neutrophilic vasculitis of arterioles and capillaries of the skin and kidney (to include glomerular capillaries). Fibrinoid necrosis of septal capillaries within the lung and resultant focal alveolar hemorrhage and edema has been widely reported in the US and Europe⁷. Finally, cases of myocarditis in piglets are often associated with lymphohistiocytic coronary arteritis and periarteritis.^{7,8}

Within the last several years, a novel swine circovirus (PCV-3) has been identified by independent groups that has been identified with cardiac and multisystemic infection.^{10,11} In one study, both individual swine and a 2% of a thousand-animal herd displayed common lesions of lymphohistiocytic myocarditis and cardiac arteriolitis. Metagenomic testing identified a new circovirus showing 55% and 33% with bat circovirus and porcine circoviruses.¹¹ A separate group in Kansas identified a similar virus, also identified as PCV-3 in sows that died acutely with lesions consistent with porcine dermatitis and nephritis syndrome.¹⁰



Heart, piglet. A variety of cells including cardiomyocytes, macrophages, and multinucleated giant cells stain positively for PCV-2 antigen. (anti-PCV2, 400X)

The moderator reviewed circoviruses in general, in pigs, dogs, and bears among other species, and a differential diagnosis for the lesion in this suckling piglet, including porcine circovirus-3, parvovirus, and aphthovirus was discussed.

References:

1. Cushing T, Steffen D, Duhamel GE. Pathology in Practice. *JAVMA* 2013; 242(3):317-319.
2. Ellis J, Krakowka S, Lairmore M, et al. Reproduction of lesions of postweaning multisystemic wasting syndrome in gnotobiotic piglets. *Journal of Veterinary Diagnostic Investigation* 1999;11:3-14.
3. Hirai T, Nunoya T, Ihara T, Kusanagi K, Kato T, Shibuya K. Acute hepatitis in a piglet experimentally inoculated with tissue homogenates from pigs with postweaning multisystemic wasting syndrome. *Journal of Veterinary Medical Science* 2003;65:1041-1045
4. Kennedy S, Moffet D, McNeilly F, et al. Reproduction of lesions

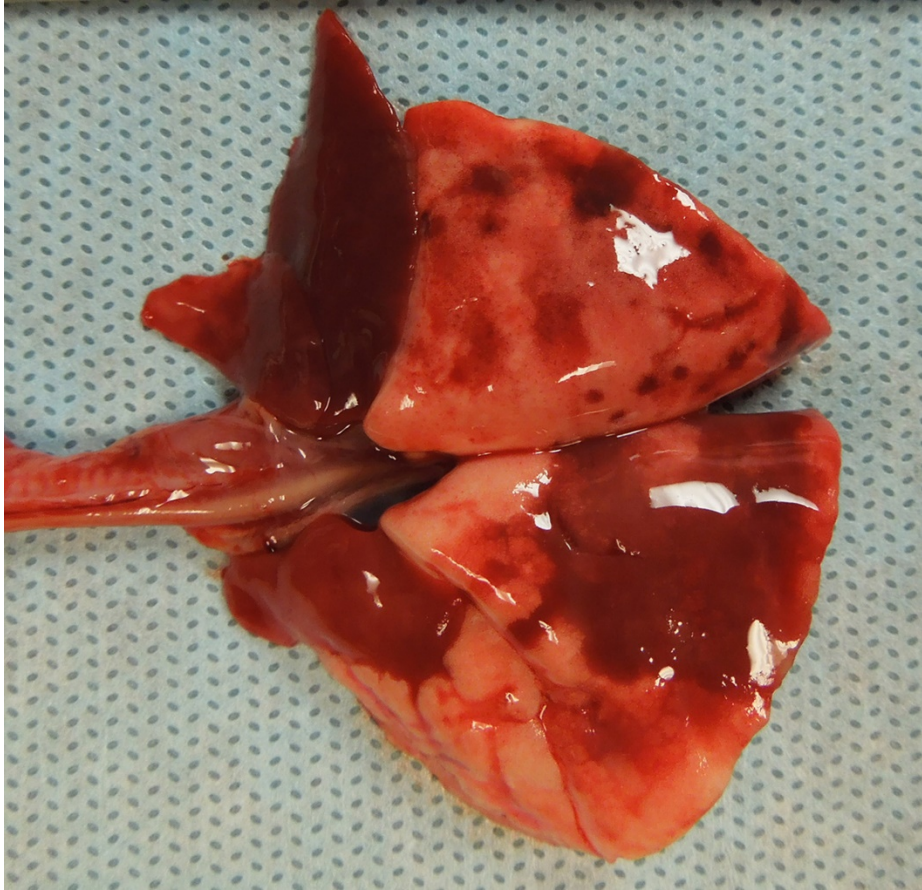
- of postweaning multisystemic wasting syndrome by infection of conventional pigs with porcine circovirus 2 alone or in combination with porcine parvovirus. *Journal of Comparative Pathology* 2000;122:9-24.
5. Loynachan AT. 2012. Cardiovascular and Hematopoietic Systems – Diseases of the Myocardium. In Zimmerman JJ, Karriker LA, Ramirez A, et al. (Eds.), *Diseases of Swine*. Ames, IA: Wiley-Blackwell. p. 192-193.
 6. Mikami O, Nakajima H, Kawashima K, et al. Nonsuppurative myocarditis caused by porcine circovirus type 2 in a weak born piglet. *Journal of Veterinary Medical Science* 2005;67:735-738.
 7. Opriessnig T, Langohr I. Current state of knowledge on porcine circovirus type 2-associated lesions. *Veterinary Pathology* 2013;50:23-38.
 8. Opriessnig T, Janke B, Halbur P. Cardiovascular lesions in pigs naturally or experimentally infected with porcine circovirus type 2. *Journal of Comparative Pathology* 2006;134:105-110.
 9. Palinski R, Pineyro P, Shang P, Yuan F, Guo R, Fang Y, Byers E, Hause BM. A novel porcine circovirus distantly related to known circoviruses is associated with porcine dermatitis and nephropathy syndrome and reproductive failure. *J Virol* 2017 91(10:e01879-16.
 10. Phan TG, Giannitti F, Rossow S, Marhaler D, Knutson T, Li L, Deng X, Resende T, Vannuci F, Delwart. Detection of a novel circovirus PCV-3 in pigs with cardiac and multi-systemic inflammation. *Virol J* 2016; 13:184.
 11. Sanchez R, Nauwynck H, McNeilly F, et al. Porcine circovirus 2 infection in swine fetuses inoculated at different stages of gestation. *Veterinary Microbiology* 2001;83:169-176.
 12. Sheykhi A, Sheiki N, Charkhkar S, Brujeni GN. Detection and characterization of circovirus in canary flocks. *Avian Dis* 2018; 62:137-142.

CASE III: D12-44205-1A or B UMN VDL (JPC 4032592).

Signalment: One-month-old, intact male, white Hartley guinea pig (*Cavia porcellus*).

History: The guinea pig, purchased and shipped from a source colony, was placed in quarantine for an acclimation period of 7 days. The guinea pig was released from quarantine on day 7, placed on study day 9 involving an induction dose (6 intradermal injections of 0.1 ml of test article extract in normal saline, normal saline and/or Freund's Complete Adjuvant). The guinea pig lost body condition and exhibited progressive respiratory distress over days 10 and 11. The guinea pig was found dead on day 12.

Gross Pathology: The guinea pig was in good nutritional condition with mild postmortem autolysis. The thoracic cavity contained approximately 0.5 ml of watery, red, clear fluid. The left and right cranial lung lobes were diffusely dark red, heavy and wet. Sections of the left and right cranial lung lobes sank in 10% neutral buffered formalin.



Lung, guinea pig: The right and left cranial lung lobes, right middle lung lobe, right accessory lung lobe were diffusely dark red and firm. The left and right caudal lung lobes contained multifocal to coalescing, dark red, firm, irregular, smooth, flat foci. (Photo courtesy of Veterinary Diagnostic Laboratory, University of Minnesota, www.vdl@umn.edu)

The right middle and right accessory lung lobes were diffusely dark red and firm. The left and right caudal lung lobes contained multifocal to coalescing, dark red, firm, irregular, smooth, flat foci.

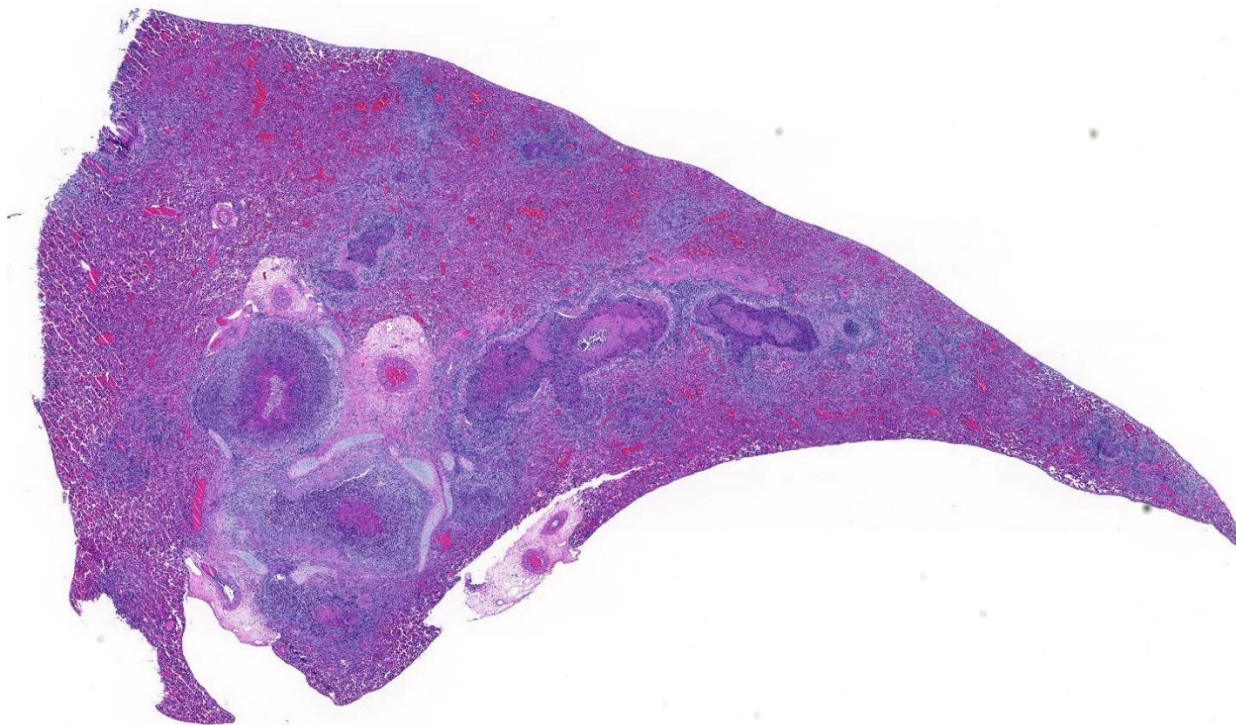
Laboratory results: Bacteriology: Lung - No bacteria isolated

Guinea pig adenovirus quantitative real-time polymerase chain reaction (qPCR) testing and aerobic culture of lung were performed at Charles River Research Animal Diagnostic Services. The lung sample was positive for guinea pig adenovirus via qPCR. Aerobic culture of the left cranial lung lobe yielded rare colonies of *Escherichia coli*.

Microscopic Description:

Multifocally, comprising 60 – 70% of the tissue section, within the bronchi, bronchioles and alveoli, there are infiltrates of numerous degenerate and nondegenerate neutrophils, macrophages, lymphocytes, few plasma cells and extravasated erythrocytes. The lumina of the bronchi and bronchioles are frequently mildly to moderately ectatic, containing large amounts of cellular and karyorrhectic debris, extravasated erythrocytes, fibrin and sloughed degenerate to necrotic respiratory epithelial cells that

occasionally contain a single, large, 5 – 15 um diameter basophilic intranuclear inclusion body. Multifocally bronchi and bronchioles are lined by flattened, attenuated, degenerate to necrotic epithelium that frequently form epithelial syncytia or are multinucleated. Multifocally alveolar septa are mildly to moderately expanded by lymphocytes, mononuclear cells, type II pneumocytes and congested blood vessels. Multifocally interstitium is mildly to moderately expanded by neutrophils, lymphocytes and plasma cells as well as edema. The tunica media of multiple small to medium caliber vessels and muscularis of



Lung; guinea pig. Multifocally bronchi, bronchioles and alveoli are filled with necrotic material and a cellular infiltrate which extends into the surrounding parenchyma. (HE, 14X)

the bronchi and bronchioles exhibits vacuolar degeneration of the smooth muscle.

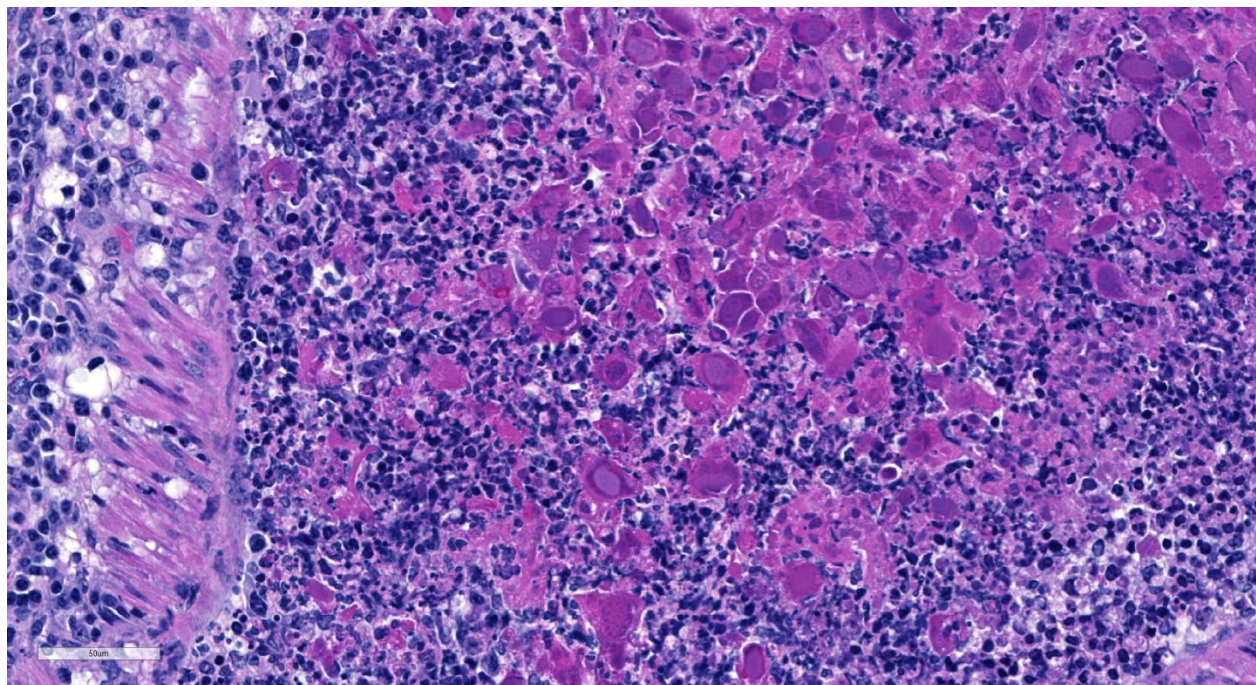
Immunohistochemistry for general adenovirus on tissue sections of lung were prepared by the Veterinary Medical Diagnostic Laboratory of the University of Missouri. Multifocally lumina of bronchioles contain numerous red to dark red, strongly immunopositive adenovirus particles, both free within the lumen admixed with cellular debris and within nuclei and cytoplasm of sloughed necrotic epithelial cells.

Electron microscopy was performed at the University of Minnesota Veterinary Diagnostic Laboratory. Bronchiolar lumina contain necrotic cells with markedly enlarged nuclei exhibiting discontinuous nuclear membranes, clumping of chromatin and lacking a clear distinction between the

nucleus and the cytoplasm. The necrotic cells contain numerous loosely arranged, nonenveloped, round to icosahedral, 70 – 90 nm diameter, variably electron dense, icosahedral viral particles consistent with adenovirus.

Contributor's Morphologic Diagnoses: Lung, bronchopneumonia, necrosuppurative, with intraepithelial intranuclear inclusion bodies (adenovirus), multifocal, marked, subacute.

Contributor's Comment: Adenoviruses are non-enveloped, linear double stranded DNA viruses with icosahedral symmetry. Adenoviruses infect a wide variety of animals with clinical signs ranging from subclinical to enteric or respiratory manifestations. Guinea pig adenovirus (GpAV) has been classified as a distinct serotype within the genus Mastadenovirus.



Lung; guinea pig. Numerous necrotic bronchiolar epithelial cells contain a single large basophilic intranuclear inclusion. (HE 400X)

GpAV has the highest level of homology with other animal mastadenoviruses (mammalian adenoviruses) and human subgroups A, C and F.^{5,14} Adenoviruses derived from birds (Aviadenovirus, Atadenovirus), frogs (Siadenovirus), fish (Ichtadenovirus) and some reptiles (Atadenovirus) are serologically distinct from Mastadenoviruses.⁹

Guinea pig adenovirus was first reported in 1981 in guinea pigs from 2 commercial breeders and a closed colony, as the cause of necrotizing bronchitis and bronchiolitis with low morbidity and high mortality.¹¹ The adenovirus observed in this outbreak was described as viral particles of 58 – 72 nm diameter, in a hexagonal crystalline array, observed as large, basophilic, intranuclear inclusion bodies by light microscopy. Additional outbreaks of GpAV in guinea pigs were characterized by necrotizing bronchitis and bronchiolitis with similar prominent basophilic intranuclear inclusions in

sloughed, necrotic epithelial cells.¹ Inclusions contained typical adenoviral particles of 68 – 72 nm diameter, arranged individually or in crystalline arrays. GpAV infection was experimentally reproduced via intranasal inoculation of newborn guinea pigs and was found to be noninfectious in additional mammalian species of hamsters and rats.^{7,10} Subclinical infection has been reported, but the asymptomatic animals were found to have microscopic lesions of minimal bronchial epithelial necrosis with typical large basophilic intranuclear inclusions.⁴

Bronchopneumonia due to GpAV is typically of low morbidity with up to 100% mortality. Clinically affected animals are often young, but infections have also been reported in adult guinea pigs in breeding colonies.^{5,6,13} Infection of guinea pigs often presents as sudden death or death after a short period of malaise. On gross necropsy, the cranial lung lobes are usually consolidated or diffusely red, while the caudal lung lobes show

multifocal consolidation. Histopathology findings are characterized by a necrotizing bronchitis and bronchiolitis with sloughing of necrotic epithelial cells into the airways, often resulting in occlusion of the affected airways with necrotic cells admixed with cell debris, leukocytes and fibrin. The necrotic epithelial cells often exhibit karyomegaly with extremely large or bizarre basophilic, round to oval, 7 – 15 μ m diameter, intranuclear inclusion bodies.^{1,7,11}

Diagnosis of GpAV infection can be confirmed via immunohistochemistry, electron microscopy, serology or polymerase chain reaction. Other differentials for pneumonia in guinea pigs include parainfluenza virus, cytomegalovirus and bacteria such as *Bordetella bronchiseptica*, *Streptococcus* species, *Staphylococcus* species and *Pseudomonas aeruginosa*.¹³

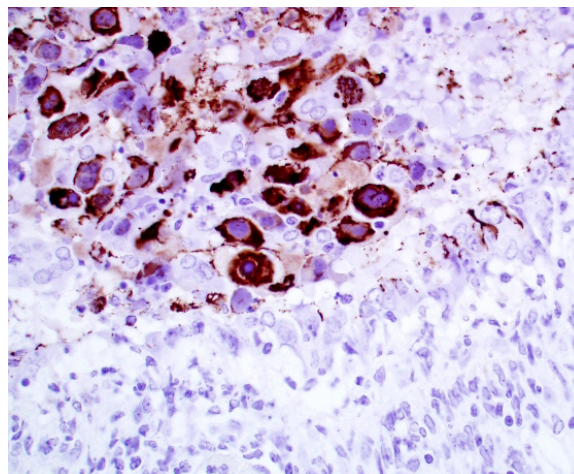
Contributing Institution:

Veterinary Diagnostic Laboratory,
University of Minnesota,
www.vdl@umn.edu

JPC Diagnosis: Lung: Bronchitis and bronchiolitis, necrotizing, diffuse, severe with diffuse lymphohistiocytic peribronchiolitis and atelectasis, and numerous karyomegalic viral inclusions

JPC Comment: Adenoviruses are common viruses in a wide range of animal species, and display tropism for a wide range of tissues – endothelium (dog, deer cattle), liver (chicken, primates), and in immunosuppressed animals (and humans), a vast array of cell types may be targeted.

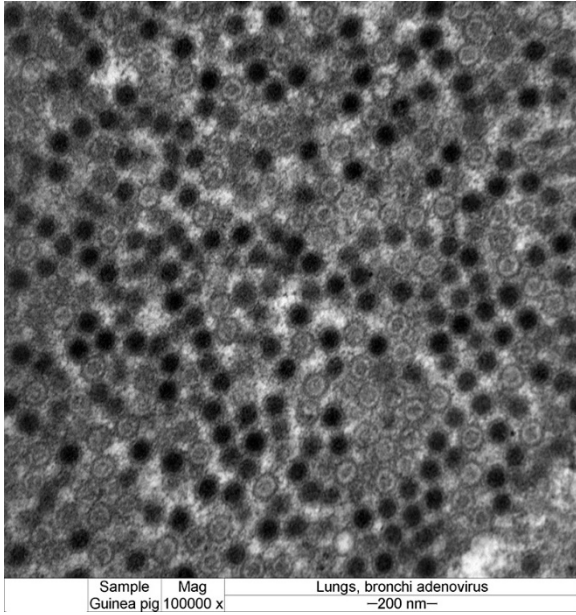
A number of pneumotropic adenoviruses may result in a similar clinical and histologic picture, although immunosuppression may be required for lesion development. Canine adenovirus-2 may result in pulmonary damage in (usually immunosuppressed, often



Lung: guinea pig. Cellular debris and necrotic epithelial cells within bronchiolar lumen exhibit strong immunopositivity to adenovirus. (Photo courtesy of Veterinary Diagnostic Laboratory, University of Minnesota, www.vdl@umn.edu)

by canine distemper virus) individuals. In experimental infections in young beagles, bronchiolitis obliterans was seen 3-4 weeks following infection² (although long-term followup was not conducted to see if the lesions resolved.) Bovine adenovirus-3 will also result in a severe necrotizing bronchiolitis with viral intranuclear inclusions in calves administered dexamethasone.¹²

Pneumotropic adenoviral infections are well-known in primate species. In 1953 adenoviruses were first isolated by Rowe who was studying the growth of poliovirus in adenoidal tissue. Today, over 60 human adenovirus serotypes have been identified. Disease in humans varies with age, immune status and population characteristics. Adenoviral pneumonia associated with serotypes 3,7,14, 21, and 55 have been associated with potentially fatal outcomes, and infants, immunosuppressed individuals, and the elderly are especially hard hit. Extrapulmonary complications include meningoencephalitis, hepatitis myocarditis, nephritis, neutropenia, and DIC.⁸



Lung; guinea pig. Within necrotic bronchiolar epithelial cells are numerous 70 – 90 nm diameter, variably electron dense, round to icosahedral viral particles. (Photo courtesy of Veterinary Diagnostic Laboratory, University of Minnesota, www.vdl@umn.edu)

An outbreak in a national primate center in 2009 in a closed colony of titi monkeys (*Callicebus* sp.). 23 of 65 developed upper respiratory symptoms which progressed to fulminant pneumonia and hepatitis; 19 of these animals died. A novel, highly divergent adenovirus (TMAdV) was isolated, sharing only <57% nucleotide identity with other known adenoviruses. The virus was also isolated from a researcher who demonstrated respiratory symptoms for 4 weeks, and a close family member who had never been to the primate colony.¹⁵

In 1997, an outbreak of adenoviral pneumonia resulted in respiratory illness in 9 infant olive baboons, with two fatalities. Six untypeable adenoviruses were isolated from these animals during the course of the illness; one novel adenovirus (BaAdV-3) was determined to be the cause of the disease.³

Conference attendees noted the presence of abundant viral antigen within the cytoplasm

of epithelial cells within the necrotic bronchioles, with relative sparing of nuclei containing karyomegalic inclusions in the image of the immunohistochemical stain provided by the contributor (Fig 2-4). The significance of this change was not apparent.

References:

1. Brennecke LH, Dreier TM, Stokes WS. Naturally occurring virus-associated respiratory disease in two guinea pigs. 1983;**20**:488-491.
2. Castleman WL. Bronchiolitis obliterans and pneumonia induced in young dogs by experimental adenovirus infection. *Am J Pathol* 1985; 119(3):495-504.
3. Chiu CY, Yagi S, Lu X, Yu G, Chen EC, Liu M, Dick EJ, Carey KD, Erd DD, Leland MM, Patterson JL. A novel adenovirus species associated with an acute respiratory outbreak in a baboon colony and evidence of coincident human infection. *mBio* 2013; 4(2):e00084-13.
4. Crippa L, Giusti AM, Sironi G, et al. Asymptomatic adenoviral respiratory tract infection in guinea pigs. 1997;**47**(2):197-199.
5. Feldman SH, Sikes R, Eckhoff G. Comparison of the deduced amino acid sequence of guinea pig adenovirus hexon protein with that of other Mastadenoviruses. *Comp Med.* 2001;**51**(2):120-126.
6. Harris IE, Portas BH, Goydich W. Adenoviral bronchopneumonia of guinea pigs. *Aust Vet Journal.* 1985;**62**(9):317-318.
7. Kaup, FJ, Naumann S, I Kunstyr, et al. Experimental viral pneumonia in guinea pigs: An ultrastructural study. 1984;**21**:521-527.
8. Khanal S, Ghimire P, Dharmoon AS. The repertoire of adenovirus in

- human disease: the innocuous to the deadly. *Biomedicines* 2018; 6:30 doi: 10.3390/biomedicines6010030
9. King, AMQ, Adams MJ, Carstens EB, et al. Virus Taxonomy. London, UK: International Committee on Taxonomy of Viruses, Elsevier Inc; 2012.
 10. Kunstyr I, Maess J, Naumann S, et al. Adenovirus pneumonia in guinea pigs: an experimental reproduction of the disease. 1984;**18**:55-60.
 11. Naumann S, Kunstyr I, Langer I, et al. Lethal pneumonia in guinea pigs associated with a virus. *Lab Animals*. 1981;**15**:235-242.
 12. Narita M, Yamada M, Tsuboi T, Kawashima. Bovine adenovirus type 3 pneumonia in dexamethasone-treated calves. *Vet Pathol* 40:128-135.
 13. Percy DH, Barthold SW. Pathology of Laboratory Rodents and Rabbits, Third Edition. Ames, Iowa: Blackwell Publishing Professional; 2007.
 14. Pring-Akerblom P, Blazek K, Schramlova J, et al. Polymerase chain reaction for detection of guinea pig adenovirus. *J Vet Diagn Invest*. 1997;**9**:232-236.
 15. Yu G, Yagi S, Carrion R, Chen EC, Liu M, Brasky KM, Lanford RD, Kelly KR, Bales KL, Schnurr DP, Canfield DR, Patterson JG, Chiu CY. Experimental cross-species infection of common marmosets by titi monkey adenovirus. *PLoS One* 2013; 8(7):e68558

CASE IV: 14A310 (JPC 4083744).

Signalment: 13.05 yr, female, Indian rhesus monkey, *Macaca mulatta*

History: Presented from the field cage in dystocia and an infant was successfully delivered by C-section but the dam died in recovery.

Gross Pathology: Hemorrhagic meninges primarily over the cerebellum, enterocolitis, hemorrhage in both adrenals.

Laboratory results: I-stat Results:

Na	144 meq/L	Ph	7.152
K	3.5 meq/L	PCO2	47.3 mmHg
Cl	111 meq/L	HCO3	16.6 mmol/L
TCO2	18 mmol/L	BEECF	12 mmol/L
BUN	18 mg/dL	ANGAP20	mmol/L

Bacterial culture of the meninges:
Streptococcus pneumoniae

Microscopic Description:

In the cortex of the adrenal, primarily the zona fasciculata is severely congested and hemorrhagic with loss of cortical cell cords and pooling of RBC between surviving the fibrovascular supporting framework. Adjacent cortical cells are swollen and rare capillaries contain minimal aggregates of neutrophils and mononuclear leukocytes.

Contributor's Morphologic Diagnoses:

Acute severe adrenal cortical hemorrhage with mild degeneration and minimal necrosis, rhesus macaque

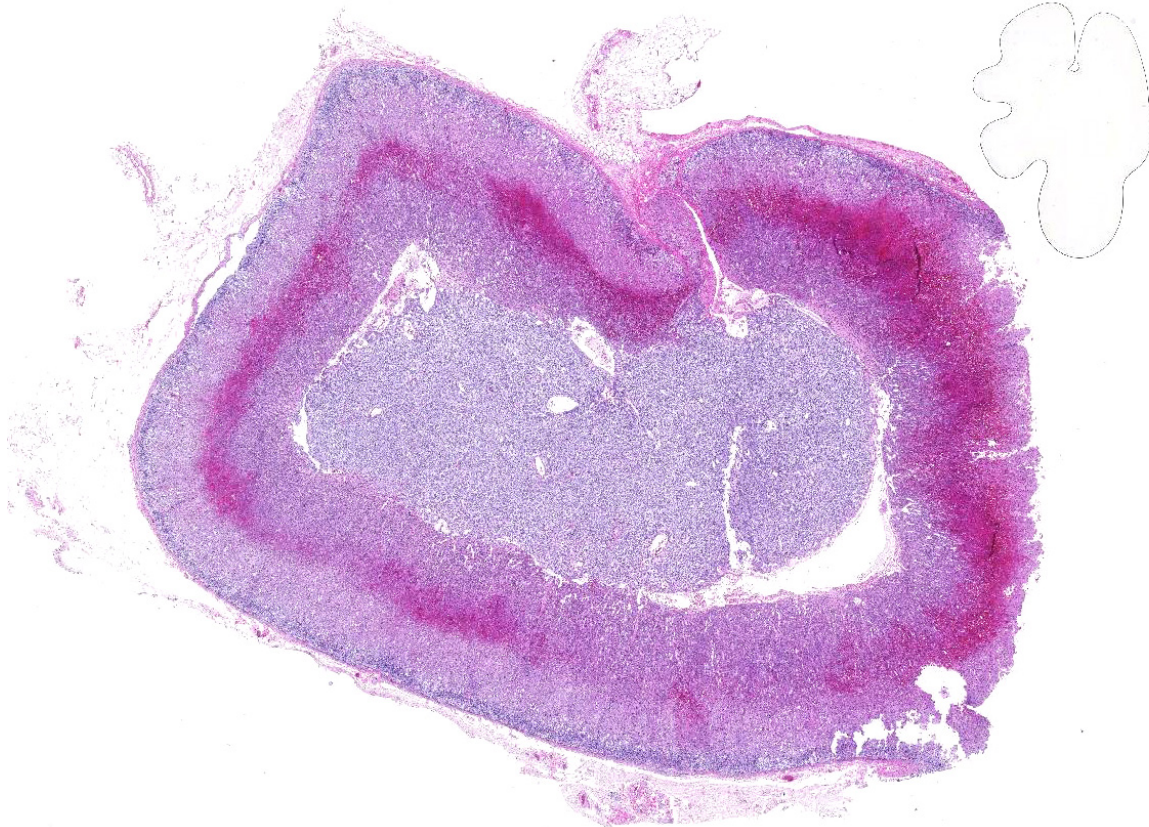
Contributor's Comment: The cesarean section for this animal was complicated by an



Adrenal gland, rhesus macaque. Hemorrhage was present within the adrenal cortex. (Photo courtesy of Tulane National Primate Research Center, Department of Comparative Pathology, 18703 Three Rivers Rd, Covington, LA 70433, <http://tulane.edu/tnprc/>)

abscess in the midbrain and meningitis from which *Streptococcus pneumoniae* was cultured. Meningococcus in humans is often a cause of acute adrenocortical insufficiency² although we see adrenal hemorrhage infrequently in our primate colony (62 cases in last 30 years). Worldwide, cerebral

tuberculosis is the most often associated with pituitary and adrenal dysfunction³. The Waterhouse-Friderichsen syndrome in humans is described as a rare complication of bacteremia due to pneumococci, staphylococci, *Neisseria meningitides*, *Pseudomonas aeruginosa*, or *Haemophilus influenza* and also cytomegalovirus infection that results in systemic hemorrhages including purpura of the skin, with hemorrhage of the adrenal, serous membranes and other organs consistent with development of disseminated intravascular coagulation (DIC).^{1,4,8} The basis for the hemorrhage, suggested to originate from the venous sinusoids of the medulla and suffuse into the cortex could be due to direct bacterial seeding of the endothelium, DIC, endotoxin-induced vasculitis or hypersensitivity vasculitis.²



Adrenal gland, rhesus macaque. There is multifocal to coalescing hemorrhage within the deep zona fascicularis and superficial zona reticularis. (HE, 10X)

Contributing Institution:

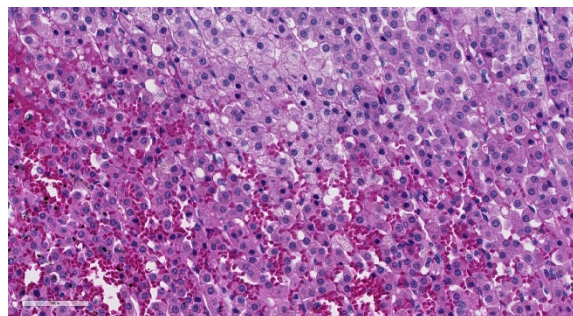
Tulane National Primate Research Center
 Department of Comparative Pathology
 18703 Three Rivers Rd
 Covington, LA 70433
<http://tulane.edu/tnprc/>

JPC Diagnosis: Adrenal gland, zona fasciculata and reticularis: Necrosis, multifocal, marked, with hemorrhage.

JPC Comment: The Waterhouse-Friderichsen syndrome (WFS) is a well-known entity (named for English physician Rupert Waterhouse (1873-1958) and Danish pediatrician Carl Friderichsen (1886-1979) in humans, non-human primates, and several other species. It was first described in 1911 as adrenal hemorrhage and subsequent adrenal crisis related to sepsis.⁸

In humans, this syndrome is usually associated with fulminant sepsis associated with pneumococcal or meningococcal bacteremia (with *Streptococcus pneumoniae* and *Neisseria meningitidis* the most commonly cultured bacilli, respectively) often in patients with splenic disorder or asplenia. Other reported bacterial causes include *N. gonorrhoeae*, *Pseudomonas aeruginosa*, *E. coli*, *Hemophilus influenzae*, and *S. aureus*.⁶ It is often associated with hypotensive shock, disseminated intravascular coagulation, purpura fulminans, and adrenal gland failure. In affected individuals, adrenal hemorrhage may vary from microscopic hemorrhage at the corticomedullary junction to massive, grossly identifiable hemorrhage effacing the entire cortex. Several anatomic factors facilitate the hemorrhage: high rate of blood flow, contribution of several arteries to a single organ-wide capillary plexus, and a single large central vein draining this organ.⁸ WFS in humans is an emergency situation,

clinically characterized by rapidly falling levels of cortisol – high doses of corticosteroids are usually administered as well as antibiotics directed at the bacterial agent.⁵ Mortality, even in treated cases, often exceeds 50%. While historically a postmortem diagnosis, the adrenal hemorrhage that characterizes WFS in humans may now be identified by ultrasonography and CT scans, increasing the odds of successful treatment.⁵



Adrenal gland, rhesus macaque. Within areas of hemorrhage in the zona reticularis, cortical cells are mildly shrunken, condensed, eosinophilic, and nuclei are hyperchromatic, but necrotic cells are rare. (HE, 400X)

In 2009, Hukkanen et al.⁷ published a retrospective of five cases of systemic inflammatory response syndrome (SIRS) including the Waterhouse-Friedrichsen syndrome, acute respiratory distress syndrome (ARDS), disseminated intravascular coagulation (DIC) and multiple organ dysfunction in five cases including both pigtailed macaques and olive baboons. In these animals, predisposing factors were similar to those in humans – major surgery, obstetric complications, and infection. The syndrome is thought to be seen in “high-responders” – subsets of nonhuman primates (and humans) which may produce 10 to 100 fold greater cytokines (IL-1b, IL-6, and IL-8 as well as TnF-alpha in response to infectious stimuli.⁷

References:

1. Adem PV, Montgomery CP, Husain AN, Koogler, TK, Arangelovich V, Humilier M, Boyle-Vavra S, Daum RS. Staphylococcus aureus sepsis and the Waterhouse-Friderichsen syndrome in children. *N Engl J Med* 353:1245-2451, 2005.
2. Cotran RS, Kumar V, Collins T. (1999). *Robins Pathologic Basis of Disease* (6th ed) p 1160.
3. Dhanwal DK, Kumar S, Vyas A, Saxena A. Hypothalamic pituitary dysfunction in acute nonmycobacterial infections of central nervous system. *Indian J Endocrinol Metab* 15 (Suppl 3): S233-S237, 2011.
4. Emori K, Takeuchi N, Soneda J. A case of Waterhouse-Friderichsen syndrome resulting from an invasive pneumococcal infection in a patient with a hypoplastic spleen. *Case Reports in Crit Care* 2016; art. ID 4708086.
5. Fox B. Disseminated intravascular coagulation and the Waterhouse-Friderichsen syndrome. *Arch Dis Childhood* 46:680-685, 1971.
6. Hale AJ, LaSalvia M, Kirby JE, Kimball A, Baden R. Fatal purpura fulminans and Waterhouse-Friderichsen syndrome from fulminant *Streptococcus pneumoniae* sepsis in an asplenic young adult. *IDCases* 2016: 6:1-4.
7. Hukkanen RR, Liggitt HD, Murnane RD, Frevert CW. Systemic inflammatory response syndrome in non-human primates culminating in multiple organ failure, acute lung injury, and disseminated intravascular coagulation. *Toxicol Pathol* 2009; 37(6):799-904.
8. Verzeletti A, Bonfanti C, Leide A, Assalini E, De Francesco MA, Piccinelli G, De Ferrari. *Streptococcus pneumoniae* detection long time after death in a fatal case of Waterhouse-Friderichsen syndrome. *Am J Forens Med* 2017:38(1)18-19.
9. Vincentelli C, Molina EG, Robinson MJ. Fatal pneumococcal Waterhouse-Friderichsen syndrome in a vaccinated adult with congenital asplenia. *Amer J Emerg Med* 27:751.e3-751.e5, 2009.

Self-Assessment - WSC 2018-2019 Conference 17

1. Which of the following would be considered a case of primary vasculitis in the dog?
 - a. Bacterial endocarditis
 - b. Beagle pain syndrome
 - c. Snakebite
 - d. Multicentric lymphoma

2. In which of the following is PCV-associated myocarditis most often seen?
 - a. Fetuses
 - b. Weanlings
 - c. Feeder pigs
 - d. Sows

3. Guinea pig adenovirus most often result in the death of which of the following cell types?
 - a. Endothelium
 - b. Respiratory epithelium
 - c. Gastric mucosal epithelium
 - d. Bone marrow precursors

4. Waterhouse-Friderichsen syndrome results in hemorrhage within which organ?
 - a. Lung
 - b. Liver
 - c. Pancreas
 - d. Adrenal gland

5. Which of the following is not a predisposing factor for the systemic inflammatory response syndrome ?
 - a. Infection
 - b. Trauma
 - c. Obstetric complication
 - d. Major surgery

Please email your completed assessment to Ms. Jessica Gold at Jessica.d.gold2.ctr@mail.mil for grading. Passing score is 80%. This program (RACE program number) is approved by the AAVSB RACE to offer a total of 0.5 CE Credits, with a maximum of 12.5 CE Credits being available to any individual Veterinary Medical Professionals for the 2017-2018 Wednesday Slide Conference. This RACE approval is for the subject matter categories of: SCIENTIFIC using the delivery method of NON-INTERACTIVE DISTANCE. This approval is valid in jurisdictions which recognize AAVSB RACE; however, participants are responsible for ascertaining each board's CE requirements. RACE does not "accredit", "endorse" or "certify" any program or person, nor does RACE approval validate the content of the program.

Please email your completed assessment to Ms. Jessica Gold at Jessica.d.gold2.ctr@mail.mil for grading. Passing score is 80%. This program (RACE program number) is approved by the AAVSB RACE to offer a total of 0.5 CE Credits, with a maximum of 12.5 CE Credits being available to any individual Veterinary Medical Professionals for the 2017-2018 Wednesday Slide Conference. This RACE approval is for the subject matter categories of: SCIENTIFIC using the delivery method of NON-INTERACTIVE DISTANCE. This approval is valid in jurisdictions which recognize AAVSB RACE; however, participants are responsible for ascertaining each board's CE requirements. RACE does not "accredit", "endorse" or "certify" any program or person, nor does RACE approval validate the content of the program.

**Joint Pathology Center
Veterinary Pathology Services**



WEDNESDAY SLIDE CONFERENCE 2018-2019

C o n f e r e n c e 1 8

6 February 2019

Conference Moderator:

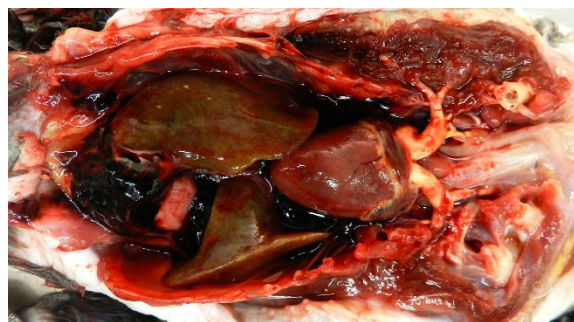
Andrew Cartoceti, DVM, DACVP
Staff Pathologist
National Zoologic Park
Washington DC, 20008

CASE I: 13-161654 (JPC 4048673).

Signalment: 25 year-old, female intact Congo African Grey Parrot (*Psittacus erithacus erithacus*)

History: This parrot was a permanent resident of a pet shop collection and was fed a diet of pellets, seeds, apples, and peanuts. The previous medical history included a prolapsed oviduct in May of 2013 with egg retention, but the bird was otherwise healthy. The bird was presented to the referring veterinarian in November of 2013 for a recent onset of lethargy, anorexia, and feather picking. On presentation, blood work abnormalities included increased bile acids and hyperproteinemia (absolute values were not provided).

Gross Pathology: Both brachiocephalic arteries are prominent, diffusely yellow, hard and do not collapse. On section, the luminal surface is expanded by a locally extensive 1mm thick, rough, yellow plaque (atherosclerosis).



Presentation, parrot: The arteries are thickened and yellow and there is marked hepatomegaly. (Photo courtesy of Cornell University – Animal Health and Diagnostic Center, 240 Farrier Road, Ithaca, NY 14850)

The coelomic cavity contains multiple aggregates of dark red gelatinous material that cover the viscera. The spleen is uniformly enlarged measuring 4.7 x4.5 cm and diffusely mottled white to light tan to red. The liver is enlarged with rounded margins and the parenchyma is diffusely mottled green to black to tan with dozens of random 0.1 cm round white foci (necrosis, presumptive).

Laboratory results: University of Miami – Avian and Wildlife Laboratory

- Increased beta and gamma globulins on electrophoresis consistent with acute inflammation and active humoral immune response
- High titer (1:25) for *Chlamydophila psittaci*

Microscopic Description:

HEART (not submitted): Randomly scattered throughout the parenchyma are small foci of cardiomyocyte loss with replacement by foamy macrophages and lymphocytes.

VESSEL, NOS: Arteries: Diffusely the tunica intima and media is disorganized with the tunica media expanded by abundant foam cells creating an irregular luminal surface. Occasionally the tunica media contains multifocal clear acicular clefts (cholesterol) that are variably surrounded by foamy macrophages and includes locally extensive regions of cellular loss with replacement by large clear spaces (fatty infiltrate) and several foci of chondroid metaplasia. The tunica



Heart and great arteries, parrot: The arteries are thickened, do not collapse under their own weight and yellow and there is marked hepatomegaly. (Photo courtesy of Cornell University – Animal Health and Diagnostic Center, 240 Farrier Road, Ithaca, NY 14850)

intima and media contain numerous small aggregates of granular amorphous deeply basophilic material (mineral). In cross section the arteriolar lumen is occluded up to 60% by a confluent mass composed of a deeper region of large foam cells, acicular clear clefts (cholesterol), large clear spaces (fatty infiltration), multifocal aggregates of mineral, and islands of chondroid matrix covered by a thin variably present endothelial lining (atheroma).

LIVER (not submitted): Randomly scattered throughout the hepatic parenchyma large coalescing areas of hepatocyte loss with the remaining hepatocytes being pale eosinophilic with loss of nuclear detail (necrosis). Admixed within these foci are small numbers of macrophages with fewer plasma cells and lymphocytes and rare heterophils. Surrounding hepatocytes contain fine granular golden brown cytoplasmic pigment (lipofuscin). The remaining hepatocytes show moderate anisocytosis and anisokaryosis, with occasional binucleate cells.

SPLEEN (not submitted): Diffusely expanding the red pulp are large coalescing aggregates of foamy macrophages admixed with few degenerate and non-degenerate heterophils.

Contributor's Morphologic Diagnoses:

Arteries: Severe, diffuse, chronic atherosclerosis

Heart: Mild, multifocal, lymphohistocytic myocarditis

Liver: Severe, multifocal to coalescing, chronic, hepatocellular necrosis with granulomatous, lymphoplasmacytic hepatitis

Spleen: Severe, multifocal, chronic, granulomatous splenitis



Liver: The liver is enlarged, with a cobblestoned mottled parenchyma. (Photo courtesy of Cornell University – Animal Health and Diagnostic Center, 240 Farrier Road, Ithaca, NY 14850)

Contributor's Comment: The histologic features seen here are consistent with atherosclerosis of a grade IV out of VII,⁵ although grade varies between submitted sections. The changes in the liver and spleen are seen with *Chlamydophila psittaci* infection, but other systemic bacterial infections (e.g. *Escherichia coli*, *Salmonella* sp, *Mycobacterium* sp, *Staphylococcus* sp, and *Streptococcus* sp) can create similar changes. Antemortem testing for *Chlamydophila psittaci* were consistent with an active infection. In this case the cause for coelomic hemorrhage remained unclear, as thrombotic events and vessel rupture are uncommon complications of atherosclerosis in the avian species.

Atherosclerosis is a chronic inflammatory fibroproliferative disorder, which commonly causes spontaneous disease in psittacines, as well as numerous other avian species. Most notably the Japanese Quail (*Coturnix coturnix japonica*) and pigeon (*Columa livia domestica*) have been used as inducible experimental models for the human disease.^{2,3,11} The pathogenesis of disease has been largely explained by the response-to-

injury hypothesis. Here the principle inciting cause is endothelial damage, secondary to endothelial dysfunction and oxidative stress that creates a local atherogenic environment^{2,5}. Endothelial dysfunction is characterized by a chronic state of endothelial cell activation leading to increased production of procoagulative and proinflammatory factors.² In a recent study endothelial cell changes were appreciated in mild pre-atheroma lesions; giving further support to the hypothesis that endothelial damage precedes lipid deposition.⁵ A recent experimental model showed that type VIII collagen is up-regulated in atherosclerotic lesions and allows for smooth muscle cell proliferation and migration, which is important for fibrous cap formation.⁷

Currently the association between histologic severity and clinical disease course is unknown. As atherosclerosis in psittacines represents a similar spontaneous disease progression to that seen in humans, a similar grading scheme based on the American Heart Association's human grading scheme has been proposed for better characterization and future prognostication of disease. This scheme divides atherosclerotic lesions into seven grades based on the light microscopic,

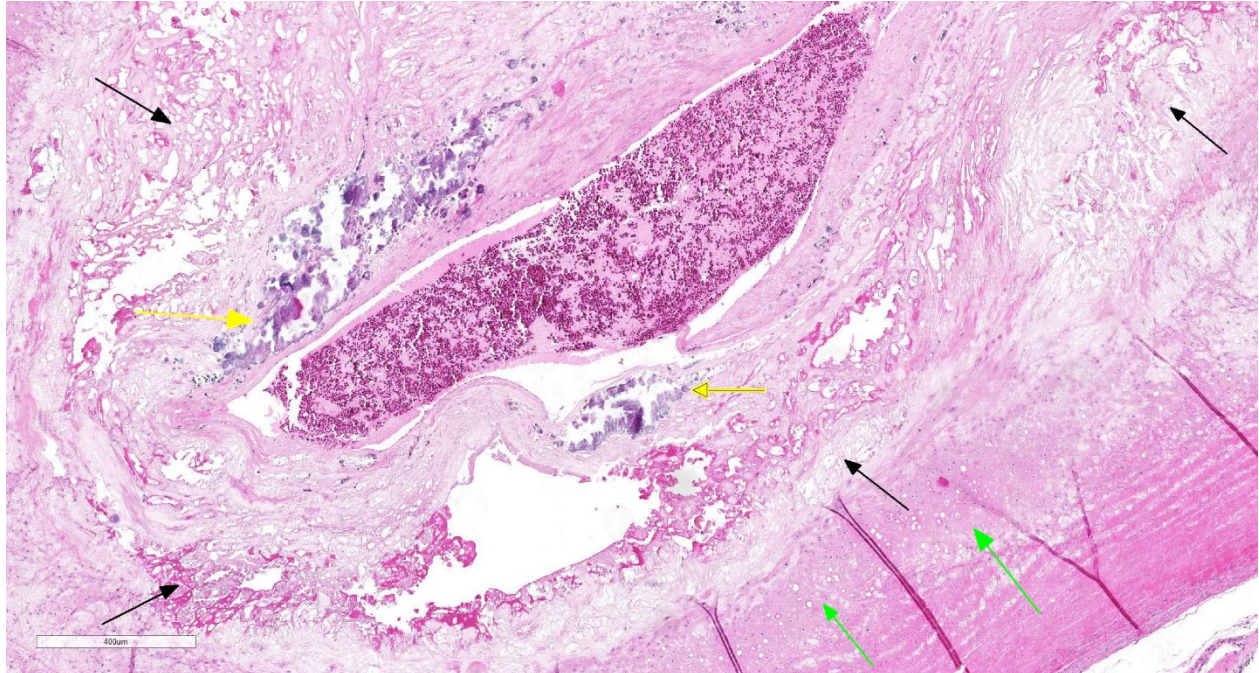


Muscular artery, parrot. The tunica intima is effaced and the tunica media is markedly expanded by a complex atheroma. (HE 20X).

histochemical, and electron microscopic features, with grades greater than IV of VII being considered clinically significant.⁵

Several risk factors have been proposed for the development of atherosclerosis in psittacines. Diet has been implicated, as many animal models for experimental disease are diet-inducible. In one study increasing the cholesterol within the feed of Quaker parrots (*Myiopsitta monachus*) by 1% induced clinically significant lesions within 4-6 months.⁶ With hypercholesterolemia, lipoproteins themselves can allow for activation of endothelial cells and leukocyte adhesion. Oxidized lipoproteins act as strong chemoattractants for monocytes. Once they enter the vascular wall and transform, to macrophages, they express scavenger receptors that allow for uptake of additional low density lipoproteins (LDLs) and stimulation of smooth muscle cells to foam cells². In addition increased age, female sex,

concurrent reproductive or hepatic disease, and the genera *Psittacus*, *Amazona*, and *Nymphicus* were found to increase the risk of development of severe atherosclerotic lesions.⁴ The synthesis and transport of VLDLs and vitellogenin to the oocyte and future egg yolk in response to estrogen may be the underlying pathogenesis for this predisposition in female birds.² As VLDLs have been shown to be pro-inflammatory.² Infectious agents have been implicated as risk factors for lesion development. In one study there was a significant association between *Chlamydophila psittaci* antigen in the blood and development of atherosclerosis, however this correlation was not appreciated in one large retrospective study. However it is interesting to note that this patient had concurrent histologic findings and antemortem test findings consistent with active *Chlamydophila psittaci* infection. Marek's disease (herpes virus infection) has



Muscular artery, parrot. Higher magnification of the atherosclerotic plaque reveals a thick, often artifactually cleaved layer of foam cells, cholesterol clefts and abundant collagen (black arrows), mineral (yellow arrows), and at the periphery, foci of cartilaginous metaplasia. (HE 66X).

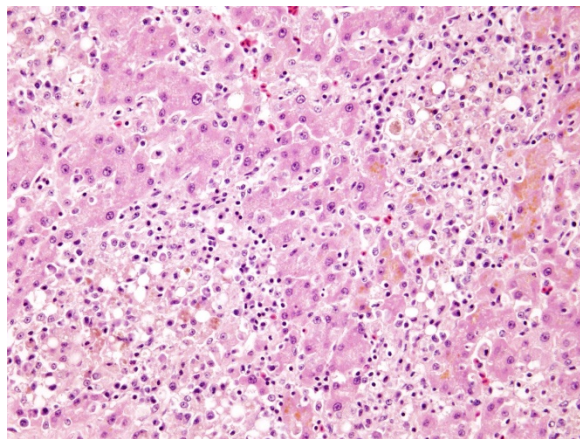
been shown in chickens to promote atherosclerotic lesion formation.²

Underlying genetic factors can predispose a patient to endothelial dysfunction. In one study in White Carneau Pigeons there was a divergence in the genes responsible for cytoskeleton remodeling, proteasome activity, cellular respiration, and immune response. These genes were postulated to predisposition to the development of atherosclerotic lesions.¹ The importance of gene divergence in other avian species has not been investigated.

Contributing Institution:

Cornell University – Animal Health and Diagnostic Center
240 Farrier Road
Ithaca, NY 14850

JPC Diagnosis: Elastic artery: Atherosclerosis, circumferential, diffuse, severe, with marked mural fibrosis, cartilaginous metaplasia and mineralization.



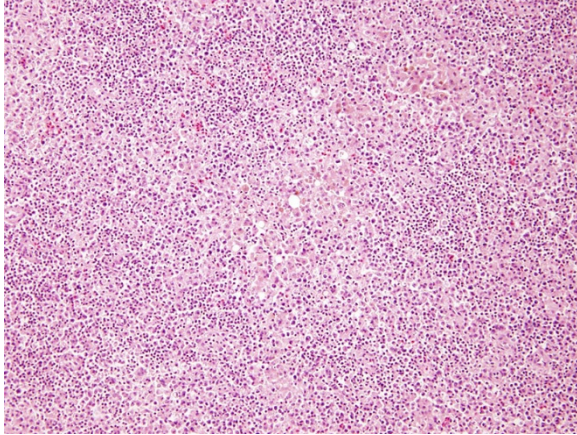
Liver: There are multifocal to coalescing foci of granulomatous inflammation containing large numbers of macrophages with fewer often peripheral lymphocytes and plasma cells. Remaining hepatocytes often contain abundant lipofuscin. (HE 200X) (Photo courtesy of Cornell University – Animal Health and Diagnostic Center, 240 Farrier Road, Ithaca, NY 14850)

2. Elastic artery, adventitial adipose tissue: Atrophy, diffuse, severe.

JPC Comment: The contributor has provided an excellent discussion of atherosclerosis in psittacines and other avian species, highlighting a number of abnormalities which are involved in this complex condition. Species such as humans, non-human primates, pigs, rabbits and hamsters are considered susceptible to atherosclerosis and its predisposing factor, hypercholesterolemia. Other laboratory animals such as mice, rats, dogs and shrews exhibit resistance to these conditions.⁹

The recent literature abounds with studies on various areas of research into animal models of atherosclerosis, in a number of areas of current interest in the pathogenesis of human atherosclerosis – genetic abnormalities, the contribution of inflammation and inflammatory mediators on the development of atheromatous plaques, endothelial dysfunction, and diet/dyslipidemia. Genetic abnormalities, such as the deficiency of low-density lipoprotein receptors (LDLR), are widespread in humans (with over 1700 separate genetic mutations to date)⁹ and have been a subject of investigation since the use of the Watanabe rabbit in the 1970's. Today, genetic manipulation of knockout mice and rabbits involved in the pathway of production and degradation of the LDLR continues to further research in this area.⁹

Diet-induced atherosclerosis (or enhancement of disease in atherosclerosis – resistant species) is a time-honored research avenue which is still being applied today to new animal models. The Gottingen minipig has been a model for atherosclerosis for the last decade. Diets high in fat/cholesterol and cholate have the potential for inducing advanced coronary and atherosclerotic



Liver: There are also foci of granulomatous inflammation within the spleen as well. (Photo courtesy of Cornell University – Animal Health and Diagnostic Center, 240 Farrier Road, Ithaca, NY 14850)

lesions in the species¹⁰, as has been demonstrated in a number of other species over the years, to include laboratory rodents as well as non-human primates.

An excellent review from a species perspective on atherosclerosis was part of a recent review of aging changes in great apes.⁸ In contrast to early literature stating that chimpanzees were suitable animal models for coronary atherosclerosis (especially if subjected to atherogenic diets), the actual incidence of coronary atherosclerosis is quite low in apes in well-managed colonies and collection; however more data needs to be collected on aortic atherosclerosis in these species.⁸

We are unable to confirm the diagnosis of chlamydia in this case, as liver and splenic tissue were not part of the submission. The connection between chronic inflammation and atherosclerosis is well-documented in the literature; however, the connection between the two lesions in this animal and its significance would be very difficult to assess.

Early on in the discussion, the moderator pointed out the difficulty in even establishing that whether this section represented an

elastic or a muscular artery. Without the use of special stains, the mural changes make it difficult to visually quantitate the amount of elastin within the wall. Muscular arteries, which deliver blood to specific organs, tend to have walls composed primarily of smooth muscle, while elastic arteries have a higher concentration of elastic fibers. Both the moderators from this week and last week conference agreed that the differentiation of elastic versus muscular arteries is extremely difficult in very diseased vessels.

The moderator reviewed atherosensitive species including rabbits, guinea pigs, birds, and pigs, as well as atheroresistant species - dogs, cats, cattle, goats, and unmanipulated mice/rats. In psittacines, the disease is common in Amazons, African greys, cockatiels and Quaker parrotss. The participants also discussed the response to injury (endothelial damage and the generation of a procoagulative and pro-inflammatory state) versus the response to retention theory (binding of LDL's by arterial extracellular matrix and promotion of further endothelial damage and recruitment of additional lipids and leukocytes) in atherogenesis. The moderator also reviewed the currently published grading system for atherosclerosis in psittacines.⁶

References:

1. Anderson JL, Ashwell CM, Smith SC, et al. Atherosclerosis-susceptible and atherosclerosis-resistant pigeon aortic cells express different genes in vivo. *Poultry Science*. 2013;92(10):2668-80. doi: 10.3382/ps.2013-03306.
2. Beaufrère H. Atherosclerosis: Comparative Pathogenesis, Lipoprotein Metabolism, and Avian and Exotic Companion Mammal Models. *Journal of Exotic Pet Medicine*. 2013;22(4):320-35. doi: 10.1053/j.jepm.2013.10.016.

3. Beaufrère H. Avian Atherosclerosis: Parrots and Beyond. *Journal of Exotic Pet Medicine*. 2013;22(4):336-47. doi: 10.1053/j.jepm.2013.10.015.
4. Beaufrère H, Ammersbach M, Reavill DR, et al. Prevalence of and risk factors associated with atherosclerosis in psittacine birds. *Journal of the American Veterinary Medical Association*. 2013;242(12):1696-704. doi: 10.2460/javma.242.12.1696.
5. Beaufrere H, Nevarez JG, Holder K, et al. Characterization and classification of psittacine atherosclerotic lesions by histopathology, digital image analysis, transmission and scanning electron microscopy. *Avian pathology : Journal of the WVPA*. 2011;40(5):531-44. doi: 10.1080/03079457.2011.607427. PubMed PMID: 21879992.
6. Beaufrere H, Nevarez JG, Wakamatsu N, et al. Experimental diet-induced atherosclerosis in Quaker parrots (*Myiopsitta monachus*). *Veterinary pathology*. 2013;50(6):1116-26. doi: 10.1177/0300985813488958. PubMed PMID: 23696447.
7. Lopes J, Adiguzel E, Gu S, et al. Type VIII collagen mediates vessel wall remodeling after arterial injury and fibrous cap formation in atherosclerosis. *Am J Pathol*. 2013;182(6):2241-53. doi: 10.1016/j.ajpath.2013.02.011. PubMed PMID: 23567639; PubMed Central PMCID: PMC3668035.
8. Lowenstine LJ, McManamon R, Terio KA. Comparative pathology of aging great apes: bonobos, chimpanzees, gorillas, and orangutans. *Vet Pathol* 2016; 53(2): 250-256.
9. Lu R, Yuan T, Wang Y, Zhang T, Yuan U, Wu D, Zhou M, He Z, Lu Y, Chen YU, Fan J, Liang J, Cheng Y. Spontaneous severe hypercholesterolemia and atherosclerosis lesions in rabbits with deficiency of low-

density lipoprotein receptor (LDLR0 on exon 7. *Ebiomedicine* 36(2018) 29-38.

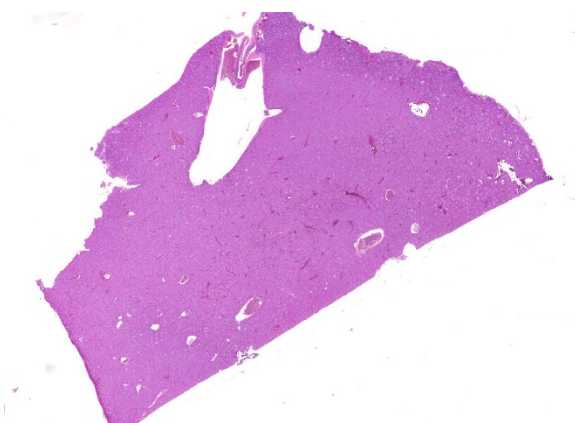
10. Ludvigsen TP, Kirk KE, Christofferssen BO, Pedersen HD, Martinussen T, Kildegaard JU, Heegaard PMH, Lykkesfeldt J, Olsen LH. Gotten miniid model of diet-induced atherosclerosis: influence of mild streptozotocin-induced diabetes on lesion severity and markers of inflammation evaluated in obese, obese and diabetic, and lean control animals. *J Translat Med'* 2015; 13:312-324.

11. Pilny AA, Quesenberry KE, Bartick-Sedrish TE, Latimer KS, Berghaus RD. Evaluation of *Chlamydia psittaci* infection and other risk factors for atherosclerosis in pet psittacine birds. *JAVMA*. 2012;240(12):1474-80.

CASE II: B or blank (JPC 4066242).

Signalment: 40 year old male Orange-winged Amazon parrot, *Amazona amazonica*

History: A 40 year old male Orange-winged Amazon parrot (*Amazona amazonica*) presented to the Ontario Veterinary College, Health Sciences Center, Avian and Exotics service for a one day history of severe



Liver, amazon parrot. Subgross examination reveals numerous small areas of pallor scattered throughout the section. (HE, 7X)

weakness, falling from his perch and inability to right himself or stand. The bird was initially purchased as a hatchling, and lived with the current owners for the last 40 years. There were no other birds in the house. The bird had a previous clinical history of feather plucking and hypovitaminosis A.

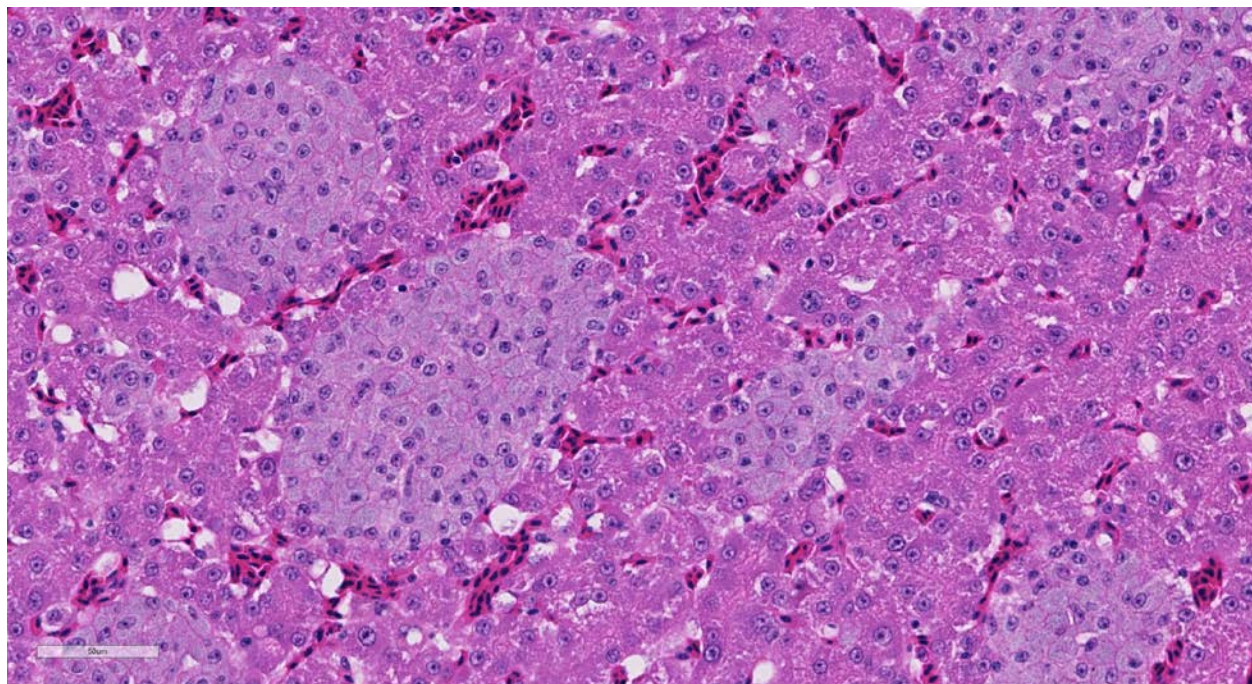
On physical examination, the bird was dull and lethargic. There was mild overgrowth of the rhamphotheca and nails. Complete blood count and serum biochemistry revealed leukocytosis (white blood cells $28.2 \times 10^9/L$ [reference $1.2-10.1 \times 10^9/L$], heterophils $21.96 \times 10^9/L$ [78 %; reference 21.9-40.7 %]⁵) and increased concentration of liver enzymes (AST 1012 U/L [reference range 150-344 U/L]²). Due to the age of the patient and severity of clinical signs, the owners declined further diagnostics and the bird was euthanized.

Gross Pathology: The bird was in thin body condition, with decreased subcutaneous fat stores and mildly depleted pectoral muscle mass. The majority of the contour feathers were missing from the ventrum, but down feathers were still present. The gnathotheca was overgrown, with flaking of keratin at the lateral edges. On internal examination, the liver was enlarged and mottled tan-red. The liver weighed 9 grams (2.8 % of body weight). The gastrointestinal tract was empty, with the exception of a small amount of gravel in the ventriculus.

Laboratory Results:

Sections of liver and brain were stained with Ziehl Neelsen acid-fast stain, revealing myriad acid-fast bright red intracytoplasmic bacilli, morphologically compatible with mycobacteria.

Samples of liver and spleen were sent to an external laboratory (Public Health Laboratory, Toronto) for culture and



Liver, amazon parrot. High magnification demonstrates the presence of numerous foci of non-caseating granulomatous inflammation throughout the section. Macrophages contain numerous intracytoplasmic bacilli which impart an amphophilic color to the cytoplasm. (HE, 400X)

mycobacteria species identification. On tissue smears of both organs, 4+ acid-fast bacilli were seen. GenoType® Mycobacterium molecular genetic test systems (Hain Lifescience) identified the bacilli as *Mycobacterium genavense*. No mycobacteria were isolated after 7 weeks of mycobacterial culture.

Microscopic Description:

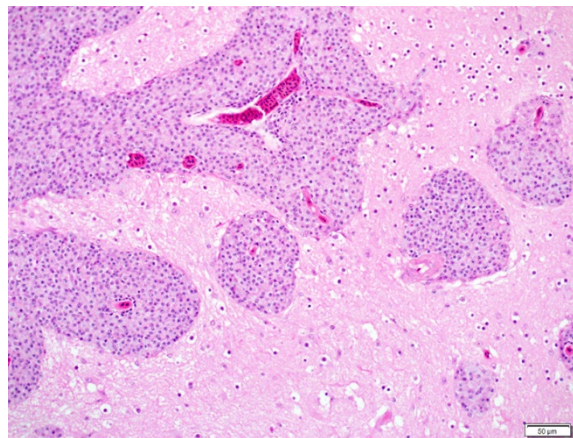
Liver: There are numerous, multiple, well-demarcated, expansile to coalescing, variably-sized (up to 250 µm in diameter) nodular infiltrates scattered randomly throughout the hepatic parenchyma, comprising up to 40% of the tissue. The infiltrates are composed of relatively uniform, approximately 15 µm diameter polygonal round cells morphologically compatible with epithelioid macrophages, with distinct cell margins and abundant faintly basophilic cytoplasm containing large numbers of faintly discernable, 1-2 µm long organisms. Nuclei are round and eccentric, with finely stippled chromatin and prominent basophilic nucleoli. Rare larger nodules contain central aggregates of pyknotic cellular debris and amorphous eosinophilic fibrillar material (necrosis).

Brain (tissue not included on slides submitted): Similar infiltrates of macrophages are present beneath the leptomeninges and within Virchow-Robins spaces throughout the sections of brain examined.

Contributor's Morphologic Diagnoses:

Liver: Hepatitis, multifocal nodular, histiocytic with intracytoplasmic bacilli (*Mycobacterium genavense*).

Contributor's Comment: A presumptive diagnosis of mycobacterial hepatitis (avian mycobacteriosis) was initially made based on the presence of intracytoplasmic acid-fast



Brain, amazon parrot. Infiltrates of similar bacilli-laden macrophages expand Virchow-Robins spaces. (HE, 100X)

bacilli. As there was potential zoonotic risk in this case,¹ samples of liver and spleen were submitted for mycobacterial culture and species identification at a local public health laboratory (Public Health Laboratory, Toronto). The lab identified acid-fast bacilli on direct smears of the tissues and speciated the sample using GenoType Mycobacterium test, which can differentiate between 16 different mycobacterial species (including *Mycobacterium genavense*).⁶ Despite the large numbers of bacilli noted histopathologically and on tissue smear, the laboratory was unable to isolate the mycobacteria after 7 weeks of culture.

Avian mycobacteriosis is one of the most common diseases of birds world-wide, affecting pet birds, domestic poultry, zoo collections and wild avian species.⁸ The disease is often insidious, presenting as a chronic wasting disease with relatively non-specific clinical signs or sudden death with no premonitory signs at all.^{1,3,8,10} Antemortem diagnosis is challenging, and diagnosis is often made on characteristic post-mortem and histopathological findings, with or without confirmatory culture and speciation.^{7, 8} Lesions may exist as multifocal, multi-organ granuloma

formation, intestinal paratuberculosis-like histiocytic infiltration, or grossly apparent organomegaly.⁸ The gross and histological appearance may be impacted by the species of bird affected, or the immune status of the affected bird.⁸

Mycobacterium genavense has been reported to be the most common mycobacterial species isolated from pet birds,^{4,8} but *Mycobacterium avium* subsp. *avium* and *Mycobacterium intracellulare* are other commonly identified species. Other mycobacterial species (of which there are at least ten identified in various species of birds) are uncommon.⁷ Mycobacteria are often ubiquitous in the environment, and can be isolated from acidic or wet soil or contaminated water sources.⁸ Environmental contamination is the presumed source of the organism, and infection is contracted by ingestion of the bacteria. Disease susceptibility is variable depending on the species of bird, with a species predilection (amongst pet birds) for amazons, parakeets, pionus parrots and budgerigars.⁸ The propensity for a bird to develop disease likely depends on several compounding factors, including nutritional status, stress and overall immune status. Once infected, mycobacteria are phagocytosed by macrophages, often within the intestinal tract, and stimulate a cell-mediated immune response. The exact mechanism of survival of mycobacteria in avian macrophages is not completely understood, but is thought to be the result of impaired enzyme function and phagosome-lysosome fusion.⁸

Contributing Institution:

Animal Health Laboratory, University of Guelph, Guelph, Ontario, Canada

<http://ahl.uoguelph.ca>

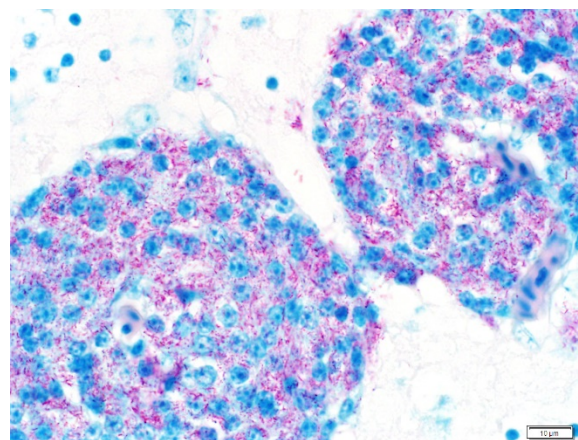
JPC Diagnosis: Liver: Hepatitis, granulomatous (histiocytic), multifocal to

coalescing, marked with numerous intracytoplasmic bacilli.

JPC Comment: The contributor has provided an excellent and concise review of mycobacteriosis (often incorrectly referred to as “avian tuberculosis”) in birds. Mycobacteriosis is the result of infection by non-tuberculous mycobacteria – over 160 species of ubiquitous environmental bacteria, a small percentage of which have been documented to cause disease in humans and other species. In humans, pulmonary disease is the most common manifestation, and there is well-documented variation in the most common clinical isolates based on location, even within individual countries.⁹

Once a problem in commercial poultry, today mycobacteriosis is a rare finding due not only to improved husbandry conditions, but most importantly, the rapid turnover of birds from hatching to market – which essentially does not leave enough time for the development of this chronic disease.

A very interesting study performed at the Zoological Society of San Diego (ZSSD) investigated the characteristics and risk



Brain, amazon parrot. An acid fast stain reveals numerous acid-fast-positive bacilli in the cytoplasm of macrophages within Virchow-Robin's spaces. (ZN, 400X)

factors associated with avian mycobacteriosis in often rare and expensive species.¹⁰ The true incidence in many zoo populations is likely underestimated as a result of the chronic nature and long latency period. While previously considered largely an intestinal disease in zoo birds, retrospective study at the ZSSD identified respiratory lesions in 76% of cases, and 27% of cases with only respiratory signs (contrasting with 58% of cases which had intestinal lesions and only 8% with intestinal lesions only) citing a need for screening for respiratory disease as well. The study showed that animals imported into the ZSSD had higher odds of being infected than those born on the property – previous exposure to infected birds prior to import, as well as immunosuppression related to shipping stress (and other forms of stress including conspecific aggression and concurrent disease were considered as potential reasons for this finding. Additional factors included birds that were moved more often between enclosures, species of infected birds, and likely species of infecting mycobacteria.¹⁰

The moderator noted the presence of occasional karyomegalic hepatocytes in this section, musing that these may be polyploid and may reflect the age of the bird. The moderator's preference in the morphologic diagnosis of this lesion is histiocytic which is absolutely acceptable, understandable, and has launched heated discussions around the world for many years. Conference participants showed amazing restraint and tolerance in this instance. The moderator concluded the discussion with a review of mycobacterial disease in a number of species, to include fish, amphibia, reptiles, ruminants, and elephants.

References:

1. Boseret G, Losson B, Mainil JG, Thiry E, Saegerman C. Zoonoses in pet birds: review and perspectives. *Vet Res.* 2013, 44: 36.
2. Harr KE. Clinical chemistry of companion avian species: a review. *Vet Clin Path.* 2002, 31 (3): 140-151.
3. Hoop RK, Bottger EC, Ossent P, Salfinger M. Mycobacteriosis due to *Mycobacterium genavense* in six pet birds. *J Clin Microbiol.* 1993, 31 (4): 990-993.
4. Medenhall MK, Ford SL, Emerson CL, Wells RA, Gines LG, Eriks IS. Detection and differentiation of *Mycobacterium avium* and *Mycobacterium genavense* by polymerase chain reaction and restriction enzyme digestion analysis. *J Vet Diagn Invest.* 2000, 12: 57-60.
5. Polo FJ, Peinado VI, Viscor G, Palomeque J. Hematologic and plasma chemistry values in captive psittacine birds. *Avian Diseases.* 1997, 42: 523-535.
6. Ruiz R, Gutierrez J, Zerolo FJ, Casal M. GenoType mycobacterium assay for identification of mycobacterial species isolated from human clinical samples by using liquid medium. *J Clin Microbiol.* 2002, 40 (8): 3076-3078
7. Shivaprasad HL, Palmieri C. Pathology of mycobacteriosis in birds. *Vet Clin Exot Anim.* 2012, 15: 41-55.
8. Tell LA, Woods L, Cromie RL. Mycobacteriosis in birds. *Rev sci tech Off int Epiz.* 2001, 20 (1): 180-203.
9. Wassilew N, Hoffmann H, Andrejak C, Lange C. Pulmonary disease caused by non-tuberculous mycobacteria. *Respiration* 2016;91:386-402.

10. Witte CL, Hungerford LL, Papendick R, Stalis IH, Rideout BA. Investigation of characteristics and factors associated with avian mycobacteriosis in zoo birds. *J Vet Diagn Invest.* 2008, 20: 186-196.

CASE III: 1013/15 (JPC 4085103).

Signalment: 18-year-old, female, bird, blue-eyed cockatoo (*Cacatua sanguinea*)

History: Bird suddenly presented respiratory distress and apathy, culminating in death few hours later. The bird was born in a house where it lived for seven years, and then moved to a small zoo where it lived for 11 years. This blue-eyed cockatoo shared premises with other bird species and, eventually, was transferred to a visiting area inside another aviary. The daily diet was a commercial ration (MegaZoo, Vale Verde, Minas Gerais, Brazil) and varied tropical fruits. Febendazole (4%) diluted in water or oral administration of ivermectin and albendazol was given once a year.

Gross Pathology: Grossly, lungs were markedly hyperemic and edematous. Visceral pleura was whitish and mildly thickened. The pericardial space and coelomic cavity contained small amount of a transparent fluid. In addition, there were moderate splenomegaly and multifocal black foci in the ovary.

Laboratory Results: None.

Microscopic Description:

In the lungs, there was marked hyperemia and air spaces contained homogenous to fibrillar eosinophilic material. In some sections there were many erythrocytes within parabronchi. Cellularity was increased throughout the lungs, resulting in mild

thickening of air capillary walls. In several perivascular areas there was mild to moderate infiltration of lymphocytes, histiocytes and few plasma cells. There was multifocal *micro-thrombosis* within capillaries. In some sections, lymphocytes, histiocytes and fewer plasma cells were also seen in the interstitium. Associate to these lesions, there were many sinuous schizonts lining the periphery of the capillaries. These schizonts were elongated, and ranged from 15 to 20 μm in length and from about 7 to 10 μm in cross-sectional diameter. There were some basophilic mature free merozoites within capillary lumen, which were most evident on the cross-sections.

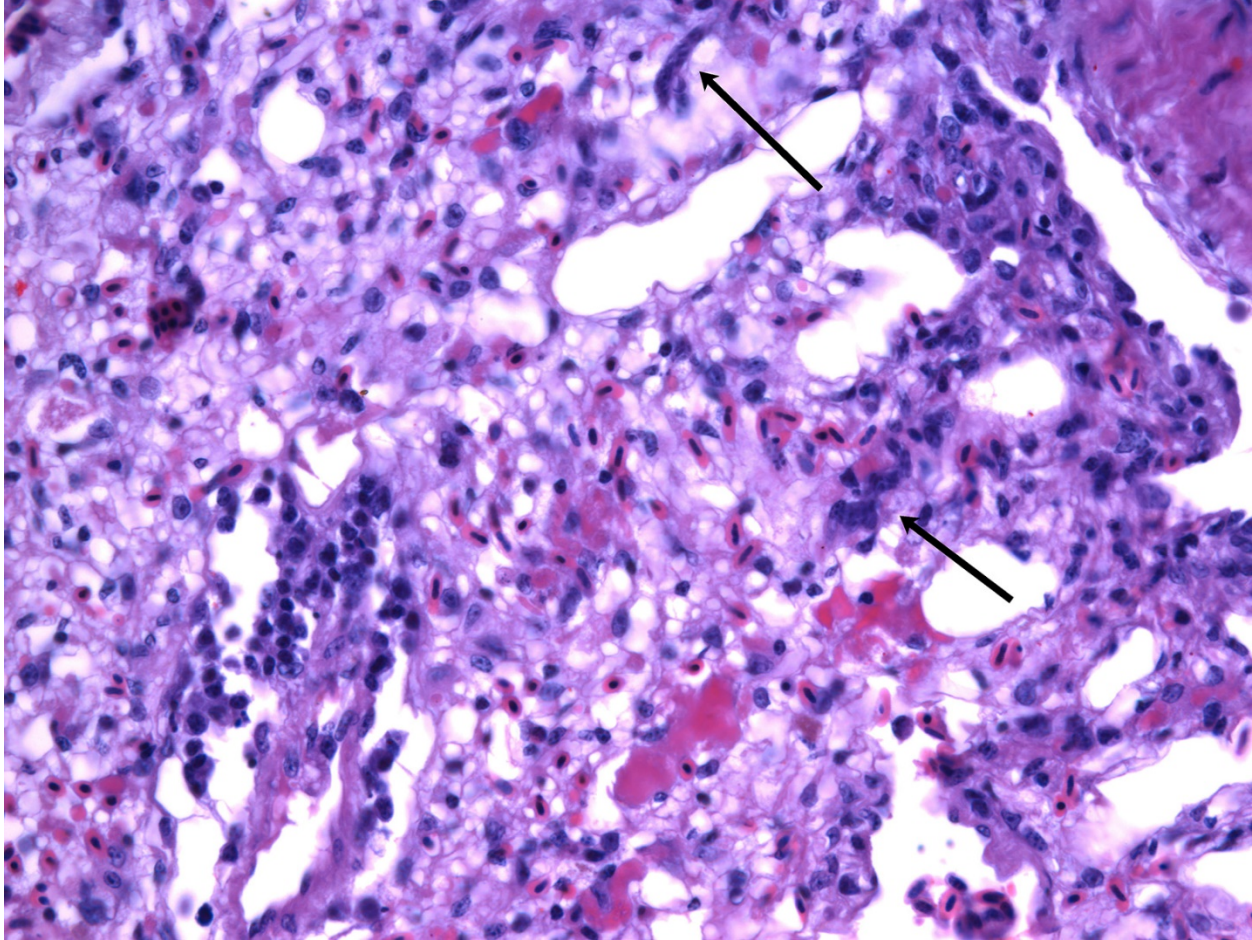
Other organs (not submitted): in the heart there was mild to moderate, multifocal perivascular infiltration of lymphocytes and plasma cells. The liver had moderate to marked increase in the cellularity due to accumulation of histiocytes, lymphocytes and plasma cells in the sinusoids. In the kidneys, there was multifocal, mild interstitial and perivascular infiltration of lymphocytes and plasma cells. In the spleen, there was mild increased in the differentiation of lymphocytes to plasma cells. In the ovary, there was multifocal melanosis.

Contributor's Morphologic Diagnoses:

Lungs: pneumonia interstitial lymphoplasmacytic acute, diffuse, moderate, with protozoa morphologically compatible with *Sarcocystis falcatula*.

Contributor's Comment: Clinical history, gross and histologic lesions associated with sinuous schizonts in the lungs, suggests that this bird had fatal pulmonary sarcocystosis, presumed to be due to *Sarcocystis falcatula*.

Sarcocystis falcatula utilizes two-host life cycle. The only known definitive host in North America is the opossum (*Didelphis*



Lung, cockatoo: There is diffuse mild edema, multifocal microthrombosis and perivascular infiltration of lymphocytes, plasma cells and histiocytes. There are multifocal immature *Sarcocystis* schizonts (arrows). (HE, 400X) (Photo courtesy of: Universidade Federal de Minas Gerais School of Veterinary Medicine – www.vet.ufmg.br)

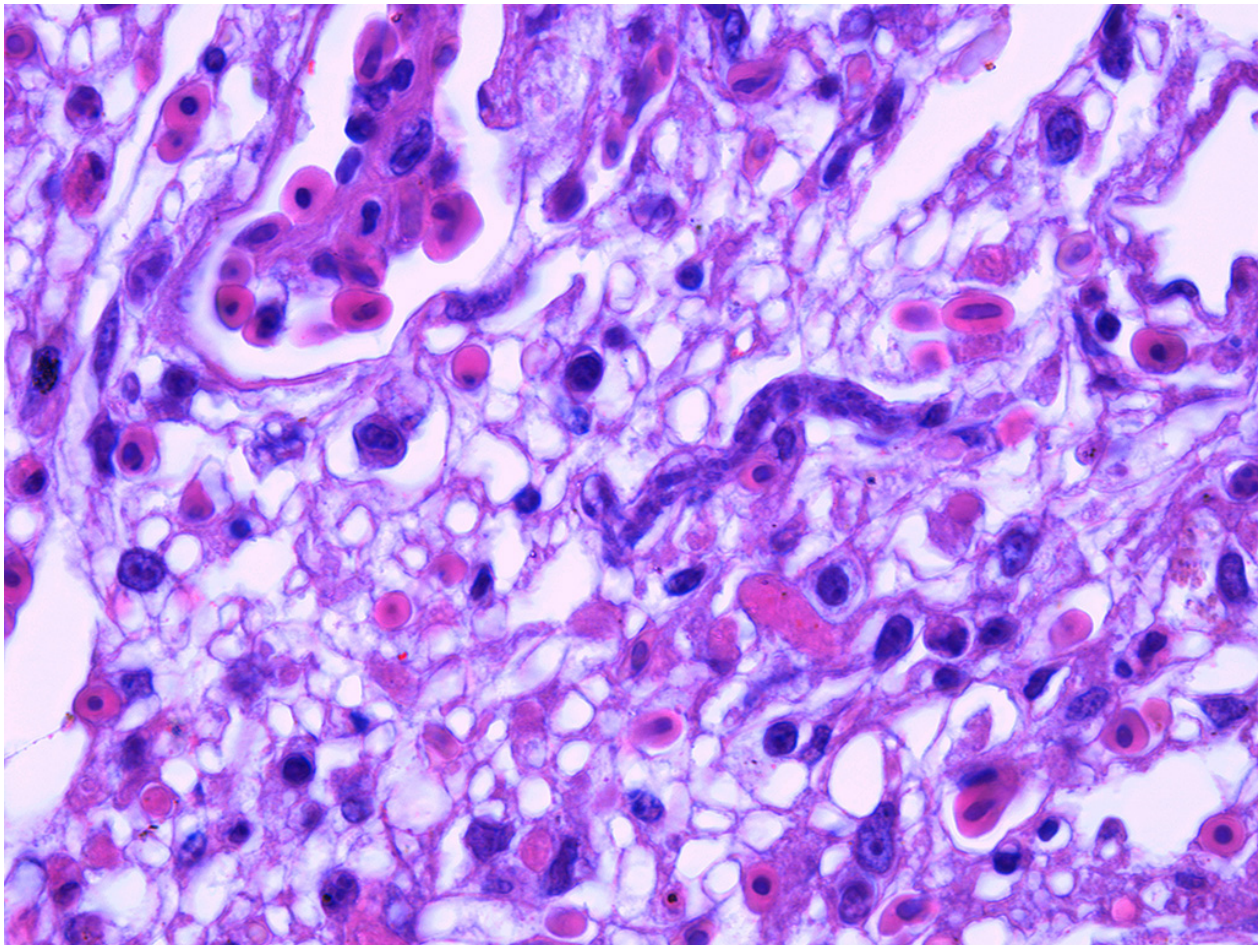
virginiana).¹² South American opossums (*D. marsupialis* and *D. albiventris*) can be the definitive hosts for *S. falcatula*, and *S. falcatula*-like protozoans.^{2,3} The aviaries where this bird was kept were enclosed by wire mesh on all sides, including the roof and the contact with feces of wild animals probably occurred. The wild opossum (*Didelphis albiventris*) inhabits the forest surrounding the area of the small zoo, and is frequently seen at night in the area near the enclosures.

Asexual reproduction occurs in the intermediate host and is characterized by schizogony (merogony) and formation of sarcocysts in skeletal muscle. *Sarcocystis*

falcatula can use a large variety of bird species as intermediate hosts, including Passeriformes,⁹ Psittaciformes,^{1,8} and Columbiformes.^{5,16} *S. falcatula* is highly pathogenic to intermediate hosts, especially to psittacines, because of its prolonged schizogony (5 months or more) and its fatal pulmonary presentation with many immature schizonts.^{1,3,7} The merogony phase in the intermediate hosts takes place in arteries, capillaries, veins, and venules of lungs, liver, kidney and brain.^{12,13} Ultimately, the merozoites give rise to sarcocysts in striated muscle. Then, mature sarcocysts can be found in cardiac and skeletal muscles.¹³

Clinical signs of acute fatal pulmonary sarcocystosis include severe dyspnea, anorexia, lethargy and loss of weight prior to death.^{12,16} Pulmonary sarcocystosis was described in different species of birds such as pigeons¹⁶, cockatiels¹, ring-necked parakeets and African grey parrots⁵. Like this blue-eyed cockatoo, similar clinical presentations and lesions are usually found in other captive birds of Psittacidae family (Psittacinae and Arinae subfamily). Mature sarcocysts in the pectoral muscles were found in a free ranged macaw (*Anodorhynchus hyacinthinus*) and in a dusky parrot (*Pionus fuscus*) necropsied in our lab.

Pulmonary lesions were the most prominent finding in this bird and, according to Smith et al.^{12,13} are directly related to the pathogenesis of *Sarcocystis* infection, because endothelial cell invasion by schizonts occurs during asexual multiplication. The schizogony of this protozoan parasite in all bird species usually begins in the endothelium of capillaries and venules in the lamina propria of the small intestine.⁷ In parrots and parakeets, pulmonary schizogony is more intense than in other organs. In contrast, schizogony in pigeons is more intense in the liver.^{14,16} There are two hypotheses for these differences: the host cellular immune



Lung, cockatoo: Higher magnification demonstrating mild perivascular infiltration of lymphocytes and histiocytes, fibrin and an immature *Sarcocystis* schizont. (HE, 1000X) (Photo courtesy of: Universidade Federal de Minas Gerais School of Veterinary Medicine – www.vet.ufmg.br)

response for controlling *Sarcocystis* infection differs among bird species¹⁵, the type of host cell infected influencing the growth and persistence of *S. falcatula* merozoites⁶ and amount of sporocysts ingested by a bird⁷. Pulmonary hyperemia and edema result from stenosis of the capillaries and venules caused by the protozoan parasite, in addition to microthrombi formation induced by endothelial lesions during schizogony.¹²

The species of *Sarcocystis* that infected the bird in the study could not be determined and awaits further study. Sarcocystosis should be considered in the differential diagnosis of sudden death and pneumonia in captive birds. The usual occurrence of sarcocystosis is probably associated with the frequency of the definitive host and the close contact between birds and these animals.

Contributing Institution:

Veterinary School, Universidade Federal de Minas Gerais – www.vet.ufmg.br

JPC Diagnosis: Lung: Pneumonia, interstitial, histiocytic, diffuse, moderate with mild multifocal necrosis, and occasional intraendothelial apicomplexan meronts.

JPC Comment: The contributor has provided an excellent review of the pathogenesis of *Sarcocystis falcatula* infection in the bird. The recent literature contains a number of articles on the isolation of this parasite from a number of species of its definitive host (opossums native to various regions of the world), as well as details of the various manifestations of infection in a wide range of avian species, such as the recent report of necrotizing meningoencephalitis in a bare-faced ibis.⁸

Historically, *S. falcatula* was named by Stiles in 1893 from a specimen of a rose-breasted grosbeak. The parasite's life cycle (similar to

other sarcocysts, utilizing herbivores as intermediate hosts and carnivores as definitive hosts) and potential for infecting a wide variety of avian species was determined by Box and Smith in 1982. They determined that *S. falcatula* utilized only avian species as intermediate hosts and were not infective for poultry. Until 1995, it was believed that *S. falcatula* was the only sarcocyst utilizing the Virginia opossum (*Didelphis virginianus*) as its definitive host, until the discovery in 1995 of *Sarcocystis neurona* by Dubey and Lindsey, another agent which causes potentially fatal disease in intermediate hosts.⁴

Recently Dubey et. Al. have posited that there may be more than one particular species of *Sarcocystis* that cycles between avian species and opossums, suggesting than many of the earlier reports of *S. falcatula* in which molecular or immunohistochemical identification of the parasite was performed may be in question.⁴ In addition, this report discusses the potential immunohistochemical cross-reaction between the schizonts of *S. falcatula* and *S. neurona* based on the stage of the parasite used for immunization, method of preparation of zoites, stage of the parasite in test tissues, and individual variability among immunized rabbits.⁴ According to Dubey, a god in this field (and for whom *Sarcocystis jaypeedubeyi* is phonetically named), the structure of the sarcocyst wall (best viewed by ultrastructure) is the most reliable way to differentiate between two species of *Sarcocystis*, especially within the same host species.⁴

References:

1. Clubb SL, Frenkel JK. *Sarcocystis falcatula* of opossums: transmission by cockroaches with fatal pulmonary disease in psittacine birds. *J Parasitol.* 1992;78:116–124.

2. Dubey JP, Venturini L, Venturini C, Basso W, Unzaga J. Isolation of *Sarcocystis falcatula* from the South American opossum (*Didelphis albiventris*) from Argentina. *Vet Parasitol.* 1999;86:239–244.
3. Dubey JP, Lindsay DS, Rezende PCB, Costa AJ. Characterization of an unidentified *Sarcocystis falcatula*-like parasite from the South American opossum, *Didelphis albiventris* from Brazil. *J Eukaryot Microbiol.* 2000;47:538–544.
4. Dubey JP, Garner MM, Stetter MD, Marsh AE, Barr BC. Acute sarcocystic falcatula-like infection in a carmine bee eater and immunohistochemical cross-reactivity between *Sarcocystis falcatula* and *Sarcocystis neurona*. *J Parasitol* 2001; 87(4):824–832.
5. Ecco R, Luppi MM, Malta MC, Araújo MR, Guedes RM, Shivaprasad HL. An outbreak of sarcocystosis in psittacines and a pigeon in a zoological collection in Brazil. *Avian Dis.* 2008;52:706–710.
6. Elsheikha HM, Saeed MA, Fitzgerald SD, Murphy AJ, Mansfield LS. Effects of temperature and host cell type on the *in vitro* growth and development of *Sarcocystis falcatula*. *Parasitol Res.* 2003;91:22–26.
7. Hemenway MP, Avery ML, Ginn PE, Schaack S, Dame JB, Greiner EC. Influence of size of sporocyst inoculum upon the size and number of sarcocysts of *Sarcocystis falcatula* which develop in the brownheaded cowbird. *Vet. Parasitol.* 2001;95:321–326.
8. Jacobson ER, Gardner CH, Nicholson A, Page CD. Sarcocystosis encephalitis in a cockatiel. *J. Am. Vet. Med. Assoc.* 1984;185:94–96.
9. Konradt G, Bianhi MV, Leite-Filho RV, da Silva BZ, Soares RM, Pavarini SP, Driemeier D. Necrotizing meningoencephalitis caused by *Sarcocystis falcatula* in a bare faced ibis. *Parasitol Res* 2017 116(2):809–812.
10. Luznar SL, Avery ML, Dame JB, Mackay RJ, Greiner EC. Development of *Sarcocystis falcatula* in its intermediate host, the brown-headed cowbird (*Molothrus ater*). *Vet. Parasitol.* 2001;95:327–334.
11. Neill PJG, Smith JH, Box ED. Pathogenesis of *Sarcocystis falcatula* (Apicomplexa: Sarcocystidae) in the budgerigar (*Melopsittacus undulatus*), IV. Ultrastructure of developing, mature and degenerating sarcocystis. *J. Protozool.* 1989;36:430–437.
12. Smith JH, Meier JL, Neill PJG, Box ED. Pathogenesis of *Sarcocystis falcatula* in the budgerigar, I. Early pulmonary schizogony. *Lab. Invest.* 1987a;56:60–71..
13. Smith JH, Meier JL, Neill PJG, Box ED.. Pathogenesis of *Sarcocystis falcatula* in the budgerigar, II. Pulmonary pathology. *Lab Invest.* 1987b;56:72–84.
14. Smith JH, Neill PJG, Box ED. Pathogenesis of *Sarcocystis falcatula* (Apicomplexa: Sarcocystidae) in the budgerigar (*Melopsittacus undulatus*), III. Pathologic and quantitative parasitologic analysis of extrapulmonary disease. *J. Parasitol.* 1989;75:270–287.
15. Smith JH, Neill PJ, Dillard EAI, Box ED. Pathology of experimental *Sarcocystis falcatula* infections of canaries (*Serinus canaries*) and pigeons (*Columba livia*). *J Parasitol.* 1990;79:59–68.
16. Suedmeyer WK, Bermudez A, Barr BC, Marsh AE. Acute pulmonary *Sarcocystis falcatula*-like infection in three Victoria crowned pigeons (*Goura Victoria*) housed indoors. *J Zoo Wild Med.* 2001;32:252–256.

CASE IV: BA214/11 B1 (JPC 4035109).

Signalment: 2 year old, male entire, *Pogona vitticeps*, bearded dragon

History: An outbreak of fungal dermatitis occurred in a colony of bearded dragons.



Presentation, bearded dragon. A round 1.25x1.5cm cutaneous plaque is present on the dorsal midline. (Photo courtesy of: Royal (Dick) School of Veterinary Studies, Easter Bush Campus, Roslin, Midlothian, EH25 9RG, UK., www.ed.ac.uk/vet)

Seven responded successfully and six were euthanized with follow-up 3 months later apparently showing complete resolution of the disease in all animals. Several months later, this animal was presented with new skin lesions on the dorsum, left stifle and left hock which were treated with both topical preparations (F10, iodine and clotrimazole) and systemic antifungals (itraconazole). The animal's condition failed to respond to therapy and due to continued deterioration (including development of coelomic distension) it was euthanized in March 2011.

Gross Pathology: An adult (2 year old), male entire, bearded dragon, weighing 553g was presented for necropsy examination. On the midline of the dorsum, there was a large (1.27cm x 1.5cm), focal, well demarcated, raised, black, irregularly rounded midline plaque. There were similar smaller lesions, which were discoloured dark yellow to brown, located over the right elbow (1cm diameter), left elbow (8mm diameter) the lateral aspect of the right knee (5mm diameter), the plantar surface of the left foot (8mm), and the plantar surface of the right foot (1mm). The liver was mottled pink to yellow to red with three, well-demarcated,

firm, raised, pale yellow, irregularly rounded nodules ranging from 8-20mm in diameter. One nodule was incised and contained yellow to brown, granular material. There was a similar 5mm diameter lesion present within the omentum, near the spleen.

Laboratory Results: 3 months prior to euthanasia blood was evaluated to assess liver function and white cell count while on treatment. Total protein=74 g/l (Range=52-72); AST=103 U/l (Range=0-80); CK=5830 (Range=0-550); Leukocytes =0.4 cells x10⁹/L (Range=1.5-8.5). The owner was given a guarded prognosis due to the low leukocyte count. Cultures submitted previously from this colony from similar lesions were identified as *Chrysosporium anamorph* of *Nannizziosis vriesii* (CANV).

Microscopic Description:

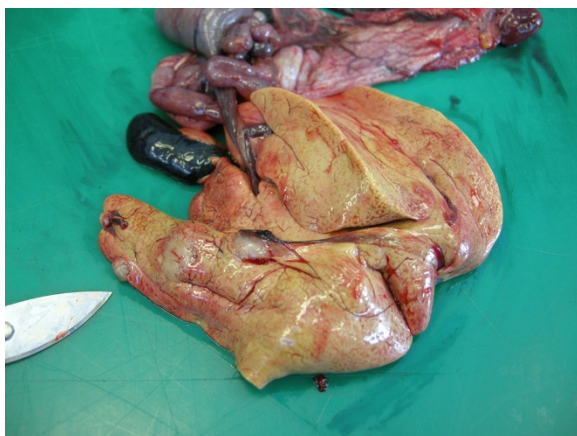
Elbow skin (1 section) –There is full thickness loss of cellular and nuclear detail extending into the dermis (necrosis). In this area, multifocal remnants of the overlying stratum corneum are present and there are scattered subcorneal accumulations of palely basophilic 1µm round to oval organisms (yeasts-presumptive). Multifocally



Scaled skin, bearded dragon. Closeup of the dorsal cutaneous plaque. (Photo courtesy of: Royal (Dick) School of Veterinary Studies, Easter Bush Campus, Roslin, Midlothian, EH25 9RG, UK., www.ed.ac.uk/vet)

throughout the necrotic tissue there are negatively stained outlines of fungal hyphae (approx 2-4um diameter with occasional septae, branching and terminal buds) with parallel walls and occasional segmentation. At the edges of the necrosis there are large numbers of epithelioid macrophages with multinucleated giant cells, heterophils and scattered lymphocytes with mild to moderate vascular congestion. Scattered haemorrhage is present. Smaller granulomas which are centrally necrotic and contain fungal organisms (as described above) are present around the edges of the necrotic region. Intact skin is mildly to moderately hyperplastic with multifocal, mild heterophilic and mononuclear inflammation within the superficial dermis.

Liver– There is a focal, large centrally necrotic area composed within the hepatic parenchyma which contains fungal organisms as previously described. Histiocytic, lymphocytic and heterophilic inflammation is present around the periphery with moderate to large numbers of multinucleated giant cells with scattered admixed fibroblasts. Multifocal, small granulomas are present around the periphery

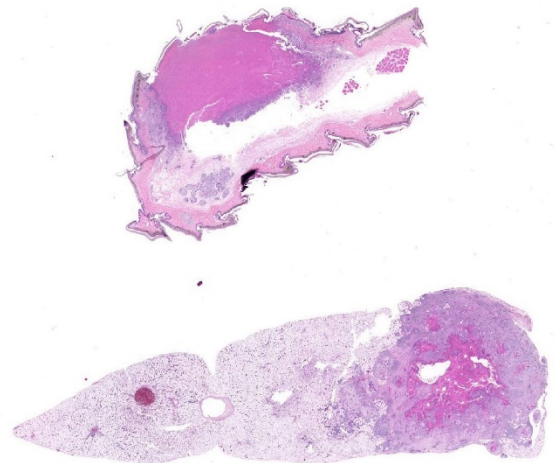


Scaled skin and liver, bearded dragon. Coalescing granulomas with a brightly eosinophilic necrotic center are present within the skin and the liver. (HE, 5X)

of the large necrotic lesion. The surrounding hepatocytes have marked, diffuse, swelling with large numbers of small to moderately sized, well demarcated, clear intracytoplasmic vacuoles (consistent with lipid) which often displace the nucleus to the periphery.

Contributor's Morphologic Diagnoses:

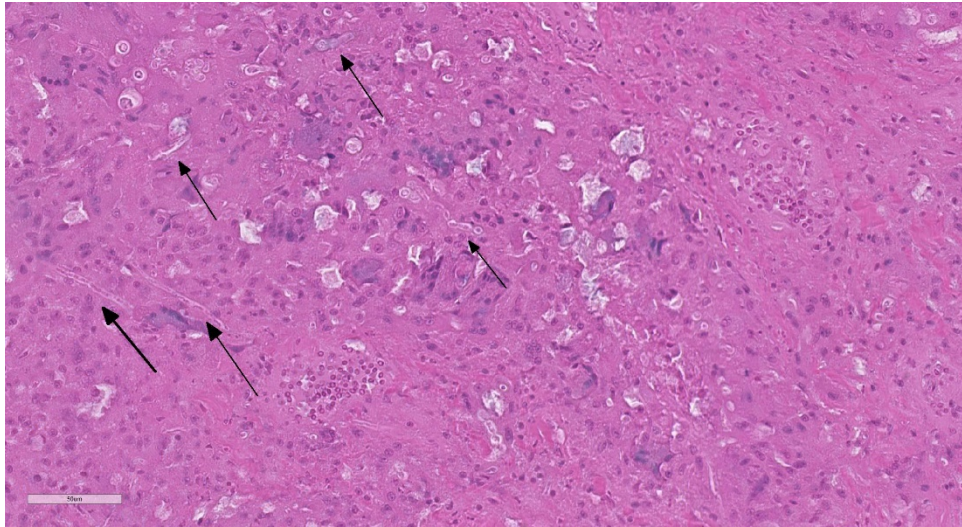
- 1) Severe, granulomatous and necrotising, ulcerative dermatomycosis and cellulitis with intra-lesional fungal organisms – elbow skin
- 2) Multifocal, severe, granulomatous hepatitis with intra-lesional fungal organisms – liver
- 3) Diffuse, moderate, hepatic lipodosis – liver



Skin, bearded dragon: There are well-formed granulomas within the dermis, with large epithelioid macrophages and more brightly eosinophilic foreign body type macrophages. These granulomas will later coalesce. (HE, 106X)

NOTE: Similar inflammation was present in sections from the dorsal skin lesion, lung and omental nodule (not included in the submission). Given the previous isolation of CANV in this colony/animal, the progression of the disease and the histological features of

the sections this was considered to be the most likely diagnosis.



Skin, bearded dragon. Within the necrotic centers, fungal hyphae and arthroconidia may be seen in bas-relief.

Contributor's Comment: Saprophytic fungi are often implicated in dermatomycoses of snakes and lizards and infections are often associated with poor husbandry, poor nutrition or immunosuppression.^{8,11} *Chrysosporium* species may be isolated from normal reptile skin but the most clinically important (and rarely isolated) is considered to be *Chrysosporium anamorph* of *Nannizziopsis vriesii* (CANV).^{8,11} This is a keratinophilic ascomycetous fungus reported to be the primary pathogen of "yellow fungus disease", an emerging disease in reptiles.¹⁻¹² CANV is a non-pigmented fungus (hyalohyphomycosis). CANV has been reported in a number of chameleon species, geckos, bearded dragons, leopard geckos, a girdled lizard, several snake species and saltwater crocodiles, among others.¹⁻¹⁶ CANV is difficult to identify on culture and may be mistaken for any of the following: *Trichophyton*, *Geotrichum*, *Malbranchea* and *Trichosporon*.^{6,12} Generally more than one animal is infected in an outbreak

(suggesting that it is contagious) especially in bearded dragons. In this species it causes

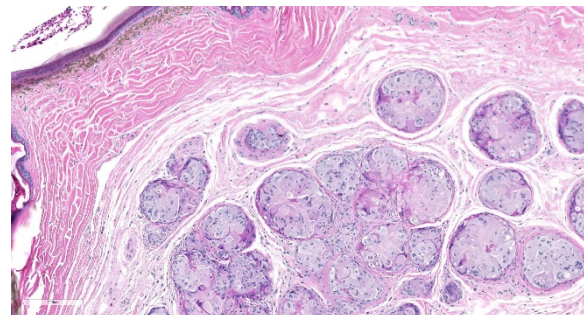
granulomatous dermatitis which often becomes systemic^{1,4,5,9}. This presents as multifocal, yellow-brown discoloured lesions on the body with crusting and/or hyperkeratotic plaques. These lesions tend to develop necrosis, leading to sloughing of the skin and ulceration. This is followed by invasion of the

musculature and bones and may progress to lethal systemic infection.

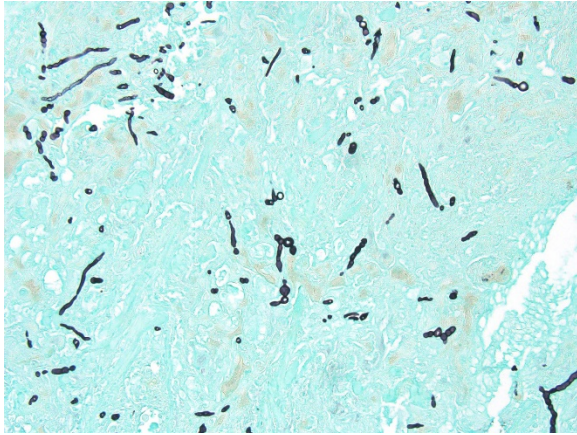
Conference participants discussed the orthokeratotic hyperkeratosis and elevation of the scale overlying the granulomas as potentially a localized form of dysecdysis.

Contributing Institution:

Royal (Dick) School of Veterinary Studies
Easter Bush Campus
Roslin, Midlothian
EH25 9RG UK. www.ed.ac.uk/vet



Skin, bearded dragon. Within the necrotic centers, fungal hyphae and arthroconidia may be seen in bas-relief.



Skin, bearded dragon: Fungal hyphae and arthroconidia (arrows) are easily demonstrated with a silver stain. (Grocott's methenamine silver, 400X)

JPC Diagnosis: 1. Scaled skin: Dermatitis, granulomatous and necrotizing multifocal to coalescing, severe, with numerous intra- and extracellular fungal hyphae and epidermal arthroconidia.

2. Liver: Hepatitis, granulomatous, focally extensive, severe, with numerous intra- and extracellular fungal hyphae.

3. Liver, hepatocytes: Lipidosis, diffuse, severe.

JPC Comment: Since the submission of this case in 2013, much has been written about the *Chrysosporium* anamorph of *Nannizziopsis vriesii* (CANV) and related pathogens (referred to as *Chrysosporium* anamorph of *Nannizziopsis vriesii* complex (CANVC) which cause disease in reptiles. Anamorphs, most often seen in the *Ascomycota*, are asexual reproductive states (i.e. these fungi do not produce a fruiting body).

CANV is a keratophilic species that lives primarily on fragments of feathers and hair in the soil. While most cases of CANV have been identified in reptiles, related species of *Chrysosporium* infection have been documented in other species – *C. pannicola* (dog, horse, human), *C. tropicum* (chickens),

Table 1. Proposed species causing infection in reptiles

<i>Chrysosporium</i> -related fungi	Reptile species
<i>Nannizziopsis</i> Currah (1985)	
<i>N. arthrosporioides</i> Stchigel et al. (2013)	Water dragon (<i>Physignathus</i> sp.)
<i>N. barbata</i> Sigler et al. (2013)	Coastal bearded dragon (<i>Pogona barbata</i>)
<i>N. chlamydospora</i> Stchigel et al. (2013)	Inland bearded dragon (<i>Pogona vitticeps</i>)
<i>N. crocodili</i> Sigler et al. (2013)	Saltwater crocodile (<i>Crocodylus porosus</i>)
<i>N. dermatidis</i> Sigler et al. (2013)	Chameleons, geckos
<i>N. draconii</i> Cabañes et al. (2013)	Inland bearded dragon
<i>N. guarroi</i> Cabañes et al. (2013)	Green iguana (<i>Iguana iguana</i>), inland bearded dragon, lizard (<i>Agama agama</i>), snake
<i>N. pluriseptata</i> Stchigel et al. (2013)	Skink lizard (<i>Eumeces inexpectatus</i>)
<i>N. vriesii</i> Currah (1985)	Lizard (<i>Ameiva</i> sp.)
<i>Paranannizziopsis</i> Sigler et al. (2013)	
<i>P. australiensis</i> Sigler et al. (2013)	Northern tuatara (<i>Sphenodon punctatus punctatus</i>), coastal bearded dragon, aquatic file snake (<i>Acrochordus</i> sp.)
<i>P. californiensis</i> Sigler et al. (2013)	Tentacled snake (<i>Erpeton tentaculatum</i>)
<i>P. crustacea</i> Sigler et al. (2013)	Tentacled snake
<i>P. longispora</i> Sigler et al. (2013)	Tentacled snake
<i>Ophidiomyces</i> Sigler et al. (2013)	
<i>O. ophiodiicola</i> Sigler et al. (2013)	Snakes

Proposed CAMVC species and infected reptile species.14,15

and *C. keratinophilum* and *C. zonatum* (human).⁵

In 2013, Stchigel et al.¹⁴ and Sigler et al.¹⁵ published a taxonomic revision of *Chrysosporium*-related fungi and their likely host specificity (Table 1).⁵ In most hosts, the lesion begins in the skin, with dermal and subcutaneous heterophilic granulomas which eventually extend into underlying bone, muscle, and disseminate to viscera, as seen in this case.¹⁶ It is difficult, if not impossible, to differentiate members of the CANV in tissue section.⁵

A related fungus, *Ophidomyces ophidiicola*, which causes similar lesions in snakes was reassigned from the CANVC in 2013 to its own genus.¹⁵ A case of this was published in the WSC earlier this year (Conference 8, Case 4).

Conference participants discussed the uniqueness of the epidermal lesion in this case. While granuloma formation is the rule in this infection, some participants interpreted with large area of necrosis within the dermis extending to the overlying epidermis as an infarct, and one participant saw hyphae involving a cutaneous vessel. The moderator commented that this was a unique presentation in his experience. Conference participants also discussed the orthokeratotic hyperkeratosis and elevation of the scale overlying the granulomas as potentially a localized form of dysecdysis.

References:

1. Abarca LM, Martorell J, Castella G, Ramis A & Cabanes EJ. Dermatormycosis in a pet inland bearded dragon (*Pogona vitticeps*) caused by a *Chrysosporium* species related to *Nannizziopsis vriesii*. *Veterinary Dermatology* 2009; 20, 295-299
2. Abarca ML, Martorell J, Castellá G, Ramis A & Cabanes EJ. Cutaneous hyalohyphomycosis caused by a *Chrysosporium* species related to *Nannizziopsis vriesii* in two green iguanas (*Iguana iguana*). *Medical Mycology* 2008; 46: 349–54.
3. Bertlesen MF, Crawshaw GJ, Sigler L, Smith DA. Fatal cutaneous mycosis in tentacled snakes (*Erpeton tentaculatum*) caused by the *Chrysosporium* anamorph of *Nannizziopsis vriesii*. *J Zoo Wildl Med* 2005; 36, 82-87
4. Bowman MR, Paré JA, Sigler L, Naeser JP, Sladky KK, Hanley CS, Helmer P, Phillips LA, Browsers A & Porter R. Deep fungal dermatitis in three inland bearded dragons (*Pogona vitticeps*) caused by the *Chrysosporium* anamorph of *Nannizziopsis vriesii*. *Medical Mycology* 2007; 45, 371-376
5. Cabanes FJ, Sutton DA, Guarro J. *Chrysosporium*-related fungi and reptiles: a fatal attraction. *PLOS Pathogens*, 2014; 10(10): 31004367.
6. Hedley J, Eatwell K, Hume L. Necrotising fungal dermatitis in a group of bearded dragons (*Pogona vitticeps*). *Veterinary Record* 2010; 166, 464-465
7. Hellebuyck T, Baert K, Pasmans F, Van Waeyenberghe L, Beernaert L, Chiers K, De Backer P, Haesebrouck F & Martel A. Cutaneous hyalohyphomycosis in a girdled lizard (*Cordylus giganteus*) caused by the *Chrysosporium* anamorph of *Nannizziopsis vriesii* and successful treatment with voriconazole. *Veterinary Dermatology* 2010; 21, 429-433
8. Jacobson ER, Cheatwood JL, Maxwell LK. Mycotic diseases of reptiles. *Seminars in Avian and Exotic Pet Medicine* 2000; 9: 94–101
9. Johnson RSP, Sangster CR, Sigler L, Hambleton S & Paré JA. Deep fungal dermatitis caused by the *Chrysosporium* anamorph of *Nannizziopsis vriesii* in

- captive coastal bearded dragons (*Pogona barbata*). *Australian Veterinary Journal* 2011; 12; 515-519.
10. Lorch JM, Knowles S, Lankton JS, Michell K, Edwards JL, Kapfer JM, Staffen RA, Wild ER, Schmidt KZ, Ballmann AE, Blodgett D, Farrell RM, Bloriosos BM, Last LA, Price SJ, Schular KL, Smith CE, Wellehan JFX, Blehert DS. Snake fungal disease; an emerging threat to wild snakes. *Phil Trans R Soc B* 2015; 371:20150457.
 11. Paré JA, Coyle KA, Sigler L, Maas AK III & Mitchell RL. Pathogenicity of the *Chrysosporium* anamorph of *Nannizziopsis vriesii* for veiled chameleons (*Chamaeleo calyptratus*). *Medical mycology* 2006; 44:25-31
 12. Paré JA, Sigler L, Rosenthal KL *et al.* Microbiology. Fungal and bacterial diseases of reptiles. In: Mader DR, ed. *Reptile Medicine and Surgery*, 2nd ed. St Louis, MO: Saunders Elsevier, 2006: 217–38
 13. Paré JA, Sigler L, Hunter DB, Summerhall RC, Smith DA & Machin KL. Cutaneous mycoses in chameleons caused by the *Chrysosporium* anamorph of *Nannizziopsis vriesii* (Apinis) Currah. *J Zoo Wildl Med* 1997;28:443-453
 14. Stchigel AM, Sutton DA, Cano-Lira JF, Cabanes FJ, Abarca L, Tintelneot K, Wickes BL, Garcia D, Guarro J.
 15. Sigler L, Hambieton S, Pare. Molecular characterization of reptile pathogens currently known as members of the *Chrysosporium* anamorph of *Nannizziopsis vriesii* complex and relationship with some human-associated isolates. *J Clin Microbiology* 2013: 51(10)3338-3357.
 16. Toplou DE, Terrell SP, Sigler L, Jacobson ER. Dermatitis and cellulitis in leopard geckos cause by the *Chrysosporium* anamorph of *Nannizziopsis vriesii*. *Vet Pathol* 2012; 50(4): 585-589.

Self-Assessment - WSC 2018-2019 Conference 18

1. Which of the following has not been identified as a predisposing factor for atherosclerosis?
 - a. Inflammation
 - b. Genetics
 - c. Hypertension
 - d. Diet

2. Chimpanzees are excellent models for coronary atherosclerosis. True or False?
 - a. True
 - b. False

3. Which of the following species of mycobacterium is the LEAST commonly identified in cases of avian mycobacteriosis?
 - a. *M. genavense*
 - b. *M. avium subsp. paratuberculosis*
 - c. *M. avium subsp. avium*
 - d. *M. intracellulare*

4. Schizogony in which organ often is a component of fatal *Sarcocystis* infection in psittacines?
 - a. Lung
 - b. Liver
 - c. Heart
 - d. Brain

5. Which of the following is not a member of the *Chrysosporium* anamorph of *Nannizziopsis vriesii* complex?
 - a. *Chrysosporium pannicola*
 - b. *Chrysosporium keratinophilum*
 - c. *Chrysosporium zonatum*
 - d. *Ophidiomyces ophidiicola*

Please email your completed assessment to Ms. Jessica Gold at Jessica.d.gold2.ctr@mail.mil for grading. Passing score is 80%. This program (RACE program number) is approved by the AAVSB RACE to offer a total of 0.5 CE Credits, with a maximum of 12.5 CE Credits being available to any individual Veterinary Medical Professionals for the 2017-2018 Wednesday Slide Conference. This RACE approval is for the subject matter categories of: SCIENTIFIC using the delivery method of NON-INTERACTIVE DISTANCE. This approval is valid in jurisdictions which recognize AAVSB RACE; however, participants are responsible for ascertaining each board's CE requirements. RACE does not "accredit", "endorse" or "certify" any program or person, nor does RACE approval validate the content of the program.

Please email your completed assessment to Ms. Jessica Gold at Jessica.d.gold2.ctr@mail.mil for grading. Passing score is 80%. This program (RACE program number) is approved by the AAVSB RACE to offer a total of 0.5 CE Credits, with a maximum of 12.5 CE Credits being available to any individual Veterinary Medical Professionals for the 2017-2018 Wednesday Slide Conference. This RACE approval is for the subject matter categories of: SCIENTIFIC using the delivery method of NON-INTERACTIVE DISTANCE. This approval is valid in jurisdictions which recognize AAVSB RACE; however, participants are responsible for ascertaining each board's CE requirements. RACE does not "accredit", "endorse" or "certify" any program or person, nor does RACE approval validate the content of the program.

**Joint Pathology Center
Veterinary Pathology Services**



WEDNESDAY SLIDE CONFERENCE 2018-2019

C o n f e r e n c e 19

13 February 2019

CASE I: 08-36807 (JPC 4048498).

Signalment: Female, Soft-shelled Turtle (*Apalone ferox*, formerly *Trionyx ferox*), Unknown age (adult)

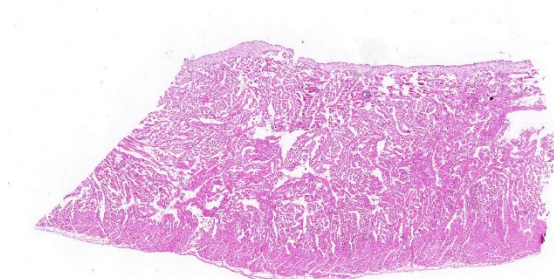
History: Found dead in an aquarium

Gross Pathology: Multifocal hyperkeratotic and raised circumscribed lesions on the skin of ventral neck and ventral body (plastron) were observed on gross examination. The carcass was found in a fair to poor body condition. Liver was enlarged and pale. Intestines had watery grayish green contents. There was accumulation of hard dry excreta in the distal large intestine (coprostitis). Several developing ova were seen in the coelomic cavity. Stomach was empty. No other grossly visible lesion.

Laboratory results: Several tissues were positive for ranavirus by PCR.

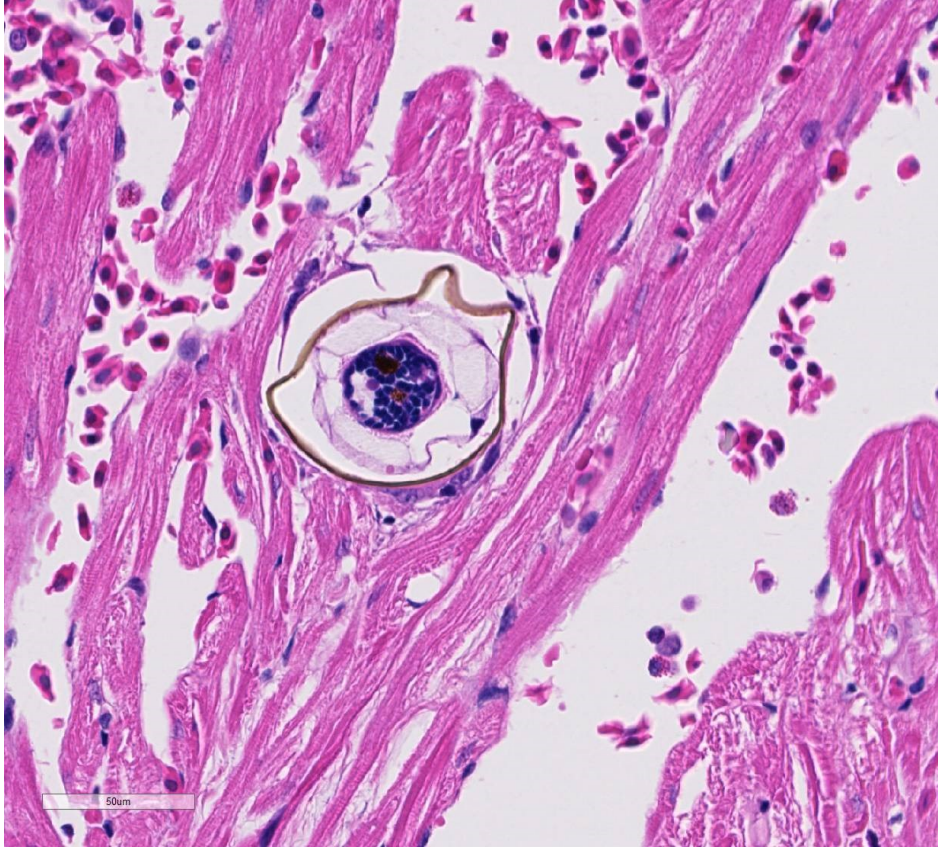
Microscopic Description:

Several myocardial fibers of the sections of heart were disrupted by parasite eggs measuring up to 100x50µm in size. The eggs had 2-3 µm in diameter yellowish refractile often fragmented wall and occasionally contained 2-4 µm in diameter blue round



Heart, turtle: A section of ventricular myocardium is submitted for examination. Multiple egg-induced granulomas may be seen from this magnification. The spongy appearance of the myocardium is normal for reptiles. (HE, 5X)

aggregates (miracidium). On the walls of few of these eggs were 5-7 µm in length projecting lateral spines. In some areas, the eggs were surrounded by multinucleated foreign body type giant cells. The eggs were diffusely disseminated in several tissues including the intestines, spleen, liver, kidney and thyroid gland (sections not included). Within vascular lumens in some sections of the heart and liver were about 150 to 300 µm in size adult trematodes. Sections of skin had deep dermal focally extensive areas of necrosis surrounded by moderate amount of collagen fibers occasionally infiltrated by few to several lymphocytes, plasma cells and macrophages. There were no other remarkable lesions.



Heart, turtle: Trematode eggs are scattered throughout the myocardium. The eggs have a thin brown shell and a miracidium within. Eggs are surrounded by one or more epithelioid or multinucleated giant cell macrophages. (HE, 400X)

Contributor's Morphologic Diagnoses:

Heart: Myocarditis, Granulomatous, mild to moderate with trematode eggs and occasional intravascular trematodes consistent with Spirorchid sp.

Granuloma, diffuse moderate to marked disseminated in several organs with trematode eggs and intravascular trematodes (spirorchid), Disseminated Spirorchidiasis.

Contributor's Comment: Intravascular trematodes (blood flukes) are reported in mammals, birds, reptiles and fish.⁵ Various species of intravascular spirorchid trematodes, including *Learedius learedi*, *Carettacola hawaiiensis*, *Hapalotrema dorsopora* and *H. postorchis* are reported in turtles. Specific species identification was

not made in the current case. Adult spirorchids inhabit the circulatory system of infected hosts. Eggs may be observed in almost every tissue in the body including the brain, heart, lung, liver, spleen, urinary bladder, shell and slat glands; and may initiate mild to severe granulomatous inflammation.

Infected animals may show debilitation, edema of the limbs, and secondary bacterial infections and death. Diagnosis is usually made at necropsy or upon identification of parasites in tissue sections.² Serology may be useful in

evaluating exposure to the infection, although it may not reflect worm burdens.⁵ Microscopic lesions reported in turtles infected with spirorchids include vasculitis (lymphoplasmacytic endarteritis), thrombosis, perivascular hemorrhage, granulomatous cystitis, enteritis, pneumonitis, hepatitis, meningitis, encephalitis, and cirrhosis.^{2,4} Remarkable vasculitis was not seen in this case. Coprostitis and poor body condition could be associated to intestinal infection with consequent maldigestion and malabsorption.

Contributing Institution:

The University of Georgia, College of Veterinary Medicine, Department of Pathology, Tifton Veterinary Diagnostic and Investigational Laboratory. Tifton, GA

31793,

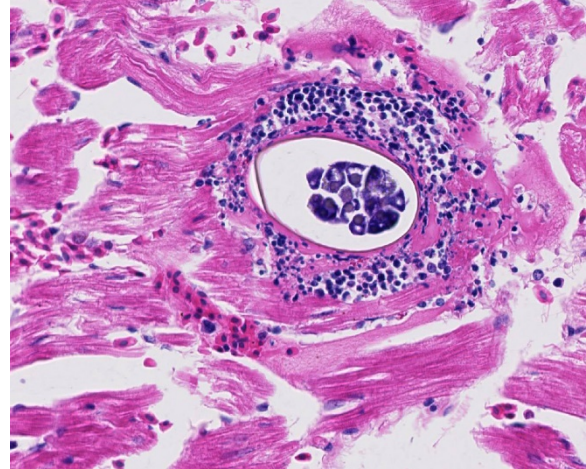
<http://www.vet.uga.edu/dlab/tifton/index.php>

JPC Diagnosis: Heart, ventricular myocardium: Trematode eggs, intravascular and intrahistiocytic, with mild multifocal cardiomyocyte degeneration.

JPC Comment: The superfamily Schistosomatoidea contains intravascular flukes in three families – Sanguinocolidae, Schistosomatidae, and Spirorchidae.

Schistosomes are grossly visible flukes which cause disease in a wide range of birds and mammals. These parasites have separate genera but the male and female are joined throughout much of their extended life cycle (ranging from 3-30 years). They feed on blood cells and globulins, which are digested in a blind digestive tract with residua regurgitated into the host's circulation.¹ In humans, schistosomiasis (Bilharzia) affects millions of people with up to 200 million on prevention annually.³ The most widespread and pathogenic human schistosomes are *S.mansoni*, *S. japonicum*, and *S. haematobium*. *S. mansoni* and *S. japonicum* live within mesenteric veins, and their eggs are trapped within intestinal walls, resulting in acute bloody diarrhea, and chronic, hepatosplenic granulomatous disease and fibrosis. The eggs of these two flukes are excreted in the feces. *S. haematobium* lives within the venous plexi adjacent to the urinary bladder resulting in urinary bladder ulceration and hematuria, and chronically in proliferative and fibrosis lesion of the urinary bladder, and less commonly, ureters. Its eggs are excreted in the urine.¹

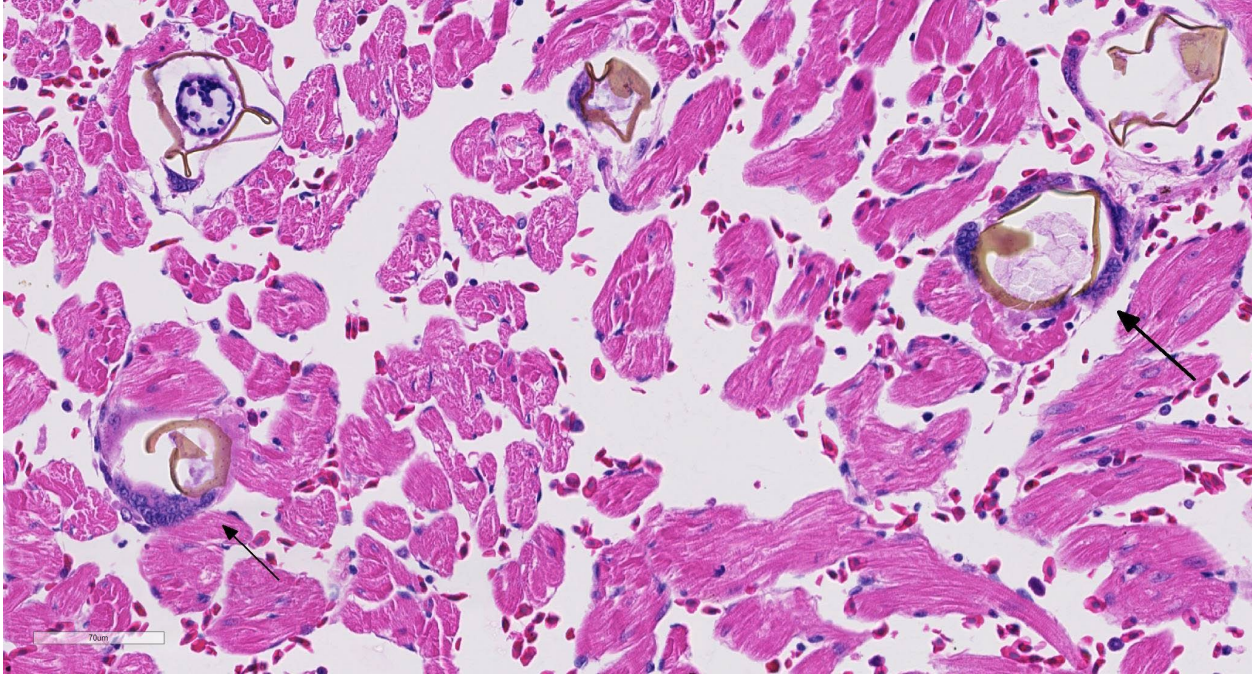
The family Spirorchidae, parasites of turtles include 16 recognized genera, and the flukes live within the cardiovascular system. Eggs of these parasites lodge within all organs of the body, forming microgranulomas (as seen



Heart, turtle: Rarely, degenerating eggs incite acute inflammation within the myocardium (HE, 400X)

in this slide.) The life cycle of spirorchid flukes of freshwater turtles involves a pulmonate snail; that of marine turtles is largely unknown, although a common species of blood fluke, *Learedius learedi*, has been identified in the limpet *Fissurella nodosa*.⁶

Of particular current interest is how the lifecycle of blood flukes is completed at all, without direct access of female flukes to intestinal (or in some cases) urinary bladder. Eggs are laid directly into the bloodstream, and form microgranulomas within tissues. Over the last decade, researchers in the area of human schistosomiasis have begun to unravel the way that flukes and their eggs exploit the immune system to get into the external environment.³ After egg shell components facilitate endothelial adhesion within intestinal vessels, the microgranuloma surrounding the egg actually facilitates the translocation process from intestinal vessels, through the lamina propria and mucosal epithelium and ultimately into the intestinal lumen. The importance of the immune system has been demonstrated by the low fecal egg counts seen in infected immunosuppressed mice; recent research has also focused on the importance of the



Heart, turtle: Degenerate or fragmented eggs are surrounded by multinucleated foreign body-type macrophages. (HE, 400X)

intestinal microbiome as well. It is likely that a similar process occurs within *Spirorchis*-infected turtles as well.³

The moderator discussed an upcoming paper (currently in press) which identifies a fatal outbreak of spirorchid parasites in black pond turtles from Thailand.

References:

1. Gryseels, B. Schistosomiasis. *Infect Dis Clin N Am* 2012; 26:383-397.
2. Jacobson, ER. Parasites and parasitic diseases of reptiles. Spirorchidae In: Jacobson (Edit). *Infectious diseases and pathology of reptiles. Color atlas and text.* 2007; 583-584. Taylor and Francis CRC press.
3. Schwartz C, Fallon PG. Schistosoma “eggs-iting the host: granuloma formation and egg excretion. *Frontiers in Immunol* 2018;
4. Wolke RE, Brooks DR, George A. Spirorchidiasis in Loggerhead Sea Turtles

(*Caretta caretta*): *Pathology. J Wildl Dis* 1982; 18 (2): 175-185.

5. Work TM, Balazs GH, Schumacher JL, Amarisa M. Epizootiology of spirorchiid infection in green turtles (*Chelonia mydas*) in Hawaii. *J Parasitol* 2005; 91(4): 871–876.

6. Yonkers SB, Schneider R, Reavill DR, Archer LL, Childress AL, Wellehan JFX. Coinfection with a novel fibropapilloma-associated herpesvirus and a novel *Spirorchis* sp. in an eastern box turtle in Florida.

CASE II: TAMU-2 2014 (JPC 4054746).

Signalment: Adult, female, Leopard Tortoise (*Stigmochelys pardalis*)

History: Animal presented to clinic for dyspnea, oral/ocular/nasal discharge, lethargy, anorexia and mucoid cloacal discharge. Eyes matted shut. No fecal/urinary production. This recently purchased tortoise arrived emaciated and



Colon, leopard tortoise. There is diffuse, severe necrotizing colitis. (Photo courtesy of Department of Veterinary Pathobiology, College of Vet Med and Biomedical Sciences, Texas A&M University, College Station, TX USA 77843-4467)

anorectic with oculonasal discharge. Animal had anemia, hyperuricemia, hypercalcemia and hyperkalemia, and renal disease was suspected. Radiographs indicated possible pneumonia. Treated for 3 days, when owner opted for humane euthanasia.

Gross Pathology: The carapace had “pyramiding” indicating metabolic disease. Other significant gross lesions included: fat pad loss (emaciation), severe enterocolitis, hepatic lipidosis, pleuritis and pulmonary emphysema, and bilateral conjunctivitis.

Laboratory results: PCV 17 with ++ polychromasia WBC - 9500, 69% heterophils, 13% lymphocytes, 15% monocytes, 2% eosinophils 1% basophils K+ 8.5 mmol/L, Uric Acid >25mg/dL, Bile Acids= 35 umol/L, Ca+ 20 mg/dL

Microscopic Description:

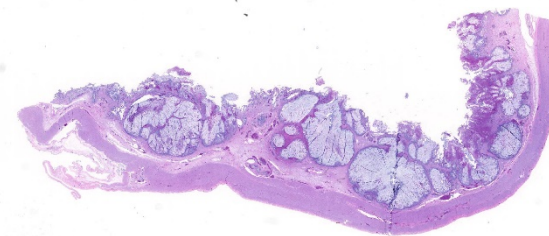
A section of terminal colon is presented. The long folds are an anatomic normal. Large segments of mucosa, especially the length of the folds, are covered by necrotic mucosa, cell debris and heterophils and macrophages, and saccules of the colon are distended by mucus with a mild, necrotic, pleocellular detritus and numerous bacteria. Viable

mucosa is disorganized and not the normal, simple, columnar epithelium. Colonic epithelium is piling up. Cells have large, hypochromic nuclei with prominent nucleoli and with somewhat granular, poorly defined eosinophilic cytoplasm. Small numbers of granulocytes exocytose. The submucosa has distended vessels (congestion) with some extravasated erythrocytes, and tissues are rarified (edema) with a mild to moderate granulocytic, histiocytic and lymphocytic infiltrate. The muscularis is intact, and coelomitis is not noted.

In the necrotic cell debris and in the viable epithelium are many, 20-35µ amoeba trophozoites with usually a single endosome and granular or globular cytoplasm (*Entamoeba* sp.). Additionally, many of the epithelial nuclei have variable numbers (1 to 8) of eosinophilic meronts. Pairs and clusters of these meronts, and clusters like merozoites of these coccidian are noted. Rare megaschizonts may be seen.

Contributor’s Morphologic Diagnoses: Necrogranulocytic/heterophilic, hyperplastic and mucinous colitis with amoeba and intranuclear coccidian.

Contributor’s Comment: This is apparently a common presentation in land tortoises, based on cases published.³ The animal was euthanized; however, she had a severe enterocolitis. The severity of the GI



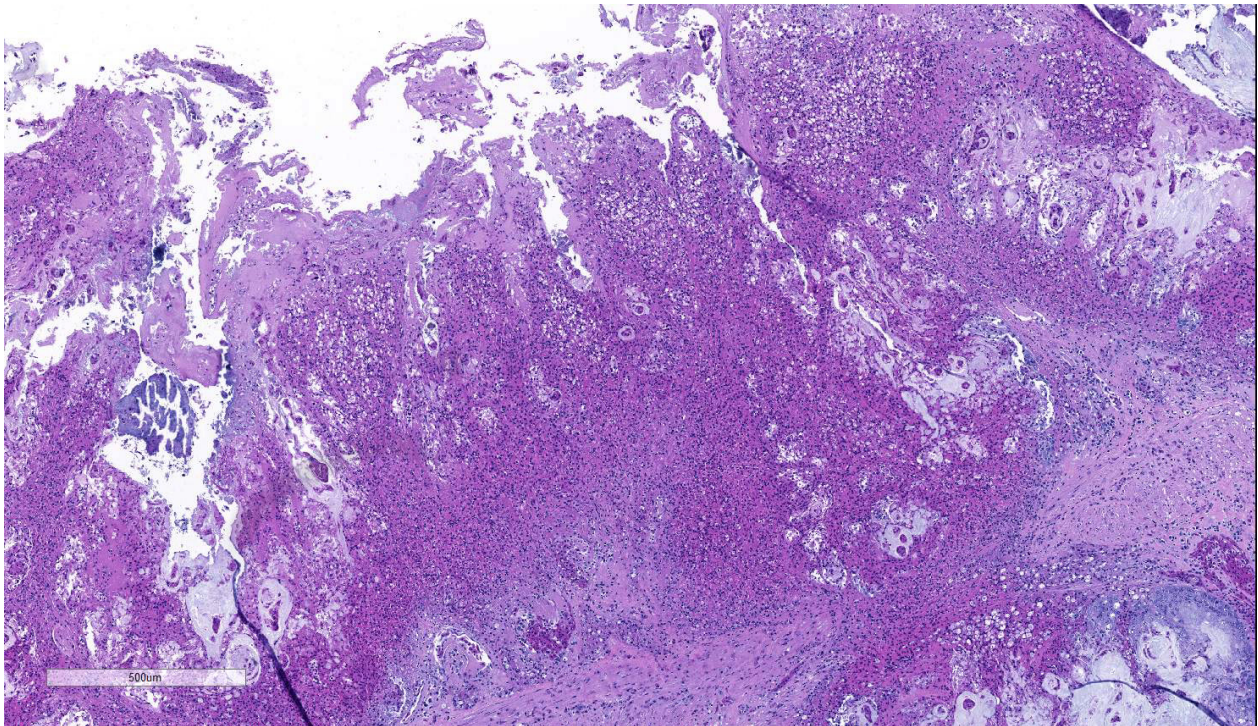
Colon, leopard tortoise. There is multifocal necrosis of the colonic mucosa which is replaced by eosinophilic coagulum. (HE, 7X)

lesion and the two associated pathogens were the reasons for the choice of our tissue selection. The coexistence of the presumed *Entamoeba* and intranuclear coccidian is not unique to our case, because it is reported.

Because no bacterial pathogens or their toxins (*Salmonella*, *Clostridium*, *Citrobacter* etc.) were recovered from this tortoise, the *Entamoeba* was considered a significant pathogen.^{2,6,9,13} *Entamoeba invadens* has been isolated from a leopard tortoise, but it should be remembered that this organism is considered a commensal to most species of chelonids. Epizootics associated with large numbers of amoebae in reptiles are reported⁶, but many are not tested with molecular procedures. It has been reported that the morphology of amoeba especially the morphology of the trophozoite in tissue is not adequate to speciate this protozoa.^{2,13} Diagnosticians must start testing, culturing

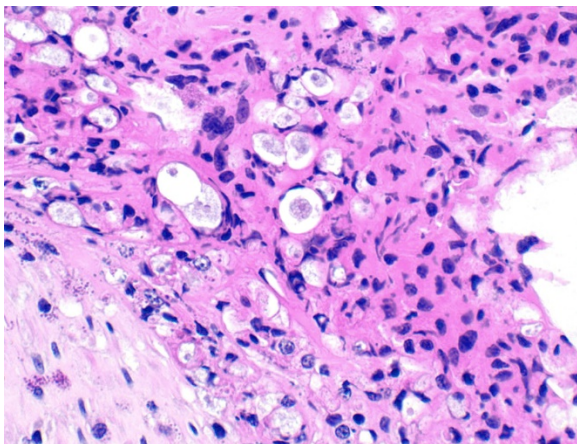
and collecting fecal cysts and typing these organisms to establish *bona fide* pathogenic strains. It is interesting that seven species of tetranucleated-cyst-producing *Entamoeba* (*E. invadens* has 2-4 nuclei in cysts) have been associated with chelonian hosts.

In this particular case, deep ulcers were not seen in the colon, and amoeba were not associated with hepatic lesions; however, *Entamoeba* was presumed to be a significant pathogen in the colon, even though it did not burrow deeply because such large numbers of organisms are visible in viable colon as well as in the necrotic debris. One report of entamoebiasis in a leopard tortoise was associated with a myositis (not seen in our case).¹⁰ A similar, verminous colonic lesion has been reported associated with *Proatractis* sp., but no embedded parasites were seen in our case.¹⁰

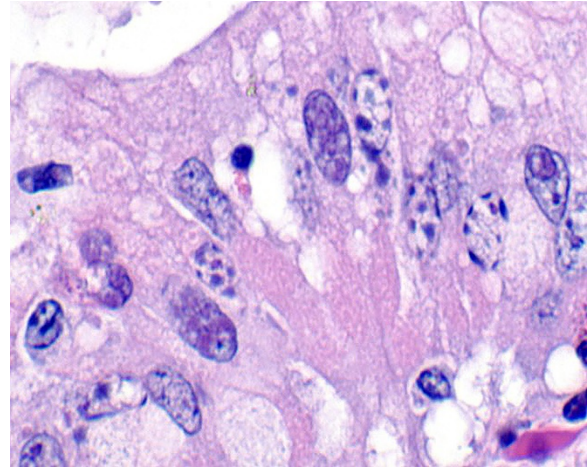


Colon, leopard tortoise. Higher magnification of necrotic areas of the colonic mucosa. (HE, 47X) (Photo courtesy of: Department of Veterinary Pathobiology, College of Vet Med and Biomedical Sciences, Texas A&M University, College Station, TX USA 7784

Intranuclear coccidia are reported in chelonians.^{1,3,5,7,8,12} The identity of the intranuclear coccidian is not known, but one report suggests it is a member of the Sarcocystidae while another suggests their case organism may be closely related to an *Eimeria*.^{1,5,12} Multisystemic infections similar to our case also are reported in leopard tortoises. The proliferative lesion of the colon is presumed to be due to the coccidian, perhaps similar to the proliferative lesion seen in sheep and goats with eimeriosis. Coccidia affected several systems in this individual. The colonic intranuclear forms are varied.^{3,5,7} The renal coccidial infection was striking in our case and no doubt was responsible for the renal compromise. The conjunctivitis was associated with coccidian as well: however, we did not culture for *Mycoplasma* (especially *M. agassizii*), a conjunctivitis-associated pathogen in tortoises.⁷ The liver was lipidotic, and no cytoplasmic coccidial forms were seen in hepatocytes as reported in one published case, but intranuclear coccidians were occasionally seen in biliary epithelium. It is interesting to speculate that some nervous signs may be seen with coccidiosis as seen in cattle!



Colon, leopard tortoise. Trophozoites of Entamoeba invadens are scattered throughout the debris. (HE, 400X) (Photo courtesy of: Department of Veterinary Pathobiology, College of Vet Med and Biomedical Sciences, Texas A&M University, College Station, TX USA 77843-4467)

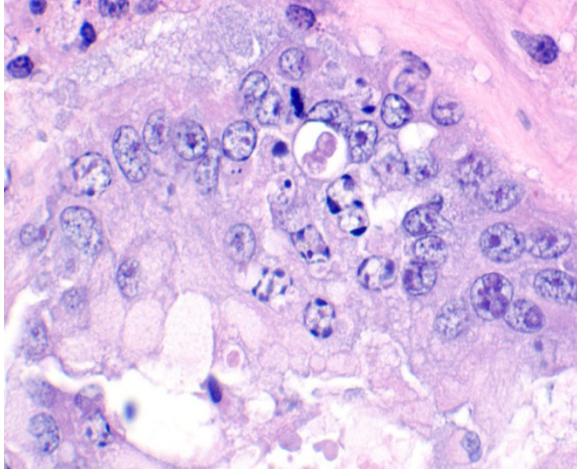


Colon, leopard tortoise. Mucosal epithelium contains variable numbers of apicomplexan zoites within their nuclei. (HE, 400X) (Photo courtesy of: Department of Veterinary Pathobiology, College of Vet Med and Biomedical Sciences, Texas A&M University, College Station, TX USA 77843-4467)

We did not test for either Type I or II chelonian herpesvirus, perhaps an oversight, but we were overwhelmed by the enterocolitis. Any herpesviral inclusions would be difficult to distinguish from intranuclear coccidian forms without EM or immunotesting. A causal relationship between chelonian herpesviruses and any of the herpesvirus related conditions is sometimes tenuous. The adenoviral nuclear inclusions, however, would seem to be distinguishable however.¹²

Contributing Institution:

Department of Veterinary Pathobiology
College of Vet Med and Biomedical Sciences
Texas A&M University
College Station, TX USA 77843-4467



Colon, Mucosal epithelium contains eosinophilic intranuclear zoites and a single oocyst (arrow). (Photo courtesy of: Department of Veterinary Pathobiology, College of Vet Med and Biomedical Sciences Texas A&M University, College Station, TX USA 77843-4467)

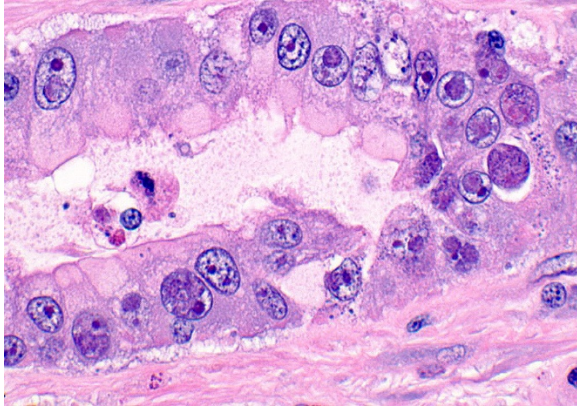
JPC Diagnosis: Colon: Colitis, necrotizing, multifocal to coalescing, subacute, severe with numerous amebic trophozoites,, and intranuclear apicomplexan zoites and schizonts.

JPC Comment: *Entamoeba invadens* is a common parasite of reptiles which occasionally affects turtles. Within collections, freshwater turtles are considered to be a source of infection for other reptile species; snakes may be especially hard hit. The genus *Entamoeba* infects many classes of vertebrates, but only a few species have been proven to cause disease. *Entamoeba suis* has been identified in swine with hemorrhagic colitis. Several species of *Entamoeba* infect man and non-human primates: *Entamoeba histolytica* the cause of “amebic dysentery” and rare cases of extraintestinal disease, as well as non-pathogenic species *E. dispar* and *E. moshkovii*.¹² Intestinal colonization occurs with encysted parasites and infection can be spread by asymptomatic carrier by oral-fecal routes. Excystation of the organism results in production of trophozoites which invade the

intestinal wall leading to ulcer formation and diarrhea.¹² Trophozoites are capable of penetrating the intestinal wall and can lead to more severe complications including liver abscesses (the most common) and, in rare cases, can spread to the brain and/or lungs, which is often fatal.¹² Recent *Entamoeba* cases in the Wednesday Slide Conference include a case of *E. invadens* in the intestine of a green anaconda (WSC 2013-2014, Conf. 21, Case 4; and *E. histolytica* in the liver of a guereza monkey – WSC 2010-2011, Conference 6, Case 1.)

Intranuclear coccidia have been sporadically reported since the 1990s and found in a wide range of chelonians to include leopard, Sulawesi, and giant tortoises, among others, as well as Eastern box turtles.¹⁰ They are considered systemic infections and widespread in chelonian collections. Clinical presentation of this disease is variable and includes mucoid nasal and/or ocular discharge (seen in this case), and it may exist as a coinfection with amebiasis (seen here), mycoplasmosis, or bacterial septicemia. Gross lesions may include generalized subcutaneous edema, coelomic effusion, necrotizing enteritis, systemic petechiation, and skin ulcers. Intranuclear coccidia may be present in a wide range of cells, including enterocytes and renal tubular epithelium as seen in this case, hepatocytes, biliary epithelium, pancreatic ductular epithelium and acinar cells, urinary bladder epithelium, nasal mucosa, and tracheal epithelium and pneumocytes.¹⁰ Recently, oro-fecal transmission has been established as the method of transmission between individuals.⁴

While most commonly identified in chelonians, intranuclear coccidia may also be seen in other species. *Cyclospora caryolytica* and *Cyclospora talpae* are present within the small intestine and liver, respectively, of moles, and other species of



Kidney, leopard tortoise. Tubular epithelium contains eosinophilic intranuclear zoites as well. (Photo courtesy of: Department of Veterinary Pathobiology, College of Vet Med and Biomedical Sciences, Texas A&M University, College Station, TX USA 77843-4467)

Cyclospora have been identified as causing watery diarrhea in Japanese Black calves.¹⁴ *Eimeria alabamensis* and *E. subspherica* have also been identified in diarrheal disease of calves, also including Japanese black calves (*E. subspherica*).¹⁴ *Eimeria hermani* and *E. stigmosa* have been observed in the enterocytes of geese.¹⁴

The moderator mentioned that the cause of pyramiding is actually due to low humidity, rather than nutritional causes (although a concurrent nutritional cause cannot be totally ruled out.)

References:

1. Alvarez WA, Gibbons PM, Rivera S, Archer LL, Childress AL, Wellehan Jr JFX, Development of a quantitative PCR for rapid and sensitive diagnosis of an intranuclear coccidian parasite in Testudines (TINC), and detection in the critically endangered Arakan forest turtle (*Heosemys depressa*). *Vet Parasitol* 193: 66-70, 2013
2. Bradford CM, Denver MC, Cranfield MR: Development of a polymerase chain reaction test for *Entamoeba invadens*. *J Zoo Wildl Med* 39: 201-7, 2008
3. Garner MM, Gardiner CH, Wellehan JFX, Johnson AJ, McNamara T, Linn M, Terrell SP, Childress A, Jacobson ER^[1]: Intranuclear coccidiosis in tortoises: Nine cases. *Vet Pathol* 43: 311-20 (2006)
4. Hoffmannova L, Kvicerova J, Bizkova K, Modry D. Intranuclear coccidiosis in tortoises – discovery of its causative agent and transmission. *Eur J Protistol* 2019; 67:71-76.
5. Innis CJ, Garner MM, Johnson AJ, Wellehan JFX, Tabaka C, Marschang RE, Nordhausen RW, Jacobson ER: Antemortem diagnosis and characterization of nasal intranuclear coccidiosis in Sulawesi tortoise (*Indotestudo forsteni*). *J Vet Diagn Invest* 19: 660-7, 2007
6. Jacobson ER, Schumacher J, Telford SR Jr, Greiner EC, Buergelt CD, Gardiner CH: Intranuclear coccidiosis in radiated tortoises (*Geochelone radiata*). *J Zoo Wildl Med* 25:95–102, 1994
7. Jacobson ER, Causes of mortality and disease in tortoises: a review. *J Zoo and Wildlife Medicine* 25: 2-17, 1994
8. Origgi FC, Jacobson ER: Diseases of the respiratory tract of chelonians. *Vet Clin No Amer Exotic Anim Prac* 3:537-49, 2000
9. Philbey AW: Amoebic enterocolitis and acute myonecrosis in leopard tortoises (*Geochelone pardalis*). *Vet Rec* 158:567-69, 2006
9. Rideout BA, Montali RJ, Phillips LG, Gardiner CH: Mortality of captive tortoises due to viviparous nematodes of the genus *Protractis* (Family Atractidae). *J Wildl Dis* 23: 103-8, 1987
10. Rodriguez CE, Duque AMH, Steinberg J, Woodburn DB. Chelonia. In Terio KA, McAloose St. Leger J, eds. *Pathology of Wildlife and Zoo Animals*. London: Elsevier Inc. pp 819-847.
11. Schmidt V, Dyachenko V, Aupperle H, Pees M, Krautwald-Junghanns EM, Daugschies A: Case report of systemic coccidiosis in a radiated tortoise (*Geochelone*

radiata). *Parasitol Res* 102: 431-36, 2008

12. Skappak C, Akierman S, Belga S, Novak K, Chadee K, Urbanski SJ, Church D, Beck PL. Invasive amoebiasis: A review of Entamoeba infection highlighted with case reports. *Can J Gastroenterol Hepatol* 2014; 28(7):355-359.

13. Stensvold CR, Lebbad M, Victory EL, Verweij JJ,^[1]_[SEP] Tannich E, Alfellani M, Legarraga P, and Clark CG: Increased sampling reveals novel lineages of *Entamoeba*: Consequences of genetic diversity and host specificity for taxonomy and molecular detection. *Protist* 162: 525-41, 2001

14. Yamada M, Hatama S, Ishikawa Y, Kadota K. Intranuclear coccidiosis caused by *Cyclospora* spp. in calves. *J Vet Diagn Invest* 2014; 26(5):678-682.

CASE III: 15-41009 (JPC 4084545).

Signalment: Adult, intact male tiger (*Panthera tigris*)

History: The animal presented for necropsy examination following euthanasia after a 3-week history of progressive pneumonia that was unresponsive to antibiotic administration.

Gross Pathology: The lungs were mottled pink to red and rubbery to firm on palpation. The right middle lung lobe was more meaty and consolidated than the other lobes. There were also multiple pale tan, round, variably sized up to 2 cm in diameter nodules interspersed throughout the pulmonary parenchyma. The bronchi within the cranioventral lungs were often filled with frothy and purulent material.

Laboratory results: Virology: The lungs were positive with fluorescent antibody testing for Canine Distemper Virus. Virus isolation was unsuccessful.

Bacteriology:

PCR on lung tissue for *Mycoplasma* sp. was negative.

Aerobic Culture and identification using MALDI-TOF -

Specimen	Isolate	Level
Lung	Acinetobacter sp.	few
<i>*Result Comment:</i> Identified by MALDI-TOF as <i>A. haemolyticus</i> with a score of 2.331.		
Lung	Escherichia coli	v rare
Lung	Ochrobactrum	v few
Lung	Pseudomonas pseudoalcaligenes	few
Lung	Gram-negative rod	v few
<i>*Result Comment:</i> Identified as <i>Rhizobium radiobacter</i> by MALDI-TOF with a score of 2.308.		
Lung	Alcaligenes faecalis	v rare

**General Test Comment:*

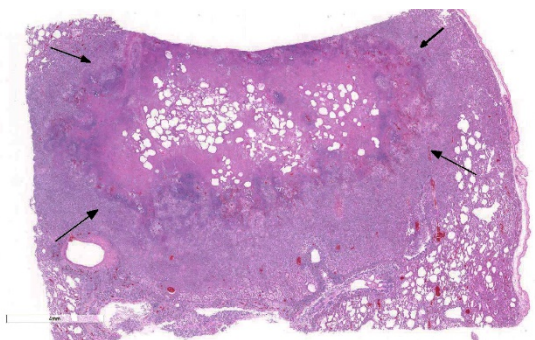
MALDI-TOF Score:

Range Description

2.300...3.000 Highly probable species identification

2.000...2.299 Secure genus identification, probable species identification

1.700...1.999 Probable genus identification



Lung, tiger: There is a focally extensive area of infarction (arrows). Much of the rest of the section is hypercellular. (HE, 5X)

Microscopic Description:

Lung: Approximately 80% of the section is affected by a profound inflammatory process. Alveolar spaces are frequently filled with many viable and degenerate neutrophils mixed with foamy macrophages, abundant eosinophilic, fibrillar material (fibrin), moderate cellular debris, and mild hemorrhage.

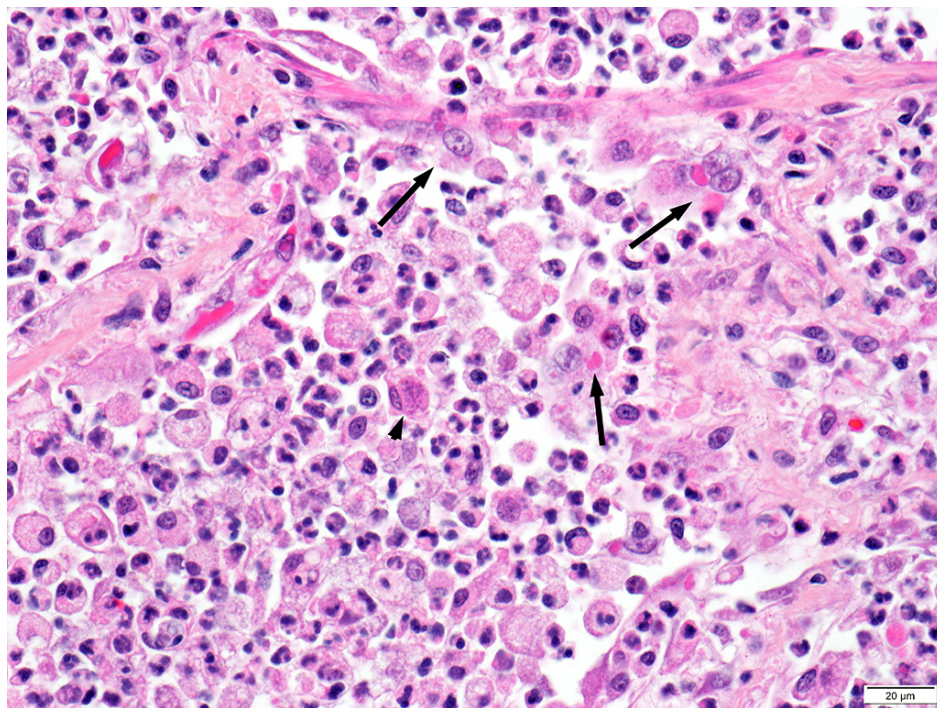
The alveolar septa are diffusely thickened up to 5 times their normal diameter by moderate numbers of similar inflammatory cells, marked type II pneumocyte hyperplasia, and moderate smooth muscle hypertrophy. Pneumocytes often form multi-nucleated syncytial cells that contain up to 7 nuclei. Many pneumocytes and syncytial cells contain one to several variably sized and shaped, eosinophilic, glassy, intracytoplasmic and intranuclear inclusion

bodies. There is multifocal, extensive necrosis with abundant pyknotic,

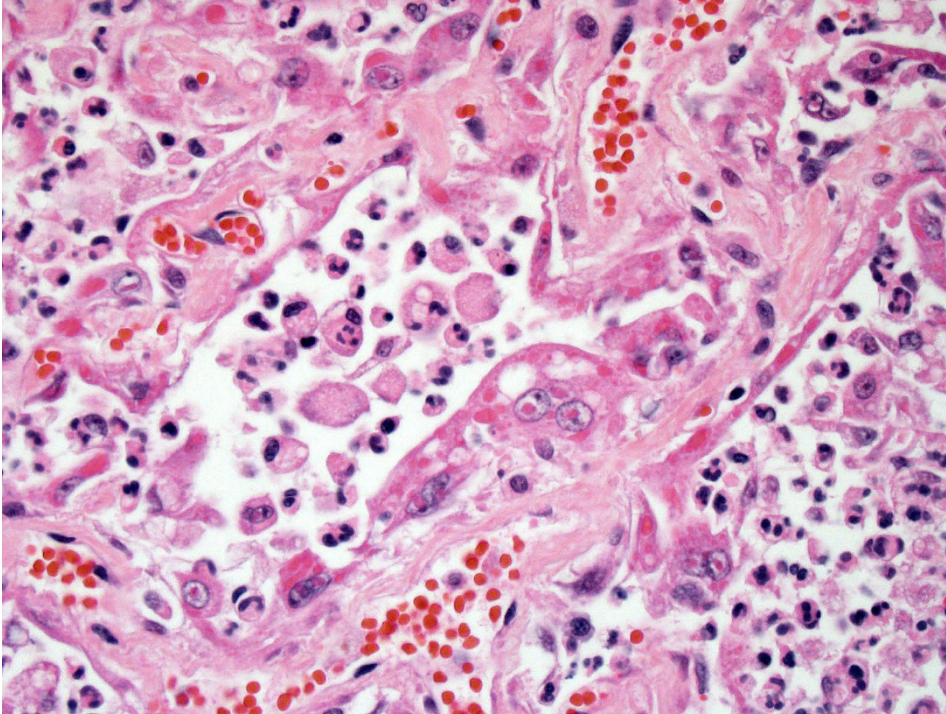
karyorrhectic, and karyolytic cellular debris, and alveoli, bronchioles and bronchi in these areas are frequently filled with innumerable degenerate neutrophils mixed with fewer macrophages and eosinophils. Many macrophages are enlarged up to 70 μm in diameter and contain an intracytoplasmic, 20 x 15 μm protozoal cysts that are filled with small, 1-2 μm bradyzoites, as well as non-encysted and similarly sized tachyzoites. Cysts and tachyzoites are also present free within the extracellular space.

Contributor's Morphologic Diagnoses:

Lung: Diffuse, marked, fibrinonecrotic, suppurative, histiocytic, bronchointerstitial pneumonia with intracytoplasmic and intranuclear epithelial inclusions (Canine Distemper Virus) and protozoal cysts and free zoites (*Toxoplasma gondii*).



*Lung, tiger: Inflammatory cells fill alveolar spaces and expand alveolar septa. Viral inclusions are present within pneumocytes and syncytial cells (arrows) and a *Toxoplasma* cyst is within a macrophage (arrowhead). (HE, 400X)*



Lung, tiger: Type II pneumocytes contain numerous intracytoplasmic and intranuclear inclusions and often have multiple nuclei (viral syncytia). (HE, 400X) (Photo courtesy of: University of Illinois College of Veterinary Medicine, Department of Pathobiology, 2522 Veterinary Medicine Basic Science Building, 2001 S. Lincoln Ave., Urbana, IL, 61802, <http://vetmed.illinois.edu/research/departments/pathobiology/>)

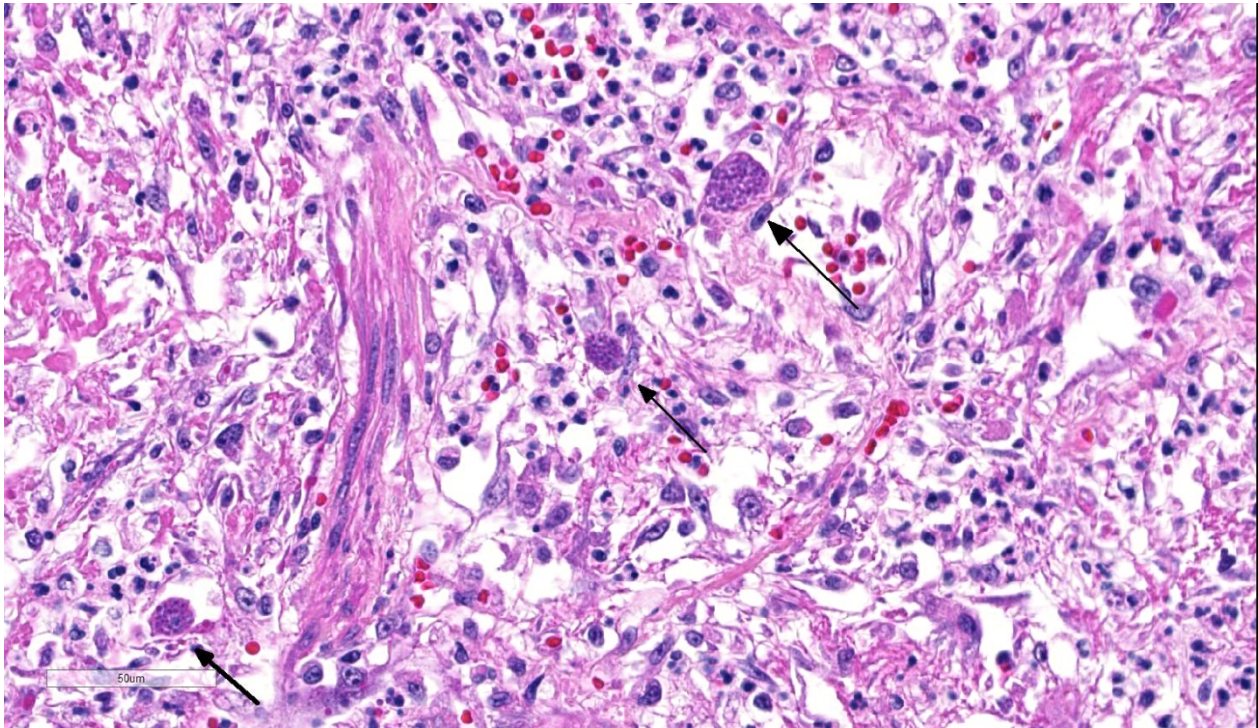
Contributor's Comment: Canine distemper virus (CDV) inclusions were also identified within the glandular epithelium of the gastric mucosa in this case. There were no identified abnormalities within the nervous system. *Toxoplasma gondii* organisms were also found within a tracheobronchial lymph node. Additional findings in this case included multiple mast cell tumors within the liver and spleen. This animal was part of a larger outbreak of CDV in a group of big cats.

CDV is in the family *Paramyxoviridae*, subfamily *Paramyxovirinae*, genus *Morbillivirus*. It is a 100–700 nm, irregularly shaped virus composed of an outer lipoprotein envelope, and inner matrix, and a nucleocapsid that contains single-stranded negative-sense RNA. Infection occurs by inhaling aerosols or close contact with

infected animals. The virus enters via the epithelium and infects upper respiratory tract macrophages which transport it to local lymphoid tissues where the virus replicates further, and spread continues unless adequate cell-mediated and humoral responses are mounted.^{7,11} Clinical signs in CDV infection most often include the respiratory, nervous, and gastrointestinal systems. Many other tissues may be affected as well. Key histologic changes in CDV infection are eosinophilic, homogenous or glassy,

variably sized intranuclear and intracytoplasmic inclusion bodies, which are most easily identified in the nervous system and epithelial tissues. In the lungs, commonly observed changes include bronchointerstitial pneumonia accompanied by viral inclusions within airway epithelium, epithelial syncytial cell formation, and type II pneumocyte hyperplasia.⁷

The host range of CDV is wide and continuing to grow. A recent retrospective review⁵ compiled all reported natural and experimental CDV infections. Susceptible animals include those from *Carnivora* (*Canidae*, *Felidae*, *Mustelidae*, *Procyonidae*, *Hyaenidae*, *Ursidae*, *Phocidae*, *Viverridae*, *Ailuridae*, *Mephitidae*, *Odobenidae*, and *Otariidae*), *Rodentia* (*Muridae*, *Cricetidae*,



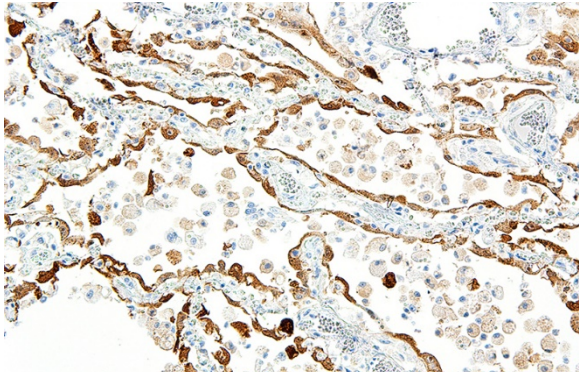
Lung, tiger: Numerous *Toxoplasma* cysts are present within areas of necrosis and/or fibrosis (arrows). (HE, 400X)

Sciuridae, and *Caviidae*), Primates (*Cercopithecidae* and *Cebidae*), *Artiodactyla* (*Suidae*, *Tayassuidae*, and *Cervidae*), and *Proboscidea* (*Elephantidae*) are susceptible to CDV.⁵

Toxoplasma gondii is a heteroxenous apicomplexan protozoan parasite that is capable of infecting virtually all homeothermic animals. It is an obligate intracellular parasite. Felids serve as definitive hosts, while other animals are intermediate hosts. Many if not all cells and tissues are susceptible to infection. Infection of non-intestinal tissues is achieved by initial ingestion of oocysts, excystation of sporozoites followed by their penetration of small intestinal mucosal and lamina propria cells, and replication within these small intestinal cells. With continued replication and formation of tachyzoites, cells eventually rupture, and tachyzoites infect new cells and are capable of spreading to distant tissues via blood or lymph.^{4,6} Necrosis predominates in

gross lesions observed and typically presents as variably sized gray foci within any tissue. Within the lung, microscopic changes closely follow that of interstitial pneumonia. Alveolar septa are initially thickened by mononuclear cells with fewer granulocytes, followed closely by type II pneumocyte hyperplasia. Alveolar lumina are filled with macrophages and fibrin. Necrosis is abundant with continued parasitic replication. Intra- or extracellular cysts and zoites within affected areas are frequently observed and are highly suggestive of toxoplasma infection.^{4,6}

Infection is believed to be widespread among humans, up to 80% in some parts of the world. (7) Seroprevalence is high in several studies involving zoo and wild animals, up to 90% in wild animals (foxes), and 52.4%, 64.5%, and 81.4% in zoo felids.^{1,3,9,10} *Toxoplasma gondii* has high zoonotic potential, and though high seroprevalence with little clinical disease indicates that most



Lung, tiger. Pneumocytes and occasional macrophages have strong cytoplasmic reactivity to canine morbillivirus immunohistochemistry. (anti-CDV, 200X) (Photo courtesy of : University of Illinois College of Veterinary Medicine, Department of Pathobiology, 2522 Veterinary Medicine Basic Science Building, 2001 S. Lincoln Ave., Urbana, IL, 61802, <http://vetmed.illinois.edu/research/departments/pathobiology/>)

infections are asymptomatic, infection in immunocompromised individuals can cause severe illness and often death. With the current case, the tiger was undoubtedly immunocompromised from concurrent CDV infection.

Contributing Institution:

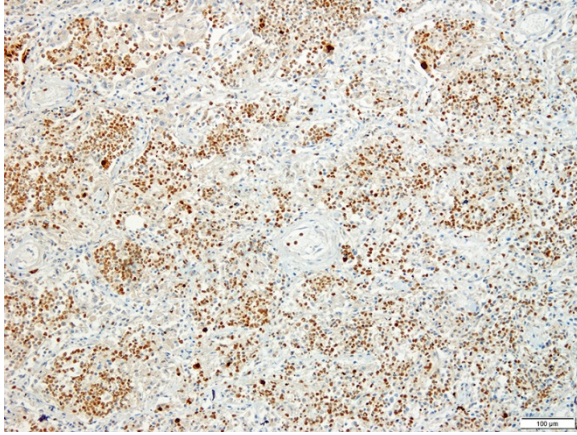
University of Illinois College of Veterinary Medicine
 Department of Pathobiology
 2522 Veterinary Medicine Basic Science Building
 2001 S. Lincoln Ave.
 Urbana, IL
 61802
<http://vetmed.illinois.edu/research/departments/pathobiology/>

JPC Diagnosis: Lung: Pneumonia, bronchiointerstitial, necrotizing and fibrinosuppurative diffuse, severe, with numerous intraepithelial intracytoplasmic and intranuclear viral inclusions viral syncytia and intraepithelial and intrahistiocytic apicomplexan zoites.

JPC Comment: Transpecies infection with canine morbillivirus is not a new

phenomenon. Canine morbillivirus infection (CDV) in non-canine host as first reported in silver jackals in 1937 in South Africa; the first cross-species infection in the U.S. (the country with the largest number of confirmed reports occurred in a badger in Colorado in 1942.⁵ Inter-Order infection was first accomplished experimentally in hamsters in the early 1960s (but required cerebral inoculation.)⁵ Natural intra-order infection occurred in the late 1970s and 1980s in primates. While transspecies infection by CDV (and high mortality) is primarily in carnivore species (prompting at least one call to rename it “Carnivore Distemper Virus”,¹² herbivorous species such as collared peccaries and non-human primates are documented as well.² Outbreaks of morbillivirus disease in seals may result from either CDV or closely related phocine distemper virus. Dolphins, harbor porpoises and pilot whales all have genetically different morbillivirus which cause similar disease (and have been transmitted to Mediterranean monk seals, but interestingly, their morbillivirus appears more closely related to the morbillivirus causing *pestis du petits* in ruminants and that which caused rinderpest.²

Rarely associated with non-human primates, CDV infection has occurred in a number of species of macaques in Japan and China since the first case occurred in Japanese macaques in 1989.⁸ CDV was responsible for up to 4000 rhesus fatalities in a breeding program in China, in which animals displayed measles-like symptoms with respiratory distress, rashes over the entire body, reddening and swelling of the footpads, conjunctivitis, and a thick nasal discharge. Interstitial fibrosis was a predominant finding at autopsy. Following sequencing of the viral genome, it showed 97% homology with other



Lung, tiger. Toxoplasma cysts and macrophages demonstrate strong cytoplasmic immunoreactivity to Toxoplasma immunohistochemistry. (anti -T. gondii, 100X). (Photo courtesy of: University of Illinois College of Veterinary Medicine, Department of Pathobiology, 2522 Veterinary Medicine Basic Science Building, 2001 S. Lincoln Ave., Urbana, IL, 61802, <http://vetmed.illinois.edu/research/departments/pathobiology/>)

CDV isolates from China. A source for this and related outbreaks was not identified.⁸

Molecular evolutionary analysis of CDV has suggested that mutations in the signaling lymphocyte activation molecule (SLAM, CD150 - the common receptor used by morbillivirus to gain entry into the host cell - and the CDV hemagglutinin (HA) protein that binds the SLAM molecule are important in cross-species infection as well as species specificity.^{2,12} An area of particular concern in the future would be the potential for CDV strains that infect primates, which already are able to use the human nectin-4 receptor for cellular entry, to mutate in the region of the viral H protein and become infective for humans.²

The moderator reviewed the history and epidemiology of morbillivirus infection in since the establishment of the veterinary school in Lyon, France in 1762 (in order to combat periodic outbreaks of rinderpest in Europe.)

References:

1. Alvarado-Esquivel C et al. Seroprevalence of toxoplasma gondii infection in captive mammals in three zoos in Mexico City, Mexico. *Journal of Zoo and Wildlife Medicine*. 2013;44(3):803-806.
2. Beineke A, Baumgartner W, Wohlsein P. Cross-species transmission of canine distemper virus-an update. *One Health* 2015; 1:49-59.
3. de Camps S et al. Seroepidemiology of toxoplasma gondii in zoo animals in selected zoos in the Midwestern United States. *Journal of Parasitology*. 2008;94(3):648-653.
4. Dubey JP and Lappin R. Toxoplasmosis and Neosporosis, In: Green CE ed. *Infectious diseases of the dog and cat*, 3rd ed. St. Louis, MO. Elsevier: 2006:754-768.
5. Martinez-Gutierrez M, Ruiz-Saenz J. Diversity of susceptible hosts in canine distemper virus infection: a systematic review and data synthesis. *BMC Vet Res*. 2016;12:78.
6. Maxie, MG. Toxoplasmosis, In: Maxie, MG ed. *Jubb, Kennedy, and Palmer's pathology of domestic animals*, 6th ed., Vol. 2. St. Louis, MO. Elsevier; 2016:236-237.
7. Maxie, MG. Canine distemper, In: Maxie, MG ed. *Jubb, Kennedy, and Palmer's pathology of domestic animals*, 6th ed., Vol. 2. St. Louis, MO. Elsevier; 2016:574-576.
8. Qui W, Zheng Y, Zhang S, Fan Q, Liu H, Zhang F, Wang W, Liao G, Hu R. Canine distemper outbreak in rhesus monkeys, China. *Emerg Inf Dis* 2011; 8:1541-1543.
9. Samuel WM, Pybus MJ, and Kocan AA. Toxoplasmosis and related

infections, In: Samuel WM, Pybus MJ, and Kocan AA eds. *Parasitic diseases of wild mammals*, 2nd ed. Ames, IA: Iowa State Press; 2001:478-519.

10. Silva JCR et al. *Toxoplasma gondii* antibodies in exotic wild felids from Brazilian zoos. *Journal of Zoo and Wildlife Medicine*. 2001;32(3):349-351.

11. Terio KA, Craft ME. 2013. Canine distemper virus (CDV) in another big cat: should CDV be renamed carnivore distemper virus? *mBio* 4(5):e00702-13. doi:10.1128/mBio.00702-13.

12. Williams, ES. Canine distemper, In: Williams ES, Barker IK, eds. *Infectious diseases of wild mammals*, 3rd ed. Ames, IA: Iowa State Press; 2001:50-59.

CASE IV: M17-69 (JPC 4102647).

Signalment: Juvenile (age unknown), female, American paddlefish (*Polyodon spathula*)

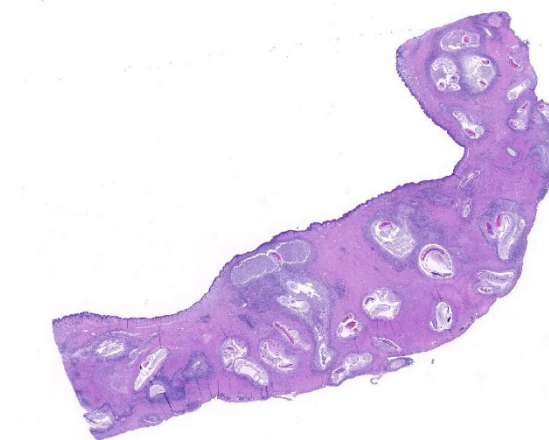
History: The fish was found dead in a stable aquarium system.

Gross Pathology: Multiple fixed tissues were received for histopathology as a mail-in necropsy. The fish was reported to be in fair to poor physical condition. Multifocal, widespread, 1-2 mm, white to tan nodules were observed on serosal and cut surfaces of the stomach and pyloric ceca during tissue trimming.

Laboratory results: N/A

Microscopic Description:

Stomach: The submucosa and muscularis are widely expanded by severe fibrosis and inflammatory infiltrates surrounding large



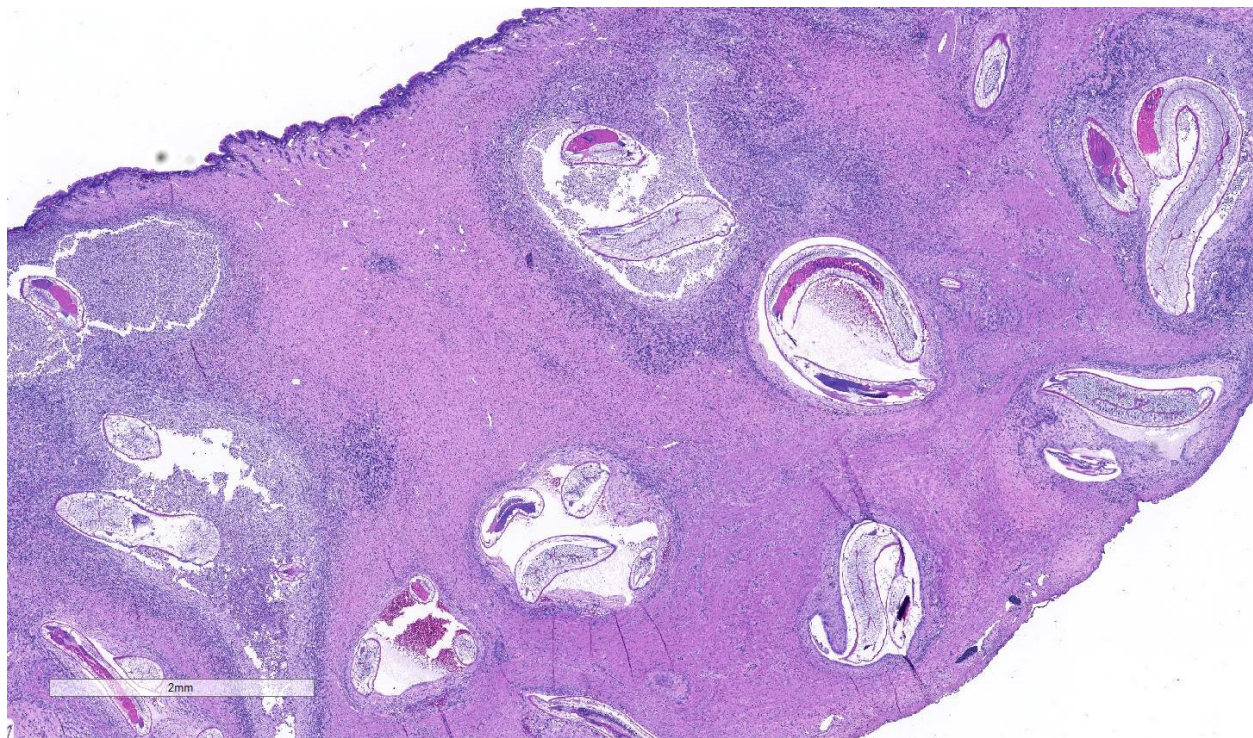
Stomach, paddlefish. Granulomas centered on larval nematodes transmurally throughout the wall. (HE, 4X)

numbers of larval nematodes. Features of the pseudocoelomate parasites include a smooth cuticle, coelomyarian/polymyarian musculature, lateral cords with eosinophilic gland cells, triradiate glandular esophagus, cecum, and large intestine lined by tall uninucleate columnar cells with a brush border. Worms are coiled within cavitated lesions partially filled by loosely associated mixtures of degenerate cells, necrotic cellular debris, erythrocytes and mixed inflammatory cells. More organized, unevenly thick mantles, composed of variable mixtures of eosinophilic granulocytes, macrophages, lymphocytes, plasma cells and fibroblasts gradually dissipate into the adjacent gastric wall. The lamina contains sparse, often short glands, with reduced cytoplasm and cytoplasmic granules, widely separated by abundant dense collagenous tissue.

Contributor's Morphologic Diagnoses:

Stomach: Gastritis, mural, widespread, chronic, severe, with glandular atrophy and loss, and larval nematodes

Contributor's Comment: The American paddlefish is a large, filter-feeding, cartilaginous, freshwater fish that is closely



Stomach, paddlefish. Higher magnification of the intestinal wall with numerous 400µm diameter larval nematodes contained within granulomas. (HE, 32X)

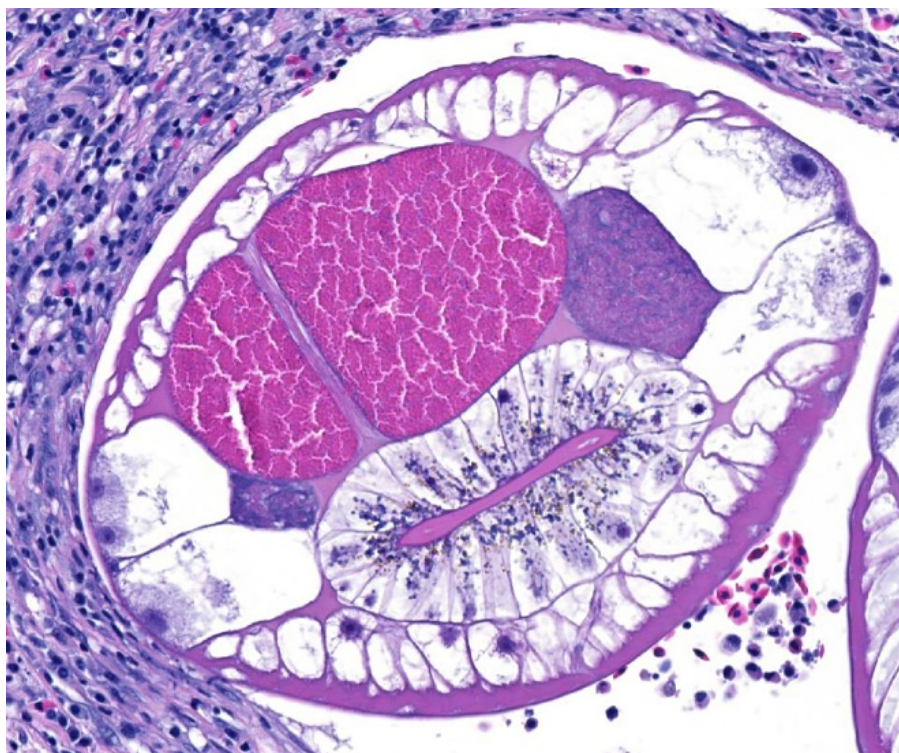
related to the sturgeons. Paddlefish roe, like that of several sturgeon species, is highly valued as caviar and supports a growing aquaculture industry.⁴ Microscopic examination revealed severe inflammatory changes and fibrosis, with glandular atrophy and loss in the stomach and cecal walls in association with large numbers of larval nematodes. Features of the worms and the associated histologic changes are compatible with descriptions of the anasakid nematode *Hysterothylacium dollfusi*, a major parasite of and impediment to the pond-culture of paddlefish.^{1,5} Although gastric ulceration was not present in the sections evaluated, the severe changes and glandular loss suggest maldigestion and malabsorption, consistent with the poor condition of this fish. Additional findings included severe hepatocellular and pancreatic acinar cell atrophy suggesting prolonged anorexia and catabolism of hepatic lipid stores. The Anisakidae are a family of intestinal

nematodes, including the well-known genera *Anisakis*, *Contracaecum* and *Pseudoterranova*. Representative *Anisakis* spp., most notably *A. simplex*, and *Pseudoterranova* spp. have the potential to cause zoonotic infections in humans (anisakidosis) when larvae are ingested in raw or insufficiently cooked fish. Anisakidosis caused by *Contracaecum* and *Hysterothylacium* spp. are rare. The life cycles of the genera are complex, involving an invertebrate first intermediate host, fish or cephalopod second intermediate host and often a bird or marine mammal final host.^{2,3}

Contributing Institution:

University of Georgia, College of Veterinary Medicine, Department of Pathology, 501 DW Brooks Drive , Athens, GA 30602, www.vet.uga.edu/VPP

JPC Diagnosis: Stomach, muscularis and serosa: Granulomas, numerous with larval



Stomach paddlefish. Larval ascarids have a thin cuticle, high polymyarian-coelomyarian musculature, prominent lateral cords with excretory cells, developing gonads, and a GI tract with tall uninnucleate columnar epithelium and a developing gonad (HE, 273X)

ascarids and mild chronic granulocytic and lymphoplasmacytic gastritis.

JPC Comment: *Anisakis* sp. and *Pseudoterranova* sp. the causative agents of anisakidosis in humans, utilize marine fish as paratenic hosts and whales and dolphins and seals and sea lions, respectively, as definitive hosts. Humans, which may develop abdominal pain, diarrhea and nausea (as well as strong allergic reactions) as accidental nonpermissive hosts. The infection of humans by species of *Anisakis* is called “anisakiasis”, while “anisakidosis” refers to infection by any member of the Anisakidae.⁶

Parasitized humans may experience abdominal pain within a few hours to a few days following ingestion of infected raw fish. Infection may occur in the stomach (where worms may be removed by gastroscopy, or

the intestine (which often requires surgery and may result in obstruction as a result of severe inflammation (which may expand the intestinal wall 3-5 times. Rare cases of “ectopic anisakiasis” may result from larval penetration within the pharynx, tongue, lung, peritoneal cavity, or pancreas. Another form of anisakidosis is gastroallergic anisakidosis, which may not present with gastrointestinal symptoms, but instead with various degrees of urticarial, angioedema, and anaphylaxis. In fact, the vomiting and diarrhea associated with allergic

reactions, may actually expel the larva from the body⁶. Interestingly, gastric allergic anisakiasis are relatively common in certain countries, including Spain and Italy, has been reported in Japan and Korea, but is rare in other parts of the world – possibly due to awareness of the condition in these parts of the world. It is not clear whether it takes live larvae or antigens from dead larvae to set off a gastroallergic reaction, as patients with previous gastroallergic anisakiasis will not react to exposure to dead larvae or antigens, while fish processing works may develop *Anisakis*-induced asthma, rhinoconjunctivitis, or dermatitis.⁶

In humans, larvae that penetrate the gastric wall, but usually die within a few days in humans. The larvae will break down in eight weeks, with eosinophils being a large component of the inflammatory lesion. Dead

Anisakis larvae may incite granuloma formation within tissues and may be associated with systemic neutrophilia or eosinophilia.⁶ The presence of inflammatory nodules may be mistaken for neoplasia, highlighting the importance of taking a good history in cases of acute onset of epigastric pain and intestinal symptoms.

In addition to reviewing anisakiasis in animals, the moderator reviewed additional large zoonotic heminthic disease, to include dracunculiasis and diphyllbothriasis.

References:

1. Gardiner CH, Poyton SL. *An Atlas of Metazoan Parasites in Animal Tissues*. Washington, DC: Armed Forces Institute of Pathology; 2006.
2. Klimpel S, Palm HW. Anisakid nematode (Ascaridoidea) life cycles and distribution: Increasing zoonotic potential in the time of climate change? In: Mehlhorn H, ed. *Progress in Parasitology*, Parasitology Research Monographs 2. Berlin: Springer-Verlag; 2011:201-222.
3. Lima dos Santos CAM, Howgate P. Fishborne zoonotic parasites and aquaculture: A review. *Aquaculture* 2011;318:253-261.
4. Mimms SD, Shelton WL, Wynne FS, Onders RJ. *Production of paddlefish*. Stoneville, MS: Southern Regional Aquaculture Center Publication 437; 1999.
5. Miyazaki T, Rogers WA, Semmens KJ. Gastro-intestinal histopathology of paddlefish, *Polyodon spathula* (Walbaum), infected with larval *Hysterothylacium dollfusi* Schmidt, Leiby & Kritsky, 1974. *J Fish Dis*. 1988;11:245-250.
6. Nieuwenhuizen NE. *Anisakis* – immunology of a foodborne parasitosis. *Parasite Immunol* 2016; 38:548-55

Self-Assessment - WSC 2018-2019 Conference 19

1. Which of the following is the intermediate host for spirorchid trematodes?
 - a. Cockroaches
 - b. Snails
 - c. Sheep
 - d. Roundworms

2. In which of the following species have intranuclear coccidia NOT been identified?
 - a. Man
 - b. Cattle
 - c. Geese
 - d. Turtles

3. Which of the following life stages is responsible for invasive entamoebiasis?
 - a. Pseudohyphae
 - b. Zoites
 - c. Cysts
 - d. Trophozoites

4. Which of the following species has not been infected by canine distemper virus (CDV)?
 - a. Seals
 - b. Macaques
 - c. Giant Pandas
 - d. Horses

5. Which of the following is the definitive host for *Anisakis simplex*?
 - a. Marine fish
 - b. Humans
 - c. Whales
 - d. Seals

Please email your completed assessment to Ms. Jessica Gold at Jessica.d.gold2.ctr@mail.mil for grading. Passing score is 80%. This program (RACE program number) is approved by the AAVSB RACE to offer a total of 0.5 CE Credits, with a maximum of 12.5 CE Credits being available to any individual Veterinary Medical Professionals for the 2017-2018 Wednesday Slide Conference. This RACE approval is for the subject matter categories of: SCIENTIFIC using the delivery method of NON-INTERACTIVE DISTANCE. This approval is valid in jurisdictions which recognize AAVSB RACE; however, participants are responsible for ascertaining each board's CE requirements. RACE does not "accredit", "endorse" or "certify" any program or person, nor does RACE approval validate the content of the program.

Please email your completed assessment to Ms. Jessica Gold at Jessica.d.gold2.ctr@mail.mil for grading. Passing score is 80%. This program (RACE program number) is approved by the AAVSB RACE to offer a total of 0.5 CE Credits, with a maximum of 12.5 CE Credits being available to any individual Veterinary Medical Professionals for the 2017-2018 Wednesday Slide Conference. This RACE approval is for the subject matter categories of: SCIENTIFIC using the delivery method of NON-INTERACTIVE DISTANCE. This approval is valid in jurisdictions which recognize AAVSB RACE; however, participants are responsible for ascertaining each board's CE requirements. RACE does not "accredit", "endorse" or "certify" any program or person, nor does RACE approval validate the content of the program.

Joint Pathology Center
Veterinary Pathology Services



WEDNESDAY SLIDE CONFERENCE 2018-2019

Conference 20

20 March 2019

Conference Moderator:

Matti Kiupel, DVM, Dr. Vet. Med., Dr. Habil, MVSc, Ph.D, DACVP, Fachtierarzt Fur Veterinar Pathologie
Veterinary Diagnostic Laboratory
4125 Beaumont Rd.
Bldg 0214, Room 152A
Lansing MI 48910

CASE I: D12-49 (JPC 4041970).

Signalment: 8-year-old, male, castrated Labrador retriever (*Canis lupus familiaris*)

History: A cutaneous mass adjacent to the prepuce was surgically removed with wide margins and submitted for histologic evaluation. Following excision, the mass recurred and continued to grow despite treatment with prednisone and vinblastine. Therapy was switched to Palladia and resulted in partial remission for one month, at which point the neoplasm began to increase in size again. Euthanasia was elected due to poor prognosis and failed response to therapy.

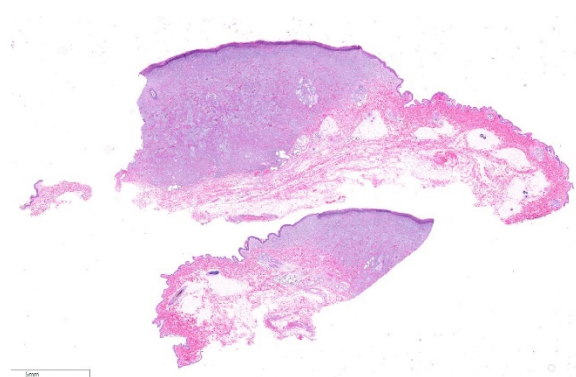
Gross Pathology: None available.

Laboratory results: None available

Microscopic Description:

Expanding the dermis and elevating the overlying ulcerated epidermis is a well

circumscribed, unencapsulated neoplasm consisting of numerous mast cells with marked anisocytosis and anisokaryosis, karyomegaly, bizarre nuclei, no apparent granules, 1-2 irregularly round nuclei, and a mitotic index of 5-6 per high power field, with bizarre mitotic figures. These cells are admixed with high numbers of eosinophils



Haired skin, dog: Sections of a dermal mast cell tumor with an ulcerated surface was submitted for examination. (HE, 5X)

and multifocal collagenolysis (flame figures). The margins appear complete.

Contributor's Morphologic Diagnoses:
Haired skin: Mast cell tumor, high grade.

Contributor's Comment: Mast cell tumors account for 15-20% of skin tumors in dogs, and are the most frequent malignant tumor of the skin. In 2011, Kiupel et al. proposed a two-tier histologic grading system to more accurately predict the biological behavior of canine cutaneous mast cell tumors.² This two-tier approach replaced the commonly used three-tier Patnaik system, and has since been shown to provide useful prognostic information with increased consistency of grading among veterinary pathologists.^{1,6}

This particular neoplasm has a very high mitotic rate with marked atypia of neoplastic cells, and serves as a prime example of a high

grade neoplasm. Clinical follow-up on this patient revealed recurrence of the neoplasm at the site of excision and failure of response to treatment.

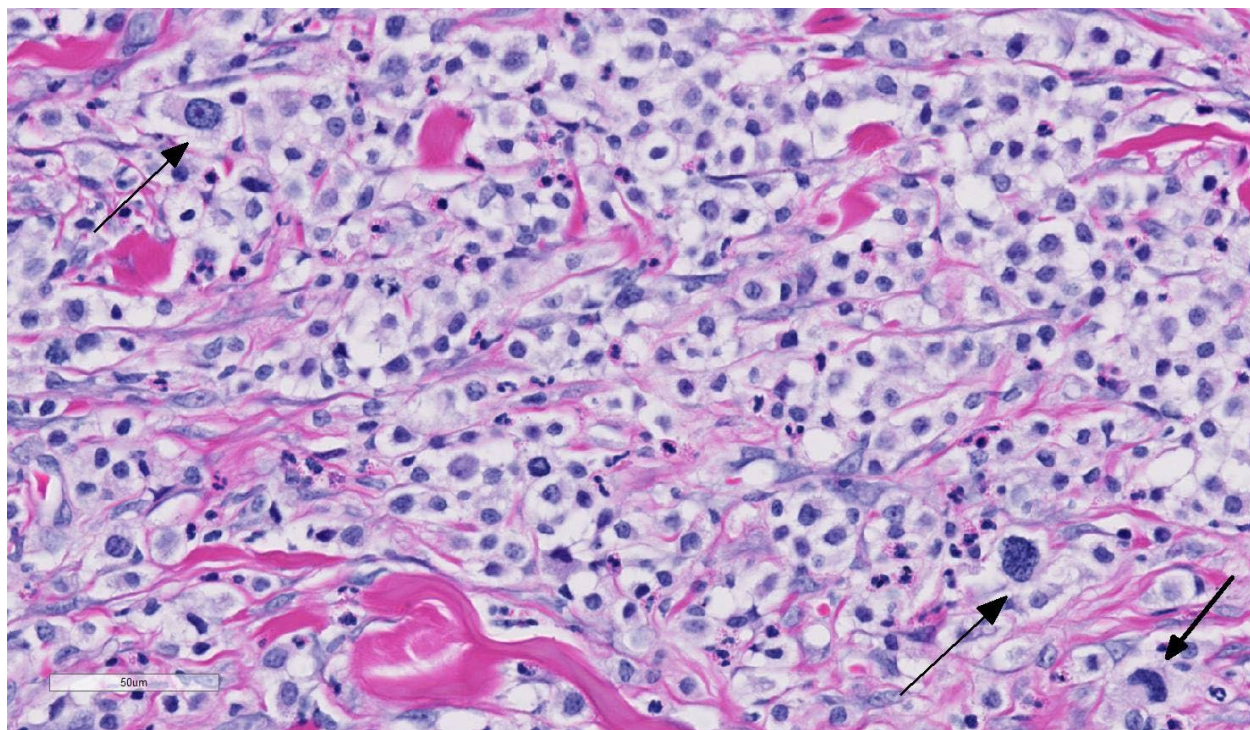
While not present in this case, it was recently reported that canine cutaneous mast cell tumors can exhibit epitheliotropism, and should be included as a differential for cutaneous round cell neoplasms with epitheliotropic behavior.⁴

Contributing Institution:

Tri-Service Research Laboratory
JBSA Ft. Sam Houston, TX

JPC Diagnosis: Haired skin: Mast cell tumor, high grade.

JPC Comment: In 2011, a 28-pathologist, 16-institution study on histologic grading of cutaneous mast cell tumors was published

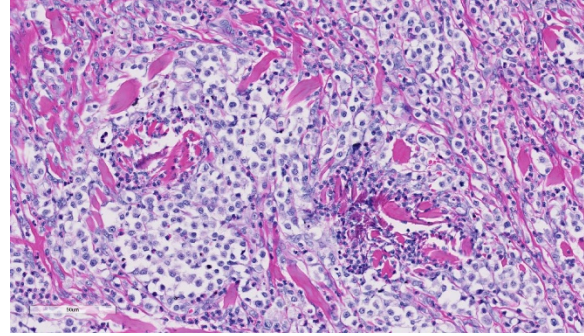


Haired skin, dog: Neoplastic cells are poorly granulated, and cells with pleomorphic nuclei exceed 3 /2.37mm² fields (arrows) (HE, 400X)

which has significantly increased concordance between pathologists in the grading and prognosis of canine mast cell tumors.² This system is currently in use at the Joint Pathology Center and in most diagnostic laboratories. The study replaced previous 3-tier studies by Bostock (1973) and Patnaik (1984), both 3-tier studies in which interobserver variation resulted in an skewing of grading toward intermediate (grade 2) grades.²

The current two-tier system classifies cutaneous mast cell tumors into low- versus high-grade. The diagnosis of high grade mast cell tumors is based on the presence of ANY ONE of the following criteria: seven mitotic figures per ten 2.37mm² fields, 3 multinucleated cells or cells with bizarre nuclei per ten 2.37mm² fields, or karyomegaly (with nuclei of at least ten per cent of neoplastic cells varying by at least two fold. In this particular case, the participants were in agreement with an elevated mitotic count as well as the presence of an increased number of cells with bizarre nuclei.² The count of mitotic figures should be performed in the areas of the slide with the highest frequency of mitotic figures.²

The kit protein is important in the proliferation, differentiation, migration and survival of mast cells. A variety of c-kit mutations have been identified in mast cell tumors, with the most common mutation (in exon 11) being associated with a significantly worse prognosis.³ In a study, 19/49 dogs with cutaneous mast cell tumors possessing a c-Kit mutation on exon 11 died within a year due to MCT-associated disease. Mutations on chromosome 8 and 9 compose less than 5% of overall mutations each, but have no impact on prognosis. PCR testing on this neoplasm was performed at the Michigan State Diagnostic Lab and was positive an



Haired skin, dog: Areas of collagen degradation are commonly seen in a number, but not all MCTs. (HE, 400X)

activation duplication mutation in exon 11 of c-Kit, but was negative for exon 8 mutations.³

While mast cell tumors may arise in any organ, the skin is the most common site for mast cell tumor development in the dog. Another classification is important in evaluating cutaneous mast cells – that of a cutaneous versus subcutaneous location. Under previous grading systems, tumor depth was considered an adverse prognostic factor. Thompson et al. in 2011⁵ evaluated followup data for 206 subcutaneous mast cell tumors (those restricted to the subcutaneous fat) and found that 6-month, 1-, 2- and 5-year survival times were 95%, 93%, 92%, and 86% respectively, indicating a significantly better prognosis for this subset of tumors. Only 4% exhibited metastasis, and 6% had local recurrence, although 56% of cases had incomplete tumor margins.⁵

References:

1. Giantin M, Vascellari M, Morello MM, et al. c-KIT messenger RNA and protein expression and mutation in canine cutaneous mast cell tumors: correlations with post-surgical prognosis. *J Vet Diagn Invest.* 2012;24(1):116-126.
2. Kiupel M, Webster JD, Bailey KL, et al. Proposal of a 2-Tier Histologic Grading

System for Canine Cutaneous Mast Cell Tumors to More Accurately Predict Biological Behavior. *Vet Pathol.* 2011;48(1):147-155.

3. Kiupel M. Mast cell tumors. In Meuten DJ, ed. *Tumors in Domestic Animals*, 5th ed. Ames, IA, Wiley Blackwell, pp. 177-177-193.

4. Oliveira FN, Elliott JW, Lewis BC, et al. Cutaneous Mast Cell Tumor With Epitheliotropism in 3 Dogs. *Vet Pathol.* 2013;50(2):234-237.

5. Thompson JJ, Pearl DL, Yager JA, Best SJ, Coomber BL Foster RA. Canine subcutaneous mast cell tumor: characterization and prognostic indices. *Vet Pathol* 2011; 48(1):156-168.

6. Vascellari M, Giantin M, Capello K, et al. Expression of Ki67, BCL-2, and COX-2 in Canine Cutaneous Mast Cell Tumors: Association With Grading and Prognosis. *Vet Pathol.* 2013;50(1):110-121.

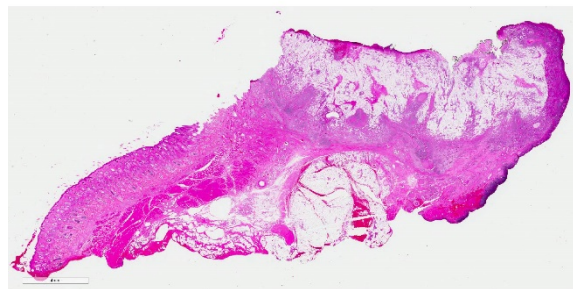
CASE II: SP-18-0001846 (JPC 4117533).

Signalment: 15-year-old, intact female, miniature horse, *Equus ferus caballus*, equine

History: This animal had a six month history of irritation of the right eye associated with a non-healing wound on the right lower eyelid. Physical examination revealed a 3cm in diameter, ovoid, ulcerated mass on the right eye lower eyelid that exuded yellow discharge.

Gross Pathology: N/A

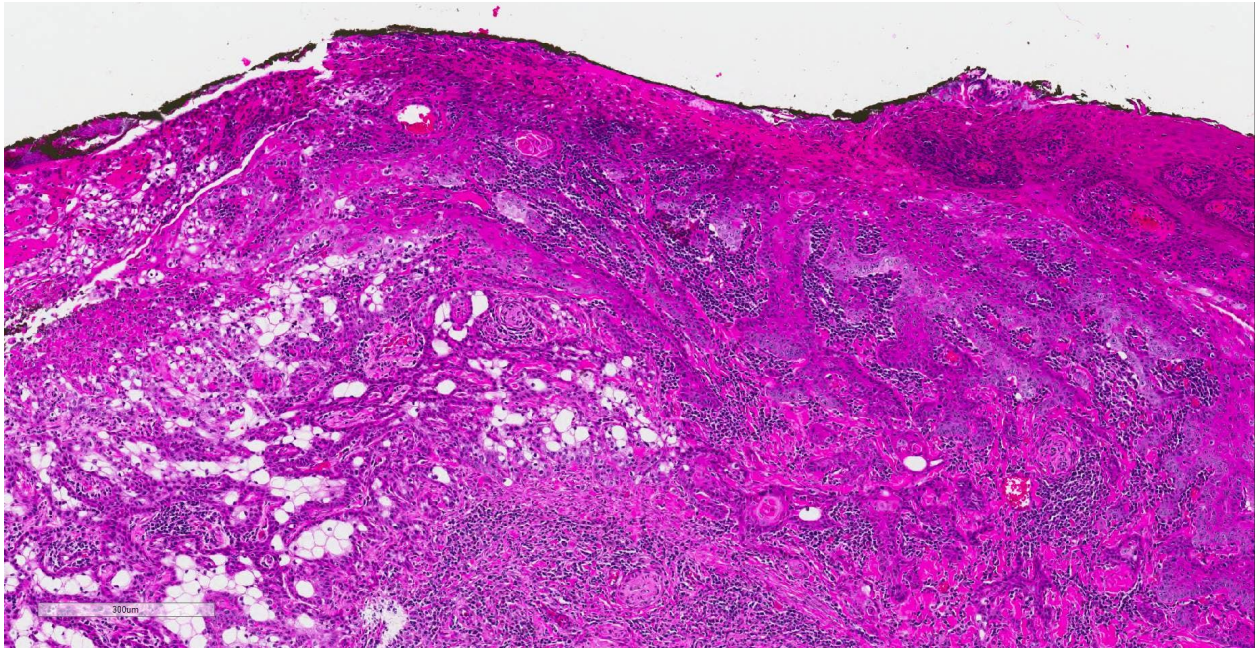
Laboratory results: N/A



Eyelid, horse. A section of ulcerated eyelid is submitted for examination. (HE, 4X)

Microscopic Description:

Histopathologic examination revealed a fairly well-demarcated, ulcerated dermal mass composed of neoplastic squamous epithelial cells arranged in anastomosing cords and nests that extended from the surface into the underlying dermis. Neoplastic cords near the surface and along the lateral margins of the mass had multifocal central keratinization. Neoplastic squamous epithelial cells merged with dense sheets of vacuolated polygonal cells towards the center of the mass. The center of the mass was also characterized by nests and cords of neoplastic cells composed of 1-3 outer layers of neoplastic squamous cells that were non-vacuolated and basaloid and rimmed central areas composed entirely of similar large vacuolated polygonal cells that formed sheets in the center of the mass. The non-vacuolated basaloid neoplastic squamous cells were round, contained a small to moderate amount of eosinophilic cytoplasm, and had round to ovoid, finely stippled nuclei that generally contained a single, large, central nucleolus. Anisokaryosis was moderate to marked, depending on the area, and there were occasional binucleated cells. There were 0-2 mitoses per high powered field. The vacuolated polygonal cells often had larger finely stippled nuclei that were peripheralized. Multifocally, nests and cords of neoplastic squamous epithelial cells invaded the underlying dense collagenous connective tissue, focally extended into the



Eyelid, horse. Anastomosing cords of squamous epithelium descend from the overlying epidermis, and at left are separated by polygonal clear cells. Numerous aggregates of lymphocytes, plasma cells, and fewer macrophages, eosinophils and neutrophils are scattered throughout the neoplasm. (HE, 123X)

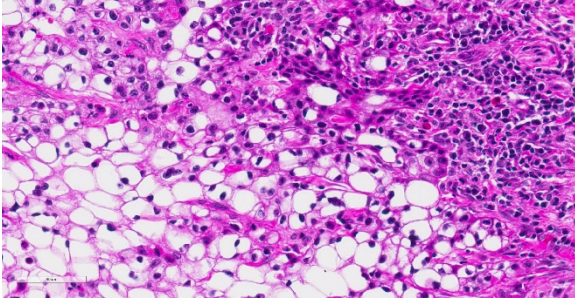
underlying skeletal muscle, and often surrounded nerves. In addition, there were multifocal perivascular and perineural inflammatory infiltrates comprised of moderate to large numbers of lymphocytes and plasma cells. In some regions, there was sebaceous gland hyperplasia along the surface of the haired skin. The dermis along the lateral margins of the neoplasm also had evidence of solar elastosis. Within the superficial dermis, there were foci of smudged degenerate collagen admixed with tangles of thickened, curled, lightly basophilic fibers that stained black with Verhoeff-van Gieson, consistent with elastin.

Immunohistochemistry for E-cadherin showed strong perimembranous labeling of neoplastic squamous, basaloid and vacuolated polygonal cells. Special staining with oil-red-O, periodic acid-Schiff (PAS), and mucicarmine did not reveal positive material within the cytoplasm of vacuolated polygonal cells.

Contributor's Morphologic Diagnoses:
Clear cell squamous cell carcinoma

Contributor's Comment: While this neoplasm was organized in varying patterns, including extensive sheets of vacuolated cells, there was overt squamous differentiation in several areas. These histologic findings, in conjunction with the immunohistochemical and histochemical staining results, were consistent with a clear cell squamous cell carcinoma (SCC). There was no true tubular or acinar formation and vacuolated polygonal cells lacked cytoplasmic lipid, glycogen, and mucus, further excluding neoplasms of sebaceous or adnexal origin.^{6-8,10,14,15}

To our knowledge, clear cell SCC has not been reported in animals. Variants of squamous cell carcinoma with clear cells have been described in dogs, but have not met the criteria of clear cell squamous cell carcinoma. A signet-ring squamous cell carcinoma was described in the scrotum of



Eyelid horse. Higher magnification of the transition between cords of squamous epithelium at right and clear cell squamous epithelium at left. (HE, 400)

one dog, but ultrastructurally clear cells contained intracytoplasmic lipid vacuoles and scattered glycogen.⁶ The uncommon canine clear cell adnexal carcinomas are also negative for oil red O, but in contrast to our case, positive for PAS.¹⁵ Other cutaneous neoplasms with clear cells that have been reported in dogs includes clear cell basal carcinoma, clear cell hidradenocarcinomas, sebaceous carcinomas, balloon cell melanomas, and liposarcomas.^{7-8,15} None of these entities is characterized by squamous differentiation, and the clear cells in adnexal neoplasms are PAS positive. In horses, clear cell differentiation has only been reported in cutaneous basal cell tumors; however, those tumors lacked the squamous differentiation observed in our case.¹⁴

In humans, clear cell SCC is a rare neoplastic entity in the skin also referred to as hydropic SCC. The clear cell appearance is caused by hydropic degeneration of neoplastic squamous cells causing accumulation of intracellular fluid and not glycogen, lipid, or mucin.^{9,13} Clear cell SCC is divided into three histologic types: keratinizing (type I), nonkeratinizing (type II), and pleomorphic (type III). The keratinizing, or type I, clear cell SCC, is defined by sheets or islands of clear neoplastic cells with peripherally displaced nuclei that are often indistinguishable from adipocytes, as well as some cells that have more vacuolated

cytoplasm and resemble sebaceous cells.¹⁰ Additionally, there are foci of keratinization or keratin pearl formation. Type II is characterized by anastomosing cords of neoplastic squamous cells with dense lymphoplasmacytic infiltrates and no keratinization, while type III demonstrates marked pleomorphism, vascular and perineural invasion, foci of squamous differentiation, and microcysts with acantholytic neoplastic cells. In all three types, there is no glycogen or mucin accumulation within clear cells, thus, clear cells are negative for PAS, mucicarmine, and alcian blue stains. AE1/AE3 and cytokeratin 7 have been used to confirm epithelial origin of the neoplastic clear cells.^{9,11} The case presented here is most consistent with a type I clear cell squamous cell carcinoma.

Squamous cell carcinomas are the most common neoplasm of the equine eye and adnexa.⁵ SCC of the eyelid typically has an aggressive, locally invasive behavior, and carries a poor prognosis.¹⁶ Metastasis is uncommon but may occur late in the course of disease and most often to the regional lymph nodes. We speculate that clear cell SCC will exhibit similar behavior, although this cannot be confirmed due to lack of follow-up in our case. The prognosis of this entity in humans is also unclear due to the scarcity of case reports. Of seven cases of clear cell SCC reported in humans, all but one have occurred on the head or neck of elderly white males who worked outdoors. One case was reported in a dark-skinned adult male who also worked outdoors. Of these reported cases, one patient died of metastatic disease, one died post-operatively, and one had recurrence after 3 months.^{1,13}

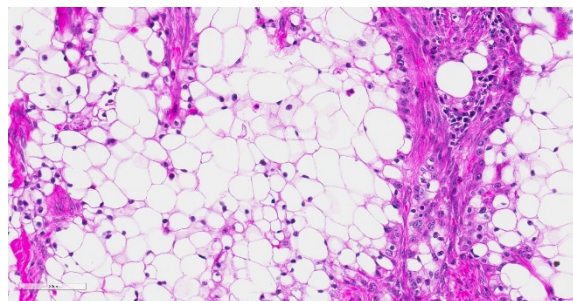
In both humans and animals, chronic ultraviolet (UV) light exposure plays an important etiologic role in the development of cutaneous SCC.^{3-4,10-11,13} Solar elastosis is a non-neoplastic UV-induced lesion

commonly observed in poorly-pigmented skin of horses and humans with or without SCC. It is defined as an accumulation of abnormal elastin in the dermis and is histologically characterized by aggregates of thick interwoven elastic fibers mixed with degenerate collagen within the superficial to mid dermis as observed in our case. The pathogenesis of elastin accumulation is unclear, but is often seen in poorly pigmented or non-pigmented skin with chronic UV exposure, or in conjunction with other solar induced changes such as solar (actinic) keratosis, epidermal plaques, and SCC. In horses, solar-associated SCC has been reported in the conjunctiva, eyelid, and vulvar epithelium, and is morphologically similar to solar-induced SCC in humans, often exhibiting solar elastosis within or adjacent to the neoplasm.³ Chronic UV-exposure evidenced by solar elastosis has been observed in human cases of clear cell SCC, and is hypothesized to play a role in the development of the disease.¹³ The solar elastosis observed in our case parallels that of human clear cell SCC, and suggests that chronic UV exposure may play an etiologic role in the development of clear cell SCC in horses as well.

Contributing Institution:

Michigan State University Veterinary Diagnostic Laboratory and Department of Pathobiology and Diagnostic Investigation, College of Veterinary Medicine, Michigan State University, East Lansing, MI, USA
<https://dcpah.msu.edu/>

JPC Diagnosis: Haired skin, eyelid: Squamous cell carcinoma, clear cell variant.



Eyelid, horse. Neoplastic cells measure up to 50um in diameter with peripheralized, hyperchromatic nuclei. HE, 400X)

JPC Comment: This is a unique neoplasm in the experience of the JPC Vet Path Service. Since the original submission of this case, it has been published as a case report in the Journal of Veterinary Diagnostic Investigation.¹⁷

This case was reviewed by human subspecialty pathologists at the JPC, who rendered the following consultation – “Interesting case. Based on morphology, we believe a lot of the clear cells are cytologically bland and there are areas of definite tubular differentiation, favoring a malignant clear cell hidradenoma. Additional myoepithelial stains would favor an adnexal origin rather than squamous cell carcinoma. Less likely would be a metastatic clear cell carcinoma such as metastatic renal cell carcinoma¹⁸. This is not favored based on morphology, but there seems to be co-expression of vimentin and cytokeratin in the section that we reviewed.”

Hidradenoma, a term far more commonly used in human rather than veterinary pathology, generally refers to neoplasms of eccrine sweat glands, which the moderator pointed out are not present in the horse (except in the portion of the hoof known as the frog). More recent investigations into the etiology of hidradenomas in humans have postulated potential origins from apocrine sweat glands as well.)

The consensus of the attendees is that while there is a focus of tubular differentiation of neoplastic cells at the deep margin, the predominant form of differentiation is toward a squamous cell morphology, and agree with the contributor's diagnosis in this case. In addition, areas of solar elastosis were noted in the superficial dermis, lending credence to the contributor's suggestion that it represents a neoplasm induced by chronic UV exposure.

References:

1. Al-Arashi MY, Byers HR. Cutaneous clear cell carcinoma in situ: clinical, histological and immunohistochemical characterization. *J Cutan Pathol*. 2006;**34**:226-233.
2. Berk DR, Lennerz JK, Bayliss SJ, Lind A, White FV, Kane AA. Mucoepidermoid carcinoma on the scalp of a child. *Pediatr Dermatol*. 2002; **24**:452-453.
3. Campbell GA, Gross TL, Adams R. Solar elastosis with squamous cell carcinoma in two horses. *Vet Pathol*. 1987;**24**:463-464.
4. Corbalán-Vélez R, Ruiz-Macia JA, Brufau C, López-Lozano JM, Martínez-Barba E, Carapeto FJ. Clear cells in cutaneous squamous cell carcinoma. *Actas Dermosifiliogr*. 2009;**100**:307-316.
5. Dugan SJ, Curtis CR, Roberts SM, Severin GA. Epidemiologic study of ocular/adnexal squamous cell carcinoma in horses. *J Am Vet Med Assoc*. 1991; **198**:251–256.
6. Espinosa de los Monteros A, Aguirre-Sanceledonio M, Ramírez GA, Castro P, Rodríguez F. Signet-ring squamous cell carcinoma in a dog. *Vet Rec*. 2003;**153**:90-92.
7. Goldschmidt MH, Dunstan RW, Stannard AA. Histological classification of epithelial and melanocytic tumors of domestic animals. In: Schulman FY, ed. World Health Organization International Histological Classification of Tumors of Domestic Animals. Washington DC: Armed Forces Institute of Pathology 1998.
8. Jabara AG, Finnie JW. Four cases of clear-cell hidradenocarcinomas in dogs. *J Comp Pathol*. 1978;**88**:525-532.
9. Kuo T. Clear cell carcinoma of the skin. A variant of the squamous cell carcinoma that simulates sebaceous carcinoma. *Am J Surg Pathol*. 1980;**4**:573–83.
10. Lawal AO, Adisa AO, Olajide MA, Olusanya AA. Clear cell variant of squamous cell carcinoma of skin: A report of a case. *J Oral Maxillofac Pathol*. 2013;**17**:110-112.
11. Rashid A, Jakobiec FA, Mandeville JT. Squamous cell carcinoma with clear-cell features of the palpebral conjunctiva. *JAMA Ophthalmol*. 2014;**132**:1019-1021.
12. Montiani-Ferreira F, Kiupel M, Muzolon P, Truppel J. Corneal squamous cell carcinoma in a dog: a case report. *Vet Ophthalmol*. 2008;**11**:269-272.
13. Rinker MH, Fenske NA, Scalf LA, Glass LF. Histologic variants of squamous cell carcinoma of the skin. *Cancer Control*. 2001;**8**:354-363.
14. Schuh JCL, Valentine BA. Equine basal cell tumors. *Vet Pathol* 1987;**24**:44-49.
15. Schulman FY, Lipscomb TP, Atkin TJ. Canine cutaneous clear cell adnexal carcinoma: histopathology, immunohistochemistry, and biologic behavior of 26 cases. *J Vet Diagn Invest*. 2005;**17**:403-411.
16. Schwink K. Factors influencing morbidity and outcome of equine ocular squamous cell carcinoma. *Equine Vet J*. 1987;**19**:198–200.
17. Stein L, Sledge D, Smedley R, Kiupel M, Thaiwong T. Squamous cell carcinoma with clear cell differentiation in an equine eyelid. *J. Vet Diagn Invest*. 2019; 259-262.
18. Williams JC, Heaney JA. Metastatic renal cell carcinoma presenting as a skin

nodule: case report and review of the literature. *J Urol.* 1994;**152**:2094–2095.

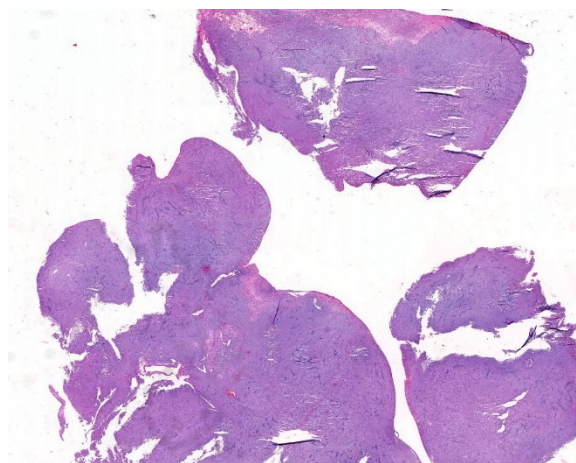
CASE III: Case 2 (JPC 4070611).

Signalment: 2 year 7 month old castrated male Labrador retriever, dog (*Canis lupis familiaris*).

History: This dog presented to the Queen Mother Hospital for Animals (Royal Veterinary College, UK) with a 4 month history of intermittent bloody discharge from his penis. The owner reported no problems with frequency, volume or the action of urination, nor did his urine appear to be discoloured. He had no previous history of illness aside from the presenting complaint. The dog had been imported from continental Europe. Urinalysis, blood biochemistry, and abdominal ultrasound were unremarkable. Haematology revealed a mild increase in lymphocytes, but was otherwise unremarkable.

Gross Pathology: Physical examination revealed a smooth swelling at the base of the penis, which upon examination under general anaesthesia appeared to be a friable mass within the prepuce. The mass was removed and submitted for histopathologic examination.

Laboratory results: Cytologic examination of five impression smears reveals high nucleated cellularity, moderate amounts of blood and low numbers of lysed cells on a pale basophilic background. High numbers of round cells are found on all smears. Cells have a round to oval nucleus, 10-15µm in diameter with finely to coarsely stippled chromatin, often a single large, round, prominent nucleolus and moderate amounts of pale blue cytoplasm, frequently containing

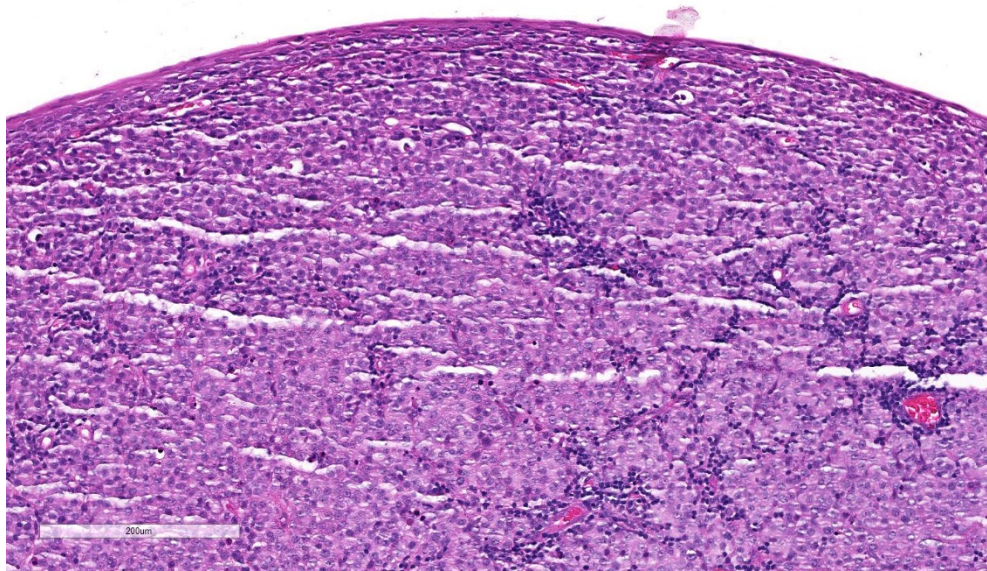


Prepuce, dog. Multiple sections of an exophytic neoplasm are submitted for examination. (HE, 4X)

moderate numbers of punctate vacuoles. Cells display mild to moderate anisocytosis and anisokaryosis, with low numbers of mitotic figures and rare binucleated forms. Low to moderate numbers of small lymphocytes are focally admixed with the tumour cells. Two smears additionally contain moderate to high numbers of squamous epithelial cells in sheets and individually, often displaying dyskeratosis. Squamous cells display mild anisocytosis and anisokaryosis, occasional bi- and rare multinucleation, and occasionally prominent nucleoli. Also occasional cells have prominent perinuclear vacuolation. These two smears also focally contain high numbers of variably degenerate neutrophils, occasionally containing intracellular cocci. Low numbers of macrophages are also found. These features are consistent with transmissible venereal tumour, with septic neutrophilic inflammation and squamous dysplasia. Other round cell tumours (e.g. of histiocytic origin) cannot be ruled out completely, but far less likely. Septic inflammation and squamous dysplasia are likely secondary changes to the presence of the tumour (e.g. ulceration).

Microscopic Description:

Multiple sections of non-haired skin, from the prepuce per history, are examined. Effacing the lamina propria, raising a multifocally eroded and attenuated stratified squamous epithelium, and extending to the lateral and deep borders of the examined sections, is an unencapsulated, poorly demarcated, round cell neoplasm. The cells are arranged in sheets and loose cords amongst a scant fibrovascular stroma. The neoplastic cells are round with indistinct cell borders, a moderate amount of eosinophilic cytoplasm containing small clear vacuoles, a central round nucleus with stippled or peripheralised chromatin, and a single prominent magenta nucleolus. Anisocytosis and anisokaryosis are mild, and 42 mitoses are observed in 10 high power (x400) fields, some of which are bizarre. Multifocally the



Prepuce, dog. Neoplastic cells abut an intact mucosal membrane. (HE, 40X)

tumour is infiltrated by moderate numbers of lymphocytes and plasma cells. Moderate to high numbers of extravasated erythrocytes and fibrin (haemorrhage) are present beneath the epithelium multifocally.

Contributor's Morphologic Diagnoses:
Prepuce; Transmissible venereal tumour.

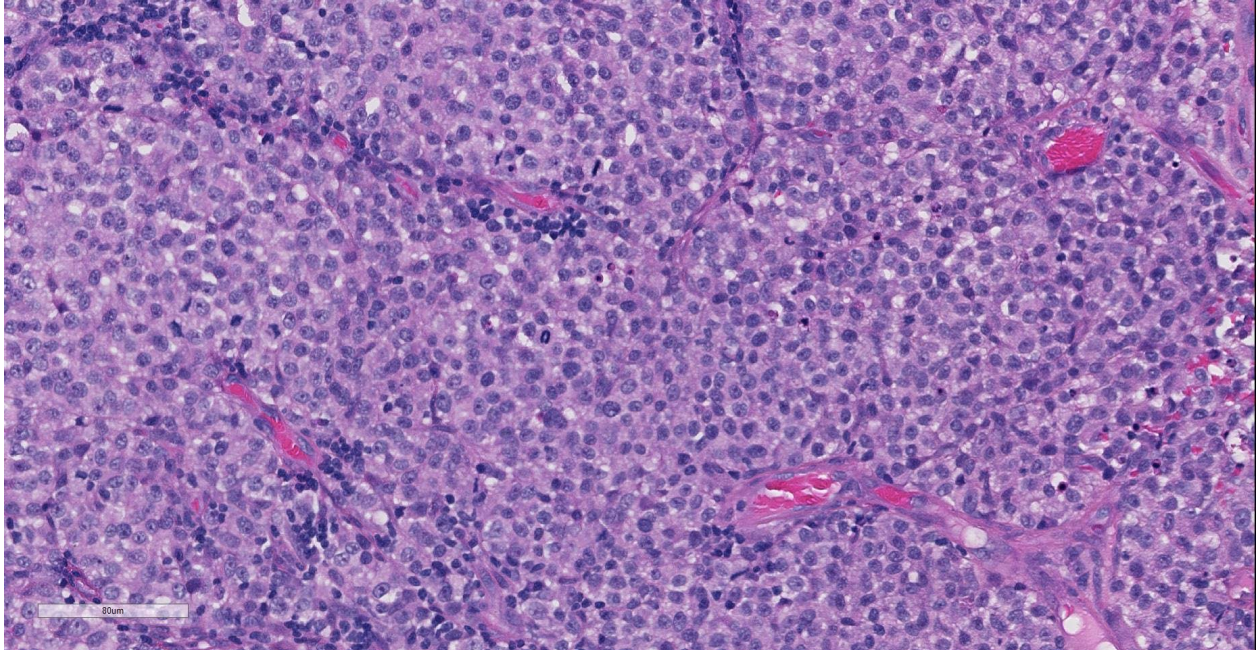
Contributor's Comment: Histopathologic and cytologic examination reveals a canine transmissible venereal tumour (CTVT). The cell of origin in CVTVs is unknown,¹ however a histiocytic origin is suspected due to positive immunolabelling for lysozyme, ACM1, a-1-antitrypsin and vimentin, and negative immunolabelling for keratin, desmin a-smooth muscle actin, CD3, IgG and IgM, and A and K light chains.^{10,13} CTVT should always be considered in cases of genital round cell tumours and primary differentials are other round cell tumours of the skin, such as histiocytoma, lymphoma and poorly granulated mast cell tumour.⁵ Haematoxylin and eosin differentiation between histiocytomas and CTVTs can be challenging, and cytology should be used, as in this case, to help confirm the diagnosis

because of better nuclear preservation in cytologic preparations.⁵

CTVT is the most common tumour of the penis of dogs,⁷ and typically affects the proximal part of the penis.³ The tumour typically presents as a single or

multinodular mass⁴ with a red

ulcerated surface.⁵ Although primarily located on the genitalia,⁵ tumours can also arise on the oral, nasal or conjunctival mucosa.⁷ Less commonly the skin is involved,⁷ particularly sites which can come into contact with the genitalia.⁵ Dogs of both sexes and all ages can be affected, and it is most common in the dorsal vagina¹⁵ of



Base of penis, dog. Neoplastic round cells have abundant vacuolated eosinophilic cytoplasm with large centrally placed round nuclei and prominent nucleoli. Mitotic rate is 3-5 per HPF, and there are infiltrates of lymphocytes within the fibrovascular stroma. (HE, 400X)

sexually mature female dogs.⁵ The pathogenesis is by physical transplantation rather than infectious means, and usually occurs during coitus.⁵ This is thought to be due to abrasions and bleeding of penile and vaginal mucosa during coitus increasing the chance of transplantation.¹³ Similar to canine cutaneous histiocytomas, the tumour has a predictable growth pattern of progressive growth, a static phase, and then regression after one to two months.^{10,13} Lymphoplasmacytic infiltration is a feature during regression⁷ and can be used to distinguish from lymphoma.^{5,13} Metastasis is rare, but has been reported in immunosuppressed animals and puppies. Metastases to the inguinal lymph nodes, brain, adenohypophysis, liver, and kidneys have been reported.^{6,13}

The global distribution of CTVT is unexplained, and is previously unreported in the UK.⁵ Two subclades of CTVT have been identified, each of which now has a broad

geographic distribution.⁵ The host does not contribute to the growth of the tumour.⁷

The neoplastic cells have 59 rather than the usual 78 chromosomes present in the cells of dogs, and this karyotypic variation is consistent between CTVTs of different animals.⁷ A 1.5kbp repetitive insertion has been identified upstream of c-myc in all CTVTs.⁷ Further investigation has revealed that CTVT first arose from a common ancestral neoplastic cell in a wolf or dog related to 'old' East Asian breeds.¹³ This is thought to have occurred 200 to 2500 years ago, thus CTVT may represent the oldest known mammalian somatic cell in continuous propagation.¹³ CTVT can be transmitted between other canids, including foxes, coyotes, jackals and wolves.¹³ Dogs appear to be resistant to challenge after natural regression of the tumour.¹⁵

CTVT was the first tumour to be transmitted experimentally, by Novinsky in 1863.¹⁵ In 1965, a transmissible sarcoma, both

spontaneous and induced by 20-methylcholanthrene, in Syrian hamsters was successfully transmitted experimentally between individuals without immunosuppression of the host.² Two other transmissible tumours have also been identified. Devil facial tumour disease is a transmissible tumour of the Tasmanian devil (*Sarcophilus harrisi*). Immunohistochemical profiling has demonstrated a Schwann cell origin of this monophyletic clonally transmissible tumour.¹¹ A Schwann cell specific myelin protein, periaxin (PRX), is used as a diagnostic marker for devil facial tumours.¹¹ Finally, a clonal contagious leukaemia in soft shelled clams (*Mya arenaria*) exhibits characteristics similar to CTVT: The genotype of neoplastic cells does not match the host animal, and there is near identical genotype of neoplastic cells between affected animals despite geographic separation, highly suggestive of horizontal transmission of leukaemia in these clams.⁸

Contributing Institution:

Department of Pathology and Pathogen Biology, The Royal Veterinary College, University of London.
<http://www.rvc.ac.uk/pathology-and-diagnostic-laboratories>

JPC Diagnosis: Prepuce: Transmissible venereal tumor.

JPC Comment: Transmissible venereal tumor occupies a unique niche in cancer biology as the most well-characterized of a small subset of neoplasms which is transmitted as living cells between hosts, rather than transformation of the host's cells.¹ The contributor has provided an excellent review of this tumor and other transmissible tumors in animal species.

The tumor, which has been reported under several names, to include transmissible venereal sarcoma, venereal granuloma,

infectious sarcoma, and Sticker's sarcoma, was first described by Hujard in 1920.⁴ In 1876, the Russian veterinarian Novinsky demonstrated the nature of the tumor with the first transplantation experiments.⁴

A 2015 paper by Sethawongsin et al¹⁶ detailed molecular identification of the specific long interspersed element (LINE) inserted upstream of the c-myc gene in CTVT cells via PCR on frozen tissue. The moderator discussed recent development of a PCR test for paraffin-embedded tissue utilizing primers of less than 100 bp which is now publicly available through the Michigan State Veterinary Diagnostic Laboratory, which may be of utility in diagnosing neoplasms not present in traditional genital locations.

The moderator also compared cytologic versus histologic appearance of these neoplasms. When taken in context of being from the genital area, the diagnosis of CTVT is not especially difficult. In this particular sample, the cytologic appearance with traditional round centrally placed nuclei, prominent, often single nucleoli, and the presence of lymphocytes and plasma cells often in perivascular location is very characteristic of this particular neoplasm. Cytologically, the presence of numerous vacuoles within the blue cytoplasm of round cells is also a fairly characteristic finding in CTVT, and some pathologists prefer cytology over histology for their diagnosis.

CTVT has evolved a number of mechanisms to evade the host response. Tumor cells downregulate DLA class II expression, but express just enough (10%) of DLA class I genes (complete masking of DLA Class I genes actually activates natural killer cells).⁴ TVT cells can also secrete immunosuppressive levels of transforming growth factor- β . During the period of regression,

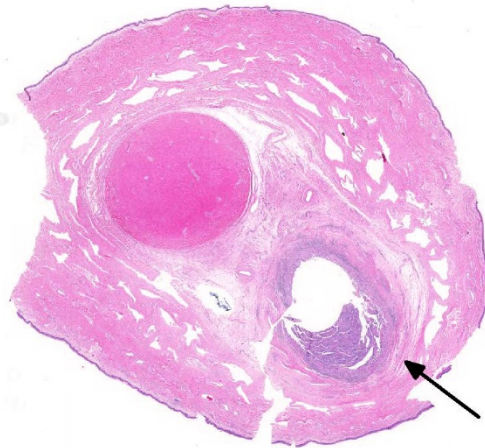
host IL-6 liberated from infiltrating lymphocytes works with host IFN- γ to re-establish DLA expression.⁴

Since the submission of this report, other clonally transmitted tumors have been reported in bivalves, including bay mussels (*Mytilus trossulus*), cockles (*Cerastoderma edule*) and golden carpet shell clams (*Polititapes aureus*).⁹ Interestingly, the neoplasm in golden carpet shell clams appears to have arisen in another species, the pullet carpet shell (*Venerupis corugata*).⁹ Even more interesting is a 2015 report by Muelenbachs et al.¹⁴ of pulmonary and lymph node neoplasms in a 41-year-old HIV-positive individual with concurrent *Hymenolepis nana* infection. Neoplasms composed of small, rapidly dividing cells uncommon in human pathology were determined, after a CDC consultation, the neoplasms were determined to contain DNA of the human cestode *Hymenolepis nana*.¹⁴

References:

1. Agnew DW, MacLachlan NJ. Tumors of the Genital System. In Meuten DJ, ed. Tumors in Domestic Species. Ames IA, Wiley Blackwell, pp 718-720.
2. Fabrizio AM. An induced transmissible sarcoma in hamsters: Eleven-year observation through 288 passages. *Cancer Res* 1965; 25:107-117.
3. Foster RA. Male reproductive system. In: Zachary JF, McGavin MD (eds.) Pathologic Basis of Veterinary Disease: 5th ed. Missouri, USA: Elsevier;2012: 1152.
4. Ganguly B, Das U, Das AK. Canine transmissible venereal tumour: a review. *Comp Oncol* 2013; 14(1):1-12.
5. Goldschmidt MH, Hendrick MJ. Tumours of the skin and soft tissues. In: Meuten DJ (ed.) Tumors in Domestic Animals: 4th ed. Iowa, USA: Iowa State Press;2002:115-117.
6. Joint Pathology Centre, Wednesday Slide Conference; 2007: 10, Case 2.
7. Kennedy PC, Cullen JM, Edwards JF, et al (eds.) Histological Classification of Tumors of the Genital System of Domestic Animals: Second Series Volume IV. Washington D.C., USA: AFIP, WHO;1998:8.3 and 11.3
8. Metzger MJ, Reinisch C, Sherry J, Goff SP. Horizontal transmission of clonal cancer cells causes leukemia in soft-shelled clams. *Cell* 2015; 161 :255-263.
9. Metzger MJ, Villalba A, Carballal MJ, Iglesias D, Sherry J, Reinisch C, Muttaray AF, Baldwin SA, Goff SP. Widespread transmission of independent cancer lineages within multiple bivalve species. *Nature* 2016; 534(7609): 705-709.
10. Mozos E, Mendez A, Gomez-Villamandos JC, Martin de las Mulas J, Perez J. Immunohistochemical characterization of canine transmissible venereal tumor. *Vet Pathol* 1996; 33:257-263.
11. Murchison EP, Tovar C, Hsu A. The Tasmanian devil transcriptome reveals Schwann cell origins of a clonally transmissible cancer. *Science* 2010; 327:84-87.

12. Murgia C, Pritchard JK, Kim SY, Fassati A, Weiss RA. Clonal origin and evolution of a transmissible cancer. *Cell* 2006; 126(3):477-487.
13. Mukaratirwa S, Gruys E. Canine transmissible venereal tumour: cytogenetic origin, immunophenotype, and immunobiology. A review. *Vet Quarterly* 2003; 25(3):101-111.
14. Muelenbachs A, Bhatnagar J, Agudelo CA, Hidron A, Eberhard ML, Mathison BA, Frace H, Ito K, Metcalfe MG, Rollin DC, Visvesvara GS, Pham CD. Malignant Transformation of *Hymenolepis nana* in a Human Host. *N Engl J Med* 2014; 373:1845:1852.
15. Schlafer DH, Miller RB. Female genital system. In: Grant Maxie M (ed.) Jubb, Kennedy, and Palmer's Pathology of Domestic Animals: 5th ed. Saunders Elsevier;2007:547-548.
16. Setthawaontsin C, Techangamsuwan S, Tankkawaattana S, Rungsippat A. cell-based polymerase chain reaction for canine transmissible venereal tumor diagnosis. *J. Vet Med Sci*



Penis, dog: The penile urethra is partially occluded by a neoplasm (arrow) and the submucosa is hypercellular. (HE, 5X)

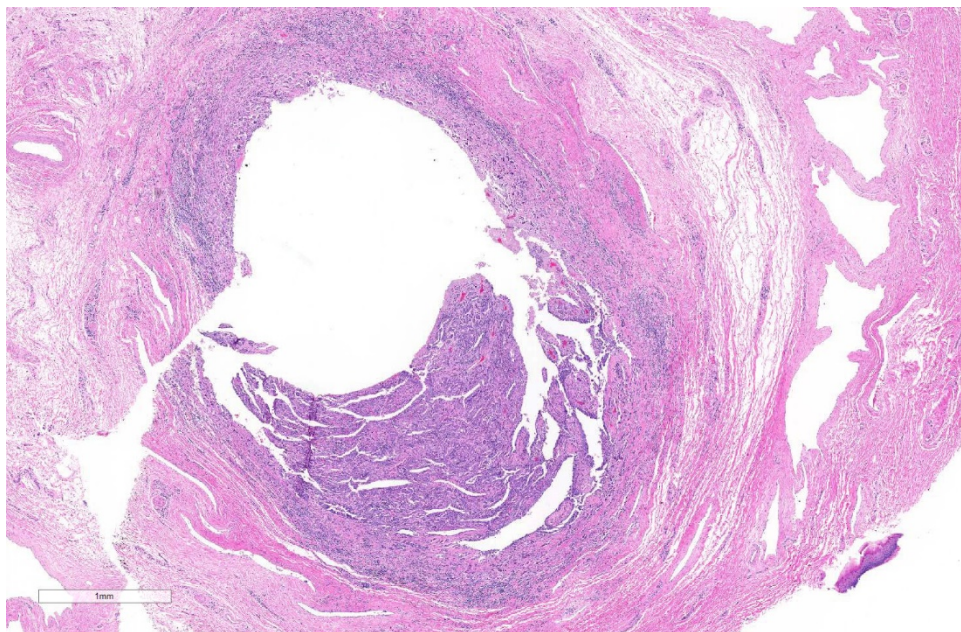
removed. Several months later Rudy presented again with hematuria. He would also dribble small spots of blood from the preputial opening when not urinating. Otherwise, the dog was bright, alert and responsive. The dog was referred to the Atlantic Veterinary College teaching hospital for further work-up. A urethroscopy was performed. Approximately 1 cm from the tip of the penis and extending approximately 2 cm further up the urethra, the mucosal surface was roughened with irregular frond-like structures extending into the narrowed lumen. Small pinch biopsies were taken of the abnormal mucosal surface. A diagnosis of urethral urothelial (or transitional) cell carcinoma was made. A partial penile amputation and an urethrostomy at the level of the bulbourethral gland was performed. The amputated portion of the penis was submitted for histopathology.

Gross Pathology: A 7.5 cm long section of the distal penis (including the glans and the distal body of the penis) is submitted for examination. The length of the urethra was opened. The mucosal lining of the distal 3

CASE IV: C9969-15 (JPC 4070611).

Signalment: 11 year old, male, castrated, Labrador retriever, *Canis lupus familiaris*, canine

History: The dog presented to referring veterinarians with hematuria and dysuria. A cystotomy was performed and calculi were



Penile urethra, dog: At higher magnification, the urethral mucosa is circumferentially ulcerated by an exophytic, and infiltrative neoplasm. (HE, 27X)

cm of the urethra was mildly roughened. Several cross-sections through the entire penis were examined.

Laboratory results Presurgical complete blood count and serum biochemistry; mild abnormalities included:

- ϕ RBC $5.26 \times 10^{12} /L$
(normal range: $5.7 - 8.4 \times 10^{12}/L$)
- ϕ Hemoglobin 127 g/L
(normal range: 135 - 198 g/L)
- ϕ Hematocrit 0.364 L/L
(normal range: 0.40 - 0.56 L/L)
- \S ALT 93 U/L
(normal range: 13 - 69 U/L)

Mild anemia was attributed to mild, chronic blood loss. Mildly increased ALT may represent mild hepatocellular leakage or possibly normal variation in this individual.

Microscopic Description:

Microscopically, the urethral lumen is narrowed and the mucosa is irregularly thickened by an infiltrative, poorly defined epithelial tumor composed of many small nests, occasional small acini and few small papillary projections covered by large polygonal neoplastic epithelial cells. These infiltrates are supported by small

amounts of dense fibrous stroma containing mild to moderate infiltrates of plasma cells, neutrophils, fewer lymphocytes and macrophages. The mucosal lining is extensively ulcerated and occasionally covered by small amounts of proteinaceous debris. Several layers of pleomorphic neoplastic epithelial cells partially line the urethral lumen in areas. Small clusters and scattered individual polygonal tumor cells frequently breach the mucosal basement membrane and infiltrate the underlying submucosa where they are accompanied by mild multifocal infiltrates of lymphocytes, plasma cells, few neutrophils, few small foci of hemorrhage and occasional macrophages rarely laden with hemosiderin. Neoplastic epithelial cells have medium to large, ovoid, nuclei with finely stippled chromatin, one to several, prominent nucleoli and moderate to large amounts of poorly defined, cytoplasm. Anisokaryosis is moderate to severe. Mitotic figures are present (7 per 10 HPF). Small clusters of neutrophils admixed with a few sloughed tumor cells are noted in the urethral lumen. Rarely, small clusters of polygonal

cells resembling tumor cells are present within lymphatics and veins within the submucosa, the corpus spongiosum and the pars longo glandis (not present in all sections). The ovoid, discrete aggregate of dense, poorly cellular, collagen dorsal to the urethra represents the distal end of the os penis.

Contributor's Morphologic Diagnoses:

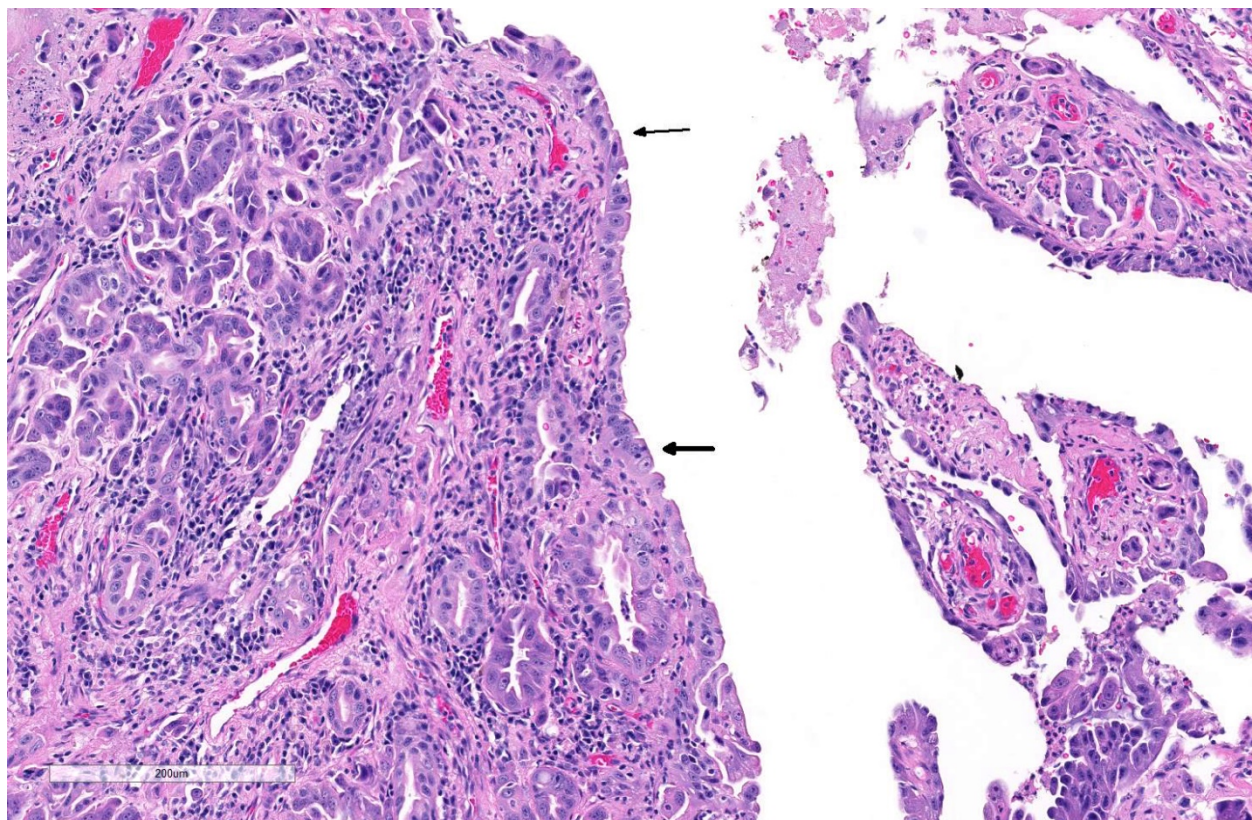
Penis: 1. Urethral urothelial (or transitional) cell carcinoma

2. Mild to moderate, lymphoplasmacytic and neutrophilic, erosive, chronic, urethritis

Contributor's Comment: The cause of hematuria and persistent blood dribbling

from the penis of this dog was a urothelial (or transitional) cell carcinoma arising within the distal urethra. Ultrasound performed at the time of surgery revealed no abnormalities in the urinary bladder and no evidence of abdominal or retroperitoneal lymph node enlargement. Thoracic radiographs were also unremarkable. Occasional small microscopic clusters of putative tumor cells were noted within vascular structures in these sections. Despite the latter finding, 2 years after partial penile amputation and complete removal of the tumor, this dog is still alive and has exhibited no clinical signs indicative of metastatic disease (per recent discussion with the rDVM).

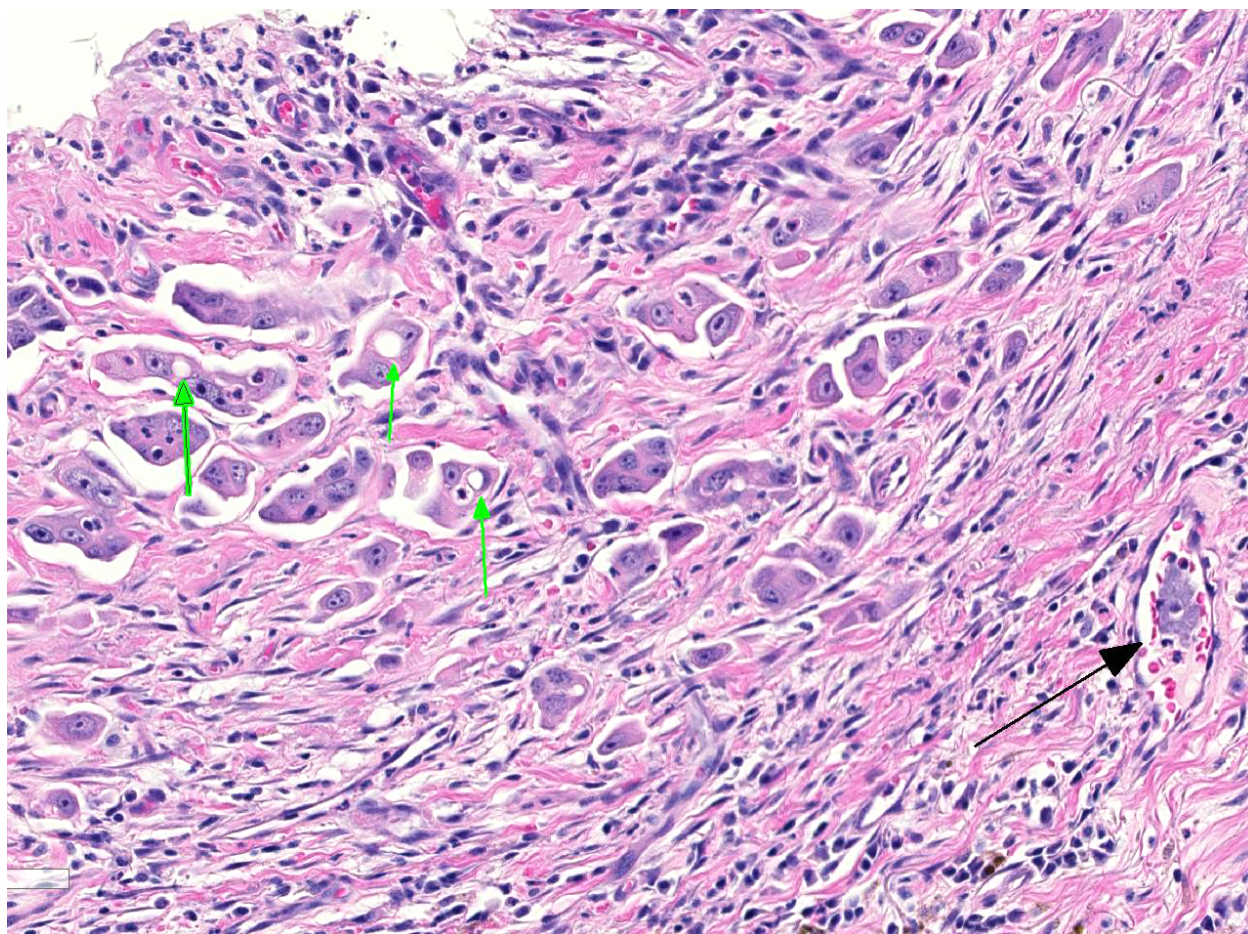
Primary urethral tumors are very rare in dogs. The vast majority of these tumors are



Penile urethra, dog: Neoplastic epithelial cells form nests, glands, and line papillary fronds in the exophytic portion of the neoplasm. The dense stroma is infiltrated by moderate numbers of lymphocytes and plasma cells with fewer neutrophils. (HE, 220X)

malignant and most are urothelial cell carcinomas. Females are generally thought more commonly affected than males. The cause is unknown but a variety of chemical carcinogens have been associated with the development of lower urinary tract tumors in dogs.² An association between chronic urethritis and urothelial tumors in females has also been shown.¹ The latter is interesting as this male dog, also had a chronic history of urinary struvite calculi. Urothelial cell carcinomas in the lower urinary tract generally occur in older dogs which often present with hematuria and dysuria. References generally report that metastasis is seen in approximately 30% of

cases; regional lymph nodes are the most common site. Approximately 1/3 of dogs with urethral tumors also have urothelial cell carcinomas in the urinary bladder. When present in both sites, affected dogs tend to have a much poorer prognosis and significantly shorter survival times.^{1,2} One retrospective study on canine lower urinary tract tumors reported that the longest survival times (median of 365 days) were achieved in dogs with no evidence of metastasis at the time of surgery, that had a solitary carcinoma located in either the urinary bladder or the urethra, and in which complete resection was achieved.²



Penile urethra, dog. In ulcerated areas of the mucosa, neoplastic cells infiltrate the inflamed submucosa. Occasional neoplastic cells contain cytoplasmic Melamed-Wolinska bodies (green arrows). Neoplastic cells are present within submucosal vessels (black arrow). (HE, 220X)

Contributing Institution:

Atlantic Veterinary College, University of Prince Edward Island / www.upei.ca

JPC Diagnosis: Penile urethra:
Transitional cell carcinoma

JPC Comment: Transitional cell (or urothelial carcinoma) account for approximately 2% of cancer in the dog. It is the most common neoplasm of the bladder, and the majority are high-grade neoplasms. It is primarily seen in older dogs between the ages of 9 and 11, and most tumors are considered high-grade neoplasms. Scottish terriers have an increased breed predisposition being 18-20X more likely to develop this tumor than other breeds. The trigone is the site of most tumor development, although the prostatic urethra and lower areas of the urethra (as seen in this case) are also commonly affected. Grossly, most neoplasms in the bladder are solitary, although they may cover a large region of the bladder making resection impossible.¹

Histologically, most tumors are readily diagnosed histologically, especially if an adequate sample is obtained. One of the more diagnostic features is the presence of Melamed-Wolinska bodies, which impart a signet ring appearance to neoplastic cells and are commonly seen in these tumors. These bodies often stain positively for uroplakin (a commonly used immunohistochemical marker for TCC).¹

Tumor growth patterns often impact on grading schemes. While most neoplasms are infiltrative indicating a high-grade, non-infiltrative neoplasms (carcinoma *in situ*) is occasionally seen or seen at the periphery of infiltrative lesions. Tumors may also be papillary or non-papillary, although this particular feature has not been identified as predictive of future behavior.¹

Invasive TCC is also extremely prone to widespread metastasis with studies demonstrating a 50-90% rate, most often to the lungs and lymph nodes. Approximately 75% are staged at T2 under the TNM system, and an addition 20% at stage 2 with invasion of adjacent organs or tissues. Cutaneous metastasis has been reported to occur in up to 10% of cases. While the presence of urethral involvement does not appear to be significantly related to the presence or absence of metastatic disease, concurrent presence of TCC within the bladder and urethra is associated with the shortest survival times.¹

As the prostatic urethra is a common site of urothelial carcinoma and local invasion, the diagnosis of prostatic carcinoma should likely include immunohistochemistry for uroplakin to rule out other forms of carcinoma. Uroplakin (uroplakin III) is an excellent marker for urothelium but may be positive in normal, hyperplastic and neoplastic urothelium. In the dog, staining is seen primarily at the surface of cell membranes in the dog and is often not uniform throughout neoplasms.¹ Other immunohistochemical markers that have been shown to have utility in the diagnosis and prognosis for human and canine TCCs include cytokeratin 7 and cyclooxygenase-2. It should be noted that there is often a loss of uroplakin and cytokeratin expression in high-grade carcinomas, especially infiltrative tumors.³

References:

1. Meuten DJ, and Meuten TLK. Tumors of the Urinary System. In: Meuton DJ, ed. *Tumors in Domestic Animals*, 5th ed. Ames, Iowa; Wiley Blackwell; 2017: 688.
2. Norris AM, Laing EJ, Valli VE, et al. Canine bladder and urethral tumors:

A retrospective study of 115 cases (1980-1985). *J Vet Int Med.* 1992: 145-153.

3. Sledge DG, Patrick DJ, Fitzgerald SD, Xie Y, Kiupel M. Difference in expression of uroplakin III, cytokeratin 7, and cyclooxygenase-2 in canine proliferative urothelial lesions of the urinary bladder. *Vet Pathol* 2015; 2(1):74-82

Self-Assessment - WSC 2018-2019 Conference 20

1. Which of the following is the NOT a criteria for the diagnosis of high-grade mast cell tumor?
 - a. Greater than foci of collagen degradation in 10 hpf
 - b. Greater than seven mitotic figures in 10 hpf
 - c. Greater than 10% of cells have nuclei larger than two-fold of the surrounding cells.
 - d. Greater than 3 pleomorphic or multinucleated cells in 10 hpf

2. Which of the following types of mast cell tumors would likely have the longest survival time?
 - a. MCT restricted to the dermis
 - b. MCT primarily in the dermis which infiltrates the subcutaneous fat
 - c. MCT primarily in the subcutaneous fat which infiltrates the overlying dermis
 - d. MCT restricted to the subcutaneous fat

3. Which of these is the most common neoplasm of the equine eyelid?
 - a. Squamous cell carcinoma
 - b. Basal cell tumor
 - c. Lymphoma
 - d. Mast cell tumor

4. How many chromosomes are present within cells in a transmissible venereal tumor?
 - a. 72
 - b. 78
 - c. 69
 - d. 59

5. Melamed-Wolinska bodies are seen in which type of epithelium?
 - a. Urothelial
 - b. Enterocyte
 - c. Thymic
 - d. Neuroepithelium

Please email your completed assessment to Ms. Jessica Gold at Jessica.d.gold2.ctr@mail.mil for grading. Passing score is 80%. This program (RACE program number) is approved by the AAVSB RACE to offer a total of 0.5 CE Credits, with a maximum of 12.5 CE Credits being available to any individual Veterinary Medical Professionals for the 2017-2018 Wednesday Slide Conference. This RACE approval is for the subject matter categories of: SCIENTIFIC using the delivery method of NON-INTERACTIVE DISTANCE. This approval is valid in jurisdictions which recognize AAVSB RACE; however, participants are responsible for ascertaining each board's CE requirements. RACE does not "accredit", "endorse" or "certify" any program or person, nor does RACE approval validate the content of the program.

Please email your completed assessment to Ms. Jessica Gold at Jessica.d.gold2.ctr@mail.mil for grading. Passing score is 80%. This program (RACE program number) is approved by the AAVSB RACE to offer a total of 0.5 CE Credits, with a maximum of 12.5 CE Credits being available to any individual Veterinary Medical Professionals for the 2017-2018 Wednesday Slide Conference. This RACE approval is for the subject matter categories of: SCIENTIFIC using the delivery method of NON-INTERACTIVE DISTANCE. This approval is valid in jurisdictions which recognize AAVSB RACE; however, participants are responsible for ascertaining each board's CE requirements. RACE does not "accredit", "endorse" or "certify" any program or person, nor does RACE approval validate the content of the program.

**Joint Pathology Center
Veterinary Pathology Services**



WEDNESDAY SLIDE CONFERENCE 2018-2019

C o n f e r e n c e 2 1

27 March 2019

Conference Moderator:

Frederic Hoerr, DVM, MS, PhD
Veterinary Diagnostic Pathology, LLC
638 South Fort Valley Road
Fort Valley, Virginia, 22652 USA

CASE I: NCAH 2013-1 (JPC 4033381).

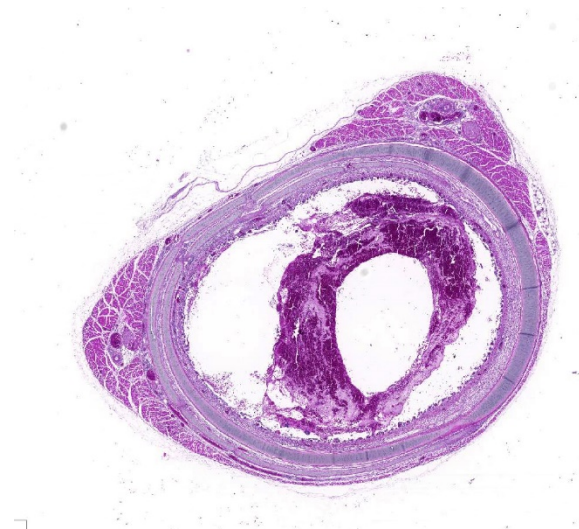
Signalment: 38 day old specific-pathogen-free chicken, *Gallus gallus domesticus*

History: The chicken was inoculated intratracheally with 0.5 mL of an experimental agent (laryngotracheitis virus). Clinical signs recorded on day 2 and 3 post inoculation include dyspnea, conjunctivitis, and depression. The bird died 4 days post inoculation.

Gross Pathology: On cut in, the tracheal lumen was partially obstructed by an opaque, thick blood-tinged exudate.

Laboratory results: N/A

Microscopic Description: Trachea: The lumen is 50% occluded by a coagulum composed of predominantly free erythrocytes admixed with eosinophilic proteinaceous fluid and fibrillar material (serum and fibrin), heterophils, and sloughed degenerate



Trachea, chicken. A section of trachea is submitted the lumen contains a large clot. (HE, 18X)

individual or syncytial epithelial cells. Syncytia contain up to 20 nuclei, often with large eosinophilic intranuclear inclusion bodies and margined chromatin. The coagulum is multifocally adhered to the extensively eroded or ulcerated tracheal mucosa with some degree of artifactual separation. Ulceration extends into the

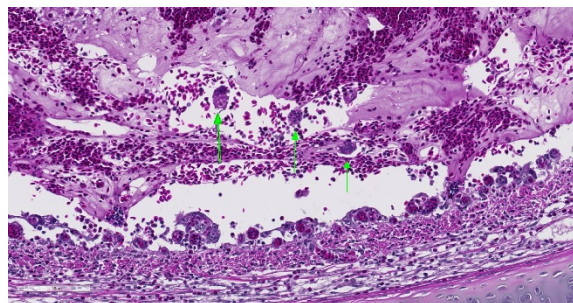
lamina propria and submucosa with complete loss of goblet cells and projection of capillaries into the lumen. The mucosa consists of loosely adhered ciliated epithelia that often form syncytia, attenuated non-ciliated epithelium, or necrotic cellular debris. The lamina propria and submucosa are expanded by clear space (edema), fibrin, heterophils, and fewer lymphocytes and plasma cells. There is diffuse vascular congestion and multifocal hemorrhage. Within the surrounding adventitia and muscular interstitia are small numbers of predominantly lymphocytes.

Contributor's Morphologic Diagnoses:

Trachea: Tracheitis, hemorrhagic and ulcerative, acute, severe with epithelial syncytia and intranuclear inclusion bodies.

Contributor's Comment:

Avian laryngotracheitis (LT) is a viral respiratory tract infection of chickens, caused by the alphaherpesvirus *Gallid herpesvirus I*, also known as laryngotracheitis virus (LTV).⁶ The disease has a worldwide distribution, but has the highest incidence in areas of concentrated poultry production.¹ LT causes increased mortality and decreased egg production in chickens, leading to economic losses for the poultry industry.⁶ The eye and respiratory tract are the usual portals of entry of LTV.⁶ Sources of infection include chickens with acute laryngotracheitis disease, latently infected chickens shedding virus, and fomites. Clinical signs generally appear 6-12 days following natural exposure. Clinical signs in severe cases include marked dyspnea, conjunctivitis, and depression.⁴ Severe forms of the disease cause high morbidity and variable mortality. Mild enzootic cases of laryngotracheitis cause unthriftiness, decreased egg production, watery eggs, conjunctivitis, and nasal discharge with low morbidity and mortality.⁶



Trachea, chicken. The mucosal epithelium is segmentally ulcerated and attenuated, and large multinucleated viral syncytia are enmeshed within the luminal clot. (HE, 200X)

Innate and cell-mediated immune responses appear to be more important than humoral responses in protection against disease.² Most alphaherpesviruses code for glycoprotein G which binds to a range of chemokines, modulating the host immune response, e.g. blocking binding of the chemokine to its host receptor.² In addition, glycoprotein G may enhance viral survival by modulating the host response toward humoral immunity rather than cell-mediated immunity.²

The diagnosis of LT can be made by histopathology, virus detection, or serology.¹ The disease is controlled through strict biosecurity measures and vaccination. Although attenuated viruses have been used by the poultry industry for years, virally vectored vaccines have recently become available, and deletion-mutant vaccines are under development.²

Differential diagnoses include infections with avian poxvirus, avian influenza virus, Newcastle disease virus, infectious bronchitis virus, fowl adenovirus, and *Aspergillus* spp.⁴

Contributing Institution:

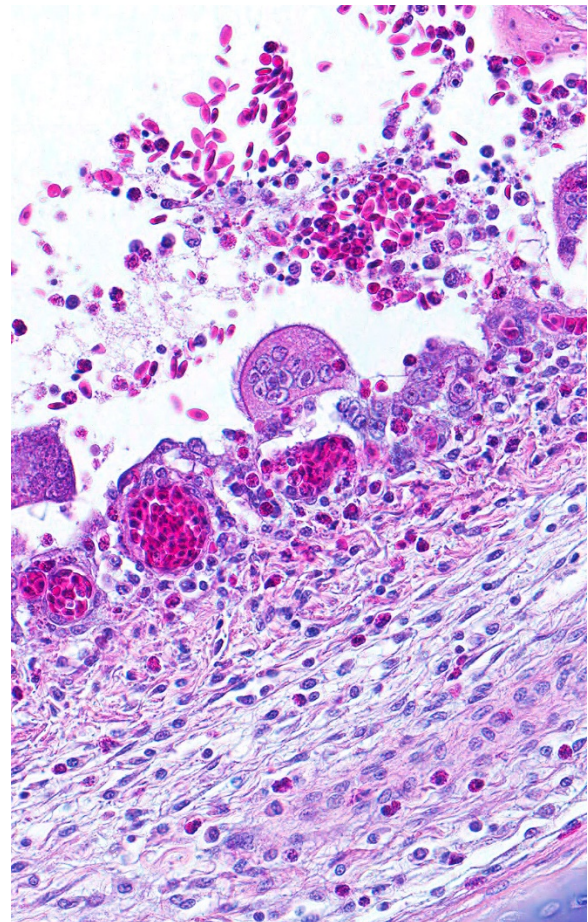
National Animal Disease Center, Ames, IA
http://ars.usda.gov/main/site_main.htm?modecode=36-25-30-00

http://www.aphis.usda.gov/animal_health/lab_info_services/about_nvsl.shtml

JPC Diagnosis: Trachea: Tracheitis, necrotizing and heterophilic, moderate with multifocal ulceration, epithelial intranuclear viral inclusion bodies and viral syncytia.

JPC Comment: The viral cause of infectious laryngotracheitis in poultry is gallid herpesvirus-1, a member of the Iltovirus (ILTovirus – get it?) genus of the subfamily Alphaerpesviridae. The disease was first reported in the 1920s, and since the advent of vaccination, two distinct clinical forms have been recognized – the classical severe form resulting in necrohemorrhagic lesions of the upper respiratory tract, and a milder form resulting in depression, reduced feed conversion and egg production, conjunctivitis, nasal discharge and sinusitis. This mild form is the most common type in the US, and is called the “vaccinal form” as analysis of the virus from many of these outbreaks demonstrate viral genome regions characteristic of vaccine strains.⁵

While effective in preventing infection, vaccines can also create latent carrier birds, which may spread virus to non-vaccinated flocks. As modified live vaccines may increase their virulence by bird to bird passage, especially those grown in chick embryos rather than in tissue culture, this may result in outbreaks of vaccinal forms of ILT when used over time in areas in which field-type strains are not endemic.⁵ Moreover, CEO vaccines, often administered in drinking water, require contact with the nasal tissues during this process, and may not result in adequate coverage of birds within a given flock. This, in turn, allows for longer circulation of the virus within said flock, increased numbers of passages within birds, and ultimately predisposes to outbreaks of vaccinal laryngotracheitis.³



Trachea, chicken. Occasionally, multinucleated viral syncytia are present within the remaining mucosal epithelium. The underlying submucosa is mildly edematous and contains moderate numbers of heterophils. (HE, 400X)

A recent publication by Sary et al⁷, demonstrated plaque-like necrotic lesions in the oral cavity, buccal mucosa, and esophagus of one laying hen and one pheasant from the same mixed species flock. Mucosal necrosis, viral inclusions, and viral syncytia which demonstrated immunopositivity for ILTV were seen in the lesions. The laying hen had additional typical lesions characteristic of ILT in the respiratory tract. This was the first description of oral lesions since very early descriptions of the disease in the 1920s.

The moderator imparted his extensive experience with this disease. He mentioned that many infections are seen in older birds

up to 40 days (heavier birds which result in increased labor costs to remove from houses in outbreaks). A marked drop in water consumption occurs 24 hours prior to the break, and many birds show conjunctivitis rather than respiratory signs – for this reason, conjunctiva should always be examined as well as trachea. In the US, the disease often peaks in the winter months, but this may not be true in other parts of the world. Vaccination does not prevent infection, but may mask or hide signs of an outbreak. The moderator thinks that the presence of viral inclusions and syncytia is diagnostic and unique for this condition; infectious bronchitis is a differential in this case gross and microscopically to an extent, but will never make syncytia.

References:

1. Bagust TJ, Jones RC, Guy JS: Avian infectious laryngotracheitis. *Rev Sci Tech* 2000; 19: 483-492.
2. Coppo MJ, Hartley CA, Devlin JM: Immune responses to infectious laryngotracheitis virus. *Dev Comp Immunol*, 2013
3. Menendez KR, Garcia M, Spatz S, Tablante NL. Molecular epidemiology of infectious laryngotracheitis: a review. *Avian Pathol* 2014; 43(2):108-117.
4. Oldoni I, Rodriguez-Avila A, Riblet SM, Zavala G, Garcia M: Pathogenicity and growth characteristics of selected infectious laryngotracheitis virus strains from the United States. *Avian Pathol* 2009;38: 47-53,
5. Ou SC, Giambone JJ. Infectious laryngotracheitis virus in chickens. *World J Virol* 2012;1(5):142-149.
6. Saif YM, Barnes HJ: Diseases of poultry, 12th ed. Blackwell Pub. Professional, Ames, Iowa, 2008
7. Sary K, Chenier S, Gagnon CA, Shavaprasad HL, Sylvester D

Boulianne M. Esophagitis and pharyngitis associated with avian infectious laryngotracheitis in backyard chickens: two cases. *Avian Dis* 2017; 61:255-260.

CASE II: A-231/15 B (JPC 4066708).

Signalment: Meat type chicken (*Gallus gallus domesticus*, broiler), 3 weeks old.

History: Sudden onset of mortality affecting 10% of the flock. Sick birds adopt a crouching position with ruffled feathers and die within 48 hours.

Gross Pathology: At necropsy, diffuse yellowish-pale, friable and swollen livers are seen. Multiple petechiae beneath the capsule are present in some livers.

Laboratory results: None given.

Microscopic Description:

There is a disruption of the hepatic parenchyma due to the presence of multifocal to coalescing randomly distributed foci of degenerated hepatocytes. These hepatocytes



Liver, chicken. The liver is swollen, pale, and there is a retiform pattern of necrosis. (Photo courtesy of: Servei de Diagnòstic de Patologia Veterinària, Facultat de Veterinària, Bellaterra (Barcelona), 08193 Spain.)

are swollen and show hypereosinophilic and highly vacuolated cytoplasm, and pyknotic nucleous with karyorrhexis and/or karyolysis. Associated to these foci and randomly scattered throughout the parenchyma some hepatocytes present marked karyomegaly with chromatin condensation at the nuclear membrane and large basophilic intranuclear inclusion bodies. Moderate lymphoplasmacytic and heterophilic inflammatory infiltrate in the periportal areas is observed. Cytoplasmic vacuolation is diffusely present in remaining hepatocytes. Occasionally, focal widening and infiltration of sinusoids with lymphocytes, heterophils and histiocytes are present.

Contributor's Morphologic Diagnosis:

Acute, severe, multifocal to coalescing necrotizing hepatitis with intranuclear inclusion bodies in hepatocytes

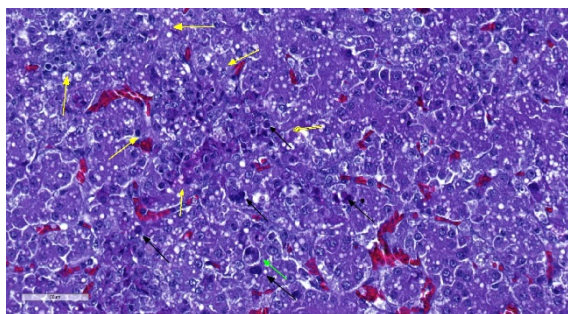
Contributor's Comment: Inclusion body hepatitis (IBH) is a viral disease produced by a member of the family Adenoviridae, genus *Aviadenovirus*,¹ which was first described in



Liver, chicken. A section of liver is submitted without discernible change at subgross magnification. (HE, 4X)

chickens by Helmboldt and Frazier in 1963.³ IBH is a ubiquitous disease in commercial and farm birds², although in the last years the infection has been proven in wild and exotic birds, producing the same characteristic hepatic lesions.³

The liver is the primary organ affected.¹ The infection produces a multifocal necrotizing hepatitis with intranuclear inclusion bodies in the hepatocytes.^{1,5} Intranuclear inclusion body description are variable: large, eosinophilic or basophilic, round or irregular shaped, but always replacing and displacing peripherally the chromatin, and producing karyomegaly.¹



Liver, chicken. At high magnification, there are multifocal areas of necrosis (yellow areas) infiltrated by low numbers of neutrophils, and adjacent Kupffer cells are debris-laden (green arrow). There are numerous large basophilic intranuclear inclusion within hepatocytes at the periphery of areas of necrosis as well as in the adjacent parenchyma. (HE, 400X)

Contributing Institution:

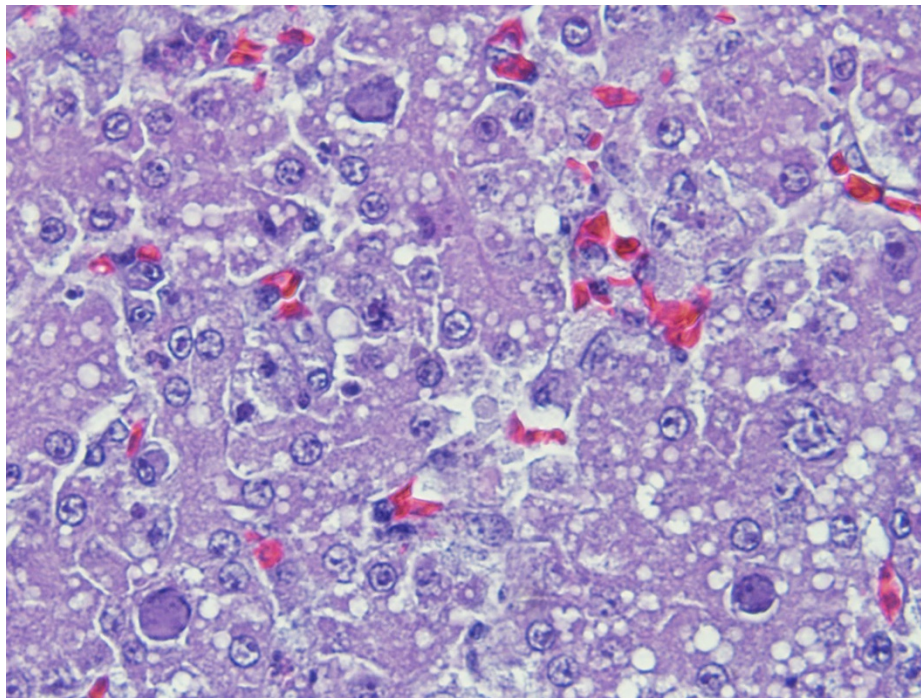
Servei de Diagnostic de Patologi Veterinaria, Facultat de Veterinaria, Bellaterra (Barcelona), 08193 Spain.

JPC Diagnosis: Liver: Hepatitis, necrotizing, multifocal and random, mild to moderate with numerous intrahepatocytic nuclear viral inclusions.

JPC Comment: Within the aviadenoviruses, there are six species (FAdV A-E and good adenoviruses, and twelve FAdV serotypes. Although all 12 serotypes

have been identified in outbreaks of inclusion body hepatitis, FAdV species D and E are most often isolated. The virus may be transmitted both vertically and horizontally, and is environmentally resistant when passed within the feces or by aerosol.

The clinical course of the disease is based on the virulence of the viral strain, age of the infected birds, as well as the presence of other viruses, to include immunosuppressive viruses such as avian circovirus and avian bunyavirus. The disease hits younger birds harder with mortalities of up to 85% in 2-day old chicks, but mortality averages 10% in 3-5 week old birds. Clinical signs are non-specific with depression and watery droppings. Grossly, livers are pale, swollen and friable. PCR for FAdV and typing is required for definitive diagnosis; the identification of FAdV in feces is not diagnostic, and FAdV are considered ubiquitous.



Liver, chicken. Large karyomegalic inclusions are present within hepatocytes throughout the section (arrows). (HE, 400X)

In more recent years, cases of hydropericardium syndrome, with and without associated IBH have been identified as resulting from infection with FAdV serotype 4. These cases are characterized by accumulation of straw-colored fluid within the pericardial sac, nephritis, and hepatitis with mortality rates of up to 70%.⁷

In addition to the inclusion body/hydropericardium syndrome, aviadenoviruses result in a number of other syndromes in chickens including necrotizing pancreatitis as well as gizzard erosions. Fowl aviadenovirus type A has been identified in outbreaks in Europe and Japan, resulting in necrosis and hemorrhage within the koilin layer, as well as adenoviral inclusions within the epithelium. Random foci of hemorrhage, unassociated with viral inclusions are also seen in this condition.

The moderator commented on the difficulties of differentiating propagating intranuclear crystalline arrays from nucleoli (which are especially prominent in turkeys), and mentioned that it is imperative to see large karyomegalic basophilic viral inclusions characteristic of adenovirus before diagnosing this condition. He also emphasized that due to the ubiquitous nature on non-pathogenic adenovirus in many flocks, isolation of an adenovirus in poultry is of little clinical importance in the

absence of disease. He also commented on the presence of glomerulonephritis in many cases of inclusion body hepatitis and the need to examine kidneys in these cases.

References:

1. Adair BM, Fitzgerald SD. Group I Adenovirus infections. In: *Diseases of Poultry*. 12th ed. Iowa State Press; 2008:252-266.
2. Garmyn A, Bosseler L, Braeckmans D, Van Erum J, Verlinden M. Adenoviral gizzard erosions in two Belgian broiler farms. *Avian Dis* 2018; 62(3):322-325.
3. Hollell JD, McDonald W, Christian RG. Inclusion body hepatitis in chickens. *Can Vet J* 1970; 11:99-101.
4. Ramis A, Marlasca MJ, Majo N, Ferrer L. Inclusion body hepatitis (IBH) in a group of eclectus parrots (*Eclectus roratus*). *Avian Pathol* 1992; 21(1):165-9.
5. Randall CR and Reece RL. *Color Atlas of Avian Histopathology*. Mosby-Wolfe, Times Mirror International Publishers Limited; 1996: 95-96.
6. Yugo DM, Hauck R, Shivaprasad HL, Meng XJ. Hepatitis virus infectious in poultry. *Avian Dis* 2016; 60:576-588.
7. Zhao J, Zhong Q, Zhao Y, Hu Y, Zhang GZ. Pathogenicity and complete genome characterization of fowl adenoviruses isolated from chickens associated with inclusion body hepatitis and hydropericardium syndrome in China. *Plos One* 2015 doi 10.1371/journal.pone.0133073

CASE III PA 38/15 (JPC 4085106).

Signalment: Italian Romagnola Duck (Roman Duck), *Anser anser*

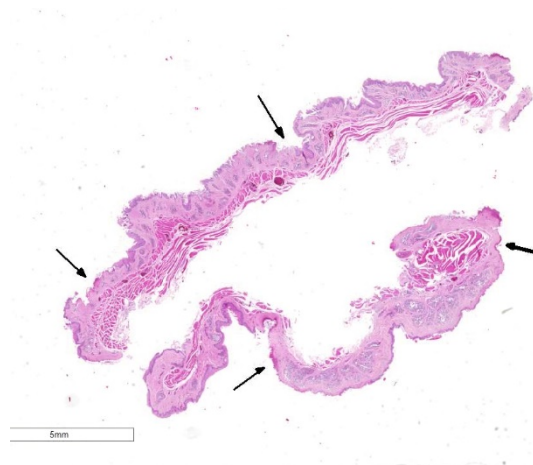
History: Multiple animals in the flock started dying suddenly without apparent cause or change in the management. The mortality is associated with a marked drop of egg deposition.

Gross Pathology: The breeder submitted only one spontaneously dead subject. The animal was a female in good postmortem and body conditions. Abundant mucous material diffusely covered the esophagus of the duck. In the proximal esophagus, beneath the mucous, multiple, multifocal to confluent, round to oval, 2 to 4mm in diameter, plaque lesions with tan-yellow discoloration and tightly attached to the mucosal surface are present. No other lesions were noted macroscopically.

Laboratory results: None

Microscopic Description:

Esophagus: Up to 70% (variable among sections) of the mucosal lining and 100% of the esophageal glands are severely ulcerated



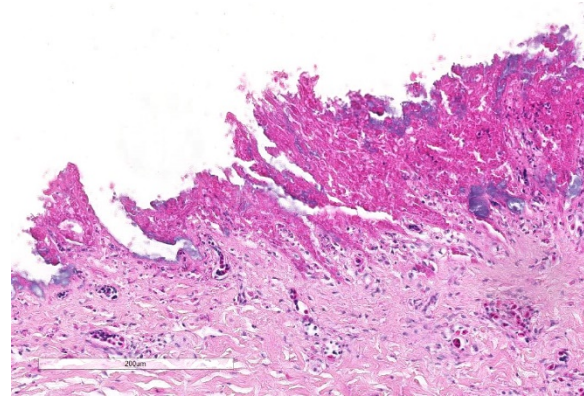
Esophagus, duck: Multiple areas of ulceration are present within the mucosa (arrows). (HE, 4X)

and lost with accumulation of necrotic debris, fibrin and degenerated heterophils.

In the mucosal lining, epithelial cells are variably severely sloughed and admixed with many viable and degenerated heterophils, lesser numbers of foamy reactive macrophages and lesser numbers of small mature lymphocytes in association with aggregates of 1-2 μm basophilic coccoid bacteria. Variable percentages of residual epithelial cells have glassy homogeneous appearance with loss of cellular details and maintenance of nuclear outlines (coagulative necrosis). Occasionally, epithelial cells have 7-10 μm in diameter, irregularly round, brightly eosinophilic intranuclear inclusion bodies that marginate the nuclear chromatin. Occasionally, intracytoplasmic inclusions are also present. Multifocally, cells of the basal layer have intracytoplasmic optically empty large vacuoles (hydropic degeneration).

Diffusely esophageal glands are ulcerated and filled by abundant pyknotic, karyolytic and karyorrhectic cellular debris (colliquative necrosis) and moderate amount of fine fibrillar material (fibrin) in association with a moderate number of foamy reactive macrophages and occasional karyolytic heterophils. In the submucosa, moderate edema, multifocal hemorrhage and mild, multifocal infiltration by a moderate numbers of heterophils and rare lymphocytes are visible. Blood vessels are diffusely and severely hyperemic.

Contributor's Morphologic Diagnosis: Esophagus. Severe multifocal to locally extensive acute necrotizing and ulcerative esophagitis with epithelial intranuclear and intracytoplasmic inclusion bodies consistent with herpesvirus inclusions.



Esophagus, duck: Ulcerated areas of the mucosa are covered by a diphtheritic membrane composed of abundant granular cell debris, fibrin, small numbers of infiltrating heterophils, and numerous bacterial colonies. (HE, 80X)

Name of the Disease: Duck plague or duck viral enteritis (DVE)

Etiology: Anatid herpesvirus-1 or DVE virus

Contributor's Comment The presence of esophageal necrosis, intranuclear and intracytoplasmic inclusion bodies, and the species affected were all information consistent with duck viral enteritis (anatid herpesvirus 1/AnHV-1).

Duck viral enteritis (DVE) is an acute, contagious and lethal disease that affects ducks, geese and swans.⁹ Currently, DVE is considered one of the most widespread and devastating diseases of waterfowl of the Anatidae family because of its ample distribution, wide host range, and relatively high morbidity and mortality.¹³ Adult ducks of Muscovy lineage (*Cairina moschata domestica*) are the most susceptible DVE.² In a recent report, the presence of DEV was found predominantly in wild ducks (*Anas platyrhynchos*) and mute swans (*Cygnus olor*), while the graylag geese (*Anser anser*), tundra bean geese (*Anser fabalis*), and grey herons (*Ardea cinerea*) were less affected.¹² The virus may have crossed between different orders and families and adapted to new hosts, developing the characteristic form

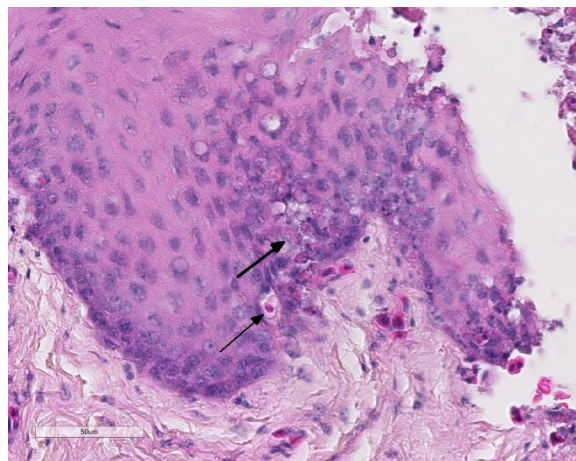
of the disease.⁸

Duck enteritis virus (DEV) is the causative agent of DVE and was alternatively known as anamid herpesvirus 1 (AnHV-1) and duck plague virus (DPV). Recent studies based on complete gene sequencing of Chinese virulent duck enteritis showed that the overall genome organization of DEV follows that of the alphaherpesviruses.¹³

DVE can be transmitted by direct contact between infected and susceptible birds or indirectly by contact with a contaminated environment.⁹ Morbidity rate may reach 67% in flocks and mortality rate may be up to 42.2% with a drop in egg production of 45% within 4 days of disease outbreak.¹¹ Mortality usually occurs from 1-5 days after the onset of clinical signs and in chronic cases, death occurs in immunosuppressed birds. Birds recovering from disease may become carriers and may shed the virus in the feces or on the surface of eggs over a period of years.¹⁰

Clinical signs of DVE include cyanosis, lethargy, listlessness, head tilt, unwillingness to eat, photophobia, ataxia and paresis, nasal discharge, ruffled feathers, bloody diarrhea and death within 2-3 hours of onset of clinical signs.^{2,5,11} Sudden death has been reported in several outbreaks.^{8,11}

Gross findings include petechial hemorrhages of serosal linings, lungs, heart, liver, spleen, kidneys, pancreas, ovarian follicles, and often small and large intestinal serosa. Hemorrhagic enteritis with intraluminal bloody contents admixed with mucus, necrotizing, ulcerative and diphtheritic inflammation of the oropharynx, proximal trachea, esophagus, small intestine and cloaca accompanied by severe hepatic degeneration and multifocal necrotizing hepatitis have also been identified in several ducks.^{2,8,11}



Esophagus, duck: Rare mucosal epithelial cells contain intranuclear inclusions (arrow). (HE, 400X)

Histological findings are characterized by necrosis in the digestive tract, reproductive and upper respiratory tract, liver, and spleen. Hemorrhages in digestive tract, spleen, and liver, and heterophils and macrophages infiltrating the lesions are visible.²

Esophageal lesions are characterized by swollen epithelial cells with a pale, dispersed, or vacuolated cytoplasm, individual epithelial cell necrosis or occasional larger foci of extensive epithelial necrosis and erosion and numerous large eosinophilic intracytoplasmic and intranuclear inclusion bodies.^{1,2} Other common findings include lymphoid depletion and necrosis in the bursa of Fabricius and vascular damage in all affected organs.¹⁴ Some authors describe the presence of two types of intranuclear inclusion bodies (IIBs) associated with herpesvirus infection: (a) small acidophilic IIBs surrounded by a clear halo and (b) slightly basophilic IIBs occupying the entire nucleus.⁸

Herpesvirus inclusion bodies are classically distinguished into two subtypes: Cowdry A inclusions are small, round eosinophilic and separated from the nuclear membrane by a halo. Cowdry B inclusions are large, glassy, eosinophilic, and centrally located, marginating nuclear material to the rim of the nucleus.⁶

Ultrastructurally, intranuclear non-enveloped viral particles measure about 110 nm in diameter with hexagonal shaped and variable electron-density in the cores. These are randomly distributed in the nucleus or aligned close to the nuclear envelope. The intracytoplasmic viral particles are arranged in clusters or as solitary enveloped virions measuring 200 to 250 nm in diameter.⁸

The definitive diagnosis of DVE is made by electron microscopy, direct immunofluorescence, PCR and immunohistochemistry.^{2,8,13,14}

The main differential diagnoses for DVE (Anatid herpesvirus-1) include viruses responsible for both intracytoplasmic and intranuclear viral inclusions, such as cytomegaloviruses (subfamily Betaherpesvirinae), gallid herpesvirus-2 (Marek's Disease virus) and paramyxoviruses.^{1,3,7}

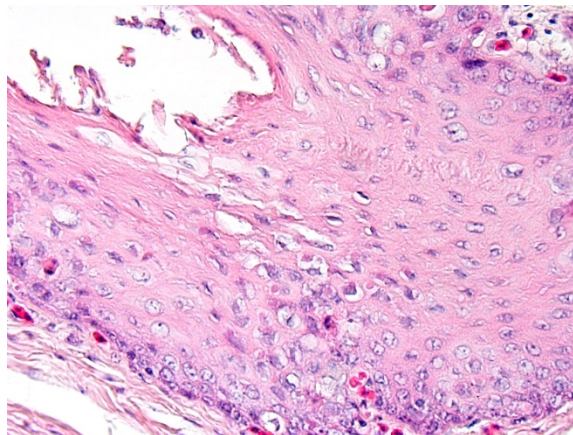
Contributing Institution:

DIMEVET-Anatomical Pathology Section
Via Celoria 10
20133 Milano
ITALY

JPC Diagnosis: Esophagus: Esophagitis, necrotizing, multifocal to coalescing, moderate with mucosal epithelium intranuclear inclusions.

JPC Comment: The contributor has done an excellent job in describing this viral disease particular to waterfowl. Duck viral enteritis, first reported in the Netherlands in 1927, was originally identified as a duck-adapted strain of avian influenza until 1942, when it was identified as a distinct viral disease of ducks following fruitless transmission attempts to galliform birds, mice, guinea pigs, rabbits rats and mice.³

The virus has caused outbreaks in the US and Europe, most often in proximity to large bodies of water where wild waterfowl may



Esophagus, duck: Rare clusters of mucosal epithelial cells contain round intracytoplasmic inclusions (HE, 400X)

mix with domestic or farmed animals. Horizontal water-borne transmission of the virus is considered to play a primary role, with vertical transmission being of questionable importance.³

Age is a particular factor, with adult breeders showing the highest mortality and birds less than 7 days resistant to infection. Being a member of the Alphaherpesvirinae, latent infections may be seen in birds, with latent infections being maintained up to 4 years in the trigeminal ganglion, lymphoid tissues, and peripheral blood lymphocytes. Convalescent birds are immune to reinfection; however, they may maintain a latent infection and migratory birds may shed the virus, initiating new outbreaks in remote areas.³

In older birds, the characteristic lesions are those of hemorrhage due to necrosis of small capillaries and venules. In younger birds, lymphoid lesions are more prevalent. The virus induces both apoptosis and necrosis of lymphocytes in lymphoid tissues throughout the body, to include the bursa, spleen, and thymus initiating at first hemorrhagic lesions and then in convalescent birds, thymic atrophy (a sign often used in condemning

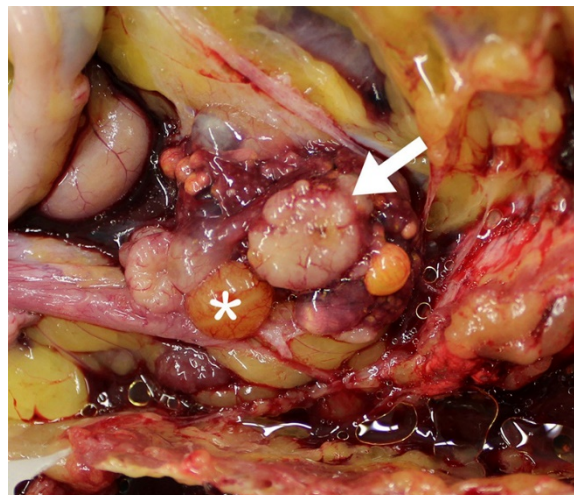
carcasses following outbreaks). Necrosis and hemorrhage of GI lymphoid tissue often results in annular bands of hemorrhage in the duodenum and ceca. The immunosuppressive effects of low-virulence duck enteritis virus (DEV) may result in an increase in secondary bacterial infections including *Riemerella anatipestifer*, *Pasteurella multocida*, and *E. coli* in younger birds. Another characteristic gross finding in outbreaks in penile phimosis.³

The presence of intranuclear and intracytoplasmic viral inclusions is an oddity in viral histopathology. As a DNA virus, viral replication occurs within the nucleus. The cytoplasmic inclusions are membrane-bound vacuoles containing enveloped virus and nuclei containing viral nucleocapsids.³

References:

1. Barr BC, Jessup DA, Docherty DE, Lowenstine LJ. Epithelial intracytoplasmic Herpes viral inclusions associated with an outbreak of duck virus enteritis. *Avian Dis.* 1992;36:164-168.
2. Campagnolo ER, Banerjee M, Panigrahy B, Jones RL. An outbreak of duck viral enteritis (duck plague) in domestic Muscovy ducks (*Cairina moschata domestica*) in Illinois. *Avian Dis.* 2001;45:522-528.
3. Shama K, Kumar N, Saminathan M, Tiwari R, Karthik K, Kumar MA, Palanivelu M, Shabbir MZ, Malik YS, Singh RK. Duck virus enteritis (duck plague) – a comprehensive update. *Vet Q* 2017 37(1):57-80.
4. Fauquet C, Mayo MA, Maniloff J, Desselberger U, Ball LA. *Virus taxonomy: eighth report of the International Committee on Taxonomy of Viruses.* San Diego, CA: Elsevier Academic Press; 2005.
5. Hanson JA, Willis NG. An outbreak of duck virus enteritis (duck plague) in Alberta. *J Wildl Dis.* 1976;12:258-262.
6. Kelly NP, Raible MD, Husain AN. Pathologic Quiz Case: An 11-day-old boy with lethargy, jaundice, fever, and melena. *Arch Pathol Lab Med.* 2000;124:469-470.
7. Knowles DP. Herpesvirales. In: MacLachlan NJ, Dubovi EJ, eds. *Fenner's Veterinary Virology.* 4th ed. London, UK: Academic Press; 2011:197–198.
8. Salguero FJ, Sanchez-Cordon PJ, Nunez A, Gomez-Villamandos JC. Histopathological and ultrastructural changes associated with herpesvirus infection in waterfowl. *Avian Pathol.* 2002;31:133-140.
9. Sandhu TS, Metwally SA. Duck Virus Enteritis (Duck Plague). In: Saif YM, Fadly AM, Glisson JR, McDougald LR, Nolan LK, Swayne DE, eds. *Diseases of Poultry.* 12th ed. Ames: Iowa State University Press; 2008: 384-393.
10. Shawky S, Schat KA. Latency sites and reactivation of duck enteritis virus. *Avian Dis.* 2002;46:308-313.

11. Uma Rani R, Muruganandan B. Outbreak of Duck Viral Enteritis in a Vaccinated Duck Flock. *Sch J Agric Vet Sci*. 2015;2:253-255.
12. Woźniakowski G, Samorek-Salamonowicz E. First survey of the occurrence of duck enteritis virus (DEV) in free-ranging Polish water birds. *Arch Virol*. 2014;159:1439-1444.
13. Wu Y, Cheng A, Wang M, et al. Complete genomic sequence of Chinese virulent duck enteritis virus. *J Virol*. 2012;86:5965.
14. Xuefeng Q, Xiaoyan Y, Anchun C, Mingshu W, Dekang Z, Renyong J. The pathogenesis of duck virus enteritis in experimentally infected ducks: a quantitative time-course study using TaqMan polymerase chain reaction. *Avian Pathol*. 2008;37:307-310.



Gonad, chicken. There is a disc-shaped structure in the ventral aspect of the ovary (arrow). Developing follicles are present (asterisk). (University of Connecticut, Connecticut Veterinary Medical Diagnostic Laboratory, Department of Pathobiology and Veterinary Science, College of Agriculture, Health and Natural Resources, <http://patho.uconn.edu>)

structures, of approximately 0.9-1.2 cm in diameter x 0.3 cm deep on the ventral aspect of the ovary. The oviduct was active but underdeveloped. The left leg was swollen distal to the hock and was approximately 2-3 times the thickness of the right leg. The subcutis was expanded, wet, gelatinous and light grey to light green.

Laboratory results: A swab from the abnormal subcutaneous tissue from the left leg was cultured aerobically and yielded a few *Escherichia coli*, a few *Staphylococcus* sp., and a few *Streptococcus* sp.

Microscopic Description:

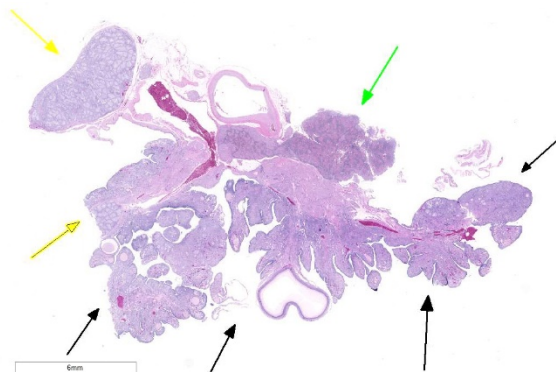
The examined gonad is comprised of both ovarian and testicular tissue, with variable degrees of differentiation. The ovarian tissue is characterized by fibrovascular stroma and finger-like projections (cortex) in which a low number of small developing follicles and one megalethical ovum are suspended. Throughout the ovarian stroma are observed multiple aggregates of lipid-laden cells (vacuolar cells), a few atretic follicles, and

CASE IV PA 16-5448 (JPC 4101316).

Signalment: Adult, female, Sussex chicken (*Gallus gallus domesticus*)

History: This adult female Sussex chicken was submitted along with two other hens; all with a reported history of lethargy, equilibrium imbalance, and watery stool.

Gross Pathology: At necropsy, the ovary was smaller than expected due to lack of large follicles (the largest was 1.0 cm in diameter). There were two gray/white, solid, disc-like



Gonad, chicken. There are three distinct types of tissue in the sample – ovary (black arrows), testis (yellow arrows), and adjacent adrenal gland (green arrow) (HE, 40X).

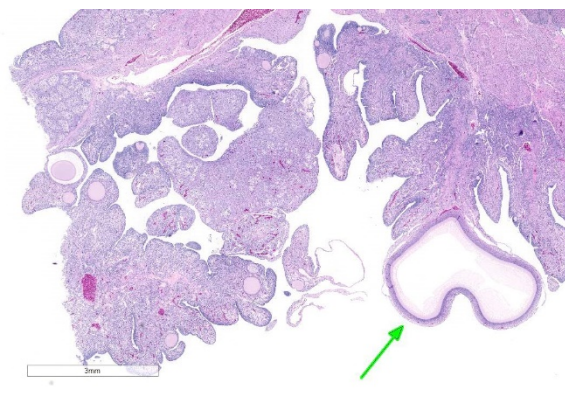
low numbers of scattered granulocytes and a few pigment-laden cells. Testicular tissue is either embedded in ovarian stroma with or without encapsulation, or attached to the ovarian tissue by a thin stalk of fibrous connective tissue. The testicular tissue is characterized by numerous, sometimes irregularly shaped tubular structures (seminiferous tubules) of varying sizes that are supported by fine to dense fibrovascular stroma. In the areas where the testicular tissue is well-demarcated/encapsulated, the tubules are fairly well-differentiated and contain developing spermatogonia, occasional multinucleated cells, and a few cells with pyknotic nuclei. Few to no late spermatids or spermatozoa are present. Adjacent to the encapsulated nodule of testicular tissue, there is a small collection of tubules lined by tall columnar epithelium (presumptive vestigial epididymis) which are devoid of spermatozoa.

Normal adrenal gland is also present along one side of the section.

Contributor's Morphologic Diagnosis:
Gonad: Ovotestis

Contributor's Comment Disorders of sexual development (DSDs) are relatively common and affect all domestic animal

species.¹⁰ The gonads, reproductive tract or external genitalia may be affected. The term intersex has been traditionally used to describe animals which exhibit some of the characteristics of both sexes.⁷ The incidence of intersex in commercial poultry flocks has been estimated at 0.05%,¹ and naturally occurring sex reversal has been reported in multiple avian species.^{1,4,9} Apparently, birds are more prone to the development of these condition for two reasons: firstly, the capability that both male and female embryos have, where cortical and medullary tissue in the developing gonads can later develop into ovary and testis respectively, is maintained after hatching.⁵ Secondly, there is a unique asymmetry during embryogenesis in female birds,² in which greater numbers of primordial germinal cells migrate to the left gonad than to the right, that persist throughout life.⁴ Sex reversal most commonly occurs in mature female birds that have had a pathologic condition resulting in atrophy of the ovary with subsequent development of seminiferous tubules in the normally rudimentary right gonad or in the medulla of the atrophic left ovary,⁵ and this has been experimentally reproduced after gonadectomy.² Mammals or birds with both ovarian and testicular tissue are classified as hermaphrodites (as opposed to pseudo-

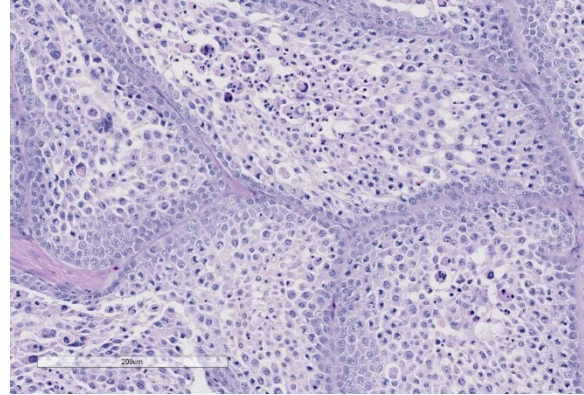


Gonad, chicken. The ovarian tissue has a decreased number of follicles with few primordial follicles in the outer cortex, several primary follicles, and a single large yellow secondary follicle (green arrow). (HE, 80X)

hermaphrodites which have the gonads of one sex and duct systems, external genitalia and some sexual characteristics of the opposite sex).⁸ The ovotestis presented here is the left gonad of an adult chicken presented to us as one of three mature Sussex hens. There was evidence of follicle development and a follicular hierarchy in the ovotestis, with the larger follicles having a stigma. However, the largest follicle was about one third of the size of those of commercial layers. The oviduct was developed to about 50% of the size of a normal fully functioning oviduct. Unfortunately, it is not known if this chicken had ever laid any eggs. The testicular tissue in our case was present in the ovarian medullary stroma, sometimes well circumscribed and encapsulated, but in one area was separated from the ovary, attached only by a thin stalk of fibrovascular tissue. Interestingly, a second chicken from this batch of three, also had an ovotestis. A high incidence (2.4%) of hermaphrodites was recorded in a flock of Cochin bantams and it was suggested that there may be a hereditary predisposition for the condition.⁵ It is not known if our two Sussex chickens were related.

In the last decade, there have been efforts to better classify DSDs by including the sex chromosome type, presence of *SRY* (in mammals; birds do not have *SRY*), gonadal type, tubular genitalia and external genital phenotype. Chromosomal typing was not performed in the present case but triploidy (ZZW) has been reported in some hens with ovotestis; triploidy can only develop at the time of fertilization.^{5,9}

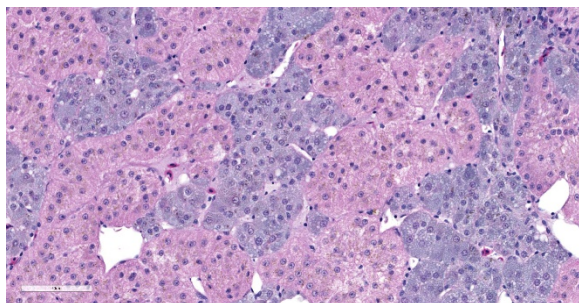
Mechanisms of sexual differentiation of the gonads appear to be highly conserved and many of the important signaling factors involved in ovarian or testicular development in mammals are also implicated in birds.² While it is known that the embryonic gonads



Gonad, chicken. Testicular tissue is composed of large abnormally shaped seminiferous tissue with numerous spermatogonia but little if any mature sperm. Multinucleated cells are present within the lumina. (HE, 176X)

in birds are bipotential for a period of time, just as they are in mammals, the sex determining system has not been fully elucidated in birds.² In mammals, the dominant acting gene is carried by the Y chromosome (*SRY* gene), and no matter how many X chromosomes are present, a single Y chromosome dictates testicular development and a genetic male gender.⁶ In birds, the female is the heterogametic sex (ZW) while the male is homogametic (ZZ).^{2,3} Three possible mechanisms of sex determination in birds have been proposed: A - The W sex chromosome carries a dominant female determinant, B - Dosage of one or more Z-linked genes, and C - Both mechanisms are at play.² The current weight of evidence tends to more strongly support mechanism A. For example, there are no cases of spontaneous male to female sex reversal in birds, and the loss of estrogen production by the left ovary allows the right gonad to take on a testis-like appearance and produce testosterone.²

Experimental work has also suggested that endogenous estrogens can have a determinant effect and variations in the levels of the hormone in the embryo can produce different effects. Exposure to estrogens feminizes the reproductive tract of the male embryo,



Adrenal gland, chicken. The adjacent adrenal gland is within normal limits. Birds do not have a discrete cortex and medulla as do mammals. (HE, 167X)

inhibition of estrogen in the female embryo disturbs development and can result in phenotypic sex reversal; both resulting in the formation of an ovotestis.^{2,3}

Contributing Institution:

University of Connecticut
 Connecticut Veterinary Medical Diagnostic Laboratory
 Department of Pathobiology and Veterinary Science
 College of Agriculture, Health and Natural Resources
<http://patho.uconn.edu>

JPC Diagnosis: Gonad: Ovotestis.

JPC Comment: The contributor has done an excellent job in reviewing the normal sexual development of the chicken as well as abnormal sexual development. In chickens and all other birds, a ZZ male/ZW female sex chromosome system exists. Until day six post-fertilization, male and female gonads are morphological indistinguishable; at this point, ZZ males develop bilateral testes and in ZW females, the left gonad develops into a functional ovary. In the developing ovary, expression of the P450 cytochrome enzyme aromatase (secreted within the ovarian medulla) has been identified as the major early determinant of sexual differentiation, as its secretion catalyses estrogen secretion and subsequent ovarian development. In the

male, the enzyme SOX9, expressed within the same window, will trigger Sertoli cell differentiation and testicular development. Treatment of chicken embryos in early development with aromatase inhibitors will result in female to male sex reversal.⁷

References:

1. Abdel-Hameed F, Shoffner RN. Intersexes and sex determination in chickens. *Science* 1971; 172:962-964.
2. Ayers KL, Smith CA, Lambeth LS. The molecular genetics of avian sex determination and its manipulation. *Genesis* 2013; 51:325-336.
3. Brunstrom B, Axelsson J, Mattsson A, Halldin K. Effect of estrogens on sex differentiation in Japanese quail and chicken. *Gen Comp Endocrinol* 2009; 163:97-103.
4. Chalmers GA. Ovotestes and sexual reversal in racing pigeons. *Can Vet J* 1986; 27:82-84.
5. Fitzgerald SD, Cardona CJ. True hermaphrodites in a flock of Cochinese bantams. *Avian Dis* 1993; 37:912-916.
6. Kumar V, Abbas AK, Aster J. *Robbins and Cotran Pathologic Basis of Disease*. Philadelphia, PA: Elsevier; 2015.
7. Lambeth LS, Cummins DM, Doran TJ, Sinclair AH, Smith CA. Overexpression of aromatase alone is sufficient for ovarian development in genetically male chicken embryos. *PLOS One* 2013, 8:6:e68362.
8. McGeady TA, Quinn PJ, Fitzpatrick ES, Ryan MT, Kilroy D, Lonergan P. *Veterinary Embryology*. Chichester, England: Wiley-Blackwell; 2017.
9. Ohno S, Kittrell WA, Christian LC, Stenius C, Witt GA. An adult triploid chicken (*Gallus domesticus*) with a

- left ovotestis. *Cytogenetics* 1963; 2:42-49.
10. Schlafer DH, Foster RA. Female Genital System. In: Maxie MG, ed. *Jubb, Kennedy and Palmer's Pathology of Domestic Animals*. 6th ed. Vol 3. Philadelphia, PA: Saunders Elsevier; 2007:358-464.

Self-Assessment - WSC 2018-2019 Conference 21

1. Which of the following is the most common form of infectious laryngotracheitis in the US?
 - a. Wild-type
 - b. Vaccinal
 - c. Velogenic
 - d. Endemic

2. Which of the following serotypes of fowl adenovirus is most often isolated in cases of hydropericardium syndrome
 - a. Serotype 2
 - b. Serotype 4
 - c. Serotype 6
 - d. Serotype 8

3. Fowl adenovirus may cause a syndrome of ulcers affecting which organ in chickens?
 - a. Crop
 - b. Vent
 - c. Ventriculus
 - d. Proventriculus

4. Which of the following is NOT a common gross finding in ducks infected with anatis herpesvirus-1 ?
 - a. Hemorrhage in multiple organs
 - b. Lymphoid necrosis
 - c. Polyserositis
 - d. Ulceration of the gastrointestinal tract

5. Birds have which of the following types of male/female chromosomes?
 - a. XX/XY
 - b. YX/YY
 - c. ZX/ZW
 - d. AvY/AvX

Please email your completed assessment to Ms. Jessica Gold at Jessica.d.gold2.ctr@mail.mil for grading. Passing score is 80%. This program (RACE program number) is approved by the AAVSB RACE to offer a total of 0.5 CE Credits, with a maximum of 12.5 CE Credits being available to any individual Veterinary Medical Professionals for the 2017-2018 Wednesday Slide Conference. This RACE approval is for the subject matter categories of: SCIENTIFIC using the delivery method of NON-INTERACTIVE DISTANCE. This approval is valid in jurisdictions which recognize AAVSB RACE; however, participants are responsible for ascertaining each board's CE requirements. RACE does not "accredit", "endorse" or "certify" any program or person, nor does RACE approval validate the content of the program.

Please email your completed assessment to Ms. Jessica Gold at Jessica.d.gold2.ctr@mail.mil for grading. Passing score is 80%. This program (RACE program number) is approved by the AAVSB RACE to offer a total of 0.5 CE Credits, with a maximum of 12.5 CE Credits being available to any individual Veterinary Medical Professionals for the 2017-2018 Wednesday Slide Conference. This RACE approval is for the subject matter categories of: SCIENTIFIC using the delivery method of NON-INTERACTIVE DISTANCE. This approval is valid in jurisdictions which recognize AAVSB RACE; however, participants are responsible for ascertaining each board's CE requirements. RACE does not "accredit", "endorse" or "certify" any program or person, nor does RACE approval validate the content of the program.

Joint Pathology Center
Veterinary Pathology Services



WEDNESDAY SLIDE CONFERENCE 2018-2019

C o n f e r e n c e 2 2

3 April 2019

Conference Moderator:

CAPT (Ret.) Christopher H. Gardiner and COL (Ret.) R. Keith Harris

San Antonio, Texas and Athens, Georgia.

CASE I: Digital Case 2 13-018-6 32 (JPC 4113194).

Signalment: Adult male, *Rattus norvegicus*, Norway rat

History: This animal was trapped and euthanized as part of the pest control program on the outskirts of the Veterinary Medical facility of the Armed Forces Research Institute of Medical Sciences (AFRIMS) in Bangkok, Thailand. The animal appeared well muscled and healthy. Necropsy findings are representative of the over 100 Norway and Black rats that have been captured, euthanized and evaluated since 2012.

Gross Pathology: Macroscopic findings in this animal consisted of small white cysts (3-5 mm) protruding from the hepatic parenchyma. In this particular case, the cysts were not incised so as to maintain the architecture of the parasitic cyst microscopically, however in other animals incision of the cyst allowed for extrusion of an individual larval cestode consistent with *Cysticercus fasciolaris*. Additional findings in this animal consisted of both adult

nematodes and cestodes within the lumen of the intestinal tract. Blood smears revealed the presence of flagellates etiologically consistent with *Trypanosoma lewisi* and fecal examination of the animal yielded myriad *Strongyle* spp. and *Strongyloides* spp. eggs. No other significant findings were observed.

Laboratory results: NA



Liver, rat #1. Numerous 3-5mm cysts protrude from the surface of the liver. (Photo courtesy of: Armed Forces Research Institute of Medical Sciences (AFRIMS). <http://afrims.amedd.army.mil/usamd-afrims.html>)

Microscopic Description:

The slide consists of three sections of liver.

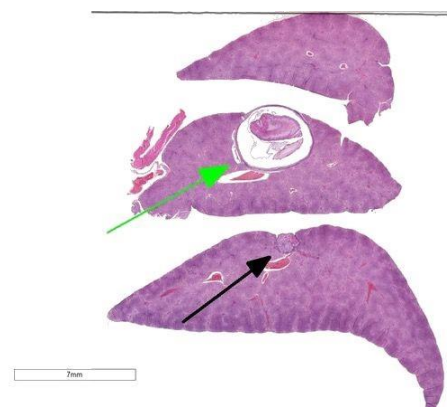
Liver: Focally, markedly expanding and extruding the hepatic capsule, replacing and compressing 20% of the parenchyma is a 3 mm, thin-walled parasitic cyst that contains several cross sections of a larval cestode including its anterior end (cysticercus). The cestode is characterized by measuring approximately 1.5 mm in diameter, lacking a pseudo coelom or a digestive tract. The parasite strobilium is bounded by an undulated tegument which contains the spongy parenchyma. There are streams of muscle fibers which separate the medullary from the cortical regions (typical of *Cyclophyllidium*), both of which are interspersed with frequent 10 μ m, ovoid structures containing central basophilic amorphous material surrounded by a clear halo (calcareous corpuscles). The section also contains a rostellum with 25 armed hooks evident. To one side of the rostellum is a muscular sucker. The cyst wall is characterized by being approximately 150-200 μ m wide composed of dense fibroblasts, an internal, circumferential, dense aggregate of lymphocytes, frequent scattered plasma cells, macrophages, fewer eosinophils and



Liver, rat #2. In a second animal, a larger cyst is visible. (Photo courtesy of: Armed Forces Research Institute of Medical Sciences (AFRIMS). <http://afirms.amedd.army.mil/usamd-afirms.html>)

occasional hemosiderophages. Multifocally, the cyst wall is disrupted by fractured foci of deeply basophilic mineral surrounded by the previously described inflammatory cells. Exterior to the cyst wall, there are frequent small caliber vessels and lymphatics which are ectatic. The extant hepatic parenchyma is affected by mild centrilobular hepatocellular lipidosis, diffuse glycogenosis and scattered sinusoidal hemosiderophages.

Within the subcapsular region of another



Liver, rat. Three sections of liver are submitted. The middle section has a large cestode larva contained within a fibrous cyst (green arrow). The bottom section has a large granuloma adherent to the capsule. (black arrow). (HE, 4X)

section on the slide is a focal lesion consisting of coalescing granulomas characterized by a central core of eosinophilic cellular debris (necrosis), deeply basophilic fragmented spicular material (mineral) or frequent 30 x 80 μ m bipolar operculated, thick-shelled, morulated nematode eggs. The central material is bounded by large epithelioid macrophages, few multinucleated giant cells, streams of reactive fibroblasts, and dense aggregates of lymphocytes, plasma cells, hemosiderophages, few eosinophils and rare mott cells. Multifocally, the fibrosis extends into the surrounding parenchyma, dissecting hepatic lobules, individualizing scattered hepatocytes, expanding rare portal areas and

is admixed with focally extensive biliary hyperplasia, and small numbers of the previously described inflammatory cells.

Contributor's Morphologic Diagnosis:

Liver: Cysticercus, focally extensive, etiology consistent with *Cysticercus fasciolaris*, *Rattus norvegicus*, rodent

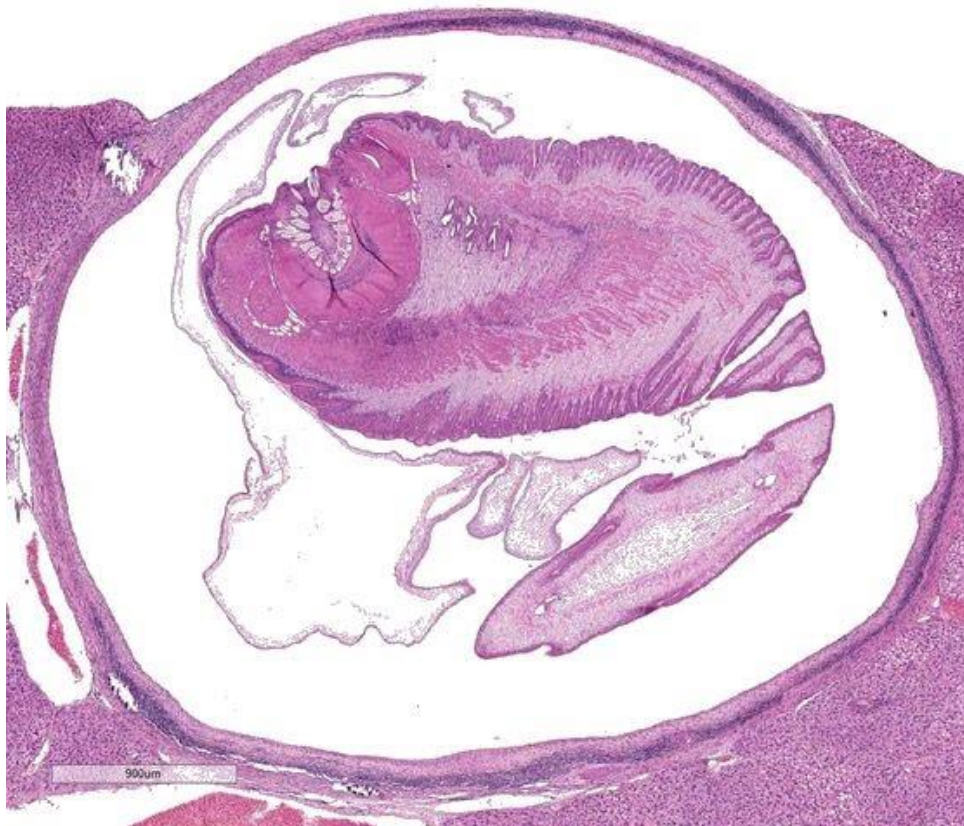
Liver: Granulomas, coalescing, focally extensive, subcapsular, with intralesional bioperculated nematode eggs etiology consistent with *Capillaria hepatica*

Contributor's Comment: Preliminary findings in an ongoing histopathological survey of trapped rats in a single point in central Bangkok have found a wide range of helminthic disease, several of which have

zoonotic potential. Multiple historical studies have been conducted in South East Asia looking at prevalence of disease in rodents evaluated however there are few that have concentrated on Thailand and Bangkok in particular.^{2,8,16} It is difficult to assess the overall rat population in this megacity in which there are estimated to be around 10 million human inhabitants, however the rats are an ever present feature of the city, especially during the wet season. The literature describes urban rat populations as being culpable for the spread of a range of zoonoses, to include *Leptospira interrogans*,^{7,8} *Yersinia pestis*,^{7,8} *Rickettsia typhi*,^{7,8} *Bartonella* spp.,^{7,14} *Streptobacillus moniliformis*,^{7,12} *Trypanosoma lewisi*,^{8,9,13,16} *Angiostrongylus cantonensis*,^{7,16,21} *Capillaria* sp.^{1,3,7,15,16,18,19,20} and *Taenia*

sp.^{3,14,16,19,21} as well as other cestodes such as *Hymenolepis* spp.^{2,3,7,21} and *Rodentolepis* spp.^{2,7}

This is purely a partial list to illustrate the enormity of the potential collision between vector and victim in a concentrated urban environment such as Bangkok. Humans are susceptible to these pathogens in a variety of ways depending on the pathogenesis of the organism in question, however with regards to the helminths, consumption of food or drinks



Liver, rat. The cyst contains a strobilocercus with an armed rostellum, a ridged cuticle, a spongy body cavity, bilayered skeletal muscle and a large thin bladder. (HE, 23X)

contaminated with rodent droppings or urine is the primary route, with a potential for infection through the eating of bushmeat. In parts of Thailand, this practice includes consumption of rat meat.

The liver of this particular animal does not present a diagnostic challenge, however, it does provide the anatomic pathologist and certainly the veterinary pathology resident with an interesting description of a parasitic coinfection.

The metacestode stage of *Taenia taeniaformis* is termed *Cysticercus fasciolaris* but also has been referred to as *Taenia crassicollis*, *Hydatigera taeniaformis* and *Strobilocercus fasciolaris*. Infection with the larval form of *Taenia solium*, *T. saginata*, *T. crassiceps*, *T. ovis*, *T. taeniaeformis* or *T. hydatigena* is termed as cysticercosis. The larvae stages of these cestodes are called cysticerci which are fluid-filled vesicles containing a single inverted protoscolex. Apart from cases of infection of the eye, the ventricles or the subarachnoid space of the brain, these cysts are bounded by a fibrous capsule and rarely an inflammatory response while the parasites are alive. Once they die, there can be a combination of chronic inflammation and mineralization of the lesions.

The definitive hosts of the parasite are members of the felid family to include domestic cats and lynx, but foxes, stoats and other carnivores have been recognized as proficient in transmitting the parasite. In this particular case in which an urban cycle is occurring, the domestic cat is the likely definitive host although the stray dog population in Bangkok is significant. A range of small mammals can act as intermediate hosts in South East Asia, to include various species of murid and cricetid rodents to include rats, and mice as well as

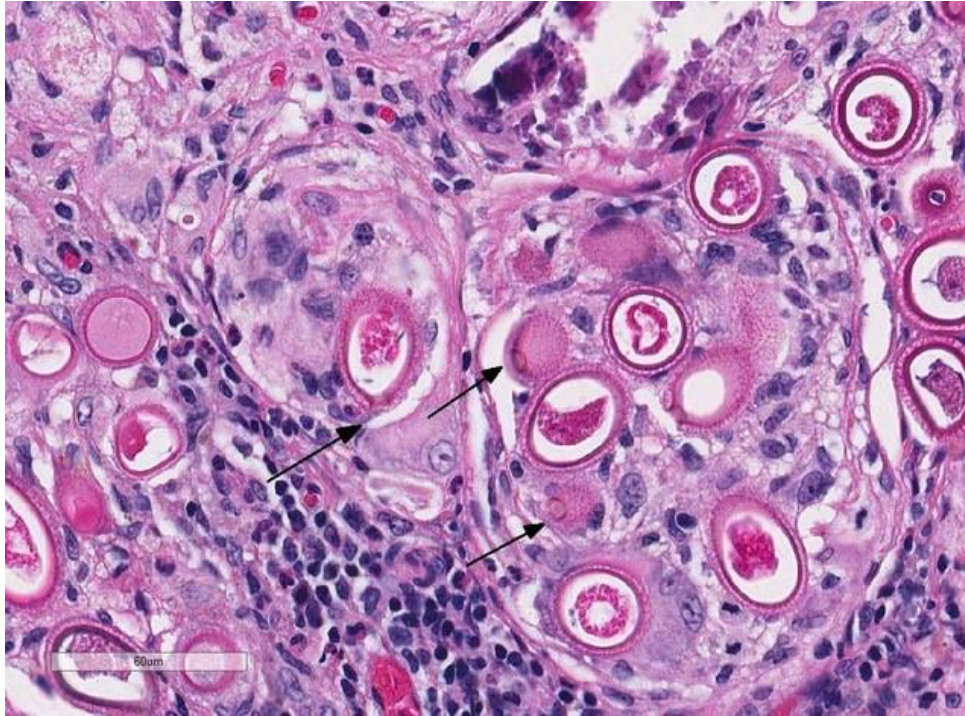
insectivores such as bandicoots and lagomorphs.

There is a single instance in the literature of human infection with the larval form of *T. taeniaformis* and as such the parasite is not felt to represent a significant zoonotic risk, although there are several reports of humans having adult parasites in their intestinal tract.²²

The second etiology noted in these sections are *Capillaria hepatica* ova (synonym *Calodium hepatica*) which were found with high frequency within granulomatous inflammation in the livers of trapped rats. Capillariasis was frequently observed within the epithelium of the squamous portions of the stomachs of rats trapped as part of this study.

C. hepatica has a direct life cycle which only requires a single host. The adult nematodes infect the liver of vertebrates and have been described in rodents, humans, pigs, a range of carnivores and non-human primates. Consumption of embryonated ova result in the larval worms migrating from the gastrointestinal tract into the liver. After a period of development which typically requires approximately 3 weeks, the mature females deposit large numbers of ova in the hepatic parenchyma, which elicit a chronic inflammatory response and granuloma formation.

Certain nematodes, such as *Gongylonema neoplasticum* (formerly *Spiroptera carcinoma*), have been implicated as being contributory to neoplastic transformation of gastric tissues. Furthermore, capillarid



Liver, rat. Nematode eggs are oval, approximate 50um x 30um, and have bipolar plugs (arrows). (HE, 357X)

nematode infections in Norway rats examined in South America were noted to display hyperplastic changes in the non-glandular stomach. These changes were associated with posited infections with *Eucoleus gastricus*; formerly *Capillaria gastrica*; *Hepaticola gastrica*.¹⁶

In humans, hepatic capillariasis typically presents as an acute eosinophilic hepatitis with potential spread to distant viscera and in rare instances has been fatal.

Specific helminthic parasitism of rats in South East Asia has been described. One study of note involved a survey of rats in Northern Thailand in the moat surrounding the ancient city of Chiang Mai.¹³ In that instance, 38 Norway rats and roof rats (*Rattus rattus*) were trapped and necropsied during a 3 month period in 1995. From this sample set, 10 different helminths were identified infection the animals. Four species of trematode, to include *Centrocestus* sp.,

Echinostoma ilocanum, *Echinostoma malayanum* and *Quinqueserialis quinqueserialis*, two species of cestode, comprising *Raillietina* sp. And *Taenia* sp., as well as four species of nematode, which were *Nippostrongylus* sp. *Angiostrongylus cantonensis*, *Rictularia* sp. and the ova of *Capillaria hepatica*.

Similarly, a more robust study

conducted in Malaysia examined the livers of over 100 rats specifically focusing on the two etiologies found in these slides. In that investigation, approximately 39% of rats were infected with *C. fasciolaris* and 45% with *C. hepaticum*, while 20% of all of the animals examined were noted to be parasitized by both etiologies.¹⁹

Contributing Institution:

Armed Forces Research Institute of Medical Sciences (AFRIMS).
<http://afrims.amedd.army.mil/usamd-afrims.html>

JPC Diagnosis: 1. Liver: Strobilocercus.

2. Liver: Granuloma, focal, with numerous aphasmid eggs.

JPC Comment: The contributor has done an excellent job in the description of many aspects of the life cycle, epidemiology, and comparative pathology of the two distinct

etiologic agents in this educational case.

Recent investigations into the pathology of *Cysticercus fasciolaris* have denoted some new and interesting facts. It is apparent that *C. fasciolaris* is best adapted to the hepatic environment, where the cyst provides adequate protection from the host response. Cysts may be seen in other tissues, such as the kidney and abdominal wall, but the cysts are poorly formed and filled with degenerate neutrophils rather than a thriving strobilocercus. In the liver, the cyst will appear to go through a distinct maturation process in which collagen types I and III are demonstrable within the wall, with type III within the inner layers and type I in outer layers. During subsequent maturation of the cyst, type I collagen predominates. It is apparent that this staging and location of different types of collagen during development is required for prolonged survival of the parasite.¹¹

Another feature of the cyst, mentioned above, is the rare but well-documented neoplastic cyst wall. First identified by Borrel in 1906, the hepatic sarcomas associated with the cyst wall of *C. fasciolaris* were first experimentally induced by Bullock and Rohdenburg in 1920, in which 25% of young rats developed sarcomas over a period of eight to fifteen months (occasionally not associated with parasites), and documented metastasis in 60% of tumors. The inability of other researchers to induce similar tumors suggests a variation in susceptibility of rat strains to develop this neoplasm.¹²

Capillaria hepatica has been identified in a number of species other than rodents which are the natural host, including cases in mammalian families Insectivora, Chiroptera, Lagomorpha, Artiodactyla, Perissodactyla, Hyracoidea, Marsupalia, Carnivora, and various primates, to include man.¹⁵ 163 cases

of human infection have been documented, to include true infections as well as spurious ones, in which unembryonated non-infective eggs are ingested and passed through the gastrointestinal tract.¹⁵ The disease in humans is similar to those seen in other aberrant mammalian hosts, with granuloma formation and marked hepatic fibrosis. Another related species, *C. philippinensis*, results in jejunal infections with mucosal invasion by the parasite. A recent report of capillariasis of *C. hepatica* infection in the horse, detailed partially calcified granulomas containing eggs were identified in the hepatic parenchyma.¹⁵

The moderator discussed the primary difference between a strobilocercus and a cysticercus, and that the neck and scolex is generally everted in tissue section with strobilocerci. The strobilocercus is generally considered a more advanced form than a cysticercus, as it more rapidly becomes an adult cestode after ingestion by the definitive host. The calcareous corpuscles in the strobilocerci were also discussed – in strobilocerci, these structures are present in the scolex and neck but not in the bladder; when pressed on the function of these structures, the moderator pointed out that it has never been definitively proven, but it was his belief that their large amount of calcium may be needed by the parasite as a buffer in the acidic nature of the enteron.

References:

1. Chaiyabutr N. Hepatic capillariasis in *Rattus norvegicus*. *J Sci Soc Thailand*. 1979; 5:49-50.
2. Chaisiri K, Chaeychomsri W, Siruntawineti J, Riba A, Herbreteau V and Morand S. Gastrointestinal Helminth Infections in Asian House Rats (*Rattus tanezumi*) from Northern and Northeastern

- Thailand. *J Trop Med Parasitol*. 2010;33:29-35.
3. Claveria FG, Causapin J, de Guzman MA, Toledo MG and Salibay C. Parasite biodiversity in *Rattus* spp caught in wet markets. *Southeast Asian J Trop Med Public Health*. 2005;36 Suppl 4:146-8.
 4. Conlan JV, Sripa B and Attwood S, Newton PN. A review of parasitic zoonoses in a changing Southeast Asia. *Vet Parasitol*. 2011;182:22-40.
 5. Gardiner CH and Poynton SL. An Atlas of Metazoan Parasites in Animal Tissues. Washington, DC: American Registry of Pathology; 1999:40-43.
 6. Gardiner CH and Poynton SL. An Atlas of Metazoan Parasites in Animal Tissues. Washington, DC: American Registry of Pathology; 1999:50-55.
 7. Himsworth CG, Parsons KL, Jardine C and Patrick DM. Rats, Cities, People, and Pathogens: A Systematic Review and Narrative Synthesis of Literature Regarding the Ecology of Rat-Associated Zoonoses in Urban Centers. *Vector-Borne Zoonot*. 2013; 13(6):349-359.
 8. Jittapalapong S, Herbreteau V, Hugot JP, Arreesrisom P, Karnchanabanthoeng A, Rerkamnuaychoke W and Morand S. Relationship of Parasites and Pathogens Diversity to Rodents in Thailand. *Kasetsart J (Nat Sci)*. 2009; 43:106-117.
 9. Joshi PP. Human trypanosomiasis in India: Is it an emerging new zoonosis? Section 1: infectious diseases. *Med Update*. 2013; 23:10-13
 10. Kamiya M, Ooi HK, Ohbayashi M and Ow-Yang CK. Bicephalic larval cestode of Taeniidae from rats in Malaysia. *Jap J Vet Res*. 1987; 35(4):275-282.
 11. Lee BW, Jeon BS, Kim HS, Kim HC, Yoon BI. *Cuscutercus fasciolaris* infection in wild rats (*Rattus norvegicus*) in Korea and formation of cysts by remodeling of collagen fibers. *J Vet Diagn Investig* 2016; 28(3):263-270.
 12. Letich, A. The experimental inquiry into the causes of cancer. *Brit Med J* 1923; 2(3262):1-7.
 13. Linardi PM and Botelho JR. Prevalence of *Trypanosoma lewisi* in *Rattus norvegicus* from Belo Horizonte, State of Minas Gerais, Brazil. *Mem Inst Oswaldo Cruz*. 2002; 97(3):411-414.
 14. McCarthy J and Moore TA. Emerging helminth zoonoses. *Int J Parasitol*. 2002; 30:1351-1360.
 15. Ochi A, Hifumi T, Ueno T, Katayama Y. *Capillaria hepatica* (*Calodium hepaticum*) infection in a horse: a case report. *BMC Vet Res* 2017; 13:384-386.
 16. Namue C and Wongsawad C. A survey of helminth infection in rats (*Rattus* spp.) from Chaing Mai moat. *Southeast Asian J Trop Med Public Health*. 1997;28 Suppl 1:179-83.
 17. Rothenburger JL, Himsworth CG, Lejeune M, Treuting PM, Leighton FA. Lesions associated with *Eucoleus* sp. in the non-glandular stomach of wild urban rats (*Rattus norvegicus*). *International Journal for Parasitology: Parasites and Wildlife*. 2014;3(2):95-101.
 18. Sarataphan N, Vongpakorn M, Nuansrichay B, Autarkool N, Keowkarnkah T, Rodtian P, Stich RW and Jittapalapong S. Diagnosis of a *Trypanosoma lewisi* -like

(Herpetosoma) infection in a sick infant from Thailand. *J Med Microbiol.* 2007; 56:1118–1121.

19. Sinniah B, Narasiman M, Habib S, Gaik Bei O. Prevalence of *Calodium hepaticum* and *Cysticercus fasciolaris* in Urban Rats and Their Histopathological Reaction in the Livers. *J Vet Med.* 2014; 2014:172829.

20. Stojčević D, Marinculić A and Mihaljević Z. Prevalence of *Capillaria hepatica* in Norway rats (*Rattus norvegicus*) in Croatia. *Veterinarski Arhiv.* 2002; 72(3):141-149.

21. Sumangali K, Rajapakse RPVJ and Rajakaruna RS. Urban rodents as potential reservoirs of zoonoses: a parasitic survey in two selected areas in Kandy district. *Ceylon J Sci (Bio Sci).* 2012; 41(1):71-77.

22. *Taenia taeniaeformis*. American Association of Veterinary Parasitologists (AAVP)

<http://www.aavp.org/wiki/cestodes/cyclophyllidea/taeniidae/taenia-taeniaeformis/>

Accessed 14 February 2018

CASE II: 401324 (JPC 4103280).

Signalment: Seven-month-old female Limousine cross bovine (*Bos taurus*).

History: The animal was presented at the Scottish Centre for Production Animal Health and Food Safety (SCPAHFS) for not recovering after an episode of fog fever. Ultrasound examination revealed prominent hyperechoic appearance of the lungs. The animal was euthanased and submitted for post mortem examination.

Gross Pathology: Caudal pulmonary lobes appear diffusely swollen; interlobular septa are prominently expanded by air.

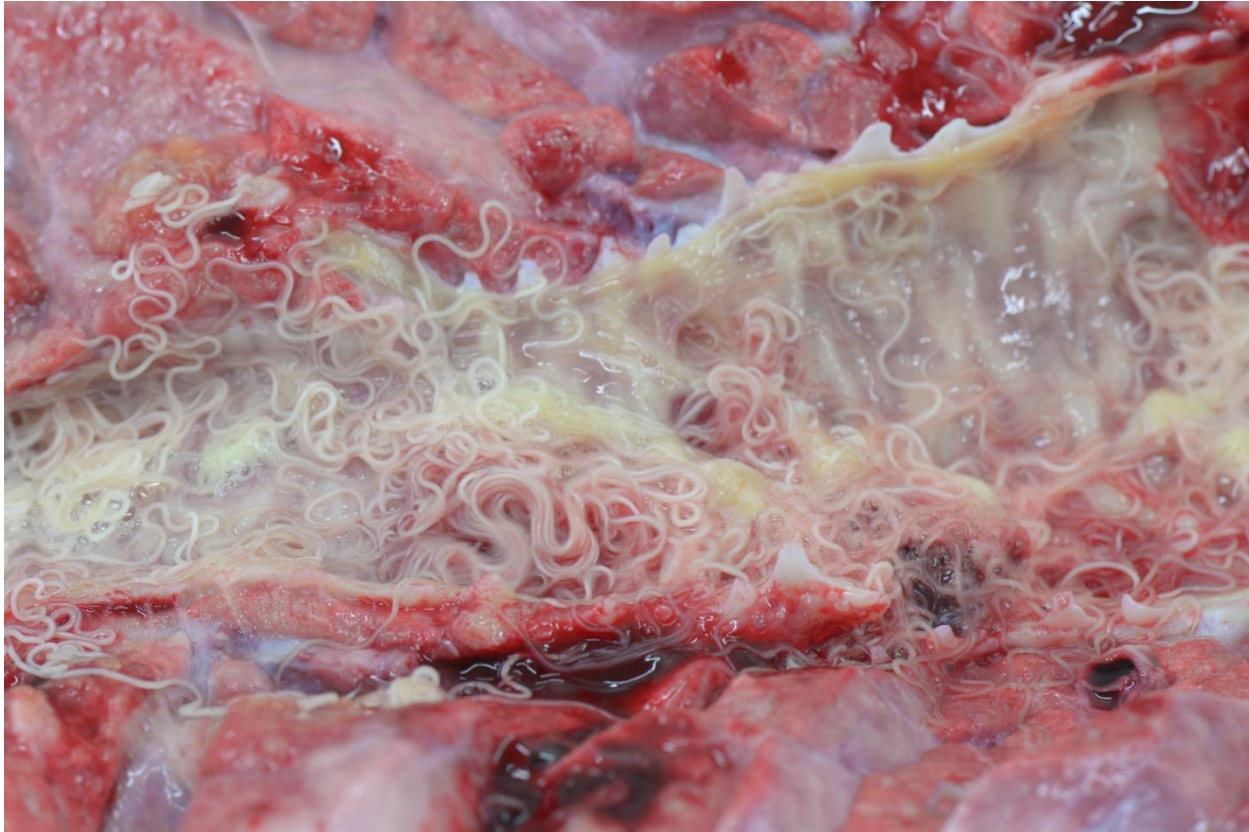


Lung, ox. The caudal pulmonary lobes are bilaterally swollen (emphysema) and there focally extensive mild thickening and dull whitish discoloration of the pleura surface. There is mild to moderate thickening of interlobular septa (interstitial emphysema). Areas of brick red discoloration and consolidation are noted in cranial and intermediate lobes and anterior portion of the caudal lobes. (Photo courtesy of: Division of Pathology, Public Health and Disease Investigation, Veterinary Diagnostic Services, School of Veterinary Medicine, College of Medical, Veterinary and Life Sciences, University of Glasgow (Garscube Campus), 464 Bearsden Road, Glasgow G61 1QH, Scotland, <http://www.gla.ac.uk/schools/vet/>)

Cranioventral lobes exhibit multifocal to extensive and coalescing areas of reddish discoloration increased firmness; a yellowish mottling is noted on the cut surface of these consolidated areas. Very large numbers of long (4-5 cm in length) thin white roundworms are lying within trachea and bronchi admixed with frothy fluid and mucoid-purulent exudate, causing a partial obstruction of the lumen.

Liver exhibits multifocal small irregular areas (approximately 1x2 up to 2x3 cm) of yellow discoloration visible on the capsular surface close to the attachment of hepatic ligaments, and extending for approximately 0.5-1 cm into the parenchyma (tension lipidosis).

Kidneys display numerous bilateral small, round, whitish foci (1-3mm in diameter), that on cut surface correspond to pale streaks extending to corticomedullary junction.



Lung, ox. Within the lumen of a large main bronchus there are large numbers of thin elongate nematodes admixed with moderate amounts of mucopurulent exudate. (Photo courtesy of: Division of Pathology, Public Health and Disease Investigation, Veterinary Diagnostic Services, School of Veterinary Medicine, College of Medical, Veterinary and Life Sciences, University of Glasgow (Garscube Campus), 464 Bearsden Road, Glasgow G61 1QH, Scotland, <http://www.gla.ac.uk/schools/vet/>)

A few scattered small (approximately 3-5 mm in diameter), dark shallow or slightly depressed lesions are evident on the abomasal mucosa.

Laboratory results: NA

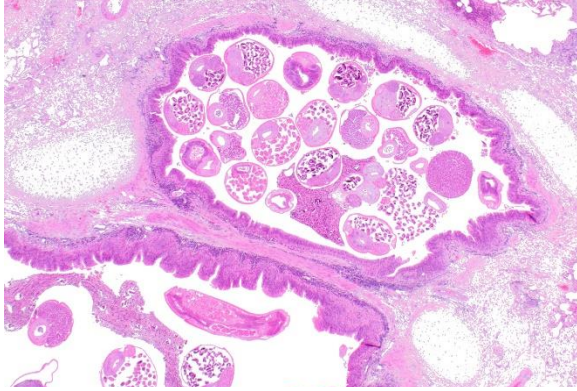
Microscopic Description:

Lung: Up to 40% of the lung tissue is obliterated by extensive and coalescing areas of inflammation.

Within the lumen of medium sized to large bronchi there are numerous adult nematodes, variable numbers of sloughed degenerate/necrotic epithelial cells and scattered larvae. Parasites are approximately 350 μ m in diameter, with an approximately 5

μ m thick cuticle, platymyarian musculature, prominent lateral cords, a pseudocoelom, reproductive organs containing embryonated eggs or larvae, and a medium-sized intestine composed of multinucleated cells lined by short microvilli. The lumen of small bronchi and bronchioles is frequently plugged with large amounts of necrotic debris admixed with numerous degenerate neutrophils and eosinophils and large numbers of nematode larvae.

Alveolar spaces are filled with large numbers of granulocytes, including eosinophils and neutrophils, and variable numbers of macrophages, admixed with variable amounts of fibrillary to finely granular material and pale eosinophilic proteinaceous



Lung, ox. Bronchial lumens are plugged with numerous cross or longitudinal sections of nematodes. Photo courtesy of: Division of Pathology, Public Health and Disease Investigation, Veterinary Diagnostic Services, School of Veterinary Medicine, College of Medical, Veterinary and Life Sciences, University of Glasgow (Garscube Campus), 464 Bearsden Road, Glasgow G61 1QH, Scotland, <http://www.gla.ac.uk/schools/vet/>

fluid (fibrin, cellular debris and edema) and numerous nematode larvae. Large numbers of plasma cells and lymphocytes expand the interstitium, along with large numbers of plump fibroblasts and increased amounts of collagen (interstitial fibrosis). Multifocal areas reveal ruptured alveolar septa with irregularly shaped clear areas resulting from coalescence of alveolar spaces (emphysema). In some areas, the inflammatory infiltrates obliterating the alveolar structures are characterised by large numbers of macrophages and variable numbers of multinucleate giant cells.

In some instances, bronchial and bronchiolar epithelium is hyperplastic (up to 6 cell layers), focal segmental squamous metaplasia is occasionally noted in larger bronchi.

Contributor's Morphologic Diagnosis:

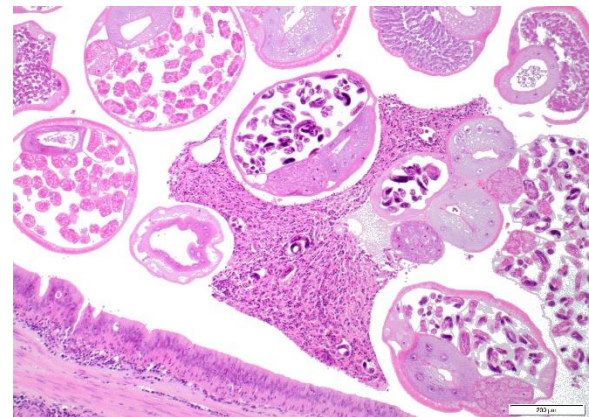
Lung: bronchopneumonia, eosinophilic and pyogranulomatous multifocal to coalescing, chronic, severe, with multifocal bronchiolar epithelial hyperplasia and squamous metaplasia, and adult and larval trichostrongyles.

Etiology: *Dictyocaulus viviparus*

Contributor's Comment: *Dictyocaulus viviparus* is a member of the superfamily *Trichostrongyloidea*, family *Dictyocaulidae*.² Trichostrongyles usually have platymyarian musculature. Characteristically, the external cuticle bears either evenly spaced or irregular longitudinal ridges. The buccal cavity in this group is not as pronounced as that of the true strongyles. Eggs of *Dictyocaulus viviparus* are embryonated (2).

The adult parasites are found in lower respiratory airways. Once delivered in the host tissue the eggs hatch rapidly. First stage *larvae* are coughed up, swallowed, and then passed in the feces. Further development into L2, and later L3, occurs in the feces on the pasture over the next 5-7 days and is strictly dependent on environmental conditions.²

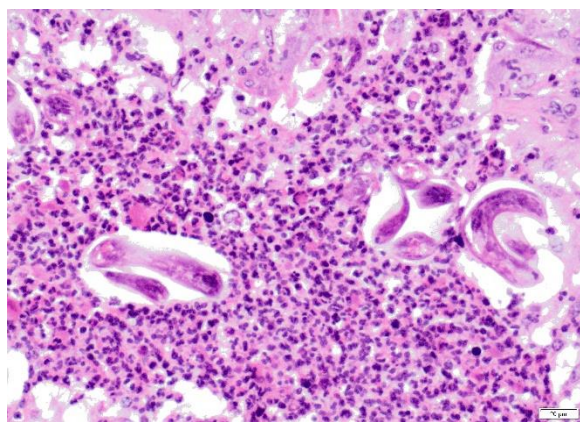
A new host is infected by ingestion of third-stage *larvae* whilst grazing. These infective *larvae* penetrate the wall of the intestine, and migrate via the lymphatics to the mesenteric nodes. In the lymph nodes they form the fourth-stage *larvae* and they enter the lungs



Lung, ox. Nematodes have a coelomic cavity, intestinal tract and uterus containing embryonated eggs or larvae; sloughed degenerate epithelial cells and larvae are also present in the lumen admixed with the nematodes. (Photo courtesy of: Division of Pathology, Public Health and Disease Investigation, Veterinary Diagnostic Services, School of Veterinary Medicine, College of Medical, Veterinary and Life Sciences, University of Glasgow (Garscube Campus), 464 Bearsden Road, Glasgow G61 1QH, Scotland, <http://www.gla.ac.uk/schools/vet/>)

about 7 days after the infection by means of lymph and blood. The final molt to the fifth stage occurs in the bronchioles, and adults develop in larger airways. Few egg-laying adults may persist in some animals and represent the source of pasture contamination in the following grazing season. Primary infections cause disease in calves during their first grazing season and clinical signs typically occur 3 to 5 months after exposure. Mortality rates depend on the degree of pasture contamination. Reinfection syndrome is observed when partially immune adult cattle on endemically affected farm have access to highly contaminated pastures. Some of the affected animals may develop fatal dyspnoea.²

Dictyocaulus viviparus is the only adult nematode known to infect the lung of the cattle and one of the most important parasites in cattle causing substantial economic losses. Current research is focused on the identification and characterization of genes associated with critical phases of the parasite life cycle and host-parasite interaction, with the purpose to exploit the gene products and



Lung, ox. Nematode larvae in alveolar spaces surrounded by an intense inflammatory response comprising large numbers of hypersegmented degenerate neutrophils. (Photo courtesy of: Division of Pathology, Public Health and Disease Investigation, Veterinary Diagnostic Services, School of Veterinary Medicine, College of Medical, Veterinary and Life Sciences, University of Glasgow (Garscube Campus), 464 Bearsden Road, Glasgow G61 1QH, Scotland, <http://www.gla.ac.uk/schools/vet/>)

related pathways as targets for vaccine design and/or drug development.^{4,5}

Contributing Institution:

Division of Pathology, Public Health and Disease Investigation
 Veterinary Diagnostic Services
 School of Veterinary Medicine
 College of Medical, Veterinary and Life Sciences
 University of Glasgow (Garscube Campus)
 464 Bearsden Road
 Glasgow G61 1QH, Scotland
<http://www.gla.ac.uk/schools/vet/>

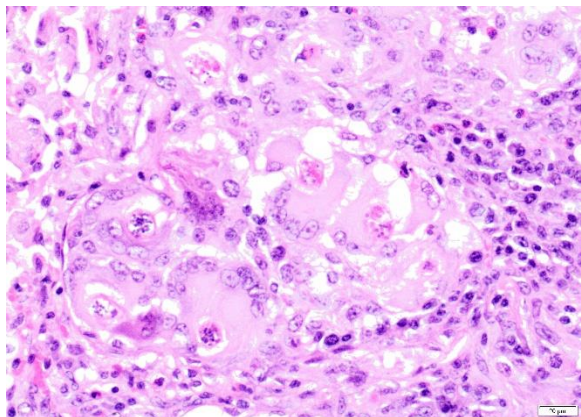
JPC Diagnosis: Lung: Bronchopneumonia, pyogranulomatous and eosinophilic, chronic, diffuse, severe, with alveolar and interlobular edema and emphysema and adult and larval metastrongyle nematodes.

JPC Comment:

While a number of lungworms may be present in larval form in the lungs of cattle, *Dictyocaulus viviparus* is the only one to establish a patent infection. *Toxocara vitulorum* and *Ascaris suum* larvae may migrate through the lungs as part of maturation and cause a transient pneumonitis, but adults will not be present in this location.¹

In the prepatent phase (prior to maturation in to adults), gross lesions in the lungs are minimal, clinical signs coincide with penetration of larvae into alveoli where they incite an intense eosinophilic reaction which blocks small bronchi and bronchioles, resulting atelectasis and clinically cough and tachypnea.¹

In the patent phase, there is usually bilaterally symmetric reddish of the caudoventral lobes with the presence of adult worms in the trachea and bronchi. In the postpatent phase, gross lesions are similar, but no adult worms



Lung, ox. Nematode larvae in alveolar spaces surrounded by a granulomatous inflammatory response with multinucleate giant cells; peripheral infiltration of macrophages, plasma cells and eosinophils is also present in this microscopic field. (Photo courtesy of: Division of Pathology, Public Health and Disease Investigation, Veterinary Diagnostic Services, School of Veterinary Medicine, College of Medical, Veterinary and Life Sciences, University of Glasgow (Garscube Campus), 464 Bearsden Road, Glasgow G61 1QH, Scotland, <http://www.gla.ac.uk/schools/vet/>)

or larvae are present. In this phase, up to 25% of severely infected animals may die as a result of a combination of severe pulmonary edema, extensive alveolar epithelial damage, and hyaline membrane formation. Histologically, animals experiencing a reinfection syndrome will develop greenish nodules up to 3-4 mm in diameter, which may be grossly visible underneath the pleura. The nodules are composed of parasitic debris and large numbers of eosinophils, macrophages, and multinucleated giant cells. In these cases, no edema or emphysema are present. More longstanding cases of reinfection syndrome may demonstrate formation of lymphoid nodules with germinal centers within the lungs.¹

References:

1. Bowman DB, Zajac AM. Parasitic Bronchitis and Pneumonia. In: Smith B, ed. Large Animal Internal Medicine, 5th ed. St. Louis MO: Elsevier, 2015:625-628.

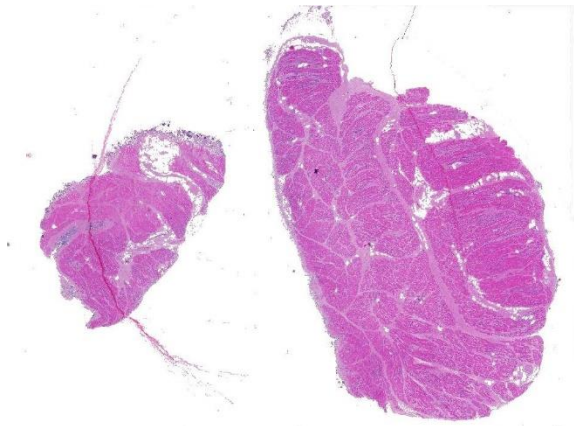
2. Caswell JL, Williams KJ Respiratory System. In: Jubb, Kennedy, and Palmer's. Pathology of Domestic Animals. 6th ed. St. Louis, MO: Elsevier; 2016: 554.
3. Gardiner CH, Poynton SL. An Atlas of Metazoan Parasites in Animal Tissues. Washington DC: Armed Forces Institute of Pathology, American Registry of Pathology; 2006: 22, 29.
4. McNulty S, Strübe C, Rosa BA, Martin JC, Tyagi R, Choi YJ, Wang Q, Hallsworth Pepin K, Zhang X, Ozersky P, Wilson RK, Sternberg PW, Gasser RB, Mitreva M. *Dictyocaulus viviparus* genome, variome and transcriptome elucidate lungworm biology and support future intervention. *Sci Rep.* 2016; 6: 20316.
5. Strube C, Buschbaum S, Schnieder T. Genes of the bovine lungworm *Dictyocaulus viviparus* associated with transition from pasture to parasitism. *Infect Genet Evol.* 2012; 12: 1178-1188.

CASE III: NP545M3 (JPC 4074226).

Signalment: Canine; Cairn terrier, 9y9m, male-castrated.

History: History of progressive lameness of the right front limb, treated with phenylbutazone and prednisone for several weeks. At presentation in a referral center, the dog showed a stiff gait, lameness of the right front limb and pain on palpation of the axillary region. Supraspinatus muscle biopsy submitted.

Gross Pathology: Subgross examination of the fixed muscle showed round blackish



Skeletal muscle, dog: Two sections of skeletal muscle are submitted for examination. (HE, 4X)

structures/organisms scattered throughout the surface.

Laboratory results: Clinical chemistry revealed increased CK values and *Anaplasma* titer of 1:2560.

Microscopic Description:

Moderately to poorly preserved muscle tissue showing moderate endomysial and perimysial fibrosis and mild multifocal muscle replacement by adipose tissue. Throughout the fascicles there are mild multifocal partially necrotizing mixed-cellular inflammatory infiltrates with predominance of histiocytes, macrophages and plasma cells accompanied by a few polymorphonuclear neutrophils. These mostly are seen in the interstitium and occasionally center on and invade necrotic myocytes. Throughout all fascicles there are numerous myocytes laden with 1-3 uncoiled sarcoplasmic nematode larvae of about 25-35 μm diameter, which in some sections show stichosomes.

Throughout muscle fascia and most superficial aspects of myofascicles, there are mycotic organisms with numerous sporangia, sporangiophores and sporangiospores, as well as some columellae. The mycelium

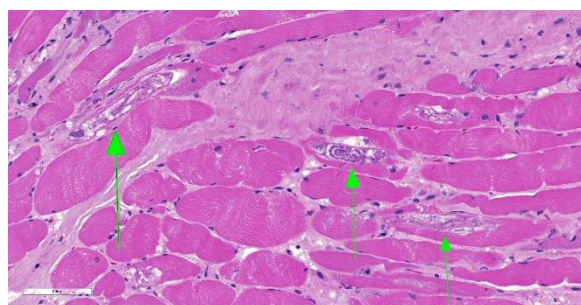
consists of mainly aseptate (coenocytic) hyphae with mostly non-parallel walls. In some slides, moreover, smaller, slender septated hyphae with dichotomous branching are seen. Fungal organisms, even in the depth of the tissue, are not accompanied by reactive tissue changes.

In addition to the fungal infestation, the surface of the biopsy shows massive bacterial colonization comprising rods, fusiform and coccoid bacteria.

Contributor's Morphologic Diagnosis:

1. Myositis, mixed-cellular, multifocal, subacute, moderate, associated with intramysial trichurid larvae (*Trichinella* spp.).
2. Superficial myofascial mucormycosis, non-reactive, diffuse, acute.
3. Bacterial contamination, mixed flora, superficial, severe.

Contributor's Comment: Even though definite histological classification is not possible, the uncoiled character and absence of nurse cells very much indicates an infection by *Trichinella pseudospiralis*, the only other common species seen in tempered climate zones. Other metazoic invaders of the muscle (as hookworms) usually do not infest within the sarcoplasm. Retrospective analysis of the medical history revealed the



Skeletal muscle, dog: Numerous myofibers contain tangential sections of uncoiled nematode larvae measuring up to 40 μm . (HE, 238X)

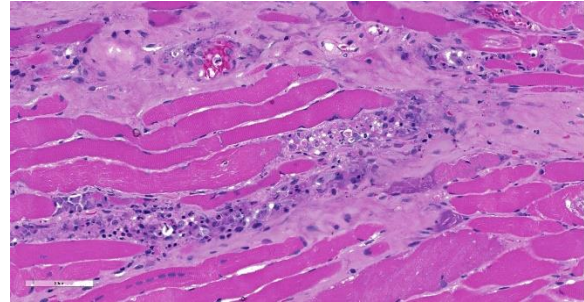
dog to be severely immunocompromised, which explains both the minimal inflammatory tissue reaction and absence of any significant inflammation in areas invaded by the described fungi. As the sample was severely autolytic and contaminated by bacteria, the presence of fungi first was considered a contamination, as well. Consultancy sought at the Federal Center for Mycotic diseases, however, excluded the possibility that this massive infestation and the development of sporangia could have resulted from a contamination within less than 36 hours. Hence, the authors consider the infection to have taken place in vivo. This assumption appears to have gained support by successful treatment of the dog with antimycotics after withdrawal of corticosteroids. Based on morphology and later confirmed by sequencing of nuclear ribosomal internal transcribed spacer (ITS) region³ fungal organism were identified resembling *Mucor* spp. The infection may have been opportunistic as a consequence to immunosuppression.

Contributing Institution:

Institut of Veterinary Pathology LMU, Munich
 Veterinaerstr. 13; 80539 Munich
 Germany
 www.patho.vetmed.uni-muenchen.de

JPC Diagnosis: Skeletal muscle: Degeneration and necrosis, multifocal, mild, with marked edema and intramyocyte nematode larvae, consistent with *Ancylostoma caninum*.

JPC Comment: Careful consideration was given to the contributor's diagnosis of trichinosis in this case, however, we prefer a diagnosis of ancylostomiasis in this case. The larvae in this section are not encysted; *Trichinella* sp. often are surrounding by a



Skeletal muscle, dog: Numerous cross and tangential sections of fungal hyphae and sporangiospores consistent with a zygomycete are admixed with bacilli at the edge of the section. The presence of these agents and lack of an immune response in an autolytic section suggest post-mortem contamination. (HE, 352X)

hyaline cyst wall ranging to 10µm during the formation of “nurse cells”. Within nurse cells, *Trichinella* sp. are generally coiled, while many of these larvae are present in longitudinal section. Larvae of *Trichinella* species also have a prominent stichosome and bacillary bands, which are absent in these larvae, which also possess lateral cords, vice the hypodermal bands seen in *Trichinella* sp. Several of the larvae also have a prominent flask-shaped esophagus characteristic of *Ancylostoma*.¹

Inatome et al. first identified that third-stage larvae of *Ancylostoma caninum* may migrate through muscle tissues and occasionally will take up residence in myofibers. Other researchers have identified other members of this genus, including *A. braziliense* and *A. tubaeformae* in host striated muscle. A detailed morphologic analysis of this finding was completed in 1975 by Lee and Beaver following oral inoculations of the mouse, cat, and monkey. In affected muscles, there are a number of degenerate and necrotic fibers, suggesting that the residence of an individual larva is not permanent within any given myofiber, and that larvae may move from one fiber to another, utilizing myofibers as a convenient way to evade the host's immune response.

A number of other nematode larvae have also been identified within striated muscle, to include *Trichinella* which undergoes significant growth after penetration and the formation of a cyst around it to protect it from the immune response. Larva of *Toxocara canis* will also migrate through muscle tissue but does not infiltrate myofibers, instead forming fibrous cysts within connective tissues.

We agree with the contributor regarding the presence a zygomycete fungus at the edge of the section, which do not appear to be the subject of an immune response, suggesting that they may be contaminants in this case.

References:

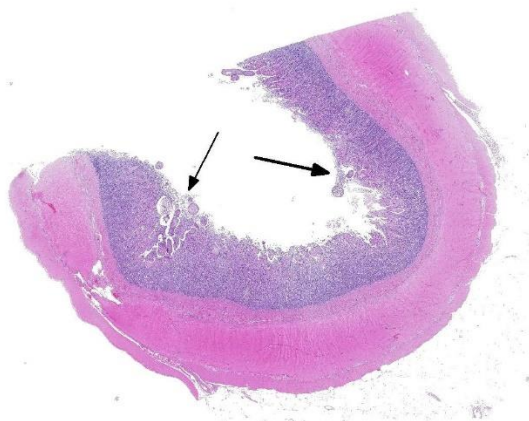
1. Gardiner CH, Poynton SL. Aphasmids. *In: An Atlas of Metazoan Parasites in Animal Tissues*. Washington DC, American Registry of Pathology, 1999: 41-44.
2. Lee, KT, Little MD, Beaver PC. Intracellular (muscle-fiber) habitat of *Ancylostoma caninum* in some mammalian hosts. *J Parasitol* 1975, 61(4): 589-598.
3. Schoch CL, Seifert KA, Huhndorf S, Robert V, Spouge JL, Levesque CA, Chen W, Fungal Barcoding Consortium Author L: Nuclear ribosomal internal transcribed spacer (ITS) region as a universal DNA barcode marker for Fungi. *Proc Natl Acad Sci U S A* **109**: 6241-6246, 2012

CASE IV: S15/8162 (JPC 4116731).

Signalment: 10Y, male intact, Whippet, *Canis lupus familiaris*, dog

History: The dog had a history of hyperadrenocorticism due to a functional pituitary adenoma and a urinary tract infection, from which *Streptococcus canis* was isolated. Additionally, the dog showed mild intermittent nasal discharge over the past few months. Suddenly the dog developed severe dyspnea and generalized weakness, after which it was referred to the clinician and treated with antibiotic and anticoagulant therapy. The dog died shortly thereafter.

Gross Pathology: The right side of the lung was severely enlarged, firm and dark red with a 2 cm long thrombus within a large branch of the *arteria pulmonalis*. Both adrenals were enlarged. The trunk muscles were mildly atrophied and the skin of the abdomen was thin and of increased fragility. Besides those changes attributed to the prolonged hyperadrenocorticism, the intestinal wall was diffusely thickened and red, with multifocal petechial hemorrhages on the serosa. Within



Intestine, dog. A single section of intestine is presented with mucosal parasites visible on subgross examination. (HE, 4X).

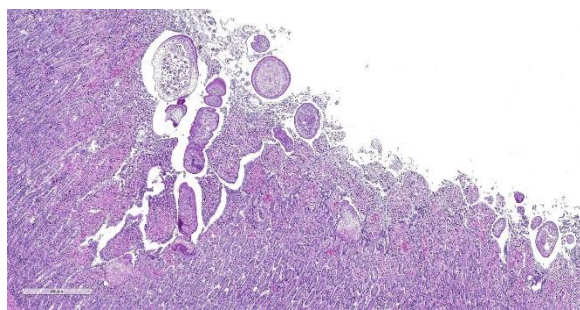
the intestinal lumen, several different adult nematodes and myriad, 2-4 mm long adult cestodes were found.

Laboratory results: Laboratory Results (clinical pathology, microbiology, PCR, ELISA, etc.):

A parasitological examination of the intestinal contents was performed:

1) Flotation: Hookworm eggs +++, Taenidae eggs +++, Toxocara sp. Eggs +++, Capillaria sp. Eggs +

2) Parasite identification of proglottids using PCR: Positive for *Echinococcus multilocularis*

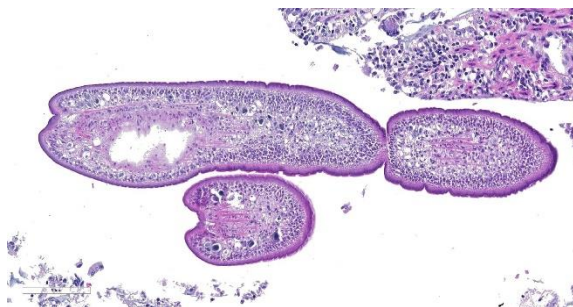


ntestine, dog. Higher magnification of embedded cestodes. (HE, 56X).

Microscopic Description:

Dog, small intestine: Multifocally, within the intestinal lumen and within the mucosa, there are several cross and longitudinal sections of adult cestode parasites of about 100-300 μm in diameter and up to 500 μm in length, with 3-5 well visible segments (proglottids). The first segment (scolex) has multiple short hooks (may not be present on all slides) attached between intestinal villi or deep into the crypts of Lieberkühn. The parasites are covered with a 3-5 μm thick amphophilic tegument with supporting basement membrane, under which there are two zones of non-striated circular (inner) and longitudinal (outer) muscle layers. Multifocally within the parasitic body parenchyma there are few round to oval, dark

basophilic, granular structures of about 10 to 15 μm in diameter (calcareous bodies). Within the mature proglottid there are numerous multilobulated, round to oval, around 30 μm in diameter large basophilic structures (testes). The most posterior, bell-shaped segment contains an egg-filled uterus (gravid proglottid). The eggs, also present freely in the intestinal lumen, are round or spherical and up to 30 μm in diameter, with a radially striated, brown embryophore. The egg lumen is filled with round to oval, up to 30 μm in diameter large oncospheres (embryonated eggs). The lamina propria and submucosa are infiltrated by a moderate amount of plasma cells, lymphocytes and few eosinophils, and multifocally there is mild fibroblast proliferation (fibrosis). Multifocally, the intestinal crypts are dilated and filled with degenerated and viable neutrophils.



Intestine, dog. Cestodes have a ridged tegument, spongy body cavity, and prominent calcareous corpuscles.. (HE, 242X).

Contributor's Morphologic Diagnosis:

Dog, small intestine: Moderate, multifocal-coalescing, subacute, lymphoplasmacytic Enteritis with intralesional adult cestodes consistent with *Echinococcus multilocularis*

Contributor's Comment: The necropsy of the dog revealed pulmonary thrombosis as the cause of death. This was attributed to the hypercoagulability, known to be associated with hyperadrenocorticism. During necropsy, we surprisingly observed that the

intestinal lumen contained large number of small, white, segmented tapeworms. Parasitological and histological investigation subsequently confirmed a severe intestinal infestation with *Echinococcus multilocularis*.

There are two major *Echinococcus* species of special importance to veterinary medicine, namely *E. multilocularis* and *E. granulosus*. *E. multilocularis* is a zoonotic cestode present in large parts of the northern hemisphere.¹¹ Transmission of *E. multilocularis* occurs in a sylvatic cycle, which is sometimes linked via infected small mammals to domestic dogs and cats.⁴ (Figure 1)

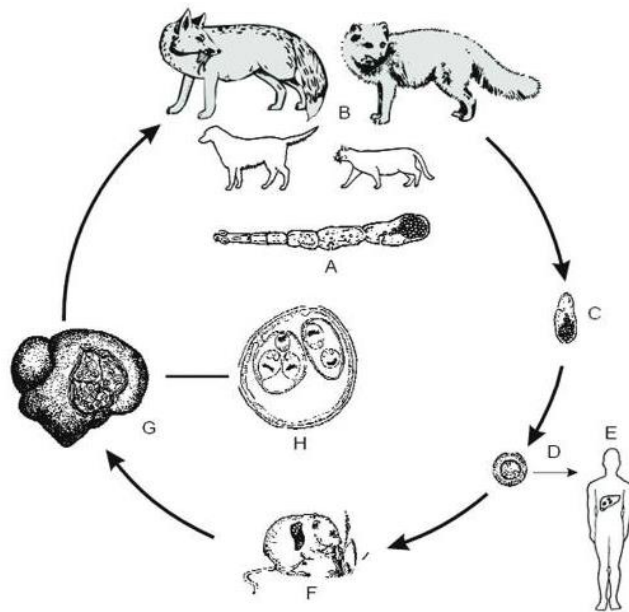


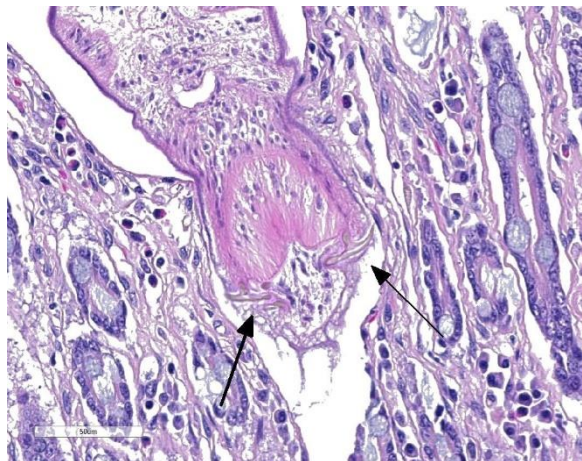
Figure 1: Life cycle of *E. multilocularis*. (A) Adult parasite. (B) Foxes as principal definitive hosts; dogs, other canids and cat can be involved in the cycle. (C) Proglottid with eggs. (D) Egg with oncosphere. (E) Infection of humans. (F) Rodent infected with metacestodes. (G) Rodent with liver metacestodes. (H) Single metacestode cyst with protoscolexes.

E. multilocularis tapeworms may be present in the small intestine of a number of species of carnivores, but predominantly affects

canids.⁷ In Europe, a high prevalence (23.9–57.3%) of *E. multilocularis* has been frequently reported in the red fox population (*Vulpes vulpes*)^{3,10,11} which is increasingly colonizing urban areas. In domestic dogs, however, this infection is rare. In a study performed in Lithuania in 2009, the prevalence within a group of 240 tested dogs was 0.8%.² Similarly, in Switzerland, echinococcosis is sporadic and most cases are diagnosed in wildlife.

Intestinal infestations of *E. multilocularis* in the definitive host usually cause little to no clinical symptoms or pathomorphological lesions. A far more severe form of infection with this parasite is alveolar echinococcosis (AE). Among the many species (>40 species) of small mammals that are susceptible to *E. multilocularis* under natural conditions, members of the family Arvicolidae (voles and lemmings) and Cricetidae (hamsters, gerbils, and related rodents) are most important. Aberrant host animals and humans can also become infected with the metacestode stage, which has the potential to cause AE, one of the most lethal helminthic infection in humans.⁵ Relatively recently, domestic dogs have also been revealed to be aberrant intermediate hosts for AE.⁵ In the intermediate host, the oncosphere penetrates the intestinal wall and enters the blood system. Via the blood stream, the oncosphere reaches different organs, especially the liver. Once the oncosphere has reached the liver it starts to develop into the metacestode stage. A characteristic feature of this stage is its exogenous tumor-like proliferation, which leads to infiltration of the affected organs and, in progressive cases, to severe disease and even death.⁴

Although we regularly see AE in zoo animals, particularly in primates, this is the first case of intestinal echinococcosis diagnosed in a domestic dog at our Institute.



Intestine, dog. The anterior end of the cestodes has an armed rostellum with numerous suckers. (HE, 400X).

The histologic slide shows several cross and longitudinal sections of well-preserved adults, which make for a great exercise in the histological descriptions of cestodes. The infestation and the development of pathological lesions within the intestine might have been exacerbated by the immunosuppressive effects of hyperadrenocorticism.

Contributing Institution:

Institute for Animal Pathology
Vetsuisse Faculty - University of Bern
122 Länggassstrasse
3001-CH Bern
Switzerland
www.itpa.vetsuisse.unibe.ch

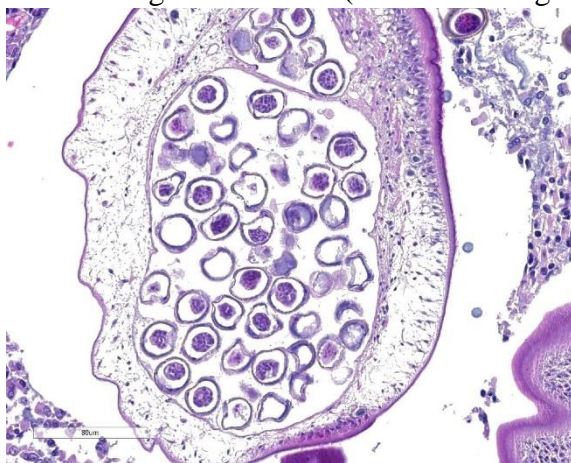
JPC Diagnosis: Jejunum: Multiple embedded adult cestodes.

JPC Comment: The contributor has provided an excellent discussion of the life cycle and pathobiology of this important and emerging zoonotic parasite in the Northern Hemisphere. While not an especially exciting descriptive exercise, this would be the first time that the adult cestode has been submitted to the WSC; five cases of the metacestode have been submitted including a

dog (WSC 2015 Conf 1, Case 4) and a rhesus macaque (WSC 2011, Conf 18, Case 2).

From a comparative standpoint, two major forms of echinococcal disease occur in humans: cystic echinococcosis (prototypically caused by *E. granulosus* in 88% of cases, but also *E. equinus*, *E. ortleppi* and *E. canadensis*), and alveolar echinococcosis (caused by *E. multilocularis*, *E. vogeli*, and *E. oligoarthrus*).⁶ Echinococcosis is one of the 17 neglected tropical diseases recognized by the World Health Organization, ranked third as the most relevant food-borne parasitic zoonosis, and affects 18,000 people each year, with most cases seen in Asia and Europe, with 91% of cases seen in China.⁹

In humans, AE is characterized by a long asymptomatic incubation period up to 15 years. Metacestodes of *E. multilocularis* generally develop in the right lobe of the liver, growing from initial lesions of several mm to large multilocular lesions ranging over 20cm in diameter. ¹Lesions in other organs arise as a result of infiltration or metastasis. Symptoms in the chronic course include jaundice, abdominal pain, fatigue and weight loss. Diagnosis of AE (based on imaging



Intestine, dog. Adult females have a uterus with developing eggs – fully developed eggs with a deep brown hyaline shell are also present. (HE, 317X).

findings) has been standardized by the WHO in a PNM system (P denoting the size of the primary hepatic lesion, N the involvement of neighboring organs, and M, the presence of metastatic lesions.) Treatment is anchored by radical resection (following principles of tumor surgery to diminish the possibility of leaving parasite residue), and the administration of benzimidazoles, such as albendazole.¹

References:

1. Brunetti E, Kern P, Vuitton DA. Expert consensus for the diagnosis and treatment of cystic and alveolar echinococcosis in humans. *Acta Tropica* 2010; 114:1-16.
2. Bružinskaitė R, Šarkūnas M, Torgerson PR, Mathis A, Deplazes P. Echinococcosis in pigs and intestinal infection with *Echinococcus* spp. in dogs in southwestern Lithuania. *Vet Parasitol.* 2009;160:237–241.
3. Bruzinskaite R, Marcinkute A, Strupas K, et al. Alveolar echinococcosis, Lithuania. *Emerg Infect Dis.* 2007;13:1618–1619.
4. Eckert J, Deplazes P. Biological, epidemiological, and clinical aspects of echinococcosis, a zoonosis of increasing concern. *Clin Microbiol Rev.* 2004;17:107–135.
5. Frey CF, Marreros N, Renneker S, et al. Dogs as victims of their own worms: Serodiagnosis of canine alveolar echinococcosis. *Parasit Vectors.* 2017;10:422.
6. Higueta NIA, Brunetti E, McCloskey C. Cystic echinococcosis. *J Clin Microbiol* 2015; 54(3)518-523.
7. Hofer S, Gloor S, Mu U, et al. High prevalence of *Echinococcus multilocularis* in urban red foxes (*Vulpes vulpes*) and voles (*Arvicola terrestris*) in the city of Zürich, Switzerland. *Parasitology.* 2000;120:135-142.
8. Malczewski A, Gawor J, Malczewska M. Infection of red foxes (*Vulpes vulpes*) with *Echinococcus multilocularis* during the years 2001–2004 in Poland. *Parasitol Res.* 2008;103:501–505.
9. Massolo A, Liccioli S, Budke C, Klein. *Echinococcus multilocularis* in North America: the great unknown. *Parasite* 2014; 21:73.
10. Maxie MG, Cullen JM, Stalker MJ. Liver and Biliary System. In: Maxie MG, ed. Jubb, Kennedy, and Palmer's Pathology of Domestic Animals. 6th ed. St. Louis, MO; 2016:319-320.
11. Otero-Abad B, Rüegg SR, Hegglin D, Deplazes P, Torgerson PR. Mathematical modelling of *Echinococcus multilocularis* abundance in foxes in Zurich, Switzerland. *Parasit Vectors.* 2017;10:21.

Self-Assessment - WSC 2018-2019 Conference 22

1. Which of the following is not true about *Cysticercus fasciolaris*?
 - a. It has a direct life cycle.
 - b. Larval forms include a single scolex.
 - c. It is a rare zoonotic disease.
 - d. Another name for this stage of *Taenia taeniaformis* is *Taenia crassicolis*.

2. In which phase of infection by *Dictyocaulus viviparus* are larval and adult worms NOT seen?
 - a. Prepatent
 - b. Patent
 - c. Postpatent
 - d. Reinfection

3. Larvae of which of the following nematodes does not penetrate myofibers?
 - a. *Trichinella spiralis*
 - b. *Toxocara canis*
 - c. *Ancylostoma caninum*
 - d. *Ancylostoma tubaeformae*

4. The definitive host of *E. multilocularis* is a ?
 - a. Dog
 - b. Human
 - c. Vole
 - d. Horse

5. Cystic echinococcosis in humans is most often caused by which of the following?
 - a. *E. granulosus*
 - b. *E. vogeli*
 - c. *E. equinus*
 - d. *E. multilocularis*

Please email your completed assessment to Ms. Jessica Gold at Jessica.d.gold2.ctr@mail.mil for grading. Passing score is 80%. This program (RACE program number) is approved by the AAVSB RACE to offer a total of 0.5 CE Credits, with a maximum of 12.5 CE Credits being available to any individual Veterinary Medical Professionals for the 2017-2018 Wednesday Slide Conference. This RACE approval is for the subject matter categories of: SCIENTIFIC using the delivery method of NON-INTERACTIVE DISTANCE. This approval is valid in jurisdictions which recognize AAVSB RACE; however, participants are responsible for ascertaining each board's CE requirements. RACE does not "accredit", "endorse" or "certify" any program or person, nor does RACE approval validate the content of the program.

Please email your completed assessment to Ms. Jessica Gold at Jessica.d.gold2.ctr@mail.mil for grading. Passing score is 80%. This program (RACE program number) is approved by the AAVSB RACE to offer a total of 0.5 CE Credits, with a maximum of 12.5 CE Credits being available to any individual Veterinary Medical Professionals for the 2017-2018 Wednesday Slide Conference. This RACE approval is for the subject matter categories of: SCIENTIFIC using the delivery method of NON-INTERACTIVE DISTANCE. This approval is valid in jurisdictions which recognize AAVSB RACE; however, participants are responsible for ascertaining each board's CE requirements. RACE does not "accredit", "endorse" or "certify" any program or person, nor does RACE approval validate the content of the program.

**Joint Pathology Center
Veterinary Pathology Services**



WEDNESDAY SLIDE CONFERENCE 2018-2019

C o n f e r e n c e 2 3

24 April 2019

Conference Moderator:

Amy Durham, BA, MS, VMD, DACVP
Associate Professor, Anatomic Pathology
Faculty Director Comparative Pathology Core
Univ. of Pennsylvania School of Veterinary Medicine

CASE I: 12-324-3 (JPC 4032713).

Signalment: 6-year-old, spayed female, Labrador Retriever cross, dog, *Canis familiaris*

History: The dog presented to the referring veterinarian with a 3-day history of inappetance, vomiting, diarrhea, and lethargy. Radiography revealed an enlarged left kidney. A nephrectomy was performed and the dog recovered uneventfully. The following day the dog became lethargic and then died.

Gross Pathology: The carcass and nephrectomized left kidney were submitted for gross examination. Necropsy examination revealed severe hemoperitoneum, and death was attributed to exsanguination from the surgical excision site. Both kidneys were markedly enlarged and had irregular contours. On section the cortex and medulla were irregularly expanded by discrete to coalescing white patches and streaks. The



Kidney, dog. The cortex contains numerous bulging white streaks. (Photo courtesy of: Diagnostic Services Unit, University of Calgary Veterinary Medicine, Clinical Skills Building, 11877 85 St. NW, Calgary AB T3R 1J3, <http://vet.ucalgary.ca/>)

liver contained approximately a dozen firm white parenchymal nodules up to 1 cm in diameter and had a diffusely accentuated lobular pattern. The mesenteric, renal and thoracic lymph nodes were moderately enlarged and, on section, lacked typical corticomedullary architecture.

Laboratory results: NA

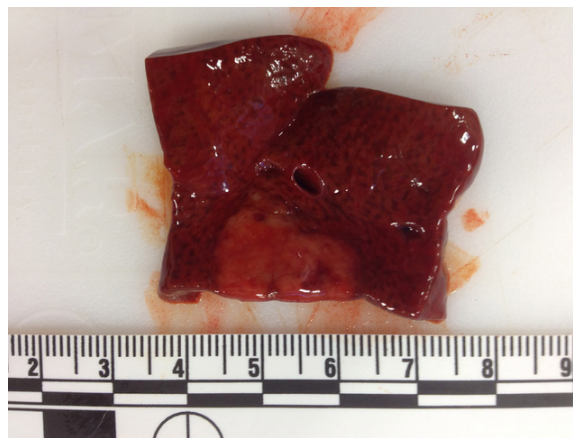
Microscopic Description:

Liver: Two sections of liver are examined. One contains a 9mm diameter nodule (described in the gross pathology section above), and the other is from an unaffected part of the liver.

The nodule is unencapsulated but well circumscribed, slightly infiltrative at its edge and surrounded by a rim of compressed hepatic parenchyma. It consists of sheets of neoplastic cells forming two distinct populations of (a) small round cells and (b) larger, highly pleomorphic cells.

The first cell population makes up approximately 80-90% of the mass. Cells are small (8-15 μm diameter) and round with centrally to eccentrically placed nuclei and a scant to moderate amount of finely granular to homogeneous eosinophilic cytoplasm. Nuclei are round or slightly indented and mildly anisokaryotic with coarsely clumped chromatin and mainly inconspicuous nucleoli. In 10 HPF there are 4 mitotic figures.

The second population of neoplastic cells consists of several hundred highly pleomorphic cells from 15-150 μm in diameter scattered randomly among the smaller cells described above. The most prominent are giant cells with abundant amphophilic to eosinophilic cytoplasm, from 1 to 10 markedly anisokaryotic nuclei, and bizarre nuclear shapes and arrangements. However, numerous forms of these cells intermediate in size or similar in size to the small round cells described above are present. Larger cells often contain variably-sized, brightly eosinophilic, smudged cytoplasmic vacuoles.



Liver, dog. The liver contains a focal 1cm nodule within the parenchyma. (Photo courtesy of: Diagnostic Services Unit, University of Calgary Veterinary Medicine, Clinical Skills Building, 11877 85 St. NW, Calgary AB T3R 1J3, <http://vet.ucalgary.ca/>)

Throughout remaining (non-nodular) hepatic parenchyma most portal tracts are heavily infiltrated by small round cells similar to those comprising the majority of the nodule described above. Centrilobular sinusoids and central veins are severely congested and centrilobular hepatocytes are atrophied or swollen with foamy cytoplasm (lipid accumulation). Kupffer cells near central veins contain abundant finely granular yellow brown pigment. Multifocally, adjacent centrilobular hepatocytes are outlined by thin, branching green-yellow lines (canalicular cholestasis).

Contributor's Morphologic Diagnoses:

Liver: 1. B cell lymphoma; 2. Megakaryocytic neoplasia

Contributor's Comment: Gross necropsy findings of bilateral irregular renomegaly, multiple pale hepatic nodules, and multifocal abdominal lymphadenomegaly led to a presumptive diagnosis of lymphoma. Histologically, hepatic portal infiltration by sheets of round cells supported this diagnosis. However, in addition to the population of presumed lymphocytes, bizarre giant and blastic cells were seen in solid hepatic



Liver, dog. Subgross examination of a well-demarcated nodular round cell neoplasm. (HE, 4X)

masses, throughout both kidneys and throughout enlarged renal lymph nodes.

IHC was performed on hepatic sections and confirmed a dual population of neoplastic cells in liver masses. The first population of small round cells had strong cytoplasmic immunopositivity for CD20 (fig. 3), a B lymphocyte marker. Cells surrounding portal areas outside the masses were also CD20 positive. The majority of the second population of larger, pleomorphic cells had moderate cytoplasmic immunopositivity for factor VIII-related antigen (fig. 4), supporting a megakaryocytic origin. Scattered among the neoplastic cells were small numbers of CD3-positive T lymphocytes (not shown).

The CD20 IHC results support a diagnosis of B cell lymphoma, a common disease in dogs. However the presence of the additional population of factor VIII-related antigen-positive cells was unusual. Their presence suggested acute megakaryoblastic leukemia (AML M7; AMegL; AML7), an acute myeloid leukemia in which the predominant blast cell is of megakaryocytic lineage. Acute megakaryoblastic leukemia (AML M7) is rare but has been reported in humans, dogs and cats. Among canine acute myeloid

leukemias it is the least common form, and has previously been described in fewer than 20 dogs. It is a rapidly progressive disease involving bone marrow, internal organs, and lymph nodes. Affected dogs exhibit anorexia, progressive weight loss, and occasionally spontaneous epistaxis. Thrombocytopenia and anemia are frequently observed. Neoplastic cells are typically immunopositive for megakaryocytic markers CD61 and factor VIII-related antigen, and the platelet marker platelet glycoprotein IIIA. They may be variably positive for leukocytic markers CD45 and CD18 and the hematopoietic precursor marker CD34, but are negative for lymphocyte, monocyte and granulocyte markers.

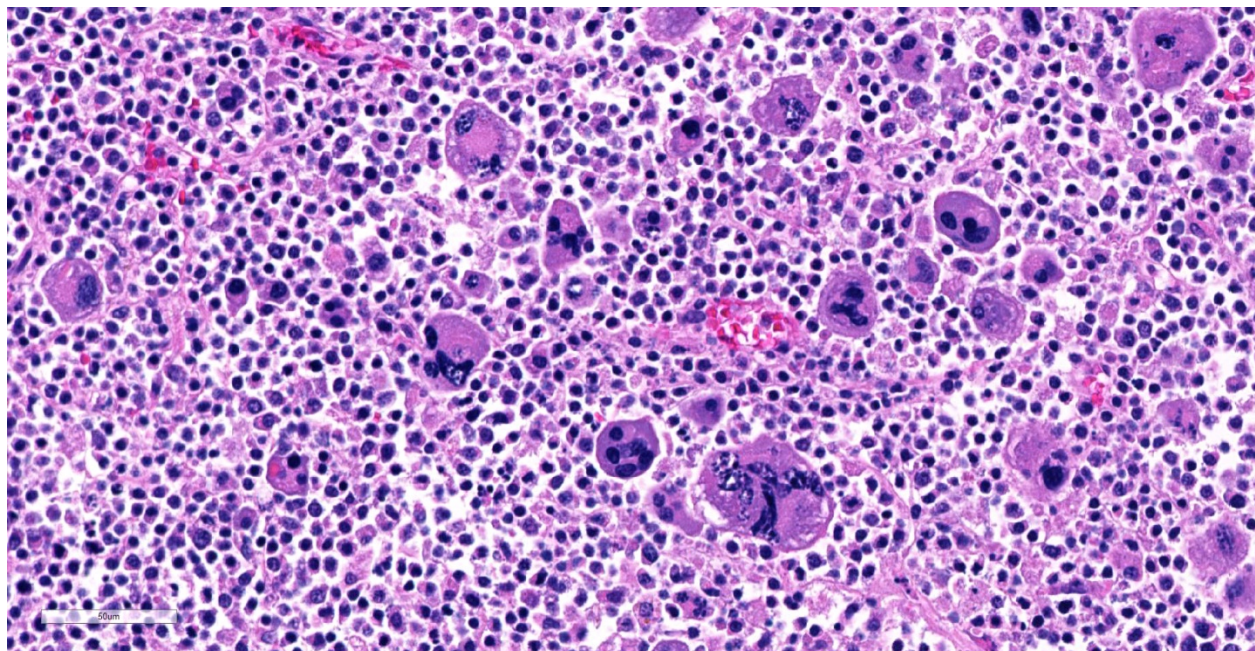
Unfortunately, a potential diagnosis of AML M7 could not be investigated further since neither blood nor bone marrow were available and because financial constraints restricted IHC use. The findings in this case suggest that two forms of hematopoietic neoplasia were present simultaneously and emphasize the need for bone marrow and blood evaluation to achieve a definitive diagnosis.

Contributing Institution:

Diagnostic Services Unit
University of Calgary Veterinary Medicine
Clinical Skills Building
11877 85 St. NW
Calgary AB T3R 1J3
<http://vet.ucalgary.ca/>

JPC Diagnosis: Malignant plasm cell tumor.

JPC Comment: This is an interesting and unique case. The neoplasm in the liver is composed of CD-20 positive B-cells (the immunostaining was confirmed at the JPC) which are the same size or 1.5x the size of an erythrocyte. Neoplastic lymphocytes have a

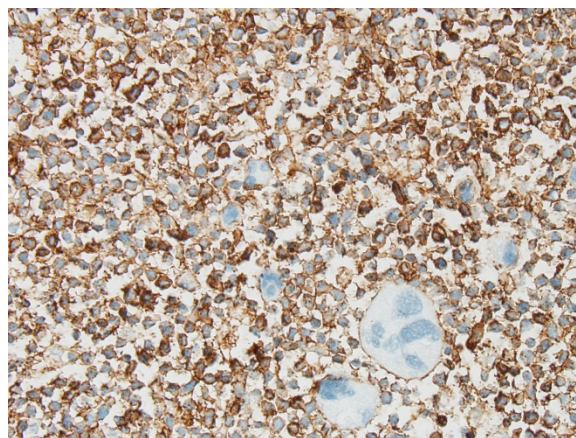


Liver, dog. The neoplasm is composed of two populations – one population of small neoplastic lymphocytes with a low mitotic rate and scattered well-differentiated megakaryocytes. (HE, 400X)

3:1 N/C ratio with a thin rim of non-granulated eosinophilic cytoplasm, and mitotic figures are rare (although preservation is not optimal and made it difficult for attendees to reach consensus on grading this neoplasm.) Nucleoli are not evident in well-preserved cells. Immunostains for CD3, PAX-5 and MUM-1 were negative in this particular population of cells.

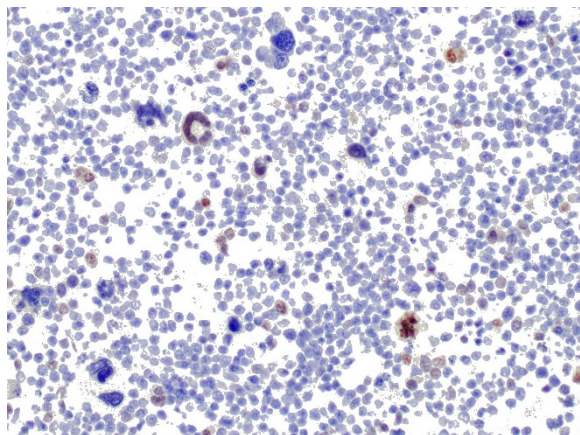
The large pleomorphic cells scattered throughout the neoplasm exhibited strong nuclear staining for MUM-1 run both at the JPC and at UPenn, suggesting that some of the neoplasm cells may be in a late stage of plasma cell differentiation, and coupled with the CD-20 staining of the smaller uninucleate cells that this neoplasm may represent a late stage B cell or malignant plasma cell tumor. This may also explain the non-specific staining of these cells with Factor VIII (as plasma cells are notorious for non-specific immunostaining). This would also help to explain the absence of these atypical cells

outside of the neoplasm (leukemic cells should be in the remainder of the section of liver as well), and the diagnosis of a neoplasm related to myeloma might help to explain the fatal bleeding identified in the clinical history.



Liver, dog. Neoplastic lymphocytes stain strongly immunopositive for CD20. (anti-CD20, 100X). (Photo courtesy of: Diagnostic Services Unit, University of Calgary Veterinary Medicine, Clinical Skills Building, 11877 85 St. NW, Calgary AB T3R 1J3, <http://vet.ucalgary.ca/>)

The small size of the B-cells, lack of prominent nuclei, and low mitotic rate led some conference participants to a diagnosis of mature peripheral B-cell lymphoma /small lymphocytic lymphoma.) B-cell CLL is primarily a neoplasm of the bone marrow which is characterized by marked lymphocytosis (of small mature lymphocytes). The course of these neoplasms is indolent, and tumors may be found in the spleen, liver, and lymph nodes.



Liver, dog. Large pleomorphic cells stain multifocally positive for MUM-1, suggesting plasmacytic differentiation. (anti-MUM-1, 400X)

There is also extensive necrosis and loss of hepatocytes throughout the section in centrilobular and some subcapsular) areas. The precise cause of this change is not evident in the examined slide but is strongly suggestive of hypoxia, perhaps due to terminal shock, anemia (perhaps as a result of marrow infiltration by a neoplasm), or resulting from local vascular impairment as a result of the presence of a neoplasm.

References:

- 1 Colbatzky F, Hermanns W: Acute Megakaryoblastic Leukemia in One Cat and Two Dogs. *Veterinary Pathology* 30: 186-194, 1993
- 2 Comazzi S, Gelain ME, Bonfanti U, Roccabianca P: Acute Megakaryoblastic

Leukemia in Dogs: A Report of Three Cases and Review of the Literature. *Journal of the American Animal Hospital Association* 46: 327-335, 2010

3 Park HM, Doster AR, Tashbaeva RE, Lee YM, Lyoo YS, Lee SJ, Kim HJ, Sur JH: Clinical, histopathological and immunohistochemical findings in a case of megakaryoblastic leukemia in a dog. *Journal of Veterinary Diagnostic Investigation* 18: 287-291, 2006

4 Valli VE, Jacobs RM, Parodi AL, Vernau W, Moore PF: *Histological Classification of Hematopoietic Tumors of Domestic Animals*, 2nd ed. Armed Forces Institute of Pathology in cooperation with the American Registry of Pathology and the World Health Organization Collaborating Center for Worldwide Reference on Comparative Oncology, Washington DC, 2002

5 Vernau W, Moore PF: An immunophenotypic study of canine leukemias and preliminary assessment of clonality by polymerase chain reaction. *Veterinary Immunology and Immunopathology* 69: 145-164, 1999

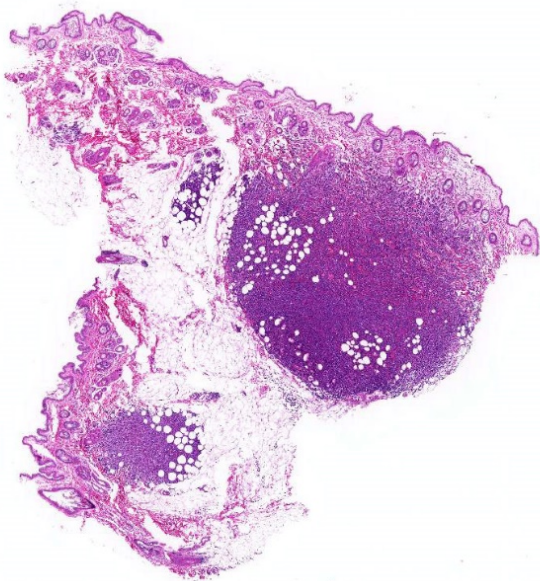
CASE II: 2014910070 (JPC 4066543).

Signalment: 8 year-8 month-old, spayed female, Italian gray hound, dog. (*Canis familiaris*)

History: The dog was presented to the veterinary clinic with skin rashes in inner thigh region. She was treated with antibiotic and antihistamine for a week. A week later, a few millimeters multiple hematomas and papules were observed from inner thigh, abdomen to neck. She was treated with another antibiotic, antiplasmin and steroid, but these lesions were not improved. Three weeks later, a skin in the neck including

papules was biopsied, and submitted to pathological examination.

Gross Pathology: The cut surface of the papule after formalin fixation was brown to dark red.



Haired skin, dog. There are multiple nodular neoplasms within the superficial dermis which extend into the underlying subcutis. (HE, 5X)

Laboratory results: B lymphocyte monoclonality is detected by lymphocyte clonality analysis.

Microscopic Description:

Histologically, a papule is composed of multiple foci. Monomorphic round tumor cells diffusely proliferate in dermis to subcutis of each focus. Tumor cells do not have epitheliotropism. Tumor cells have oval to vesicular nuclei of intermediate-large size and scant to moderate amount of cytoplasm. One small to large nucleolus and finely distributed chromatin contain in the nucleus. Giant and multiple nucleus are occasionally

seen. Mitotic figures are often observed. Mild hemorrhage is seen between tumor cells, and tumor cells frequently engulf red blood cells in the cytoplasm.

Immunohistochemically, almost all tumor cells are positive for CD20, lambda light chains. Multiple myeloma Oncogene 1, weakly positive for CD79a but negative for CD3, Kappa light chains, and Iba-1.

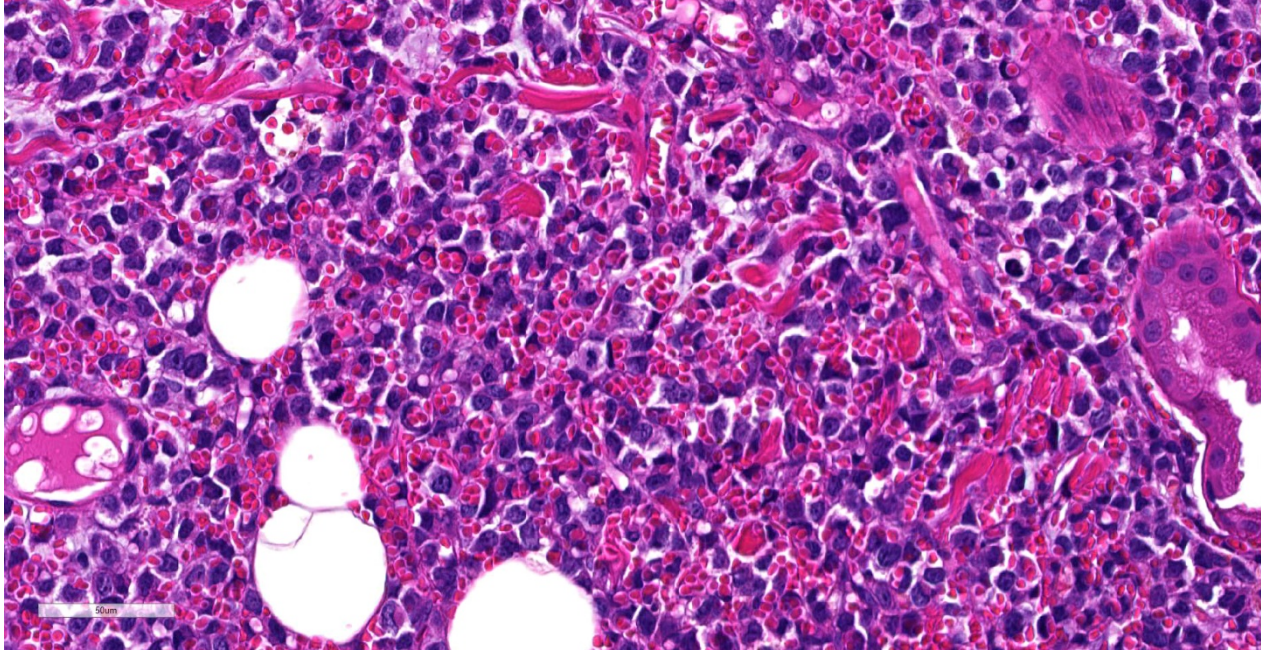
Ultrastructurally, tumor cells have nucleus with heterochromatin clumped under the nuclear membrane. Cytoplasm contain large amount of rough endoplasmic reticulum, but Golgi complex does not develop. Erythrocytes are taken into tumor cell cytoplasm. Primary and secondary lysosomes are often observed in the cytoplasm.

Contributor's Morphologic Diagnoses:

Skin: hemophagocytic cutaneous lymphoma (B cell lymphoma), canine (*Canis familiaris*)

Contributor's Comment: The present case was a round cell tumor with a characteristic of erythrophagocytosis. In animal, erythrophagia was reported most frequently in tumors of histiocytic cell origin^{6,10,14,15,17}. Thus, the primary differential diagnosis was histiocytic sarcoma. However, tumor cells often had scant cytoplasm, and showed no immunohistochemical reactivity for Iba-1 (marker of histiocytic cell).

In animals, erythrophagocytic tumors have been reported several tumors other than histiocytic sarcoma, including angiosarcoma, osteosarcoma, lymphoma, mast cell tumor, multiple myeloma and plasmacytoma^{1-3,12,13,19}.



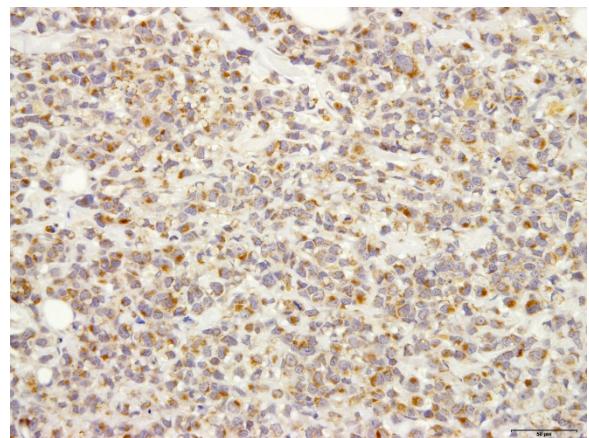
Haired skin, dog. Neoplastic lymphocytes contain one or multiple non-degenerate erythrocytes within their cytoplasm, which often indent or peripheralize the nucleus. Neoplastic cells are four to five times larger than an erythrocyte and have large nuclei with prominent nucleoli. (HE, 400X)

In present case, tumor cells did not have nuclei with a cartwheel appearance and perinuclear halo (clear zone) in cytoplasm - thus, the cellular morphology was not similar to mature plasma cell. However, tumor cells had immunoreaction for CD79a, lambda light chain and MUM-1. MUM-1 was expressed more than 94% of canine plasmacytomas and few canine B cell lymphoma¹⁶. Developed rough endoplasmic reticulum like plasma cell was seen in the cytoplasm by ultrastructural observation. It was suggested tumor cells had partially plasmacytic differentiation.

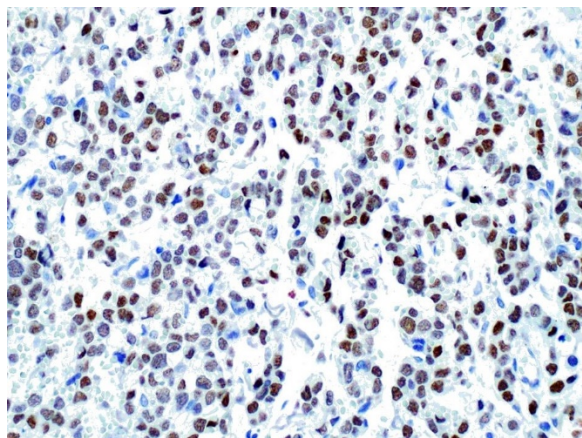
Lymphoma with plasmacytic differentiation include plasmacytoma, lymphoplasmacytic lymphoma and plasmablastic lymphoma. We compared the cellular morphology and immunohistochemical reaction between present case and those tumors with plasmacytic differentiation.

Typical plasmacytomas are composed of small to medium size round cells. The cells are characterized by moderate to slightly abundant cytoplasm with an eosinophilic or amphophilic appearance. Nuclei are round to

oval, small and irregular with single or multiple nucleoli and large, dense chromatin. Mitotic activity was varied but was usually low. The tumor cells are immunoreactive for CD79a, lambda and kappa light chains,



Haired skin, dog. Neoplastic cells are strongly immunopositive for CD-20, a B-cell marker. (Photo courtesy of Laboratory of Pathology, Faculty of Pharmaceutical Sciences, Setsunan University, 45-1 Nagaotohge-cho, Hirakata, Osaka 573-0101, Japan <http://www.setsunan.ac.jp/~p-byori/>)



Haired skin, dog. Neoplastic cells are positive for MUM-1, suggesting plasmacytic differentiation. (anti-MUM-1, 400X)

MUM-1^{7,16,18} and in a few cases are positive for CD20¹⁶.

Lymphoplasmacytic lymphoma is composed of small lymphocytes of a plasmacytoid type. The cells have characteristics of chronic lymphocyte lymphoma or lymphocytic lymphoma of intermediate type. The cells have small (slightly larger than erythrocyte) round nuclei; numerous small chromocenters, absent or small nucleoli and slight larger than scant cytoplasm. Rare immunoblasts are often present. The mitoses were very low. The tumor cells were immunoreactive for CD79a^{9,18}.

Plasmablastic lymphoma is a variant of diffuse large B-cell lymphoma, characterized by morphology and immunohistochemical criteria of plasmacytic differentiation. The cells are round or oval, of medium to large size with immunoblastic/centroblastic morphologic features or classic "plasmablastic" morphologic features, with scant to abundant cytoplasm, and a prominent central nucleolus or multiple smaller nuclei with chromatin clumped under the nuclear membrane. The mitoses were frequent. The cells do not express B cell makers such as CD20 and CD79a, but express of plasmacyte markers as MUM-1^{4,8}.

The present case has a cellular morphology similar to plasmablastic lymphoma, but

differed from it by immunohistochemical features. Thus, the present case was diagnosed as B cell lymphoma.

Canine cutaneous lymphoma is reported in about 3-8% of all canine lymphoma, and is histologically divided into epitheliotropic and non-epitheliotropic lymphoma^{5,7}. The majority of canine cutaneous non-epitheliotropic lymphomas are of T cell origin, B- cell origin is rare^{5,7}.

Animals with erythrophagocytic neoplasms in the spleen and liver often have non-regenerative anemia^{6,10-12,15,17}. In the present case, as the affected animal did not show obvious anemia at the time of a biopsy, it was suggested that our lymphoma may be localized in the skin.

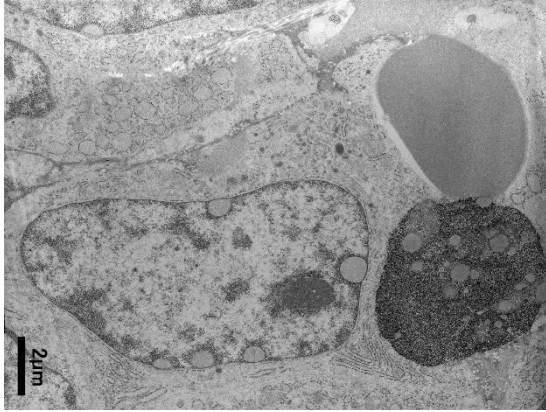
Contributing Institution:

Laboratory of Pathology, Faculty of Pharmaceutical Sciences, Setsunan University,
45-1 Nagaotohge-cho, Hirakata, Osaka 573-0101, Japan

<http://www.setsunan.ac.jp/~p-byori/>

JPC Diagnosis: Haired skin: Plasmablastic lymphoma, large cell, high grade, plasmablastic, with marked erythrophagocytosis

JPC Comment: Conference participants agreed that the morphology of this unique neoplasm is that of a large cell (neoplastic cells exceed 2x that of an erythrocyte), high grade neoplasm. Identification of the cells on HE is difficult, especially given the degree of erythrocytosis exhibited by these cells. Conference participants identify significant plasmacytic differentiation among the neoplastic cells, although mature plasma cells were scattered throughout the neoplasm, as evidenced both on the HE stain and several immunostains run at the JPC (plasma cells commonly pick up immunostains in a non-



Haired skin, dog. Electron micrograph of a neoplastic B cell with two ingested erythrocytes within its cytoplasm. The one at left appears viable; significant degenerative changes including condensation occur within the one on the right. (Photo courtesy of Laboratory of Pathology, Faculty of Pharmaceutical Sciences, Setsunan University, 45-1 Nagaotohge-cho, Hirakata, Osaka 573-0101, Japan <http://www.setsunan.ac.jp/~p-byori/>)

specific fashion to frustrate pathologists.)

The CD-20 immunostain was repeated at the JPC and neoplastic cells was strongly positive; and a MUM-1 stain performed at UPenn was also positive. An IBA-1 stain demonstrated numerous infiltrating histiocytes. IBA-1 demonstrated some histiocytes within the neoplasm, but not a large component. Based on the immunohistochemical findings in this case, the moderator assessed this neoplasm as a likely B-cell neoplasm with early plasmacytic differentiation.

While we have seen cutaneous B-cell lymphoma in the skin numerous times, the erythrophagocytosis seen in this case is unique and remarkable. A Pubmed review of erythrophagocytic forms of lymphoma noted several cases of T-cell neoplasm exhibiting erythrophagocytosis in both humans and animals, this case appears unique for its B-cell erythrophagocytic activity. As B-cells do not have intracellular machinery to break down erythrocytes into hemosiderin and

lipofuscin like macrophages, this tumor is especially striking in the presence of apparently viable erythrocytes in neoplastic cells and a lack of hemosiderin pigment.

The moderator commented that while the presence of erythrocytes within neoplastic cells is unusual, it is prudent to believe in the conventional wisdom that neoplastic cells of any lineage may engulf erythrocytes if they desire to do so.

References:

- 1 Barger AM, Skowronski MC, MacNeill AL. Cytologic identification of erythrophagocytic neoplasms in dogs. *Vet Clin Pathol.* 2012;41:587-589.
- 2 Bertazzolo W, Dell'Orco M, Bonfanti U, et al. Canine angiosarcoma: cytologic, histologic, and immunohistochemical correlations. *Vet Clin Pathol.* 2005;34:28-34.
- 3 Carter JE, Tarigo JL, Vernau W, Cecere TE, Hovis RL, Suter SE: Erythrophagocytic low-grade extranodal T-cell lymphoma in a cat. *Vet Clin Pathol.* 2008;37:416-421.
- 4 Castillo JJ, Reagan JL. Plasmablastic lymphoma: a systematic review. *Scientific World Journal.* 2011; 11:687-696.
- 5 Day MJ. Immunophenotypic characterization of cutaneous lymphoid neoplasia in the dog and cat. *J Comp Pathol.* 1995;112:79-96.
- 6 Friedrichs KR, Young KM. Histiocytic sarcoma of macrophage origin in a cat: case report with a literature review of feline histiocytic malignancies and comparison with canine hemophagocytic histiocytic sarcoma. *Vet Clin Pathol.* 2008;37:121-128.
- 7 Gross TL IP, Walder EJ, Affolter VK. Lymphocytic tumors. In: *Skin diseases of the dog and cat.* 2nd ed. Oxford, UK: Blackwell; 2005:866-893.
- 8 Hsi ED, Lorsbach RB, Fend F, Dogan A: Plasmablastic lymphoma and related disorders. *Am J Clin Pathol.* 2011;136:183-

- 194.
- 9 Jaffe VE, Harris, N.L, Stein, H, Varidiman, J. W: Pathology & Genetic Tumor of Hematopoietic and Lymphoid Tissues. In: *World Health Organization Classification of tumours*. Lyon, France: 2001:120-134,171-174.
- 10 Kraje AC, Patton CS, Edwards DF. Malignant histiocytosis in 3 cats. *J Vet Intern Med*. 2001;15:252-256.
- 11 Ledieu D, Palazzi X, Marchal T, Fournel-Fleury C. Acute megakaryoblastic leukemia with erythrophagocytosis and thrombosis in a dog. *Vet Clin Pathol*. 2005;34:52-56.
- 12 Madewell BR, Gunn C, Gribble DH: Mast cell phagocytosis of red blood cells in a cat. *Vet Pathol*. 1983;20:638-640.
- 13 Marks SL, Moore PF, Taylor DW, Munn RJ. Nonsecretory multiple myeloma in a dog: immunohistologic and ultrastructural observations. *J Vet Intern Med*. 1995;9:50-54.
- 14 Matsuda K, Nomoto H, Kawamura Y, Someya Y, Koiwa M, Taniyama H. Hemophagocytic histiocytic sarcoma in a Japanese black cow. *Vet Pathol*. 2010;47:339-342.
- 15 Moore PF, Affolter VK, Vernau W. Canine hemophagocytic histiocytic sarcoma: a proliferative disorder of CD11d+ macrophages. *Vet Pathol*. 2006;43:632-645.
- 16 Ramos-Vara JA, Miller MA, Valli VE. Immunohistochemical detection of multiple myeloma 1/interferon regulatory factor 4 (MUM1/IRF-4) in canine plasmacytoma: comparison with CD79a and CD20. *Vet Pathol*. 2007;44:875-884.
- 17 Rossi S, Gelain ME, Comazzi S. Disseminated histiocytic sarcoma with peripheral blood involvement in a Bernese Mountain dog. *Vet Clin Pathol*. 2009;38:126-130.
- 18 Valli VE, Jacobs RM, Parodi, AL, Vernau W, Moore, P.F. *Hematopoietic Tumor of Domestic Animals*. vol. VIII. Washington DC, USA: World Health Organization

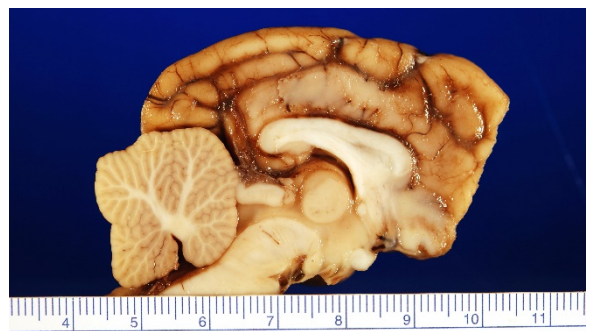
International Histological Classification of tumors of domestic animals; 2002:28-38.

19 Yearley JH, Stanton C, Olivry T, Dean GA. Phagocytic plasmacytoma in a dog. *Vet Clin Pathol*. 2007;36:293-296.

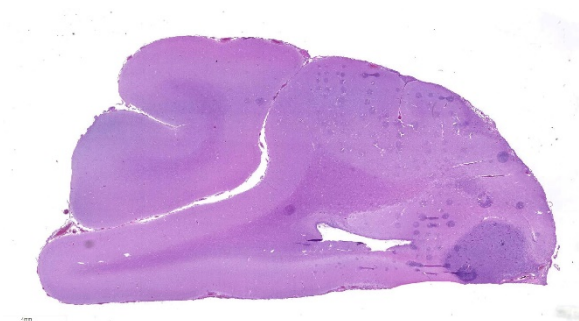
CASE III: 66619 (JPC 4066455).

Signalment: 12 year old, Male Neutered, Italian Greyhound, *Canis lupus familiaris*, Canine

History: One-week history of anxiety, nervousness, intermittent anorexia, and excessive vocalization. The vocalization was especially pronounced with regards to interactions involving the head or neck. The patient was referred to a neurologist for examination and further workup. On the morning of neurological consultation, an episode of ataxia, with a partial seizure occurred, followed by several hours of mental disorientation, the inability to sit up, and repetitive paddling activities impacting the entire left side of the body. When presented to the neurologist, the dog exhibited postural deficits on the right side.



Brain, dog: A focal 1.6x1.0 cm mass is present in the frontal lobe abutting the corpus callosum. (Photo courtesy of: Department of Molecular and Comparative Pathobiology, Johns Hopkins University, 733 N. Broadway, Suite 811, Baltimore, MD 21205, <http://www.hopkinsmedicine.org/mcp/index.html>)



Cerebral cortex, dog: A focal nodular well-demarcated neoplasm is present in the frontal lobe. (HE 4X)

Magnetic resonance imaging (MRI) showed a multifocal disease process impacting the falx cerebri rostral to the lateral ventricles and the ventrolateral right cerebrum adjacent to the meningeal surface. The ventrolateral lesion was approximately 1 cm in diameter with the falx cerebral lesions being smaller in size. Lesions coalesced at the cribriform plate.

Gross Pathology: Specimens submitted for histopathologic examination included brain (in entirety), nasal turbinate, lung, liver, spleen, and kidney. Gross examination of the brain revealed a focal extensive, 1.6 cm by 1 cm tan, firm, non-encapsulated, invasive mass in the gray matter of the frontal lobe abutting the corpus callosum, centered with an approximate midline – midline right orientation. Multifocally within the mass there are areas of malacia with a tan/red coloration (necrosis). The remainder of the submitted tissues are grossly unremarkable.

Laboratory results: NA

Microscopic Description:

Located in the grey matter of the frontal lobe is a non-encapsulated, poorly demarcated, multicentric, invasive mass of neoplastic round cells arranged in sheets and individual cells and supported on a pre-existing fibrovascular stroma. Neoplastic cells are round to oval with moderate eosinophilic finely vacuolated cytoplasm. Nuclei are

generally eccentrically located and round to reniform with coarsely stippled chromatin and up to three prominent nucleoli. There is marked anisocytosis and anisokaryosis, and mitoses number 1-3 per 40x field. Neoplastic cells are often multinucleate, with up to eight nuclei per cell. Neoplastic cells also frequently exhibit erythrophagocytosis. Throughout the mass, there are multifocally moderate numbers of infiltrating lymphocytes and plasma cells, and multifocal areas of necrosis. Multifocally, neoplastic cells invade and expand the meninges. No evidence of vascular or lymphatic invasion is appreciated.

Immunohistochemistry:

Kappa and Lambda Light Chain - Negative

CD3 – Negative

CD20 – Negative

GFAP – Negative

CD163 – Neoplastic cells exhibit variable cytoplasmic and membranous immunoreactivity

Iba1 – Neoplastic cells exhibit strong diffuse cytoplasmic immunoreactivity

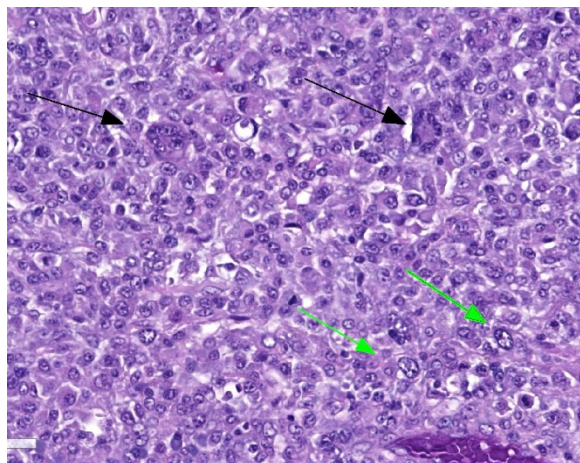
Contributor's Morphologic Diagnoses:

Brain (frontal lobe), primary malignant histiocytosis

Contributor's Comment: Histologically, the mass in this dog's brain consisted of aggressive and highly invasive round cells with multicentric extension into the meninges. On immunohistochemistry, neoplastic cells were negative for T, B, and glial cell markers and positive for macrophage/monocyte markers (Iba-1, CD-163). Overall, immunohistochemistry results along with histopathological morphology are consistent with the diagnosis of malignant histiocytosis.

Histiocytic proliferative disorders can be subdivided into local and disseminated

forms. Localized forms are referred to as histiocytic sarcomas and are common primary tumors of the liver, spleen, tongue, and stomach wall in the canine patient.⁷ Malignant histiocytosis is the term most commonly used to describe disseminated neoplastic cells of histiocytic origin. The term “diffuse histiocytic sarcoma” has also been used to designate a localized histiocytic sarcoma that has become systemic. Additionally, benign aspects of histiocytic proliferative disorders include the cutaneous histiocytoma and cutaneous and systemic histiocytosis.



Cerebral cortex, dog: The neoplasm is composed of pleomorphic round cells. Multinucleated neoplastic cells (black arrows) and karyomegalic neoplastic cells, as well as mitotic figures are present in this field. (HE 400X)

In the canine patient, malignant histiocytosis most commonly occurs in middle age to older male dogs with increased incidence in the Bernese Mountain Dog, Rottweiler, Golden Retriever, and Labrador Retriever.⁵ Overall, the spleen and liver are the most commonly impacted tissues, but other organs including the lungs, lymph nodes, bone marrow, and central nervous system can also be impacted. Primary cases involving the brain are considered rare, with an overall poor to grave prognosis due to the invasive/aggressive nature of the neoplasia.⁷

As this case documents, definitive diagnosis of histiocytic tumors can be challenging with histopathology alone, and the use of immunohistochemistry can be advantageous. Overall, malignant histiocytic tumor histopathology is characterized by sheets of highly pleomorphic cells that exhibit severe atypia along with abundant mitotic figures. Noted throughout the neoplastic cells often are multinucleated giant cells, erythrophagocytosis, and scattered populations of lymphocytes and plasma cells. Malignant histiocytic tumors exhibit positive staining with CD1c, CD11c, CD45, lysozyme, CD18, and Iba1, and do not exhibit stain uptake for B cell, T cell, and glial cell markers.^{4,7} Iba1 is a 17-kDa EF hand protein that is specifically expressed in microglia and is not reactive with neurons or astrocytes. Iba1 has been recently recognized as a macrophage marker, expressed by all subpopulations of cells of the monocyte/macrophage lineage with efficacious used in the characterization of canine and feline histiocytic tumors.⁴

Differentials for this case included: a tumor of neuroglial origin, lymphoma, plasma cell tumor, and granulomatous disease.

Contributing Institution:

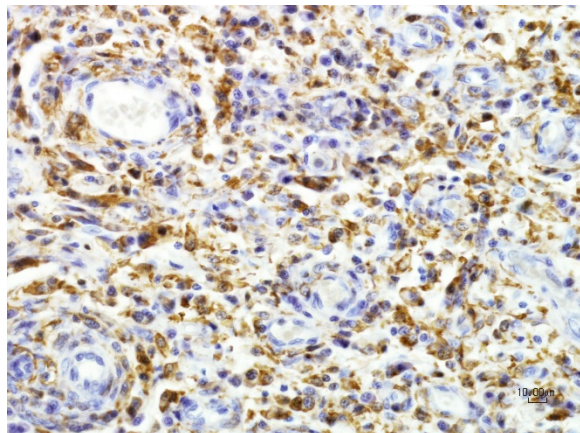
<http://www.hopkinsmedicine.org/mcp/index.html>

JPC Diagnosis: Cerebral cortex:
Histiocytic sarcoma

JPC Comment: The contributor has done an excellent job describing this rare entity in the dog. Disseminated histiocytic sarcomas (also referred to malignant histiocytosis) is not an uncommon neoplasm in the dog, but primary lesions in a single organ are.

A diagnosis of primary intracerebral histiocytic sarcoma not only requires immunophenotyping to establish the histiocytic lineage of the neoplastic cells, but

also to establish that no other similar lesions are present throughout the other tissues of the body. Recent studies in dogs have identified abnormalities in certain tumor suppressor genes (RB1, PTEN, and CDKN2A/B).³



Cerebral cortex, dog: Neoplastic cells are strongly immunopositive for IBA-1, a histiocytic marker. (anti-IBA-1 400X) (Photo courtesy of: Department of Molecular and Comparative Pathobiology, Johns Hopkins University, 733 N. Broadway, Suite 811, Baltimore, MD 21205, <http://www.hopkinsmedicine.org/mcp/index.html>)

No gender or age predispositions have been identified for the development of primary intracerebral histiocytic sarcoma, and Pembroke Welsh Corgis have been identified as a predisposed breed.³

This particular case demonstrates the traditional appearance of a primary CNS histiocytic sarcoma – a single whitish subdural lesion within the cerebrum with a broad meningeal base. Secondary or metastatic lesions are usually multiple, and often arise within the meninges.² The subdural or meningeal location of these tumors may reflect the restriction of dendritic cells (the presumptive cell of origin for this neoplasm) to the meninges and choroid plexus.²

The moderator reviewed the maturation of cells of the macrophage/monocyte lineage as

well as common manifestations of histiocytic diseases in dogs and cats including canine cutaneous histiocytosis, reactive and systemic histiocytosis, feline progressive pulmonary histiocytosis, histiocytic sarcoma and the very rare dendritic cell leukemia.

References:

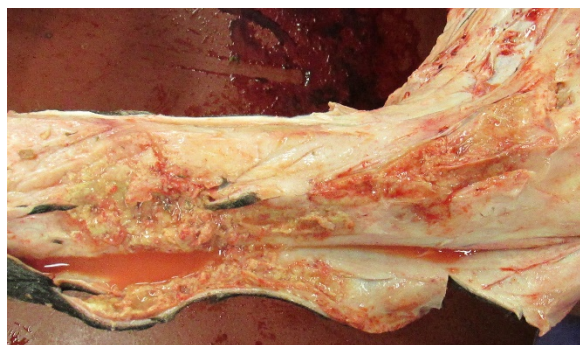
1. Chandra AM, Ginn PE. Primary malignant histiocytosis of the brain in a dog. *J Comp Pathol.* 1999;121:77–82.
2. Higgins RJ, Bollen AW, Dickinson PJ, Siso-Llonch S. Tumors of the nervous system. *In: Meuten DJ, ed. Tumors in Domestic Animals.* Ames, IA, Wiley Blackwell, 2017, pp. 877, 878.
3. Moore, PF. A review of histiocytic diseases of dogs and cats. *Vet Pathol* 2014;51:167-184.
4. Pierezan F, Mansell J, Ambrus A and Rodrigues Hoffmann A. Immunohistochemical Expression of Ionized Calcium Binding Adapter Molecule 1 in Cutaneous Histiocytic Proliferative, Neoplastic and Inflammatory Disorders of Dogs and Cats. *J. Comp. Pathol.* 2014, Vol. 151
5. Thio T, Hilbe M, Grest P and Pospischil A. Malignant Histiocytosis of the Brain in Three Dogs. *J. Comp. Path.* 2006, Vol. 134, 241–244
6. Uchida K, Morozumi M, Yamaguchi R, and Tateyama S. Diffuse Leptomeningeal Malignant Histiocytosis in the Brain and Spinal Cord of a Tibetan Terrier. *Vet Pathol* 38:219–222 (2001)
7. Zimmerman K, Almy F, Carter L, Higgins M, Rossmeisl J, Inzana K, Duncan R. Cerebrospinal fluid from a 10-year-old dog with a single seizure episode. *Veterinary*

CASE IV: UMC172 (JPC 4099791).

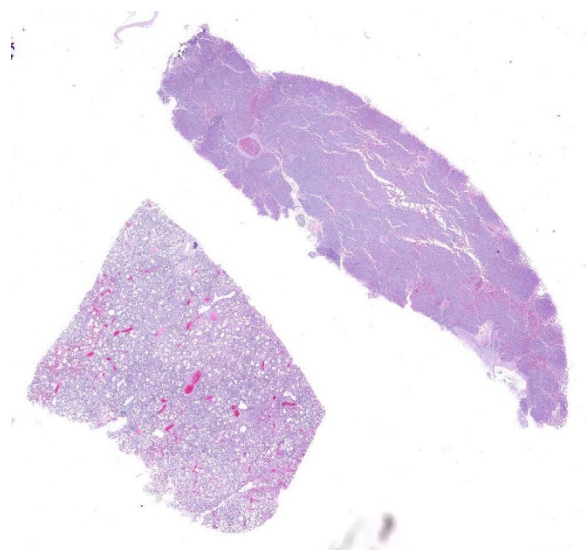
Signalment: 21 year old Thoroughbred gelding (*Equus caballus*)

History: This 21 year old Thoroughbred gelding was euthanized and submitted for necropsy due to a severe, chronic, non-healing wound on its right hind leg.

Gross Pathology: A 530kg body weight, aged adult, bay gelding, in moderate body condition (4/9 body condition score) is necropsied. The medial right hind limb is diffusely swollen from the inguinal region down to the level of the fetlock. A punctate fistula is noted on the medially, slightly below the fetlock joint. Considerable dense fibrous tissue is evident in the subcutis of the tibia and metatarsals. Roughly 100 ml watery translucent yellow orange fluid pools in the subcutis during dissection. Extending from the medial hock to the medial fetlock is soft, tan, friable tissue that oozes fluid. The process does not affect the bone, itself tendon sheaths or the joint fluids of the hock, fetlock or pastern. Other gross lesions include ulcers



Right rear leg, horse: The right front leg, when incised, demonstrates the extension of the chronic pyogranulomatous cellulitis. (Photo courtesy of: Veterinary Medical Diagnostic Lab and Department of Veterinary Pathobiology . <http://vmdl.missouri.edu/> <http://vpbio.missouri.edu/>)



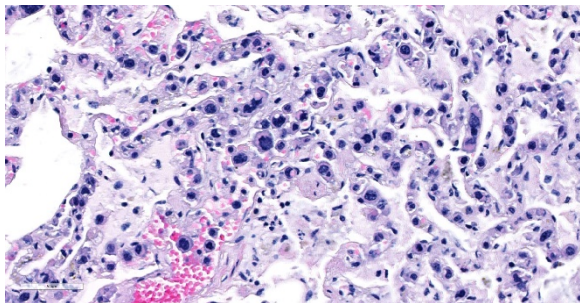
Liver, lung, horse: Sections of liver and lung are submitted for examination. (HE, 5X)

in the squamous portion of the stomach, and a large free-floating abdominal blood clot, thought to be a result of trauma sustained during euthanasia. The abnormalities in the organs submitted to the conference were unexpected.

Laboratory results: NA

Microscopic Description:

Large and small pulmonary vessels are congested, and there are contained numerous large nucleated cells located in alveolar capillaries. However, the cells are much less frequently present in larger arteries or veins. The cells have a defined outline and are polygonal in shape. They have large (even in relationship to cell size) polyhedral to reniform nuclei, with condensed chromatin. Occasional cells are multinucleate. Erythrophagia is common. Rare intravascular mitoses are found. In the liver, similar cells distend hepatic sinusoids, with atrophy of hepatic cords and degeneration. As in the lung, they have distinct cytoplasmic borders, large hyperchromatic nuclei and are erythrophagocytic. Additional similar



Lung, horse. Alveolar capillaries contain numerous large round cells with indented, often hyperchromatic nuclei. (HE, 400X)

cellular infiltrates were found in the spleen and in vessels but not in the parenchyma of the bone marrow.

Immunohistochemistry identified the cells as CD3-positive. Positively staining cells have a linear arrangement in the marrow due to their intravascular location, which is not readily appreciated in the photo. CD20 staining identified a few small lymphocytes in the marrow itself. Numerous Iba-1 positive cells were present and appeared to be parenchymal, but co-localization of this marker with CD3 was not tested.

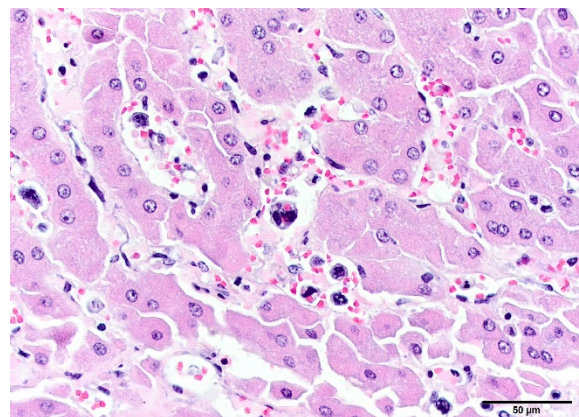
Contributor's Morphologic Diagnoses:

Lung and liver: Intravascular (angiotrophic) lymphoma, multiple organs

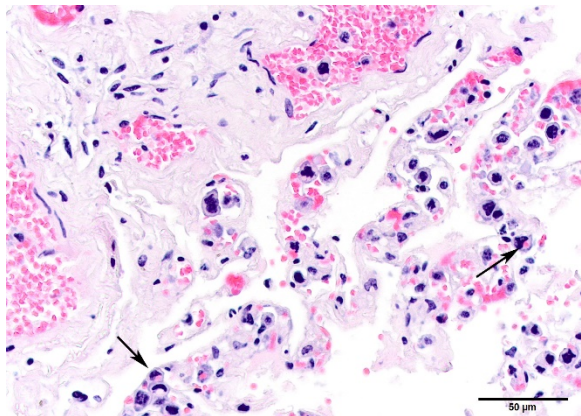
Contributor's Comment: Finding an intravascular lymphoma was entirely unexpected in this horse, which had been euthanized for intractable chronic cellulitis of one rear leg. Lymphoma is the most common malignant neoplasm of the hematopoietic system of horses, with the multicentric form being most common. B cell and T cell-rich B cell neoplasms are most common.¹ Angiotrophic or intravascular lymphoma, also call lymphoid granulomatosis, is one of the least common types of lymphoma in any species. Different types of lymphoma are

now considered specific diseases rather than a single entity.

Intravascular lymphoma is a rare disease and may be of B cell, T cell, or NK cell origin, in order of increasing rareness in people.^{2,4} Neoplastic cells are found only in small and medium-sized vessels, and it has been speculated that they cannot interact with the vascular wall to exit the circulation.² In people, especially in the western hemisphere, most cases are large B cell lymphomas. They are often difficult to diagnose hematologically. In Asian countries, the T cell phenotype is more common.⁴ T cell tumors have been associated with HIV infection.² Patients with intravascular lymphoma commonly present with fever, and fever due to this neoplasm might have been attributed to the leg infection in this horse. Hemophagia is very common, although in the past it had been attributed to red cell consumption macrophages in the tumor rather than tumor cells. No antemortem hematologic data was available for this patient. In our case, it is clear that the neoplastic cells are engulfing red cells. However, double immunolabeling was not done, and the possibility remains that this lymphoma could express both markers. Intravascular lymphoma cells typically reside



Liver, horse: Similar neoplastic cells are present within liver sinusoids and also exhibit erythrophagocytic activity. (Photo courtesy of: Veterinary Medical Diagnostic Lab and Department of Veterinary Pathobiology. <http://vmdl.missouri.edu/>)



Lung horse: Intravascular neoplastic lymphocytes occasionally exhibit erythrophagocytosis (arrows). (Photo courtesy of: Veterinary Medical Diagnostic Lab and Department of Veterinary Pathobiology. <http://vmdl.missouri.edu/>)

in small arteries veins and capillaries instead of large vessels;⁶ this characteristic was present in the horse. Intravascular or angiotropic lymphoma has been called by others a “homeless lymphoma” and apparently lacks the ability to exit the vasculature. It is thought that lack of β -integrin or ICAM homing receptor may explain the inability of these cells to exit the intravascular space.

This neoplasm has a short list of differential diagnoses, includes histiocytic sarcoma/leukemia, lymphoid leukemia and intravascular lymphoma. Intravascular lymphoma has been described in an Australian horse that presented with anemia due to hemophagic syndrome.⁴ Participants in this case were split between a diagnosis of leukemia or intravascular lymphoma, both of which are viable diagnoses in the absence of bloodwork or the ability to evaluate peripheral blood or bone marrow specimens. The moderator brought up an interesting clinical aspect of intravascular lymphomas in animals, as that peripheral blood smears of intravascular lymphoma are often devoid of neoplastic cells, while leukemias will show a

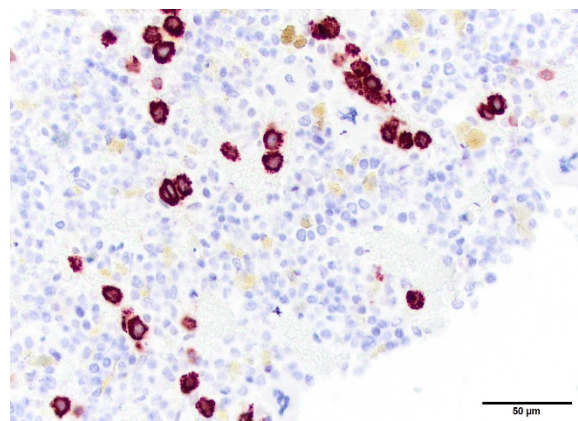
lymphocytosis as well as abnormal cells on a peripheral blood draw. Attendees also commented on the relative paucity of neoplastic cells in this particular case, while previous cases that they had seen (albeit all in dogs), contained numerous circulating neoplastic cells which often filled vessels in multiple organs. This may simply be a species difference.

The consensus of the participants is that the JPC diagnosis of “intravascular lymphoma with erythrophagocytosis” would be most appropriate in this case, as the poor preservation of the lung section as well as the pleomorphic nature of the cells precludes a more specific diagnosis in this case without the use of immunohistochemical markers.

Contributing Institution:

Veterinary Medical Diagnostic Lab and Department of Veterinary Pathobiology
<http://vmdl.missouri.edu/>,
<http://vpbio.missouri.edu/>

JPC Diagnosis: Lung, liver: Intravascular lymphoma, with erythrophagocytosis.



Bone marrow: CD3 staining of tumor cells. The linear arrangement is a result of intravascular localization. (Photo courtesy of: Veterinary Medical Diagnostic Lab and Department of Veterinary Pathobiology. <http://vmdl.missouri.edu/>)

JPC Comment: The contributor has supplied an excellent writeup of a unique case. Based solely on the morphology of the pleomorphic lymphocytes within the sinusoids and alveolar capillaries and their unfamiliarity with the syndrome in the horse, conference attendees preferred a diagnosis of intravascular lymphoma (IVL) until phenotyping information became available as the case was discussed.

Intravascular lymphoma is a rare entity in all species including humans. In humans, most cases of angiotropic are of B-cell origin. In the dog, in which the majority of this rare neoplasm has been reported, it is usually of T-cell origin. A previous case of cerebral intravascular lymphoma of presumptive T-cell origin was presented in WSC 2013-2014, Conference 6, case 2; dogs are also predisposed to develop this neoplasm within the nervous system.⁵

In the single previously reported case of IVL in a mare, antemortem diagnosis was not made, a common finding in IVL likely resulting of the variable involvement of somewhat random organs often seen in this condition. In that report, a mare with a viable 8-month fetus rapidly developed extravascular hemolysis and regenerative anemia as a result of erythrophagocytosis by an activated reticuloendothelial system (hemophagocytic syndrome), rather than by neoplastic cells as seen in this case.

A possible reason for the intravascular nature of the neoplastic cells comes from human cases, in which neoplastic B cells have demonstrated deficiencies in β_1 - (CD29) or β_2 -integrin (CD18) deficiencies. β -integrins are important in the leukocyte adhesion cascade, enabling leukocytes to exit blood vessels and migrate through tissue in order to participate in inflammation. The lack of these molecules may render neoplastic

lymphocytes unable to exit vessels, resulting in high numbers within the vasculature.⁵

References:

1. Valli VEO, Kiupel M, Bienzle D. Hematopoietic System. In Maxie G, ed. *Jubb, Kennedy, and Palmer's Pathology of Domestic Animals Vol 3*, 6th ed. Elsevier, Inc. St. Louis; 2016:237-238.
2. Ponzoni M, Ferreri AJM. Intravascular lymphoma: a neoplasm of "homeless lymphocytes. *Hematol Oncol*. 2006;**24**:105-112.
3. Raidal SL, Clatk, P, Raidal SP. Angiotropic T-cell lymphoma as a cause of regenerative anemia in a horse. *J Vet Intern Med*. 2006;**20**:1009-1013.
4. Sukpanichnant S, Visuthisakchai S. Intravascular lymphomatosis: a study of 20 cases in Thailand and review of the literature. *Clinical lymphoma & Myeloma*. 2006; **6**(4):319-328.
5. WSC 2013-2014, Conference 6, Case 2; http://www.askjpc.org/wsc/wsc_showcase4.php?id=djZ2eEQwNDZoc1NZZUNDTXB5R3IUZz09
6. Yao X, Sadd A, Chitambar CR. Intravascular B-cell lymphoma, and exclusively small vessel disease? Case report and review of the literature. *Leuk Res*. 2010;**34**:275-77.

Self-Assessment - WSC 2018-2019 Conference 23

1. Megakaryocytes will stain positively for which of the following markers?
 - a. CD20
 - b. MUM-1
 - c. Lysozyme
 - d. Factor VIII related antigen

2. In which of the following neoplasms is erythrophagocytosis most commonly seen?
 - a. T-cell lymphoma
 - b. B-cell lymphoma
 - c. Histiocytic sarcoma
 - d. Mast cell tumor

3. Histiocytic sarcoma will stain positively with which of the following Immunostains?
 - a. IBA-1
 - b. CD3
 - c. GFAP
 - d. CD79

4. Most cases of intravascular lymphoma are of what type in the dog?
 - a. T-cell
 - b. B-cell
 - c. NK cell
 - d. Large granular leukocytes

5. Why are lymphocytes confined to the vasculature in intravascular lymphoma?
 - a. Lack of critical leukocyte adhesion molecules
 - b. Their large size
 - c. Inappropriate cluster differentiation molecules
 - d. Lack of nerve

Please email your completed assessment to Ms. Jessica Gold at Jessica.d.gold2.ctr@mail.mil for grading. Passing score is 80%. This program (RACE program number) is approved by the AAVSB RACE to offer a total of 0.5 CE Credits, with a maximum of 12.5 CE Credits being available to any individual Veterinary Medical Professionals for the 2017-2018 Wednesday Slide Conference. This RACE approval is for the subject matter categories of: SCIENTIFIC using the delivery method of NON-INTERACTIVE DISTANCE. This approval is valid in jurisdictions which recognize AAVSB RACE; however, participants are responsible for ascertaining each board's CE requirements. RACE does not "accredit", "endorse" or "certify" any program or person, nor does RACE approval validate the content of the program.

Please email your completed assessment to Ms. Jessica Gold at Jessica.d.gold2.ctr@mail.mil for grading. Passing score is 80%. This program (RACE program number) is approved by the AAVSB RACE to offer a total of 0.5 CE Credits, with a maximum of 12.5 CE Credits being available to any individual Veterinary Medical Professionals for the 2017-2018 Wednesday Slide Conference. This RACE approval is for the subject matter categories of: SCIENTIFIC using the delivery method of NON-INTERACTIVE DISTANCE. This approval is valid in jurisdictions which recognize AAVSB RACE; however, participants are responsible for ascertaining each board's CE requirements. RACE does not "accredit", "endorse" or "certify" any program or person, nor does RACE approval validate the content of the program.

Joint Pathology Center
Veterinary Pathology Services



WEDNESDAY SLIDE CONFERENCE 2018-2019

Conference 24

10 April 2019

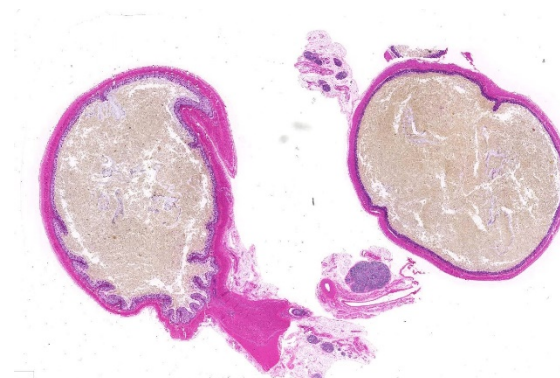
Conference Moderator:

Julie Engiles, BA, VMD, DACVP
Associate Professor, Anatomic Pathology
Section Head – Avian and Mammalian Pathology
Univ. of Pennsylvania School of Veterinary Medicine

CASE I: W837-12 (JPC 4088206).

Signalment 1 day old, female, Quarterhorse, equine (*Equus caballus*)

History: The foal was presented for development of colic several hours after birth. The foal was white with small areas of grey/black coloration on the tail base, lip and ear; the mare had a solid bay coat with a small area of white flecking on the left shoulder and the stallion was paint. The foal was suckling but passage of meconium was not observed. Reduced gastrointestinal sounds were noted on auscultation, but the examination was otherwise unremarkable. No meconium was palpated within the rectum. A moderate amount of intestinal gas was noted on abdominal radiographs. The colic failed to resolve with supportive treatment and the abdomen became progressive distended and tympanic over the next 12 hours. Due to continued deterioration, the foal was



Colon, day-old foal. The colonic lumen is distended with meconium and the wall appears diffusely and transmurally thinned. It is unclear if the distention is due to dilation proximal to a more affected segment). (HE, 4X)

ethanized and submitted for post-mortem examination.

Gross Pathology: The rectum and small colon appeared to be diffusely small and pale. The large colon was filled with meconium and also appeared to be segmentally mildly stenotic along the right dorsal section, though the entire gastrointestinal tract was patent.

The small intestine was distended with gas and liquid meconium distally, while the stomach and proximal duodenum contained ingested milk. All other body systems were unremarkable.

Laboratory results: NA

Microscopic Description:

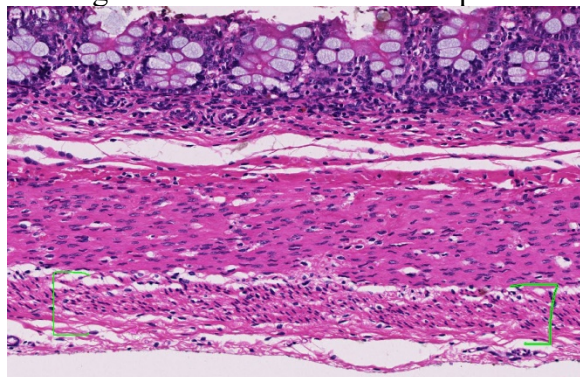
Within the colon, there is complete absence of ganglion cells within the gut wall, together with a severe paucity of myenteric (Auerbach's) ganglia and submucosal nerves (Meissner's). The submucosa was reduced, but in the tissue that remained there was increased prominence of stromal cells.

Contributor's Morphologic Diagnoses:

Ileocolonic aganglionosis, severe, diffuse, chronic (consistent with overo lethal foal syndrome)

Contributor's Comment:

Lethal White Foal Syndrome (LWFS) is a disease associated with horse breeds that register white coat spotting patterns. Breeding between particular spotted horses, generally described as 'frame overo', produce some foals that, in contrast to their parents, are all white or nearly all white and die shortly after birth of severe intestinal blockage.¹ The frame overo coat pattern is

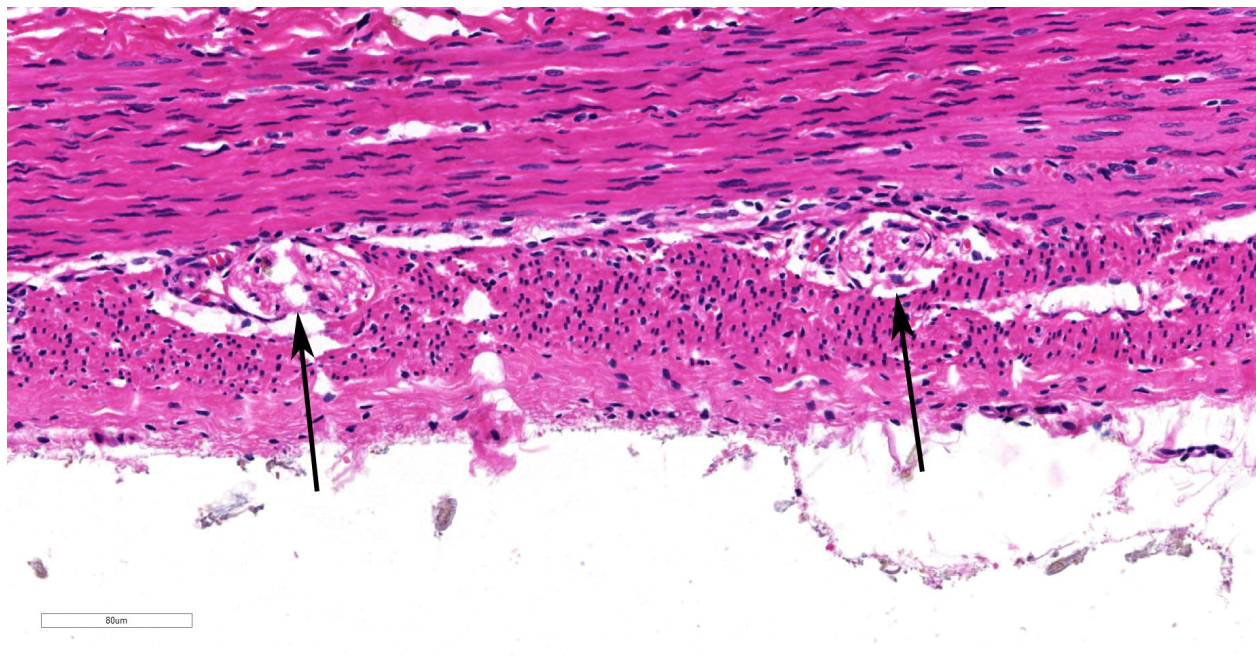


Colon, day-old foal. The muscularis is markedly thinned, the outer longitudinal layer (green brackets) in particular. (HE, 238X)

described as white markings on the lateral and ventral aspects of the neck and torso, whereas a pattern with more white on the dorsal cervical and lumbar regions and the legs is called 'tobiano'.³

Overo lethal white syndrome occurs in newborn foals is associated with the 'overo' coat pattern that receives a copy of the mutated OLW gene (Ile118Lys EDNR-B) from each parent.⁸ Two heterozygote carriers of the mutated gene must be mated to produce a homozygous lethal white foal. Color patterns with highest incidence (> 94%) of heterozygotes were frame overo, highly white calico overo, and frame blend overo. White-patterned bloodlines with lowest incidence of heterozygotes (< 21 %) were tobiano, sabino, minimally white calico overo, splashed white overo, non-frame blend overo, and breeding-stock solid. The mutation was not detected in solid-colored horses from breeds without white patterning.^{4,6,8}

Phenotypically, the altered gene causes lack of skin pigmentation and white coat colour which was strongly associated with endothelin receptor B (EDNR-B) genotype. Endothelin receptors are important in neural crest cell migration. Neural crest cells are precursor cells to a variety of cell types including melanocytes, neural and glial cells of the peripheral, including the enteric, nervous systems.⁹ A consequence of a foal carrying two copies of the mutated EDNR-B gene is that neural crest cells do not migrate to the skin or the gut appropriately, thus resulting in foals being born with a white hair coat and aganglionosis of the submucosal and myenteric ganglia of the distal part of the small intestine and of the large intestine, resulting in intestinal immotility and colic, similar to human Hirschsprung's disease.^{3,4}



Colon, day-old foal. A cross section through the myenteric plexus shows a single hypocellular nerve fiber without any adjacent ganglion cells. (HE, 313X)

The condition Hirschsprung's disease in human children, seen in 1 in 5000 live births, and can be familial or sporadic. In these children often only a segment of the colon or the distal rectum is involved and leads to congenital megacolon. Familial Hirschsprung's disease has been associated with one or more mutations in three separate genes: 1) the RET proto-oncogene, 2) the endothelin-3 (EDN-3) gene, and 3) the endothelin-B receptor (EDNR-B) gene.² Endothelin-3 knockout mice have congenital megacolon due to colonic aganglionosis and coat color spotting due to regional lack of epidermal melanocytes. Endothelin-B receptor knockout mice have the same phenotype.⁴ Mutation of this receptor gene has also been shown to be responsible for familial Hirschsprung's disease in Mennonite families.⁶ Affected humans also occasionally exhibit abnormalities in skin pigmentation.

White patterning in horses has been strongly associated with EDNR-B genotype. Determination of EDNR-B genotype by use

of a DNA-based test is the only way to determine with certainty whether white-patterned horses can produce a foal affected with OLWS.³ (3).

DNA-based test that identifies horses that are heterozygous for the Overo lethal white gene has been developed. The allele-specific polymerase chain reaction test locates and amplifies the specific mutated site in the endothelin receptor B gene (EDNR-B gene).³ The test for this mutant allele can be utilized in all breeds where heterozygous animals may be unknowingly bred to each other including the Paint Horse, Pinto horse, Quarter Horse, Miniature Horse, and Thoroughbred.

Contributing Institution:

Veterinary Pathology, Faculty of Veterinary and Agricultural Sciences, University of Melbourne <http://www.fvas.unimelb.edu.au>

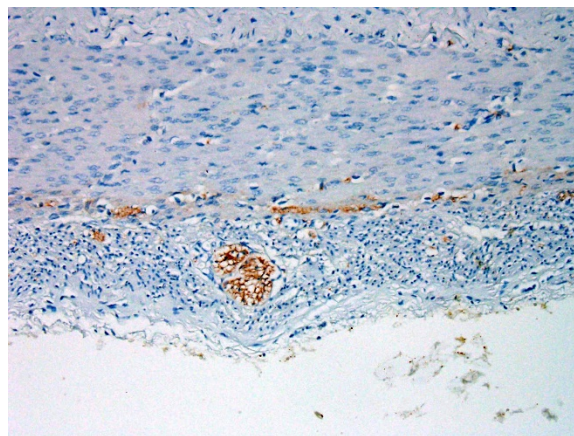
JPC Diagnosis: Colon: Aganglionosis,

diffuse, severe, with marked hypoplasia of the muscular tunics.

JPC Comment: The contributor has done an excellent job in describing the molecular basis of lethal white foal syndrome and Hirschsprung's disease, its human equivalent. Hirschsprung's disease was named after Danish pediatrician Harald Hirschsprung, who first described the condition in two infants in 1886.

Today, a number of mouse models are available for colonic aganglionosis, which exploit mutations in the endothelin 3 receptor, as well as glial cell line-derived neurotrophic factor (GDNF) and its receptor, tyrosine kinase.⁵ In addition to colonic aganglionosis and lack of appropriate colonic contractions, these mutations also result in white spotting of the coat, giving rise to the term "lethal spotting mice". According to the Jackson Laboratory, lethal white spotting mice and similar homozygous "piebald mice" usually die within the third week of life.⁷

Another "lethal white" syndrome is seen in guinea pigs. While the genetic basis of this disease has not been worked out, the overall picture strongly suggests defective migration of neural crest cells during embryogenesis. Similar to the syndrome seen in overo foals, the condition arises in approximately 25% of guinea pigs born to parents carrying the red "roan" allele. While aganglionosis has not been documented in affected guinea pigs, affected individuals manifest albinism, microphthalmia, cataracts, hypodontia and malocclusion, intestinal malabsorption, and diminished immune responses.¹⁰ They are, however, reputed to have excellent personalities.



Colon, day-old foal. A cross section through the myenteric plexus demonstrates the absence of neurons. (anti-NSE, 400X)

The thickness of the muscular tunics was a subject of spirited discussion, with some of the attendees favoring a hypoplastic change due to lack of innervation during development, and some favoring a thinning due to distention from accumulated waste and sampling proximal to the a more profound obstruction.

References:

1. Barker I.K., Baker D.C, Brown C.C: The alimentary system. In: Jubb KVF, Kennedy PC, Palmer N eds *Pathology of Domestic Animals*, 5th ed., vol. 2. Elsevier Saunders, 2007:85-86.
2. Kusafuka T, Puri P: Mutations of the endothelin-B receptor and endothelin-3 genes in Hirschsprung's disease. *Pediatr Surg Int* 1997; 12:19-23.
3. Lightbody, T. Foal with overo lethal white syndrome born to a registered quarter horse mare. *Can Vet J.* 1994; 43(9): 715-717
4. Metallinos DL et al., "A missense mutation in the endothelin-B receptor gene is associated with Lethal White Foal Syndrome: an equine version of

- Hirschsprung disease.” *Mamm Genome*. 1998; 9: 426-31. PMID: 9585428
5. Roberts RR, Bornstein JC, Bergner AJ, Young HM. Disturbances of colonic motility in mouse models of Hirschsprung’s disease. *Am J Physiol Gastrointest Liver Physiol* 2018; 294:G996-G1008.
 6. Santschi EM, Purdy AK, Valberg SJ, Vrotsos PD, Kaese H, Mickelson JR. Endothelin receptor B polymorphism associated with lethal white foal syndrome in horses. *Mamm Genome* 1998; 4:306–309
 7. The Jackson Laboratory Mouse strain Datasheet 000262 - <https://www.jax.org/strain/000262>
 8. Vrotsos P.D., Santschi E.M, Mickelson J.R: The Impact of the Mutation Causing Overo Lethal White Syndrome on White Patterning in Horses. *Proceedings of the annual convention of the American association of equine practitioners*. 47:385-391
 9. Webb A.A., Cullen C.L. Coat color and coat color pattern-related neurologic and neuro-ophthalmic diseases. *Can Vet J*. 2010 Jun; 51(6): 653–657.
 10. Williams, BH. Non-infections diseases in guinea pigs. *In: Suckow MA, Stevens KA, Wilson RP, eds. The laboratory rabbit, guinea pig, hamster, and other rodents*. London, Academic Press, 2012, p. 686-702.

CASE II: P/2014-95 (JPC 4066219).

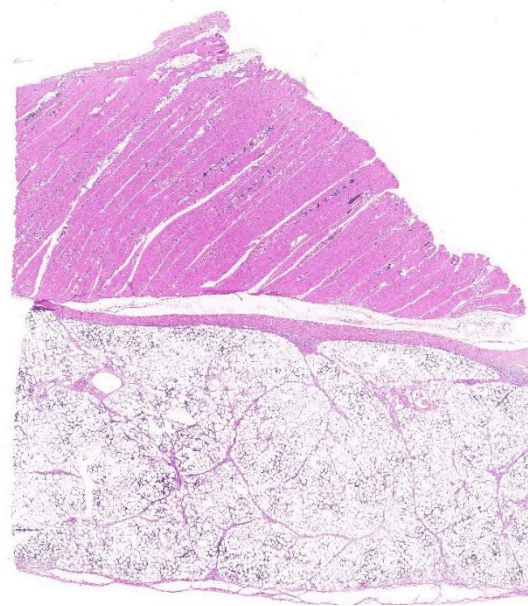
Signalment: 7-week-old, female Cob-X, horse, *Equus caballus*.

History: The filly was presented with lethargy and unwillingness to suckle over the last few days. On clinical examination she exhibited tachycardia, tachypnea, fever, increased capillary refill time, pink mucous membranes, loud and harsh respiratory sounds, and had a pasty fecal consistency. She was treated with antibiotics and nonsteroidal anti-inflammatory drugs (NSAIDs).

The following day, the foal was much the same, yet drinking milk from bucket. Additionally, she exhibited a stiff gait, which was more obvious on the hindlimbs when compared to the forelimbs. Her treatment with antibiotics and NSAIDs was continued and supplemented by intravenous fluid therapy.

The next day the foal became recumbent and died.

In the previous weeks, a number of foals, five of which died, had deteriorated with similar symptoms at the yard down the road, which belonged to the same owner. During the days following submission of the filly for post



Abdominal wall, foal. A section containing skeletal muscle and abdominal fat is submitted for examination. (HE, 5X)

mortem examination, also other foals at the same yard started to show symptoms.

Gross Pathology: Upon gross examination, the cause of death in this foal was not apparent. The adipose tissue in this foal diffusely appeared yellow and, where associated with the mesentery, slightly nodular. Additionally, there was a mild to moderate catarrhal enteritis and very mild ascites.

Laboratory results: NA

Microscopic Description:

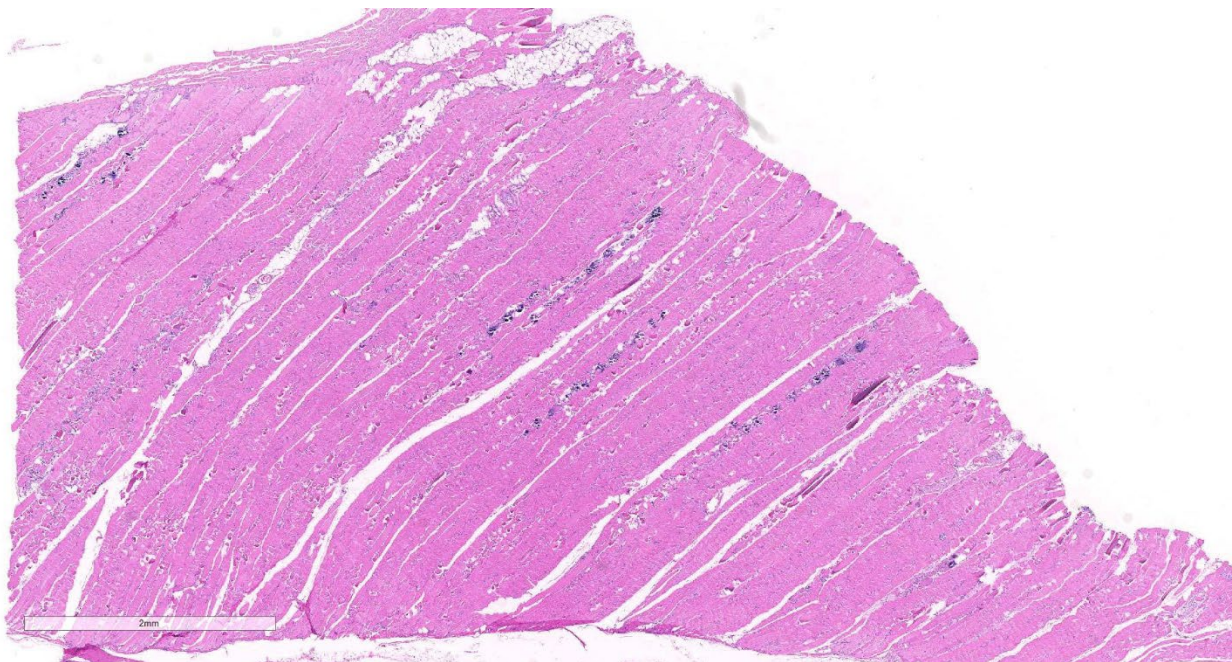
In a multifocal distribution, the striated (skeletal) myofibers are homogeneously eosinophilic, devoid of striations and frequently fragmented, exhibiting irregular contours (hyaline degeneration). Some of these fibers stain strongly eosinophilic (Zenker's degeneration), whilst others exhibit a punctate intracytoplasmic basophilic stain (mineralization). Occasional

degenerative myofibers are being infiltrated by macrophages.

In a multifocal to coalescing distribution, the interstitium of the overlying adipose tissue contains moderate numbers of neutrophils admixed with lesser numbers of macrophages and small to moderate amounts of granular basophilic material (mineralization). Numerous adipocytes, mainly in close association with the inflammatory infiltrates exhibit a blurring of their cytoplasmic vacuoles with pale eosinophilic or basophilic staining (necrosis), whilst in others small clusters of neutrophils are present within lipid vacuoles. Multifocally, the stromal tissue supporting the sheets of mature adipocytes is mildly to moderately expanded by small numbers of plump spindle cells (activated fibroblasts).

Contributor's Morphologic Diagnoses:

Myofiber degeneration, segmental, acute to subacute, multifocal to coalescing, moderate to marked; abdominal wall with



Abdominal wall, foal. Myofiber necrosis and mineralization are visible in skeletal muscle even at low magnification (HE, 18X)

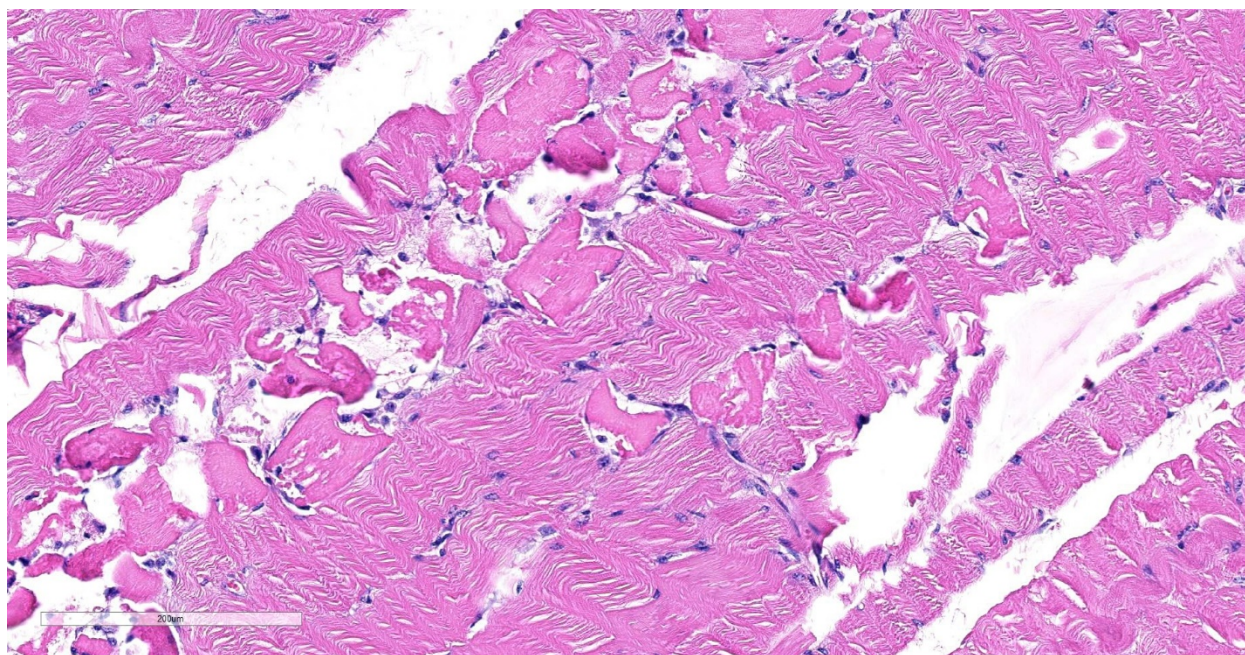
- a) Myofiber mineralization, multifocal, moderate; and
 - b) Myositis, histiocytic, subacute, multifocal, mild.
- 1.) Adipocyte necrosis, acute to subacute, multifocal to coalescing, moderate; abdominal wall with
- a) Steatitis, neutrophilic and histiocytic, subacute, multifocal to coalescing, moderate to marked; and
 - a) Mineralization, multifocal, mild to moderate; and
 - b) Fibrosis, subacute, multifocal, mild.

Contributor's Comment: The combination of muscle degeneration and fat necrosis with prominent inflammatory changes in the fat (also termed “yellow fat disease”) is a disorder seen in equine and donkey foals ranging from one day to 12 weeks^{2,7} and young equids up 3 years^{1,5}, and is thought to be the results of a deficiency of vitamin E and/or selenium, or a diet high in unsaturated

fatty acids¹. However, possibly also a more complex aetiology may need to be considered, since vitamin E/selenium supplementation in these patients often is only of very little or no curative value and these foals may also exhibit normal tissue selenium or glutathione peroxidase concentrations⁶.

Whilst the metabolism of vitamin E and selenium is incompletely understood, the pathogenesis for the muscular changes observed in these foals is considered to be based on lipid peroxidation and damage to proteins of mitochondria, endoplasmic reticulum and the cytosol by radicals due to a relative lack of radical-quenching systems. Both vitamin E and selenium play a role in radical scavenging via the glutathione peroxidase/glutathione reductase system.⁷

Following injury to the cellular membranes by free radicals, these membranes are unable to upkeep the homeostasis. Mitochondria take up the surplus of calcium following the



Abdominal wall, foal. There are multifocal areas of skeletal muscle necrosis, with vacuolation and fragmentation. (HE, 194X)

intracellular influx of this, which negatively affects their ability to produce energy. Energy is required for the recapture of calcium-ions following muscle contracture, with the increase in calcium further resulting in a hypercontractile state which in turn results in coagulative destruction of the myofilaments.⁷

Similarly, the changes to the adipose tissue are considered to be the result of progressive peroxidation¹. The relative distribution of necrosis and mineralization, however, in comparison to the extent of steatitis may vary between the different sites examined.⁶

Affected foals are considered to likely be born to selenium-deficient mares or possibly also vitamin E-deficient mares.^{1,6} Interestingly “yellow fat disease” has a relatively high incidence in Shetland ponies and cold-blooded horses indicating a possibly hereditary predisposition of these regarding for example transplacental passage and liver storage of selenium or colostral vitamin E, or that these horse groups may be relatively over-represented amongst suboptimally fed equids.¹

Clinically, affected foals and horses exhibit depression, fever, tachycardia and variable tachypnea.^{1,2,5} Additionally, mild to moderate abdominal discomfort and tenderness, painful swelling of the nuchal ligament, groin and axillary regions, stiffness and muscular weakness are present, which may affect their ability to suckle.^{3,5,6,7} Their feces are of abnormal consistency.^{1,2}

In biochemistry, lactate dehydrogenase, creatine kinase and aspartate aminotransferase are increased,^{1,2,3} whilst serum vitamin E or selenium is decreased.^{1,3,5}

Upon gross examination, affected foals/horses exhibit hardened, multinodular

and focally hemorrhagic adipose tissues of the nuchal ligament, the coronary sulci, the subcutis and throughout the abdominal cavity with or without yellow-brown discoloration and which may be chalky on cross-section.^{1,2,3,5} Subcutaneous oedema, and discoloration and striation of the skeletal muscles may also be seen.^{1,3,6} Some horses exhibit evidence of a chronic enteritis and bronchopneumonia.¹

The histological changes comprise necrosis of fat cells combined with a steatitis and mineralisation, and degeneration and mineralisation of muscle fibres combined with inflammatory infiltrates.^{1,5,7} Severely affected foals exhibit a monophasic myopathy, whilst subacute cases exhibit polyphasic changes.⁵

Interestingly, the myocardial changes are variable and range from no changes to loss of striations, mineralization and small foci of myocardial necrosis.^{1,5} Degenerative changes to the adrenal cortex with necrosis, calcification and replacement fibrosis of the zona fasciculata have also been reported.⁴

The moderator reviewed features of fat necrosis in histologic section (in the absence of saponification, which was minimal in the adipose tissue on this slide., to include loss of adipocyte nuclei, color change from basophilic to eosinophilic cell membranes, and extension of inflammation into adipocyte cytoplasm.

Contributing Institution:

Veterinary Pathology
Department of Veterinary Medicine
University of Cambridge, UK
<http://www.vet.cam.ac.uk>

JPC Diagnosis: 1. Skeletal muscle: Degeneration and necrosis, polyphasic, multifocal to coalescing, with mineralization.

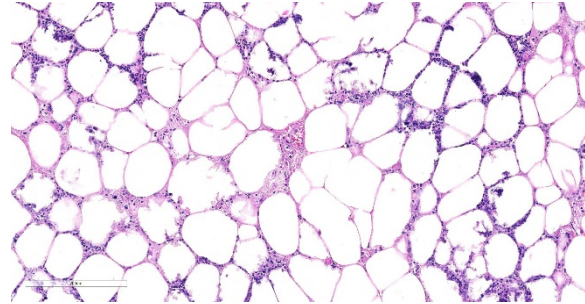
2. Fat: Steatitis, necrotizing, multifocal to coalescing, marked.

JPC Comment: The contributor has done an outstanding job of reviewing the syndrome of Vitamin E/selenium deficiency in the foal, and this section is an outstanding example of the damage that may be seen in multiple tissues.

Vitamin E/selenium imbalance may have one of the most diverse repertoire of damage in many animal species, with some animals (such as pigs) manifesting in a multitude of syndromes. Most species will demonstrated muscle necrosis, often both skeletal and cardiac, in the face of Vitamin E deficiency. Decreased reproductive efficiency is also a common finding across species. Panniculitis may be seen as a result of dietary Vit E deficiency in cats, mink, foals, swine as a result of feeding high-fish diets, but is also seen in certain waterbirds, such as herons. In dogs, a vitamin E-deficient diet may result in ceroidosis of intestinal smooth muscle, so-called “brown dog gut”.

Vascular damage may be seen in animals with Vitamin E deficiency, to include cerebellar hemorrhage and necrosis in turkey poults, as well as exudative diathesis in poultry and swine, in which fluid exudes from blood vessels yielding a soft edematous overlying tissue. Vitamin E deficiency may also result in hemolytic anemia in a number of species, including humans and non-human primates. Vitamin E deficiency in guinea pigs may result leukoencephalomalacia in feti. Cutaneous manifestations of Vitamin E deficiency include alopecia and seborrhea dermatitis in goats, as well as alopecia in calves on Vitamin E-deficient milk replacer.⁴

Growing pigs may suffer a number of manifestations of Vit E/Selenium imbalance, including massive hepatic necrosis (hepatosis



Abdominal wall, foal. There is multifocal dystrophic calcification of necrotic myofibers. (HE, 194X)

dietetica), arteriolar degeneration and thrombosis (mulberry heart disease), exudative diathesis, and white muscle disease. These syndromes rarely occur concurrently in the same animal.

Vitamin E was discovered in 1922 by Drs. Herbert Evans and Katharine Bishop, who identified it as a dietary fertility factor for laboratory rats. In fact, the name “tocopherol” is derived from the Greek meaning “to carry a pregnancy”. It is obviously a necessary dietary factor for all animal species. As a widely used mendicant on the human market, it has enjoyed great popularity as a dietary supplement and ingredient in topical products for the skin in humans, largely without documented benefits. The benefits of megadosing on Vitamin E, begun in the 1930’s and 1940’s by the Shupe brothers (who extolled its virtues in treating heart disease) have yet to be proven beneficial in treating cardiovascular disease or a wide range of other diseases for which it has been purposed.

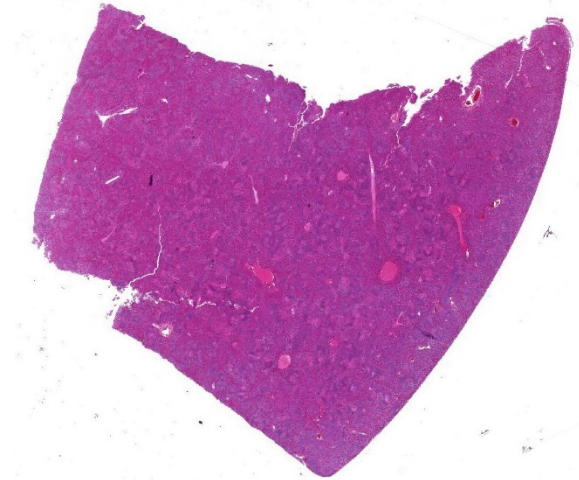
Participants remarked on the lack of saponification in the areas of necrotic fat on this slide. In the absence of obvious saponification, a lack of vital staining, loss of adipocytes nuclei, and extension of inflammatory cells within the cytoplasmic border of affected adipocytes are all clues to the potential viability of damaged adipocytes.

References:

1. De Bruin CM, Veldhuis Kroeze EJB, Sloet van Oldruitenborgh-Oosterbaan MM. Yellow fat disease in equids. *Equine Vet Educ* 2006;18(1):38-44.
2. Dixon RJ, Nuttal WO, Carthew DA. A case of steatitis and myonecrosis in a donkey foal. *New Zeal Vet J* 1983;31:62.
3. Foreman JH, Potter KA, Bayly WM et al. Generalised steatitis associated with selenium deficiency and normal vitamin E status in a foal. *JAVMA* 1986;189(1):83-86.
4. Mauldin EA, Peters-Kennedy J. Integumentary System. In: Maxie, GM, ed. Jubb Kennedy and Palmer's Pathology of Domestic Animals, 6th ed. St. Louis, Elsevier, 2017. Vol 1, p 583.
5. Platt H, Whitwell KE. Clinical and pathological observations on generalized steatitis in foals. *J Comp Path* 1971;81:499-508.
6. Valentine BA, McGavin MD. Skeletal Muscle. In: Zachary JF, McGavin MD, eds Pathologic Basis of Veterinary Disease. 5th ed. St Louis, MO; Elsevier Mosby;2012.900-901.
7. Van Vleet F, Valentine BA. Muscle and Tendon. In: Maxie MG, ed. Jubb, Kennedy and Palmer's Pathology of Domestic animals. 5th ed. Vol. 1. Philadelphia, PA: Elsevier Saunders; 2007. 242.

CASE III: S643/17 (JPC 4101752).

Signalment: Foal, 3 weeks of age, female, crossbred horse, *Equus caballus*



Liver, foal. A section of liver is presented for examination. (HE, 4X)

History: This foal was born without any complication in March 2017 and developed normal the following days. At the third week of life, the animal was put with other horses and foals on the pasture. The following morning, the foal was lethargic and dyspneic with a body temperature of 40 °C. A veterinarian was called in immediately. The foal was treated with NSAIDs. The body temperature declined within 30 minutes. Another 30 minutes later, the foal showed tachycardia (100/min), reduced breathing rate (3/min) with cyanosis of mucous membranes and died spontaneously. All other horses and foals in the flock were healthy the entire time.

Gross Pathology: Postmortem examination was performed immediately the same morning. The foal was in good body condition and developmental stage. A marked jaundice was visible with intensely yellowish staining of mucous membranes, connective tissue and fasciae as well as the intima of large vessels. The liver was severely enlarged, mottled reddish brown with a friable consistency. White spots were not visible within the parenchyma. The spleen was mildly enlarged. Beside alveolar edema and emphysema of the lungs, other

organs and tissues including heart, brain, thymus, umbilicus, and joints were unremarkable macroscopically.

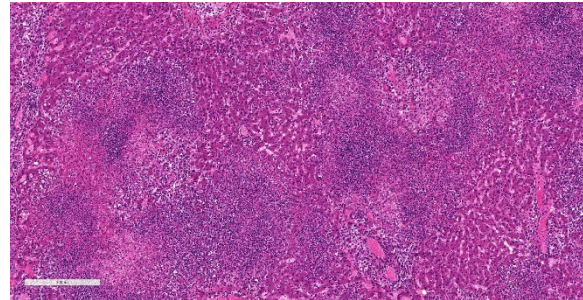
Laboratory results: Virology (detection of cytopathogenic viruses in cell culture): negative

Bacteriology (aerobic and anaerobic culture): numerous colonies of *E. coli* and *Pseudomonas* sp. in all organs, few colonies *Clostridium perfringens* in the small intestine, and unspecific bacteria (e.g. *Acinetobacter johnsonii*, aerobic *Bacillus* sp., *Enterobacter ludwigii*, *Providencia rettgeri*) in liver, lung, intestine, spleen and brain

PCR/liver: Amplification of a 633 bp fragment of *Clostridium piliforme* (GenBank accession number L07416) (Fig.1)

Microscopic Description:

Liver: Affecting 80% of hepatic parenchyma are multifocally to coalescing and randomly distributed areas of lytic necrosis characterized by loss of cellular detail and replacement of hepatocytes by nuclear and cellular debris admixed with fibrillar to beaded eosinophilic material (fibrin) and erythrocytes (hemorrhage). Foci measure up to 1.2 mm in diameter and are variably infiltrated by intact and degenerated neutrophils and fewer macrophages. Hepatocytes adjacent to the necrotic areas exhibit either hypereosinophilia with maintenance of cell border and karyorrhectic or pyknotic nuclei (coagulative necrosis). Other hepatocytes are swollen with pale eosinophilic and often finely vacuolated cytoplasm (degeneration). In some hepatocytes at the periphery of the necrosis numerous barely visible filamentous, pale basophilic bacilli (0.5 x 5 μ m) can be seen. Portal areas are moderately infiltrated by lymphocytes, plasma cells, macrophages and fewer neutrophils.



Liver, foal. Multifocal to coalescing areas of lytic necrosis occupy about half of the section. (HE, 81X)

Using Warthin-Starry stain argyrophilic filamentous bacteria are visualized within hepatocytes at the periphery of necrotic areas and within the debris (Fig. 2).

Contributor's Morphologic Diagnoses: Liver: Hepatitis, random, necrotizing and suppurative, acute, multifocal to coalescing, severe with intracellular argyrophilic filamentous bacteria. Tyzzer's disease.

Contributor's Comment: A fatality in a young foal with a rapid course of disease, fever and jaundice, focused the postmortem examination on infectious diseases with highly virulent pathogens. Differentials after necropsy were infection with EHV-1 and bacterial sepsis (e.g. Enterobacteriaceae, *Actinobacillus equuli*). The typical histomorphology with random areas of necrosis and detection of argyrophilic bacteria were highly suggestive of Tyzzer's disease. This was confirmed by PCR detecting a 633 bp fragment of *Clostridium piliforme* in a liver sample of this foal.

Clostridium piliforme, formerly known as *Bacillus piliformis*, is a gram-negative filamentous bacillus that is not cultivable in cell free media. In domestic animals, young foals are most often affected. Often, they are found dead or die after short illness.³ Wild rodents are believed to be the reservoir of the bacterium.

In 2013 Swerczek¹¹ reviewed 148 cases of Tyzzer's disease from central Kentucky and highlighted the predispositions, risk factors, and the mode of transmission. Foals in the first month of age are most frequently affected and at the highest risk for Tyzzer's disease. Adult horses are believed to be resistant. There are more cases in spring in association with heavy rainfall. Interestingly, on 18th of March, two days before this foal came to the pasture, heavy rainfall started in the region of the herd in the western part of Germany (35 l/m² rain in 48 hours). It is suggested that foals are infected by consuming feed contaminated with environmental spores of *Clostridium piliforme* or by ingestion of feces of the mares. Foals show coprophagy only from the second to the fifth week of life.¹⁰

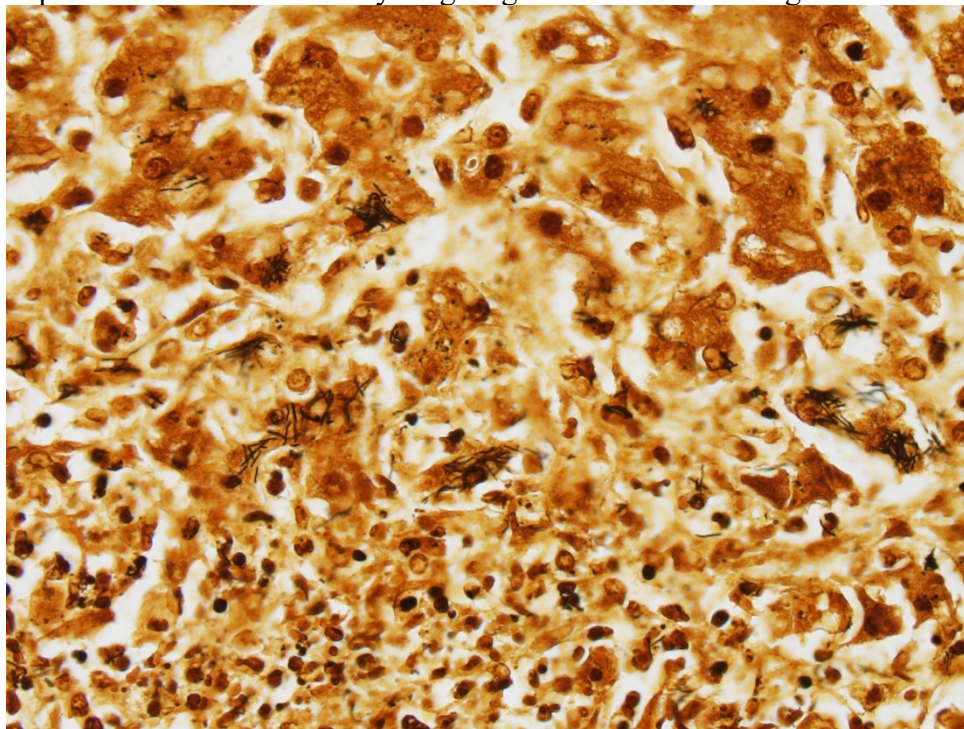
Some cases of Tyzzer's disease were reported in calves⁴ and in young dogs and

cats, some of them suffering from immunosuppression.^{3,6,12}

Mongolian gerbils are exquisitely susceptible to fatal Tyzzer's disease, and many other laboratory animals (e.g. mice, rats, lagomorphs, hamsters, guinea pigs) are at risk for the infection with *Clostridium piliforme*.¹ Cases were reported in marsupials² and birds.^{5,7} The infection is extremely rare in nonhuman primates and humans.⁹ Recently, a case of Tyzzer's disease was reported in a captive born cotton-top tamarin. A necrotizing typhlocolitis, accompanied by myocarditis was found additionally to the hepatic lesions.⁸

In the following weeks, no other cases of Tyzzer's disease occurred in the herd of the affected foal.

We are grateful to Dr. W. Herbst, Institute of



Liver, foal. Numerous sheaves of 1x4 intracytoplasmic bacilli consistent with Clostridium piliforme are present within the cytoplasm of intact hepatocytes at the periphery of areas of necrosis. (Warthin Starry 4.0, 400X)

Hygiene and Infectious Diseases of Animals, University of Giessen, for performing the PCR.

Contributing

Institution:

Institut fuer Veterinaer-Pathologie, Justus-Liebig-Universitaet Giessen
Frankfurter Str. 96,
35392 Giessen,
Germany

http://www.uni-giessen.de/cms/fbz/fb10/institute_klinikum/institute/pathologie

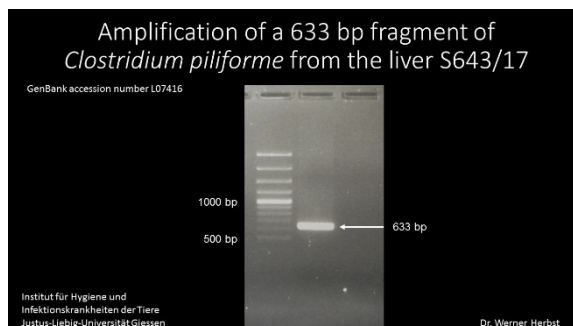
JPC Diagnosis: Liver: Hepatitis, necrotizing, multifocal to coalescing, severe, with intracytoplasmic filamentous bacilli.

JPC Comment: The contributor has provided an excellent review of Tyzzer's disease in a variety of species, and the previous case of Tyzzer's disease in this year's WSC Conference (Conf. 4, Case 1) in the colon of a cat should be reviewed for additional information on this often fatal disease.

In the foal, the disease is considered highly fatal but not contagious. Disease is seen between 1 and 6 weeks, with an average of 20 days.¹¹ Outbreaks, first identified in Kentucky in 1964, may claim multiple animals on a farm, and are likely the result of soil contamination by these resistant bacilli and ingestion by foals. Another postulated route of infection is directly from the mare's feces. It is thought that increased nutrition of nursing mares may result in a bloom of *C. piliforme* within the intestine. *C. piliforme* infection is extremely rare in adult healthy horse, but will result in an increased numbers within feces, and coprophagic foals may receive a large oral inoculum in this fashion.¹¹

As opposed to the diseases in laboratory species, most cases of Tyzzer's disease in the horse are primarily hepatic in nature. Enteric lesions may be present, but diarrhea is rare, and myocardial lesions are also very rare.

The moderator and attendees discussed the use of terms subacute and acute when describing this lesion. While a consensus was not reached, and both sides provided viable arguments, the moderator stressed the



A 633bp fragment of C. piliforme was identified by PCR from the liver of this foal. (Photo courtesy of Dr. Werner Herbst, Institute für Hygiene und Infektionskrankheiten der Tiere Justus-Liebig-Universität Giessen)

need for precision in the usage of such terms in reporting out equine cases, especially in insurance cases.

References:

1. Barthold SW, Griffey SM, Percy DH. Pathology of laboratory rodents and rabbits, 4th Edition. John Wiley & Sons. 2016
2. Canfield PJ, Hartley WJ. Tyzzer's disease (*Bacillus piliformis*) in Australian marsupials. *J Comp Pathol.* 1991;**105**(2):167-173.
3. Cullen JM, Stalker MJ. Liver and biliary system. In: Maxie MG, ed. Jubb, Kennedy and Palmers Pathology of Domestic Animals. 6th ed. Vol 2. Elsevier, St. Louis, Missouri; 2015:258-352.
4. Ikegami T, Shirota K, Une Y, Nomura Y, Wada Y, Goto K, et al. Naturally occurring Tyzzer's disease in a calf. *Vet Pathol.* 1999;**36**:253-255.
5. Mete A, Eigenheer A, Goodnight A, Woods L. *Clostridium piliforme* encephalitis in a weaver bird (*Ploceus*

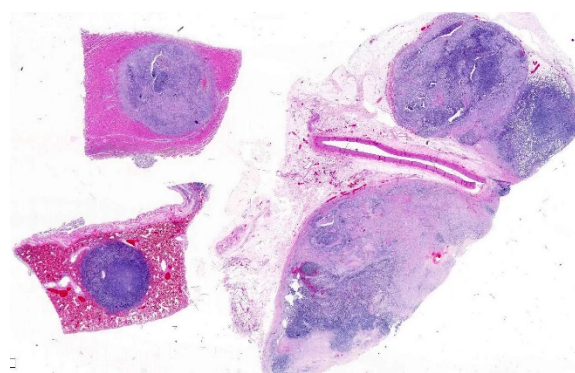
- castaneiceps). J Vet Diagn Invest. 2011;**23**(6):1240-1242.
6. Neto RT, Uzal FA, Hodzic E, Persiani M, Jolissaint S, Alcaraz A, Carvalho FR. Coinfection with *Clostridium piliforme* and Felid herpesvirus 1 in a kitten. J Vet Diagn Invest. 2015;**27**(4):547-551.
 7. Raymond JT, Topham K, Shirota K, Ikeda T, Garner MM. Tyzzer's disease in a neonatal rainbow lorikeet (*Trichoglossus haematodus*). Vet Pathol. 2001;**38**(3):326-327.
 8. Sasseville VG, Simon MA, Chalifoux LV, Lin KC, Mansfield KG. Naturally occurring Tyzzer's disease in cotton-top tamarins (*Saguinus oedipus*). Comp Med. 2007;**57**(1):125-127.
 9. Smith KJ, Skelton HG, Hilyard EJ, Hadfield T, Moeller RS, Tuur S, Decker C, Wagner KF, Angritt P. *Bacillus piliformis* infection (Tyzzer's disease) in a patient infected with HIV-1: confirmation with 16S ribosomal RNA sequence analysis. J Am Acad Dermatol. 1996;**34**(2 Pt 2):343-348.
 10. Soave O, Brand CD. Coprophagy in animals: a review. Cornell Vet. 1991;**81**(4):357-364.
 11. Swerczek TW. Tyzzer's disease in foals: retrospective studies from 1969 to 2010. Can Vet J. 2013;**54**(9):876-880.
 12. Young JK, Baker DC, Burney DP. Naturally occurring Tyzzer's disease in a puppy. Vet Pathol. 1995;**32**:63-65.

CASE IV: 16L-2013 (JPC 4085442).

Signalment: 1 year 5 month old female neutered Newfoundland (*Canis lupus familiaris*) dog.

History: The animal presented to the Department of Veterinary Neurology at the University of Liverpool's small animal teaching hospital with a history of chronic right pelvic limb monoparesis and lameness that had significantly worsened in the last 2-3 weeks prior to presentation along with severe weight loss. The referring veterinary surgeon had performed CBC and biochemistry which were unremarkable; gracilis muscle biopsy that revealed muscle atrophy of unknown etiology. On clinical examination patella reflex was absent in the right hind limb with mildly reduced withdrawal reflex. Magnetic resonance imaging (MRI) was performed and revealed an infiltrative paravertebral mass and due to the guarded prognosis euthanasia was performed and a full post mortem completed.

Gross Pathology: There was a large lumbar to sacral paravertebral multi-lobulated tan firm infiltrative mass within the paravertebral right muscles extending from the level of L4 to the sacrum and expanding into the retroperitoneal space measuring 18 x 6 x 9



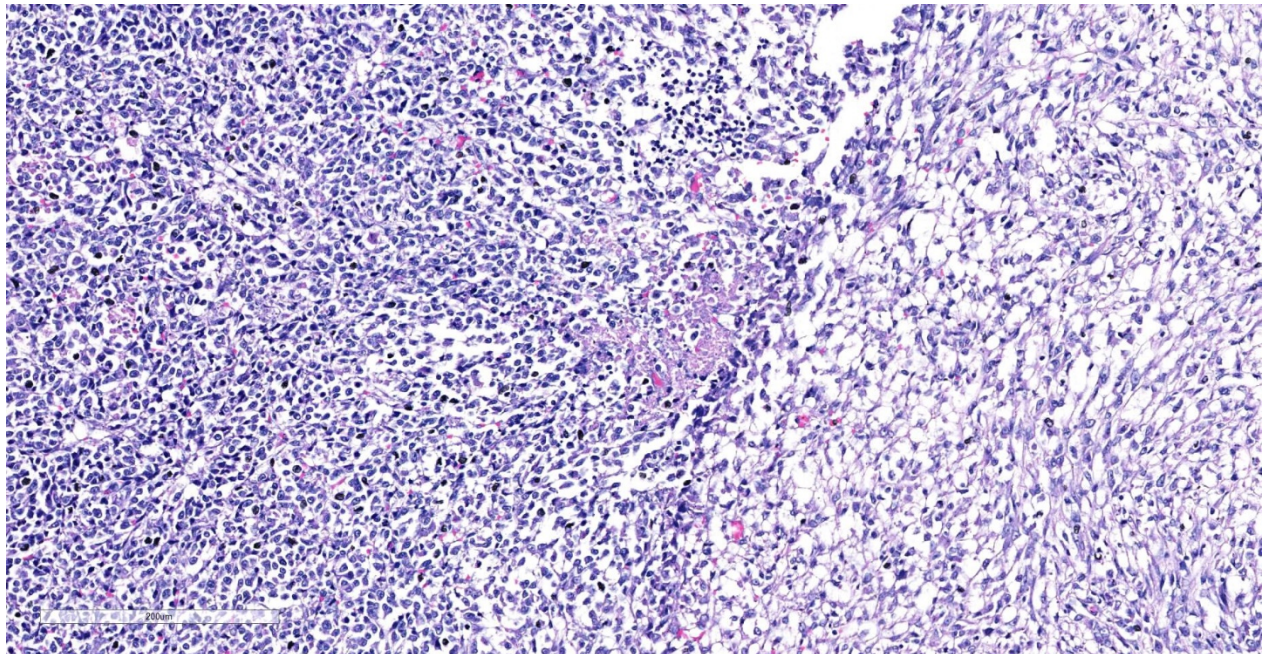
Spinal musculature (per contributor), heart, lung. dog: Sections from multiple tissues, each with a neoplasm in it, are presented for evaluation.

cm. The mass invaded the right side of L5-L7 vertebrae. Similar tan masses up to 2 cm in diameter were observed randomly scattered in the liver, pancreas, omentum, lung and myocardium. There was also enlargement of the right ovary by a tan firm mass measuring 7 x 4.5 x 2 cm. Multifocal masses with full thickness ulcerations were observed in the gastric mucosa of the fundic region.

Laboratory results: MRI of lumbar spine: there was a large (18 x 6 x 9 cm) irregularly shaped and multilobulated complex soft tissue mass located in the paraspinal soft tissue ventral to the caudal lumbar spine extending from the level of L4 to the sacrum. The mass filled the right side of the epidural space and wrapped around the cauda equine and the caudal spinal cord. The mass invaded the right side of L5-L& vertebrae. The mass caused ventral displacement of the abdominal organs and compression of the aorta and caudal vena cava.

Cytology: large numbers of neoplastic cells arranged in loose aggregates, moderately

cohesive sheets or individualized amid a finely stippled pink background. Occasional macrophages with erythrophagia and intracytoplasmic hemosiderin are scattered throughout. Neoplastic cells are pleomorphic spanning in morphology from small round cells with a high nuclear to cytoplasmic ratio, round nucleus, granular chromatin and scant blue cytoplasm to polygonal cells with more abundant and often vacuolated cytoplasm to clearly fusate cells with oval to reniform nuclei sometimes embedded amid scant pink extracellular matrix and occasionally surrounded by capillaries. Nucleoli are consistently large and pale blue, in number of one to three. Mitoses are occasionally seen. Rarely, small variably sized round dark blue granules (possible hemosiderin) are noted within the cytoplasm. Occasionally, erythrocytes are closely associated with these cells or a single erythrocyte is seen intracellularly. Anisocytosis and anisokaryosis are moderate. Rare elongated multinucleated cells are noted (either neoplastic cells or ('strap cells')). In one slide small fragments of skeletal muscle myocytes



Paravertebral muscle tumor: Neoplastic skeletal muscle cells assume two morphologies in this field - a alveolar pattern (left) and more typical spindle at right. (HE, 178X)

with occasional centralized nuclei are noted scattered amid the neoplastic cells.

Cytological findings are most suggestive of a sarcoma possible rhabdomyosarcoma.

Trucut biopsy: Focally within the section, cells arranged in linear streams within a moderate amount of collagenous stroma, are elongated with indistinct cell borders, variably sized from 40 x 20 µm up to 300 x 200 µm with abundant pale to brightly eosinophilic cytoplasm, sometimes containing striations, and multiple, up to 7, central to para-central nuclei. Chromatin is finely stippled to coarsely clumped, often with a central prominent nucleolus. Adjacent to this there are extensive to polygonal, with indistinct cell borders, approximately 30 x 10 µm with abundant eosinophilic cytoplasm and a central elongated vesiculated nucleus. Chromatin is finely stippled and nucleoli are often indistinct. There is scant fibrovascular stroma and scattered necrotic cells. Mitotic figures are rare. There is mild to moderate multifocal mixed (neutrophils-dominated) inflammation.

Immunohistochemistry:

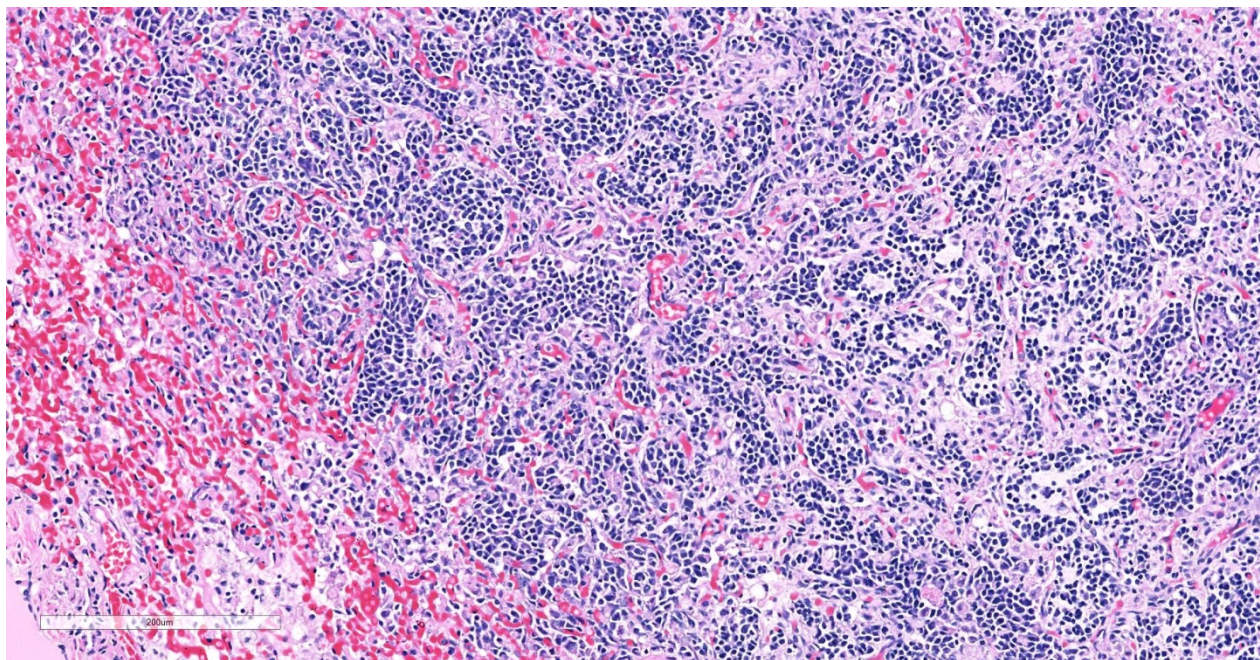
Immunohistochemistry for pancytokeratin, vimentin and myoglobin was performed on sections of the skeletal muscle mass, the mass in the myocardium and on the mass in the lung. The neoplasm was strongly positive for vimentin and negative for pancytokeratin. There were approximately 40% of neoplastic cells that were positive for myoglobin.

Microscopic Description:

Skeletal muscle: Completely effacing the skeletal muscle there is a non-encapsulated, poorly demarcated, densely-cellular and infiltrative neoplasm. The neoplasm is biphasic with one population of cells arranged haphazardly into streams and the second population arranged into sheets. Cells

of the first population are spindled with indistinct cell borders, approximately 15-40 µm with abundant pale eosinophilic cytoplasm and usually a single centrally placed nucleus. Occasionally these cells are large and contain many up to 6 nuclei arranged in a row (strap cell, fig. 4, variable between slides). Chromatin is finely stippled to coarsely clumped, and nucleoli vary from indistinct to a prominent single nucleolus to up to 3 nucleoli. Anisocytosis and anisokaryosis are marked and mitotic index is 1 per 10HPF. The second population is interwoven with the first and is composed of sometimes densely packed sheets and other times with a looser arranged alveolar-like structure (fig. 5) with cells sloughed into a lumen both with a fine fibrovascular stroma. Cells are round with mostly distinct cell borders, approximately 20-30 µm diameter with a moderate amount of eosinophilic cytoplasm and a large round to oval central to para-centrally placed nucleus (rhabdomyoblasts). Occasionally cells are multinucleated and several nuclei are aligned in a row. Chromatin is finely stippled and dense to coarsely clumped and open with nucleoli variable from indistinct up to 3 per nucleus. Anisocytosis and anisokaryosis are marked and mitotic index is 6 per 10 HPF. Multifocally throughout the neoplasm there are large areas of necrosis and smaller areas of hemorrhage.

Heart: Within the myocardium there is an approximately 6 mm diameter well demarcated, non-encapsulated densely cellular neoplasm. The neoplastic cells are arranged haphazardly in streams and with a smaller population arranged in sheets with a moderate quantity of fibrovascular stroma. Cells arranged in streams are spindled with indistinct borders, approximately 5 x 30 µm with abundant eosinophilic cytoplasm and an elongated centrally placed nucleus. While cells arranged in sheets are round to



Lung, dog. Within the lung, neoplastic cells assume a very definitive alveolar pattern. (HE, 176X)

polygonal with distinct cell borders, approximately 10-20 μm in diameter with a moderate amount of eosinophilic cytoplasm and a large round to polygonal central to para-centrally placed nucleus. Occasionally in both populations there are large elongated multinucleated cells with nuclei arranged in a row (strap cells, variable between slides). Chromatin is finely stippled to coarsely clumped with from indistinct up to 3 nucleoli per nucleus. Anisocytosis and anisokaryosis are marked and mitotic index is 9 per 10 HPF which are often bizarre.

Multifocally scattered throughout the neoplasm there are areas of lytic necrosis admixed with small amounts of haemorrhage. Also scattered throughout the neoplasm there are areas of deeply basophilic irregular vacuolated material.

Lung: In the lung there is and approximately 5 mm diameter non-encapsulated, reasonably well demarcated but infiltrative, densely cellular neoplasm. The neoplasm is tri-phasic with cells arranged in sheets, streams,

cords and packets and sometimes reproducing alveolar-like structures divided by abundant fibrovascular stroma. Cells are hyperchromatic, round to polygonal to spindled with mostly distinct cell borders, approximately 10 μm diameter up to 15 x 30 μm and 10 x 40 μm with a moderate amount of eosinophilic cytoplasm and a central to para centrally placed, round to polygonal to elongated hyperbasophilic nucleus. Chromatin is finely stippled to coarsely clumped and there are indistinct up to 3 nucleoli per nucleus. Cells are highly pleomorphic and mitotic index is 23 per 10 HPF often with bizarre mitotic figures. There are large areas of coagulative necrosis multifocally within the neoplasm and smaller areas of hemorrhage. The lung is diffusely moderately hyperemic.

Contributor's Morphologic Diagnoses:

Skeletal muscle rhabdomyosarcoma, alveolar type
Heart metastatic rhabdomyosarcoma
Lung metastatic rhabdomyosarcoma

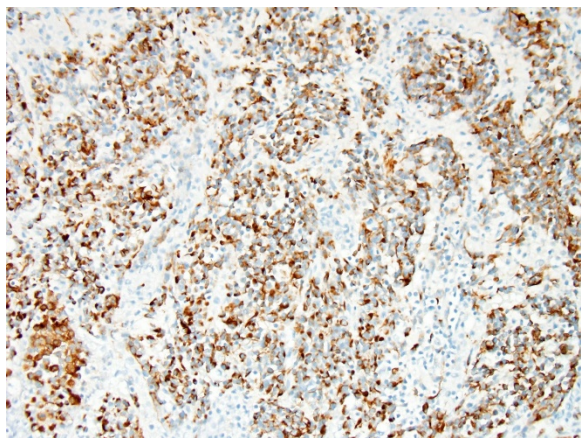
Contributor's Comment: Rhabdomyosarcoma (RMS) is the malignant neoplasm derived from skeletal muscle. They are highly variable in-terms of age of onset, location, gross and histological appearance^{1,2,3,4,5,10}. RMS are common in human children and juvenile dogs under 2 years old². Both the human and veterinary RMS can be separated into different categories depending on the various degrees of differentiation towards skeletal muscle. The veterinary RMS can be subclassified as follows^{2,4,5,6,7}:

- **Embryonal RMS:** embryonal RMS can be further divided due to the cell morphology into Myotubular, Rhabdomyoblastic and Spindle cell. Another embryonal RMS is the Botryoid embryonal RMS. All embryonal RMS are most frequently encountered in juvenile animals (less than 2 years old).
 - Myotubular – this is a RMS that is dominated by classical multinucleated strap cells with frequently observable cross-striations.
 - Rhabdomyoblastic – is composed of mostly small round to polygonal cells with abundant eosinophilic cytoplasm and only occasionally cells with cross striations. This may be confused with the solid variant of the alveolar RMS.
 - Spindle cell – The RMS is composed of mostly spindle shaped cell in low cellularity often arranged in a storiform pattern.
 - Botryoid RMS – RMS that is usually found in the trigone region of the urinary bladder with predominance in the

female population and large breed dogs. The term botryoid is used due to the macroscopic grape like appearance. The tumor must be contained in the submucosa.

- **Alveolar RMS-** the alveolar pattern is determined by the presence of an area of neoplastic cells that are arranged in a glandular like pattern to give “alveolar” spaces. There is also a solid variant where the cells are in dense sheets. Often in the alveolar RMS there will only be a small area displaying the “alveolar” pattern and the rest of the neoplasm is in sheets or anaplastic. Neoplastic cells tend to be round with small to moderate amounts of eosinophilic cytoplasm and multinucleated giant cells (strap cells) that are common in the embryonal RMS are uncommon in the alveolar variant.
- **Pleomorphic RMS-** rare as only RMS that do not display any features of embryonal or alveolar RMS can be termed truly pleomorphic. The histological features are of a mesenchymal neoplasm with marked anisocytosis and anisokaryosis and bizarre mitotic figures. The pleomorphic RMS tends to be observed in adult rather than juvenile animals.

RMS is one of the most common neoplasms in human children under 15 years old with there being a difference in survival time between embryonal and alveolar variants^{1,6,7,8,9}. It is therefore important to be able to differentiate between the subtypes. The prognostic impact of dividing RMS into subclasses has not yet been determined for



Lung, dog. Neoplastic cells within the lung stain strongly immunopositive with desmin. (anti-desmin, 200X)

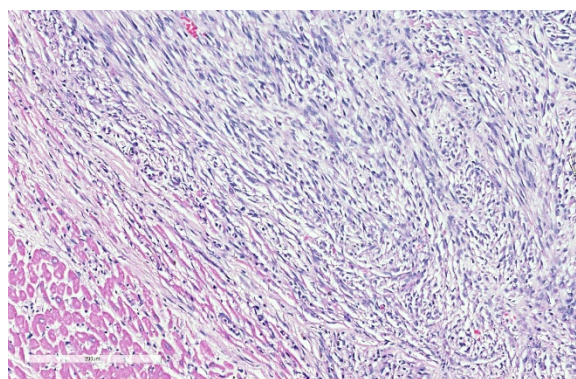
veterinary species however in human medicine the pleomorphic and the alveolar variants have the worse prognosis with the embryonal variants having a more favorable outcome⁶.

Differential diagnosis for RMS are nephroblastoma, germ cell tumors, malignant peripheral nerve sheath tumors and anaplastic sarcomas^{2,6}. It can be extremely difficult to differentiate some RMS on histological cell morphology alone especially if there are low numbers of strap cells. Therefore further diagnostic techniques such as immunohistochemistry and electron microscopy are often required^{2,4}. Due to RMS being a mesenchymal proliferation neoplastic cells label strongly for vimentin. Desmin may be useful but labelling can be uneven in both human and veterinary species. Smooth muscle actin can be used to rule out leiomyosarcomas². Myoglobin expression may be decreased or lost on undifferentiated rhabdomyosarcomas.

Immunohistochemistry was performed on our case which was strongly positive for vimentin and many neoplastic cells were positive for myoglobin and all neoplastic cells were negative for pan-cytokeratin.

The case presented here is most likely the alveolar variant of a rhabdomyosarcoma due to the areas within the primary and the metastatic neoplasms having alveoli-like structures. All rhabdomyosarcomas have a degree of pleomorphism and only if there is no evidence of embryonal or alveolar differentiation then the pleomorphic variant can be diagnosed⁶. A variant described in human medicine but not in veterinary medicine is the spindle cell/sclerosing rhabdomyosarcoma¹¹. The spindle cell/sclerosing RMS is described as being composed fascicles of spindle cells or primitive round cells embedded in sclerotic matrix with varying numbers of rhabdomyoblasts¹¹ which can often mimic the classic alveolar pattern⁹ and is consistent with some areas in the case presented here.

Clinical features of all RMS vary depending on the location of the neoplasm. Embryonal RMS (except botryoid RMS) are usually observed in the head and neck regions². Alveolar RMS can be found in a wide range of regions and pleomorphic RMS tend to be within the skeletal muscle^{2,4}.



Heart dog. Neoplastic cells within the heart assume a more traditional spindle cell "myotube appearance. (HE, 176X)

Contributing Institution:

University of Liverpool, Leahurst Campus,
Chester High Road, Neston, Wirral, UK;
<https://www.liverpool.ac.uk/vetpathology/>

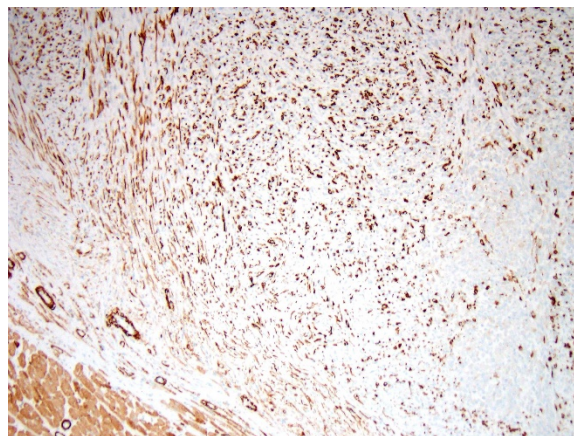
JPC Diagnosis: Paraspinal fibrovascular
tissue (per contributor):
Rhabdomyosarcoma, alveolar type.

Heart, lung: Rhabdomyosarcoma, alveolar
type, metastatic

JPC Comment: The contributor has
provided an excellent review of the
subclassification of rhabdomyosarcoma in
human and veterinary species, and in doing
so, has illustrated the difficulty so often
encountered in trying to classify them. This
is also a process that, as mentioned by the
contributor, is not of as much importance in
veterinary medicine as it is in human
medicine, where prognostic information is
based on precise classification.

The neoplasm in this case shows two
definitive phenotypic morphologies – that of
a spindle cell tumor (myotubular) with few
classic strap cells, as well as the nesting and
packeting of cells with a polygonal
appearance, the so-called alveolar pattern
(presence in the lung here notwithstanding).
The primary neoplasm of the paraspinal
musculature demonstrates both patterns,
while in the metastatic nodule in the lung the
alveolar pattern predominates, and in the
heart, the spindle cell pattern predominates
(likely attesting to different
microenvironments in various metastatic
sites).

A number of immunohistochemical markers
were applied on this section, although the
morphology of the neoplasm is strongly
suggestive of a skeletal muscle, and the
metastatic nodules meet the most critical



Heart dog. Neoplastic cells within the heart stain strongly immunopositive with muscle specific actin. (anti-MSA, 200X)

determinant of malignancy. Vimentin was
not used in this case due to the obvious
spindle cell morphology – quite a number of
human pathologists at the JPC eschew the use
of vimentin in many subspecialties. The
appropriate choice of immunostains in
muscle neoplasms may not only indicate a
diagnosis, but also yield clues as to the degree
of differentiation. Desmin and muscle-
specific actin are non-specific muscle
markers that will stain smooth and cardiac
muscle as well as myofibroblasts. Smooth
muscle actin should not stain skeletal muscle
but may be an important part of an
immunopanel to rule out smooth muscle
tumors. Myoglobin is expressed in skeletal
and cardiac muscle, but not smooth muscle,
and may or may not be expressed in skeletal
muscle malignancies, especially poorly
differentiated tumors. Myogenin and myoD1
are skeletal muscle-specific nuclear products
which are expressed early in development,
and may be critical in identifying poorly
differentiated neoplasms in veterinary
medicine, and have shown utility in
differentiating embryonal and alveolar
rhabdomyosarcomas in human cases.

The stalwart procedure of identifying cross-
striations on a Masson's trichrome or

phosphotungstic acid hematoxylin (PTAH) stain or ultrastructural analysis has largely been supplanted by the use of immunostains and lack of disposable time and patience by today's veterinary pathologist.

The precise diagnosis in this case was also a subject of lively discussion. Some attendees favored a simple diagnosis of rhabdomyosarcoma, suggesting that the biphasic nature of this neoplasm may simply be a factor of sampling (as is often seen in osteosarcoma), or perhaps factors associated with metastatic environment. Ultimately, upon review of gross necropsy findings and current classification (as listed above), the group agrees with the contributor based on the distribution of metastases in multiple tissues as well as the alveolar pattern seem most prominently in the pulmonary metastatic focus.

References:

1. Akkoc A, Ozyigit MO, Yilmaz R, *et al.* Cardiac metastasizing rhabdomyosarcoma in a great Dane. *Vet Rec.* 2006;**156**:803-804.
2. Caserto BG. A comparative review of canine and human rhabdomyosarcoma with emphasis on classification and pathogenesis. *Vet Pathol.* 2013;**55**(5):806-826.
3. Ginel PJ, Martín de las Mulas J, Lucena R, *et al.* Skeletal muscle rhabdomyosarcoma in a dog. *Vet Rec.* 2002;**151**:736-738.
4. Maxie MG. Jubb, Kennedy, and Palmer's Pathology of domestic animals. *Elsevier.* 2016;**1**(3):241-244.
5. Morris JS, Bostock DE, McInnes EF, *et al.* Histopathological survey of neoplasms in flat-coated retrievers, 1990 to 1998. *Vet Rec.* 2000;**147**:291-295.
6. Newton WA, Gehan EA, Webber BL, *et al.* Classification of rhabdomyosarcomas and related sarcomas. *Cancer.* 1995;**76**(6):1073-1085.
7. Parham DM. Pathologic classification of rhabdomyosarcomas and correlations with molecular studies. *Mod Pathol.* 2001;**14**(5):506-514.
8. Parham MD, Barr FG. Classification of rhabdomyosarcoma and its molecular basis. *Adv Anat Pathol.* 2013;**20**(6):387-397.
9. Rudzinski ER, Anderson JR, Hawkins DS, *et al.* The World Health Organization classification of skeletal muscle tumors in pediatric rhabdomyosarcoma. *Arch Pathol Lab Med.* 2015;**139**(10):1281-1287.
10. Yhee J, Kim D, Hwang D, *et al.* Hematogenous metastasis of embryonal rhabdomyosarcoma originating from skeletal muscle in a young dog. *J Vet Diagn Invest.* 2008;**20**:243-246.
11. Zhao Z, Yin Y, Zhang J, *et al.* Spindle cell/sclerosing rhabdomyosarcoma: case series from a single institution emphasizing morphology, immunohistochemistry

and follow up. *Int J Clin Exp Pathol.*
2015;**8**(11):13814-13820.

Self-Assessment - WSC 2018-2019 Conference 24

1. Which of the following mutations is responsible for colonic aganglionosis in overo foals?
 - a. FGF-4
 - b. SLC4A2
 - c. Endothelin-3
 - d. Doublecortin

2. Which of the following is not usually seen with Vitamin E deficiency in horses?
 - a. Cerebellar hemorrhage
 - b. Hardened, hemorrhagic adipose tissue
 - c. Discoloration and striation of the skeletal muscle
 - d. Chronic enteritis

3. Which of the following is NOT true about equine Tyzzer's disease?
 - a. It is primarily a disease that affects the liver.
 - b. Foals are more susceptible than adult horses.
 - c. It is a disease only of mammals.
 - d. The bacilli may persist for long times in the environment.

4. Which is the most likely route of infection of *C. piliforme* in foals?
 - a. Oral
 - b. Conjunctival
 - c. Inhalation
 - d. Wound contamination

5. Which of the following Immunostains is selective for skeletal muscle?
 - a. Myoglobin
 - b. Muscle specific actin
 - c. Myogenin
 - d. Desmin

Please email your completed assessment to Ms. Jessica Gold at Jessica.d.gold2.ctr@mail.mil for grading. Passing score is 80%. This program (RACE program number) is approved by the AA VSB RACE to offer a total of 0.5 CE Credits, with a maximum of 12.5 CE Credits being available to any individual Veterinary Medical Professionals for the 2017-2018 Wednesday Slide Conference. This RACE approval is for the subject matter categories of: SCIENTIFIC using the delivery method of NON-INTERACTIVE DISTANCE. This approval is valid in jurisdictions which recognize AA VSB RACE; however, participants are responsible for ascertaining each board's CE requirements. RACE does not "accredit", "endorse" or "certify" any program or person, nor does RACE approval validate the content of the program.

Please email your completed assessment to Ms. Jessica Gold at Jessica.d.gold2.ctr@mail.mil for grading. Passing score is 80%. This program (RACE program number) is approved by the AAVSB RACE to offer a total of 0.5 CE Credits, with a maximum of 12.5 CE Credits being available to any individual Veterinary Medical Professionals for the 2017-2018 Wednesday Slide Conference. This RACE approval is for the subject matter categories of: SCIENTIFIC using the delivery method of NON-INTERACTIVE DISTANCE. This approval is valid in jurisdictions which recognize AAVSB RACE; however, participants are responsible for ascertaining each board's CE requirements. RACE does not "accredit", "endorse" or "certify" any program or person, nor does RACE approval validate the content of the program.

**Joint Pathology Center
Veterinary Pathology Services**



WEDNESDAY SLIDE CONFERENCE 2018-2019

C o n f e r e n c e 2 5

1 May 2019

CASE I: N261/13 (JPC 4037902).

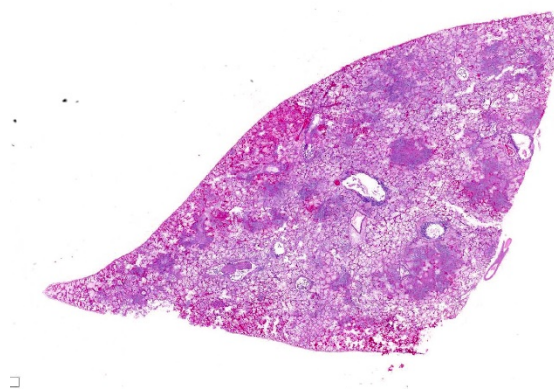
Signalment: 5 month old, female, Devon rex, *Felis domesticus*, feline.

History: This young, fully vaccinated, pedigree Devon rex cat with no previous history of illness became acutely ill with pyrexia and severe dyspnea, the morning following its attendance at a cat show where it had won both classes of competition for which it had been entered. Despite immediate veterinary attention and antibiotic treatment, the animal died within 36 hrs and was submitted for necropsy.

Gross Pathology: The carcass is well preserved with adequate body fat reserves. Periocular and perinasal regions are encrusted with light brown discharge. Tracheal and bronchial lumens filled with frothy mucopurulent exudate. There is multifocal consolidation in all lung lobes: on sectioning coalescing pale firm foci are present. The kidneys are bilaterally congested at the cortico-medullary junction. The stomach contains mucus only. Feces of normal color and consistency in rectum. The urinary bladder is empty.

Laboratory results: Both *Bordetella bronchiseptica* and *Mycoplasma felis* were cultured from samples of lung.

Microscopic Description: Multifocally, there is extensive necrosis of contiguous alveolar walls with filling of associated airspace with cell debris, protein-rich fluid/fibrin, and admixed intact and degenerate inflammatory cells (predominantly neutrophils with fewer macrophages and lymphocytes). Myriad loosely scattered to clumped basophilic coccobacilli (bacteria), and small numbers of



Lung, cat. Approximately 33% of the section is effaced by areas of hypercellularity centered on small airways, and there are multifocal, largely subpleural areas of hemorrhage and edema. (HE, 4X)

erythrocytes also noted in these areas. Bronchioles frequently contain similar inflammatory debris and bacteria, and focally, necrosis of bronchiolar epithelia is detected. Widespread hyperemia with small number of medium-caliber blood vessels variously exhibiting fibrinoid necrosis and leucocytoclastic vasculitis. Occasional thrombi noted (not visible in all sections).

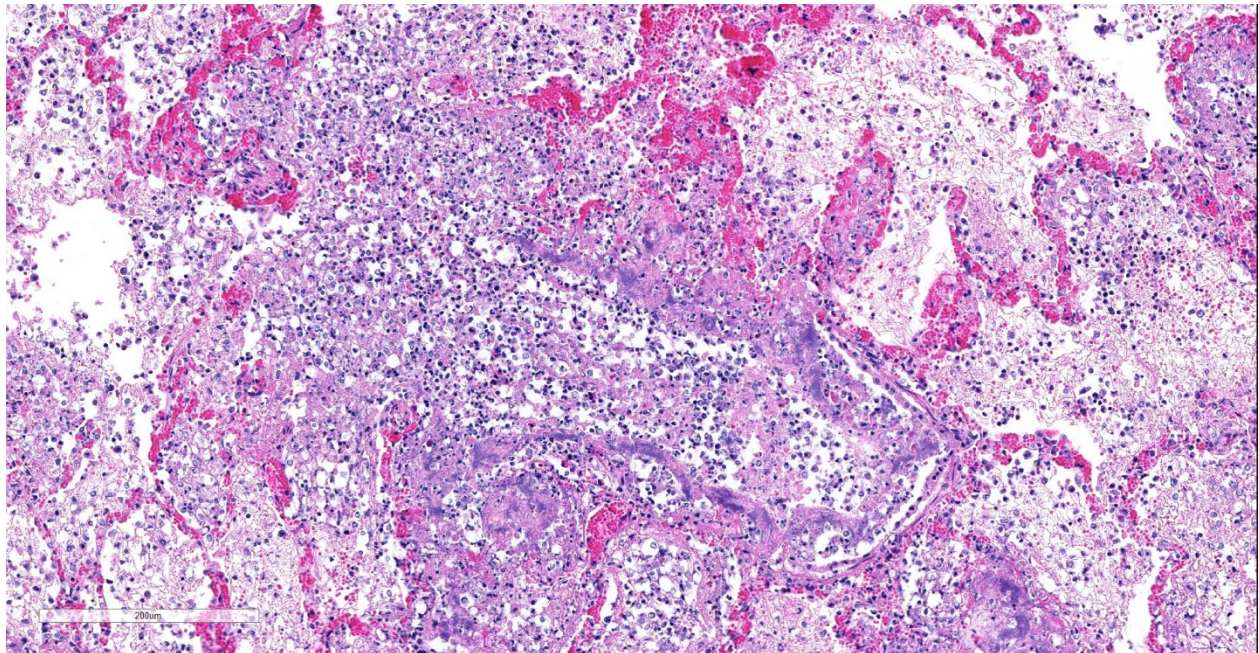
Contributor's Morphologic Diagnoses:

Lung: necrotizing bronchopneumonia, acute, severe with myriad bacteria (identified as *Bordetella bronchiseptica* on culture).

Contributor's Comment: *Bordetella bronchiseptica* is a gram-negative coccobacillus commonly carried in the nasopharynx of healthy cats. In a survey of respiratory pathogens in multi-cat (≥ 5 cats) households, *B. bronchiseptica* was detected by PCR in 5% of cats from households with disease, and in 1.3% of cats without.⁶ Considered a somewhat uncommon pathogen

in this species, infection typically manifests when pulmonary defenses are impaired by feline calicivirus or herpes virus infections, or by stressful environmental conditions (while occasional structures possibly suspicious of basophilic intra-nuclear inclusions were observed in bronchiolar gland epithelium in this case, these were considered equivocal: immunohistochemistry was not performed).^{2,4,10} The clinical consequences on infection can vary dramatically: from mild pyrexia, coughing and sneezing to severe pneumonia and death as seen in this case.

Details of the pathogenesis of infection in the cat are inferred from studies in other species. Bacterial virulence is regulated by the *Bordetella virulence gene (bvg) operon*, which orchestrates the expression of the adhesin filamentous haemagglutinin (FHA), pertactin, and the fimbriae that facilitate adherence to the ciliated epithelium, as well as to macrophages and neutrophils within the



Lung, cat. Areas of inflammation are centered on necrotic airways, which are filled with numerous viable and degenerate neutrophils, cell debris, fibrin, and bacterial colonies. The exudate has ruptured through the wall and spilled into the surrounding alveoli. (HE, 163X)

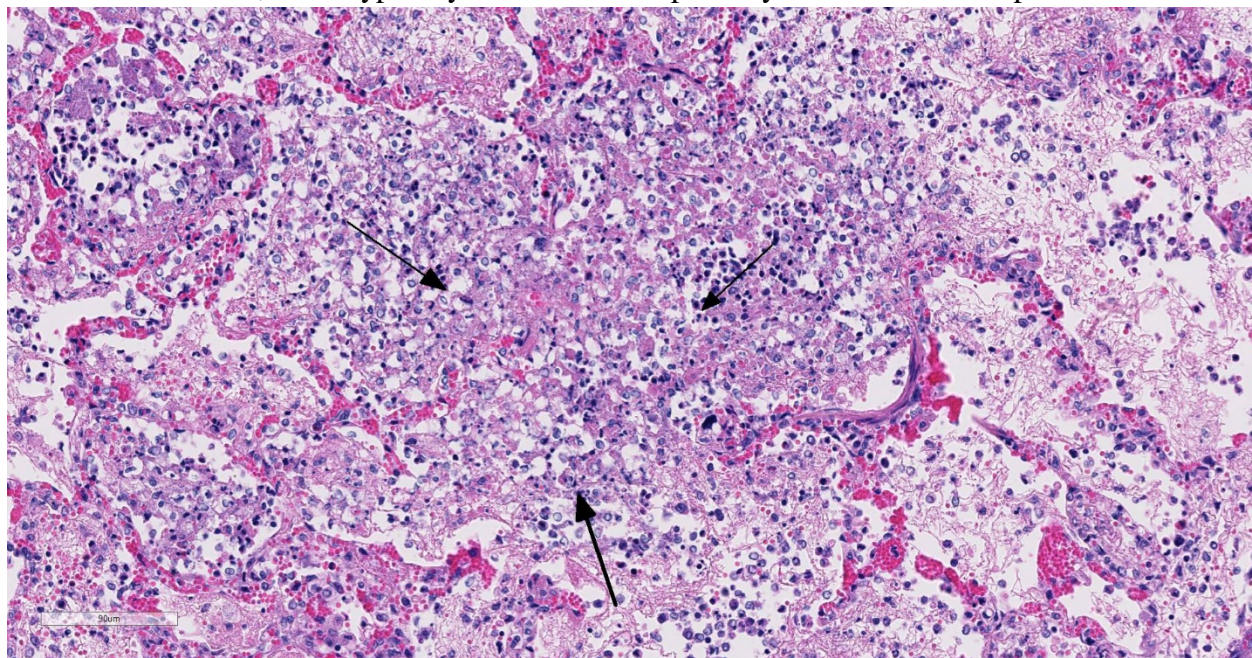
lungs.^{2,6} Following attachment the pathogen secretes the RTX adenylate cyclase toxin (hemolysin) that results in impaired leucocyte phagocytosis and oxidative burst, and may induce their apoptosis. A lipooligosaccharide with endotoxin activity and a soluble peptidoglycan-derived tracheal cytotoxin are also produced that induce ciliostasis and the apoptosis of ciliated epithelial cells.^{2,6}

Bacterial culture (as in this case) and PCR are used to conform the diagnosis, although both lack sensitivity.^{6,9} In regions where vaccines against *B. bronchiseptica* are available, it is recommended that cats should not be routinely vaccinated, given the typically mild disease that occurs. However, vaccination is encouraged in units such as shelters where populations are in continuous turnover, and thus at increased risk of infectious disease.⁶ Organisms are shed in oral and nasal secretions of infected cats and infected dogs are considered an infection risk for cats.^{5,6} Rare zoonosis, typically in

immunocompromised individuals, have been reported.^{8,11}

Mycoplasma felis can colonize the upper respiratory tract of cats, but evidence suggests it is not a significant primary pathogen. Molecular detection techniques have found *Mycoplasma* spp in the lower respiratory tract of 15.4% of cats with respiratory disease, with *M. felis*, *M. gateae* and *M. feliminutum* the species identified. However, the pathogenic significance of their presence remains unclear.⁷ It is likely that *M. felis* contributed to the severity of the pneumonia in this case through opportunist secondary involvement.

This case represented a sudden and highly traumatic loss for the owner concerned as they witnessed the rapid clinical deterioration and death of their prize-winning animal over a period of 36 hrs. We may speculate that contact with other cats at the cat show provided a source of the infection, and how possibly the stress of transport or attendance



Lung, cat. Within affected areas there are discontinuous alveolar septa, characteristic of septal necrosis (black arrows.) (HE, 313X)

at this event could have precipitated disease. In any event, the rapidity of disease progression suggests the strain of *B. bronchiseptica* involved was particularly virulent.

Contributing Institution:

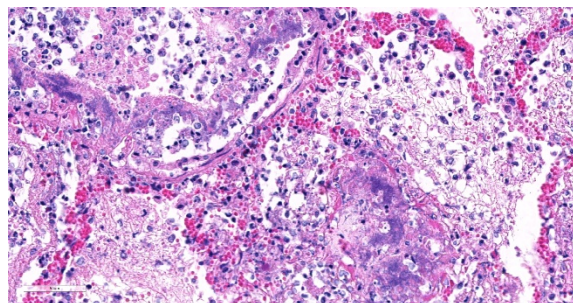
Room 012, Veterinary Sciences Centre,
School of Veterinary Medicine, University
College Dublin, Belfield, Dublin 2, Ireland
<http://www.ucd.ie/vetmed/>

JPC Diagnosis: Lung: Bronchopneumonia, fibrinosuppurative and necrotizing, multifocal to coalescing, severe, with numerous bacterial colonies.

JPC Comment: The contributor has provided an excellent review of *Bordetella bronchiseptica* in this case, as well as the pathogenesis of the disease across species lines. *Bordetella bronchiseptica* is an important, if sporadic, pathogen of the respiratory system in a wide range of mammalian species. Previous WSC cases include *Bordetella bronchopneumonia* infection in a chinchilla (WSC 2014-2015, Conf 18, Case 4), an African green monkey (WSC 2011-2012, Conf 22, Case 3), squirrel monkeys (WSC 2007-2008, Conf 9, Case 3), pigs (WSC 1996-1997, Conf 20, Case 2), a rabbit (WSC 1995-1996), among others.

There are three species of *Bordetella* of veterinary importance, including *B. bronchiseptica* (whose dermonecrotic toxin also causes atrophic rhinitis in pigs and rabbits), *B. hinzii* which causes limited respiratory disease in turkey poults and rare septicemia in humans, and *B. pertussis* a potent pathogen in humans which may cause lower respiratory disease in lambs.

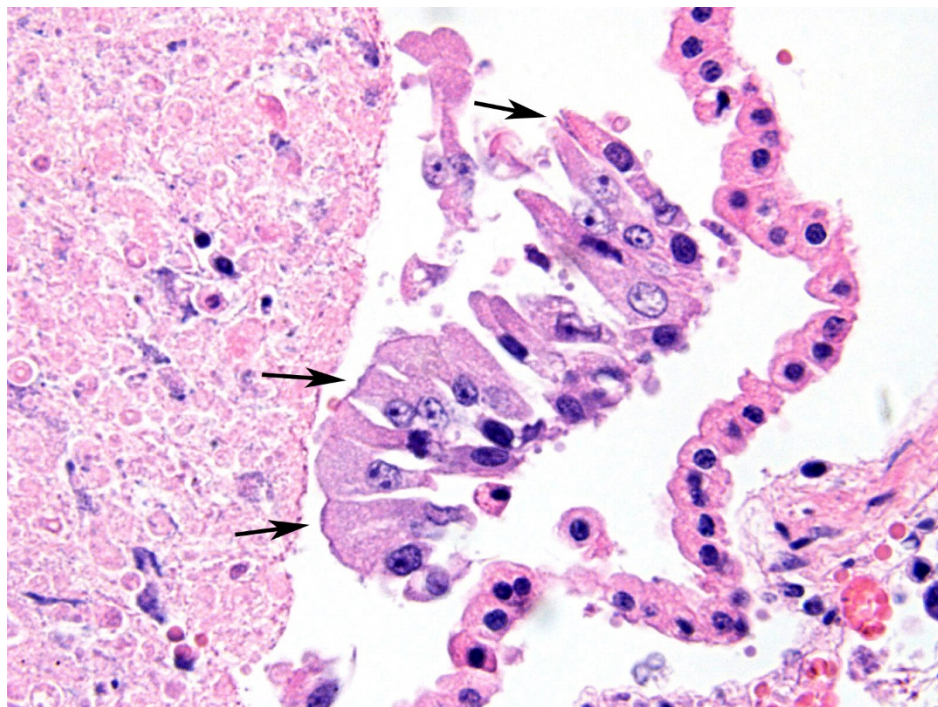
Well known for its involvement in non-fatal tracheobronchitis (aka “kennel cough”), a recent publication⁹ has detailed *Bordetella*'s



Lung, cat. Large colonies of bacilli are present within airways and alveoli in close proximity. (HE, 400X)

role in fatal pneumonia as exemplified in this case. *B. bronchiseptica* has been identified in between 12 and 78% of dogs with lower respiratory tract infections, and 5-13% of cats.⁹ At a major university veterinary school, a retrospective study identified *B. bronchiseptica* via immunohistochemistry and/or bacterial culture in 8 of 36 of canine and 14 of 31 feline cases of fatal bronchopneumonia. Upon close review, bacteria could be visualized among the cilia in 4 of 36 canine cases and 5 of 31 feline cases.⁹ Close review of columnar epithelium in this case also disclosed the presence of cilia-associated bacteria; it was seen only on intact cells, as necrotic or attenuated epithelium has probably already lost its cilia. This may be an important finding in such cases, as the lesions associated with the bronchopneumonia in these cases, in the authors' opinion, were not specific for any particular pathogen.

Bordetella bronchiseptica can be an opportunistic pathogen in humans as well, particularly immunosuppressed individuals and cystic fibrosis patients. *B. bronchiseptica* and *B. pertussis*, (the causative agent of whooping cough) exhibit little genetic variation,¹ with *B. pertussis* being a more recent derived, human adapted bacterium derived as a consequence of gene deletions and loss of genetic regulatory functions. Both organisms possess the *Bordetella* virulence gene as discussed



Lung, cat: Careful evaluation of the HE slide may disclose the presence of bacilli lining cilia of columnar airway epithelium (arrows). Necrotic or attenuated epithelium likely lack cilia, so are not worthy of inspection. (HE, 600X)

above. In a large children's CF center, 7 patients had multiple repeated isolates of *B. bronchiseptica* from their airways. All patients had documented exposure to pets or lived on a farm or an operating kennel, resulting in an overall infection of as many as 12% of children in the center at any time.¹

One of the issues associated with persistence of *Bordetella* infections in human patients leading to vaccine failures and re-emergence of disease has been recently elucidated – the ability for this bacterium to produce biofilms.³ This is yet another feature of the BvgAS gene, which regulates the expression of genes encoding surface membrane, secreted, and regulatory proteins from host cells, as well as filamentous hemagglutinin, pertactin, fimbriae and various toxins which contribute to the extracellular matrix comprising the *Bordetella* biofilm.³

The moderator reviewed the general patterns

of pneumonia in the lung across animal species. In this particular case, attendees were split on whether the appropriate morphologic diagnosis would be bronchopneumonia (based on the traditional pathogenesis of this aerogenous bacteria and the obvious necrosis within airways) or bronchiointerstitial, based on the widespread necrosis of alveolar septa, pulmonary vessels, and exudative

alveolitis in much of the section

References:

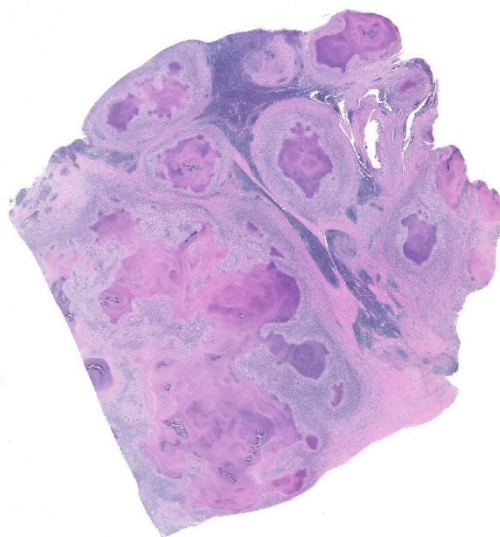
1. Brady C, Ackerman P, Johnson M, McNamara J. *Bordetella bronchiseptica* in a pediatric cystic fibrosis center. *J Cystic Fibrosis*, 2014 13:43-48
2. Caswell JL, Williams KJ: The Respiratory System. In: Jubb, Kennedy and Palmer's Pathology of Domestic Animals, ed. Maxie MG, 5th ed., vol. 2, Philadelphia, PA: Elsevier; 2007: 216-219.
3. Cattelan N, Dubey P, Arnal L, Yantorno OM, Deora R. *FEMS Pathog Dis* 2016; doi 10.1093/femspd/ftv108.
4. Coutts AJ, Dawson S, Binns S, Hart CA, Gaskell CJ, Gaskell RM. Studies

- on natural transmission of *Bordetella bronchiseptica* in cats. *Vet Microbiol* **48**:19–27, 1996.
5. Dawson S, Gaskell CJ, McCracken CM, Gaskell RM, Hart CA, Jones D. *Bordetella bronchiseptica* infection in cats following contact with infected dogs. *Vet Rec* **146**: 46–48, 2000.
 6. Egberink H, Addie D, Belák S, Boucraut-Baralon C, Frymus T, Gruffydd-Jones T, Hartmann K, Hosie MJ, Lloret A, Lutz H, Marsilio F, Grazia Pennisi M, Radford AD, Thiry E, Truyen U, Horzinek MC. *Bordetella Bronchiseptica* Infection in Cats: ABCD guidelines on prevention and management. *J Fel Med Surg* **11**:610-614, 2009.
 7. Reed N, Simpson K, Ayling R, Nicholas R, Gunn-Moore D. *Mycoplasma* species in cats with lower airway disease: improved detection and species identification using a polymerase chain reaction assay. *J Fel Med Surg* **14**: 833–840, 2012.
 8. Register KB, Sukumar N, Palavecino EL, Rubin BK, Deora R. *Bordetella bronchiseptica* in a paediatric cystic fibrosis patient: Possible transmission from a household cat. *Zoonoses Public Hlth* **59**: 246–250, 2012.
 9. Taha-Abdelaziz K, Bassel LL, Harness ML, Clark ME, Register KB, Caswell JL. Cilia-associated bacteria in fatal *Brodetella bronchiseptica* pneumonia of dogs and cats. *J Vet Diagn Investig* 2016; 28(4)369-376.
 10. Welsh RD. *Bordetella bronchiseptica* infections in cats. *J Am Anim Hosp Assoc* **32**: 153–158, 1996.
 11. Woolfrey BF, Moody JA. Human infections associated with *Bordetella bronchiseptica*. *Clin Microbiol Rev* **4**: 243–255, 1991.

CASE II: 2014 Case 2 (JPC 4050143).

Signalment: Juvenile (<30 months), unreported gender, unreported breed, *Bos taurus*, bovine.

History: The bovine was presented for slaughter at a United States Department of Agriculture (USDA) federally inspected slaughter facility and passed antemortem inspection. The carcass was retained for further diagnostic testing after lesions suspicious for bovine tuberculosis were observed in lymph nodes of the head, thoracic, and abdominal cavities and lungs during postmortem inspection.



Lymph node, ox: The node is effaced by multiple, often coalescing granulomas. (HE, 5X)

Gross Pathology: None

Laboratory results: PCR from formalin-fixed, paraffin-embedded tissues were positive for IS6110 (*Mycobacterium tuberculosis* complex) and negative for IS900 (*M. avium paratuberculosis*) and 16S rDNA (*M. avium* complex). Culture recovered *M. bovis*.

Microscopic Description:

Lymph node. Up to 80% of the parenchyma (there is some slide variability) is effaced by coalescing to locally extensive granulomas. Granulomas are composed of central areas of caseous necrosis and variable amounts of basophilic granular material (mineral) rimmed by large numbers of epithelioid macrophages and multinucleated giant cells surrounded peripherally by lower numbers of lymphocytes, plasma cells, fibroblasts, and fibrous connective tissue. Giant cells have up to 10 peripheral nuclei (Langhans type). There are rare, ~5µm long, acid-fast bacilli

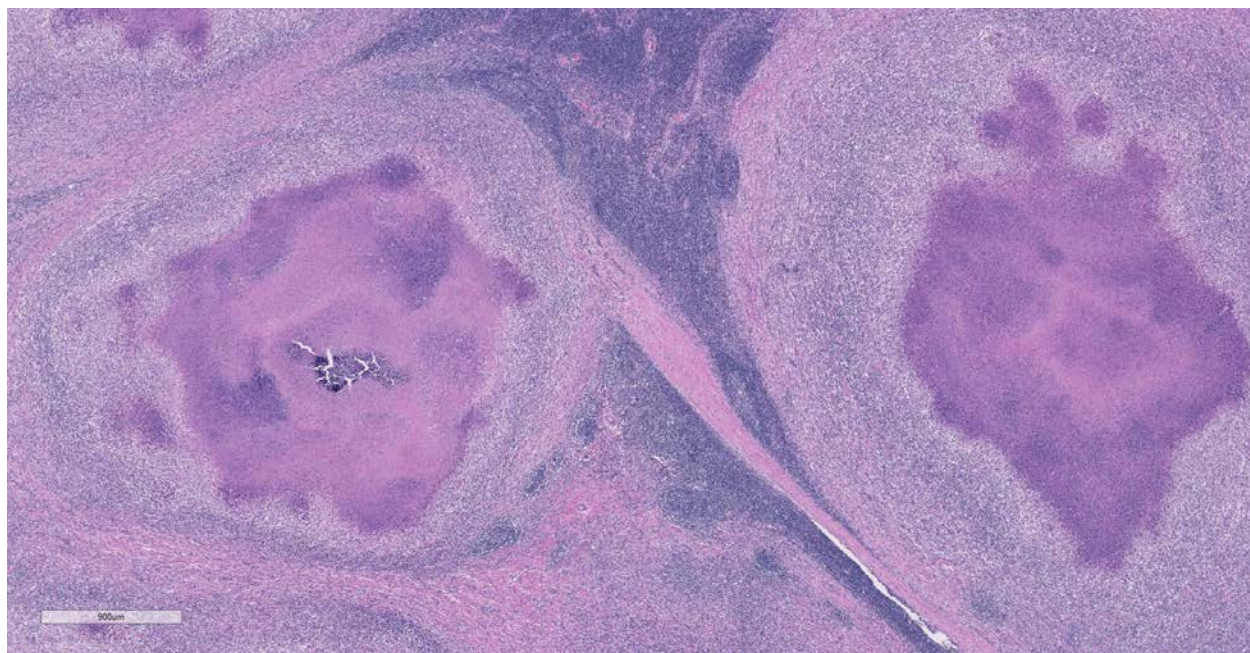
within areas of necrosis and the cytoplasm of macrophages and giant cells.

Contributor's Morphologic Diagnoses:

Lymph node: Lymphadenitis, necrogranulomatous, locally extensive, chronic, severe, *Bos taurus*.

Contributor's Comment:

Mycobacterium bovis causes tuberculosis in many mammals, including cattle and is a zoonotic disease. Cattle slaughtered for consumption in the United States in federally inspected abattoirs undergo inspection by personnel from the Food Safety Inspection Service (FSIS) of the USDA to insure they are safe and wholesome for entry into the market. In accordance with the USDA's Bovine Tuberculosis Eradication Program, FSIS personnel retain carcasses when lesions resembling tuberculosis are identified. Suspect granulomas from these cattle are collected and submitted to the National Veterinary



Lymph node, ox: Granulomas have a thick, often central core of cellular debris, which is occasionally mineralized. The intervening remnant node is hyperplastic. (HE, 23X)

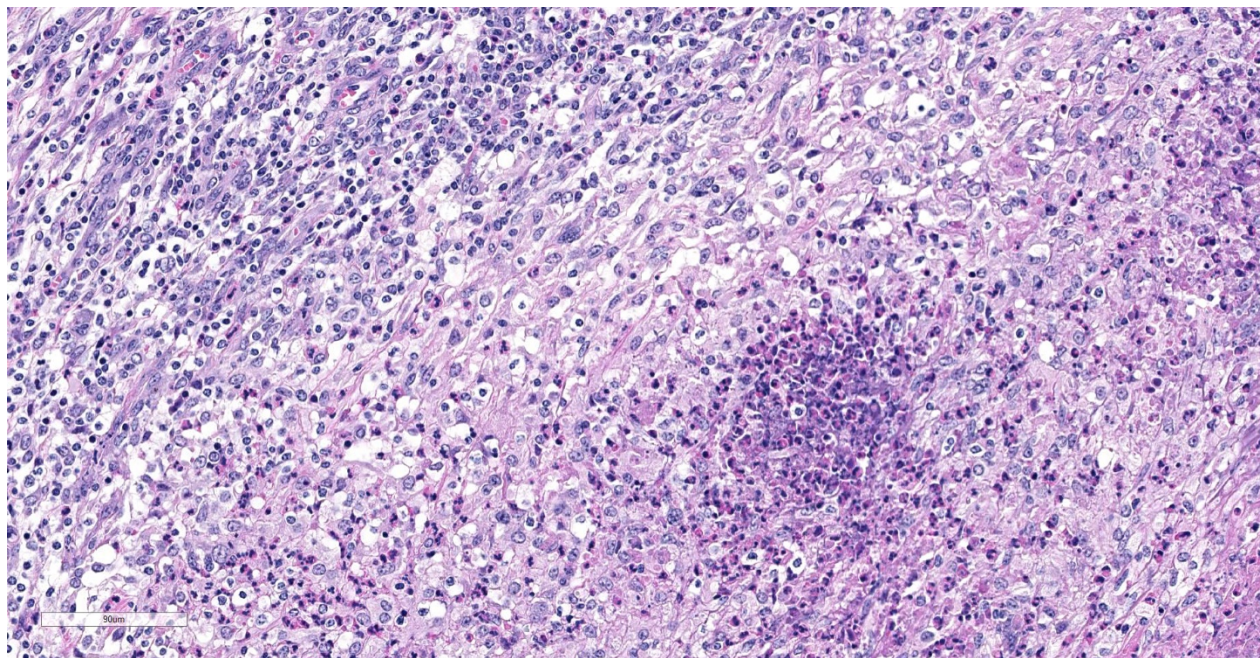
Services Laboratories (NVSL) for histopathology and culture.⁸

Microscopic lesions consistent with tuberculosis in cattle are often multicentric and coalescing with central areas of caseous necrosis and mineral. Epithelioid macrophages with small to moderate numbers of Langhans-type multinucleated giant cells surround the necrosis with smaller numbers of peripheral lymphocytes, plasma cells, and occasional neutrophils.² The typical tuberculous lesion caused by *Mycobacterium bovis* has rare to occasionally moderate numbers of acid-fast bacteria present within the cytoplasm of macrophages and giant cells as well as in areas of necrosis.²

Bovine cases that are histologically compatible with tuberculosis undergo additional testing at NVSL by means of PCR on formalin-fixed, paraffin-embedded (FFPE) tissue to test for mycobacterial DNA. Because the scope of the TB eradication

program is focused on identifying *M. bovis*, primers used in the PCR are limited to those for *M. tuberculosis* complex (MTBC, of which *M. bovis* is a member), *M. avium* complex (MAC, common environmental mycobacteria) and *M. avium paratuberculosis* (MAP, the bacterium that causes Johne's disease in cattle). A recent report⁷ of mycobacteria cultured from clinical samples submitted to the NVSL stated that the majority of mycobacteria cultured from cattle were *M. bovis* (32%) followed by *M. avium* complex (25.5%). The next most common species, *M. fortuitum*/*M. fortuitum* complex, comprised 10.1%.⁷

The microscopic features of the current case were consistent with bovine tuberculosis and FFPE tissue was tested by PCR for mycobacterial DNA using our primers for MTBC, MAC, and MAP. PCR was positive for the MTBC primer sets and negative for MAC and MAP. False negative results for mycobacterial DNA can occur in some cases. The more common reasons for false negative



Lymph node, ox: The periphery of the node contains numerous epithelioid macrophages and aggregates of neutrophils, and more peripherally (HE, 238X)

PCR results include tissue being fixed in formalin for an extended period of time (>7 days) and and/or extremely low numbers of AFB present in the lesion or tissue section. Formalin fixation causes irreversible cross-linking between DNA and protein, which becomes worse as the tissue fixes over time.³

Culture, which is considered the gold standard for definitive diagnosis of bovine tuberculosis² and can take up to 10 weeks to complete with slow-growing mycobacteria, recovered *M. bovis*.

Mycobacterium bovis is a member of the *M. tuberculosis* complex, which includes *M. tuberculosis*, *M. africanum*, *M. canettii*, *M. pinnipedii*, *M. caprae*, *M. microti*,⁵ and the newly described *M. mungi*.¹ *M. bovis* can cause disease in cattle as well as humans and other domesticated and wild mammals. Currently, *M. bovis* is endemic in various populations of wildlife and are a source for re-infection of domesticated animals in regions of the United States (white-tailed deer, *Odocoileus virginianus*), Spain (wild boar, *Sus scrofa*), United Kingdom (Eurasian

badgers, *Meles meles*), and New Zealand (brushtail possums, *Trichosurus vulpecula*).⁶

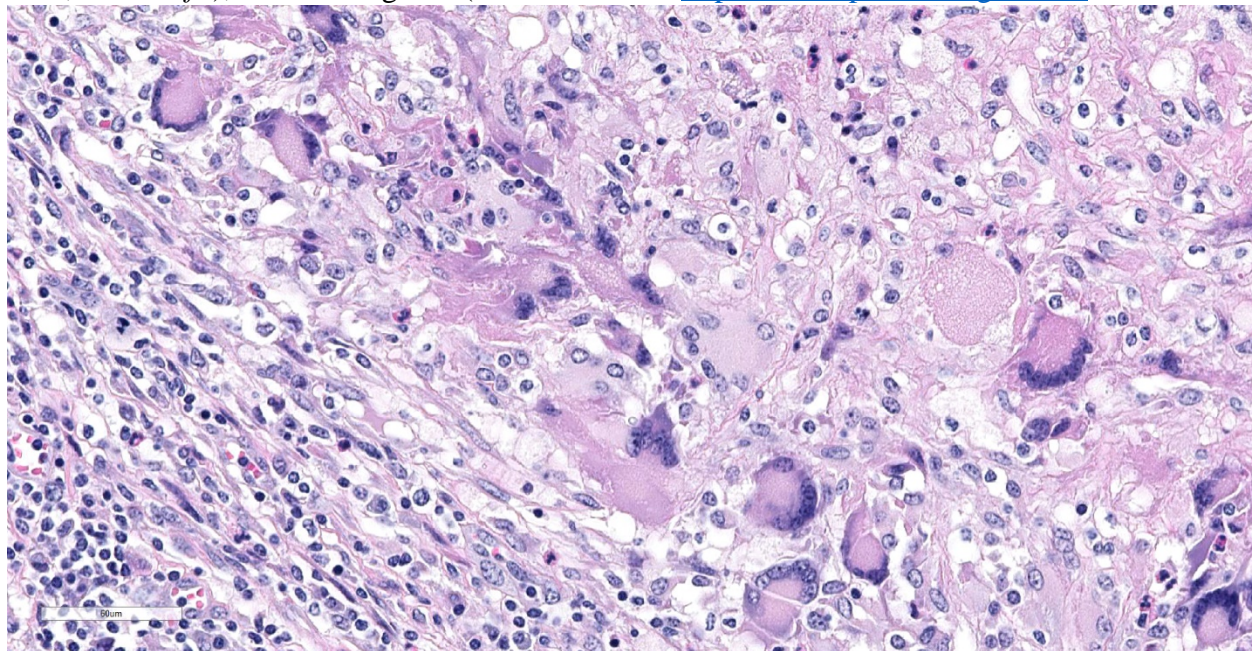
Disease manifestation can vary, but *M. bovis* typically causes granulomatous inflammation in the lungs and lymph nodes of the head (retropharyngeal), chest (tracheobronchial and mediastinal) and/or abdomen (mesenteric), often reflecting the route of transmission (inhalation or ingestion).^{2,7} Grossly, the classic tubercle is encapsulated, pale yellow, and often has a caseous core that may be variably mineralized.² Clinically, the only sign of infection may be chronic weight loss (wasting), weakness, loss of appetite, fluctuating fever, cough, exercise intolerance, and lymphadenomegaly.⁹ Most animals that are infected with *M. bovis* do not develop clinical disease.²

Contributing Institution:

National Centers for Animal Health, Ames, IA

http://www.ars.usda.gov/main/site_main.htm?modecode=36-25-30-00

<http://www.aphis.usda.gov/nvsl>



Lymph node, ox: Numerous Langhans giant cells are present at the periphery of the granulomas. (HE, 238X)

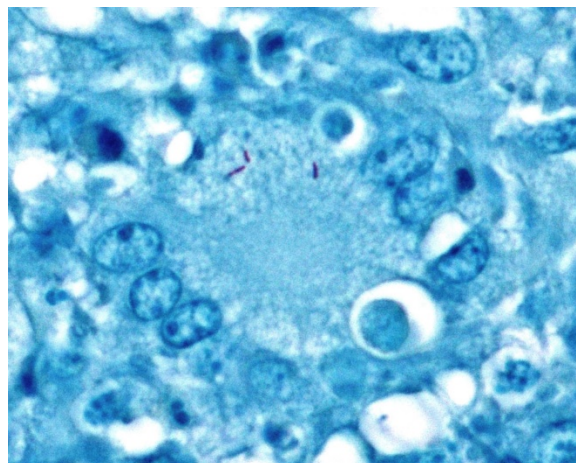
JPC Diagnosis: Lymph node: Lymphadenitis, granulomatous, multifocal to coalescing, severe, with diffuse moderate follicular and paracortical hyperplasia.

JPC Comment: The contributor does an excellent job reviewing the thorough protocol used to investigate tissue suspected of - *Mycobacterium bovis* infection at the National Veterinary Services Laboratory, an important link in food safety in the United States.

M. bovis is a member of the growing *M. tuberculosis* complex as described above. A recent publication⁴ noted the divergent pathogenesis in non-bovine hosts in several countries of the world which have been incriminated in maintaining infection in local livestock.

In the North America, the white-tailed deer, and to a lesser extent, elk harbor the infection and potentiate the infection through contact with cattle in their pasturing area. Infected lymph nodes in deer often have soft centers, resembling abscesses; however neutrophils, as seen in cattle, are not a feature of the lesion.⁴ Approximately 30-35% of infections exhibit spread to the thoracic viscera, and often the pleural surfaces, where they form pearlescent nodules reminiscent of mesothelioma.

In England and Ireland, the Eurasian badger (*Meles meles*) has been indicted as a major factor in outbreaks of cattle with bovine tuberculosis. In the badger, respiratory infection is most common with 50% cases showing pulmonary infection, and 35% of cases involving lymph node. Elongate radial lesions may be seen in the kidneys, and miliary lesions may be seen in the liver and spleen. Many infected badgers show no visible gross lesions.⁴



Lymph node, ox. Three acid-fast bacilli, approximately 5-7µm, within the cytoplasm of a multinucleated giant cell. Modified Ziehl-Neelsen., 1000X)

In western Europe, wild boars serve as wildlife reservoirs of *Mycobacterium bovis*. This species, well known as highly susceptible to *M. bovis*, has been used as a sentinel species to screen for *M. bovis* in Hawaii and New Zealand. Disseminated infection is the rule in this species, with lesions in multiple anatomic regions, including cranial lymph nodes and mandibular lymph nodes, lungs, liver, and spleen.⁴

In New Zealand, the brushtail possum (*Trichosurus vulpecula*) is considered a source of infection for cattle. Highly susceptible, they manifest the disease by infection of subcutaneous lymph nodes, forming draining fistulous tracts. Terminally ill possums attract cattle by wandering erratically across pastures, and curious cattle may sniff and lick them, thereby receiving exposure to the bacteria. In these regions, infected wild ferrets may also be infected, but their role in spreading the infection to cattle is controversial – a reduction in possum population in these areas results in a proportional decrease in infection of this carnivore, suggesting that the ferret is a spillover host at best.⁴

The participants agreed that an alternate JPC diagnosis of multiple lymph node granulomas would be acceptable as well. As this was the last conference of the 2018-2019 year, the box containing the age-old discussion of “granulomatous versus granuloma” was quickly slammed shut.

References:

- 1 Alexander KA, Laver PN, Michel AL, Williams M, van Helden PD, Warren RM, Gey van Pittius NC: Novel *Mycobacterium tuberculosis* complex pathogen, *M. mungi*. *Emerg Infect Dis* **16**: 1296-1299, 2010
- 2 Caswell JL, Williams KJ: Respiratory system. *In*: Jubb, Kennedy, and Palmer's Pathology of Domestic Animals, ed. Maxie MG, pp. 523-653. Saunders Elsevier, St. Louis, 2007
- 3 Fang SG, Wan QH, Fujihara N: Formalin removal from archival tissue by critical point drying. *Biotechniques* **33**: 604-611, 2002
- 4 Fitzgerald SD and Kaneene JB. Wildlife reservoirs of bovine tuberculosis worldwide: hosts, pathology, surveillance, and control. *Vet Pathol* 2013; 50(3):488-499.
- 5 Olsen I, Barletta RG, Thoen CO: *Mycobacterium*. *In*: Pathogenesis of Bacterial Infections in Animals, pp. 113-132. Wiley-Blackwell, 2010
- 6 Palmer MV, Thacker TC, Waters WR, Gortázar C, Corner LAL: *Mycobacterium bovis*: A model pathogen at the interface of livestock, wildlife, and humans. *Vet Med Int* **2012**: 17, 2012
- 7 Palmer MV, Waters WR: Advances in bovine tuberculosis diagnosis and pathogenesis: What policy makers

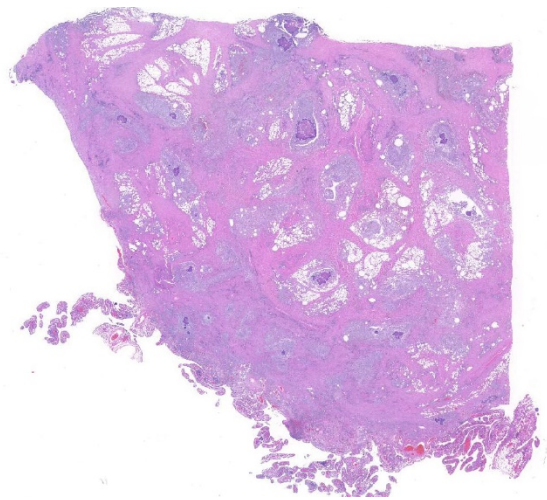
need to know. *Vet Microbiol* **112**: 181-190, 2006

- 8 Thacker T, Robbe-Austerman S, Harris B, Palmer MV, Waters WR: Isolation of mycobacteria from clinical samples collected in the United States from 2004 to 2011. *BMC Vet Res* **9**:100, 2013
- 9 Thoen CO: Overview of tuberculosis and other mycobacterial infections. *In*: The Merck Veterinary Manual Online, eds. Aiello SE, Moses MA. 2012

CASE III: S-2017-20 (JPC 4100993).

Signalment: 6-year and 5-month old female neutered crossbreed dog (*Canis lupus familiaris*).

History: A 6-year 5 months-old female neutered Springer Spaniel Cross presented for investigation of pyrexia of unknown origin of 5 months duration. The owner also noted lethargy and mild gastrointestinal signs during this time (inappetence and diarrhoea). Previously the patient had responded well to oral prednisolone and potentiated amoxicillin, however symptoms recurred



Omentum, dog. The omentum is markedly expanded, and largely effaced by multifocal to coalescing pyogranulomas. (HE, 4X)

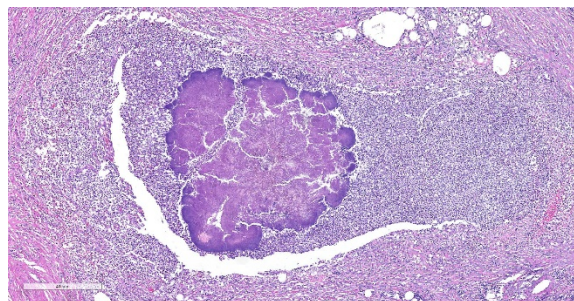
after the treatment was stopped. On physical examination, marked pyrexia of 40.3C was noted, with tachycardia of 160 beats per minute and normal synchronous pulses. A normal respiratory rate of 32 breaths per minute with normal respiratory effort was noted. Auscultation of the thorax was unremarkable. Mucous membranes were pink and moist, with CRT <2s. Mild discomfort was noted on deep palpation of the cranial abdomen, which was subjectively mildly bloated. Rectal examination was unremarkable and peripheral lymph nodes were within normal limits. Abdominal ultrasound showed free fluid within the abdomen. At exploratory laparotomy the abdomen was diffusely filled with creamy pink fluid and there were multiple masses in the omentum and mesentery of the jejunum, which were sampled for histopathology.

Gross Pathology: In a multifocal to coalescing pattern, the greater omentum was expanded by irregular, tan to brown to dark red and moderately firm mass-like lesions with cream to tan, multifocally red cut surfaces. The adjacent omentum was tan to brown, and soft.

Laboratory results: Haematology: WBC count $18.2 \times 10^9/L$ (ref 6-17), otherwise unremarkable. Biochemistry: C-reactive protein 26.3mg/L (ref 0-8.2) and hypoalbuminaemia 17g/L (ref 25-41). ALT was mildly decreased and AST was mildly increased. Abdominal fluid sample: Cytology of aspirated abdominal fluid showed neutrophilic macrophagic inflammation with phagocytosed bacteria and was consistent with a septic exudate. Culture of omental masses: *Actinomyces* spp. was cultured.

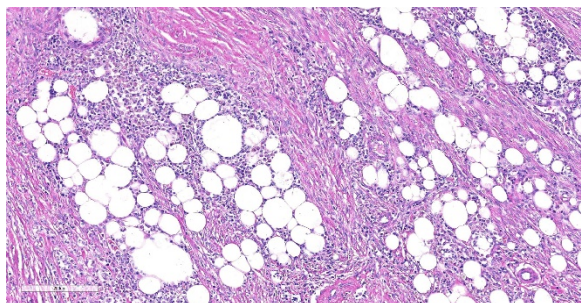
Microscopic Description:

Expanding and effacing the collagenous connective tissue and adipose tissue of the omentum, in a multifocal to coalescing



Omentum, dog. Pyogranulomas are centered on large colonies of filamentous bacilli which range up to a mm in diameter. (HE, 63X)

distribution, are large numbers of macrophages, neutrophils and lesser numbers of lymphocytes, which are often forming moderately sized to large groups. Small to moderate numbers of plasma cells are present multifocally, often at the periphery of these groups and multifocally within the connective tissue and adipose. Large numbers of macrophages and neutrophils often surround large colonies of filamentous Gram-positive bacteria, measuring approximately $1 \times 3-7 \mu m$. Bacteria are admixed with large (approximately $500 \mu m$ diameter) accumulations of finely granular basophilic to eosinophilic material which radiates outwards from a central focus (Splendore-Hoeppli material; “sulphur granules”). These colonies often show a rosette-like arrangement and are visible subgrossly. Small amounts of eosinophilic material, cellular debris, haemorrhage and small numbers of haemosiderin-laden macrophages (haemosiderophages) multifocally surround the colonies. Further to the periphery of these foci are haphazardly arranged, hypertrophied fibroblasts embedded in fibrous connective tissue which often progresses to thick bands of mature fibrous connective tissue, containing scattered to moderate numbers of neutrophils, lymphocytes, plasma cells, and fewer macrophages.



Omentum, dog. There is mild granulomatous inflammation focused on areas of remnant adipose tissue. (HE, 150X)

The omentum is lined by flattened to multifocally plump mesothelial cells and exhibits multifocal ulceration. Underlying ulcerated areas there are frequent plump reactive fibroblasts, aligned in parallel to each other and perpendicular to adjacent, newly formed blood vessels (angiogenesis) and to the ulcerated surface (granulation tissue formation). At the edges of the section the omentum exhibits a multifocal folded appearance and contains numerous, frequently congested, blood vessels and is expanded by variable numbers of macrophages, lymphocytes, neutrophils, plasma cells, and fibroblasts.

Contributor's Morphologic Diagnoses:

Greater omentum: Peritonitis, pyogranulomatous, lymphocytic, and plasmacytic, chronic, locally extensive, severe; with:

- a. Numerous accumulations of Splendore-Hoeppli material with intralesional microcolonies of Gram-positive filamentous rod bacteria, morphology consistent with *Actinomyces* spp.;
- b. Granulation tissue formation, chronic, multifocal, marked; and
- c. Fibrosis, chronic, multifocal, marked.

Contributor's Comment: The histopathological findings in this case were consistent with abdominal actinomycosis, a diagnosis that was supported by the microbiology results. The patient had an abdominal drain placed at the time of exploratory laparotomy and was subsequently hospitalized for 6 days. Antibiotic treatment with amoxicillin-clavulanic acid commenced following receipt of the histopathology and culture results, and treatment resulted in good clinical improvement and a positive outcome.

Actinomycosis is caused by filamentous, gram-positive bacteria from the family Actinomycetaceae, genus *Actinomyces*, and to a lesser extent to the related genus *Arcanobacterium*. These bacteria are normally present in the mucous membranes, especially in the oropharynx, and in the genital and gastrointestinal tracts, having however the potential to cause opportunistic infection when inoculated into tissues in association with other bacteria when there is mechanical disruption of normal mucosal barriers (such as deeply penetrating wounds or migration of foreign material).^{7,14}

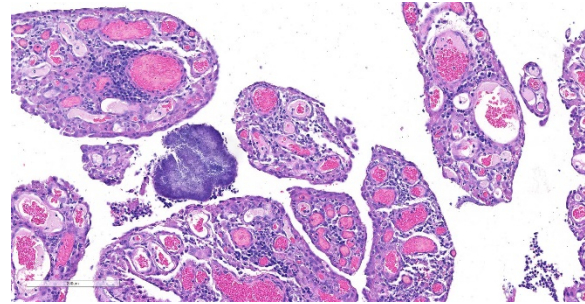
Canine actinomycosis is most common in young adult to middle-aged large breed dogs (median age of 5 years old) that have outdoor access, especially retriever and hunting breeds. The development of actinomycosis in outdoor dogs is frequently related to exposure to plant penetrating material, such as grass awns.^{7,14} After ingestion or inhalation, plant awns become contaminated with *Actinomyces* spp. and other bacteria from the oropharynx, and then migrate to various sites.^{6,7,14}

Actinomyces spp. can also be inoculated into tissues by bite injury. Other co-infecting aerobic and anaerobic bacteria from the oral cavity or intestinal tract impair normal host

defenses and reduce oxygen tension, which allows *Actinomyces* spp. to endure.^{7,14} Abdominal actinomycosis, as seen in this case, may develop when ingested foreign bodies penetrate the gastrointestinal tract, which leads to the formation of intra-abdominal mass lesions and ascites or it can also occur due to direct extension from subcutaneous tissues or hematogenous spread of the organism to abdominal organs such as the liver.^{9,14}

Actinomyces spp. that have fimbriae can bind to specific cell surface receptors on other bacteria, especially streptococci, and this bacterial co-aggregation prevents the capacity of neutrophils to phagocytize the organisms.^{13,14} Dense colonies of *Actinomyces* spp. form, and these 'Sulfur' granules can be macroscopically visible in exudates in actinomycosis as small yellow free granules.¹⁵ The colonies are progressively encircled by concentric accumulations of neutrophils, macrophages, and plasma cells, with the ensuing development of pyogranulomatous inflammation¹⁴ and are often bordered by star-like or club-shaped-like amorphous eosinophilic material (Splendore-Hoeppli material).

The connective tissue is destroyed by proteolytic enzymes from the associated bacteria, macrophages and degranulated neutrophils, which allows the inflammatory process to extend through normal tissue planes. Less frequently *Actinomyces* spp. spreads hematogenously to distant sites. In some cases, the inflammatory reaction is accompanied by mass formation and extensive fibrosis, as in this case. The most common clinical forms of actinomycosis in dogs and cats involve the cervicofacial region, thorax, abdomen, and subcutaneous tissue, but central nervous system infections including meningitis and



Omentum, dog. At the edge of the section, there are mesothelial lined papillary projections of fibrous connective tissue, and bacterial colonies ("granules") within the extracellular space. (HE, 150X)

meningoencephalitis,^{5,14} and ocular infections such as keratitis and endophthalmitis,³ may also occur.

In cattle, actinomycosis, caused by *Actinomyces bovis*, often affects the bones of the jaw, with development of granulomatous and fibrosing osteomyelitis ('lumpy jaw'). Less commonly it can also affect the musculature of the tongue, leading to the development of chronic fibrosing nodular myositis.¹⁶ *Actinomyces* spp. may also cause hepatic abscesses in different species.⁴ In swine, *Actinomyces suis* has been associated with the development of pyogranulomatous mastitis¹⁰ and *Actinomyces hyovaginalis* has been associated with necrotic pulmonary lesions in the same species.² In horses, *Actinomyces* spp. can cause abscesses, which are most commonly located in the submandibular and retropharyngeal regions⁸ and *Actinomyces denticolens* has been associated with the development of submandibular lymphadenitis.¹

Contributing Institution:

Department of Veterinary Medicine, University of Cambridge, Madingley Road, Cambridge CB3 0ES, UK.

<http://www.vet.cam.ac.uk/>

JPC Diagnosis: Omentum: Peritonitis and

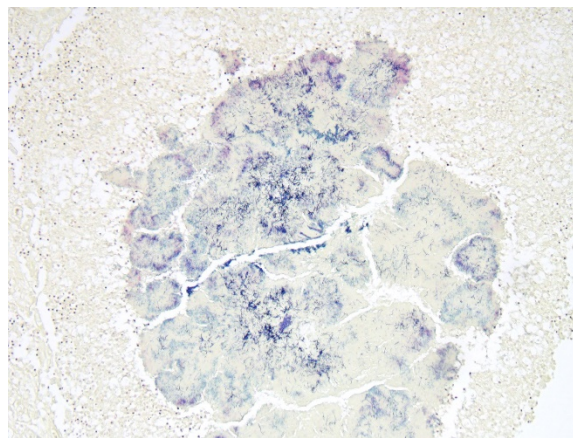
steatitis, chronic-active and pyogranulomatous, multifocal to coalescing, severe, with large colonies of filamentous bacilli and marked mesothelial hyperplasia

JPC Comment: The contributor has provided an excellent review of actinomycotic infection in the dog and a wider range of species. *Actinomyces* is a genus of gram-positive bacteria, with new species being identified on a regular basis in species as diverse as mammals and mollusks.

Members of the genus *Actinomyces* are well documented in health and disease in humans as well. A number of species of *Actinomyces*, including *A. odontolyticus*, *A. oris*, and *A. naeshlundii*, are common commensals in the oral cavity, and are components of the biofilm on teeth at all ages. A number of commensal actinomycetes colonize the gastrointestinal tract, where they are proposed to help in the breakdown of complex sugars as well as producing antibiotics to maintain balance of the bacterial flora.¹²

The pathology of actinomycosis in humans was first identified in 1892 by Kruse, when the bacterium was known as *Streptomyces israelii* (now *A. israelii*).¹¹ Twenty-five species of pathogenic actinomycetes have now been identified in humans. These species of *Actinomyces* are endogenous inhabitants of mucosal membranes which are introduced into deeper tissues by trauma, surgery, or the introduction of foreign bodies. In humans, actinomycosis is classified as orocervicofacial, thoracic, and abdominal. *Omentum, dog: Filamentous bacilli stain positively with a tissue gram stain. (Brown and Brenn, 400X)*

More than half of all cases of human actinomycosis are orocervicofacial, an unsurprising fact considering the ubiquity of multiple species in the oral cavity, and many



infections are polymicrobial in nature. Unlike dogs, the basis for thoracic infection is usually aspiration of oropharyngeal secretions, and results in pulmonary abscessation. Extrapulmonary extension into the thorax (common in small animals) is relatively uncommon in humans, with sepsis being a more common result. Abdominal infections are often the result of abdominal surgery or invasive infection such as appendicitis; pelvic infections have been associated with prolonged use of intrauterine devices for contraception. Less common manifestations are cutaneous and musculoskeletal infections (generally caused by traumatic implantation, and cerebral and disseminated actinomycosis (usually resulting from sepsis). An excellent review of human infection, to include specific forms of infection and associated actinomycotic species was published by Kononen et al. in 2015.¹¹

The moderator discussed the nature of Splendore-Hoeppli material and various theories concerning its makeup, and possible mechanisms of infection the dog and cat, as well as actinomycotic infections in other species.

References:

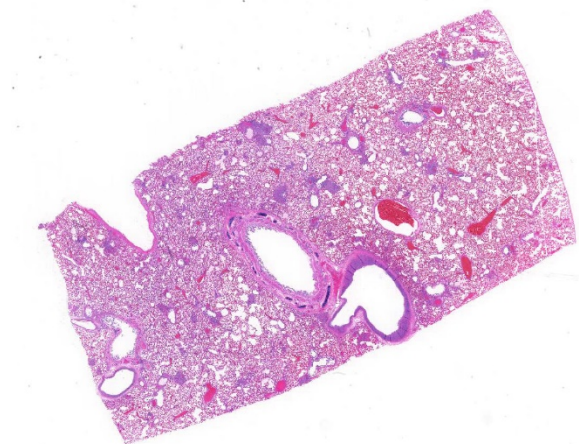
1. Albini S, Korczak BM, Abril C, et al. Mandibular lymphadenopathy caused by *Actinomyces denticolens* mimicking stranglers in three horses. *Vet Rec.* 2008;162(5):158-9.
2. Aalbæk B, Christensen H, Bisgaard M, et al. *Actinomyces hyovaginalis* Associated with disseminated necrotic lung lesions in slaughter pactionomyces veterinary igs. *J Comp Pathol.* 2003;129 (1):70–77.
3. Barnes LD, Grahn BH. Actinomyces endophthalmitis and pneumonia in a dog. *Can Vet J.* 2007;48(11):1155-8.
4. Brown DL, Van Wettere AJ, Cullen JM – Hepatobiliary System and Exocrine Pancreas In: Zachary FJ, ed. *Pathologic Basis of Veterinary Disease*: Elsevier Saunders, 2017:442.
5. Couto SS, Dickinson PJ, Jang S, et al. Pyogranulomatous meningoencephalitis due to *Actinomyces* sp. in a dog. *Vet Pathol.* 2000;37(6):650-2.
6. Edwards DF, Nyland TG, Weigel JP. Thoracic, abdominal, and vertebral actinomycosis. Diagnosis and long-term therapy in three dogs. *J Vet Intern Med.* 1988;2(4):184-91.
7. Edwards DF. Actinomycosis and nocardiosis. In: Greene CE, ed. *Infectious Diseases of the Dog and Cat*. 1st ed. Philadelphia: WB Saunders, 1990:585–590.
8. Fielding CL, Magdesian KG, Morgan RA, Ruby RE, Sprayberry KA. Actinomyces species as a cause of abscesses in nine horses. *Vet Rec.* 2008;162(1):18-20.
9. Gavhane, D.S., Moregaonkar, S.D., Mhase, A.K., Sawale, G.K. and Kadam, D.P.A Case of Chronic Abdominal Actinomycosis with Severe Hepatic Involvement in a Dog. *Israel J Vet Med.* 2016; 71(1):58.
10. Hoyles L, Falsen E, Holmström G, et al. Actinomyces suimastitidis sp. nov., isolated from pig mastitis. *Int J Syst Evol Microbiol.* 2001;51(Pt 4):1323-6.
11. Kononen E, Wade WG. Actinomyces and related organisms in human infections. *Clin Microbiol Rev* doi: 10.1128/CMR.00100-14.
12. Li J, Li Y, Zhou Y, Wang C, Wu B, Wan J. Actinomyces and alimentary tract diseases a review of it. *Biomed Res Int* 2018; <https://doi.org/10.1155/2018/3820215>
13. Ochiai K, Kurita-Ochiai T, Kamino Y, et al. Effect of co-aggregation on the pathogenicity of oral bacteria. *J Med Microbiol.* 1993;39(3):183-90.
14. Sykes J. Bacterial diseases - Actinomycosis In: Sykes J, ed. *Canine and Feline Infectious Diseases*. St Louis, MO: Elsevier Saunders, 2014:399-408.
15. Uzal FA, Plattner BL, Hostetter JM. Alimentary system. In: Maxie MG, ed. *Pathology of Domestic Animals, Volume 2*. 6th ed. St Louis, MO: Elsevier, 2015:253.
16. Valentine B – Skeletal Muscle In: Zachary FJ, ed. *Pathologic Basis of Veterinary Disease*. 6th ed. St Louis, MO: Elsevier Saunders, 2017:926, 942.

CASE IV: 12H5674 (JPC 4032439).

Signalment: A six year old, spayed female Pembroke Welsh Corgi dog (*Canis lupus familiaris*).

History: The dog presented with tachypnea, increased respiratory effort, cardiomegaly, panhypoproteinemia, mild anemia.

Gross Pathology: The dog had areas of ecchymoses around the peripheral veins and clotted blood in the right nasal cavity and ethmoid conchae. Feces were black and tarry. Lungs were diffusely firm and dark red. There were pinpoint multifocal white circular structures diffuse across the lung surface. Other findings included: subendocardial



Lung, dog. At low magnification, there are areas of hypercellularity around small arterioles. (HE, 7X)

petechiae and petechiae cranial to the trigone of the bladder.

Laboratory results: The dog had a slight increase in neutrophils (11.81; range 3.0-11.4 x 10³/ul), monocytes (2.35; range 0.15-1.35 x 10³/ul), reduced hematocrit (36.9; range 37.0-55%), reduced platelets (43; range 200-500 x 10³/ul), increased ALT (223; range 24-90 IU/L), BUN (>180; range 10-30 mg/dl), decreased calcium (8.6; range 9.7-11.3 mg/dl), increased phosphorus (10.7; range 3.2-6.0 mg/dl), increased glucose (202; range 68-115 mg/dl), decreased sodium (122; range 141-151 mEq/L), decreased total protein (4.6; range 5.2-7.1 gm/dl).

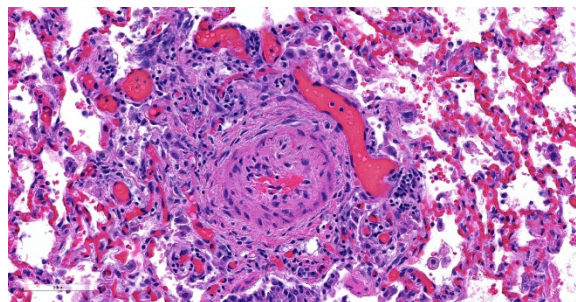
v variable numbers of lymphocytes (plexiform pulmonary arteriopathy). Multifocal alveoli are variably-filled with seroproteinaceous fluid and/or hemorrhage along with increased numbers of alveolar macrophages. There is moderate multifocal to diffuse vascular congestion.

Contributor's Morphologic Diagnoses: Lung, arteriolitis and arteritis, proliferative, lymphocytic and fibrosing with plexiform change, chronic moderate to severe

Lung, hemorrhage, congestion, and edema, multifocal, moderate

Contributor's Comment: The arterial lesions coupled with the clinical and laboratory results are suggestive of plexiform pulmonary arteriopathy.^{2,6} The dog lacked heartworms and lacked evidence of a left to right cardiac shunt and thus the changes are consistent with idiopathic pulmonary arterial hypertension (IPAH).⁶ In a limited number of dogs (six) with pulmonary arteriopathy and hypertension 67% were female, as in this case. The pulmonary vascular changes likely led to or were caused by pulmonary hypertension resulting in right heart failure suggested by radiographic and ultrasound findings that included right ventricular dilation and hepatic centrilobular congestion. Hemorrhage and congestion are present in the lung and are likely due to pulmonary hypertension possibly exacerbated by the thrombocytopenia. The hypoproteinemia and azotemia could not be fully explained. Right heart failure can lead to renal dysfunction but typically not glomerular leakage.

Some cases of IPAH have a mild inflammatory component in the arterioles which was evident in this case as well.⁶ It could not be determined if the inflammation was secondary or incidental to the



Lung, dog. There is intimal hyperplasia and expansion of the tunica media by smooth muscle hyperplasia and increased amounts of collagen and extracellular matrix. Surrounding affected areioles, there is a proliferation of thin-walled arteriolar branches. (HE, 282X)

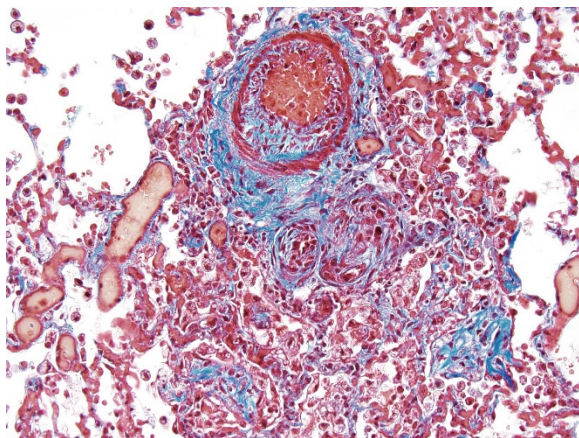
proliferative change or if there is some antigen (self or infectious agent) that triggered the lymphocytic infiltration.

Contributing Institution:

Department of Veterinary Pathology
College of Veterinary Medicine
Iowa State University
Ames, Iowa 50010-1250

JPC Diagnosis: Lung, small arterioles: Plexiform (plexogenic) arteritis with marked intimal and medial hyperplasia and fibrosis, recanalization, and multifocal fibrinoid necrosis and exudative alveolitis.

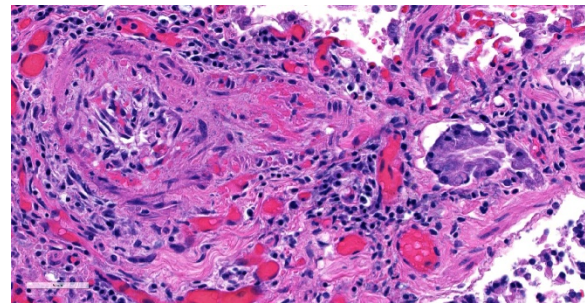
JPC Comment: Plexiform (plexogenic) arterial lesions are striking histologic lesions which are associated with pulmonary hypertension in man and animals. In general terms, plexiform lesions is a form of “dilatation” lesion developing in late stages of pulmonary hypertension, following a precipitous decrease in pulmonary blood flow and resultant irreversible pulmonary hypertension. While many small arterioles will show evidence of prolonged hypertension, to include intimal hyperplasia, smooth muscle hyperplasia and disarray, and medial and adventitial fibrosis and in some



Lung, dog: Plexiform lesion demonstrate marked asymmetric intimal hyperplasia and medial and adventitial fibrosis, as well a proliferation of smaller arterioles (also fibrotic) at the periphery. (Masson's, 400X)

cases fibrinoid necrosis (all present in this section), the plexiform lesion is a unique finding. This lesion is the result of a localized sac-like dilation of a branch of a muscular artery, in which fibrin accumulates from necrosis in the wall of the parent artery.¹ Over time, this fibrin is organized into small vessels populated by cells from the parent artery as well. This pathogenesis also explains why the proliferating vessels are not circumferential but often present eccentrically on only one side of affected arterioles.¹

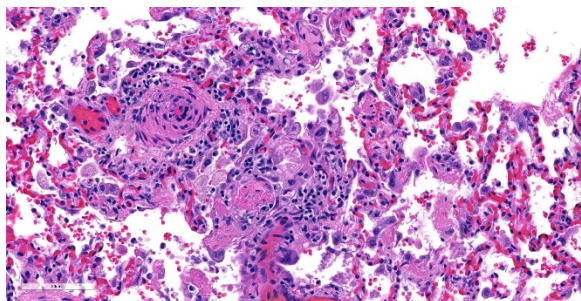
These lesions have been well studied by



Lung, dog. Affected vessels occasionally contain extruded brightly eosinophilic protein and cellular debris within their walls (fibrinoid necrosis.) (HE, 400X)

sequential biopsies taken during the closure of congenital shunts in humans, and many of the associated lesions are seen in this section. The first lesion is increased muscularity of the wall of small arterioles (medial hypertrophy). This is often followed over time by an intimal cellular proliferation, in which smooth muscle cells penetrate the internal elastic lamina and their proliferation at this point may occlude the lumen. They are often accompanied by a proliferation of both collagen and elastin fibers within the intima as well.⁴ At this point, dilatation lesions will develop proximally and concurrent fibrinoid necrosis in the wall of the artery begins the final development of the plexiform lesion as described above.⁴

In humans, plexogenic arteriopathy may arise



Lung dog – There is often polymerized fibrin, increased numbers of alveolar macrophages, polymerized fibrin, and patchy type II pneumocyte hyperplasia within proximity of plexiform lesions. (HE 282X)

as a result of congenital cardiac shunting, but may also be seen with acquired cardiac shunts, hepatic cirrhosis with portal hypertension, schistosomiasis, and oral ingestion of drugs for anorexia.⁴

The first description of pulmonary plexiform arteriopathy (PPA), also in a Welsh Corgi, was published in 2004, and its etiology was attributed to an untreated patent ductus arteriosus (the animal was 21 months at its death.)² PPA was also identified in 4 of 6 animals in another study of dogs with idiopathic pulmonary hypertension. Plexiform lesions were identified primarily at branching points of terminal to alveolar duct arteries.⁶

Plexiform lesions have also been identified in a line of rapidly growing broiler chickens which had a high incidence of idiopathic pulmonary arterial hypertension; however, as opposed to other species, plexiform lesions could be identified immediately post-hatch and did not require a period of pulmonary arterial hypertension.⁵ A line of genetically engineered mutant mice that develop plexiform arteriopathy has been developed as a result of decreased expression of intersectin-1s.³

References:

1. Heath D, Smith P. Plexiform lesions with giant cells. *Thorax* 1982; 37:394-395.
2. Kolm US, Amberger CN, Boujon CE, Lombard CW. Plexogenic pulmonary arteriopathy in a Pembroke Welsh Corgi. *J Small Anim Prac* 45(9):461-466, 2004
3. Patel M, Predescu D, Bardita C, Chen J, Jegathan N, Pritchard M, DiBartolo S, Machado, R, Predescu S. Modulation of intersectin-1s lung expression induces obliterative remodeling and severe plexiform arteriopathy in the murine pulmonary vascular bed. *Am J Pathol* 2017; 187(3):529-542
4. Wagenvoort CA. Plexiform arteriopathy. *Thorax* 1994; 49:S39-245.
5. Wideman RF, Mason JG, Anthony NB, Cross D. Plexogenic arteriopathy in broiler lungs: Evaluation of line, age and sex influences. *Poultry Sci* 2015; 94:628-638.
6. Zabka TS, Campbell FE, Wilson DE. Pulmonary arteriopathy and idiopathic pulmonary arterial hypertension in six dogs. *Vet Pathol* 43(4): 510-522, 2006

Self-Assessment - WSC 2018-2019 Conference 25

1. Which of the following species has *Bordetella bronchiseptica* not been identified in?
 - a. Humans
 - b. Pigs
 - c. Snakes
 - d. Rabbits

2. Which of the following is NOT a member of the *M. tuberculosis* group?
 - a. *M. microti*
 - b. *M. bovis*
 - c. *M. genavense*
 - d. *M. caprae*

3. Which of the following exhibits draining fistulous tracts in the skin as a result of infection with *M. bovis*?
 - a. Feral swine
 - b. Brushtail possums
 - c. White-tailed deer
 - d. Eurasian badgers

4. Which is the most likely route of infection for actinomyces across species?
 - a. Traumatic implantation
 - b. Respiratory
 - c. Orofecal
 - d. Conjunctival inoculation

5. Which of the following Immunostains is selective for skeletal muscle?
 - a. Myoglobin
 - b. Muscle specific actin
 - c. Myogenin
 - d. Desmin

Please email your completed assessment to Ms. Jessica Gold at Jessica.d.gold2.ctr@mail.mil for grading. Passing score is 80%. This program (RACE program number) is approved by the AA VSB RACE to offer a total of 0.5 CE Credits, with a maximum of 12.5 CE Credits being available to any individual Veterinary Medical Professionals for the 2017-2018 Wednesday Slide Conference. This RACE approval is for the subject matter categories of: SCIENTIFIC using the delivery method of NON-INTERACTIVE DISTANCE. This approval is valid in jurisdictions which recognize AA VSB RACE; however, participants are responsible for ascertaining each board's CE requirements. RACE does not "accredit", "endorse" or "certify" any program or person, nor does RACE approval validate the content of the program.